PART II

BIOENERGETICS AND METABOLISM

Metabolism is a highly coordinated cellular activity in which many multienzyme systems (metabolic pathways) cooperate to (1) obtain chemical energy by capturing solar energy or degrading energy-rich nutrients from the environment; (2) convert nutrient molecules into the cell's own characteristic molecules, including precursors of macromolecules; (3) polymerize monomeric precursors into macromolecules: proteins, nucleic acids, and polysaccharides; and (4) synthesize and degrade biomolecules required for specialized cellular functions, such as membrane lipids, intracellular messengers, and pigments.

Although metabolism embraces hundreds of different enzyme-catalyzed reactions, our major concern in Part II is the central metabolic pathways, which are few in number and remarkably similar in all forms of life. Living organisms can be divided into two large groups according to the chemical form in which they obtain carbon from the environment. **Autotrophs** (such as photosynthetic bacteria, green algae, and vascular plants) can use carbon dioxide from the atmosphere as their sole source of carbon, from which they construct all their carbon-containing biomolecules (see Fig. 1–5). Some autotrophic organisms, such as cyanobacteria, can also use atmospheric nitrogen to generate all their nitrogenous components. **Heterotrophs** cannot use atmospheric carbon dioxide and must obtain carbon from their environment in the form of relatively complex organic molecules such as glucose. Multicellular animals and most microorganisms are heterotrophic. Autotrophic cells and organisms are relatively self-sufficient, whereas heterotrophic cells and organisms, with their requirements for carbon in more complex forms, must subsist on the products of other organisms.

Many autotrophic organisms are photosynthetic and obtain their energy from sunlight, whereas heterotrophic organisms obtain their energy from the degradation of organic nutrients produced by autotrophs. In our biosphere, autotrophs and heterotrophs live together in a vast, interdependent cycle in which autotrophic organisms use atmospheric carbon dioxide to build their organic biomolecules, some of them generating

oxygen from water in the process. Heterotrophs in turn use the organic products of autotrophs as nutrients and return carbon dioxide to the atmosphere. Some of the oxidation reactions that produce carbon dioxide also consume oxygen, converting it to water. Thus carbon, oxygen, and water are constantly cycled between the heterotrophic and autotrophic worlds, with solar energy as the driving force for this global process **(Fig. 1)**.

All living organisms also require a source of nitrogen, which is necessary for the synthesis of amino acids, nucleotides, and other compounds. Bacteria and plants can generally use either ammonia or nitrate as their sole source of nitrogen, but vertebrates must obtain nitrogen in the form of amino acids or other organic compounds. Only a few organisms—the cyanobacteria and many species of soil bacteria that live symbiotically on the roots of some plants—are capable of converting ("fixing") atmospheric nitrogen (N_2) into ammonia. Other bacteria (the nitrifying bacteria) oxidize ammonia to nitrites and nitrates; yet others convert nitrate to N_2. The anammox bacteria convert ammonia and nitrite to N_2. Thus, in addition to the global carbon and oxygen cycles, a nitrogen cycle operates in the biosphere, turning over huge amounts of nitrogen **(Fig. 2)**. The cycling of carbon, oxygen, and nitrogen, which ultimately involves all species, depends on a proper balance between the activities of the producers (autotrophs) and consumers (heterotrophs) in our biosphere.

These cycles of matter are driven by an enormous flow of energy into and through the biosphere, beginning with the capture of solar energy by photosynthetic organisms and use of this energy to generate energy-rich carbohydrates and other organic nutrients; these nutrients are then used as energy sources by

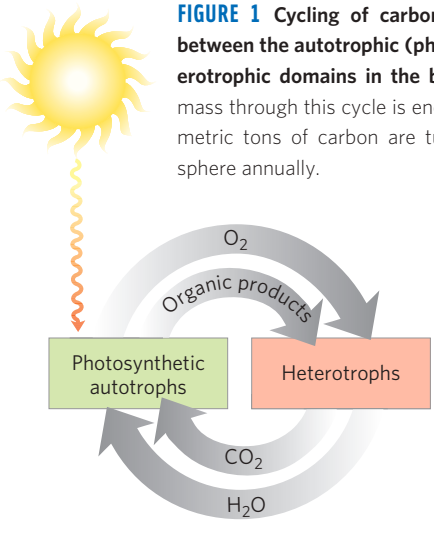

FIGURE 1 Cycling of carbon dioxide and oxygen between the autotrophic (photosynthetic) and heterotrophic domains in the biosphere. The flow of mass through this cycle is enormous; about 4×10^{11} metric tons of carbon are turned over in the biosphere annually.

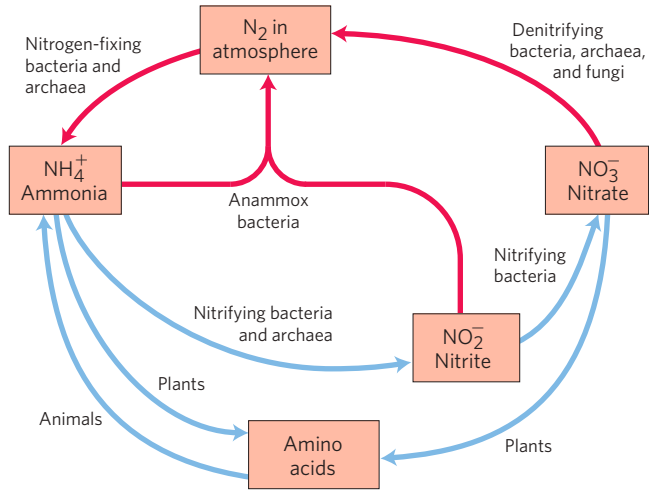

FIGURE 2 Cycling of nitrogen in the biosphere. Gaseous nitrogen (N_2) makes up 80% of the earth's atmosphere.

heterotrophic organisms. In metabolic processes, and in all energy transformations, there is a loss of useful energy (free energy) and an inevitable increase in the amount of unusable energy (heat and entropy). In contrast to the cycling of matter, therefore, energy flows one way through the biosphere; organisms cannot regenerate useful energy from energy dissipated as heat and entropy. Carbon, oxygen, and nitrogen recycle continuously, but energy is constantly transformed into unusable forms such as heat.

Metabolism, the sum of all the chemical transformations taking place in a cell or organism, occurs through a series of enzyme-catalyzed reactions that constitute **metabolic pathways**. Each of the consecutive steps in a metabolic pathway brings about a specific, small chemical change, usually the removal, transfer, or addition of a particular atom or functional group. The precursor is converted into a product through a series of metabolic intermediates called **metabolites**. The term **intermediary metabolism** is often applied to the combined activities of all the metabolic pathways that interconvert precursors, metabolites, and products of low molecular weight (generally, $M_r < 1{,}000$).

Catabolism is the degradative phase of metabolism in which organic nutrient molecules (carbohydrates, fats, and proteins) are converted into smaller, simpler end products (such as lactic acid, CO_2, and NH_3). Catabolic pathways release energy, some of which is conserved in the formation of ATP and reduced electron carriers (NADH, NADPH, and $FADH_2$); the rest is lost as heat. In **anabolism**, also called biosynthesis, small, simple precursors are built up into larger and more complex molecules, including lipids, polysaccharides, proteins,

and nucleic acids. Anabolic reactions require an input of energy, generally in the form of the phosphoryl group transfer potential of ATP and the reducing power of NADH, NADPH, and $FADH_2$ **(Fig. 3)**.

Some metabolic pathways are linear, and some are branched, yielding multiple useful end products from a single precursor or converting several starting materials into a single product. In general, catabolic pathways are *convergent* and anabolic pathways *divergent* **(Fig. 4)**. Some pathways are cyclic: one starting component of the pathway is regenerated in a series of reactions that converts another starting component into a product. We shall see examples of each type of pathway in the following chapters.

Most cells have the enzymes to carry out both the degradation and the synthesis of the important categories of biomolecules—fatty acids, for example. The simultaneous synthesis and degradation of fatty acids would be wasteful, however, and this is prevented by reciprocally regulating the anabolic and catabolic reaction sequences: when one sequence is active, the other is suppressed. Such regulation could not occur if anabolic and catabolic pathways were catalyzed by exactly the same set of enzymes, operating in one direction for anabolism, the opposite direction for catabolism: inhibition of an enzyme involved in catabolism would also inhibit the reaction sequence in the anabolic direction. Catabolic and anabolic pathways that connect the same two end points (glucose ⟶⟶ pyruvate, and pyruvate ⟶⟶ glucose, for example) may employ many of the same enzymes, but invariably at least one of the steps is catalyzed by different enzymes in the catabolic and anabolic directions, and these enzymes are the sites of separate regulation. Moreover, for both anabolic and catabolic pathways to be essentially irreversible, the reactions unique to each direction must include at least one that is thermodynamically very favorable—in other words, a reaction for which the reverse reaction is very unfavorable. As a further contribution to the separate regulation of catabolic and anabolic reaction sequences, paired catabolic and anabolic pathways commonly take place in different cellular compartments: for example, fatty acid catabolism in mitochondria, fatty acid synthesis in the cytosol. The concentrations of intermediates, enzymes, and regulators can be maintained at different levels in these different compartments. Because metabolic pathways are subject to kinetic control by substrate concentration, separate pools of anabolic and catabolic intermediates also contribute to the control of metabolic rates. Devices that separate anabolic and catabolic processes will be of particular interest in our discussions of metabolism.

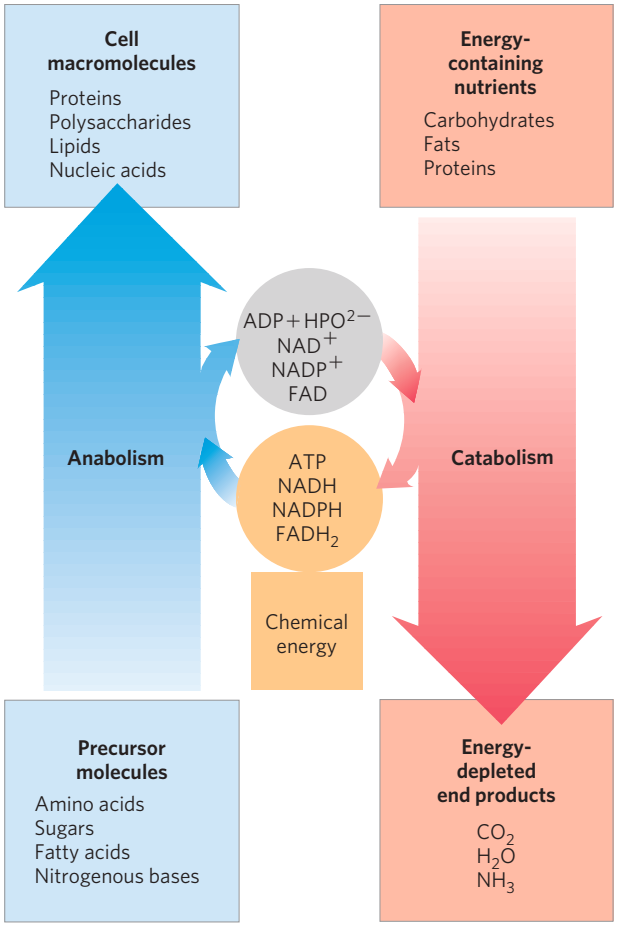

FIGURE 3 Energy relationships between catabolic and anabolic pathways. Catabolic pathways deliver chemical energy in the form of ATP, NADH, NADPH, and $FADH_2$. These energy carriers are used in anabolic pathways to convert small precursor molecules into cellular macromolecules.

Metabolic pathways are regulated at several levels, from within the cell and from outside. The most immediate regulation is by the availability of substrate; when the intracellular concentration of an enzyme's substrate is near or below K_m (as is commonly the case), the rate of the reaction depends strongly on substrate concentration (see Fig. 6–11). A second type of rapid control from within is allosteric regulation (p. 226) by a metabolic intermediate or coenzyme—an amino acid or ATP, for example—that signals the cell's internal metabolic state. When the cell contains an amount of, say, aspartate sufficient for its immediate needs or when the cellular level of ATP indicates that further fuel consumption is unnecessary at the moment, these signals allosterically inhibit the activity of one or more enzymes in the relevant pathway. In multicellular organisms, the metabolic activities of different tissues are regulated and integrated by growth factors and hormones that act from outside

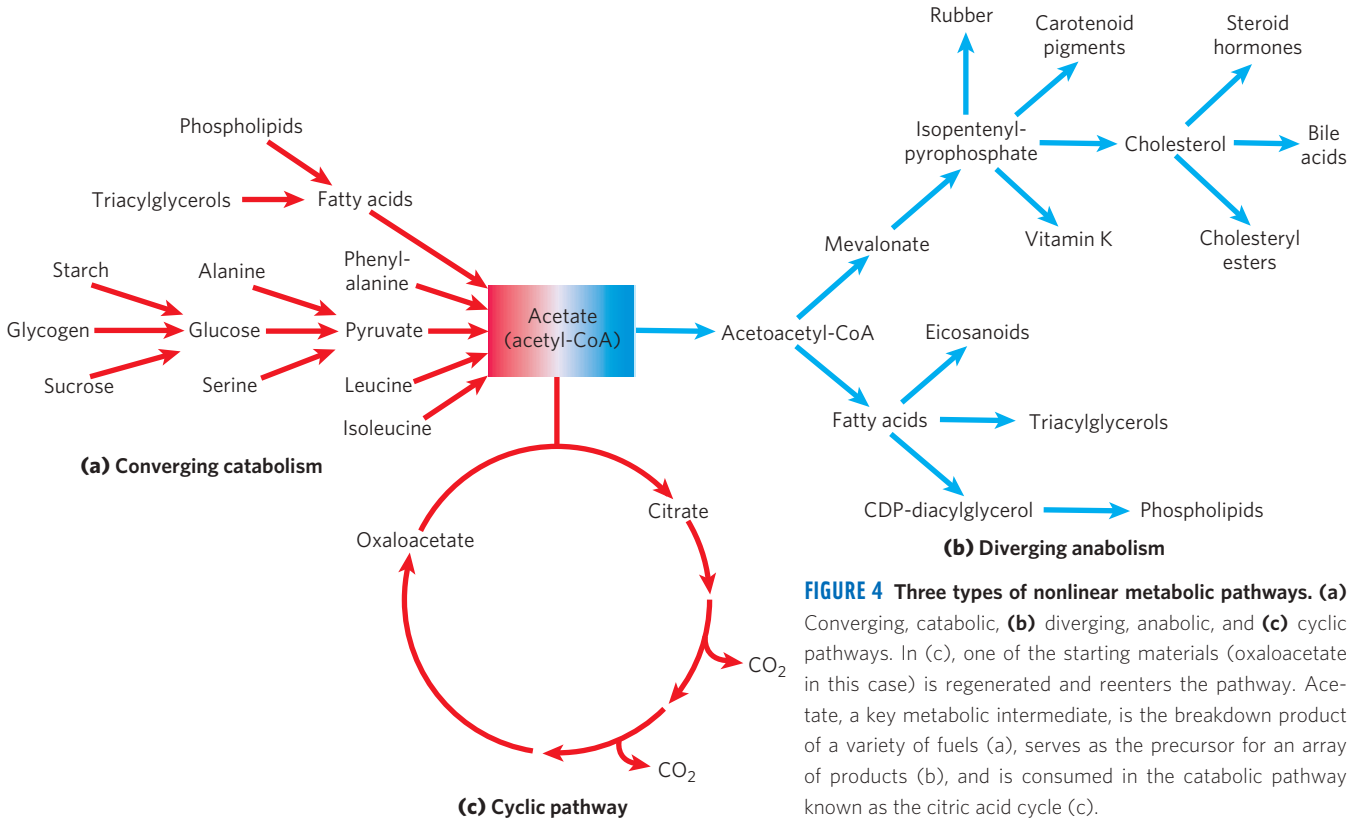

FIGURE 4 **Three types of nonlinear metabolic pathways. (a)** Converging, catabolic, **(b)** diverging, anabolic, and **(c)** cyclic pathways. In (c), one of the starting materials (oxaloacetate in this case) is regenerated and reenters the pathway. Acetate, a key metabolic intermediate, is the breakdown product of a variety of fuels (a), serves as the precursor for an array of products (b), and is consumed in the catabolic pathway known as the citric acid cycle (c).

the cell. In some cases, this regulation occurs virtually instantaneously (sometimes in less than a millisecond) through changes in the levels of intracellular messengers that modify the activity of existing enzyme molecules by allosteric mechanisms or by covalent modification such as phosphorylation. In other cases, the extracellular signal changes the cellular concentration of an enzyme by altering the rate of its synthesis or degradation, so the effect is seen only after minutes or hours.

We begin Part II with a discussion of the basic energetic principles that govern all metabolism (Chapter 13). We then consider the major catabolic pathways by which cells obtain energy from the oxidation of various fuels (Chapters 14 through 19). Chapter 19 is the pivotal point of our discussion of metabolism; it concerns chemiosmotic energy coupling, a universal mechanism in which a transmembrane electrochemical potential, produced either by substrate oxidation or by light absorption, drives the synthesis of ATP.

Chapters 20 through 22 describe the major anabolic pathways by which cells use the energy in ATP to produce carbohydrates, lipids, amino acids, and nucleotides from simpler precursors. In Chapter 23 we step back from our detailed look at the metabolic pathways—as they occur in all organisms, from *Escherichia coli* to humans—and consider how they are regulated and integrated in mammals by hormonal mechanisms.

As we undertake our study of intermediary metabolism, a final word. Keep in mind that the myriad reactions described in these pages take place in, and play crucial roles in, living organisms. As you encounter each reaction and each pathway, ask, What does this chemical transformation do for the organism? How does this pathway interconnect with the other pathways operating simultaneously in the same cell to produce the energy and products required for cell maintenance and growth? How do the multilayered regulatory mechanisms cooperate to balance metabolic and energy inputs and outputs, achieving the dynamic steady state of life? Studied with this perspective, metabolism provides fascinating and revealing insights into life, with countless applications in medicine, agriculture, and biotechnology.

13

Bioenergetics and Biochemical Reaction Types

Living cells and organisms must perform work to stay alive, to grow, and to reproduce. The ability to harness energy and to channel it into biological work is a fundamental property of all living organisms; it must have been acquired very early in cellular evolution. Modern organisms carry out a remarkable variety of energy transductions, conversions of one form of energy to another. They use the chemical energy in fuels to bring about the synthesis of complex, highly ordered macromolecules from simple precursors. They also convert the chemical energy of fuels into concentration gradients and electrical gradients, into motion and heat, and, in a few organisms such as fireflies and deep-sea fish, into light. Photosynthetic organisms transduce light energy into all these other forms of energy.

The chemical mechanisms that underlie biological energy transductions have fascinated and challenged biologists for centuries. The French chemist Antoine Lavoisier recognized that animals somehow transform chemical fuels (foods) into heat and that this process of respiration is essential to life. He observed that

Antoine Lavoisier, 1743–1794

> . . . in general, respiration is nothing but a slow combustion of carbon and hydrogen, which is entirely similar to that which occurs in a lighted lamp or candle, and that, from this point of view, animals that respire are true combustible bodies that burn and consume themselves. . . . One may say that this analogy between combustion and respiration has not escaped the notice of the poets, or rather the philosophers of antiquity, and which they had expounded and interpreted. This fire stolen from heaven, this torch of Prometheus, does not only represent an ingenious and poetic idea, it is a faithful picture of the operations of nature, at least for animals that breathe; one may therefore say, with the ancients, that the torch of life lights itself at the moment the infant breathes for the first time, and it does not extinguish itself except at death.*

In the twentieth century, we began to understand much of the chemistry underlying that "torch of life." Biological energy transductions obey the same chemical and physical laws that govern all other natural processes. It is therefore essential for a student of biochemistry to understand these laws and how they apply to the flow of energy in the biosphere.

In this chapter we first review the laws of thermodynamics and the quantitative relationships among free energy, enthalpy, and entropy. We then review the common types of biochemical reactions that occur in living cells, reactions that harness, store, transfer, and release the energy taken up by organisms from their surroundings. Our focus then shifts to reactions that have special roles in biological energy exchanges, particularly those involving ATP. We finish by considering the importance of oxidation-reduction reactions in living cells, the energetics of biological electron transfers, and the electron carriers commonly employed as cofactors in these processes.

*From a memoir by Armand Seguin and Antoine Lavoisier, dated 1789, quoted in Lavoisier, A. (1862) *Oeuvres de Lavoisier*, Imprimerie Impériale, Paris.

13.1 Bioenergetics and Thermodynamics

Bioenergetics is the quantitative study of **energy transductions**—changes of one form of energy into another—that occur in living cells, and of the nature and function of the chemical processes underlying these transductions. Although many of the principles of thermodynamics have been introduced in earlier chapters and may be familiar to you, a review of the quantitative aspects of these principles is useful here.

Biological Energy Transformations Obey the Laws of Thermodynamics

Many quantitative observations made by physicists and chemists on the interconversion of different forms of energy led, in the nineteenth century, to the formulation of two fundamental laws of thermodynamics. The first law is the principle of the conservation of energy: *for any physical or chemical change, the total amount of energy in the universe remains constant; energy may change form or it may be transported from one region to another, but it cannot be created or destroyed.* The second law of thermodynamics, which can be stated in several forms, says that the universe always tends toward increasing disorder: *in all natural processes, the entropy of the universe increases.*

"Now, in the *second* law of thermodynamics . . . "

Living organisms consist of collections of molecules much more highly organized than the surrounding materials from which they are constructed, and organisms maintain and produce order, seemingly immune to the second law of thermodynamics. But living organisms do not violate the second law; they operate strictly within it. To discuss the application of the second law to biological systems, we must first define those systems and their surroundings.

The reacting system is the collection of matter that is undergoing a particular chemical or physical process; it may be an organism, a cell, or two reacting compounds. The reacting system and its surroundings together constitute the universe. In the laboratory, some chemical or physical processes can be carried out in isolated or closed systems, in which no material or energy is exchanged with the surroundings. Living cells and organisms, however, are open systems, exchanging both material and energy with their surroundings; living systems are never at equilibrium with their surroundings, and the constant transactions between system and surroundings explain how organisms can create order within themselves while operating within the second law of thermodynamics.

In Chapter 1 (p. 23) we defined three thermodynamic quantities that describe the energy changes occurring in a chemical reaction:

Gibbs free energy, ***G***, expresses the amount of an energy capable of doing work during a reaction at constant temperature and pressure. When a reaction proceeds with the release of free energy (that is, when the system changes so as to possess less free energy), the free-energy change, ΔG, has a negative value and the reaction is said to be exergonic. In endergonic reactions, the system gains free energy and ΔG is positive.

Enthalpy, ***H***, is the heat content of the reacting system. It reflects the number and kinds of chemical bonds in the reactants and products. When a chemical reaction releases heat, it is said to be exothermic; the heat content of the products is less than that of the reactants and ΔH has, by convention, a negative value. Reacting systems that take up heat from their surroundings are endothermic and have positive values of ΔH.

Entropy, ***S***, is a quantitative expression for the randomness or disorder in a system (see Box 1–3). When the products of a reaction are less complex and more disordered than the reactants, the reaction is said to proceed with a gain in entropy.

The units of ΔG and ΔH are joules/mole or calories/mole (recall that 1 cal = 4.184 J); units of entropy are joules/mole·Kelvin (J/mol·K) (Table 13–1).

Under the conditions existing in biological systems (including constant temperature and pressure), changes in free energy, enthalpy, and entropy are related to each other quantitatively by the equation

$$\Delta G = \Delta H - T\,\Delta S \qquad (13\text{–}1)$$

in which ΔG is the change in Gibbs free energy of the reacting system, ΔH is the change in enthalpy of the system, T is the absolute temperature, and ΔS is the change in entropy of the system. By convention, ΔS has a positive sign when entropy increases and ΔH, as noted above, has a negative sign when heat is released by the system to its surroundings. Either of these conditions,

TABLE 13–1 Some Physical Constants and Units Used in Thermodynamics

Boltzmann constant, $\mathbf{k} = 1.381 \times 10^{-23}$ J/K
Avogadro's number, $N = 6.022 \times 10^{23}$ mol^{-1}
Faraday constant, $\mathcal{F} = 96{,}480$ J/V·mol
Gas constant, $R = 8.315$ J/mol·K
$(= 1.987$ cal/mol·K$)$
Units of ΔG and ΔH are J/mol (or cal/mol)
Units of ΔS are J/mol·K (or cal/mol·K)
1 cal = 4.184 J
Units of absolute temperature, T, are Kelvin, K
25 °C = 298 K
At 25 °C, $RT = 2.478$ kJ/mol
$(= 0.592$ kcal/mol$)$

which are typical of energetically favorable processes, tend to make ΔG negative. In fact, ΔG of a spontaneously reacting system is always negative.

The second law of thermodynamics states that the entropy *of the universe* increases during all chemical and physical processes, but it does not require that the entropy increase take place *in the reacting system* itself. The order produced within cells as they grow and divide is more than compensated for by the disorder they create in their surroundings in the course of growth and division (see Box 1–3, case 2). In short, living organisms preserve their internal order by taking from the surroundings free energy in the form of nutrients or sunlight, and returning to their surroundings an equal amount of energy as heat and entropy.

Cells Require Sources of Free Energy

Cells are isothermal systems—they function at essentially constant temperature (and also function at constant pressure). Heat flow is not a source of energy for cells, because heat can do work only as it passes to a zone or object at a lower temperature. The energy that cells can and must use is free energy, described by the Gibbs free-energy function G, which allows prediction of the direction of chemical reactions, their exact equilibrium position, and the amount of work they can (in theory) perform at constant temperature and pressure. Heterotrophic cells acquire free energy from nutrient molecules, and photosynthetic cells acquire it from absorbed solar radiation. Both kinds of cells transform this free energy into ATP and other energy-rich compounds capable of providing energy for biological work at constant temperature.

Standard Free-Energy Change Is Directly Related to the Equilibrium Constant

The composition of a reacting system (a mixture of chemical reactants and products) tends to continue changing until equilibrium is reached. At the equilibrium concentration of reactants and products, the rates of the forward and reverse reactions are exactly equal and no further net change occurs in the system. The concentrations of reactants and products *at equilibrium* define the equilibrium constant, K_{eq} (p. 25). In the general reaction aA + bB $\rightleftharpoons$ cC + dD, where a, b, c, and d are the number of molecules of A, B, C, and D participating, the equilibrium constant is given by

$$K_{eq} = \frac{[C]^c[D]^d}{[A]^a[B]^b} \qquad (13\text{–}2)$$

where [A], [B], [C], and [D] are the molar concentrations of the reaction components at the point of equilibrium.

When a reacting system is not at equilibrium, the tendency to move toward equilibrium represents a driving force, the magnitude of which can be expressed as the free-energy change for the reaction, ΔG. Under standard conditions (298 K = 25 °C), when reactants and products are initially present at 1 M concentrations or, for gases, at partial pressures of 101.3 kilopascals (kPa), or 1 atm, the force driving the system toward equilibrium is defined as the standard free-energy change, $\Delta G°$. By this definition, the standard state for reactions that involve hydrogen ions is $[H^+] = 1$ M, or pH 0. Most biochemical reactions, however, occur in well-buffered aqueous solutions near pH 7; both the pH and the concentration of water (55.5 M) are essentially constant.

KEY CONVENTION: For convenience of calculations, biochemists define a standard state different from that used in chemistry and physics: in the biochemical standard state, $[H^+]$ is 10^{-7} M (pH 7) and $[H_2O]$ is 55.5 M. For reactions that involve Mg^{2+} (which include most of those with ATP as a reactant), $[Mg^{2+}]$ in solution is commonly taken to be constant at 1 mM. ■

Physical constants based on this biochemical standard state are called **standard transformed constants** and are written with a prime (such as $\Delta G'°$ and K'_{eq}) to distinguish them from the untransformed constants used by chemists and physicists. (Note that most other textbooks use the symbol $\Delta G°'$ rather than $\Delta G'°$. Our use of $\Delta G'°$, recommended by an international committee of chemists and biochemists, is intended to emphasize that the transformed free energy, $\Delta G'$, is the criterion for equilibrium.) For simplicity, we will hereafter refer to these transformed constants as **standard free-energy changes**.

KEY CONVENTION: In another simplifying convention used by biochemists, when H_2O, H^+, and/or Mg^{2+} are reactants or products, their concentrations are not included in equations such as Equation 13–2 but are instead incorporated into the constants K'_{eq} and $\Delta G'°$. ■

Just as K'_{eq} is a physical constant characteristic for each reaction, so too is $\Delta G'°$ a constant. As we noted in

Chapter 6, there is a simple relationship between K'_{eq} and $\Delta G'^{\circ}$:

$$\Delta G'^{\circ} = -RT \ln K'_{eq} \qquad (13\text{–}3)$$

The standard free-energy change of a chemical reaction is simply an alternative mathematical way of expressing its equilibrium constant. Table 13–2 shows the relationship between $\Delta G'^{\circ}$ and K'_{eq}. If the equilibrium constant for a given chemical reaction is 1.0, the standard free-energy change of that reaction is 0.0 (the natural logarithm of 1.0 is zero). If K'_{eq} of a reaction is greater than 1.0, its $\Delta G'^{\circ}$ is negative. If K'_{eq} is less than 1.0, $\Delta G'^{\circ}$ is positive. Because the relationship between $\Delta G'^{\circ}$ and K'_{eq} is exponential, relatively small changes in $\Delta G'^{\circ}$ correspond to large changes in K'_{eq}.

It may be helpful to think of the standard free-energy change in another way. $\Delta G'^{\circ}$ is the difference between the free-energy content of the products and the free-energy content of the reactants, under standard conditions. When $\Delta G'^{\circ}$ is negative, the products contain less free energy than the reactants and the reaction will proceed spontaneously under standard conditions; all chemical reactions tend to go in the direction that results in a decrease in the free energy of the system. A positive value of $\Delta G'^{\circ}$ means that the products of the reaction contain more free energy than the reactants, and this reaction will tend to go in the reverse direction if we start with 1.0 M concentrations of all components (standard conditions). Table 13–3 summarizes these points.

TABLE 13–2 Relationship between Equilibrium Constants and Standard Free-Energy Changes of Chemical Reactions

	$\Delta G'^{\circ}$	
K'_{eq}	(kJ/mol)	(kcal/mol)*
10^{3}	−17.1	−4.1
10^{2}	−11.4	−2.7
10^{1}	−5.7	−1.4
1	0.0	0.0
10^{-1}	5.7	1.4
10^{-2}	11.4	2.7
10^{-3}	17.1	4.1
10^{-4}	22.8	5.5
10^{-5}	28.5	6.8
10^{-6}	34.2	8.2

*Although joules and kilojoules are the standard units of energy and are used throughout this text, biochemists and nutritionists sometimes express $\Delta G'^{\circ}$ values in kilocalories per mole. We have therefore included values in both kilojoules and kilocalories in this table and in Tables 13–4 and 13–6. To convert kilojoules to kilocalories, divide the number of kilojoules by 4.184.

TABLE 13–3 Relationships among K'_{eq}, $\Delta G'^{\circ}$, and the Direction of Chemical Reactions

When K'_{eq} is . . .	$\Delta G'^{\circ}$ is . . .	Starting with all components at 1 M, the reaction . . .
>1.0	negative	proceeds forward
1.0	zero	is at equilibrium
<1.0	positive	proceeds in reverse

WORKED EXAMPLE 13–1 Calculation of $\Delta G'^{\circ}$

Calculate the standard free-energy change of the reaction catalyzed by the enzyme phosphoglucomutase

$$\text{Glucose 1-phosphate} \rightleftharpoons \text{glucose 6-phosphate}$$

given that, starting with 20 mM glucose 1-phosphate and no glucose 6-phosphate, the final equilibrium mixture at 25°C and pH 7.0 contains 1.0 mM glucose 1-phosphate and 19 mM glucose 6-phosphate. Does the reaction in the direction of glucose 6-phosphate formation proceed with a loss or a gain of free energy?

Solution: First we calculate the equilibrium constant:

$$K'_{eq} = \frac{[\text{glucose 6-phosphate}]}{[\text{glucose 1-phosphate}]} = \frac{19\ \text{mM}}{1.0\ \text{mM}} = 19$$

We can now calculate the standard free-energy change:

$$\begin{aligned}\Delta G'^{\circ} &= -RT \ln K'_{eq} \\ &= -(8.315\ \text{J/mol}\cdot\text{K})(298\ \text{K})(\ln 19) \\ &= -7.3\ \text{kJ/mol}\end{aligned}$$

Because the standard free-energy change is negative, the conversion of glucose 1-phosphate to glucose 6-phosphate proceeds with a loss (release) of free energy. (For the reverse reaction, $\Delta G'^{\circ}$ has the same magnitude but the *opposite* sign.)

Table 13–4 gives the standard free-energy changes for some representative chemical reactions. Note that hydrolysis of simple esters, amides, peptides, and glycosides, as well as rearrangements and eliminations, proceed with relatively small standard free-energy changes, whereas hydrolysis of acid anhydrides is accompanied by relatively large decreases in standard free energy. The complete oxidation of organic compounds such as glucose or palmitate to CO_2 and H_2O, which in cells requires many steps, results in very large decreases in standard free energy. However, standard free-energy changes such as those in Table 13–4 indicate how much free energy is available from a reaction under *standard conditions*. To describe the energy released under the conditions existing in cells, an expression for the *actual* free-energy change is essential.

TABLE 13–4 Standard Free-Energy Changes of Some Chemical Reactions

Reaction type	$\Delta G'^\circ$ (kJ/mol)	$\Delta G'^\circ$ (kcal/mol)
Hydrolysis reactions		
Acid anhydrides		
Acetic anhydride + $H_2O \longrightarrow$ 2 acetate	−91.1	−21.8
ATP + $H_2O \longrightarrow$ ADP + P_i	−30.5	−7.3
ATP + $H_2O \longrightarrow$ AMP + PP_i	−45.6	−10.9
PP_i + $H_2O \longrightarrow 2P_i$	−19.2	−4.6
UDP-glucose + $H_2O \longrightarrow$ UMP + glucose 1-phosphate	−43.0	−10.3
Esters		
Ethyl acetate + $H_2O \longrightarrow$ ethanol + acetate	−19.6	−4.7
Glucose 6-phosphate + $H_2O \longrightarrow$ glucose + P_i	−13.8	−3.3
Amides and peptides		
Glutamine + $H_2O \longrightarrow$ glutamate + NH_4^+	−14.2	−3.4
Glycylglycine + $H_2O \longrightarrow$ 2 glycine	−9.2	−2.2
Glycosides		
Maltose + $H_2O \longrightarrow$ 2 glucose	−15.5	−3.7
Lactose + $H_2O \longrightarrow$ glucose + galactose	−15.9	−3.8
Rearrangements		
Glucose 1-phosphate $\longrightarrow$ glucose 6-phosphate	−7.3	−1.7
Fructose 6-phosphate $\longrightarrow$ glucose 6-phosphate	−1.7	−0.4
Elimination of water		
Malate $\longrightarrow$ fumarate + H_2O	3.1	0.8
Oxidations with molecular oxygen		
Glucose + $6O_2 \longrightarrow 6CO_2 + 6H_2O$	−2,840	−686
Palmitate + $23O_2 \longrightarrow 16CO_2 + 16H_2O$	−9,770	−2,338

Actual Free-Energy Changes Depend on Reactant and Product Concentrations

We must be careful to distinguish between two different quantities: the actual free-energy change, ΔG, and the standard free-energy change, $\Delta G'^\circ$. Each chemical reaction has a characteristic standard free-energy change, which may be positive, negative, or zero, depending on the equilibrium constant of the reaction. The standard free-energy change tells us in which direction and how far a given reaction must go to reach equilibrium *when the initial concentration of each component is 1.0 M,* the pH is 7.0, the temperature is 25 °C, and the pressure is 101.3 kPa (1 atm). Thus $\Delta G'^\circ$ is a constant: it has a characteristic, unchanging value for a given reaction. But the *actual* free-energy change, ΔG, is a function of reactant and product concentrations and of the temperature prevailing during the reaction, none of which will necessarily match the standard conditions as defined above. Moreover, the ΔG of any reaction proceeding spontaneously toward its equilibrium is always negative, becomes less negative as the reaction proceeds, and is zero at the point of equilibrium, indicating that no more work can be done by the reaction.

ΔG and $\Delta G'^\circ$ for any reaction $aA + bB \rightleftharpoons cC + dD$ are related by the equation

$$\Delta G = \Delta G'^\circ + RT \ln \frac{[C]^c[D]^d}{[A]^a[B]^b} \qquad (13\text{–}4)$$

in which the terms in red are those *actually prevailing* in the system under observation. The concentration terms in this equation express the effects commonly called mass action, and the term $[C]^c[D]^d/[A]^a[B]^b$ is called the **mass-action ratio**, ***Q***. Thus Equation 13–4 can be expressed as $\Delta G = \Delta G'^\circ + RT \ln Q$. As an example, let

us suppose that the reaction A + B $\rightleftharpoons$ C + D is taking place under the standard conditions of temperature (25 °C) and pressure (101.3 kPa) but that the concentrations of A, B, C, and D are *not* equal and none of the components is present at the standard concentration of 1.0 M. To determine the actual free-energy change, ΔG, under these nonstandard conditions of concentration as the reaction proceeds from left to right, we simply enter the *actual* concentrations of A, B, C, and D in Equation 13–4; the values of *R, T,* and $\Delta G'^\circ$ are the standard values. ΔG is negative and approaches zero as the reaction proceeds, because the actual concentrations of A and B decrease and the concentrations of C and D increase. Notice that when a reaction is at equilibrium—when there is no force driving the reaction in either direction and ΔG is zero—Equation 13–4 reduces to

$$0 = \Delta G = \Delta G'^\circ + RT \ln \frac{[C]_{eq}[D]_{eq}}{[A]_{eq}[B]_{eq}}$$

or

$$\Delta G'^\circ = -RT \ln K'_{eq}$$

which is the equation relating the standard free-energy change and equilibrium constant (Eqn 13–3).

The criterion for spontaneity of a reaction is the value of ΔG, not $\Delta G'^\circ$. A reaction with a positive $\Delta G'^\circ$ can go in the forward direction *if* ΔG *is negative.* This is possible if the term *RT* ln ([products]/[reactants]) in Equation 13–4 is negative and has a larger absolute value than $\Delta G'^\circ$. For example, the immediate removal of the products of a reaction can keep the ratio [products]/[reactants] well below 1, such that the term *RT* ln ([products]/[reactants]) has a large, negative value. $\Delta G'^\circ$ and ΔG are expressions of the *maximum* amount of free energy that a given reaction can *theoretically* deliver—an amount of energy that could be realized only if a perfectly efficient device were available to trap or harness it. Given that no such device is possible (some energy is always lost to entropy during any process), the amount of work done by the reaction at constant temperature and pressure is always less than the theoretical amount.

Another important point is that some thermodynamically favorable reactions (that is, reactions for which $\Delta G'^\circ$ is large and negative) do not occur at measurable rates. For example, combustion of firewood to CO_2 and H_2O is very favorable thermodynamically, but firewood remains stable for years because the activation energy (see Figs 6–2 and 6–3) for the combustion reaction is higher than the energy available at room temperature. If the necessary activation energy is provided (with a lighted match, for example), combustion will begin, converting the wood to the more stable products CO_2 and H_2O and releasing energy as heat and light. The heat released by this exothermic reaction provides the activation energy for combustion of neighboring regions of the firewood; the process is self-perpetuating.

In living cells, reactions that would be extremely slow *if uncatalyzed* are caused to proceed not by supplying additional heat but by lowering the activation energy through use of an enzyme. An enzyme provides an alternative reaction pathway with a lower activation energy than the uncatalyzed reaction, so that at room temperature a large fraction of the substrate molecules have enough thermal energy to overcome the activation barrier, and the reaction rate increases dramatically. *The free-energy change for a reaction is independent of the pathway by which the reaction occurs*; it depends only on the nature and concentration of the initial reactants and the final products. *Enzymes cannot, therefore, change equilibrium constants*; but they can and do increase the *rate* at which a reaction proceeds in the direction dictated by thermodynamics (see Section 6.2).

Standard Free-Energy Changes Are Additive

In the case of two sequential chemical reactions, A $\rightleftharpoons$ B and B $\rightleftharpoons$ C, each reaction has its own equilibrium constant and each has its characteristic standard free-energy change, $\Delta G'^\circ_1$ and $\Delta G'^\circ_2$. As the two reactions are sequential, B cancels out to give the overall reaction A $\rightleftharpoons$ C, which has its own equilibrium constant and thus its own standard free-energy change, $\Delta G'^\circ_{total}$. *The* $\Delta G'^\circ$ *values of sequential chemical reactions are additive.* For the overall reaction A $\rightleftharpoons$ C, $\Delta G'^\circ_{total}$ is the sum of the individual standard free-energy changes, $\Delta G'^\circ_1$ and $\Delta G'^\circ_2$, of the two reactions: $\Delta G'^\circ_{total} = \Delta G'^\circ_1 + \Delta G'^\circ_2$.

(1)	A $\longrightarrow$ B	$\Delta G'^\circ_1$
(2)	B $\longrightarrow$ C	$\Delta G'^\circ_2$
Sum:	A $\longrightarrow$ C	$\Delta G'^\circ_1 + \Delta G'^\circ_2$

This principle of bioenergetics explains how a thermodynamically unfavorable (endergonic) reaction can be driven in the forward direction by coupling it to a highly exergonic reaction through a common intermediate. For example, the synthesis of glucose 6-phosphate is the first step in the utilization of glucose by many organisms:

$$\text{Glucose} + P_i \longrightarrow \text{glucose 6-phosphate} + H_2O \qquad \Delta G'^\circ = 13.8 \text{ kJ/mol}$$

The positive value of $\Delta G'^\circ$ predicts that under standard conditions the reaction will tend not to proceed spontaneously in the direction written. Another cellular reaction, the hydrolysis of ATP to ADP and P_i, is very exergonic:

$$ATP + H_2O \longrightarrow ADP + P_i \quad \Delta G'^\circ = -30.5 \text{ kJ/mol}$$

These two reactions share the common intermediates P_i and H_2O and may be expressed as sequential reactions:

(1)	Glucose + P_i $\longrightarrow$ glucose 6-phosphate + H_2O
(2)	ATP + H_2O $\longrightarrow$ ADP + P_i
Sum:	ATP + glucose $\longrightarrow$ ADP + glucose 6-phosphate

The overall standard free-energy change is obtained by adding the $\Delta G'^\circ$ values for individual reactions:

$$\Delta G'^\circ = 13.8 \text{ kJ/mol} + (-30.5 \text{ kJ/mol}) = -16.7 \text{ kJ/mol}$$

The overall reaction is exergonic. In this case, energy stored in ATP is used to drive the synthesis of glucose 6-phosphate, even though its formation from glucose and inorganic phosphate (P_i) is endergonic. The *pathway* of glucose 6-phosphate formation from glucose by phosphoryl transfer from ATP is different from reactions (1) and (2) above, but the net result is the same as the sum of the two reactions. In thermodynamic calculations, all that matters is the state of the system at the beginning of the process and its state at the end; the route between the initial and final states is immaterial.

We have said that $\Delta G'^\circ$ is a way of expressing the equilibrium constant for a reaction. For reaction (1) above,

$$K'_{eq_1} = \frac{[\text{glucose 6-phosphate}]}{[\text{glucose}]\,[P_i]} = 3.9 \times 10^{-3}\ \text{M}^{-1}$$

Notice that H_2O is not included in this expression, as its concentration (55.5 M) is assumed to remain unchanged by the reaction. The equilibrium constant for the hydrolysis of ATP is

$$K'_{eq_2} = \frac{[\text{ADP}]\,[P_i]}{[\text{ATP}]} = 2.0 \times 10^{5}\ \text{M}$$

The equilibrium constant for the two coupled reactions is

$$\begin{aligned} K'_{eq_3} &= \frac{[\text{glucose 6-phosphate}]\,[\text{ADP}]\,[P_i]}{[\text{glucose}]\,[P_i]\,[\text{ATP}]} \\ &= (K'_{eq_1})(K'_{eq_2}) = (3.9 \times 10^{-3}\ \text{M}^{-1})(2.0 \times 10^{5}\ \text{M}) \\ &= 7.8 \times 10^{2} \end{aligned}$$

This calculation illustrates an important point about equilibrium constants: although the $\Delta G'^\circ$ values for two reactions that sum to a third, overall reaction are *additive*, the K'_{eq} for the overall reaction is the *product* of the individual K'_{eq} values for the two reactions. Equilibrium constants are *multiplicative*. By coupling ATP hydrolysis to glucose 6-phosphate synthesis, the K'_{eq} for formation of glucose 6-phosphate from glucose has been raised by a factor of about 2×10^5.

This common-intermediate strategy is employed by all living cells in the synthesis of metabolic intermediates and cellular components. Obviously, the strategy works only if compounds such as ATP are continuously available. In the following chapters we consider several of the most important cellular pathways for producing ATP.

SUMMARY 13.1 Bioenergetics and Thermodynamics

- Living cells constantly perform work. They require energy for maintaining their highly organized structures, synthesizing cellular components, generating electric currents, and many other processes.
- Bioenergetics is the quantitative study of energy relationships and energy conversions in biological systems. Biological energy transformations obey the laws of thermodynamics.
- All chemical reactions are influenced by two forces: the tendency to achieve the most stable bonding state (for which enthalpy, H, is a useful expression) and the tendency to achieve the highest degree of randomness, expressed as entropy, S. The net driving force in a reaction is ΔG, the free-energy change, which represents the net effect of these two factors: $\Delta G = \Delta H - T\Delta S$.
- The standard transformed free-energy change, $\Delta G'^\circ$, is a physical constant that is characteristic for a given reaction and can be calculated from the equilibrium constant for the reaction: $\Delta G'^\circ = -RT \ln K'_{eq}$.
- The actual free-energy change, ΔG, is a variable that depends on $\Delta G'^\circ$ and on the concentrations of reactants and products: $\Delta G = \Delta G'^\circ + RT \ln$ ([products]/[reactants]).
- When ΔG is large and negative, the reaction tends to go in the forward direction; when ΔG is large and positive, the reaction tends to go in the reverse direction; and when $\Delta G = 0$, the system is at equilibrium.
- The free-energy change for a reaction is independent of the pathway by which the reaction occurs. Free-energy changes are additive; the net chemical reaction that results from successive reactions sharing a common intermediate has an overall free-energy change that is the sum of the ΔG values for the individual reactions.

13.2 Chemical Logic and Common Biochemical Reactions

The biological energy transductions we are concerned with in this book are chemical reactions. Cellular chemistry does not encompass every kind of reaction learned in a typical organic chemistry course. Which reactions take place in biological systems and which do not is determined by (1) their relevance to that particular metabolic system and (2) their rates. Both considerations play major roles in shaping the metabolic pathways we consider throughout the rest of the book. A relevant reaction is one that makes use of an available substrate and converts it to a useful product. However, even a potentially relevant reaction may not occur. Some chemical transformations are too slow (have activation energies that are too high) to contribute to living systems even with the aid of powerful enzyme catalysts. The reactions that do occur in cells represent a toolbox that evolution has used to construct metabolic pathways that circumvent the "impossible" reactions. Learning to

recognize the plausible reactions can be a great aid in developing a command of biochemistry.

Even so, the number of metabolic transformations taking place in a typical cell can seem overwhelming. Most cells have the capacity to carry out thousands of specific, enzyme-catalyzed reactions: for example, transformation of a simple nutrient such as glucose into amino acids, nucleotides, or lipids; extraction of energy from fuels by oxidation; and polymerization of monomeric subunits into macromolecules.

To study these reactions, some organization is essential. There are patterns within the chemistry of life; you do not need to learn every individual reaction to comprehend the molecular logic of biochemistry. Most of the reactions in living cells fall into one of five general categories: (1) reactions that make or break carbon–carbon bonds; (2) internal rearrangements, isomerizations, and eliminations; (3) free-radical reactions; (4) group transfers; and (5) oxidation-reductions. We discuss each of these in more detail below and refer to some examples of each type in later chapters. Note that the five reaction types are not mutually exclusive; for example, an isomerization reaction may involve a free-radical intermediate.

Before proceeding, however, we should review two basic chemical principles. First, a covalent bond consists of a shared pair of electrons, and the bond can be broken in two general ways **(Fig. 13–1)**. In **homolytic cleavage**, each atom leaves the bond as a **radical**, carrying one unpaired electron. In **heterolytic cleavage**,

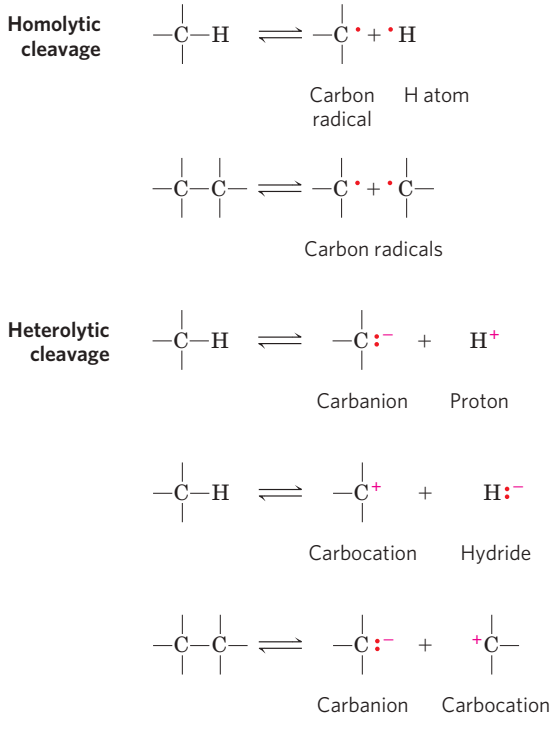

FIGURE 13–1 Two mechanisms for cleavage of a C—C or C—H bond. In a homolytic cleavage, each atom keeps one of the bonding electrons, resulting in the formation of carbon radicals (carbons having unpaired electrons) or uncharged hydrogen atoms. In a heterolytic cleavage, one of the atoms retains both bonding electrons. This can result in the formation of carbanions, carbocations, protons, or hydride ions.

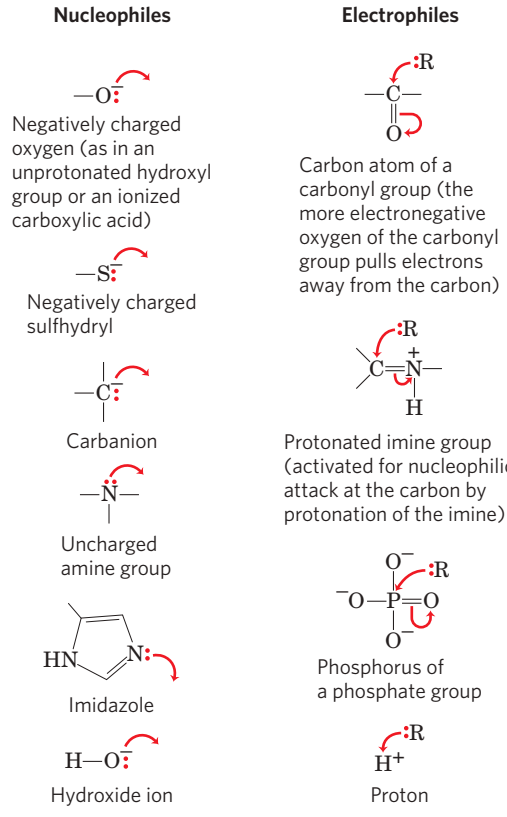

FIGURE 13–2 Common nucleophiles and electrophiles in biochemical reactions. Chemical reaction mechanisms, which trace the formation and breakage of covalent bonds, are communicated with dots and curved arrows, a convention known informally as "electron pushing." A covalent bond consists of a shared pair of electrons. Nonbonded electrons important to the reaction mechanism are designated by dots (:). Curved arrows (↷) represent the movement of electron pairs. For movement of a single electron (as in a free radical reaction), a single-headed (fishhook-type) arrow is used (↷). Most reaction steps involve an unshared electron pair.

which is more common, one atom retains both bonding electrons. The species most often generated when C—C and C—H bonds are cleaved are illustrated in Figure 13–1. Carbanions, carbocations, and hydride ions are highly unstable; this instability shapes the chemistry of these ions, as we shall see.

The second basic principle is that many biochemical reactions involve interactions between **nucleophiles** (functional groups rich in and capable of donating electrons) and **electrophiles** (electron-deficient functional groups that seek electrons). Nucleophiles combine with and give up electrons to electrophiles. Common biological nucleophiles and electrophiles are shown in **Figure 13–2**. Note that a carbon atom can act as either a nucleophile or an electrophile, depending on which bonds and functional groups surround it.

Reactions That Make or Break Carbon–Carbon Bonds Heterolytic cleavage of a C—C bond yields a **carbanion** and a **carbocation** (Fig. 13–1). Conversely, the formation of a C—C bond involves the combination of a nucleophilic carbanion and an electrophilic carbocation. Carbanions

and carbocations are generally so unstable that their formation as reaction intermediates can be energetically inaccessible even with enzyme catalysts. For the purpose of cellular biochemistry they are impossible reactions—unless chemical assistance is provided in the form of functional groups containing electronegative atoms (O and N) that can alter the electronic structure of adjacent carbon atoms so as to stabilize and facilitate the formation of carbanion and carbocation intermediates.

Carbonyl groups are particularly important in the chemical transformations of metabolic pathways. The carbon of a carbonyl group has a partial positive charge due to the electron-withdrawing property of the carbonyl oxygen, and thus is an electrophilic carbon **(Fig. 13–3a)**. A carbonyl group can thus facilitate the formation of a carbanion on an adjoining carbon by delocalizing the carbanion's negative charge (Fig. 13–3b). An imine group (see Fig. 1–16) can serve a similar function (Fig. 13–3c). The capacity of carbonyl and imine groups to delocalize electrons can be further enhanced by a general acid catalyst or by a metal ion such as Mg^{2+} (Fig. 13–3d).

The importance of a carbonyl group is evident in three major classes of reactions in which C—C bonds are formed or broken **(Fig. 13–4)**: aldol condensations, Claisen ester condensations, and decarboxylations. In each type of reaction, a carbanion intermediate is stabilized by a carbonyl group, and in many cases another carbonyl provides the electrophile with which the nucleophilic carbanion reacts.

An **aldol condensation** is a common route to the formation of a C—C bond; the aldolase reaction, which converts a six-carbon compound to two three-carbon compounds in glycolysis, is an aldol condensation in reverse (see Fig. 14–6). In a **Claisen condensation**, the carbanion is stabilized by the carbonyl of an adjacent thioester; an example is the synthesis of citrate in the citric acid cycle (see Fig. 16–9). Decarboxylation also commonly involves the formation of a carbanion stabilized by a carbonyl group; the acetoacetate decarboxylase reaction that occurs in the formation of ketone bodies during fatty acid catabolism provides an example (see Fig. 17–19). Entire metabolic pathways are organized around the introduction of a carbonyl group in a particular location so that a nearby carbon–carbon bond can be formed or cleaved. In some reactions, an imine or a specialized cofactor such as pyridoxal phosphate plays the electron-withdrawing role of the carbonyl group.

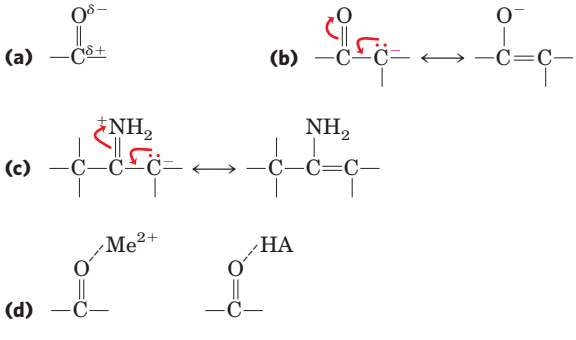

FIGURE 13–3 Chemical properties of carbonyl groups. (a) The carbon atom of a carbonyl group is an electrophile by virtue of the electron-withdrawing capacity of the electronegative oxygen atom, which results in a structure in which the carbon has a partial positive charge. **(b)** Within a molecule, delocalization of electrons into a carbonyl group stabilizes a carbanion on an adjacent carbon, facilitating its formation. **(c)** Imines function much like carbonyl groups in facilitating electron withdrawal. **(d)** Carbonyl groups do not always function alone; their capacity as electron sinks often is augmented by interaction with either a metal ion (Me^{2+}, such as Mg^{2+}) or a general acid (HA).

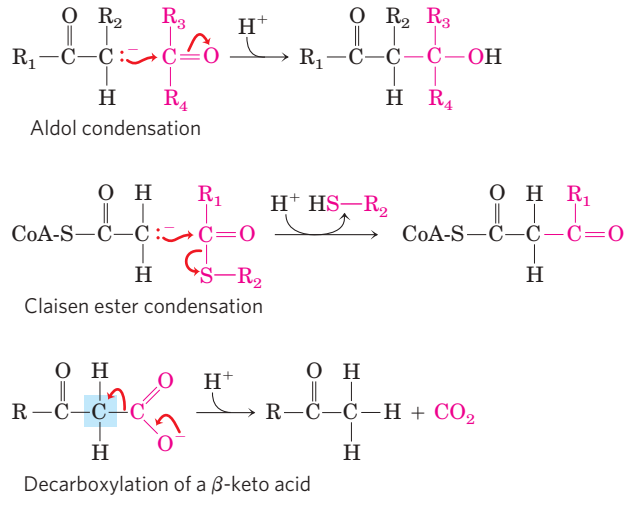

FIGURE 13–4 Some common reactions that form and break C—C bonds in biological systems. For both the aldol condensation and the Claisen condensation, a carbanion serves as nucleophile and the carbon of a carbonyl group serves as electrophile. The carbanion is stabilized in each case by another carbonyl at the adjoining carbon. In the decarboxylation reaction, a carbanion is formed on the carbon shaded blue as the CO_2 leaves. The reaction would not occur at an appreciable rate without the stabilizing effect of the carbonyl adjacent to the carbanion carbon. Wherever a carbanion is shown, a stabilizing resonance with the adjacent carbonyl, as shown in Figure 13–3b, is assumed. An imine (Fig. 13–3c) or other electron-withdrawing group (including certain enzymatic cofactors such as pyridoxal) can replace the carbonyl group in the stabilization of carbanions.

The carbocation intermediate occurring in some reactions that form or cleave C—C bonds is generated by the elimination of a very good leaving group, such as pyrophosphate (see Group Transfer Reactions below). An example is the prenyltransferase reaction **(Fig. 13–5)**, an early step in the pathway of cholesterol biosynthesis.

Internal Rearrangements, Isomerizations, and Eliminations

Another common type of cellular reaction is an intramolecular rearrangement in which redistribution of electrons results in alterations of many different types without a change in the overall oxidation state of the molecule. For example, different groups in a molecule may undergo oxidation-reduction, with no net change in oxidation state of the molecule; groups at a double bond may undergo a cis-trans rearrangement; or the positions of double bonds may be transposed. An example of an isomerization entailing oxidation-reduction is the formation of

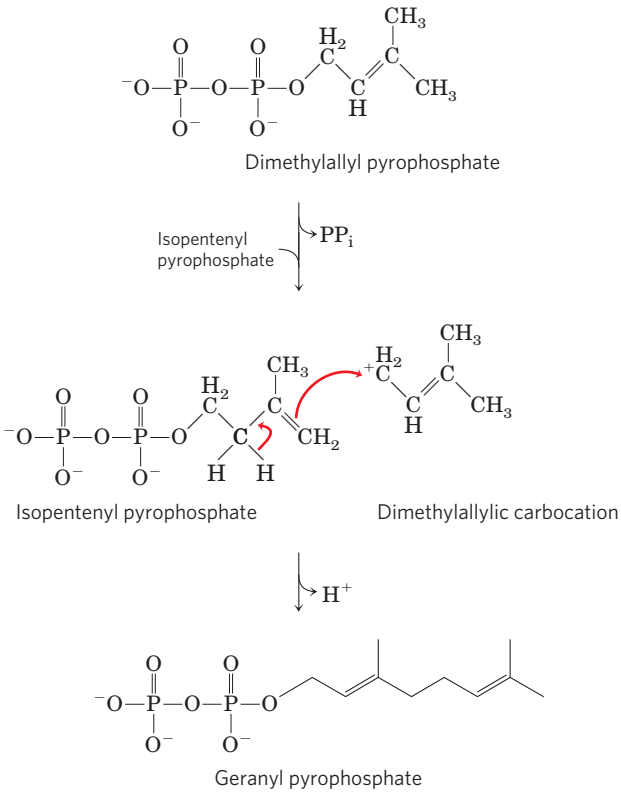

FIGURE 13–5 Carbocations in carbon–carbon bond formation. In one of the early steps in cholesterol biosynthesis, the enzyme prenyltransferase catalyzes condensation of isopentenyl pyrophosphate and dimethylallyl pyrophosphate to form geranyl pyrophosphate (see Fig. 21-36). The reaction is initiated by elimination of pyrophosphate from the dimethylallyl pyrophosphate to generate a carbocation, stabilized by resonance with the adjacent C═C bond.

fructose 6-phosphate from glucose 6-phosphate in glycolysis **(Fig. 13–6)**; this reaction is discussed in detail in Chapter 14): C-1 is reduced (aldehyde to alcohol) and C-2 is oxidized (alcohol to ketone). Figure 13–6b shows the details of the electron movements in this type of isomerization. A cis-trans rearrangement is illustrated by the prolyl cis-trans isomerase reaction in the folding of certain proteins (see Fig. 4–8). A simple transposition of a C═C bond occurs during metabolism of oleic acid, a common fatty acid (see Fig. 17–10). Some spectacular examples of double-bond repositioning occur in the biosynthesis of cholesterol (see Fig. 21–33).

An example of an elimination reaction that does not affect overall oxidation state is the loss of water from an alcohol, resulting in the introduction of a C═C bond:

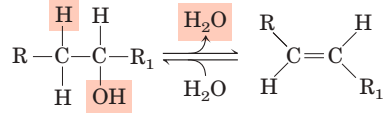

Similar reactions can result from eliminations in amines.

Free-Radical Reactions Once thought to be rare, the homolytic cleavage of covalent bonds to generate free radicals has now been found in a wide range of biochemical processes. These include: isomerizations that make use of adenosylcobalamin (vitamin B_{12}) or *S*-adenosylmethionine, which are initiated with a 5′-deoxyadenosyl radical (see the methylmalonyl-CoA mutase reaction in Box 17–2); certain radical-initiated decarboxylation reactions **(Fig. 13–7)**; some reductase reactions, such as that catalyzed by ribonucleotide reductase (see Fig. 22–41);

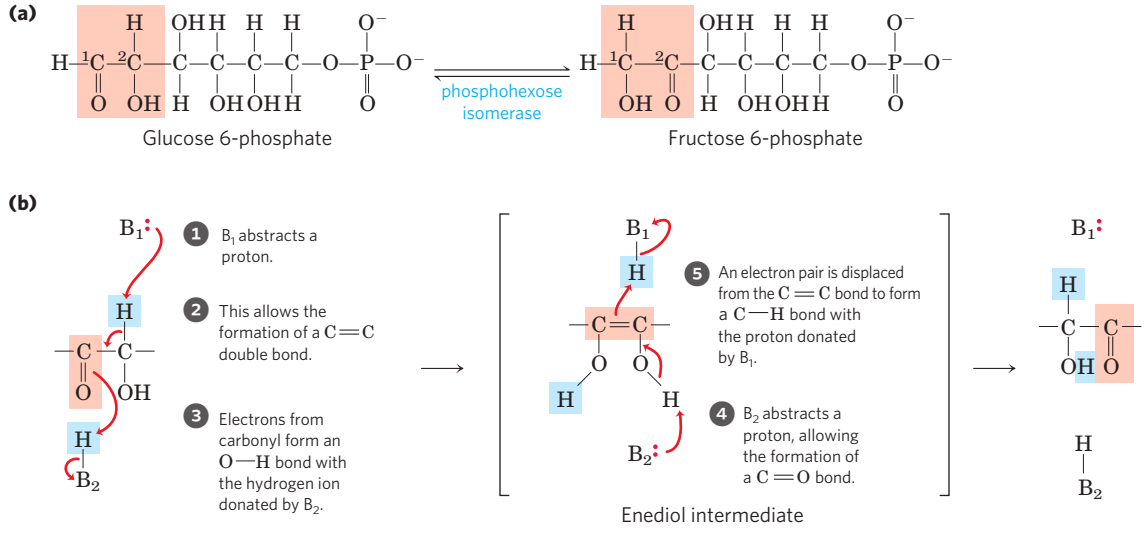

FIGURE 13–6 Isomerization and elimination reactions. (a) The conversion of glucose 6-phosphate to fructose 6-phosphate, a reaction of sugar metabolism catalyzed by phosphohexose isomerase. **(b)** This reaction proceeds through an enediol intermediate. Light red screens follow the path of oxidation from left to right. B_1 and B_2 are ionizable groups on the enzyme; they are capable of donating and accepting protons (acting as general acids or general bases) as the reaction proceeds.

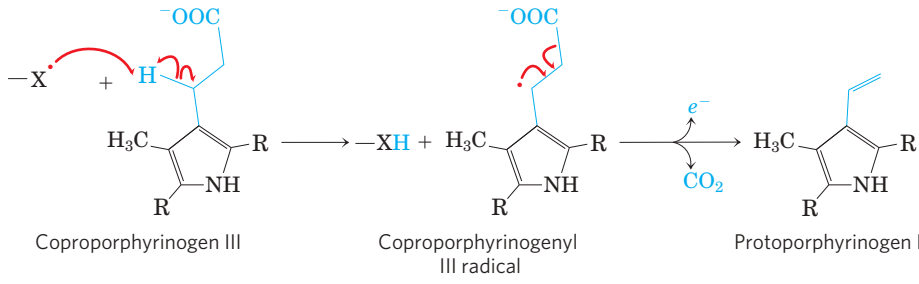

FIGURE 13–7 A free radical–initiated decarboxylation reaction. The biosynthesis of heme (see Fig. 22–26) in *Escherichia coli* includes a decarboxylation step in which propionyl side chains on the coproporphyrinogen III intermediate are converted to the vinyl side chains of protoporphyrinogen IX. When the bacteria are grown anaerobically the enzyme oxygen-independent coproporphyrinogen III oxidase, also called HemN protein, promotes decarboxylation via the free-radical mechanism shown here. The acceptor of the released electron is not known. For simplicity, only the relevant portions of the large coproporphyrinogen III and protoporphyrinogen molecules are shown; the entire structures are given in Figure 22–26. When *E. coli* are grown in the presence of oxygen, this reaction is an oxidative decarboxylation and is catalyzed by a different enzyme.

and some rearrangement reactions, such as that catalyzed by DNA photolyase (see Fig. 25–26).

Group Transfer Reactions The transfer of acyl, glycosyl, and phosphoryl groups from one nucleophile to another is common in living cells. Acyl group transfer generally involves the addition of a nucleophile to the carbonyl carbon of an acyl group to form a tetrahedral intermediate:

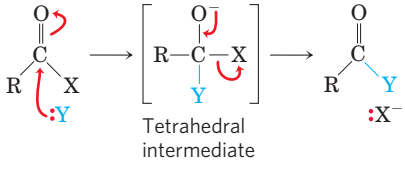

The chymotrypsin reaction is one example of acyl group transfer (see Fig. 6–22). Glycosyl group transfers involve nucleophilic substitution at C-1 of a sugar ring, which is the central atom of an acetal. In principle, the substitution could proceed by an S_N1 or S_N2 pathway, as described in Figure 6–28 for the enzyme lysozyme.

Phosphoryl group transfers play a special role in metabolic pathways, and these transfer reactions are discussed in detail in Section 13.3. A general theme in metabolism is the attachment of a good leaving group to a metabolic intermediate to "activate" the intermediate for subsequent reaction. Among the better leaving groups in nucleophilic substitution reactions are inorganic orthophosphate (the ionized form of H_3PO_4 at neutral pH, a mixture of $H_2PO_4^-$ and HPO_4^{2-}, commonly abbreviated P_i) and inorganic pyrophosphate ($P_2O_7^{4-}$, abbreviated PP_i); esters and anhydrides of phosphoric acid are effectively activated for reaction. Nucleophilic substitution is made more favorable by the attachment of a phosphoryl group to an otherwise poor leaving group such as —OH. Nucleophilic substitutions in which the phosphoryl group ($—PO_3^{2-}$) serves as a leaving group occur in hundreds of metabolic reactions.

Phosphorus can form five covalent bonds. The conventional representation of P_i **(Fig. 13–8a)**, with three P—O bonds and one P═O bond, is a convenient

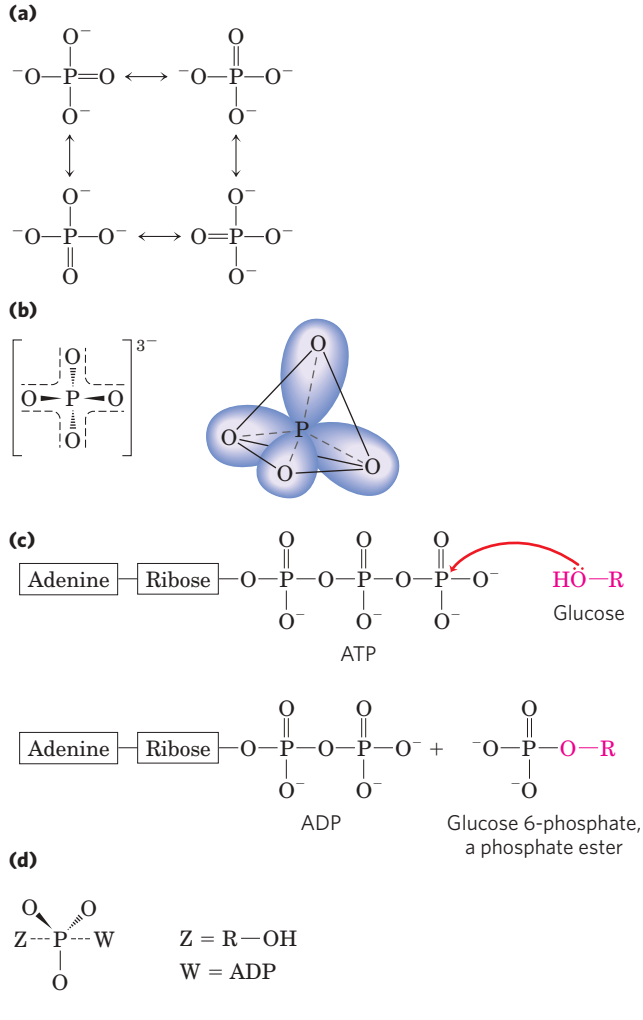

FIGURE 13–8 Phosphoryl group transfers: some of the participants. **(a)** In one (inadequate) representation of P_i, three oxygens are single-bonded to phosphorus, and the fourth is double-bonded, allowing the four different resonance structures shown here. **(b)** The resonance structures of P_i can be represented more accurately by showing all four phosphorus-oxygen bonds with some double-bond character; the hybrid orbitals so represented are arranged in a tetrahedron with P at its center. **(c)** When a nucleophile Z (in this case, the —OH on C-6 of glucose) attacks ATP, it displaces ADP (W). In this S_N2 reaction, a pentacovalent intermediate **(d)** forms transiently.

but inaccurate picture. In P_i, four equivalent phosphorus–oxygen bonds share some double-bond character, and the anion has a tetrahedral structure (Fig. 13–8b). Because oxygen is more electronegative than phosphorus, the sharing of electrons is unequal: the central phosphorus bears a partial positive charge and can therefore act as an electrophile. In a great many metabolic reactions, a phosphoryl group ($—PO_3^{2-}$) is transferred from ATP to an alcohol, forming a phosphate ester (Fig. 13–8c), or to a carboxylic acid, forming a mixed anhydride. When a nucleophile attacks the electrophilic phosphorus atom in ATP, a relatively stable pentacovalent structure forms as a reaction intermediate (Fig. 13–8d). With departure of the leaving group (ADP), the transfer of a phosphoryl group is complete. The large family of enzymes that catalyze phosphoryl group transfers with ATP as donor are called **kinases** (Greek *kinein*, "to move"). Hexokinase, for example, "moves" a phosphoryl group from ATP to glucose.

Phosphoryl groups are not the only groups that activate molecules for reaction. Thioalcohols (thiols), in which the oxygen atom of an alcohol is replaced with a sulfur atom, are also good leaving groups. Thiols activate carboxylic acids by forming thioesters (thiol esters). In later chapters we discuss several reactions, including those catalyzed by the fatty acyl synthases in lipid synthesis (see Fig. 21–2), in which nucleophilic substitution at the carbonyl carbon of a thioester results in transfer of the acyl group to another moiety.

Oxidation-Reduction Reactions Carbon atoms can exist in five oxidation states, depending on the elements with which they share electrons **(Fig. 13–9)**, and transitions between these states are of crucial importance in metabolism (oxidation-reduction reactions are the topic of Section 13.4). In many biological oxidations, a compound loses two electrons and two hydrogen ions (that is, two hydrogen atoms); these reactions are commonly called dehydrogenations and the enzymes that catalyze them are called dehydrogenases **(Fig. 13–10)**. In some, but not all, biological oxidations, a carbon atom becomes covalently bonded to an oxygen atom. The enzymes that catalyze these oxidations are generally called oxidases or, if the oxygen atom is derived directly from molecular oxygen (O_2) oxygenases.

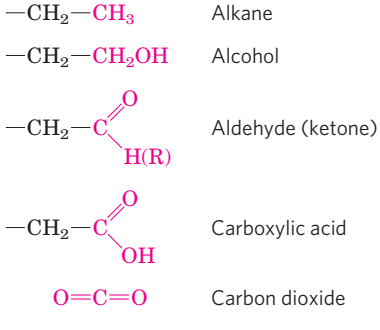

FIGURE 13–9 The oxidation levels of carbon in biomolecules. Each compound is formed by oxidation of the red carbon in the compound shown immediately above. Carbon dioxide is the most highly oxidized form of carbon found in living systems.

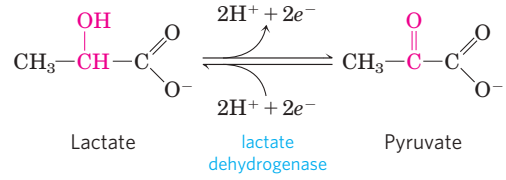

FIGURE 13–10 An oxidation-reduction reaction. Shown here is the oxidation of lactate to pyruvate. In this dehydrogenation, two electrons and two hydrogen ions (the equivalent of two hydrogen atoms) are removed from C-2 of lactate, an alcohol, to form pyruvate, a ketone. In cells the reaction is catalyzed by lactate dehydrogenase and the electrons are transferred to the cofactor nicotinamide adenine dinucleotide (NAD). This reaction is fully reversible; pyruvate can be reduced by electrons transferred from the cofactor.

Every oxidation must be accompanied by a reduction, in which an electron acceptor acquires the electrons removed by oxidation. Oxidation reactions generally release energy (think of camp fires: the compounds in wood are oxidized by oxygen molecules in the air). Most living cells obtain the energy needed for cellular work by oxidizing metabolic fuels such as carbohydrates or fat (photosynthetic organisms can also trap and use the energy of sunlight). The catabolic (energy-yielding) pathways described in Chapters 14 through 19 are oxidative reaction sequences that result in the transfer of electrons from fuel molecules, through a series of electron carriers, to oxygen. The high affinity of O_2 for electrons makes the overall electron-transfer process highly exergonic, providing the energy that drives ATP synthesis—the central goal of catabolism.

Many of the reactions within these five classes are facilitated by cofactors, in the form of coenzymes and metals (vitamin B_{12}, *S*-adenosylmethionine, folate, nicotinamide, and iron are some examples). Cofactors bind to enzymes—in some cases reversibly, in other cases almost irreversibly—and confer on them the capacity to promote a particular kind of chemistry (p. 190). Most cofactors participate in a narrow range of closely related reactions. In the following chapters, we will introduce and discuss each important cofactor at the point where we first encounter it. The cofactors provide another way to organize the study of biochemical processes, since the reactions facilitated by a given cofactor generally are mechanistically related.

Biochemical and Chemical Equations Are Not Identical

Biochemists write metabolic equations in a simplified way, and this is particularly evident for reactions involving ATP. Phosphorylated compounds can exist in several ionization states and, as we have noted, the different species can bind Mg^{2+}. For example, at pH 7 and 2 mM Mg^{2+}, ATP exists in the forms ATP^{4-}, $HATP^{3-}$, H_2ATP^{2-}, $MgHATP^{-}$, and Mg_2ATP. In thinking about the biological role of ATP, however, we are not always interested in all this detail, and so we consider ATP as an entity made up of a sum of species, and we write its hydrolysis as the biochemical equation

$$ATP + H_2O \longrightarrow ADP + P_i$$

where ATP, ADP, and P_i are sums of species. The corresponding standard transformed equilibrium constant, $K'_{eq} = [ADP][P_i]/[ATP]$, depends on the pH and the concentration of free Mg^{2+}. Note that H^+ and Mg^{2+} do not appear in the biochemical equation because they are held constant. Thus a biochemical equation does not necessarily balance H, Mg, or charge, although it does balance all other elements involved in the reaction (C, N, O, and P in the equation above).

We can write a chemical equation that *does* balance for all elements and for charge. For example, when ATP is hydrolyzed at a pH above 8.5 in the absence of Mg^{2+}, the chemical reaction is represented by

$$ATP^{4-} + H_2O \longrightarrow ADP^{3-} + HPO_4^{2-} + H^+$$

The corresponding equilibrium constant, $K'_{eq} = [ADP^{3-}][HPO_4^{2-}][H^+]/[ATP^{4-}]$, depends only on temperature, pressure, and ionic strength.

Both ways of writing a metabolic reaction have value in biochemistry. Chemical equations are needed when we want to account for all atoms and charges in a reaction, as when we are considering the mechanism of a chemical reaction. Biochemical equations are used to determine in which direction a reaction will proceed spontaneously, given a specified pH and $[Mg^{2+}]$, or to calculate the equilibrium constant of such a reaction.

Throughout this book we use biochemical equations, unless the focus is on chemical mechanism, and we use values of $\Delta G'^{\circ}$ and K'_{eq} as determined at pH 7 and 1 mM Mg^{2+}.

SUMMARY 13.2 Chemical Logic and Common Biochemical Reactions

- Living systems make use of a large number of chemical reactions that can be classified into five general types.
- Carbonyl groups play a special role in reactions that form or cleave C—C bonds. Carbanion intermediates are common and are stabilized by adjacent carbonyl groups or, less often, by imines or certain cofactors.
- A redistribution of electrons can produce internal rearrangements, isomerizations, and eliminations. Such reactions include intramolecular oxidation-reduction, change in cis-trans arrangement at a double bond, and transposition of double bonds.
- Homolytic cleavage of covalent bonds to generate free radicals occurs in some pathways, such as in certain isomerization, decarboxylation, reductase, and rearrangement reactions.
- Phosphoryl transfer reactions are an especially important type of group transfer in cells, required for the activation of molecules for reactions that would otherwise be highly unfavorable.
- Oxidation-reduction reactions involve the loss or gain of electrons: one reactant gains electrons and is reduced, while the other loses electrons and is oxidized. Oxidation reactions generally release energy and are important in catabolism.

13.3 Phosphoryl Group Transfers and ATP

Having developed some fundamental principles of energy changes in chemical systems and reviewed the common classes of reactions, we can now examine the energy cycle in cells and the special role of ATP as the energy currency that links catabolism and anabolism (see Fig. 1–29). Heterotrophic cells obtain free energy in a chemical form by the catabolism of nutrient molecules, and they use that energy to make ATP from ADP and P_i. ATP then donates some of its chemical energy to endergonic processes such as the synthesis of metabolic intermediates and macromolecules from smaller precursors, the transport of substances across membranes against concentration gradients, and mechanical motion. This donation of energy from ATP generally involves the covalent participation of ATP in the reaction that is to be driven, with the eventual result that ATP is converted to ADP and P_i or, in some reactions, to AMP and 2 P_i. We discuss here the chemical basis for the large free-energy changes that accompany hydrolysis of ATP and other high-energy phosphate compounds, and we show that most cases of energy donation by ATP involve group transfer, not simple hydrolysis of ATP. To illustrate the range of energy transductions in which ATP provides the energy, we consider the synthesis of information-rich macromolecules, the transport of solutes across membranes, and motion produced by muscle contraction.

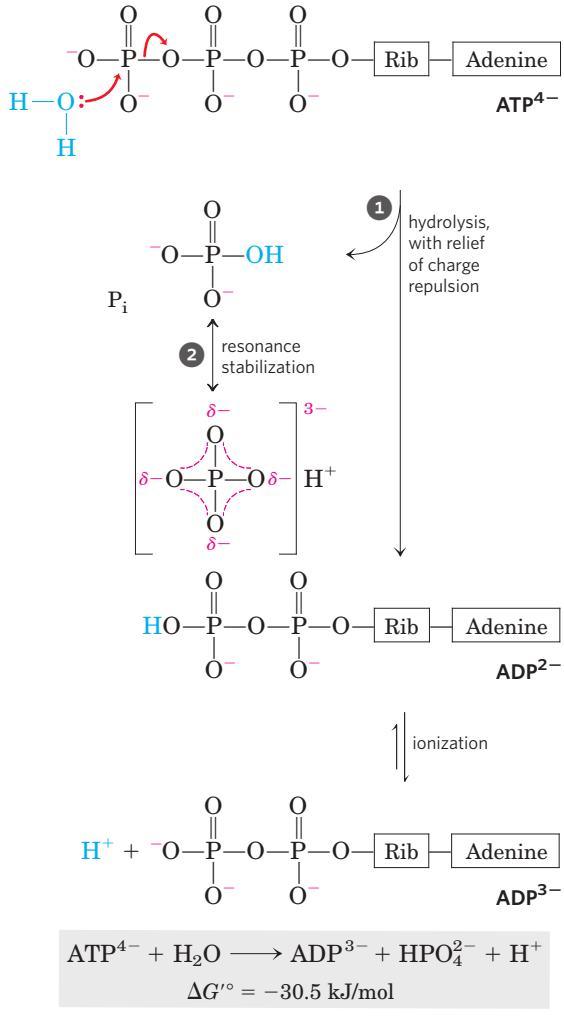

$$ATP^{4-} + H_2O \longrightarrow ADP^{3-} + HPO_4^{2-} + H^+$$
$$\Delta G'^\circ = -30.5 \text{ kJ/mol}$$

FIGURE 13–11 Chemical basis for the large free-energy change associated with ATP hydrolysis. ❶ The charge separation that results from hydrolysis relieves electrostatic repulsion among the four negative charges on ATP. ❷ The product inorganic phosphate (P_i) is stabilized by formation of a resonance hybrid, in which each of the four phosphorus-oxygen bonds has the same degree of double-bond character and the hydrogen ion is not permanently associated with any one of the oxygens. (Some degree of resonance stabilization also occurs in phosphates involved in ester or anhydride linkages, but fewer resonance forms are possible than for P_i.) A third factor (not shown) that favors ATP hydrolysis is the greater degree of solvation (hydration) of the products P_i and ADP relative to ATP, which further stabilizes the products relative to the reactants.

The Free-Energy Change for ATP Hydrolysis Is Large and Negative

Figure 13–11 summarizes the chemical basis for the relatively large, negative, standard free energy of hydrolysis of ATP. The hydrolytic cleavage of the terminal phosphoric acid anhydride (phosphoanhydride) bond in ATP separates one of the three negatively charged phosphates and thus relieves some of the electrostatic repulsion in ATP; the P_i released is stabilized by the formation of several resonance forms not possible in ATP.

The free-energy change for ATP hydrolysis is −30.5 kJ/mol under standard conditions, but the *actual* free energy of hydrolysis (ΔG) of ATP in living cells is very different: the cellular concentrations of ATP, ADP, and P_i are not identical and are much lower than the 1.0 M of standard conditions (Table 13–5). Furthermore, Mg^{2+} in the cytosol binds to ATP and ADP **(Fig. 13–12)**, and for most enzymatic reactions that involve ATP as phosphoryl group donor, the true substrate is $MgATP^{2-}$. The relevant $\Delta G'^\circ$ is therefore that for $MgATP^{2-}$ hydrolysis. We can calculate ΔG for ATP hydrolysis using data such as those in Table 13–5. The actual free energy of hydrolysis of ATP under intracellular conditions is often called its **phosphorylation potential**, ΔG_p.

TABLE 13–5 Adenine Nucleotide, Inorganic Phosphate, and Phosphocreatine Concentrations in Some Cells

	Concentration (mM)*				
	ATP	ADP†	AMP	P_i	PCr
Rat hepatocyte	3.38	1.32	0.29	4.8	0
Rat myocyte	8.05	0.93	0.04	8.05	28
Rat neuron	2.59	0.73	0.06	2.72	4.7
Human erythrocyte	2.25	0.25	0.02	1.65	0
E. coli cell	7.90	1.04	0.82	7.9	0

*For erythrocytes the concentrations are those of the cytosol (human erythrocytes lack a nucleus and mitochondria). In the other types of cells the data are for the entire cell contents, although the cytosol and the mitochondria have very different concentrations of ADP. PCr is phosphocreatine, discussed on p. 526.

†This value reflects total concentration; the true value for free ADP may be much lower (p. 519).

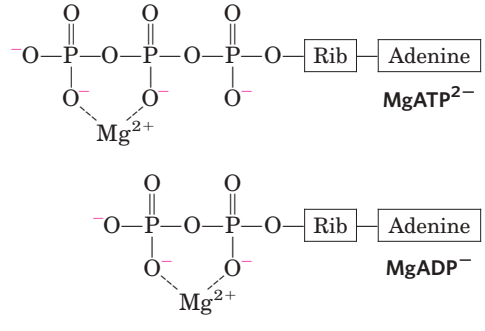

FIGURE 13–12 Mg^{2+} and ATP. Formation of Mg^{2+} complexes partially shields the negative charges and influences the conformation of the phosphate groups in nucleotides such as ATP and ADP.

WORKED EXAMPLE 13–2 Calculation of ΔG_p

Calculate the actual free energy of hydrolysis of ATP, ΔG_p, in human erythrocytes. The standard free energy of hydrolysis of ATP is −30.5 kJ/mol, and the concentrations of ATP, ADP, and P_i in erythrocytes are as shown in Table 13–5. Assume that the pH is 7.0 and the temperature is 37 °C (body temperature). What does this reveal about the amount of energy required to *synthesize* ATP under the same cellular conditions?

Solution: The concentrations of ATP, ADP, and P_i in human erythrocytes are 2.25, 0.25, and 1.65 mM, respectively. The actual free energy of hydrolysis of ATP under these conditions is given by the relationship (see Eqn 13–4)

$$\Delta G_p = \Delta G'^\circ + RT \ln \frac{[ADP][P_i]}{[ATP]}$$

Substituting the appropriate values we get

$$\begin{aligned}\Delta G_p &= -30.5 \text{ kJ/mol} + \left[(8.315 \text{ J/mol} \cdot \text{K})(310 \text{ K}) \ln \frac{(0.25 \times 10^{-3})(1.65 \times 10^{-3})}{(2.25 \times 10^{-3})}\right] \\ &= -30.5 \text{ kJ/mol} + (2.58 \text{ kJ/mol}) \ln 1.8 \times 10^{-4} \\ &= -30.5 \text{ kJ/mol} + (2.58 \text{ kJ/mol})(-8.6) \\ &= -30.5 \text{ kJ/mol} - 22 \text{ kJ/mol} \\ &= -52 \text{ kJ/mol}\end{aligned}$$

(Note that the final answer has been rounded to the correct number of significant figures (52.5 rounded to 52), following rules for rounding a number that ends in a 5 to the nearest even number.) Thus ΔG_p, the actual free-energy change for ATP hydrolysis in the intact erythrocyte (−52 kJ/mol), is much larger than the standard free-energy change (−30.5 kJ/mol). By the same token, the free energy required to *synthesize* ATP from ADP and P_i under the conditions prevailing in the erythrocyte would be 52 kJ/mol.

Because the concentrations of ATP, ADP, and P_i differ from one cell type to another, ΔG_p for ATP likewise differs among cells. Moreover, in any given cell, ΔG_p can vary from time to time, depending on the metabolic conditions and how they influence the concentrations of ATP, ADP, P_i, and H^+ (pH). We can calculate the actual free-energy change for any given metabolic reaction as it occurs in a cell, providing we know the concentrations of all the reactants and products and other factors (such as pH, temperature, and $[Mg^{2+}]$) that may affect the actual free-energy change.

To further complicate the issue, the *total* concentrations of ATP, ADP, P_i, and H^+ in a cell may be substantially higher than the *free* concentrations, which are the thermodynamically relevant values. The difference is due to tight binding of ATP, ADP, and P_i to cellular proteins. For example, the free [ADP] in resting muscle has been variously estimated at between 1 and 37 μM. Using the value 25 μM in Worked Example 13–2, we would get a ΔG_p of −64 kJ/mol. Calculation of the exact value of ΔG_p, however, is perhaps less instructive than the generalization we can make about actual free-energy changes: in vivo, the energy released by ATP hydrolysis is greater than the standard free-energy change, $\Delta G'^\circ$.

In the following discussions we use the $\Delta G'^\circ$ value for ATP hydrolysis because this allows comparison, on the same basis, with the energetics of other cellular reactions. Always keep in mind, however, that in living cells ΔG is the relevant quantity—for ATP hydrolysis and all other reactions—and may be quite different from $\Delta G'^\circ$.

Here we must make an important point about cellular ATP levels. We have shown (and will discuss further) how the chemical properties of ATP make it a suitable form of energy currency in cells. But it is not merely the molecule's intrinsic chemical properties that give it this ability to drive metabolic reactions and other energy-requiring processes. Even more important is that, in the course of evolution, there has been a very strong selective pressure for regulatory mechanisms that *hold cellular ATP concentrations far above the equilibrium concentrations* for the hydrolysis reaction. When the ATP level drops, not only does the *amount* of fuel decrease, but the fuel itself *loses its potency:* ΔG for its hydrolysis (that is, its phosphorylation potential, ΔG_p) is diminished. As our discussions of the metabolic pathways that produce and consume ATP will show, living cells have developed elaborate mechanisms—often at what might seem to us the expense of efficiency and common sense—to maintain high concentrations of ATP.

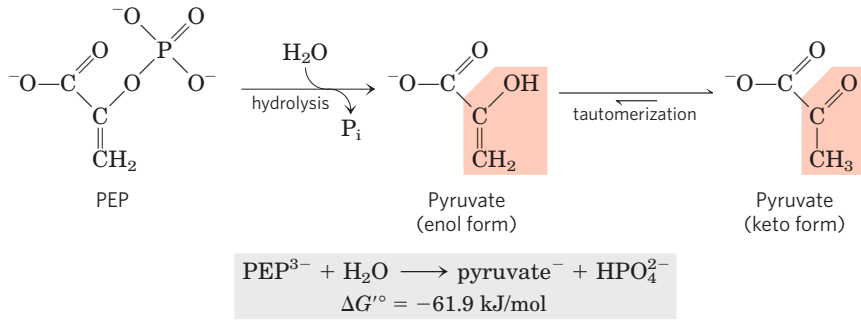

$$PEP^{3-} + H_2O \longrightarrow pyruvate^- + HPO_4^{2-}$$
$$\Delta G'^\circ = -61.9 \text{ kJ/mol}$$

FIGURE 13–13 Hydrolysis of phosphoenolpyruvate (PEP). Catalyzed by pyruvate kinase, this reaction is followed by spontaneous tautomerization of the product, pyruvate. Tautomerization is not possible in PEP, and thus the products of hydrolysis are stabilized relative to the reactants. Resonance stabilization of P_i also occurs, as shown in Figure 13–11.

Other Phosphorylated Compounds and Thioesters Also Have Large Free Energies of Hydrolysis

Phosphoenolpyruvate (PEP; **Fig. 13–13**) contains a phosphate ester bond that undergoes hydrolysis to yield the enol form of pyruvate, and this direct product can tautomerize to the more stable keto form. Because the reactant (PEP) has only one form (enol) and the product (pyruvate) has two possible forms, the product is stabilized relative to the reactant. This is the greatest contributing factor to the high standard free energy of hydrolysis of phosphoenolpyruvate: $\Delta G'^\circ = -61.9$ kJ/mol.

Another three-carbon compound, 1,3-bisphosphoglycerate **(Fig. 13–14)**, contains an anhydride bond between the C-1 carboxyl group and a number that ends in a phosphoric acid. Hydrolysis of this acyl phosphate is accompanied by a large, negative, standard free-energy change ($\Delta G'^\circ = -49.3$ kJ/mol), which can, again, be explained in terms of the structure of reactant and products. When H_2O is added across the anhydride bond of 1,3-bisphosphoglycerate, one of the direct products, 3-phosphoglyceric acid, can lose a proton to give the carboxylate ion, 3-phosphoglycerate, which has two equally probable resonance forms (Fig. 13–14). Removal of the direct product (3-phosphoglyceric acid) and formation of the resonance-stabilized ion favor the forward reaction.

In phosphocreatine **(Fig. 13–15)**, the P—N bond can be hydrolyzed to generate free creatine and P_i. The release of P_i and the resonance stabilization of creatine favor the forward reaction. The standard free-energy change of phosphocreatine hydrolysis is again large, −43.0 kJ/mol.

In all these phosphate-releasing reactions, the several resonance forms available to P_i (Fig. 13–11) stabilize this product relative to the reactant, contributing to an already negative free-energy change. Table 13–6 lists

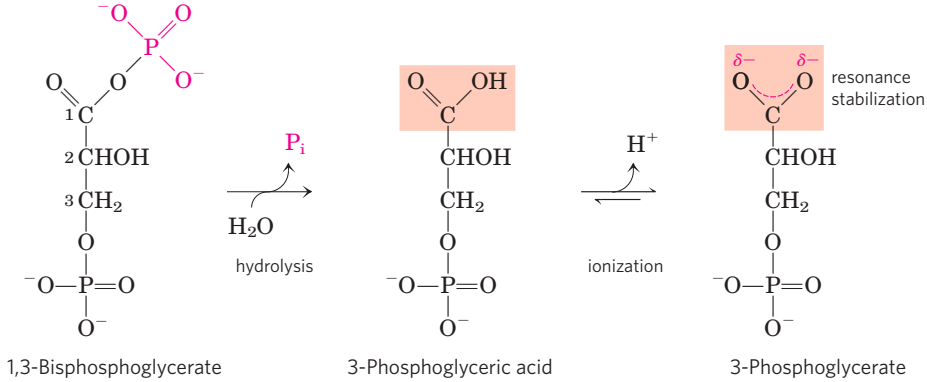

$$1,3\text{-Bisphosphoglycerate}^{4-} + H_2O \longrightarrow 3\text{-phosphoglycerate}^{3-} + HPO_4^{2-} + H^+$$
$$\Delta G'^\circ = -49.3 \text{ kJ/mol}$$

FIGURE 13–14 Hydrolysis of 1,3-bisphosphoglycerate. The direct product of hydrolysis is 3-phosphoglyceric acid, with an undissociated carboxylic acid. Its dissociation allows resonance structures that stabilize the product relative to the reactants. Resonance stabilization of P_i further contributes to the negative free-energy change.

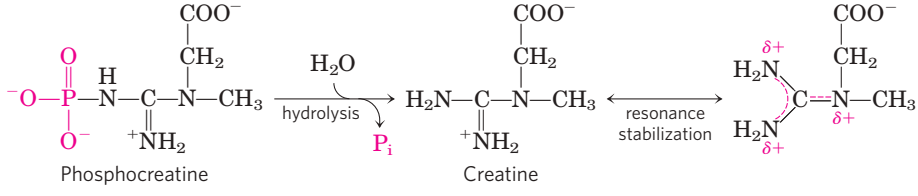

$$Phosphocreatine^{2-} + H_2O \longrightarrow creatine + HPO_4^{2-}$$
$$\Delta G'^\circ = -43.0 \text{ kJ/mol}$$

FIGURE 13–15 Hydrolysis of phosphocreatine. Breakage of the P—N bond in phosphocreatine produces creatine, which is stabilized by formation of a resonance hybrid. The other product, P_i, is also resonance stabilized.

TABLE 13–6 Standard Free Energies of Hydrolysis of Some Phosphorylated Compounds and Acetyl-CoA (a Thioester)

	$\Delta G'^\circ$ (kJ/mol)	$\Delta G'^\circ$ (kcal/mol)
Phosphoenolpyruvate	−61.9	−14.8
1,3-Bisphosphoglycerate (→ 3-phosphoglycerate + P_i)	−49.3	−11.8
Phosphocreatine	−43.0	−10.3
ADP (→ AMP + P_i)	−32.8	−7.8
ATP (→ ADP + P_i)	−30.5	−7.3
ATP (→ AMP + PP_i)	−45.6	−10.9
AMP (→ adenosine + P_i)	−14.2	−3.4
PP_i (→ $2P_i$)	−19.2	−4.0
Glucose 3-phosphate	−20.9	−5.0
Fructose 6-phosphate	−15.9	−3.8
Glucose 6-phosphate	−13.8	−3.3
Glycerol 3-phosphate	−9.2	−2.2
Acetyl-CoA	−31.4	−7.5

Source: Data mostly from Jencks, W.P. (1976) in *Handbook of Biochemistry and Molecular Biology,* 3rd edn (Fasman, G.D., ed.), *Physical and Chemical Data,* Vol. 1, pp. 296–304, CRC Press, Boca Raton, FL. The value for the free energy of hydrolysis of PP_i is from Frey, P.A. & Arabshahi, A. (1995) Standard free-energy change for the hydrolysis of the α-β-phosphoanhydride bridge in ATP. *Biochemistry* 34, 11,307–11,310.

the standard free energies of hydrolysis for some biologically important phosphorylated compounds.

Thioesters, in which a sulfur atom replaces the usual oxygen in the ester bond, also have large, negative, standard free energies of hydrolysis. Acetyl-coenzyme A, or acetyl-CoA **(Fig. 13–16)**, is one of many thioesters important in metabolism. The acyl group in these compounds is activated for transacylation, condensation, or oxidation-reduction reactions. Thioesters undergo much less resonance stabilization than do oxygen esters; consequently, the difference in free energy between the

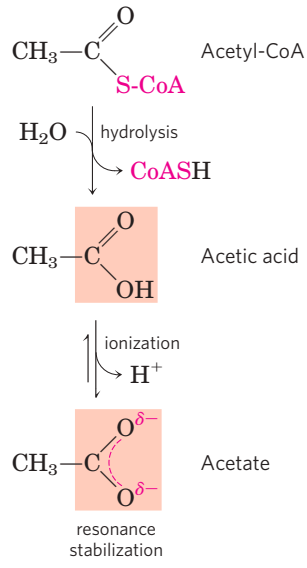

$$\text{Acetyl-CoA} + H_2O \longrightarrow \text{acetate}^- + \text{CoA} + H^+$$
$$\Delta G'^\circ = -31.4 \text{ kJ/mol}$$

FIGURE 13–16 Hydrolysis of acetyl-coenzyme A. Acetyl-CoA is a thioester with a large, negative, standard free energy of hydrolysis. Thioesters contain a sulfur atom in the position occupied by an oxygen atom in oxygen esters. The complete structure of coenzyme A (CoA, or CoASH) is shown in Figure 8–38.

reactant and its hydrolysis products, which *are* resonance-stabilized, is greater for thioesters than for comparable oxygen esters **(Fig. 13–17)**. In both cases, hydrolysis of the ester generates a carboxylic acid, which can ionize and assume several resonance forms. Together, these factors result in the large, negative $\Delta G'^\circ$ (−31.4 kJ/mol) for acetyl-CoA hydrolysis.

To summarize, for hydrolysis reactions with large, negative, standard free-energy changes, the products are more stable than the reactants for one or more of the following reasons: (1) the bond strain in reactants due to electrostatic repulsion is relieved by charge separation, as for ATP; (2) the products are stabilized by ionization, as for ATP, acyl phosphates, and thioesters; (3) the

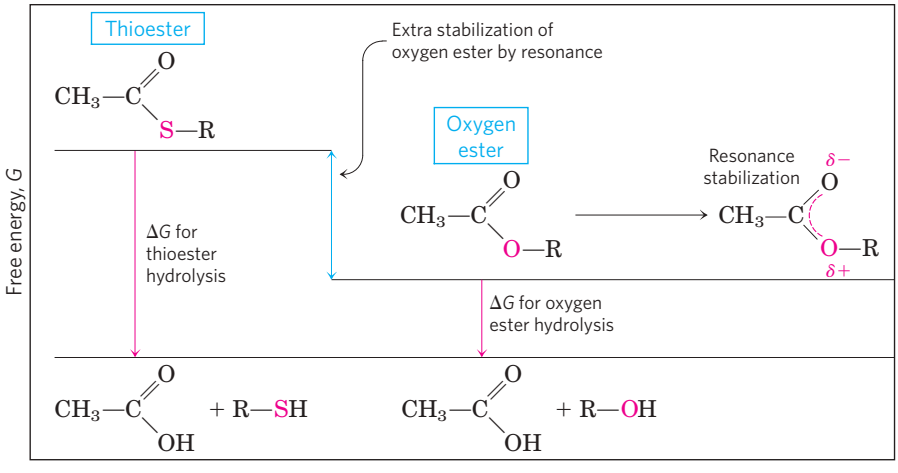

FIGURE 13–17 Free energy of hydrolysis for thioesters and oxygen esters. The *products* of both types of hydrolysis reaction have about the same free-energy content (G), but the thioester has a higher free-energy content than the oxygen ester. Orbital overlap between the O and C atoms allows resonance stabilization in oxygen esters; orbital overlap between S and C atoms is poorer and provides little resonance stabilization.

products are stabilized by isomerization (tautomerization), as for PEP; and/or (4) the products are stabilized by resonance, as for creatine released from phosphocreatine, carboxylate ion released from acyl phosphates and thioesters, and phosphate (P_i) released from anhydride or ester linkages.

ATP Provides Energy by Group Transfers, Not by Simple Hydrolysis

Throughout this book you will encounter reactions or processes for which ATP supplies energy, and the contribution of ATP to these reactions is commonly indicated as in **Figure 13–18a**, with a single arrow showing the conversion of ATP to ADP and P_i (or, in some cases, of ATP to AMP and pyrophosphate, PP_i). When written this way, these reactions of ATP seem to be simple hydrolysis reactions in which water displaces P_i (or PP_i), and one is tempted to say that an ATP-dependent reaction is "driven by the hydrolysis of ATP." This is *not* the case. ATP hydrolysis per se usually accomplishes nothing but the liberation of heat, which cannot drive a chemical process in an isothermal system. A single reaction arrow such as that in Figure 13–18a almost invariably represents a two-step process (Fig. 13–18b) in which part of the ATP molecule, a phosphoryl or pyrophosphoryl group or the adenylate moiety (AMP), is first transferred to a substrate molecule or to an amino acid residue in an enzyme, becoming covalently attached to the substrate or the enzyme and raising its free-energy content. Then, in a second step, the phosphate-containing moiety transferred in the first step is displaced, generating P_i, PP_i, or AMP. Thus ATP participates *covalently* in the enzyme-catalyzed reaction to which it contributes free energy.

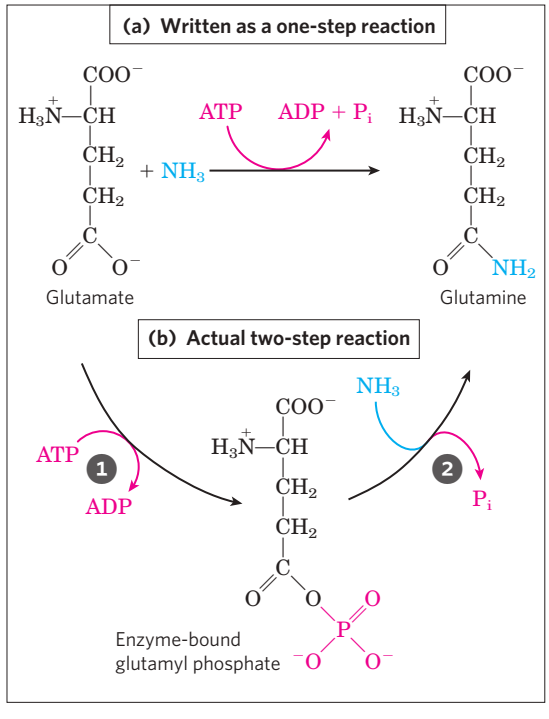

FIGURE 13–18 ATP hydrolysis in two steps. (a) The contribution of ATP to a reaction is often shown as a single step, but is almost always a two-step process. **(b)** Shown here is the reaction catalyzed by ATP-dependent glutamine synthetase. ❶ A phosphoryl group is transferred from ATP to glutamate, then ❷ the phosphoryl group is displaced by NH_3 and released as P_i.

Some processes *do* involve direct hydrolysis of ATP (or GTP), however. For example, noncovalent binding of ATP (or GTP), followed by its hydrolysis to ADP (or GDP) and P_i, can provide the energy to cycle some proteins between two conformations, producing mechanical motion. This occurs in muscle contraction (see Fig. 5–31), and in the movement of enzymes along DNA (see Fig. 25–31) or of ribosomes along messenger RNA (see Fig. 27–31). The energy-dependent reactions catalyzed by helicases, RecA protein, and some topoisomerases (Chapter 25) also involve direct hydrolysis of phosphoanhydride bonds. The AAA+ ATPases involved in DNA replication and other processes described in Chapter 25 use ATP hydrolysis to cycle associated proteins between active and inactive forms. GTP-binding proteins that act in signaling pathways directly hydrolyze GTP to drive conformational changes that terminate signals triggered by hormones or by other extracellular factors (Chapter 12).

The phosphate compounds found in living organisms can be divided somewhat arbitrarily into two groups, based on their standard free energies of hydrolysis **(Fig. 13–19)**. **"**High-energy" compounds have a $\Delta G'^\circ$ of hydrolysis more negative than −25 kJ/mol; "low-energy" compounds have a less negative $\Delta G'^\circ$. Based on this criterion, ATP, with a $\Delta G'^\circ$ of hydrolysis of −30.5 kJ/mol (−7.3 kcal/mol), is a high-energy compound; glucose 6-phosphate, with a $\Delta G'^\circ$ of hydrolysis of −13.8 kJ/mol (−3.3 kcal/mol), is a low-energy compound.

The term "high-energy phosphate bond," long used by biochemists to describe the P—O bond broken in hydrolysis reactions, is incorrect and misleading as it wrongly suggests that the bond itself contains the energy. In fact, the breaking of all chemical bonds requires an *input* of energy. The free energy released by hydrolysis of phosphate compounds does not come from the specific bond that is broken; it results from the products of the reaction having a lower free-energy content than the reactants. For simplicity, we will sometimes use the term "high-energy phosphate compound" when referring to ATP or other phosphate compounds with a large, negative, standard free energy of hydrolysis.

As is evident from the additivity of free-energy changes of sequential reactions (see Section 13.1), any phosphorylated compound can be synthesized by coupling the synthesis to the breakdown of another phosphorylated compound with a more negative free energy of hydrolysis. For example, because cleavage of P_i from phosphoenolpyruvate releases more energy than is needed to drive the condensation of P_i with ADP, the

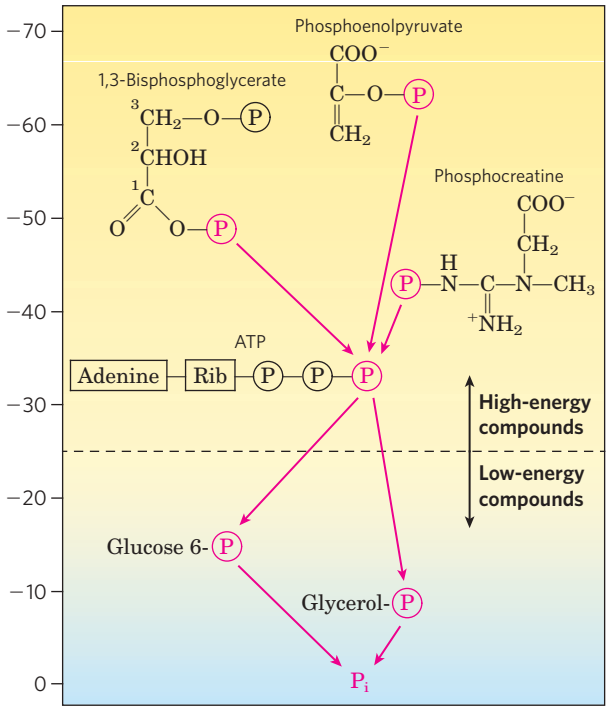

FIGURE 13–19 Ranking of biological phosphate compounds by standard free energies of hydrolysis. This shows the flow of phosphoryl groups, represented by Ⓟ, from high-energy phosphoryl group donors via ATP to acceptor molecules (such as glucose and glycerol) to form their low-energy phosphate derivatives. (The location of each compound's donor phosphoryl group along the scale approximately indicates the $\Delta G'°$ of hydrolysis.) This flow of phosphoryl groups, catalyzed by kinases, proceeds with an overall loss of free energy under intracellular conditions. Hydrolysis of low-energy phosphate compounds releases P_i, which has an even lower phosphoryl group transfer potential (as defined in the text).

direct donation of a phosphoryl group from PEP to ADP is thermodynamically feasible:

		$\Delta G'°$ (kJ/mol)
(1)	PEP + H_2O ⟶ pyruvate + P_i	−61.9
(2)	ADP + P_i ⟶ ATP + H_2O	+30.5
Sum:	PEP + ADP ⟶ pyruvate + ATP	−31.4

Notice that while the overall reaction is represented as the algebraic sum of the first two reactions, the overall reaction is actually a third, distinct reaction that does not involve P_i; PEP donates a *phosphoryl* group *directly* to ADP. We can describe phosphorylated compounds as having a high or low phosphoryl group transfer potential, on the basis of their standard free energies of hydrolysis (as listed in Table 13–6). The phosphoryl group transfer potential of PEP is very high, that of ATP is high, and that of glucose 6-phosphate is low (Fig. 13–19).

Much of catabolism is directed toward the synthesis of high-energy phosphate compounds, but their formation is not an end in itself; they are the means of activating a very wide variety of compounds for further chemical transformation. The transfer of a phosphoryl group to a compound effectively puts free energy into that compound, so that it has more free energy to give up during subsequent metabolic transformations. We described above how the synthesis of glucose 6-phosphate is accomplished by phosphoryl group transfer from ATP. In the next chapter we see how this phosphorylation of glucose activates, or "primes," the glucose for catabolic reactions that occur in nearly every living cell. Because of its intermediate position on the scale of group transfer potential, ATP can carry energy from high-energy phosphate compounds produced by catabolism to compounds such as glucose, converting them into more reactive species. ATP thus serves as the universal energy currency in all living cells.

One more chemical feature of ATP is crucial to its role in metabolism: although in aqueous solution ATP is thermodynamically unstable and is therefore a good phosphoryl group donor, it is *kinetically* stable. Because of the huge activation energies (200 to 400 kJ/mol) required for uncatalyzed cleavage of its phosphoanhydride bonds, ATP does not spontaneously donate phosphoryl groups to water or to the hundreds of other potential acceptors in the cell. Only when specific enzymes are present to lower the energy of activation does phosphoryl group transfer from ATP proceed. The cell is therefore able to regulate the disposition of the energy carried by ATP by regulating the various enzymes that act on it.

ATP Donates Phosphoryl, Pyrophosphoryl, and Adenylyl Groups

The reactions of ATP are generally S_N2 nucleophilic displacements (see Section 13.2) in which the nucleophile may be, for example, the oxygen of an alcohol or carboxylate, or a nitrogen of creatine or of the side chain of arginine or histidine. Each of the three phosphates of ATP is susceptible to nucleophilic attack **(Fig. 13–20)**, and each position of attack yields a different type of product.

Nucleophilic attack by an alcohol on the γ phosphate (Fig. 13–20a) displaces ADP and produces a new phosphate ester. Studies with ^{18}O-labeled reactants have shown that the bridge oxygen in the new compound is

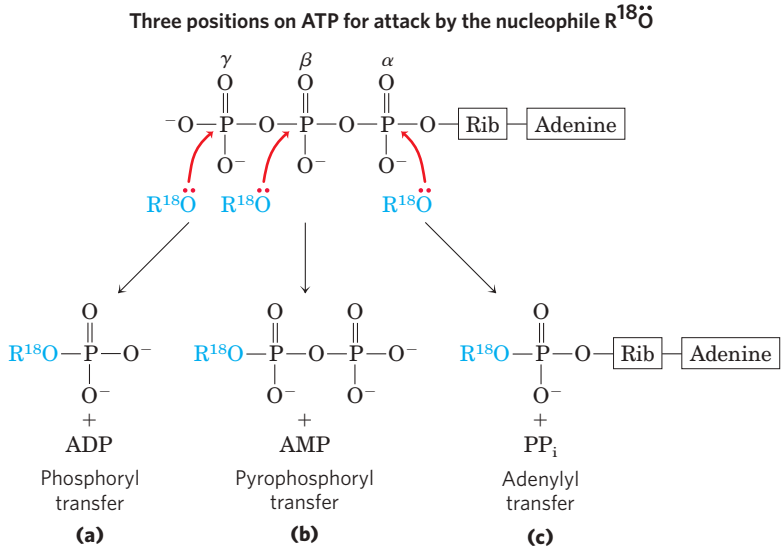

FIGURE 13–20 Nucleophilic displacement reactions of ATP. Any of the three P atoms (α, β, or γ) may serve as the electrophilic target for nucleophilic attack—in this case, by the labeled nucleophile R—^{18}O:. The nucleophile may be an alcohol (ROH), a carboxyl group ($RCOO^-$), or a phosphoanhydride (a nucleoside mono- or diphosphate, for example). **(a)** When the oxygen of the nucleophile attacks the γ position, the bridge oxygen of the product is labeled, indicating that the group transferred from ATP is a phosphoryl ($-PO_3^{2-}$), not a phosphate ($-OPO_3^{2-}$). **(b)** Attack on the β position displaces AMP and leads to the transfer of a pyrophosphoryl (not pyrophosphate) group to the nucleophile. **(c)** Attack on the α position displaces PP_i and transfers the adenylyl group to the nucleophile.

derived from the alcohol, not from ATP; the group transferred from ATP is therefore a phosphoryl ($-PO_3^{2-}$), not a phosphate ($-OPO_3^{2-}$). Phosphoryl group transfer from ATP to glutamate (Fig. 13–18) or to glucose (p. 219) involves attack at the γ position of the ATP molecule.

Attack at the β phosphate of ATP displaces AMP and transfers a pyrophosphoryl (not pyrophosphate) group to the attacking nucleophile (Fig. 13–20b). For example, the formation of 5-phosphoribosyl-1-pyrophosphate (p. 892), a key intermediate in nucleotide synthesis, results from attack of an —OH of the ribose on the β phosphate.

Nucleophilic attack at the α position of ATP displaces PP_i and transfers adenylate (5′-AMP) as an adenylyl group (Fig. 13–20c); the reaction is an **adenylylation** (a-den′-i-li-la′-shun, one of the most ungainly words in the biochemical language). Notice that hydrolysis of the α–β phosphoanhydride bond releases considerably more energy (~46 kJ/mol) than hydrolysis of the β–γ bond (~31 kJ/mol) (Table 13–6). Furthermore, the PP_i formed as a byproduct of the adenylylation is hydrolyzed to two P_i by the ubiquitous enzyme **inorganic pyrophosphatase**, releasing 19 kJ/mol and thereby providing a further energy "push" for the adenylylation reaction. In effect, both phosphoanhydride bonds of ATP are split in the overall reaction. Adenylylation reactions are therefore thermodynamically very favorable. When the energy of ATP is used to drive a particularly unfavorable metabolic reaction, adenylylation is often the mechanism of energy coupling. Fatty acid activation is a good example of this energy-coupling strategy.

The first step in the activation of a fatty acid—either for energy-yielding oxidation or for use in the synthesis of more complex lipids—is the formation of its thiol ester (see Fig. 17–5). The direct condensation of a fatty acid with coenzyme A is endergonic, but the formation of fatty acyl–CoA is made exergonic by stepwise removal of *two* phosphoryl groups from ATP. First, adenylate (AMP) is transferred from ATP to the carboxyl group of the fatty acid, forming a mixed anhydride (fatty acyl adenylate) and liberating PP_i. The thiol group of coenzyme A then displaces the adenylyl group and forms a thioester with the fatty acid. The sum of these two reactions is energetically equivalent to the exergonic hydrolysis of ATP to AMP and PP_i ($\Delta G'^\circ = -45.6$ kJ/mol) and the endergonic formation of fatty acyl–CoA ($\Delta G'^\circ = 31.4$ kJ/mol). The formation of fatty acyl–CoA is made energetically favorable by hydrolysis of the PP_i by inorganic pyrophosphatase. Thus, in the activation of a fatty acid, both phosphoanhydride bonds of ATP are broken. The resulting $\Delta G'^\circ$ is the sum of the $\Delta G'^\circ$ values for the breakage of these bonds, or -45.6 kJ/mol + (-19.2) kJ/mol:

$$ATP + 2H_2O \longrightarrow AMP + 2P_i \qquad \Delta G'^\circ = -64.8 \text{ kJ/mol}$$

The activation of amino acids before their polymerization into proteins (see Fig. 27–19) is accomplished by an analogous set of reactions in which a transfer RNA molecule takes the place of coenzyme A. An interesting use of the cleavage of ATP to AMP and PP_i occurs in the firefly, which uses ATP as an energy source to produce light flashes (Box 13–1).

Assembly of Informational Macromolecules Requires Energy

When simple precursors are assembled into high molecular weight polymers with defined sequences (DNA, RNA, proteins), as described in detail in Part III, energy is required both for the condensation of monomeric units and for the creation of *ordered* sequences. The precursors for DNA and RNA synthesis are nucleoside triphosphates, and polymerization is accompanied by cleavage of the phosphoanhydride linkage between the α and β phosphates, with the release of PP_i (Fig. 13–20). The moieties transferred to the growing polymer in these reactions are adenylate (AMP), guanylate (GMP), cytidylate (CMP), or uridylate (UMP) for RNA synthesis, and their deoxy analogs (with TMP in place

BOX 13–1 Firefly Flashes: Glowing Reports of ATP

Bioluminescence requires considerable amounts of energy. In the firefly, ATP is used in a set of reactions that converts chemical energy into light energy. In the 1950s, from many thousands of fireflies collected by children in and around Baltimore, William McElroy and his colleagues at the Johns Hopkins University isolated the principal biochemical components: luciferin, a complex carboxylic acid, and luciferase, an enzyme. The generation of a light flash requires activation of luciferin by an enzymatic reaction involving pyrophosphate cleavage of ATP to form luciferyl adenylate (Fig. 1). In the presence of molecular oxygen and luciferase, the luciferin undergoes a multistep oxidative decarboxylation to oxyluciferin. This process is accompanied by emission of light. The color of the light flash differs with the firefly species and seems to be determined by differences in the structure of the luciferase. Luciferin is regenerated from oxyluciferin in a subsequent series of reactions.

In the laboratory, pure firefly luciferin and luciferase are used to measure minute quantities of ATP by the intensity of the light flash produced. As little as a few picomoles (10^{-12} mol) of ATP can be measured in this way. Next-gen pyrosequencing of DNA relies on flashes of light from the luciferin-luciferase reaction to detect the presence of ATP after addition of nucleotides to a growing strand of DNA (see Fig. 9–25).

The firefly, a beetle of the *Lampyridae* family.

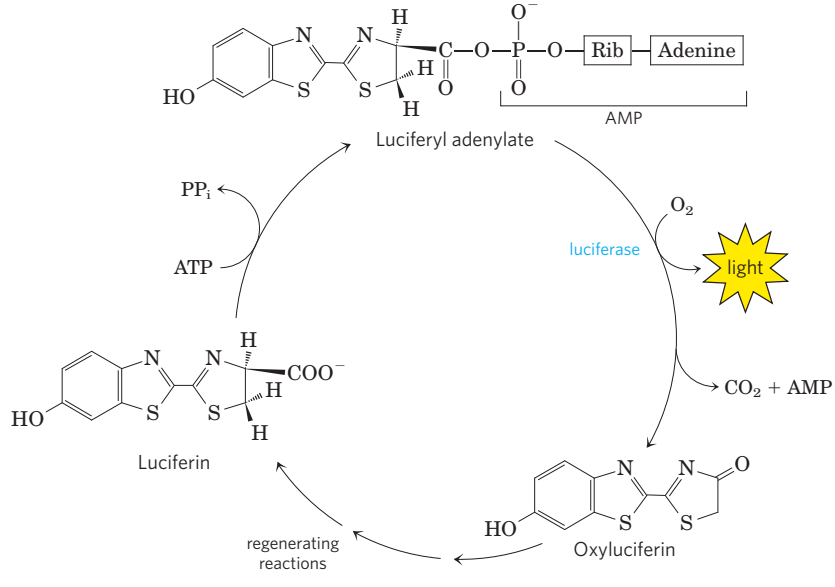

FIGURE 1 Important components in the firefly bioluminescence cycle.

of UMP) for DNA synthesis. As noted above, the activation of amino acids for protein synthesis involves the donation of adenylyl groups from ATP, and we shall see in Chapter 27 that several steps of protein synthesis on the ribosome are also accompanied by GTP hydrolysis. In all these cases, the exergonic breakdown of a nucleoside triphosphate is coupled to the endergonic process of synthesizing a polymer of a specific sequence.

ATP Energizes Active Transport and Muscle Contraction

ATP can supply the energy for transporting an ion or a molecule across a membrane into another aqueous compartment where its concentration is higher (see Fig. 11–38). Transport processes are major consumers of energy; in human kidney and brain, for example, as much as two-thirds of the energy consumed at rest is used to pump Na^+ and K^+ across plasma membranes via the Na^+K^+ ATPase. The transport of Na^+ and K^+ is driven by cyclic phosphorylation and dephosphorylation of the transporter protein, with ATP as the phosphoryl group donor. Na^+-dependent phosphorylation of the Na^+K^+ ATPase forces a change in the protein's conformation, and K^+-dependent dephosphorylation favors return to the original conformation. Each cycle in the transport process results in the conversion of ATP to ADP and P_i, and it is the free-energy change of ATP hydrolysis that drives the cyclic changes in protein conformation that result in the electrogenic pumping of Na^+ and K^+. Note that in this case ATP interacts covalently by phosphoryl group transfer to the enzyme, not the substrate.

In the contractile system of skeletal muscle cells, myosin and actin are specialized to transduce the chemical energy of ATP into motion (see Fig. 5–31). ATP binds tightly but noncovalently to one conformation of

myosin, holding the protein in that conformation. When myosin catalyzes the hydrolysis of its bound ATP, the ADP and P_i dissociate from the protein, allowing it to relax into a second conformation until another molecule of ATP binds. The binding and subsequent hydrolysis of ATP (by myosin ATPase) provide the energy that forces cyclic changes in the conformation of the myosin head. The change in conformation of many individual myosin molecules results in the sliding of myosin fibrils along actin filaments (see Fig. 5–30), which translates into macroscopic contraction of the muscle fiber. As we noted earlier, this production of mechanical motion at the expense of ATP is one of the few cases in which ATP hydrolysis per se, rather than group transfer from ATP, is the source of the chemical energy in a coupled process.

Transphosphorylations between Nucleotides Occur in All Cell Types

Although we have focused on ATP as the cell's energy currency and donor of phosphoryl groups, all other nucleoside triphosphates (GTP, UTP, and CTP) and all deoxynucleoside triphosphates (dATP, dGTP, dTTP, and dCTP) are energetically equivalent to ATP. The standard free-energy changes associated with hydrolysis of their phosphoanhydride linkages are very nearly identical with those shown in Table 13–6 for ATP. In preparation for their various biological roles, these other nucleotides are generated and maintained as the nucleoside triphosphate (NTP) forms by phosphoryl group transfer to the corresponding nucleoside diphosphates (NDPs) and monophosphates (NMPs).

ATP is the primary high-energy phosphate compound produced by catabolism, in the processes of glycolysis, oxidative phosphorylation, and, in photosynthetic cells, photophosphorylation. Several enzymes then carry phosphoryl groups from ATP to the other nucleotides. **Nucleoside diphosphate kinase**, found in all cells, catalyzes the reaction

$$\text{ATP} + \text{NDP (or dNDP)} \overset{Mg^{2+}}{\rightleftharpoons} \text{ADP} + \text{NTP (or dNTP)} \qquad \Delta G'^{\circ} \approx 0$$

Although this reaction is fully reversible, the relatively high [ATP]/[ADP] ratio in cells normally drives the reaction to the right, with the net formation of NTPs and dNTPs. The enzyme actually catalyzes a two-step phosphoryl group transfer, which is a classic case of a double-displacement (Ping-Pong) mechanism (**Fig. 13–21**; see also Fig. 6–13b). First, phosphoryl group transfer from ATP to an active-site His residue produces a phosphoenzyme intermediate; then the phosphoryl group is transferred from the Ⓟ–His residue to an NDP acceptor. Because the enzyme is nonspecific for the base in the NDP and works equally well on dNDPs and NDPs, it can synthesize all NTPs and dNTPs, given the corresponding NDPs and a supply of ATP.

Phosphoryl group transfers from ATP result in an accumulation of ADP; for example, when muscle is contracting vigorously, ADP accumulates and interferes with ATP-dependent contraction. During periods of intense demand for ATP, the cell lowers the ADP concentration, and at the same time replenishes ATP, by the action of **adenylate kinase**:

$$2\text{ADP} \overset{Mg^{2+}}{\rightleftharpoons} \text{ATP} + \text{AMP} \qquad \Delta G'^{\circ} \approx 0$$

This reaction is fully reversible, so after the intense demand for ATP ends, the enzyme can recycle AMP by converting it to ADP, which can then be phosphorylated to ATP in mitochondria. A similar enzyme, guanylate kinase, converts GMP to GDP at the expense of ATP. By pathways such as these, energy conserved in the catabolic production of ATP is used to supply the cell with all required NTPs and dNTPs.

Phosphocreatine (PCr; Fig. 13–15), also called creatine phosphate, serves as a ready source of phosphoryl groups for the quick synthesis of ATP from ADP. The PCr concentration in skeletal muscle is approximately 30 mM, nearly 10 times the concentration of ATP, and in other tissues such as smooth muscle, brain, and kidney [PCr] is 5 to 10 mM. The enzyme **creatine kinase** catalyzes the reversible reaction

$$\text{ADP} + \text{PCr} \overset{Mg^{2+}}{\rightleftharpoons} \text{ATP} + \text{Cr} \qquad \Delta G'^{\circ} = -12.5\ \text{kJ/mol}$$

When a sudden demand for energy depletes ATP, the PCr reservoir is used to replenish ATP at a rate considerably faster than ATP can be synthesized by catabolic pathways. When the demand for energy slackens, ATP produced by catabolism is used to replenish the PCr

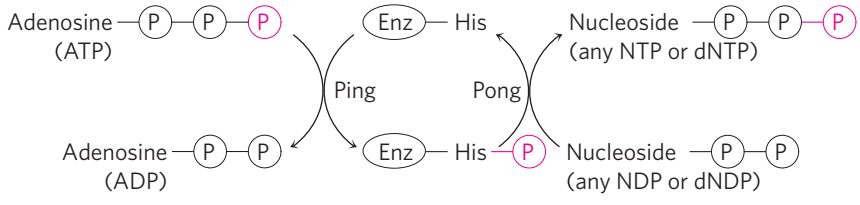

FIGURE 13–21 Ping-Pong mechanism of nucleoside diphosphate kinase. The enzyme binds its first substrate (ATP in our example), and a phosphoryl group is transferred to the side chain of a His residue. ADP departs, and another nucleoside (or deoxynucleoside) diphosphate replaces it, and this is converted to the corresponding triphosphate by transfer of the phosphoryl group from the phosphohistidine residue.

reservoir by reversal of the creatine kinase reaction (see Box 23–2). Organisms in the lower phyla employ other PCr-like molecules (collectively called **phosphagens**) as phosphoryl reservoirs.

Inorganic Polyphosphate Is a Potential Phosphoryl Group Donor

Inorganic polyphosphate, polyP (or $(polyP)_n$, where n is the number of orthophosphate residues), is a linear polymer composed of many tens or hundreds of P_i residues linked through phosphoanhydride bonds. This polymer, present in all organisms, may accumulate to high levels in some cells. In yeast, for example, the amount of polyP that accumulates in the vacuoles would represent, if distributed uniformly throughout the cell, a concentration of 200 mM! (Compare this with the concentrations of other phosphoryl group donors listed in Table 13–5.)

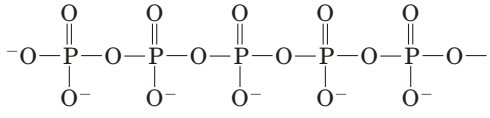

Inorganic polyphosphate (polyP)

One potential role for polyP is to serve as a phosphagen, a reservoir of phosphoryl groups that can be used to generate ATP, as creatine phosphate is used in muscle. PolyP has about the same phosphoryl group transfer potential as PP_i. The shortest polyphosphate, PP_i ($n = 2$), can serve as the energy source for active transport of H^+ across the vacuolar membrane in plant cells. For at least one form of the enzyme phosphofructokinase in plants, PP_i is the phosphoryl group donor, a role played by ATP in animals and microbes (p. 550). The finding of high concentrations of polyP in volcanic condensates and steam vents suggests that it could have served as an energy source in prebiotic and early cellular evolution.

In bacteria, the enzyme **polyphosphate kinase-1** (PPK-1) catalyzes the reversible reaction

$$ATP + (polyP)_n \overset{Mg^{2+}}{\rightleftharpoons} ADP + (polyP)_{n+1}$$

$$\Delta G'^\circ = -20 \text{ kJ/mol}$$

by a mechanism involving an enzyme-bound Ⓟ–His intermediate (recall the mechanism of nucleoside diphosphate kinase, described in Fig. 13–21). A second enzyme, **polyphosphate kinase-2** (PPK-2), catalyzes the reversible synthesis of GTP (or ATP) from polyphosphate and GDP (or ADP):

$$GDP + (polyP)_{n+1} \overset{Mn^{2+}}{\rightleftharpoons} GTP + (polyP)_n$$

PPK-2 is believed to act primarily in the direction of GTP and ATP synthesis, and PPK-1 in the direction of polyphosphate synthesis. PPK-1 and PPK-2 are present in a wide variety of bacteria, including many pathogenic species.

In bacteria, elevated levels of polyP have been shown to promote expression of genes involved in adaptation of the organism to conditions of starvation or other threats to survival. In *Escherichia coli*, for example, polyP accumulates when cells are starved for amino acids or P_i, and this accumulation confers a survival advantage. Deletion of the genes for polyphosphate kinases diminishes the ability of certain pathogenic bacteria to invade animal tissues. The enzymes may therefore prove to be suitable targets in the development of new antimicrobial drugs.

No yeast gene encodes a PPK-like protein, but four genes—unrelated to bacterial PPK genes—are necessary for the synthesis of polyphosphate. The mechanism for polyphosphate synthesis in eukaryotes seems to be quite different from that in bacteria.

SUMMARY 13.3 Phosphoryl Group Transfers and ATP

- ATP is the chemical link between catabolism and anabolism. It is the energy currency of the living cell. The exergonic conversion of ATP to ADP and P_i, or to AMP and PP_i, is coupled to many endergonic reactions and processes.
- Direct hydrolysis of ATP is the source of energy in some processes driven by conformational changes, but in general it is not ATP hydrolysis but the transfer of a phosphoryl, pyrophosphoryl, or adenylyl group from ATP to a substrate or enzyme that couples the energy of ATP breakdown to endergonic transformations of substrates.
- Through these group transfer reactions, ATP provides the energy for anabolic reactions, including the synthesis of informational macromolecules, and for the transport of molecules and ions across membranes against concentration gradients and electrical potential gradients.
- To maintain its high group transfer potential, ATP concentration must be held far above the equilibrium concentration by energy-yielding reactions of catabolism.
- Cells contain other metabolites with large, negative, free energies of hydrolysis, including phosphoenolpyruvate, 1,3-bisphosphoglycerate, and phosphocreatine. These high-energy compounds, like ATP, have a high phosphoryl group transfer potential. Thioesters also have high free energies of hydrolysis.
- Inorganic polyphosphate, present in all cells, may serve as a reservoir of phosphoryl groups with high group transfer potential.

13.4 Biological Oxidation-Reduction Reactions

The transfer of phosphoryl groups is a central feature of metabolism. Equally important is another kind of transfer, electron transfer in oxidation-reduction reactions. These reactions involve the loss of electrons by one chemical species, which is thereby oxidized, and the gain of electrons by another, which is reduced. The flow of electrons in oxidation-reduction reactions is responsible, directly or indirectly, for all work done by living organisms. In nonphotosynthetic organisms, the sources of electrons are reduced compounds (foods); in photosynthetic organisms, the initial electron donor is a chemical species excited by the absorption of light. The path of electron flow in metabolism is complex. Electrons move from various metabolic intermediates to specialized electron carriers in enzyme-catalyzed reactions. The carriers in turn donate electrons to acceptors with higher electron affinities, with the release of energy. Cells contain a variety of molecular energy transducers, which convert the energy of electron flow into useful work.

We begin by discussing how work can be accomplished by an electromotive force (emf), then consider the theoretical and experimental basis for measuring energy changes in oxidation reactions in terms of emf and the relationship between this force, expressed in volts, and the free-energy change, expressed in joules. We conclude by describing the structures and oxidation-reduction chemistry of the most common of the specialized electron carriers, which you will encounter repeatedly in later chapters.

The Flow of Electrons Can Do Biological Work

Every time we use a motor, an electric light or heater, or a spark to ignite gasoline in a car engine, we use the flow of electrons to accomplish work. In the circuit that powers a motor, the source of electrons can be a battery containing two chemical species that differ in affinity for electrons. Electrical wires provide a pathway for electron flow from the chemical species at one pole of the battery, through the motor, to the chemical species at the other pole of the battery. Because the two chemical species differ in their affinity for electrons, electrons flow spontaneously through the circuit, driven by a force proportional to the difference in electron affinity, the **electromotive force**, **emf**. The emf (typically a few volts) can accomplish work if an appropriate energy transducer—in this case a motor—is placed in the circuit. The motor can be coupled to a variety of mechanical devices to do useful work.

Living cells have an analogous biological "circuit," with a relatively reduced compound such as glucose as the source of electrons. As glucose is enzymatically oxidized, the released electrons flow spontaneously through a series of electron-carrier intermediates to another chemical species, such as O_2. This electron flow is exergonic, because O_2 has a higher affinity for electrons than do the electron-carrier intermediates. The resulting emf provides energy to a variety of molecular energy transducers (enzymes and other proteins) that do biological work. In the mitochondrion, for example, membrane-bound enzymes couple electron flow to the production of a transmembrane pH difference and a transmembrane electrical potential, accomplishing osmotic and electrical work. The proton gradient thus formed has potential energy, sometimes called the proton-motive force by analogy with electromotive force. Another enzyme, ATP synthase in the inner mitochondrial membrane, uses the proton-motive force to do chemical work: synthesis of ATP from ADP and P_i as protons flow spontaneously across the membrane. Similarly, membrane-localized enzymes in *E. coli* convert emf to proton-motive force, which is then used to power flagellar motion. The principles of electrochemistry that govern energy changes in the macroscopic circuit with a motor and battery apply with equal validity to the molecular processes accompanying electron flow in living cells.

Oxidation-Reductions Can Be Described as Half-Reactions

Although oxidation and reduction must occur together, it is convenient when describing electron transfers to consider the two halves of an oxidation-reduction reaction separately. For example, the oxidation of ferrous ion by cupric ion,

$$Fe^{2+} + Cu^{2+} \rightleftharpoons Fe^{3+} + Cu^{+}$$

can be described in terms of two half-reactions:

$$(1) \quad Fe^{2+} \rightleftharpoons Fe^{3+} + e^{-}$$
$$(2) \quad Cu^{2+} + e^{-} \rightleftharpoons Cu^{+}$$

The electron-donating molecule in an oxidation-reduction reaction is called the reducing agent or reductant; the electron-accepting molecule is the oxidizing agent or oxidant. A given agent, such as an iron cation existing in the ferrous (Fe^{2+}) or ferric (Fe^{3+}) state, functions as a conjugate reductant-oxidant pair (redox pair), just as an acid and corresponding base function as a conjugate acid-base pair. Recall from Chapter 2 that in acid-base reactions we can write a general equation: proton donor $\rightleftharpoons$ H^+ + proton acceptor. In redox reactions we can write a similar general equation: electron donor (reductant) $\rightleftharpoons$ e^- + electron acceptor (oxidant). In the reversible half-reaction (1) above, Fe^{2+} is the electron donor and Fe^{3+} is the electron acceptor; together, Fe^{2+} and Fe^{3+} constitute a **conjugate redox pair**.

The electron transfers in the oxidation-reduction reactions of organic compounds are not fundamentally different from those of inorganic species. Consider the oxidation of a reducing sugar (an aldehyde or ketone) by cupric ion:

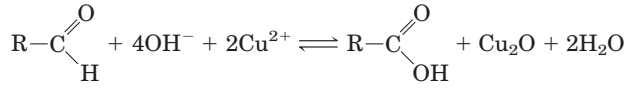

This overall reaction can be expressed as two half-reactions:

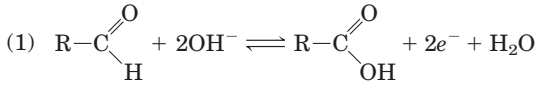

(1) $R{-}C(=O){-}H + 2OH^- \rightleftharpoons R{-}C(=O){-}OH + 2e^- + H_2O$

(2) $2Cu^{2+} + 2e^- + 2OH^- \rightleftharpoons Cu_2O + H_2O$

Because two electrons are removed from the aldehyde carbon, the second half-reaction (the one-electron reduction of cupric to cuprous ion) must be doubled to balance the overall equation.

Biological Oxidations Often Involve Dehydrogenation

The carbon in living cells exists in a range of oxidation states **(Fig. 13–22)**. When a carbon atom shares an electron pair with another atom (typically H, C, S, N, or O), the sharing is unequal in favor of the more electronegative atom. The order of increasing electronegativity is H < C < S < N < O. In oversimplified but useful terms, the more electronegative atom "owns" the bonding electrons it shares with another atom. For example, in methane (CH_4), carbon is more electronegative than the four hydrogens bonded to it, and the C atom therefore "owns" all eight bonding electrons (Fig. 13–22). In ethane, the electrons in the C—C bond are shared equally, so each C atom "owns" only seven of its eight bonding electrons. In ethanol, C-1 is less electronegative than the oxygen to which it is bonded, and the O atom therefore "owns" both electrons of the C—O bond, leaving C-1 with only five bonding electrons. With each formal loss of "owned" electrons, the carbon atom has undergone oxidation—even when no oxygen is involved, as in the conversion of an alkane (—CH_2—CH_2—) to an alkene (—CH=CH—). In this case, oxidation (loss of electrons) is coincident with the loss of hydrogen. In biological systems, as we noted earlier in the chapter, oxidation is often synonymous with **dehydrogenation** and many enzymes that catalyze oxidation reactions are **dehydrogenases**. Notice that the more reduced compounds in Figure 13–22 (top) are richer in hydrogen than in oxygen, whereas the more oxidized compounds (bottom) have more oxygen and less hydrogen.

Not all biological oxidation-reduction reactions involve carbon. For example, in the conversion of molecular nitrogen to ammonia, $6H^+ + 6e^- + N_2 \rightarrow 2NH_3$, the nitrogen atoms are reduced.

Electrons are transferred from one molecule (electron donor) to another (electron acceptor) in one of four ways:

1. Directly as *electrons*. For example, the Fe^{2+}/Fe^{3+} redox pair can transfer an electron to the Cu^+/Cu^{2+} redox pair:

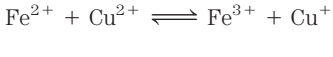

$Fe^{2+} + Cu^{2+} \rightleftharpoons Fe^{3+} + Cu^+$

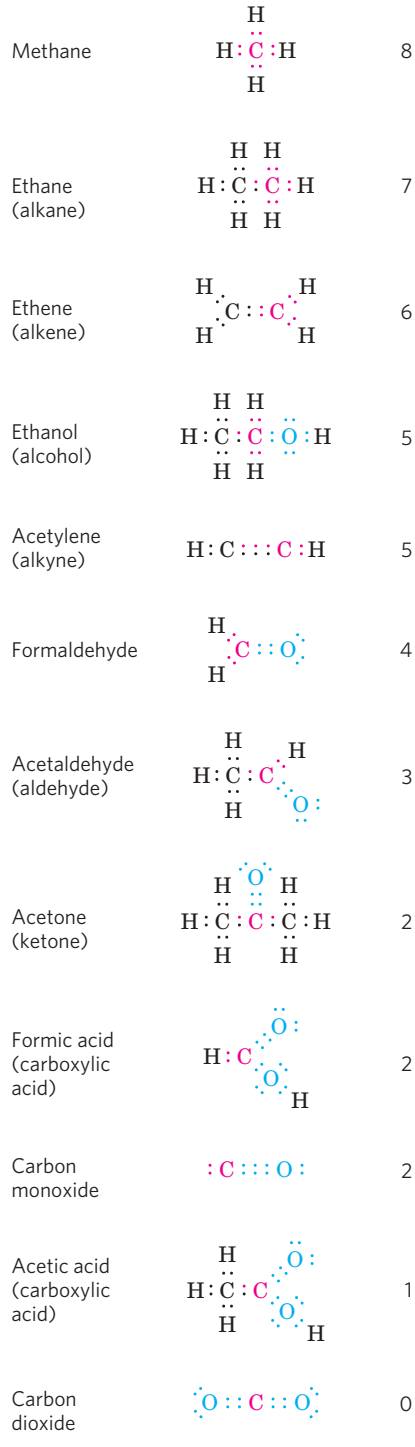

FIGURE 13–22 Different levels of oxidation of carbon compounds in the biosphere. To approximate the level of oxidation of these compounds, focus on the red carbon atom and its bonding electrons. When this carbon is bonded to the less electronegative H atom, both bonding electrons (red) are assigned to the carbon. When carbon is bonded to another carbon, bonding electrons are shared equally, so one of the two electrons is assigned to the red carbon. When the red carbon is bonded to the more electronegative O atom, the bonding electrons are assigned to the oxygen. The number to the right of each compound is the number of electrons "owned" by the red carbon, a rough expression of the degree of oxidation of that compound. As the red carbon undergoes oxidation (loses electrons), the number gets smaller.

2. As *hydrogen atoms.* Recall that a hydrogen atom consists of a proton (H^+) and a single electron (e^-). In this case we can write the general equation

$$AH_2 \rightleftharpoons A + 2e^- + 2H^+$$

where AH_2 is the hydrogen/electron donor. (Do not mistake the above reaction for an acid dissociation, which involves a proton and no electron.) AH_2 and A together constitute a conjugate redox pair (A/AH_2), which can reduce another compound B (or redox pair, B/BH_2) by transfer of hydrogen atoms:

$$AH_2 + B \rightleftharpoons A + BH_2$$

3. As a *hydride ion* ($:H^-$), which has two electrons. This occurs in the case of NAD-linked dehydrogenases, described below.

4. Through direct *combination with oxygen.* In this case, oxygen combines with an organic reductant and is covalently incorporated in the product, as in the oxidation of a hydrocarbon to an alcohol:

$$R{-}CH_3 + \tfrac{1}{2}O_2 \longrightarrow R{-}CH_2{-}OH$$

The hydrocarbon is the electron donor and the oxygen atom is the electron acceptor.

All four types of electron transfer occur in cells. The neutral term **reducing equivalent** is commonly used to designate a single electron equivalent participating in an oxidation-reduction reaction, no matter whether this equivalent is an electron per se or part of a hydrogen atom or a hydride ion, or whether the electron transfer takes place in a reaction with oxygen to yield an oxygenated product. Because biological fuel molecules are usually enzymatically dehydrogenated to lose *two* reducing equivalents at a time, and because each oxygen atom can accept two reducing equivalents, biochemists by convention regard the unit of biological oxidations as two reducing equivalents passing from substrate to oxygen.

Reduction Potentials Measure Affinity for Electrons

When two conjugate redox pairs are together in solution, electron transfer from the electron donor of one pair to the electron acceptor of the other may proceed spontaneously. The tendency for such a reaction depends on the relative affinity of the electron acceptor of each redox pair for electrons. The **standard reduction potential**, $\boldsymbol{E}^\circ$, a measure (in volts) of this affinity, can be determined in an experiment such as that described in **Figure 13–23**. Electrochemists have chosen as a standard of reference the half-reaction

$$H^+ + e^- \longrightarrow \tfrac{1}{2}H_2$$

The electrode at which this half-reaction occurs (called a half-cell) is arbitrarily assigned an E° of 0.00 V.

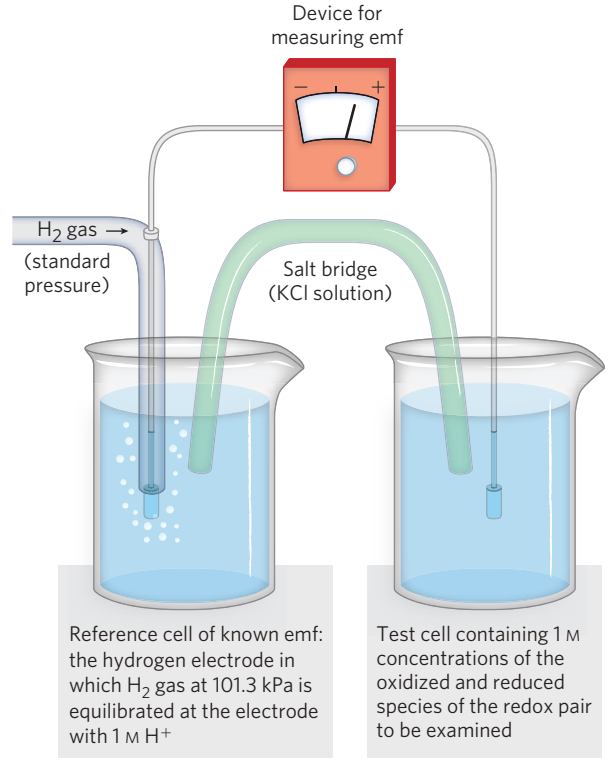

FIGURE 13–23 Measurement of the standard reduction potential (E'°) of a redox pair. Electrons flow from the test electrode to the reference electrode, or vice versa. The ultimate reference half-cell is the hydrogen electrode, as shown here, at pH 0. The electromotive force (emf) of this electrode is designated 0.00 V. At pH 7 in the test cell (and 25 °C), E'° for the hydrogen electrode is −0.414 V. The direction of electron flow depends on the relative electron "pressure" or potential of the two cells. A salt bridge containing a saturated KCl solution provides a path for counter-ion movement between the test cell and the reference cell. From the observed emf and the known emf of the reference cell, the experimenter can find the emf of the test cell containing the redox pair. The cell that gains electrons has, by convention, the more positive reduction potential.

When this hydrogen electrode is connected through an external circuit to another half-cell in which an oxidized species and its corresponding reduced species are present at standard concentrations (25 °C, each solute at 1 M, each gas at 101.3 kPa), electrons tend to flow through the external circuit from the half-cell of lower E° to the half-cell of higher E°. By convention, a half-cell that takes electrons from the standard hydrogen cell is assigned a positive value of E°, and one that donates electrons to the hydrogen cell, a negative value. When any two half-cells are connected, that with the larger (more positive) E° will get reduced; it has the greater reduction potential.

The reduction potential of a half-cell depends not only on the chemical species present but also on their activities, approximated by their concentrations. About a century ago, Walther Nernst derived an equation that

relates standard reduction potential ($E°$) to the actual reduction potential (E) at any concentration of oxidized and reduced species in a living cell:

$$E = E° + \frac{RT}{n\mathcal{F}} \ln \frac{[\text{electron acceptor}]}{[\text{electron donor}]} \qquad (13\text{–}5)$$

where R and T have their usual meanings, n is the number of electrons transferred per molecule, and $\mathcal{F}$ is the Faraday constant (Table 13–1). At 298 K (25 °C), this expression reduces to

$$E = E° + \frac{0.026\text{V}}{n} \ln \frac{[\text{electron acceptor}]}{[\text{electron donor}]} \qquad (13\text{–}6)$$

KEY CONVENTION: Many half-reactions of interest to biochemists involve protons. As in the definition of $\Delta G'°$, biochemists define the standard state for oxidation-reduction reactions as pH 7 and express a standard transformed reduction potential, $E'°$, the standard reduction potential at pH 7 and 25 °C. By convention, $\Delta E'°$ for any redox reaction is given as $E'°$ of the electron acceptor minus $E'°$ of the electron donor. ■

The standard reduction potentials given in Table 13–7 and used throughout this book are values for $E'°$ and are therefore valid only for systems at neutral pH. Each value represents the potential difference when the conjugate redox pair, at 1 M concentrations, 25 °C, and pH 7, is connected with the standard (pH 0) hydrogen electrode. Notice in Table 13–7 that when the conjugate pair $2H^+/H_2$ at pH 7 is connected with the standard hydrogen electrode (pH 0), electrons tend to flow from the pH 7 cell to the standard (pH 0) cell; the measured $E'°$ for the $2H^+/H_2$ pair is −0.414 V.

Standard Reduction Potentials Can Be Used to Calculate Free-Energy Change

Why are reduction potentials so useful to the biochemist? When E values have been determined for any two half-cells, relative to the standard hydrogen electrode, we also know their reduction potentials relative to each other. We can then predict the direction in which electrons will tend to flow when the two half-cells are connected through an external circuit or when components of both half-cells are present in the same solution. Electrons tend to flow to the half-cell with the more positive E, and the strength of that tendency is proportional to ΔE, the difference in reduction potential. The energy made available by this spontaneous electron flow (the free-energy change, ΔG, for the oxidation-reduction reaction) is proportional to ΔE:

$$\Delta G = -n\mathcal{F}\Delta E \quad \text{or} \quad \Delta G'° = -n\mathcal{F}\,\Delta E'° \qquad (13\text{–}7)$$

where n is the number of electrons transferred in the reaction. With this equation we can calculate the actual free-energy change for any oxidation-reduction reaction from the values of $E'°$ in a table of reduction potentials (Table 13–7) and the concentrations of reacting species.

TABLE 13–7 Standard Reduction Potentials of Some Biologically Important Half-Reactions

Half-reaction	$E'°$ (V)
$\frac{1}{2}O_2 + 2H^+ + 2e^- \longrightarrow H_2O$	0.816
$Fe^{3+} + e^- \longrightarrow Fe^{2+}$	0.771
$NO_3^- + 2H^+ + 2e^- \longrightarrow NO_2^- + H_2O$	0.421
Cytochrome f (Fe^{3+}) + e^- ⟶ cytochrome f (Fe^{2+})	0.365
$Fe(CN)_6^{3-}$ (ferricyanide) + $e^- \longrightarrow Fe(CN)_6^{4-}$	0.36
Cytochrome a_3 (Fe^{3+}) + e^- ⟶ cytochrome a_3 (Fe^{2+})	0.35
$O_2 + 2H^+ + 2e^- \longrightarrow H_2O_2$	0.295
Cytochrome a (Fe^{3+}) + e^- ⟶ cytochrome a (Fe^{2+})	0.29
Cytochrome c (Fe^{3+}) + e^- ⟶ cytochrome c (Fe^{2+})	0.254
Cytochrome c_1 (Fe^{3+}) + e^- ⟶ cytochrome c_1 (Fe^{2+})	0.22
Cytochrome b (Fe^{3+}) + e^- ⟶ cytochrome b (Fe^{2+})	0.077
Ubiquinone + $2H^+ + 2e^-$ ⟶ ubiquinol + H_2	0.045
Fumarate^{2-} + $2H^+ + 2e^-$ ⟶ succinate^{2-}	0.031
$2H^+ + 2e^- \longrightarrow H_2$ (at standard conditions, pH 0)	0.000
Crotonyl-CoA + $2H^+ + 2e^-$ ⟶ butyryl-CoA	−0.015
Oxaloacetate^{2-} + $2H^+ + 2e^-$ ⟶ malate^{2-}	−0.166
Pyruvate$^-$ + $2H^+ + 2e^-$ ⟶ lactate$^-$	−0.185
Acetaldehyde + $2H^+ + 2e^-$ ⟶ ethanol	−0.197
FAD + $2H^+ + 2e^-$ ⟶ $FADH_2$	−0.219*
Glutathione + $2H^+ + 2e^-$ ⟶ 2 reduced glutathione	−0.23
$S + 2H^+ + 2e^- \longrightarrow H_2S$	−0.243
Lipoic acid + $2H^+ + 2e^-$ ⟶ dihydrolipoic acid	−0.29
$NAD^+ + H^+ + 2e^- \longrightarrow NADH$	−0.320
$NADP^+ + H^+ + 2e^- \longrightarrow NADPH$	−0.324
Acetoacetate + $2H^+ + 2e^-$ ⟶ β-hydroxybutyrate	−0.346
α-Ketoglutarate + $CO_2 + 2H^+ + 2e^-$ ⟶ isocitrate	−0.38
$2H^+ + 2e^- \longrightarrow H_2$ (at pH 7)	−0.414
Ferredoxin (Fe^{3+}) + e^- ⟶ ferredoxin (Fe^{2+})	−0.432

Source: Data mostly from Loach, R.A. (1976) in *Handbook of Biochemistry and Molecular Biology,* 3rd edn (Fasman, G.D., ed.), *Physical and Chemical Data,* Vol. 1, pp. 122–130, CRC Press, Boca Raton, FL.

* This is the value for free FAD; FAD bound to a specific flavoprotein (e.g., succinate dehydrogenase) has a different $E'°$ that depends on its protein environment.

WORKED EXAMPLE 13–3 Calculation of $\Delta G'^\circ$ and ΔG of a Redox Reaction

Calculate the standard free-energy change, $\Delta G'^\circ$, for the reaction in which acetaldehyde is reduced by the biological electron carrier NADH:

$$\text{Acetaldehyde} + \text{NADH} + \text{H}^+ \longrightarrow \text{ethanol} + \text{NAD}^+$$

Then calculate the *actual* free-energy change, ΔG, when [acetaldehyde] and [NADH] are 1.00 M, and [ethanol] and [NAD^+] are 0.100 M. The relevant half-reactions and their E'° values are:

$$(1)\quad \text{Acetaldehyde} + 2\text{H}^+ + 2e^- \longrightarrow \text{ethanol} \qquad E'^\circ = -0.197\ \text{V}$$

$$(2)\quad \text{NAD}^+ + 2\text{H}^+ + 2e^- \longrightarrow \text{NADH} + \text{H}^+ \qquad E'^\circ = -0.320\ \text{V}$$

Remember that, by convention, $\Delta E'^\circ$ is E'° of the electron acceptor minus E'° of the electron donor.

Solution: Because acetaldehyde is accepting electrons ($n = 2$) from NADH, $\Delta E'^\circ = -0.197\ \text{V} - (-0.320\ \text{V}) = 0.123\ \text{V}$. Therefore,

$$\Delta G'^\circ = -n\mathcal{F}\,\Delta E'^\circ = -2(96.5\ \text{kJ/V}\cdot\text{mol})(0.123\ \text{V}) = -23.7\ \text{kJ/mol}$$

This is the free-energy change for the oxidation-reduction reaction at 25 °C and pH 7, when acetaldehyde, ethanol, NAD^+, and NADH are all present at 1.00 M concentrations.

To calculate ΔG when [acetaldehyde] and [NADH] are 1.00 M, and [ethanol] and [NAD^+] are 0.100 M, we can use Equation 13–4 and the standard free-energy change we calculated above:

$$\Delta G = \Delta G'^\circ + RT\ln\frac{[\text{ethanol}][\text{NAD}^+]}{[\text{acetaldehyde}][\text{NADH}]}$$
$$= -23.7\ \text{kJ/mol} + (8.315\ \text{J/mol}\cdot\text{K})(298\ \text{K})\ln\frac{(0.100\ \text{M})(0.100\ \text{M})}{(1.00\ \text{M})(1.00\ \text{M})}$$
$$= -23.7\ \text{kJ/mol} + (2.48\ \text{J/mol})\ln 0.01$$
$$= -35.1\ \text{kJ/mol}$$

This is the actual free-energy change at the specified concentrations of the redox pairs.

Cellular Oxidation of Glucose to Carbon Dioxide Requires Specialized Electron Carriers

The principles of oxidation-reduction energetics described above apply to the many metabolic reactions that involve electron transfers. For example, in many organisms, the oxidation of glucose supplies energy for the production of ATP. The complete oxidation of glucose:

$$C_6H_{12}O_6 + 6O_2 \longrightarrow 6CO_2 + 6H_2O$$

has a $\Delta G'^\circ$ of −2,840 kJ/mol. This is a much larger release of free energy than is required for ATP synthesis in cells (50 to 60 kJ/mol; see Worked Example 13–2). Cells convert glucose to CO_2 not in a single, high-energy-releasing reaction but rather in a series of controlled reactions, some of which are oxidations. The free energy released in these oxidation steps is of the same order of magnitude as that required for ATP synthesis from ADP, with some energy to spare. Electrons removed in these oxidation steps are transferred to coenzymes specialized for carrying electrons, such as NAD^+ and FAD (described below).

A Few Types of Coenzymes and Proteins Serve as Universal Electron Carriers

The multitude of enzymes that catalyze cellular oxidations channel electrons from their hundreds of different substrates into just a few types of universal electron carriers. The reduction of these carriers in catabolic processes results in the conservation of free energy released by substrate oxidation. NAD, NADP, FMN, and FAD are water-soluble coenzymes that undergo reversible oxidation and reduction in many of the electron-transfer reactions of metabolism. The nucleotides NAD and NADP move readily from one enzyme to another; the flavin nucleotides FMN and FAD are usually very tightly bound to the enzymes, called flavoproteins, for which they serve as prosthetic groups. Lipid-soluble quinones such as ubiquinone and plastoquinone act as electron carriers and proton donors in the nonaqueous environment of membranes. Iron-sulfur proteins and cytochromes, which have tightly bound prosthetic groups that undergo reversible oxidation and reduction, also serve as electron carriers in many oxidation-reduction reactions. Some of these proteins are water-soluble, but others are peripheral or integral membrane proteins (see Fig. 11–7).

We conclude this chapter by describing some chemical features of nucleotide coenzymes and some of the enzymes (dehydrogenases and flavoproteins) that use them. The oxidation-reduction chemistry of quinones, iron-sulfur proteins, and cytochromes is discussed in Chapter 19.

NADH and NADPH Act with Dehydrogenases as Soluble Electron Carriers

Nicotinamide adenine dinucleotide (NAD; NAD^+ in its oxidized form) and its close analog nicotinamide adenine dinucleotide phosphate (NADP; $NADP^+$ when oxidized) are composed of two nucleotides joined through their phosphate groups by a phosphoanhydride bond **(Fig. 13–24a)**. Because the nicotinamide ring resembles pyridine, these compounds are sometimes called **pyridine nucleotides**. The vitamin niacin is the source of the nicotinamide moiety in nicotinamide nucleotides.

Both coenzymes undergo reversible reduction of the nicotinamide ring (Fig. 13–24). As a substrate molecule undergoes oxidation (dehydrogenation), giving up two hydrogen atoms, the oxidized form of the nucleotide

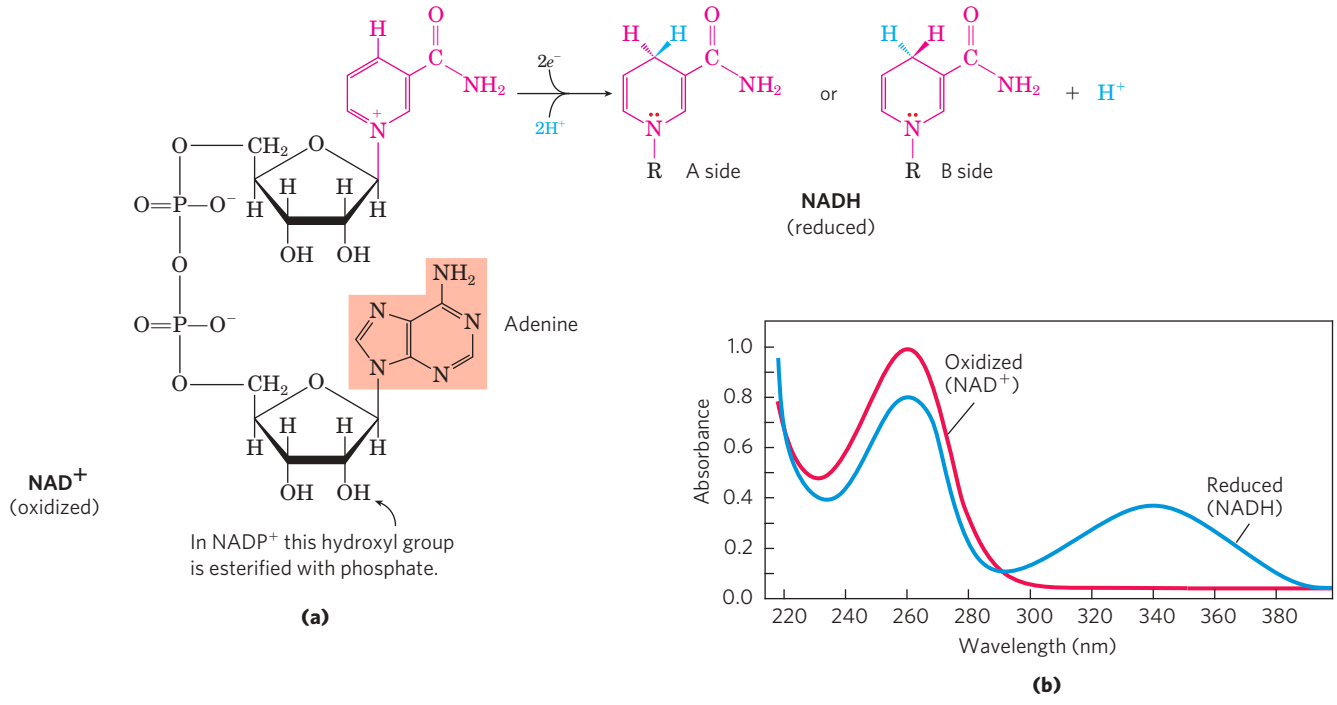

FIGURE 13–24 NAD and NADP. (a) Nicotinamide adenine dinucleotide, NAD^+, and its phosphorylated analog $NADP^+$ undergo reduction to NADH and NADPH, accepting a hydride ion (two electrons and one proton) from an oxidizable substrate. The hydride ion is added to either the front (the A side) or the back (the B side) of the planar nicotinamide ring (see Table 13-8). **(b)** The UV absorption spectra of NAD^+ and NADH. Reduction of the nicotinamide ring produces a new, broad absorption band with a maximum at 340 nm. The production of NADH during an enzyme-catalyzed reaction can be conveniently followed by observing the appearance of the absorbance at 340 nm (molar extinction coefficient $\varepsilon_{340} = 6{,}200\ \text{M}^{-1}\,\text{cm}^{-1}$).

(NAD^+ or $NADP^+$) accepts a hydride ion ($:H^-$, the equivalent of a proton and two electrons) and is reduced (to NADH or NADPH). The second proton removed from the substrate is released to the aqueous solvent. The half-reactions for these nucleotide cofactors are

$$NAD^+ + 2e^- + 2H^+ \longrightarrow NADH + H^+$$
$$NADP^+ + 2e^- + 2H^+ \longrightarrow NADPH + H^+$$

Reduction of NAD^+ or $NADP^+$ converts the benzenoid ring of the nicotinamide moiety (with a fixed positive charge on the ring nitrogen) to the quinonoid form (with no charge on the nitrogen). The reduced nucleotides absorb light at 340 nm; the oxidized forms do not (Fig. 13–24b); this difference in absorption is used by biochemists to assay reactions involving these coenzymes. Note that the plus sign in the abbreviations NAD^+ and $NADP^+$ does *not* indicate the net charge on these molecules (in fact, both are negatively charged); rather, it indicates that the nicotinamide ring is in its oxidized form, with a positive charge on the nitrogen atom. In the abbreviations NADH and NADPH, the "H" denotes the added hydride ion. To refer to these nucleotides without specifying their oxidation state, we use NAD and NADP.

The total concentration of NAD^+ + NADH in most tissues is about 10^{-5} M; that of $NADP^+$ + NADPH is about 10^{-6} M. In many cells and tissues, the ratio of NAD^+ (oxidized) to NADH (reduced) is high, favoring hydride transfer from a substrate *to* NAD^+ to form NADH. By contrast, NADPH is generally present at a higher concentration than $NADP^+$, favoring hydride transfer *from* NADPH to a substrate. This reflects the specialized metabolic roles of the two coenzymes: NAD^+ generally functions in oxidations—usually as part of a catabolic reaction; NADPH is the usual coenzyme in reductions—nearly always as part of an anabolic reaction. A few enzymes can use either coenzyme, but most show a strong preference for one over the other. Also, the processes in which these two cofactors function are segregated in eukaryotic cells: for example, oxidations of fuels such as pyruvate, fatty acids, and α-keto acids derived from amino acids occur in the mitochondrial matrix, whereas reductive biosynthetic processes such as fatty acid synthesis take place in the cytosol. This functional and spatial specialization allows a cell to maintain two distinct pools of electron carriers, with two distinct functions.

More than 200 enzymes are known to catalyze reactions in which NAD^+ (or $NADP^+$) accepts a hydride ion from a reduced substrate, or NADPH (or NADH) donates a hydride ion to an oxidized substrate. The general reactions are

$$AH_2 + NAD^+ \longrightarrow A + NADH + H^+$$
$$A + NADPH + H^+ \longrightarrow AH_2 + NADP^+$$

where AH_2 is the reduced substrate and A the oxidized substrate. The general name for an enzyme of this type is **oxidoreductase**; they are also commonly called dehydrogenases. For example, alcohol dehydrogenase catalyzes the first step in the catabolism of ethanol, in which ethanol is oxidized to acetaldehyde:

$$\underset{\text{Ethanol}}{CH_3CH_2OH} + NAD^+ \longrightarrow \underset{\text{Acetaldehyde}}{CH_3CHO} + NADH + H^+$$

Notice that one of the carbon atoms in ethanol has lost a hydrogen; the compound has been oxidized from an alcohol to an aldehyde (refer again to Fig. 13–22 for the oxidation states of carbon).

When NAD^+ or $NADP^+$ is reduced, the hydride ion could in principle be transferred to either side of the nicotinamide ring: the front (A side) or the back (B side), as represented in Figure 13–24a. Studies with isotopically labeled substrates have shown that a given enzyme catalyzes either an A-type or a B-type transfer, but not both. For example, yeast alcohol dehydrogenase and lactate dehydrogenase of vertebrate heart transfer a hydride ion to (or remove a hydride ion from) the A side of the nicotinamide ring; they are classed as type A dehydrogenases to distinguish them from another group of enzymes that transfer a hydride ion to (or remove a hydride ion from) the B side of the nicotinamide ring (Table 13–8). The specificity for one side or another can be very striking; lactate dehydrogenase, for example, prefers the A side over the B side by a factor of 5×10^7! The basis for this preference lies in the exact positioning of the enzyme groups involved in hydrogen bonding with the $—CONH_2$ group of the nicotinamide.

Most dehydrogenases that use NAD or NADP bind the cofactor in a conserved protein domain called the Rossmann fold (named for Michael Rossmann, who deduced the structure of lactate dehydrogenase and first described this structural motif). The Rossmann fold typically consists of a six-stranded parallel β sheet and four associated α helices **(Fig. 13–25)**.

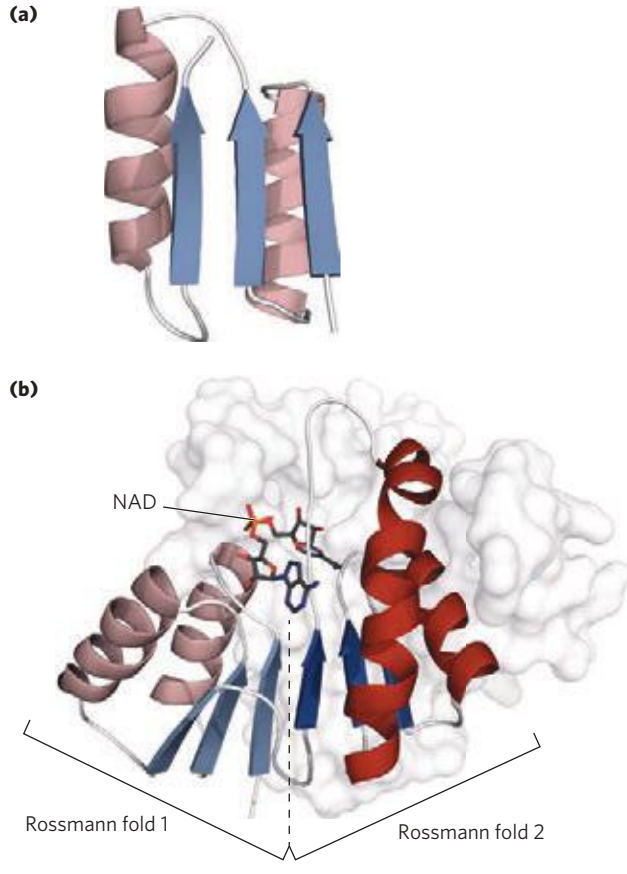

FIGURE 13–25 The Rossmann fold. This structural motif is found in the NAD-binding site of many dehydrogenases. **(a)** It consists of a pair of structurally similar motifs (only one of which is shown here), each having three parallel β sheets and two α helices (β-α-β-α-β). **(b)** The nucleotide-binding domain of the enzyme lactate dehydrogenase (derived from PDB ID 3LDH) with NAD (ball-and-stick structure) bound in an extended conformation through hydrogen bonds and salt bridges to the paired β-α-β-α-β motifs of the Rossmann fold (shades of red and blue).

The association between a dehydrogenase and NAD or NADP is relatively loose; the coenzyme readily diffuses from one enzyme to another, acting as a water-soluble

TABLE 13–8 Stereospecificity of Dehydrogenases That Employ NAD^+ or $NADP^+$ as Coenzymes

Enzyme	Coenzyme	Stereochemical specificity for nicotinamide ring (A or B)	Text page
Isocitrate dehydrogenase	NAD^+	A	643
α-Ketoglutarate dehydrogenase	NAD^+	B	644
Glucose 6-phosphate dehydrogenase	$NADP^+$	B	577
Malate dehydrogenase	NAD^+	A	647
Glutamate dehydrogenase	NAD^+ or $NADP^+$	B	702
Glyceraldehyde 3-phosphate dehydrogenase	NAD^+	B	553
Lactate dehydrogenase	NAD^+	A	563
Alcohol dehydrogenase	NAD^+	A	565

carrier of electrons from one metabolite to another. For example, in the production of alcohol during fermentation of glucose by yeast cells, a hydride ion is removed from glyceraldehyde 3-phosphate by one enzyme (glyceraldehyde 3-phosphate dehydrogenase, a type B enzyme) and transferred to NAD^+. The NADH produced then leaves the enzyme surface and diffuses to another enzyme (alcohol dehydrogenase, a type A enzyme), which transfers a hydride ion to acetaldehyde, producing ethanol:

(1) Glyceraldehyde 3-phosphate + NAD^+ ⟶ 3-phosphoglycerate + NADH + H^+

(2) Acetaldehyde + NADH + H^+ ⟶ ethanol + NAD^+

Sum: Glyceraldehyde 3-phosphate + acetaldehyde ⟶ 3-phosphoglycerate + ethanol

Notice that in the overall reaction there is no net production or consumption of NAD^+ or NADH; the coenzymes function catalytically and are recycled repeatedly without a net change in the concentration of NAD^+ + NADH.

Dietary Deficiency of Niacin, the Vitamin Form of NAD and NADP, Causes Pellagra

As we noted in Chapter 6, and will discuss further in the chapters to follow, most coenzymes are derived from the substances we call vitamins. The pyridine-like rings of NAD and NADP are derived from the vitamin **niacin** (nicotinic acid; **Fig. 13–26**), which is synthesized from tryptophan. Humans generally cannot synthesize sufficient quantities of niacin, and this is especially so for individuals with diets low in tryptophan (maize, for example, has a low tryptophan content). Niacin deficiency, which affects all the NAD(P)-dependent dehydrogenases, causes the serious human disease pellagra (Italian for "rough skin") and a related disease in dogs, blacktongue. These diseases are characterized by the "three Ds": dermatitis, diarrhea, and dementia, followed in many cases by death. A century ago, pellagra was a common human disease; in the southern United States, where maize was a dietary staple, about 100,000 people were afflicted and about 10,000 died as a result of this disease between 1912 and 1916. In 1920 Joseph Goldberger showed pellagra to be caused by a dietary insufficiency, and in 1937 Frank Strong, D. Wayne Woolley, and Conrad Elvehjem identified niacin as the curative agent for blacktongue. Supplementation of the human diet with this inexpensive compound has eradicated pellagra in the populations of the developed world, with one significant exception: people with alcoholism, or who drink excessive amounts of alcohol. In these individuals, intestinal absorption of niacin is much reduced, and caloric needs are often met with distilled spirits that are virtually devoid of vitamins, including niacin. In some parts of the world, including the Deccan Plateau in India, pellagra still occurs in the general population, especially among people living in poverty. ■

Frank Strong, 1908–1993

D. Wayne Woolley, 1914–1966

Conrad Elvehjem, 1901–1962

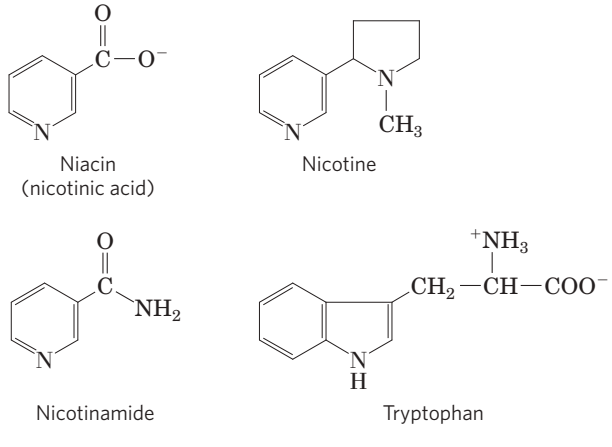

FIGURE 13–26 Niacin (nicotinic acid) and its derivative nicotinamide. The biosynthetic precursor of these compounds is tryptophan. In the laboratory, nicotinic acid was first produced by oxidation of the natural product nicotine—thus the name. Both nicotinic acid and nicotinamide cure pellagra, but nicotine (from cigarettes or elsewhere) has no curative activity.

Flavin Nucleotides Are Tightly Bound in Flavoproteins

Flavoproteins (Table 13–9) are enzymes that catalyze oxidation-reduction reactions using either flavin mononucleotide (FMN) or flavin adenine dinucleotide (FAD) as coenzyme **(Fig. 13–27)**. These coenzymes, the **flavin nucleotides**, are derived from the vitamin riboflavin. The fused ring structure of flavin nucleotides (the isoalloxazine ring) undergoes reversible reduction, accepting either one or two electrons in the form of one or two hydrogen atoms (each atom an electron plus a proton) from a reduced substrate. The fully reduced forms are abbreviated $FADH_2$ and $FMNH_2$. When a fully oxidized flavin nucleotide accepts only one electron (one hydrogen atom), the semiquinone form of the isoalloxazine ring is produced, abbreviated $FADH^•$ and $FMNH^•$. Because flavin nucleotides have a slightly different chemical specialty from that of the nicotinamide

TABLE 13–9 Some Enzymes (Flavoproteins) That Employ Flavin Nucleotide Coenzymes

Enzyme	Flavin nucleotide	Text page(s)
Acyl-CoA dehydrogenase	FAD	673
Dihydrolipoyl dehydrogenase	FAD	637
Succinate dehydrogenase	FAD	646
Glycerol 3-phosphate dehydrogenase	FAD	759
Thioredoxin reductase	FAD	917
NADH dehydrogenase (Complex I)	FMN	738–739
Glycolate oxidase	FMN	813

coenzymes—the ability to participate in either one- or two-electron transfers—flavoproteins are involved in a greater diversity of reactions than the NAD(P)-linked dehydrogenases.

Like the nicotinamide coenzymes (Fig. 13–24), the flavin nucleotides undergo a shift in a major absorption band on reduction (again, useful to biochemists who want to monitor reactions involving these coenzymes). Flavoproteins that are fully reduced (two electrons accepted) generally have an absorption maximum near 360 nm. When partially reduced (one electron), they acquire another absorption maximum at about 450 nm; when fully oxidized, the flavin has maxima at 370 and 440 nm.

The flavin nucleotide in most flavoproteins is bound rather tightly to the protein, and in some enzymes, such as succinate dehydrogenase, it is bound covalently. Such tightly bound coenzymes are properly called prosthetic groups. They do not transfer electrons by diffusing from one enzyme to another; rather, they provide a means by which the flavoprotein can temporarily hold electrons while it catalyzes electron transfer from a reduced substrate to an electron acceptor. One important feature of the flavoproteins is the variability in the standard reduction potential ($E'°$) of the bound flavin nucleotide. Tight association between the enzyme and prosthetic group confers on the flavin ring a reduction potential typical of that particular flavoprotein, sometimes quite different from the reduction potential of the free flavin nucleotide. FAD bound to succinate dehydrogenase, for example, has an $E'°$ close to 0.0 V, compared with −0.219 V for free FAD; $E'°$ for other flavoproteins ranges from −0.40 V to + 0.06 V. Flavoproteins are often very complex; some have, in addition to a flavin nucleotide, tightly bound inorganic ions (iron or molybdenum, for example) capable of participating in electron transfers.

Certain flavoproteins act in a quite different role, as light receptors. **Cryptochromes** are a family of flavoproteins, widely distributed in the eukaryotic phyla, that mediate the effects of blue light on plant development and the effects of light on mammalian circadian rhythms (oscillations in physiology and biochemistry, with a 24-hour period). The cryptochromes are homologs of another family of flavoproteins, the photolyases. Found in both bacteria and eukaryotes, **photolyases** use the energy of absorbed light to repair chemical defects in DNA.

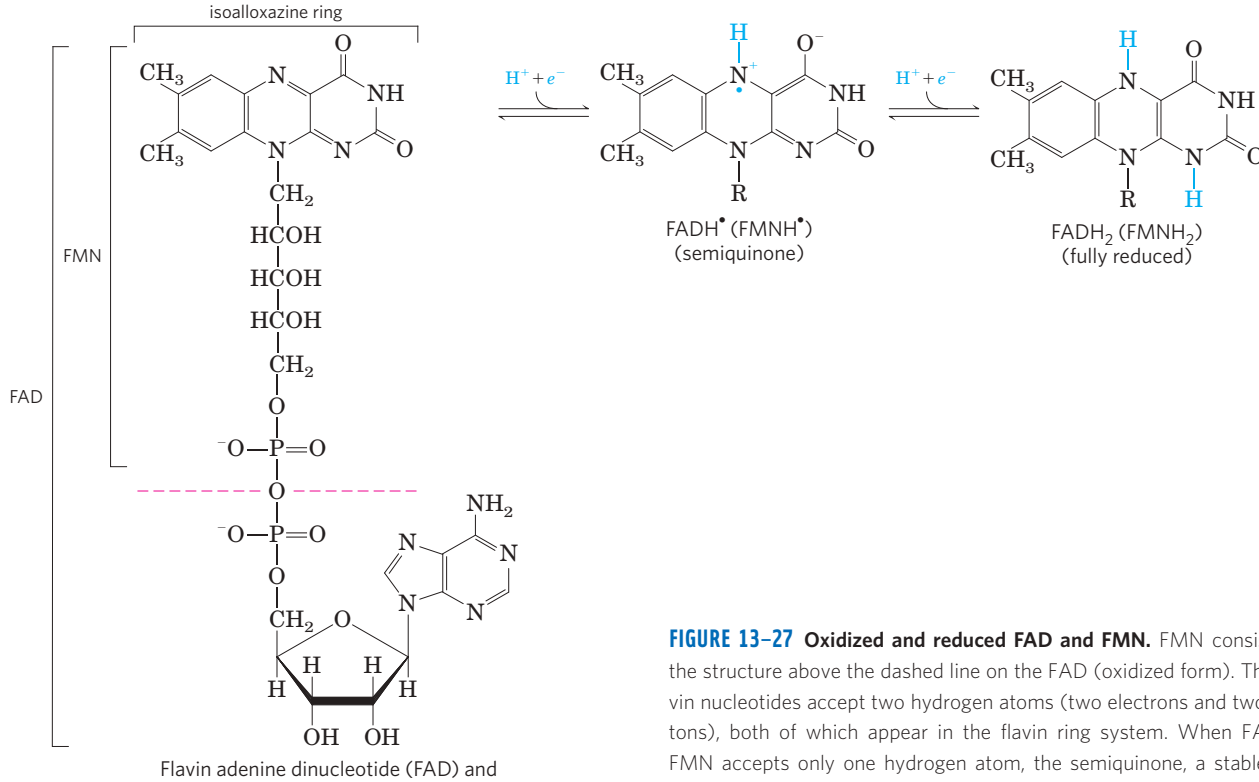

Flavin adenine dinucleotide (FAD) and flavin mononucleotide (FMN)

FIGURE 13–27 Oxidized and reduced FAD and FMN. FMN consists of the structure above the dashed line on the FAD (oxidized form). The flavin nucleotides accept two hydrogen atoms (two electrons and two protons), both of which appear in the flavin ring system. When FAD or FMN accepts only one hydrogen atom, the semiquinone, a stable free radical, forms.

We examine the function of flavoproteins as electron carriers in Chapter 19, when we consider their roles in oxidative phosphorylation (in mitochondria) and photophosphorylation (in chloroplasts), and we describe the photolyase reactions in Chapter 25.

SUMMARY 13.4 Biological Oxidation-Reduction Reactions

- In many organisms, a central energy-conserving process is the stepwise oxidation of glucose to CO_2, in which some of the energy of oxidation is conserved in ATP as electrons are passed to O_2.
- Biological oxidation-reduction reactions can be described in terms of two half-reactions, each with a characteristic standard reduction potential, $E'°$.
- When two electrochemical half-cells, each containing the components of a half-reaction, are connected, electrons tend to flow to the half-cell with the higher reduction potential. The strength of this tendency is proportional to the difference between the two reduction potentials (ΔE) and is a function of the concentrations of oxidized and reduced species.
- The standard free-energy change for an oxidation-reduction reaction is directly proportional to the difference in standard reduction potentials of the two half-cells: $\Delta G'° = -n\,\mathcal{F}\,\Delta E'°$.
- Many biological oxidation reactions are dehydrogenations in which one or two hydrogen atoms ($H^+ + e^-$) are transferred from a substrate to a hydrogen acceptor. Oxidation-reduction reactions in living cells involve specialized electron carriers.
- NAD and NADP are the freely diffusible coenzymes of many dehydrogenases. Both NAD^+ and $NADP^+$ accept two electrons and one proton.
- FAD and FMN, the flavin nucleotides, serve as tightly bound prosthetic groups of flavoproteins. They can accept either one or two electrons and one or two protons. Flavoproteins also serve as light receptors in cryptochromes and photolyases.

Key Terms

Terms in bold are defined in the glossary.

autotroph 501
heterotroph 501
metabolism 502
metabolic pathways 502
metabolite 502
intermediary metabolism 502
catabolism 502
anabolism 502
standard transformed constants 507
homolytic cleavage 512
radical 512
heterolytic cleavage 512
nucleophile 512
electrophile 512
carbanion 512
carbocation 512
aldol condensation 513
Claisen condensation 513
kinases 516
phosphorylation potential (ΔG_p) 518
thioester 521
adenylylation 524
inorganic pyrophosphatase 524
nucleoside diphosphate kinase 526
adenylate kinase 526
creatine kinase 526
phosphagens 527
polyphosphate kinase-1, kinase-2 527
electromotive force (emf) 528
conjugate redox pair 528
dehydrogenation 529
dehydrogenases 529
reducing equivalent 530
standard reduction potential ($E'°$) 530
pyridine nucleotide 532
oxidoreductase 534
flavoprotein 535
flavin nucleotides 535
cryptochrome 536
photolyase 536

Further Reading

Bioenergetics and Thermodynamics

Atkins, P.W. (1984) *The Second Law*, Scientific American Books, Inc., New York.
A well-illustrated and elementary discussion of the second law and its implications.

Atkinson, D.E. (1977) *Cellular Energy Metabolism and Its Regulation*, Academic Press, Inc., New York.
A classic treatment of the roles of ATP, ADP, and AMP in controlling the rate of catabolism.

Bergethon, P.R. (1998) *The Physical Basis of Biochemistry*, Springer Verlag, New York.
Chapters 11 through 13 of this book, and the books by Tinoco et al. and van Holde et al. (below), are excellent general references for physical biochemistry, with good discussions of the applications of thermodynamics to biochemistry.

Edsall, J.T. & Gutfreund, H. (1983) *Biothermodynamics: The Study of Biochemical Processes at Equilibrium*, John Wiley & Sons, Inc., New York.

Hammes, G. (2000) *Thermodynamics and Kinetics for the Biological Sciences*, John Wiley & Sons, Inc., New York.
Clearly written, well illustrated, with excellent examples and problems.

Harold, F.M. (1986) *The Vital Force: A Study of Bioenergetics*, W.H. Freeman and Company, New York.
A beautifully clear discussion of thermodynamics in biological processes.

Harris, D.A. (1995) *Bioenergetics at a Glance*, Blackwell Science, Oxford.
A short, clearly written account of cellular energetics, including introductory chapters on thermodynamics.

Haynie, D.T. (2001) *Biological Thermodynamics*, Cambridge University Press, Cambridge.
Highly accessible discussions of thermodynamics and kinetics in biological systems.

Loewenstein, W.R. (1999) *The Touchstone of Life: Molecular Information, Cell Communication, and the Foundations of Life*, Oxford University Press, New York.
Beautifully written discussion of the relationship between entropy and information.

Nicholls, D.G. & Ferguson, S.J. (2002) *Bioenergetics 3*, Academic Press, Inc., New York.
Clear, well-illustrated, intermediate-level discussion of the theory of bioenergetics and the mechanisms of energy transductions.

Tinoco, I., Jr., Sauer, K., Wang, J.C., & Puglisi, J.D. (2002) *Physical Chemistry: Principles and Applications in Biological Sciences*, 4th edn, Prentice-Hall, Inc., Upper Saddle River, NJ.
Chapters 2 through 5 cover thermodynamics.

van Holde, K.E., Johnson, C., & Ho, P.S. (2006) *Principles of Physical Biochemistry*, 2nd edn, Prentice-Hall, Inc., Upper Saddle River, NJ.
Chapters 2 and 3 are especially relevant.

Chemical Logic and Common Biochemical Reactions

Frey, P.A. (2001) Radical mechanisms of enzymatic catalysis. *Annu. Rev. Biochem.* **70**, 121–148.
A very useful survey of reactions that proceed by free-radical mechanisms.

Frey, P.A. & Hegeman, A.D. (2006) *Enzymatic Reaction Mechanisms*, Oxford University Press, New York.
An authoritative and up-to-date resource on the reactions that occur in living systems.

Gutteridge, A. & Thornton, J.M. (2005) Understanding nature's catalytic toolkit. *Trends Biochem. Sci.* **11**, 622–629.

Kraut, D.A., Carroll, K.S., & Herschlag, D. (2003) Challenges in enzyme mechanism and energetics. *Annu. Rev. Biochem.* **72**, 517–571.
A good summary of the principles of enzyme catalysis as currently understood, and what we still do not understand.

Phosphoryl Group Transfers and ATP

Alberty, R.A. (1994) Biochemical thermodynamics. *Biochim. Biophys. Acta* **1207**, 1–11.
Explains the distinction between biochemical and chemical equations, and the calculation and meaning of transformed thermodynamic properties for ATP and other phosphorylated compounds.

Bridger, W.A. & Henderson, J.F. (1983) *Cell ATP,* John Wiley & Sons, Inc., New York.
The chemistry of ATP, its place in metabolic regulation, and its catabolic and anabolic roles.

Brown, M.R.W. & Kornberg, A. (2004) Inorganic polyphosphate in the origin and survival of species. *Proc. Natl. Acad. Sci. USA* **101**, 16,085–16,087.

Fraley, C.D., Rashid, M.H., Lee, S.S.K., Gottschalk, R., Harrison, J., Wood, P.J., Brown, M.R.W, & Kornberg, A. (2007) A polyphosphate kinase 1 (ppk1) mutant of *Pseudomonas aeruginosa* exhibits multiple ultrastructural and functional defects. *Proc. Natl. Acad. Sci. USA* **104**, 3526–3531.

Frey, P.A. & Arabshahi, A. (1995) Standard free-energy change for the hydrolysis of the α–β-phosphoanhydride bridge in ATP. *Biochemistry* **34**, 11,307–11,310.

Hanson, R.W. (1989) The role of ATP in metabolism. *Biochem. Educ.* **17**, 86–92.
Excellent summary of the chemistry and biology of ATP.

Kalckar, H.M. (1991) Fifty years of biological research: from oxidative phosphorylation to energy requiring transport regulation. *Annu. Rev. Biochem.* **60**, 1–37.
Intermediate-level discussion of the history of ATP studies, in which the author was a major player.

Kornberg, A. (1999) Inorganic polyphosphate: a molecule of many functions. *Annu. Rev. Biochem.* **68**, 89–125.

Lipmann, F. (1941) Metabolic generation and utilization of phosphate bond energy. *Adv. Enzymol.* **11**, 99–162.
The classic description of the role of high-energy phosphate compounds in biology.

Pullman, B. & Pullman, A. (1960) Electronic structure of energy-rich phosphates. *Radiat. Res.,* Suppl. 2, 160–181.
An advanced discussion of the chemistry of ATP and other "energy-rich" compounds.

Rees, D.C. & Howard, J.B. (1999) Structural bioenergetics and energy transduction mechanisms. *J. Mol. Biol.* **293**, 343–350.
Discussion of the structural basis for the efficient coupling of two energetic processes by way of changes in conformational states.

Veech, R.L., Lawson, J.W.R., Cornell, N.W., & Krebs, H.A. (1979) Cytosolic phosphorylation potential. *J. Biol. Chem.* **254**, 6538–6547.
Experimental determination of ATP, ADP, and P_i concentrations in brain, muscle, and liver, and a discussion of the difficulties in determining the real free-energy change for ATP synthesis in cells.

Westheimer, F.H. (1987) Why nature chose phosphates. *Science* **235**, 1173–1178.
A chemist's description of the unique suitability of phosphate esters and anhydrides for metabolic transformations.

Biological Oxidation-Reduction Reactions

Cashmore, A.R., Jarillo, J.A., Wu, Y.J., & Liu, D. (1999) Cryptochromes: blue light receptors for plants and animals. *Science* **284**, 760–765.

Dolphin, D., Avramović, O., & Poulson, R. (eds). (1987) *Pyridine Nucleotide Coenzymes: Chemical, Biochemical, and Medical Aspects*, John Wiley & Sons, Inc., New York.
An excellent two-volume collection of authoritative reviews. Among the most useful are the chapters by Kaplan, Westheimer, Veech, and Ohno and Ushio.

Fraaije, M.W. & Mattevi, A. (2000) Flavoenzymes: diverse catalysts with recurrent features. *Trends Biochem. Sci.* **25**, 126–132.

Hosler, J.P., Ferguson-Miller, S., & Mills, D.S. (2006) Energy transduction: proton transfer through the respiratory complexes. *Annu. Rev. Biochem.* **75**, 165–187.

Massey, V. (1994) Activation of molecular oxygen by flavins and flavoproteins. *J. Biol. Chem.* **269**, 22,459–22,462.
A short review of the chemistry of flavin-oxygen interactions in flavoproteins.

Rees, D.C. (2002) Great metalloclusters in enzymology. *Annu. Rev. Biochem.* **71**, 221–246.
Advanced review of the types of metal ion clusters found in enzymes and their modes of action.

Roehm, K.-H. (2001) Electron carriers: proteins and cofactors in oxidative phosphorylation. In *Encyclopedia of Life Sciences*, John Wiley & Sons, Inc./Wiley InterScience, www.els.net.
Good overview of the different classes of electron carriers that participate in respiration.

Williams, R.E. & Bruce, N.C. (2002) New uses for an old enzyme—the old yellow enzyme family of flavoenzymes. *Microbiology* **148**, 1607–1614.

Problems

1. Entropy Changes during Egg Development Consider a system consisting of an egg in an incubator. The white and yolk of the egg contain proteins, carbohydrates, and lipids. If fertilized, the egg is transformed from a single cell to a complex organism. Discuss this irreversible process in terms of the entropy changes in the system, surroundings, and universe. Be sure that you first clearly define the system and surroundings.

2. Calculation of $\Delta G'^{\circ}$ from an Equilibrium Constant Calculate the standard free-energy change for each of the following metabolically important enzyme-catalyzed reactions, using the equilibrium constants given for the reactions at 25 °C and pH 7.0.

(a) Glutamate + oxaloacetate $\overset{\text{aspartate aminotransferase}}{\rightleftharpoons}$ aspartate + α-ketoglutarate $\quad K'_{eq} = 6.8$

(b) Dihydroxyacetone phosphate $\overset{\text{triose phosphate isomerase}}{\rightleftharpoons}$ glyceraldehyde 3-phosphate $\quad K'_{eq} = 0.0475$

(c) Fructose 6-phosphate + ATP $\overset{\text{phosphofructokinase}}{\rightleftharpoons}$ fructose 1,6-bisphosphate + ADP $\quad K'_{eq} = 254$

3. Calculation of the Equilibrium Constant from $\Delta G'^\circ$ Calculate the equilibrium constant K'_{eq} for each of the following reactions at pH 7.0 and 25 °C, using the $\Delta G'^\circ$ values in Table 13–4.

(a) Glucose 6-phosphate + H_2O $\overset{\text{glucose 6-phosphatase}}{\rightleftharpoons}$ glucose + P_i

(b) Lactose + H_2O $\overset{\beta\text{-galactosidase}}{\rightleftharpoons}$ glucose + galactose

(c) Malate $\overset{\text{fumarase}}{\rightleftharpoons}$ fumarate + H_2O

4. Experimental Determination of K'_{eq} and $\Delta G'^\circ$ If a 0.1 M solution of glucose 1-phosphate at 25 °C is incubated with a catalytic amount of phosphoglucomutase, the glucose 1-phosphate is transformed to glucose 6-phosphate. At equilibrium, the concentrations of the reaction components are

Glucose 1-phosphate $\rightleftharpoons$ glucose 6-phosphate

4.5×10^{-3} M $\qquad$ 9.6×10^{-2} M

Calculate K'_{eq} and $\Delta G'^\circ$ for this reaction.

5. Experimental Determination of $\Delta G'^\circ$ for ATP Hydrolysis A direct measurement of the standard free-energy change associated with the hydrolysis of ATP is technically demanding because the minute amount of ATP remaining at equilibrium is difficult to measure accurately. The value of $\Delta G'^\circ$ can be calculated indirectly, however, from the equilibrium constants of two other enzymatic reactions having less favorable equilibrium constants:

Glucose 6-phosphate + H_2O ⟶ glucose + P_i $\quad K'_{eq} = 270$

ATP + glucose ⟶ ADP + glucose 6-phosphate $\quad K'_{eq} = 890$

Using this information for equilibrium constants determined at 25 °C, calculate the standard free energy of hydrolysis of ATP.

6. Difference between $\Delta G'^\circ$ and ΔG Consider the following interconversion, which occurs in glycolysis (Chapter 14):

Fructose 6-phosphate $\rightleftharpoons$ glucose 6-phosphate $\quad K'_{eq} = 1.97$

(a) What is $\Delta G'^\circ$ for the reaction (K'_{eq} measured at 25 °C)?

(b) If the concentration of fructose 6-phosphate is adjusted to 1.5 M and that of glucose 6-phosphate is adjusted to 0.50 M, what is ΔG?

(c) Why are $\Delta G'^\circ$ and ΔG different?

7. Free Energy of Hydrolysis of CTP Compare the structure of the nucleoside triphosphate CTP with the structure of ATP.

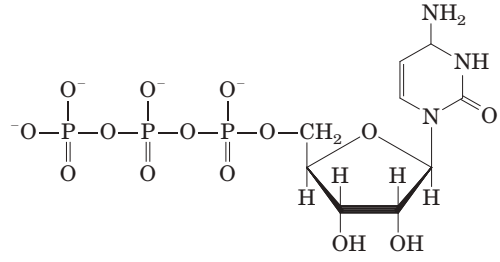

Cytidine triphosphate (CTP)

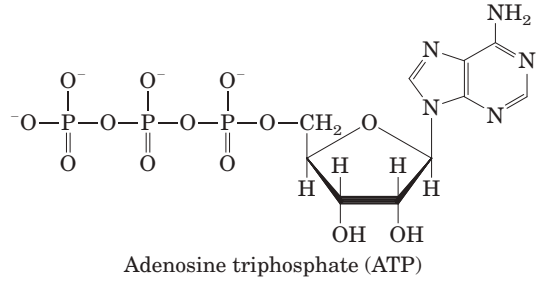

Adenosine triphosphate (ATP)

Now predict the K'_{eq} and $\Delta G'^\circ$ for the following reaction:

ATP + CDP ⟶ ADP + CTP

8. Dependence of ΔG on pH The free energy released by the hydrolysis of ATP under standard conditions is −30.5 kJ/mol. If ATP is hydrolyzed under standard conditions except at pH 5.0, is more or less free energy released? Explain. Use the Living Graph to explore this relationship.

9. The $\Delta G'^\circ$ for Coupled Reactions Glucose 1-phosphate is converted into fructose 6-phosphate in two successive reactions:

Glucose 1-phosphate ⟶ glucose 6-phosphate

Glucose 6-phosphate ⟶ fructose 6-phosphate

Using the $\Delta G'^\circ$ values in Table 13–4, calculate the equilibrium constant, K'_{eq}, for the sum of the two reactions:

Glucose 1-phosphate ⟶ fructose 6-phosphate

10. Effect of [ATP]/[ADP] Ratio on Free Energy of Hydrolysis of ATP Using Equation 13–4, plot ΔG against ln Q (mass-action ratio) at 25 °C for the concentrations of ATP, ADP, and P_i in the table below. $\Delta G'^\circ$ for the reaction is −30.5 kJ/mol. Use the resulting plot to explain why metabolism is regulated to keep the ratio [ATP]/[ADP] high.

	Concentration (mM)				
ATP	5	3	1	0.2	5
ADP	0.2	2.2	4.2	5.0	25
P_i	10	12.1	14.1	14.9	10

11. Strategy for Overcoming an Unfavorable Reaction: ATP-Dependent Chemical Coupling The phosphorylation of glucose to glucose 6-phosphate is the initial step in the

catabolism of glucose. The direct phosphorylation of glucose by P_i is described by the equation

$$\text{Glucose} + P_i \longrightarrow \text{glucose 6-phosphate} + H_2O \qquad \Delta G'^\circ = 13.8 \text{ kJ/mol}$$

(a) Calculate the equilibrium constant for the above reaction at 37 °C. In the rat hepatocyte the physiological concentrations of glucose and P_i are maintained at approximately 4.8 mM. What is the equilibrium concentration of glucose 6-phosphate obtained by the direct phosphorylation of glucose by P_i? Does this reaction represent a reasonable metabolic step for the catabolism of glucose? Explain.

(b) In principle, at least, one way to increase the concentration of glucose 6-phosphate is to drive the equilibrium reaction to the right by increasing the intracellular concentrations of glucose and P_i. Assuming a fixed concentration of P_i at 4.8 mM, how high would the intracellular concentration of glucose have to be to give an equilibrium concentration of glucose 6-phosphate of 250 μM (the normal physiological concentration)? Would this route be physiologically reasonable, given that the maximum solubility of glucose is less than 1 M?

(c) The phosphorylation of glucose in the cell is coupled to the hydrolysis of ATP; that is, part of the free energy of ATP hydrolysis is used to phosphorylate glucose:

(1) $\text{Glucose} + P_i \longrightarrow \text{glucose 6-phosphate} + H_2O \qquad \Delta G'^\circ = 13.8 \text{ kJ/mol}$

(2) $ATP + H_2O \longrightarrow ADP + P_i \qquad \Delta G'^\circ = -30.5 \text{ kJ/mol}$

Sum: $\text{Glucose} + ATP \longrightarrow \text{glucose 6-phosphate} + ADP$

Calculate K'_{eq} at 37 °C for the overall reaction. For the ATP-dependent phosphorylation of glucose, what concentration of glucose is needed to achieve a 250 μM intracellular concentration of glucose 6-phosphate when the concentrations of ATP and ADP are 3.38 mM and 1.32 mM, respectively? Does this coupling process provide a feasible route, at least in principle, for the phosphorylation of glucose in the cell? Explain.

(d) Although coupling ATP hydrolysis to glucose phosphorylation makes thermodynamic sense, we have not yet specified how this coupling is to take place. Given that coupling requires a common intermediate, one conceivable route is to use ATP hydrolysis to raise the intracellular concentration of P_i and thus drive the unfavorable phosphorylation of glucose by P_i. Is this a reasonable route? (Think about the solubility products of metabolic intermediates.)

(e) The ATP-coupled phosphorylation of glucose is catalyzed in hepatocytes by the enzyme glucokinase. This enzyme binds ATP and glucose to form a glucose-ATP-enzyme complex, and the phosphoryl group is transferred directly from ATP to glucose. Explain the advantages of this route.

12. Calculations of $\Delta G'^\circ$ for ATP-Coupled Reactions From data in Table 13–6 calculate the $\Delta G'^\circ$ value for the following reactions

(a) $\text{Phosphocreatine} + ADP \longrightarrow \text{creatine} + ATP$

(b) $ATP + \text{fructose} \longrightarrow ADP + \text{fructose 6-phosphate}$

13. Coupling ATP Cleavage to an Unfavorable Reaction To explore the consequences of coupling ATP hydrolysis under physiological conditions to a thermodynamically unfavorable biochemical reaction, consider the hypothetical transformation $X \rightarrow Y$, for which $\Delta G'^\circ = 20.0$ kJ/mol.

(a) What is the ratio [Y]/[X] at equilibrium?

(b) Suppose X and Y participate in a sequence of reactions during which ATP is hydrolyzed to ADP and P_i. The overall reaction is

$$X + ATP + H_2O \longrightarrow Y + ADP + P_i$$

Calculate [Y]/[X] for this reaction at equilibrium. Assume that the temperature is 25 °C and the equilibrium concentrations of ATP, ADP, and P_i are 1 M.

(c) We know that [ATP], [ADP], and [P_i] are *not* 1 M under physiological conditions. Calculate [Y]/[X] for the ATP-coupled reaction when the values of [ATP], [ADP], and [P_i] are those found in rat myocytes (Table 13–5).

14. Calculations of ΔG at Physiological Concentrations Calculate the actual, physiological ΔG for the reaction

$$\text{Phosphocreatine} + ADP \longrightarrow \text{creatine} + ATP$$

at 37 °C, as it occurs in the cytosol of neurons, with phosphocreatine at 4.7 mM, creatine at 1.0 mM, ADP at 0.73 mM, and ATP at 2.6 mM.

15. Free Energy Required for ATP Synthesis under Physiological Conditions In the cytosol of rat hepatocytes, the temperature is 37 °C and the mass-action ratio, Q, is

$$\frac{[ATP]}{[ADP][P_i]} = 5.33 \times 10^2 \text{ M}^{-1}$$

Calculate the free energy required to synthesize ATP in a rat hepatocyte.

16. Chemical Logic In the glycolytic pathway, a six-carbon sugar (fructose 1,6-bisphosphate) is cleaved to form two three-carbon sugars, which undergo further metabolism (see Fig. 14–6). In this pathway, an isomerization of glucose 6-phosphate to fructose 6-phosphate (shown below) occurs two steps before the cleavage reaction (the intervening step is phosphorylation of fructose 6-phosphate to fructose 1,6-bisphosphate (p. 549)).

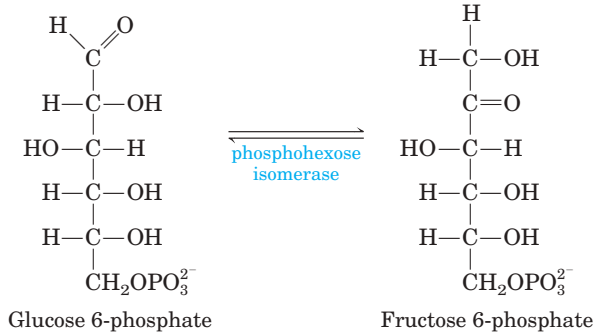

Glucose 6-phosphate Fructose 6-phosphate

What does the isomerization step accomplish from a chemical perspective? (Hint: Consider what might happen if the C—C bond cleavage were to proceed without the preceding isomerization.)

17. Enzymatic Reaction Mechanisms I Lactate dehydrogenase is one of the many enzymes that require NADH as coenzyme. It catalyzes the conversion of pyruvate to lactate:

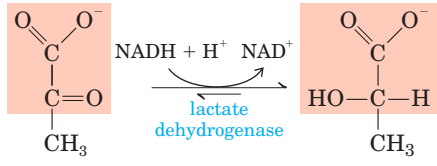

Draw the mechanism of this reaction (show electron-pushing arrows). (Hint: This is a common reaction throughout metabolism; the mechanism is similar to that catalyzed by other dehydrogenases that use NADH, such as alcohol dehydrogenase.)

18. Enzymatic Reaction Mechanisms II Biochemical reactions often look more complex than they really are. In the pentose phosphate pathway (Chapter 14), sedoheptulose 7-phosphate and glyceraldehyde 3-phosphate react to form erythrose 4-phosphate and fructose 6-phosphate in a reaction catalyzed by transaldolase.

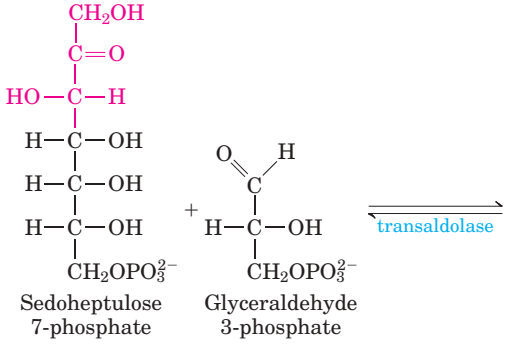

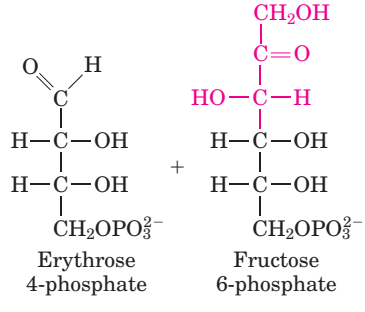

Draw a mechanism for this reaction (show electron-pushing arrows). (Hint: Take another look at aldol condensations, then consider the name of this enzyme.)

19. Daily ATP Utilization by Human Adults

(a) A total of 30.5 kJ/mol of free energy is needed to synthesize ATP from ADP and P_i when the reactants and products are at 1 M concentrations and the temperature is 25 °C (standard state). Because the actual physiological concentrations of ATP, ADP, and P_i are not 1 M, and the temperature is 37 °C, the free energy required to synthesize ATP under physiological conditions is different from $\Delta G'°$. Calculate the free energy required to synthesize ATP in the human hepatocyte when the physiological concentrations of ATP, ADP, and P_i are 3.5, 1.50, and 5.0 mM, respectively.

(b) A 68 kg (150 lb) adult requires a caloric intake of 2,000 kcal (8,360 kJ) of food per day (24 hours). The food is metabolized and the free energy is used to synthesize ATP, which then provides energy for the body's daily chemical and mechanical work. Assuming that the efficiency of converting food energy into ATP is 50%, calculate the weight of ATP used by a human adult in 24 hours. What percentage of the body weight does this represent?

(c) Although adults synthesize large amounts of ATP daily, their body weight, structure, and composition do not change significantly during this period. Explain this apparent contradiction.

20. Rates of Turnover of γ and β Phosphates of ATP If a small amount of ATP labeled with radioactive phosphorus in the terminal position, [γ-^{32}P]ATP, is added to a yeast extract, about half of the ^{32}P activity is found in P_i within a few minutes, but the concentration of ATP remains unchanged. Explain. If the same experiment is carried out using ATP labeled with ^{32}P in the central position, [β-^{32}P]ATP, the ^{32}P does not appear in P_i within such a short time. Why?

21. Cleavage of ATP to AMP and PP_i during Metabolism Synthesis of the activated form of acetate (acetyl-CoA) is carried out in an ATP-dependent process:

$$\text{Acetate} + \text{CoA} + \text{ATP} \longrightarrow \text{acetyl-CoA} + \text{AMP} + PP_i$$

(a) The $\Delta G'°$ for hydrolysis of acetyl-CoA to acetate and CoA is −32.2 kJ/mol and that for hydrolysis of ATP to AMP and PP_i is −30.5 kJ/mol. Calculate $\Delta G'°$ for the ATP-dependent synthesis of acetyl-CoA.

(b) Almost all cells contain the enzyme inorganic pyrophosphatase, which catalyzes the hydrolysis of PP_i to P_i. What effect does the presence of this enzyme have on the synthesis of acetyl-CoA? Explain.

22. Energy for H^+ Pumping The parietal cells of the stomach lining contain membrane "pumps" that transport hydrogen ions from the cytosol (pH 7.0) into the stomach, contributing to the acidity of gastric juice (pH 1.0). Calculate the free energy required to transport 1 mol of hydrogen ions through these pumps. (Hint: See Chapter 11.) Assume a temperature of 37 °C.

23. Standard Reduction Potentials The standard reduction potential, $E'°$, of any redox pair is defined for the half-cell reaction:

$$\text{Oxidizing agent} + n \text{ electrons} \longrightarrow \text{reducing agent}$$

The $E'°$ values for the NAD^+/NADH and pyruvate/lactate conjugate redox pairs are −0.32 V and −0.19 V, respectively.

(a) Which redox pair has the greater tendency to lose electrons? Explain.

(b) Which pair is the stronger oxidizing agent? Explain.

(c) Beginning with 1 M concentrations of each reactant and product at pH 7 and 25 °C, in which direction will the following reaction proceed?

$$\text{Pyruvate} + \text{NADH} + H^+ \rightleftharpoons \text{lactate} + NAD^+$$

(d) What is the standard free-energy change ($\Delta G'°$) for the conversion of pyruvate to lactate?

(e) What is the equilibrium constant (K'_{eq}) for this reaction?

24. Energy Span of the Respiratory Chain Electron transfer in the mitochondrial respiratory chain may be represented by the net reaction equation

$$NADH + H^+ + \tfrac{1}{2}O_2 \rightleftharpoons H_2O + NAD^+$$

(a) Calculate $\Delta E'°$ for the net reaction of mitochondrial electron transfer. Use $E'°$ values from Table 13–7.

(b) Calculate $\Delta G'°$ for this reaction.

(c) How many ATP molecules can *theoretically* be generated by this reaction if the free energy of ATP synthesis under cellular conditions is 52 kJ/mol?

25. Dependence of Electromotive Force on Concentrations Calculate the electromotive force (in volts) registered by an electrode immersed in a solution containing the following mixtures of NAD^+ and NADH at pH 7.0 and 25 °C, with reference to a half-cell of $E'°$ 0.00 V.

(a) 1.0 mM NAD^+ and 10 mM NADH

(b) 1.0 mM NAD^+ and 1.0 mM NADH

(c) 10 mM NAD^+ and 1.0 mM NADH

26. Electron Affinity of Compounds List the following in order of increasing tendency to accept electrons: (a) α-ketoglutarate + CO_2 (yielding isocitrate); (b) oxaloacetate; (c) O_2; (d) $NADP^+$.

27. Direction of Oxidation-Reduction Reactions Which of the following reactions would you expect to proceed in the direction shown, under standard conditions, in the presence of the appropriate enzymes?

(a) Malate + NAD^+ $\longrightarrow$ oxaloacetate + NADH + H^+

(b) Acetoacetate + NADH + H^+ $\longrightarrow$ β-hydroxybutyrate + NAD^+

(c) Pyruvate + NADH + H^+ $\longrightarrow$ lactate + NAD^+

(d) Pyruvate + β-hydroxybutyrate $\longrightarrow$ lactate + acetoacetate

(e) Malate + pyruvate $\longrightarrow$ oxaloacetate + lactate

(f) Acetaldehyde + succinate $\longrightarrow$ ethanol + fumarate

Data Analysis Problem

28. Thermodynamics Can Be Tricky Thermodynamics is a challenging area of study and one with many opportunities for confusion. An interesting example is found in an article by Robinson, Hampson, Munro, and Vaney, published in *Science* in 1993. Robinson and colleagues studied the movement of small molecules between neighboring cells of the nervous system through cell-to-cell channels (gap junctions). They found that the dyes Lucifer yellow (a small, negatively charged molecule) and biocytin (a small zwitterionic molecule) moved in only one direction between two particular types of glia (nonneuronal cells of the nervous system). Dye injected into astrocytes would rapidly pass into adjacent astrocytes, oligodendrocytes, or Müller cells, but dye injected into oligodendrocytes or Müller cells passed slowly if at all into astrocytes. All of these cell types are connected by gap junctions.

Although it was not a central point of their article, the authors presented a molecular model for how this unidirectional transport might occur, as shown in their Figure 3:

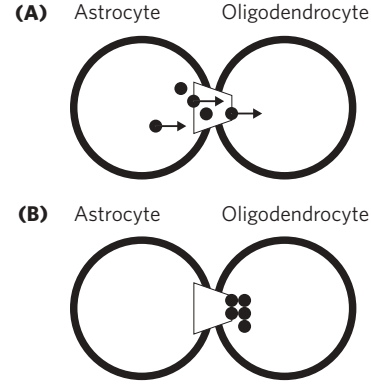

The figure legend reads: "Model of the unidirectional diffusion of dye between coupled oligodendrocytes and astrocytes, based on differences in connection pore diameter. Like a fish in a fish trap, dye molecules (black circles) can pass from an astrocyte to an oligodendrocyte (A) but not back in the other direction (B)."

Although this article clearly passed review at a well-respected journal, several letters to the editor (1994) followed, showing that Robinson and coauthors' model violated the second law of thermodynamics.

(a) Explain how the model violates the second law. Hint: Consider what would happen to the entropy of the system if one started with equal concentrations of dye in the astrocyte and oligodendrocyte connected by the "fish trap" type of gap junctions.

(b) Explain why this model cannot work for small molecules, although it may allow one to catch fish.

(c) Explain why a fish trap *does* work for fish.

(d) Provide two plausible mechanisms for the unidirectional transport of dye molecules between the cells that do not violate the second law of thermodynamics.

References

Letters to the editor. (1994) *Science* **265**, 1017–1019.

Robinson, S.R., Hampson, E.C.G.M., Munro, M.N., & Vaney, D.I. (1993) Unidirectional coupling of gap junctions between neuroglia. *Science* **262**, 1072–1074.

14

Glycolysis, Gluconeogenesis, and the Pentose Phosphate Pathway

Glucose occupies a central position in the metabolism of plants, animals, and many microorganisms. It is relatively rich in potential energy, and thus a good fuel; the complete oxidation of glucose to carbon dioxide and water proceeds with a standard free-energy change of −2,840 kJ/mol. By storing glucose as a high molecular weight polymer such as starch or glycogen, a cell can stockpile large quantities of hexose units while maintaining a relatively low cytosolic osmolarity. When energy demands increase, glucose can be released from these intracellular storage polymers and used to produce ATP either aerobically or anaerobically.

Glucose is not only an excellent fuel, it is also a remarkably versatile precursor, capable of supplying a huge array of metabolic intermediates for biosynthetic reactions. A bacterium such as *Escherichia coli* can obtain from glucose the carbon skeletons for every amino acid, nucleotide, coenzyme, fatty acid, or other metabolic intermediate it needs for growth. A comprehensive study of the metabolic fates of glucose would encompass hundreds or thousands of transformations. In animals and vascular plants, glucose has four major fates: it may be used in the synthesis of complex polysaccharides destined for the extracellular space; stored in cells (as a polysaccharide or as sucrose); oxidized to a three-carbon compound (pyruvate) via glycolysis to provide ATP and metabolic intermediates; or oxidized via the pentose phosphate (phosphogluconate) pathway to yield ribose 5-phosphate for nucleic acid synthesis and NADPH for reductive biosynthetic processes **(Fig. 14–1)**.

Organisms that do not have access to glucose from other sources must make it. Photosynthetic organisms make glucose by first reducing atmospheric CO_2 to trioses, then converting the trioses to glucose. Nonphotosynthetic cells make glucose from simpler three- and four-carbon precursors by the process of gluconeogenesis, effectively reversing glycolysis in a pathway that uses many of the glycolytic enzymes.

In this chapter we describe the individual reactions of glycolysis, gluconeogenesis, and the pentose phosphate pathway and the functional significance of each pathway. We also describe the various metabolic fates of the pyruvate produced by glycolysis. They include the fermentations that are used by many organisms in anaerobic niches to produce ATP and that are exploited industrially as sources of ethanol, lactic acid, and other commercially useful products. And we look at the pathways that feed various sugars from mono-, di-, and polysaccharides into the glycolytic pathway. The discussion of glucose metabolism continues in Chapter 15, where we

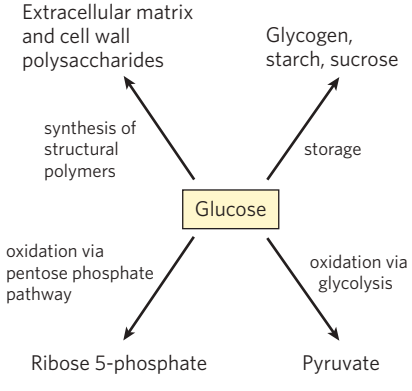

FIGURE 14–1 Major pathways of glucose utilization. Although not the only possible fates for glucose, these four pathways are the most significant in terms of the amount of glucose that flows through them in most cells.

use the processes of carbohydrate synthesis and degradation to illustrate the many mechanisms by which organisms regulate metabolic pathways. The biosynthetic pathways from glucose to extracellular matrix and cell wall polysaccharides and storage polysaccharides are discussed in Chapter 20.

14.1 Glycolysis

In **glycolysis** (from the Greek *glykys*, "sweet" or "sugar," and *lysis*, "splitting"), a molecule of glucose is degraded in a series of enzyme-catalyzed reactions to yield two molecules of the three-carbon compound pyruvate. During the sequential reactions of glycolysis, some of the free energy released from glucose is conserved in the form of ATP and NADH. Glycolysis was the first metabolic pathway to be elucidated and is probably the best understood. From Eduard Buchner's discovery in 1897 of fermentation in broken extracts of yeast cells until the elucidation of the whole pathway in yeast (by Otto Warburg and Hans von Euler-Chelpin) and in muscle (by Gustav Embden and Otto Meyerhof) in the 1930s, the reactions of glycolysis in extracts of yeast and muscle were a major focus of biochemical research. The philosophical shift that accompanied these discoveries was announced by Jacques Loeb in 1906:

> Through the discovery of Buchner, Biology was relieved of another fragment of mysticism. The splitting up of sugar into CO_2 and alcohol is no more the effect of a "vital principle" than the splitting up of cane sugar by invertase. The history of this problem is instructive, as it warns us against considering problems as beyond our reach because they have not yet found their solution.

The development of methods of enzyme purification, the discovery and recognition of the importance of coenzymes such as NAD, and the discovery of the pivotal metabolic role of ATP and other phosphorylated compounds all came out of studies of glycolysis. The glycolytic enzymes of many species have long since been purified and thoroughly studied.

Glycolysis is an almost universal central pathway of glucose catabolism, the pathway with the largest flux of carbon in most cells. The glycolytic breakdown of glucose is the sole source of metabolic energy in some mammalian tissues and cell types (erythrocytes, renal medulla, brain, and sperm, for example). Some plant tissues that are modified to store starch (such as potato tubers) and some aquatic plants (watercress, for example) derive most of their energy from glycolysis; many anaerobic microorganisms are entirely dependent on glycolysis.

Fermentation is a general term for the *anaerobic* degradation of glucose or other organic nutrients to obtain energy, conserved as ATP. Because living organisms first arose in an atmosphere without oxygen, anaerobic breakdown of glucose is probably the most ancient biological mechanism for obtaining energy from organic fuel molecules. And as genome sequencing of a wide variety of organisms has revealed, some archaea and some parasitic microorganisms lack one or more of the enzymes of glycolysis but retain the core of the pathway; they presumably carry out variant forms of glycolysis. In the course of evolution, the chemistry of this reaction sequence has been completely conserved; the glycolytic enzymes of vertebrates are closely similar, in amino acid sequence and three-dimensional structure, to their homologs in yeast and spinach. Glycolysis differs among species only in the details of its regulation and in the subsequent metabolic fate of the pyruvate formed. The thermodynamic principles and the types of regulatory mechanisms that govern glycolysis are common to all pathways of cell metabolism. The glycolytic pathway, of central importance in itself, can also serve as a model for many aspects of the pathways discussed throughout this book.

Before examining each step of the pathway in some detail, we take a look at glycolysis as a whole.

An Overview: Glycolysis Has Two Phases

The breakdown of the six-carbon glucose into two molecules of the three-carbon pyruvate occurs in 10 steps, the first 5 of which constitute the *preparatory phase* **(Fig. 14–2a)**. In these reactions, glucose is first phosphorylated at the hydroxyl group on C-6 (step ❶). The D-glucose 6-phosphate thus formed is converted to D-fructose 6-phosphate (step ❷), which is again phosphorylated, this time at C-1, to yield D-fructose 1,6-bisphosphate (step ❸). For both phosphorylations, ATP is the phosphoryl group donor. As all sugar derivatives in glycolysis are the D isomers, we will usually omit the D designation except when emphasizing stereochemistry.

Fructose 1,6-bisphosphate is split to yield two three-carbon molecules, dihydroxyacetone phosphate and glyceraldehyde 3-phosphate (step ❹); this is the "lysis" step that gives the pathway its name. The dihydroxyacetone phosphate is isomerized to a second molecule of glyceraldehyde 3-phosphate (step ❺),

Hans Von Euler-Chelpin, 1873–1964

Gustav Embden, 1874–1933

Otto Meyerhof, 1884–1951

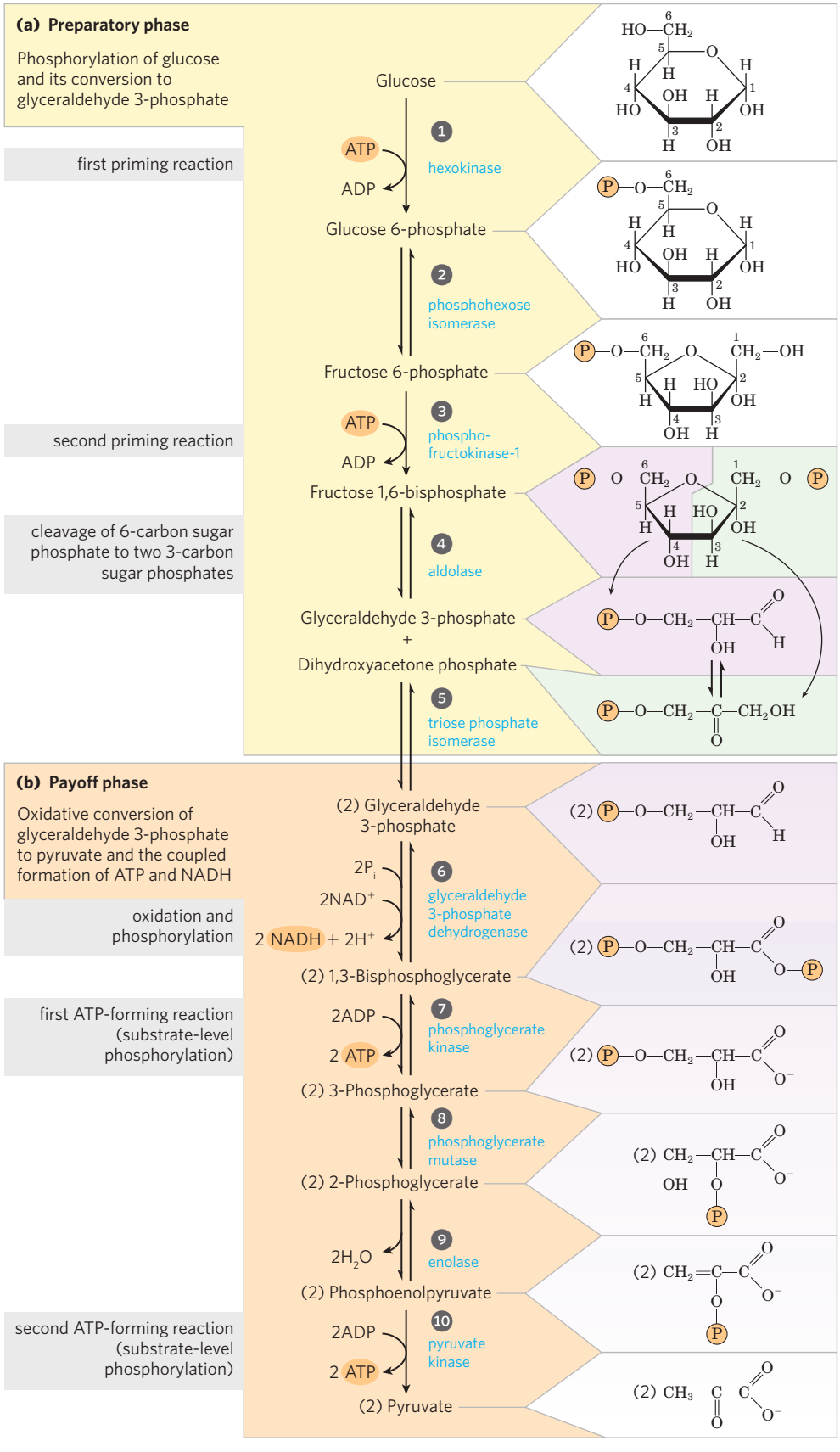

FIGURE 14–2 The two phases of glycolysis. For each molecule of glucose that passes through the preparatory phase **(a)**, two molecules of glyceraldehyde 3-phosphate are formed; both pass through the payoff phase **(b)**. Pyruvate is the end product of the second phase of glycolysis. For each glucose molecule, two ATP are consumed in the preparatory phase and four ATP are produced in the payoff phase, giving a net yield of two ATP per molecule of glucose converted to pyruvate. The numbered reaction steps correspond to the numbered headings in the text discussion. Keep in mind that each phosphoryl group, represented here as Ⓟ, has two negative charges ($-PO_3^{2-}$).

ending the first phase of glycolysis. Note that two molecules of ATP are invested before the cleavage of glucose into two three-carbon pieces; there will be a good return on this investment. To summarize: in the preparatory phase of glycolysis the energy of ATP is invested, raising the free-energy content of the intermediates, and the carbon chains of all the metabolized hexoses are converted to a common product, glyceraldehyde 3-phosphate.

The energy gain comes in the *payoff phase* of glycolysis (Fig. 14–2b). Each molecule of glyceraldehyde 3-phosphate is oxidized and phosphorylated by inorganic phosphate (*not* by ATP) to form 1,3-bisphosphoglycerate (step ❻). Energy is then released as the two molecules of 1,3-bisphosphoglycerate are converted to two molecules of pyruvate (steps ❼ through ❿). Much of this energy is conserved by the coupled phosphorylation of four molecules of ADP to ATP. The net yield is two molecules of ATP per molecule of glucose used, because two molecules of ATP were invested in the preparatory phase. Energy is also conserved in the payoff phase in the formation of two molecules of the electron carrier NADH per molecule of glucose.

In the sequential reactions of glycolysis, three types of chemical transformations are particularly noteworthy: (1) degradation of the carbon skeleton of glucose to yield pyruvate; (2) phosphorylation of ADP to ATP by compounds with high phosphoryl group transfer potential, formed during glycolysis; and (3) transfer of a hydride ion to NAD^+, forming NADH. The overall chemical logic of the pathway is described in **Figure 14–3**.

Fates of Pyruvate With the exception of some interesting variations in the bacterial realm, the pyruvate formed by glycolysis is further metabolized via one of three catabolic routes. In aerobic organisms or tissues, under aerobic conditions, glycolysis is only the first stage in the complete degradation of glucose **(Fig. 14–4)**. Pyruvate is oxidized, with loss of its carboxyl group as CO_2, to yield the acetyl group of acetyl-coenzyme A; the acetyl group is then oxidized completely to CO_2 by the citric acid cycle (Chapter 16). The electrons from these oxidations are passed to O_2 through a chain of carriers in mitochondria, to form H_2O. The energy from the electron-transfer reactions drives the synthesis of ATP in mitochondria (Chapter 19).

The second route for pyruvate is its reduction to lactate via **lactic acid fermentation**. When vigorously contracting skeletal muscle must function under low-oxygen conditions (**hypoxia**), NADH cannot be reoxidized to NAD^+, but NAD^+ is required as an electron acceptor for the further oxidation of pyruvate. Under these conditions pyruvate is reduced to lactate, accepting electrons from NADH and thereby regenerating the NAD^+ necessary for glycolysis to continue. Certain tissues and cell types (retina and erythrocytes, for example) convert glucose to lactate even under aerobic conditions, and lactate is also the product of glycolysis under anaerobic conditions in some microorganisms (Fig. 14–4).

The third major route of pyruvate catabolism leads to ethanol. In some plant tissues and in certain invertebrates, protists, and microorganisms such as brewer's or baker's yeast, pyruvate is converted under hypoxic or anaerobic conditions to ethanol and CO_2, a process called **ethanol (alcohol) fermentation** (Fig. 14–4).

The oxidation of pyruvate is an important catabolic process, but pyruvate has anabolic fates as well. It can, for example, provide the carbon skeleton for the synthesis of the amino acid alanine or for the synthesis of fatty acids. We return to these anabolic reactions of pyruvate in later chapters.

ATP and NADH Formation Coupled to Glycolysis During glycolysis some of the energy of the glucose molecule is conserved in ATP, while much remains in the product, pyruvate. The overall equation for glycolysis is

$$\text{Glucose} + 2NAD^+ + 2ADP + 2P_i \longrightarrow 2\ \text{pyruvate} + 2NADH + 2H^+ + 2ATP + 2H_2O \quad (14\text{–}1)$$

For each molecule of glucose degraded to pyruvate, two molecules of ATP are generated from ADP and P_i, and two molecules of NADH are produced by the reduction of NAD^+. The hydrogen acceptor in this reaction is NAD^+ (see Fig. 13–24), bound to a Rossmann fold as shown in Figure 13–25. The reduction of NAD^+ proceeds by the enzymatic transfer of a hydride ion ($:H^-$) from the aldehyde group of glyceraldehyde 3-phosphate to the nicotinamide ring of NAD^+, yielding the reduced coenzyme NADH. The other hydrogen atom of the substrate molecule is released to the solution as H^+.

We can now resolve the equation of glycolysis into two processes—the conversion of glucose to pyruvate, which is exergonic:

$$\text{Glucose} + 2NAD^+ \longrightarrow 2\ \text{pyruvate} + 2NADH + 2H^+ \quad (14\text{–}2)$$
$$\Delta G'^\circ_1 = -146\ \text{kJ/mol}$$

and the formation of ATP from ADP and P_i, which is endergonic:

$$2ADP + 2P_i \longrightarrow 2ATP + 2H_2O \quad (14\text{–}3)$$
$$\Delta G'^\circ_2 = 2(30.5\ \text{kJ/mol}) = 61.0\ \text{kJ/mol}$$

The sum of Equations 14–2 and 14–3 gives the overall standard free-energy change of glycolysis, $\Delta G'^\circ_s$:

$$\Delta G'^\circ_s = \Delta G'^\circ_1 + \Delta G'^\circ_2 = -146\ \text{kJ/mol} + 61.0\ \text{kJ/mol} = -85\ \text{kJ/mol}$$

Under standard conditions, and under the (nonstandard) conditions that prevail in a cell, glycolysis is an essentially irreversible process, driven to completion by a large net decrease in free energy.

Energy Remaining in Pyruvate Glycolysis releases only a small fraction of the total available energy of the glucose

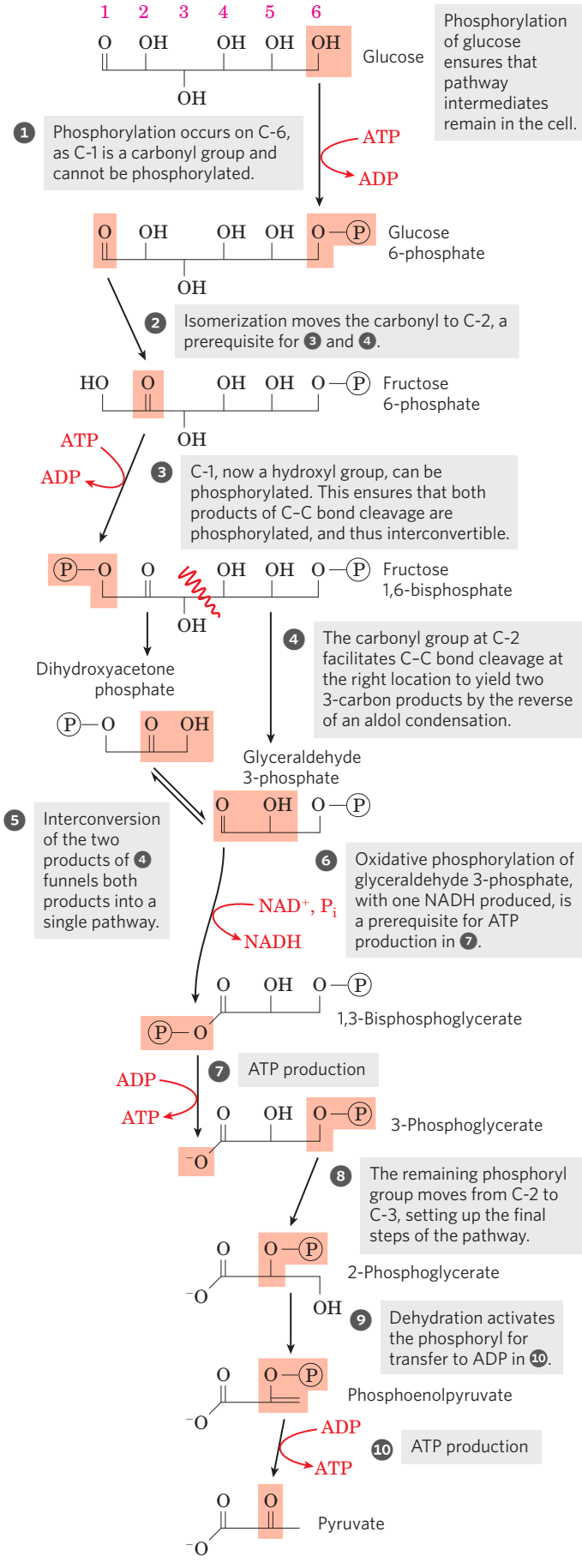

molecule; the two molecules of pyruvate formed by glycolysis still contain most of the chemical potential energy of glucose, energy that can be extracted by oxidative reactions in the citric acid cycle (Chapter 16) and oxidative phosphorylation (Chapter 19).

Importance of Phosphorylated Intermediates Each of the nine glycolytic intermediates between glucose and pyruvate is phosphorylated (Fig. 14–2). The phosphoryl groups seem to have three functions.

1. Because the plasma membrane generally lacks transporters for phosphorylated sugars, the phosphorylated glycolytic intermediates cannot leave the cell. After the initial phosphorylation, no further energy is necessary to retain phosphorylated intermediates in the cell, despite the large difference in their intracellular and extracellular concentrations.
2. Phosphoryl groups are essential components in the enzymatic conservation of metabolic energy. Energy released in the breakage of phosphoanhydride bonds (such as those in ATP) is partially conserved in the formation of phosphate esters such as glucose 6-phosphate. High-energy phosphate compounds formed in glycolysis (1,3-bisphosphoglycerate and phosphoenolpyruvate) donate phosphoryl groups to ADP to form ATP.
3. Binding energy resulting from the binding of phosphate groups to the active sites of enzymes lowers the activation energy and increases the specificity of the enzymatic reactions (Chapter 6). The phosphate groups of ADP, ATP, and the glycolytic intermediates form complexes with Mg^{2+}, and the substrate binding sites of many glycolytic enzymes are specific for these Mg^{2+} complexes. Most glycolytic enzymes require Mg^{2+} for activity.

FIGURE 14–3 The chemical logic of the glycolytic pathway. In this simplified version of the pathway, each molecule is shown in a linear form, with carbon and hydrogen atoms not depicted, in order to highlight chemical transformations. Remember that glucose and fructose are present mostly in their cyclized forms in solution, although they are transiently present in linear form at the active sites of some of the enzymes in this pathway.

The preparatory phase, steps 1 to 5, converts the six-carbon glucose into two three-carbon units, each of them phosphorylated. Oxidation of the three-carbon units is initiated in the payoff phase. To produce pyruvate, the chemical steps must occur in the order shown.

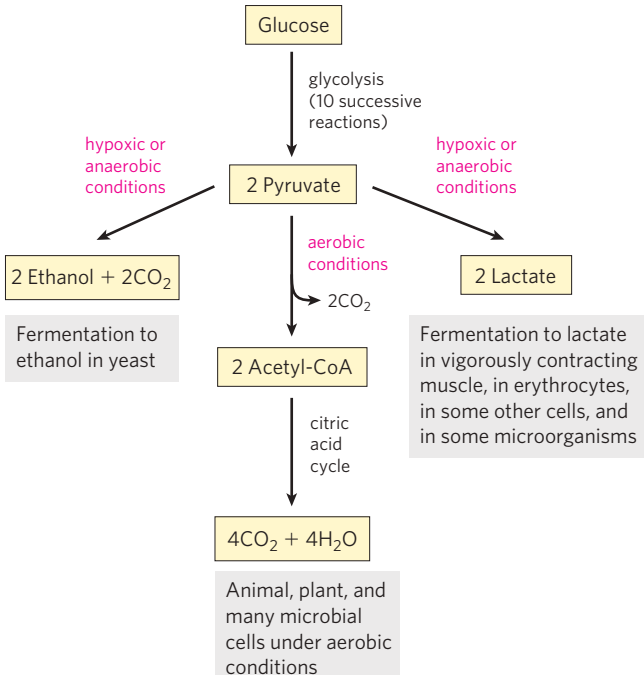

FIGURE 14–4 Three possible catabolic fates of the pyruvate formed in glycolysis. Pyruvate also serves as a precursor in many anabolic reactions, not shown here.

The Preparatory Phase of Glycolysis Requires ATP

In the preparatory phase of glycolysis, two molecules of ATP are invested and the hexose chain is cleaved into two triose phosphates. The realization that *phosphorylated* hexoses were intermediates in glycolysis came slowly and serendipitously. In 1906, Arthur Harden and William Young tested their hypothesis that inhibitors of proteolytic enzymes would stabilize the glucose-fermenting enzymes in yeast extract. They added blood serum (known to contain inhibitors of proteolytic enzymes) to yeast extracts and observed the predicted stimulation of glucose metabolism. However, in a control experiment intended to show that boiling the serum destroyed the stimulatory activity, they discovered that boiled serum was just as effective at stimulating glycolysis! Careful examination and testing of the contents of the boiled serum revealed that inorganic phosphate was responsible for the stimulation. Harden and Young soon discovered that glucose added to their yeast extract was converted to a hexose bisphosphate (the "Harden-Young ester," eventually identified as fructose 1,6-bisphosphate). This was the beginning of a long series of investigations on the role of organic esters and anhydrides of phosphate in biochemistry, which has led to our current understanding of the central role of phosphoryl group transfer in biology.

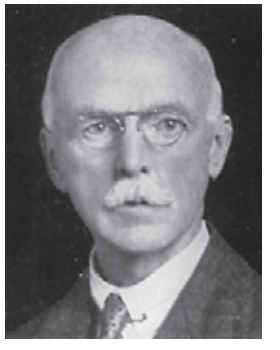
Arthur Harden, 1865–1940

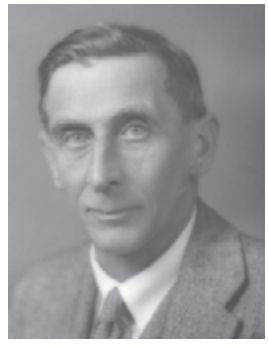
William Young, 1878–1942

1 Phosphorylation of Glucose In the first step of glycolysis, glucose is activated for subsequent reactions by its phosphorylation at C-6 to yield **glucose 6-phosphate**, with ATP as the phosphoryl donor:

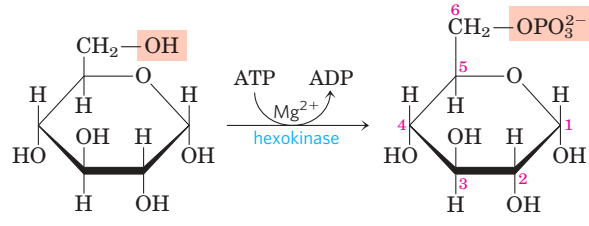

$\Delta G'^{\circ} = -16.7$ kJ/mol

This reaction, which is irreversible under intracellular conditions, is catalyzed by **hexokinase**. Recall that kinases are enzymes that catalyze the transfer of the terminal phosphoryl group from ATP to an acceptor nucleophile (see Fig. 13–20). Kinases are a subclass of transferases (see Table 6–3). The acceptor in the case of hexokinase is a hexose, normally D-glucose, although hexokinase also catalyzes the phosphorylation of other common hexoses, such as D-fructose and D-mannose, in some tissues.

Hexokinase, like many other kinases, requires Mg^{2+} for its activity, because the true substrate of the enzyme is not ATP^{4-} but the $MgATP^{2-}$ complex (see Fig. 13–12). Mg^{2+} shields the negative charges of the phosphoryl groups in ATP, making the terminal phosphorus atom an easier target for nucleophilic attack by an —OH of glucose. Hexokinase undergoes a profound change in shape, an induced fit, when it binds glucose; two domains of the protein move about 8 Å closer to each other when ATP binds (see Fig. 6–25). This movement brings bound ATP closer to a molecule of glucose also bound to the enzyme and blocks the access of water (from the solvent), which might otherwise enter the active site and attack (hydrolyze) the phosphoanhydride bonds of ATP. Like the other nine enzymes of glycolysis, hexokinase is a soluble, cytosolic protein.

Hexokinase is present in nearly all organisms. The human genome encodes four different hexokinases (I to IV), all of which catalyze the same reaction. Two or more enzymes that catalyze the same reaction but are encoded by different genes are called **isozymes** (see Box 15–2). One of the isozymes present in hepatocytes, hexokinase IV (also called glucokinase), differs from

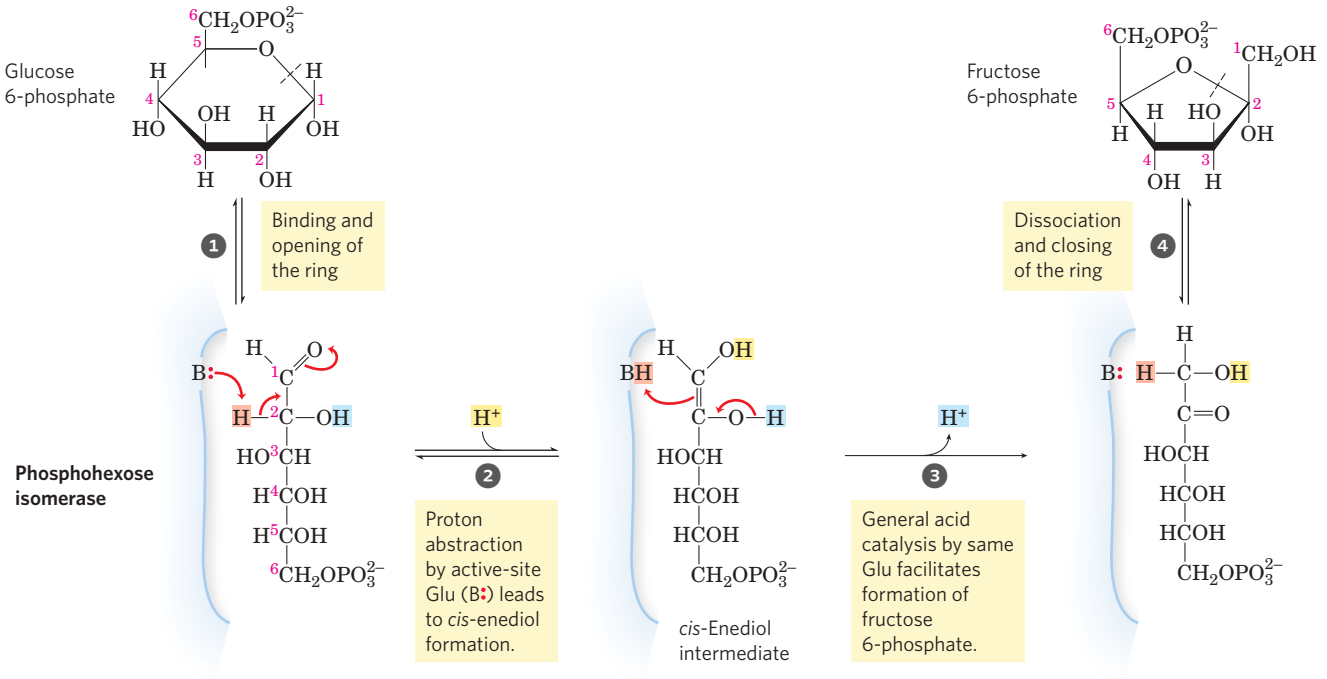

MECHANISM FIGURE 14–5 The phosphohexose isomerase reaction. The ring opening and closing reactions (steps 1 and 4) are catalyzed by an active-site His residue, by mechanisms omitted here for simplicity. The proton (light red) initially at C-2 is made more easily abstractable by electron withdrawal by the adjacent carbonyl and nearby hydroxyl groups. After its transfer from C-2 to the active-site Glu residue (a weak acid), the proton is freely exchanged with the surrounding solution; that is, the proton abstracted from C-2 in step 2 is not necessarily the same one that is added to C-1 in step 3.

Phosphohexose Isomerase Mechanism

other forms of hexokinase in kinetic and regulatory properties, with important physiological consequences that are described in Section 15.3.

2 Conversion of Glucose 6-Phosphate to Fructose 6-Phosphate The enzyme **phosphohexose isomerase** (**phosphoglucose isomerase**) catalyzes the reversible isomerization of glucose 6-phosphate, an aldose, to **fructose 6-phosphate**, a ketose:

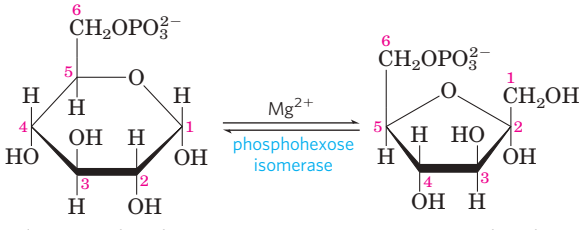

$\Delta G'^{\circ} = 1.7$ kJ/mol

The mechanism for this reaction involves an enediol intermediate **(Fig. 14–5)**. The reaction proceeds readily in either direction, as might be expected from the relatively small change in standard free energy.

3 Phosphorylation of Fructose 6-Phosphate to Fructose 1,6-Bisphosphate In the second of the two priming reactions of glycolysis, **phosphofructokinase-1 (PFK-1)** catalyzes the transfer of a phosphoryl group from ATP to fructose 6-phosphate to yield **fructose 1,6-bisphosphate**:

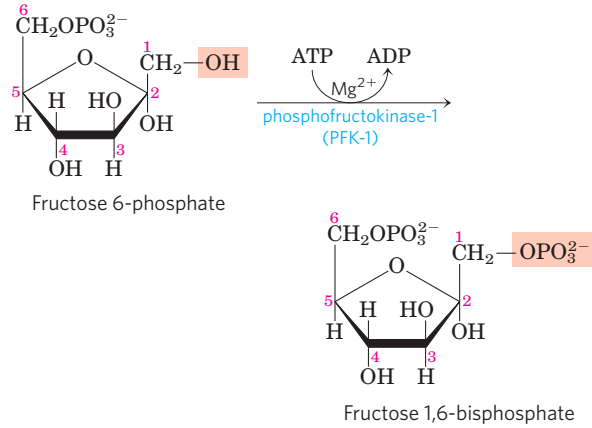

$\Delta G'^{\circ} = -14.2$ kJ/mol

KEY CONVENTION: Compounds that contain two phosphate or phosphoryl groups attached at different positions in the molecule are named *bisphosphates* (or *bisphospho* compounds); for example, fructose 1,6-bisphosphate and 1,3-bisphosphoglycerate. Compounds with two phosphates linked together as a pyrophosphoryl group are named *diphosphates*; for example, adenosine diphosphate (ADP). Similar rules apply for the naming of *trisphosphates* (such as inositol 1,4,5-trisphosphate; see p. 450) and *triphosphates* (such as adenosine triphosphate, ATP). ■

The enzyme that forms fructose 1,6-bisphosphate is called PFK-1 to distinguish it from a second enzyme (PFK-2) that catalyzes the formation of fructose 2,6-bisphosphate from fructose 6-phosphate in a separate pathway (the roles of PFK-2 and fructose 2,6-bisphosphate are discussed in Chapter 15). The PFK-1 reaction is essentially irreversible under cellular conditions, and it is the first "committed" step in the glycolytic pathway; glucose 6-phosphate and fructose 6-phosphate have other possible fates, but fructose 1,6-bisphosphate is targeted for glycolysis.

Some bacteria and protists and perhaps all plants have a phosphofructokinase that uses pyrophosphate (PP_i), not ATP, as the phosphoryl group donor in the synthesis of fructose 1,6-bisphosphate:

Fructose 6-phosphate + $\xrightarrow{Mg^{2+}}$ fructose 1,6-bisphosphate + P_i

$\Delta G'^\circ = -2.9$ kJ/mol

Phosphofructokinase-1 is subject to complex allosteric regulation; its activity is increased whenever the cell's ATP supply is depleted or when the ATP breakdown products, ADP and AMP (particularly the latter), accumulate. The enzyme is inhibited whenever the cell has ample ATP and is well supplied by other fuels such as fatty acids. In some organisms, fructose 2,6-bisphosphate (not to be confused with the PFK-1 reaction product, fructose 1,6-bisphosphate) is a potent allosteric activator of PFK-1. Ribulose 5-phosphate, an intermediate in the pentose phosphate pathway discussed later in this chapter, also activates phosphofructokinase indirectly. The multiple layers of regulation of this step in glycolysis are discussed in greater detail in Chapter 15.

❹ Cleavage of Fructose 1,6-Bisphosphate The enzyme **fructose 1,6-bisphosphate aldolase**, often called simply **aldolase**, catalyzes a reversible aldol condensation (see Fig. 13–4). Fructose 1,6-bisphosphate is cleaved to yield two different triose phosphates, **glyceraldehyde 3-phosphate**, an aldose, and **dihydroxyacetone phosphate**, a ketose:

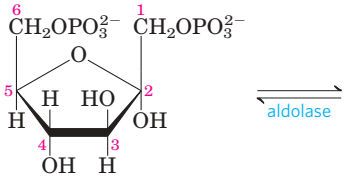

Fructose 1,6-bisphosphate

aldolase

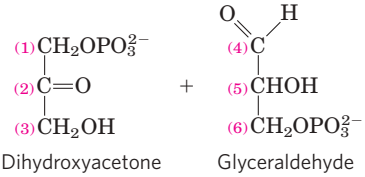

Dihydroxyacetone phosphate

Glyceraldehyde 3-phosphate

$\Delta G'^\circ = 23.8$ kJ/mol

There are two classes of aldolases. Class I aldolases, found in animals and plants, use the mechanism shown in **Figure 14–6**. Class II enzymes, in fungi and bacteria, do not form the Schiff base intermediate. Instead, a zinc ion at the active site is coordinated with the carbonyl oxygen at C-2; the Zn^{2+} polarizes the carbonyl group and stabilizes the enolate intermediate created in the C—C bond cleavage step (see Fig. 6–17).

Although the aldolase reaction has a strongly positive standard free-energy change in the direction of fructose 1,6-bisphosphate cleavage, at the lower concentrations of reactants present in cells the actual free-energy change is small and the aldolase reaction is readily reversible. We shall see later that aldolase acts in the reverse direction during the process of gluconeogenesis (see Fig. 14–17).

❺ Interconversion of the Triose Phosphates Only one of the two triose phosphates formed by aldolase, glyceraldehyde 3-phosphate, can be directly degraded in the subsequent steps of glycolysis. The other product, dihydroxyacetone phosphate, is rapidly and reversibly converted to glyceraldehyde 3-phosphate by the fifth enzyme of the glycolytic sequence, **triose phosphate isomerase**:

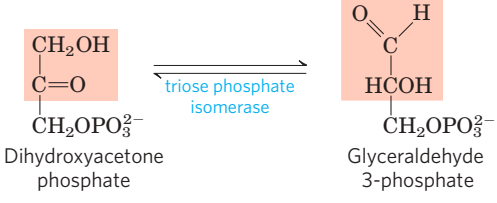

Dihydroxyacetone phosphate

Glyceraldehyde 3-phosphate

$\Delta G'^\circ = 7.5$ kJ/mol

The reaction mechanism is similar to the reaction promoted by phosphohexose isomerase in step ❷ of glycolysis (Fig. 14–5). After the triose phosphate isomerase reaction, the carbon atoms derived from C-1, C-2, and C-3 of the starting glucose are chemically indistinguishable from C-6, C-5, and C-4, respectively **(Fig. 14–7)**; the two "halves" of glucose have both yielded glyceraldehyde 3-phosphate.

This reaction completes the preparatory phase of glycolysis. The hexose molecule has been phosphorylated at C-1 and C-6 and then cleaved to form two molecules of glyceraldehyde 3-phosphate.

The Payoff Phase of Glycolysis Yields ATP and NADH

The payoff phase of glycolysis (Fig. 14–2b) includes the energy-conserving phosphorylation steps in which some of the chemical energy of the glucose molecule is conserved in the form of ATP and NADH. Remember that one molecule of glucose yields two molecules of glyceraldehyde 3-phosphate, and both halves of the

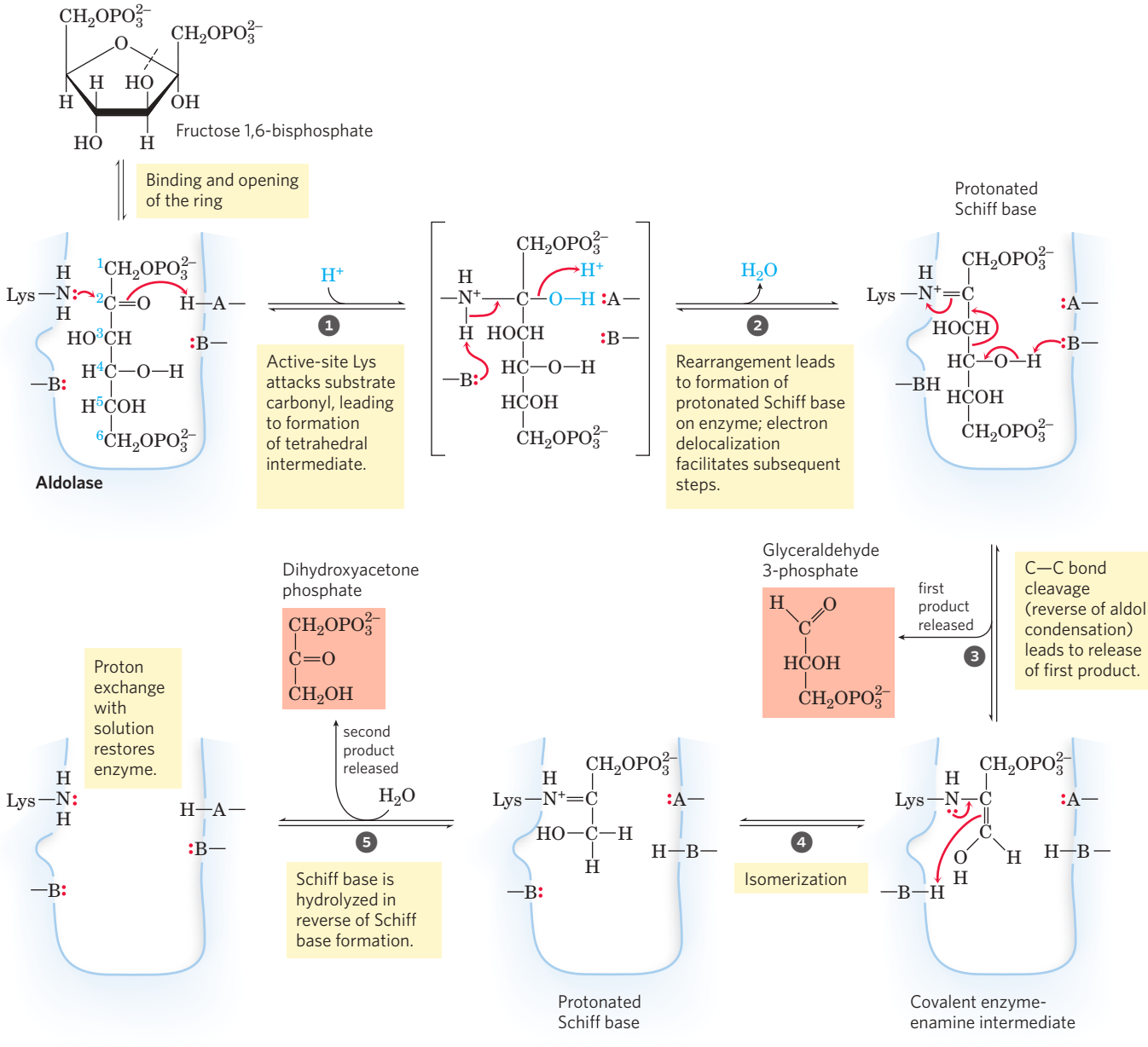

MECHANISM FIGURE 14–6 The class I aldolase reaction. The reaction shown here is the reverse of an aldol condensation. Note that cleavage between C-3 and C-4 depends on the presence of the carbonyl group at C-2, which is converted to an imine on the enzyme. A and B represent amino acid residues that serve as general acid (A) or base (B).

glucose molecule follow the same pathway in the second phase of glycolysis. The conversion of two molecules of glyceraldehyde 3-phosphate to two molecules of pyruvate is accompanied by the formation of four molecules of ATP from ADP. However, the net yield of ATP per molecule of glucose degraded is only two, because two ATP were invested in the preparatory phase of glycolysis to phosphorylate the two ends of the hexose molecule.

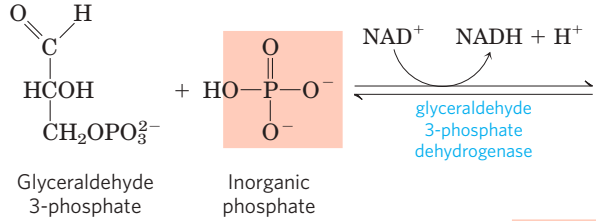

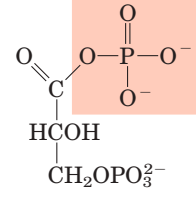

6 Oxidation of Glyceraldehyde 3-Phosphate to 1,3-Bisphosphoglycerate The first step in the payoff phase is the oxidation of glyceraldehyde 3-phosphate to **1,3-bisphosphoglycerate**, catalyzed by **glyceraldehyde 3-phosphate dehydrogenase**:

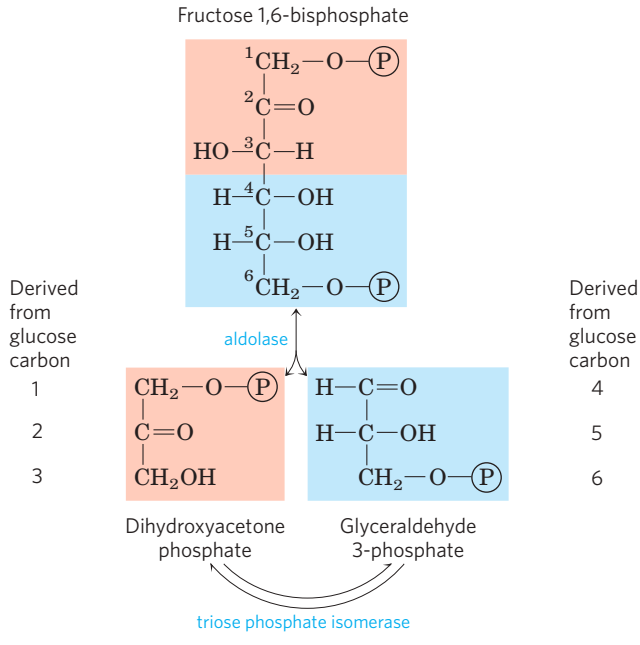

FIGURE 14–7 Fate of the glucose carbons in the formation of glyceraldehyde 3-phosphate. (a) The origin of the carbons in the two three-carbon products of the aldolase and triose phosphate isomerase reactions. The end product of the two reactions is glyceraldehyde 3-phosphate (two molecules). **(b)** Each carbon of glyceraldehyde 3-phosphate is derived from either of two specific carbons of glucose. Note that the numbering of the carbon atoms of glyceraldehyde 3-phosphate differs from that of the glucose from which it is derived. In glyceraldehyde 3-phosphate, the most complex functional group (the carbonyl) is specified as C-1. This numbering change is important for interpreting experiments with glucose in which a single carbon is labeled with a radioisotope. (See Problems 6 and 9 at the end of this chapter.)

This is the first of the two energy-conserving reactions of glycolysis that eventually lead to the formation of ATP. The aldehyde group of glyceraldehyde 3-phosphate is oxidized, not to a free carboxyl group but to a carboxylic acid anhydride with phosphoric acid. This type of anhydride, called an **acyl phosphate**, has a very high standard free energy of hydrolysis ($\Delta G'^\circ = -49.3$ kJ/mol; see Fig. 13–14, Table 13–6). Much of the free energy of oxidation of the aldehyde group of glyceraldehyde 3-phosphate is conserved by formation of the acyl phosphate group at C-1 of 1,3-bisphosphoglycerate.

Glyceraldehyde 3-phosphate is covalently bound to the dehydrogenase during the reaction **(Fig. 14–8)**. The aldehyde group of glyceraldehyde 3-phosphate reacts with the —SH group of an essential Cys residue in the active site, in a reaction analogous to the formation of a hemiacetal (see Fig. 7–5), in this case producing a *thio*-hemiacetal. Reaction of the essential Cys residue with a heavy metal such as Hg^{2+} irreversibly inhibits the enzyme.

The amount of NAD^+ in a cell ($\leq 10^{-5}$ M) is far smaller than the amount of glucose metabolized in a few minutes. Glycolysis would soon come to a halt if the NADH formed in this step of glycolysis were not continuously reoxidized and recycled. We return to a discussion of this recycling of NAD^+ later in the chapter.

❼ Phosphoryl Transfer from 1,3-Bisphosphoglycerate to ADP The enzyme **phosphoglycerate kinase** transfers the high-energy phosphoryl group from the carboxyl group of 1,3-bisphosphoglycerate to ADP, forming ATP and **3-phosphoglycerate**:

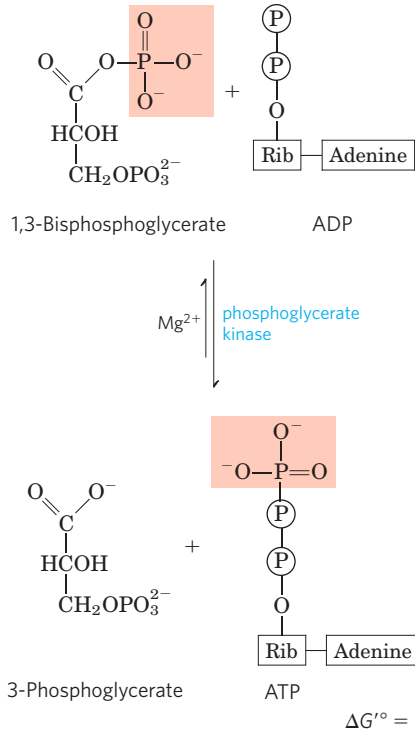

Notice that phosphoglycerate kinase is named for the reverse reaction, in which it transfers a phosphoryl

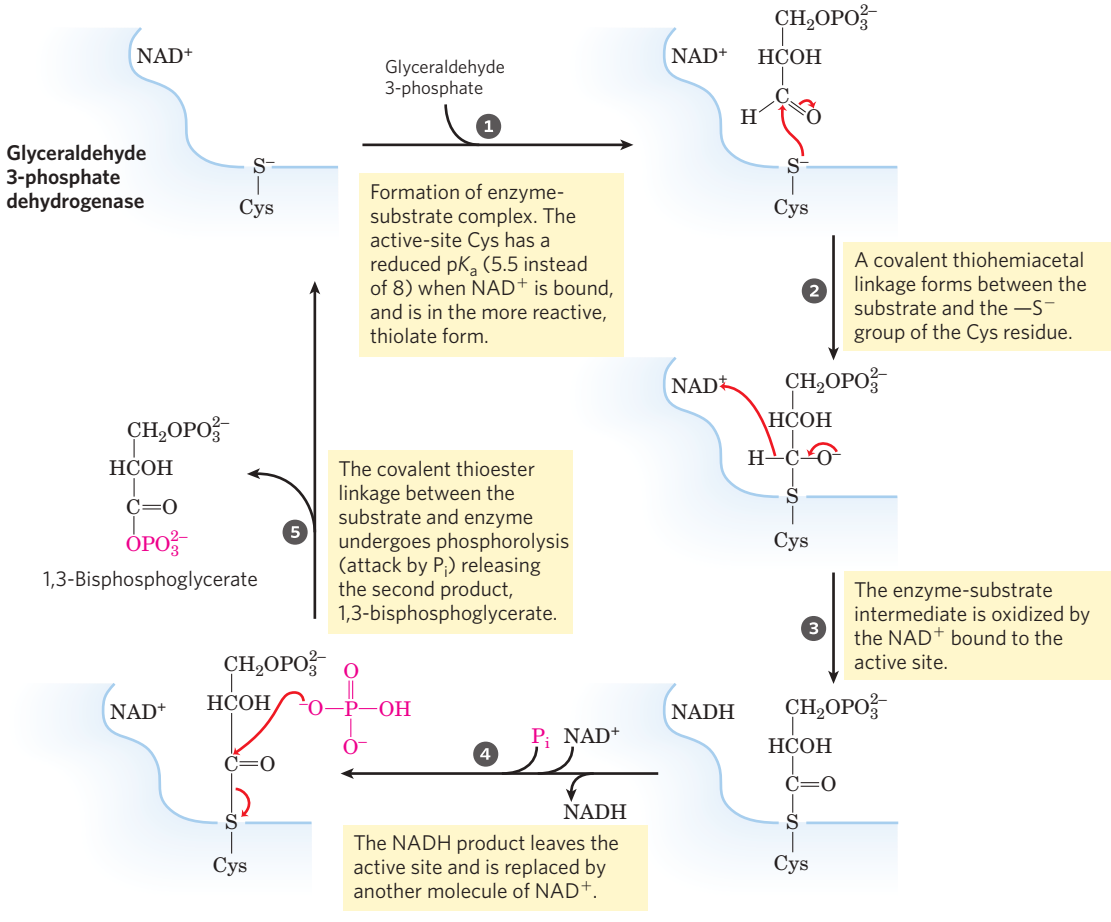

MECHANISM FIGURE 14–8 **The glyceraldehyde 3-phosphate dehydrogenase reaction.**

group from ATP to 3-phosphoglycerate. Like all enzymes, it catalyzes the reaction in both directions. This enzyme acts in the direction suggested by its name during gluconeogenesis (see Fig. 14–17) and during photosynthetic CO_2 assimilation (see Fig. 20–4). In glycolysis, the reaction it catalyzes proceeds as shown above, in the direction of ATP synthesis.

Steps 6 and 7 of glycolysis together constitute an energy-coupling process in which 1,3-bisphosphoglycerate is the common intermediate; it is formed in the first reaction (which would be endergonic in isolation), and its acyl phosphate group is transferred to ADP in the second reaction (which is strongly exergonic). The sum of these two reactions is

$$\text{Glyceraldehyde 3-phosphate} + \text{ADP} + \text{P}_\text{i} + \text{NAD}^+ \rightleftharpoons \text{3-phosphoglycerate} + \text{ATP} + \text{NADH} + \text{H}^+$$
$$\Delta G'^\circ = -12.2 \text{ kJ/mol}$$

Thus the overall reaction is exergonic.

Recall from Chapter 13 that the actual free-energy change, ΔG, is determined by the standard free-energy change, $\Delta G'^\circ$, and the mass-action ratio, Q, which is the ratio [products]/[reactants] (see Eqn 13–4). For step 6

$$\Delta G = \Delta G'^\circ + RT \ln Q$$
$$= \Delta G'^\circ + RT \ln \frac{[\text{1,3-bisphosphoglycerate}][\text{NADH}]}{[\text{glyceraldehyde 3-phosphate}][\text{P}_\text{i}][\text{NAD}^+]}$$

Notice that $[H^+]$ is not included in Q. In biochemical calculations, $[H^+]$ is assumed to be a constant (10^{-7} M), and this constant is included in the definition of $\Delta G'^\circ$ (p. 507).

When the mass-action ratio is less than 1.0, its natural logarithm has a negative sign. In the cytosol, where these reactions are taking place, the ratio [NADH]/[NAD^+] is a small fraction, contributing to a low Q. Step 7, by consuming the product of step 6 (1,3-bisphosphoglycerate), keeps [1,3-bisphosphoglycerate] relatively low in the steady state and thereby keeps Q for the overall energy-coupling process small. When Q is small, the contribution of ln Q can make ΔG strongly negative. This is simply another way of showing how the two reactions, steps 6 and 7, are coupled through a common intermediate.

The outcome of these coupled reactions, both reversible under cellular conditions, is that the energy released on oxidation of an aldehyde to a carboxylate group is conserved by the coupled formation of ATP from ADP and P_i. The formation of ATP by phosphoryl group transfer from a substrate such as 1,3-bisphosphoglycerate is referred to as a **substrate-level phosphorylation**, to distinguish this mechanism from **respiration-linked phosphorylation**. Substrate-level phosphorylations involve soluble enzymes and chemical intermediates (1,3-bisphosphoglycerate in this case). Respiration-linked phosphorylations, on the other hand,

involve membrane-bound enzymes and transmembrane gradients of protons (Chapter 19).

8 Conversion of 3-Phosphoglycerate to 2-Phosphoglycerate The enzyme **phosphoglycerate mutase** catalyzes a reversible shift of the phosphoryl group between C-2 and C-3 of glycerate; Mg^{2+} is essential for this reaction:

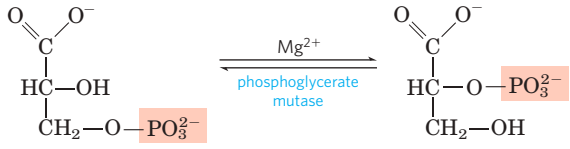

3-Phosphoglycerate 2-Phosphoglycerate

$\Delta G'^\circ = 4.4$ kJ/mol

The reaction occurs in two steps **(Fig. 14–9)**. A phosphoryl group initially attached to a His residue of the mutase is transferred to the hydroxyl group at C-2 of 3-phosphoglycerate, forming 2,3-bisphosphoglycerate (2,3-BPG). The phosphoryl group at C-3 of 2,3-BPG is then transferred to the same His residue, producing 2-phosphoglycerate and regenerating the phosphorylated enzyme. Phosphoglycerate mutase is initially phosphorylated by phosphoryl transfer from 2,3-BPG, which is required in small quantities to initiate the catalytic cycle and is continuously regenerated by that cycle.

9 Dehydration of 2-Phosphoglycerate to Phosphoenolpyruvate In the second glycolytic reaction that generates a compound with high phosphoryl group transfer potential (the first was step 6), **enolase** promotes reversible removal of a molecule of water from 2-phosphoglycerate to yield **phosphoenolpyruvate (PEP)**:

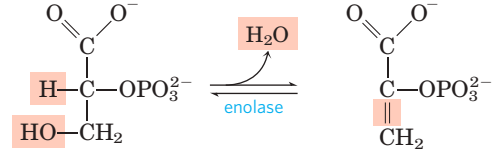

2-Phosphoglycerate Phosphoenolpyruvate

$\Delta G'^\circ = 7.5$ kJ/mol

The mechanism of the enolase reaction involves an enolic intermediate stabilized by Mg^{2+} (see Fig. 6–26). The reaction converts a compound with a relatively low phosphoryl group transfer potential ($\Delta G'^\circ$ for hydrolysis of 2-phosphoglycerate is −17.6 kJ/mol) to one with high phosphoryl group transfer potential ($\Delta G'^\circ$ for PEP hydrolysis is −61.9 kJ/mol) (see Fig. 13–13, Table 13–6).

10 Transfer of the Phosphoryl Group from Phosphoenolpyruvate to ADP The last step in glycolysis is the transfer of the phosphoryl group from phosphoenolpyruvate to ADP, catalyzed by **pyruvate kinase**, which requires K^+ and either Mg^{2+} or Mn^{2+}:

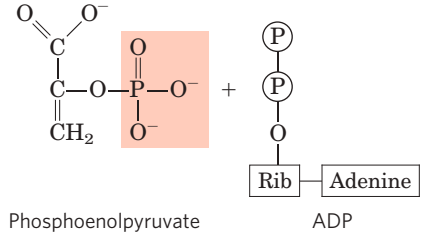

Phosphoenolpyruvate ADP

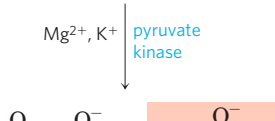

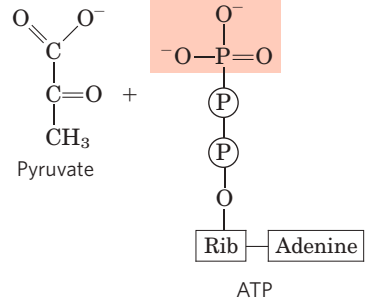

Pyruvate ATP

$\Delta G'^\circ = -31.4$ kJ/mol

MECHANISM FIGURE 14–9 **The phosphoglycerate mutase reaction.**

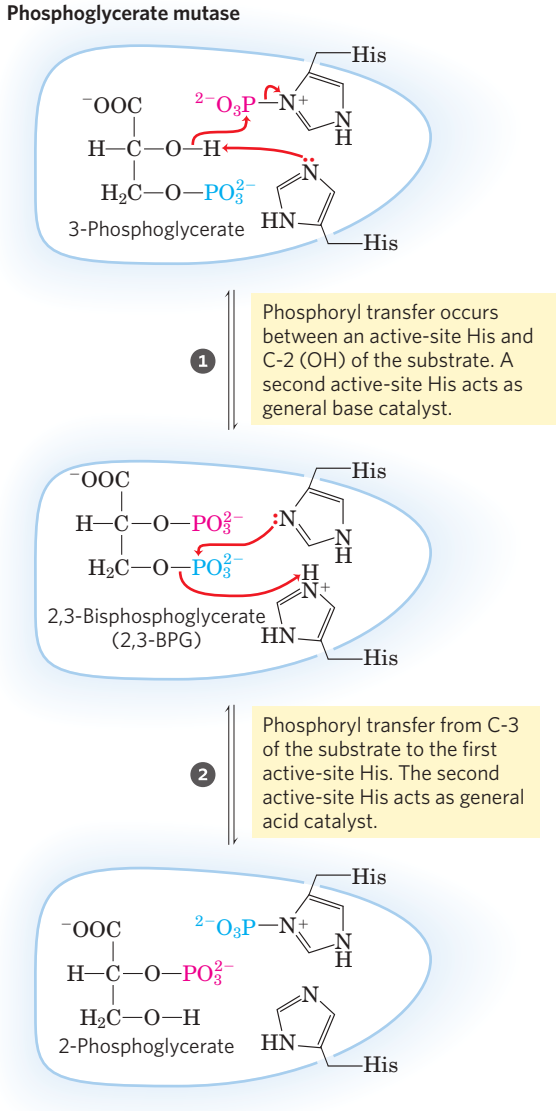

In this substrate-level phosphorylation, the product **pyruvate** first appears in its enol form, then tautomerizes rapidly and nonenzymatically to its keto form, which predominates at pH 7:

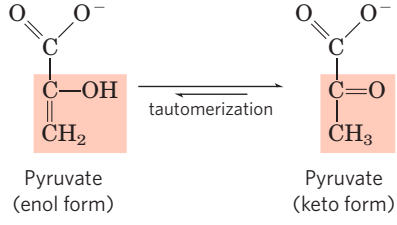

The overall reaction has a large, negative standard free-energy change, due in large part to the spontaneous conversion of the enol form of pyruvate to the keto form (see Fig. 13–13). About half of the energy released by PEP hydrolysis ($\Delta G'^{\circ} = -61.9$ kJ/mol) is conserved in the formation of the phosphoanhydride bond of ATP ($\Delta G'^{\circ} = -30.5$ kJ/mol), and the rest (−31.4 kJ/mol) constitutes a large driving force pushing the reaction toward ATP synthesis. We discuss the regulation of pyruvate kinase in Chapter 15.

The Overall Balance Sheet Shows a Net Gain of ATP

We can now construct a balance sheet for glycolysis to account for (1) the fate of the carbon skeleton of glucose, (2) the input of P_i and ADP and output of ATP, and (3) the pathway of electrons in the oxidation-reduction reactions. The left-hand side of the following equation shows all the inputs of ATP, NAD^+, ADP, and P_i (consult Fig. 14–2), and the right-hand side shows all the outputs (keep in mind that each molecule of glucose yields two molecules of pyruvate):

$$\text{Glucose} + 2\text{ATP} + 2\text{NAD}^+ + 4\text{ADP} + 2\text{P}_i \longrightarrow 2\text{ pyruvate} + 2\text{ADP} + 2\text{NADH} + 2\text{H}^+ + 4\text{ATP} + 2\text{H}_2\text{O}$$

Canceling out common terms on both sides of the equation gives the overall equation for glycolysis under aerobic conditions:

$$\text{Glucose} + 2\text{NAD}^+ + 2\text{ADP} + 2\text{P}_i \longrightarrow 2\text{ pyruvate} + 2\text{NADH} + 2\text{H}^+ + 2\text{ATP} + 2\text{H}_2\text{O}$$

The two molecules of NADH formed by glycolysis in the cytosol are, under aerobic conditions, reoxidized to NAD^+ by transfer of their electrons to the electron-transfer chain, which in eukaryotic cells is located in the mitochondria. The electron-transfer chain passes these electrons to their ultimate destination, O_2:

$$2\text{NADH} + 2\text{H}^+ + \text{O}_2 \longrightarrow 2\text{NAD}^+ + 2\text{H}_2\text{O}$$

Electron transfer from NADH to O_2 in mitochondria provides the energy for synthesis of ATP by respiration-linked phosphorylation (Chapter 19).

In the overall glycolytic process, one molecule of glucose is converted to two molecules of pyruvate (the pathway of carbon). Two molecules of ADP and two of P_i are converted to two molecules of ATP (the pathway of phosphoryl groups). Four electrons, as two hydride ions, are transferred from two molecules of glyceraldehyde 3-phosphate to two of NAD^+ (the pathway of electrons).

Glycolysis Is under Tight Regulation

During his studies on the fermentation of glucose by yeast, Louis Pasteur discovered that both the rate and the total amount of glucose consumption were many times greater under anaerobic than aerobic conditions. Later studies of muscle showed the same large difference in the rates of anaerobic and aerobic glycolysis. The biochemical basis of this "Pasteur effect" is now clear. The ATP yield from glycolysis under anaerobic conditions (2 ATP per molecule of glucose) is much smaller than that from the complete oxidation of glucose to CO_2 under aerobic conditions (30 or 32 ATP per glucose; see Table 19–5). About 15 times as much glucose must therefore be consumed anaerobically as aerobically to yield the same amount of ATP.

The flux of glucose through the glycolytic pathway is regulated to maintain nearly constant ATP levels (as well as adequate supplies of glycolytic intermediates that serve biosynthetic roles). The required adjustment in the rate of glycolysis is achieved by a complex interplay among ATP consumption, NADH regeneration, and allosteric regulation of several glycolytic enzymes—including hexokinase, PFK-1, and pyruvate kinase—and by second-to-second fluctuations in the concentration of key metabolites that reflect the cellular balance between ATP production and consumption. On a slightly longer time scale, glycolysis is regulated by the hormones glucagon, epinephrine, and insulin, and by changes in the expression of the genes for several glycolytic enzymes. An especially interesting case of abnormal regulation of glycolysis is seen in cancer. The German biochemist Otto Warburg first observed in 1928 that tumors of nearly all types carry out glycolysis at a much higher rate than normal tissue, *even when oxygen is available*. This "Warburg effect" is the basis for several methods of detecting and treating cancer (Box 14–1).

Warburg is generally considered the preeminent biochemist of the first half of the twentieth century. He made seminal contributions to many other areas of biochemistry, including respiration, photosynthesis, and the enzymology of intermediary metabolism. Beginning in 1930, Warburg and his associates purified and crystallized seven of the enzymes of glycolysis. They developed an experimental tool that revolutionized biochemical studies of oxidative metabolism: the Warburg manometer, which directly measured the oxygen consumption of tissues by monitoring changes in gas volume, and thus allowed quantitative measurement of any enzyme with oxidase activity.


Otto Warburg, 1883–1970

BOX 14–1 MEDICINE High Rate of Glycolysis in Tumors Suggests Targets for Chemotherapy and Facilitates Diagnosis

In many types of tumors found in humans and other animals, glucose uptake and glycolysis proceed about 10 times faster than in normal, noncancerous tissues. Most tumor cells grow under hypoxic conditions (i.e., with limited oxygen supply) because, at least initially, they lack the capillary network to supply sufficient oxygen. Cancer cells located more than 100 to 200 μm from the nearest capillaries must depend on glycolysis alone (without further oxidation of pyruvate) for much of their ATP production. The energy yield (2 ATP per glucose) is far lower than can be obtained by the complete oxidation of pyruvate to CO_2 in mitochondria (about 30 ATP per glucose; Chapter 19). So, to make the same amount of ATP, tumor cells must take up much more glucose than do normal cells, converting it to pyruvate and then to lactate as they recycle NADH. It is likely that two early steps in the transformation of a normal cell into a tumor cell are (1) the change to dependence on glycolysis for ATP production, and (2) the development of tolerance to a low pH in the extracellular fluid (caused by release of the end product of glycolysis, lactic acid). In general, the more aggressive the tumor, the greater is its rate of glycolysis.

This increase in glycolysis is achieved at least in part by increased synthesis of the glycolytic enzymes and of the plasma membrane transporters GLUT1 and GLUT3 (see Table 11–3) that carry glucose into cells. (Recall that GLUT1 and GLUT3 are not dependent on insulin.) The **hypoxia-inducible transcription factor (HIF-1)** is a protein that acts at the level of mRNA synthesis to stimulate the production of at least eight glycolytic enzymes and the glucose transporters when oxygen supply is limited (Fig. 1). With the resulting high rate of glycolysis, the tumor cell can survive anaerobic conditions until the supply of blood vessels has caught up with tumor growth. Another protein induced by HIF-1 is the peptide hormone VEGF (vascular endothelial growth factor), which stimulates the outgrowth of blood vessels (angiogenesis) toward the tumor.

There is also evidence that the tumor suppressor protein p53, which is mutated in most types of cancer (see Section 12.12), controls the synthesis and assembly of mitochondrial proteins essential to the passage of electrons to O_2. Cells with mutant p53 are defective in mitochondrial electron transport and are forced to rely more heavily on glycolysis for ATP production (Fig. 1).

This heavier reliance of tumors than of normal tissue on glycolysis suggests a possibility for anticancer therapy: inhibitors of glycolysis might target and kill tumors by depleting their supply of ATP. Three inhibitors of hexokinase have shown promise as chemotherapeutic agents: 2-deoxyglucose, lonidamine, and 3-bromopyruvate. By preventing the formation

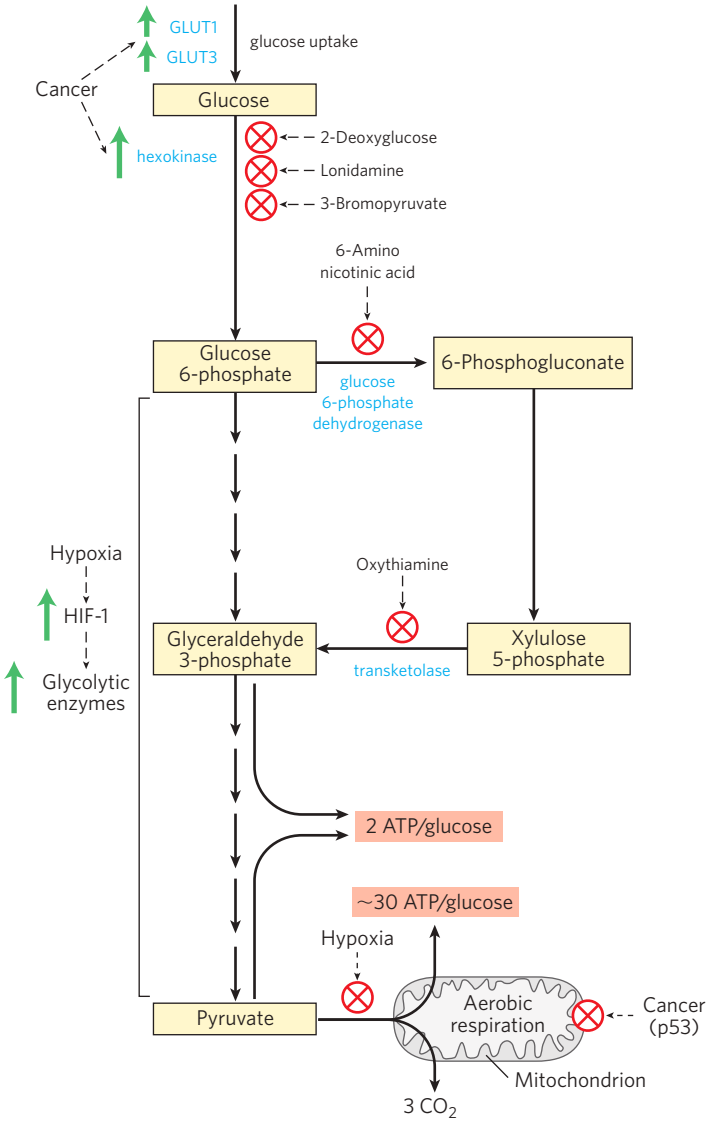

FIGURE 1 The anaerobic metabolism of glucose in tumor cells yields far less ATP (2 per glucose) than the complete oxidation to CO_2 that takes place in healthy cells under aerobic conditions (~30 ATP per glucose), so a tumor cell must consume much more glucose to produce the same amount of ATP. Glucose transporters and most of the glycolytic enzymes are overproduced in tumors. Compounds that inhibit hexokinase, glucose 6-phosphate dehydrogenase, or transketolase block ATP production by glycolysis, thus depriving the cancer cell of energy and killing it.

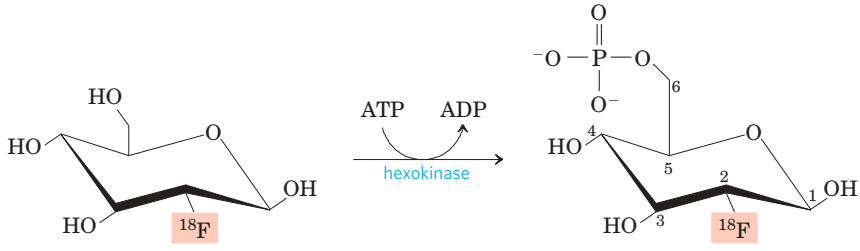

[^{18}F]2-Fluoro-2-deoxyglucose (FdG)

[^{18}F]6-Phospho-2-fluoro-2-deoxyglucose (6-Phospho-FdG)

FIGURE 2 Phosphorylation of ^{18}F-labeled 2-fluoro-2-deoxyglucose by hexokinase traps the FdG in cells (as 6-phospho-FdG), where its presence can be detected by positron emission from ^{18}F.

of glucose 6-phosphate, these compounds not only deprive tumor cells of glycolytically produced ATP but also prevent the formation of pentose phosphates via the pentose phosphate pathway, which also begins with glucose 6-phosphate. Without pentose phosphates, a cell cannot synthesize the nucleotides essential to DNA and RNA synthesis and thus cannot grow or divide. Another anticancer drug already approved for clinical use is imatinib (Gleevec), described in Box 12–5. It inhibits a specific tyrosine kinase, preventing the increased synthesis of hexokinase normally triggered by that kinase. The thiamine analog oxythiamine, which blocks the action of a transketolase-like enzyme that converts xylulose 5-phosphate to glyceraldehyde 3-phosphate (Fig. 1), is in preclinical trials as an antitumor drug.

The high glycolytic rate in tumor cells also has diagnostic usefulness. The relative rates at which tissues take up glucose can be used in some cases to pinpoint the location of tumors. In positron emission tomography (PET), individuals are injected with a harmless, isotopically labeled glucose analog that is taken up but not metabolized by tissues. The labeled compound is 2-fluoro-2-deoxyglucose (FdG), in which the hydroxyl group at the C-2 of glucose is replaced with ^{18}F (Fig. 2). This compound is taken up via GLUT transporters and is a good substrate for hexokinase, but it cannot be converted to the enediol intermediate in the phosphohexose isomerase reaction (see Fig. 14–5) and therefore accumulates as 6-phospho-FdG. The extent of its accumulation depends on its rate of uptake and phosphorylation, which as noted above is typically 10 or more times higher in tumors than in normal tissue. Decay of ^{18}F yields positrons (two per ^{18}F atom) that can be detected by a series of sensitive detectors positioned around the body, which allows accurate localization of accumulated 6-phospho-FdG (Fig. 3).

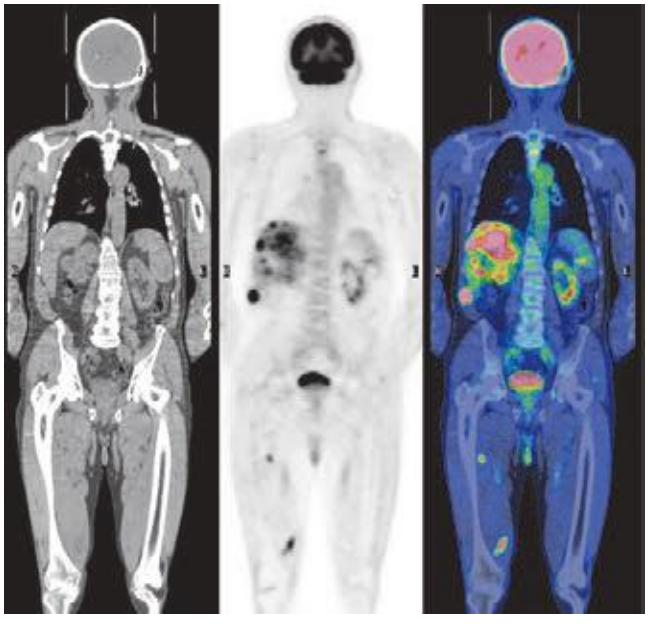

FIGURE 3 Detection of cancerous tissue by positron emission tomography (PET). The adult male patient had undergone surgical removal of a primary skin cancer (malignant melanoma). The image on the left, obtained by whole-body computed tomography (CT scan), shows the location of the soft tissues and bones. The central panel is a PET scan after the patient had ingested ^{18}F-labeled 2-fluoro-2-deoxyglucose (FdG). Dark spots indicate regions of high glucose utilization. As expected, the brain and bladder are heavily labeled—the brain because it uses most of the glucose consumed in the body, and the bladder because the ^{18}F-labeled 6-phospho-FdG is excreted in the urine. When the intensity of the label in the PET scan is translated into false color (the intensity increases from green to yellow to red) and the image is superimposed on the CT scan, the fused image (right) reveals cancer in the bones of the upper spine, in the liver, and in some regions of muscle, all the result of cancer spreading from the primary malignant melanoma.

Trained in carbohydrate chemistry in the laboratory of the great Emil Fischer (who won the Nobel Prize in Chemistry in 1902), Warburg himself won the Nobel Prize in Physiology or Medicine in 1931. Several of Warburg's students and colleagues also were awarded Nobel Prizes: Otto Meyerhof in 1922, Hans Krebs and Fritz Lipmann in 1953, and Hugo Theorell in 1955. Meyerhof's laboratory provided training for Lipmann, and for several other Nobel Prize winners: Severo Ochoa (1959), Andre Lwoff (1965), and George Wald (1967).

Glucose Uptake Is Deficient in Type 1 Diabetes Mellitus

The metabolism of glucose in mammals is limited by the rate of glucose uptake into cells and its phosphorylation by hexokinase. Glucose uptake from the blood is mediated by the GLUT family of glucose transporters (see Table 11–3). The transporters of hepatocytes (GLUT1, GLUT2) and of brain neurons (GLUT3) are always present in plasma membranes. In contrast, the main glucose transporter in the cells of skeletal muscle, cardiac muscle, and adipose tissue (GLUT4) is sequestered in small intracellular vesicles and moves into the plasma membrane only in response to an insulin signal **(Fig. 14–10)**. We discussed this insulin signaling mechanism in Chapter 12 (see Fig. 12–16). Thus in skeletal muscle, heart, and adipose tissue, glucose uptake and metabolism depend on the normal release of insulin by pancreatic β cells in response to elevated blood glucose (see Fig. 23–26).

Individuals with type 1 diabetes mellitus (also called insulin-dependent diabetes) have too few β cells and cannot release sufficient insulin to trigger glucose uptake by the cells of skeletal muscle, heart, or adipose tissue. Thus, after a meal containing carbohydrates, glucose accumulates to abnormally high levels in the blood, a condition known as hyperglycemia. Unable to take up glucose, muscle and fat tissue use the fatty acids of stored triacylglycerols as their principal fuel. In the liver, acetyl-CoA derived from this fatty acid breakdown is converted to "ketone bodies"—acetoacetate and β-hydroxybutyrate—which are exported and carried to other tissues to be used as fuel (Chapter 17). These compounds are especially critical to the brain, which uses ketone bodies as alternative fuel when glucose is unavailable. (Fatty acids cannot pass through the blood-brain barrier and thus are not a fuel for brain neurons.)

In untreated type 1 diabetes, overproduction of acetoacetate and β-hydroxybutyrate leads to their accumulation in the blood, and the consequent lowering of blood pH produces **ketoacidosis**, a life-threatening condition. Insulin injection reverses this sequence of events: GLUT4 moves into the plasma membranes of hepatocytes and adipocytes, glucose is taken up into the cells and phosphorylated, and the blood glucose level falls, greatly reducing the production of ketone bodies.

Diabetes mellitus has profound effects on the metabolism of both carbohydrates and fats. We return to this topic in Chapter 23, after considering lipid metabolism (Chapters 17 and 21). ■

SUMMARY 14.1 Glycolysis

- Glycolysis is a near-universal pathway by which a glucose molecule is oxidized to two molecules of pyruvate, with energy conserved as ATP and NADH.
- All 10 glycolytic enzymes are in the cytosol, and all 10 intermediates are phosphorylated compounds of three or six carbons.
- In the preparatory phase of glycolysis, ATP is invested to convert glucose to fructose 1,6-bisphosphate. The bond between C-3 and C-4 is then broken to yield two molecules of triose phosphate.
- In the payoff phase, each of the two molecules of glyceraldehyde 3-phosphate derived from glucose undergoes oxidation at C-1; the energy of this oxidation reaction is conserved in the form of one NADH and two ATP per triose phosphate oxidized. The net equation for the overall process is

$$\text{Glucose} + 2\text{NAD}^+ + 2\text{ADP} + 2\text{P}_i \longrightarrow 2\ \text{pyruvate} + 2\text{NADH} + 2\text{H}^+ + 2\text{ATP} + 2\text{H}_2\text{O}$$

- Glycolysis is tightly regulated in coordination with other energy-yielding pathways to ensure a steady supply of ATP.
- In type 1 diabetes, defective uptake of glucose by muscle and adipose tissue has profound effects on the metabolism of carbohydrates and fats.

14.2 Feeder Pathways for Glycolysis

Many carbohydrates besides glucose meet their catabolic fate in glycolysis, after being transformed into one of the glycolytic intermediates. The most significant are the storage polysaccharides glycogen and starch, either within cells (endogenous) or obtained in the diet; the disaccharides maltose, lactose, trehalose, and sucrose; and the monosaccharides fructose, mannose, and galactose **(Fig. 14–11)**.

Dietary Polysaccharides and Disaccharides Undergo Hydrolysis to Monosaccharides

For most humans, starch is the major source of carbohydrates in the diet (Fig. 14–11). Digestion begins in the mouth, where salivary **α-amylase** hydrolyzes the internal (α1→4) glycosidic linkages of starch, producing short polysaccharide fragments or oligosaccharides. (Note that in this *hydrolysis* reaction, water, not P_i, is the attacking species.) In the stomach, salivary α-amylase is inactivated

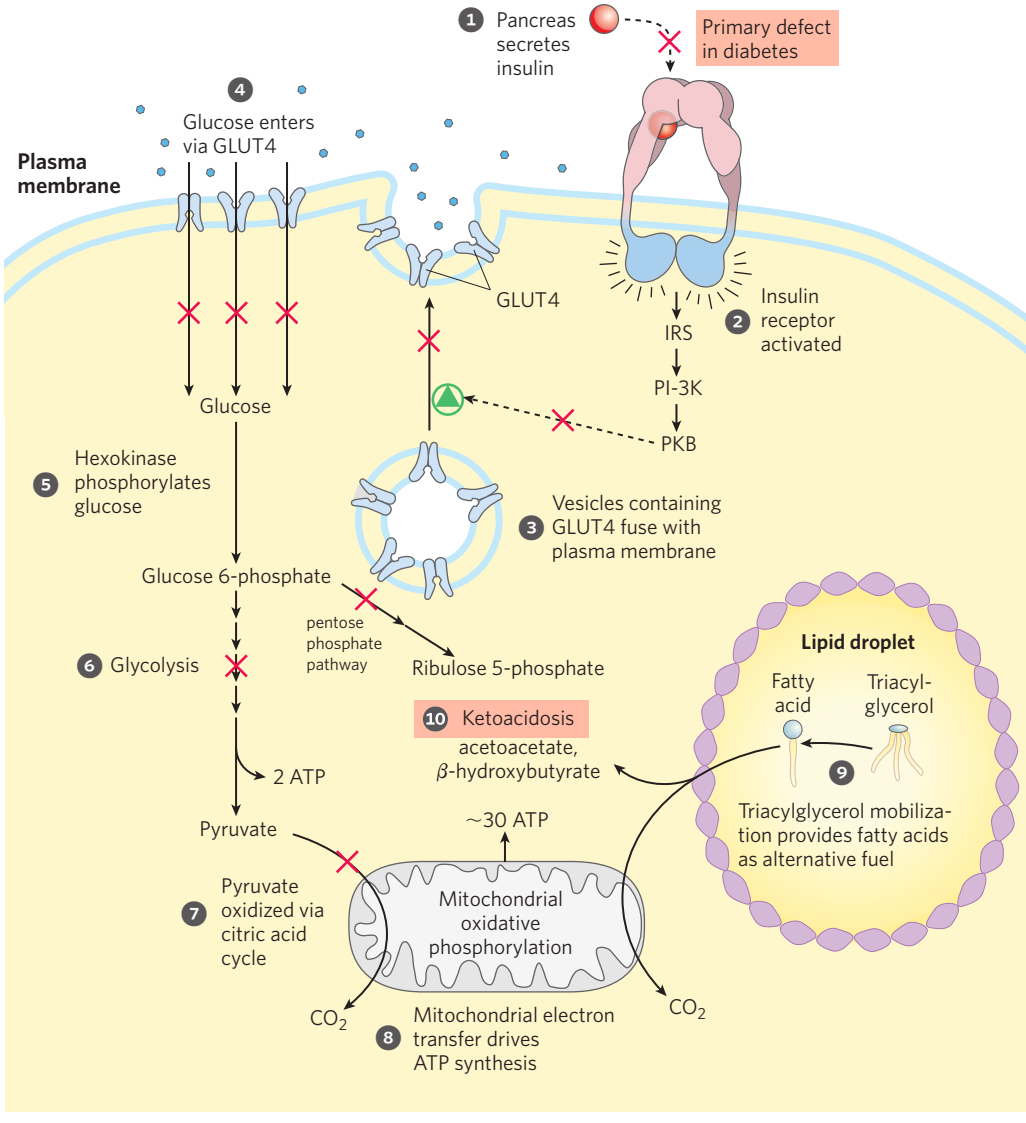

FIGURE 14–10 Effect of type 1 diabetes on carbohydrate and fat metabolism in an adipocyte. Normally, insulin triggers the insertion of GLUT4 transporters into the plasma membrane by the fusion of GLUT4-containing vesicles with the membrane, allowing glucose uptake from the blood. When blood levels of insulin drop, GLUT4 is resequestered in vesicles by endocytosis. In type 1 (insulin-dependent) diabetes mellitus, the insertion of GLUT4 into membranes, as well as other processes normally stimulated by insulin, are inhibited as indicated by **X**. The lack of insulin prevents glucose uptake via GLUT4; as a consequence, cells are deprived of glucose, and blood glucose is elevated. Lacking glucose for energy supply, adipocytes break down triacylglycerols stored in fat droplets and supply the resulting fatty acids to other tissues for mitochondrial ATP production. Two byproducts of fatty acid oxidation in the liver (acetoacetate and β-hydroxybutyrate, see p. 686) accumulate and are released into the blood, providing fuel for the brain but also decreasing blood pH, causing ketoacidosis. The same sequence of events takes place in muscle, except that myocytes do not store triacylglycerols and instead take up fatty acids that are released into the blood by adipocytes.

by the low pH, but a second form of α-amylase, secreted by the pancreas into the small intestine, continues the breakdown process. Pancreatic α-amylase yields mainly maltose and maltotriose (the di- and trisaccharides of glucose) and oligosaccharides called limit dextrins, fragments of amylopectin containing (α1→6) branch points. Maltose and dextrins are degraded to glucose by enzymes of the intestinal brush border (the fingerlike microvilli of intestinal epithelial cells, which greatly increase the area of the intestinal surface). Dietary glycogen has essentially the same structure as starch, and its digestion proceeds by the same pathway.

As we noted in Chapter 7, most animals cannot digest cellulose for lack of the enzyme cellulase, which attacks the (β1→4) glycosidic bonds of cellulose. In ruminant animals, the extended stomach includes a chamber in which symbiotic microorganisms that produce cellulase break down cellulose into glucose molecules. These microorganisms use the resulting glucose in an anaerobic fermentation that produces large quantities

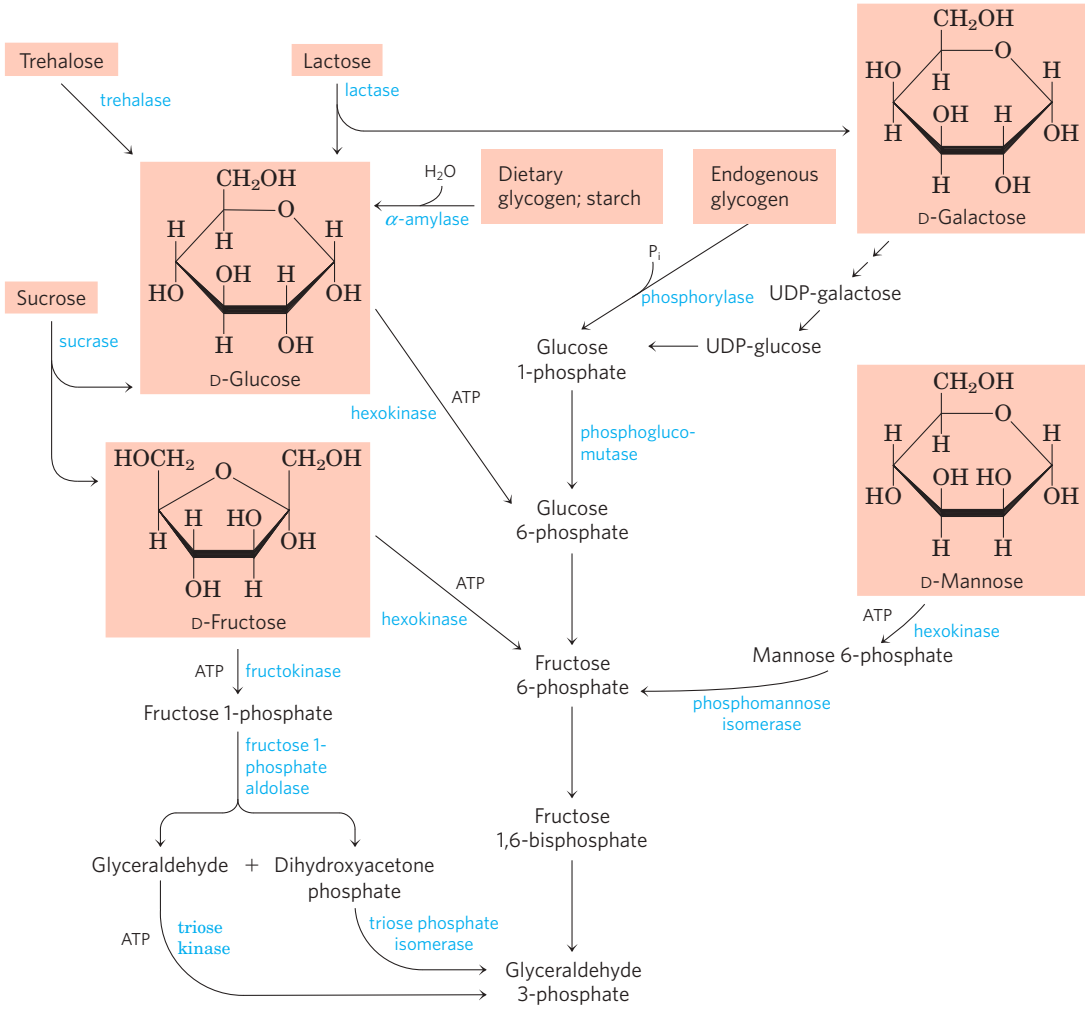

FIGURE 14–11 **Entry of dietary glycogen, starch, disaccharides, and hexoses into the preparatory stage of glycolysis.**

of propionate. This propionate serves as the starting material for gluconeogenesis, which produces much of the lactose in milk.

Endogenous Glycogen and Starch Are Degraded by Phosphorolysis

Glycogen stored in animal tissues (primarily liver and skeletal muscle), in microorganisms, or in plant tissues can be mobilized for use within the same cell by a *phosphorolytic* reaction catalyzed by **glycogen phosphorylase** (**starch phosphorylase** in plants) **(Fig. 14–12)**. These enzymes catalyze an attack by P_i on the ($\alpha 1 \rightarrow 4$) glycosidic linkage that joins the last two glucose residues at a nonreducing end, generating glucose 1-phosphate and a polymer one glucose unit shorter. *Phosphorolysis* preserves some of the energy of the glycosidic bond in the phosphate ester glucose 1-phosphate. Glycogen phosphorylase (or starch phosphorylase) acts repetitively until it approaches an ($\alpha 1 \rightarrow 6$) branch point (see Fig. 7–13), where its action stops. A **debranching enzyme** removes the branches. The mechanisms and control of glycogen degradation are described in greater detail in Chapter 15.

Glucose 1-phosphate produced by glycogen phosphorylase is converted to glucose 6-phosphate by **phosphoglucomutase**, which catalyzes the reversible reaction

$$\text{Glucose 1-phosphate} \rightleftharpoons \text{glucose 6-phosphate}$$

Phosphoglucomutase employs essentially the same mechanism as phosphoglycerate mutase (Fig. 14–9): both entail a bisphosphate intermediate, and the enzyme is transiently phosphorylated in each catalytic cycle. The general name **mutase** is given to enzymes that catalyze the transfer of a functional group from one position to another in the same molecule. Mutases are a subclass of **isomerases**, enzymes that interconvert stereoisomers or structural or positional isomers (see Table 6–3). The glucose 6-phosphate formed in the phosphoglucomutase reaction can enter glycolysis or another pathway such as the pentose phosphate pathway, described in Section 14.5.

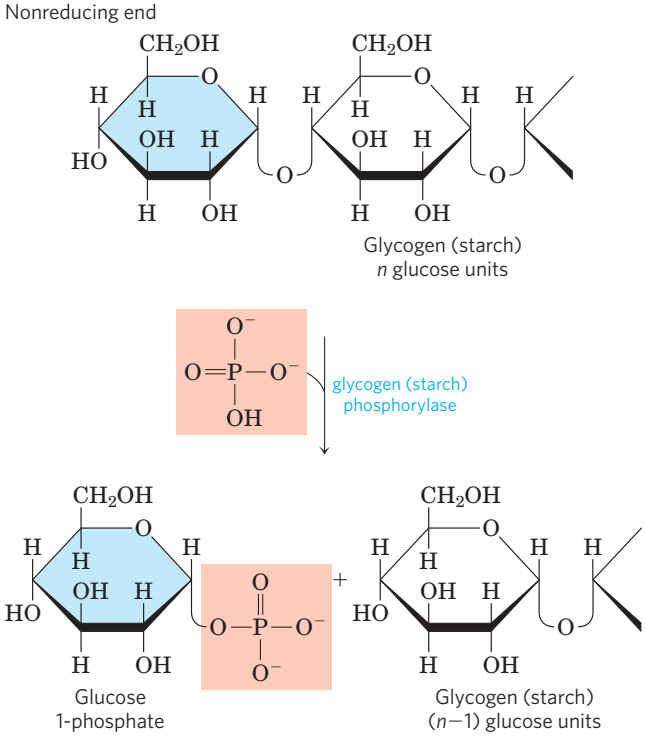

FIGURE 14–12 Breakdown of intracellular glycogen by glycogen phosphorylase. The enzyme catalyzes attack by inorganic phosphate (pink) on the terminal glucosyl residue (blue) at the nonreducing end of a glycogen molecule, releasing glucose 1-phosphate and generating a glycogen molecule shortened by one glucose residue. The reaction is a *phosphorolysis* (not hydrolysis).

WORKED EXAMPLE 14–1 Energy Savings for Glycogen Breakdown by Phosphorolysis

Calculate the energy savings (in ATP molecules per glucose monomer) achieved by breaking down glycogen by *phosphorolysis* rather than *hydrolysis* to begin the process of glycolysis.

Solution: Phosphorolysis produces a phosphorylated glucose (glucose 1-phosphate), which is then converted to glucose 6-phosphate—without expenditure of the cellular energy (1 ATP) needed for formation of glucose 6-phosphate from free glucose. Thus only 1 ATP is consumed per glucose monomer in the preparatory phase, compared with 2 ATP when glycolysis starts with free glucose. The cell therefore gains 3 ATP per glucose monomer (4 ATP produced in the payoff phase minus 1 ATP used in the preparatory phase), rather than 2—a saving of 1 ATP per glucose monomer.

Breakdown of dietary polysaccharides such as glycogen and starch in the gastrointestinal tract by phosphorolysis rather than hydrolysis would produce no energy gain: sugar phosphates are not transported into the cells that line the intestine, but must first be dephosphorylated to the free sugar.

Disaccharides must be hydrolyzed to monosaccharides before entering cells. Intestinal disaccharides and dextrins are hydrolyzed by enzymes attached to the outer surface of the intestinal epithelial cells:

$$\text{Dextrin} + n\text{H}_2\text{O} \xrightarrow[\text{dextrinase}]{} n \text{ D-glucose}$$

$$\text{Maltose} + \text{H}_2\text{O} \xrightarrow[\text{maltase}]{} 2 \text{ D-glucose}$$

$$\text{Lactose} + \text{H}_2\text{O} \xrightarrow[\text{lactase}]{} \text{D-galactose} + \text{D-glucose}$$

$$\text{Sucrose} + \text{H}_2\text{O} \xrightarrow[\text{sucrase}]{} \text{D-fructose} + \text{D-glucose}$$

$$\text{Trehalose} + \text{H}_2\text{O} \xrightarrow[\text{trehalase}]{} 2 \text{ D-glucose}$$

The monosaccharides so formed are actively transported into the epithelial cells (see Fig. 11–43), then passed into the blood to be carried to various tissues, where they are phosphorylated and funneled into the glycolytic sequence.

Lactose intolerance, common among adults of most human populations except those originating in Northern Europe and some parts of Africa, is due to the disappearance after childhood of most or all of the lactase activity of the intestinal epithelial cells. Without intestinal lactase, lactose cannot be completely digested and absorbed in the small intestine, and it passes into the large intestine, where bacteria convert it to toxic products that cause abdominal cramps and diarrhea. The problem is further complicated because undigested lactose and its metabolites increase the osmolarity of the intestinal contents, favoring retention of water in the intestine. In most parts of the world where lactose intolerance is prevalent, milk is not used as a food by adults, although milk products predigested with lactase are commercially available in some countries. In certain human disorders, several or all of the intestinal disaccharidases are missing. In these cases, the digestive disturbances triggered by dietary disaccharides can sometimes be minimized by a controlled diet. ■

Other Monosaccharides Enter the Glycolytic Pathway at Several Points

In most organisms, hexoses other than glucose can undergo glycolysis after conversion to a phosphorylated derivative. D-Fructose, present in free form in many fruits and formed by hydrolysis of sucrose in the small intestine of vertebrates, is phosphorylated by hexokinase:

$$\text{Fructose} + \text{ATP} \xrightarrow{Mg^{2+}} \text{fructose 6-phosphate} + \text{ADP}$$

This is a major pathway of fructose entry into glycolysis in the muscles and kidney. In the liver, fructose enters by a different pathway. The liver enzyme **fructokinase** catalyzes the phosphorylation of fructose at C-1 rather than C-6:

$$\text{Fructose} + \text{ATP} \xrightarrow{Mg^{2+}} \text{fructose 1-phosphate} + \text{ADP}$$

The fructose 1-phosphate is then cleaved to glyceraldehyde and dihydroxyacetone phosphate by **fructose 1-phosphate aldolase**:

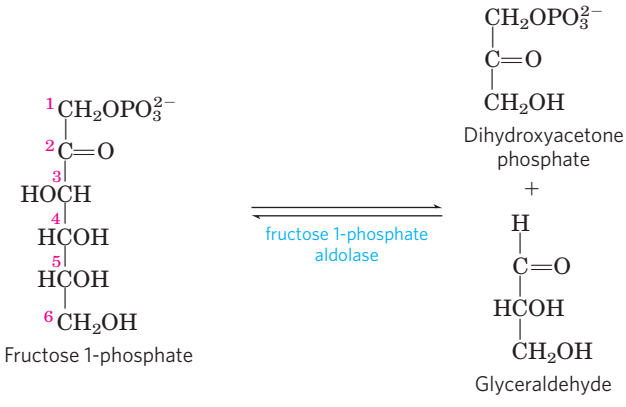

Dihydroxyacetone phosphate is converted to glyceraldehyde 3-phosphate by the glycolytic enzyme triose phosphate isomerase. Glyceraldehyde is phosphorylated by ATP and **triose kinase** to glyceraldehyde 3-phosphate:

$$\text{Glyceradehyde} + \text{ATP} \xrightarrow{Mg^{2+}} \text{glyceraldehyde 3-phosphate} + \text{ADP}$$

Thus both products of fructose 1-phosphate hydrolysis enter the glycolytic pathway as glyceraldehyde 3-phosphate.

D-Galactose, a product of the hydrolysis of lactose (milk sugar), passes in the blood from the intestine to the liver, where it is first phosphorylated at C-1, at the expense of ATP, by the enzyme **galactokinase**:

$$\text{Galactose} + \text{ATP} \xrightarrow{Mg^{2+}} \text{galactose 1-phosphate} + \text{ADP}$$

The galactose 1-phosphate is then converted to its epimer at C-4, glucose 1-phosphate, by a set of reactions in which **uridine diphosphate** (UDP) functions as a coenzyme-like carrier of hexose groups **(Fig. 14–13)**. The epimerization involves first the oxidation of the C-4 —OH group to a ketone, then reduction of the ketone to an —OH, with inversion of the configuration at C-4. NAD is the cofactor for both the oxidation and the reduction.

A defect in any of the three enzymes in this pathway causes **galactosemia** in humans. In galactokinase-deficiency galactosemia, high galactose concentrations are found in blood and urine. Affected individuals develop cataracts in infancy, caused by deposition of the galactose metabolite galactitol in the lens.

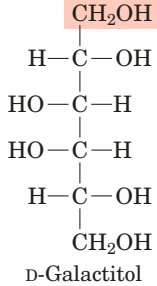

The other symptoms in this disorder are relatively mild, and strict limitation of galactose in the diet greatly diminishes their severity.

Transferase-deficiency galactosemia is more serious; it is characterized by poor growth in childhood, speech abnormality, mental deficiency, and liver damage

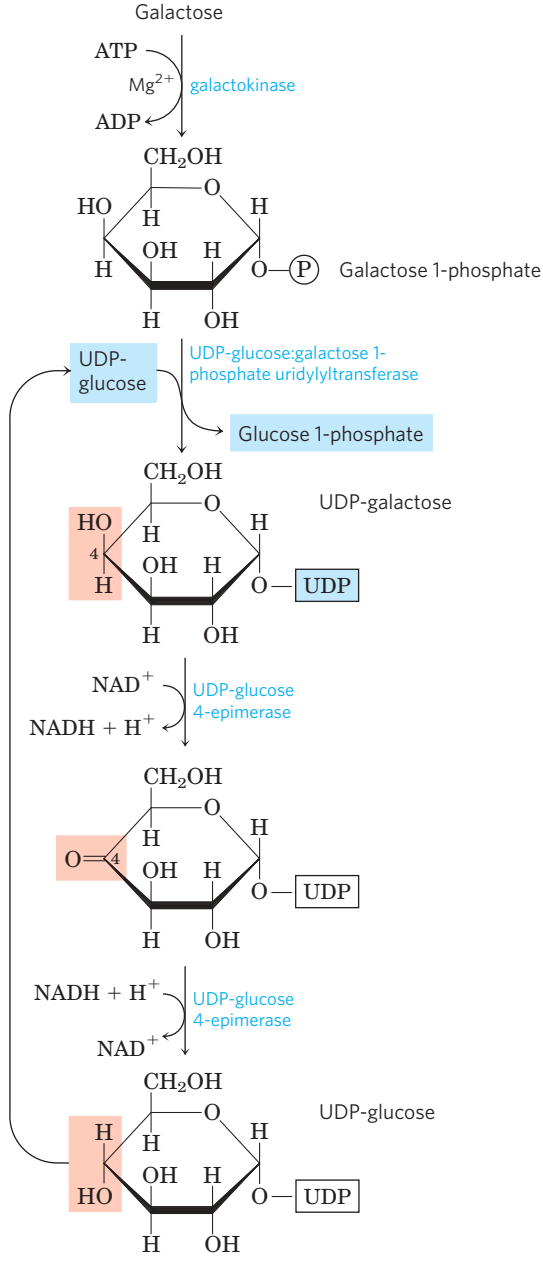

FIGURE 14–13 Conversion of galactose to glucose 1-phosphate. The conversion proceeds through a sugar-nucleotide derivative, UDP-galactose, which is formed when galactose 1-phosphate displaces glucose 1-phosphate from UDP-glucose. UDP-galactose is then converted by UDP-glucose 4-epimerase to UDP-glucose, in a reaction that involves oxidation of C-4 (light red) by NAD^+, then reduction of C-4 by NADH; the result is inversion of the configuration at C-4. The UDP-glucose is recycled through another round of the same reaction. The net effect of this cycle is the conversion of galactose 1-phosphate to glucose 1-phosphate; there is no net production or consumption of UDP-galactose or UDP-glucose.

that may be fatal, even when galactose is withheld from the diet. Epimerase-deficiency galactosemia leads to similar symptoms, but is less severe when dietary galactose is carefully controlled. ■

D-Mannose, released in the digestion of various polysaccharides and glycoproteins of foods, can be phosphorylated at C-6 by hexokinase:

$$\text{Mannose} + \text{ATP} \xrightarrow{Mg^{2+}} \text{mannose 6-phosphate} + \text{ADP}$$

Mannose 6-phosphate is isomerized by **phosphomannose isomerase** to yield fructose 6-phosphate, an intermediate of glycolysis.

SUMMARY 14.2 Feeder Pathways for Glycolysis

- Endogenous glycogen and starch, storage forms of glucose, enter glycolysis in a two-step process. Phosphorolytic cleavage of a glucose residue from an end of the polymer, forming glucose 1-phosphate, is catalyzed by glycogen phosphorylase or starch phosphorylase. Phosphoglucomutase then converts the glucose 1-phosphate to glucose 6-phosphate, which can enter glycolysis.
- Ingested polysaccharides and disaccharides are converted to monosaccharides by intestinal hydrolytic enzymes, and the monosaccharides then enter intestinal cells and are transported to the liver or other tissues.
- A variety of D-hexoses, including fructose, galactose, and mannose, can be funneled into glycolysis. Each is phosphorylated and converted to glucose 6-phosphate, fructose 6-phosphate, or fructose 1-phosphate.
- Conversion of galactose 1-phosphate to glucose 1-phosphate involves two nucleotide derivatives: UDP-galactose and UDP-glucose. Genetic defects in any of the three enzymes that catalyze conversion of galactose to glucose 1-phosphate result in galactosemias of varying severity.

14.3 Fates of Pyruvate under Anaerobic Conditions: Fermentation

Under aerobic conditions, the pyruvate formed in the final step of glycolysis is oxidized to acetate (acetyl-CoA), which enters the citric acid cycle and is oxidized to CO_2 and H_2O. The NADH formed by dehydrogenation of glyceraldehyde 3-phosphate is ultimately reoxidized to NAD^+ by passage of its electrons to O_2 in mitochondrial respiration. Under hypoxic (low-oxygen) conditions, however—as in very active skeletal muscle, in submerged plant tissues, in solid tumors, or in lactic acid bacteria—NADH generated by glycolysis cannot be reoxidized by O_2. Failure to regenerate NAD^+ would leave the cell with no electron acceptor for the oxidation of glyceraldehyde 3-phosphate, and the energy-yielding reactions of glycolysis would stop. NAD^+ must therefore be regenerated in some other way.

The earliest cells lived in an atmosphere almost devoid of oxygen and had to develop strategies for deriving energy from fuel molecules under anaerobic conditions. Most modern organisms have retained the ability to continually regenerate NAD^+ during anaerobic glycolysis by transferring electrons from NADH to form a reduced end product such as lactate or ethanol.

Pyruvate Is the Terminal Electron Acceptor in Lactic Acid Fermentation

When animal tissues cannot be supplied with sufficient oxygen to support aerobic oxidation of the pyruvate and NADH produced in glycolysis, NAD^+ is regenerated from NADH by the reduction of pyruvate to **lactate**. As mentioned earlier, some tissues and cell types (such as erythrocytes, which have no mitochondria and thus cannot oxidize pyruvate to CO_2) produce lactate from glucose even under aerobic conditions. The reduction of pyruvate in this pathway is catalyzed by **lactate dehydrogenase**, which forms the L isomer of lactate at pH 7:

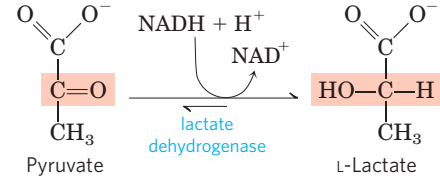

$\Delta G'^\circ = -25.1$ kJ/mol

The overall equilibrium of the reaction strongly favors lactate formation, as shown by the large negative standard free-energy change.

In glycolysis, dehydrogenation of the two molecules of glyceraldehyde 3-phosphate derived from each molecule of glucose converts two molecules of NAD^+ to two of NADH. Because the reduction of two molecules of pyruvate to two of lactate regenerates two molecules of NAD^+, there is no net change in NAD^+ or NADH:

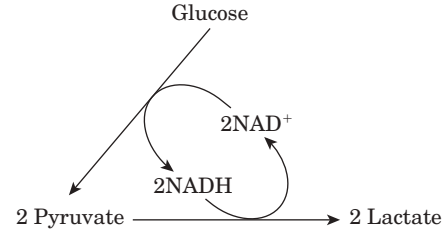

The lactate formed by active skeletal muscles (or by erythrocytes) can be recycled; it is carried in the blood to the liver, where it is converted to glucose during the recovery from strenuous muscular activity. When lactate is produced in large quantities during vigorous muscle contraction (during a sprint, for example), the

acidification that results from ionization of lactic acid in muscle and blood limits the period of vigorous activity. The best-conditioned athletes can sprint at top speed for no more than a minute (Box 14–2).

Although conversion of glucose to lactate includes two oxidation-reduction steps, there is no net change in the oxidation state of carbon; in glucose ($C_6H_{12}O_6$) and lactic acid ($C_3H_6O_3$), the H:C ratio is the same.

BOX 14–2 Athletes, Alligators, and Coelacanths: Glycolysis at Limiting Concentrations of Oxygen

Most vertebrates are essentially aerobic organisms; they convert glucose to pyruvate by glycolysis, then use molecular oxygen to oxidize the pyruvate completely to CO_2 and H_2O. Anaerobic catabolism of glucose to lactate occurs during short bursts of extreme muscular activity, for example in a 100 m sprint, during which oxygen cannot be carried to the muscles fast enough to oxidize pyruvate. Instead, the muscles use their stored glucose (glycogen) as fuel to generate ATP by fermentation, with lactate as the end product. In a sprint, lactate in the blood builds up to high concentrations. It is slowly converted back to glucose by gluconeogenesis in the liver in the subsequent rest or recovery period, during which oxygen is consumed at a gradually diminishing rate until the breathing rate returns to normal. The excess oxygen consumed in the recovery period represents a repayment of the oxygen debt. This is the amount of oxygen required to supply ATP for gluconeogenesis during recovery respiration, in order to regenerate the glycogen "borrowed" from liver and muscle to carry out intense muscular activity in the sprint. The cycle of reactions that includes glucose conversion to lactate in muscle and lactate conversion to glucose in liver is called the Cori cycle, for Carl and Gerty Cori, whose studies in the 1930s and 1940s clarified the pathway and its role (see Box 15–4).

The circulatory systems of most small vertebrates can carry oxygen to their muscles fast enough to avoid having to use muscle glycogen anaerobically. For example, migrating birds often fly great distances at high speeds without rest and without incurring an oxygen debt. Many running animals of moderate size also maintain an essentially aerobic metabolism in their skeletal muscle. However, the circulatory systems of larger animals, including humans, cannot completely sustain aerobic metabolism in skeletal muscles over long periods of intense muscular activity. These animals generally are slow-moving under normal circumstances and engage in intense muscular activity only in the gravest emergencies, because such bursts of activity require long recovery periods to repay the oxygen debt.

Alligators and crocodiles, for example, are normally sluggish animals. Yet when provoked they are capable of lightning-fast charges and dangerous lashings of their powerful tails. Such intense bursts of activity are short and must be followed by long periods of recovery. The fast emergency movements require lactic acid fermentation to generate ATP in skeletal muscles. The stores of muscle glycogen are rapidly expended in intense muscular activity, and lactate reaches very high concentrations in myocytes and extracellular fluid. Whereas a trained athlete can recover from a 100 m sprint in 30 min or less, an alligator may require many hours of rest and extra oxygen consumption to clear the excess lactate from its blood and regenerate muscle glycogen after a burst of activity.

Other large animals, such as the elephant and rhinoceros, have similar metabolic characteristics, as do diving mammals such as whales and seals. Dinosaurs and other huge, now-extinct animals probably had to depend on lactic acid fermentation to supply energy for muscular activity, followed by very long recovery periods during which they were vulnerable to attack by smaller predators better able to use oxygen and thus better adapted to continuous, sustained muscular activity.

Deep-sea explorations have revealed many species of marine life at great ocean depths, where the oxygen concentration is near zero. For example, the primitive coelacanth, a large fish recovered from depths of 4,000 m or more off the coast of South Africa, has an essentially anaerobic metabolism in virtually all its tissues. It converts carbohydrates to lactate and other products, most of which must be excreted. Some marine vertebrates ferment glucose to ethanol and CO_2 in order to generate ATP.

Nevertheless, some of the energy of the glucose molecule has been extracted by its conversion to lactate—enough to give a net yield of two molecules of ATP for every glucose molecule consumed. **Fermentation** is the general term for such processes, which extract energy (as ATP) but do not consume oxygen or change the concentrations of NAD^+ or NADH. Fermentations are carried out by a wide range of organisms, many of which occupy anaerobic niches, and they yield a variety of end products, some of which find commercial uses.

Ethanol Is the Reduced Product in Ethanol Fermentation

Yeast and other microorganisms ferment glucose to ethanol and CO_2, rather than to lactate. Glucose is converted to pyruvate by glycolysis, and the pyruvate is converted to ethanol and CO_2 in a two-step process:

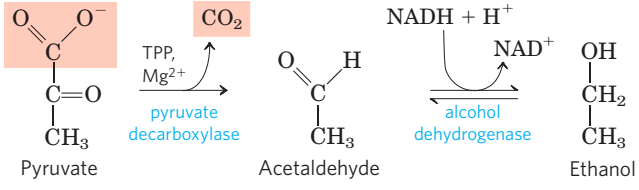

In the first step, pyruvate is decarboxylated in an irreversible reaction catalyzed by **pyruvate decarboxylase**. This reaction is a simple decarboxylation and does not involve the net oxidation of pyruvate. Pyruvate decarboxylase requires Mg^{2+} and has a tightly bound coenzyme, thiamine pyrophosphate, which is discussed below. In the second step, acetaldehyde is reduced to ethanol through the action of **alcohol dehydrogenase**, with the reducing power furnished by NADH derived from the dehydrogenation of glyceraldehyde 3-phosphate. This reaction is a well-studied case of hydride transfer from NADH **(Fig. 14–14)**. Ethanol and CO_2 are thus the end products of ethanol fermentation, and the overall equation is

$$\text{Glucose} + 2\text{ADP} + 2\text{P}_\text{i} \longrightarrow 2\ \text{ethanol} + 2\text{CO}_2 + 2\text{ATP} + 2\text{H}_2\text{O}$$

As in lactic acid fermentation, there is no net change in the ratio of hydrogen to carbon atoms when glucose (H:C ratio = 12/6 = 2) is fermented to two ethanol and two CO_2 (combined H:C ratio = 12/6 = 2). In all fermentations, the H:C ratio of the reactants and products remains the same.

Pyruvate decarboxylase is present in brewer's and baker's yeast (*Saccharomyces cerevisiae*) and in all other organisms that ferment glucose to ethanol, including some plants. The CO_2 produced by pyruvate decarboxylation in brewer's yeast is responsible for the characteristic carbonation of champagne. The ancient art of brewing beer involves several enzymatic processes in addition to the reactions of ethanol fermentation (Box 14–3). In baking, CO_2 released by pyruvate decarboxylase when yeast is mixed with a fermentable sugar causes dough to rise. The enzyme is absent in

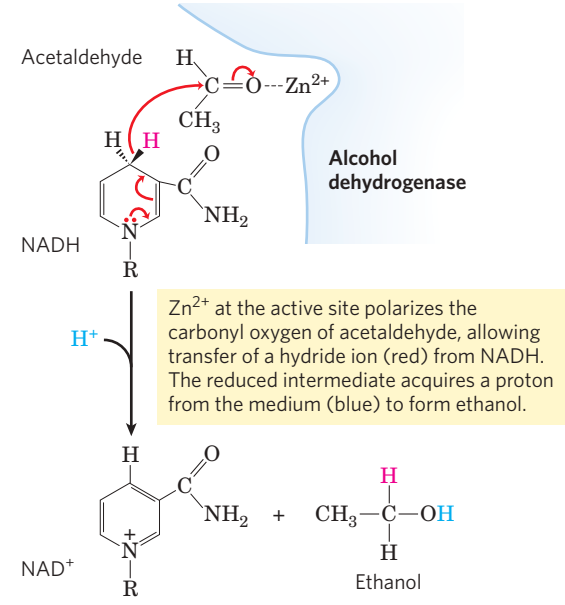

MECHANISM FIGURE 14–14 **The alcohol dehydrogenase reaction.** Alcohol Dehydrogenase Mechanism

vertebrate tissues and in other organisms that carry out lactic acid fermentation.

Alcohol dehydrogenase is present in many organisms that metabolize ethanol, including humans. In the liver it catalyzes the oxidation of ethanol, either ingested or produced by intestinal microorganisms, with the concomitant reduction of NAD^+ to NADH. In this case, the reaction proceeds in the direction opposite to that involved in the production of ethanol by fermentation.

Thiamine Pyrophosphate Carries "Active Acetaldehyde" Groups

The pyruvate decarboxylase reaction provides our first encounter with **thiamine pyrophosphate (TPP)** **(Fig. 14–15)**, a coenzyme derived from vitamin B_1. Lack of vitamin B_1 in the human diet leads to the condition known as beriberi, characterized by an accumulation of body fluids (swelling), pain, paralysis, and ultimately death. ■

Thiamine pyrophosphate plays an important role in the cleavage of bonds adjacent to a carbonyl group, such as the decarboxylation of α-keto acids, and in chemical rearrangements in which an activated acetaldehyde group is transferred from one carbon atom to another (Table 14–1). The functional part of TPP, the thiazolium ring, has a relatively acidic proton at C-2. Loss of this proton produces a carbanion that is the active species in TPP-dependent reactions (Fig. 14–15). The carbanion readily adds to carbonyl groups, and the thiazolium ring is thereby positioned to act as an "electron sink" that greatly facilitates reactions such as the decarboxylation catalyzed by pyruvate decarboxylase.

BOX 14–3 Ethanol Fermentations: Brewing Beer and Producing Biofuels

Beer brewing was a science learned early in human history, and later refined for larger-scale production. Brewers prepare beer by ethanol fermentation of the carbohydrates in cereal grains (seeds) such as barley, carried out by yeast glycolytic enzymes. The carbohydrates, largely polysaccharides, must first be degraded to disaccharides and monosaccharides. In a process called malting, the barley seeds are allowed to germinate until they form the hydrolytic enzymes required to break down their polysaccharides, at which point germination is stopped by controlled heating. The product is malt, which contains enzymes that catalyze the hydrolysis of the β linkages of cellulose and other cell wall polysaccharides of the barley husks, and enzymes such as α-amylase and maltase.

The brewer next prepares the wort, the nutrient medium required for fermentation by yeast cells. The malt is mixed with water and then mashed or crushed. This allows the enzymes formed in the malting process to act on the cereal polysaccharides to form maltose, glucose, and other simple sugars, which are soluble in the aqueous medium. The remaining cell matter is then separated, and the liquid wort is boiled with hops to give flavor. The wort is cooled and then aerated.

Now the yeast cells are added. In the aerobic wort the yeast grows and reproduces very rapidly, using energy obtained from available sugars. No ethanol forms during this stage, because the yeast, amply supplied with oxygen, oxidizes the pyruvate formed by glycolysis to CO_2 and H_2O via the citric acid cycle. When all the dissolved oxygen in the vat of wort has been consumed, the yeast cells switch to anaerobic metabolism, and from this point they ferment the sugars into ethanol and CO_2. The fermentation process is controlled in part by the concentration of the ethanol formed, by the pH, and by the amount of remaining sugar. After fermentation has been stopped, the cells are removed and the "raw" beer is ready for final processing.

In the final steps of brewing, the amount of foam (or head) on the beer, which results from dissolved proteins, is adjusted. Normally this is controlled by proteolytic enzymes that arise in the malting process. If these enzymes act on the proteins too long, the beer will have very little head and will be flat; if they do not act long enough, the beer will not be clear when it is cold. Sometimes proteolytic enzymes from other sources are added to control the head.

Much of the technology developed for large-scale production of alcoholic beverages is now finding application to a wholly different problem: the production of ethanol as a renewable fuel. With the continuing depletion of the known stores of fossil fuels and the rising cost of fuel for internal combustion engines, there is increased interest in the use of ethanol as a fuel substitute or extender. The principal advantage of ethanol as a fuel is that it can be produced from relatively *inexpensive* and *renewable* resources rich in sucrose, starch, or cellulose—starch from corn or wheat, sucrose from beets or cane, and cellulose from straw, forest industry waste, or municipal solid waste. Typically, the raw material (feedstock) is first converted chemically to monosaccharides, then fed to a hardy strain of yeast in an industrial-scale fermenter (Fig. 1). The fermentation can yield not only ethanol for fuel but also side products such as proteins that can be used as animal feed.

FIGURE 1 Industrial-scale fermentations to produce biofuel and other products are typically carried out in tanks that hold thousands of liters of medium.

Fermentations Are Used to Produce Some Common Foods and Industrial Chemicals

Our progenitors learned millennia ago to use fermentation in the production and preservation of foods. Certain microorganisms present in raw food products ferment the carbohydrates and yield metabolic products that give the foods their characteristic forms, textures, and tastes. Yogurt, already known in biblical times, is produced when the bacterium *Lactobacillus bulgaricus* ferments the carbohydrate in milk, producing lactic acid; the resulting drop in pH causes the milk proteins to precipitate, producing the thick texture and sour taste of unsweetened yogurt. Another bacterium,

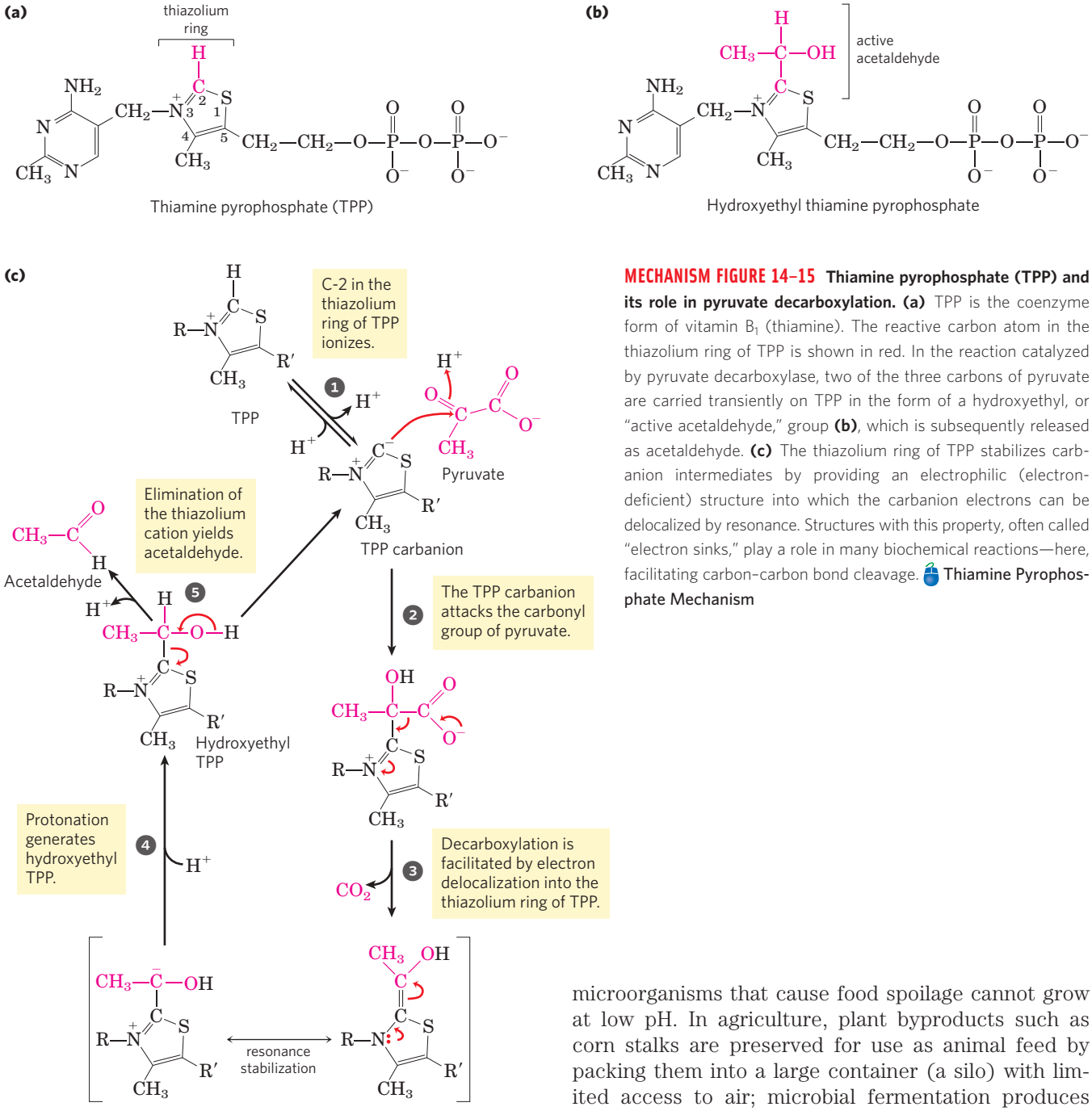

MECHANISM FIGURE 14–15 Thiamine pyrophosphate (TPP) and its role in pyruvate decarboxylation. (a) TPP is the coenzyme form of vitamin B_1 (thiamine). The reactive carbon atom in the thiazolium ring of TPP is shown in red. In the reaction catalyzed by pyruvate decarboxylase, two of the three carbons of pyruvate are carried transiently on TPP in the form of a hydroxyethyl, or "active acetaldehyde," group **(b)**, which is subsequently released as acetaldehyde. **(c)** The thiazolium ring of TPP stabilizes carbanion intermediates by providing an electrophilic (electron-deficient) structure into which the carbanion electrons can be delocalized by resonance. Structures with this property, often called "electron sinks," play a role in many biochemical reactions—here, facilitating carbon–carbon bond cleavage. Thiamine Pyrophosphate Mechanism

Propionibacterium freudenreichii, ferments milk to produce propionic acid and CO_2; the propionic acid precipitates milk proteins, and bubbles of CO_2 cause the holes characteristic of Swiss cheese. Many other food products are the result of fermentations: pickles, sauerkraut, sausage, soy sauce, and a variety of national favorites, such as kimchi (Korea), tempoyak (Indonesia), kefir (Russia), dahi (India), and pozol (Mexico). The drop in pH associated with fermentation also helps to preserve foods, because most of the microorganisms that cause food spoilage cannot grow at low pH. In agriculture, plant byproducts such as corn stalks are preserved for use as animal feed by packing them into a large container (a silo) with limited access to air; microbial fermentation produces acids that lower the pH. The silage that results from this fermentation process can be kept as animal feed for long periods without spoilage.

In 1910 Chaim Weizmann (later to become the first president of Israel) discovered that the bacterium *Clostridium acetobutyricum* ferments starch to butanol and acetone. This discovery opened the field of industrial fermentations, in which some readily available material rich in carbohydrate (corn starch or molasses, for example) is supplied to a pure culture of a specific microorganism, which ferments it into a product of greater commercial value. The ethanol used to make "gasohol" is produced by microbial fermentation, as are formic, acetic, propionic, butyric, and succinic acids,

TABLE 14–1 Some TPP-Dependent Reactions

Enzyme	Pathway(s)	Bond cleaved	Bond formed
Pyruvate decarboxylase	Ethanol fermentation	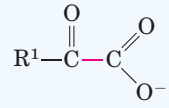	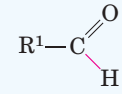
Pyruvate dehydrogenase α-Ketoglutarate dehydrogenase	Synthesis of acetyl-CoA Citric acid cycle	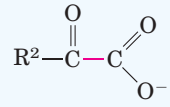	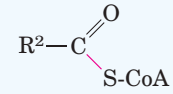
Transketolase	Carbon-assimilation reactions Pentose phosphate pathway	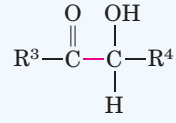	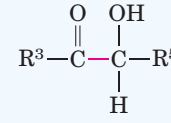

and glycerol, methanol, isopropanol, butanol, and butanediol. These fermentations are generally carried out in huge closed vats in which temperature and access to air are controlled to favor the multiplication of the desired microorganism and to exclude contaminating organisms. The beauty of industrial fermentations is that complicated, multistep chemical transformations are carried out in high yields and with few side products by chemical factories that reproduce themselves—microbial cells. For some industrial fermentations, technology has been developed to immobilize the cells in an inert support, to pass the starting material continuously through the bed of immobilized cells, and to collect the desired product in the effluent—an engineer's dream!

SUMMARY 14.3 Fates of Pyruvate under Anaerobic Conditions: Fermentation

- The NADH formed in glycolysis must be recycled to regenerate NAD^+, which is required as an electron acceptor in the first step of the payoff phase. Under aerobic conditions, electrons pass from NADH to O_2 in mitochondrial respiration.
- Under anaerobic or hypoxic conditions, many organisms regenerate NAD^+ by transferring electrons from NADH to pyruvate, forming lactate. Other organisms, such as yeast, regenerate NAD^+ by reducing pyruvate to ethanol and CO_2. In these anaerobic processes (fermentations), there is no *net* oxidation or reduction of the carbons of glucose.
- A variety of microorganisms can ferment sugar in fresh foods, resulting in changes in pH, taste, and texture, and preserving food from spoilage. Fermentations are used in industry to produce a wide variety of commercially valuable organic compounds from inexpensive starting materials.

14.4 Gluconeogenesis

The central role of glucose in metabolism arose early in evolution, and this sugar remains the nearly universal fuel and building block in modern organisms, from microbes to humans. In mammals, some tissues depend almost completely on glucose for their metabolic energy. For the human brain and nervous system, as well as the erythrocytes, testes, renal medulla, and embryonic tissues, glucose from the blood is the sole or major fuel source. The brain alone requires about 120 g of glucose each day—more than half of all the glucose stored as glycogen in muscle and liver. However, the supply of glucose from these stores is not always sufficient; between meals and during longer fasts, or after vigorous exercise, glycogen is depleted. For these times, organisms need a method for synthesizing glucose from noncarbohydrate precursors. This is accomplished by a pathway called **gluconeogenesis** ("new formation of sugar"), which converts pyruvate and related three- and four-carbon compounds to glucose.

Gluconeogenesis occurs in all animals, plants, fungi, and microorganisms. The reactions are essentially the same in all tissues and all species. The important precursors of glucose in animals are three-carbon compounds such as lactate, pyruvate, and glycerol, as well as certain amino acids **(Fig. 14–16)**. In mammals, gluconeogenesis takes place mainly in the liver, and to a lesser extent in renal cortex and in the epithelial cells that line the inside of the small intestine. The glucose produced passes into the blood to supply other tissues. After vigorous exercise, lactate produced by anaerobic glycolysis in skeletal muscle returns to the liver and is converted to glucose, which moves back to muscle and is converted to glycogen—a circuit called the Cori cycle (Box 14–2; see also Fig. 23–19). In plant seedlings, stored fats and proteins are converted, via paths that include gluconeogenesis, to the disaccharide sucrose for transport throughout the developing

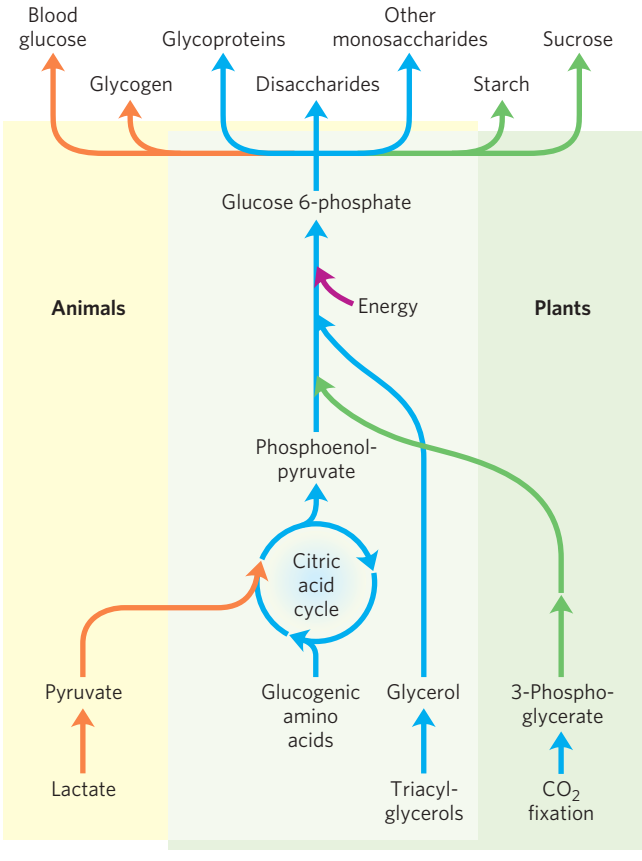

FIGURE 14–16 Carbohydrate synthesis from simple precursors. The pathway from phosphoenolpyruvate to glucose 6-phosphate is common to the biosynthetic conversion of many different precursors of carbohydrates in animals and plants. The path from pyruvate to phosphoenolpyruvate leads through oxaloacetate, an intermediate of the citric acid cycle, which we discuss in Chapter 16. Any compound that can be converted to either pyruvate or oxaloacetate can therefore serve as starting material for gluconeogenesis. This includes alanine and aspartate, which are convertible to pyruvate and oxaloacetate, respectively, and other amino acids that can also yield three- or four-carbon fragments, the so-called glucogenic amino acids (see Table 14–4; see also Fig. 18–15). Plants and photosynthetic bacteria are uniquely able to convert CO_2 to carbohydrates, using the Calvin cycle (see Section 20.1).

plant. Glucose and its derivatives are precursors for the synthesis of plant cell walls, nucleotides and coenzymes, and a variety of other essential metabolites. In many microorganisms, gluconeogenesis starts from simple organic compounds of two or three carbons, such as acetate, lactate, and propionate, in their growth medium.

Although the reactions of gluconeogenesis are the same in all organisms, the metabolic context and the regulation of the pathway differ from one species to another and from tissue to tissue. In this section we focus on gluconeogenesis as it occurs in the mammalian liver. In Chapter 20 we show how photosynthetic organisms use this pathway to convert the primary products of photosynthesis into glucose, to be stored as sucrose or starch.

Gluconeogenesis and glycolysis are not identical pathways running in opposite directions, although they do share several steps **(Fig. 14–17)**; 7 of the 10 enzymatic reactions of gluconeogenesis are the reverse of glycolytic reactions. However, three reactions of glycolysis are essentially irreversible in vivo and cannot

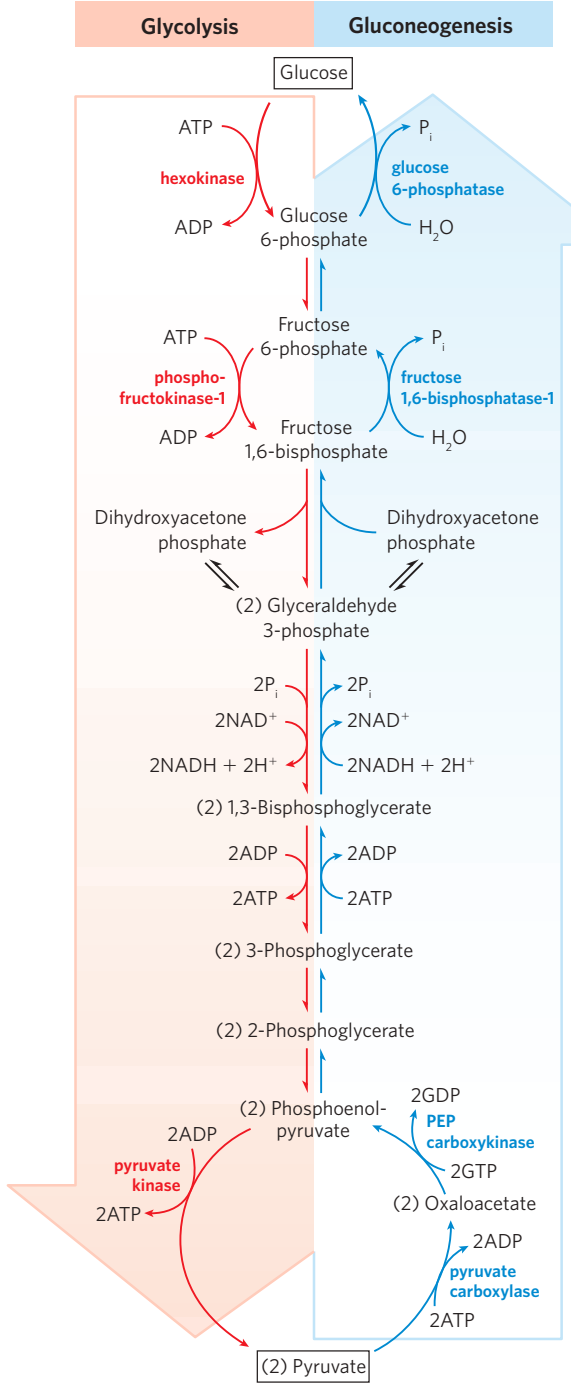

FIGURE 14–17 Opposing pathways of glycolysis and gluconeogenesis in rat liver. The reactions of glycolysis are on the left side, in red; the opposing pathway of gluconeogenesis is on the right, in blue. The major sites of regulation of gluconeogenesis shown here are discussed later in this chapter, and in detail in Chapter 15. Figure 14–20 illustrates an alternative route for oxaloacetate produced in mitochondria.

be used in gluconeogenesis: the conversion of glucose to glucose 6-phosphate by hexokinase, the phosphorylation of fructose 6-phosphate to fructose 1,6-bisphosphate by phosphofructokinase-1, and the conversion of phosphoenolpyruvate to pyruvate by pyruvate kinase (Fig. 14–17). In cells, these three reactions are characterized by a large negative free-energy change, whereas other glycolytic reactions have a ΔG near 0 (Table 14–2). In gluconeogenesis, the three irreversible steps are bypassed by a separate set of enzymes, catalyzing reactions that are sufficiently exergonic to be effectively irreversible in the direction of glucose synthesis. Thus, both glycolysis and gluconeogenesis are irreversible processes in cells. In animals, both pathways occur largely in the cytosol, necessitating their reciprocal and coordinated regulation. Separate regulation of the two pathways is brought about through controls exerted on the enzymatic steps unique to each.

We begin by considering the three bypass reactions of gluconeogenesis. (Keep in mind that "bypass" refers throughout to the bypass of irreversible glycolytic reactions.)

Conversion of Pyruvate to Phosphoenolpyruvate Requires Two Exergonic Reactions

The first of the bypass reactions in gluconeogenesis is the conversion of pyruvate to phosphoenolpyruvate (PEP). This reaction cannot occur by simple reversal of the pyruvate kinase reaction of glycolysis (p. 554), which has a large, negative free-energy change and is therefore irreversible under the conditions prevailing in intact cells (Table 14–2, step 10). Instead, the phosphorylation of pyruvate is achieved by a roundabout sequence of reactions that in eukaryotes requires enzymes in both the cytosol and mitochondria. As we shall see, the pathway shown in Figure 14–17 and described in detail here is one of two routes from pyruvate to PEP; it is the predominant path when pyruvate or alanine is the glucogenic precursor. A second pathway, described later, predominates when lactate is the glucogenic precursor.

Pyruvate is first transported from the cytosol into mitochondria or is generated from alanine within mitochondria by transamination, in which the α-amino group is transferred from alanine (leaving pyruvate) to an α-keto carboxylic acid (transamination reactions are discussed in detail in Chapter 18). Then **pyruvate carboxylase**, a mitochondrial enzyme that requires the coenzyme **biotin**, converts the pyruvate to oxaloacetate **(Fig. 14–18)**:

$$\text{Pyruvate} + HCO_3^- + \text{ATP} \longrightarrow \text{oxaloacetate} + \text{ADP} + P_i \quad (14\text{–}4)$$

The carboxylation reaction involves biotin as a carrier of activated bicarbonate, as shown in **Figure 14–19**; the reaction mechanism is shown in Figure 16–17. (Note that HCO_3^- is formed by ionization of carbonic acid formed from $CO_2 + H_2O$.) HCO_3^- is phosphorylated by ATP to form a mixed anhydride (a carboxyphosphate); then biotin displaces the phosphate in the formation of carboxybiotin.

Pyruvate carboxylase is the first regulatory enzyme in the gluconeogenic pathway, requiring acetyl-CoA as a positive effector. (Acetyl-CoA is produced by fatty acid oxidation (Chapter 17), and its accumulation signals the availability of fatty acids as fuel.) As we shall see in Chapter 16 (see Fig. 16–16), the pyruvate carboxylase reaction can replenish intermediates in another central metabolic pathway, the citric acid cycle.

Because the mitochondrial membrane has no transporter for oxaloacetate, before export to the cytosol the oxaloacetate formed from pyruvate must be reduced to malate by mitochondrial **malate dehydrogenase**, at the expense of NADH:

TABLE 14–2 Free-Energy Changes of Glycolytic Reactions in Erythrocytes

Glycolytic reaction step	$\Delta G'°$ (kJ/mol)	ΔG (kJ/mol)
1 Glucose + ATP ⟶ glucose 6-phosphate + ADP	−16.7	−33.4
2 Glucose 6-phosphate ⇌ fructose 6-phosphate	1.7	0 to 25
3 Fructose 6-phosphate + ATP ⟶ fructose 1,6-bisphosphate + ADP	−14.2	−22.2
4 Fructose 1,6-bisphosphate ⇌ dihydroxyacetone phosphate + glyceraldehyde 3-phosphate	23.8	−6 to 0
5 Dihydroxyacetone phosphate ⇌ glyceraldehyde 3-phosphate	7.5	0 to 4
6 Glyceraldehyde 3-phosphate + P_i + NAD^+ ⇌ 1,3-bisphosphoglycerate + NADH + H^+	6.3	−2 to 2
7 1,3-Bisphosphoglycerate + ADP ⇌ 3-phosphoglycerate + ATP	−18.8	0 to 2
8 3-Phosphoglycerate ⇌ 2-phosphoglycerate	4.4	0 to 0.8
9 2-Phosphoglycerate ⇌ phosphoenolpyruvate + H_2O	7.5	0 to 3.3
10 Phosphoenolpyruvate + ADP ⟶ pyruvate + ATP	−31.4	−16.7

Note: $\Delta G'°$ is the standard free-energy change, as defined in Chapter 13 (pp. 507–508). ΔG is the free-energy change calculated from the actual concentrations of glycolytic intermediates present under physiological conditions in erythrocytes, at pH 7. The glycolytic reactions bypassed in gluconeogenesis are shown in red. Biochemical equations are not necessarily balanced for H or charge (p. 517).

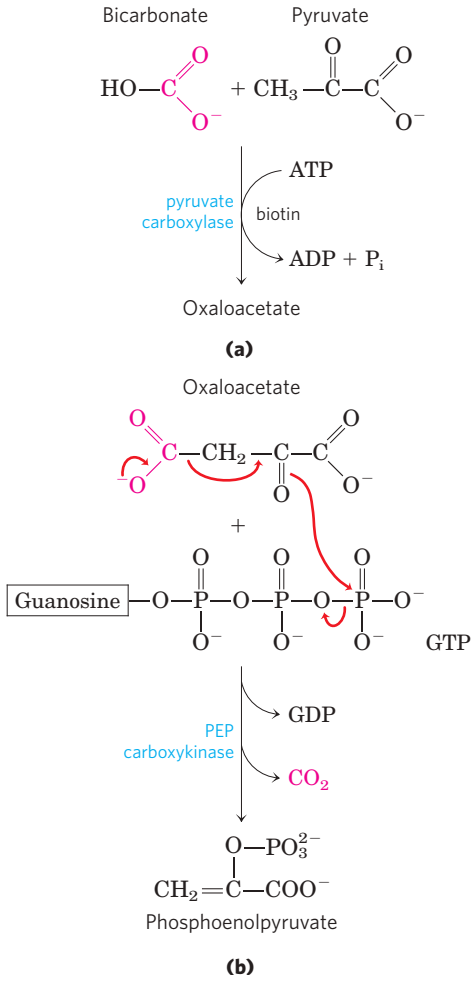

FIGURE 14–18 Synthesis of phosphoenolpyruvate from pyruvate. (a) In mitochondria, pyruvate is converted to oxaloacetate in a biotin-requiring reaction catalyzed by pyruvate carboxylase. **(b)** In the cytosol, oxaloacetate is converted to phosphoenolpyruvate by PEP carboxykinase. The CO_2 incorporated in the pyruvate carboxylase reaction is lost here as CO_2. The decarboxylation leads to a rearrangement of electrons that facilitates attack of the carbonyl oxygen of the pyruvate moiety on the γ phosphate of GTP.

$$\text{Oxaloacetate} + \text{NADH} + \text{H}^+ \rightleftharpoons \text{L-malate} + \text{NAD}^+ \quad (14\text{–}5)$$

The standard free-energy change for this reaction is quite high, but under physiological conditions (including a very low concentration of oxaloacetate) $\Delta G \approx 0$ and the reaction is readily reversible. Mitochondrial malate dehydrogenase functions in both gluconeogenesis and the citric acid cycle, but the overall flow of metabolites in the two processes is in opposite directions.

Malate leaves the mitochondrion through a specific transporter in the inner mitochondrial membrane (see Fig. 19–31), and in the cytosol it is reoxidized to oxaloacetate, with the production of cytosolic NADH:

$$\text{Malate} + \text{NAD}^+ \longrightarrow \text{oxaloacetate} + \text{NADH} + \text{H}^+ \quad (14\text{–}6)$$

The oxaloacetate is then converted to PEP by **phosphoenolpyruvate carboxykinase** (Fig. 14–18). This Mg^{2+}-dependent reaction requires GTP as the phosphoryl group donor:

$$\text{Oxaloacetate} + \text{GTP} \rightleftharpoons \text{PEP} + \text{CO}_2 + \text{GDP} \quad (14\text{–}7)$$

The reaction is reversible under intracellular conditions; the formation of one high-energy phosphate compound (PEP) is balanced by the hydrolysis of another (GTP).

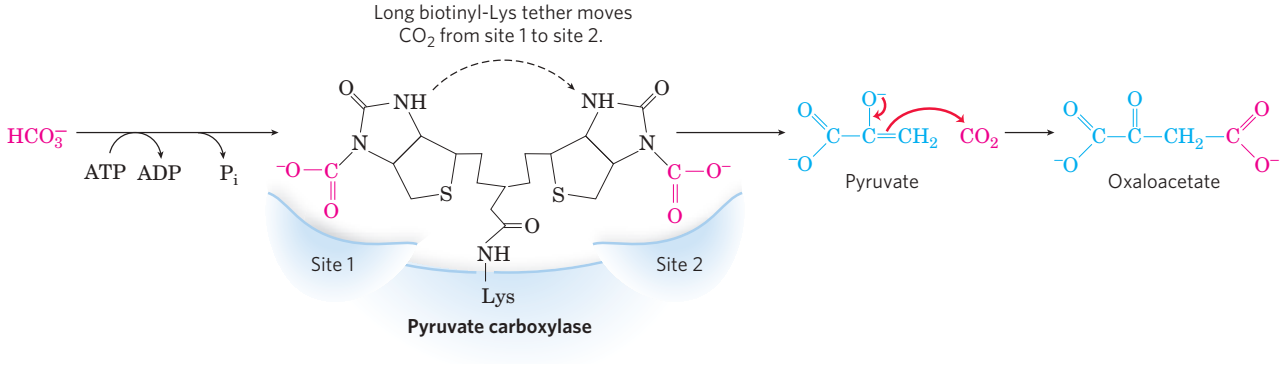

FIGURE 14–19 Role of biotin in the pyruvate carboxylase reaction. The cofactor biotin is covalently attached to the enzyme through an amide linkage to the ε-amino group of a Lys residue, forming a biotinyl-enzyme. The reaction occurs in two phases, which occur at two different sites in the enzyme. At catalytic site 1, bicarbonate ion is converted to CO_2 at the expense of ATP. Then CO_2 reacts with biotin, forming carboxybiotinyl-enzyme. The long arm composed of biotin and the Lys side chain to which it is attached then carry the CO_2 of carboxybiotinyl-enzyme to catalytic site 2 on the enzyme surface, where CO_2 is released and reacts with the pyruvate, forming oxaloacetate and regenerating the biotinyl-enzyme. The general role of flexible arms in carrying reaction intermediates between enzyme active sites is described in Figure 16–18 and the mechanistic details of the pyruvate carboxylase reaction are shown in Figure 16–17. Similar mechanisms occur in other biotin-dependent carboxylation reactions, such as those catalyzed by propionyl-CoA carboxylase (see Fig. 17–12) and acetyl-CoA carboxylase (see Fig. 21–1).

The overall equation for this set of bypass reactions, the sum of Equations 14–4 through 14–7, is

$$\text{Pyruvate} + \text{ATP} + \text{GTP} + \text{HCO}_3^- \longrightarrow \text{PEP} + \text{ADP} + \text{GDP} + \text{P}_i + \text{CO}_2 \quad (14\text{–}8)$$
$$\Delta G'^\circ = 0.9 \text{ kJ/mol}$$

Two high-energy phosphate equivalents (one from ATP and one from GTP), each yielding about 50 kJ/mol under cellular conditions, must be expended to phosphorylate one molecule of pyruvate to PEP. In contrast, when PEP is converted to pyruvate during glycolysis, only one ATP is generated from ADP. Although the standard free-energy change ($\Delta G'^\circ$) of the two-step path from pyruvate to PEP is 0.9 kJ/mol, the actual free-energy change (ΔG), calculated from measured cellular concentrations of intermediates, is very strongly negative (–25 kJ/mol); this results from the ready consumption of PEP in other reactions such that its concentration remains relatively low. The reaction is thus effectively irreversible in the cell.

Note that the CO_2 added to pyruvate in the pyruvate carboxylase step is the same molecule that is lost in the PEP carboxykinase reaction (Fig. 14–18b). This carboxylation-decarboxylation sequence represents a way of "activating" pyruvate, in that the decarboxylation of oxaloacetate facilitates PEP formation. In Chapter 21 we shall see how a similar carboxylation-decarboxylation sequence is used to activate acetyl-CoA for fatty acid biosynthesis (see Fig. 21–1).

There is a logic to the route of these reactions through the mitochondrion. The [NADH]/[NAD^+] ratio in the cytosol is 8×10^{-4}, about 10^5 times lower than in mitochondria. Because cytosolic NADH is consumed in gluconeogenesis (in the conversion of 1,3-bisphosphoglycerate to glyceraldehyde 3-phosphate; Fig. 14–17), glucose biosynthesis cannot proceed unless NADH is available. The transport of malate from the mitochondrion to the cytosol and its reconversion there to oxaloacetate effectively moves reducing equivalents to the cytosol, where they are scarce. This path from pyruvate to PEP therefore provides an important balance between NADH produced and consumed in the cytosol during gluconeogenesis.

A second pyruvate → PEP bypass predominates when lactate is the glucogenic precursor **(Fig. 14–20)**. This pathway makes use of lactate produced by glycolysis in erythrocytes or anaerobic muscle, for example, and it is particularly important in large vertebrates after vigorous exercise (Box 14–2). The conversion of lactate to pyruvate in the cytosol of hepatocytes yields NADH, and the export of reducing equivalents (as malate) from mitochondria is therefore unnecessary. After the pyruvate produced by the lactate dehydrogenase reaction is transported into the mitochondrion, it is converted to oxaloacetate by pyruvate carboxylase, as described above. This oxaloacetate, however, is converted directly to PEP by a mitochondrial isozyme of PEP carboxykinase, and the PEP is transported out of the mitochondrion to continue on the gluconeogenic path. The mitochondrial and cytosolic isozymes of PEP carboxykinase are encoded by separate genes in the nuclear chromosomes, providing another example of two distinct enzymes catalyzing the same reaction but having different cellular locations or metabolic roles (recall the isozymes of hexokinase).

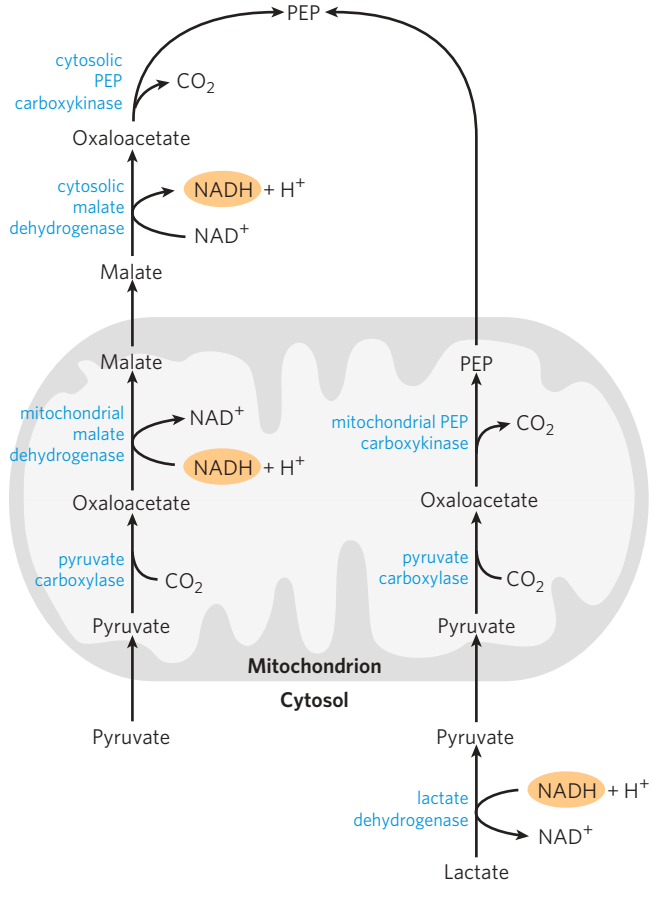

FIGURE 14–20 Alternative paths from pyruvate to phosphoenolpyruvate. The relative importance of the two pathways depends on the availability of lactate or pyruvate and the cytosolic requirements for NADH for gluconeogenesis. The path on the right predominates when lactate is the precursor, because cytosolic NADH is generated in the lactate dehydrogenase reaction and does not have to be shuttled out of the mitochondrion (see text). The requirements of ATP for pyruvate carboxylase and GTP for PEP carboxykinase (see Fig. 14–17) are omitted for simplicity.

Conversion of Fructose 1,6-Bisphosphate to Fructose 6-Phosphate Is the Second Bypass

The second glycolytic reaction that cannot participate in gluconeogenesis is the phosphorylation of fructose 6-phosphate by PFK-1 (Table 14–2, step 3). Because this reaction is highly exergonic and therefore irreversible in intact cells, the generation of fructose 6-phosphate from fructose 1,6-bisphosphate (Fig. 14–17) is catalyzed by a different enzyme, Mg^{2+}-dependent **fructose 1,6-bisphosphatase (FBPase-1)**, which promotes the

essentially irreversible *hydrolysis* of the C-1 phosphate (*not* phosphoryl group transfer to ADP):

$$\text{Fructose 1,6-bisphosphate} + H_2O \longrightarrow \text{fructose 6-phosphate} + P_i \qquad \Delta G'^\circ = -16.3 \text{ kJ/mol}$$

FBPase-1 is so named to distinguish it from another, similar enzyme (FBPase-2) with a regulatory role, which we discuss in Chapter 15.

Conversion of Glucose 6-Phosphate to Glucose Is the Third Bypass

The third bypass is the final reaction of gluconeogenesis, the dephosphorylation of glucose 6-phosphate to yield glucose (Fig. 14–17). Reversal of the hexokinase reaction (p. 548) would require phosphoryl group transfer from glucose 6-phosphate to ADP, forming ATP, an energetically unfavorable reaction (Table 14–2, step 1). The reaction catalyzed by **glucose 6-phosphatase** does not require synthesis of ATP; it is a simple hydrolysis of a phosphate ester:

$$\text{Glucose 6-phosphate} + H_2O \longrightarrow \text{glucose} + P_i \qquad \Delta G'^\circ = -13.8 \text{ kJ/mol}$$

This Mg^{2+}-activated enzyme is found on the lumenal side of the endoplasmic reticulum of hepatocytes, renal cells, and epithelial cells of the small intestine (see Fig. 15–30), but not in other tissues, which are therefore unable to supply glucose to the blood. If other tissues had glucose 6-phosphatase, this enzyme's activity would hydrolyze the glucose 6-phosphate needed within those tissues for glycolysis. Glucose produced by gluconeogenesis in the liver or kidney or ingested in the diet is delivered to these other tissues, including brain and muscle, through the bloodstream.

Gluconeogenesis Is Energetically Expensive, but Essential

The sum of the biosynthetic reactions leading from pyruvate to free blood glucose (Table 14–3) is

$$2 \text{ Pyruvate} + 4ATP + 2GTP + 2NADH + 2H^+ + 4H_2O \longrightarrow \text{glucose} + 4ADP + 2GDP + 6P_i + 2NAD^+ \qquad (14\text{–}9)$$

For each molecule of glucose formed from pyruvate, six high-energy phosphate groups are required, four from ATP and two from GTP. In addition, two molecules of NADH are required for the reduction of two molecules of 1,3-bisphosphoglycerate. Clearly, Equation 14–9 is not simply the reverse of the equation for conversion of glucose to pyruvate by glycolysis, which would require only two molecules of ATP:

$$\text{Glucose} + 2ADP + 2P_i + NAD^+ \longrightarrow 2 \text{ pyruvate} + 2ATP + 2NADH + 2H^+ + 2H_2O$$

The synthesis of glucose from pyruvate is a relatively expensive process. Much of this high energy cost is necessary to ensure the irreversibility of gluconeogenesis. Under intracellular conditions, the overall free-energy change of glycolysis is at least −63 kJ/mol. Under the same conditions the overall ΔG of gluconeogenesis is −16 kJ/mol. Thus both glycolysis and gluco-neogenesis are essentially irreversible processes in cells. A second advantage to investing energy to convert pyruvate to glucose is that if pyruvate were instead excreted, its considerable potential for ATP production by complete, aerobic oxidation would be lost (more than 10 ATP are produced per pyruvate, as we shall see in Chapter 16).

TABLE 14–3 Sequential Reactions in Gluconeogenesis Starting from Pyruvate

Pyruvate + HCO_3^- + ATP ⟶ oxaloacetate + ADP + P_i	×2
Oxaloacetate + GTP ⇌ phosphoenolpyruvate + CO_2 + GDP	×2
Phosphoenolpyruvate + H_2O ⇌ 2-phosphoglycerate	×2
2-Phosphoglycerate ⇌ 3-phosphoglycerate	×2
3-Phosphoglycerate + ATP ⇌ 1,3-bisphosphoglycerate + ADP	×2
1,3-Bisphosphoglycerate + NADH + H^+ ⇌ glyceraldehyde 3-phosphate + NAD^+ + P_i	×2
Glyceraldehyde 3-phosphate ⇌ dihydroxyacetone phosphate	
Glyceraldehyde 3-phosphate + dihydroxyacetone phosphate ⇌ fructose 1,6-bisphosphate	
Fructose 1,6-bisphosphate ⟶ fructose 6-phosphate + P_i	
Fructose 6-phosphate ⇌ glucose 6-phosphate	
Glucose 6-phosphate + H_2O ⟶ glucose + P_i	
Sum: 2 Pyruvate + 4ATP + 2GTP + 2NADH + $2H^+$ + $4H_2O$ ⟶ glucose + 4ADP + 2GDP + $6P_i$ + $2NAD^+$	

Note: The bypass reactions are in red; all other reactions are reversible steps of glycolysis. The figures at the right indicate that the reaction is to be counted twice, because two three-carbon precursors are required to make a molecule of glucose. The reactions required to replace the cytosolic NADH consumed in the glyceraldehyde 3-phosphate dehydrogenase reaction (the conversion of lactate to pyruvate in the cytosol or the transport of reducing equivalents from mitochondria to the cytosol in the form of malate) are not considered in this summary. Biochemical equations are not necessarily balanced for H and charge (p. 517).

Citric Acid Cycle Intermediates and Some Amino Acids Are Glucogenic

The biosynthetic pathway to glucose described above allows the net synthesis of glucose not only from pyruvate but also from the four-, five-, and six-carbon intermediates of the citric acid cycle (Chapter 16). Citrate, isocitrate, α-ketoglutarate, succinyl-CoA, succinate, fumarate, and malate—all are citric acid cycle intermediates that can undergo oxidation to oxaloacetate (see Fig. 16–7). Some or all of the carbon atoms of most amino acids derived from proteins are ultimately catabolized to pyruvate or to intermediates of the citric acid cycle. Such amino acids can therefore undergo net conversion to glucose and are said to be **glucogenic** (Table 14–4). Alanine and glutamine, the principal molecules that transport amino groups from extrahepatic tissues to the liver (see Fig. 18–9), are particularly important glucogenic amino acids in mammals. After removal of their amino groups in liver mitochondria, the carbon skeletons remaining (pyruvate and α-ketoglutarate, respectively) are readily funneled into gluconeogenesis.

Mammals Cannot Convert Fatty Acids to Glucose

No net conversion of fatty acids to glucose occurs in mammals. As we shall see in Chapter 17, the catabolism of most fatty acids yields only acetyl-CoA. Mammals cannot use acetyl-CoA as a precursor of glucose, because the pyruvate dehydrogenase reaction is irreversible and cells have no other pathway to convert acetyl-CoA to pyruvate. Plants, yeast, and many bacteria do have a pathway (the glyoxylate cycle; see Fig. 16–22) for converting acetyl-CoA to oxaloacetate, so these organisms can use fatty acids as the starting material for gluconeogenesis. This is important during the germination of seedlings, for example; before leaves develop and photosynthesis can provide energy and carbohydrates, the seedling relies on stored seed oils for energy production and cell wall biosynthesis.

Although mammals cannot convert fatty acids to carbohydrate, they can use the small amount of glycerol produced from the breakdown of fats (triacyl*glycerols*) for gluconeogenesis. Phosphorylation of glycerol by glycerol kinase, followed by oxidation of the central carbon, yields dihydroxyacetone phosphate, an intermediate in gluconeogenesis in liver.

As we shall see in Chapter 21, glycerol phosphate is an essential intermediate in triacylglycerol synthesis in adipocytes, but these cells lack glycerol kinase and so cannot simply phosphorylate glycerol. Instead, adipocytes carry out a truncated version of gluconeogenesis, known as **glyceroneogenesis**: the conversion of pyruvate to dihydroxyacetone phosphate via the early reactions of gluconeogenesis, followed by reduction of the dihydroxyacetone phosphate to glycerol phosphate (see Fig. 21–21).

TABLE 14–4 Glucogenic Amino Acids, Grouped by Site of Entry

Pyruvate	**Succinyl-CoA**
Alanine	Isoleucine*
Cysteine	Methionine
Glycine	Threonine
Serine	Valine
Threonine	**Fumarate**
Tryptophan*	Phenylalanine*
α-Ketoglutarate	Tyrosine*
Arginine	**Oxaloacetate**
Glutamate	Asparagine
Glutamine	Aspartate
Histidine	
Proline	

Note: All these amino acids are precursors of blood glucose or liver glycogen, because they can be converted to pyruvate or citric acid cycle intermediates. Of the 20 common amino acids, only leucine and lysine are unable to furnish carbon for net glucose synthesis.

*These amino acids are also ketogenic (see Fig. 18–15).

Glycolysis and Gluconeogenesis Are Reciprocally Regulated

If glycolysis (the conversion of glucose to pyruvate) and gluconeogenesis (the conversion of pyruvate to glucose) were allowed to proceed simultaneously at high rates, the result would be the consumption of ATP and the production of heat. For example, PFK-1 and FBPase-1 catalyze opposing reactions:

$$\text{ATP} + \text{fructose 6-phosphate} \xrightarrow[\text{PFK-1}]{} \text{ADP} + \text{fructose 1,6-bisphosphate}$$

$$\text{Fructose 1,6-bisphosphate} + H_2O \xrightarrow[\text{FBPase-1}]{} \text{fructose 6-phosphate} + P_i$$

The sum of these two reactions is

$$\text{ATP} + H_2O \longrightarrow \text{ADP} + P_i + \text{heat}$$

These two enzymatic reactions, and several others in the two pathways, are regulated allosterically and by covalent modification (phosphorylation). In Chapter 15 we take up the mechanisms of this regulation in detail. For now, suffice it to say that the pathways are regulated so that when the flux of glucose through glycolysis goes up, the flux of pyruvate toward glucose goes down, and vice versa.

SUMMARY 14.4 Gluconeogenesis

- Gluconeogenesis is a ubiquitous multistep process in which glucose is produced from lactate,

pyruvate, or oxaloacetate, or any compound (including citric acid cycle intermediates) that can be converted to one of these intermediates. Seven of the steps in gluconeogenesis are catalyzed by the same enzymes used in glycolysis; these are the reversible reactions.

- Three irreversible steps in glycolysis are bypassed by reactions catalyzed by gluconeogenic enzymes: (1) conversion of pyruvate to PEP via oxaloacetate, catalyzed by pyruvate carboxylase and PEP carboxykinase; (2) dephosphorylation of fructose 1,6-bisphosphate by FBPase-1; and (3) dephosphorylation of glucose 6-phosphate by glucose 6-phosphatase.
- Formation of one molecule of glucose from pyruvate requires 4 ATP, 2 GTP, and 2 NADH; it is expensive.
- In mammals, gluconeogenesis in the liver, kidney, and small intestine provides glucose for use by the brain, muscles, and erythrocytes.
- Pyruvate carboxylase is stimulated by acetyl-CoA, increasing the rate of gluconeogenesis when the cell has adequate supplies of other substrates (fatty acids) for energy production.
- Animals cannot convert acetyl-CoA derived from fatty acids into glucose; plants and microorganisms can.
- Glycolysis and gluconeogenesis are reciprocally regulated to prevent wasteful operation of both pathways at the same time.

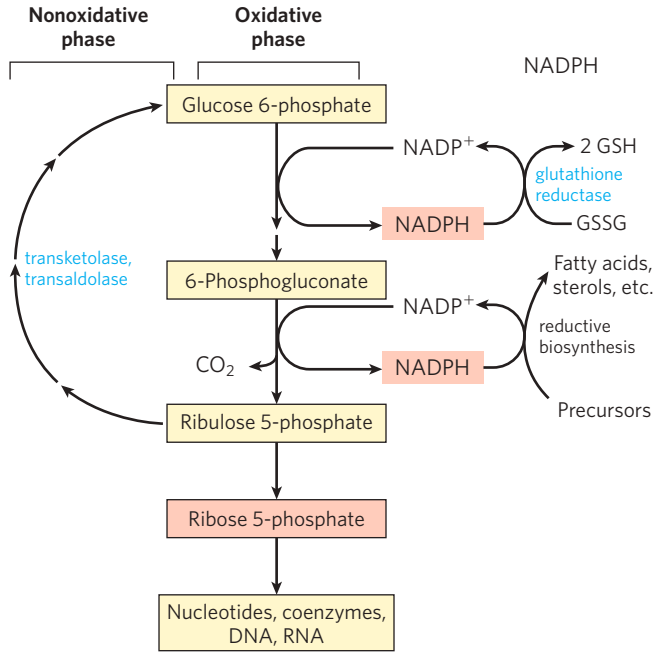

FIGURE 14–21 General scheme of the pentose phosphate pathway. NADPH formed in the oxidative phase is used to reduce glutathione, GSSG (see Box 14–4) and to support reductive biosynthesis. The other product of the oxidative phase is ribose 5-phosphate, which serves as a precursor for nucleotides, coenzymes, and nucleic acids. In cells that are not using ribose 5-phosphate for biosynthesis, the nonoxidative phase recycles six molecules of the pentose into five molecules of the hexose glucose 6-phosphate, allowing continued production of NADPH and converting glucose 6-phosphate (in six cycles) to CO_2.

14.5 Pentose Phosphate Pathway of Glucose Oxidation

In most animal tissues, the major catabolic fate of glucose 6-phosphate is glycolytic breakdown to pyruvate, much of which is then oxidized via the citric acid cycle, ultimately leading to the formation of ATP. Glucose 6-phosphate does have other catabolic fates, however, which lead to specialized products needed by the cell. Of particular importance in some tissues is the oxidation of glucose 6-phosphate to pentose phosphates by the **pentose phosphate pathway** (also called the **phosphogluconate pathway** or the **hexose monophosphate pathway**; **Fig. 14–21**). In this oxidative pathway, $NADP^+$ is the electron acceptor, yielding NADPH. Rapidly dividing cells, such as those of bone marrow, skin, and intestinal mucosa, and those of tumors, use the pentose ribose 5-phosphate to make RNA, DNA, and such coenzymes as ATP, NADH, $FADH_2$, and coenzyme A.

In other tissues, the essential product of the pentose phosphate pathway is not the pentoses but the electron donor NADPH, needed for reductive biosynthesis or to counter the damaging effects of oxygen radicals. Tissues that carry out extensive fatty acid synthesis (liver, adipose, lactating mammary gland) or very active synthesis of cholesterol and steroid hormones (liver, adrenal glands, gonads) require the NADPH provided by this pathway. Erythrocytes and the cells of the lens and cornea are directly exposed to oxygen and thus to the damaging free radicals generated by oxygen. By maintaining a reducing atmosphere (a high ratio of NADPH to $NADP^+$ and a high ratio of reduced to oxidized glutathione), such cells can prevent or undo oxidative damage to proteins, lipids, and other sensitive molecules. In erythrocytes, the NADPH produced by the pentose phosphate pathway is so important in preventing oxidative damage that a genetic defect in glucose 6-phosphate dehydrogenase, the first enzyme of the pathway, can have serious medical consequences (Box 14–4). ■

The Oxidative Phase Produces Pentose Phosphates and NADPH

The first reaction of the pentose phosphate pathway **(Fig. 14–22)** is the oxidation of glucose 6-phosphate by **glucose 6-phosphate dehydrogenase (G6PD)** to form 6-phosphoglucono-δ-lactone, an intramolecular ester. $NADP^+$ is the electron acceptor, and the

BOX 14–4 MEDICINE Why Pythagoras Wouldn't Eat Falafel: Glucose 6-Phosphate Dehydrogenase Deficiency

Fava beans, an ingredient of falafel, have been an important food source in the Mediterranean and Middle East since antiquity. The Greek philosopher and mathematician Pythagoras prohibited his followers from dining on fava beans, perhaps because they make many people sick with a condition called favism, which can be fatal. In favism, erythrocytes begin to lyse 24 to 48 hours after ingestion of the beans, releasing free hemoglobin into the blood. Jaundice and sometimes kidney failure can result. Similar symptoms can occur with ingestion of the antimalarial drug primaquine or of sulfa antibiotics, or following exposure to certain herbicides. These symptoms have a genetic basis: glucose 6-phosphate dehydrogenase (G6PD) deficiency, which affects about 400 million people worldwide. Most G6PD-deficient individuals are asymptomatic; only the combination of G6PD deficiency and certain environmental factors produces the clinical manifestations.

Glucose 6-phosphate dehydrogenase catalyzes the first step in the pentose phosphate pathway (see Fig. 14–22), which produces NADPH. This reductant, essential in many biosynthetic pathways, also protects cells from oxidative damage by hydrogen peroxide (H_2O_2) and superoxide free radicals, highly reactive oxidants generated as metabolic byproducts and through the actions of drugs such as primaquine and natural products such as divicine—the toxic ingredient of fava beans. During normal detoxification, H_2O_2 is converted to H_2O by reduced glutathione and glutathione peroxidase, and the oxidized glutathione is converted back to the reduced form by glutathione reductase and NADPH (Fig. 1). H_2O_2 is also broken down to H_2O and O_2 by catalase, which also requires NADPH. In G6PD-deficient individuals, the NADPH production is diminished and detoxification of H_2O_2 is inhibited. Cellular damage results: lipid peroxidation leading to breakdown of erythrocyte membranes and oxidation of proteins and DNA.

The geographic distribution of G6PD deficiency is instructive. Frequencies as high as 25% occur in tropical Africa, parts of the Middle East, and Southeast Asia, areas where malaria is most prevalent. In addition to such epidemiological observations, in vitro studies show that growth of one malaria parasite, *Plasmodium falciparum*, is inhibited in G6PD-deficient erythrocytes. The parasite is very sensitive to oxidative damage and is killed by a level of oxidative stress that is tolerable to a G6PD-deficient human host. Because the advantage of resistance to malaria balances the disadvantage of lowered resistance to oxidative damage, natural selection sustains the G6PD-deficient genotype in human populations where malaria is prevalent. Only under overwhelming oxidative stress, caused by drugs, herbicides, or divicine, does G6PD deficiency cause serious medical problems.

An antimalarial drug such as primaquine is believed to act by causing oxidative stress to the parasite. It is ironic that antimalarial drugs can cause human illness through the same biochemical mechanism that provides resistance to malaria. Divicine also acts as an antimalarial drug, and ingestion of fava beans may protect against malaria. By refusing to eat falafel, many Pythagoreans with normal G6PD activity may have unwittingly increased their risk of malaria!

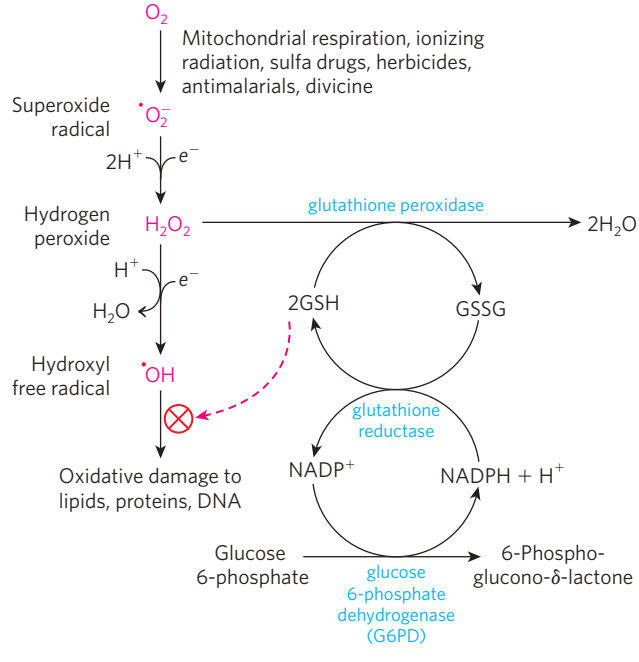

FIGURE 1 Role of NADPH and glutathione in protecting cells against highly reactive oxygen derivatives. Reduced glutathione (GSH) protects the cell by destroying hydrogen peroxide and hydroxyl free radicals. Regeneration of GSH from its oxidized form (GSSG) requires the NADPH produced in the glucose 6-phosphate dehydrogenase reaction.

overall equilibrium lies far in the direction of NADPH formation. The lactone is hydrolyzed to the free acid 6-phosphogluconate by a specific **lactonase**, then 6-phosphogluconate undergoes oxidation and decarboxylation by **6-phosphogluconate dehydrogenase** to form the ketopentose ribulose 5-phosphate; the reaction generates a second molecule of NADPH. (This ribulose 5-phosphate is important in the regulation of glycolysis and gluconeogenesis, as we shall see in Chapter 15.) **Phosphopentose isomerase** converts

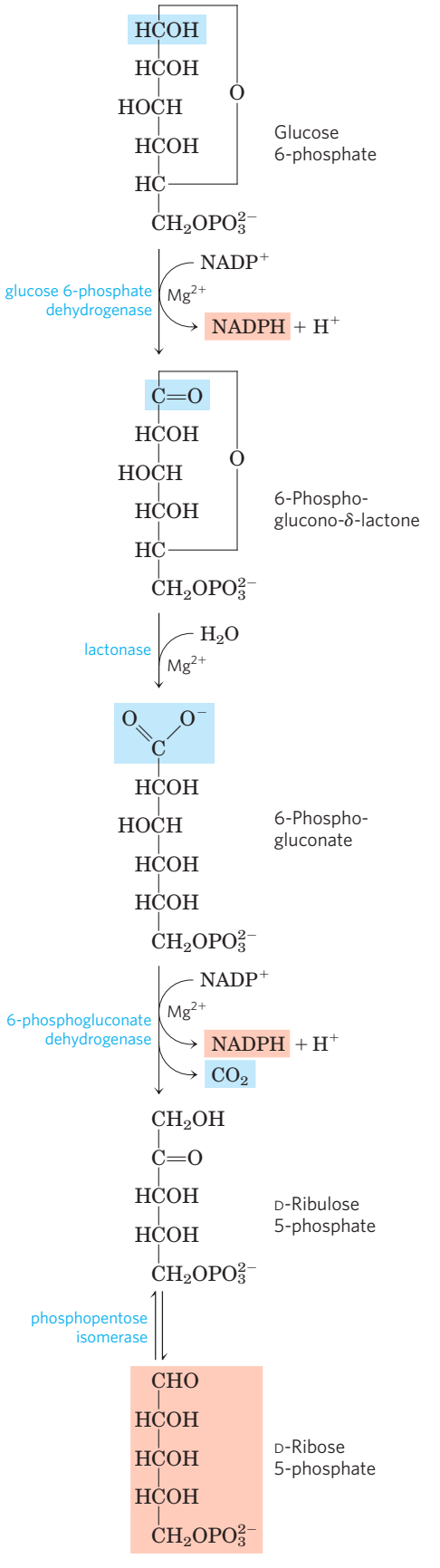

FIGURE 14–22 **Oxidative reactions of the pentose phosphate pathway.** The end products are ribose 5-phosphate, CO_2, and NADPH.

ribulose 5-phosphate to its aldose isomer, ribose 5-phosphate. In some tissues, the pentose phosphate pathway ends at this point, and its overall equation is

$$\text{Glucose 6-phosphate} + 2\text{NADP}^+ + \text{H}_2\text{O} \longrightarrow \text{ribose 5-phosphate} + \text{CO}_2 + 2\text{NADPH} + 2\text{H}^+$$

The net result is the production of NADPH, a reductant for biosynthetic reactions, and ribose 5-phosphate, a precursor for nucleotide synthesis.

The Nonoxidative Phase Recycles Pentose Phosphates to Glucose 6-Phosphate

In tissues that require primarily NADPH, the pentose phosphates produced in the oxidative phase of the pathway are recycled into glucose 6-phosphate. In this nonoxidative phase, ribulose 5-phosphate is first epimerized to xylulose 5-phosphate:

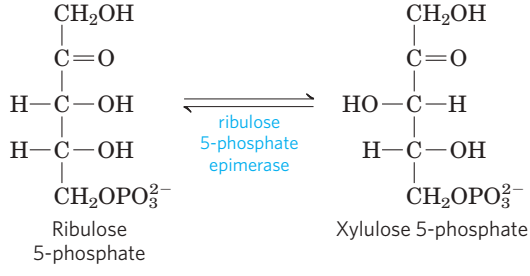

Then, in a series of rearrangements of the carbon skeletons **(Fig. 14–23)**, six five-carbon sugar phosphates are converted to five six-carbon sugar phosphates, completing the cycle and allowing continued oxidation of glucose 6-phosphate with production of NADPH. Continued recycling leads ultimately to the conversion of glucose 6-phosphate to six CO_2. Two enzymes unique to the pentose phosphate pathway act in these interconversions of sugars: transketolase and transaldolase. **Transketolase** catalyzes the transfer of a two-carbon fragment from a ketose donor to an aldose acceptor **(Fig. 14–24a)**. In its first appearance in the pentose phosphate pathway, transketolase transfers C-1 and C-2 of xylulose 5-phosphate to ribose 5-phosphate, forming the seven-carbon product sedoheptulose 7-phosphate (Fig. 14–24b). The remaining three-carbon fragment from xylulose is glyceraldehyde 3-phosphate.

Next, **transaldolase** catalyzes a reaction similar to the aldolase reaction of glycolysis: a three-carbon fragment is removed from sedoheptulose 7-phosphate and condensed with glyceraldehyde 3-phosphate, forming fructose 6-phosphate and the tetrose erythrose 4-phosphate **(Fig. 14–25)**. Now transketolase acts again, forming fructose 6-phosphate and glyceraldehyde 3-phosphate from erythrose 4-phosphate and xylulose 5-phosphate **(Fig. 14–26)**. Two molecules of glyceraldehyde 3-phosphate formed by two iterations of these

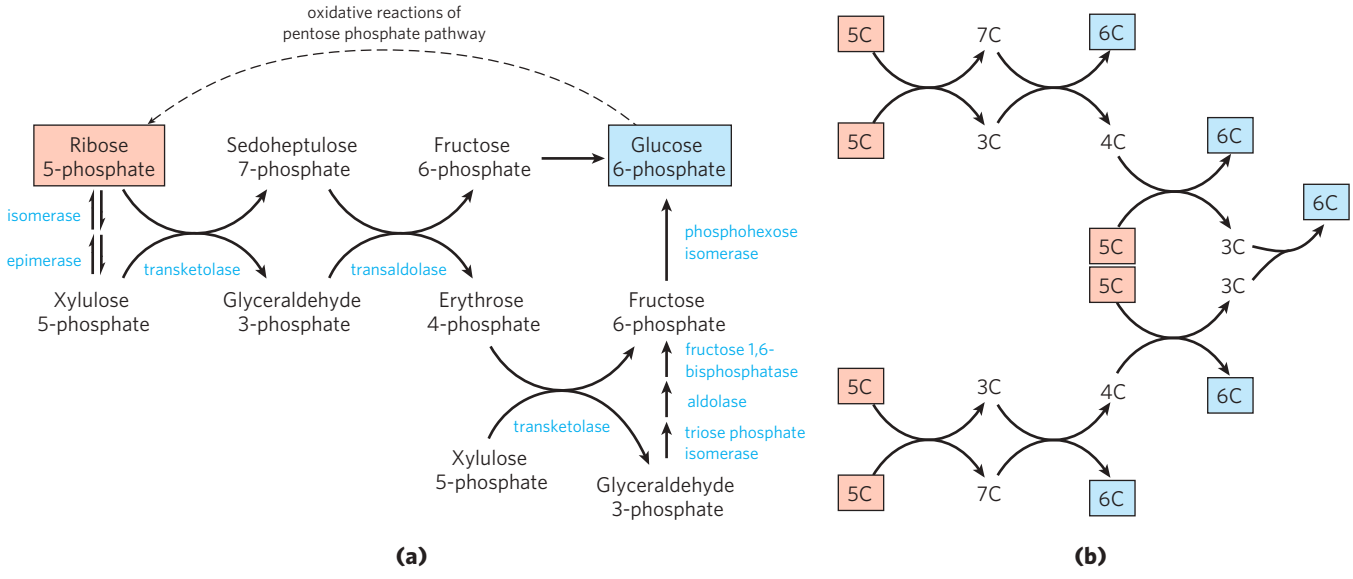

FIGURE 14–23 **Nonoxidative reactions of the pentose phosphate pathway. (a)** These reactions convert pentose phosphates to hexose phosphates, allowing the oxidative reactions (see Fig. 14–22) to continue. Transketolase and transaldolase are specific to this pathway; the other enzymes also serve in the glycolytic or gluconeogenic pathways. **(b)** A schematic diagram showing the pathway from six pentoses (5C) to five hexoses (6C). Note that this involves two sets of the interconversions shown in **(a)**. Every reaction shown here is reversible; unidirectional arrows are used only to make clear the direction of the reactions during continuous oxidation of glucose 6-phosphate. In the light-independent reactions of photosynthesis, the direction of these reactions is reversed (see Fig. 20–10).

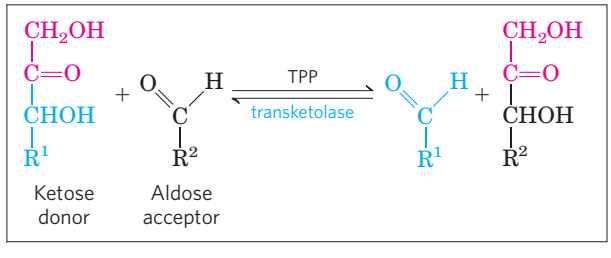

(a)

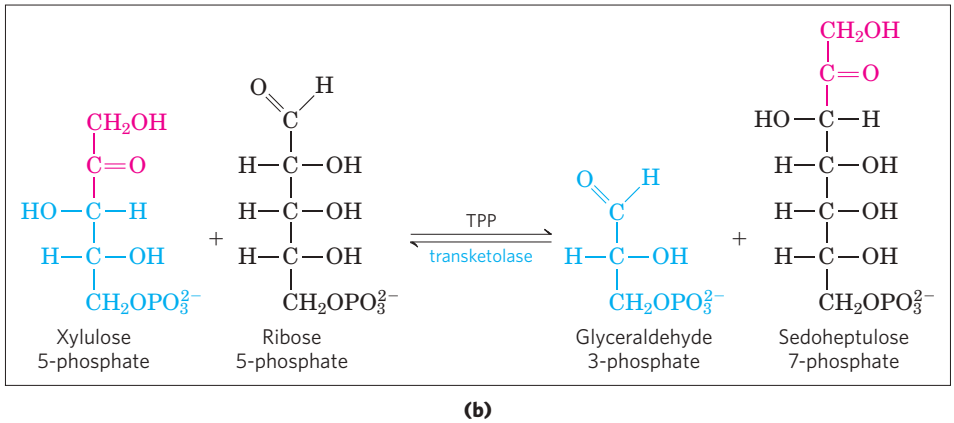

(b)

FIGURE 14–24 **The first reaction catalyzed by transketolase. (a)** The general reaction catalyzed by transketolase is the transfer of a two-carbon group, carried temporarily on enzyme-bound TPP, from a ketose donor to an aldose acceptor. **(b)** Conversion of two pentose phosphates to a triose phosphate and a seven-carbon sugar phosphate, sedoheptulose 7-phosphate.

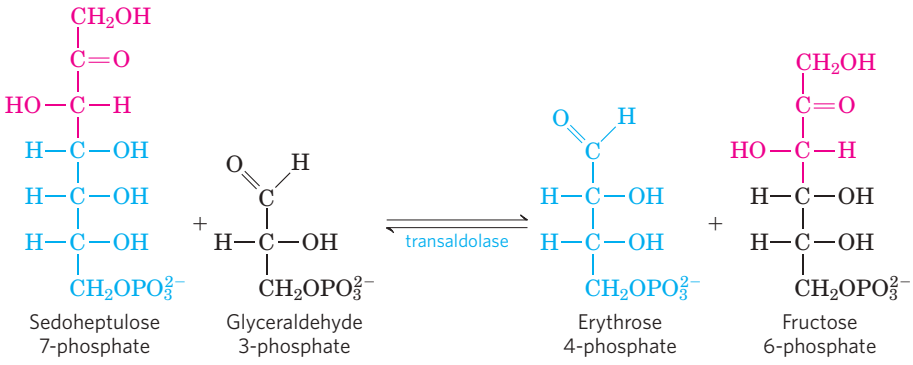

FIGURE 14–25 **The reaction catalyzed by transaldolase.**

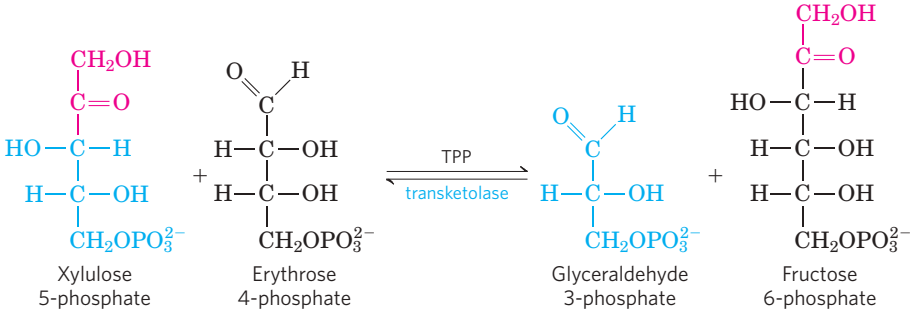

FIGURE 14–26 **The second reaction catalyzed by transketolase.**

reactions can be converted to a molecule of fructose 1,6-bisphosphate as in gluconeogenesis (Fig. 14–17), and finally FBPase-1 and phosphohexose isomerase convert fructose 1,6-bisphosphate to glucose 6-phosphate. Overall, six pentose phosphates have been converted to five hexose phosphates (Fig. 14–23b)—the cycle is now complete!

Transketolase requires the cofactor thiamine pyrophosphate (TPP), which stabilizes a two-carbon carbanion in this reaction **(Fig. 14–27a)**, just as it does in the pyruvate decarboxylase reaction (Fig. 14–15). Transaldolase uses a Lys side chain to form a Schiff base with the carbonyl group of its substrate, a ketose, thereby stabilizing a carbanion (Fig. 14–27b) that is central to the reaction mechanism.

The process described in Figure 14–22 is known as the **oxidative pentose phosphate pathway**. The first and third steps are oxidations with large, negative standard free-energy changes and are essentially irreversible in the cell. The reactions of the nonoxidative part of the pentose phosphate pathway (Fig. 14–23) are readily reversible and thus also provide a means of converting hexose phosphates to pentose phosphates. As we shall see in Chapter 20, a process that converts hexose phosphates to pentose phosphates is crucial to the photosynthetic assimilation of CO_2 by plants. That pathway, the **reductive pentose phosphate pathway**, is essentially the reversal of the reactions shown in Figure 14–23 and employs many of the same enzymes.

All the enzymes in the pentose phosphate pathway are located in the cytosol, like those of glycolysis and most of those of gluconeogenesis. In fact, these three pathways are connected through several shared intermediates and enzymes. The glyceraldehyde 3-phosphate formed by the action of transketolase is readily

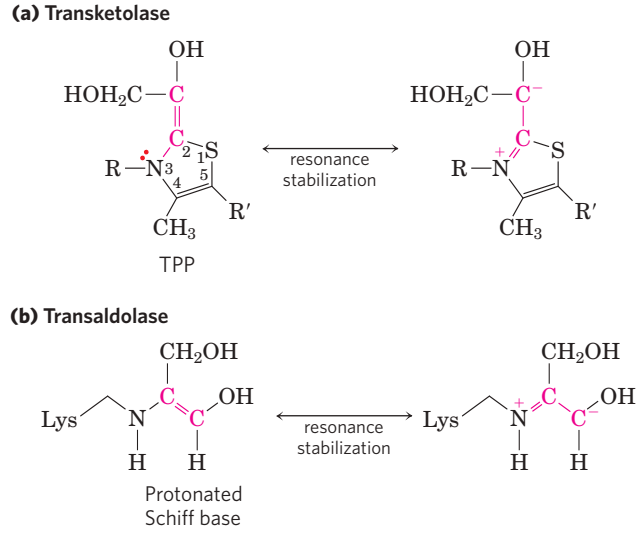

FIGURE 14–27 **Carbanion intermediates stabilized by covalent interactions with transketolase and transaldolase. (a)** The ring of TPP stabilizes the carbanion in the dihydroxyethyl group carried by transketolase; see Fig. 14–15 for the chemistry of TPP action. **(b)** In the transaldolase reaction, the protonated Schiff base formed between the ε-amino group of a Lys side chain and the substrate stabilizes the C-3 carbanion formed after aldol cleavage.

converted to dihydroxyacetone phosphate by the glycolytic enzyme triose phosphate isomerase, and these two trioses can be joined by the aldolase as in gluconeogenesis, forming fructose 1,6-bisphosphate. Alternatively, the triose phosphates can be oxidized to pyruvate by the glycolytic reactions. The fate of the trioses is determined by the cell's relative needs for pentose phosphates, NADPH, and ATP.

Wernicke-Korsakoff Syndrome Is Exacerbated by a Defect in Transketolase

Wernicke-Korsakoff syndrome is a disorder caused by a severe deficiency of thiamine, a component of TPP. The syndrome is more common among people with alcoholism than in the general population, because chronic, heavy alcohol consumption interferes with the intestinal absorption of thiamine. The syndrome can be exacerbated by a mutation in the gene for transketolase that results in an enzyme with a lowered affinity for TPP—an affinity one-tenth that of the normal enzyme. This defect makes individuals much more sensitive to a thiamine deficiency: even a moderate thiamine deficiency (tolerable in individuals with an unmutated transketolase) can drop the level of TPP below that needed to saturate the enzyme. The result is a slowing down of the whole pentose phosphate pathway. In people with Wernicke-Korsakoff syndrome this results in a worsening of symptoms, which can include severe memory loss, mental confusion, and partial paralysis. ■

Glucose 6-Phosphate Is Partitioned between Glycolysis and the Pentose Phosphate Pathway

Whether glucose 6-phosphate enters glycolysis or the pentose phosphate pathway depends on the current needs of the cell and on the concentration of $NADP^+$ in the cytosol. Without this electron acceptor, the first reaction of the pentose phosphate pathway (catalyzed by G6PD) cannot proceed. When a cell is rapidly converting NADPH to $NADP^+$ in biosynthetic reductions, the level of $NADP^+$ rises, allosterically stimulating G6PD and thereby increasing the flux of glucose 6-phosphate through the pentose phosphate pathway **(Fig. 14–28)**. When the demand for NADPH slows, the level of $NADP^+$ drops, the pentose phosphate pathway slows, and glucose 6-phosphate is instead used to fuel glycolysis.

SUMMARY 14.5 Pentose Phosphate Pathway of Glucose Oxidation

- The *oxidative* pentose phosphate pathway (phosphogluconate pathway, or hexose monophosphate pathway) brings about oxidation and decarboxylation at C-1 of glucose 6-phosphate, reducing $NADP^+$ to NADPH and producing pentose phosphates.

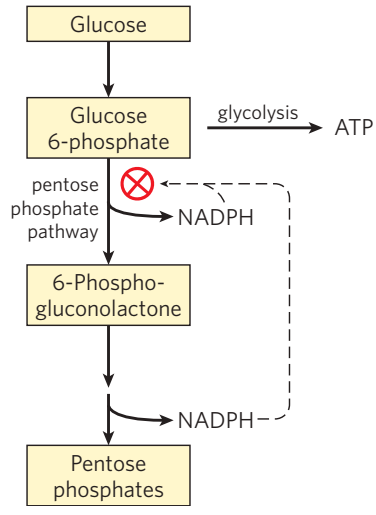

FIGURE 14–28 Role of NADPH in regulating the partitioning of glucose 6-phosphate between glycolysis and the pentose phosphate pathway. When NADPH is forming faster than it is being used for biosynthesis and glutathione reduction (see Fig. 14–21), [NADPH] rises and inhibits the first enzyme in the pentose phosphate pathway. As a result, more glucose 6-phosphate is available for glycolysis.

- NADPH provides reducing power for biosynthetic reactions, and ribose 5-phosphate is a precursor for nucleotide and nucleic acid synthesis. Rapidly growing tissues and tissues carrying out active biosynthesis of fatty acids, cholesterol, or steroid hormones send more glucose 6-phosphate through the pentose phosphate pathway than do tissues with less demand for pentose phosphates and reducing power.
- The first phase of the pentose phosphate pathway consists of two oxidations that convert glucose 6-phosphate to ribulose 5-phosphate and reduce $NADP^+$ to NADPH. The second phase comprises nonoxidative steps that convert pentose phosphates to glucose 6-phosphate, which begins the cycle again.
- In the second phase, transketolase (with TPP as cofactor) and transaldolase catalyze the interconversion of three-, four-, five-, six-, and seven-carbon sugars, with the reversible conversion of six pentose phosphates to five hexose phosphates. In the carbon-assimilating reactions of photosynthesis, the same enzymes catalyze the reverse process, the *reductive* pentose phosphate pathway: conversion of five hexose phosphates to six pentose phosphates.
- A genetic defect in transketolase that lowers its affinity for TPP exacerbates the Wernicke-Korsakoff syndrome.
- Entry of glucose 6-phosphate either into glycolysis or into the pentose phosphate pathway is largely determined by the relative concentrations of $NADP^+$ and NADPH.

Key Terms

Terms in bold are defined in the glossary.

glycolysis 544
fermentation 544
lactic acid fermentation 546
hypoxia 546
ethanol (alcohol) fermentation 546
isozymes 549
acyl phosphate 552
substrate-level phosphorylation 553
respiration-linked phosphorylation 553
phosphoenolpyruvate (PEP) 554
mutases 560
isomerases 560
lactose intolerance 561
galactosemia 562
thiamine pyrophosphate (TPP) 565
gluconeogenesis 568
biotin 570
pentose phosphate pathway 575
phosphogluconate pathway 575
hexose monophosphate pathway 575

Further Reading

General

Fruton, J.S. (1999) *Proteins, Genes, and Enzymes: The Interplay of Chemistry and Biology*, Yale University Press, New Haven.
This text includes a detailed historical account of research on glycolysis.

Glycolysis

Boiteux, A. & Hess, B. (1981) Design of glycolysis. *Philos. Trans. R. Soc. Lond. Ser. B Biol. Sci.* **293**, 5–22.
Intermediate-level review of the pathway and the classic view of its control.

Dandekar, T., Schuster, S., Snel, B., Huynen, M., & Bork, P. (1999) Pathway alignment: application to the comparative analysis of glycolytic enzymes. *Biochem. J.* **343**, 115–124.
Intermediate-level review of the bioinformatic view of the evolution of glycolysis.

Dang, C.V. & Semenza, G.L. (1999) Oncogenic alterations of metabolism. *Trends Biochem. Sci.* **24**, 68–72.
Brief review of the molecular basis for increased glycolysis in tumors.

Erlandsen, H., Abola, E.E., & Stevens, R.C. (2000) Combining structural genomics and enzymology: completing the picture in metabolic pathways and enzyme active sites. *Curr. Opin. Struct. Biol.* **10**, 719–730.
Intermediate-level review of the structures of the glycolytic enzymes.

Gatenby, R.A. & Gillies, R.J. (2004) Why do cancers have high aerobic glycolysis? *Nat. Rev. Cancer* **4**, 891–899.

Hardie, D.G. (2000) Metabolic control: a new solution to an old problem. *Curr. Biol.* **10**, R757–R759.

Harris, A.L. (2002) Hypoxia—a key regulatory factor in tumour growth. *Nat. Rev. Cancer* **2**, 38–47.

Heinrich, R., Melendez-Hevia, E., Montero, F., Nuno, J.C., Stephani, A., & Waddell, T.D. (1999) The structural design of glycolysis: an evolutionary approach. *Biochem. Soc. Trans.* **27**, 294–298.

Herling, A., König, M., Bulik, S., & Holzhütter, H.G. (2011) Enzymatic features of the glucose metabolism in tumor cells. *FEBS J.* **278**, 2436–2459.

Keith, B. & Simon, M.C. (2007) Hypoxia-inducible factors, stem cells, and cancer. *Cell* **129**, 465–472.
Intermediate-level review.

Knowles, J. & Albery, W.J. (1977) Perfection in enzyme catalysis: the energetics of triose phosphate isomerase. *Acc. Chem. Res.* **10**, 105–111.

Kresge, N., Simoni, R.D., & Hill, R.L. (2005) Otto Fritz Meyerhof and the elucidation of the glycolytic pathway. *J. Biol. Chem.* **280**, e3.
Brief review of classic papers, which are also available online.

Kritikou, E. (2006) p53 turns on the energy switch. *Nat. Rev. Mol. Cell Biol.* **7**, 552–553.

Pelicano, H., Martin, D.S., Zu, R-H., & Huang, P. (2006) Glycolysis inhibition for anticancer treatment. *Oncogene* **25**, 4633–4646.
Intermediate-level review.

Phillips, D., Blake, C.C.F., & Watson, H.C. (eds). (1981) The Enzymes of Glycolysis: Structure, Activity and Evolution. *Philos. Trans. R. Soc. Lond. Ser. B Biol. Sci.* **293**, 1–214.
A collection of excellent reviews on the enzymes of glycolysis, written at a level challenging but comprehensible to a beginning student of biochemistry.

Plaxton, W.C. (1996) The organization and regulation of plant glycolysis. *Annu. Rev. Plant Physiol. Plant Mol. Biol.* **47**, 185–214.
Very helpful review of the subcellular localization of glycolytic enzymes and the regulation of glycolysis in plants.

Rose, I. (1981) Chemistry of proton abstraction by glycolytic enzymes (aldolase, isomerases, and pyruvate kinase). *Philos. Trans. R. Soc. Lond. Ser. B Biol. Sci.* **293**, 131–144.
Intermediate-level review of the mechanisms of these enzymes.

Shirmer, T. & Evans, P.R. (1990) Structural basis for the allosteric behavior of phosphofructokinase. *Nature* **343**, 140–145.

Smith, T.A. (2000) Mammalian hexokinases and their abnormal expression in cancer. *Br. J. Biomed. Sci.* **57**, 170–178.
A review of the four hexokinase isozymes of mammals: their properties and tissue distributions and their expression during the development of tumors.

Feeder Pathways for Glycolysis

Elsas, L.J. & Lai, K. (1998) The molecular biology of galactosemia. *Genet. Med.* **1**, 40–48.

Novelli, G. & Reichardt, J.K. (2000) Molecular basis of disorders of human galactose metabolism: past, present, and future. *Mol. Genet. Metab.* **71**, 62–65.

Petry, K.G. & Reichardt, J.K. (1998) The fundamental importance of human galactose metabolism: lessons from genetics and biochemistry. *Trends Genet.* **14**, 98–102.

Van Beers, E.H., Buller, H.A., Grand, R.J., Einerhand, A.W.C., & Dekker, J. (1995) Intestinal brush border glycohydrolases: structure, function, and development. *Crit. Rev. Biochem. Mol. Biol.* **30**, 197–262.

Fermentations

Demain, A.L., Davies, J.E., Atlas, R.M., Cohen, G., Hershberger, C.L., Hu, W.-S., Sherman, D.H., Willson, R.C., & Wu, J.H.D. (eds). (1999) *Manual of Industrial Microbiology and Biotechnology*, American Society for Microbiology, Washington, DC.
Classic introduction to all aspects of industrial fermentations.

Liese, A., Seelbach, K., & Wandrey, C. (eds). (2006) *Industrial Biotransformations*, John Wiley & Sons, New York.
The use of microorganisms in industry for the synthesis of valuable products from inexpensive starting materials.

Sticklen, M.B. (2008) Plant genetic engineering for biofuel production: towards affordable cellulosic ethanol. *Nat. Rev. Genet.* **9**, 433–443.

Gluconeogenesis

Aschenback, J.R., Kristensen, N.B., Donkin, S.S., Hammon, H.M., & Penner, G.B. (2010) Gluconeogenesis in dairy cows: the secret of making sweet milk from sour dough. *IUBMB Life* **62**, 869–877.

Gerich, J.E., Meyer, C., Woerle, H.J., & Stumvoll, M. (2001) Renal gluconeogenesis: its importance in human glucose homeostasis. *Diabetes Care* **24**, 382–391.

Intermediate-level review of the contribution of kidney tissue to gluconeogenesis.

Gleeson, T. (1996) Post-exercise lactate metabolism: a comparative review of sites, pathways, and regulation. *Annu. Rev. Physiol.* **58**, 565–581.

Hers, H.G. & Hue, L. (1983) Gluconeogenesis and related aspects of glycolysis. *Annu. Rev. Biochem.* **52**, 617–653.

Matte, A., Tari, L.W., Goldie, H., & Delbaere, L.T.J. (1997) Structure and mechanism of phosphoenolpyruvate carboxykinase. *J. Biol. Chem.* **272**, 8105–8108.

Oxidative Pentose Phosphate Pathway

Chayen, J., Howat, D.W., & Bitensky, L. (1986) Cellular biochemistry of glucose 6-phosphate and 6-phosphogluconate dehydrogenase activities. *Cell Biochem. Funct.* **4**, 249–253.

Horecker, B.L. (1976) Unraveling the pentose phosphate pathway. In *Reflections on Biochemistry* (Kornberg, A., Cornudella, L., Horecker, B.L., & Oro, J., eds), pp. 65–72, Pergamon Press, Inc., Oxford.

Kletzien, R.F., Harris, P.K., & Foellmi, L.A. (1994) Glucose 6-phosphate dehydrogenase: a "housekeeping" enzyme subject to tissue-specific regulation by hormones, nutrients, and oxidant stress. *FASEB J.* **8**, 174–181.

An intermediate-level review.

Kresge, N., Simoni, R.D., & Hill, R.L. (2005) Bernard L. Horecker's contributions to elucidating the pentose phosphate pathway. *J. Biol. Chem.* **280**, e26.

Brief review of classic papers, which are also available online.

Martini, G. & Ursini, M.V. (1996) A new lease on life for an old enzyme. *BioEssays* **18**, 631–637.

An intermediate-level review of glucose 6-phosphate dehydrogenase, the effects of mutations in this enzyme in humans, and the effects of knock-out mutations in mice.

Notaro, R., Afolayan, A., & Luzzatto, L. (2000) Human mutations in glucose 6-phosphate dehydrogenase reflect evolutionary history. *FASEB J.* **14**, 485–494.

Perl, A., Hanczko, R., Relarico, T., Oaks, Z., & Landas, S. (2011) Oxidative stress, inflammation and carcinogenesis are controlled through the pentose phosphate pathway by transaldolase. *Trends Mol. Med.* **17**, 395–403.

Saggerson, D. (2009) Getting to grips with the pentose phosphate pathway in 1953. *Biochem J.* (doi:10.1042/BJ20081961).

Vulliamy, T., Mehta, A., Luzzatto, L. (2006) Glucose 6-Phosphate Dehydrogenas Deficiency. In *Scriver's Online Metabolic and Molecular Bases of Inherited Disease* (Valle, D., Beaudet, A.L., Vogelstein, B., Kinzler, K.W., Antonarakis, S.E., Ballabio, A., eds) (http://dx.doi.org/10.1036/ommbid.212).

This classic medical encyclopedia, last published in 2001 as a four-volume set, is now maintained online (www.ommbid.com). It contains definitive descriptions of the clinical, biochemical, and genetic aspects of hundreds of human metabolic diseases—an authoritative source and fascinating reading.

Wood, T. (1985) *The Pentose Phosphate Pathway*, Academic Press, Inc., Orlando, FL.

Wood, T. (1986) Physiological functions of the pentose phosphate pathway. *Cell Biochem. Funct.* **4**, 241–247.

Problems

1. Equation for the Preparatory Phase of Glycolysis Write balanced biochemical equations for all the reactions in the catabolism of glucose to two molecules of glyceraldehyde 3-phosphate (the preparatory phase of glycolysis), including the standard free-energy change for each reaction. Then write the overall or net equation for the preparatory phase of glycolysis, with the net standard free-energy change.

2. The Payoff Phase of Glycolysis in Skeletal Muscle In working skeletal muscle under anaerobic conditions, glyceraldehyde 3-phosphate is converted to pyruvate (the payoff phase of glycolysis), and the pyruvate is reduced to lactate. Write balanced biochemical equations for all the reactions in this process, with the standard free-energy change for each reaction. Then write the overall or net equation for the payoff phase of glycolysis (with lactate as the end product), including the net standard free-energy change.

3. GLUT Transporters Compare the localization of GLUT4 with that of GLUT2 and GLUT3, and explain why these localizations are important in the response of muscle, adipose tissue, brain, and liver to insulin.

4. Ethanol Production in Yeast When grown anaerobically on glucose, yeast (*S. cerevisiae*) converts pyruvate to acetaldehyde, then reduces acetaldehyde to ethanol using electrons from NADH. Write the equation for the second reaction, and calculate its equilibrium constant at 25°C, given the standard reduction potentials in Table 13–7.

5. Energetics of the Aldolase Reaction Aldolase catalyzes the glycolytic reaction

Fructose 1,6-bisphosphate ⟶
glyceraldehyde 3-phosphate + dihydroxyacetone phosphate

The standard free-energy change for this reaction in the direction written is +23.8 kJ/mol. The concentrations of the three intermediates in the hepatocyte of a mammal are: fructose 1,6-bisphosphate, 1.4×10^{-5} M; glyceraldehyde 3-phosphate, 3×10^{-6} M; and dihydroxyacetone phosphate, 1.6×10^{-5} M. At body temperature (37°C), what is the actual free-energy change for the reaction?

6. Pathway of Atoms in Fermentation A "pulse-chase" experiment using ^{14}C-labeled carbon sources is carried out on a yeast extract maintained under strictly anaerobic conditions to produce ethanol. The experiment consists of incubating a small amount of ^{14}C-labeled substrate (the pulse) with the yeast extract just long enough for each intermediate in the fermentation pathway to become labeled. The label is then

"chased" through the pathway by the addition of excess unlabeled glucose. The chase effectively prevents any further entry of labeled glucose into the pathway.

(a) If [1-^{14}C]glucose (glucose labeled at C-1 with ^{14}C) is used as a substrate, what is the location of ^{14}C in the product ethanol? Explain.

(b) Where would ^{14}C have to be located in the starting glucose to ensure that all the ^{14}C activity is liberated as $^{14}CO_2$ during fermentation to ethanol? Explain.

7. Heat from Fermentations Large-scale industrial fermenters generally require constant, vigorous cooling. Why?

8. Fermentation to Produce Soy Sauce Soy sauce is prepared by fermenting a salted mixture of soybeans and wheat with several microorganisms, including yeast, over a period of 8 to 12 months. The resulting sauce (after solids are removed) is rich in lactate and ethanol. How are these two compounds produced? To prevent the soy sauce from having a strong vinegary taste (vinegar is dilute acetic acid), oxygen must be kept out of the fermentation tank. Why?

9. Equivalence of Triose Phosphates ^{14}C-Labeled glyceraldehyde 3-phosphate was added to a yeast extract. After a short time, fructose 1,6-bisphosphate labeled with ^{14}C at C-3 and C-4 was isolated. What was the location of the ^{14}C label in the starting glyceraldehyde 3-phosphate? Where did the second ^{14}C label in fructose 1,6-bisphosphate come from? Explain.

10. Glycolysis Shortcut Suppose you discovered a mutant yeast whose glycolytic pathway was shorter because of the presence of a new enzyme catalyzing the reaction

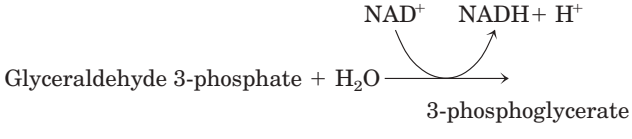

Would shortening the glycolytic pathway in this way benefit the cell? Explain.

11. Role of Lactate Dehydrogenase During strenuous activity, the demand for ATP in muscle tissue is vastly increased. In rabbit leg muscle or turkey flight muscle, the ATP is produced almost exclusively by lactic acid fermentation. ATP is formed in the payoff phase of glycolysis by two reactions, promoted by phosphoglycerate kinase and pyruvate kinase. Suppose skeletal muscle were devoid of lactate dehydrogenase. Could it carry out strenuous physical activity; that is, could it generate ATP at a high rate by glycolysis? Explain.

12. Efficiency of ATP Production in Muscle The transformation of glucose to lactate in myocytes releases only about 7% of the free energy released when glucose is completely oxidized to CO_2 and H_2O. Does this mean that anaerobic glycolysis in muscle is a wasteful use of glucose? Explain.

13. Free-Energy Change for Triose Phosphate Oxidation The oxidation of glyceraldehyde 3-phosphate to 1,3-bisphosphoglycerate, catalyzed by glyceraldehyde 3-phosphate dehydrogenase, proceeds with an unfavorable equilibrium constant ($K'_{eq} = 0.08$; $\Delta G'° = 6.3$ kJ/mol), yet the flow through this point in the glycolytic pathway proceeds smoothly. How does the cell overcome the unfavorable equilibrium?

14. Arsenate Poisoning Arsenate is structurally and chemically similar to inorganic phosphate (P_i), and many enzymes that require phosphate will also use arsenate. Organic compounds of arsenate are less stable than analogous phosphate compounds, however. For example, acyl *arsenates* decompose rapidly by hydrolysis:

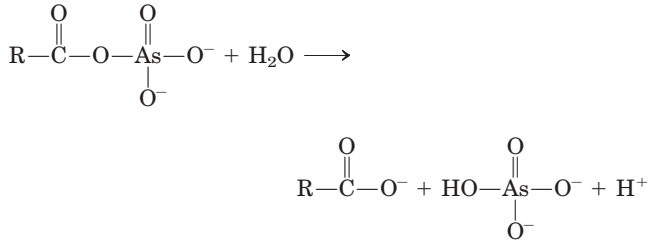

On the other hand, acyl *phosphates*, such as 1,3-bisphosphoglycerate, are more stable and undergo further enzyme-catalyzed transformation in cells.

(a) Predict the effect on the net reaction catalyzed by glyceraldehyde 3-phosphate dehydrogenase if phosphate were replaced by arsenate.

(b) What would be the consequence to an organism if arsenate were substituted for phosphate? Arsenate is very toxic to most organisms. Explain why.

15. Requirement for Phosphate in Ethanol Fermentation In 1906 Harden and Young, in a series of classic studies on the fermentation of glucose to ethanol and CO_2 by extracts of brewer's yeast, made the following observations. (1) Inorganic phosphate was essential to fermentation; when the supply of phosphate was exhausted, fermentation ceased before all the glucose was used. (2) During fermentation under these conditions, ethanol, CO_2, and a hexose bisphosphate accumulated. (3) When arsenate was substituted for phosphate, no hexose bisphosphate accumulated, but the fermentation proceeded until all the glucose was converted to ethanol and CO_2.

(a) Why did fermentation cease when the supply of phosphate was exhausted?

(b) Why did ethanol and CO_2 accumulate? Was the conversion of pyruvate to ethanol and CO_2 essential? Why? Identify the hexose bisphosphate that accumulated. Why did it accumulate?

(c) Why did the substitution of arsenate for phosphate prevent the accumulation of the hexose bisphosphate yet allow fermentation to ethanol and CO_2 to go to completion? (See Problem 14.)

16. Role of the Vitamin Niacin Adults engaged in strenuous physical activity require an intake of about 160 g of carbohydrate daily but only about 20 mg of niacin for optimal nutrition. Given the role of niacin in glycolysis, how do you explain the observation?

17. Synthesis of Glycerol Phosphate The glycerol 3-phosphate required for the synthesis of glycerophospholipids can be synthesized from a glycolytic intermediate. Propose a reaction sequence for this conversion.

18. Severity of Clinical Symptoms Due to Enzyme Deficiency The clinical symptoms of two forms of galactosemia—deficiency of galactokinase or of UDP-glucose:galactose 1-phosphate uridylyltransferase—show radically different severity. Although both types produce gastric discomfort after milk ingestion, deficiency of the transferase also leads to liver, kidney, spleen, and brain dysfunction and eventual death. What products accumulate in the blood and tissues with each type of enzyme deficiency? Estimate the relative toxicities of these products from the above information.

19. Muscle Wasting in Starvation One consequence of starvation is a reduction in muscle mass. What happens to the muscle proteins?

20. Pathway of Atoms in Gluconeogenesis A liver extract capable of carrying out all the normal metabolic reactions of the liver is briefly incubated in separate experiments with the following ^{14}C-labeled precursors.

(a) [^{14}C]Bicarbonate, $HO-{}^{14}C(=O)-O^-$

(b) [1-^{14}C]Pyruvate, $CH_3-C(=O)-{}^{14}COO^-$

Trace the pathway of each precursor through gluconeogenesis. Indicate the location of ^{14}C in all intermediates and in the product, glucose.

21. Energy Cost of a Cycle of Glycolysis and Gluconeogenesis What is the cost (in ATP equivalents) of transforming glucose to pyruvate via glycolysis and back again to glucose via gluconeogenesis?

22. Relationship between Gluconeogenesis and Glycolysis Why is it important that gluconeogenesis is not the exact reversal of glycolysis?

23. Energetics of the Pyruvate Kinase Reaction Explain in bioenergetic terms how the conversion of pyruvate to phosphoenolpyruvate in gluconeogenesis overcomes the large, negative, standard free-energy change of the pyruvate kinase reaction in glycolysis.

24. Glucogenic Substrates A common procedure for determining the effectiveness of compounds as precursors of glucose in mammals is to starve the animal until the liver glycogen stores are depleted and then administer the compound in question. A substrate that leads to a *net* increase in liver glycogen is termed glucogenic, because it must first be converted to glucose 6-phosphate. Show by means of known enzymatic reactions which of the following substances are glucogenic.

(a) Succinate, $^-OOC-CH_2-CH_2-COO^-$

(b) Glycerol, $CH_2(OH)-CH(OH)-CH_2(OH)$

(c) Acetyl-CoA, $CH_3-C(=O)-S\text{-}CoA$

(d) Pyruvate, $CH_3-C(=O)-COO^-$

(e) Butyrate, $CH_3-CH_2-CH_2-COO^-$

25. Ethanol Affects Blood Glucose Levels The consumption of alcohol (ethanol), especially after periods of strenuous activity or after not eating for several hours, results in a deficiency of glucose in the blood, a condition known as hypoglycemia. The first step in the metabolism of ethanol by the liver is oxidation to acetaldehyde, catalyzed by liver alcohol dehydrogenase:

$$CH_3CH_2OH + NAD^+ \longrightarrow CH_3CHO + NADH + H^+$$

Explain how this reaction inhibits the transformation of lactate to pyruvate. Why does this lead to hypoglycemia?

26. Blood Lactate Levels during Vigorous Exercise The concentrations of lactate in blood plasma before, during, and after a 400 m sprint are shown in the graph.

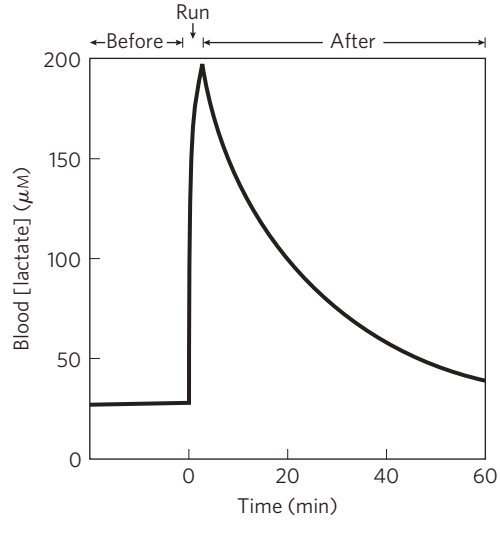

(a) What causes the rapid rise in lactate concentration?

(b) What causes the decline in lactate concentration after completion of the sprint? Why does the decline occur more slowly than the increase?

(c) Why is the concentration of lactate not zero during the resting state?

27. Relationship between Fructose 1,6-Bisphosphatase and Blood Lactate Levels A congenital defect in the liver enzyme fructose 1,6-bisphosphatase results in abnormally high levels of lactate in the blood plasma. Explain.

28. Effect of Phloridzin on Carbohydrate Metabolism Phloridzin, a toxic glycoside from the bark of the pear tree, blocks the normal reabsorption of glucose from the kidney tubule, thus

causing blood glucose to be almost completely excreted in the urine. In an experiment, rats fed phloridzin and sodium succinate excreted about 0.5 mol of glucose (made by gluconeogenesis) for every 1 mol of sodium succinate ingested. How is the succinate transformed to glucose? Explain the stoichiometry.

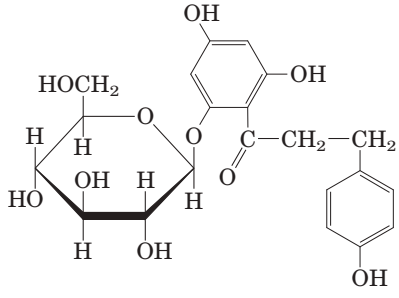

Phloridzin

29. Excess O_2 Uptake during Gluconeogenesis Lactate absorbed by the liver is converted to glucose, with the input of 6 mol of ATP for every mole of glucose produced. The extent of this process in a rat liver preparation can be monitored by administering [^{14}C]lactate and measuring the amount of [^{14}C]glucose produced. Because the stoichiometry of O_2 consumption and ATP production is known (about 5 ATP per O_2), we can predict the extra O_2 consumption above the normal rate when a given amount of lactate is administered. However, when the extra O_2 used in the synthesis of glucose from lactate is actually measured, it is always higher than predicted by known stoichiometric relationships. Suggest a possible explanation for this observation.

30. Role of the Pentose Phosphate Pathway If the oxidation of glucose 6-phosphate via the pentose phosphate pathway were being used primarily to generate NADPH for biosynthesis, the other product, ribose 5-phosphate, would accumulate. What problems might this cause?

Data Analysis Problem

31. Engineering a Fermentation System Fermentation of plant matter to produce ethanol for fuel is one potential method for reducing the use of fossil fuels and thus the CO_2 emissions that lead to global warming. Many microorganisms can break down cellulose then ferment the glucose to ethanol. However, many potential cellulose sources, including agricultural residues and switchgrass, also contain substantial amounts of arabinose, which is not as easily fermented.

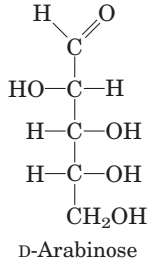

D-Arabinose

Escherichia coli is capable of fermenting arabinose to ethanol, but it is not naturally tolerant of high ethanol levels, thus limiting its utility for commercial ethanol production. Another bacterium, *Zymomonas mobilis,* is naturally tolerant of high levels of ethanol but cannot ferment arabinose. Deanda, Zhang, Eddy, and Picataggio (1996) described their efforts to combine the most useful features of these two organisms by introducing the *E. coli* genes for the arabinose-metabolizing enzymes into *Z. mobilis.*

(a) Why is this a simpler strategy than the reverse: engineering *E. coli* to be more ethanol-tolerant?

Deanda and colleagues inserted five *E. coli* genes into the *Z. mobilis* genome: *araA*, coding for L-arabinose isomerase, which interconverts L-arabinose and L-ribulose; *araB*, L-ribulokinase, which uses ATP to phosphorylate L-ribulose at C-5; *araD*, L-ribulose 5-phosphate epimerase, which interconverts L-ribulose 5-phosphate and L-xylulose 5-phosphate; *talB*, transaldolase; and *tktA*, transketolase.

(b) For each of the three *ara* enzymes, briefly describe the chemical transformation it catalyzes and, where possible, name an enzyme discussed in this chapter that carries out an analogous reaction.

The five *E. coli* genes inserted in *Z. mobilis* allowed the entry of arabinose into the nonoxidative phase of the pentose phosphate pathway (Fig. 14–23), where it was converted to glucose 6-phosphate and fermented to ethanol.

(c) The three *ara* enzymes eventually converted arabinose into which sugar?

(d) The product from part (c) feeds into the pathway shown in Figure 14–23. Combining the five *E. coli* enzymes listed above with the enzymes of this pathway, describe the overall pathway for the fermentation of six molecules of arabinose to ethanol.

(e) What is the stoichiometry of the fermentation of six molecules of arabinose to ethanol and CO_2? How many ATP molecules would you expect this reaction to generate?

(f) *Zymomonas mobilis* uses a slightly different pathway for ethanol fermentation from the one described in this chapter. As a result, the expected ATP yield is only 1 ATP per molecule of arabinose. Although this is less beneficial for the bacterium, it is better for ethanol production. Why?

Another sugar commonly found in plant matter is xylose.

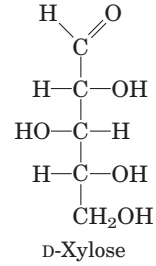

D-Xylose

(g) What additional enzymes would you need to introduce into the modified *Z. mobilis* strain described above to enable it to use xylose as well as arabinose to produce ethanol? You don't need to name the enzymes (they may not even exist in the real world!); just give the reactions they would need to catalyze.

Reference

Deanda, K., Zhang, M., Eddy, C., & Picataggio, S. (1996) Development of an arabinose-fermenting *Zymomonas mobilis* strain by metabolic pathway engineering. *Appl. Environ. Microbiol.* **62**, 4465–4470.

this page left intentionally blank

15

Principles of Metabolic Regulation

Metabolic regulation, a central theme in biochemistry, is one of the most remarkable features of living organisms. Of the thousands of enzyme-catalyzed reactions that can take place in a cell, there is probably not one that escapes some form of regulation. This need to regulate every aspect of cellular metabolism becomes clear as one examines the complexity of metabolic reaction sequences. Although it is convenient for the student of biochemistry to divide metabolic processes into "pathways" that play discrete roles in the cell's economy, no such separation exists in the living cell. Rather, every pathway we discuss in this book is inextricably intertwined with all the other cellular pathways in a multidimensional network of reactions **(Fig. 15–1)**. For example, in Chapter 14 we discussed four possible fates for **glucose 6-phosphate** in a hepatocyte: breakdown by glycolysis for the production of ATP, breakdown in the pentose phosphate pathway for the production of NADPH and pentose phosphates, use in the synthesis of complex polysaccharides of the extracellular matrix, or hydrolysis to glucose and phosphate to replenish blood glucose. In fact, glucose 6-phosphate has other possible fates in hepatocytes, too; it may, for example, be used to synthesize other sugars, such as glucosamine, galactose, galactosamine, fucose, and neuraminic acid, for use in protein glycosylation, or it may be partially degraded to provide acetyl-CoA for fatty acid and sterol synthesis. And the bacterium *Escherichia coli* can use glucose to produce the carbon skeleton of *every one* of its several thousand types of molecules. When any cell uses glucose 6-phosphate for one purpose, that "decision" affects all the other pathways for which glucose 6-phosphate is a precursor or intermediate: any change in the allocation of glucose 6-phosphate to one pathway affects, directly or indirectly, the flow of metabolites through all the others.

Such changes in allocation are common in the life of a cell. Louis Pasteur was the first to describe the more than 10-fold increase in glucose consumption by a yeast culture when it was shifted from aerobic to anaerobic conditions. This "Pasteur effect" occurs without a significant change in the concentrations of ATP or most of the hundreds of metabolic intermediates and products derived from glucose. A similar effect occurs in the cells of skeletal muscle when a sprinter leaves the starting blocks. The ability of a cell to carry out all these interlocking metabolic processes simultaneously—obtaining every product in the amount needed and at the right time, in the face of major perturbations from outside, and without generating leftovers—is an *astounding* accomplishment.

In this chapter we use the metabolism of glucose to illustrate some general principles of metabolic regulation. First we look at the general roles of regulation in achieving metabolic homeostasis and introduce metabolic control analysis, a system for analyzing complex metabolic interactions quantitatively. We then describe the specific regulatory properties of the individual enzymes of glucose metabolism; for glycolysis and gluconeogenesis, we described the catalytic activities of the enzymes in Chapter 14. Here we also discuss both the catalytic and regulatory properties of the enzymes of glycogen synthesis and breakdown, one of the best-studied cases of metabolic regulation. Note that in selecting carbohydrate metabolism to illustrate the principles of metabolic regulation, we have artificially separated the metabolism of fats and carbohydrates. In fact, these two activities are very tightly integrated, as we shall see in Chapter 23.

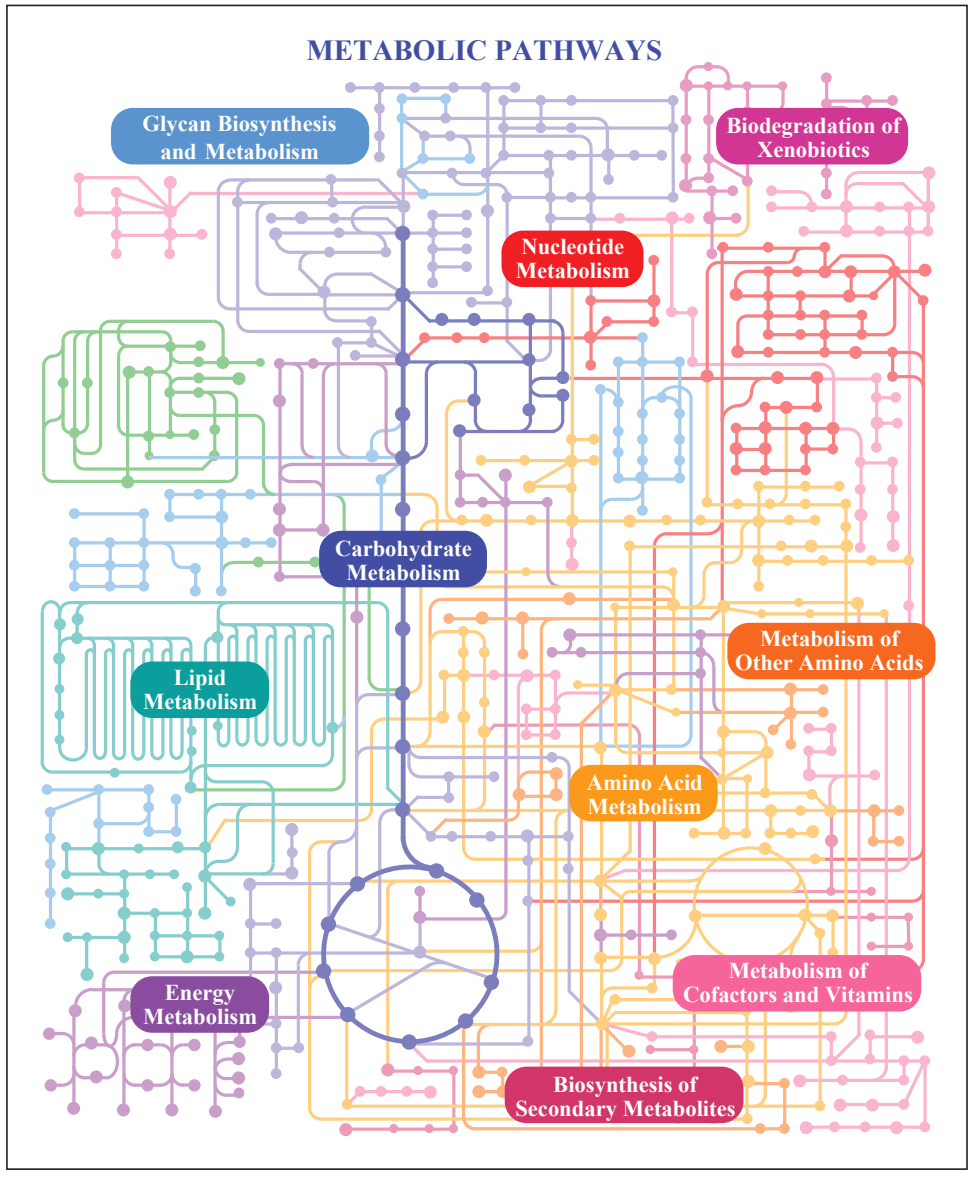

FIGURE 15–1 Metabolism as a three-dimensional meshwork. A typical eukaryotic cell has the capacity to make about 30,000 different proteins, which catalyze thousands of different reactions involving many hundreds of metabolites, most shared by more than one "pathway." In this much-simplified overview of metabolic pathways, each dot represents an intermediate compound and each connecting line represents an enzymatic reaction. For a more realistic and far more complex diagram of metabolism, see the online KEGG PATHWAY database (www.genome.ad.jp/kegg/pathway/map/map01100.html); in this interactive map, each dot can be clicked to obtain extensive data about the compound and the enzymes for which it is a substrate. The cover of this book shows the interlocking reactions that occur in the mitochondrion.

15.1 Regulation of Metabolic Pathways

The pathways of glucose metabolism provide, in the catabolic direction, the energy essential to oppose the forces of entropy and, in the anabolic direction, biosynthetic precursors and a storage form of metabolic energy. These reactions are so important to survival that very complex regulatory mechanisms have evolved to ensure that metabolites move through each pathway in the correct direction and at the correct rate to match exactly the cell's or the organism's changing circumstances. By a variety of mechanisms operating on different time scales, adjustments are made in the rate of metabolite flow through an entire pathway when external circumstances change.

Circumstances do change, sometimes dramatically. For example, the demand for ATP in insect flight muscle increases 100-fold in a few seconds when the insect takes flight. In humans, the availability of oxygen may decrease due to hypoxia (diminished delivery of oxygen to tissues) or ischemia (diminished flow of blood to tissues). The relative proportions of carbohydrate, fat, and protein in the diet vary from meal to meal, and the supply of fuels obtained in the diet is intermittent, requiring metabolic adjustments between meals and during periods of starvation. Wound healing

requires huge amounts of energy and biosynthetic precursors.

Cells and Organisms Maintain a Dynamic Steady State

Fuels such as glucose enter a cell, and waste products such as CO_2 leave, but the mass and the gross composition of a typical cell, organ, or adult animal do not change appreciably over time; cells and organisms exist in a dynamic steady state. For each metabolic reaction in a pathway, the substrate is provided by the preceding reaction at the same rate at which it is converted to product. Thus, although the rate (v) of metabolite flow, or **flux**, through this step of the pathway may be high and variable, the concentration of substrate, S, remains constant. So, for the two-step reaction

$$A \xrightarrow{v_1} S \xrightarrow{v_2} P$$

when $v_1 = v_2$, [S] is constant. For example, changes in v_1 for the entry of glucose from various sources into the blood are balanced by changes in v_2 for the uptake of glucose from the blood into various tissues, so the concentration of glucose in the blood ([S]) is held nearly constant at 5 mM. This is **homeostasis** at the molecular level. The failure of homeostatic mechanisms is often at the root of human disease. In diabetes mellitus, for example, the regulation of blood glucose concentration is defective as a result of the lack of or insensitivity to insulin, with profound medical consequences.

When the external perturbation is not merely transient, or when one kind of cell develops into another, the adjustments in cell composition and metabolism can be more dramatic and may require significant and lasting changes in the allocation of energy and synthetic precursors to bring about a new dynamic steady state. Consider, for example, the differentiation of stem cells in the bone marrow into erythrocytes. The precursor cell contains a nucleus, mitochondria, and little or no hemoglobin, whereas the fully differentiated erythrocyte contains prodigious amounts of hemoglobin but has neither nucleus nor mitochondria; the cell's composition has permanently changed in response to external developmental signals, with accompanying changes in metabolism. This **cellular differentiation** requires precise regulation of the levels of cellular proteins.

In the course of evolution, organisms have acquired a remarkable collection of regulatory mechanisms for maintaining homeostasis at the molecular, cellular, and organismal levels, as reflected in the proportion of genes that encode regulatory machinery. In humans, about 4,000 genes (~12% of all genes) encode regulatory proteins, including a variety of receptors, regulators of gene expression, and more than 500 different protein kinases! In many cases, the regulatory mechanisms overlap: one enzyme is subject to regulation by several different mechanisms.

Both the Amount and the Catalytic Activity of an Enzyme Can Be Regulated

The flux through an enzyme-catalyzed reaction can be modulated by changes in the *number* of enzyme molecules or by changes in the *catalytic activity* of each enzyme molecule already present. Such changes occur on time scales from milliseconds to many hours, in response to signals from within or outside the cell. Very rapid allosteric changes in enzyme activity are generally triggered locally, by changes in the local concentration of a small molecule—a substrate of the pathway in which that reaction is a step (say, glucose for glycolysis), a product of the pathway (ATP from glycolysis), or a key metabolite or cofactor (such as NADH) that indicates the cell's metabolic state. Second messengers (such as cyclic AMP and Ca^{2+}) generated intracellularly in response to extracellular signals (hormones, cytokines, and so forth) also mediate allosteric regulation, on a slightly slower time scale set by the rate of the signal-transduction mechanism (see Chapter 12).

Extracellular signals (**Fig. 15–2**, ❶) may be hormonal (insulin or epinephrine, for example) or neuronal (acetylcholine), or may be growth factors or cytokines. The number of molecules of a given enzyme in a cell is a function of the relative rates of synthesis and degradation of that enzyme. The rate of synthesis can be adjusted by the activation (in response to some outside signal) of a transcription factor (Fig. 15–2, ❷; described in more detail in Chapter 28). **Transcription factors** are nuclear proteins that, when activated, bind specific DNA regions (**response elements**) near a gene's promoter (its transcriptional starting point) and activate or repress the transcription of that gene, leading to increased or decreased synthesis of the encoded protein. Activation of a transcription factor is sometimes the result of its binding of a specific ligand and sometimes the result of its phosphorylation or dephosphorylation. Each gene is controlled by one or more response elements that are recognized by specific transcription factors. Genes that have several response elements are therefore controlled by several different transcription factors responding to several different signals. Groups of genes encoding proteins that act together, such as the enzymes of glycolysis or gluconeogenesis, often share common response element sequences, so that a single signal, acting through a particular transcription factor, turns all of these genes on and off together. The regulation of carbohydrate metabolism by specific transcription factors is described in Section 15.3.

The stability of messenger RNAs—their resistance to degradation by cellular ribonucleases (Fig. 15–2, ❸)—varies, and the amount of a given mRNA in the cell is a function of its rates of synthesis and degradation (Chapter 26). The rate at which an mRNA is translated into a protein by ribosomes (Fig. 15–2, ❹) is also regulated, and depends on several factors described in detail in Chapter 27. Note that an n-fold increase in an mRNA

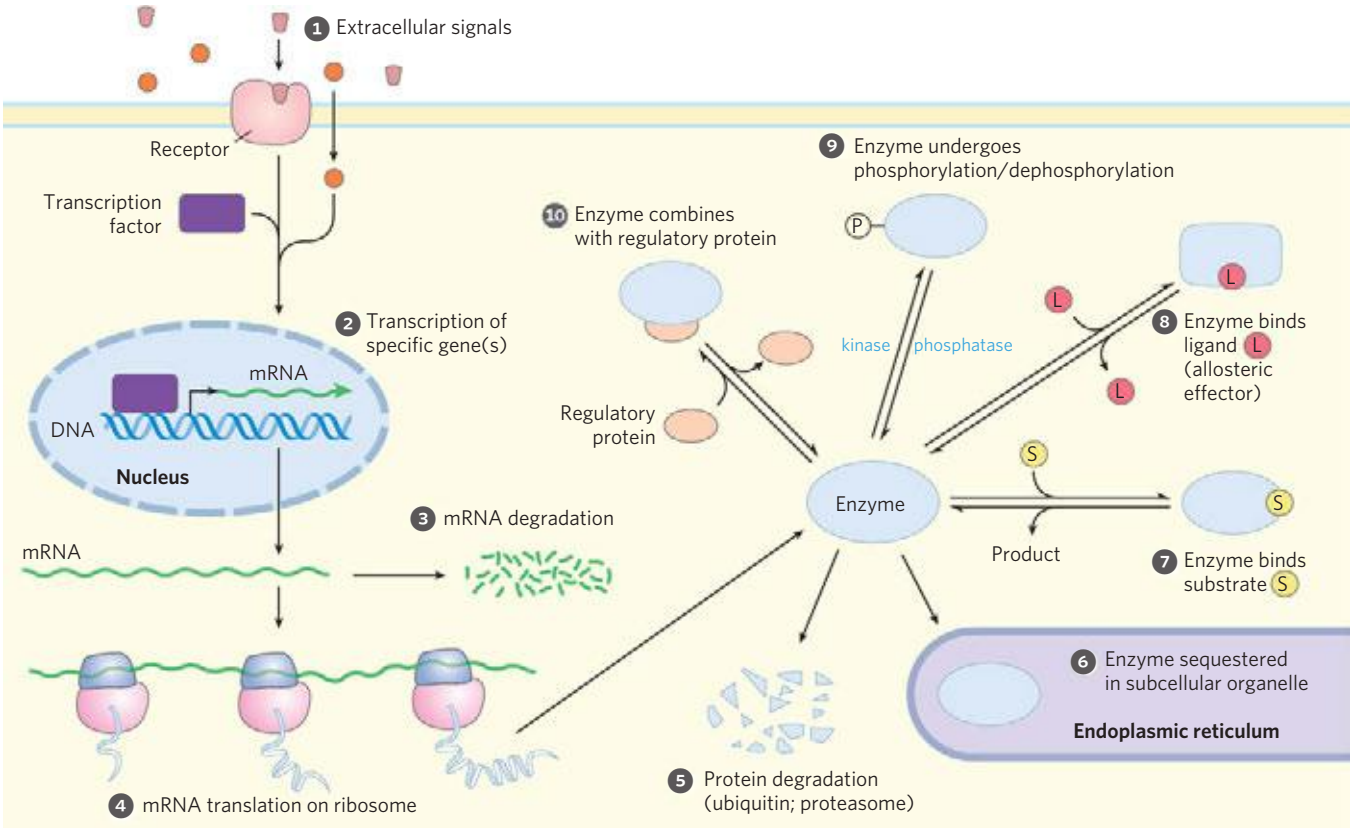

FIGURE 15–2 Factors affecting the activity of enzymes. The total activity of an enzyme can be changed by altering the *number* of its molecules in the cell, or its *effective* activity in a subcellular compartment (❶ through ❻), or by modulating the *activity* of existing molecules (❼ through ❿), as detailed in the text. An enzyme may be influenced by a combination of such factors.

does not always mean an n-fold increase in its protein product.

Once synthesized, protein molecules have a finite lifetime, which may range from minutes to many days (Table 15–1). The rate of protein degradation (Fig. 15–2, ❺) differs from one enzyme to another and depends on the conditions in the cell. Some proteins are tagged by the covalent attachment of ubiquitin for degradation in proteasomes, as discussed in Chapter 27 (see, for example, the case of cyclin, in Fig. 12–47). Rapid **turnover** (synthesis followed by degradation) is energetically expensive, but proteins with a short half-life can reach new steady state levels much faster than those with a long half-life, and the benefit of this quick responsiveness must balance or outweigh the cost to the cell.

TABLE 15–1 Average Half-Life of Proteins in Mammalian Tissues

Tissue	Average half-life (days)
Liver	0.9
Kidney	1.7
Heart	4.1
Brain	4.6
Muscle	10.7

Yet another way to alter the *effective* activity of an enzyme is to sequester the enzyme and its substrate in different compartments (Fig. 15–2, ❻). In muscle, for example, hexokinase cannot act on glucose until the sugar enters the myocyte from the blood, and the rate at which it enters depends on the activity of glucose transporters (see Table 11–3) in the plasma membrane. Within cells, membrane-bounded compartments segregate certain enzymes and enzyme systems, and the transport of substrate across these intracellular membranes may be the limiting factor in enzyme action.

By these several mechanisms for regulating enzyme level, cells can dramatically change their complement of enzymes in response to changes in metabolic circumstances. In vertebrates, liver is the most adaptable tissue; a change from a high-carbohydrate to a high-lipid diet, for example, affects the transcription of hundreds of genes and thus the levels of hundreds of proteins. These global changes in gene expression can be quantified by the use of DNA microarrays (see Fig. 9–23) that display the entire complement of mRNAs present in a given cell type or organ (the **transcriptome**) or by two-dimensional gel electrophoresis (see Fig. 3–21) that displays the protein complement of a cell type or organ (its **proteome**). Both techniques offer great insights into metabolic regulation. The effect of changes in the proteome is often a change in the total ensemble

of low molecular weight metabolites, the **metabolome (Fig. 15–3)**. The metabolome of *E. coli* growing on glucose is dominated by a few classes of metabolites: glutamate (49%); nucleotides (mainly ribonucleoside triphosphates) (15%); intermediates of glycolysis, the citric acid cycle, and the pentose phosphate pathway (central pathways of carbon metabolism) (15%); and redox cofactors and glutathiones (9%).

Once the regulatory mechanisms that involve protein synthesis and degradation have produced a certain number of molecules of each enzyme in a cell, the activity of those enzymes can be further regulated in several other ways: by the concentration of substrate, the presence of allosteric effectors, covalent modifications, or binding of regulatory proteins—all of which can change the activity of an individual enzyme molecule (Fig. 15–2, ❼ to ❿).

All enzymes are sensitive to the concentration of their substrate(s) (Fig. 15–2, ❼). Recall that in the simplest case (an enzyme that follows Michaelis-Menten kinetics), the initial rate of the reaction is half-maximal when the substrate is present at a concentration equal to K_m (that is, when the enzyme is half-saturated with substrate). Activity drops off at lower [S], and when [S] $<<$ K_m, the reaction rate is linearly dependent on [S].

The relationship between [S] and K_m is important because intracellular concentrations of substrate are often in the same range as, or lower than, K_m. The activity of hexokinase, for example, changes with [glucose], and intracellular [glucose] varies with the concentration of glucose in the blood. As we will see, the different forms (isozymes) of hexokinase have different K_m values and are therefore affected differently by changes in intracellular [glucose], in ways that make sense physiologically. For a number of phosphoryl transfers from ATP, and for redox reactions using NADPH or NAD^+, the metabolite concentration is well above the K_m **(Fig. 15–4)**; these cofactors are not likely to be the limiting factors in such reactions.

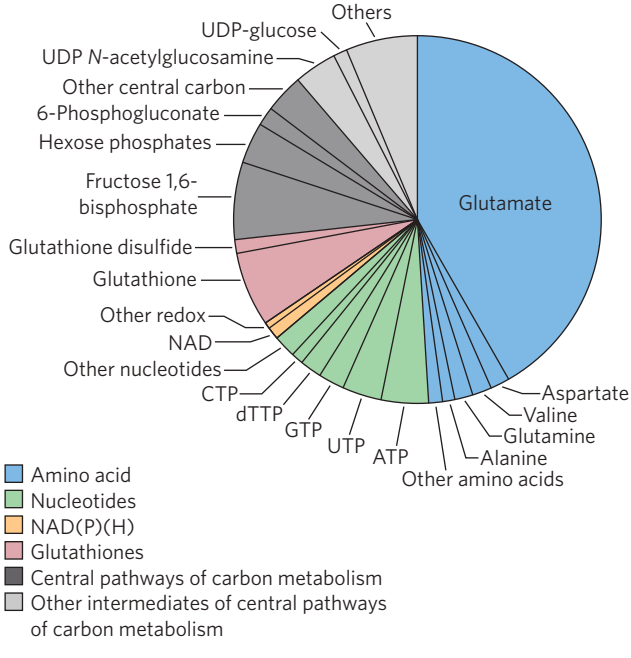

FIGURE 15–3 The metabolome of *E. coli* growing on glucose. Summary of the amounts of 103 metabolites measured by a combination of liquid chromatography and tandem mass spectrometry (LC-MS/MS).

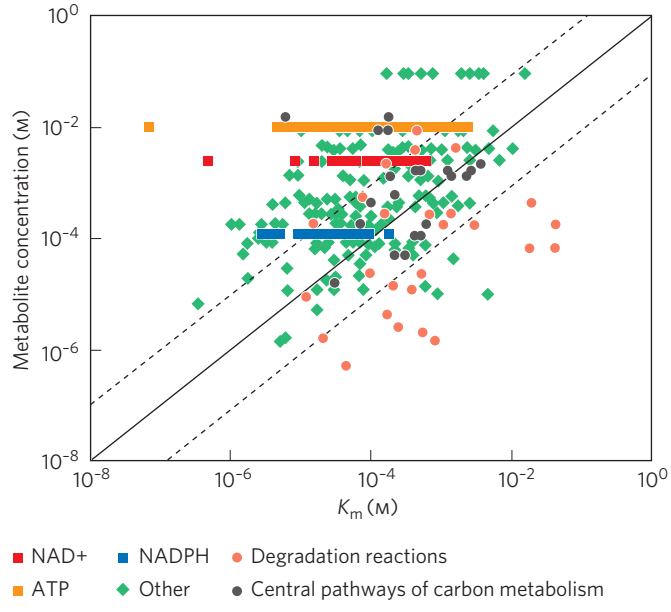

FIGURE 15–4 Comparison of K_m and substrate concentration for some metabolic enzymes. Measured metabolite concentrations for *E. coli* growing on glucose are plotted against the known K_m for enzymes that consume that metabolite. The solid line is the line of unity (where metabolite concentration = K_m), and the dashed lines each denote a tenfold deviation from the line of unity.

WORKED EXAMPLE 15–1 Activity of a Glucose Transporter

If K_t (the equivalent of K_m) for the glucose transporter in liver (GLUT2) is 40 mM, calculate the effect on the rate of glucose flux into a hepatocyte of increasing the blood glucose concentration from 3 mM to 10 mM.

Solution: We use Equation 11–1 (p. 406) to find the initial velocity (flux) of glucose uptake.

$$V_0 = \frac{V_{max}[S]_{out}}{K_t + [S]_{out}}$$

At 3 mM glucose

$$V_0 = V_{max}\ (3\ mM)/(40\ mM + 3\ mM)$$
$$= V_{max}\ (3\ mM/43\ mM) = 0.07\ V_{max}$$

At 10 mM glucose

$$V_0 = V_{max}\ (10\ mM)/(40\ mM + 10\ mM)$$
$$= V_{max}\ (10\ mM/50\ mM) = 0.20\ V_{max}$$

So a rise in blood glucose from 3 mM to 10 mM increases the rate of glucose influx into a hepatocyte by a factor of $0.20/0.07 \approx 3$.

Enzyme activity can be either increased or decreased by an allosteric effector (Fig. 15–2, ❽; see Fig. 6–34). Allosteric effectors typically convert hyperbolic kinetics to sigmoid kinetics, or vice versa (see Fig. 15–16b, for example). In the steepest part of the sigmoid curve, a small change in the concentration of substrate, or of allosteric effector, can have a large impact on reaction rate. Recall from Chapter 5 (p. 167) that the cooperativity of an allosteric enzyme can be expressed as a Hill coefficient, with higher coefficients meaning greater cooperativity. For an allosteric enzyme with a Hill coefficient of 4, activity increases from 10% V_{max} to 90% V_{max} with only a 3-fold increase in [S], compared with the 81-fold rise in [S] needed by an enzyme with no cooperative effects (Hill coefficient of 1; Table 15–2).

Covalent modifications of enzymes or other proteins (Fig. 15–2, ❾) occur within seconds or minutes of a regulatory signal, typically an extracellular signal. By far the most common modifications are phosphorylation and dephosphorylation **(Fig. 15–5)**; up to half the proteins in a eukaryotic cell are phosphorylated under some circumstances. Phosphorylation by a specific protein kinase may alter the electrostatic features of an enzyme's active site, cause movement of an inhibitory region of the enzyme out of the active site, alter the enzyme's interaction with other proteins, or force conformational changes that translate into changes in V_{max} or K_m. For covalent modification to be useful in regulation, the cell must be able to restore the altered enzyme to its original activity state. A family of phosphoprotein phosphatases, at least some of which are themselves under regulation, catalyzes the dephosphorylation of proteins.

Finally, many enzymes are regulated by association with and dissociation from another, regulatory protein (Fig. 15–2, ❿). For example, the cyclic AMP–dependent protein kinase (PKA; see Fig. 12–6) is inactive until cAMP binding separates catalytic from regulatory (inhibitory) subunits of the enzyme.

These several mechanisms for altering the flux through a step in a metabolic pathway are not mutually exclusive. It is very common for a single enzyme to be regulated at the level of transcription and by both allosteric and covalent mechanisms. The combination provides fast, smooth, effective regulation in response to a very wide array of perturbations and signals.

TABLE 15–2 Relationship between Hill Coefficient and the Effect of Substrate Concentration on Reaction Rate for Allosteric Enzymes

Hill coefficient (n_H)	Required change in [S] to increase V_0 from 10% to 90% V_{max}
0.5	×6,600
1.0	×81
2.0	×9
3.0	×4.3
4.0	×3

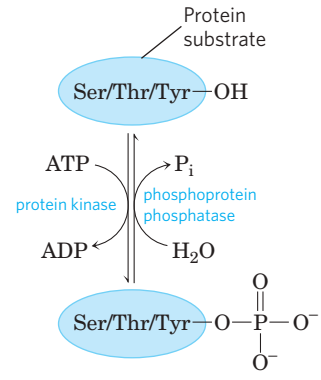

FIGURE 15–5 Protein phosphorylation and dephosphorylation. Protein kinases transfer a phosphoryl group from ATP to a Ser, Thr, or Tyr residue in an enzyme or other protein substrate. Protein phosphatases remove the phosphoryl group as P_i.

In the discussions that follow, it is useful to think of changes in enzymatic activity as serving two distinct though complementary roles. We use the term **metabolic regulation** to refer to processes that serve to maintain homeostasis at the molecular level—to hold some cellular parameter (concentration of a metabolite, for example) at a steady level over time, even as the flow of metabolites through the pathway changes. The term **metabolic control** refers to a process that leads to a change in the output of a metabolic pathway over time, in response to some outside signal or change in circumstances. The distinction, although useful, is not always easy to make.

Reactions Far from Equilibrium in Cells Are Common Points of Regulation

For some steps in a metabolic pathway the reaction is close to equilibrium, with the cell in its dynamic steady state **(Fig. 15–6)**. The net flow of metabolites through these steps is the small difference between the rates of the forward and reverse reactions, rates that are very similar when a reaction is near equilibrium. Small changes in

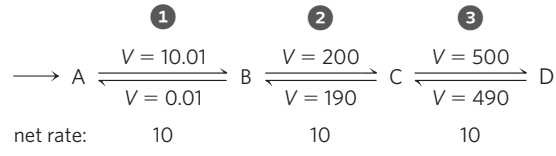

FIGURE 15–6 Near-equilibrium and nonequilibrium steps in a metabolic pathway. Steps ❷ and ❸ of this pathway are near equilibrium in the cell; for each step, the rate (V) of the forward reaction is only slightly greater than the reverse rate, so the net forward rate (10) is relatively low and the free-energy change, ΔG, is close to zero. An increase in [C] or [D] can reverse the direction of these steps. Step ❶ is maintained in the cell far from equilibrium; its forward rate greatly exceeds its reverse rate. The net rate of step ❶ (10) is much larger than the reverse rate (0.01) and is identical to the net rates of steps ❷ and ❸ when the pathway is operating in the steady state. Step ❶ has a large, negative ΔG.

TABLE 15–3 Equilibrium Constants, Mass-Action Coefficients, and Free-Energy Changes for Enzymes of Carbohydrate Metabolism

Enzyme	K'_{eq}	Mass-action ratio, Q		Reaction near equilibrium in vivo?*	$\Delta G'^{\circ}$ (kJ/mol)	ΔG (kJ/mol) in heart
		Liver	Heart			
Hexokinase	1×10^{3}	2×10^{-2}	8×10^{-2}	No	−17	−27
PFK-1	1.0×10^{3}	9×10^{-2}	3×10^{-2}	No	−14	−23
Aldolase	1.0×10^{-4}	1.2×10^{-6}	9×10^{-6}	Yes	+24	−6.0
Triose phosphate isomerase	4×10^{-2}	—†	2.4×10^{-1}	Yes	+7.5	+3.8
Glyceraldehyde 3-phosphate dehydrogenase + phosphoglycerate kinase	2×10^{3}	6×10^{2}	9.0	Yes	−13	+3.5
Phosphoglycerate mutase	1×10^{-1}	1×10^{-1}	1.2×10^{-1}	Yes	+4.4	+0.6
Enolase	3	2.9	1.4	Yes	−3.2	−0.5
Pyruvate kinase	2×10^{4}	7×10^{-1}	40	No	−31	−17
Phosphoglucose isomerase	4×10^{-1}	3.1×10^{-1}	2.4×10^{-1}	Yes	+2.2	−1.4
Pyruvate carboxylase + PEP carboxykinase	7	1×10^{-3}	—†	No	−5.0	−23
Glucose 6-phosphatase	8.5×10^{2}	1.2×10^{2}	—†	Yes	−17	−5.0

Source: K'_{eq} and Q from Newsholme, E.A. & Start, C. (1973) *Regulation in Metabolism*, Wiley Press, New York, pp. 97, 263. ΔG and $\Delta G'^{\circ}$ were calculated from these data.

*For simplicity, any reaction for which the absolute value of the calculated ΔG is less than 6 is considered near equilibrium.

†Data not available.

substrate or product concentration can produce large changes in the net rate, and can even change the direction of the net flow. We can identify these near-equilibrium reactions in a cell by comparing the **mass-action ratio**, Q, with the equilibrium constant for the reaction, K'_{eq}. Recall that for the reaction $A + B \rightarrow C + D$, $Q = [C][D]/[A][B]$. When Q and K'_{eq} are within 1 to 2 orders of magnitude of each other, the reaction is near equilibrium. This is the case for 6 of the 10 steps in the glycolytic pathway (Table 15–3).

Other reactions are far from equilibrium in the cell. For example, K'_{eq} for the phosphofructokinase-1 (PFK-1) reaction is about 1,000, but Q ([fructose 1,6-bisphosphate][ADP]/[fructose 6-phosphate][ATP]) in a hepatocyte in the steady state is about 0.1 (Table 15–3). It is *because* the reaction is so far from equilibrium that the process is exergonic under cellular conditions and tends to go in the forward direction. The reaction is held far from equilibrium because, under prevailing cellular conditions of substrate, product, and effector concentrations, the rate of conversion of fructose 6-phosphate to fructose 1,6-bisphosphate is limited by the activity of PFK-1, which is itself limited by the number of PFK-1 molecules present and by the actions of allosteric effectors. Thus the net forward rate of the enzyme-catalyzed reaction is equal to the net flow of glycolytic intermediates through other steps in the pathway, and the reverse flow through PFK-1 remains near zero.

The cell *cannot* allow reactions with large equilibrium constants to reach equilibrium. If [fructose 6-phosphate], [ATP], and [ADP] in the cell were held at typical levels (low millimolar concentrations) and the PFK-1 reaction were allowed to reach equilibrium by an increase in [fructose 1,6-bisphosphate], the concentration of fructose 1,6-bisphosphate would rise into the molar range, wreaking osmotic havoc on the cell. Consider another case: if the reaction $ATP \rightarrow ADP + P_i$ were allowed to approach equilibrium in the cell, the actual free-energy change ($\Delta G'$) for that reaction (ΔG_p; see Worked Example 13–2, p. 519) would approach zero, and ATP would lose the high phosphoryl group transfer potential that makes it valuable to the cell. It is therefore essential that enzymes catalyzing ATP breakdown and other highly exergonic reactions in a cell be sensitive to regulation, so that when metabolic changes are forced by external circumstances, the flow through these enzymes will be adjusted to ensure that [ATP] remains far above its equilibrium level. When such metabolic changes occur, the activities of enzymes in all interconnected pathways adjust to keep these critical steps away from equilibrium. Thus, not surprisingly, many enzymes (such as PFK-1) that catalyze highly exergonic reactions are subject to a variety of subtle regulatory mechanisms. The multiplicity of these adjustments is so great that we cannot predict by examining the properties of any one enzyme in a pathway whether that enzyme has a strong influence on net flow through the entire pathway. This complex problem can be approached by metabolic control analysis, as described in Section 15.2.

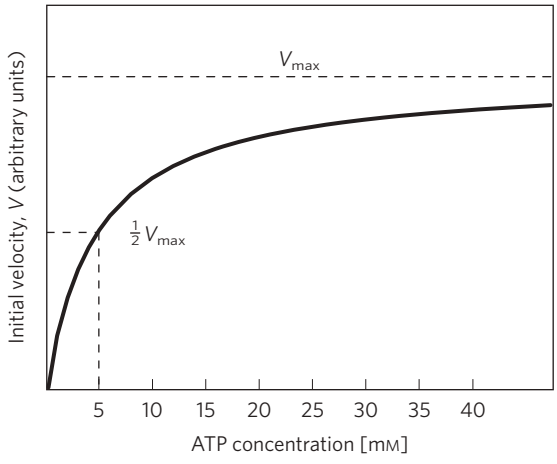

FIGURE 15–7 Effect of ATP concentration on the initial reaction velocity of a typical ATP-dependent enzyme. These experimental data yield a K_m for ATP of 5 mM. The concentration of ATP in animal tissues is ~5 mM.

Adenine Nucleotides Play Special Roles in Metabolic Regulation

After the protection of its DNA from damage, perhaps nothing is more important to a cell than maintaining a constant supply and concentration of ATP. Many ATP-using enzymes have K_m values between 0.1 and 1 mM, and the ATP concentration in a typical cell is about 5 to 10 mM (Fig. 15–4). If [ATP] were to drop significantly, these enzymes would be less than fully saturated by their substrate (ATP), and the rates of hundreds of reactions that involve ATP would decrease **(Fig. 15–7)**; the cell would probably not survive this *kinetic* effect on so many reactions.

There is also an important *thermodynamic* effect of lowered [ATP]. Because ATP is converted to ADP or AMP when "spent" to accomplish cellular work, the [ATP]/[ADP] ratio profoundly affects all reactions that employ these cofactors. (The same is true for other important cofactors, such as NADH/NAD^+ and NADPH/$NADP^+$.) For example, consider the reaction catalyzed by hexokinase:

$$\text{ATP} + \text{glucose} \longrightarrow \text{ADP} + \text{glucose 6-phosphate}$$

$$K'_{eq} = \frac{[\text{ADP}]_{eq}[\text{glucose 6-phosphate}]_{eq}}{[\text{ATP}]_{eq}[\text{glucose}]_{eq}} = 2 \times 10^3$$

Note that this expression holds true *only* when reactants and products are at their *equilibrium* concentrations, where $\Delta G' = 0$. At any other set of concentrations, $\Delta G'$ is not zero. Recall (from Chapter 13) that the ratio of products to substrates (the mass action ratio, Q) determines the magnitude and sign of $\Delta G'$ and therefore the driving force, $\Delta G'$, of the reaction:

$$\Delta G' = \Delta G'^\circ + RT \ln \frac{[\text{ADP}][\text{glucose 6-phosphate}]}{[\text{ATP}][\text{glucose}]}$$

Because an alteration of this driving force profoundly influences every reaction that involves ATP, organisms have evolved under strong pressure to develop regulatory mechanisms responsive to the [ATP]/[ADP] ratio.

AMP concentration is an even more sensitive indicator of a cell's energetic state than is [ATP]. Normally cells have a far higher concentration of ATP (5 to 10 mM) than of AMP (<0.1 mM). When some process (say, muscle contraction) consumes ATP, AMP is produced in two steps. First, hydrolysis of ATP produces ADP, then the reaction catalyzed by **adenylate kinase** produces AMP:

$$2\text{ADP} \longrightarrow \text{AMP} + \text{ATP}$$

If ATP is consumed such that its concentration drops 10%, the *relative* increase in [AMP] is much greater than that of [ADP] (Table 15–4). It is not surprising, therefore, that many regulatory processes are keyed to changes in [AMP]. Probably the most important mediator of regulation by AMP is **AMP-activated protein kinase (AMPK)**, which responds to an increase in [AMP] by phosphorylating key proteins and thus regulating their activities. The rise in [AMP] may be caused by a reduced nutrient supply or by increased exercise. The action of AMPK (not to be confused with the *cyclic* AMP–dependent protein kinase; see Section 15.5) increases glucose transport and activates glycolysis and fatty acid oxidation, while suppressing energy-requiring processes such as the synthesis of fatty acids, cholesterol, and protein **(Fig. 15–8)**. We discuss AMPK further, and the detailed mechanisms by which it effects these changes, in Chapter 23.

In addition to ATP, hundreds of metabolic intermediates also must be present at appropriate concentrations in the cell. To take just one example: the glycolytic intermediates dihydroxyacetone phosphate and 3-phosphoglycerate are precursors of triacylglycerols and serine, respectively. When these products are needed, the rate of glycolysis must be adjusted to provide them without reducing the glycolytic production of ATP. The same

TABLE 15–4 Relative Changes in [ATP] and [AMP] When ATP Is Consumed

Adenine nucleotide	Concentration before ATP depletion (mM)	Concentration after ATP depletion (mM)	Relative change
ATP	5.0	4.5	10%
ADP	1.0	1.0	0
AMP	0.1	0.6	600%

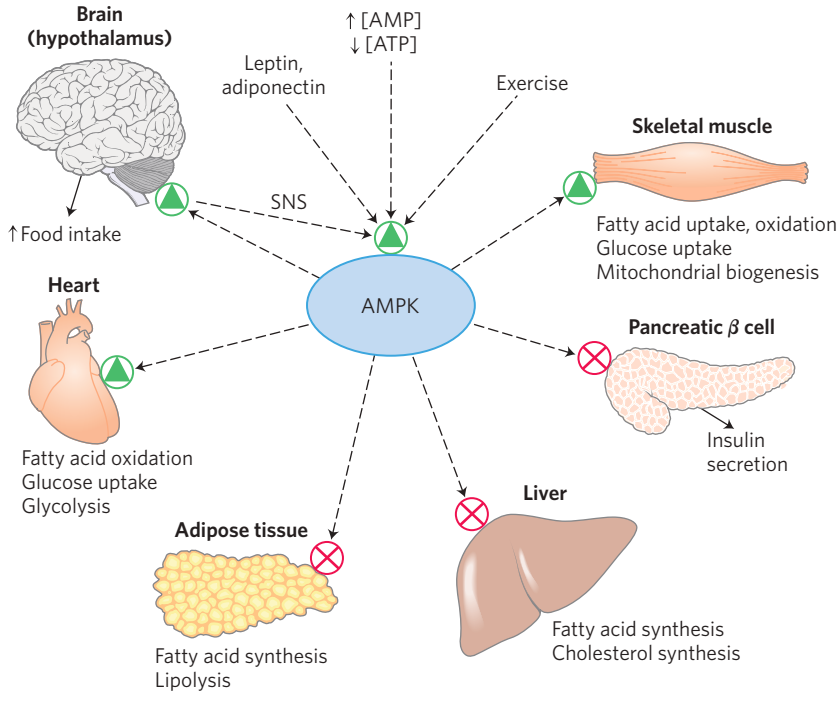

FIGURE 15–8 Role of AMP-activated protein kinase (AMPK) in carbohydrate and fat metabolism. AMPK is activated by elevated [AMP] or decreased [ATP], by exercise, by the sympathetic nervous system (SNS), or by peptide hormones produced in adipose tissue (leptin and adiponectin, described in more detail in Chapter 23). When activated, AMPK phosphorylates target proteins and shifts metabolism in a variety of tissues away from energy-consuming processes such as the synthesis of glycogen, fatty acids, and cholesterol; shifts metabolism in extrahepatic tissues to the use of fatty acids as a fuel; and triggers gluconeogenesis in the liver to provide glucose for the brain. In the hypothalamus, AMPK stimulates feeding behavior to provide more dietary fuel.

is true for maintaining the levels of other important cofactors, such as NADH and NADPH: changes in their mass action ratios (that is, in the ratio of reduced to oxidized cofactor) have global effects on metabolism.

Of course, priorities at the *organismal* level have also driven the evolution of regulatory mechanisms. In mammals, the brain has virtually no stored source of energy, depending instead on a constant supply of glucose from the blood. If blood glucose drops from its normal concentration of 4 to 5 mM to half that level, mental confusion results, and a fivefold reduction in blood glucose can lead to coma and death. To buffer against changes in blood glucose concentration, release of the hormones insulin and glucagon, elicited by high or low blood glucose, respectively, triggers metabolic changes that tend to return the blood glucose concentration to normal.

Other selective pressures must also have operated throughout evolution, selecting for regulatory mechanisms that accomplish the following:

1. Maximize the efficiency of fuel utilization by preventing the simultaneous operation of pathways in opposite directions (such as glycolysis and gluconeogenesis).
2. Partition metabolites appropriately between alternative pathways (such as glycolysis and the pentose phosphate pathway).
3. Draw on the fuel best suited for the immediate needs of the organism (glucose, fatty acids, glycogen, or amino acids).
4. Slow down biosynthetic pathways when their products accumulate.

The remaining chapters of this book present many examples of each kind of regulatory mechanism.

SUMMARY 15.1 Regulation of Metabolic Pathways

- In a metabolically active cell in a steady state, intermediates are formed and consumed at equal rates. When a transient perturbation alters the rate of formation or consumption of a metabolite, compensating changes in enzyme activities return the system to the steady state.
- Cells regulate their metabolism by a variety of mechanisms over a time scale ranging from less than a millisecond to days, either by changing the activity of existing enzyme molecules or by changing the number of molecules of a specific enzyme.
- Various signals activate or inactivate transcription factors, which act in the nucleus to regulate gene expression. Changes in the transcriptome lead to changes in the proteome, and ultimately in the metabolome of a cell or tissue.

- In multistep processes such as glycolysis, certain reactions are essentially at equilibrium in the steady state; the rates of these reactions rise and fall with substrate concentration. Other reactions are far from equilibrium; these steps are typically the points of regulation of the overall pathway.
- Regulatory mechanisms maintain nearly constant levels of key metabolites such as ATP and NADH in cells and glucose in the blood, while matching the use or production of glucose to the organism's changing needs.
- The levels of ATP and AMP are a sensitive reflection of a cell's energy status, and when the [ATP]/[AMP] ratio decreases, the AMP-activated protein kinase (AMPK) triggers a variety of cellular responses to raise [ATP] and lower [AMP].

15.2 Analysis of Metabolic Control

Eduard Buchner, 1860–1917

Detailed studies of metabolic regulation were not feasible until the basic chemical steps in a pathway had been clarified and the responsible enzymes characterized. Beginning with Eduard Buchner's discovery (c. 1900) that an extract of broken yeast cells could convert glucose to ethanol and CO_2, a major thrust of biochemical research was to deduce the steps by which this transformation occurred and to purify and characterize the enzymes that catalyzed each step. By the middle of the twentieth century, all 10 enzymes of the glycolytic pathway had been purified and characterized. In the next 50 years much was learned about the regulation of these enzymes by intracellular and extracellular signals, through the kinds of allosteric and covalent mechanisms described in this chapter. The conventional wisdom was that in a linear pathway such as glycolysis, catalysis by one enzyme must be the slowest and must therefore determine the rate of metabolite flow, or flux, through the whole pathway. For glycolysis, PFK-1 was considered the rate-limiting enzyme, because it was known to be closely regulated by fructose 2,6-bisphosphate and other allosteric effectors.

With the advent of genetic engineering technology, it became possible to test this "single rate-determining step" hypothesis by increasing the concentration of the enzyme that catalyzes the "rate-limiting step" in a pathway and determining whether flux through the pathway increases proportionally. Most often it does not; the simple solution (a single rate-determining step) is wrong. It has now become clear that in most pathways the control of flux is distributed among several enzymes, and the extent to which each contributes to the control varies with metabolic circumstances—the supply of the starting material (say, glucose), the supply of oxygen, the need for other products derived from intermediates of the pathway (say, glucose 6-phosphate for the pentose phosphate pathway in cells synthesizing large amounts of nucleotides), the effects of metabolites with regulatory roles, and the hormonal status of the organism (such as the levels of insulin and glucagon), among other factors.

Why are we interested in what limits the flux through a pathway? To understand the action of hormones or drugs, or the pathology that results from a failure of metabolic regulation, we must know where control is exercised. If researchers wish to develop a drug that stimulates or inhibits a pathway, the logical target is the enzyme that has the greatest impact on the flux through that pathway. And the bioengineering of a microorganism to overproduce a product of commercial value (p. 321) requires a knowledge of what limits the flux of metabolites toward that product.

The Contribution of Each Enzyme to Flux through a Pathway Is Experimentally Measurable

There are several ways to determine experimentally how a change in the activity of one enzyme in a pathway affects metabolite flux through that pathway. Consider the experimental results shown in **Figure 15–9**. When a sample of rat liver was homogenized to release all soluble enzymes, the extract carried out the glycolytic conversion of glucose to fructose 1,6-bisphosphate at a measurable rate. (This experiment, for simplicity, focused on just the first part of the glycolytic pathway.) When increasing amounts of purified hexokinase IV

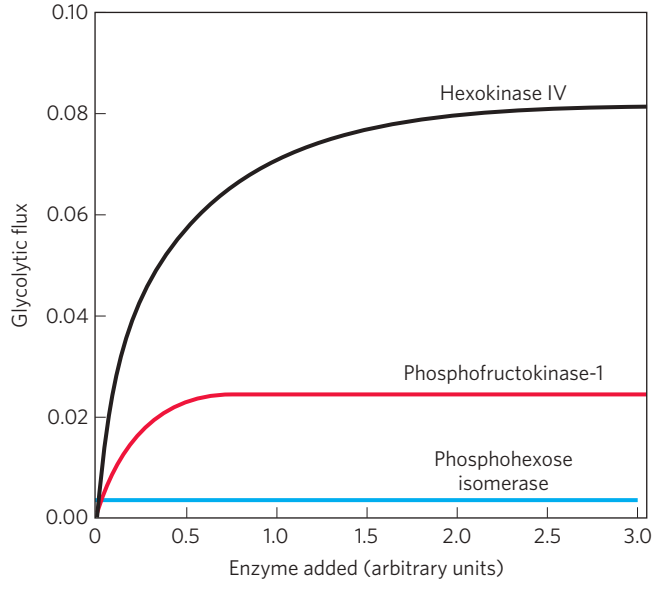

FIGURE 15–9 Dependence of glycolytic flux in a rat liver homogenate on added enzymes. Purified enzymes in the amounts shown on the *x* axis were added to an extract of liver carrying out glycolysis in vitro. The flux through the pathway is shown on the *y* axis.

(glucokinase) were added to the extract, the rate of glycolysis progressively increased. The addition of purified PFK-1 to the extract also increased the rate of glycolysis, but not as dramatically as did hexokinase. Addition of purified phosphohexose isomerase was without effect. These results suggest that hexokinase and PFK-1 both contribute to setting the flux through the pathway (hexokinase more than PFK-1), and that phosphohexose isomerase does not.

Similar experiments can be done on intact cells or organisms, using specific inhibitors or activators to change the activity of one enzyme while observing the effect on flux through the pathway. The amount of an enzyme can also be altered genetically; bioengineering can produce a cell that makes extra copies of the enzyme under investigation or has a version of the enzyme that is less active than the normal enzyme. Increasing the concentration of an enzyme genetically sometimes has significant effects on flux; sometimes it has no effect.

Three critical parameters, which together describe the responsiveness of a pathway to changes in metabolic circumstances, lie at the center of **metabolic control analysis**. We turn now to a qualitative description of these parameters and their meaning in the context of a living cell. Box 15–1 provides a more rigorous quantitative discussion.

The Flux Control Coefficient Quantifies the Effect of a Change in Enzyme Activity on Metabolite Flux through a Pathway

Quantitative data on metabolic flux, obtained as described in Figure 15–9, can be used to calculate a **flux control coefficient**, ***C***, for each enzyme in a pathway. This coefficient expresses the relative contribution of each enzyme to setting the rate at which metabolites flow through the pathway—that is, the **flux**, ***J***. C can have any value from 0.0 (for an enzyme with no impact on the flux) to 1.0 (for an enzyme that wholly determines the flux). An enzyme can also have a *negative* flux control coefficient. In a branched pathway, an enzyme in one branch, by drawing intermediates away from the other branch, can have a negative impact on the flux through that other branch **(Fig. 15–10)**. C is not a constant, and it is not intrinsic to a single enzyme; it is a function of the whole system of enzymes, and its value depends on the concentrations of substrates and effectors.

When real data from the experiment on glycolysis in a rat liver extract (Fig. 15–9) were subjected to this kind of analysis, investigators found flux control coefficients (for enzymes at the concentrations found in the extract) of 0.79 for hexokinase, 0.21 for PFK-1, and 0.0 for phosphohexose isomerase. It is not just fortuitous that these values add up to 1.0; we can show that for any complete pathway, the sum of the flux control coefficients must equal unity.

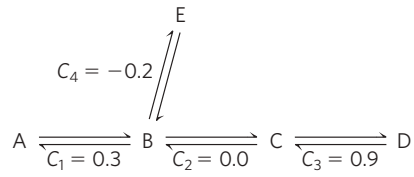

FIGURE 15–10 Flux control coefficient, *C*, in a branched metabolic pathway. In this simple pathway, the intermediate B has two alternative fates. To the extent that reaction B → E draws B away from the pathway A → D, it controls that pathway, which will result in a *negative* flux control coefficient for the enzyme that catalyzes step B → E. Note that the sum of all four coefficients equals 1.0, as it must for any defined system of enzymes.

The Elasticity Coefficient Is Related to an Enzyme's Responsiveness to Changes in Metabolite or Regulator Concentrations

A second parameter, the **elasticity coefficient**, ε, expresses quantitatively the responsiveness of a single enzyme to changes in the concentration of a metabolite or regulator; it is a function of the enzyme's intrinsic kinetic properties. For example, an enzyme with typical Michaelis-Menten kinetics shows a hyperbolic response to increasing substrate concentration **(Fig. 15–11)**. At low concentrations of substrate (say, 0.1 K_m), each increment in substrate concentration results in a comparable increase in enzymatic activity, yielding an ε near 1.0. At relatively high substrate concentrations (say, 10 K_m), increasing the substrate concentration has little effect on the reaction rate, because the enzyme is already saturated with substrate. The elasticity in this case approaches zero. For allosteric enzymes that show positive cooperativity, ε may exceed 1.0, but it cannot exceed the Hill coefficient, which is typically between 1.0 and 4.0.

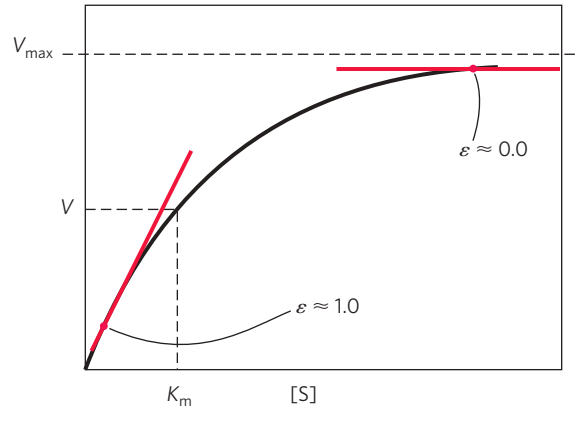

FIGURE 15–11 Elasticity coefficient, ε, of an enzyme with typical Michaelis-Menten kinetics. At substrate concentrations far below the K_m, each increase in [S] produces a correspondingly large increase in the reaction velocity, V. For this region of the curve, the enzyme has an ε of about 1.0. At [S] >> K_m, increasing [S] has little effect on V; ε here is close to 0.0.

BOX 15–1 METHODS Metabolic Control Analysis: Quantitative Aspects

The factors that influence the flow of intermediates (flux) through a pathway may be determined quantitatively by experiment and expressed in terms useful for predicting the change in flux when some factor involved in the pathway changes. Consider the simple reaction sequence in Figure 1, in which a substrate X (say, glucose) is converted in several steps to a product Z (perhaps pyruvate, formed glycolytically). An enzyme late in the pathway is a dehydrogenase (ydh) that acts on substrate Y. Because the action of a dehydrogenase is easily measured (see Fig. 13–24), we can use the flux (J) through this step (J_{ydh}) to measure the flux through the whole path. We manipulate experimentally the level of an early enzyme in the pathway (xase, which acts on the substrate X) and measure the flux through the path (J_{ydh}) for several levels of the enzyme xase.

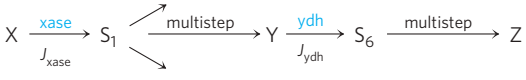

FIGURE 1 Flux through a hypothetical multienzyme pathway.

The relationship between the flux through the pathway from X to Z in the intact cell and the concentration of each enzyme in the path should be hyperbolic, with virtually no flux at infinitely low enzyme activity and near-maximum flux at very high enzyme activity. In a plot of J_{ydh} against the concentration of xase, E_{xase}, the change in flux with a small change in enzyme level is $\partial J_{ydh}/\partial E_{xase}$, which is simply the slope of the tangent to the curve at any concentration of enzyme, E_{xase}, and which tends toward zero at saturating E_{xase}. At low E_{xase}, the slope is steep; the flux increases with each incremental increase in enzyme activity. At very high E_{xase}, the slope is much smaller; the system is less responsive to added xase because it is already present in excess over the other enzymes in the pathway.

To show quantitatively the dependence of flux through the pathway, ∂J_{ydh}, on ∂E_{xase}, we could use the ratio $\partial J_{ydh}/\partial E_{xase}$. However, its usefulness is limited because its value depends on the units used to express flux and enzyme activity. By expressing the *fractional* changes in flux and enzyme activity, $\partial J_{ydh}/J_{ydh}$ and $\partial E_{xase}/E_{xase}$, we obtain a unitless expression for the **flux control coefficient**, $\boldsymbol{C}$, in this case $C^{J_{ydh}}_{xase}$:

$$C^{J_{ydh}}_{xase} \approx \frac{\partial J_{ydh}}{J_{ydh}} \Big/ \frac{\partial E_{xase}}{E_{xase}} \qquad (1)$$

This can be rearranged to

$$C^{J_{ydh}}_{xase} \approx \frac{\partial J_{ydh}}{\partial E_{xase}} \cdot \frac{E_{xase}}{J_{ydh}}$$

which is mathematically identical to

$$C^{J_{ydh}}_{xase} \approx \frac{\partial \ln J_{ydh}}{\partial \ln E_{xase}}$$

This equation suggests a simple graphical means for determining the flux control coefficient: $C^{J_{ydh}}_{xase}$ is the slope of the tangent to the plot of ln J_{ydh} versus ln E_{xase}, which can be obtained by replotting the experimental data in Figure 2a to obtain Figure 2b. Notice that $C^{J_{ydh}}_{xase}$ is not a constant; it depends on the starting E_{xase} from which the change in enzyme level takes place. For the cases shown in Figure 2, $C^{J_{ydh}}_{xase}$ is about 1.0 at the lowest E_{xase}, but only about 0.2 at high E_{xase}. A value near 1.0 for $C^{J_{ydh}}_{xase}$ means that the enzyme's concentration wholly determines the flux through the pathway; a value near 0.0 means that the enzyme's concentration does not limit the flux through the path. Unless the flux control coefficient is greater than about 0.5, changes in the activity of the enzyme will not have a strong effect on the flux.

The **elasticity**, $\boldsymbol{\varepsilon}$, of an enzyme is a measure of how that enzyme's catalytic activity changes when the concentration of a metabolite—substrate, product, or effector—changes. It is obtained from an experimental plot of the rate of the reaction catalyzed by the enzyme versus the concentration of the metabolite, at metabolite concentrations that prevail in the cell. By arguments analogous to those used to

The Response Coefficient Expresses the Effect of an Outside Controller on Flux through a Pathway

We can also derive a quantitative expression for the relative impact of an outside factor (such as a hormone or growth factor), which is neither a metabolite nor an enzyme in the pathway, on the flux through the pathway. The experiment would measure the flux through the pathway (glycolysis, in this case) at various levels of the parameter P (the insulin concentration, for example) to obtain the **response coefficient**, $\boldsymbol{R}$, which expresses the change in pathway flux when P ([insulin]) changes.

The three coefficients C, ε, and R are related in a simple way: the responsiveness (R) of a pathway to an outside factor that affects a certain enzyme is a function of (1) how sensitive the pathway is to changes in the activity of that enzyme (the flux control coefficient, C) and (2) how sensitive that specific enzyme is to changes in the outside controlling factor (the elasticity, ε):

$$R = C \cdot \varepsilon$$

Each enzyme in the pathway can be examined in this way, and the effects of any of several outside factors on flux through the pathway can be separately determined.

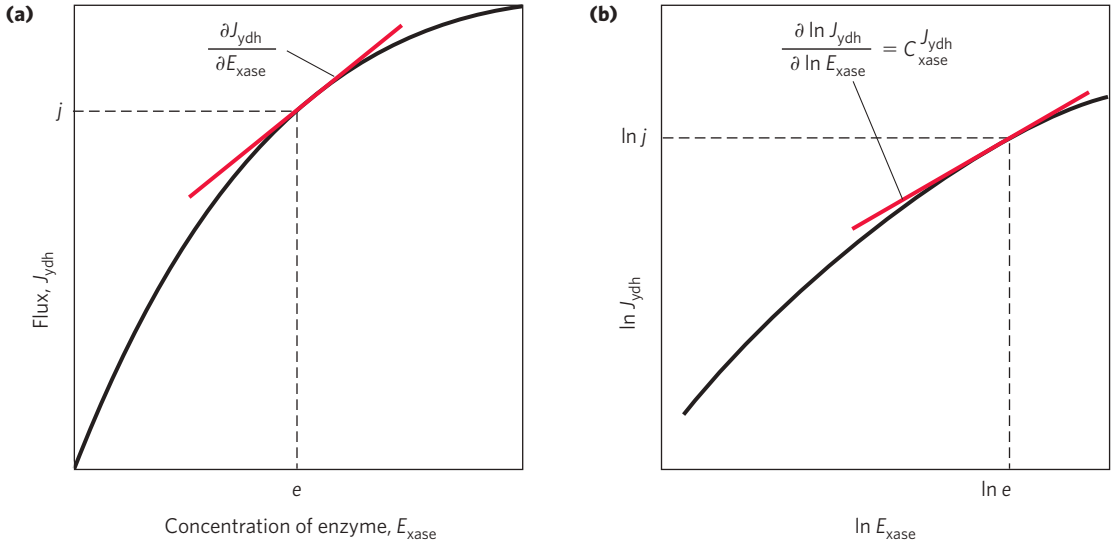

FIGURE 2 The flux control coefficient. **(a)** Typical variation of the pathway flux, J_{ydh}, measured at the step catalyzed by the enzyme ydh, as a function of the amount of the enzyme xase, E_{xase}, which catalyzes an earlier step in the pathway. The flux control coefficient at (*e*,*j*) is the product of the slope of the tangent to the curve, $\partial J_{ydh}/\partial E_{xase}$, and the ratio (scaling factor) *e*/*j*. **(b)** On a double-logarithmic plot of the same curve, the flux control coefficient is the slope of the tangent to the curve.

derive C, we can show ε to be the slope of the tangent to a plot of ln V versus ln [substrate, or product, or effector]:

$$\varepsilon_S^{xase} = \frac{\partial V_{xase}}{\partial S} \cdot \frac{S}{V_{xase}} = \frac{\partial \ln |V_{xase}|}{\partial \ln S}$$

For an enzyme with typical Michaelis-Menten kinetics, the value of ε ranges from about 1 at substrate concentrations far below K_m to near 0 as V_{max} is approached. Allosteric enzymes can have elasticities greater than 1.0, but not larger than their Hill coefficient (p. 167).

Finally, the effect of controllers outside the pathway itself (that is, not metabolites) can be measured and expressed as the **response coefficient**, ***R***. The change in flux through the pathway is measured for changes in the concentration of the controlling parameter P, and R is defined in a form analogous to that of Equation 1, yielding the expression

$$R_P^{J_{ydh}} = \frac{\partial J_{ydh}}{\partial P} \cdot \frac{P}{J_{ydh}}$$

Using the same logic and graphical methods as described above for determining C, we can obtain R as the slope of the tangent to the plot of ln J versus ln P.

The three coefficients we have described are related in this simple way:

$$R_P^{J_{ydh}} = C_{xase}^{J_{ydh}} \cdot \varepsilon_P^{xase}$$

Thus the responsiveness of each enzyme in a pathway to a change in an outside controlling factor is a simple function of two things: the control coefficient, a variable that expresses the extent to which that enzyme influences the flux under a given set of conditions, and the elasticity, an intrinsic property of the enzyme that reflects its sensitivity to substrate and effector concentrations.

Thus, in principle, we can predict how the flux of substrate through a series of enzymatic steps will change when there is a change in one or more controlling factors external to the pathway. Box 15–1 shows how these qualitative concepts are treated quantitatively.

Metabolic Control Analysis Has Been Applied to Carbohydrate Metabolism, with Surprising Results

Metabolic control analysis provides a framework within which we can think quantitatively about regulation, interpret the significance of the regulatory properties of each enzyme in a pathway, identify the steps that most affect the flux through the pathway, and distinguish between *regulatory* mechanisms that act to maintain metabolite concentrations and *control* mechanisms that actually alter the flux through the pathway. Analysis of the glycolytic pathway in yeast, for example, has revealed an unexpectedly low flux control coefficient for PFK-1, which, as we have noted, has been viewed as the main point of flux control—the "rate-determining step"—in glycolysis. Experimentally raising the level of PFK-1 fivefold led to a change in flux through glycolysis of less than 10%, suggesting that the real role of PFK-1

regulation is not to control flux through glycolysis but to mediate metabolite homeostasis—to prevent large changes in metabolite concentrations when the flux through glycolysis increases in response to elevated blood glucose or insulin. Recall that the study of glycolysis in a liver extract (Fig. 15–9) also yielded a flux control coefficient that contradicted the conventional wisdom; it showed that hexokinase, not PFK-1, is most influential in setting the flux through glycolysis. We must note here that a liver extract is far from equivalent to a hepatocyte; the ideal way to study flux control is by manipulating one enzyme at a time in the living cell. This is already feasible in many cases.

Investigators have used nuclear magnetic resonance (NMR) as a noninvasive means to determine the concentrations of glycogen and metabolites in the five-step pathway from glucose in the blood to glycogen in myocytes **(Fig. 15–12)** in rat and human muscle. They found that the flux control coefficient for glycogen synthase was smaller than that for either the glucose transporter (GLUT4) or hexokinase. (We discuss glycogen synthase and other enzymes of glycogen metabolism in Sections 15.4 and 15.5.) This finding contradicts the conventional wisdom that glycogen synthase is the locus of flux control and suggests that the importance of the phosphorylation/dephosphorylation of glycogen synthase is related instead to the maintenance of metabolite homeostasis—that is, *regulation*, not *control*. Two metabolites in this pathway, glucose and glucose 6-phosphate, are key intermediates in other pathways, including glycolysis, the pentose phosphate pathway, and the synthesis of glucosamine. Metabolic control analysis suggests that when the blood glucose level rises, insulin acts in muscle to (1) increase glucose transport into cells by conveying GLUT4 to the plasma membrane, (2) induce the synthesis of hexokinase, and (3) activate glycogen synthase by covalent alteration (see Fig. 15–41). The first two effects of insulin increase glucose flux through the pathway (control), and the third serves to adapt the activity of glycogen synthase so that metabolite levels (glucose 6-phosphate, for example) will not change dramatically with the increased flux (regulation).

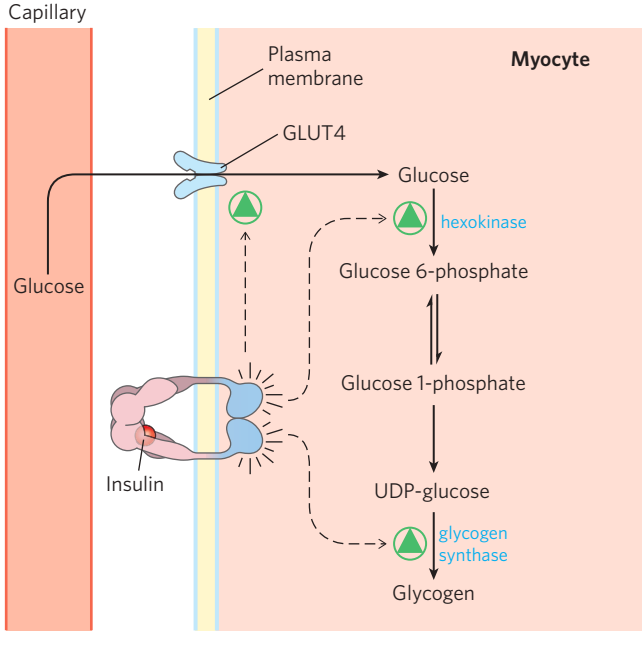

FIGURE 15–12 Control of glycogen synthesis from blood glucose in muscle. Insulin affects three of the five steps in this pathway, but it is the effects on transport and hexokinase activity, not the change in glycogen synthase activity, that increase the flux toward glycogen.

Metabolic Control Analysis Suggests a General Method for Increasing Flux through a Pathway

How could an investigator engineer a cell to increase the flux through one pathway without altering the concentrations of other metabolites or the fluxes through other pathways? More than three decades ago Henrik Kacser predicted, on the basis of metabolic control analysis, that this could be accomplished by increasing the concentrations of every enzyme in a pathway. The prediction has been confirmed in several experimental tests, and it also fits with the way cells normally control fluxes through a pathway. For example, rats fed a high-protein diet dispose of excess amino groups by converting them to urea in the urea cycle (Chapter 18). After such a dietary shift, the urea output increases fourfold, and the amount of all eight enzymes in the urea cycle increases two- to threefold. Similarly, when increased fatty acid oxidation is triggered by activation of peroxisome proliferator-activated receptor γ (PPARγ, a ligand-activated transcription factor; see Fig. 21–22), synthesis of the *whole set* of fatty acid oxidative enzymes is increased. With the growing use of DNA microarrays to study the expression of whole sets of genes in response to various perturbations, we should soon learn whether this is the general mechanism by which cells make long-term adjustments in flux through specific pathways.

SUMMARY 15.2 Analysis of Metabolic Control

- Metabolic control analysis shows that control of the rate of metabolite flux through a pathway is distributed among several of the enzymes in that path.
- The flux control coefficient, C, is an experimentally determined measure of the effect of an enzyme's concentration on flux through a multienzyme pathway. It is characteristic of the whole system, not intrinsic to the enzyme.
- The elasticity coefficient, ε, of an enzyme is an experimentally determined measure of its responsiveness to changes in the concentration of a metabolite or regulator molecule.
- The response coefficient, R, is a measure of the experimentally determined change in flux through

a pathway in response to a regulatory hormone or second messenger. It is a function of C and ε: $R = C \cdot \varepsilon$.

- Some regulated enzymes control the flux through a pathway, while others rebalance the level of metabolites in response to the change in flux. The first activity is *control*; the second, rebalancing activity is *regulation*.
- Metabolic control analysis predicts, and experiments have confirmed, that flux toward a specific product is most effectively increased by raising the concentration of all enzymes in the pathway.

15.3 Coordinated Regulation of Glycolysis and Gluconeogenesis

In mammals, **gluconeogenesis** occurs primarily in the liver, where its role is to provide glucose for export to other tissues when glycogen stores are exhausted and when no dietary glucose is available. As we discussed in Chapter 14, gluconeogenesis employs several of the enzymes that act in glycolysis, but it is not simply the reversal of glycolysis. Seven of the glycolytic reactions are freely reversible, and the enzymes that catalyze these reactions also function in gluconeogenesis **(Fig. 15–13)**. Three reactions of glycolysis are so exergonic as to be essentially irreversible: those catalyzed by hexokinase, PFK-1, and pyruvate kinase. All three reactions have a large, negative $\Delta G'$ (Table 15–3 shows the values in heart muscle). Gluconeogenesis uses detours around each of these irreversible steps; for example, the conversion of fructose 1,6-bisphosphate to fructose 6-phosphate is catalyzed by fructose 1,6-bisphosphatase (FBPase-1). Each of these bypass reactions also has a large, negative $\Delta G'$.

At each of the three points where glycolytic reactions are bypassed by alternative, gluconeogenic reactions, simultaneous operation of both pathways would consume ATP without accomplishing any chemical or biological work. For example, PFK-1 and FBPase-1 catalyze opposing reactions:

$$\text{ATP} + \text{fructose 6-phosphate} \xrightarrow{\text{PFK-1}} \text{ADP} + \text{fructose 1,6-bisphosphate}$$

$$\text{Fructose 1,6-bisphosphate} + \text{H}_2\text{O} \xrightarrow{\text{FBPase-1}} \text{fructose 6-phosphate} + \text{P}_\text{i}$$

The sum of these two reactions is:

$$\text{ATP} + \text{H}_2\text{O} \longrightarrow \text{ADP} + \text{P}_\text{i} + \text{heat}$$

that is, hydrolysis of ATP without any useful metabolic work being done. Clearly, if these two reactions were allowed to proceed simultaneously at a high rate in the same cell, a large amount of chemical energy would be dissipated as heat. This uneconomical process has been called a **futile cycle**. However, as we shall see later, such cycles may provide advantages for controlling pathways, and the term **substrate cycle** is a better description. Similar substrate cycles also occur with the other two sets of bypass reactions of gluconeogenesis (Fig. 15–13).

We look now in some detail at the mechanisms that regulate glycolysis and gluconeogenesis at the three points where these pathways diverge.

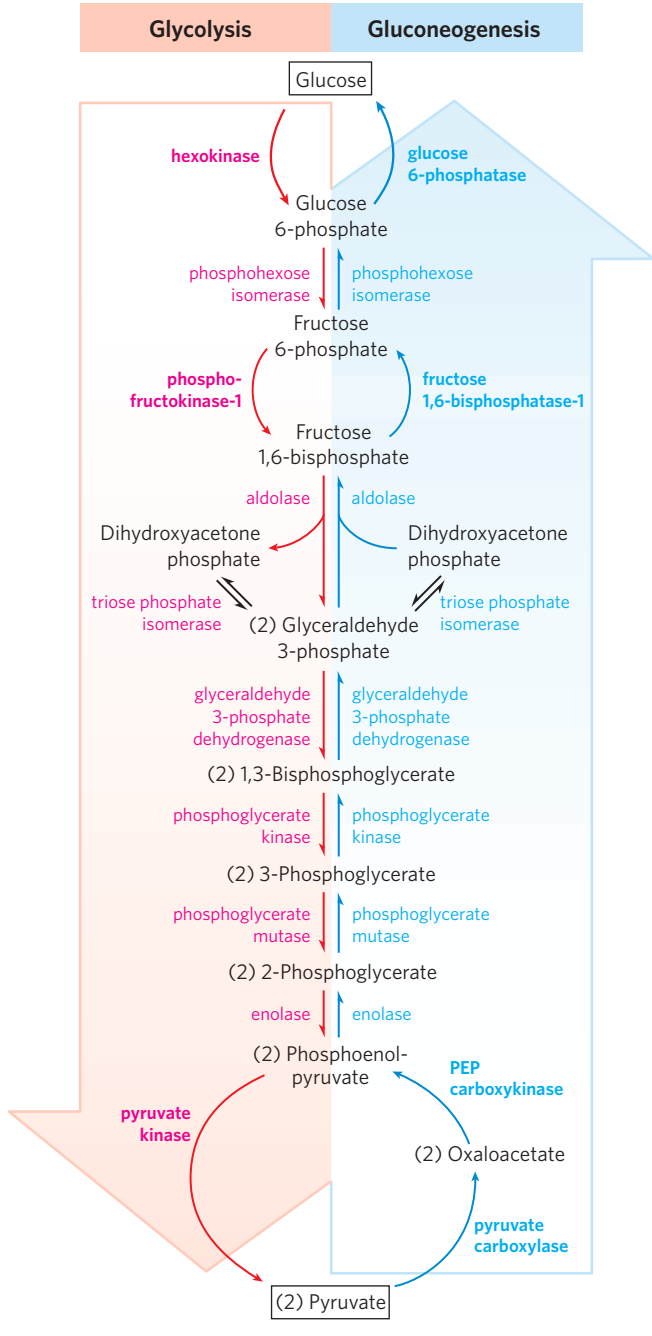

FIGURE 15–13 Glycolysis and gluconeogenesis. Opposing pathways of glycolysis (pink) and gluconeogenesis (blue) in rat liver. Three steps are catalyzed by different enzymes in gluconeogenesis (the "bypass reactions") and glycolysis; seven steps are catalyzed by the same enzymes in the two pathways. Cofactors have been omitted for simplicity.

Hexokinase Isozymes of Muscle and Liver Are Affected Differently by Their Product, Glucose 6-Phosphate

Hexokinase, which catalyzes the entry of glucose into the glycolytic pathway, is a regulatory enzyme. Humans have four isozymes (designated I to IV), encoded by four different genes. **Isozymes** are different proteins that catalyze the same reaction (Box 15–2). The predominant hexokinase isozyme of myocytes (**hexokinase II**) has a high affinity for glucose—it is half-saturated at about 0.1 mM. Because glucose entering myocytes from the blood (where the glucose concentration is 4 to 5 mM) produces an intracellular glucose concentration high enough to saturate hexokinase II, the enzyme normally acts at or near its maximal rate. Muscle **hexokinase I** and hexokinase II are allosterically inhibited by their product, glucose 6-phosphate, so whenever the cellular concentration of glucose 6-phosphate rises above its normal level, these isozymes are temporarily and reversibly inhibited, bringing the rate of glucose 6-phosphate formation into balance with the rate of its utilization and reestablishing the steady state.

BOX 15–2 Isozymes: Different Proteins That Catalyze the Same Reaction

The four forms of hexokinase found in mammalian tissues are but one example of a common biological situation: the same reaction catalyzed by two or more different molecular forms of an enzyme. These multiple forms, called isozymes or isoenzymes, may occur in the same species, in the same tissue, even in the same cell. The different forms (isoforms) of the enzyme generally differ in kinetic or regulatory properties, in the cofactor they use (NADH or NADPH for dehydrogenase isozymes, for example), or in their subcellular distribution (soluble or membrane-bound). Isozymes may have similar, but not identical, amino acid sequences, and in many cases they clearly share a common evolutionary origin.

One of the first enzymes found to have isozymes was lactate dehydrogenase (LDH; p. 563), which in vertebrate tissues exists as at least five different isozymes separable by electrophoresis. All LDH isozymes contain four polypeptide chains (each of M_r 33,500), each type containing a different ratio of two kinds of polypeptides. The M (for muscle) chain and the H (for heart) chain are encoded by two different genes.

In skeletal muscle the predominant isozyme contains four M chains, and in heart the predominant isozyme contains four H chains. Other tissues have some combination of the five possible types of LDH isozymes:

Type	Composition	Location
LDH_1	HHHH	Heart and erythrocyte
LDH_2	HHHM	Heart and erythrocyte
LDH_3	HHMM	Brain and kidney
LDH_4	HMMM	Skeletal muscle and liver
LDH_5	MMMM	Skeletal muscle and liver

The differences in the isozyme content of tissues can be used to assess the timing and extent of heart damage due to myocardial infarction (heart attack). Damage to heart tissue results in the release of heart LDH into the blood. Shortly after a heart attack, the blood level of total LDH increases, and there is more LDH_2 than LDH_1. After 12 hours the amounts of LDH_1 and LDH_2 are very similar, and after 24 hours there is more LDH_1 than LDH_2. This switch in the $[LDH_1]/[LDH_2]$ ratio, combined with increased concentrations in the blood of another heart enzyme, creatine kinase, is very strong evidence of a recent myocardial infarction. ■

The different LDH isozymes have significantly different values of V_{max} and K_m, particularly for pyruvate. The properties of LDH_4 favor rapid reduction of very low concentrations of pyruvate to lactate in skeletal muscle, whereas those of isozyme LDH_1 favor rapid oxidation of lactate to pyruvate in the heart.

In general, the distribution of different isozymes of a given enzyme reflects at least four factors:

1. *Different metabolic patterns in different organs.* For glycogen phosphorylase, the isozymes in skeletal muscle and liver have different regulatory properties, reflecting the different roles of glycogen breakdown in these two tissues.
2. *Different locations and metabolic roles for isozymes in the same cell.* The isocitrate dehydrogenase isozymes of the cytosol and the mitochondrion are an example (Chapter 16).
3. *Different stages of development in embryonic or fetal tissues and in adult tissues.* For example, the fetal liver has a characteristic isozyme distribution of LDH, which changes as the organ develops into its adult form. Some enzymes of glucose catabolism in malignant (cancer) cells occur as their fetal, not adult, isozymes.
4. *Different responses of isozymes to allosteric modulators.* This difference is useful in fine-tuning metabolic rates. Hexokinase IV (glucokinase) of liver and the hexokinase isozymes of other tissues differ in their sensitivity to inhibition by glucose 6-phosphate.

The different hexokinase isozymes of liver and muscle reflect the different roles of these organs in carbohydrate metabolism: muscle consumes glucose, using it for energy production, whereas liver maintains blood glucose homeostasis by consuming or producing glucose, depending on the prevailing blood glucose concentration. The predominant hexokinase isozyme of liver is **hexokinase IV** (glucokinase), which differs in three important respects from hexokinases I–III of muscle. First, the glucose concentration at which hexokinase IV is half-saturated (about 10 mM) is higher than the usual concentration of glucose in the blood. Because an efficient glucose transporter in hepatocytes (**GLUT2**) rapidly equilibrates the glucose concentrations in cytosol and blood (see Fig. 11–31 for the kinetics of the same transporter, GLUT1, in erythrocytes), the high K_m of hexokinase IV allows its direct regulation by the level of blood glucose **(Fig. 15–14)**. When blood glucose is high, as it is after a meal rich in carbohydrates, excess glucose is transported into hepatocytes, where hexokinase IV converts it to glucose 6-phosphate. Because hexokinase IV is not saturated at 10 mM glucose, its activity continues to increase as the glucose concentration rises to 10 mM or more. Under conditions of low blood glucose, the glucose concentration in a hepatocyte is low relative to the K_m of hexokinase IV, and the glucose generated by gluconeogenesis leaves the cell before being trapped by phosphorylation.

Second, hexokinase IV is not inhibited by glucose 6-phosphate, and it can therefore continue to operate when the accumulation of glucose 6-phosphate completely inhibits hexokinases I–III. Finally, hexokinase IV is subject to inhibition by the reversible binding of a regulatory protein specific to liver **(Fig. 15–15)**. The binding is much tighter in the presence of the allosteric effector fructose 6-phosphate. Glucose competes with fructose 6-phosphate for binding and causes dissociation of the regulatory protein from the hexokinase, relieving the inhibition. Immediately after a carbohydrate-rich meal, when blood glucose is high, glucose enters the hepatocyte via GLUT2 and activates hexokinase IV by this mechanism. During a fast, when blood glucose drops

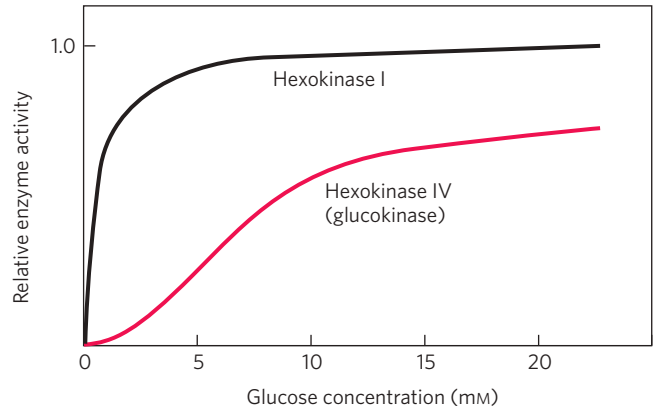

FIGURE 15–14 Comparison of the kinetic properties of hexokinase IV (glucokinase) and hexokinase I. Note the sigmoidicity for hexokinase IV and the much lower K_m for hexokinase I. When blood glucose rises above 5 mM, hexokinase IV activity increases, but hexokinase I is already operating near V_{max} and cannot respond to an increase in glucose concentration. Hexokinases I, II, and III have similar kinetic properties.

below 5 mM, fructose 6-phosphate triggers the inhibition of hexokinase IV by the regulatory protein, so the liver does not compete with other organs for the scarce glucose. The mechanism of inhibition by the regulatory protein is interesting: the protein anchors hexokinase IV inside the nucleus, where it is segregated from the other enzymes of glycolysis in the cytosol (Fig. 15–15). When the glucose concentration in the cytosol rises, it equilibrates with glucose in the nucleus by transport through the nuclear pores. Glucose causes dissociation of the regulatory protein, and hexokinase IV enters the cytosol and begins to phosphorylate glucose.

Hexokinase IV (Glucokinase) and Glucose 6-Phosphatase Are Transcriptionally Regulated

Hexokinase IV is also regulated at the level of protein synthesis. Circumstances that call for greater energy production (low [ATP], high [AMP], vigorous muscle contraction) or for greater glucose consumption (high blood glucose, for example) cause increased transcription of the hexokinase IV gene. Glucose 6-phosphatase, the

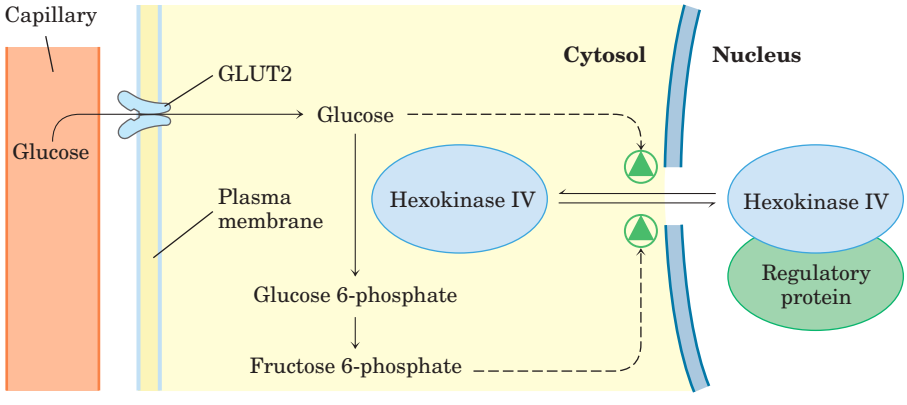

FIGURE 15–15 Regulation of hexokinase IV (glucokinase) by sequestration in the nucleus. The protein inhibitor of hexokinase IV is a nuclear binding protein that draws hexokinase IV into the nucleus when the fructose 6-phosphate concentration in liver is high and releases it to the cytosol when the glucose concentration is high.

gluconeogenic enzyme that bypasses the hexokinase step of glycolysis, is transcriptionally regulated by factors that call for increased production of glucose (low blood glucose, glucagon signaling). The transcriptional regulation of these two enzymes (along with other enzymes of glycolysis and gluconeogenesis) is described below.

Phosphofructokinase-1 and Fructose 1,6-Bisphosphatase Are Reciprocally Regulated

As we have noted, glucose 6-phosphate can flow either into glycolysis or through any of several other pathways, including glycogen synthesis and the pentose phosphate pathway. The metabolically irreversible reaction catalyzed by PFK-1 is the step that commits glucose to glycolysis. In addition to its substrate-binding sites, this complex enzyme has several regulatory sites at which allosteric activators or inhibitors bind.

ATP is not only a substrate for PFK-1 but also an end product of the glycolytic pathway. When high cellular [ATP] signals that ATP is being produced faster than it is being consumed, ATP inhibits PFK-1 by binding to an allosteric site and lowering the affinity of the enzyme for its substrate fructose 6-phosphate **(Fig. 15–16)**. ADP and AMP, which increase in concentration as consumption of ATP outpaces production, act allosterically to relieve this inhibition by ATP. These effects combine to produce higher enzyme activity when ADP or AMP accumulates and lower activity when ATP accumulates.

Citrate (the ionized form of citric acid), a key intermediate in the aerobic oxidation of pyruvate, fatty acids, and amino acids, is also an allosteric regulator of PFK-1; high citrate concentration increases the inhibitory effect of ATP, further reducing the flow of glucose through glycolysis. In this case, as in several others encountered later, citrate serves as an intracellular signal that the cell is meeting its current needs for energy-yielding metabolism by the oxidation of fats and proteins.

The corresponding step in gluconeogenesis is the conversion of fructose 1,6-bisphosphate to fructose 6-phosphate **(Fig. 15–17)**. The enzyme that catalyzes this reaction, FBPase-1, is strongly inhibited (allosterically) by AMP; when the cell's supply of ATP is low (corresponding to high [AMP]), the ATP-requiring synthesis of glucose slows.

Thus these opposing steps in the glycolytic and gluconeogenic pathways—those catalyzed by PFK-1 and FBPase-1—are regulated in a coordinated and reciprocal manner. In general, when sufficient concentrations of acetyl-CoA or citrate (the product of acetyl-CoA condensation with oxaloacetate) are present, or when a high proportion of the cell's adenylate is in the form of ATP, gluconeogenesis is favored. When the level of AMP increases, it promotes glycolysis by stimulating PFK-1 (and, as we shall see in Section 15.5, promotes glycogen degradation by activating glycogen phosphorylase).

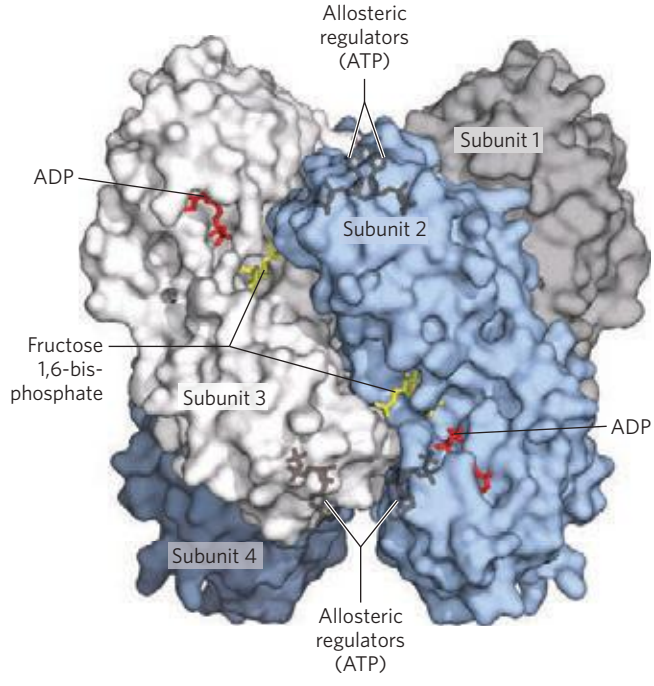

(a)

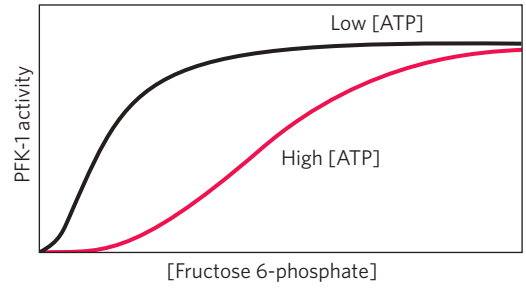

(b)

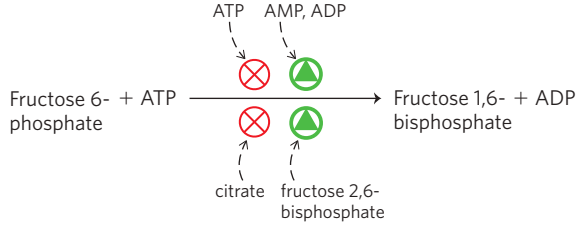

(c)

FIGURE 15–16 Phosphofructokinase-1 (PFK-1) and its regulation. **(a)** Surface contour image of *E. coli* PFK-1, showing portions of its four identical subunits (PDB ID 1PFK). Each subunit has its own catalytic site, where the products ADP and fructose 1,6-bisphosphate (red and yellow stick structures, respectively) are almost in contact, and its own binding sites for the allosteric regulator ATP, buried in the protein in the positions indicated. **(b)** Allosteric regulation of muscle PFK-1 by ATP, shown by a substrate-activity curve. At low [ATP], the $K_{0.5}$ for fructose 6-phosphate is relatively low, enabling the enzyme to function at a high rate at relatively low [fructose 6-phosphate]. (Recall from Chapter 6 that $K_{0.5}$ is the K_m term for regulatory enzymes.) When [ATP] is high, $K_{0.5}$ for fructose 6-phosphate is greatly increased, as indicated by the sigmoid relationship between substrate concentration and enzyme activity. **(c)** Summary of the regulators affecting PFK-1 activity.

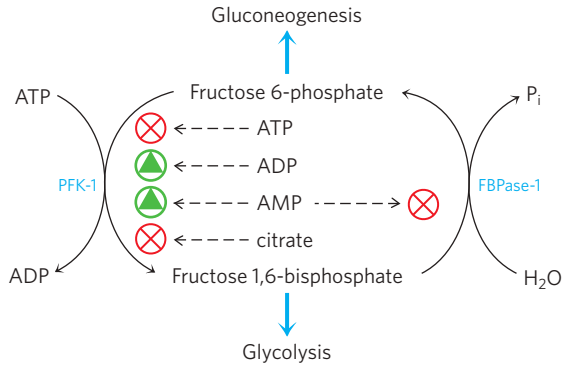

FIGURE 15–17 Regulation of fructose 1,6-bisphosphatase (FBPase-1) and phosphofructokinase-1 (PFK-1). The important role of fructose 2,6-bisphosphate in the regulation of this substrate cycle is detailed in subsequent figures.

Fructose 2,6-Bisphosphate Is a Potent Allosteric Regulator of PFK-1 and FBPase-1

The special role of the liver in maintaining a constant blood glucose level requires additional regulatory mechanisms to coordinate glucose production and consumption. When the blood glucose level decreases, the hormone **glucagon** signals the liver to produce and release more glucose and to stop consuming it for its own needs. One source of glucose is glycogen stored in the liver; another source is gluconeogenesis, using pyruvate, lactate, glycerol, or certain amino acids as starting material. When blood glucose is high, insulin signals the liver to use glucose as a fuel and as a precursor for the synthesis and storage of glycogen and triacylglycerol.

The rapid hormonal regulation of glycolysis and gluconeogenesis is mediated by **fructose 2,6-bisphosphate**, an allosteric effector for the enzymes PFK-1 and FBPase-1:

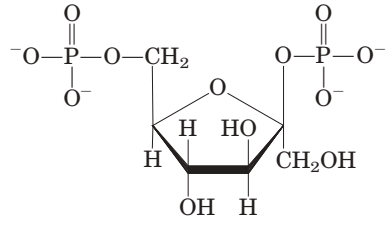

Fructose 2,6-bisphosphate

When fructose 2,6-bisphosphate binds to its allosteric site on PFK-1, it increases the enzyme's affinity for its substrate fructose 6-phosphate and reduces its affinity for the allosteric inhibitors ATP and citrate **(Fig. 15–18)**. At the physiological concentrations of its substrates, ATP and fructose 6-phosphate, and of its other positive and

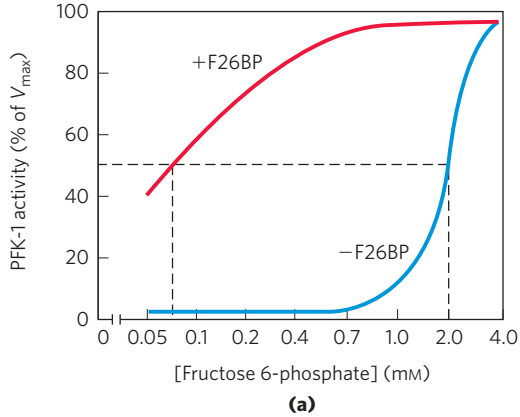

(a)

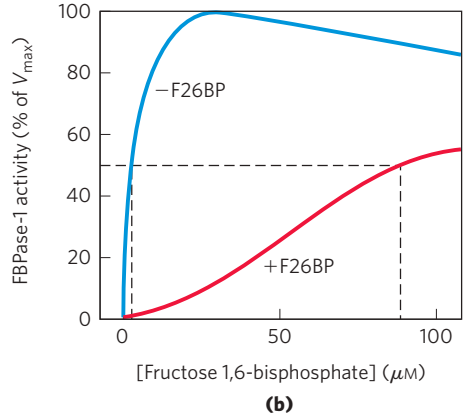

(b)

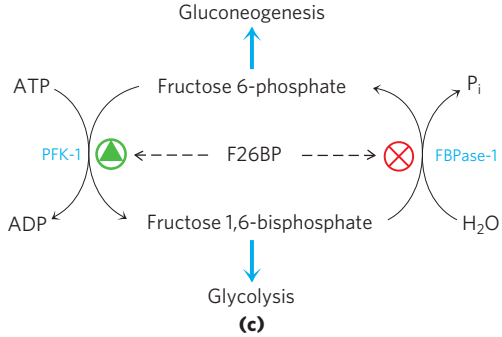

(c)

FIGURE 15–18 Role of fructose 2,6-bisphosphate in regulation of glycolysis and gluconeogenesis. Fructose 2,6-bisphosphate (F26BP) has opposite effects on the enzymatic activities of phosphofructokinase-1 (PFK-1, a glycolytic enzyme) and fructose 1,6-bisphosphatase (FBPase-1, a gluconeogenic enzyme). **(a)** PFK-1 activity in the absence of F26BP (blue curve) is half-maximal when the concentration of fructose 6-phosphate is 2 mM (that is, $K_{0.5}$ = 2 mM). When 0.13 μM F26BP is present (red curve), the $K_{0.5}$ for fructose 6-phosphate is only 0.08 mM. Thus F26BP activates PFK-1 by increasing its apparent affinity for fructose 6-phosphate (see Fig. 15-16b). **(b)** FBPase-1 activity is inhibited by as little as 1 μM F26BP and is strongly inhibited by 25 μM. In the absence of this inhibitor (blue curve) the $K_{0.5}$ for fructose 1,6-bisphosphate is 5 μM, but in the presence of 25 μM F26BP (red curve) the $K_{0.5}$ is >70 μM. Fructose 2,6-bisphosphate also makes FBPase-1 more sensitive to inhibition by another allosteric regulator, AMP. **(c)** Summary of regulation by F26BP.

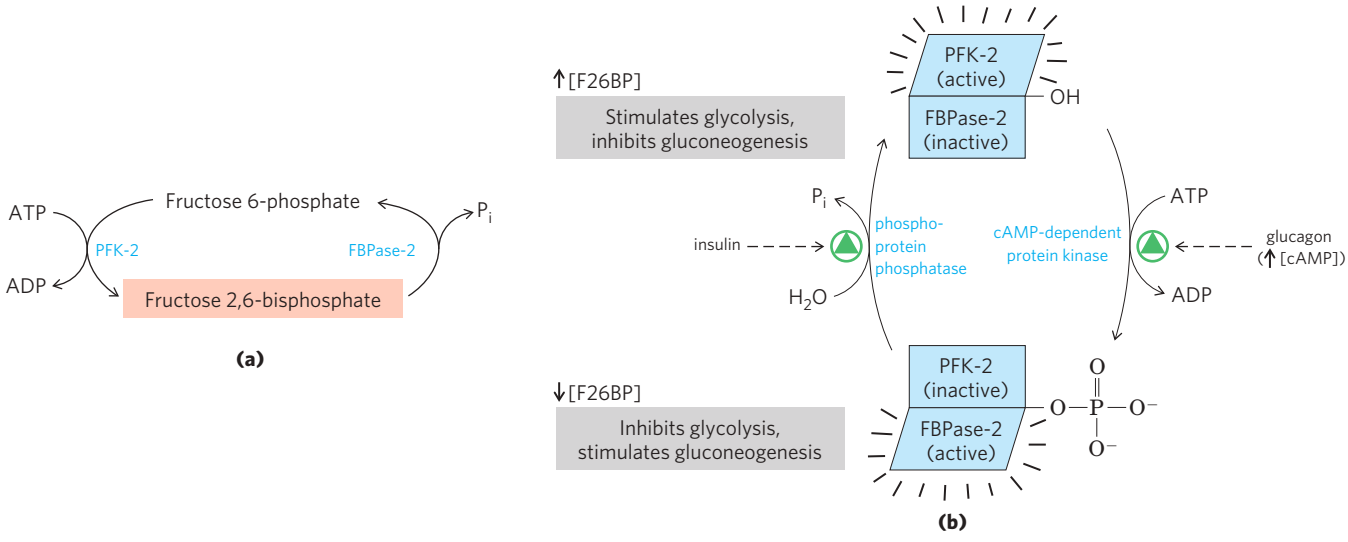

FIGURE 15–19 Regulation of fructose 2,6-bisphosphate level. (a) The cellular concentration of the regulator fructose 2,6-bisphosphate (F26BP) is determined by the rates of its synthesis by phosphofructokinase-2 (PFK-2) and its breakdown by fructose 2,6-bisphosphatase (FBPase-2). **(b)** Both enzyme activities are part of the same polypeptide chain, and they are reciprocally regulated by insulin and glucagon.

negative effectors (ATP, AMP, citrate), PFK-1 is virtually inactive in the absence of fructose 2,6-bisphosphate. Fructose 2,6-bisphosphate has the opposite effect on FBPase-1: it reduces its affinity for its substrate (Fig. 15–18b), thereby slowing gluconeogenesis.

The cellular concentration of the allosteric regulator fructose 2,6-bisphosphate is set by the relative rates of its formation and breakdown **(Fig. 15–19a)**. It is formed by phosphorylation of fructose 6-phosphate, catalyzed by **phosphofructokinase-2 (PFK-2)**, and is broken down by **fructose 2,6-bisphosphatase (FBPase-2)**. (Note that these enzymes are distinct from PFK-1 and FBPase-1, which catalyze the formation and breakdown, respectively, of fructose 1,6-bisphosphate.) PFK-2 and FBPase-2 are two separate enzymatic activities of a single, bifunctional protein. The balance of these two activities in the liver, which determines the cellular level of fructose 2,6-bisphosphate, is regulated by glucagon and insulin (Fig. 15–19b).

As we saw in Chapter 12 (p. 446), glucagon stimulates the adenylyl cyclase of liver to synthesize 3′,5′-cyclic AMP (cAMP) from ATP. Cyclic AMP then activates cAMP-dependent protein kinase, which transfers a phosphoryl group from ATP to the bifunctional protein PFK-2/FBPase-2. Phosphorylation of this protein enhances its FBPase-2 activity and inhibits its PFK-2 activity. Glucagon thereby lowers the cellular level of fructose 2,6-bisphosphate, inhibiting glycolysis and stimulating gluconeogenesis. The resulting production of more glucose enables the liver to replenish blood glucose in response to glucagon. Insulin has the opposite effect, stimulating the activity of a phosphoprotein phosphatase that catalyzes removal of the phosphoryl group from the bifunctional protein PFK-2/FBPase-2, activating its PFK-2 activity, increasing the level of fructose 2,6-bisphosphate, stimulating glycolysis, and inhibiting gluconeogenesis.

Xylulose 5-Phosphate Is a Key Regulator of Carbohydrate and Fat Metabolism

Another regulatory mechanism also acts by controlling the level of fructose 2,6-bisphosphate. In the mammalian liver, xylulose 5-phosphate (p. 577), a product of the pentose phosphate pathway (hexose monophosphate pathway), mediates the increase in glycolysis that follows ingestion of a high-carbohydrate meal. The xylulose 5-phosphate concentration rises as glucose entering the liver is converted to glucose 6-phosphate and enters both the glycolytic and pentose phosphate pathways. Xylulose 5-phosphate activates phosphoprotein phosphatase 2A (PP2A; **Fig. 15–20**), which dephosphorylates the bifunctional PFK-2/FBPase-2 enzyme (Fig. 15–19). Dephosphorylation activates PFK-2 and inhibits FBPase-2, and the resulting rise in fructose 2,6-bisphosphate concentration stimulates glycolysis and inhibits gluconeogenesis. The increased glycolysis boosts the production of acetyl-CoA, while the increased flow of hexose through the pentose phosphate pathway generates NADPH. Acetyl-CoA and NADPH are the starting materials for fatty acid synthesis, which has long been known to increase dramatically in response to intake of a high-carbohydrate meal. Xylulose 5-phosphate also increases the synthesis of *all* the enzymes required for fatty acid synthesis, meeting the prediction from metabolic control analysis. We return to this effect in our discussion of the integration of carbohydrate and lipid metabolism in Chapter 23.

The Glycolytic Enzyme Pyruvate Kinase Is Allosterically Inhibited by ATP

At least three isozymes of pyruvate kinase are found in vertebrates, differing in their tissue distribution and their response to modulators. High concentrations of

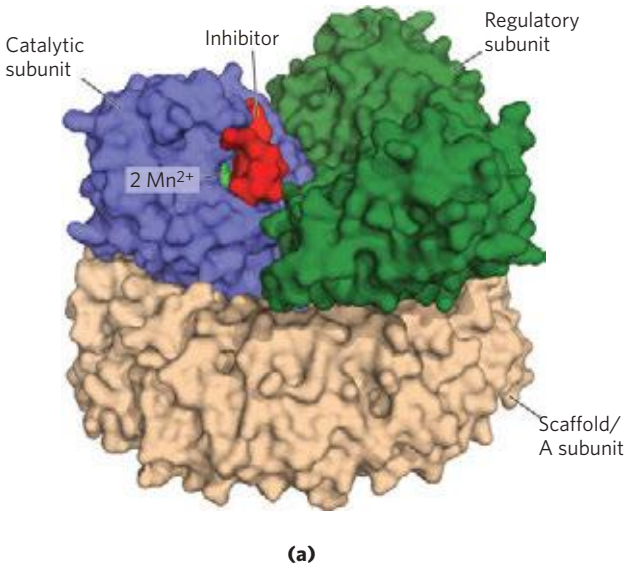

FIGURE 15–20 Structure and action of phosphoprotein phosphatase 2A (PP2A). (a) The catalytic subunit has two Mn^{2+} ions in its active site, positioned close to the substrate-recognition surface formed by the interface between the catalytic subunit and the regulatory subunit (PDB ID 2NPP). Microcystin-LR, shown here in red, is a specific inhibitor of PP2A. The catalytic and regulatory subunits rest in a scaffold (the A subunit) that positions them relative to each other and shapes the substrate-recognition site. **(b)** PP2A recognizes several target proteins, its specificity provided by the regulatory subunit. Each of several regulatory subunits fits the scaffold containing the catalytic subunit, and each regulatory subunit creates its unique substrate-binding site.

ATP, acetyl-CoA, and long-chain fatty acids (signs of abundant energy supply) allosterically inhibit all isozymes of pyruvate kinase **(Fig. 15–21)**. The liver isozyme (L form), but not the muscle isozyme (M form), is subject to further regulation by phosphorylation. When low blood glucose causes glucagon release, cAMP-dependent protein kinase phosphorylates the L isozyme of pyruvate kinase, inactivating it. This slows the use of

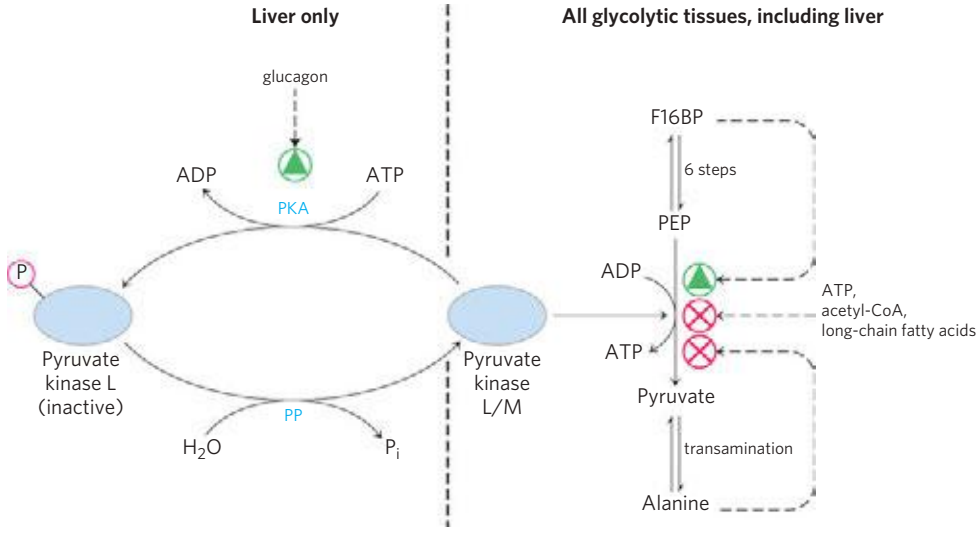

FIGURE 15–21 Regulation of pyruvate kinase. The enzyme is allosterically inhibited by ATP, acetyl-CoA, and long-chain fatty acids (all signs of an abundant energy supply), and the accumulation of fructose 1,6-bisphosphate triggers its activation. Accumulation of alanine, which can be synthesized from pyruvate in one step, allosterically inhibits pyruvate kinase, slowing the production of pyruvate by glycolysis. The liver isozyme (L form) is also regulated hormonally. Glucagon activates cAMP-dependent protein kinase (PKA; see Fig. 15–37), which phosphorylates the pyruvate kinase L isozyme, inactivating it. When the glucagon level drops, a protein phosphatase (PP) dephosphorylates pyruvate kinase, activating it. This mechanism prevents the liver from consuming glucose by glycolysis when blood glucose is low; instead, the liver exports glucose. The muscle isozyme (M form) is not affected by this phosphorylation mechanism.

glucose as a fuel in liver, sparing it for export to the brain and other organs. In muscle, the effect of increased [cAMP] is quite different. In response to epinephrine, cAMP activates glycogen breakdown and glycolysis and provides the fuel needed for the fight-or-flight response.

The Gluconeogenic Conversion of Pyruvate to Phosphoenolpyruvate Is under Multiple Types of Regulation

In the pathway leading from pyruvate to glucose, the first control point determines the fate of pyruvate in the mitochondrion: its conversion either to acetyl-CoA (by the pyruvate dehydrogenase complex) to fuel the citric acid cycle (Chapter 16) or to oxaloacetate (by pyruvate carboxylase) to start the process of gluconeogenesis **(Fig. 15–22)**. When fatty acids are readily available as fuels, their breakdown in liver mitochondria yields acetyl-CoA, a signal that further oxidation of glucose for fuel is not necessary. Acetyl-CoA is a positive allosteric modulator of pyruvate carboxylase and a negative modulator of pyruvate dehydrogenase, through stimulation of a protein kinase that inactivates the dehydrogenase. When the cell's energy needs are being met, oxidative phosphorylation slows, [NADH] rises relative to [NAD^+] and inhibits the citric acid cycle, and acetyl-CoA accumulates. The increased concentration of acetyl-CoA inhibits the pyruvate dehydrogenase complex, slowing the formation of acetyl-CoA from pyruvate, and stimulates gluconeogenesis by activating pyruvate carboxylase, allowing conversion of excess pyruvate to oxaloacetate (and, eventually, glucose).

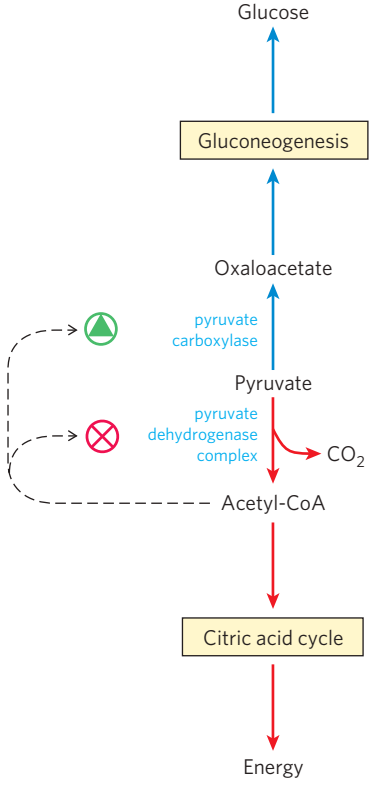

FIGURE 15–22 Two alternative fates for pyruvate. Pyruvate can be converted to glucose and glycogen via gluconeogenesis or oxidized to acetyl-CoA for energy production. The first enzyme in each path is regulated allosterically; acetyl-CoA, produced either by fatty acid oxidation or by the pyruvate dehydrogenase complex, stimulates pyruvate carboxylase and inhibits pyruvate dehydrogenase.

Oxaloacetate formed in this way is converted to phosphoenolpyruvate (PEP) in the reaction catalyzed by PEP carboxykinase (Fig. 15–13). In mammals, the regulation of this key enzyme occurs primarily at the level of its synthesis and breakdown, in response to dietary and hormonal signals. Fasting or high glucagon levels act through cAMP to increase the rate of transcription and to stabilize the mRNA. Insulin, or high blood glucose, has the opposite effects. We discuss this transcriptional regulation in more detail below. Generally triggered by a signal from outside the cell (diet, hormones), these changes take place on a time scale of minutes to hours.

Transcriptional Regulation of Glycolysis and Gluconeogenesis Changes the Number of Enzyme Molecules

Most of the regulatory actions discussed thus far are mediated by fast, quickly reversible mechanisms: allosteric effects, covalent alteration (phosphorylation) of the enzyme, or binding of a regulatory protein. Another set of regulatory processes involves changes in the number of molecules of an enzyme in the cell, through changes in the balance of enzyme synthesis and breakdown, and our discussion now turns to regulation of transcription through signal-activated transcription factors.

In Chapter 12 we encountered nuclear receptors and transcription factors in the context of insulin signaling. Insulin acts through its receptor in the plasma membrane to turn on at least two distinct signaling pathways, each involving activation of a protein kinase. The MAP kinase ERK, for example, phosphorylates the transcription factors SRF and Elk1 (see Fig. 12–15), which then stimulate the synthesis of enzymes needed for cell growth and division. Protein kinase B (PKB; also called Akt) phosphorylates another set of transcription factors (PDX1, for example), and these stimulate the synthesis of enzymes that metabolize carbohydrates and the fats formed and stored following excess carbohydrate intake in the diet. In pancreatic β cells, PDX1 also stimulates the synthesis of insulin itself.

More than 150 genes are transcriptionally regulated by insulin; humans have at least seven general types of insulin response elements, each recognized by a subset of transcription factors activated by insulin under various conditions. Insulin stimulates the transcription of the genes that encode hexokinases II and IV, PFK-1, pyruvate kinase, and PFK-2/FBPase-2 (all involved in glycolysis and its regulation); several enzymes of fatty acid synthesis; and glucose 6-phosphate dehydrogenase and 6-phosphogluconate dehydrogenase, enzymes of the pentose phosphate pathway that generate the NADPH

TABLE 15–5 Some of the Genes Regulated by Insulin

Change in gene expression	Pathway
Increased expression	
Hexokinase II	Glycolysis
Hexokinase IV	Glycolysis
Phosphofructokinase-1 (PFK-1)	Glycolysis
Pyruvate kinase	Glycolysis
PFK-2/FBPase-2	Regulation of glycolysis/gluconeogenesis
Glucose 6-phosphate dehydrogenase	Pentose phosphate pathway (NADPH)
6-Phosphogluconate dehydrogenase	Pentose phosphate pathway (NADPH)
Pyruvate dehydrogenase	Fatty acid synthesis
Acetyl-CoA carboxylase	Fatty acid synthesis
Malic enzyme	Fatty acid synthesis (NADPH)
ATP-citrate lyase	Fatty acid synthesis (provides acetyl-CoA)
Fatty acid synthase complex	Fatty acid synthesis
Stearoyl-CoA dehydrogenase	Fatty acid desaturation
Acyl-CoA–glycerol transferases	Triacylglycerol synthesis
Decreased expression	
PEP carboxykinase	Gluconeogenesis
Glucose 6-phosphatase (catalytic subunit)	Glucose release to blood

required for fatty acid synthesis. Insulin also slows the expression of the genes for two enzymes of gluconeogenesis: PEP carboxykinase and glucose 6-phosphatase (Table 15–5).

One transcription factor important to carbohydrate metabolism is **ChREBP** (**carbohydrate response element binding protein**; **Fig. 15–23**), which is expressed primarily in liver, adipose tissue, and kidney. It serves to coordinate the synthesis of enzymes needed for carbohydrate and fat synthesis. ChREBP in its inactive state is phosphorylated, and is located in the cytosol. When the phosphoprotein phosphatase PP2A (Fig. 15–20) removes a phosphoryl group from ChREBP, the transcription factor can enter the nucleus. Here, nuclear PP2A removes another phosphoryl group, and ChREBP now joins with a partner protein, Mlx, and turns on the synthesis of several enzymes: pyruvate kinase, fatty acid synthase, and acetyl-CoA carboxylase, the first enzyme in the path to fatty acid synthesis.

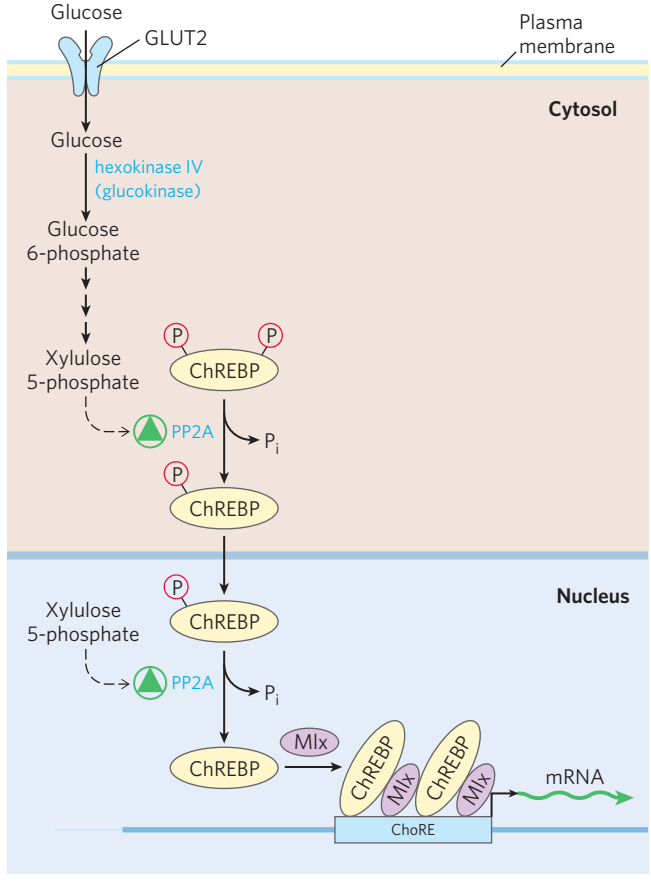

FIGURE 15–23 Mechanism of gene regulation by the transcription factor ChREBP. When ChREBP in the cytosol of a hepatocyte is phosphorylated on a Ser and a Thr residue, it cannot enter the nucleus. Dephosphorylation of Ⓟ-Ser by protein phosphatase PP2A allows ChREBP to enter the nucleus, where a second dephosphorylation, of Ⓟ-Thr, activates ChREBP so that it can associate with its partner protein, Mlx. ChREBP-Mlx now binds to the carbohydrate response element (ChoRE) in the promoter and stimulates transcription. PP2A is allosterically activated by xylulose 5-phosphate, an intermediate in the pentose phosphate pathway.

Controlling the activity of PP2A—and thus, ultimately, the synthesis of this group of metabolic enzymes—is xylulose 5-phosphate, an intermediate of the pentose phosphate pathway (Fig. 14–23). When blood glucose concentration is high, glucose enters the liver and is phosphorylated by hexokinase IV. The glucose 6-phosphate thus formed can enter either the glycolytic pathway or the pentose phosphate pathway. If the latter, two initial oxidations produce xylulose 5-phosphate, which serves as a signal that the glucose-utilizing pathways are well-supplied with substrate. It accomplishes this by allosterically activating PP2A, which then dephosphorylates ChREBP, allowing the transcription factor to turn on the expression of genes for enzymes of glycolysis and fat synthesis (Fig. 15–23). Glycolysis yields pyruvate, and conversion of pyruvate to acetyl-CoA provides the starting material for fatty acid synthesis: acetyl-CoA carboxylase converts acetyl-CoA to malonyl-CoA, the first committed intermediate in the path to fatty acids. The fatty acid synthase complex produces fatty acids for export to adipose tissue and storage as triacylglycerols (Chapter 21). In this way, excess dietary carbohydrate is stored as fat.

Another transcription factor in the liver, **SREBP-1c**, a member of the family of **sterol regulatory element binding proteins** (see Fig. 21–44), turns on the synthesis of pyruvate kinase, hexokinase IV, lipoprotein lipase, acetyl-CoA carboxylase, and the fatty acid synthase complex that will convert acetyl-CoA (produced from pyruvate) into fatty acids for storage in adipocytes. The synthesis of SREBP-1c is stimulated by insulin and depressed by glucagon. SREBP-1c also suppresses the expression of several gluconeogenic enzymes: glucose 6-phosphatase, PEP carboxykinase, and FBPase-1.

The transcription factor **CREB** (**cyclic AMP response element binding protein**) turns on the synthesis of glucose 6-phosphatase and PEP carboxykinase in response to the increase in [cAMP] triggered by glucagon. In contrast, insulin-stimulated *inactivation* of other transcription factors turns off several gluconeogenic enzymes in the liver: PEP carboxykinase, fructose 1,6-bisphosphatase, the glucose 6-phosphate transporter of the endoplasmic reticulum, and glucose 6-phosphatase. For example, **FOXO1 (forkhead box other)** stimulates the synthesis of gluconeogenic enzymes and suppresses the synthesis of the enzymes of glycolysis, the pentose phosphate pathway, and triacylglycerol synthesis **(Fig. 15–24)**. In its unphosphorylated form, FOXO1 acts as a nuclear transcription factor. In response to insulin, FOXO1 leaves the nucleus and in the cytosol is phosphorylated by PKB, then tagged with ubiquitin and degraded by the proteasome. Glucagon prevents this phosphorylation by PKB, and FOXO1 remains active in the nucleus.

Complicated though the processes outlined above may seem, regulation of the genes encoding enzymes of carbohydrate and fat metabolism is proving far more complex and more subtle than we have shown here. Multiple transcription factors can act on the same gene promoter; multiple protein kinases and phosphatases can activate or inactivate these transcription factors; and a variety of protein accessory factors modulate the action of the transcription factors. This complexity is apparent, for example, in the gene encoding PEP carboxykinase, a very well-studied case of transcriptional control. Its promoter region **(Fig. 15–25)** has 15 or more response elements that are recognized by at least a dozen known transcription factors, with more likely to be discovered. The transcription factors act in combination on this promoter region, and on hundreds of other gene promoters, to fine-tune the levels of hundreds of metabolic enzymes, coordinating their activity in the metabolism of carbohydrates and fats. The critical importance of transcription factors in metabolic regulation is made clear by observing the effects of mutations in their genes. For example, at least five different types of maturity-onset diabetes of the young (MODY) are associated with mutations in specific transcription factors (Box 15–3).

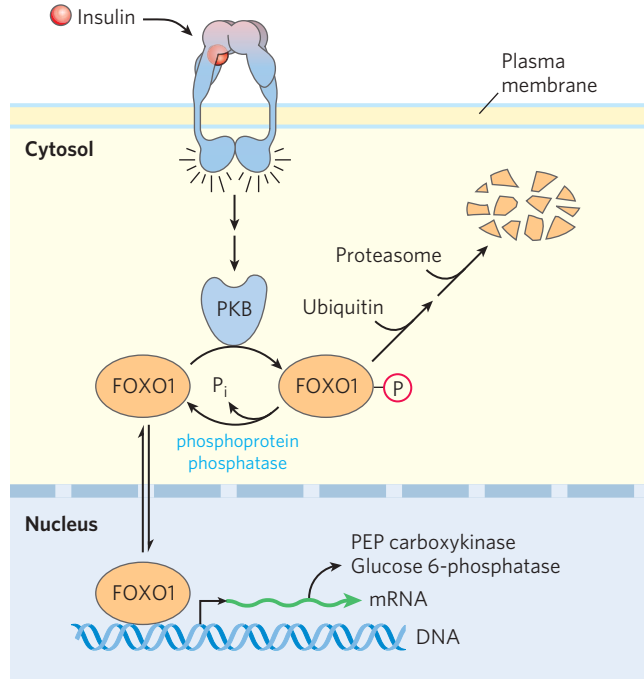

FIGURE 15–24 Mechanism of gene regulation by the transcription factor FOXO1. Insulin activates the signaling cascade shown in Figure 12–16, leading to activation of protein kinase B (PKB). FOXO1 in the cytosol is phosphorylated by PKB, and the phosphorylated transcription factor is tagged by the attachment of ubiquitin for degradation by proteasomes. FOXO1 that remains unphosphorylated or is dephosphorylated can enter the nucleus, bind to a response element, and trigger transcription of the associated genes. Insulin therefore has the effect of turning *off* the expression of these genes, which include PEP carboxykinase and glucose 6-phosphatase.

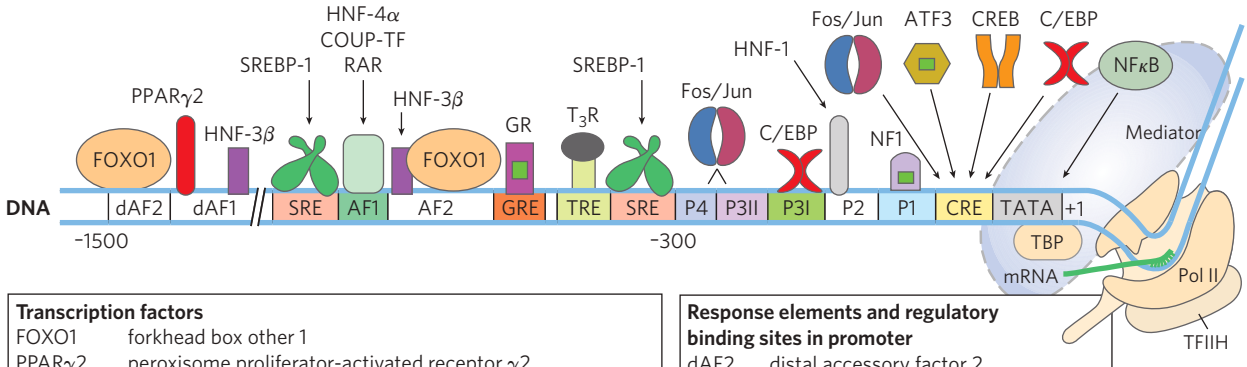

Transcription factors	
FOXO1	forkhead box other 1
PPARγ2	peroxisome proliferator-activated receptor γ2
HNF-3β	hepatic nuclear factor-3β
SREBP-1	sterol regulatory element binding protein-1
HNF-4α	hepatic nuclear factor-4α
COUP-TF	chicken ovalbumin upstream promoter–transcription factor
RAR	retinoic acid receptor
GR	glucocorticoid receptor
T_3R	thyroid hormone receptor
C/EBP	CAAT/enhance binding protein
HNF-1	hepatic nuclear factor-1
NF1	nuclear factor 1
ATF3	activating transcription factor 3
CREB	cAMP response element binding protein
NFκB	nuclear factor κB
TBP	TATA-box binding protein
TFIIH	transcription factor IIH

Response elements and regulatory binding sites in promoter	
dAF2	distal accessory factor 2
dAF1	distal accessory factor 1
SRE	sterol regulatory element
AF1	accessory factor 1
AF2	accessory factor 2
GRE	glucocorticoid regulatory element
TRE	thyroid hormone regulatory element
CRE	cAMP regulatory element

FIGURE 15–25 The PEP carboxykinase promoter region, showing the complexity of regulatory input to this gene. This diagram shows the transcription factors (smaller icons, bound to the DNA) known to regulate the transcription of the PEP carboxykinase gene. The extent to which this gene is expressed depends on the combined input affecting all of these factors, which can reflect the availability of nutrients, blood glucose level, and other circumstances that affect the cell's need for this enzyme at any particular time. P1, P2, P3I, P3II, and P4 are protein-binding sites identified by DNase I footprinting (see Box 26–1). The TATA box is the assembly point for the RNA polymerase II (Pol II) transcription complex.

BOX 15–3 MEDICINE Genetic Mutations That Lead to Rare Forms of Diabetes

The term "diabetes" describes a variety of medical conditions that have in common an excessive production of urine. In Box 11–1 we described diabetes insipidus, in which defective water reabsorption in the kidney results from a mutation in the gene for aquaporin. "Diabetes mellitus" refers specifically to disease in which the ability to metabolize glucose is defective, due either to the failure of the pancreas to produce insulin or to tissue resistance to the actions of insulin.

There are two common types of diabetes mellitus. Type 1, also called insulin-dependent diabetes mellitus (IDDM), is caused by autoimmune attack on the insulin-producing β cells of the pancreas. Individuals with IDDM must take insulin by injection or inhalation to compensate for their missing β cells. IDDM develops in childhood or in the teen years; an older name for the disease is juvenile diabetes. Type 2, also called non–insulin-dependent diabetes mellitus (NIDDM), typically develops in adults over 40 years old. It is far more common than IDDM, and its occurrence in the population is strongly correlated with obesity. The current epidemic of obesity in the more developed countries brings with it the promise of an epidemic of NIDDM, providing a strong incentive to understand the relationship between obesity and the onset of NIDDM at the genetic and biochemical levels. After completing our look at the metabolism of fats and proteins in later chapters, we will return (in Chapter 23) to the discussion of diabetes, which has a broad effect on metabolism: of carbohydrates, fats, and proteins.

Here we consider another type of diabetes in which carbohydrate and fat metabolism is deranged: mature onset diabetes of the young (MODY), in which genetic mutation affects a transcription factor important in carrying the insulin signal into the nucleus, or affects an enzyme that responds to insulin. In MODY2, a mutation in the hexokinase IV (glucokinase) gene affects the liver and pancreas, tissues in which this is the main isoform of hexokinase. The glucokinase of pancreatic β cells functions as a glucose sensor. Normally, when blood glucose

(*Continued on the next page*)

BOX 15–3 MEDICINE Genetic Mutations That Lead to Rare Forms of Diabetes (*Continued*)

rises, so does the glucose level in β cells, and because glucokinase has a relatively high K_m for glucose, its activity increases with rising blood glucose levels. Metabolism of the glucose 6-phosphate formed in this reaction raises the ATP level in β cells, and this triggers insulin release by the mechanism shown in Fig. 23–27. In healthy individuals, blood glucose concentrations of ~5 mM trigger this insulin release. But individuals with inactivating mutations in both copies of the glucokinase gene have very high thresholds for insulin release, and consequently, from birth, they have severe hyperglycemia—permanent neonatal diabetes. In individuals with one mutated and one normal copy of the glucokinase gene, the glucose threshold for insulin release rises to about 7 mM. As a result these individuals have blood glucose levels only slightly above normal: they generally have only mild hyperglycemia and no symptoms. This condition (MODY2) is generally discovered by accident during routine blood glucose analysis.

There are at least five other types of MODY, each the result of an inactivating mutation in one or another of the transcription factors essential to the normal development and function of pancreatic β cells. Individuals with these mutations have varying degrees of reduced insulin production and the associated defects in blood glucose homeostasis. In MODY1 and MODY3, the defects are severe enough to produce the long-term complications associated with IDDM and NIDDM—cardiovascular problems, kidney failure, and blindness. MODY4, 5, and 6 are less severe forms of the disease. Altogether, MODY disorders represent a small percentage of NIDDM cases. Also very rare are individuals with mutations in the insulin gene itself; they have defects in insulin signaling of varying severity.

SUMMARY 15.3 Coordinated Regulation of Glycolysis and Gluconeogenesis

- Gluconeogenesis and glycolysis share seven enzymes, catalyzing the freely reversible reactions of the pathways. For the other three steps, the forward and reverse reactions are catalyzed by different enzymes, and these are the points of regulation of the two pathways.
- Hexokinase IV (glucokinase) has kinetic properties related to its special role in the liver: releasing glucose to the blood when blood glucose is low, and taking up and metabolizing glucose when blood glucose is high.
- PFK-1 is allosterically inhibited by ATP and citrate. In most mammalian tissues, including liver, fructose 2,6-bisphosphate is an allosteric activator of this enzyme.
- Pyruvate kinase is allosterically inhibited by ATP, and the liver isozyme also is inhibited by cAMP-dependent phosphorylation.
- Gluconeogenesis is regulated at the level of pyruvate carboxylase (which is activated by acetyl-CoA) and FBPase-1 (which is inhibited by fructose 2,6-bisphosphate and AMP).
- To limit substrate cycling between glycolysis and gluconeogenesis, the two pathways are under reciprocal allosteric control, mainly achieved by the opposing effects of fructose 2,6-bisphosphate on PFK-1 and FBPase-1.
- Glucagon or epinephrine decreases [fructose 2,6-bisphosphate], by raising [cAMP] and bringing about phosphorylation of the bifunctional enzyme PFK-2/FBPase-2. Insulin increases [fructose 2,6-bisphosphate] by activating a phosphoprotein phosphatase that dephosphorylates and thus activates PFK-2.
- Xylulose 5-phosphate, an intermediate of the pentose phosphate pathway, activates phosphoprotein phosphatase PP2A, which dephosphorylates several target proteins, including PFK-2/FBPase-2, tilting the balance toward glucose uptake, glycogen synthesis, and lipid synthesis in the liver.
- Transcription factors including ChREBP, CREB, SREBP, and FOXO1 act in the nucleus to regulate the expression of specific genes coding for enzymes of the glycolytic and gluconeogenic pathways. Insulin and glucagon act antagonistically in activating these transcription factors, thus turning on and off large numbers of genes.

15.4 The Metabolism of Glycogen in Animals

Our discussion of metabolic regulation, using carbohydrate metabolism as the primary example, now turns to the synthesis and breakdown of glycogen. In this section we focus on the metabolic pathways; in Section 15.5 we turn to the regulatory mechanisms.

In organisms from bacteria to plants to vertebrates, excess glucose is converted to polymeric forms for storage—glycogen in vertebrates and many microorganisms, starch in plants. In vertebrates, glycogen is found primarily in the liver and skeletal muscle; it may repre-

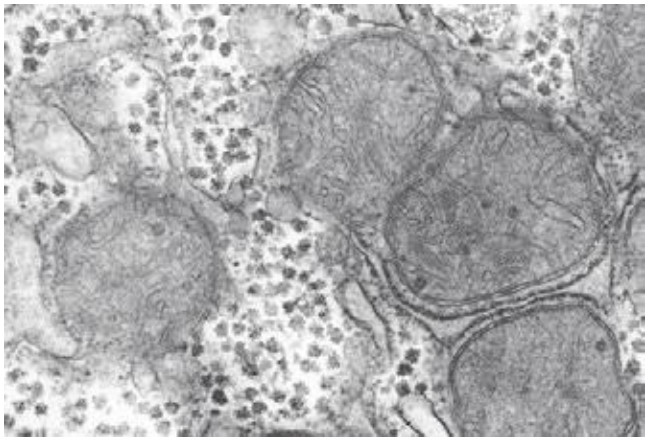

FIGURE 15–26 Glycogen granules in a hepatocyte. Glycogen, a storage form of carbohydrate, appears as electron-dense particles, often in aggregates or rosettes. In hepatocytes glycogen is closely associated with tubules of the smooth endoplasmic reticulum. Many mitochondria are also evident in this micrograph.

sent up to 10% of the weight of liver and 1% to 2% of the weight of muscle. If this much glucose were dissolved in the cytosol of a hepatocyte, its concentration would be about 0.4 M, enough to dominate the osmotic properties of the cell. When stored as a large polymer (glycogen), however, the same mass of glucose has a concentration of only 0.01 μM. Glycogen is stored in large cytosolic granules. The elementary particle of glycogen, the β-particle, is about 21 nm in diameter and consists of up to 55,000 glucose residues with about 2,000 nonreducing ends. Twenty to 40 of these particles cluster together to form α-rosettes, easily seen with the microscope in tissue samples from well-fed animals **(Fig. 15–26)** but essentially absent after a 24-hour fast.

The glycogen in muscle is there to provide a quick source of energy for either aerobic or anaerobic metabolism. Muscle glycogen can be exhausted in less than an hour during vigorous activity. Liver glycogen serves as a reservoir of glucose for other tissues when dietary glucose is not available (between meals or during a fast); this is especially important for the neurons of the brain, which cannot use fatty acids as fuel. Liver glycogen can be depleted in 12 to 24 hours. In humans, the total amount of energy stored as glycogen is far less than the amount stored as fat (triacylglycerol) (see Table 23–5), but fats cannot be converted to glucose in mammals and cannot be catabolized anaerobically.

Glycogen granules are complex aggregates of glycogen and the enzymes that synthesize it and degrade it, as well as the machinery for regulating these enzymes. The general mechanisms for storing and mobilizing glycogen are the same in muscle and liver, but the enzymes differ in subtle yet important ways that reflect the different roles of glycogen in the two tissues. Glycogen is also obtained in the diet and broken down in the gut, and this involves a separate set of hydrolytic enzymes that convert glycogen to free glucose. (Dietary starch is hydrolyzed in a similar way.) We begin our discussion with the breakdown of glycogen to glucose 1-phosphate (**glycogenolysis**), then turn to synthesis of glycogen (**glycogenesis**).

Glycogen Breakdown Is Catalyzed by Glycogen Phosphorylase

In skeletal muscle and liver, the glucose units of the outer branches of glycogen enter the glycolytic pathway through the action of three enzymes: glycogen phosphorylase, glycogen debranching enzyme, and phosphoglucomutase. Glycogen phosphorylase catalyzes the reaction in which an (α1→4) glycosidic linkage between two glucose residues at a nonreducing end of glycogen undergoes attack by inorganic phosphate (P_i), removing the terminal glucose residue as **α-D-glucose 1-phosphate (Fig. 15–27)**. This *phosphorolysis* reaction is

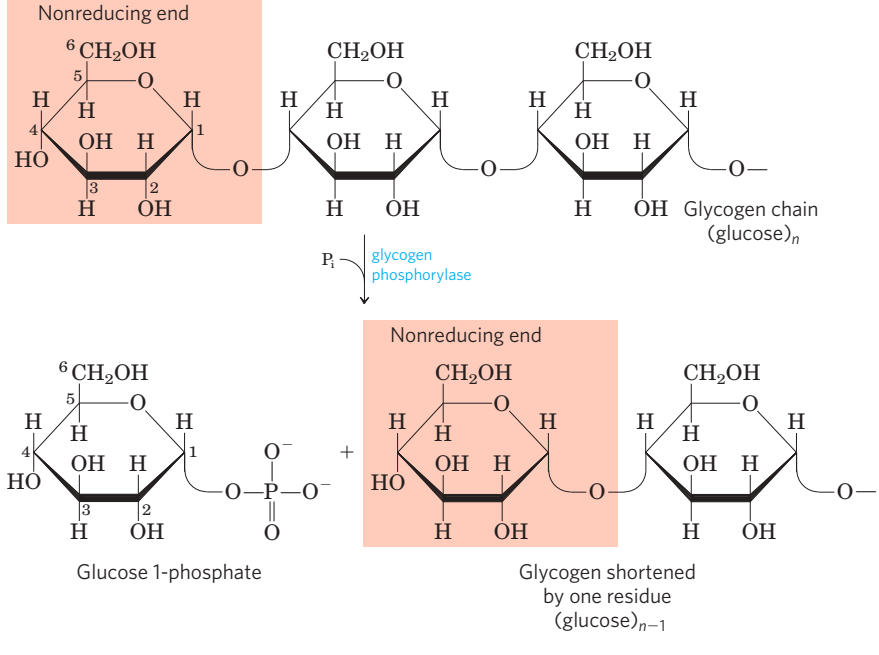

FIGURE 15–27 Removal of a glucose residue from the nonreducing end of a glycogen chain by glycogen phosphorylase. This process is repetitive; the enzyme removes successive glucose residues until it reaches the fourth glucose unit from a branch point (see Fig. 15–28).

different from the *hydrolysis* of glycosidic bonds by amylase during intestinal degradation of dietary glycogen and starch. In phosphorolysis, some of the energy of the glycosidic bond is preserved in the formation of the phosphate ester, glucose 1-phosphate (see Section 14.2).

Pyridoxal phosphate is an essential cofactor in the glycogen phosphorylase reaction; its phosphate group acts as a general acid catalyst, promoting attack by P_i on the glycosidic bond. (This is an unusual role for pyridoxal phosphate; its more typical role is as a cofactor in amino acid metabolism; see Fig. 18–6.)

Glycogen phosphorylase acts repetitively on the nonreducing ends of glycogen branches until it reaches a point four glucose residues away from an (α1→6) branch point (see Fig. 7–13), where its action stops. Further degradation by glycogen phosphorylase can occur only after the **debranching enzyme**, formally known as **oligo (α1→6) to (α1→4) glucantransferase**, catalyzes two successive reactions that transfer branches **(Fig. 15–28)**. Once these branches are transferred and the glucosyl residue at C-6 is hydrolyzed, glycogen phosphorylase activity can continue.

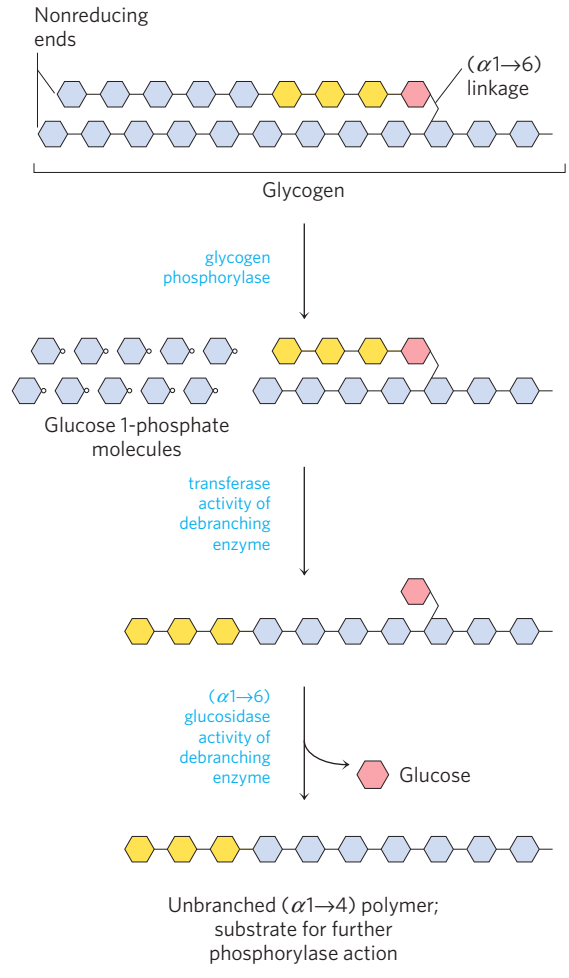

FIGURE 15–28 Glycogen breakdown near an (α1→6) branch point. Following sequential removal of terminal glucose residues by glycogen phosphorylase (see Fig. 15–27), glucose residues near a branch are removed in a two-step process that requires a bifunctional debranching enzyme. First, the transferase activity of the enzyme shifts a block of three glucose residues from the branch to a nearby nonreducing end, to which they are reattached in (α1→4) linkage. The single glucose residue remaining at the branch point, in (α1→6) linkage, is then released as free glucose by the debranching enzyme's (α1→6) glucosidase activity. The glucose residues are shown in shorthand form, which omits the —H, —OH, and —CH_2OH groups from the pyranose rings.

Glucose 1-Phosphate Can Enter Glycolysis or, in Liver, Replenish Blood Glucose

Glucose 1-phosphate, the end product of the glycogen phosphorylase reaction, is converted to glucose 6-phosphate by **phosphoglucomutase**, which catalyzes the reversible reaction

$$\text{Glucose 1-phosphate} \rightleftharpoons \text{glucose 6-phosphate}$$

Initially phosphorylated at a Ser residue, the enzyme donates a phosphoryl group to C-6 of the substrate, then accepts a phosphoryl group from C-1 **(Fig. 15–29)**.

The glucose 6-phosphate formed from glycogen in skeletal muscle can enter glycolysis and serve as an energy source to support muscle contraction. In liver, glycogen breakdown serves a different purpose: to release glucose into the blood when the blood glucose

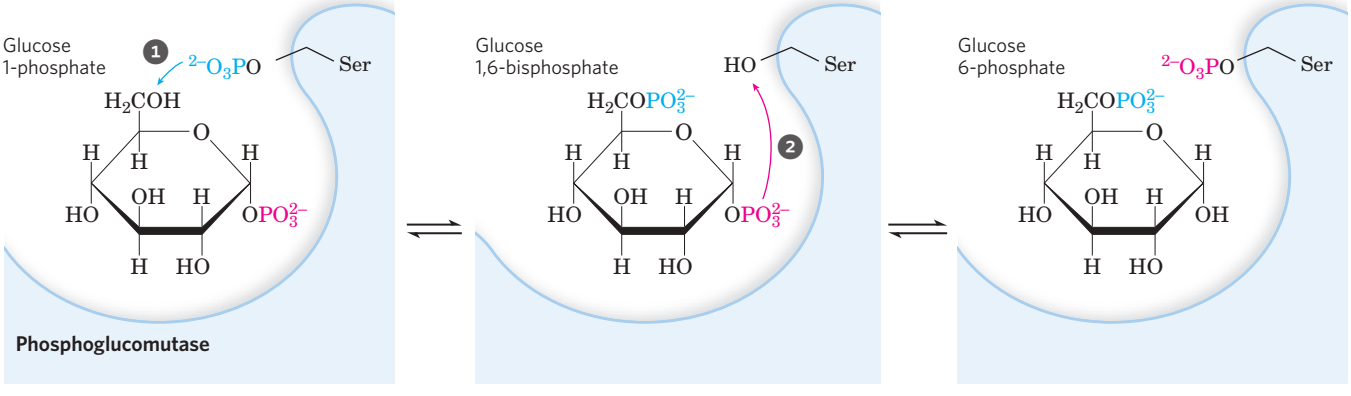

FIGURE 15–29 Reaction catalyzed by phosphoglucomutase. The reaction begins with the enzyme phosphorylated on a Ser residue. In step 1, the enzyme donates its phosphoryl group (blue) to glucose 1-phosphate, producing glucose 1,6-bisphosphate. In step 2, the phosphoryl group at C-1 of glucose 1,6-bisphosphate (red) is transferred back to the enzyme, reforming the phosphoenzyme and producing glucose 6-phosphate.

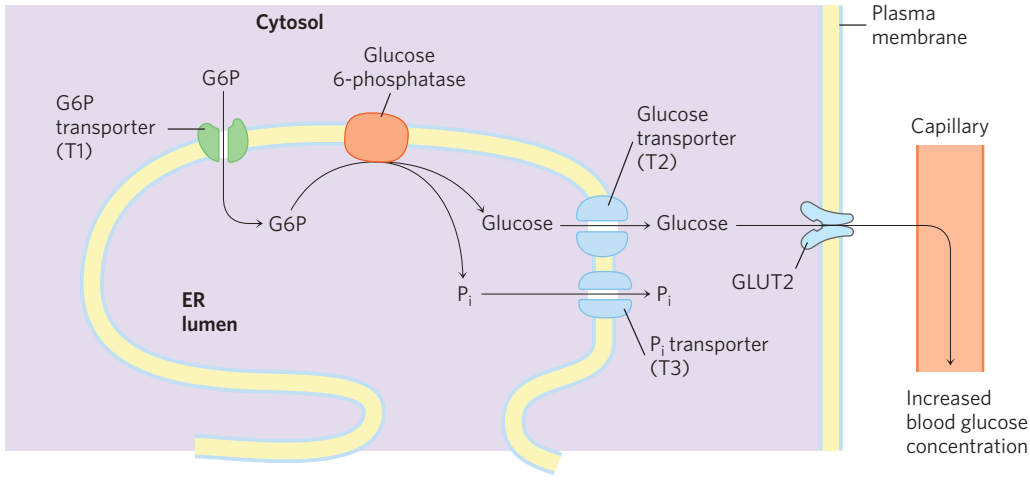

FIGURE 15–30 Hydrolysis of glucose 6-phosphate by glucose 6-phosphatase of the ER. The catalytic site of glucose 6-phosphatase faces the lumen of the ER. A glucose 6-phosphate (G6P) transporter (T1) carries the substrate from the cytosol to the lumen, and the products glucose and P_i pass to the cytosol on specific transporters (T2 and T3). Glucose leaves the cell via the GLUT2 transporter in the plasma membrane.

level drops, as it does between meals. This requires the enzyme glucose 6-phosphatase, present in liver and kidney but not in other tissues. The enzyme is an integral membrane protein of the endoplasmic reticulum, predicted to contain nine transmembrane helices, with its active site on the lumenal side of the ER. Glucose 6-phosphate formed in the cytosol is transported into the ER lumen by a specific transporter (T1) **(Fig. 15–30)** and hydrolyzed at the lumenal surface by the glucose 6-phosphatase. The resulting P_i and glucose are thought to be carried back into the cytosol by two different transporters (T2 and T3), and the glucose leaves the hepatocyte via the plasma membrane transporter, GLUT2. Notice that by having the active site of glucose 6-phosphatase inside the ER lumen, the cell separates this reaction from the process of glycolysis, which takes place in the cytosol and would be aborted by the action of glucose 6-phosphatase. Genetic defects in either glucose 6-phosphatase or T1 lead to serious derangement of glycogen metabolism, resulting in type Ia glycogen storage disease (Box 15–4).

Because muscle and adipose tissue lack glucose 6-phosphatase, they cannot convert the glucose 6-phosphate formed by glycogen breakdown to glucose, and these tissues therefore do not contribute glucose to the blood.

The Sugar Nucleotide UDP-Glucose Donates Glucose for Glycogen Synthesis

Luis Leloir, 1906–1987

Many of the reactions in which hexoses are transformed or polymerized involve **sugar nucleotides**, compounds in which the anomeric carbon of a sugar is activated by attachment to a nucleotide through a phosphate ester linkage. Sugar nucleotides are the substrates for polymerization of monosaccharides into disaccharides, glycogen, starch, cellulose, and more complex extracellular polysaccharides. They are also key intermediates in the production of the aminohexoses and deoxyhexoses found in some of these polysaccharides, and in the synthesis of vitamin C (l-ascorbic acid). The role of sugar nucleotides in the biosynthesis of glycogen and many other carbohydrate derivatives was discovered in 1953 by the Argentine biochemist Luis Leloir.

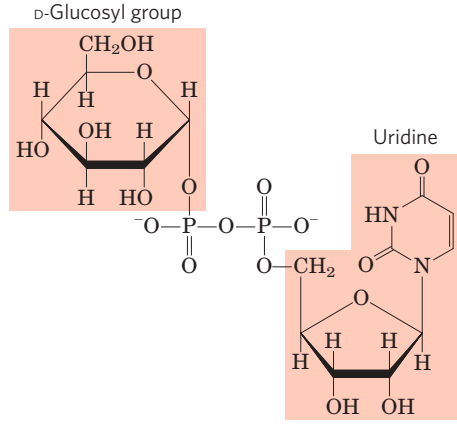

UDP-glucose
(a sugar nucleotide)

The suitability of sugar nucleotides for biosynthetic reactions stems from several properties:

1. Their formation is metabolically irreversible, contributing to the irreversibility of the synthetic pathways in which they are intermediates. The condensation of a nucleoside triphosphate with a hexose 1-phosphate to form a sugar nucleotide has a small positive free-energy change, but the reaction releases PP_i, which is rapidly hydrolyzed by inorganic pyrophosphatase **(Fig. 15–31)**, in a reaction that is strongly exergonic ($\Delta G'^\circ = -19.2$ kJ/mol). This keeps the cellular concentration of PP_i low, ensuring that the actual free-energy change in the cell is favorable. In effect, rapid removal of the product, driven by the large, negative free-energy change of PP_i

BOX 15–4 Carl and Gerty Cori: Pioneers in Glycogen Metabolism and Disease

Much of what is written in present-day biochemistry textbooks about the metabolism of glycogen was discovered between about 1925 and 1950 by the remarkable husband and wife team of Carl F. Cori and Gerty T. Cori. Both trained in medicine in Europe at the end of World War I (she completed premedical studies and medical school in one year!). They left Europe together in 1922 to establish research laboratories in the United States, first for nine years in Buffalo, New York, at what is now the Roswell Park Memorial Institute, then from 1931 until the end of their lives at Washington University in St. Louis.

In their early physiological studies of the origin and fate of glycogen in animal muscle, the Coris demonstrated the conversion of glycogen to lactate in tissues, movement of lactate in the blood to the liver, and, in the liver, reconversion of lactate to glycogen—a pathway that came to be known as the Cori cycle (see Fig. 23–19). Pursuing these observations at the biochemical level, they showed that glycogen was mobilized in a phosphorolysis reaction catalyzed by the enzyme they discovered, glycogen phosphorylase. They identified the product of this reaction (the "Cori ester") as glucose 1-phosphate and showed that it could be reincorporated into glycogen in the reverse reaction. Although this did not prove to be the reaction by which glycogen is synthesized in cells, it was the first in vitro demonstration of the synthesis of a macromolecule from simple monomeric subunits, and it inspired others to search for polymerizing enzymes. Arthur Kornberg, discoverer of the first DNA polymerase, said of his experience in the Coris' lab, "Glycogen phosphorylase, not base pairing, was what led me to DNA polymerase."

The Coris in Gerty Cori's laboratory, around 1947.

Gerty Cori became interested in human genetic diseases in which too much glycogen is stored in the liver. She was able to identify the biochemical defect in several of these diseases and to show that the diseases could be diagnosed by assays of the enzymes of glycogen metabolism in small samples of tissue obtained by biopsy. Table 1 summarizes what we now know about 13 genetic diseases of this sort. ■

Carl and Gerty Cori shared the Nobel Prize in Physiology or Medicine in 1947 with Bernardo Houssay of Argentina, who was cited for his studies of hormonal regulation of carbohydrate metabolism. The Cori laboratories in St. Louis became an international center of biochemical research in the 1940s and 1950s, and at least six scientists who trained with the Coris became Nobel laureates: Arthur Kornberg (for DNA synthesis, 1959), Severo Ochoa (for RNA synthesis, 1959), Luis Leloir (for the role of sugar nucleotides in polysaccharide synthesis, 1970), Earl Sutherland (for the discovery of cAMP in the regulation of carbohydrate metabolism, 1971), Christian de Duve (for subcellular fractionation, 1974), and Edwin Krebs (for the discovery of phosphorylase kinase, 1991).

hydrolysis, pulls the synthetic reaction forward, a common strategy in biological polymerization reactions.

2. Although the chemical transformations of sugar nucleotides do not involve the atoms of the nucleotide itself, the nucleotide moiety has many groups that can undergo noncovalent interactions with enzymes; the additional free energy of binding can contribute significantly to catalytic activity (Chapter 6; see also pp. 306–307).
3. Like phosphate, the nucleotidyl group (UMP or AMP, for example) is an excellent leaving group, facilitating nucleophilic attack by activating the sugar carbon to which it is attached.
4. By "tagging" some hexoses with nucleotidyl groups, cells can set them aside in a pool for one purpose (glycogen synthesis, for example), separate from hexose phosphates destined for another purpose (such as glycolysis).

TABLE 1 Glycogen Storage Diseases of Humans

Type (name)	Enzyme affected	Primary organ affected	Symptoms
Type 0	Glycogen synthase	Liver	Low blood glucose, high ketone bodies, early death
Type Ia (von Gierke)	Glucose 6-phosphatase	Liver	Enlarged liver, kidney failure
Type Ib	Microsomal glucose 6-phosphate translocase	Liver	As in type Ia; also high susceptibility to bacterial infections
Type Ic	Microsomal P_i transporter	Liver	As in type Ia
Type II (Pompe)	Lysosomal glucosidase	Skeletal and cardiac muscle	Infantile form: death by age 2; juvenile form: muscle defects (myopathy); adult form: as in muscular dystrophy
Type IIIa (Cori or Forbes)	Debranching enzyme	Liver, skeletal and cardiac muscle	Enlarged liver in infants; myopathy
Type IIIb	Liver debranching enzyme (muscle enzyme normal)	Liver	Enlarged liver in infants
Type IV (Andersen)	Branching enzyme	Liver, skeletal muscle	Enlarged liver and spleen, myoglobin in urine
Type V (McArdle)	Muscle phosphorylase	Skeletal muscle	Exercise-induced cramps and pain; myoglobin in urine
Type VI (Hers)	Liver phosphorylase	Liver	Enlarged liver
Type VII (Tarui)	Muscle PFK-1	Muscle, erythrocytes	As in type V; also hemolytic anemia
Type VIb, VIII, or IX	Phosphorylase kinase	Liver, leukocytes, muscle	Enlarged liver
Type XI (Fanconi-Bickel)	Glucose transporter (GLUT2)	Liver	Failure to thrive, enlarged liver, rickets, kidney dysfunction

Glycogen synthesis takes place in virtually all animal tissues but is especially prominent in the liver and skeletal muscles. The starting point for synthesis of glycogen is glucose 6-phosphate. As we have seen, this can be derived from free glucose in a reaction catalyzed by the isozymes hexokinase I and hexokinase II in muscle and hexokinase IV (glucokinase) in liver:

$$\text{D-Glucose} + \text{ATP} \longrightarrow \text{D-glucose 6-phosphate} + \text{ADP}$$

However, some ingested glucose takes a more roundabout path to glycogen. It is first taken up by erythrocytes and converted to lactate glycolytically; the lactate is then taken up by the liver and converted to glucose 6-phosphate by gluconeogenesis.

To initiate glycogen synthesis, the glucose 6-phosphate is converted to glucose 1-phosphate in the phosphoglucomutase reaction:

$$\text{Glucose 6-phosphate} \rightleftharpoons \text{glucose 1-phosphate}$$

The product of this reaction is converted to UDP-glucose by the action of **UDP-glucose pyrophosphorylase**, in a key step of glycogen biosynthesis:

$$\text{Glucose 1-phosphate} + \text{UTP} \longrightarrow \text{UDP-glucose} + PP_i$$

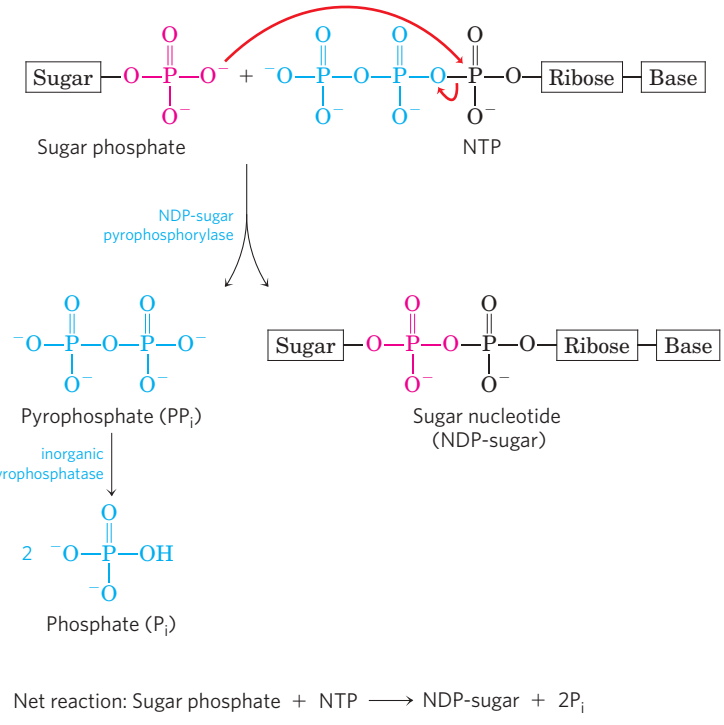

FIGURE 15–31 Formation of a sugar nucleotide. A condensation reaction occurs between a nucleoside triphosphate (NTP) and a sugar phosphate. The negatively charged oxygen on the sugar phosphate serves as a nucleophile, attacking the α phosphate of the nucleoside triphosphate and displacing pyrophosphate. The reaction is pulled in the forward direction by the hydrolysis of PP_i by inorganic pyrophosphatase.

Notice that this enzyme is named for the reverse reaction; in the cell, the reaction proceeds in the direction of UDP-glucose formation, because pyrophosphate is rapidly hydrolyzed by inorganic pyrophosphatase (Fig. 15–31).

UDP-glucose is the immediate donor of glucose residues in the reaction catalyzed by **glycogen synthase**, which promotes the transfer of the glucose residue from UDP-glucose to a nonreducing end of a branched glycogen molecule **(Fig. 15–32)**. The overall equilibrium of the path from glucose 6-phosphate to glycogen lengthened by one glucose unit greatly favors synthesis of glycogen.

Glycogen synthase cannot make the (α1⟶6) bonds found at the branch points of glycogen; these are

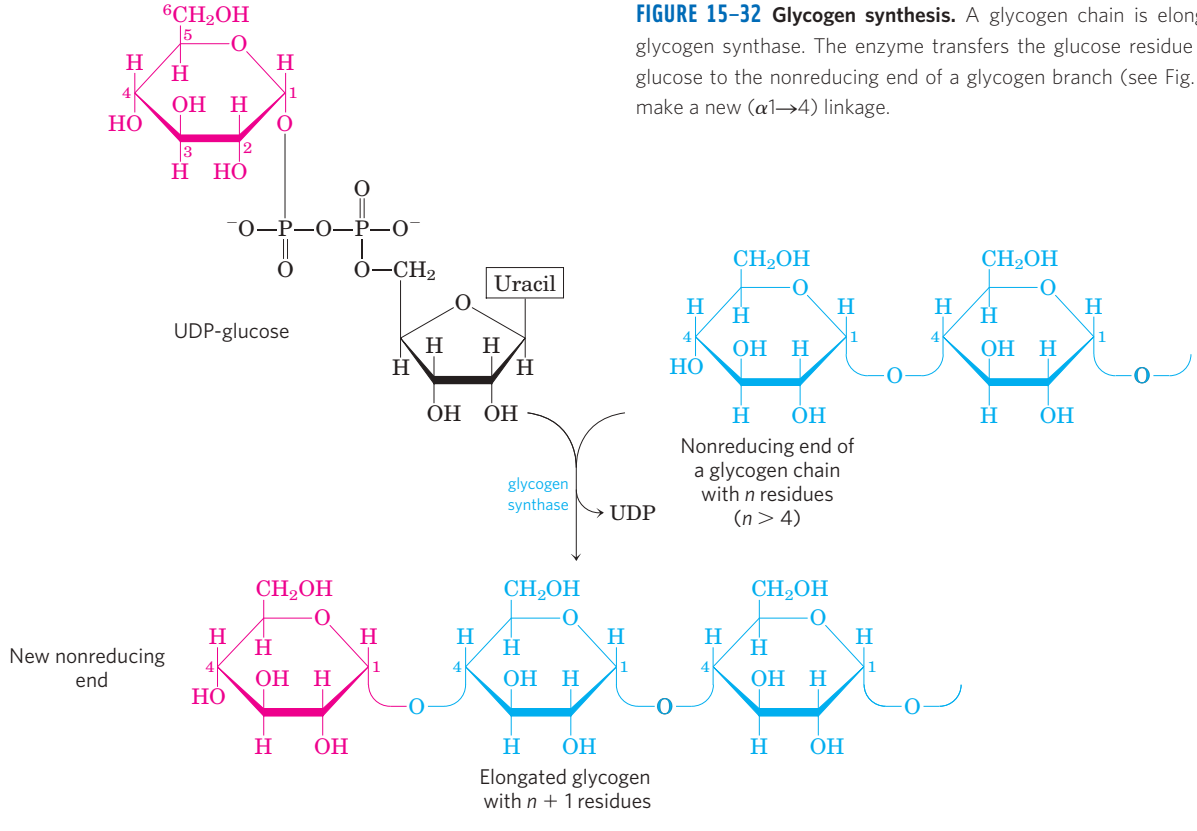

FIGURE 15–32 Glycogen synthesis. A glycogen chain is elongated by glycogen synthase. The enzyme transfers the glucose residue of UDP-glucose to the nonreducing end of a glycogen branch (see Fig. 7–13) to make a new (α1⟶4) linkage.

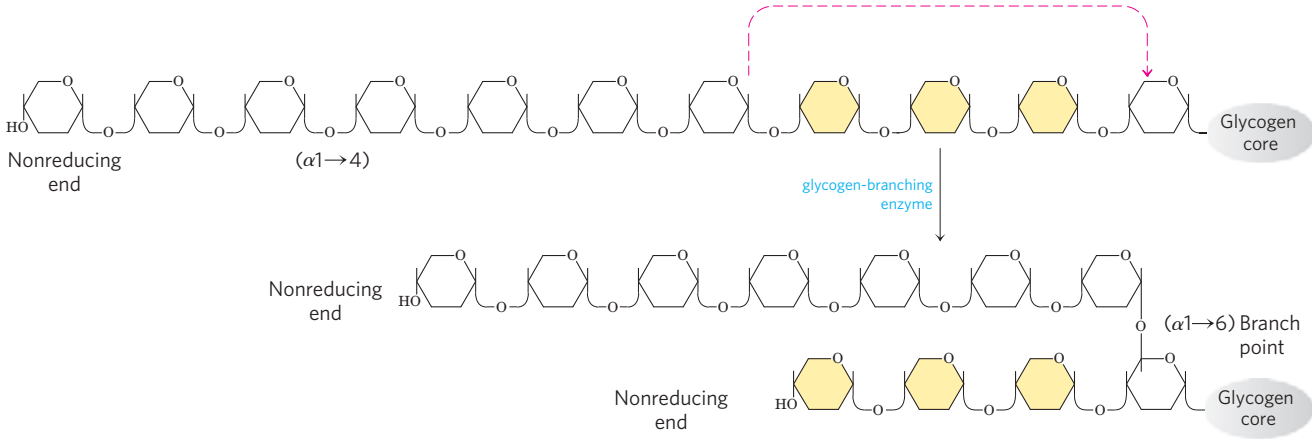

FIGURE 15–33 Branch synthesis in glycogen. The glycogen-branching enzyme (also called amylo (1→4) to (1→6) transglycosylase, or glycosyl-(4→6) transferase) forms a new branch point during glycogen synthesis.

formed by the glycogen-branching enzyme, also called **amylo (1→4) to (1→6) transglycosylase**, or glycosyl-(4→6) transferase. The glycogen-branching enzyme catalyzes transfer of a terminal fragment of 6 or 7 glucose residues from the nonreducing end of a glycogen branch having at least 11 residues to the C-6 hydroxyl group of a glucose residue at a more interior position of the same or another glycogen chain, thus creating a new branch **(Fig. 15–33)**. Further glucose residues may be added to the new branch by glycogen synthase. The biological effect of branching is to make the glycogen molecule more soluble and to increase the number of nonreducing ends. This increases the number of sites accessible to glycogen phosphorylase and glycogen synthase, both of which act only at nonreducing ends.

Glycogenin Primes the Initial Sugar Residues in Glycogen

Glycogen synthase cannot initiate a new glycogen chain de novo. It requires a primer, usually a preformed (α1→4) polyglucose chain or branch having at least eight glucose residues. So, how is a *new* glycogen molecule initiated? The intriguing protein **glycogenin** **(Fig. 15–34)** is both the primer on which new chains are assembled and the enzyme that catalyzes their assembly. The first step in the synthesis of a new glycogen molecule is the transfer of a glucose residue from UDP-glucose to the hydroxyl group of Tyr^{194} of glycogenin, catalyzed by the protein's intrinsic glucosyltransferase activity **(Fig. 15–35)**. The nascent chain is extended by the sequential addition of seven more glucose residues, each derived from UDP-glucose; the reactions are catalyzed by the chain-extending activity of glycogenin. At this point, glycogen synthase takes over, further extending the glycogen chain. Glycogenin remains buried within the β-particle, covalently attached to the single reducing end of the glycogen molecule (Fig. 15–35b). Medical consequences of a mutation in the gene for glycogenin that knocks out that protein's polymerizing activity include muscle weakness and fatigue, depleted glycogen in the liver, and an irregular heartbeat (cardiac arrhythmia).

SUMMARY 15.4 The Metabolism of Glycogen in Animals

- Glycogen is stored in muscle and liver as large particles. Contained within the particles are the

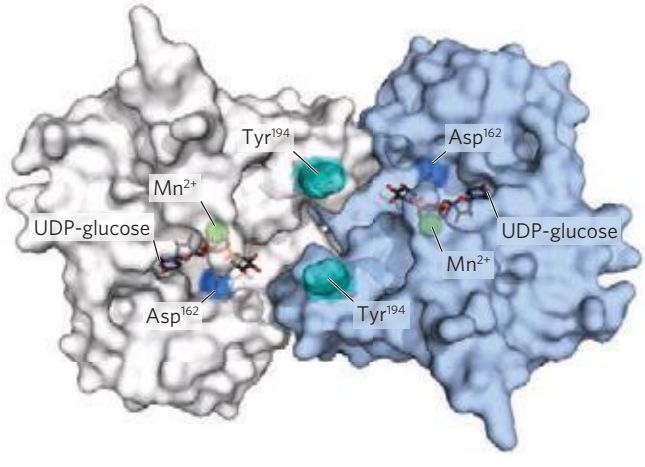

FIGURE 15–34 Glycogenin structure. (PDB 1D 1LL2) Muscle glycogenin (M_r 37,000) forms dimers in solution. Humans have a second isoform in liver, glycogenin-2. The substrate, UDP-glucose, is bound to a Rossmann fold near the amino terminus and is some distance from the Tyr^{194} residues—15 Å from the Tyr in the same monomer, 12 Å from the Tyr in the dimeric partner. Each UDP-glucose is bound through its phosphates to a Mn^{2+} ion, which is essential to catalysis. Mn^{2+} is believed to function as an electron-pair acceptor (Lewis acid) to stabilize the leaving group, UDP. The glycosidic bond in the product has the same configuration about the C-1 of glucose as the substrate UDP-glucose, suggesting that the transfer of glucose from UDP to Tyr^{194} occurs in two steps. The first step is probably a nucleophilic attack by Asp^{162}, forming a temporary intermediate with inverted configuration. A second nucleophilic attack by Tyr^{194} then restores the starting configuration.

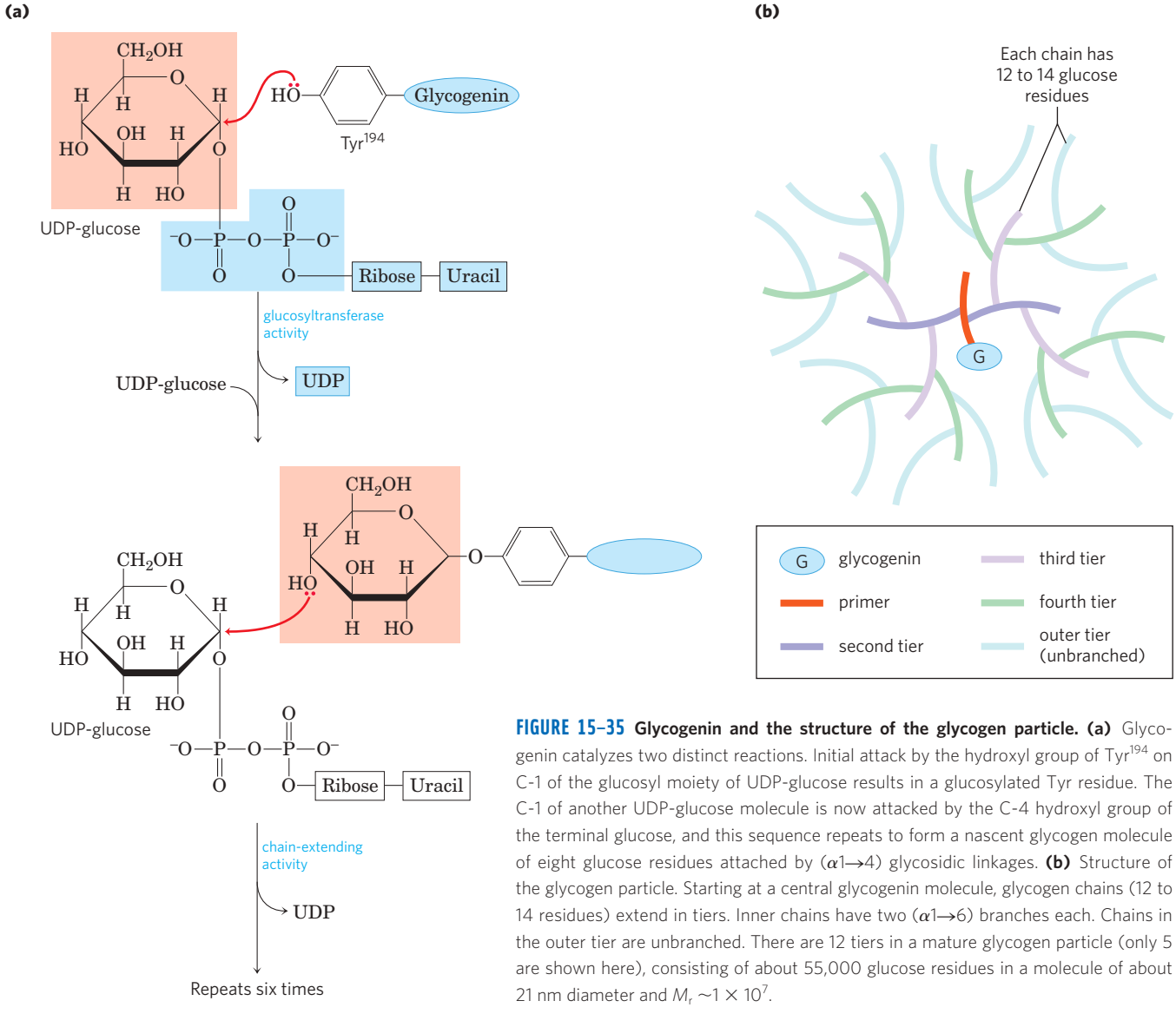

FIGURE 15–35 Glycogenin and the structure of the glycogen particle. (a) Glycogenin catalyzes two distinct reactions. Initial attack by the hydroxyl group of Tyr^{194} on C-1 of the glucosyl moiety of UDP-glucose results in a glucosylated Tyr residue. The C-1 of another UDP-glucose molecule is now attacked by the C-4 hydroxyl group of the terminal glucose, and this sequence repeats to form a nascent glycogen molecule of eight glucose residues attached by (α1→4) glycosidic linkages. **(b)** Structure of the glycogen particle. Starting at a central glycogenin molecule, glycogen chains (12 to 14 residues) extend in tiers. Inner chains have two (α1→6) branches each. Chains in the outer tier are unbranched. There are 12 tiers in a mature glycogen particle (only 5 are shown here), consisting of about 55,000 glucose residues in a molecule of about 21 nm diameter and M_r ~1 × 10^7.

enzymes that metabolize glycogen, as well as regulatory enzymes.

- Glycogen phosphorylase catalyzes phosphorolytic cleavage at the nonreducing ends of glycogen chains, producing glucose 1-phosphate. The debranching enzyme transfers branches onto main chains and releases the residue at the (α1→6) branch as free glucose.
- Phosphoglucomutase interconverts glucose 1-phosphate and glucose 6-phosphate. Glucose 6-phosphate can enter glycolysis or, in liver, can be converted to free glucose by glucose 6-phosphatase in the endoplasmic reticulum, then released to replenish blood glucose.
- The sugar nucleotide UDP-glucose donates glucose residues to the nonreducing end of glycogen in the reaction catalyzed by glycogen synthase. A separate branching enzyme produces the (α1→6) linkages at branch points.
- New glycogen particles begin with the autocatalytic formation of a glycosidic bond between the glucose of UDP-glucose and a Tyr residue in the protein glycogenin, followed by addition of several glucose residues to form a primer that can be acted on by glycogen synthase.

15.5 Coordinated Regulation of Glycogen Synthesis and Breakdown

As we have seen, the mobilization of stored glycogen is brought about by glycogen phosphorylase, which degrades glycogen to glucose 1-phosphate (Fig. 15–27). Glycogen phosphorylase provides an especially instructive case of enzyme regulation. It was one of the first known examples of an allosterically regulated enzyme and the first enzyme shown to be controlled by reversible phosphorylation. It was also one of the first allosteric

enzymes for which the detailed three-dimensional structures of the active and inactive forms were revealed by x-ray crystallographic studies. Glycogen phosphorylase is also another illustration of how isozymes play their tissue-specific roles.

Glycogen Phosphorylase Is Regulated Allosterically and Hormonally

Earl W. Sutherland, Jr., 1915–1974

In the late 1930s, Carl and Gerty Cori (Box 15–4) discovered that the glycogen phosphorylase of skeletal muscle exists in two interconvertible forms: **glycogen phosphorylase *a***, which is catalytically active, and **glycogen phosphorylase *b***, which is less active **(Fig. 15–36)**. Subsequent studies by Earl Sutherland showed that phosphorylase *b* predominates in resting muscle, but during vigorous muscular activity epinephrine triggers phosphorylation of a specific Ser residue in phosphorylase *b*, converting it to its more active form, phosphorylase *a*. (Note that glycogen phosphorylase is often referred to simply as phosphorylase—so honored because it was the first phosphorylase to be discovered; the shortened name has persisted in common usage and in the literature.)

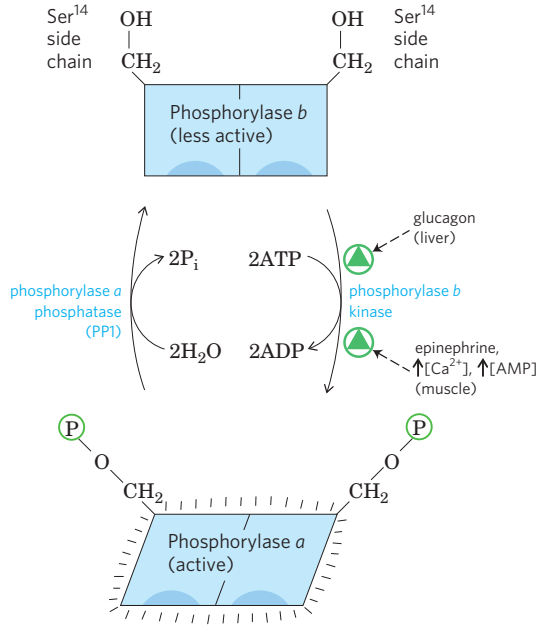

FIGURE 15–36 Regulation of muscle glycogen phosphorylase by covalent modification. In the more active form of the enzyme, phosphorylase *a*, Ser^{14} residues, one on each subunit, are phosphorylated. Phosphorylase *a* is converted to the less active form, phosphorylase *b*, by enzymatic loss of these phosphoryl groups, catalyzed by phosphorylase *a* phosphatase (also known as phosphoprotein phosphatase 1, PP1). Phosphorylase *b* can be reconverted (reactivated) to phosphorylase *a* by the action of phosphorylase *b* kinase. (See also Fig. 6–42 on glycogen phosphorylase regulation.)

The enzyme (phosphorylase *b* kinase) responsible for activating phosphorylase by transferring a phosphoryl group to its Ser residue is itself activated by epinephrine or glucagon through a series of steps shown in **Figure 15–37**. Sutherland discovered the second messenger cAMP, which increases in concentration in response to stimulation by epinephrine (in muscle) or glucagon (in liver). Elevated [cAMP] initiates an **enzyme cascade**, in which a catalyst activates a catalyst, which activates a catalyst (see Section 12.1). Such cascades allow for large amplification of the initial signal (see pink boxes in Fig. 15–37). The rise in [cAMP] activates cAMP-dependent protein kinase, also called protein kinase A (PKA). PKA then phosphorylates and activates **phosphorylase *b* kinase**, which catalyzes the phosphorylation of Ser residues in each of the two identical subunits of glycogen phosphorylase, activating it and thus stimulating glycogen breakdown. In muscle, this provides fuel for glycolysis to sustain muscle contraction for the fight-or-flight response signaled by epinephrine. In liver, glycogen breakdown counters the low blood glucose signaled by glucagon, releasing glucose. These different roles are reflected in subtle differences in the regulatory mechanisms in muscle and liver. The glycogen phosphorylases of liver and muscle are isozymes, encoded by different genes and differing in their regulatory properties.

In muscle, superimposed on the regulation of phosphorylase by covalent modification are two allosteric control mechanisms (Fig. 15–37). Ca^{2+}, the signal for muscle contraction, binds to and activates phosphorylase *b* kinase, promoting conversion of phosphorylase *b* to the active *a* form. Ca^{2+} binds to phosphorylase *b* kinase through its δ subunit, which is calmodulin (see Fig. 12–11). AMP, which accumulates in vigorously contracting muscle as a result of ATP breakdown, binds to and activates phosphorylase, speeding the release of glucose 1-phosphate from glycogen. When ATP levels are adequate, ATP blocks the allosteric site to which AMP binds, inactivating phosphorylase.

When the muscle returns to rest, a second enzyme, **phosphorylase *a* phosphatase**, also called **phosphoprotein phosphatase 1 (PP1)**, removes the phosphoryl groups from phosphorylase *a*, converting it to the less active form, phosphorylase *b*.

Like the enzyme of muscle, the glycogen phosphorylase of liver is regulated hormonally (by phosphorylation/dephosphorylation) and allosterically. The dephosphorylated form is essentially inactive. When the blood glucose level is too low, glucagon (acting through the cascade mechanism shown in Fig. 15–37) activates phosphorylase *b* kinase, which in turn converts phosphorylase *b* to its active *a* form, initiating the release of

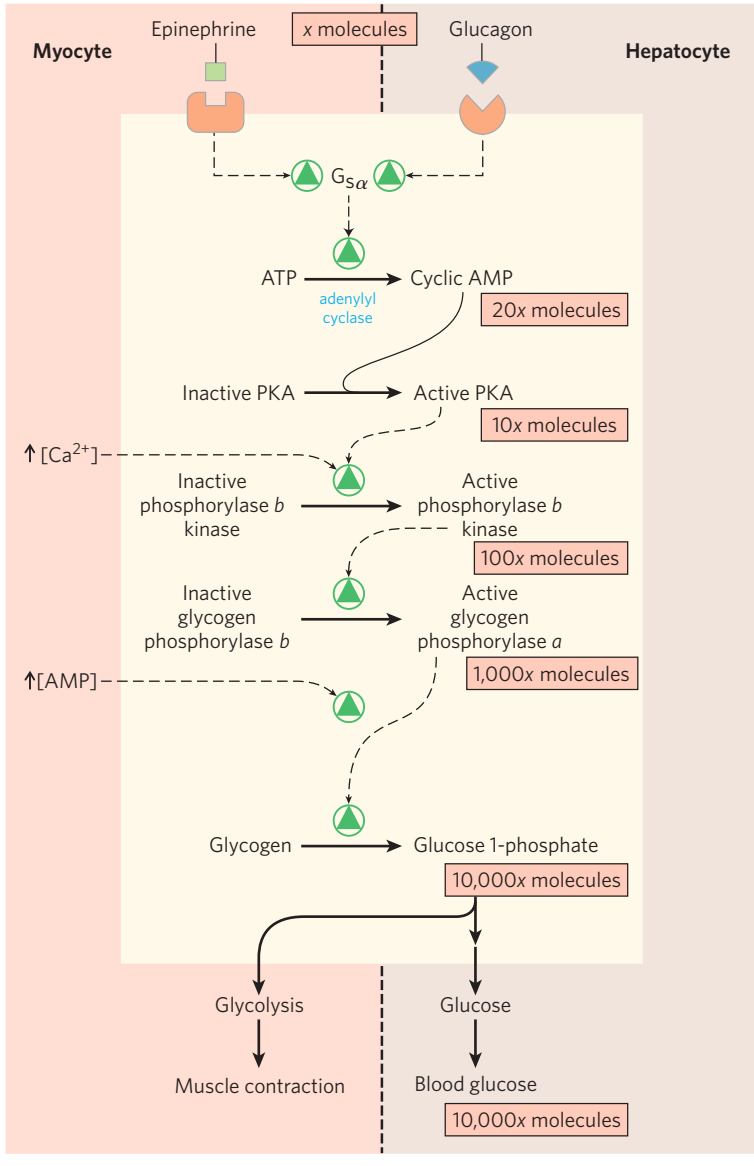

FIGURE 15–37 Cascade mechanism of epinephrine and glucagon action. By binding to specific surface receptors, either epinephrine acting on a myocyte (left) or glucagon acting on a hepatocyte (right) activates a GTP-binding protein, $G_{s\alpha}$ (see Fig. 12–4). Active $G_{s\alpha}$ triggers a rise in [cAMP], activating PKA. This sets off a cascade of phosphorylations; PKA activates phosphorylase *b* kinase, which then activates glycogen phosphorylase. Such cascades effect a large amplification of the initial signal; the figures in pink boxes are probably low estimates of the actual increase in number of molecules at each stage of the cascade. The resulting breakdown of glycogen provides glucose, which in the myocyte can supply ATP (via glycolysis) for muscle contraction and in the hepatocyte is released into the blood to counter the low blood glucose.

glucose into the blood. When blood glucose levels return to normal, glucose enters hepatocytes and binds to an inhibitory allosteric site on phosphorylase *a*. This binding also produces a conformational change that exposes the phosphorylated Ser residues to PP1, which catalyzes their dephosphorylation and inactivates the phosphorylase **(Fig. 15–38)**. The allosteric site for glucose allows liver glycogen phosphorylase to act as its own glucose sensor and to respond appropriately to changes in blood glucose.

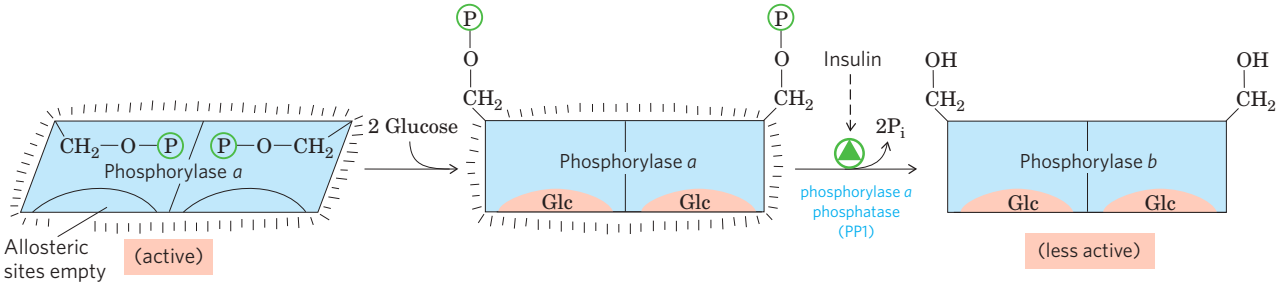

FIGURE 15–38 Glycogen phosphorylase of liver as a glucose sensor. Glucose binding to an allosteric site of the phosphorylase *a* isozyme of liver induces a conformational change that exposes its phosphorylated Ser residues to the action of phosphorylase *a* phosphatase (PP1). This phosphatase converts phosphorylase *a* to phosphorylase *b*, sharply reducing the activity of phosphorylase and slowing glycogen breakdown in response to high blood glucose. Insulin also acts indirectly to stimulate PP1 and slow glycogen breakdown.

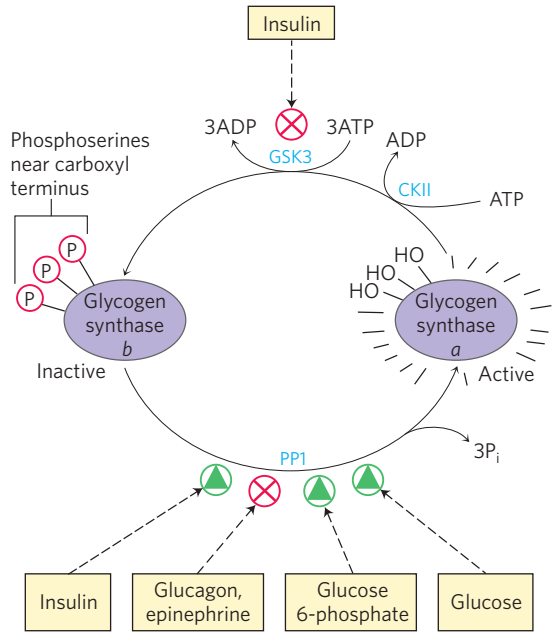

FIGURE 15–39 Effects of GSK3 on glycogen synthase activity. Glycogen synthase *a*, the active form, has three Ser residues near its carboxyl terminus, which are phosphorylated by glycogen synthase kinase 3 (GSK3). This converts glycogen synthase to the inactive (*b*) form. GSK3 action requires prior phosphorylation (priming) by casein kinase (CKII). Insulin triggers activation of glycogen synthase *b* by blocking the activity of GSK3 (see the pathway for this action in Fig. 12–16) and activating a phosphoprotein phosphatase (PP1 in muscle, another phosphatase in liver). In muscle, epinephrine activates PKA, which phosphorylates the glycogen-targeting protein GM (see Fig. 15–42) on a site that causes dissociation of PP1 from glycogen. Glucose 6-phosphate favors dephosphorylation of glycogen synthase by binding to it and promoting a conformation that is a good substrate for PP1. Glucose also promotes dephosphorylation; the binding of glucose to glycogen phosphorylase *a* forces a conformational change that favors dephosphorylation to glycogen phosphorylase *b*, thus allowing the action of PP1 (see Fig. 15–41).

Glycogen Synthase Is Also Regulated by Phosphorylation and Dephosphorylation

Like glycogen phosphorylase, glycogen synthase can exist in phosphorylated and dephosphorylated forms **(Fig. 15–39)**. Its active form, **glycogen synthase *a***, is unphosphorylated. Phosphorylation of the hydroxyl side chains of several Ser residues of both subunits converts glycogen synthase *a* to **glycogen synthase *b***, which is inactive unless its allosteric activator, glucose 6-phosphate, is present. Glycogen synthase is remarkable for its ability to be phosphorylated on various residues by at least 11 different protein kinases. The most important regulatory kinase is **glycogen synthase kinase 3 (GSK3)**, which adds phosphoryl groups to three Ser residues near the carboxyl terminus of glycogen synthase, strongly inactivating it. The action of GSK3 is hierarchical; it cannot phosphorylate glycogen synthase until another protein kinase, **casein kinase II (CKII)**, has first phosphorylated the glycogen synthase on a nearby residue, an event called **priming (Fig. 15–40a)**.

In liver, conversion of glycogen synthase *b* to the active form is promoted by PP1, which is bound to the glycogen particle. PP1 removes the phosphoryl groups from the three Ser residues phosphorylated by GSK3. Glucose 6-phosphate binds to an allosteric site on

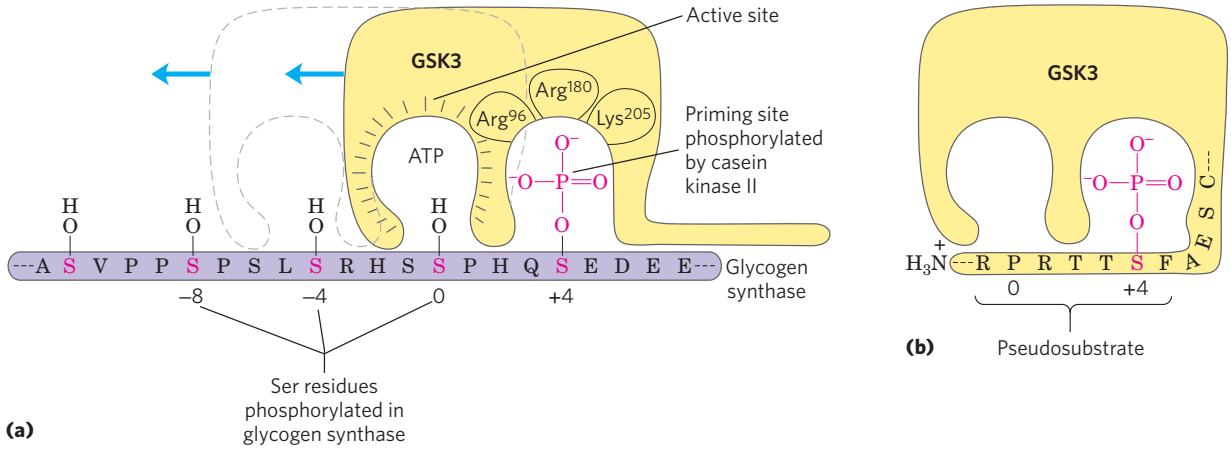

FIGURE 15–40 Priming of GSK3 phosphorylation of glycogen synthase. **(a)** Glycogen synthase kinase 3 first associates with its substrate (glycogen synthase) by interaction between three positively charged residues (Arg^{96}, Arg^{180}, Lys^{205}) and a phosphoserine residue at position +4 in the substrate. (For orientation, the Ser or Thr residue to be phosphorylated in the substrate is assigned the index 0. Residues on the amino-terminal side of this residue are numbered −1, −2, and so forth; residues on the carboxyl-terminal side are numbered +1, +2, and so forth.) This association aligns the active site of the enzyme with a Ser residue at position 0, which it phosphorylates. This creates a new priming site, and the enzyme moves down the protein to phosphorylate the Ser residue at position −4, and then the Ser at −8. **(b)** GSK3 has a Ser residue near its amino terminus that can be phosphorylated by PKA or PKB (see Fig. 15–41). This produces a "pseudosubstrate" region in GSK3 that folds into the priming site and makes the active site inaccessible to another protein substrate, inhibiting GSK3 until the priming phosphoryl group of its pseudosubstrate region is removed by PP1. Other proteins that are substrates for GSK3 also have a priming site at position +4, which must be phosphorylated by another protein kinase before GSK3 can act on them. (See also Figs 6–37 and 12–22b on glycogen synthase regulation.)

glycogen synthase *b*, making the enzyme a better substrate for dephosphorylation by PP1 and causing its activation. By analogy with glycogen phosphorylase, which acts as a glucose sensor, glycogen synthase can be regarded as a glucose 6-phosphate sensor. In muscle, a different phosphatase may have the role played by PP1 in liver, activating glycogen synthase by dephosphorylating it.

Glycogen Synthase Kinase 3 Mediates Some of the Actions of Insulin

As we saw in Chapter 12, one way in which insulin triggers intracellular changes is by activating a protein kinase (PKB) that in turn phosphorylates and inactivates GSK3 (**Fig. 15–41**; see also Fig. 12–16). Phosphorylation of a Ser residue near the amino terminus of GSK3 converts that region of the protein to a pseudosubstrate, which folds into the site at which the priming phosphorylated Ser residue normally binds (Fig. 15–40b). This prevents GSK3 from binding the priming site of a real substrate, thereby inactivating the enzyme and tipping the balance in favor of dephosphorylation of glycogen synthase by PP1. Glycogen phosphorylase can also affect the phosphorylation of glycogen synthase: active glycogen phosphorylase directly inhibits PP1, preventing it from activating glycogen synthase (Fig. 15–39).

Although first discovered in its role in glycogen metabolism (hence the name glycogen synthase kinase), GSK3 clearly has a much broader role than the regulation of glycogen synthase. It mediates signaling by insulin and other growth factors and nutrients, and it acts in the specification of cell fates during embryonic development. Among its targets are cytoskeletal proteins and proteins essential for mRNA and protein synthesis. These targets, like glycogen synthase, must first undergo a priming phosphorylation by another protein kinase before they can be phosphorylated by GSK3.

Phosphoprotein Phosphatase 1 Is Central to Glycogen Metabolism

A single enzyme, PP1, can remove phosphoryl groups from all three of the enzymes phosphorylated in response to glucagon (liver) and epinephrine (liver and muscle): phosphorylase kinase, glycogen phosphorylase, and glycogen synthase. Insulin stimulates glycogen synthesis by activating PP1 and by inactivating GSK3.

Phosphoprotein phosphatase 1 does not exist free in the cytosol, but is tightly bound to its target proteins by one of a family of **glycogen-targeting proteins** that bind glycogen and each of the three enzymes, glycogen phosphorylase, phosphorylase kinase, and glycogen synthase **(Fig. 15–42)**. PP1 is itself subject to covalent and allosteric regulation: it is inactivated when phosphorylated by PKA and is allosterically activated by glucose 6-phosphate.

Allosteric and Hormonal Signals Coordinate Carbohydrate Metabolism Globally

Having looked at the mechanisms that regulate individual enzymes, we can now consider the overall shifts in carbohydrate metabolism that occur in the well-fed state, during fasting, and in the fight-or-flight response—signaled by insulin, glucagon, and epinephrine, respectively. We need to contrast two cases in which regulation serves different ends: (1) the role of hepatocytes in supplying glucose to the blood, and (2) the selfish use of carbohydrate fuels by nonhepatic

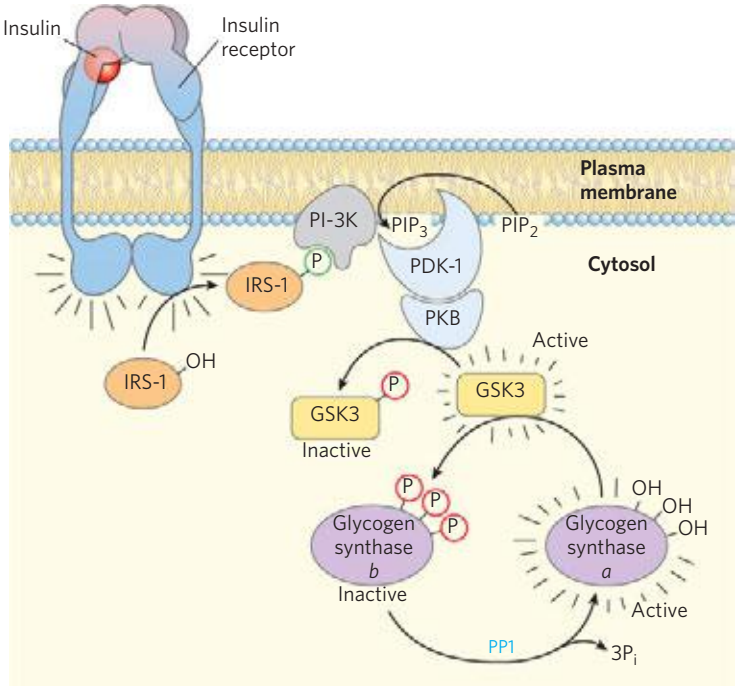

FIGURE 15–41 The path from insulin to GSK3 and glycogen synthase. Insulin binding to its receptor activates a tyrosine protein kinase in the receptor, which phosphorylates insulin receptor substrate-1 (IRS-1). The phosphotyrosine in this protein is then bound by phosphatidylinositol 3-kinase (PI-3K), which converts phosphatidylinositol 4,5-bisphosphate (PIP_2) in the membrane to phosphatidylinositol 3,4,5-trisphosphate (PIP_3). A protein kinase (PDK-1) that is activated when bound to PIP_3 activates a second protein kinase (PKB), which phosphorylates glycogen synthase kinase 3 (GSK3) in its pseudosubstrate region, inactivating it by the mechanism shown in Figure 15–40b. The inactivation of GSK3 allows phosphoprotein phosphatase 1 (PP1) to dephosphorylate and thus activate glycogen synthase. In this way, insulin stimulates glycogen synthesis. (See Fig. 12–16 for more details on insulin action.)

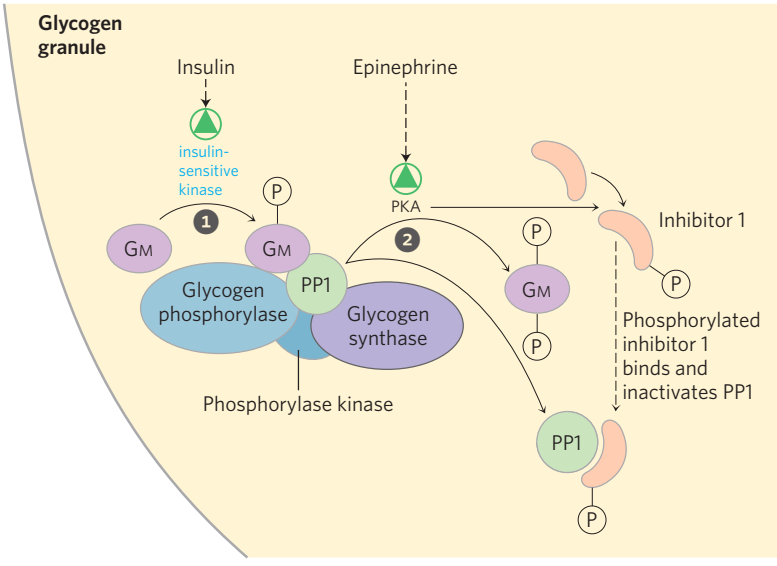

FIGURE 15–42 Glycogen-targeting protein GM. The glycogen-targeting protein GM is one of a family of proteins that bind other proteins (including PP1) to glycogen particles. GM can be phosphorylated at two different sites in response to insulin or epinephrine. ❶ Insulin-stimulated phosphorylation of GM site 1 activates PP1, which dephosphorylates phosphorylase kinase, glycogen phosphorylase, and glycogen synthase. ❷ Epinephrine-stimulated phosphorylation of GM site 2 causes dissociation of PP1 from the glycogen particle, preventing its access to glycogen phosphorylase and glycogen synthase. PKA also phosphorylates a protein (inhibitor 1) that, when phosphorylated, inhibits PP1. By these means, insulin inhibits glycogen breakdown and stimulates glycogen synthesis, and epinephrine (or glucagon in the liver) has the opposite effects.

tissues, typified by skeletal muscle (myocytes), to support their own activities.

After ingestion of a carbohydrate-rich meal, the elevation of blood glucose triggers insulin release (**Fig. 15–43**, top). In a hepatocyte, insulin has two immediate effects: it inactivates GSK3, acting through the cascade shown in Figure 15–41, and activates a protein phosphatase, perhaps PP1. These two actions fully activate glycogen synthase. PP1 also inactivates glycogen phosphorylase *a* and phosphorylase kinase by dephosphorylating both, effectively stopping glycogen breakdown. Glucose enters the hepatocyte through the high-capacity transporter GLUT2, always present in the plasma membrane, and the elevated intracellular glucose leads to dissociation of hexokinase IV (glucokinase) from its nuclear regulatory protein (Fig. 15–15). Hexokinase IV enters the cytosol and phosphorylates glucose, stimulating glycolysis and supplying the precursor for glycogen synthesis. Under these conditions, hepatocytes use the excess glucose in the blood to synthesize glycogen, up to the limit of about 10% of the total weight of the liver.

Between meals, or during an extended fast, the drop in blood glucose triggers the release of glucagon, which, acting through the cascade shown in Figure 15–37, activates PKA. PKA mediates all the effects of glucagon (Fig. 15–43, bottom). It phosphorylates phosphorylase kinase, activating it and leading to the activation of glycogen phosphorylase. It phosphorylates glycogen synthase, inactivating it and blocking glycogen synthesis. It phosphorylates PFK-2/FBPase-2, leading to a

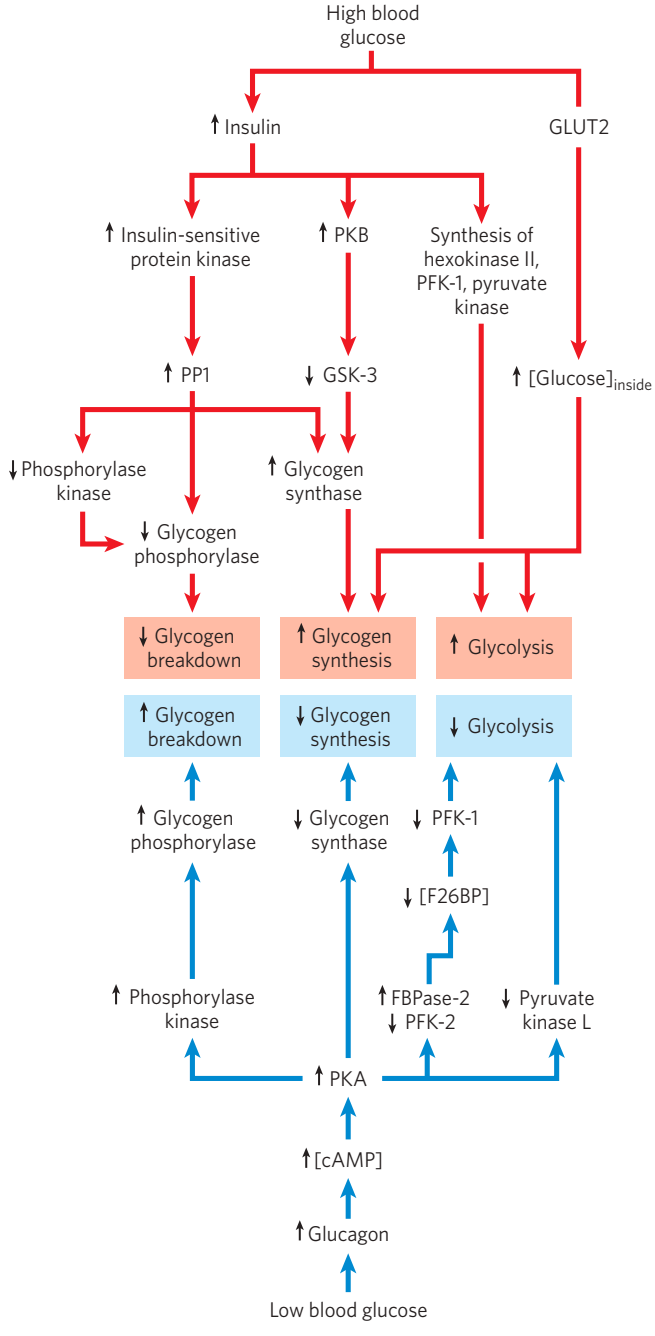

FIGURE 15–43 Regulation of carbohydrate metabolism in the liver. Arrows indicate causal relationships between the changes they connect. For example, an arrow from ↓A to ↑B means that a decrease in A causes an increase in B. Red arrows connect events that result from high blood glucose; blue arrows connect events that result from low blood glucose.

drop in the concentration of the regulator fructose 2,6-bisphosphate, which has the effect of inactivating the glycolytic enzyme PFK-1 and activating the gluconeogenic enzyme FBPase-1. And it phosphorylates and inactivates the glycolytic enzyme pyruvate kinase. Under these conditions, the liver produces glucose 6-phosphate by glycogen breakdown and by gluconeogenesis, and it stops using glucose to fuel glycolysis or make glycogen, maximizing the amount of glucose it can release to the blood. This release of glucose is possible only in liver and kidney, because other tissues lack glucose 6-phosphatase (Fig. 15–30).

The physiology of skeletal muscle differs from that of liver in three ways important to our discussion of metabolic regulation **(Fig. 15–44)**: (1) muscle uses its stored glycogen only for its own needs; (2) as it goes from rest to vigorous contraction, muscle undergoes very large changes in its demand for ATP, which is supported by glycolysis; (3) muscle lacks the enzymatic machinery for gluconeogenesis. The regulation of carbohydrate metabolism in muscle reflects these differences from liver. First, myocytes lack receptors for glucagon. Second, the muscle isozyme of pyruvate kinase is not phosphorylated by PKA, so glycolysis is not turned off when [cAMP] is high. In fact, cAMP *increases* the rate of glycolysis in muscle, probably by activating glycogen phosphorylase. When epinephrine is released into the blood in a fight-or-flight situation, PKA is activated by the rise in [cAMP] and phosphorylates and activates glycogen phosphorylase kinase. The resulting phosphorylation and activation of glycogen phosphorylase results in faster glycogen breakdown. Epinephrine is not released under low-stress conditions, but with each neuronal stimulation of muscle contraction, cytosolic [Ca^{2+}] rises briefly and activates phosphorylase kinase through its calmodulin subunit.

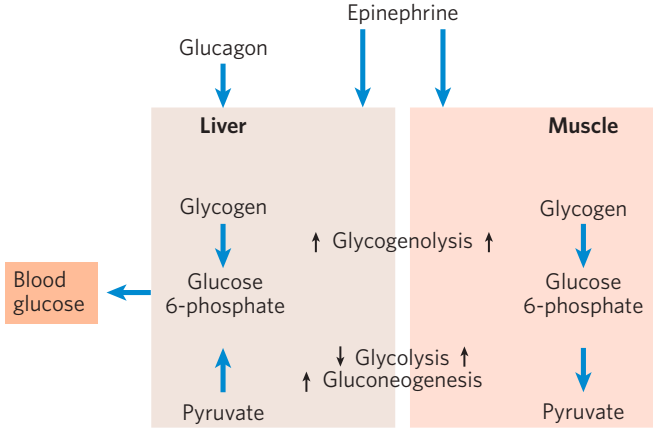

FIGURE 15–44 Difference in the regulation of carbohydrate metabolism in liver and muscle. In liver, either glucagon (indicating low blood glucose) or epinephrine (signaling the need to fight or flee) has the effect of maximizing the output of glucose into the bloodstream. In muscle, epinephrine increases glycogen breakdown and glycolysis, which together provide fuel to produce the ATP needed for muscle contraction.

Elevated insulin triggers increased glycogen synthesis in myocytes by activating PP1 and inactivating GSK3. Unlike hepatocytes, myocytes have a reserve of GLUT4 sequestered in intracellular vesicles. Insulin triggers their movement to the plasma membrane (see Fig. 12–16), where they allow increased glucose uptake. In response to insulin, therefore, myocytes help to lower blood glucose by increasing their rates of glucose uptake, glycogen synthesis, and glycolysis.

Carbohydrate and Lipid Metabolism Are Integrated by Hormonal and Allosteric Mechanisms

As complex as the regulation of carbohydrate metabolism is, it is far from the whole story of fuel metabolism. The metabolism of fats and fatty acids is very closely tied to that of carbohydrates. Hormonal signals such as insulin and changes in diet or exercise are equally important in regulating fat metabolism and integrating it with that of carbohydrates. We return to this overall metabolic integration in mammals in Chapter 23, after first considering the metabolic pathways for fats and amino acids (Chapters 17 and 18). The message we wish to convey here is that metabolic pathways are overlaid with complex regulatory controls that are exquisitely sensitive to changes in metabolic circumstances. These mechanisms act to adjust the flow of metabolites through various metabolic pathways, as needed by the cell and organism, and to do so without causing major changes in the concentrations of intermediates shared with other pathways.

SUMMARY 15.5 Coordinated Regulation of Glycogen Synthesis and Breakdown

- Glycogen phosphorylase is activated in response to glucagon or epinephrine, which raise [cAMP] and activate PKA. PKA phosphorylates and activates phosphorylase kinase, which converts glycogen phosphorylase *b* to its active *a* form. Phosphoprotein phosphatase 1 (PP1) reverses the phosphorylation of glycogen phosphorylase *a*, inactivating it. Glucose binds to the liver isozyme of glycogen phosphorylase *a*, favoring its dephosphorylation and inactivation.
- Glycogen synthase *a* is inactivated by phosphorylation catalyzed by GSK3. Insulin blocks GSK3. PP1, which is activated by insulin, reverses the inhibition by dephosphorylating glycogen synthase *b*.
- Insulin increases glucose uptake into myocytes and adipocytes by triggering movement of the glucose transporter GLUT4 to the plasma membrane.
- Insulin stimulates the synthesis of hexokinases II and IV, PFK-1, pyruvate kinase, and several

enzymes involved in lipid synthesis. Insulin stimulates glycogen synthesis in muscle and liver.

- In liver, glucagon stimulates glycogen breakdown and gluconeogenesis while blocking glycolysis, thereby sparing glucose for export to the brain and other tissues.
- In muscle, epinephrine stimulates glycogen breakdown and glycolysis, providing ATP to support contraction.

Key Terms

Terms in bold are defined in the glossary.

glucose 6-phosphate 587
flux, J 589
homeostasis 589
cellular differentiation 589
transcription factor 589
response element 589
turnover 590
transcriptome 590
proteome 590
metabolome 591
metabolic regulation 592
metabolic control 592
mass-action ratio, Q 593
adenylate kinase 594
AMP-activated protein kinase (AMPK) 594
flux control coefficient, C 597, 598
elasticity coefficient, ε 597, 598
response coefficient, R 598
gluconeogenesis 601
futile cycle 601
substrate cycle 601
hexokinase II 602
hexokinase I 602
hexokinase IV 603
GLUT2 603
glucagon 605
fructose 2,6-bisphosphate 605
phosphofructokinase-2 (PFK-2) 606
fructose 2,6-bisphosphatase (FBPase-2) 606
carbohydrate response element binding protein (ChREBP) 609
sterol regulatory element binding protein (SREBP) 610
cyclic AMP response element binding protein (CREB) 610
forkhead box other (FOXO1) 610
glycogenolysis 613
glycogenesis 613
glucose 1-phosphate 613
debranching enzyme 614
oligo (α1→6) to (α1→4) glucantransferase 614
phosphoglucomutase 614
sugar nucleotides 615
UDP-glucose pyrophosphorylase 617
amylo (1→4) to (1→6) transglycosylase 619
glycogenin 619
glycogen phosphorylase a 621
glycogen phosphorylase b 621
enzyme cascade 621
phosphorylase b kinase 621
phosphoprotein phosphatase 1 (PP1) 621
glycogen synthase a 623
glycogen synthase b 623
glycogen synthase kinase 3 (GSK3) 623
casein kinase II (CKII) 623
priming 623
glycogen-targeting proteins 624

Further Reading

Regulation of Metabolic Pathways

Desvergne, B., Michalik, L., & Wahli, W. (2006) Transcriptional regulation of metabolism. *Physiol. Rev*. **86**, 465–514.
Advanced and comprehensive review.

Gibson, D. & Harris, R.A. (2001) *Metabolic Regulation in Mammals*, Taylor & Francis, New York.
Excellent, readable account of metabolic regulation.

Li, X. & Snyder, M. (2011) Metabolites as global regulators: a new view of protein regulation. *Bioessays* **33**, 485–489.

Naïmi, M., Arous, C., & Obberghen, E. (2010) Energetic cell sensors: a key to metabolic homeostasis. *Trends Endocrinol. Med.* **21**, 75–82.

Storey, K.B. (ed.). (2004) *Functional Metabolism: Regulation and Adaptation*, Wiley-Liss, Inc., Hoboken, NJ.
Excellent discussion of the principles of metabolic regulation, signal transduction, transcriptional control, and energy metabolism in health and disease.

Analysis of Metabolic Control

Castrillo, J.I. & Oliver, S.G. (2007) Metabolic control in the eukaryotic cell, a systems biology perspective. *Meth. Microbiol.* **36**, 527–549. doi:10.1016/S0580-9517(06)36021-7

Fell, D.A. (1992) Metabolic control analysis: a survey of its theoretical and experimental development. *Biochem. J.* **286**, 313–330.
Clear statement of the principles of metabolic control analysis.

Fell, D.A. (1997) *Understanding the Control of Metabolism*, Portland Press, Ltd., London.
An excellent, clear exposition of metabolic regulation, from the point of view of metabolic control analysis. If you read only one treatment on metabolic control analysis, this should be it.

Heinrich, R. & Rapoport, T.A. (1974) A linear steady-state treatment of enzymatic chains: general properties, control and effector strength. *Eur. J. Biochem*. **42**, 89–95.
Early statement of principles of metabolic control analysis. See also the paper by Kacser & Burns, listed below.

Jeffrey, F.M.H., Rajagopal, A., Maloy, C.R., & Sherry, A.D. (1991) ^{13}C-NMR: a simple yet comprehensive method for analysis of intermediary metabolism. *Trends Biochem. Sci*. **16**, 5–10.
Brief, intermediate-level review.

Kacser, H. & Burns, J.A. (1973) The control of flux. *Symp. Soc. Exp. Biol*. **32**, 65–104.
A classic paper in the field. See also the paper by Heinrich & Rapoport, listed above.

Kacser, H., Burns, J.A., & Fell, D.A. (1995) The control of flux: 21 years on. *Biochem. Soc. Trans*. **23**, 341–366.

Saavedra, E., Rodriguez-Enriquesz, S., Quezada, H., Jasso-Chavez, R., & Moreno-Sanchez, R. (2011) Rational design of strategies based on metabolic control analysis. In *Comprehensive Biotechnology*, 2nd edn, Vol. 1 (Moo-Young, M., Butler, M., Webb. C., Moreira, A., Grodzinski, B., Cui, Z.E., and Agathos, S., eds), pp. 511–524. Pergamon Press, Elmsford, NY.

Schilling, C.H., Schuster, S., Palsson, B.O., & Heinrich, R. (1999) Metabolic pathway analysis: basic concepts and scientific applications in the post-genomic era. *Biotechnol. Prog*. **15**, 296–303.
Short, advanced discussion of theoretical treatments that attempt to find ways of manipulating metabolism to optimize the formation of metabolic products.

Schuster, S., Fell, D.A., & Dandekar, T. (2000) A general definition of metabolic pathways useful for systematic organization and analysis of complex metabolic networks. *Nat. Biotechnol*. **18**, 326–332.
An interesting and provocative analysis of the interplay between the pentose phosphate pathway and glycolysis, from a theoretical standpoint.

Sohn, S.B., Kim, T.Y., Kim, J.M., Park, J.M., & Lee, S.Y. (2011) Metabolic control. In *Comprehensive Biotechnology*, 2nd edn, Vol. 2 (Moo-Young, M., Butler, M., Webb, C., Moreira, A., Grodzinski, B., Cui, Z.F., and Agathos, S., eds), pp. 853–861. Pergamon Press, Elmsford, NY.

Varma, A. & Palsson, B.O. (1994) Metabolic flux balancing: basic concepts, scientific and practical use. *Bio/Technology* **12**, 994–98.

Westerhoff, H.V., Hofmeyr, J.-H.S., & Kholodenko, B.N. (1994) Getting to the inside of cells using metabolic control analysis. *Biophys. Chem.* **50**, 273–283.

Coordinated Regulation of Glycolysis and Gluconeogenesis

Armoni, M., Harel, C., & Karnieli, E. (2007) Transcriptional regulation of the GLUT4 gene: from PPAR-gamma and FOXO1 to FFA and inflammation. *Trends Endocrinol. Metab.* **18**, 100–107.

Barthel, A., Schmoll, D., & Unterman, T.G. (2005) FoxO proteins in insulin action and metabolism. *Trends Endocrinol. Metab.* **16**, 183–189.

Intermediate-level review of the transcription factor's effects on carbohydrate metabolism.

Brady, M.J., Pessin, J.E., & Saltiel, A.R. (1999) Spatial compartmentalization in the regulation of glucose metabolism by insulin. *Trends Endocrinol. Metab.* **10**, 408–413.

Intermediate-level review.

Carling, D. (2004) The AMP-activated protein kinase cascade—a unifying system for energy control. *Trends Biochem. Sci.* **29**, 18–24.

Intermediate-level review of AMPK and its role in energy metabolism.

de la Iglesia, N., Mukhtar, M., Seoane, J., Guinovart, J.J., & Agius, L. (2000) The role of the regulatory protein of glucokinase in the glucose sensory mechanism of the hepatocyte. *J. Biol. Chem.* **275**, 10,597–10,603.

Report of the experimental determination of the flux control coefficients for glucokinase and the glucokinase regulatory protein in hepatocytes.

Dean, L. & McEntyre, J. (2004) *The Genetic Landscape of Diabetes*, National Center for Biotechnology Information, www.ncbi.nlm.nih.gov/books/bv.fcgi?rid=diabetes.

An excellent, highly readable, downloadable book (free). It includes an introduction to diabetes, a history of studies of diabetes, and chapters on the genetic factors in IDDM, NIDDM, and MODY.

Desverne, B., Michalik, L., & Wahli, W. (2006) Transcriptional regulation of metabolism. *Physiol. Rev.* **86**, 465–514.

Extensive, advanced review of transcription factors, including those that regulate carbohydrate and fat metabolism.

Grüning, N.-M., Lehrach, H., & Ralser, M. (2010) Regulatory crosstalk of the metabolic network. *Trends Biochem. Sci.* **35**, 220–227.

Hardie, D.G. (2007) AMP-activated protein kinase as a drug target. *Annu. Rev. Pharmacol. Toxicol.* **47**, 185–210.

Advanced review, with emphasis on the possible role of this enzyme in type II diabetes.

Herman, M.A. & Kahn, B.B. (2006) Glucose transport and sensing in the maintenance of glucose homeostasis and metabolic harmony. *J. Clin. Invest.* **116**, 1767–1775.

Beautifully illustrated, intermediate-level review.

Hers, H.G. & Van Schaftingen, E. (1982) Fructose 2,6-bisphosphate 2 years after its discovery. *Biochem. J.* **206**, 1–12.

Classic description of this regulatory molecule and its role in regulating carbohydrate metabolism.

Hue, L. & Rider, M.H. (1987) Role of fructose 2,6-bisphosphate in the control of glycolysis in mammalian tissues. *Biochem. J.* **245**, 313–324.

Jorgensen, S.B., Richter, E.A., & Wojtaszewski, J.F.P. (2006) Role of AMPK in skeletal muscle metabolic regulation and adaptation in relation to exercise. *J. Physiol.* **574**, 17–31.

Kahn, B.B., Alquier, T., Carling, D., & Hardie, D.G. (2005) AMP-activated protein kinase: ancient energy gauge provides clues to modern understanding of metabolism. *Cell Metab.* **1**, 15–25.

Well-illustrated, intermediate-level review.

Long, Y.C. & Zierath, J.R. (2006) AMP-activated protein kinase signaling in metabolic regulation. *J. Clin. Invest.* **116**, 1776–1783.

Advanced, short review of AMPK role in metabolism, including data on knockout mice.

Nordlie, R.C., Foster, J.D., & Lange, A.J. (1999) Regulation of glucose production by the liver. *Annu. Rev. Nutr.* **19**, 379–406.

Advanced review.

Okar, D.A., Manzano, A., Navarro-Sabate, A., Riera, L., Bartrons, R., & Lange, A.J. (2001) PFK-2/FBPase-2: maker and breaker of the essential biofactor fructose-2,6-bisphosphate. *Trends Biochem. Sci.* **26**, 30–35.

Pilkis, S.J. & Granner, D.K. (1992) Molecular physiology of the regulation of hepatic gluconeogenesis and glycolysis. *Annu. Rev. Physiol.* **54**, 885–909.

Postic, C., Dentin, R., Denechaud, P.-D., & Girard, J. (2007) ChREBP, a transcriptional regulator of glucose and lipid metabolism. *Annu. Rev. Nutr.* **27**, 179–192.

Advanced review of the role of transcription factor ChREBP in carbohydrate metabolism.

Rider, M.H. & Bartrons, R. (2010) Fructose 2,6-bisphosphate: the last milestone of the 20th century in metabolic control? *Biochem. J.* doi:10.1042/BJ20091921.

Schirmer, T. & Evans, P.R. (1990) Structural basis of the allosteric behavior of phosphofructokinase. *Nature* **343**, 140–145.

Sola-Penna, M., Da Silva, D., Coelho, W.S., Marinho-Carvalho, M.M., & Zancan, P. (2010) Regulation of mammalian muscle type 6-phosphofructo-1-kinase and its implication for the control of metabolism. *IUBMB Life* **62**, 791–796.

Towle, H.C. (2005) Glucose as a regulator of eukaryotic gene transcription. *Trends Endocrinol. Metab.* **16**, 489–494.

Intermediate-level review.

Towler, M.C. & Hardie, D.G. (2007) AMP-activated protein kinase in metabolic control and insulin signaling. *Circ. Res.* **100**, 328–341.

van Shaftingen, E. & Gerin, I. (2002) The glucose-6-phosphatase system. *Biochem. J.* **362**, 513–532.

Veech, R.L. (2003) A humble hexose monophosphate pathway metabolite regulates short- and long-term control of lipogenesis. *Proc. Natl. Acad. Sci. USA* **100**, 5578–5580.

Short review of the work from K. Uyeda's laboratory on the role of xylulose 5-phosphate in carbohydrate and fat metabolism; Uyeda's papers are cited in this review.

Yamada, K. & Noguchi, T. (1999) Nutrient and hormonal regulation of pyruvate kinase gene expression. *Biochem. J.* **337**, 1–11.

The Metabolism of Glycogen in Animals

Moslemi, A.-R., Lindberg, C., Nilsson, J., Tajsharghi, H., Andersson, B., & Oldfors, A. (2010) Glycogenin-1 deficiency and inactivated priming of glycogen synthesis. *N. Engl. J. Med.* **362**, 1203–1210.

Whelan, W.J. (1976) On the origin of primer for glycogen synthesis. *Trends Biochem. Sci.* **1**, 13–15.

Intermediate review of the discovery, properties, and role of glycogenin.

Coordinated Regulation of Glycogen Synthesis and Breakdown

Aiston, S., Hampson, L., Gomez-Foix, A.M., Guinovart, J.J., & Agius, L. (2001) Hepatic glycogen synthesis is highly sensitive to phosphorylase activity: evidence from metabolic control analysis. *J. Biol. Chem.* **276**, 23,858–23,866.

Jope, R.S. & Johnson, G.V.W. (2004) The glamour and gloom of glycogen synthase kinase-3. *Trends Biochem. Sci.* **29**, 95–102.
Intermediate-level, well-illustrated review.

Problems

1. Measurement of Intracellular Metabolite Concentrations Measuring the concentrations of metabolic intermediates in a living cell presents great experimental difficulties—usually a cell must be destroyed before metabolite concentrations can be measured. Yet enzymes catalyze metabolic interconversions very rapidly, so a common problem associated with these types of measurements is that the findings reflect not the physiological concentrations of metabolites but the equilibrium concentrations. A reliable experimental technique requires all enzyme-catalyzed reactions to be instantaneously stopped in the intact tissue so that the metabolic intermediates do not undergo change. This objective is accomplished by rapidly compressing the tissue between large aluminum plates cooled with liquid nitrogen (−190 °C), a process called **freeze-clamping**. After freezing, which stops enzyme action instantly, the tissue is powdered and the enzymes are inactivated by precipitation with perchloric acid. The precipitate is removed by centrifugation, and the clear supernatant extract is analyzed for metabolites. To calculate intracellular concentrations, the intracellular volume is determined from the total water content of the tissue and a measurement of the extracellular volume.

The intracellular concentrations of the substrates and products of the phosphofructokinase-1 reaction in isolated rat heart tissue are given in the table below.

Metabolite	Concentration (μM)*
Fructose 6-phosphate	87.0
Fructose 1,6-bisphosphate	22.0
ATP	11,400
ADP	1,320

Source: From Williamson, J.R. (1965) Glycolytic control mechanisms I: inhibition of glycolysis by acetate and pyruvate in the isolated, perfused rat heart. *J. Biol. Chem.* **240**, 2308–2321.

*Calculated as μmol/mL of intracellular water.

(a) Calculate Q, [fructose 1,6-bisphosphate][ADP]/[fructose 6-phosphate][ATP], for the PFK-1 reaction under physiological conditions.

(b) Given a $\Delta G'^{\circ}$ for the PFK-1 reaction of −14.2 kJ/mol, calculate the equilibrium constant for this reaction.

(c) Compare the values of Q and K'_{eq}. Is the physiological reaction near or far from equilibrium? Explain. What does this experiment suggest about the role of PFK-1 as a regulatory enzyme?

2. Are All Metabolic Reactions at Equilibrium?

(a) Phosphoenolpyruvate (PEP) is one of the two phosphoryl group donors in the synthesis of ATP during glycolysis. In human erythrocytes, the steady-state concentration of ATP is 2.24 mM, that of ADP is 0.25 mM, and that of pyruvate is 0.051 mM. Calculate the concentration of PEP at 25 °C, assuming that the pyruvate kinase reaction (see Fig. 13–13) is at equilibrium in the cell.

(b) The physiological concentration of PEP in human erythrocytes is 0.023 mM. Compare this with the value obtained in (a). Explain the significance of this difference.

3. Effect of O_2 Supply on Glycolytic Rates The regulated steps of glycolysis in intact cells can be identified by studying the catabolism of glucose in whole tissues or organs. For example, the glucose consumption by heart muscle can be measured by artificially circulating blood through an isolated intact heart and measuring the concentration of glucose before and after the blood passes through the heart. If the circulating blood is deoxygenated, heart muscle consumes glucose at a steady rate. When oxygen is added to the blood, the rate of glucose consumption drops dramatically, then is maintained at the new, lower rate. Explain.

4. Regulation of PFK-1 The effect of ATP on the allosteric enzyme PFK-1 is shown below. For a given concentration of fructose 6-phosphate, the PFK-1 activity increases with increasing concentrations of ATP, but a point is reached beyond which increasing the concentration of ATP inhibits the enzyme.

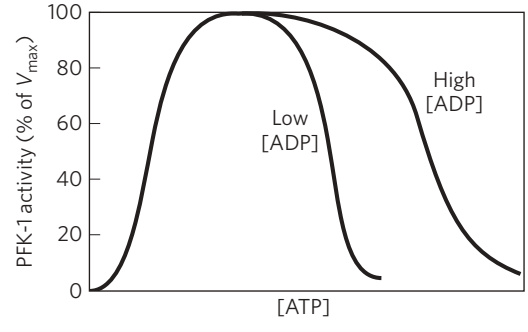

(a) Explain how ATP can be both a substrate and an inhibitor of PFK-1. How is the enzyme regulated by ATP?

(b) In what ways is glycolysis regulated by ATP levels?

(c) The inhibition of PFK-1 by ATP is diminished when the ADP concentration is high, as shown in the illustration. How can this observation be explained?

5. Cellular Glucose Concentration The concentration of glucose in human blood plasma is maintained at about 5 mM. The concentration of free glucose inside a myocyte is much lower. Why is the concentration so low in the cell? What happens to glucose after entry into the cell? Glucose is administered intravenously as a food source in certain clinical situations. Given that the transformation of glucose to glucose 6-phosphate consumes ATP, why not administer intravenous glucose 6-phosphate instead?

6. Enzyme Activity and Physiological Function The V_{max} of the glycogen phosphorylase from skeletal muscle is much greater than the V_{max} of the same enzyme from liver tissue.

(a) What is the physiological function of glycogen phosphorylase in skeletal muscle? In liver tissue?

(b) Why does the V_{max} of the muscle enzyme need to be greater than that of the liver enzyme?

7. Glycogen Phosphorylase Equilibrium Glycogen phosphorylase catalyzes the removal of glucose from glycogen. The $\Delta G'^{\circ}$ for this reaction is 3.1 kJ/mol.

(a) Calculate the ratio of [P_i] to [glucose 1-phosphate] when the reaction is at equilibrium. (Hint: The removal of glucose units from glycogen does not change the glycogen concentration.)

(b) The measured ratio [P_i]/[glucose 1-phosphate] in myocytes under physiological conditions is more than 100:1. What does this indicate about the direction of metabolite flow through the glycogen phosphorylase reaction in muscle?

(c) Why are the equilibrium and physiological ratios different? What is the possible significance of this difference?

8. Regulation of Glycogen Phosphorylase In muscle tissue, the rate of conversion of glycogen to glucose 6-phosphate is determined by the ratio of phosphorylase *a* (active) to phosphorylase *b* (less active). Determine what happens to the rate of glycogen breakdown if a muscle preparation containing glycogen phosphorylase is treated with (a) phosphorylase kinase and ATP; (b) PP1; (c) epinephrine.

9. Glycogen Breakdown in Rabbit Muscle The intracellular use of glucose and glycogen is tightly regulated at four points. To compare the regulation of glycolysis when oxygen is plentiful and when it is depleted, consider the utilization of glucose and glycogen by rabbit leg muscle in two physiological settings: a resting rabbit, with low ATP demands, and a rabbit that sights its mortal enemy, the coyote, and dashes into its burrow. For each setting, determine the relative levels (high, intermediate, or low) of AMP, ATP, citrate, and acetyl-CoA and describe how these levels affect the flow of metabolites through glycolysis by regulating specific enzymes. In periods of stress, rabbit leg muscle produces much of its ATP by anaerobic glycolysis (lactate fermentation) and very little by oxidation of acetyl-CoA derived from fat breakdown.

10. Glycogen Breakdown in Migrating Birds Unlike the rabbit with its short dash, migratory birds require energy for extended periods of time. For example, ducks generally fly several thousand miles during their annual migration. The flight muscles of migratory birds have a high oxidative capacity and obtain the necessary ATP through the oxidation of acetyl-CoA (obtained from fats) via the citric acid cycle. Compare the regulation of muscle glycolysis during short-term intense activity, as in the fleeing rabbit, and during extended activity, as in the migrating duck. Why must the regulation in these two settings be different?

11. Enzyme Defects in Carbohydrate Metabolism Summaries of four clinical case studies follow. For each case determine which enzyme is defective and designate the appropriate treatment, from the lists provided at the end of the problem. Justify your choices. Answer the questions contained in each case study. (You may need to refer to information in Chapter 14.)

Case A The patient develops vomiting and diarrhea shortly after milk ingestion. A lactose tolerance test is administered. (The patient ingests a standard amount of lactose, and the glucose and galactose concentrations of blood plasma are measured at intervals. In individuals with normal carbohydrate metabolism, the levels increase to a maximum in about 1 hour, then decline.) The patient's blood glucose and galactose concentrations do not increase during the test. Why do blood glucose and galactose increase and then decrease during the test in healthy individuals? Why do they fail to rise in the patient?

Case B The patient develops vomiting and diarrhea after ingestion of milk. His blood is found to have a low concentration of glucose but a much higher than normal concentration of reducing sugars. The urine tests positive for galactose. Why is the concentration of reducing sugar in the blood high? Why does galactose appear in the urine?

Case C The patient complains of painful muscle cramps when performing strenuous physical exercise but has no other symptoms. A muscle biopsy indicates a muscle glycogen concentration much higher than normal. Why does glycogen accumulate?

Case D The patient is lethargic, her liver is enlarged, and a biopsy of the liver shows large amounts of excess glycogen. She also has a lower than normal blood glucose level. What is the reason for the low blood glucose in this patient?

Defective Enzyme
(a) Muscle PFK-1
(b) Phosphomannose isomerase
(c) Galactose 1-phosphate uridylyltransferase
(d) Liver glycogen phosphorylase
(e) Triose kinase
(f) Lactase in intestinal mucosa
(g) Maltase in intestinal mucosa
(h) Muscle debranching enzyme
Treatment
1. Jogging 5 km each day
2. Fat-free diet
3. Low-lactose diet
4. Avoiding strenuous exercise
5. Large doses of niacin (the precursor of NAD^+)
6. Frequent feedings (smaller portions) of a normal diet

12. Effects of Insufficient Insulin in a Person with Diabetes A man with insulin-dependent diabetes is brought to the emergency room in a near-comatose state. While vacationing in an isolated place, he lost his insulin medication and has not taken any insulin for two days.

(a) For each tissue listed below, is each pathway faster, slower, or unchanged in this patient, compared with the normal level when he is getting appropriate amounts of insulin?

(b) For each pathway, describe at least one control mechanism responsible for the change you predict.

Tissue and Pathways
1. Adipose: fatty acid synthesis
2. Muscle: glycolysis; fatty acid synthesis; glycogen synthesis
3. Liver: glycolysis; gluconeogenesis; glycogen synthesis; fatty acid synthesis; pentose phosphate pathway

13. Blood Metabolites in Insulin Insufficiency For the patient described in Problem 12, predict the levels of the following metabolites in his blood *before* treatment in the emergency room, relative to levels maintained during adequate insulin treatment: (a) glucose; (b) ketone bodies; (c) free fatty acids.

14. Metabolic Effects of Mutant Enzymes Predict and explain the effect on glycogen metabolism of each of the following defects caused by mutation: (a) loss of the cAMP-binding site on the regulatory subunit of protein kinase A (PKA); (b) loss of the protein phosphatase inhibitor (inhibitor 1 in Fig. 15–42); (c) overexpression of phosphorylase *b* kinase in liver; (d) defective glucagon receptors in liver.

15. Hormonal Control of Metabolic Fuel Between your evening meal and breakfast, your blood glucose drops and your liver becomes a net producer rather than consumer of glucose. Describe the hormonal basis for this switch, and explain how the hormonal change triggers glucose production by the liver.

16. Altered Metabolism in Genetically Manipulated Mice Researchers can manipulate the genes of a mouse so that a single gene in a single tissue either produces an inactive protein (a "knockout" mouse) or produces a protein that is always (constitutively) active. What effects on metabolism would you predict for mice with the following genetic changes: (a) knockout of glycogen debranching enzyme in the liver; (b) knockout of hexokinase IV in liver; (c) knockout of FBPase-2 in liver; (d) constitutively active FBPase-2 in liver; (e) constitutively active AMPK in muscle; (f) constitutively active ChREBP in liver?

Data Analysis Problem

17. Optimal Glycogen Structure Muscle cells need rapid access to large amounts of glucose during heavy exercise. This glucose is stored in liver and skeletal muscle in polymeric form as particles of glycogen. The typical glycogen particle contains about 55,000 glucose residues (see Fig. 15–35b). Meléndez-Hevia, Waddell, and Shelton (1993) explored some theoretical aspects of the structure of glycogen, as described in this problem.

(a) The cellular concentration of glycogen in liver is about 0.01 μM. What cellular concentration of free glucose would be required to store an equivalent amount of glucose? Why would this concentration of free glucose present a problem for the cell?

Glucose is released from glycogen by glycogen phosphorylase, an enzyme that can remove glucose molecules, one at a time, from one end of a glycogen chain. Glycogen chains are branched (see Figs 15–28 and 15–35b), and the degree of branching—the number of branches per chain—has a powerful influence on the rate at which glycogen phosphorylase can release glucose.

(b) Why would a degree of branching that was too low (i.e., below an optimum level) reduce the rate of glucose release? (Hint: Consider the extreme case of no branches in a chain of 55,000 glucose residues.)

(c) Why would a degree of branching that was too high also reduce the rate of glucose release? (Hint: Think of the physical constraints.)

Meléndez-Hevia and colleagues did a series of calculations and found that two branches per chain (see Fig. 15–35b) was optimal for the constraints described above. This is what is found in glycogen stored in muscle and liver.

To determine the optimum number of glucose residues per chain, Meléndez-Hevia and coauthors considered two key parameters that define the structure of a glycogen particle: t = the number of tiers of glucose chains in a particle (the molecule in Fig. 15–35b has five tiers); g_c = the number of glucose residues in each chain. They set out to find the values of t and g_c that would maximize three quantities: (1) the amount of glucose stored in the particle (G_T) per unit volume; (2) the number of unbranched glucose chains (C_A) per unit volume (i.e., number of chains in the outermost tier, readily accessible to glycogen phosphorylase); and (3) the amount of glucose available to phosphorylase in these unbranched chains (G_{PT}).

(d) Show that $C_A = 2^{t-1}$. This is the number of chains available to glycogen phosphorylase before the action of the debranching enzyme.

(e) Show that C_T, the total number of chains in the particle, is given by $C_T = 2^t - 1$. Thus $G_T = g_c(C_T) = g_c(2^t - 1)$, the total number of glucose residues in the particle.

(f) Glycogen phosphorylase cannot remove glucose from glycogen chains that are shorter than five glucose residues. Show that $G_{PT} = (g_c - 4)(2^{t-1})$. This is the amount of glucose readily available to glycogen phosphorylase.

(g) Based on the size of a glucose residue and the location of branches, the thickness of one tier of glycogen is $0.12\ g_c$ nm + 0.35 nm. Show that the volume of a particle, V_s, is given by the equation $V_s = \frac{4}{3}\pi t^3(0.12g_c + 0.35)^3\ \text{nm}^3$.

Meléndez-Hevia and coauthors then determined the optimum values of t and g_c—those that gave the maximum value of a quality function, f, that maximizes G_T, C_A, and G_{PT}, while minimizing V_s: $f = \frac{G_T C_A G_{PT}}{V_S}$. They found that the optimum value of g_c is independent of t.

(h) Choose a value of t between 5 and 15 and find the optimum value of g_c. How does this compare with the g_c found in liver glycogen (see Fig. 15–35b)? (Hint: You may find it useful to use a spreadsheet program.)

Reference

Meléndez-Hevia, E., Waddell, T.G., & Shelton, E.D. (1993) Optimization of molecular design in the evolution of metabolism: the glycogen molecule. *Biochem. J.* **295**, 477–483.

this page left intentionally blank

16

The Citric Acid Cycle

As we saw in Chapter 14, some cells obtain energy (ATP) by fermentation, breaking down glucose in the absence of oxygen. For most eukaryotic cells and many bacteria, which live under aerobic conditions and oxidize their organic fuels to carbon dioxide and water, glycolysis is but the first stage in the complete oxidation of glucose. Rather than being reduced to lactate, ethanol, or some other fermentation product, the pyruvate produced by glycolysis is further oxidized to H_2O and CO_2. This aerobic phase of catabolism is called **respiration**. In the broader physiological or macroscopic sense, respiration refers to a multicellular organism's uptake of O_2 and release of CO_2. Biochemists and cell biologists, however, use the term in a narrower sense to refer to the molecular processes by which *cells* consume O_2 and produce CO_2—processes more precisely termed **cellular respiration**.

Cellular respiration occurs in three major stages **(Fig. 16–1)**. In the first, organic fuel molecules—glucose, fatty acids, and some amino acids—are oxidized to yield two-carbon fragments in the form of the acetyl group of acetyl-coenzyme A (acetyl-CoA). In the second stage, the acetyl groups are fed into the citric acid cycle, which enzymatically oxidizes them to CO_2; the energy released is conserved in the reduced electron carriers NADH and $FADH_2$. In the third stage of respiration, these reduced coenzymes are themselves oxidized, giving up protons (H^+) and electrons. The electrons are transferred to O_2—the final electron acceptor—via a chain of electron-carrying molecules known as the respiratory chain. In the course of electron transfer, the large amount of energy released is conserved in the form of ATP, by a process called oxidative phosphorylation (Chapter 19). Respiration is more complex than glycolysis and is believed to have evolved much later, after the appearance of cyanobacteria. The metabolic activities of cyanobacteria account for the rise of oxygen levels in the earth's atmosphere, a dramatic turning point in evolutionary history.

We consider first the conversion of pyruvate to acetyl groups, then the entry of those groups into the **citric acid cycle**, also called the **tricarboxylic acid (TCA) cycle** or the **Krebs cycle** (after its discoverer, Hans Krebs). We next examine the cycle reactions and the enzymes that catalyze them. Because intermediates of the citric acid cycle are also siphoned off as biosynthetic precursors, we go on to consider some ways in which these intermediates are replenished. The citric acid cycle is a hub in metabolism, with degradative pathways leading in and anabolic pathways leading out, and it is closely regulated in coordination with other pathways. The chapter ends with a description of the glyoxylate pathway, a metabolic sequence in some organisms that employs several of the same enzymes and reactions used in the citric acid cycle, bringing about the net synthesis of glucose from stored triacylglycerols.

Hans Krebs, 1900–1981

16.1 Production of Acetyl-CoA (Activated Acetate)

In aerobic organisms, glucose and other sugars, fatty acids, and most amino acids are ultimately oxidized to CO_2 and H_2O via the citric acid cycle and the respiratory chain. Before entering the citric acid cycle, the carbon skeletons of sugars and fatty acids are degraded to the acetyl group of acetyl-CoA, the form in which the cycle accepts most of its fuel input. Many amino acid carbons also enter the cycle this way, although several amino acids are degraded to other cycle intermediates. Here

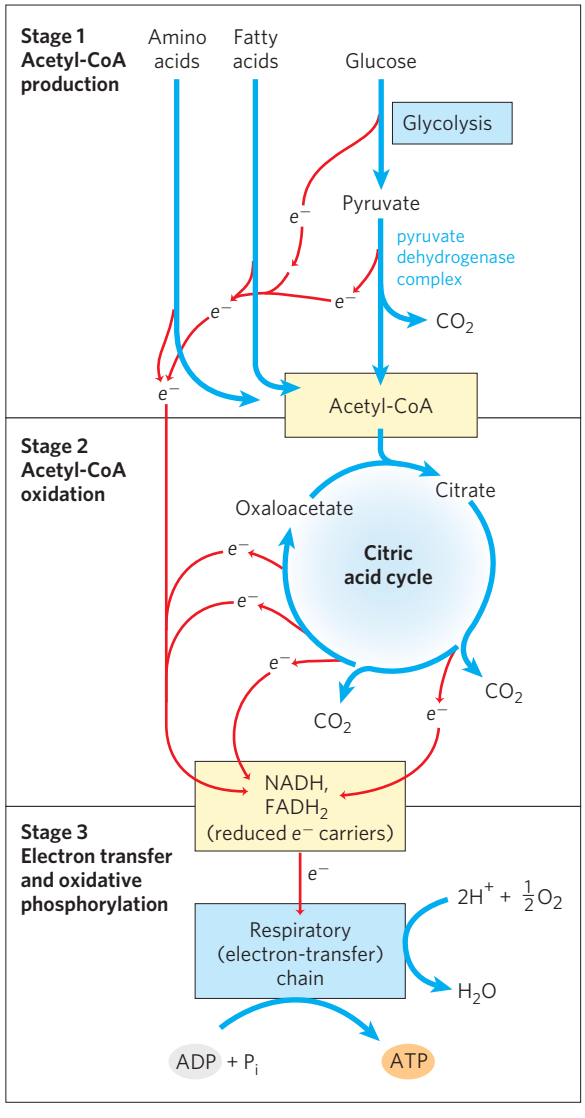

FIGURE 16–1 Catabolism of proteins, fats, and carbohydrates in the three stages of cellular respiration. Stage 1: oxidation of fatty acids, glucose, and some amino acids yields acetyl-CoA. Stage 2: oxidation of acetyl groups in the citric acid cycle includes four steps in which electrons are abstracted. Stage 3: electrons carried by NADH and $FADH_2$ are funneled into a chain of mitochondrial (or, in bacteria, plasma membrane-bound) electron carriers—the respiratory chain—ultimately reducing O_2 to H_2O. This electron flow drives the production of ATP.

we focus on how pyruvate, derived from glucose and other sugars by glycolysis, is oxidized to acetyl-CoA and CO_2 by the **pyruvate dehydrogenase (PDH) complex**, a cluster of enzymes—multiple copies of each of three enzymes—located in the mitochondria of eukaryotic cells and in the cytosol of bacteria.

A careful examination of this enzyme complex is rewarding in several respects. The PDH complex is a classic, much-studied example of a multienzyme complex in which a series of chemical intermediates remain bound to the enzyme molecules as a substrate is transformed into the final product. Five cofactors, four derived from vitamins, participate in the reaction mechanism. The regulation of this enzyme complex also illustrates how a combination of covalent modification and allosteric mechanism results in precisely regulated flux through a metabolic step. Finally, the PDH complex is the prototype for two other important enzyme complexes: α-ketoglutarate dehydrogenase, of the citric acid cycle, and the branched-chain α-keto acid dehydrogenase, of the oxidative pathways of several amino acids (see Fig. 18–28). The remarkable similarity in the protein structure, cofactor requirements, and reaction mechanisms of these three complexes doubtless reflects a common evolutionary origin.

Pyruvate Is Oxidized to Acetyl-CoA and CO_2

The overall reaction catalyzed by the pyruvate dehydrogenase complex is an **oxidative decarboxylation**, an irreversible oxidation process in which the carboxyl group is removed from pyruvate as a molecule of CO_2 and the two remaining carbons become the acetyl group of acetyl-CoA **(Fig. 16–2)**. The NADH formed in this reaction gives up a hydride ion ($:H^-$) to the respiratory chain (Fig. 16–1), which carries the two electrons to oxygen or, in anaerobic microorganisms, to an alternative electron acceptor such as nitrate or sulfate. The transfer of electrons from NADH to oxygen ultimately generates 2.5 molecules of ATP per pair of electrons. The irreversibility of the PDH complex reaction has been demonstrated by isotopic labeling experiments: the complex cannot reattach radioactively labeled CO_2 to acetyl-CoA to yield carboxyl-labeled pyruvate.

The Pyruvate Dehydrogenase Complex Requires Five Coenzymes

The combined dehydrogenation and decarboxylation of pyruvate to the acetyl group of acetyl-CoA (Fig. 16–2) requires the sequential action of three different enzymes and five different coenzymes or prosthetic groups—thiamine pyrophosphate (TPP), flavin adenine dinucleotide (FAD), coenzyme A (CoA, sometimes denoted CoA-SH, to emphasize the role of the —SH group), nicotinamide adenine dinucleotide (NAD), and lipoate. Four different vitamins required in human nutrition are vital components of this system: thiamine (in TPP), riboflavin (in FAD), niacin (in NAD), and pantothenate (in CoA). We have

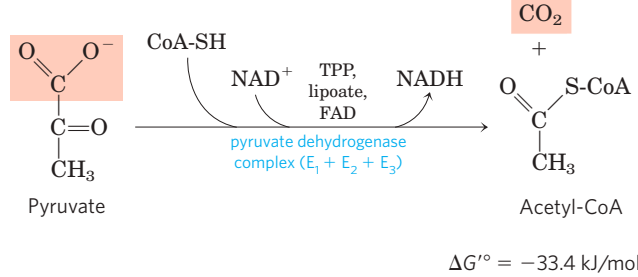

$\Delta G'^\circ = -33.4$ kJ/mol

FIGURE 16–2 Overall reaction catalyzed by the pyruvate dehydrogenase complex. The five coenzymes participating in this reaction, and the three enzymes that make up the enzyme complex, are discussed in the text.

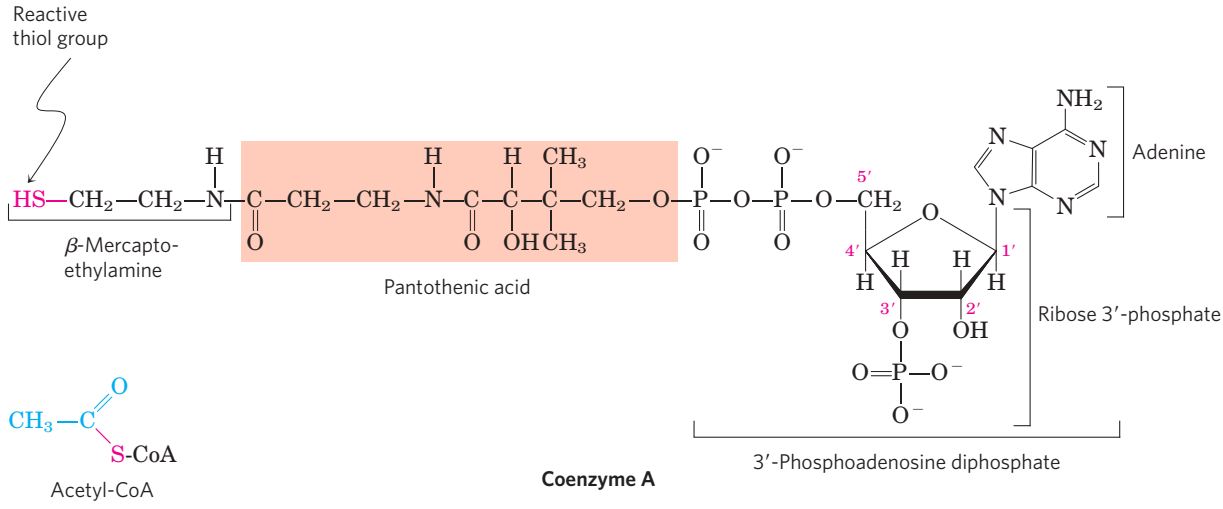

FIGURE 16–3 Coenzyme A (CoA). A hydroxyl group of pantothenic acid is joined to a modified ADP moiety by a phosphate ester bond, and its carboxyl group is attached to β-mercaptoethylamine in amide linkage. The hydroxyl group at the 3′ position of the ADP moiety has a phosphoryl group not present in free ADP. The —SH group of the mercaptoethylamine moiety forms a thioester with acetate in acetyl-coenzyme A (acetyl-CoA) (lower left).

already described the roles of FAD and NAD as electron carriers (Chapter 13), and we have encountered TPP as the coenzyme of pyruvate decarboxylase (see Fig. 14–15).

Coenzyme A **(Fig. 16–3)** has a reactive thiol (—SH) group that is critical to the role of CoA as an acyl carrier in a number of metabolic reactions. Acyl groups are covalently linked to the thiol group, forming **thioesters**. Because of their relatively high standard free energies of hydrolysis (see Figs 13–16, 13–17), thioesters have a high acyl group transfer potential and can donate their acyl groups to a variety of acceptor molecules. The acyl group attached to coenzyme A may thus be thought of as "activated" for group transfer.

The fifth cofactor of the PDH complex, **lipoate (Fig. 16–4)**, has two thiol groups that can undergo reversible oxidation to a disulfide bond (—S—S—), similar to that between two Cys residues in a protein. Because of its capacity to undergo oxidation-reduction reactions, lipoate can serve both as an electron (hydrogen) carrier and as an acyl carrier, as we shall see.

The Pyruvate Dehydrogenase Complex Consists of Three Distinct Enzymes

The PDH complex contains three enzymes—**pyruvate dehydrogenase** (E_1), **dihydrolipoyl transacetylase** (E_2), and **dihydrolipoyl dehydrogenase** (E_3)—each present in multiple copies. The number of copies of each enzyme and therefore the size of the complex varies among species. The PDH complex isolated from mammals is about 50 nm in diameter—more than five times the size of an entire ribosome and big enough to be visualized with the electron microscope **(Fig. 16–5a)**. In the bovine enzyme, 60 identical copies of E_2 form a pentagonal dodecahedron (the core) with a diameter of about 25 nm (Fig. 16–5b). (The core of the *Escherichia coli* enzyme contains 24 copies of E_2.) E_2 is the point of connection for the prosthetic group lipoate, attached through an amide bond to the ε-amino group of a Lys residue (Fig. 16–4). E_2 has three functionally distinct domains (Fig. 16–5c): the amino-terminal *lipoyl domain*, containing the lipoyl-Lys residue(s); the central E_1- and E_3-*binding domain*; and the inner-core *acyltransferase domain*, which contains the acyltransferase active site. The yeast PDH complex has a single lipoyl domain with a lipoate attached, but the

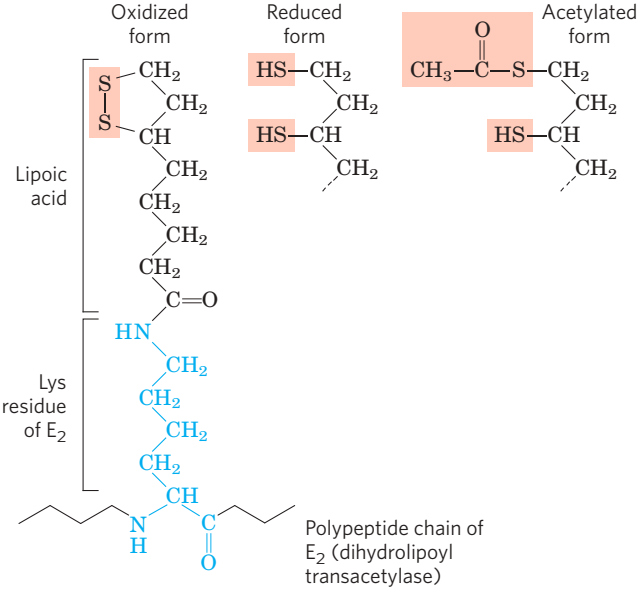

FIGURE 16–4 Lipoic acid (lipoate) in amide linkage with a Lys residue. The lipoyllysyl moiety is the prosthetic group of dihydrolipoyl transacetylase (E_2 of the PDH complex). The lipoyl group occurs in oxidized (disulfide) and reduced (dithiol) forms and acts as a carrier of both hydrogen and an acetyl (or other acyl) group.

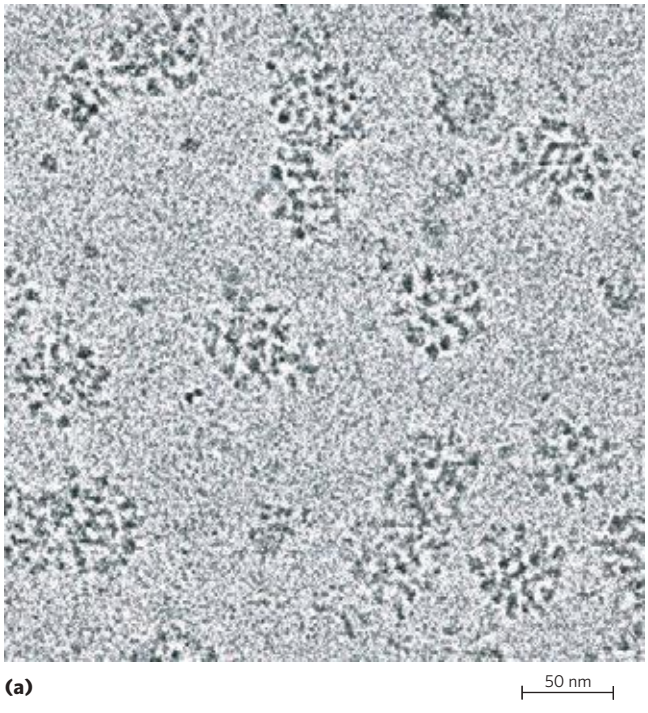

FIGURE 16–5 The pyruvate dehydrogenase complex. (a) Cryoelectron micrograph of PDH complexes isolated from bovine kidney. In cryoelectron microscopy, biological samples are viewed at extremely low temperatures; this avoids potential artifacts introduced by the usual process of dehydrating, fixing, and staining. **(b)** Three-dimensional image of PDH complex, showing the subunit structure: E_1, pyruvate dehydrogenase; E_2, dihydrolipoyl transacetylase; and E_3, dihydrolipoyl dehydrogenase. This image is reconstructed by analysis of a large number of images such as those in (a), combined with crystallographic studies of individual subunits. The core (green) consists of 60 molecules of E_2, arranged in 20 trimers to form a pentagonal dodecahedron. The lipoyl domain of E_2 (blue) reaches outward to touch the active sites of E_1 molecules (yellow) arranged on the E_2 core. Several E_3 subunits (red) are also bound to the core, where the swinging arm on E_2 can reach their active sites. An asterisk marks the site where a lipoyl group is attached to the lipoyl domain of E_2. To make the structure clearer, about half of the complex has been cut away from the front. This model was prepared by Z. H. Zhou and colleagues (2001); in another model, proposed by J. L. S. Milne and colleagues (2002), the E_3 subunits are located more toward the periphery (see Further Reading). **(c)** E_2 consists of three types of domains linked by short polypeptide linkers: a catalytic acyltransferase domain; a binding domain, involved in the binding of E_2 to E_1 and E_3; and one or more (depending on the species) lipoyl domains.

mammalian complex has two, and *E. coli* has three (Fig. 16–5c). The domains of E_2 are separated by linkers, sequences of 20 to 30 amino acid residues, rich in Ala and Pro and interspersed with charged residues; these linkers tend to assume their extended forms, holding the three domains apart.

The active site of E_1 has bound TPP, and that of E_3 has bound FAD. Also part of the complex are two regulatory proteins, a protein kinase and a phosphoprotein phosphatase, discussed below. This basic E_1–E_2–E_3 structure has been conserved during evolution and used in a number of similar metabolic reactions, including the oxidation of α-ketoglutarate in the citric acid cycle (described below) and the oxidation of α-keto acids derived from the breakdown of the branched-chain amino acids valine, isoleucine, and leucine (see Fig. 18–28). Within a given species, E_3 of PDH is identical to E_3 of the other two enzyme complexes. The attachment of lipoate to the end of a Lys side chain in E_2 produces a long, flexible arm that can move from the active site of E_1 to the active sites of E_2 and E_3, a distance of perhaps 5 nm or more.

In Substrate Channeling, Intermediates Never Leave the Enzyme Surface

Figure 16–6 shows schematically how the pyruvate dehydrogenase complex carries out the five consecutive reactions in the decarboxylation and dehydrogenation of pyruvate. Step ❶ is essentially identical to the reaction catalyzed by pyruvate decarboxylase (see Fig. 14–15c); C-1 of pyruvate is released as CO_2, and C-2, which in pyruvate has the oxidation state of an aldehyde, is attached to TPP as a hydroxyethyl group. This first step is the slowest and therefore limits the rate of

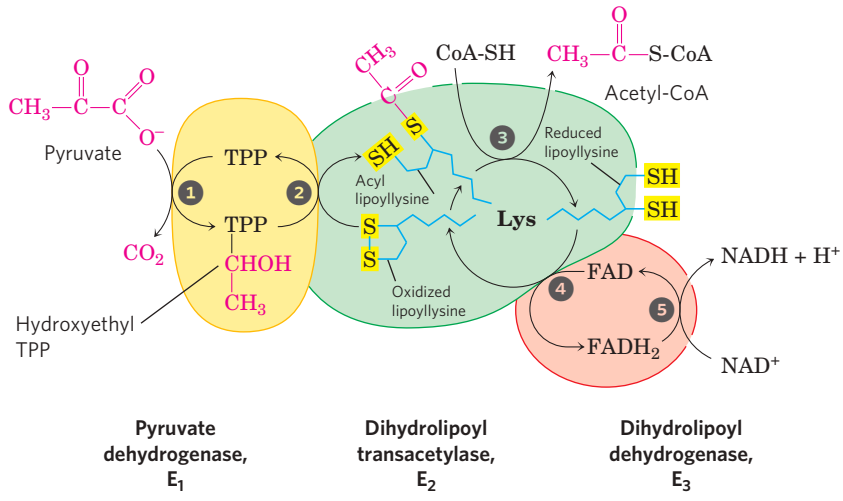

FIGURE 16–6 Oxidative decarboxylation of pyruvate to acetyl-CoA by the PDH complex. The fate of pyruvate is traced in red. In step ❶ pyruvate reacts with the bound thiamine pyrophosphate (TPP) of pyruvate dehydrogenase (E_1), undergoing decarboxylation to the hydroxyethyl derivative (see Fig. 14–15). Pyruvate dehydrogenase also carries out step ❷, the transfer of two electrons and the acetyl group from TPP to the oxidized form of the lipoyllysyl group of the core enzyme, dihydrolipoyl transacetylase (E_2), to form the acetyl thioester of the reduced lipoyl group. Step ❸ is a transesterification in which the —SH group of CoA replaces the —SH group of E_2 to yield acetyl-CoA and the fully reduced (dithiol) form of the lipoyl group. In step ❹ dihydrolipoyl dehydrogenase (E_3) promotes transfer of two hydrogen atoms from the reduced lipoyl groups of E_2 to the FAD prosthetic group of E_3, restoring the oxidized form of the lipoyllysyl group of E_2. In step ❺ the reduced $FADH_2$ of E_3 transfers a hydride ion to NAD^+, forming NADH. The enzyme complex is now ready for another catalytic cycle. (Subunit colors correspond to those in Fig. 16–5b.)

the overall reaction. It is also the point at which the PDH complex exercises its substrate specificity. In step ❷ the hydroxyethyl group is oxidized to the level of a carboxylic acid (acetate). The two electrons removed in this reaction reduce the —S—S— of a lipoyl group on E_2 to two thiol (—SH) groups. The acetyl moiety produced in this oxidation-reduction reaction is first esterified to one of the lipoyl —SH groups, then transesterified to CoA to form acetyl-CoA (step ❸). Thus the energy of oxidation drives the formation of a high-energy thioester of acetate. The remaining reactions catalyzed by the PDH complex (by E_3, in steps ❹ and ❺) are electron transfers necessary to regenerate the oxidized (disulfide) form of the lipoyl group of E_2 to prepare the enzyme complex for another round of oxidation. The electrons removed from the hydroxyethyl group derived from pyruvate pass through FAD to NAD^+.

Central to the mechanism of the PDH complex are the swinging lipoyllysyl arms of E_2, which accept from E_1 the two electrons and the acetyl group derived from pyruvate, passing them to E_3. All these enzymes and coenzymes are clustered, allowing the intermediates to react quickly without diffusing away from the surface of the enzyme complex. The five-reaction sequence shown in Figure 16–6 is thus an example of **substrate channeling**. The intermediates of the multistep sequence never leave the complex, and the local concentration of the substrate of E_2 is kept very high. Channeling also prevents theft of the activated acetyl group by other enzymes that use this group as substrate. As we shall see, a similar tethering mechanism for the channeling of substrate between active sites is used in some other enzymes, with lipoate, biotin, or a CoA-like moiety serving as cofactors.

As one might predict, mutations in the genes for the subunits of the PDH complex, or a dietary thiamine deficiency, can have severe consequences. Thiamine-deficient animals are unable to oxidize pyruvate normally. This is of particular importance to the brain, which usually obtains all its energy from the aerobic oxidation of glucose in a pathway that necessarily includes the oxidation of pyruvate. Beriberi, a disease that results from thiamine deficiency, is characterized by loss of neural function. This disease occurs primarily in populations that rely on a diet consisting mainly of white (polished) rice, which lacks the hulls in which most of the thiamine of rice is found. People who habitually consume large amounts of alcohol can also develop thiamine deficiency, because much of their dietary intake consists of the vitamin-free "empty calories" of distilled spirits. An elevated level of pyruvate in the blood is often an indicator of defects in pyruvate oxidation due to one of these causes. ■

SUMMARY 16.1 Production of Acetyl-CoA (Activated Acetate)

- Pyruvate, the product of glycolysis, is converted to acetyl-CoA, the starting material for the citric acid cycle, by the pyruvate dehydrogenase complex.
- The PDH complex is composed of multiple copies of three enzymes: pyruvate dehydrogenase, E_1 (with its bound cofactor TPP); dihydrolipoyltransacetylase, E_2 (with its covalently bound lipoyl group); and

dihydrolipoyl dehydrogenase, E_3 (with its cofactors FAD and NAD).

- E_1 catalyzes first the decarboxylation of pyruvate, producing hydroxyethyl-TPP, and then the oxidation of the hydroxyethyl group to an acetyl group. The electrons from this oxidation reduce the disulfide of lipoate bound to E_2, and the acetyl group is transferred into thioester linkage with one —SH group of reduced lipoate.
- E_2 catalyzes the transfer of the acetyl group to coenzyme A, forming acetyl-CoA.
- E_3 catalyzes the regeneration of the disulfide (oxidized) form of lipoate; electrons pass first to FAD, then to NAD^+.
- The long lipoyllysyl arm swings from the active site of E_1 to E_2 to E_3, tethering the intermediates to the enzyme complex to allow substrate channeling.
- The organization of the PDH complex is very similar to that of the enzyme complexes that catalyze the oxidation of α-ketoglutarate and the branched-chain α-keto acids.

16.2 Reactions of the Citric Acid Cycle

We are now ready to trace the process by which acetyl-CoA undergoes oxidation. This chemical transformation is carried out by the citric acid cycle, the first *cyclic* pathway we have encountered **(Fig. 16–7)**. To begin a turn of the cycle, acetyl-CoA donates its acetyl group to the four-carbon compound oxaloacetate to form the six-carbon citrate. Citrate is then transformed into isocitrate, also a six-carbon molecule, which is dehydrogenated with loss of CO_2 to yield the five-carbon compound α-ketoglutarate (also called oxoglutarate). α-Ketoglutarate undergoes loss of a second molecule of CO_2 and ultimately yields the four-carbon compound succinate. Succinate is then enzymatically converted in three steps into the four-carbon oxaloacetate—which is then ready to react with another molecule of acetyl-CoA. In each turn of the cycle, one acetyl group (two carbons) enters as acetyl-CoA and two molecules of CO_2 leave; one molecule of oxaloacetate is used to form citrate and one molecule of oxaloacetate is regenerated. No net removal of oxaloacetate occurs; one molecule of oxaloacetate can theoretically bring about oxidation of an infinite number of acetyl groups, and, in fact, oxaloacetate is present in cells in very low concentrations. Four of the eight steps in this process are oxidations, in which the energy of oxidation is very efficiently conserved in the form of the reduced coenzymes NADH and $FADH_2$.

As noted earlier, although the citric acid cycle is central to energy-yielding metabolism its role is not limited to energy conservation. Four- and five-carbon intermediates of the cycle serve as precursors for a wide variety of products. To replace intermediates removed for this purpose, cells employ anaplerotic (replenishing) reactions, which are described below.

Eugene Kennedy and Albert Lehninger showed in 1948 that, in eukaryotes, the entire set of reactions of the citric acid cycle takes place in mitochondria. Isolated mitochondria were found to contain not only all the enzymes and coenzymes required for the citric acid cycle, but also all the enzymes and proteins necessary for the last stage of respiration—electron transfer and ATP synthesis by oxidative phosphorylation. As we shall see in later chapters, mitochondria also contain the enzymes for the oxidation of fatty acids and some amino acids to acetyl-CoA, and the oxidative degradation of other amino acids to α-ketoglutarate, succinyl-CoA, or oxaloacetate. Thus, in nonphotosynthetic eukaryotes, the mitochondrion is the site of most energy-yielding oxidative reactions and of the coupled synthesis of ATP. In photosynthetic eukaryotes, mitochondria are the major site of ATP production in the dark, but in daylight chloroplasts produce most of the organism's ATP. In most bacteria, the enzymes of the citric acid cycle are in the cytosol, and the plasma membrane plays a role analogous to that of the inner mitochondrial membrane in ATP synthesis (Chapter 19).

The Sequence of Reactions in the Citric Acid Cycle Makes Chemical Sense

Acetyl-CoA produced in the breakdown of carbohydrates, fats, and proteins must be completely oxidized to CO_2 if the maximum potential energy is to be extracted from these fuels. However, the direct oxidation of acetate (or acetyl-CoA) to CO_2 is not biochemically feasible. Decarboxylation of this two-carbon acid would yield CO_2 and methane (CH_4). Methane is chemically rather stable, and except for certain methanotrophic bacteria that grow in methane-rich niches, organisms do not have the cofactors and enzymes needed to oxidize methane. Methylene groups (—CH_2—), however, are readily metabolized by enzyme systems present in most organisms. In typical oxidation sequences, two adjacent methylene groups (—CH_2—CH_2—) are involved, at least one of which is adjacent to a carbonyl group. As we noted in Chapter 13 (p. 513), carbonyl groups are particularly important in the chemical transformations of metabolic pathways. The carbon of the carbonyl group has a partial positive charge due to the electron-withdrawing property of the carbonyl oxygen and is therefore an electrophilic center. A carbonyl group can facilitate the formation of a carbanion on an adjoining carbon by delocalizing the carbanion's negative charge. We see in the citric acid cycle an example of the oxidation of a methylene group as succinate is oxidized (steps ❻ to ❽ in Fig. 16–7), forming a carbonyl (in oxaloacetate) that is more chemically reactive than either a methylene group or methane.

In short, if acetyl-CoA is to be oxidized efficiently, the methyl group of the acetyl-CoA must be attached to

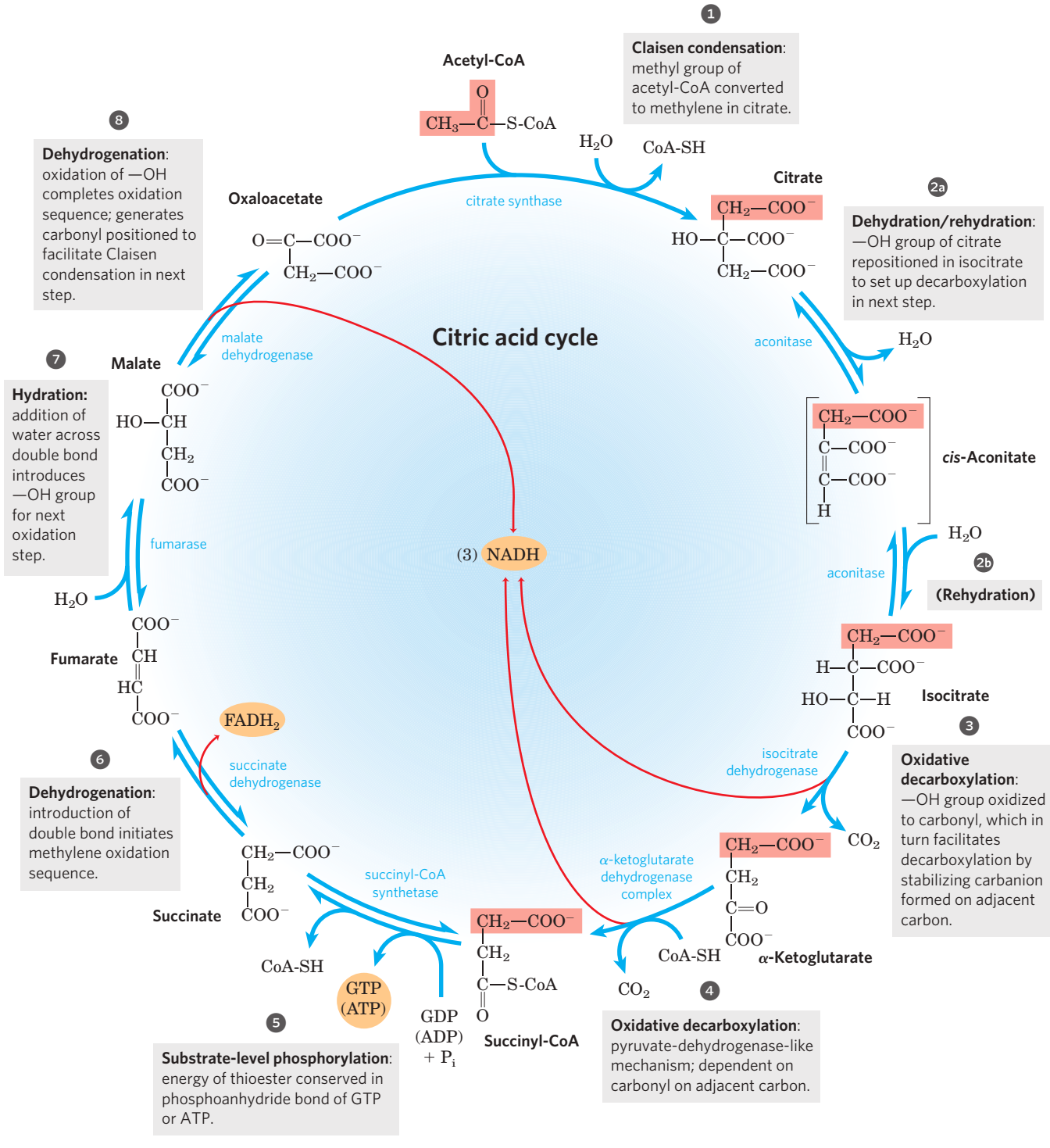

FIGURE 16–7 Reactions of the citric acid cycle. The carbon atoms shaded in pink are those derived from the acetate of acetyl-CoA in the first turn of the cycle; these are *not* the carbons released as CO_2 in the first turn. Note that in succinate and fumarate, the two-carbon group derived from acetate can no longer be specifically denoted; because succinate and fumarate are symmetric molecules, C-1 and C-2 are indistinguishable from C-4 and C-3. The number beside each reaction step corresponds to a numbered heading on pages 640–647). The red arrows show where energy is conserved by electron transfer to FAD or NAD^+, forming $FADH_2$ or NADH + H^+. Steps ❶, ❸, and ❹ are essentially irreversible in the cell; all other steps are reversible. The nucleoside triphosphate product of step ❺ may be either ATP or GTP, depending on which succinyl-CoA synthetase isozyme is the catalyst.

something. The first step of the citric acid cycle neatly solves the problem of the unreactive methyl group by means of the condensation of acetyl-CoA with oxaloacetate. The carbonyl of oxaloacetate acts as an electrophilic center, which is attacked by the methyl carbon of acetyl-CoA in a Claisen condensation (p. 513) to form citrate (step ❶ in Fig. 16–7). The methyl group of acetate has been converted into a methylene in citric acid. This tricarboxylic acid then readily undergoes a series of oxidations that eliminate two carbons as CO_2. Note

that all steps featuring the breakage or formation of carbon–carbon bonds (steps ❶, ❸, and ❹) rely on properly positioned carbonyl groups. As in all metabolic pathways, there is a chemical logic to the sequence of steps in the citric acid cycle: each step either involves an energy-conserving oxidation or is a necessary prelude to the oxidation, placing functional groups in position to facilitate oxidation or oxidative decarboxylation. As you learn the steps of the cycle, keep in mind the chemical rationale for each; it will make the process easier to understand and remember.

The Citric Acid Cycle Has Eight Steps

In examining the eight successive reaction steps of the citric acid cycle, we place special emphasis on the chemical transformations taking place as citrate formed from acetyl-CoA and oxaloacetate is oxidized to yield CO_2 and the energy of this oxidation is conserved in the reduced coenzymes NADH and $FADH_2$.

❶ Formation of Citrate The first reaction of the cycle is the condensation of acetyl-CoA with **oxaloacetate** to form **citrate**, catalyzed by **citrate synthase**:

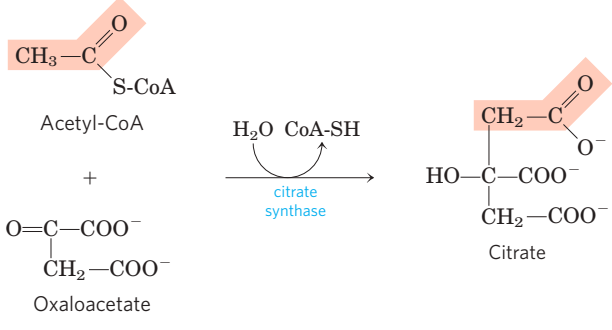

$\Delta G'^{\circ} = -32.2$ kJ/mol

In this reaction the methyl carbon of the acetyl group is joined to the carbonyl group (C-2) of oxaloacetate. Citroyl-CoA is a transient intermediate formed on the active site of the enzyme (see Fig. 16–9). It rapidly undergoes hydrolysis to free CoA and citrate, which are released from the active site. The hydrolysis of this high-energy thioester intermediate makes the forward reaction highly exergonic. The large, negative standard free-energy change of the citrate synthase reaction is essential to the operation of the cycle because, as noted earlier, the concentration of oxaloacetate is normally very low. The CoA liberated in this reaction is recycled to participate in the oxidative decarboxylation of another molecule of pyruvate by the PDH complex.

Citrate synthase from mitochondria has been crystallized and visualized by x-ray diffraction in the presence and absence of its substrates and inhibitors **(Fig. 16–8)**. Each subunit of the homodimeric enzyme is a single polypeptide with two domains, one large and rigid, the other smaller and more flexible, with the active site between

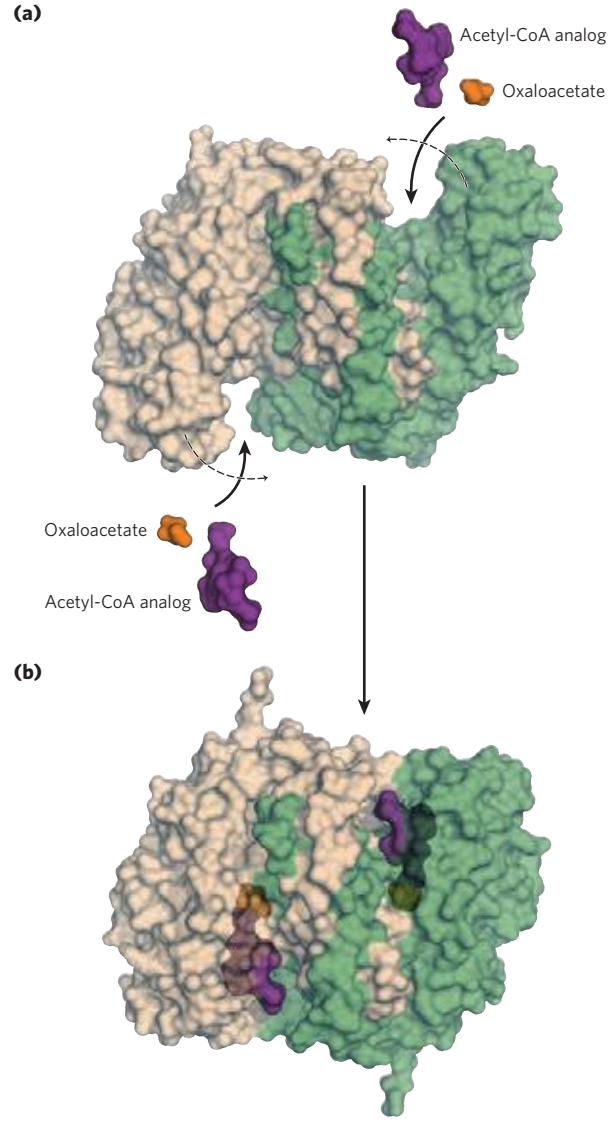

FIGURE 16–8 Structure of citrate synthase. The flexible domain of each subunit undergoes a large conformational change on binding oxaloacetate, creating a binding site for acetyl-CoA. **(a)** Open form of the enzyme alone (PDB ID 5CSC); **(b)** closed form with bound oxaloacetate and a stable analog of acetyl-CoA (carboxymethyl-CoA) (derived from PDB ID 5CTS). In these representations one subunit is colored tan and one green.

them. Oxaloacetate, the first substrate to bind to the enzyme, induces a large conformational change in the flexible domain, creating a binding site for the second substrate, acetyl-CoA. When citroyl-CoA has formed in the enzyme active site, another conformational change brings about thioester hydrolysis, releasing CoA-SH. This induced fit of the enzyme first to its substrate and then to its reaction intermediate decreases the likelihood of premature and unproductive cleavage of the thioester bond of acetyl-CoA. Kinetic studies of the enzyme are consistent with this ordered bisubstrate mechanism (see Fig. 6–13). The reaction catalyzed by citrate synthase is essentially a Claisen condensation (p. 513), involving a thioester (acetyl-CoA) and a ketone (oxaloacetate) **(Fig. 16–9)**.

❷ Formation of Isocitrate via *cis*-Aconitate The enzyme **aconitase** (more formally, **aconitate hydratase**) catalyzes the reversible transformation of citrate to **isocitrate**, through the intermediary formation of the tricarboxylic acid ***cis*-aconitate**, which normally does not dissociate from the active site. Aconitase can promote the reversible addition of H_2O to the double bond of enzyme-bound *cis*-aconitate in two different ways, one leading to citrate and the other to isocitrate:

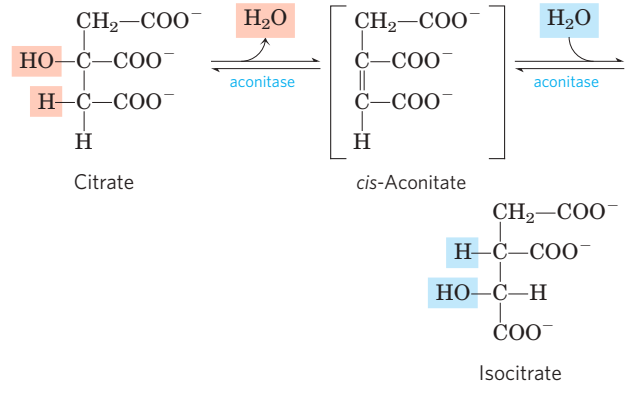

$\Delta G'^{\circ} = 13.3$ kJ/mol

Although the equilibrium mixture at pH 7.4 and 25 °C contains less than 10% isocitrate, in the cell the reaction is pulled to the right because isocitrate is rapidly consumed in the next step of the cycle, lowering its steady-state concentration. Aconitase contains an **iron-sulfur center (Fig. 16–10)**, which acts both in the binding of the substrate at the active site and in the catalytic addition or removal of H_2O. In iron-depleted cells, aconitase loses its iron-sulfur center and acquires a new role in the regulation of iron homeostasis. Aconitase is one of many enzymes known to "moonlight" in a second role (Box 16–1).

❸ Oxidation of Isocitrate to α-Ketoglutarate and CO_2 In the next step, **isocitrate dehydrogenase** catalyzes oxidative decarboxylation of isocitrate to form ***α*-ketoglutarate (Fig. 16–11)**. Mn^{2+} in the active site interacts with the carbonyl group of the intermediate

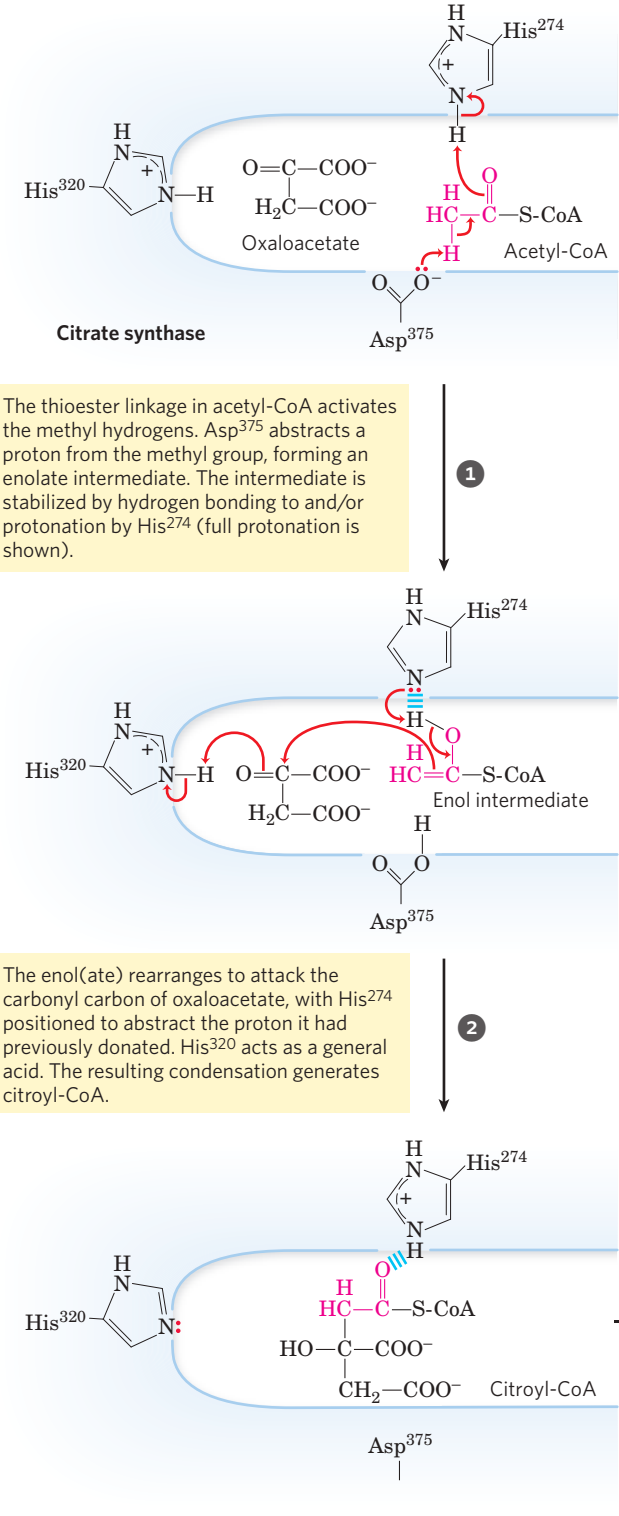

MECHANISM FIGURE 16–9 Citrate synthase. In the mammalian citrate synthase reaction, oxaloacetate binds first, in a strictly ordered reaction sequence. This binding triggers a conformation change that opens up the binding site for acetyl-CoA. Oxaloacetetate is specifically oriented in the active site of citrate synthase by interaction of its two carboxylates with two positively charged Arg residues (not shown here). **Citrate Synthase Mechanism**

BOX 16–1 Moonlighting Enzymes: Proteins with More Than One Job

The "one gene–one enzyme" dictum, put forward by George Beadle and Edward Tatum in 1940 (see Chapter 24), went unchallenged for much of the twentieth century, as did the associated assumption that each protein had only one role. But in recent years, many striking exceptions to this simple formula have been discovered—cases in which a single protein encoded by a single gene clearly is **"moonlighting,"** doing more than one job in the cell. Aconitase is one such protein: it acts both as an enzyme and as a regulator of protein synthesis.

Eukaryotic cells have two isozymes of aconitase. The mitochondrial isozyme converts citrate to isocitrate in the citric acid cycle. The cytosolic isozyme has two distinct functions. It catalyzes the conversion of citrate to isocitrate, providing the substrate for a cytosolic isocitrate dehydrogenase that generates NADPH as reducing power for fatty acid synthesis and other anabolic processes in the cytosol. It also has a role in cellular iron homeostasis.

All cells must obtain iron for the activity of the many proteins that require it as a cofactor. In humans, severe iron deficiency results in anemia, an insufficient supply of erythrocytes and a reduced oxygen-carrying capacity that can be life-threatening. Too much iron is also harmful: it accumulates in and damages the liver in hemochromatosis and other diseases. Iron obtained in the diet is carried in the blood by the protein **transferrin** and enters cells via endocytosis mediated by the **transferrin receptor**. Once inside cells, iron is used in the synthesis of hemes, cytochromes, Fe-S proteins, and other Fe-dependent proteins, and excess iron is stored bound to the protein **ferritin**. The levels of transferrin, transferrin receptor, and ferritin are therefore crucial to cellular iron homeostasis. The synthesis of these three proteins is regulated in response to iron availability—and aconitase, in its moonlighting job, plays a key regulatory role.

Aconitase has an essential Fe-S cluster at its active site (see Fig. 16–10). When a cell is depleted of iron, this Fe-S cluster is disassembled and the enzyme loses its aconitase activity. But the apoenzyme (apoaconitase, lacking its Fe-S cluster) so formed has now acquired its second activity—the ability to bind to specific sequences in the mRNAs for the transferrin receptor and ferritin, thus regulating protein synthesis at the translational level. Two **iron regulatory proteins**, **IRP1** and **IRP2**, were independently discovered as regulators of iron metabolism. As it turned out, IRP1 is identical to cytosolic apoaconitase, and IRP2 is very closely related to IRP1 in structure and function, but unlike IRP1 it cannot be converted to enzymatically active aconitase. Both IRP1 and IRP2 bind to regions in the mRNAs encoding ferritin and the transferrin receptor, with effects on iron mobilization and iron uptake. These mRNA sequences are part of hairpin structures (p. 292) called **iron response elements** (**IREs**),

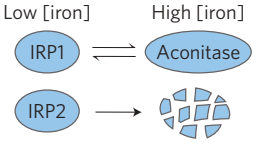

IRP bound to iron response element (IRE)?		Yes	No
5′ Ferritin mRNA IRE — $AAA(A)_n$ 3′	Ferritin mRNA translation Ferritin synthesis	Repressed Decreased	Activated Increased
5′ Transferrin receptor (TfR) mRNA IREs — $AAA(A)_n$ 3′	TfR mRNA stability TfR synthesis	Increased Increased	Decreased Decreased

FIGURE 1 Effect of IRP1 and IRP2 on the mRNAs for ferritin and the transferrin receptor.

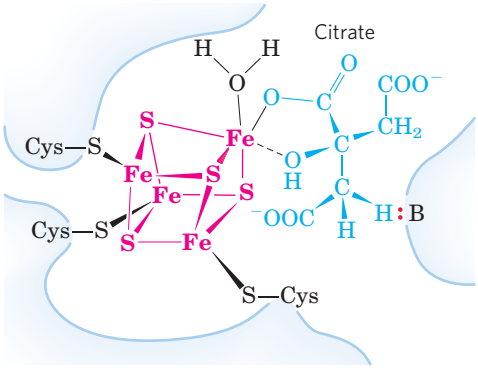

FIGURE 16–10 Iron-sulfur center in aconitase. The iron-sulfur center is in red, the citrate molecule in blue. Three Cys residues of the enzyme bind three iron atoms; the fourth iron is bound to one of the carboxyl groups of citrate and also interacts noncovalently with a hydroxyl group of citrate (dashed bond). A basic residue (:B) in the enzyme helps to position the citrate in the active site. The iron-sulfur center acts in both substrate binding and catalysis. The general properties of iron-sulfur proteins are discussed in Chapter 19 (see Fig. 19–5).

located at the 5′ and 3′ ends of the mRNAs (Fig. 1). When bound to the 5′-untranslated IRE sequence in the ferritin mRNA, IRPs block ferritin synthesis; when bound to the 3′-untranslated IRE sequences in the transferrin receptor mRNA, they stabilize the mRNA, preventing its degradation and thus allowing the synthesis of more copies of the receptor protein per mRNA molecule. So, in iron-deficient cells, iron uptake becomes more efficient and iron storage (bound to ferritin) is reduced. When cellular iron concentrations return to normal levels, IRP1 is converted to aconitase, and IRP2 undergoes proteolytic degradation, ending the low-iron response.

The enzymatically active aconitase and the moonlighting, regulatory apoaconitase have different structures. As the active aconitase, the protein has two lobes that close around the Fe-S cluster; as IRP1, the two lobes open, exposing the mRNA-binding site (Fig. 2).

Aconitase is just one of a growing list of enzymes known (or believed) to moonlight in a second role. Many of the glycolytic enzymes are included in this group. Pyruvate kinase acts in the nucleus to regulate the transcription of genes that respond to thyroid hormone. Glyceraldehyde 3-phosphate dehydrogenase moonlights both as uracil DNA glycosylase, effecting the repair of damaged DNA, and as a regulator of histone H2B transcription. The crystallins in the lens of the vertebrate eye are several moonlighting glycolytic enzymes, including phosphoglycerate kinase, triose phosphate isomerase, and lactate dehydrogenase.

Until recently, the discovery that a protein has more than one function was largely a matter of serendipity: two groups of investigators studying two unrelated questions discovered that "their" proteins had similar properties, compared them carefully, and found them to be identical. With the growth of annotated protein and DNA sequence databases, researchers can now deliberately look for moonlighting proteins by searching the databases for any other protein with the same sequence as the one under study, but with a different function. This also means that in the databases, a protein annotated as having a given function doesn't necessarily have *only* that function. Protein moonlighting may also explain some puzzling findings: experiments in which a protein with a known function is made inactive by a mutation, and the resulting mutant organisms show a phenotype with no obvious relation to that function.

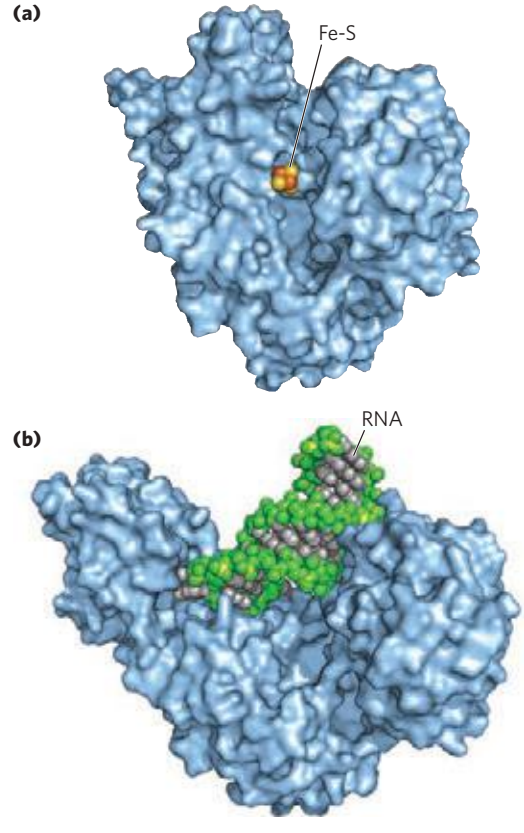

FIGURE 2 Two forms of cytosolic aconitase/IRP1 with two distinct functions. **(a)** In aconitase, the two major lobes are closed and the Fe-S cluster is buried; the protein has been made transparent here to show the Fe-S cluster (PDB ID 2B3Y). **(b)** In IRP1, the lobes open up, exposing a binding site for the mRNA hairpin of the substrate (PDB ID 2IPY).

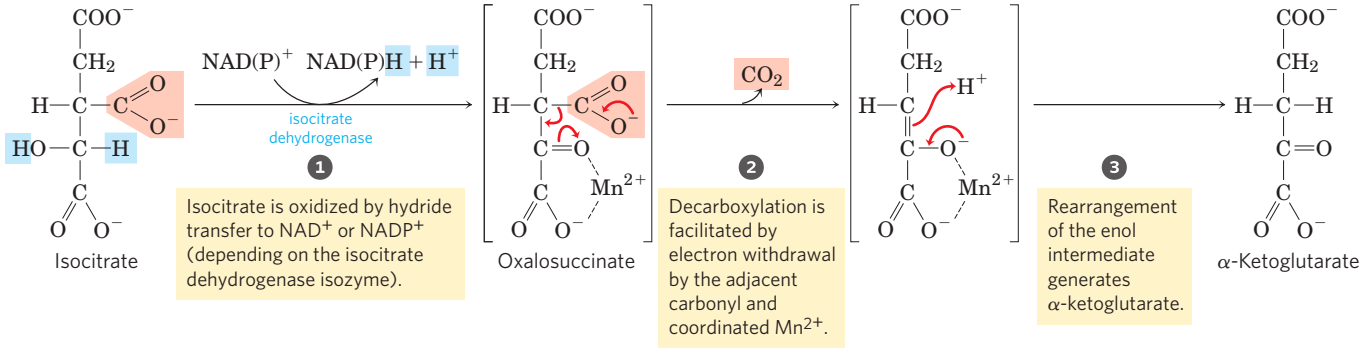

MECHANISM FIGURE 16–11 Isocitrate dehydrogenase. In this reaction, the substrate, isocitrate, loses one carbon by oxidative decarboxylation. See Figure 14–14 for more information on hydride transfer reactions involving NAD^+ and $NADP^+$.

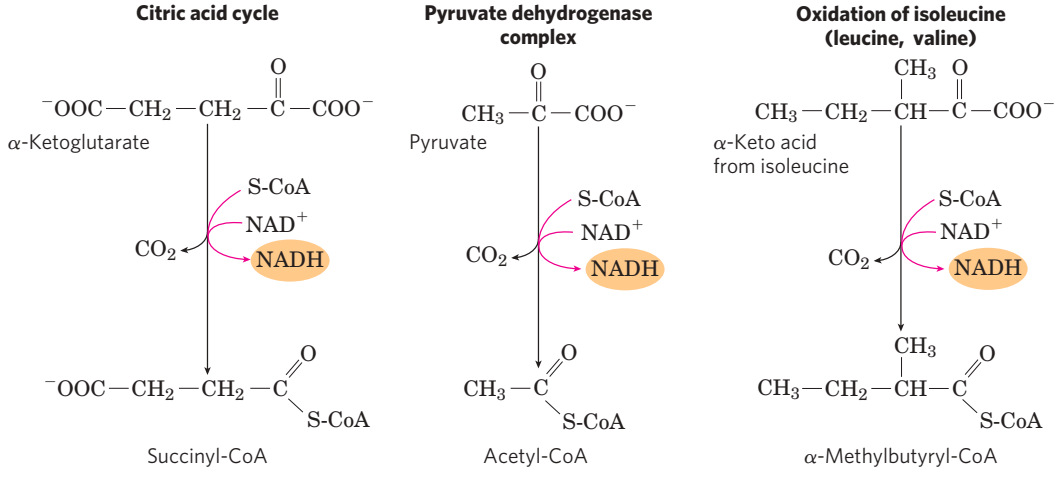

FIGURE 16–12 A conserved mechanism for oxidative decarboxylation. The pathways shown employ the same five cofactors (thiamine pyrophosphate, coenzyme A, lipoate, FAD, and NAD^+), closely similar multienzyme complexes, and the same enzymatic mechanism to carry out oxidative decarboxylations of pyruvate (by the pyruvate dehydrogenase complex), α-ketoglutarate (in the citric acid cycle), and the carbon skeletons of the three branched-chain amino acids, isoleucine (shown here), leucine, and valine. A fourth reaction, catalyzed by glycine decarboxylase, involves a very similar mechanism (see Fig. 20-22).

oxalosuccinate, which is formed transiently but does not leave the binding site until decarboxylation converts it to α-ketoglutarate. Mn^{2+} also stabilizes the enol formed transiently by decarboxylation.

There are two different forms of isocitrate dehydrogenase in all cells, one requiring NAD^+ as electron acceptor and the other requiring $NADP^+$. The overall reactions are otherwise identical. In eukaryotic cells, the NAD-dependent enzyme occurs in the mitochondrial matrix and serves in the citric acid cycle. The main function of the NADP-dependent enzyme, found in both the mitochondrial matrix and the cytosol, may be the generation of NADPH, which is essential for reductive anabolic reactions.

❹ Oxidation of α-Ketoglutarate to Succinyl-CoA and CO_2 The next step is another oxidative decarboxylation, in which α-ketoglutarate is converted to **succinyl-CoA** and CO_2 by the action of the **α-ketoglutarate dehydrogenase complex**; NAD^+ serves as electron acceptor and CoA as the carrier of the succinyl group. The energy of oxidation of α-ketoglutarate is conserved in the formation of the thioester bond of succinyl-CoA:

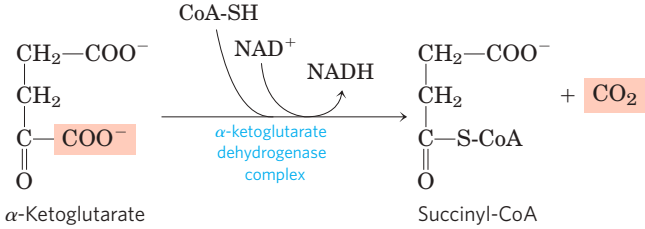

$\Delta G'^\circ = -33.5$ kJ/mol

This reaction is virtually identical to the pyruvate dehydrogenase reaction discussed above and to the reaction sequence responsible for the breakdown of branched-chain amino acids **(Fig. 16–12)**. The α-ketoglutarate dehydrogenase complex closely resembles the PDH complex in both structure and function. It includes three enzymes, homologous to E_1, E_2, and E_3 of the PDH complex, as well as enzyme-bound TPP, bound lipoate, FAD, NAD, and coenzyme A. Both complexes are certainly derived from a common evolutionary ancestor. Although the E_1 components of the two complexes are structurally similar, their amino acid sequences differ and, of course, they have different binding specificities: E_1 of the PDH complex binds pyruvate, and E_1 of the α-ketoglutarate dehydrogenase complex binds α-ketoglutarate. The E_2 components of the two complexes are also very similar, both having covalently bound lipoyl moieties. The subunits of E_3 are identical in the two enzyme complexes. The complex that degrades branched-chain α-keto acids (see Fig. 18–28) catalyzes the same reaction sequence using the same five cofactors. This is a clear case of **divergent evolution**, in which the genes for an enzyme with one substrate specificity give rise, during evolution, to closely related enzymes with different substrate specificities but the same enzymatic mechanism.

❺ Conversion of Succinyl-CoA to Succinate Succinyl-CoA, like acetyl-CoA, has a thioester bond with a strongly negative standard free energy of hydrolysis ($\Delta G'^\circ \approx -36$ kJ/mol). In the next step of the citric acid cycle, energy released in the breakage of this bond is used to drive the synthesis of a phosphoanhydride bond in

either GTP or ATP, with a net $\Delta G'^\circ$ of only −2.9 kJ/mol. **Succinate** is formed in the process:

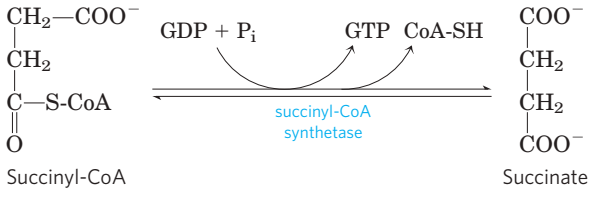

$\Delta G'^\circ = -2.9$ kJ/mol

The enzyme that catalyzes this reversible reaction is called **succinyl-CoA synthetase** or **succinic thiokinase**; both names indicate the participation of a nucleoside triphosphate in the reaction (Box 16–2).

This energy-conserving reaction involves an intermediate step in which the enzyme molecule itself becomes phosphorylated at a His residue in the active site **(Fig. 16–13a)**. This phosphoryl group, which has a high group transfer potential, is transferred to ADP (or GDP) to form ATP (or GTP). Animal cells have two isozymes of succinyl-CoA synthetase, one specific for ADP and the other for GDP. The enzyme has two subunits, α (M_r 32,000), which has the Ⓟ–His residue (His^{246}) and the binding site for CoA, and β (M_r 42,000), which confers specificity for either ADP or GDP. The active site is at the interface between subunits. The crystal structure of succinyl-CoA synthetase reveals two "power helices" (one from each subunit), oriented so that their electric dipoles situate partial positive charges close to the negatively charged Ⓟ–His (Fig. 16–13b), stabilizing the phosphoenzyme intermediate. (Recall the similar role of helix dipoles in stabilizing K^+ ions in the K^+ channel; see Fig. 11–47.)

The formation of ATP (or GTP) at the expense of the energy released by the oxidative decarboxylation of α-ketoglutarate is a substrate-level phosphorylation, like the synthesis of ATP in the glycolytic reactions catalyzed by glyceraldehyde 3-phosphate dehydrogenase and pyruvate kinase (see Fig. 14–2). The GTP formed by succinyl-CoA synthetase can donate its terminal phosphoryl group to ADP to form ATP, in a reversible reaction catalyzed by **nucleoside diphosphate kinase** (p. 526):

$$GTP + ADP \rightleftharpoons GDP + ATP \qquad \Delta G'^\circ = 0 \text{ kJ/mol}$$

Thus the net result of the activity of either isozyme of succinyl-CoA synthetase is the conservation of energy as ATP. There is no change in free energy for the nucleoside diphosphate kinase reaction; ATP and GTP are energetically equivalent.

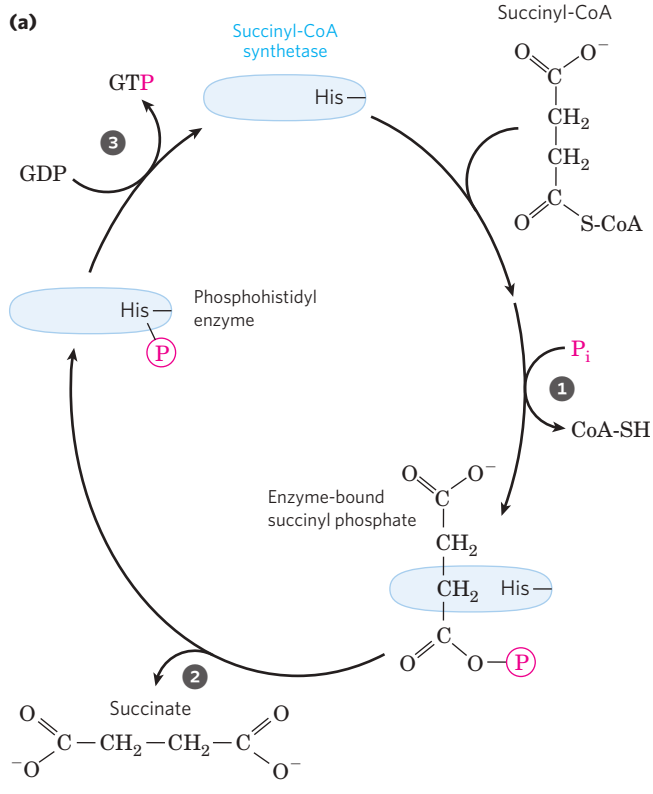

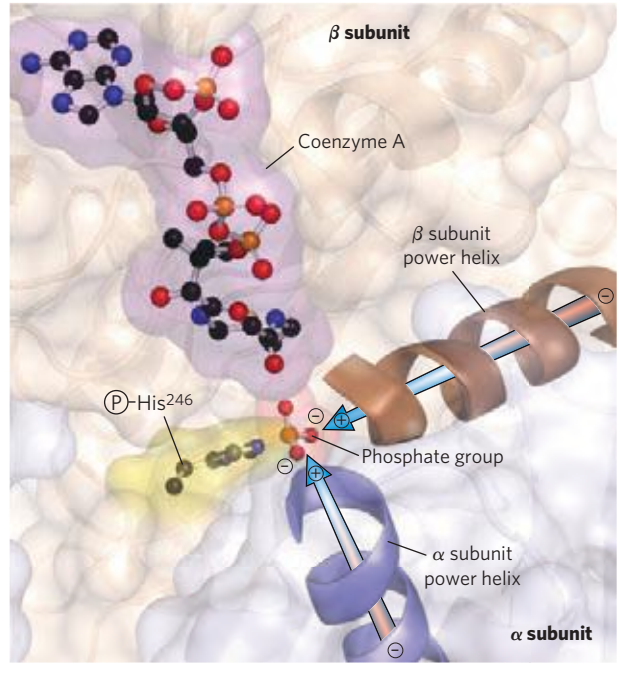

FIGURE 16–13 The succinyl-CoA synthetase reaction. (a) In step ❶ a phosphoryl group replaces the CoA of succinyl-CoA bound to the enzyme, forming a high-energy acyl phosphate. In step ❷ the succinyl phosphate donates its phosphoryl group to a His residue of the enzyme, forming a high-energy phosphohistidyl enzyme. In step ❸ the phosphoryl group is transferred from the His residue to the terminal phosphate of GDP (or ADP), forming GTP (or ATP). **(b)** Active site of succinyl-CoA synthetase of *E. coli* (derived from PDB ID 1SCU). The active site includes part of both the α (blue) and the β (brown) subunits. The power helices (blue, brown) place the partial positive charges of the helix dipole near the phosphate group of Ⓟ-His^{246} in the α chain, stabilizing the phosphohistidyl enzyme. The bacterial and mammalian enzymes have similar amino acid sequences and three-dimensional structures.

BOX 16–2 Synthases and Synthetases; Ligases and Lyases; Kinases, Phosphatases, and Phosphorylases: Yes, the Names Are Confusing!

Citrate synthase is one of many enzymes that catalyze condensation reactions, yielding a product more chemically complex than its precursors. **Synthases** catalyze condensation reactions in which no nucleoside triphosphate (ATP, GTP, and so forth) is required as an energy source. **Synthetases** catalyze condensations that *do* use ATP or another nucleoside triphosphate as a source of energy for the synthetic reaction. Succinyl-CoA synthetase is such an enzyme. **Ligases** (from the Latin *ligare*, "to tie together") are enzymes that catalyze condensation reactions in which two atoms are joined, using ATP or another energy source. (Thus synthetases are ligases.) DNA ligase, for example, closes breaks in DNA molecules, using energy supplied by either ATP or NAD^+; it is widely used in joining DNA pieces for genetic engineering. Ligases are not to be confused with **lyases**, enzymes that catalyze cleavages (or, in the reverse direction, additions) in which electronic rearrangements occur. The PDH complex, which oxidatively cleaves CO_2 from pyruvate, is a member of the large class of lyases.

The name **kinase** is applied to enzymes that transfer a phosphoryl group from a nucleoside triphosphate such as ATP to an acceptor molecule—a sugar (as in hexokinase and glucokinase), a protein (as in glycogen phosphorylase kinase), another nucleotide (as in nucleoside diphosphate kinase), or a metabolic intermediate such as oxaloacetate (as in PEP carboxykinase). The reaction catalyzed by a kinase is a *phosphorylation*. On the other hand, *phosphorolysis* is a displacement reaction in which phosphate is the attacking species and becomes covalently attached at the point of bond breakage. Such reactions are catalyzed by **phosphorylases**. Glycogen phosphorylase, for example, catalyzes the phosphorolysis of glycogen, producing glucose 1-phosphate. *Dephosphorylation,* the removal of a phosphoryl group from a phosphate ester, is catalyzed by **phosphatases**, with water as the attacking species. Fructose bisphosphatase-1 converts fructose 1,6-bisphosphate to fructose 6-phosphate in gluconeogenesis, and phosphorylase *a* phosphatase removes phosphoryl groups from phosphoserine in phosphorylated glycogen phosphorylase. Whew!

Unfortunately, these descriptions of enzyme types overlap, and many enzymes are commonly called by two or more names. Succinyl-CoA synthetase, for example, is also called succinate thiokinase; the enzyme is both a synthetase in the citric acid cycle and a kinase when acting in the direction of succinyl-CoA synthesis. This raises another source of confusion in the naming of enzymes. An enzyme may have been discovered by the use of an assay in which, say, A is converted to B. The enzyme is then named for that reaction. Later work may show, however, that in the cell, the enzyme functions primarily in converting B to A. Commonly, the first name continues to be used, although the metabolic role of the enzyme would be better described by naming it for the reverse reaction. The glycolytic enzyme pyruvate kinase illustrates this situation (p. 554). To a beginner in biochemistry, this duplication in nomenclature can be bewildering. International committees have made heroic efforts to systematize the nomenclature of enzymes (see Table 6–3 for a brief summary of the system), but some systematic names have proved too long and cumbersome and are not frequently used in biochemical conversation.

We have tried throughout this book to use the enzyme name most commonly used by working biochemists and to point out cases in which an enzyme has more than one widely used name. For current information on enzyme nomenclature, refer to the recommendations of the Nomenclature Committee of the International Union of Biochemistry and Molecular Biology (www.chem.qmw.ac.uk/iubmb/nomenclature/).

6 Oxidation of Succinate to Fumarate The succinate formed from succinyl-CoA is oxidized to **fumarate** by the flavoprotein **succinate dehydrogenase**:

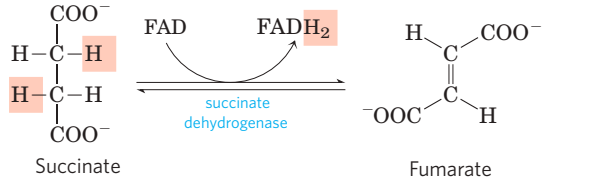

$\Delta G'° = 0$ kJ/mol

In eukaryotes, succinate dehydrogenase is tightly bound to the mitochondrial inner membrane; in bacteria, to the plasma membrane. The enzyme contains three different iron-sulfur clusters and one molecule of covalently bound FAD (see Fig. 19–10). Electrons pass from succinate through the FAD and iron-sulfur centers before entering the chain of electron carriers in the mitochondrial inner membrane (the plasma membrane in bacteria). Electron flow from succinate through these carriers to the final electron acceptor, O_2, is coupled to the synthesis of about 1.5 ATP molecules per pair of electrons (respiration-linked phosphorylation). Malonate,

an analog of succinate not normally present in cells, is a strong competitive inhibitor of succinate dehydrogenase, and its addition to mitochondria blocks the activity of the citric acid cycle.

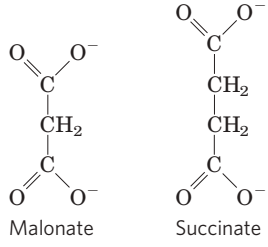

❼ Hydration of Fumarate to Malate The reversible hydration of fumarate to **L-malate** is catalyzed by **fumarase** (formally, **fumarate hydratase**). The transition state in this reaction is a carbanion:

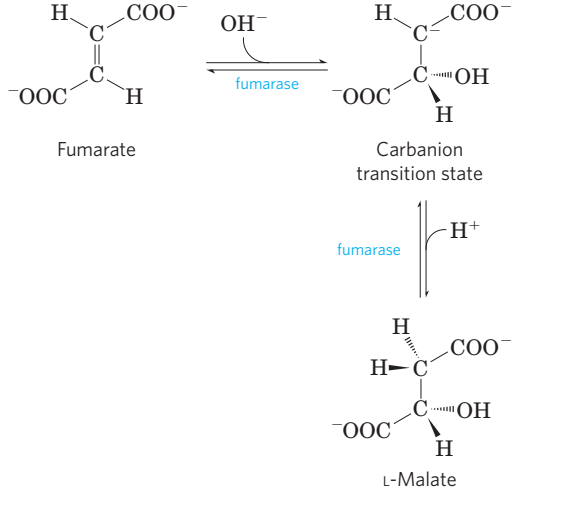

$\Delta G'^{\circ} = -3.8$ kJ/mol

This enzyme is highly stereospecific; it catalyzes hydration of the trans double bond of fumarate but not the cis double bond of maleate (the cis isomer of fumarate). In the reverse direction (from L-malate to fumarate), fumarase is equally stereospecific: D-malate is not a substrate.

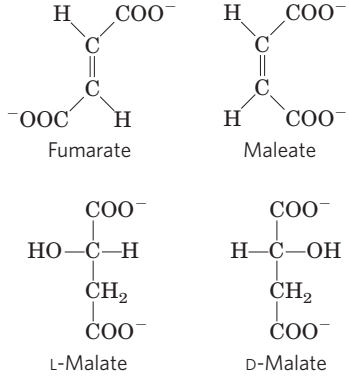

❽ Oxidation of Malate to Oxaloacetate In the last reaction of the citric acid cycle, NAD-linked **L-malate dehydrogenase** catalyzes the oxidation of L-malate to oxaloacetate:

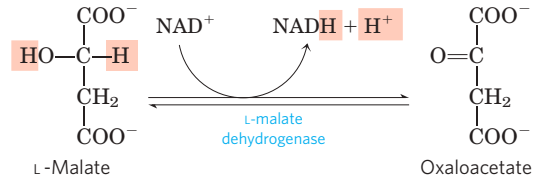

$\Delta G'^{\circ} = 29.7$ kJ/mol

The equilibrium of this reaction lies far to the left under standard thermodynamic conditions, but in intact cells oxaloacetate is continually removed by the highly exergonic citrate synthase reaction (step ❷ of Fig. 16–7). This keeps the concentration of oxaloacetate in the cell extremely low ($<10^{-6}$ M), pulling the malate dehydrogenase reaction toward the formation of oxaloacetate.

Although the individual reactions of the citric acid cycle were initially worked out in vitro, using minced muscle tissue, the pathway and its regulation have also been studied extensively in vivo. By using radioactively labeled precursors such as [^{14}C]pyruvate and [^{14}C]acetate, researchers have traced the fate of individual carbon atoms through the citric acid cycle. Some of the earliest experiments with isotopes produced an unexpected result, however, which aroused considerable controversy about the pathway and mechanism of the citric acid cycle. In fact, these experiments at first seemed to show that citrate was not the first tricarboxylic acid to be formed. Box 16–3 gives some details of this episode in the history of citric acid cycle research. Metabolic flux through the cycle can now be monitored in living tissue by using ^{13}C-labeled precursors and whole-tissue NMR spectroscopy. Because the NMR signal is unique to the compound containing the ^{13}C, biochemists can trace the movement of precursor carbons into each cycle intermediate and into compounds derived from the intermediates. This technique has great promise for studies of regulation of the citric acid cycle and its interconnections with other metabolic pathways such as glycolysis.

The Energy of Oxidations in the Cycle Is Efficiently Conserved

We have now covered one complete turn of the citric acid cycle **(Fig. 16–14)**. A two-carbon acetyl group entered the cycle by combining with oxaloacetate. Two carbon atoms emerged from the cycle as CO_2 from the oxidation of isocitrate and α-ketoglutarate. The energy released by these oxidations was conserved in the reduction of three NAD^+ and one FAD and the production of one ATP or GTP. At the end of the cycle a molecule of oxaloacetate was regenerated. Note that the two carbon atoms appearing as CO_2 are not the same two carbons that entered in the form of the acetyl group; additional turns around the cycle are required to release these carbons as CO_2 (Fig. 16–7).

Although the citric acid cycle directly generates only one ATP per turn (in the conversion of succinyl-CoA

BOX 16–3 Citrate: A Symmetric Molecule That Reacts Asymmetrically

When compounds enriched in the heavy-carbon isotope ^{13}C and the radioactive carbon isotopes ^{11}C and ^{14}C became available about 60 years ago, they were soon put to use in tracing the pathway of carbon atoms through the citric acid cycle. One such experiment initiated the controversy over the role of citrate. Acetate labeled in the carboxyl group (designated [1-^{14}C] acetate) was incubated aerobically with an animal tissue preparation. Acetate is enzymatically converted to acetyl-CoA in animal tissues, and the pathway of the labeled carboxyl carbon of the acetyl group in the cycle reactions could thus be traced. α-Ketoglutarate was isolated from the tissue after incubation, then degraded by known chemical reactions to establish the position(s) of the isotopic carbon.

Condensation of unlabeled oxaloacetate with carboxyl-labeled acetate would be expected to produce citrate labeled in one of the two primary carboxyl groups. Citrate is a symmetric molecule, its two terminal carboxyl groups being chemically indistinguishable. Therefore, half the labeled citrate molecules were expected to yield α-ketoglutarate labeled in the α-carboxyl group and the other half to yield α-ketoglutarate labeled in the γ-carboxyl group; that is, the α-ketoglutarate isolated was expected to be a mixture of the two types of labeled molecules (Fig. 1, pathways ❶ and ❷). Contrary to this expectation, the labeled α-ketoglutarate isolated from the tissue suspension contained ^{14}C only in the γ-carboxyl group (Fig. 1, pathway ❶). The investigators concluded that citrate (or any other symmetric molecule) could not be an intermediate in the pathway from acetate to α-ketoglutarate. Rather, an asymmetric tricarboxylic acid, presumably *cis*-aconitate or isocitrate, must be the first product formed from condensation of acetate and oxaloacetate.

In 1948, however, Alexander Ogston pointed out that although citrate has no chiral center (see Fig. 1–20), it has the *potential* to react asymmetrically if an enzyme with which it interacts has an active site that is asymmetric. He suggested that the active site of aconitase may have three points to which the citrate must be bound and that the citrate must undergo a specific three-point attachment to these binding points. As seen in Figure 2, the binding of citrate to three such points could happen in only one way, and this would account for the formation of only one type of labeled α-ketoglutarate. Organic molecules such as citrate that have no chiral center but are potentially capable of reacting asymmetrically with an asymmetric active site are now called **prochiral molecules**.

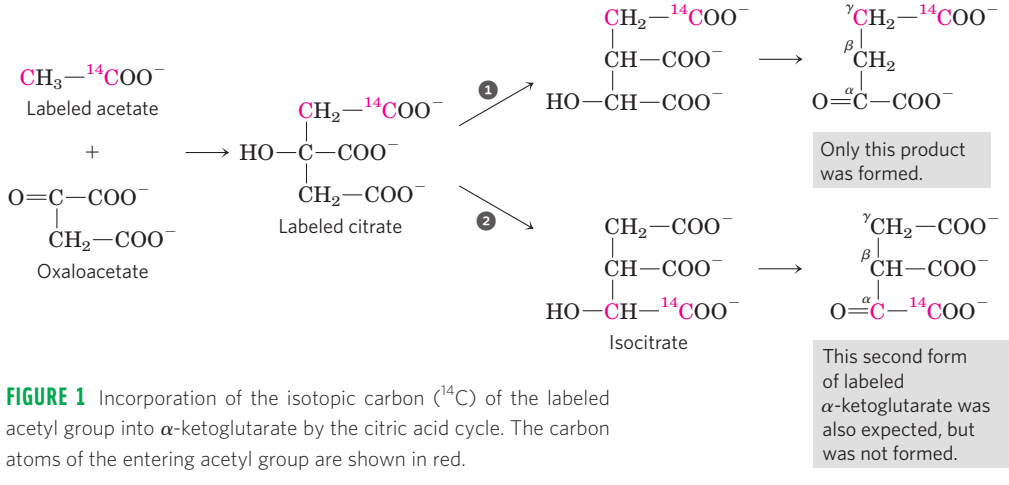

FIGURE 1 Incorporation of the isotopic carbon (^{14}C) of the labeled acetyl group into α-ketoglutarate by the citric acid cycle. The carbon atoms of the entering acetyl group are shown in red.

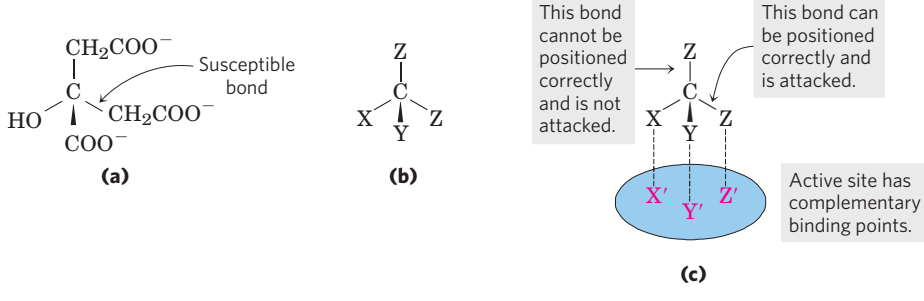

FIGURE 2 The prochiral nature of citrate. **(a)** Structure of citrate; **(b)** schematic representation of citrate: X = −OH; Y = COO^-; Z = $-CH_2COO^-$. **(c)** Correct complementary fit of citrate to the binding site of aconitase. There is only one way in which the three specified groups of citrate can fit on the three points of the binding site. Thus only one of the two $-CH_2COO^-$ groups is bound by aconitase.

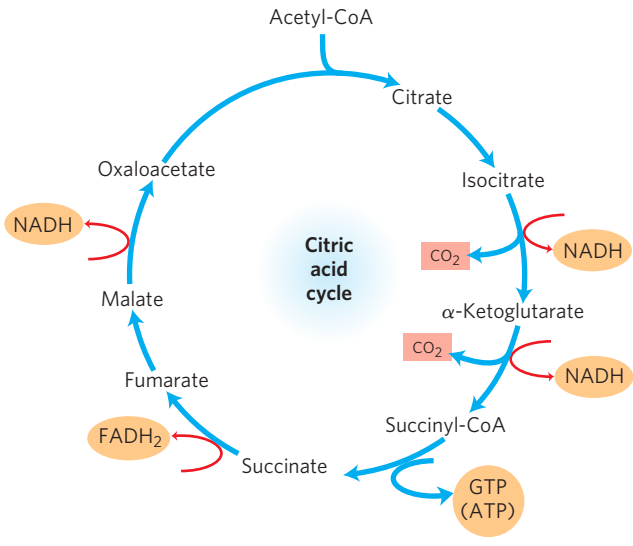

FIGURE 16–14 Products of one turn of the citric acid cycle. At each turn of the cycle, three NADH, one $FADH_2$, one GTP (or ATP), and two CO_2 are released in oxidative decarboxylation reactions. Here and in several following figures, all cycle reactions are shown as proceeding in one direction only, but keep in mind that most of the reactions are reversible (see Fig. 16–7).

to succinate), the four oxidation steps in the cycle provide a large flow of electrons into the respiratory chain via NADH and $FADH_2$ and thus lead to formation of a large number of ATP molecules during oxidative phosphorylation.

We saw in Chapter 14 that the energy yield from the production of two molecules of pyruvate from one molecule of glucose in glycolysis is 2 ATP and 2 NADH. In oxidative phosphorylation (Chapter 19), passage of two electrons from NADH to O_2 drives the formation of about 2.5 ATP, and passage of two electrons from $FADH_2$ to O_2 yields about 1.5 ATP. This stoichiometry allows us to calculate the overall yield of ATP from the complete oxidation of glucose. When both pyruvate molecules are oxidized to 6 CO_2 via the pyruvate dehydrogenase complex and the citric acid cycle, and the electrons are transferred to O_2 via oxidative phosphorylation, as many as 32 ATP are obtained per glucose (Table 16–1). In round numbers, this represents the conservation of 32×30.5 kJ/mol = 976 kJ/mol or 34% of the theoretical maximum of about 2,840 kJ/mol available from the complete oxidation of glucose. These calculations employ the standard free-energy changes; when corrected for the actual free energy required to form ATP within cells (see Worked Example 13–2, p. 519), the calculated efficiency of the process is closer to 65%.

Why Is the Oxidation of Acetate So Complicated?

The eight-step cyclic process for oxidation of simple two-carbon acetyl groups to CO_2 may seem unnecessarily cumbersome and not in keeping with the biological principle of maximum economy. The role of the citric acid cycle is not confined to the oxidation of acetate, however. This pathway is the hub of intermediary metabolism. Four- and five-carbon end products of many catabolic processes feed into the cycle to serve as fuels. Oxaloacetate and α-ketoglutarate, for example, are produced from aspartate and glutamate, respectively, when proteins are degraded. Under some metabolic circumstances, intermediates are drawn out of the

TABLE 16–1 Stoichiometry of Coenzyme Reduction and ATP Formation in the Aerobic Oxidation of Glucose via Glycolysis, the Pyruvate Dehydrogenase Complex Reaction, the Citric Acid Cycle, and Oxidative Phosphorylation

Reaction	Number of ATP or reduced coenzyme directly formed	Number of ATP ultimately formed*
Glucose ⟶ glucose 6-phosphate	−1 ATP	−1
Fructose 6-phosphate ⟶ fructose 1,6-bisphosphate	−1 ATP	−1
2 Glyceraldehyde 3-phosphate ⟶ 2 1,3-bisphosphoglycerate	2 NADH	3 or 5†
2 1,3-Bisphosphoglycerate ⟶ 2 3-phosphoglycerate	2 ATP	2
2 Phosphoenolpyruvate ⟶ 2 pyruvate	2 ATP	2
2 Pyruvate ⟶ 2 acetyl-CoA	2 NADH	5
2 Isocitrate ⟶ 2 α-ketoglutarate	2 NADH	5
2 α-Ketoglutarate ⟶ 2 succinyl-CoA	2 NADH	5
2 Succinyl-CoA ⟶ 2 succinate	2 ATP (or 2 GTP)	2
2 Succinate ⟶ 2 fumarate	2 $FADH_2$	3
2 Malate ⟶ 2 oxaloacetate	2 NADH	5
Total		30–32

*This is calculated as 2.5 ATP per NADH and 1.5 ATP per $FADH_2$. A negative value indicates consumption.

†This number is either 3 or 5, depending on the mechanism used to shuttle NADH equivalents from the cytosol to the mitochondrial matrix; see Figures 19–30 and 19–31.

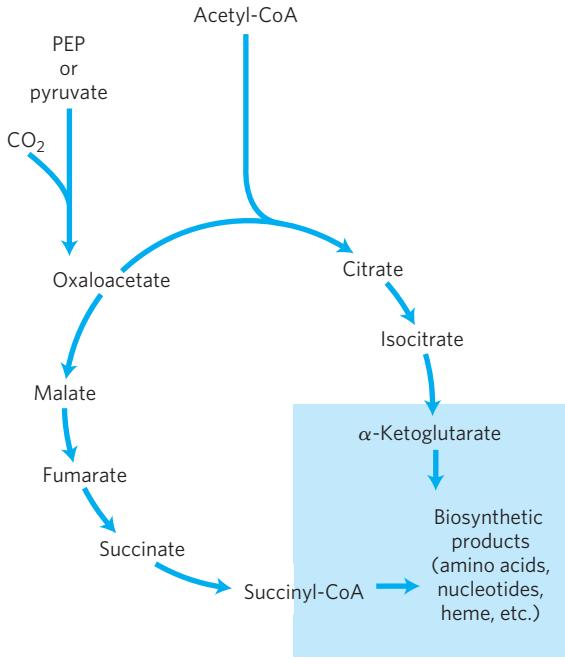

FIGURE 16–15 Biosynthetic precursors produced by an incomplete citric acid cycle in anaerobic bacteria. These anaerobes lack α-ketoglutarate dehydrogenase and therefore cannot carry out the complete citric acid cycle. α-Ketoglutarate and succinyl-CoA serve as precursors in a variety of biosynthetic pathways. (See Fig. 16–14 for the "normal" direction of these reactions in the citric acid cycle.)

cycle to be used as precursors in a variety of biosynthetic pathways.

The citric acid cycle, like all other metabolic pathways, is the product of evolution, and much of this evolution occurred before the advent of aerobic organisms. It does not necessarily represent the *shortest* pathway from acetate to CO_2, but it is the pathway that has, over time, conferred the greatest selective advantage. Early anaerobes most probably used some of the reactions of the citric acid cycle in linear biosynthetic processes. In fact, some modern anaerobic microorganisms use an incomplete citric acid cycle as a source of, not energy, but biosynthetic precursors **(Fig. 16–15)**. These organisms use the first three reactions of the cycle to make α-ketoglutarate but, lacking α-ketoglutarate dehydrogenase, they cannot carry out the complete set of citric acid cycle reactions. They do have the four enzymes that catalyze the reversible conversion of oxaloacetate to succinyl-CoA and can produce malate, fumarate, succinate, and succinyl-CoA from oxaloacetate in a reversal of the "normal" (oxidative) direction of flow through the cycle. This pathway is a fermentation, with the NADH produced by isocitrate oxidation recycled to NAD^+ by reduction of oxaloacetate to succinate.

With the evolution of cyanobacteria that produced O_2 from water, the earth's atmosphere became aerobic and organisms were under selective pressure to develop aerobic metabolism, which, as we have seen, is much more efficient than anaerobic fermentation.

Citric Acid Cycle Components Are Important Biosynthetic Intermediates

In aerobic organisms, the citric acid cycle is an **amphibolic pathway**, one that serves in both catabolic and anabolic processes. Besides its role in the oxidative catabolism of carbohydrates, fatty acids, and amino acids, the cycle provides precursors for many biosynthetic pathways **(Fig. 16–16)**, through reactions that served the same purpose in anaerobic ancestors. α-Ketoglutarate and oxaloacetate can, for example, serve as precursors of the amino acids aspartate and glutamate by simple transamination (Chapter 22). Through aspartate and glutamate, the carbons of oxaloacetate and α-ketoglutarate are then used to build other amino acids, as well as purine and pyrimidine nucleotides. Oxaloacetate is converted to glucose in gluconeogenesis (see Fig. 15–13). Succinyl-CoA is a central intermediate in the synthesis of the porphyrin ring of heme groups, which serve as oxygen carriers (in hemoglobin and myoglobin) and electron carriers (in cytochromes) (see Fig. 22–25). And the citrate produced in some organisms is used commercially for a variety of purposes.

Anaplerotic Reactions Replenish Citric Acid Cycle Intermediates

As intermediates of the citric acid cycle are removed to serve as biosynthetic precursors, they are replenished by **anaplerotic reactions** (Fig. 16–16; Table 16–2). Under normal circumstances, the reactions by which cycle intermediates are siphoned off into other pathways and those by which they are replenished are in dynamic balance, so that the concentrations of the citric acid cycle intermediates remain almost constant.

Table 16–2 shows the most common anaplerotic reactions, all of which, in various tissues and organisms, convert either pyruvate or phosphoenolpyruvate to oxaloacetate or malate. The most important anaplerotic reaction in mammalian liver and kidney is the reversible carboxylation of pyruvate by CO_2 to form oxaloacetate, catalyzed by **pyruvate carboxylase**. When the citric acid cycle is deficient in oxaloacetate or any other intermediates, pyruvate is carboxylated to produce more oxaloacetate. The enzymatic addition of a carboxyl group to pyruvate requires energy, which is supplied by ATP—the free energy required to attach a carboxyl group to pyruvate is about equal to the free energy available from ATP.

Pyruvate carboxylase is a regulatory enzyme and is virtually inactive in the absence of acetyl-CoA, its positive allosteric modulator. Whenever acetyl-CoA, the fuel for the citric acid cycle, is present in excess, it stimulates the pyruvate carboxylase reaction to produce more oxaloacetate, enabling the cycle to use more acetyl-CoA in the citrate synthase reaction.

The other anaplerotic reactions shown in Table 16–2 are also regulated to keep the level of intermediates

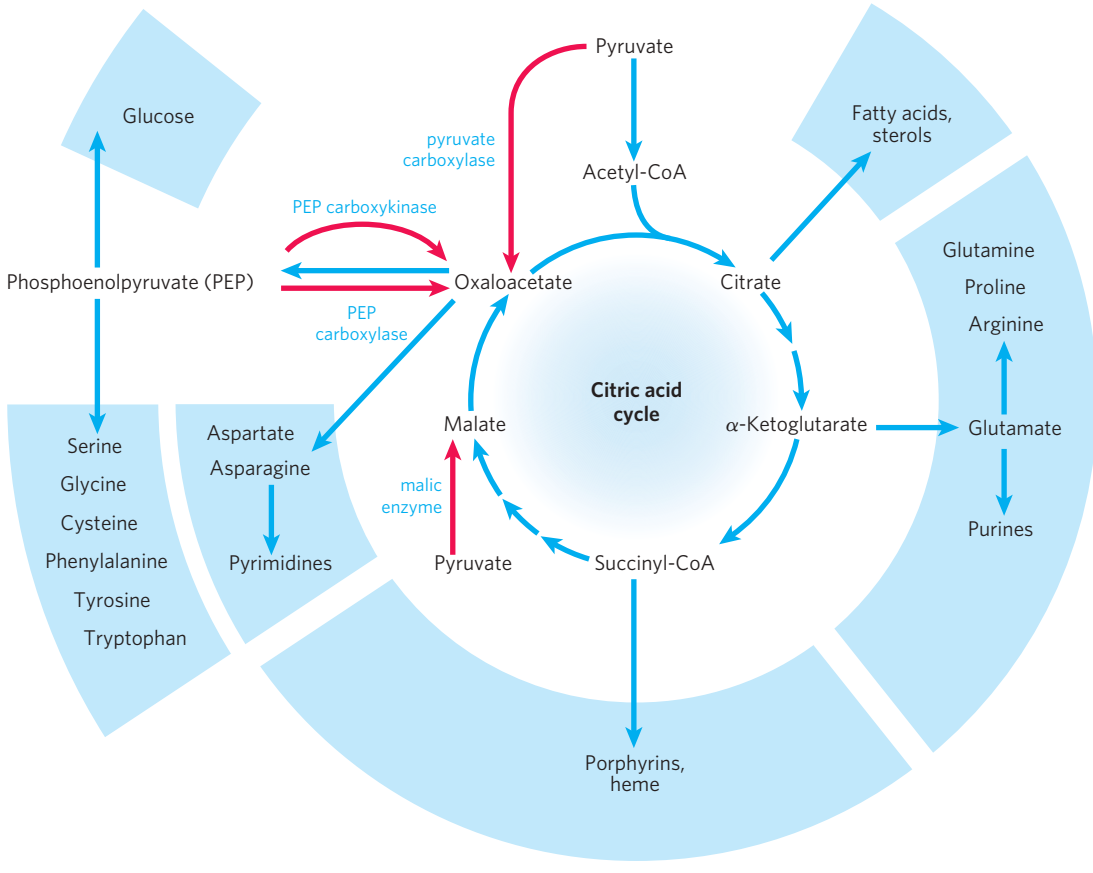

FIGURE 16–16 Role of the citric acid cycle in anabolism. Intermediates of the citric acid cycle are drawn off as precursors in many biosynthetic pathways. Shown in red are four anaplerotic reactions that replenish depleted cycle intermediates (see Table 16–2).

high enough to support the activity of the citric acid cycle. Phosphoenolpyruvate (PEP) carboxylase, for example, is activated by the glycolytic intermediate fructose 1,6-bisphosphate, which accumulates when the citric acid cycle operates too slowly to process the pyruvate generated by glycolysis.

Biotin in Pyruvate Carboxylase Carries CO_2 Groups

The pyruvate carboxylase reaction requires the vitamin **biotin** **(Fig. 16–17)**, which is the prosthetic group of the enzyme. Biotin plays a key role in many carboxylation reactions. It is a specialized carrier of one-carbon groups in their most oxidized form: CO_2. (The transfer of one-carbon groups in more reduced forms is mediated by other cofactors, notably tetrahydrofolate and *S*-adenosylmethionine, as described in Chapter 18.) Carboxyl groups are activated in a reaction that consumes ATP and joins CO_2 to enzyme-bound biotin. This "activated" CO_2 is then passed to an acceptor (pyruvate in this case) in a carboxylation reaction.

Pyruvate carboxylase has four identical subunits, each containing a molecule of biotin covalently attached through an amide linkage to the ε-amino

TABLE 16–2 Anaplerotic Reactions

Reaction	Tissue(s)/organism(s)
$\text{Pyruvate} + HCO_3^- + \text{ATP} \xrightleftharpoons{\text{pyruvate carboxylase}} \text{oxaloacetate} + \text{ADP} + P_i$	Liver, kidney
$\text{Phosphoenolpyruvate} + CO_2 + \text{GDP} \xrightleftharpoons{\text{PEP carboxykinase}} \text{oxaloacetate} + \text{GTP}$	Heart, skeletal muscle
$\text{Phosphoenolpyruvate} + HCO_3^- \xrightleftharpoons{\text{PEP carboxylase}} \text{oxaloacetate} + P_i$	Higher plants, yeast, bacteria
$\text{Pyruvate} + HCO_3^- + \text{NAD(P)H} \xrightleftharpoons{\text{malic enzyme}} \text{malate} + \text{NAD(P)}^+$	Widely distributed in eukaryotes and bacteria

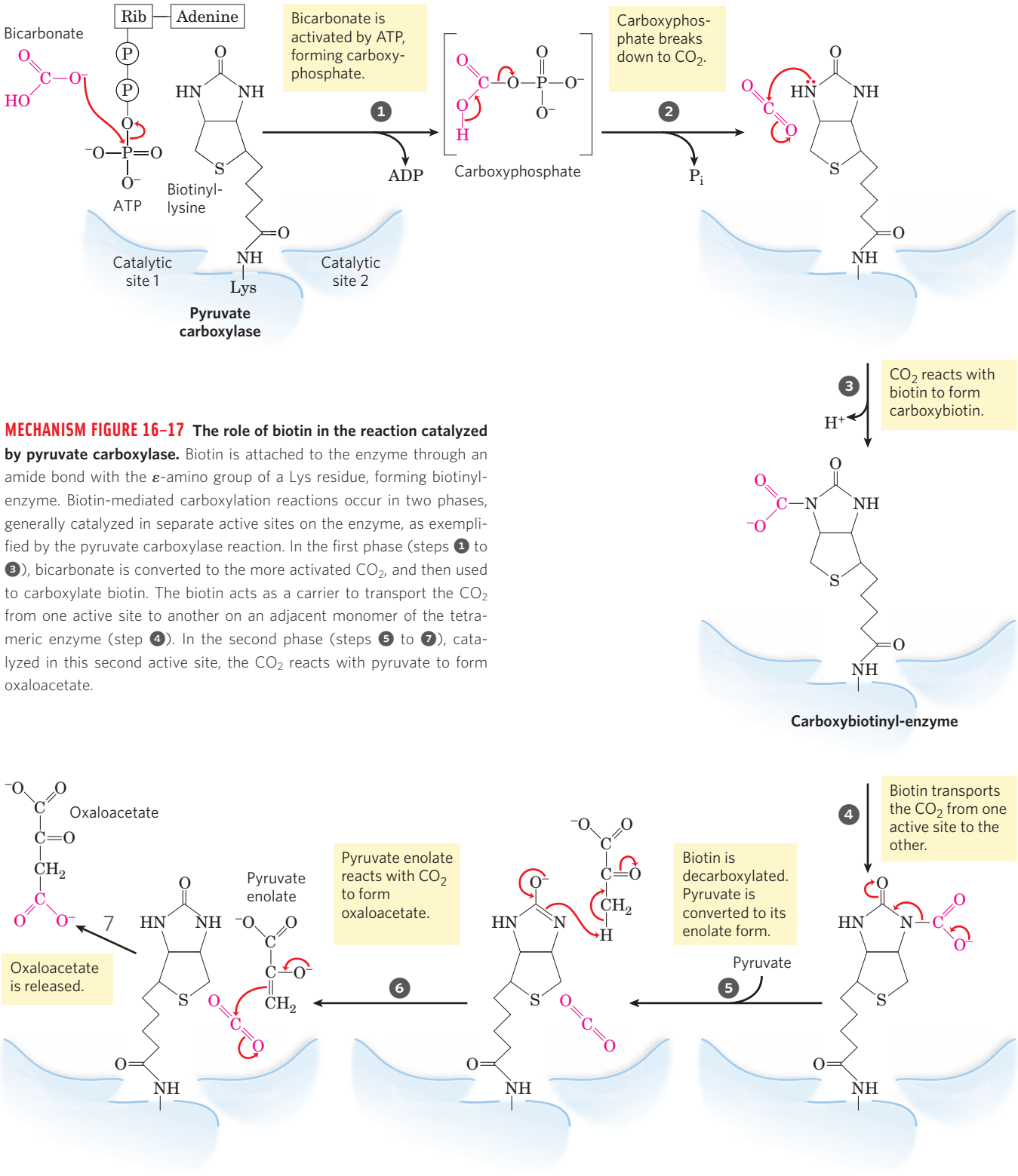

MECHANISM FIGURE 16–17 The role of biotin in the reaction catalyzed by pyruvate carboxylase. Biotin is attached to the enzyme through an amide bond with the ε-amino group of a Lys residue, forming biotinyl-enzyme. Biotin-mediated carboxylation reactions occur in two phases, generally catalyzed in separate active sites on the enzyme, as exemplified by the pyruvate carboxylase reaction. In the first phase (steps ❶ to ❸), bicarbonate is converted to the more activated CO_2, and then used to carboxylate biotin. The biotin acts as a carrier to transport the CO_2 from one active site to another on an adjacent monomer of the tetrameric enzyme (step ❹). In the second phase (steps ❺ to ❼), catalyzed in this second active site, the CO_2 reacts with pyruvate to form oxaloacetate.

group of a specific Lys residue in the enzyme active site. Carboxylation of pyruvate proceeds in two steps (Fig. 16–17): first, a carboxyl group derived from HCO_3^- is attached to biotin, then the carboxyl group is transferred to pyruvate to form oxaloacetate. These two steps occur at separate active sites; the long flexible arm of biotin transfers activated carboxyl groups from the first active site (on one monomer of the tetramer) to the second (on the adjacent monomer), functioning much like the long lipoyllysyl arm of E_2 in the PDH complex (Fig. 16–6) and the long arm of the CoA-like moiety in the acyl carrier protein involved in

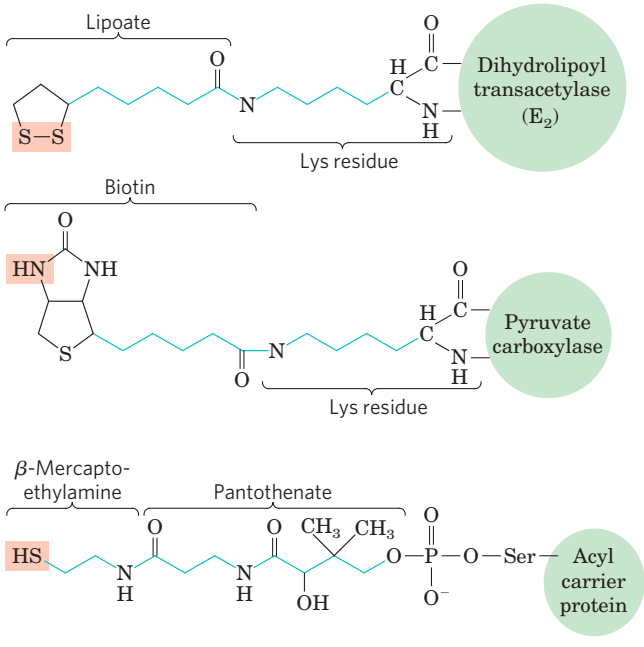

FIGURE 16–18 Biological tethers. The cofactors lipoate, biotin, and the combination of β-mercaptoethylamine and pantothenate form long, flexible arms (blue) on the enzymes to which they are covalently bound, acting as tethers that move intermediates from one active site to the next. The group shaded light red is in each case the point of attachment of the activated intermediate to the tether.

fatty acid synthesis (see Fig. 21–5); these are compared in **Figure 16–18**. Lipoate, biotin, and pantothenate all enter cells on the same transporter; all become covalently attached to proteins by similar reactions; and all provide a flexible tether that allows bound reaction intermediates to move from one active site to another in an enzyme complex, without dissociating from it—all, that is, participate in substrate channeling.

Biotin is a vitamin required in the human diet; it is abundant in many foods and is synthesized by intestinal bacteria. Biotin deficiency is rare, but can sometimes be caused by a diet rich in raw eggs. Egg whites contain a large amount of the protein **avidin** (M_r 70,000), which binds very tightly to biotin and prevents its absorption in the intestine. The avidin of egg whites may be a defense mechanism for the potential chick embryo, inhibiting the growth of bacteria. When eggs are cooked, avidin is denatured (and thereby inactivated) along with all other egg white proteins. Purified avidin is a useful reagent in biochemistry and cell biology. A protein that contains covalently bound biotin (derived experimentally or produced in vivo) can be recovered by affinity chromatography (see Fig. 3–17c) based on biotin's strong affinity for avidin. The protein is then eluted from the column with an excess of free biotin. The very high affinity of biotin for avidin is also used in the laboratory in the form of a molecular glue that can hold two structures together (see Fig. 19–27).

SUMMARY 16.2 Reactions of the Citric Acid Cycle

- The citric acid cycle (Krebs cycle, TCA cycle) is a nearly universal central catabolic pathway in which compounds derived from the breakdown of carbohydrates, fats, and proteins are oxidized to CO_2, with most of the energy of oxidation temporarily held in the electron carriers $FADH_2$ and NADH. During aerobic metabolism, these electrons are transferred to O_2 and the energy of electron flow is trapped as ATP.
- Acetyl-CoA enters the citric acid cycle (in the mitochondria of eukaryotes, the cytosol of bacteria) as citrate synthase catalyzes its condensation with oxaloacetate to form citrate.
- In seven sequential reactions, including two decarboxylations, the citric acid cycle converts citrate to oxaloacetate and releases two CO_2. The pathway is cyclic in that the intermediates of the cycle are not used up; for each oxaloacetate consumed in the path, one is produced.
- For each acetyl-CoA oxidized by the citric acid cycle, the energy gain consists of three molecules of NADH, one $FADH_2$, and one nucleoside triphosphate (either ATP or GTP).
- Besides acetyl-CoA, any compound that gives rise to a four- or five-carbon intermediate of the citric acid cycle—for example, the breakdown products of many amino acids—can be oxidized by the cycle.
- The citric acid cycle is amphibolic, serving in both catabolism and anabolism; cycle intermediates can be drawn off and used as the starting material for a variety of biosynthetic products.
- When intermediates are shunted from the citric acid cycle to other pathways, they are replenished by several anaplerotic reactions, which produce four-carbon intermediates by carboxylation of three-carbon compounds; these reactions are catalyzed by pyruvate carboxylase, PEP carboxykinase, PEP carboxylase, and malic enzyme. Enzymes that catalyze carboxylations commonly employ biotin to activate CO_2 and to carry it to acceptors such as pyruvate or phosphoenolpyruvate.

16.3 Regulation of the Citric Acid Cycle

As we have seen in Chapter 15, the regulation of key enzymes in metabolic pathways, by allosteric effectors and by covalent modification, ensures the production of intermediates at the rates required to keep the cell in a stable steady state while avoiding wasteful overproduction. The flow of carbon atoms from pyruvate into and through the citric acid cycle is under tight regulation at two levels: the conversion of pyruvate to acetyl-CoA, the starting material for the cycle (the

pyruvate dehydrogenase complex reaction), and the entry of acetyl-CoA into the cycle (the citrate synthase reaction). Acetyl-CoA is also produced by pathways other than the PDH complex reaction—most cells produce acetyl-CoA from the oxidation of fatty acids and certain amino acids—and the availability of intermediates from these other pathways is important in the regulation of pyruvate oxidation and of the citric acid cycle. The cycle is also regulated at the isocitrate dehydrogenase and α-ketoglutarate dehydrogenase reactions.

Production of Acetyl-CoA by the Pyruvate Dehydrogenase Complex Is Regulated by Allosteric and Covalent Mechanisms

The PDH complex of mammals is strongly inhibited by ATP and by acetyl-CoA and NADH, the products of the reaction catalyzed by the complex **(Fig. 16–19)**. The allosteric inhibition of pyruvate oxidation is greatly enhanced when long-chain fatty acids are available. AMP, CoA, and NAD^+, all of which accumulate when too little acetate flows into the citric acid cycle, allosterically activate the PDH complex. Thus, this enzyme activity is turned off when ample fuel is available in the form of fatty acids and acetyl-CoA and when the cell's [ATP]/[ADP] and [NADH]/[NAD^+] ratios are high, and it is turned on again when energy demands are high and the cell requires greater flux of acetyl-CoA into the citric acid cycle.

In mammals, these allosteric regulatory mechanisms are complemented by a second level of regulation: covalent protein modification. The PDH complex is inhibited by reversible phosphorylation of a specific Ser residue on one of the two subunits of E_1. As noted earlier, in addition to the enzymes E_1, E_2, and E_3, the mammalian PDH complex contains two regulatory proteins whose sole purpose is to regulate the activity of the complex. Pyruvate dehydrogenase kinase phosphorylates and thereby inactivates E_1, and a specific phosphoprotein phosphatase removes the phosphoryl group by hydrolysis and thereby activates E_1. The kinase is allosterically activated by ATP: when [ATP] is high (reflecting a sufficient supply of energy), the PDH complex is inactivated by phosphorylation of E_1. When [ATP] declines, kinase activity decreases and phosphatase action removes the phosphoryl groups from E_1, activating the complex.

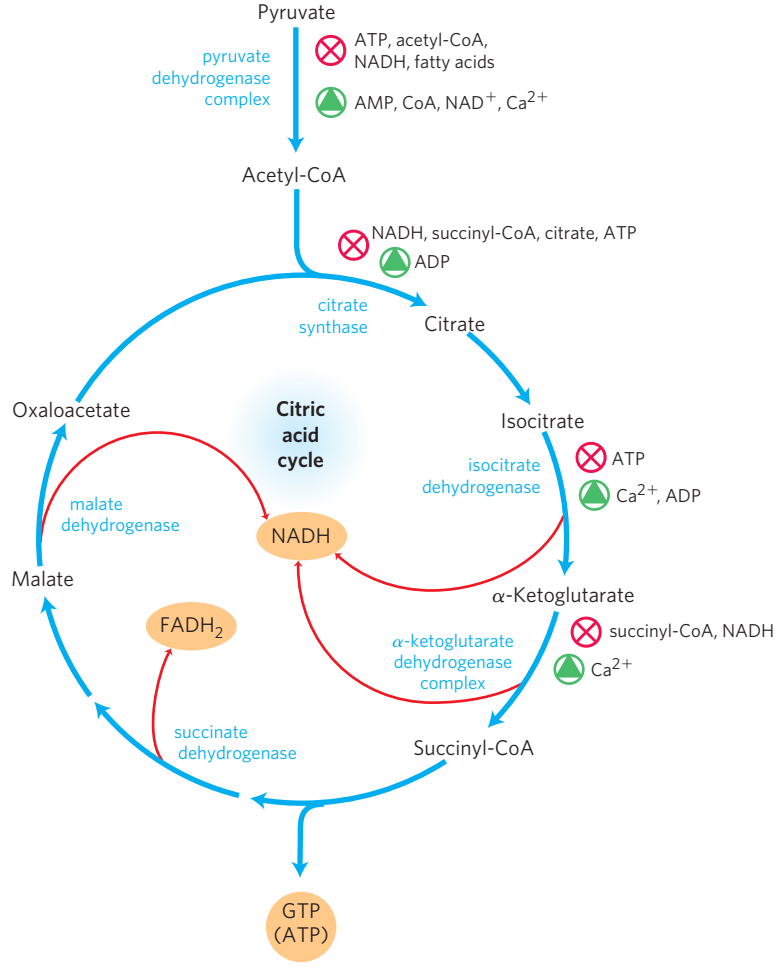

FIGURE 16–19 Regulation of metabolite flow from the PDH complex through the citric acid cycle in mammals. The PDH complex is allosterically inhibited when [ATP]/[ADP], [NADH]/[NAD^+], and [acetyl-CoA]/[CoA] ratios are high, indicating an energy-sufficient metabolic state. When these ratios decrease, allosteric activation of pyruvate oxidation results. The rate of flow through the citric acid cycle can be limited by the availability of the citrate synthase substrates, oxaloacetate and acetyl-CoA, or of NAD^+, which is depleted by its conversion to NADH, slowing the three NAD-dependent oxidation steps. Feedback inhibition by succinyl-CoA, citrate, and ATP also slows the cycle by inhibiting early steps. In muscle tissue, Ca^{2+} signals contraction and, as shown here, stimulates energy-yielding metabolism to replace the ATP consumed by contraction.

The PDH complex of plants, located in the mitochondrial matrix and in plastids, is inhibited by its products, NADH and acetyl-CoA. The plant mitochondrial enzyme is also regulated by reversible phosphorylation; pyruvate inhibits the kinase, thus activating the PDH complex, and NH_4^+ stimulates the kinase, causing inactivation of the complex. The PDH complex of *E. coli* is under allosteric regulation similar to that of the mammalian enzyme, but it does not seem to be regulated by phosphorylation.

The Citric Acid Cycle Is Regulated at Its Three Exergonic Steps

The flow of metabolites through the citric acid cycle is under stringent regulation. Three factors govern the rate of flux through the cycle: substrate availability, inhibition by accumulating products, and allosteric feedback inhibition of the enzymes that catalyze early steps in the cycle.

Each of the three strongly exergonic steps in the cycle—those catalyzed by citrate synthase, isocitrate dehydrogenase, and α-ketoglutarate dehydrogenase (Fig. 16–19)—can become the rate-limiting step under some circumstances. The availability of the substrates for citrate synthase (acetyl-CoA and oxaloacetate) varies with the metabolic state of the cell and sometimes limits the rate of citrate formation. NADH, a product of isocitrate and α-ketoglutarate oxidation, accumulates under some conditions, and at high [NADH]/[NAD^+] both dehydrogenase reactions are severely inhibited by mass action. Similarly, in the cell, the malate dehydrogenase reaction is essentially at equilibrium (that is, it is substrate-limited), and when [NADH]/[NAD^+] is high the concentration of oxaloacetate is low, slowing the first step in the cycle. Product accumulation inhibits all three limiting steps of the cycle: succinyl-CoA inhibits α-ketoglutarate dehydrogenase (and also citrate synthase); citrate blocks citrate synthase; and the end product, ATP, inhibits both citrate synthase and isocitrate dehydrogenase. The inhibition of citrate synthase by ATP is relieved by ADP, an allosteric activator of this enzyme. In vertebrate muscle, Ca^{2+}, the signal for contraction and for a concomitant increase in demand for ATP, activates both isocitrate dehydrogenase and α-ketoglutarate dehydrogenase, as well as the PDH complex. In short, the concentrations of substrates and intermediates in the citric acid cycle set the flux through this pathway at a rate that provides optimal concentrations of ATP and NADH.

Under normal conditions, the rates of glycolysis and of the citric acid cycle are integrated so that only as much glucose is metabolized to pyruvate as is needed to supply the citric acid cycle with its fuel, the acetyl groups of acetyl-CoA. Pyruvate, lactate, and acetyl-CoA are normally maintained at steady-state concentrations. The rate of glycolysis is matched to the rate of the citric acid cycle not only through its inhibition by high levels of ATP and NADH, which are common to both the glycolytic and respiratory stages of glucose oxidation, but also by the concentration of citrate. Citrate, the product of the first step of the citric acid cycle, is an important allosteric inhibitor of phosphofructokinase-1 in the glycolytic pathway (see Fig. 15–16).

Substrate Channeling through Multienzyme Complexes May Occur in the Citric Acid Cycle

Although the enzymes of the citric acid cycle are usually described as soluble components of the mitochondrial matrix (except for succinate dehydrogenase, which is membrane-bound), growing evidence suggests that within the mitochondrion these enzymes exist as multienzyme complexes. The classic approach of enzymology—purification of individual proteins from extracts of broken cells—was applied with great success to the citric acid cycle enzymes. However, the first casualty of cell breakage is higher-level organization within the cell—the noncovalent, reversible interaction of one protein with another, or of an enzyme with some structural component such as a membrane, microtubule, or microfilament. When cells are broken open, their contents, including enzymes, are diluted 100- or 1,000-fold **(Fig. 16–20)**.

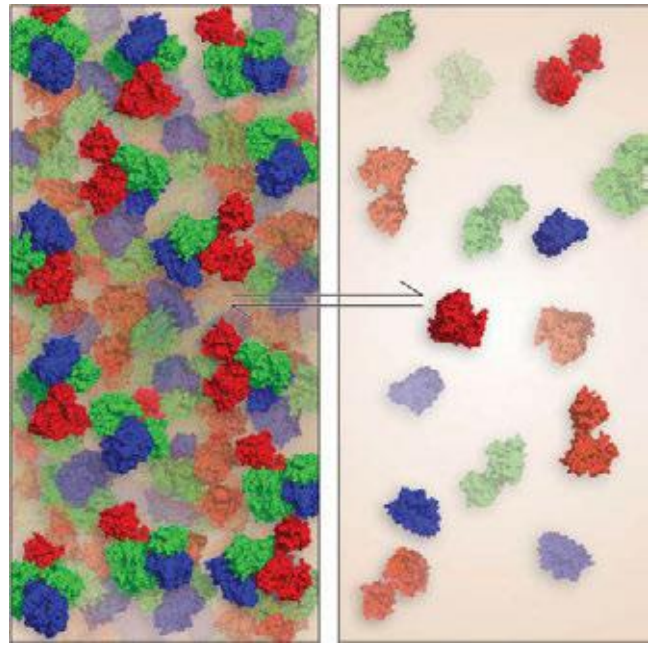

In the cytosol, high concentrations of enzymes 1, 2, and 3 favor their association.

In extract of broken cells, dilution by buffer reduces the concentrations of enzymes 1, 2, and 3, favoring their dissociation.

FIGURE 16–20 Dilution of a solution containing a noncovalently bound protein complex—such as one consisting of three enzymes (illustrated here in red, blue, and green)—favors dissociation of the complex into its constituents.

Several types of evidence suggest that, in cells, multienzyme complexes ensure efficient passage of the product of one enzyme reaction to the next enzyme in the pathway. Such complexes are called **metabolons**. Certain enzymes of the citric acid cycle have been isolated together as supramolecular complexes, or have been found associated with the inner mitochondrial membrane, or have been shown to diffuse in the mitochondrial matrix more slowly than expected for the individual protein in solution. There is strong evidence for substrate channeling through multienzyme complexes in other metabolic pathways, and many enzymes thought of as "soluble" probably function in the cell as highly organized complexes that channel intermediates. We will encounter other examples of channeling when we discuss the biosynthesis of amino acids and nucleotides in Chapter 22.

Some Mutations in Enzymes of the Citric Acid Cycle Lead to Cancer

When the mechanisms for regulating a pathway such as the citric acid cycle are overwhelmed by a major metabolic perturbation, the result can be serious disease. Mutations in citric acid cycle enzymes are very rare in humans and other mammals, but those that do occur are devastating. Genetic defects in the fumarase gene lead to tumors of smooth muscle (leiomas) and kidney; mutations in succinate dehydrogenase lead to tumors of the adrenal gland (pheochromocytomas). In cultured cells with these mutations, fumarate (in the case of fumarase mutations) and, to a lesser extent, succinate (in the case of succinate dehydrogenase mutations) accumulate, and this accumulation induces the hypoxia-inducible transcription factor HIF-1α (see Box 14–1). The mechanism of tumor formation may be the production of a pseudohypoxic state. In cells with these mutations, there is an up-regulation of genes normally regulated by HIF-1α. These effects of mutations in the fumarase and succinate dehydrogenase genes define them as tumor suppressor genes (p. 489).

Another remarkable connection between citric acid cycle intermediates and cancer is the finding that in many glial cell tumors (gliomas), the NADPH-dependent isocitrate dehydrogenase has an unusual genetic defect. The mutant enzyme loses its normal activity (converting isocitrate to α-ketoglutarate) but *gains* a new activity: it converts α-ketoglutarate to 2-hydroxyglutarate **(Fig. 16–21)**, which accumulates in the tumor cells. α-Ketoglutarate and Fe^{3+} are essential cofactors for a family of histone demethylases that alter gene expression by removing methyl groups from Arg and Lys residues in the histones that organize nuclear DNA. By competing with α-ketoglutarate for binding to the histone demethylases, 2-hydroxyglutarate inhibits their activity. The inhibition of the histone demethylases in turn interferes with normal gene regulation, leading to unrestricted glial cell growth. ■

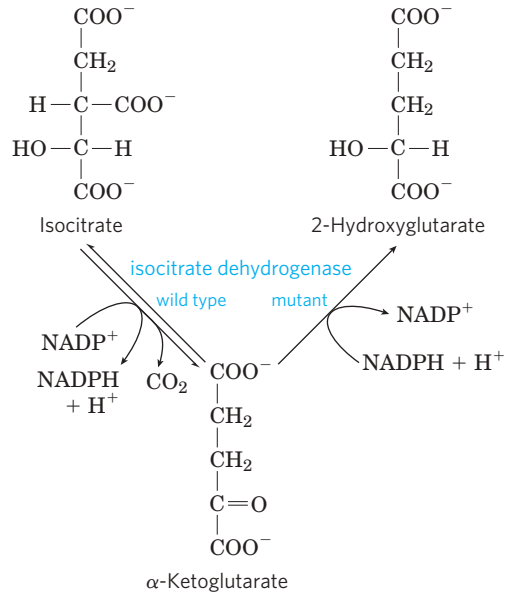

FIGURE 16-21 A mutant isocitrate dehydrogenase acquires a new activity. Wild-type isocitrate dehydrogenase catalyzes the conversion of isocitrate to α-ketoglutarate, but mutations that alter the binding site for isocitrate cause loss of the normal enzymatic activity and gain of a new activity: conversion of α-ketoglutarate to 2-hydroxyglutarate. Accumulation of this product inhibits histone demethylase, altering gene regulation and leading to glial cell tumors in the brain.

SUMMARY 16.3 Regulation of the Citric Acid Cycle

- The overall rate of the citric acid cycle is controlled by the rate of conversion of pyruvate to acetyl-CoA and by the flux through citrate synthase, isocitrate dehydrogenase, and α-ketoglutarate dehydrogenase. These fluxes are largely determined by the concentrations of substrates and products: the end products ATP and NADH are inhibitory, and the substrates NAD^+ and ADP are stimulatory.
- The production of acetyl-CoA for the citric acid cycle by the PDH complex is inhibited allosterically by metabolites that signal a sufficiency of metabolic energy (ATP, acetyl-CoA, NADH, and fatty acids) and stimulated by metabolites that indicate a reduced energy supply (AMP, NAD^+, CoA).
- Complexes of consecutive enzymes in a pathway allow substrate channeling between them.

16.4 The Glyoxylate Cycle

Vertebrates cannot convert fatty acids, or the acetate derived from them, to carbohydrates. Conversion of phosphoenolpyruvate to pyruvate (p. 554) and of pyruvate to acetyl-CoA (Fig. 16–2) are so exergonic as to be essentially irreversible. If a cell cannot convert

acetate into phosphoenolpyruvate, acetate cannot serve as the starting material for the gluconeogenic pathway, which leads from phosphoenolpyruvate to glucose (see Fig. 15–13). Without this capacity, then, a cell or organism is unable to convert fuels or metabolites that are degraded to acetate (fatty acids and certain amino acids) into carbohydrates.

As noted in the discussion of anaplerotic reactions (Table 16–2), phosphoenolpyruvate can be synthesized from oxaloacetate in the reversible reaction catalyzed by PEP carboxykinase:

$$\text{Oxaloacetate} + \text{GTP} \rightleftharpoons \text{phosphoenolpyruvate} + CO_2 + \text{GDP}$$

Because the carbon atoms of acetate molecules that enter the citric acid cycle appear eight steps later in oxaloacetate, it might seem that this pathway could generate oxaloacetate from acetate and thus generate phosphoenolpyruvate for gluconeogenesis. However, as an examination of the stoichiometry of the citric acid cycle shows, there is no *net* conversion of acetate to oxaloacetate; in vertebrates, for every two carbons that enter the cycle as acetyl-CoA, two leave as CO_2. In many organisms other than vertebrates, the glyoxylate cycle serves as a mechanism for converting acetate to carbohydrate.

The Glyoxylate Cycle Produces Four-Carbon Compounds from Acetate

In plants, certain invertebrates, and some microorganisms (including *E. coli* and yeast) acetate can serve both as an energy-rich fuel and as a source of phosphoenolpyruvate for carbohydrate synthesis. In these organisms, enzymes of the **glyoxylate cycle** catalyze the net conversion of acetate to succinate or other four-carbon intermediates of the citric acid cycle:

$$2\ \text{Acetyl-CoA} + \text{NAD}^+ + 2H_2O \longrightarrow \text{succinate} + 2\text{CoA} + \text{NADH} + H^+$$

In the glyoxylate cycle, acetyl-CoA condenses with oxaloacetate to form citrate, and citrate is converted to isocitrate, exactly as in the citric acid cycle. The next step, however, is not the breakdown of isocitrate by isocitrate dehydrogenase but the cleavage of isocitrate by **isocitrate lyase**, forming succinate and **glyoxylate**. The glyoxylate then condenses with a second molecule of acetyl-CoA to yield malate, in a reaction catalyzed by **malate synthase**. The malate is subsequently oxidized to oxaloacetate, which can condense with another molecule of acetyl-CoA to start another turn of the cycle **(Fig. 16–22)**. Each turn of the glyoxylate cycle consumes two molecules of acetyl-CoA and produces one molecule of succinate, which is then available for biosynthetic purposes. The succinate may be converted through fumarate and malate into oxaloacetate, which can then be converted to phosphoenolpyruvate by PEP carboxykinase, and thus to glucose by gluconeogenesis. Vertebrates do not have the enzymes specific to the glyoxylate cycle (isocitrate lyase and malate synthase) and therefore cannot bring about the net synthesis of glucose from lipids.

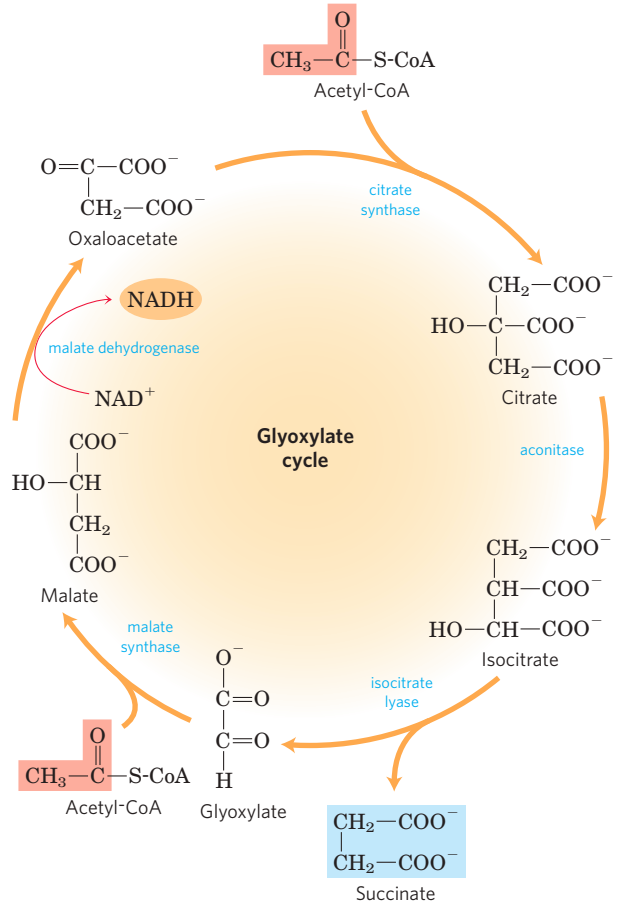

FIGURE 16–22 Glyoxylate cycle. The citrate synthase, aconitase, and malate dehydrogenase of the glyoxylate cycle are isozymes of the citric acid cycle enzymes; isocitrate lyase and malate synthase are unique to the glyoxylate cycle. Notice that two acetyl groups (light red) enter the cycle and four carbons leave as succinate (blue). The glyoxylate cycle was elucidated by Hans Kornberg and Neil Madsen in the laboratory of Hans Krebs.

In plants, the enzymes of the glyoxylate cycle are sequestered in membrane-bounded organelles called glyoxysomes, which are specialized peroxisomes **(Fig. 16–23)**. Those enzymes common to the citric acid and glyoxylate cycles have two isozymes, one specific to mitochondria, the other to glyoxysomes. Glyoxysomes are not present in all plant tissues at all times. They develop in lipid-rich seeds during germination, before the developing plant acquires the ability to make glucose by photosynthesis. In addition to glyoxylate cycle enzymes, glyoxysomes contain all the enzymes needed for the degradation of the fatty acids stored in seed oils (see Fig. 17–14). Acetyl-CoA formed from lipid breakdown is converted to succinate via the glyoxylate cycle, and the succinate is exported to mitochondria, where citric acid cycle enzymes transform it to malate. A cytosolic isozyme

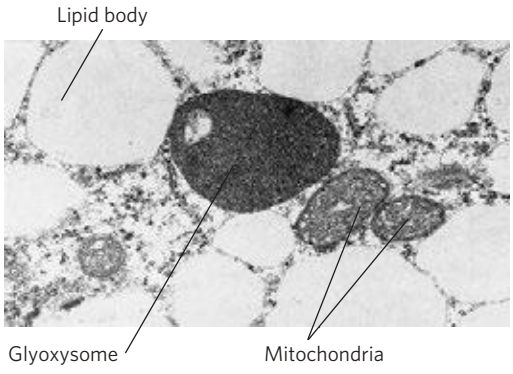

FIGURE 16–23 Electron micrograph of a germinating cucumber seed, showing a glyoxysome, mitochondria, and surrounding lipid bodies.

of malate dehydrogenase oxidizes malate to oxaloacetate, a precursor for gluconeogenesis. Germinating seeds can therefore convert the carbon of stored lipids into glucose.

The Citric Acid and Glyoxylate Cycles Are Coordinately Regulated

In germinating seeds, the enzymatic transformations of dicarboxylic and tricarboxylic acids occur in three intracellular compartments: mitochondria, glyoxysomes, and the cytosol. There is a continuous interchange of metabolites among these compartments **(Fig. 16–24)**.

The carbon skeleton of oxaloacetate from the citric acid cycle (in the mitochondrion) is carried to the glyoxysome in the form of aspartate. Aspartate is converted to oxaloacetate, which condenses with acetyl-CoA derived from fatty acid breakdown. The citrate thus formed is converted to isocitrate by aconitase, then split into glyoxylate and succinate by isocitrate lyase. The succinate returns to the mitochondrion, where it reenters the citric acid cycle and is transformed into malate, which enters the cytosol and is oxidized (by cytosolic malate dehydrogenase) to oxaloacetate. Oxaloacetate is converted via gluconeogenesis into hexoses and sucrose, which can be transported to the growing roots and shoot. Four distinct pathways participate in these conversions: fatty acid breakdown to acetyl-CoA (in glyoxysomes), the glyoxylate cycle (in glyoxysomes), the citric acid cycle (in mitochondria), and gluconeogenesis (in the cytosol).

The sharing of common intermediates requires that these pathways be coordinately regulated. Isocitrate is a crucial intermediate, at the branch point between the glyoxylate and citric acid cycles **(Fig. 16–25)**. Isocitrate dehydrogenase is regulated by covalent modification: a specific protein kinase phosphorylates and thereby inactivates the dehydrogenase. This inactivation shunts isocitrate to the glyoxylate cycle, where it begins the synthetic route toward glucose. A phosphoprotein phosphatase removes the phosphoryl group from isocitrate dehydrogenase, reactivating the enzyme and sending more isocitrate through the energy-yielding

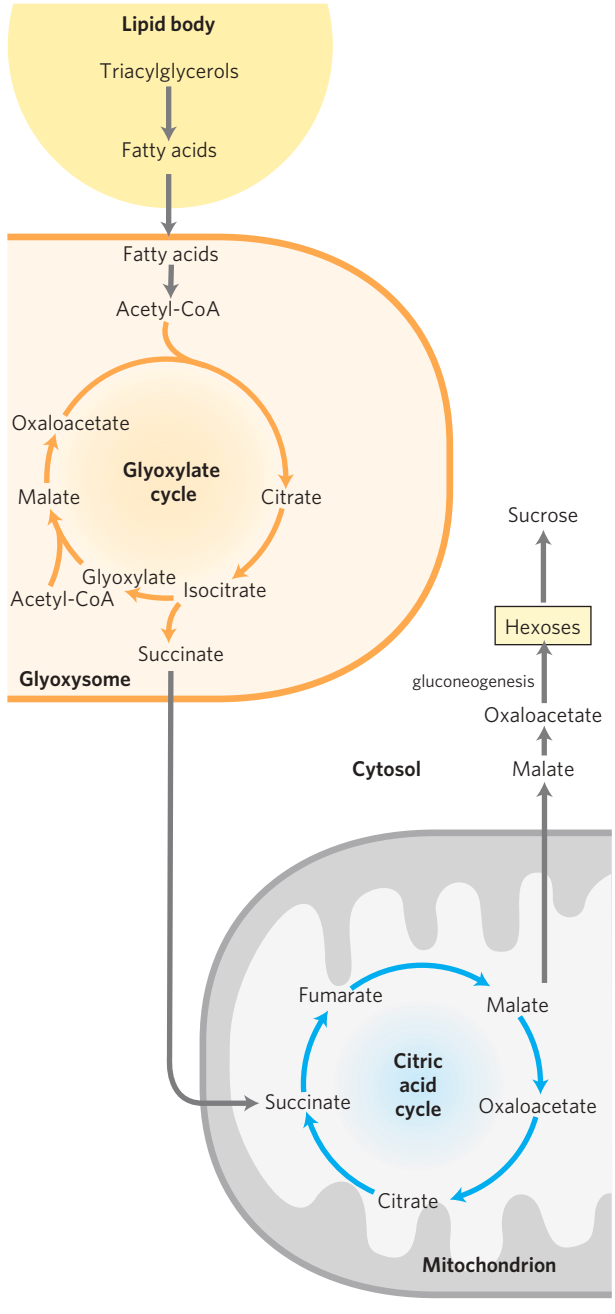

FIGURE 16–24 Relationship between the glyoxylate and citric acid cycles. The reactions of the glyoxylate cycle (in glyoxysomes) proceed simultaneously with, and mesh with, those of the citric acid cycle (in mitochondria), as intermediates pass between these compartments. The conversion of succinate to oxaloacetate is catalyzed by citric acid cycle enzymes. The oxidation of fatty acids to acetyl-CoA is described in Chapter 17; the synthesis of hexoses from oxaloacetate is described in Chapter 20.

citric acid cycle. The regulatory protein kinase and phosphoprotein phosphatase are separate enzymatic activities of a single polypeptide.

Some bacteria, including *E. coli*, have the full complement of enzymes for the glyoxylate and citric acid cycles in the cytosol and can therefore grow on acetate as their sole source of carbon and energy. The phosphoprotein phosphatase that activates isocitrate dehydrogenase

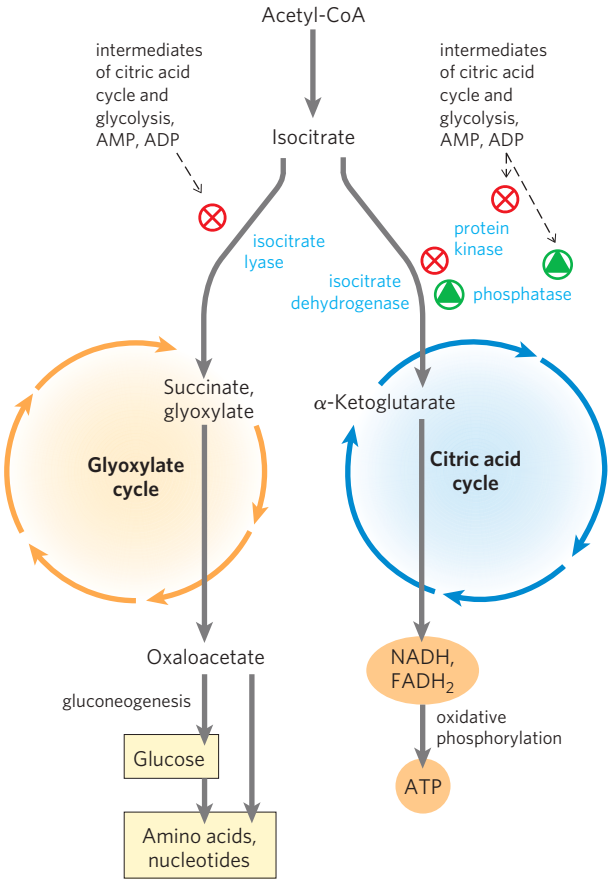

FIGURE 16–25 Coordinated regulation of glyoxylate and citric acid cycles. Regulation of isocitrate dehydrogenase activity determines the partitioning of isocitrate between the glyoxylate and citric acid cycles. When the enzyme is inactivated by phosphorylation (by a specific protein kinase), isocitrate is directed into biosynthetic reactions via the glyoxylate cycle. When the enzyme is activated by dephosphorylation (by a specific phosphatase), isocitrate enters the citric acid cycle and ATP is produced.

is stimulated by intermediates of the citric acid cycle and glycolysis and by indicators of reduced cellular energy supply (Fig. 16–25). The same metabolites *inhibit* the protein kinase activity of the bifunctional polypeptide. Thus, the accumulation of intermediates of the central energy-yielding pathways—indicating energy depletion—results in the activation of isocitrate dehydrogenase. When the concentration of these regulators falls, signaling a sufficient flux through the energy-yielding citric acid cycle, isocitrate dehydrogenase is inactivated by the protein kinase.

The same intermediates of glycolysis and the citric acid cycle that activate isocitrate dehydrogenase are allosteric inhibitors of isocitrate lyase. When energy-yielding metabolism is sufficiently fast to keep the concentrations of glycolytic and citric acid cycle intermediates low, isocitrate dehydrogenase is inactivated, the inhibition of isocitrate lyase is relieved, and isocitrate flows into the glyoxylate pathway, to be used in the biosynthesis of carbohydrates, amino acids, and other cellular components.

SUMMARY 16.4 The Glyoxylate Cycle

- The glyoxylate cycle is active in the germinating seeds of some plants and in certain microorganisms that can live on acetate as the sole carbon source. In plants, the pathway takes place in glyoxysomes in seedlings. It involves several citric acid cycle enzymes and two additional enzymes: isocitrate lyase and malate synthase.
- In the glyoxylate cycle, the bypassing of the two decarboxylation steps of the citric acid cycle makes possible the *net* formation of succinate, oxaloacetate, and other cycle intermediates from acetyl-CoA. Oxaloacetate thus formed can be used to synthesize glucose via gluconeogenesis.
- Vertebrates lack the glyoxylate cycle and cannot synthesize glucose from acetate or the fatty acids that give rise to acetyl-CoA.
- The partitioning of isocitrate between the citric acid cycle and the glyoxylate cycle is controlled at the level of isocitrate dehydrogenase, which is regulated by reversible phosphorylation.

Key Terms

Terms in bold are defined in the glossary.

respiration 633
cellular respiration 633
citric acid cycle 633
tricarboxylic acid (TCA) cycle 633
Krebs cycle 633
pyruvate dehydrogenase (PDH) complex 634
oxidative decarboxylation 634
thioester 635
lipoate 635
substrate channeling 637
iron-sulfur center 641
moonlighting enzymes 642
α-ketoglutarate dehydrogenase complex 644
nucleoside diphosphate kinase 645
synthases 646
synthetases 646
ligases 646
lyases 646
kinases 646
phosphorylases 646
phosphatases 646
prochiral molecule 648
amphibolic pathway 650
anaplerotic reaction 650
biotin 651
avidin 653
metabolon 656
glyoxylate cycle 657

Further Reading

General

Holmes, F.L. (1990, 1993) *Hans Krebs*, Vol 1: *Formation of a Scientific Life, 1900–1933*; Vol. 2: *Architect of Intermediary Metabolism, 1933–1937*, Oxford University Press, Oxford.

A scientific and personal biography of Krebs by an eminent historian of science, with a thorough description of the work that revealed the urea and citric acid cycles.

Kay, J. & Weitzman, P.D.J. (eds). (1987) *Krebs' Citric Acid Cycle: Half a Century and Still Turning*, Biochemical Society Symposium **54**, The Biochemical Society, London.

A multiauthor book on the citric acid cycle, including molecular genetics, regulatory mechanisms, variations on the cycle in microorganisms from unusual ecological niches, and evolution of the pathway. Especially relevant are the chapters by H. Gest (Evolutionary Roots of the Citric Acid Cycle in Prokaryotes), W. H. Holms (Control of Flux through the Citric Acid Cycle and the Glyoxylate Bypass in *Escherichia coli*), and R. N. Perham et al. (α-Keto Acid Dehydrogenase Complexes).

Pyruvate Dehydrogenase Complex

Harris, R.A., Bowker-Kinley, M.M., Huang, B., & Wu, P. (2002) Regulation of the activity of the pyruvate dehydrogenase complex. *Adv. Enzyme Regul.* **42**, 249–259.

Milne, J.L.S., Shi, D., Rosenthal, P.B., Sunshine, J.S., Domingo, G.J., Wu, X., Brooks, B.R., Perham, R.N., Henderson, R., & Subramaniam, S. (2002) Molecular architecture and mechanism of an icosahedral pyruvate dehydrogenase complex: a multifunctional catalytic machine. *EMBO J.* **21**, 5587–5598.

Beautiful illustration of the power of image reconstruction methodology with cryoelectron microscopy, here used to develop a plausible model for the structure of the PDH complex. Compare this model with that in the paper by Zhou et al. (below).

Perham, R.N. (2000) Swinging arms and swinging domains in multifunctional enzymes: catalytic machines for multistep reactions. *Annu. Rev. Biochem.* **69**, 961–1004.

Review of the roles of swinging arms containing lipoate, biotin, and pantothenate in substrate channeling through multienzyme complexes.

Zhou, Z.H., McCarthy, D.B., O'Conner, C.M., Reed, L.J., & Stoops, J.K. (2001) The remarkable structural and functional organization of the eukaryotic pyruvate dehydrogenase complexes. *Proc. Natl. Acad. Sci. USA* **98**, 14,802–14,807.

Another striking paper in which image reconstruction with cryoelectron microscopy yields a model of the PDH complex. Compare this model with that in the paper by Milne et al. (above).

Citric Acid Cycle Enzymes

de la Fuente, J.M., Ramírez-Rodríguez, V., Cabrera-Ponce, J.L., & Herrera-Estrella, L. (1997) Aluminum tolerance in transgenic plants by alteration of citrate synthesis. *Science* **276**, 1566–1568.

Fraser, M.D., James, M.N., Bridger, W.A., & Wolodko, W.T. (1999) A detailed structural description of *Escherichia coli* succinyl-CoA synthetase. *J. Mol. Biol.* **285**, 1633–1653. (See also the erratum in *J. Mol. Biol.* **288**, 501 (1998).)

Goward, C.R. & Nicholls, D.J. (1994) Malate dehydrogenase: a model for structure, evolution, and catalysis. *Protein Sci.* **3**, 1883–1888.

A good, short review.

Hagerhall, C. (1997) Succinate:quinone oxidoreductases: variations on a conserved theme. *Biochim. Biophys. Acta* **1320**, 107–141.

A review of the structure and function of succinate dehydrogenases.

Hanson, R.W. (2009) Thematic minireview series: a perspective on the biology of phosphoenolpyruvate carboxykinase 55 years after its discovery. *J. Biol. Chem.* **284**, 27,021–27,023.

The editorial introduction to a series of minireviews in this journal issue on PEP carboxykinase.

Jitrapakdee, S., St. Maurice, M., Rayment, I., Cleland, W.W., Wallace, J.C., & Attwood, P.V. (2008) Structure, mechanism and regulation of pyruvate carboxylase. *Biochem. J.* **413**, 369–387.

Ma, J.F., Ryan, P.R., & Delhaize, E. (2001) Aluminium tolerance in plants and the complexing role of organic acids. *Trends Plant Sci.* **6**, 273–278.

Matte, A., Tari, L.W., Goldie, H., & Delbaere, L.T.J. (1997) Structure and mechanism of phosphoenolpyruvate carboxykinase. *J. Biol. Chem.* **272**, 8105–8108.

Ovadi, J. & Srere, P. (2000) Macromolecular compartmentation and channeling. *Int. Rev. Cytol.* **192**, 255–280.

Advanced review of the evidence for channeling and metabolons.

Prensner, J.R. & Chinnaiyan, A.M. (2011) Metabolism unhinged: IDH mutations in cancer. *Nat. Med.* **17**, 291–293.

Brief review of the mutations of isocitrate dehydrogenase associated with cancer.

Remington, S.J. (1992) Structure and mechanism of citrate synthase. *Curr. Top. Cell. Regul.* **33**, 209–229.

A thorough review of this enzyme.

Singer, T.P. & Johnson, M.K. (1985) The prosthetic groups of succinate dehydrogenase: 30 years from discovery to identification. *FEBS Lett.* **190**, 189–198.

A description of the structure and role of the iron-sulfur centers in this enzyme.

Weigand, G. & Remington, S.J. (1986) Citrate synthase: structure, control, and mechanism. *Annu. Rev. Biophys. Biophys. Chem.* **15**, 97–117.

Wolodko, W.T., Fraser, M.E., James, M.N.G., & Bridger, W.A. (1994) The crystal structure of succinyl-CoA synthetase from *Escherichia coli* at 2.5-Å resolution. *J. Biol. Chem.* **269**, 10,883–10,890.

Yang, J., Kalhan, S.C., & Hanson, R.W. (2009) What is the metabolic role of phosphenolpyruvate carboxykinase? *J. Biol. Chem.* **284**, 27,025–27,029.

A minireview of the several roles played by this enzyme.

Moonlighting Enzymes

Eisenstein, R.S. (2000) Iron regulatory proteins and the molecular control of mammalian iron metabolism. *Annu. Rev. Nutr.* **20**, 627–662.

Flores, C.-L. & Gancedo, C. (2011) Unraveling moonlighting functions with yeasts. *IUBMB Life* **63**, 457–462.

Jeffery, C.J. (1999) Moonlighting proteins. *Trends Biochem. Sci.* **24**, 8–11.

Kim, J.-W. & Dang, C.V. (2006) Multifaceted roles of glycolytic enzymes. *Trends Biochem. Sci.* **30**, 142–150.

Intermediate-level review of moonlighting enzymes.

Rouault, T.A. (2006) The role of iron regulatory proteins in mammalian iron homeostasis and disease. *Nat. Chem. Biol.* **2**, 406–414.

An advanced review.

Regulation of the Citric Acid Cycle

Briere, J.-J., Favier, J., Gimenez-Roqueplo, A.-P., & Rustin, P. (2006) Tricarboxylic acid cycle dysfunction as a cause of human diseases and tumor formation. *Am. J. Physiol. Cell Physiol.* **291**, 1114–1120.

Intermediate-level review of clinical effects of mutations in succinate dehydrogenase, fumarase, and α-ketoglutarate dehydrogenase.

Hansford, R.G. (1980) Control of mitochondrial substrate oxidation. *Curr. Top. Bioenerget.* **10**, 217–278.

A detailed review of the regulation of the citric acid cycle.

Kaplan, N.O. (1985) The role of pyridine nucleotides in regulating cellular metabolism. *Curr. Top. Cell. Regul.* **26**, 371–381.

An excellent general discussion of the importance of the [NADH]/[NAD^+] ratio in cellular regulation.

King, A., Selak, M.A., & Gottlieb, E. (2006) Succinate dehydrogenase and fumarate hydratase: linking mitochondrial dysfunction and cancer. *Oncogene* **25**, 4675–4682.

Reed, L.J., Damuni, Z., & Merryfield, M.L. (1985) Regulation of mammalian pyruvate and branched-chain α-keto acid dehydrogenase

complexes by phosphorylation-dephosphorylation. *Curr. Top. Cell. Regul.* **27**, 41–49.

Glyoxylate Cycle

Eastmond, P.J. & Graham, I.A. (2001) Re-examining the role of the glyoxylate cycle in oilseeds. *Trends Plant Sci.* **6**, 72–77.

Intermediate-level review of studies of the glyoxylate cycle in *Arabidopsis*.

Holms, W.H. (1986) The central metabolic pathways of *Escherichia coli:* relationship between flux and control at a branch point, efficiency of conversion to biomass, and excretion of acetate. *Curr. Top. Cell. Regul.* **28**, 69–106.

Problems

1. Balance Sheet for the Citric Acid Cycle The citric acid cycle has eight enzymes: citrate synthase, aconitase, isocitrate dehydrogenase, α-ketoglutarate dehydrogenase, succinyl-CoA synthetase, succinate dehydrogenase, fumarase, and malate dehydrogenase.

(a) Write a balanced equation for the reaction catalyzed by each enzyme.

(b) Name the cofactor(s) required by each enzyme reaction.

(c) For each enzyme determine which of the following describes the type of reaction(s) catalyzed: condensation (carbon–carbon bond formation); dehydration (loss of water); hydration (addition of water); decarboxylation (loss of CO_2); oxidation-reduction; substrate-level phosphorylation; isomerization.

(d) Write a balanced net equation for the catabolism of acetyl-CoA to CO_2.

2. Net Equation for Glycolysis and the Citric Acid Cycle Write the net biochemical equation for the metabolism of a molecule of glucose by glycolysis and the citric acid cycle, including all cofactors.

3. Recognizing Oxidation and Reduction Reactions One biochemical strategy of many living organisms is the stepwise oxidation of organic compounds to CO_2 and H_2O and the conservation of a major part of the energy thus produced in the form of ATP. It is important to be able to recognize oxidation-reduction processes in metabolism. Reduction of an organic molecule results from the hydrogenation of a double bond (Eqn 1, below) or of a single bond with accompanying cleavage (Eqn 2). Conversely, oxidation results from dehydrogenation. In biochemical redox reactions, the coenzymes NAD and FAD dehydrogenate/hydrogenate organic molecules in the presence of the proper enzymes.

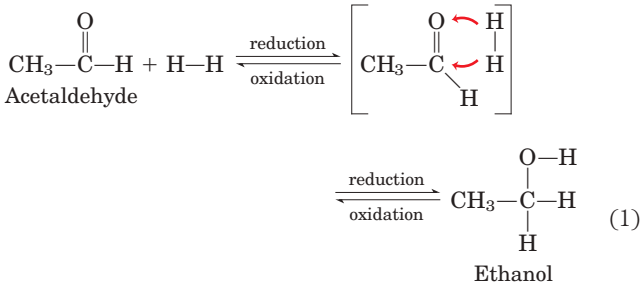

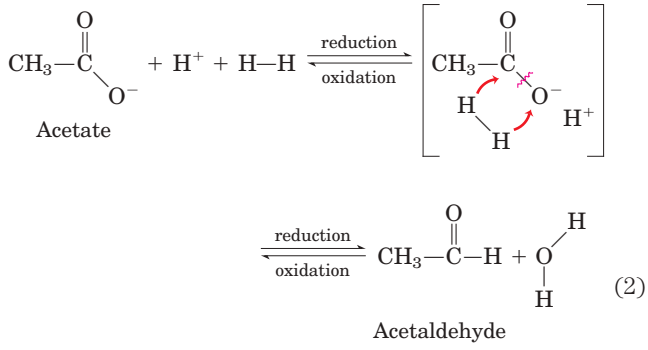

For each of the metabolic transformations in (a) through (h), determine whether oxidation or reduction has occurred. Balance each transformation by inserting H—H and, where necessary, H_2O.

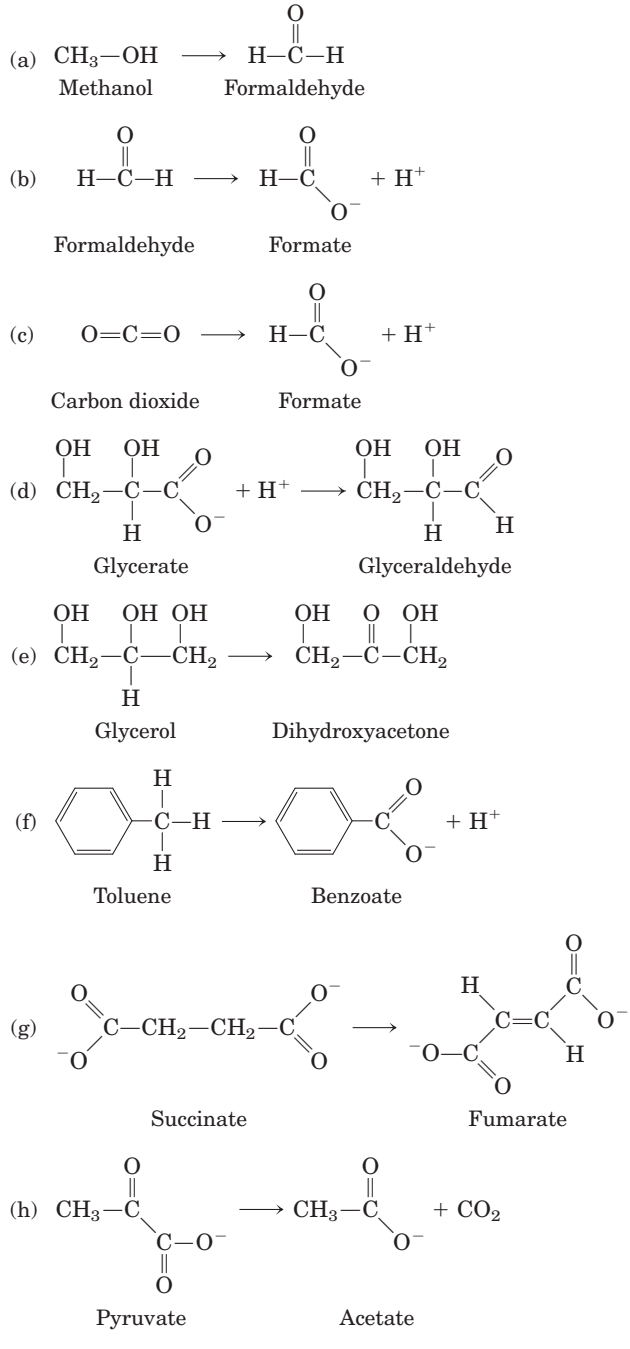

4. Relationship between Energy Release and the Oxidation State of Carbon A eukaryotic cell can use glucose ($C_6H_{12}O_6$) and hexanoic acid ($C_6H_{14}O_2$) as fuels for cellular respiration. On the basis of their structural formulas, which substance releases more energy per gram on complete combustion to CO_2 and H_2O?

5. Nicotinamide Coenzymes as Reversible Redox Carriers The nicotinamide coenzymes (see Fig. 13–24) can undergo reversible oxidation-reduction reactions with specific substrates in the presence of the appropriate dehydrogenase. In these reactions, NADH + H^+ serves as the hydrogen source, as described in Problem 3. Whenever the coenzyme is oxidized, a substrate must be simultaneously reduced:

$$\underset{\text{Oxidized}}{\text{Substrate}} + \underset{\text{Reduced}}{\text{NADH}} + H^+ \rightleftharpoons \underset{\text{Reduced}}{\text{product}} + \underset{\text{Oxidized}}{NAD^+}$$

For each of the reactions in (a) through (f), determine whether the substrate has been oxidized or reduced or is unchanged in oxidation state (see Problem 3). If a redox change has occurred, balance the reaction with the necessary amount of NAD^+, NADH, H^+, and H_2O. The objective is to recognize when a redox coenzyme is necessary in a metabolic reaction.

(a) $CH_3CH_2OH \longrightarrow CH_3-C(=O)-H$

Ethanol — Acetaldehyde

(b) $CH_2(OPO_3^{2-})-CH(OH)-C(=O)-OPO_3^{2-} \longrightarrow CH_2(OPO_3^{2-})-CH(OH)-C(=O)-H + HPO_4^{2-}$

1,3-Bisphosphoglycerate — Glyceraldehyde 3-phosphate

(c) $CH_3-C(=O)-C(=O)-O^- \longrightarrow CH_3-C(=O)-H + CO_2$

Pyruvate — Acetaldehyde

(d) $CH_3-C(=O)-C(=O)-O^- \longrightarrow CH_3-C(=O)-O^- + CO_2$

Pyruvate — Acetate

(e) $^-OOC-CH_2-C(=O)-COO^- \longrightarrow ^-OOC-CH_2-C(OH)(H)-COO^-$

Oxaloacetate — Malate

(f) $CH_3-C(=O)-CH_2-C(=O)-O^- + H^+ \longrightarrow CH_3-C(=O)-CH_3 + CO_2$

Acetoacetate — Acetone

6. Pyruvate Dehydrogenase Cofactors and Mechanism Describe the role of each cofactor involved in the reaction catalyzed by the pyruvate dehydrogenase complex.

7. Thiamine Deficiency Individuals with a thiamine-deficient diet have relatively high levels of pyruvate in their blood. Explain this in biochemical terms.

8. Isocitrate Dehydrogenase Reaction What type of chemical reaction is involved in the conversion of isocitrate to α-ketoglutarate? Name and describe the role of any cofactors. What other reaction(s) of the citric acid cycle are of this same type?

9. Stimulation of Oxygen Consumption by Oxaloacetate and Malate In the early 1930s, Albert Szent-Györgyi reported the interesting observation that the addition of small amounts of oxaloacetate or malate to suspensions of minced pigeon breast muscle stimulated the oxygen consumption of the preparation. Surprisingly, the amount of oxygen consumed was about seven times more than the amount necessary for complete oxidation (to CO_2 and H_2O) of the added oxaloacetate or malate. Why did the addition of oxaloacetate or malate stimulate oxygen consumption? Why was the amount of oxygen consumed so much greater than the amount necessary to completely oxidize the added oxaloacetate or malate?

10. Formation of Oxaloacetate in a Mitochondrion In the last reaction of the citric acid cycle, malate is dehydrogenated to regenerate the oxaloacetate necessary for the entry of acetyl-CoA into the cycle:

$$\text{L-Malate} + NAD^+ \longrightarrow \text{oxaloacetate} + \text{NADH} + H^+$$
$$\Delta G'^\circ = 30.0 \text{ kJ/mol}$$

(a) Calculate the equilibrium constant for this reaction at 25 °C.

(b) Because $\Delta G'^\circ$ assumes a standard pH of 7, the equilibrium constant calculated in (a) corresponds to

$$K'_{eq} = \frac{[\text{oxaloacetate}][\text{NADH}]}{[\text{L-malate}][NAD^+]}$$

The measured concentration of L-malate in rat liver mitochondria is about 0.20 mM when $[NAD^+]/[\text{NADH}]$ is 10. Calculate the concentration of oxaloacetate at pH 7 in these mitochondria.

(c) To appreciate the magnitude of the mitochondrial oxaloacetate concentration, calculate the number of oxaloacetate molecules in a single rat liver mitochondrion. Assume the mitochondrion is a sphere of diameter 2.0 μm.

11. Cofactors for the Citric Acid Cycle Suppose you have prepared a mitochondrial extract that contains all of the soluble enzymes of the matrix but has lost (by dialysis) all the low molecular weight cofactors. What must you add to the extract so that the preparation will oxidize acetyl-CoA to CO_2?

12. Riboflavin Deficiency How would a riboflavin deficiency affect the functioning of the citric acid cycle? Explain your answer.

13. Oxaloacetate Pool What factors might decrease the pool of oxaloacetate available for the activity of the citric acid cycle? How can the pool of oxaloacetate be replenished?

14. Energy Yield from the Citric Acid Cycle The reaction catalyzed by succinyl-CoA synthetase produces the high-energy

compound GTP. How is the free energy contained in GTP incorporated into the cellular ATP pool?

15. Respiration Studies in Isolated Mitochondria Cellular respiration can be studied in isolated mitochondria by measuring oxygen consumption under different conditions. If 0.01 M sodium malonate is added to actively respiring mitochondria that are using pyruvate as fuel source, respiration soon stops and a metabolic intermediate accumulates.

(a) What is the structure of this intermediate?

(b) Explain why it accumulates.

(c) Explain why oxygen consumption stops.

(d) Aside from removal of the malonate, how can this inhibition of respiration be overcome? Explain.

16. Labeling Studies in Isolated Mitochondria The metabolic pathways of organic compounds have often been delineated by using a radioactively labeled substrate and following the fate of the label.

(a) How can you determine whether glucose added to a suspension of isolated mitochondria is metabolized to CO_2 and H_2O?

(b) Suppose you add a brief pulse of [3-^{14}C]pyruvate (labeled in the methyl position) to the mitochondria. After one turn of the citric acid cycle, what is the location of the ^{14}C in the oxaloacetate? Explain by tracing the ^{14}C label through the pathway. How many turns of the cycle are required to release all the [3-^{14}C]pyruvate as CO_2?

17. Pathway of CO_2 in Gluconeogenesis In the first bypass step of gluconeogenesis, the conversion of pyruvate to phosphoenolpyruvate (PEP), pyruvate is carboxylated by pyruvate carboxylase to oxaloacetate, which is subsequently decarboxylated to PEP by PEP carboxykinase (Chapter 14). Because the addition of CO_2 is directly followed by the loss of CO_2, you might expect that in tracer experiments, the ^{14}C of $^{14}CO_2$ would not be incorporated into PEP, glucose, or any intermediates in gluconeogenesis. However, investigators find that when a rat liver preparation synthesizes glucose in the presence of $^{14}CO_2$, ^{14}C slowly appears in PEP and eventually at C-3 and C-4 of glucose. How does the ^{14}C label get into the PEP and glucose? (Hint: During gluconeogenesis in the presence of $^{14}CO_2$, several of the four-carbon citric acid cycle intermediates also become labeled.)

18. [1-^{14}C]Glucose Catabolism An actively respiring bacterial culture is briefly incubated with [1-^{14}C]glucose, and the glycolytic and citric acid cycle intermediates are isolated. Where is the ^{14}C in each of the intermediates listed below? Consider only the initial incorporation of ^{14}C, in the first pass of labeled glucose through the pathways.

(a) Fructose 1,6-bisphosphate

(b) Glyceraldehyde 3-phosphate

(c) Phosphoenolpyruvate

(d) Acetyl-CoA

(e) Citrate

(f) α-Ketoglutarate

(g) Oxaloacetate

19. Role of the Vitamin Thiamine People with beriberi, a disease caused by thiamine deficiency, have elevated levels of blood pyruvate and α-ketoglutarate, especially after consuming a meal rich in glucose. How are these effects related to a deficiency of thiamine?

20. Synthesis of Oxaloacetate by the Citric Acid Cycle Oxaloacetate is formed in the last step of the citric acid cycle by the NAD^+-dependent oxidation of L-malate. Can a net synthesis of oxaloacetate from acetyl-CoA occur using only the enzymes and cofactors of the citric acid cycle, without depleting the intermediates of the cycle? Explain. How is oxaloacetate that is lost from the cycle (to biosynthetic reactions) replenished?

21. Oxaloacetate Depletion Mammalian liver can carry out gluconeogenesis using oxaloacetate as the starting material (Chapter 14). Would the operation of the citric acid cycle be affected by extensive use of oxaloacetate for gluconeogenesis? Explain your answer.

22. Mode of Action of the Rodenticide Fluoroacetate Fluoroacetate, prepared commercially for rodent control, is also produced by a South African plant. After entering a cell, fluoroacetate is converted to fluoroacetyl-CoA in a reaction catalyzed by the enzyme acetate thiokinase:

$$F-CH_2COO^- + CoA\text{-}SH + ATP \longrightarrow F-CH_2C(=O)-S\text{-}CoA + AMP + PP_i$$

The toxic effect of fluoroacetate was studied in an experiment using intact isolated rat heart. After the heart was perfused with 0.22 mM fluoroacetate, the measured rate of glucose uptake and glycolysis decreased, and glucose 6-phosphate and fructose 6-phosphate accumulated. Examination of the citric acid cycle intermediates revealed that their concentrations were below normal, except for citrate, with a concentration 10 times higher than normal.

(a) Where did the block in the citric acid cycle occur? What caused citrate to accumulate and the other cycle intermediates to be depleted?

(b) Fluoroacetyl-CoA is enzymatically transformed in the citric acid cycle. What is the structure of the end product of fluoroacetate metabolism? Why does it block the citric acid cycle? How might the inhibition be overcome?

(c) In the heart perfusion experiments, why did glucose uptake and glycolysis decrease? Why did hexose monophosphates accumulate?

(d) Why is fluoroacetate poisoning fatal?

23. Synthesis of L-Malate in Wine Making The tartness of some wines is due to high concentrations of L-malate. Write a sequence of reactions showing how yeast cells synthesize L-malate from glucose under anaerobic conditions in the presence of dissolved CO_2 (HCO_3^-). Note that the overall reaction for this fermentation cannot involve the consumption of nicotinamide coenzymes or citric acid cycle intermediates.

24. Net Synthesis of α-Ketoglutarate α-Ketoglutarate plays a central role in the biosynthesis of several amino acids. Write a sequence of enzymatic reactions that could result in the net synthesis of α-ketoglutarate from pyruvate. Your

proposed sequence must not involve the net consumption of other citric acid cycle intermediates. Write an equation for the overall reaction and identify the source of each reactant.

25. Amphibolic Pathways Explain, giving examples, what is meant by the statement that the citric acid cycle is amphibolic.

26. Regulation of the Pyruvate Dehydrogenase Complex In animal tissues, the rate of conversion of pyruvate to acetyl-CoA is regulated by the ratio of active, phosphorylated to inactive, unphosphorylated PDH complex. Determine what happens to the rate of this reaction when a preparation of rabbit muscle mitochondria containing the PDH complex is treated with (a) pyruvate dehydrogenase kinase, ATP, and NADH; (b) pyruvate dehydrogenase phosphatase and Ca^{2+}; (c) malonate.

27. Commercial Synthesis of Citric Acid Citric acid is used as a flavoring agent in soft drinks, fruit juices, and many other foods. Worldwide, the market for citric acid is valued at hundreds of millions of dollars per year. Commercial production uses the mold *Aspergillus niger*, which metabolizes sucrose under carefully controlled conditions.

(a) The yield of citric acid is strongly dependent on the concentration of $FeCl_3$ in the culture medium, as indicated in the graph. Why does the yield decrease when the concentration of Fe^{3+} is above or below the optimal value of 0.5 mg/L?

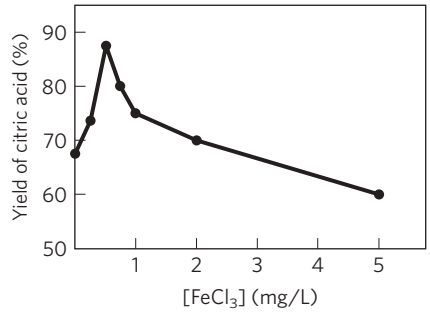

(b) Write the sequence of reactions by which *A. niger* synthesizes citric acid from sucrose. Write an equation for the overall reaction.

(c) Does the commercial process require the culture medium to be aerated—that is, is this a fermentation or an aerobic process? Explain.

28. Regulation of Citrate Synthase In the presence of saturating amounts of oxaloacetate, the activity of citrate synthase from pig heart tissue shows a sigmoid dependence on the concentration of acetyl-CoA, as shown in the graph below. When succinyl-CoA is added, the curve shifts to the right and the sigmoid dependence is more pronounced.

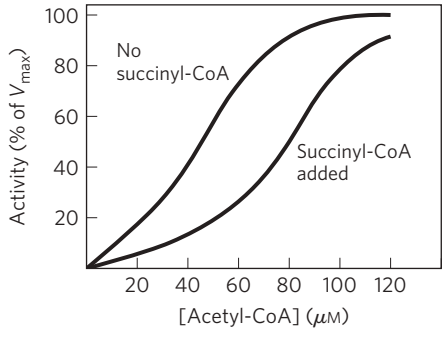

On the basis of these observations, suggest how succinyl-CoA regulates the activity of citrate synthase. (Hint: See Fig. 6–34.) Why is succinyl-CoA an appropriate signal for regulation of the citric acid cycle? How does the regulation of citrate synthase control the rate of cellular respiration in pig heart tissue?

29. Regulation of Pyruvate Carboxylase The carboxylation of pyruvate by pyruvate carboxylase occurs at a very low rate unless acetyl-CoA, a positive allosteric modulator, is present. If you have just eaten a meal rich in fatty acids (triacylglycerols) but low in carbohydrates (glucose), how does this regulatory property shut down the oxidation of glucose to CO_2 and H_2O but increase the oxidation of acetyl-CoA derived from fatty acids?

30. Relationship between Respiration and the Citric Acid Cycle Although oxygen does not participate directly in the citric acid cycle, the cycle operates only when O_2 is present. Why?

31. Effect of [NADH]/[NAD$^+$] on the Citric Acid Cycle How would you expect the operation of the citric acid cycle to respond to a rapid increase in the [NADH]/[NAD$^+$] ratio in the mitochondrial matrix? Why?

32. Thermodynamics of Citrate Synthase Reaction in Cells Citrate is formed by the condensation of acetyl-CoA with oxaloacetate, catalyzed by citrate synthase:

$$\text{Oxaloacetate} + \text{acetyl-CoA} + H_2O \rightleftharpoons \text{citrate} + \text{CoA} + H^+$$

In rat heart mitochondria at pH 7.0 and 25 °C, the concentrations of reactants and products are: oxaloacetate, 1 μM; acetyl-CoA, 1 μM; citrate, 220 μM; and CoA, 65 μM. The standard free-energy change for the citrate synthase reaction is −32.2 kJ/mol. What is the direction of metabolite flow through the citrate synthase reaction in rat heart cells? Explain.

33. Reactions of the Pyruvate Dehydrogenase Complex Two of the steps in the oxidative decarboxylation of pyruvate (steps ❹ and ❺ in Fig. 16–6) do not involve any of the three carbons of pyruvate yet are essential to the operation of the PDH complex. Explain.

34. Citric Acid Cycle Mutants There are many cases of human disease in which one or another enzyme activity is lacking due to genetic mutation. However, cases in which individuals lack one of the enzymes of the citric acid cycle are extremely rare. Why?

35. Partitioning between the Citric Acid and Glyoxylate Cycles In an organism (such as *E. coli*) that has both the citric acid cycle and the glyoxylate cycle, what determines which of these pathways isocitrate will enter?

Data Analysis Problem

36. How the Citric Acid Cycle Was Determined The detailed biochemistry of the citric acid cycle was determined by several researchers over a period of decades. In a 1937 article, Krebs and Johnson summarized their work and the work of others in the first published description of this pathway.

The methods used by these researchers were very different from those of modern biochemistry. Radioactive tracers were not commonly available until the 1940s, so Krebs and other researchers had to use nontracer techniques to work out the pathway. Using freshly prepared samples of pigeon breast muscle, they determined oxygen consumption by suspending minced muscle in buffer in a sealed flask and measuring the volume (in μL) of oxygen consumed under different conditions. They measured levels of substrates (intermediates) by treating samples with acid to remove contaminating proteins, then assaying the quantities of various small organic molecules. The two key observations that led Krebs and colleagues to propose a citric acid *cycle* as opposed to a *linear pathway* (like that of glycolysis) were made in the following experiments.

Experiment I. They incubated 460 mg of minced muscle in 3 mL of buffer at 40 °C for 150 minutes. Addition of *citrate* increased O_2 consumption by 893 μL compared with samples without added citrate. They calculated, based on the O_2 consumed during respiration of other carbon-containing compounds, that the expected O_2 consumption for complete respiration of this quantity of citrate was only 302 μL.

Experiment II. They measured O_2 consumption by 460 mg of minced muscle in 3 mL of buffer when incubated with *citrate* and/or with *1-phosphoglycerol* (glycerol 1-phosphate; this was known to be readily oxidized by cellular respiration) at 40 °C for 140 minutes. The results are shown in the table.

Sample	Substrate(s) added	μL O_2 absorbed
1	No extra	342
2	0.3 mL 0.2 M 1-phosphoglycerol	757
3	0.15 mL 0.02 M citrate	431
4	0.3 mL 0.2 M 1-phosphoglycerol and 0.15 mL 0.02 M citrate	1,385

(a) Why is O_2 consumption a good measure of cellular respiration?

(b) Why does sample 1 (unsupplemented muscle tissue) consume some oxygen?

(c) Based on the results for samples 2 and 3, can you conclude that 1-phosphoglycerol and citrate serve as substrates for cellular respiration in this system? Explain your reasoning.

(d) Krebs and colleagues used the results from these experiments to argue that citrate was "catalytic"—that it helped the muscle tissue samples metabolize 1-phosphoglycerol more completely. How would you use their data to make this argument?

(e) Krebs and colleagues further argued that citrate was not simply consumed by these reactions, but had to be *regenerated*. Therefore, the reactions had to be a *cycle* rather than a linear pathway. How would you make this argument?

Other researchers had found that *arsenate* (AsO_4^{3-}) inhibits α-ketoglutarate dehydrogenase and that *malonate* inhibits succinate dehydrogenase.

(f) Krebs and coworkers found that muscle tissue samples treated with arsenate and citrate would consume citrate only in the presence of oxygen; under these conditions, oxygen was consumed. Based on the pathway in Figure 16–7, what was the citrate converted to in this experiment, and why did the samples consume oxygen?

In their article, Krebs and Johnson further reported the following. (1) In the presence of arsenate, 5.48 mmol of citrate was converted to 5.07 mmol of α-ketoglutarate. (2) In the presence of malonate, citrate was quantitatively converted to large amounts of succinate and small amounts of α-ketoglutarate. (3) Addition of oxaloacetate in the absence of oxygen led to production of a large amount of citrate; the amount was increased if glucose was also added.

Other workers had found the following pathway in similar muscle tissue preparations:

Succinate ⟶ fumarate ⟶ malate ⟶ oxaloacetate ⟶ pyruvate

(g) Based only on the data presented in this problem, what is the order of the intermediates in the citric acid cycle? How does this compare with Figure 16–7? Explain your reasoning.

(h) Why was it important to show the *quantitative* conversion of citrate to α-ketoglutarate?

The Krebs and Johnson article also contains other data that filled in most of the missing components of the cycle. The only component left unresolved was the molecule that reacted with oxaloacetate to form citrate.

Reference

Krebs, H.A. & Johnson, W.A. (1937) The role of citric acid in intermediate metabolism in animal tissues. *Enzymologia* **4**, 148–156. [Reprinted (1980) in *FEBS Lett.* **117** (Suppl.), K2–K10.]

this page left intentionally blank

17

Fatty Acid Catabolism

The oxidation of long-chain fatty acids to acetyl-CoA is a central energy-yielding pathway in many organisms and tissues. In mammalian heart and liver, for example, it provides as much as 80% of the energetic needs under all physiological circumstances. The electrons removed from fatty acids during oxidation pass through the respiratory chain, driving ATP synthesis; the acetyl-CoA produced from the fatty acids may be completely oxidized to CO_2 in the citric acid cycle, resulting in further energy conservation. In some species and in some tissues, the acetyl-CoA has alternative fates. In liver, acetyl-CoA may be converted to ketone bodies—water-soluble fuels exported to the brain and other tissues when glucose is not available. In higher plants, acetyl-CoA serves primarily as a biosynthetic precursor, only secondarily as fuel. Although the biological role of fatty acid oxidation differs from organism to organism, the mechanism is essentially the same. The repetitive four-step process, called **β oxidation**, by which fatty acids are converted into acetyl-CoA is the main topic of this chapter.

In Chapter 10 we described the properties of triacylglycerols (also called triglycerides or neutral fats) that make them especially suitable as storage fuels. The long alkyl chains of their constituent fatty acids are essentially hydrocarbons, highly reduced structures with an energy of complete oxidation (~38 kJ/g) more than twice that for the same weight of carbohydrate or protein. This advantage is compounded by the extreme insolubility of lipids in water; cellular triacylglycerols aggregate in lipid droplets, which do not raise the osmolarity of the cytosol, and they are unsolvated. (In storage polysaccharides, by contrast, water of solvation can account for two-thirds of the overall weight of the stored molecules.) And because of their relative chemical inertness, triacylglycerols can be stored in large quantity in cells without the risk of undesired chemical reactions with other cellular constituents.

The properties that make triacylglycerols good storage compounds, however, present problems in their role as fuels. Because they are insoluble in water, ingested triacylglycerols must be emulsified before they can be digested by water-soluble enzymes in the intestine, and triacylglycerols absorbed in the intestine or mobilized from storage tissues must be carried in the blood bound to proteins that counteract their insolubility. To overcome the relative stability of the C—C bonds in a fatty acid, the carboxyl group at C-1 is activated by attachment to coenzyme A, which allows stepwise oxidation of the fatty acyl group at the C-3, or β, position—hence the name β oxidation.

We begin this chapter with a brief discussion of the sources of fatty acids and the routes by which they travel to the site of their oxidation, with special emphasis on the process in vertebrates. We then describe the chemical steps of fatty acid oxidation in mitochondria. The complete oxidation of fatty acids to CO_2 and H_2O takes place in three stages: the oxidation of long-chain fatty acids to two-carbon fragments, in the form of acetyl-CoA (β oxidation); the oxidation of acetyl-CoA to CO_2 in the citric acid cycle (Chapter 16); and the transfer of electrons from reduced electron carriers to the mitochondrial respiratory chain (Chapter 19). In this chapter we focus on the first of these stages. We begin our discussion of β oxidation with the simple case in which a fully saturated fatty acid with an even number of carbon atoms is degraded to acetyl-CoA. We then look briefly at the extra transformations necessary for the degradation of unsaturated fatty acids and fatty acids with an odd number of carbons. Finally, we discuss variations on the β-oxidation theme in specialized organelles—peroxisomes and glyoxysomes—and two less common pathways of fatty acid catabolism, ω and α oxidation. The chapter concludes with a description of an alternative fate for the acetyl-CoA formed by β oxidation in vertebrates: the production of ketone bodies in the liver.

17.1 Digestion, Mobilization, and Transport of Fats

Cells can obtain fatty acid fuels from three sources: fats consumed in the diet, fats stored in cells as lipid droplets, and fats synthesized in one organ for export to another. Some species use all three sources under various circumstances, others use one or two. Vertebrates, for example, obtain fats in the diet, mobilize fats stored in specialized tissue (adipose tissue, consisting of cells called adipocytes), and, in the liver, convert excess dietary carbohydrates to fats for export to other tissues. On average, 40% or more of the daily energy requirement of humans in highly industrialized countries is supplied by dietary triacylglycerols (although most nutritional guidelines recommend no more than 30% of daily caloric intake from fats). Triacylglycerols provide more than half the energy requirements of some organs, particularly the liver, heart, and resting skeletal muscle. Stored triacylglycerols are virtually the sole source of energy in hibernating animals and migrating birds. Protists obtain fats by consuming organisms lower in the food chain, and some also store fats as cytosolic lipid droplets. Vascular plants mobilize fats stored in seeds during germination, but do not otherwise depend on fats for energy.

Dietary Fats Are Absorbed in the Small Intestine

In vertebrates, before ingested triacylglycerols can be absorbed through the intestinal wall they must be converted from insoluble macroscopic fat particles to finely dispersed microscopic micelles. This solubilization is carried out by bile salts, such as taurocholic acid (p. 370), which are synthesized from cholesterol in the liver, stored in the gallbladder, and released into the small intestine after ingestion of a fatty meal. Bile salts are amphipathic compounds that act as biological detergents, converting dietary fats into mixed micelles of bile salts and triacylglycerols (**Fig. 17–1**, step ❶). Micelle formation enormously increases the fraction of lipid molecules accessible to the action of water-soluble lipases in the intestine, and lipase action converts triacylglycerols to monoacylglycerols (monoglycerides) and diacylglycerols (diglycerides), free fatty acids, and glycerol (step ❷). These products of lipase action diffuse into the epithelial cells lining the intestinal surface (the intestinal mucosa) (step ❸), where they are reconverted to triacylglycerols and packaged

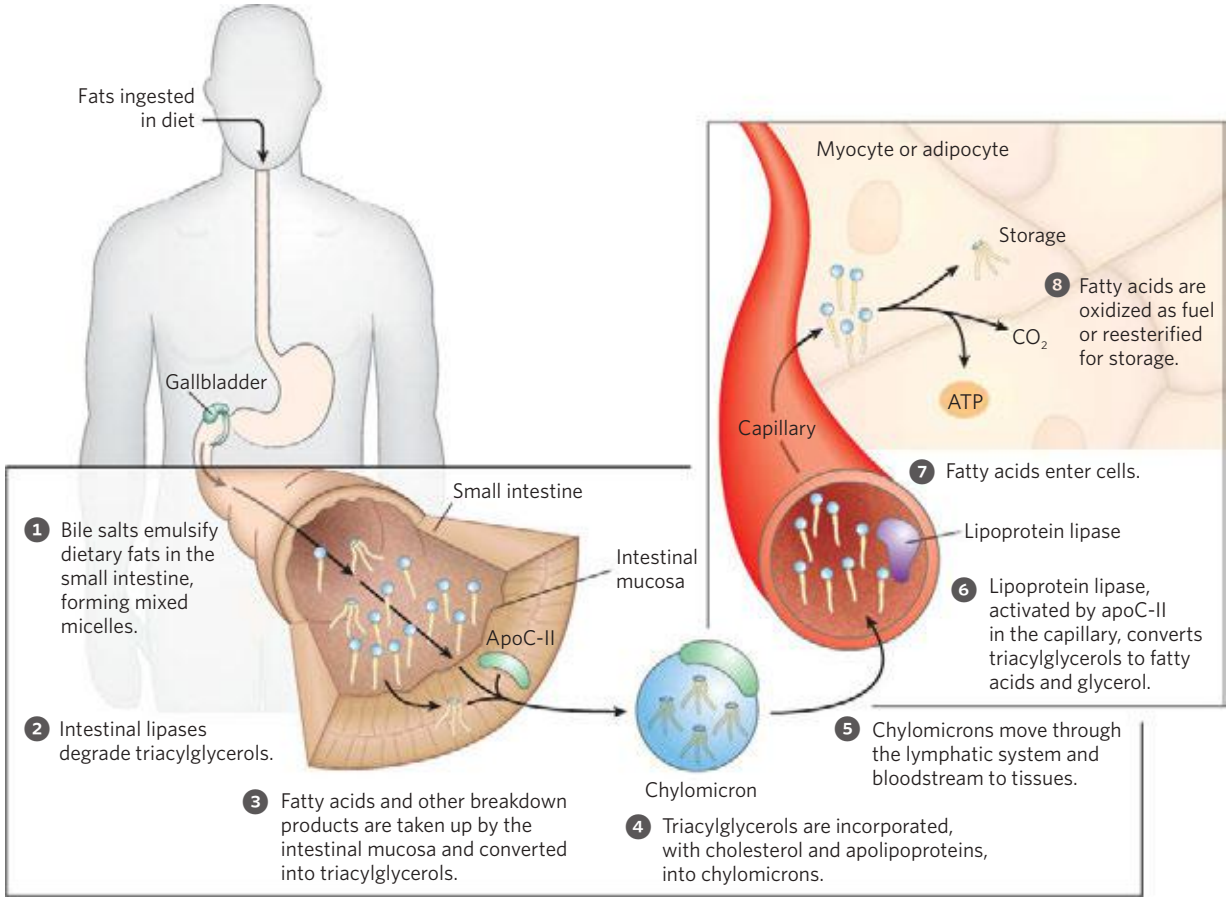

FIGURE 17–1 Processing of dietary lipids in vertebrates. Digestion and absorption of dietary lipids occur in the small intestine, and the fatty acids released from triacylglycerols are packaged and delivered to muscle and adipose tissues. The eight steps are discussed in the text.

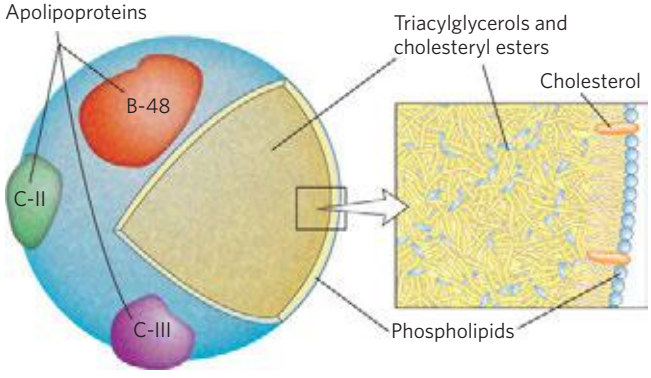

FIGURE 17–2 Molecular structure of a chylomicron. The surface is a layer of phospholipids, with head groups facing the aqueous phase. Triacylglycerols sequestered in the interior (yellow) make up more than 80% of the mass. Several apolipoproteins that protrude from the surface (B-48, C-III, C-II) act as signals in the uptake and metabolism of chylomicron contents. The diameter of chylomicrons ranges from about 100 to 500 nm.

with dietary cholesterol and specific proteins into lipoprotein aggregates called **chylomicrons** (**Fig. 17–2**; see also Fig. 17–1, step ❹).

Apolipoproteins are lipid-binding proteins in the blood, responsible for the transport of triacylglycerols, phospholipids, cholesterol, and cholesteryl esters between organs. Apolipoproteins ("apo" means "detached" or "separate," designating the protein in its lipid-free form) combine with lipids to form several classes of **lipoprotein** particles, spherical aggregates with hydrophobic lipids at the core and hydrophilic protein side chains and lipid head groups at the surface. Various combinations of lipid and protein produce particles of different densities, ranging from chylomicrons and very-low-density lipoproteins (VLDL) to very-high-density lipoproteins (VHDL), which can be separated by ultracentrifugation. The structures of these lipoprotein particles and their roles in lipid transport are detailed in Chapter 21.

The protein moieties of lipoproteins are recognized by receptors on cell surfaces. In lipid uptake from the intestine, chylomicrons, which contain apolipoprotein C-II (apoC-II), move from the intestinal mucosa into the lymphatic system, and then enter the blood, which carries them to muscle and adipose tissue (Fig. 17–1, step ❺). In the capillaries of these tissues, the extracellular enzyme **lipoprotein lipase**, activated by apoC-II, hydrolyzes triacylglycerols to fatty acids and glycerol (step ❻), which are taken up by cells in the target tissues (step ❼). In muscle, the fatty acids are oxidized for energy; in adipose tissue, they are reesterified for storage as triacylglycerols (step ❽).

The remnants of chylomicrons, depleted of most of their triacylglycerols but still containing cholesterol and apolipoproteins, travel in the blood to the liver, where they are taken up by endocytosis, mediated by receptors for their apolipoproteins. Triacylglycerols that enter the liver by this route may be oxidized to provide energy or to provide precursors for the synthesis of ketone bodies, as described in Section 17.3. When the diet contains more fatty acids than are needed immediately for fuel or as precursors, the liver converts them to triacylglycerols, which are packaged with specific apolipoproteins into VLDLs. The VLDLs are transported in the blood to adipose tissues, where the triacylglycerols are removed and stored in lipid droplets within adipocytes.

Hormones Trigger Mobilization of Stored Triacylglycerols

Neutral lipids are stored in adipocytes (and in steroid-synthesizing cells of the adrenal cortex, ovary, and testis) in the form of lipid droplets, with a core of sterol esters and triacylglycerols surrounded by a monolayer of phospholipids. The surface of these droplets is coated with **perilipins**, a family of proteins that restrict access to lipid droplets, preventing untimely lipid mobilization. When hormones signal the need for metabolic energy, triacylglycerols stored in adipose tissue are mobilized (brought out of storage) and transported to tissues (skeletal muscle, heart, and renal cortex) in which fatty acids can be oxidized for energy production. The hormones epinephrine and glucagon, secreted in response to low blood glucose levels or impending activity, stimulate the enzyme adenylyl cyclase in the adipocyte plasma membrane **(Fig. 17–3)**, which produces the intracellular second messenger cyclic AMP (cAMP; see Fig. 12–4). Cyclic AMP–dependent protein kinase (PKA) triggers changes that open the lipid droplet up to the action of three lipases, which act on tri-, di-, and monoacylglycerols, releasing fatty acids and glycerol.

The fatty acids thus released (**free fatty acids, FFA**) pass from the adipocyte into the blood, where they bind to the blood protein **serum albumin** (Fig. 17–3). This protein (M_r 66,000), which makes up about half of the total serum protein, noncovalently binds as many as 10 fatty acids per protein monomer. Bound to this soluble protein, the otherwise insoluble fatty acids are carried to tissues such as skeletal muscle, heart, and renal cortex. In these target tissues, fatty acids dissociate from albumin and are moved by plasma membrane transporters into cells to serve as fuel. The glycerol liberated by lipase action is phosphorylated and oxidized to dihydroxyacetone phosphate, which can enter the glycolytic or gluconeogenic pathways. Alternatively, glycerol phosphate can be used in triacylglycerol or phospholipid synthesis.

About 95% of the biologically available energy of triacylglycerols resides in their three long-chain fatty acids; only 5% is contributed by the glycerol moiety. The glycerol released by lipase action is phosphorylated

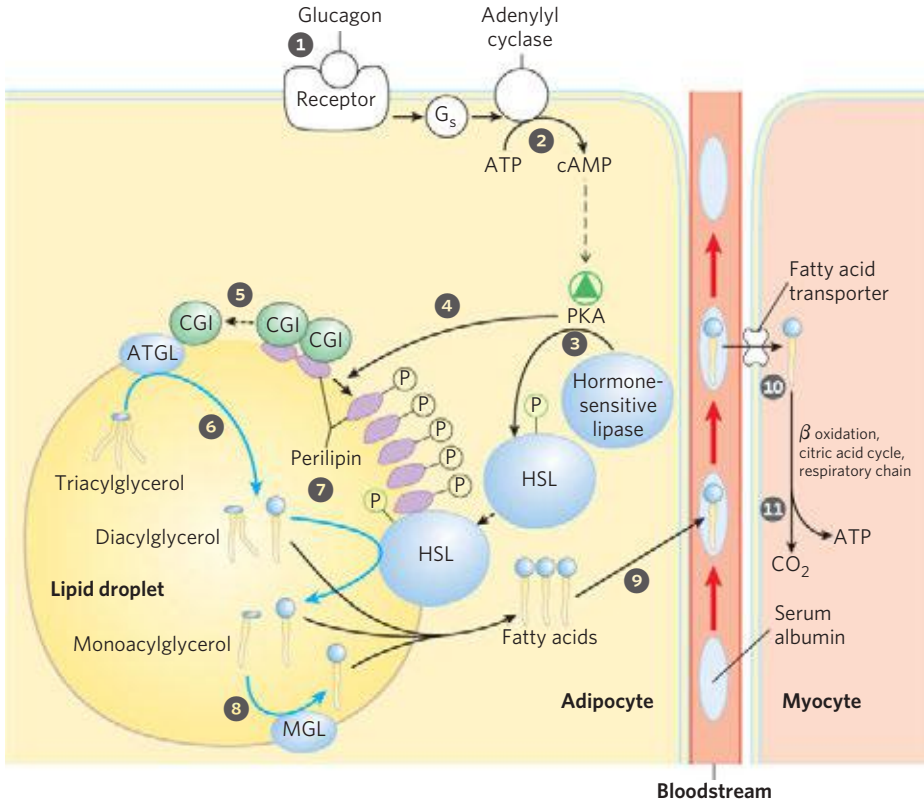

FIGURE 17–3 Mobilization of triacylglycerols stored in adipose tissue. When low levels of glucose in the blood trigger the release of glucagon, ❶ the hormone binds its receptor in the adipocyte membrane and thus ❷ stimulates adenylyl cyclase, via a G protein, to produce cAMP. This activates PKA, which phosphorylates ❸ the hormone-sensitive lipase (HSL) and ❹ perilipin molecules on the surface of the lipid droplet. Phosphorylation of perilipin causes ❺ dissociation of the protein CGI from perilipin. CGI then associates with the enzyme adipose triacylglycerol lipase (ATGL), activating it. Active ATGL ❻ converts triacylglycerols to diacylglycerols. The phosphorylated perilipin associates with phosphorylated HSL, allowing it access to the surface of the lipid droplet, where ❼ it converts diacylglycerols to monoacylglycerols. A third lipase, monoacylglycerol lipase (MGL) ❽, hydrolyzes monoacylglycerols. ❾ Fatty acids leave the adipocyte, bind serum albumin in the blood, and are carried in the blood; they are released from the albumin and ❿ enter a myocyte via a specific fatty acid transporter. ⓫ In the myocyte, fatty acids are oxidized to CO_2, and the energy of oxidation is conserved in ATP, which fuels muscle contraction and other energy-requiring metabolism in the myocyte.

by **glycerol kinase** **(Fig. 17–4)**, and the resulting glycerol 3-phosphate is oxidized to dihydroxyacetone phosphate. The glycolytic enzyme triose phosphate isomerase converts this compound to glyceraldehyde 3-phosphate, which is oxidized via glycolysis.

Fatty Acids Are Activated and Transported into Mitochondria

The enzymes of fatty acid oxidation in animal cells are located in the mitochondrial matrix, as demonstrated in 1948 by Eugene P. Kennedy and Albert Lehninger. The fatty acids with chain lengths of 12 or fewer carbons enter mitochondria without the help of membrane transporters. Those with 14 or more carbons, which constitute the majority of the FFA obtained in the diet or released from adipose tissue, cannot pass directly through the mitochondrial membranes—they must first undergo the three enzymatic reactions of the **carnitine shuttle**. The first reaction is catalyzed by a family of isozymes (different isozymes specific for fatty acids having short, intermediate, or long carbon chains) present in the outer mitochondrial membrane, the **acyl-CoA synthetases**, which promote the general reaction

$$\text{Fatty acid} + \text{CoA} + \text{ATP} \rightleftharpoons \text{fatty acyl–CoA} + \text{AMP} + \text{PP}_i$$

Thus, acyl–CoA synthetases catalyze the formation of a thioester linkage between the fatty acid carboxyl group and the thiol group of coenzyme A to yield a **fatty acyl–CoA**, coupled to the cleavage of ATP to AMP and PP_i. (Recall the description of this reaction in Chapter 13, to illustrate how the free energy released by cleavage of phosphoanhydride bonds in ATP could be coupled to the formation of a high-energy compound; p. 524.) The reaction occurs in two steps and involves a fatty acyl–adenylate intermediate **(Fig. 17–5)**.

Fatty acyl–CoAs, like acetyl-CoA, are high-energy compounds; their hydrolysis to FFA and CoA has a large, negative standard free-energy change ($\Delta G'^\circ = -31$ kJ/mol). The formation of a fatty acyl–CoA is made more favorable by the hydrolysis of *two* high-energy bonds in ATP; the pyrophosphate formed in the activation reaction is immediately hydrolyzed by inorganic pyrophosphatase (left side of Fig. 17–5), which pulls

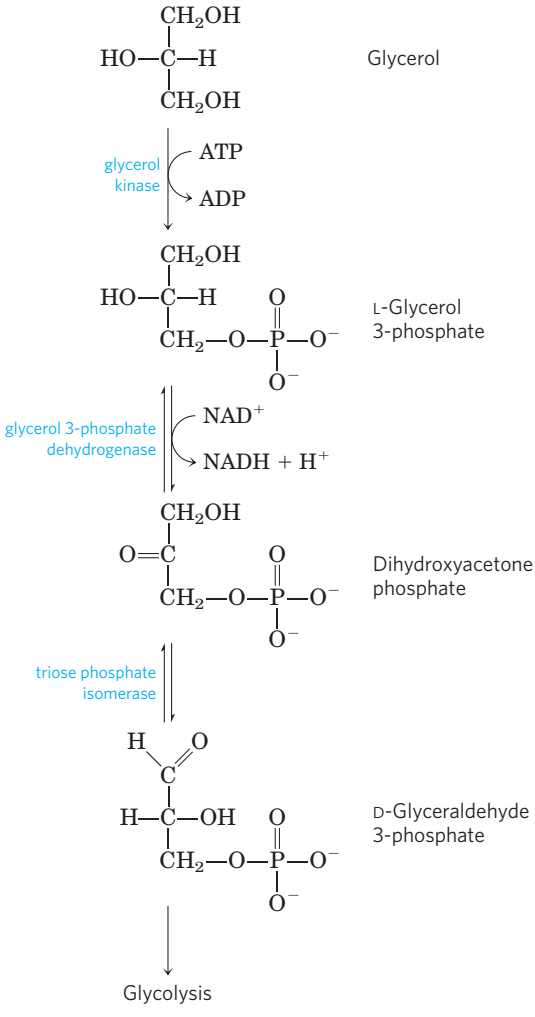

FIGURE 17–4 **Entry of glycerol into the glycolytic pathway.**

the preceding activation reaction in the direction of fatty acyl–CoA formation. The overall reaction is

$$\text{Fatty acid} + \text{CoA} + \text{ATP} \longrightarrow \text{fatty acyl–CoA} + \text{AMP} + 2\text{P}_\text{i} \quad (17\text{–}1)$$
$$\Delta G'^\circ = -34 \text{ kJ/mol}$$

Fatty acyl–CoA esters formed at the cytosolic side of the outer mitochondrial membrane can be transported into the mitochondrion and oxidized to produce ATP, or they can be used in the cytosol to synthesize membrane lipids. Fatty acids destined for mitochondrial oxidation are transiently attached to the hydroxyl group of **carnitine** to form fatty acyl–carnitine—the second reaction of the shuttle.

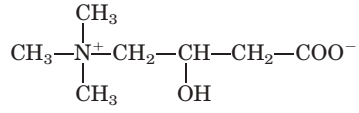

This transesterification is catalyzed by **carnitine acyltransferase I**, in the outer membrane. Either the acyl-CoA passes through the outer membrane and is converted to the carnitine ester in the intermembrane space **(Fig. 17–6)**, or the carnitine ester is formed on the cytosolic face of the outer membrane, then moved across the outer membrane to the intermembrane space—the current evidence does not reveal which. In either case, passage into the intermembrane space (the space between the outer and inner membranes) occurs through large pores (formed by the protein porin) in the outer membrane. The fatty acyl–carnitine ester then enters the matrix by facilitated diffusion through the **acyl-carnitine/carnitine transporter** of the inner mitochondrial membrane (Fig. 17–6).

In the third and final step of the carnitine shuttle, the fatty acyl group is enzymatically transferred from carnitine to intramitochondrial coenzyme A by **carnitine acyltransferase II**. This isozyme, located on the inner face of the inner mitochondrial membrane, regenerates fatty acyl–CoA and releases it, along with free carnitine, into the matrix (Fig. 17–6). Carnitine reenters the intermembrane space via the acylcarnitine/carnitine transporter.

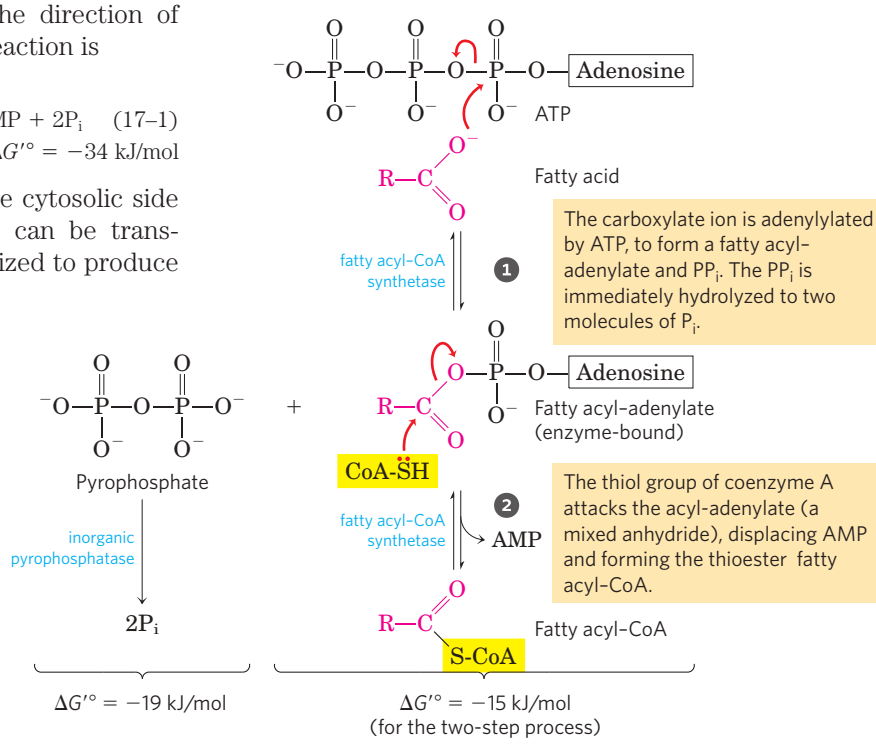

MECHANISM FIGURE 17–5 **Conversion of a fatty acid to a fatty acyl-CoA.** The conversion is catalyzed by fatty acyl-CoA synthetase and inorganic pyrophosphatase. Fatty acid activation by formation of the fatty acyl-CoA derivative occurs in two steps. The overall reaction is highly exergonic. Fatty Acyl-CoA Synthetase Mechanism

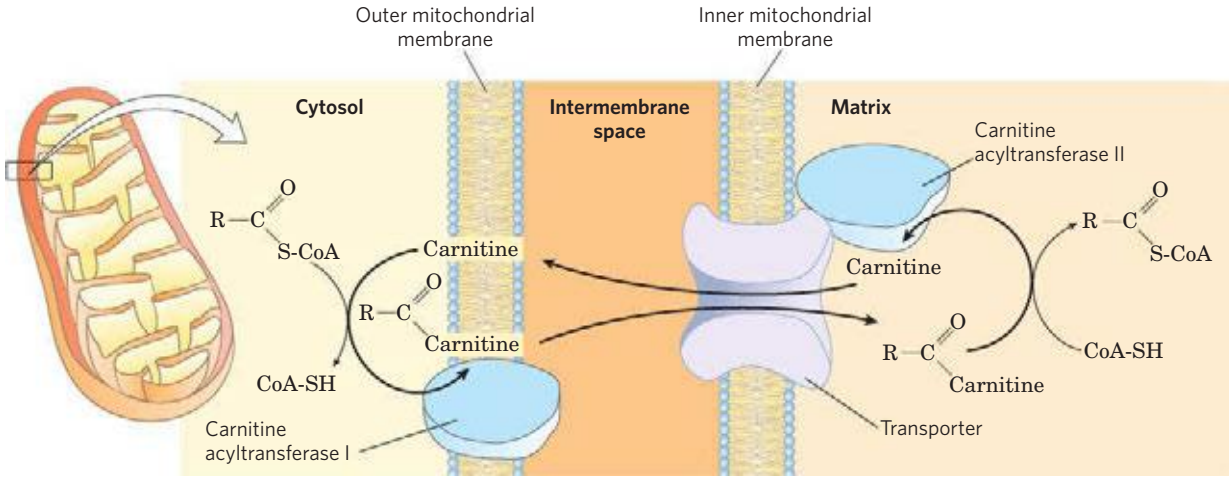

FIGURE 17–6 Fatty acid entry into mitochondria via the acyl-carnitine/carnitine transporter. After fatty acyl-carnitine is formed at the outer membrane or in the intermembrane space, it moves into the matrix by facilitated diffusion through the transporter in the inner membrane. In the matrix, the acyl group is transferred to mitochondrial coenzyme A, freeing carnitine to return to the intermembrane space through the same transporter. Acyltransferase I is inhibited by malonyl-CoA, the first intermediate in fatty acid synthesis (see Fig. 21–2). This inhibition prevents the simultaneous synthesis and degradation of fatty acids.

This three-step process for transferring fatty acids into the mitochondrion—esterification to CoA, transesterification to carnitine followed by transport, and transesterification back to CoA—links two separate pools of coenzyme A and of fatty acyl–CoA, one in the cytosol, the other in mitochondria. These pools have different functions. Coenzyme A in the mitochondrial matrix is largely used in oxidative degradation of pyruvate, fatty acids, and some amino acids, whereas cytosolic coenzyme A is used in the biosynthesis of fatty acids (see Fig. 21–10). Fatty acyl–CoA in the cytosolic pool can be used for membrane lipid synthesis or can be moved into the mitochondrial matrix for oxidation and ATP production. Conversion to the carnitine ester commits the fatty acyl moiety to the oxidative fate.

The carnitine-mediated entry process is the rate-limiting step for oxidation of fatty acids in mitochondria and, as discussed later, is a regulation point. Once inside the mitochondrion, the fatty acyl–CoA is acted upon by a set of enzymes in the matrix.

SUMMARY 17.1 Digestion, Mobilization, and Transport of Fats

- The fatty acids of triacylglycerols furnish a large fraction of the oxidative energy in animals. Dietary triacylglycerols are emulsified in the small intestine by bile salts, hydrolyzed by intestinal lipases, absorbed by intestinal epithelial cells, reconverted into triacylglycerols, then formed into chylomicrons by combination with specific apolipoproteins.
- Chylomicrons deliver triacylglycerols to tissues, where lipoprotein lipase releases free fatty acids for entry into cells. Triacylglycerols stored in adipose tissue are mobilized by a hormone-sensitive triacylglycerol lipase. The released fatty acids bind to serum albumin and are carried in the blood to the heart, skeletal muscle, and other tissues that use fatty acids for fuel.
- Once inside cells, fatty acids are activated at the outer mitochondrial membrane by conversion to fatty acyl–CoA thioesters. Fatty acyl–CoA that is to be oxidized enters mitochondria in three steps, via the carnitine shuttle.

17.2 Oxidation of Fatty Acids

As noted earlier, mitochondrial oxidation of fatty acids takes place in three stages **(Fig. 17–7)**. In the first stage—β oxidation—fatty acids undergo oxidative removal of successive two-carbon units in the form of acetyl-CoA, starting from the carboxyl end of the fatty acyl chain. For example, the 16-carbon palmitic acid (palmitate at pH 7) undergoes seven passes through the oxidative sequence, in each pass losing two carbons as acetyl-CoA. At the end of seven cycles the last two carbons of palmitate (originally C-15 and C-16) remain as acetyl-CoA. The overall result is the conversion of the 16-carbon chain of palmitate to eight two-carbon acetyl groups of acetyl-CoA molecules. Formation of each acetyl-CoA requires removal of four hydrogen atoms (two pairs of electrons and four H^+) from the fatty acyl moiety by dehydrogenases.

In the second stage of fatty acid oxidation, the acetyl groups of acetyl-CoA are oxidized to CO_2 in the citric acid cycle, which also takes place in the mitochondrial matrix. Acetyl-CoA derived from fatty acids thus enters a final common pathway of oxidation with the acetyl-CoA derived from glucose via glycolysis and pyruvate oxidation (see Fig. 16–1). The first two stages of fatty acid oxidation produce the reduced electron carriers NADH and $FADH_2$, which in the third stage donate electrons to the mitochondrial respiratory chain, through which the

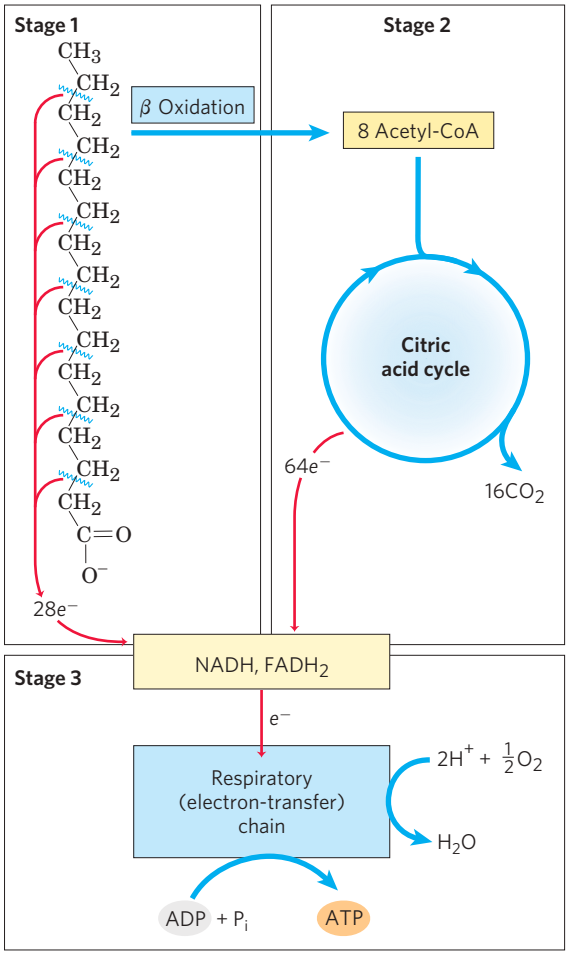

FIGURE 17–7 Stages of fatty acid oxidation. Stage 1: A long-chain fatty acid is oxidized to yield acetyl residues in the form of acetyl-CoA. This process is called β oxidation. Stage 2: The acetyl groups are oxidized to CO_2 via the citric acid cycle. Stage 3: Electrons derived from the oxidations of stages 1 and 2 pass to O_2 via the mitochondrial respiratory chain, providing the energy for ATP synthesis by oxidative phosphorylation.

electrons pass to oxygen with the concomitant phosphorylation of ADP to ATP (Fig. 17–7). The energy released by fatty acid oxidation is thus conserved as ATP.

We now take a closer look at the first stage of fatty acid oxidation, beginning with the simple case of a saturated fatty acyl chain with an even number of carbons, then turning to the slightly more complicated cases of unsaturated and odd-number chains. We also consider the regulation of fatty acid oxidation, the β-oxidative processes as they occur in organelles other than mitochondria, and, finally, two less-general modes of fatty acid catabolism, α oxidation and ω oxidation.

The β Oxidation of Saturated Fatty Acids Has Four Basic Steps

Four enzyme-catalyzed reactions make up the first stage of fatty acid oxidation **(Fig. 17–8a)**. First, dehydrogenation of fatty acyl–CoA produces a double bond between the α and β carbon atoms (C-2 and C-3), yielding a ***trans*-Δ^2-enoyl-CoA** (the symbol Δ^2 designates the position of the double bond; you may want to review fatty acid nomenclature, p. 357.) Note that the new double bond has the trans configuration, whereas the double bonds in naturally occurring unsaturated fatty acids are normally in the cis configuration. We consider the significance of this difference later.

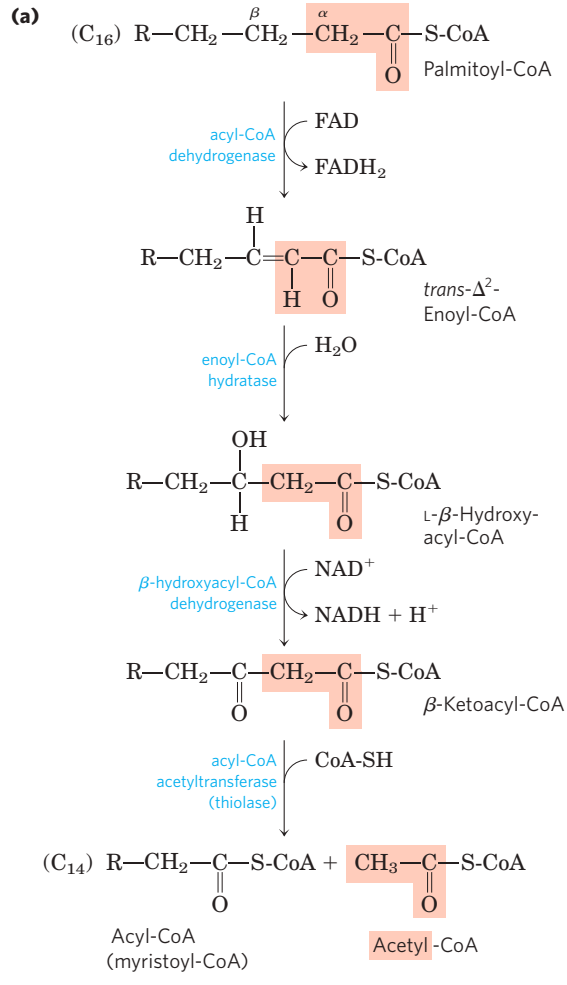

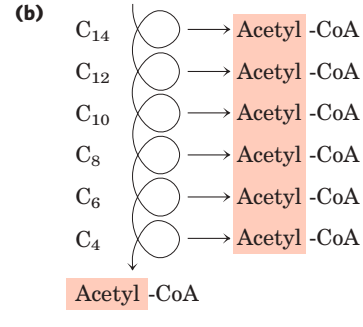

FIGURE 17–8 The β-oxidation pathway. (a) In each pass through this four-step sequence, one acetyl residue (shaded in pink) is removed in the form of acetyl-CoA from the carboxyl end of the fatty acyl chain—in this example palmitate (C_{16}), which enters as palmitoyl-CoA. **(b)** Six more passes through the pathway yield seven more molecules of acetyl-CoA, the seventh arising from the last two carbon atoms of the 16-carbon chain. Eight molecules of acetyl-CoA are formed in all.

This first step is catalyzed by three isozymes of **acyl-CoA dehydrogenase**, each specific for a range of fatty-acyl chain lengths: very-long-chain acyl-CoA dehydrogenase (VLCAD), acting on fatty acids of 12 to 18 carbons; medium-chain (MCAD), acting on fatty acids of 4 to 14 carbons; and short-chain (SCAD), acting on fatty acids of 4 to 8 carbons. All three isozymes are flavoproteins with FAD (see Fig. 13–27) as a prosthetic group. The electrons removed from the fatty acyl–CoA are transferred to FAD, and the reduced form of the dehydrogenase immediately donates its electrons to an electron carrier of the mitochondrial respiratory chain, the **electron-transferring flavoprotein (ETF)** (see Fig. 19–8). The oxidation catalyzed by an acyl-CoA dehydrogenase is analogous to succinate dehydrogenation in the citric acid cycle (p. 646); in both reactions the enzyme is bound to the inner membrane, a double bond is introduced into a carboxylic acid between the α and β carbons, FAD is the electron acceptor, and electrons from the reaction ultimately enter the respiratory chain and pass to O_2, with the concomitant synthesis of about 1.5 ATP molecules per electron pair.

In the second step of the β-oxidation cycle (Fig. 17–8a), water is added to the double bond of the *trans*-Δ^2-enoyl-CoA to form the L stereoisomer of **β-hydroxyacyl-CoA (3-hydroxyacyl-CoA)**. This reaction, catalyzed by **enoyl-CoA hydratase**, is formally analogous to the fumarase reaction in the citric acid cycle, in which H_2O adds across an α–β double bond (p. 647).

In the third step, L-β-hydroxyacyl-CoA is dehydrogenated to form **β-ketoacyl-CoA**, by the action of **β-hydroxyacyl-CoA dehydrogenase**; NAD^+ is the electron acceptor. This enzyme is absolutely specific for the L stereoisomer of hydroxyacyl-CoA. The NADH formed in the reaction donates its electrons to **NADH dehydrogenase**, an electron carrier of the respiratory chain, and ATP is formed from ADP as the electrons pass to O_2. The reaction catalyzed by β-hydroxyacyl-CoA dehydrogenase is closely analogous to the malate dehydrogenase reaction of the citric acid cycle (p. 647).

The fourth and last step of the β-oxidation cycle is catalyzed by **acyl-CoA acetyltransferase**, more commonly called **thiolase**, which promotes reaction of β-ketoacyl-CoA with a molecule of free coenzyme A to split off the carboxyl-terminal two-carbon fragment of the original fatty acid as acetyl-CoA. The other product is the coenzyme A thioester of the fatty acid, now shortened by two carbon atoms (Fig. 17–8a). This reaction is called thiolysis, by analogy with the process of hydrolysis, because the β-ketoacyl-CoA is cleaved by reaction with the thiol group of coenzyme A. The thiolase reaction is a reverse Claisen condensation (see Fig. 13–4).

The last three steps of this four-step sequence are catalyzed by either of two sets of enzymes, with the enzymes employed depending on the length of the fatty acyl chain. For fatty acyl chains of 12 or more carbons, the reactions are catalyzed by a multienzyme complex associated with the inner mitochondrial membrane, the **trifunctional protein (TFP)**. TFP is a heterooctamer of $\alpha_4\beta_4$ subunits. Each α subunit contains two activities, the enoyl-CoA hydratase and the β-hydroxyacyl-CoA dehydrogenase; the β subunits contain the thiolase activity. This tight association of three enzymes may allow efficient substrate channeling from one active site to the next, without diffusion of the intermediates away from the enzyme surface. When TFP has shortened the fatty acyl chain to 12 or fewer carbons, further oxidations are catalyzed by a set of four soluble enzymes in the matrix.

As noted earlier, the single bond between methylene (—CH_2—) groups in fatty acids is relatively stable. The β-oxidation sequence is an elegant mechanism for destabilizing and breaking these bonds. The first three reactions of β oxidation create a much less stable C—C bond, in which the α carbon (C-2) is bonded to *two* carbonyl carbons (the β-ketoacyl-CoA intermediate). The ketone function on the β carbon (C-3) makes it a good target for nucleophilic attack by the —SH of coenzyme A, catalyzed by thiolase. The acidity of the α hydrogen and the resonance stabilization of the carbanion generated by the departure of this hydrogen make the terminal —CH_2—CO—S-CoA a good leaving group, facilitating breakage of the α–β bond.

We have already seen a reaction sequence nearly identical with these four steps of fatty acid oxidation, in the citric acid cycle reaction steps between succinate and oxaloacetate (see Fig. 16–7). A nearly identical reaction sequence occurs again in the pathways by which the branched-chain amino acids (isoleucine, leucine, and valine) are oxidized as fuels (see Fig. 18–28). **Figure 17–9** shows the common features of these three sequences, almost certainly an example of the conservation of a mechanism by gene duplication and evolution of a new specificity in the enzyme products of the duplicated genes.

The Four β-Oxidation Steps Are Repeated to Yield Acetyl-CoA and ATP

In one pass through the β-oxidation sequence, one molecule of acetyl-CoA, two pairs of electrons, and four protons (H^+) are removed from the long-chain fatty acyl–CoA, shortening it by two carbon atoms. The equation for one pass, beginning with the coenzyme A ester of our example, palmitate, is

$$\text{Palmitoyl-CoA} + \text{CoA} + \text{FAD} + \text{NAD}^+ + \text{H}_2\text{O} \longrightarrow \text{myristoyl-CoA} + \text{acetyl-CoA} + \text{FADH}_2 + \text{NADH} + \text{H}^+ \quad (17\text{–}2)$$

Following removal of one acetyl-CoA unit from palmitoyl-CoA, the coenzyme A thioester of the shortened fatty acid (now the 14-carbon myristate) remains. The myristoyl-CoA can now go through another set of four β-oxidation reactions, exactly analogous to the first, to yield a second molecule of acetyl-CoA and lauroyl-CoA, the coenzyme A thioester of the 12-carbon laurate. Altogether, seven passes through the β-oxidation sequence are required to oxidize one molecule of palmitoyl-CoA to eight molecules of acetyl-CoA (Fig. 17–8b). The overall equation is

$$\text{Palmitoyl-CoA} + 7\text{CoA} + 7\text{FAD} + 7\text{NAD}^+ + 7\text{H}_2\text{O} \longrightarrow 8\ \text{acetyl-CoA} + 7\text{FADH}_2 + 7\text{NADH} + 7\text{H}^+ \quad (17\text{–}3)$$

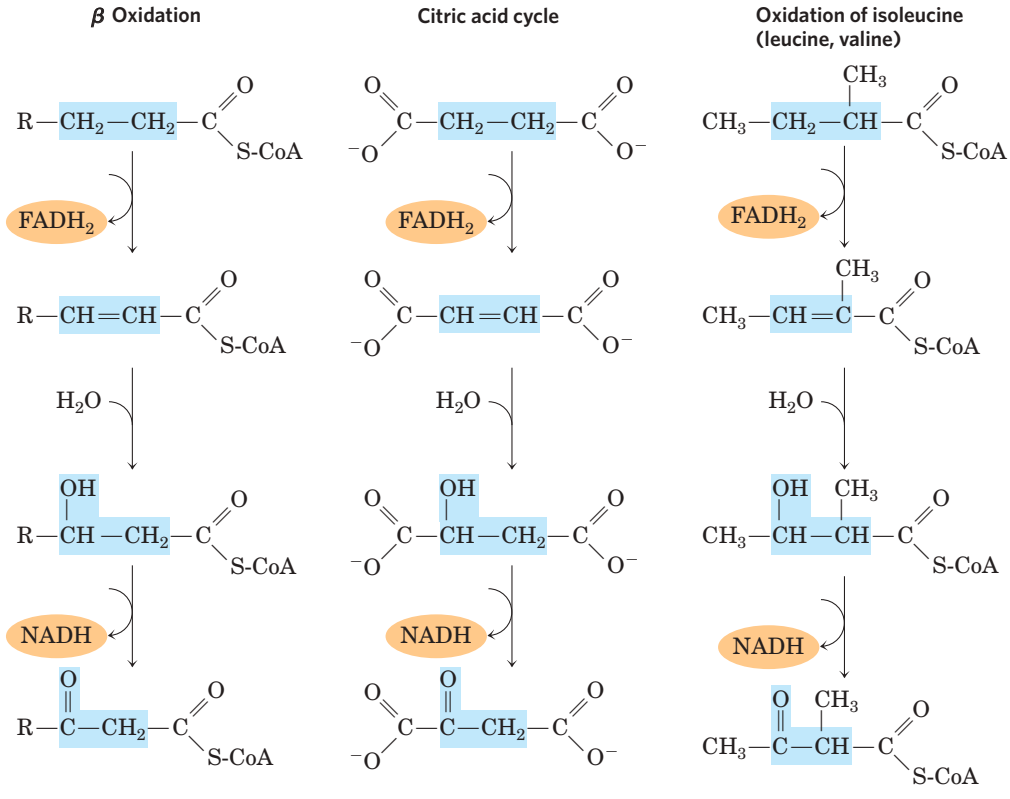

FIGURE 17–9 A conserved reaction sequence to introduce a carbonyl function on the carbon β to a carboxyl group. The β-oxidation pathway for fatty acyl-CoAs, the pathway from succinate to oxaloacetate in the citric acid cycle, and the pathway by which the deaminated carbon skeletons from isoleucine, leucine, and valine are oxidized as fuels, use the same reaction sequence.

Each molecule of $FADH_2$ formed during oxidation of the fatty acid donates a pair of electrons to ETF of the respiratory chain, and about 1.5 molecules of ATP are generated during the ensuing transfer of each electron pair to O_2. Similarly, each molecule of NADH formed delivers a pair of electrons to the mitochondrial NADH dehydrogenase, and the subsequent transfer of each pair of electrons to O_2 results in formation of about 2.5 molecules of ATP. Thus four molecules of ATP are formed for each two-carbon unit removed in one pass through the sequence. Note that water is also produced in this process. Transfer of electrons from NADH or $FADH_2$ to O_2 yields one H_2O per electron pair. Reduction of O_2 by NADH also consumes one H^+ per NADH molecule: $NADH + H^+ + \frac{1}{2}O_2 \longrightarrow NAD^+ + H_2O$. In hibernating animals, fatty acid oxidation provides metabolic energy, heat, and water—all essential for survival of an animal that neither eats nor drinks for long periods (Box 17–1). Camels obtain water to supplement the meager supply available in their natural environment by oxidation of fats stored in their hump.

The overall equation for the oxidation of palmitoyl-CoA to eight molecules of acetyl-CoA, including the electron transfers and oxidative phosphorylations, is

$$\text{Palmitoyl-CoA} + 7\text{CoA} + 7O_2 + 28P_i + 28\text{ADP} \longrightarrow 8\text{ acetyl-CoA} + 28\text{ATP} + 7H_2O \qquad (17\text{–}4)$$

Acetyl-CoA Can Be Further Oxidized in the Citric Acid Cycle

The acetyl-CoA produced from the oxidation of fatty acids can be oxidized to CO_2 and H_2O by the citric acid cycle. The following equation represents the balance sheet for the second stage in the oxidation of palmitoyl-CoA, together with the coupled phosphorylations of the third stage:

$$8\text{ Acetyl-CoA} + 16O_2 + 80P_i + 80\text{ADP} \longrightarrow 8\text{CoA} + 80\text{ATP} + 16CO_2 + 16H_2O \qquad (17\text{–}5)$$

Combining Equations 17–4 and 17–5, we obtain the overall equation for the complete oxidation of palmitoyl-CoA to carbon dioxide and water:

$$\text{Palmitoyl-CoA} + 23O_2 + 108P_i + 108\text{ADP} \longrightarrow \text{CoA} + 108\text{ATP} + 16CO_2 + 23H_2O \qquad (17\text{–}6)$$

Table 17–1 summarizes the yields of NADH, $FADH_2$, and ATP in the successive steps of palmitoyl-CoA oxidation. Note that because the activation of palmitate to palmitoyl-CoA breaks both phosphoanhydride bonds in ATP (Fig. 17–5), the energetic cost of activating a fatty acid is equivalent to two ATP, and the net gain per molecule of palmitate is 106 ATP. The standard free-energy change for the oxidation of palmitate to CO_2 and H_2O is about 9,800 kJ/mol. Under standard conditions, the energy recovered as the phosphate bond energy of ATP is 106×30.5 kJ/mol = 3,230 kJ/mol, about 33% of the

BOX 17–1 Fat Bears Carry Out β Oxidation in Their Sleep

Many animals depend on fat stores for energy during hibernation, during migratory periods, and in other situations involving radical metabolic adjustments. One of the most pronounced adjustments of fat metabolism occurs in hibernating grizzly bears. These animals remain in a continuous state of dormancy for periods as long as seven months. Unlike most hibernating species, the bear maintains a body temperature of between 32 and 35°C, close to the normal (nonhibernating) level. Although expending about 25,000 kJ/day (6,000 kcal/day), the bear does not eat, drink, urinate, or defecate for months at a time.

Experimental studies have shown that hibernating grizzly bears use body fat as their sole fuel. Fat oxidation yields sufficient energy for maintenance of body temperature, active synthesis of amino acids and proteins, and other energy-requiring activities, such as membrane transport. Fat oxidation also releases large amounts of water, as described in the text, which replenishes water lost in breathing. The glycerol released by degradation of triacylglycerols is converted into blood glucose by gluconeogenesis. Urea formed during breakdown of amino acids is reabsorbed in the kidneys and recycled, the amino groups reused to make new amino acids for maintaining body proteins.

Bears store an enormous amount of body fat in preparation for their long sleep. An adult grizzly consumes about 38,000 kJ/day during the late spring and summer, but as winter approaches it feeds 20 hours a day, consuming up to 84,000 kJ daily. This change in feeding is a response to a seasonal change in hormone secretion. Large amounts of triacylglycerols are formed from the huge intake of carbohydrates during the fattening-up period. Other hibernating species, including the tiny dormouse, also accumulate large amounts of body fat.

A grizzly bear prepares its hibernation nest near the McNeil River in Canada.

TABLE 17–1 Yield of ATP during Oxidation of One Molecule of Palmitoyl-CoA to CO_2 and H_2O

Enzyme catalyzing the oxidation step	Number of NADH or $FADH_2$ formed	Number of ATP ultimately formed*
Acyl-CoA dehydrogenase	7 $FADH_2$	10.5
β-Hydroxyacyl-CoA dehydrogenase	7 NADH	17.5
Isocitrate dehydrogenase	8 NADH	20
α-Ketoglutarate dehydrogenase	8 NADH	20
Succinyl-CoA synthetase		8†
Succinate dehydrogenase	8 $FADH_2$	12
Malate dehydrogenase	8 NADH	20
Total		108

*These calculations assume that mitochondrial oxidative phosphorylation produces 1.5 ATP per $FADH_2$ oxidized and 2.5 ATP per NADH oxidized.

†GTP produced directly in this step yields ATP in the reaction catalyzed by nucleoside diphosphate kinase (p. 526).

theoretical maximum. However, when the free-energy changes are calculated from actual concentrations of reactants and products under intracellular conditions (see Worked Example 13–2, p. 519), the free-energy recovery is more than 60%; the energy conservation is remarkably efficient.

Oxidation of Unsaturated Fatty Acids Requires Two Additional Reactions

The fatty acid oxidation sequence just described is typical when the incoming fatty acid is saturated (that is, has only single bonds in its carbon chain). However, most of the fatty acids in the triacylglycerols and phospholipids of animals and plants are unsaturated, having one or more double bonds. These bonds are in the cis configuration and cannot be acted upon by enoyl-CoA hydratase, the enzyme catalyzing the addition of H_2O to the trans double bond of the Δ^2-enoyl-CoA generated during β oxidation. Two auxiliary enzymes are needed for β oxidation of the common unsaturated fatty acids: an isomerase and a reductase. We illustrate these auxiliary reactions with two examples.

Oleate is an abundant 18-carbon monounsaturated fatty acid with a cis double bond between C-9 and C-10 (denoted Δ^9). In the first step of oxidation, oleate is converted to oleoyl-CoA and, like the saturated fatty acids, enters the mitochondrial matrix via the carnitine shuttle (Fig. 17–6). Oleoyl-CoA then undergoes three passes through the fatty acid oxidation cycle to yield three molecules of acetyl-CoA and the coenzyme A ester of a Δ^3, 12-carbon unsaturated fatty acid, *cis*-Δ^3-dodecenoyl-CoA **(Fig. 17–10)**. This product cannot serve as a substrate for enoyl-CoA hydratase, which acts only on trans double bonds. The auxiliary enzyme **Δ^3,Δ^2-enoyl-CoA isomerase** isomerizes the *cis*-Δ^3-enoyl-CoA to the *trans*-Δ^2-enoyl-CoA, which is converted by enoyl-CoA hydratase into the corresponding L-β-hydroxyacyl-CoA (*trans*-Δ^2-dodecenoyl-CoA). This intermediate is now acted upon by the remaining enzymes of β oxidation to yield acetyl-CoA and the coenzyme A ester of a 10-carbon saturated fatty acid, decanoyl-CoA. The latter undergoes four more passes through the β-oxidation pathway to yield five more molecules of acetyl-CoA. Altogether, nine acetyl-CoAs are produced from one molecule of the 18-carbon oleate.

The other auxiliary enzyme (a reductase) is required for oxidation of polyunsaturated fatty acids—for example, the 18-carbon linoleate, which has a *cis*-Δ^9,*cis*-Δ^{12} configuration **(Fig. 17–11)**. Linoleoyl-CoA undergoes three passes through the β-oxidation sequence to yield three molecules of acetyl-CoA and the coenzyme A ester of a 12-carbon unsaturated fatty acid with a *cis*-Δ^3,*cis*-Δ^6 configuration. This intermediate cannot be used by the enzymes of the β-oxidation pathway; its double bonds are in the wrong position

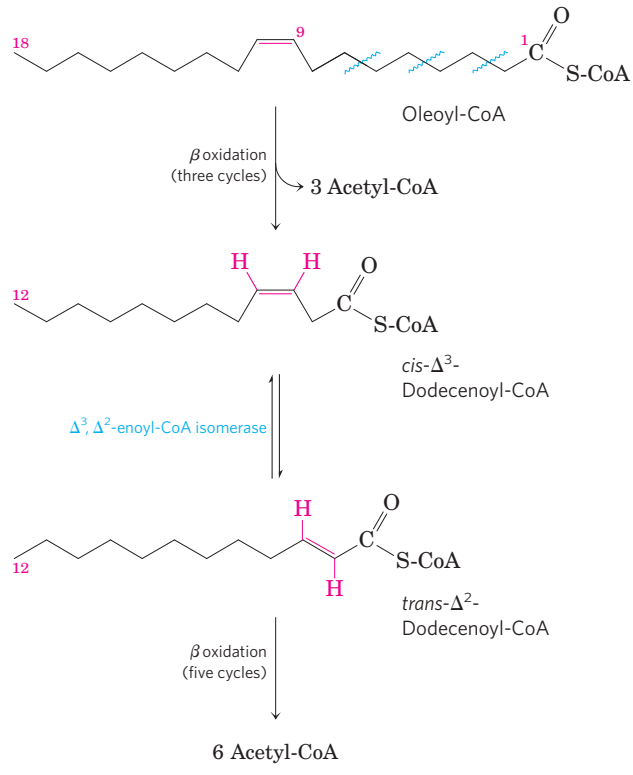

FIGURE 17–10 Oxidation of a monounsaturated fatty acid. Oleic acid, as oleoyl-CoA (Δ^9), is the example used here. Oxidation requires an additional enzyme, enoyl-CoA isomerase, to reposition the double bond, converting the cis isomer to a trans isomer, a normal intermediate in β oxidation.

and have the wrong configuration (cis, not trans). However, the combined action of enoyl-CoA isomerase and **2,4-dienoyl-CoA reductase**, as shown in Figure 17–11, allows reentry of this intermediate into the β-oxidation pathway and its degradation to six acetyl-CoAs. The overall result is conversion of linoleate to nine molecules of acetyl-CoA.

Complete Oxidation of Odd-Number Fatty Acids Requires Three Extra Reactions

Although most naturally occurring lipids contain fatty acids with an even number of carbon atoms, fatty acids with an odd number of carbons are common in the lipids of many plants and some marine organisms. Cattle and other ruminant animals form large amounts of the three-carbon **propionate** (CH_3—CH_2—COO^-) during fermentation of carbohydrates in the rumen. The propionate is absorbed into the blood and oxidized by the liver and other tissues. And small quantities of propionate are added as a mold inhibitor to some breads and cereals, thus entering the human diet.

Long-chain odd-number fatty acids are oxidized in the same pathway as the even-number acids, beginning at the carboxyl end of the chain. However, the substrate for the last pass through the β-oxidation sequence is a fatty acyl–CoA with a five-carbon fatty acid. When this

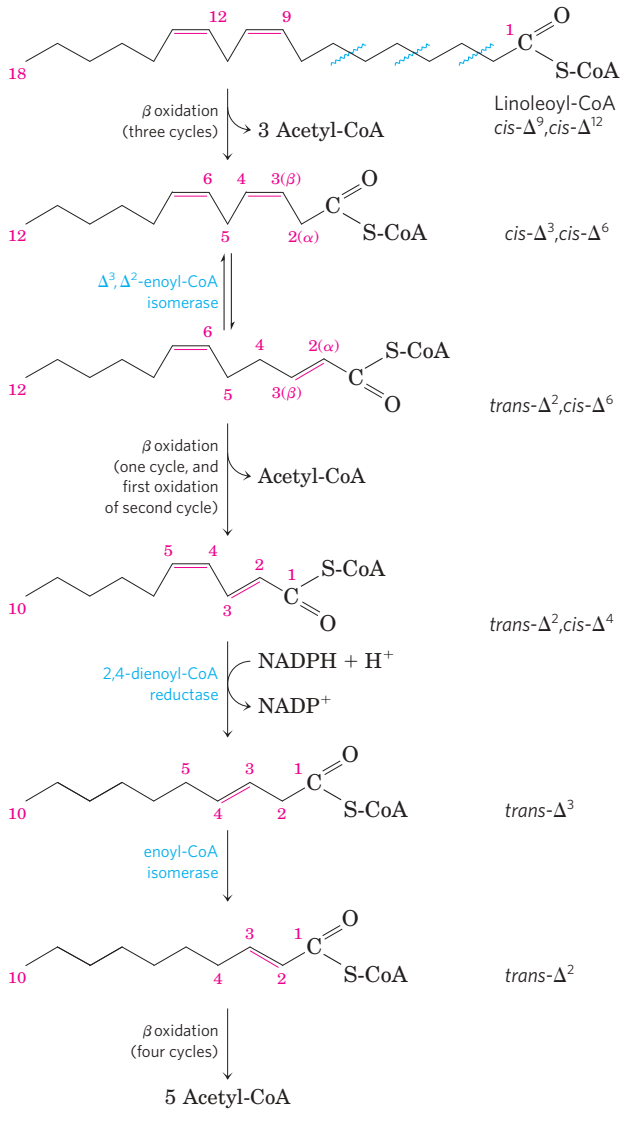

FIGURE 17–11 Oxidation of a polyunsaturated fatty acid. The example here is linoleic acid, as linoleoyl-CoA ($\Delta^{9,12}$). Oxidation requires a second auxiliary enzyme in addition to enoyl-CoA isomerase: NADPH-dependent 2,4-dienoyl-CoA reductase. The combined action of these two enzymes converts a *trans*-Δ^2,*cis*-Δ^4-dienoyl-CoA intermediate to the *trans*-Δ^2-enoyl-CoA substrate necessary for β oxidation.

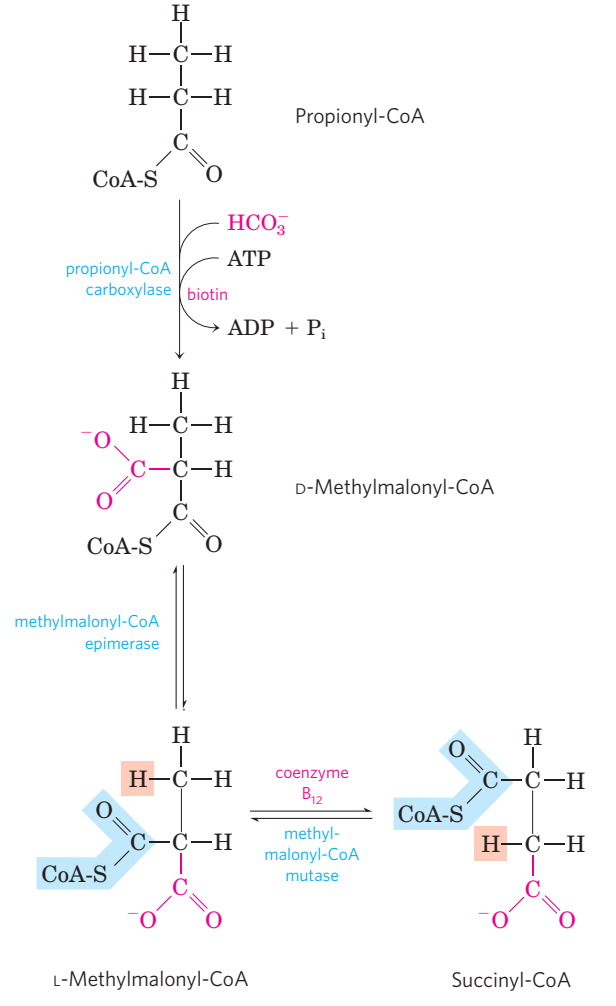

FIGURE 17–12 Oxidation of propionyl-CoA produced by β oxidation of odd-number fatty acids. The sequence involves the carboxylation of propionyl-CoA to D-methylmalonyl-CoA and conversion of the latter to succinyl-CoA. This conversion requires epimerization of D- to L-methylmalonyl-CoA, followed by a remarkable reaction in which substituents on adjacent carbon atoms exchange positions (see Box 17–2).

is oxidized and cleaved, the products are acetyl-CoA and **propionyl-CoA**. The acetyl-CoA can be oxidized in the citric acid cycle, of course, but propionyl-CoA enters a different pathway having three enzymes.

Propionyl-CoA is first carboxylated to form the D stereoisomer of **methylmalonyl-CoA (Fig. 17–12)** by **propionyl-CoA carboxylase**, which contains the cofactor biotin. In this enzymatic reaction, as in the pyruvate carboxylase reaction (see Fig. 16–17), CO_2 (or its hydrated ion, HCO_3^-) is activated by attachment to biotin before its transfer to the substrate, in this case the propionate moiety. Formation of the carboxybiotin intermediate requires energy, which is provided by ATP. The D-methylmalonyl-CoA thus formed is enzymatically epimerized to its L stereoisomer by **methylmalonyl-CoA epimerase** (Fig. 17–12). The L-methylmalonyl-CoA then undergoes an intramolecular rearrangement to form succinyl-CoA, which can enter the citric acid cycle. This rearrangement is catalyzed by **methylmalonyl-CoA mutase**, which requires as its coenzyme **5′-deoxyadenosylcobalamin**, or **coenzyme B_{12}**, which is derived from vitamin B_{12} (cobalamin). Box 17–2 describes the role of coenzyme B_{12} in this remarkable exchange reaction.

Fatty Acid Oxidation Is Tightly Regulated

Oxidation of fatty acids consumes a precious fuel, and it is regulated so as to occur only when the need for energy requires it. In the liver, fatty acyl–CoA formed in the cytosol has two major pathways open to it: (1) β oxidation by enzymes in mitochondria or (2) conversion

into triacylglycerols and phospholipids by enzymes in the cytosol. The pathway taken depends on the rate of transfer of long-chain fatty acyl–CoA into mitochondria. The three-step process (carnitine shuttle) by which fatty acyl groups are carried from cytosolic fatty acyl–CoA into the mitochondrial matrix (Fig. 17–6) is rate-limiting for fatty acid oxidation and is an important point of regulation. Once fatty acyl groups have entered the mitochondrion, they are committed to oxidation to acetyl-CoA.

Malonyl-CoA, the first intermediate in the cytosolic biosynthesis of long-chain fatty acids from acetyl-CoA (see Fig. 21–2), increases in concentration whenever the animal is well supplied with carbohydrate; excess glucose that cannot be oxidized or stored as glycogen is converted in the cytosol into fatty acids for storage as triacylglycerol. The inhibition of carnitine acyltransferase I by malonyl-CoA **(Fig. 17–13)** ensures that the oxidation of fatty acids is inhibited whenever the liver is amply supplied with glucose as fuel and is actively making triacylglycerols from excess glucose.

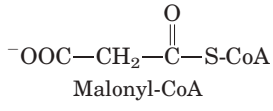

Two of the enzymes of β oxidation are also regulated by metabolites that signal energy sufficiency. When the [NADH]/[NAD^+] ratio is high, β-hydroxyacyl-CoA dehydrogenase is inhibited; in addition, high concentrations of acetyl-CoA inhibit thiolase.

Recall from Chapter 15 that during periods of vigorous muscle contraction or during fasting, the fall in [ATP] and the rise in [AMP] activate AMPK, the AMP-activated protein kinase. AMPK phosphorylates several target enzymes, including acetyl-CoA carboxylase, which catalyzes malonyl-CoA synthesis. This phosphorylation and thus inhibition of acetyl-CoA carboxylase lowers the concentration of malonyl-CoA, relieving the inhibition of fatty acyl–carnitine transport into mitochondria (Fig. 17–13) and allowing β oxidation to replenish the supply of ATP.

Transcription Factors Turn on the Synthesis of Proteins for Lipid Catabolism

In addition to the various short-term regulatory mechanisms that modulate the activity of existing enzymes, transcriptional regulation can change the number of molecules of the enzymes of fatty acid oxidation on a longer time scale, minutes to hours. The **PPAR** family of nuclear receptors are transcription factors that affect many metabolic processes in response to a variety of fatty acid–like ligands. (They were originally recognized as *p*eroxisome *p*roliferator-*a*ctivated *r*eceptors, then were found to function more broadly.) PPARα acts in muscle, adipose tissue, and liver to turn on a set of genes essential for fatty acid oxidation, including the

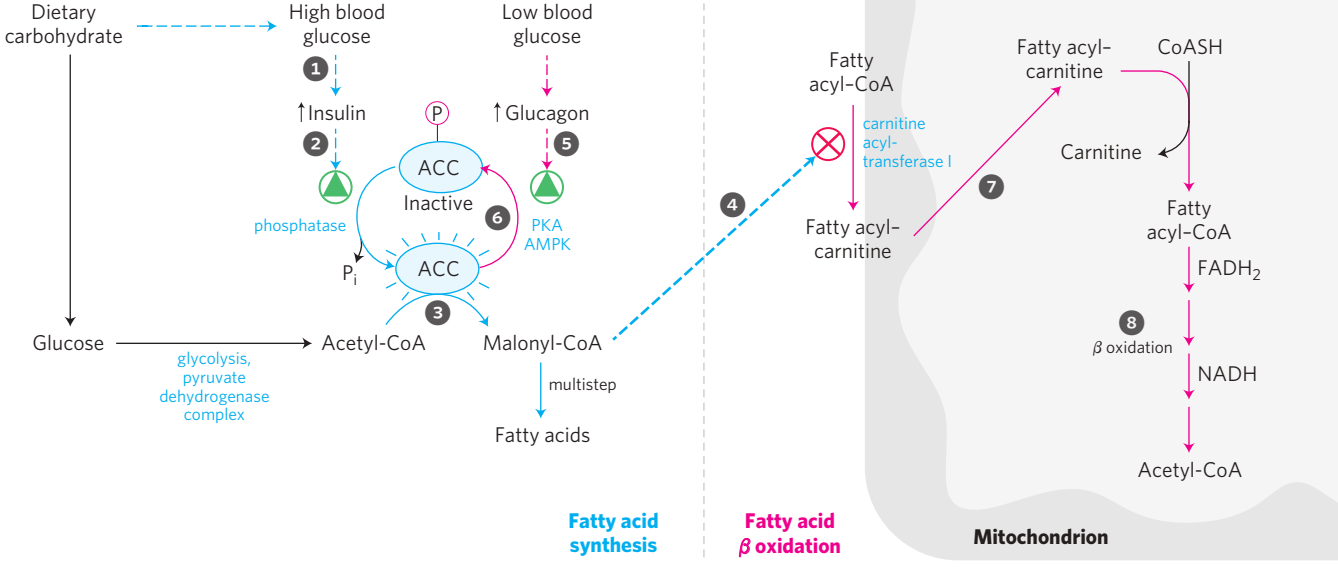

FIGURE 17–13 Coordinated regulation of fatty acid synthesis and breakdown. When the diet provides a ready source of carbohydrate as fuel, β oxidation of fatty acids is unnecessary and is therefore down-regulated. Two enzymes are key to the coordination of fatty acid metabolism: acetyl-CoA carboxylase (ACC), the first enzyme in the synthesis of fatty acids (see Fig. 21–1), and carnitine acyltransferase I, which limits the transport of fatty acids into the mitochondrial matrix for β oxidation (see Fig. 17–6). Ingestion of a high-carbohydrate meal raises the blood glucose level and thus ❶ triggers the release of insulin. ❷ Insulin-dependent protein phosphatase dephosphorylates ACC, activating it. ❸ ACC catalyzes the formation of malonyl-CoA (the first intermediate of fatty acid synthesis), and ❹ malonyl-CoA inhibits carnitine acyltransferase I, thereby preventing fatty acid entry into the mitochondrial matrix. When blood glucose levels drop between meals, ❺ glucagon release activates cAMP-dependent protein kinase (PKA), which ❻ phosphorylates and inactivates ACC. The concentration of malonyl-CoA falls, the inhibition of fatty acid entry into mitochondria is relieved, and ❼ fatty acids enter the mitochondrial matrix and ❽ become the major fuel. Because glucagon also triggers the mobilization of fatty acids in adipose tissue, a supply of fatty acids begins arriving in the blood.

BOX 17–2 Coenzyme B_{12}: A Radical Solution to a Perplexing Problem

In the methylmalonyl-CoA mutase reaction (see Fig. 17–12), the group —CO—S-CoA at C-2 of the original propionate exchanges position with a hydrogen atom at C-3 of the original propionate (Fig. 1a). Coenzyme B_{12} is the cofactor for this reaction, as it is for almost all enzymes that catalyze reactions of this general type (Fig. 1b). These coenzyme B_{12}–dependent processes are among the very few enzymatic reactions in biology in which there is an exchange of an alkyl or substituted alkyl group (X) with a hydrogen atom on an adjacent carbon, *with no mixing of the transferred hydrogen atom with the hydrogen of the solvent*, H_2O. How can the hydrogen atom move between two carbons without mixing with the enormous excess of hydrogen atoms in the solvent?

Coenzyme B_{12} is the cofactor form of vitamin B_{12}, which is unique among all the vitamins in that it contains not only a complex organic molecule but an essential trace element, cobalt. The complex **corrin ring system** of vitamin B_{12} (colored blue in Fig. 2), to which cobalt (as Co^{3+}) is coordinated, is chemically related to the porphyrin ring system of heme and heme proteins (see Fig. 5–1). A fifth coordination position of cobalt is filled by dimethylbenzimidazole ribonucleotide (shaded yellow), bound covalently by its 3′-phosphate group to a side chain of the corrin ring, through aminoisopropanol. The formation of this complex cofactor occurs in one of only two known reactions in which triphosphate is cleaved from ATP (Fig. 3); the other reaction is the formation of *S*-adenosylmethionine from ATP and methionine (see Fig. 18–18).

Vitamin B_{12} as usually isolated is called **cyanocobalamin**, because it contains a cyano group (picked up during purification) attached to cobalt in the sixth coordination position. In **5′-deoxyadenosylcobalamin**, the cofactor for methylmalonyl-CoA mutase, the cyano group is replaced by the **5′-deoxyadenosyl** group (red in Fig. 2), covalently bound through C-5′ to the cobalt. The three-dimensional structure of the cofactor was determined by Dorothy Crowfoot Hodgkin in 1956, using x-ray crystallography.

Dorothy Crowfoot Hodgkin, 1910–1994

The key to understanding how coenzyme B_{12} catalyzes hydrogen exchange lies in the properties of the covalent bond between cobalt and C-5′ of the deoxyadenosyl group (Fig. 2). This is a relatively weak bond; its bond dissociation energy is about 110 kJ/mol, compared with 348 kJ/mol for a typical C—C bond or 414 kJ/mol for a C—H bond. Merely illuminating the

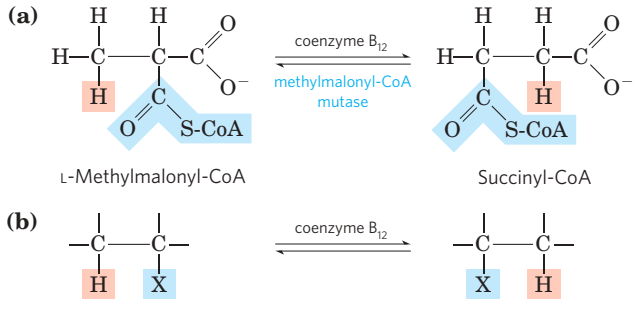

FIGURE 1

compound with visible light is enough to break this Co—C bond. (This extreme photolability probably accounts for the absence of vitamin B_{12} in plants.) Dissociation produces a 5′-deoxyadenosyl radical and the Co^{2+} form of the vitamin. The chemical function of 5′-deoxyadenosylcobalamin is to generate free radicals in this way, thus initiating a series of transformations such as that illustrated in Figure 4—a postulated mechanism for the reaction catalyzed by methylmalonyl-CoA

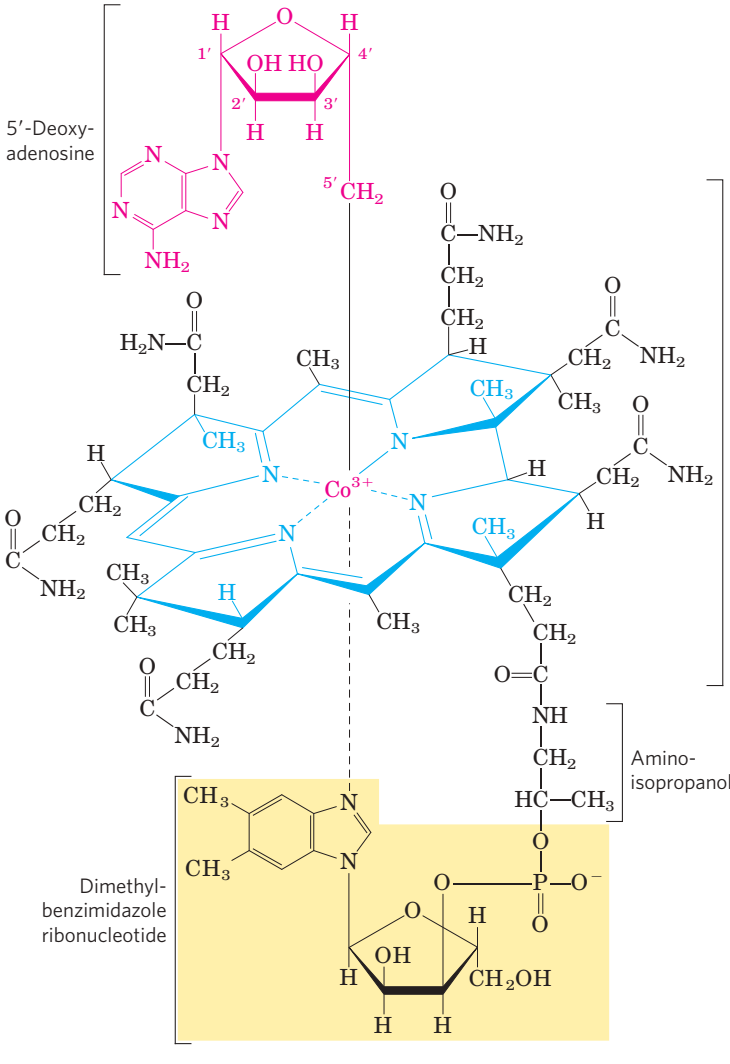

FIGURE 2

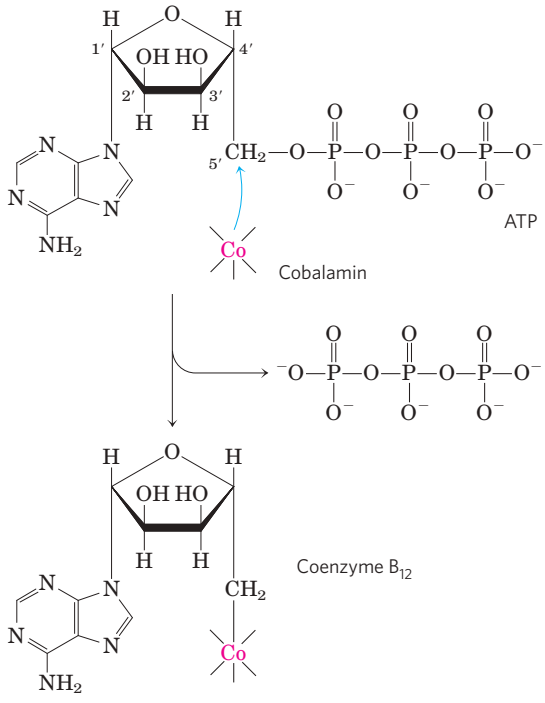

FIGURE 3

mutase and several other coenzyme B_{12}–dependent transformations. In this postulated mechanism, the migrating hydrogen atom never exists as a free species and is thus never free to exchange with the hydrogen of surrounding water molecules.

Vitamin B_{12} deficiency results in serious disease. This vitamin is not made by plants or animals and can be synthesized only by a few species of microorganisms. It is required by healthy people in only minute amounts, about 3 μg/day. The serious disease **pernicious anemia** results from failure to absorb vitamin B_{12} efficiently from the intestine, where it is synthesized by intestinal bacteria or obtained from digestion of meat. Individuals with this disease do not produce sufficient amounts of **intrinsic factor**, a glycoprotein essential to vitamin B_{12} absorption. The pathology in pernicious anemia includes reduced production of erythrocytes, reduced levels of hemoglobin, and severe, progressive impairment of the central nervous system. Administration of large doses of vitamin B_{12} alleviates these symptoms in at least some cases. ■

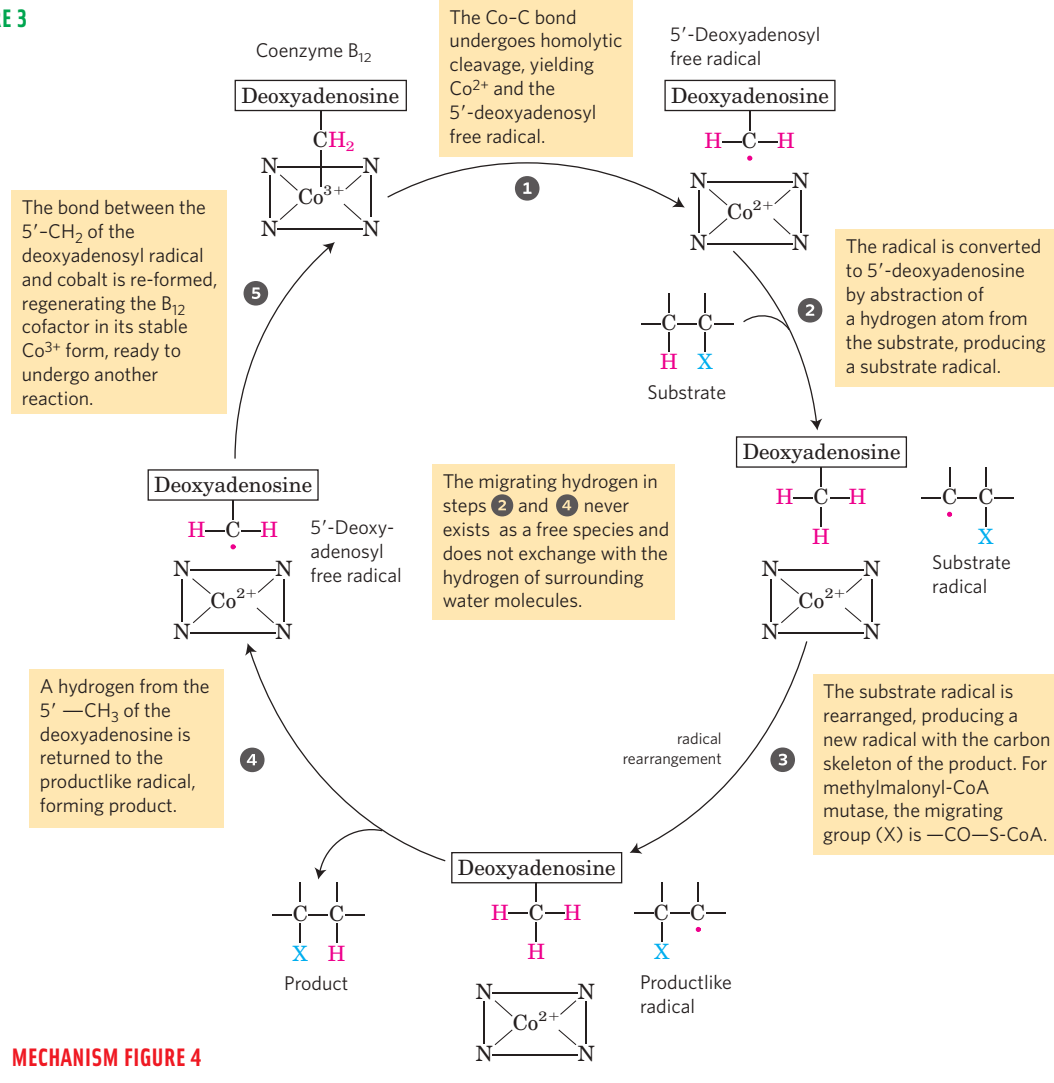

MECHANISM FIGURE 4

fatty acid transporter, carnitine acyltransferases I and II, fatty acyl–CoA dehydrogenases for short, medium, long, and very long acyl chains, and related enzymes. This response is triggered when a cell or organism has an increased demand for energy from fat catabolism, such as during a fast between meals or under conditions of longer-term starvation. Glucagon, released in response to low blood glucose, can act through cAMP and the transcription factor CREB to turn on certain genes for lipid catabolism.

Another situation that is accompanied by major changes in the expression of the enzymes of fatty acid oxidation is the transition from fetal to neonatal metabolism in the heart. In the fetus the principal fuels are glucose and lactate, but in the neonatal heart, fatty acids are the main fuel. At the time of this transition, PPARα is activated and in turn activates the genes essential for fatty acid metabolism. As we will see in Chapter 23, two other transcription factors in the PPAR family also play crucial roles in setting the enzyme complements—and therefore the metabolic activities—of specific tissues at particular times (see Fig. 23–42).

The major site of fatty acid oxidation, at rest and during exercise, is skeletal muscle. Endurance training increases PPARα expression in muscle, leading to increased levels of fatty acid–oxidizing enzymes and increased oxidative capacity of the muscle.

Genetic Defects in Fatty Acyl–CoA Dehydrogenases Cause Serious Disease

Stored triacylglycerols are typically the chief source of energy for muscle contraction, and an inability to oxidize fatty acids from triacylglycerols has serious consequences for health. The most common genetic defect in fatty acid catabolism in U.S. and northern European populations is due to a mutation in the gene encoding the **medium-chain acyl-CoA dehydrogenase (MCAD)**. Among northern Europeans, the frequency of carriers (individuals with this recessive mutation on one of the two homologous chromosomes) is about 1 in 40, and about 1 individual in 10,000 has the disease—that is, has two copies of the mutant MCAD allele and is unable to oxidize fatty acids of 6 to 12 carbons. The disease is characterized by recurring episodes of a syndrome that includes fat accumulation in the liver, high blood levels of octanoic acid (8:0), low blood glucose (hypoglycemia), sleepiness, vomiting, and coma. The pattern of organic acids in the urine helps in the diagnosis of this disease: the urine commonly contains high levels of 6-carbon to 10-carbon dicarboxylic acids (produced by ω oxidation) and low levels of urinary ketone bodies (we discuss ω oxidation below and ketone bodies in Section 17.3). Although individuals may have no symptoms between episodes, the episodes are very serious; mortality from this disease is 25% to 60% in early childhood. If the genetic defect is detected shortly after birth, the infant can be started on a low-fat, high-carbohydrate diet. With early detection and careful management of the diet—including avoiding long intervals between meals, to prevent the body from turning to its fat reserves for energy—the prognosis for these individuals is good.

More than 20 other human genetic defects in fatty acid transport or oxidation have been documented, most much less common than the defect in MCAD. One of the most severe disorders results from loss of the long-chain β-hydroxyacyl-CoA dehydrogenase activity of the trifunctional protein, TFP. Other disorders include defects in the α or β subunits that affect all three activities of TFP and cause serious heart disease and abnormal skeletal muscle. ■

Peroxisomes Also Carry Out β Oxidation

The mitochondrial matrix is the major site of fatty acid oxidation in animal cells, but in certain cells other compartments also contain enzymes capable of oxidizing fatty acids to acetyl-CoA, by a pathway similar but not identical to that in mitochondria. In plant cells, the major site of β oxidation is not mitochondria but peroxisomes.

In **peroxisomes**, membrane-enclosed organelles of animal and plant cells, the intermediates for β oxidation of fatty acids are coenzyme A derivatives, and the process consists of four steps, as in mitochondrial β oxidation **(Fig. 17–14)**: (1) dehydrogenation, (2) addition of water to the resulting double bond, (3) oxidation of the β-hydroxyacyl-CoA to a ketone, and (4) thiolytic cleavage by coenzyme A. (The identical reactions also occur in glyoxysomes, as discussed below.)

One difference between the peroxisomal and mitochondrial pathways is in the chemistry of the first step. In peroxisomes, the flavoprotein acyl-CoA oxidase that introduces the double bond passes electrons directly to O_2, producing H_2O_2 (Fig. 17–14). (Thus the name peroxisomes.) This strong and potentially damaging oxidant is immediately cleaved to H_2O and O_2 by **catalase**. Recall that in mitochondria, the electrons removed in the first oxidation step pass through the respiratory chain to O_2 to produce H_2O, and this process is accompanied by ATP synthesis. In peroxisomes, the energy released in the first oxidative step of fatty acid breakdown is not conserved as ATP, but is dissipated as heat.

A second important difference between mitochondrial and peroxisomal β oxidation in mammals is in the specificity for fatty acyl–CoAs; the peroxisomal system is much more active on very-long-chain fatty acids such as hexacosanoic acid (26:0) and on branched-chain fatty acids such as phytanic acid and pristanic acid (see Fig. 17–18). These less-common fatty acids are obtained in the diet from dairy products, the fat of ruminant animals, meat, and fish. Their catabolism in the peroxisome involves several auxiliary enzymes unique to this organelle. The inability to oxidize these compounds is responsible for several serious human diseases. Individuals with **Zellweger syndrome** are unable to make peroxisomes and therefore lack all the

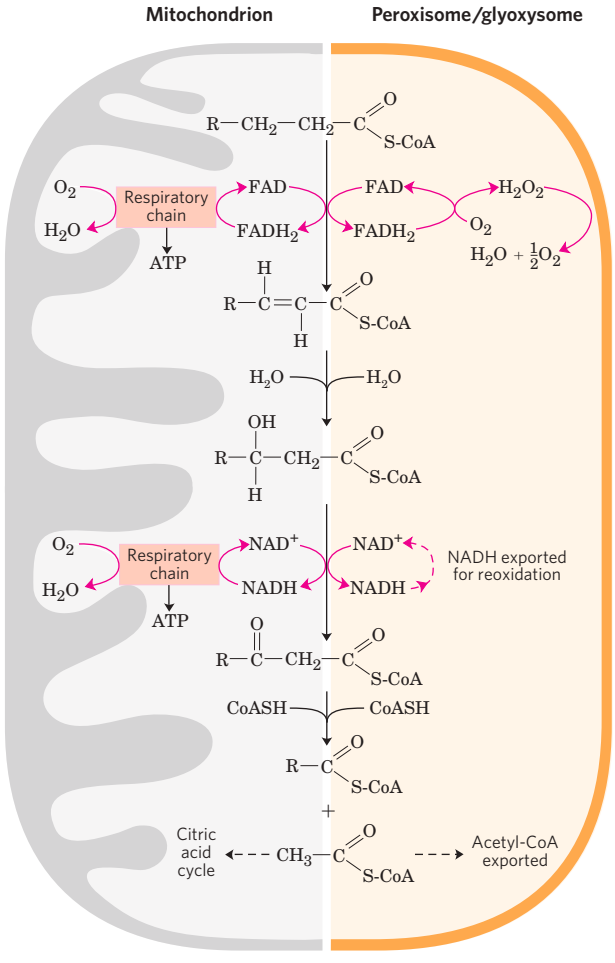

FIGURE 17–14 Comparison of β oxidation in mitochondria and in peroxisomes and glyoxysomes. The peroxisomal/glyoxysomal system differs from the mitochondrial system in three respects: (1) the peroxisomal system prefers very-long-chain fatty acids; (2) in the first oxidative step electrons pass directly to O_2, generating H_2O_2, and (3) the NADH formed in the second oxidative step cannot be reoxidized in the peroxisome or glyoxysome, so reducing equivalents are exported to the cytosol, eventually entering mitochondria. The acetyl-CoA produced by peroxisomes and glyoxysomes is also exported; the acetate from glyoxysomes (organelles found only in germinating seeds) serves as a biosynthetic precursor (see Fig. 17–15). Acetyl-CoA produced in mitochondria is further oxidized in the citric acid cycle.

metabolism unique to that organelle. In **X-linked adrenoleukodystrophy (XALD)**, peroxisomes fail to oxidize very-long-chain fatty acids, apparently for lack of a functional transporter for these fatty acids in the peroxisomal membrane. Both defects lead to accumulation in the blood of very-long-chain fatty acids, especially 26:0. XALD affects young boys before the age of 10 years, causing loss of vision, behavioral disturbances, and death within a few years. ■

In mammals, high concentrations of fats in the diet result in increased synthesis of the enzymes of peroxisomal β oxidation in the liver. Liver peroxisomes do not contain the enzymes of the citric acid cycle and cannot catalyze the oxidation of acetyl-CoA to CO_2. Instead, long-chain or branched fatty acids are catabolized to shorter-chain products, such as hexanoyl-CoA, which are exported to mitochondria and completely oxidized.

Plant Peroxisomes and Glyoxysomes Use Acetyl-CoA from β Oxidation as a Biosynthetic Precursor

In plants, fatty acid oxidation does not occur primarily in mitochondria but in the peroxisomes of leaf tissue and in the glyoxysomes of germinating seeds. Plant peroxisomes and glyoxysomes are similar in structure and function; glyoxysomes, which occur only in germinating seeds, may be considered specialized peroxisomes. The biological role of β oxidation in these organelles is to use stored lipids primarily to provide biosynthetic precursors, not energy.

During seed germination, stored triacylglycerols are converted into glucose, sucrose, and a wide variety of essential metabolites **(Fig. 17–15)**. Fatty acids released from the triacylglycerols are first activated to their coenzyme A derivatives and oxidized in glyoxysomes by the same four-step process that takes place in peroxisomes (Fig. 17–14). The acetyl-CoA produced is converted via the glyoxylate cycle to four-carbon precursors for gluconeogenesis (see Fig. 16–24). Glyoxysomes, like peroxisomes, contain high concentrations of catalase, which converts the H_2O_2 produced by β oxidation to H_2O and O_2.

The β-Oxidation Enzymes of Different Organelles Have Diverged during Evolution

Although the β-oxidation reactions in mitochondria are essentially the same as those in peroxisomes and glyoxysomes, the enzymes (isozymes) differ significantly

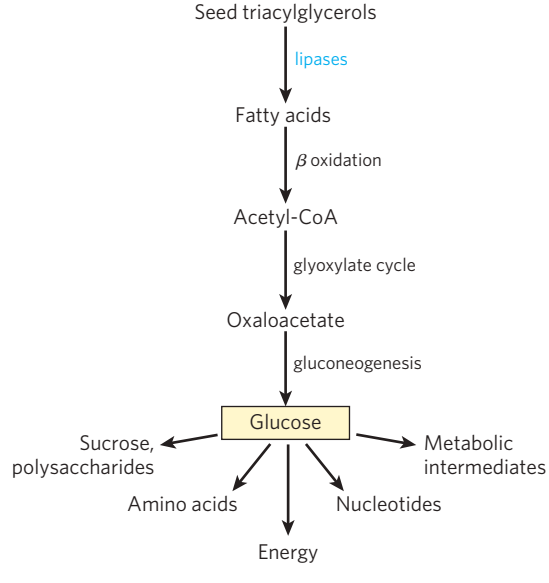

FIGURE 17–15 Triacylglycerols as glucose source in seeds. β Oxidation is one stage in a pathway that converts stored triacylglycerols to glucose in germinating seeds. For more detail, see Figure 16–24.

between the two types of organelles. The differences apparently reflect an evolutionary divergence that occurred very early, with the separation of gram-positive and gram-negative bacteria (see Fig. 1–6).

In mitochondria, the four β-oxidation enzymes that act on short-chain fatty acyl–CoAs are separate, soluble proteins (as noted earlier), similar in structure to the analogous enzymes of gram-positive bacteria **(Fig. 17–16a)**. The gram-negative bacteria have four activities in three soluble subunits (Fig. 17–16b), and the eukaryotic enzyme system that acts on long-chain fatty acids—the trifunctional protein, TFP—has three enzyme activities in two subunits that are membrane-associated (Fig. 17–16c). The β-oxidation enzymes of plant peroxisomes and glyoxysomes, however, form a complex of proteins, one of which contains four enzymatic activities in a single polypeptide chain (Fig. 17–16d). The first enzyme, acyl-CoA oxidase, is a single polypeptide chain; the **multifunctional protein (MFP)** contains the second and third enzyme activities (enoyl-CoA hydratase and hydroxyacyl-CoA dehydrogenase) as well as two auxiliary activities needed for the oxidation of unsaturated fatty acids (D-3-hydroxyacyl-CoA epimerase and Δ^3,Δ^2-enoyl-CoA isomerase); the fourth enzyme, thiolase, is a separate, soluble polypeptide.

It is interesting that the enzymes that catalyze essentially the reversal of β oxidation in the synthesis of fatty acids are also organized differently in bacteria and eukaryotes; in bacteria, the seven enzymes needed for fatty acid synthesis are separate polypeptides, but in mammals, all seven activities are part of a single, huge polypeptide chain. One advantage to the cell in having several enzymes of the same pathway encoded in a single polypeptide chain is that this solves the problem of regulating the synthesis of enzymes that must interact functionally; regulation of the expression of *one* gene ensures production of the same number of active sites for all enzymes in the path. When each enzyme activity is on a separate polypeptide, some mechanism is required to coordinate the synthesis of all the gene products. The *disadvantage* of having several activities on the same polypeptide is that the longer the polypeptide chain, the greater is the probability of a mistake in its synthesis: a single incorrect amino acid in the chain may make all the enzyme activities in that chain useless. Comparison of the gene structures for these proteins in many species may shed light on the reasons for the selection of one or the other strategy in evolution.

The ω Oxidation of Fatty Acids Occurs in the Endoplasmic Reticulum

Although mitochondrial β oxidation, in which enzymes act at the carboxyl end of a fatty acid, is by far the most important catabolic fate for fatty acids in animal cells, there is another pathway in some species, including vertebrates, that involves oxidation of the ω (omega) carbon—the carbon most distant from the carboxyl group. The enzymes unique to **ω oxidation** are located (in vertebrates) in the endoplasmic reticulum of liver and

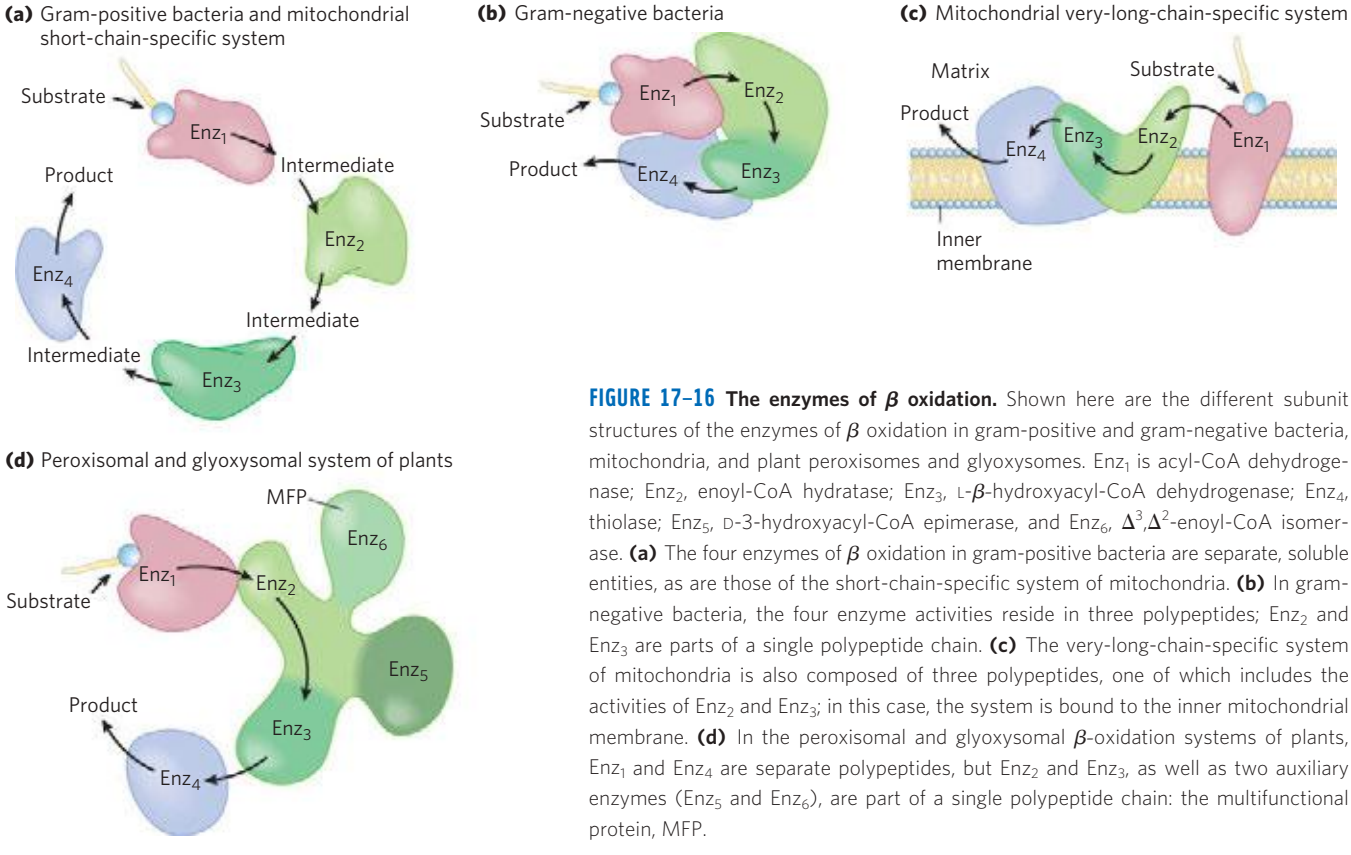

FIGURE 17–16 The enzymes of β oxidation. Shown here are the different subunit structures of the enzymes of β oxidation in gram-positive and gram-negative bacteria, mitochondria, and plant peroxisomes and glyoxysomes. Enz_1 is acyl-CoA dehydrogenase; Enz_2, enoyl-CoA hydratase; Enz_3, L-β-hydroxyacyl-CoA dehydrogenase; Enz_4, thiolase; Enz_5, D-3-hydroxyacyl-CoA epimerase, and Enz_6, Δ^3,Δ^2-enoyl-CoA isomerase. **(a)** The four enzymes of β oxidation in gram-positive bacteria are separate, soluble entities, as are those of the short-chain-specific system of mitochondria. **(b)** In gram-negative bacteria, the four enzyme activities reside in three polypeptides; Enz_2 and Enz_3 are parts of a single polypeptide chain. **(c)** The very-long-chain-specific system of mitochondria is also composed of three polypeptides, one of which includes the activities of Enz_2 and Enz_3; in this case, the system is bound to the inner mitochondrial membrane. **(d)** In the peroxisomal and glyoxysomal β-oxidation systems of plants, Enz_1 and Enz_4 are separate polypeptides, but Enz_2 and Enz_3, as well as two auxiliary enzymes (Enz_5 and Enz_6), are part of a single polypeptide chain: the multifunctional protein, MFP.

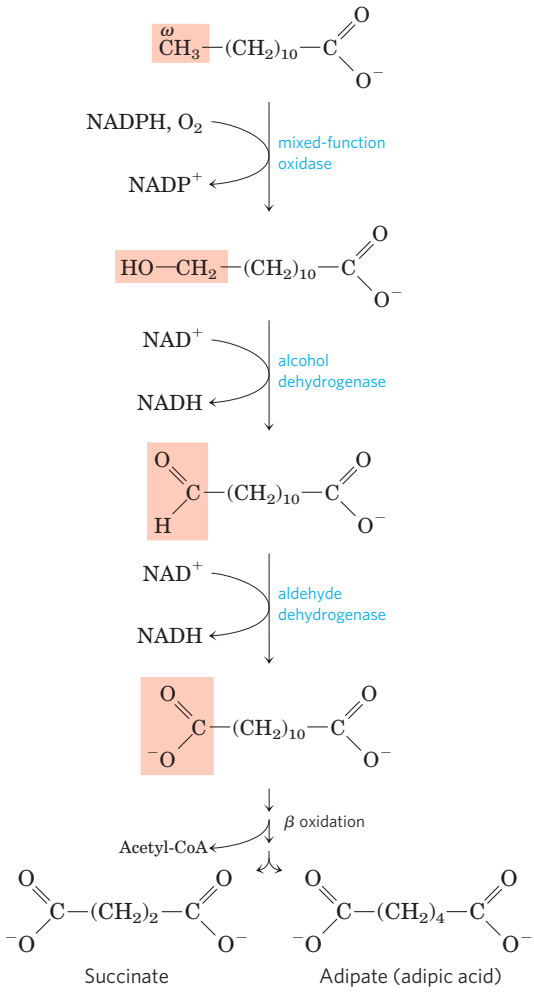

FIGURE 17–17 The ω oxidation of fatty acids in the endoplasmic reticulum. This alternative to β oxidation begins with oxidation of the carbon most distant from the β carbon—the ω (omega) carbon. The substrate is usually a medium-chain fatty acid; shown here is lauric acid (laurate). This pathway is generally not the major route for oxidative catabolism of fatty acids.

kidney, and the preferred substrates are fatty acids of 10 or 12 carbon atoms. In mammals ω oxidation is normally a minor pathway for fatty acid degradation, but when β oxidation is defective (because of mutation or a carnitine deficiency, for example) it becomes more important.

The first step introduces a hydroxyl group onto the ω carbon **(Fig. 17–17)**. The oxygen for this group comes from molecular oxygen (O_2) in a complex reaction that involves cytochrome P450 and the electron donor NADPH. Reactions of this type are catalyzed by **mixed-function oxidases**, described in Box 21–1. Two more enzymes now act on the ω carbon: **alcohol dehydrogenase** oxidizes the hydroxyl group to an aldehyde, and **aldehyde dehydrogenase** oxidizes the aldehyde group to a carboxylic acid, producing a fatty acid with a carboxyl group at each end. At this point, either end can be attached to coenzyme A, and the molecule can enter the mitochondrion and undergo β oxidation by the normal route. In each pass through the β-oxidation pathway, the "double-ended" fatty acid yields dicarboxylic acids such as succinic acid, which can enter the citric acid cycle, and adipic acid (Fig. 17–17).

Phytanic Acid Undergoes α Oxidation in Peroxisomes

The presence of a methyl group on the β carbon of a fatty acid makes β oxidation impossible, and these branched fatty acids are catabolized in peroxisomes of animal cells by **α oxidation**. In the oxidation of phytanic acid, for example **(Fig. 17–18)**, phytanoyl-CoA is hydroxylated on its α carbon, in a reaction that

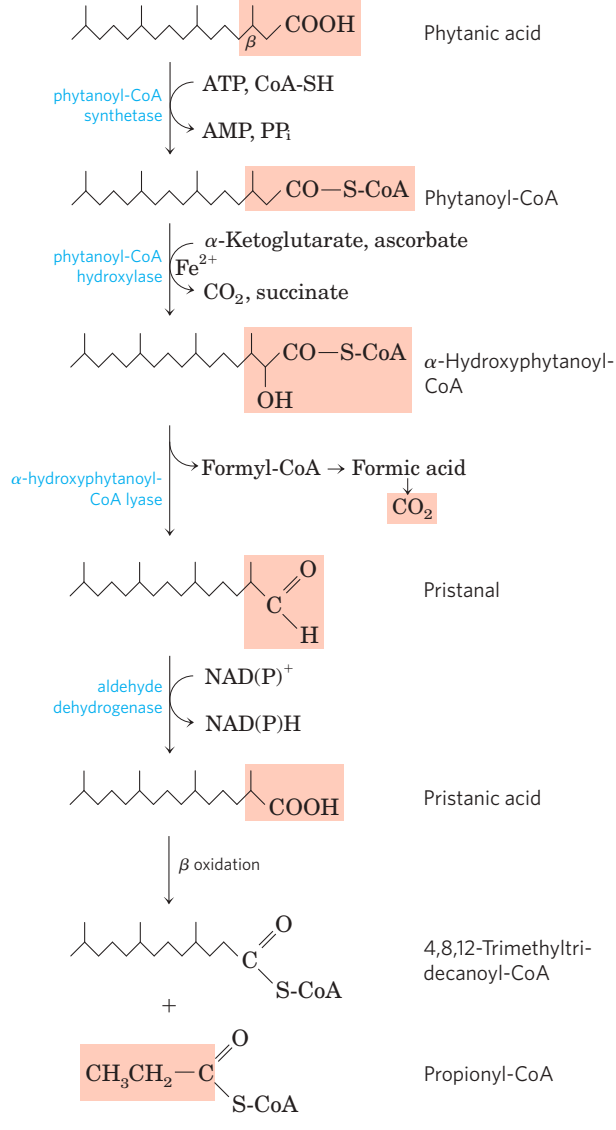

FIGURE 17–18 The α oxidation of a branched-chain fatty acid (phytanic acid) in peroxisomes. Phytanic acid has a methyl-substituted β carbon and therefore cannot undergo β oxidation. The combined action of the enzymes shown here removes the carboxyl carbon of phytanic acid to produce pristanic acid, in which the β carbon is unsubstituted, allowing β oxidation. Notice that β oxidation of pristanic acid releases propionyl-CoA, not acetyl-CoA. This is further catabolized as in Figure 17–12. (The details of the reaction that produces pristanal remain controversial.)

involves molecular oxygen; decarboxylated to form an aldehyde one carbon shorter; and then oxidized to the corresponding carboxylic acid, which now has no substituent on the β carbon and can be oxidized further by β oxidation. **Refsum disease**, resulting from a genetic defect in phytanoyl-CoA hydroxylase, leads to very high blood levels of phytanic acid and severe neurological problems, including blindness and deafness. ■

SUMMARY 17.2 Oxidation of Fatty Acids

- In the first stage of β oxidation, four reactions remove each acetyl-CoA unit from the carboxyl end of a saturated fatty acyl–CoA: (1) dehydrogenation of the α and β carbons (C-2 and C-3) by FAD-linked acyl-CoA dehydrogenases, (2) hydration of the resulting trans-Δ^2 double bond by enoyl-CoA hydratase, (3) dehydrogenation of the resulting L-β-hydroxyacyl-CoA by NAD-linked β-hydroxyacyl-CoA dehydrogenase, and (4) CoA-requiring cleavage of the resulting β-ketoacyl-CoA by thiolase, to form acetyl-CoA and a fatty acyl–CoA shortened by two carbons. The shortened fatty acyl–CoA then reenters the sequence.
- In the second stage of fatty acid oxidation, the acetyl-CoA is oxidized to CO_2 in the citric acid cycle. A large fraction of the theoretical yield of free energy from fatty acid oxidation is recovered as ATP by oxidative phosphorylation, the final stage of the oxidative pathway.
- Malonyl-CoA, an early intermediate of fatty acid synthesis, inhibits carnitine acyltransferase I, preventing fatty acid entry into mitochondria. This blocks fatty acid breakdown while synthesis is occurring.
- Genetic defects in the medium-chain acyl-CoA dehydrogenase result in serious human disease, as do mutations in other components of the β-oxidation system.
- Oxidation of unsaturated fatty acids requires two additional enzymes: enoyl-CoA isomerase and 2,4-dienoyl-CoA reductase. Odd-number fatty acids are oxidized by the β-oxidation pathway to yield acetyl-CoA and a molecule of propionyl-CoA. This is carboxylated to methylmalonyl-CoA, which is isomerized to succinyl-CoA in a reaction catalyzed by methylmalonyl-CoA mutase, an enzyme requiring coenzyme B_{12}.
- Peroxisomes of plants and animals, and glyoxysomes of plants, carry out β oxidation in four steps similar to those of the mitochondrial pathway in animals. The first oxidation step, however, transfers electrons directly to O_2, generating H_2O_2. Peroxisomes of animal tissues specialize in the oxidation of very-long-chain fatty acids and branched fatty acids. In glyoxysomes, in germinating seeds, β oxidation is one step in the conversion of stored lipids into a variety of intermediates and products.
- The reactions of ω oxidation, occurring in the endoplasmic reticulum, produce dicarboxylic fatty acyl intermediates, which can undergo β oxidation at either end to yield short dicarboxylic acids such as succinate.
- The reactions of α oxidation degrade branched fatty acids such as phytanic acid.

17.3 Ketone Bodies

In humans and most other mammals, acetyl-CoA formed in the liver during oxidation of fatty acids can either enter the citric acid cycle (stage 2 of Fig. 17–7) or undergo conversion to the "ketone bodies," **acetone**, **acetoacetate**, and **D-β-hydroxybutyrate**, for export to other tissues. (The term "bodies" is a historical artifact; the term is occasionally applied to insoluble particles, but these compounds are soluble in blood and urine.)

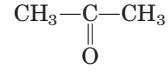

Acetone

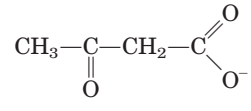

Acetoacetate

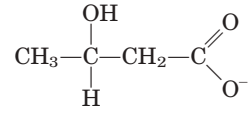

D-β-Hydroxybutyrate

Acetone, produced in smaller quantities than the other ketone bodies, is exhaled. Acetoacetate and D-β-hydroxybutyrate are transported by the blood to tissues other than the liver (extrahepatic tissues), where they are converted to acetyl-CoA and oxidized in the citric acid cycle, providing much of the energy required by tissues such as skeletal and heart muscle and the renal cortex. The brain, which preferentially uses glucose as fuel, can adapt to the use of acetoacetate or D-β-hydroxybutyrate under starvation conditions, when glucose is unavailable. The production and export of ketone bodies from the liver to extrahepatic tissues allows continued oxidation of fatty acids in the liver when acetyl-CoA is not being oxidized in the citric acid cycle.

Ketone Bodies, Formed in the Liver, Are Exported to Other Organs as Fuel

The first step in the formation of acetoacetate, occurring in the liver **(Fig. 17–19)**, is the enzymatic condensation of two molecules of acetyl-CoA, catalyzed by thiolase;

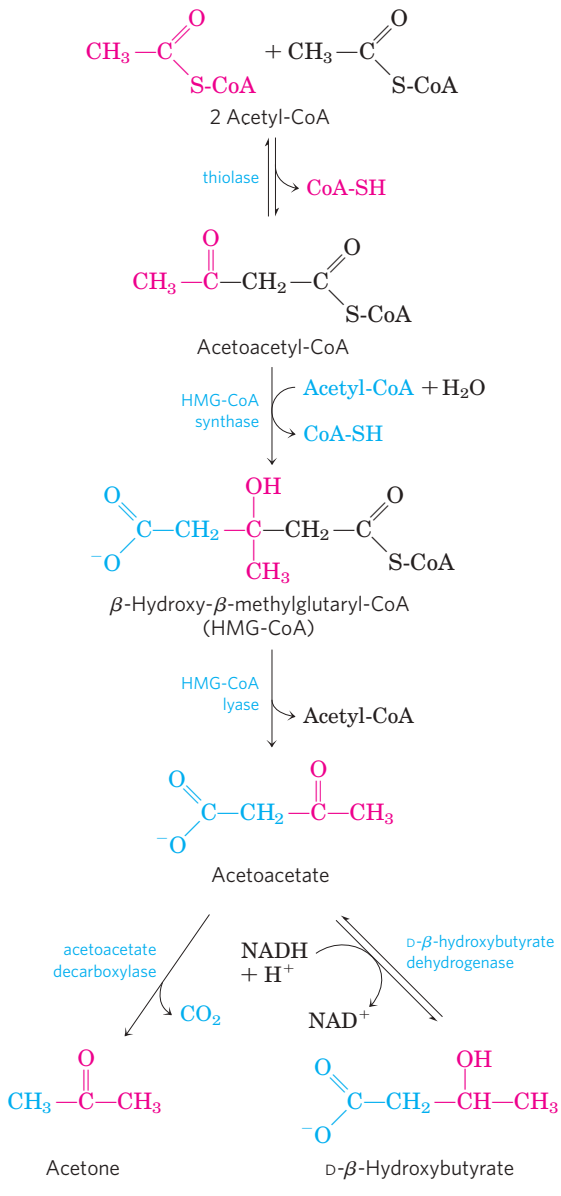

FIGURE 17–19 Formation of ketone bodies from acetyl-CoA. Healthy, well-nourished individuals produce ketone bodies at a relatively low rate. When acetyl-CoA accumulates (as in starvation or untreated diabetes, for example), thiolase catalyzes the condensation of two acetyl-CoA molecules to acetoacetyl-CoA, the parent compound of the three ketone bodies. The reactions of ketone body formation occur in the matrix of liver mitochondria. The six-carbon compound β-hydroxy-β-methylglutaryl-CoA (HMG-CoA) is also an intermediate of sterol biosynthesis, but the enzyme that forms HMG-CoA in that pathway is cytosolic. HMG-CoA lyase is present only in the mitochondrial matrix.

this is simply the reversal of the last step of β oxidation. The acetoacetyl-CoA then condenses with acetyl-CoA to form **β-hydroxy-β-methylglutaryl-CoA (HMG-CoA)**, which is cleaved to free acetoacetate and acetyl-CoA. The acetoacetate is reversibly reduced by D-β-hydroxybutyrate dehydrogenase, a mitochondrial enzyme, to D-β-hydroxybutyrate. This enzyme is specific for the D stereoisomer; it does not act on L-β-hydroxyacyl-CoAs and is not to be confused with L-β-hydroxyacyl-CoA dehydrogenase of the β-oxidation pathway.

In healthy people, acetone is formed in very small amounts from acetoacetate, which is easily decarboxylated, either spontaneously or by the action of **acetoacetate decarboxylase** (Fig. 17–19). Because individuals with untreated diabetes produce large quantities of acetoacetate, their blood contains significant amounts of acetone, which is toxic. Acetone is volatile and imparts a characteristic odor to the breath, which is sometimes useful in diagnosing diabetes. ■

In extrahepatic tissues, D-β-hydroxybutyrate is oxidized to acetoacetate by D-β-hydroxybutyrate dehydrogenase **(Fig. 17–20)**. The acetoacetate is activated to its coenzyme A ester by transfer of CoA from succinyl-CoA, an intermediate of the citric acid cycle (see Fig. 16–7), in a reaction catalyzed by ***β*-ketoacyl-CoA transferase**, also called thiophorase. The acetoacetyl-CoA is then cleaved by thiolase to yield two acetyl-CoAs, which enter the citric acid cycle. Thus the ketone bodies are used as fuels in all tissues except liver, which lacks thiophorase. The liver is therefore a producer of ketone bodies for the other tissues, but not a consumer.

The production and export of ketone bodies by the liver allows continued oxidation of fatty acids with only minimal oxidation of acetyl-CoA. When intermediates of the citric acid cycle are being siphoned off for glucose synthesis by gluconeogenesis, for example, oxidation of

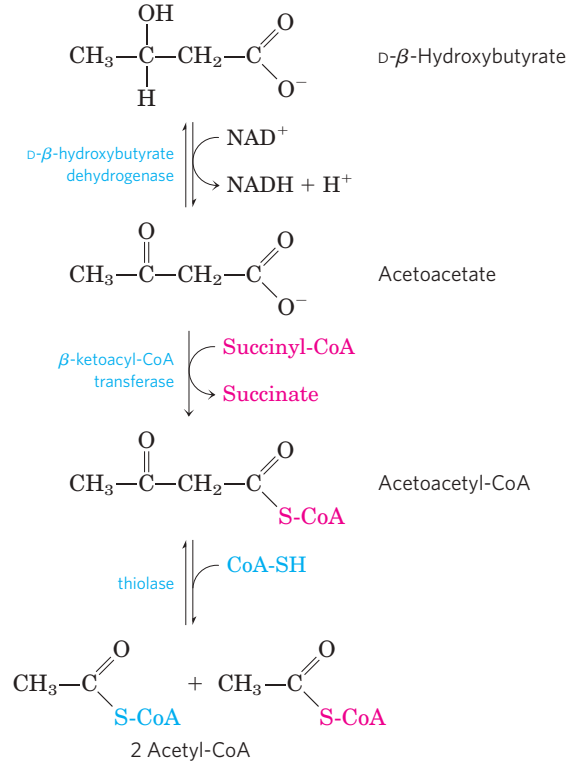

FIGURE 17–20 D-β-Hydroxybutyrate as a fuel. D-β-Hydroxybutyrate, synthesized in the liver, passes into the blood and thus to other tissues, where it is converted in three steps to acetyl-CoA. It is first oxidized to acetoacetate, which is activated with coenzyme A donated from succinyl-CoA, then split by thiolase. The acetyl-CoA thus formed is used for energy production.

cycle intermediates slows—and so does acetyl-CoA oxidation. Moreover, the liver contains only a limited amount of coenzyme A, and when most of it is tied up in acetyl-CoA, β oxidation slows for want of the free coenzyme. The production and export of ketone bodies frees coenzyme A, allowing continued fatty acid oxidation.

Ketone Bodies Are Overproduced in Diabetes and during Starvation

Starvation and untreated diabetes mellitus lead to overproduction of ketone bodies, with several associated medical problems. During starvation, gluconeogenesis depletes citric acid cycle intermediates, diverting acetyl-CoA to ketone body production **(Fig. 17–21)**. In untreated diabetes, when the insulin level is insufficient, extrahepatic tissues cannot take up glucose efficiently from the blood, either for fuel or for conversion to fat. Under these conditions, levels of malonyl-CoA (the starting material for fatty acid synthesis) fall, inhibition of carnitine acyltransferase I is relieved, and fatty acids enter mitochondria to be degraded to acetyl-CoA—which cannot pass through the citric acid cycle because cycle intermediates have been drawn off for use as substrates in gluconeogenesis. The resulting accumulation of acetyl-CoA accelerates the formation of ketone bodies beyond the capacity of extrahepatic tissues to oxidize them. The increased blood levels of acetoacetate and D-β-hydroxybutyrate lower the blood pH, causing the condition known as **acidosis**. Extreme acidosis can lead to coma and in some cases death. Ketone bodies in the blood and urine of individuals with untreated diabetes can reach extraordinary levels—a blood concentration of 90 mg/100 mL (compared with a normal level of <3 mg/100 mL) and urinary excretion of 5,000 mg/24 hr (compared with a normal rate of ≤125 mg/24 hr). This condition is called **ketosis**.

Individuals on very low-calorie diets, using the fats stored in adipose tissue as their major energy source, also have increased levels of ketone bodies in their blood and urine. These levels must be monitored to avoid the dangers of acidosis and ketosis (ketoacidosis). ■

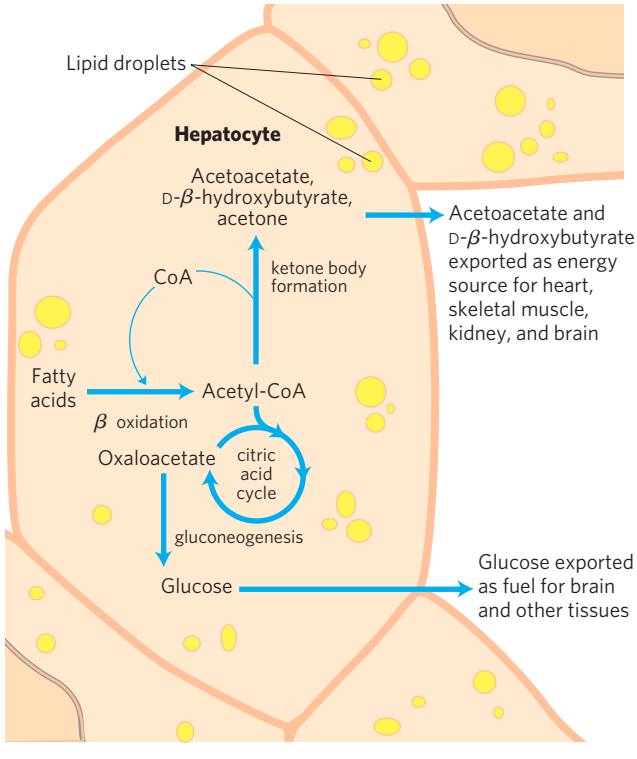

FIGURE 17–21 Ketone body formation and export from the liver. Conditions that promote gluconeogenesis (untreated diabetes, severely reduced food intake) slow the citric acid cycle (by drawing off oxaloacetate) and enhance the conversion of acetyl-CoA to acetoacetate. The released coenzyme A allows continued β oxidation of fatty acids.

SUMMARY 17.3 Ketone Bodies

- The ketone bodies—acetone, acetoacetate, and D-β-hydroxybutyrate—are formed in the liver. The latter two compounds serve as fuel molecules in extrahepatic tissues, through oxidation to acetyl-CoA and entry into the citric acid cycle.
- Overproduction of ketone bodies in uncontrolled diabetes or severely reduced calorie intake can lead to acidosis or ketosis.

Key Terms

Terms in bold are defined in the glossary.

β oxidation 667
chylomicron 669
apolipoprotein 669
lipoprotein 669
perilipin 669
free fatty acids 669
serum albumin 669
carnitine shuttle 670
carnitine acyltransferase I 671
acyl-carnitine/carnitine transporter 671
carnitine acyltransferase II 671
trifunctional protein (TFP) 674
methylmalonyl-CoA mutase 678
coenzyme B_{12} 678
malonyl-CoA 679
PPAR (peroxisome proliferator-activated receptor) 679
pernicious anemia 681
intrinsic factor 681
medium-chain acyl-CoA dehydrogenase (MCAD) 682
multifunctional protein (MFP) 684
ω oxidation 684
mixed-function oxidases 685
α oxidation 685
acidosis 688
ketosis 688

Further Reading

General

Boyer, P.D. (1983) *The Enzymes*, 3rd edn, Vol. 16: *Lipid Enzymology*, Academic Press, Inc., San Diego, CA.

Ferry, G. (1998) *Dorothy Hodgkin: A Life*, Cold Spring Harbor Laboratory Press, Cold Spring Harbor, NY.
Fascinating biography of an amazing woman.

Gurr, M.I., Harwood, J.L., & Frayn, K.N. (2002) *Lipid Biochemistry: An Introduction*, 5th edn, Blackwell Science, Oxford, UK.

Plutzky, J. (2009) The mighty mighty fatty acid. *Nat. Med.* **15**, 618–619.

Scheffler, I.E. (1999) *Mitochondria*, Wiley-Liss, New York.
An excellent book on mitochondrial structure and function.

Wood, P.A. (2006) *How Fat Works*, Harvard University Press, Cambridge, MA.
Very readable, intermediate-level account of the contributions of genetics and mouse models to the understanding of lipid metabolism and obesity.

Digestion, Mobilization, and Transport of Fats

Farese, R.V., Jr., & Walther, T.C. (2009) Lipid droplets finally get a little r-e-s-p-e-c-t. *Cell* **139**, 855–860.

Glatz, J.F.C., Luiken, J.J.F.P., & Bonen, A. (2010) Membrane fatty acid transporters as regulators of lipid metabolism: implications for metabolic disease. *Physiol. Rev.* **90**, 367–417.

Greenberg, A.S. & Coleman, R.A. (2011) Expanding roles for lipid droplets. *Trends Endocrinol. Metab.* 22, 195–196.
Editorial introduction to an issue of this journal devoted to lipid droplets.

Langin, D., Holm, C., & Lafontan, M. (1996) Adipocyte hormone-sensitive lipase: a major regulator of lipid metabolism. *Proc. Nutr. Soc.* **55**, 93–109.

Ramsay, T.G. (1996) Fat cells. *Endocrinol. Metab. Clin. N. Am.* **25**, 847–870.
A review of all aspects of fat storage and mobilization in adipocytes.

Reue, K. (2011) A thematic review series: lipid droplet storage and metabolism: from yeast to man. *J. Lipid Res.* **52**, 1865–1868.
Editorial introduction to a series of articles on lipid droplets published together in this issue.

Shaw, C.S., Clark, J., & Wagenmakers, A.J.M. (2010) The effect of exercise and nutrition on intramuscular fat metabolism and insulin sensitivity. *Annu. Rev. Nutr.* **30**, 13–34.

Steinberg, G.R. (2009) Role of the AMP-activated protein kinase in regulating fatty acid metabolism during exercise. *Appl. Physiol. Nutr. Metab.* **34**, 315–322.

Storch, J. & Rhumsey, A.D. (2010) Tissue-specific functions in the fatty acid-binding protein family (minireview) *J. Biol. Chem.* **285**, 32,679–32,683.

Wang, C.S., Hartsuck, J., & McConathy, W.J. (1992) Structure and functional properties of lipoprotein lipase. *Biochim. Biophys. Acta* **1123**, 1–17.
Advanced-level discussion of the enzyme that releases fatty acids from lipoproteins in the capillaries of muscle and adipose tissue.

Watt, M.J. & Steinberg, G.R. (2008) Regulation and function of triacylglycerol lipases in cellular metabolism. *Biochem. J.* **414**, 313–325.

Zechner, R., Kienesberger, P.C., Haemmerle, G., Zimmermann R., & Lass, A. (2009) Adipose triglyceride lipase and the lipolytic catabolism of cellular fat stores. *J. Lipid Res.* **50**, 3–21.

Mitochondrial β Oxidation

Bannerjee, R. (1997) The yin-yang of cobalamin biochemistry. *Chem. Biol.* **4**, 175–186.
A review of the biochemistry of coenzyme B_{12} reactions, including the methylmalonyl-CoA mutase reaction.

Carey, H.V., Andrews, M.T., & Martin, S.L. (2003) Mammalian hibernation: cellular and molecular responses to depressed metabolism and low temperature. *Physiol. Rev*. **83**, 1153–1181.

Desverne, B., Michalik, L., & Wahij, W. (2006) Transcriptional regulation of metabolism. *Physiol. Rev.* **86**, 465–514.
An extensive review of the regulation of metabolism, including fat metabolism, by transcription factors.

Eaton, S., Bartlett, K., & Pourfarzam, M. (1996) Mammalian mitochondrial β-oxidation. *Biochem. J.* **320**, 345–357.
A review of the enzymology of β oxidation, inherited defects in this pathway, and regulation of the process in mitochondria.

Eaton, S., Bursby, T., Middleton, B., Pourfarzam, M., Mills, K., Johnson, A.W., & Bartlett, K. (2000) The mitochondrial trifunctional protein: centre of a β-oxidation metabolon? *Biochem. Soc. Trans.* **28**, 177–182.
Short, intermediate-level review.

Evans, R.M., Barish, G.D., & Wang, Y.-X. (2004) PPARs and the complex journey to obesity. *Nat. Med.* **10**, 1–7.
A very readable, intermediate-level account of the discovery of the PPARs and their functions.

Harwood, J.L. (1988) Fatty acid metabolism. *Annu. Rev. Plant Physiol. Plant Mol. Biol.* **39**, 101–138.

Jeukendrup, A.E., Saris, W.H., & Wagenmakers, A.J. (1998) Fat metabolism during exercise: a review. Part III: effects of nutritional interventions. *Int. J. Sports Med*. **19**, 371–379.
This paper is one of a series that reviews the factors that influence fat mobilization and utilization during exercise.

Kampf, J.P. & Kleinfeld, A.M. (2007) Is membrane transport of FFA mediated by lipid, protein, or both? *Physiology* **22**, 7–14.

Kerner, J. & Hoppel, C. (1998) Genetic disorders of carnitine metabolism and their nutritional management. *Annu. Rev. Nutr.* **18**, 179–206.

Kerner, J. & Hoppel, C. (2000) Fatty acid import into mitochondria. *Biochim. Biophys. Acta* **1486**, 1–17.

Kunau, W.H., Dommes, V., & Schulz, H. (1995) β-Oxidation of fatty acids in mitochondria, peroxisomes, and bacteria: a century of continued progress. *Prog. Lipid Res.* **34**, 267–342.
A good historical account and a useful comparison of β oxidation in different systems.

Mandard, S., Muller, M., & Kersten, S. (2004) Peroxisome proliferator-activated receptor alpha target genes. *Cell. Mol. Life Sci.* **61**, 393–416.
A review of the genes controlled by PPARα.

Rinaldo, P., Matern, D., & Bennett, M.J. (2002) Fatty acid oxidation disorders. *Annu. Rev. Physiol.* **64**, 477–502.
Advanced review of metabolic defects in fat oxidation, including MCAD mutations.

Rufer, A.C., Thoma, R., Benz, J., Stihle, M., Gsell, B., De Roo, E., Banner, D.W., Mueller, F., Chomienne, O., & Hennig, M. (2006) The crystal structure of carnitine palmitoyltransferase 2 and implications for diabetes treatment. *Structure* **14**, 713–723.

Sherratt, H.S. (1994) Introduction: the regulation of fatty acid oxidation in cells. *Biochem. Soc. Trans.* **22**, 421–422.
Introduction to reviews in this journal issue of various aspects of fatty acid oxidation and its regulation.

Thorpe, C. & Kim, J.J. (1995) Structure and mechanism of action of the acyl-CoA dehydrogenases. *FASEB J.* **9**, 718–725.
Short, clear description of the three-dimensional structure and catalytic mechanism of these enzymes.

Peroxisomal β Oxidation

Graham, I.A. & Eastmond, P.J. (2002) Pathways of straight and branched chain fatty acid catabolism in higher plants. *Prog. Lipid Res*. **41**, 156–181.

Wanders, R.J.A., van Grunsven, E.G., & Jansen, G.A. (2000) Lipid metabolism in peroxisomes: enzymology, functions and dysfunctions of the fatty acid α- and β-oxidation systems in humans. *Biochem. Soc. Trans*. **28**, 141–148.

Ketone Bodies

Foster, D.W. & McGarry, J.D. (1983) The metabolic derangements and treatment of diabetic ketoacidosis. *N. Engl. J. Med.* **309**, 159–169.

McGarry, J.D. & Foster, D.W. (1980) Regulation of hepatic fatty acid oxidation and ketone body production. *Annu. Rev. Biochem.* **49**, 395–420.

Robinson, A.M. & Williamson, D.H. (1980) Physiological roles of ketone bodies as substrates and signals in mammalian tissues. *Physiol. Rev.* **60**, 143–187.

Problems

1. Energy in Triacylglycerols On a per-carbon basis, where does the largest amount of biologically available energy in triacylglycerols reside: in the fatty acid portions or the glycerol portion? Indicate how knowledge of the chemical structure of triacylglycerols provides the answer.

2. Fuel Reserves in Adipose Tissue Triacylglycerols, with their hydrocarbon-like fatty acids, have the highest energy content of the major nutrients.

(a) If 15% of the body mass of a 70.0 kg adult consists of triacylglycerols, what is the total available fuel reserve, in both kilojoules and kilocalories, in the form of triacylglycerols? Recall that 1.00 kcal = 4.18 kJ.

(b) If the basal energy requirement is approximately 8,400 kJ/day (2,000 kcal/day), how long could this person survive if the oxidation of fatty acids stored as triacylglycerols were the only source of energy?

(c) What would be the weight loss in pounds per day under such starvation conditions (1 lb = 0.454 kg)?

3. Common Reaction Steps in the Fatty Acid Oxidation Cycle and Citric Acid Cycle Cells often use the same enzyme reaction pattern for analogous metabolic conversions. For example, the steps in the oxidation of pyruvate to acetyl-CoA and of α-ketoglutarate to succinyl-CoA, although catalyzed by different enzymes, are very similar. The first stage of fatty acid oxidation follows a reaction sequence closely resembling a sequence in the citric acid cycle. Use equations to show the analogous reaction sequences in the two pathways.

4. β Oxidation: How Many Cycles? How many cycles of β oxidation are required for the complete oxidation of activated oleic acid, 18:1(Δ^9)?

5. Chemistry of the Acyl-CoA Synthetase Reaction Fatty acids are converted to their coenzyme A esters in a reversible reaction catalyzed by acyl-CoA synthetase:

$$R{-}COO^- + ATP + CoA \rightleftharpoons R{-}C(=O){-}CoA + AMP + PP_i$$

(a) The enzyme-bound intermediate in this reaction has been identified as the mixed anhydride of the fatty acid and adenosine monophosphate (AMP), acyl-AMP:

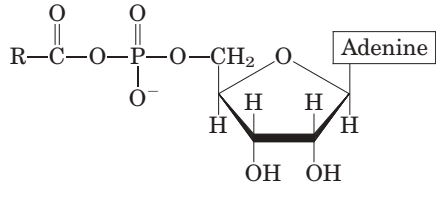

Write two equations corresponding to the two steps of the reaction catalyzed by acyl-CoA synthetase.

(b) The acyl-CoA synthetase reaction is readily reversible, with an equilibrium constant near 1. How can this reaction be made to favor formation of fatty acyl–CoA?

6. Intermediates in Oleic Acid Oxidation What is the structure of the partially oxidized fatty acyl group that is formed when oleic acid, 18:1(Δ^9), has undergone three cycles of β oxidation? What are the next two steps in the continued oxidation of this intermediate?

7. β Oxidation of an Odd-Chain Fatty Acid What are the direct products of β oxidation of a fully saturated, straight-chain fatty acid of 11 carbons?

8. Oxidation of Tritiated Palmitate Palmitate uniformly labeled with tritium (^{3}H) to a specific activity of 2.48×10^8 counts per minute (cpm) per micromole of palmitate is added to a mitochondrial preparation that oxidizes it to acetyl-CoA. The acetyl-CoA is isolated and hydrolyzed to acetate. The specific activity of the isolated acetate is 1.00×10^7 cpm/μmol. Is this result consistent with the β-oxidation pathway? Explain. What is the final fate of the removed tritium?

9. Compartmentation in β Oxidation Free palmitate is activated to its coenzyme A derivative (palmitoyl-CoA) in the cytosol before it can be oxidized in the mitochondrion. If palmitate and [^{14}C]coenzyme A are added to a liver homogenate, palmitoyl-CoA isolated from the cytosolic fraction is radioactive, but that isolated from the mitochondrial fraction is not. Explain.

10. Comparative Biochemistry: Energy-Generating Pathways in Birds One indication of the relative importance of various ATP-producing pathways is the V_{max} of certain enzymes of these pathways. The values of V_{max} of several enzymes from the pectoral muscles (chest muscles used for flying) of pigeon and pheasant are listed below.

	V_{max} (μmol substrate/min/g tissue)	
Enzyme	**Pigeon**	**Pheasant**
Hexokinase	3.0	2.3
Glycogen phosphorylase	18.0	120.0
Phosphofructokinase-1	24.0	143.0
Citrate synthase	100.0	15.0
Triacylglycerol lipase	0.07	0.01

(a) Discuss the relative importance of glycogen metabolism and fat metabolism in generating ATP in the pectoral muscles of these birds.

(b) Compare oxygen consumption in the two birds.

(c) Judging from the data in the table, which bird is the long-distance flyer? Justify your answer.

(d) Why were these particular enzymes selected for comparison? Would the activities of triose phosphate isomerase and malate dehydrogenase be equally good bases for comparison? Explain.

11. Mutant Carnitine Acyltransferase What changes in metabolic pattern would result from a mutation in the muscle carnitine acyltransferase I in which the mutant protein

has lost its affinity for malonyl-CoA but not its catalytic activity?

12. Effect of Carnitine Deficiency An individual developed a condition characterized by progressive muscular weakness and aching muscle cramps. The symptoms were aggravated by fasting, exercise, and a high-fat diet. The homogenate of a skeletal muscle specimen from the patient oxidized added oleate more slowly than did control homogenates, consisting of muscle specimens from healthy individuals. When carnitine was added to the patient's muscle homogenate, the rate of oleate oxidation equaled that in the control homogenates. The patient was diagnosed as having a carnitine deficiency.

(a) Why did added carnitine increase the rate of oleate oxidation in the patient's muscle homogenate?

(b) Why were the patient's symptoms aggravated by fasting, exercise, and a high-fat diet?

(c) Suggest two possible reasons for the deficiency of muscle carnitine in this individual.

13. Fatty Acids as a Source of Water Contrary to legend, camels do not store water in their humps, which actually consist of large fat deposits. How can these fat deposits serve as a source of water? Calculate the amount of water (in liters) that a camel can produce from 1.0 kg of fat. Assume for simplicity that the fat consists entirely of tripalmitoylglycerol.

14. Petroleum as a Microbial Food Source Some microorganisms of the genera *Nocardia* and *Pseudomonas* can grow in an environment where hydrocarbons are the only food source. These bacteria oxidize straight-chain aliphatic hydrocarbons, such as octane, to their corresponding carboxylic acids:

$$CH_3(CH_2)_6CH_3 + NAD^+ + O_2 \rightleftharpoons CH_3(CH_2)_6COOH + NADH + H^+$$

How could these bacteria be used to clean up oil spills? What would be some of the limiting factors in the efficiency of this process?

15. Metabolism of a Straight-Chain Phenylated Fatty Acid A crystalline metabolite was isolated from the urine of a rabbit that had been fed a straight-chain fatty acid containing a terminal phenyl group:

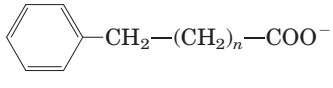

A 302 mg sample of the metabolite in aqueous solution was completely neutralized by 22.2 mL of 0.100 M NaOH.

(a) What is the probable molecular weight and structure of the metabolite?

(b) Did the straight-chain fatty acid contain an even or an odd number of methylene (—CH_2—) groups (i.e., is n even or odd)? Explain.

16. Fatty Acid Oxidation in Uncontrolled Diabetes When the acetyl-CoA produced during β oxidation in the liver exceeds the capacity of the citric acid cycle, the excess acetyl-CoA forms ketone bodies—acetone, acetoacetate, and D-β-hydroxybutyrate. This occurs in severe, uncontrolled diabetes: because the tissues cannot use glucose, they oxidize large amounts of fatty acids instead. Although acetyl-CoA is not toxic, the mitochondrion must divert the acetyl-CoA to ketone bodies. What problem would arise if acetyl-CoA were not converted to ketone bodies? How does the diversion to ketone bodies solve the problem?

17. Consequences of a High-Fat Diet with No Carbohydrates Suppose you had to subsist on a diet of whale blubber and seal blubber, with little or no carbohydrate.

(a) What would be the effect of carbohydrate deprivation on the utilization of fats for energy?

(b) If your diet were totally devoid of carbohydrate, would it be better to consume odd- or even-numbered fatty acids? Explain.

18. Even- and Odd-Chain Fatty Acids in the Diet In a laboratory experiment, two groups of rats are fed two different fatty acids as their sole source of carbon for a month. The first group gets heptanoic acid (7:0), and the second gets octanoic acid (8:0). After the experiment, a striking difference is seen between the two groups. Those in the first group are healthy and have gained weight, whereas those in the second group are weak and have lost weight as a result of losing muscle mass. What is the biochemical basis for this difference?

19. Metabolic Consequences of Ingesting ω-Fluorooleate The shrub *Dichapetalum toxicarium*, native to Sierra Leone, produces ω-fluorooleate, which is highly toxic to warm-blooded animals.

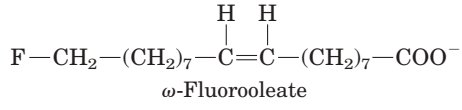

ω-Fluorooleate

This substance has been used as an arrow poison, and powdered fruit from the plant is sometimes used as a rat poison (hence the plant's common name, ratsbane). Why is this substance so toxic? (Hint: Review Chapter 16, Problem 22.)

20. Mutant Acetyl-CoA Carboxylase What would be the consequences for fat metabolism of a mutation in acetyl-CoA carboxylase that replaced the Ser residue normally phosphorylated by AMPK with an Ala residue? What might happen if the same Ser were replaced by Asp? (Hint: See Fig. 17–13.)

21. Effect of PDE Inhibitor on Adipocytes How would an adipocyte's response to epinephrine be affected by the addition of an inhibitor of cAMP phosphodiesterase (PDE)? (Hint: See Fig. 12–4.)

22. Role of FAD as Electron Acceptor Acyl-CoA dehydrogenase uses enzyme-bound FAD as a prosthetic group to dehydrogenate the α and β carbons of fatty acyl–CoA. What is the advantage of using FAD as an electron acceptor rather than NAD^+? Explain in terms of the standard reduction potentials for the Enz-FAD/$FADH_2$ ($E'^\circ = -0.219$ V) and NAD^+/NADH ($E'^\circ = -0.320$ V) half-reactions.

23. β Oxidation of Arachidic Acid How many turns of the fatty acid oxidation cycle are required for complete oxidation of arachidic acid (see Table 10–1) to acetyl-CoA?

24. Fate of Labeled Propionate If [3-^{14}C]propionate (^{14}C in the methyl group) is added to a liver homogenate, ^{14}C-labeled oxaloacetate is rapidly produced. Draw a flow chart for the pathway by which propionate is transformed to oxaloacetate, and indicate the location of the ^{14}C in oxaloacetate.

25. Phytanic Acid Metabolism When phytanic acid uniformly labeled with ^{14}C is fed to a mouse, radioactivity can be detected in malate, a citric acid cycle intermediate, within minutes. Draw a metabolic pathway that could account for this. Which of the carbon atoms in malate would contain ^{14}C label?

26. Sources of H_2O Produced in β Oxidation The complete oxidation of palmitoyl-CoA to carbon dioxide and water is represented by the overall equation

$$\text{Palmitoyl-CoA} + 23O_2 + 108P_i + 108\text{ADP} \longrightarrow \text{CoA} + 16CO_2 + 108\text{ATP} + 23H_2O$$

Water is also produced in the reaction

$$\text{ADP} + P_i \longrightarrow \text{ATP} + H_2O$$

but is not included as a product in the overall equation. Why?

27. Biological Importance of Cobalt In cattle, deer, sheep, and other ruminant animals, large amounts of propionate are produced in the rumen through the bacterial fermentation of ingested plant matter. Propionate is the principal source of glucose for these animals, via the route propionate $\longrightarrow$ oxaloacetate $\longrightarrow$ glucose. In some areas of the world, notably Australia, ruminant animals sometimes show symptoms of anemia with concomitant loss of appetite and retarded growth, resulting from an inability to transform propionate to oxaloacetate. This condition is due to a cobalt deficiency caused by very low cobalt levels in the soil and thus in plant matter. Explain.

28. Fat Loss during Hibernation Bears expend about 25×10^6 J/day during periods of hibernation, which may last as long as seven months. The energy required to sustain life is obtained from fatty acid oxidation. How much weight loss (in kilograms) has occurred after seven months? How might ketosis be minimized during hibernation? (Assume the oxidation of fat yields 38 kJ/g.)

Data Analysis Problem

29. β Oxidation of Trans Fats Unsaturated fats with trans double bonds are commonly referred to as "trans fats." There has been much discussion about the effects of dietary trans fats on health. In their investigations of the effects of trans fatty acid metabolism on health, Yu and colleagues (2004) showed that a model trans fatty acid was processed differently from its cis isomer. They used three related 18-carbon fatty acids to explore the difference in β oxidation between cis and trans isomers of the same-size fatty acid.

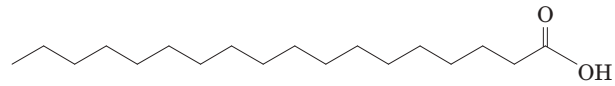

Stearic acid
(octadecenoic acid)

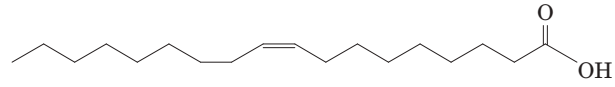

Oleic acid
(*cis*-Δ^9-octadecenoic acid)

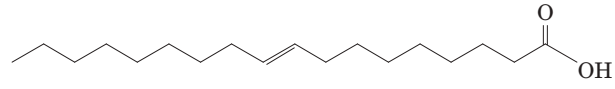

Elaidic acid
(*trans*-Δ^9-octadecenoic acid)

The researchers incubated the coenzyme A derivative of each acid with rat liver mitochondria for 5 minutes, then separated the remaining CoA derivatives in each mixture by HPLC (high-performance liquid chromatography). The results are shown below, with separate panels for the three experiments.

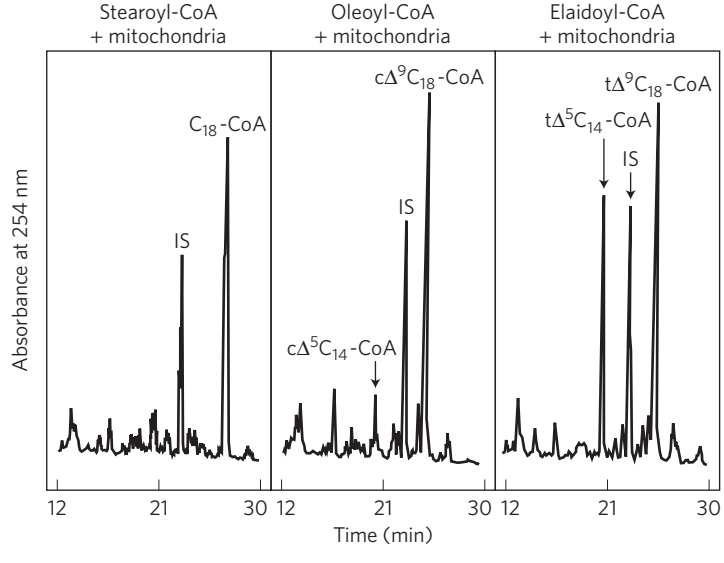

In the figure, IS indicates an internal standard (pentadecanoyl-CoA) added to the mixture, after the reaction, as a molecular marker. The researchers abbreviated the CoA derivatives as follows: stearoyl-CoA, C_{18}-CoA; *cis*-Δ^5-tetradecenoyl-CoA, cΔ^5C_{14}-CoA; oleoyl-CoA, cΔ^9C_{18}-CoA; *trans*-Δ^5-tetradecenoyl-CoA, tΔ^5C_{14}-CoA; and elaidoyl-CoA, tΔ^9C_{18}-CoA.

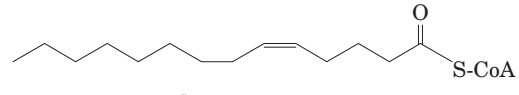

cis-Δ^5-Tetradecenoyl-CoA

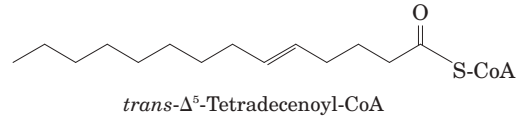

trans-Δ^5-Tetradecenoyl-CoA

(a) Why did Yu and colleagues need to use CoA derivatives rather than the free fatty acids in these experiments?

(b) Why were no lower molecular weight CoA derivatives found in the reaction with stearoyl-CoA?

(c) How many rounds of β oxidation would be required to convert the oleoyl-CoA and the elaidoyl-CoA to *cis*-Δ^5-tetradecenoyl-CoA and *trans*-Δ^5-tetradecenoyl-CoA, respectively?

There are two forms of the enzyme acyl-CoA dehydrogenase (see Fig. 17–8a): long-chain acyl-CoA dehydrogenase (LCAD) and very-long-chain acyl-CoA dehydrogenase (VLCAD). Yu and coworkers measured the kinetic parameters of both enzymes. They used the CoA derivatives of three fatty acids: tetradecanoyl-CoA (C_{14}-CoA), *cis*-Δ^5-tetradecenoyl-CoA ($c\Delta^5C_{14}$-CoA), and *trans*-Δ^5-tetradecenoyl-CoA ($t\Delta^5C_{14}$-CoA). The results are shown below. (See Chapter 6 for definitions of the kinetic parameters.)

	LCAD			VLCAD		
	C_{14}-CoA	**$c\Delta^5C_{14}$-CoA**	**$t\Delta^5C_{14}$-CoA**	**C_{14}-CoA**	**$c\Delta^5C_{14}$-CoA**	**$t\Delta^5C_{14}$-CoA**
V_{max}	3.3	3.0	2.9	1.4	0.32	0.88
K_m	0.41	0.40	1.6	0.57	0.44	0.97
k_{cat}	9.9	8.9	8.5	2.0	0.42	1.12
k_{cat}/K_m	24	22	5	4	1	1

(d) For LCAD, the K_m differs dramatically for the cis and trans substrates. Provide a plausible explanation for this observation in terms of the structures of the substrate molecules. (Hint: You may want to refer to Fig. 10–2.)

(e) The kinetic parameters of the two enzymes are relevant to the differential processing of these fatty acids *only* if the LCAD or VLCAD reaction (or both) is the rate-limiting step in the pathway. What evidence is there to support this assumption?

(f) How do these different kinetic parameters explain the different levels of the CoA derivatives found after incubation of rat liver mitochondria with stearoyl-CoA, oleoyl-CoA, and elaidoyl-CoA (shown in the three-panel figure)?

Yu and coworkers measured the substrate specificity of rat liver mitochondrial thioesterase, which hydrolyzes acyl-CoA to CoA and free fatty acid (see Chapter 21). This enzyme was approximately twice as active with C_{14}-CoA thioesters as with C_{18}-CoA thioesters.

(g) Other research has suggested that free fatty acids can pass through membranes. In their experiments, Yu and colleagues found *trans*-Δ^5-tetradecenoic acid outside mitochondria (i.e., in the medium) that had been incubated with elaidoyl-CoA. Describe the pathway that led to this extramitochondrial *trans*-Δ^5-tetradecenoic acid. Be sure to indicate where in the cell the various transformations take place, as well as the enzymes that catalyze the transformations.

(h) It is often said in the popular press that "trans fats are not broken down by your cells and instead accumulate in your body." In what sense is this statement correct and in what sense is it an oversimplification?

Reference

Yu, W., Liang, X., Ensenauer, R., Vockley, J., Sweetman, L., & Schultz, H. (2004) Leaky β-oxidation of a *trans*-fatty acid. *J. Biol. Chem.* **279**, 52,160–52,167.

this page left intentionally blank

18

Amino Acid Oxidation and the Production of Urea

We now turn our attention to the amino acids, the final class of biomolecules that, through their oxidative degradation, make a significant contribution to the generation of metabolic energy. The fraction of metabolic energy obtained from amino acids, whether they are derived from dietary protein or from tissue protein, varies greatly with the type of organism and with metabolic conditions. Carnivores can obtain (immediately following a meal) up to 90% of their energy requirements from amino acid oxidation, whereas herbivores may fill only a small fraction of their energy needs by this route. Most microorganisms can scavenge amino acids from their environment and use them as fuel when required by metabolic conditions. Plants, however, rarely if ever oxidize amino acids to provide energy; the carbohydrate produced from CO_2 and H_2O in photosynthesis is generally their sole energy source. Amino acid concentrations in plant tissues are carefully regulated to just meet the requirements for biosynthesis of proteins, nucleic acids, and other molecules needed to support growth. Amino acid catabolism does occur in plants, but its purpose is to produce metabolites for other biosynthetic pathways.

In animals, amino acids undergo oxidative degradation in three different metabolic circumstances:

1. During the normal synthesis and degradation of cellular proteins (protein turnover; Chapter 27), some amino acids that are released from protein breakdown and are not needed for new protein synthesis undergo oxidative degradation.
2. When a diet is rich in protein and the ingested amino acids exceed the body's needs for protein synthesis, the surplus is catabolized; amino acids cannot be stored.
3. During starvation or in uncontrolled diabetes mellitus, when carbohydrates are either unavailable or not properly utilized, cellular proteins are used as fuel.

Under all these metabolic conditions, amino acids lose their amino groups to form α-keto acids, the "carbon skeletons" of amino acids. The α-keto acids undergo oxidation to CO_2 and H_2O or, often more importantly, provide three- and four-carbon units that can be converted by gluconeogenesis into glucose, the fuel for brain, skeletal muscle, and other tissues.

The pathways of amino acid catabolism are quite similar in most organisms. The focus of this chapter is on the pathways in vertebrates, because these have received the most research attention. As in carbohydrate and fatty acid catabolism, the processes of amino acid degradation converge on the central catabolic pathways, with the carbon skeletons of most amino acids finding their way to the citric acid cycle. In some cases the reaction pathways of amino acid breakdown closely parallel steps in the catabolism of fatty acids (see Fig. 17–9).

One important feature distinguishes amino acid degradation from other catabolic processes described to this point: every amino acid contains an amino group, and the pathways for amino acid degradation therefore include a key step in which the α-amino group is separated from the carbon skeleton and shunted into the pathways of amino group metabolism **(Fig. 18–1)**. We deal first with amino group metabolism and nitrogen excretion, then with the fate of the carbon skeletons derived from the amino acids; along the way we see how the pathways are interconnected.

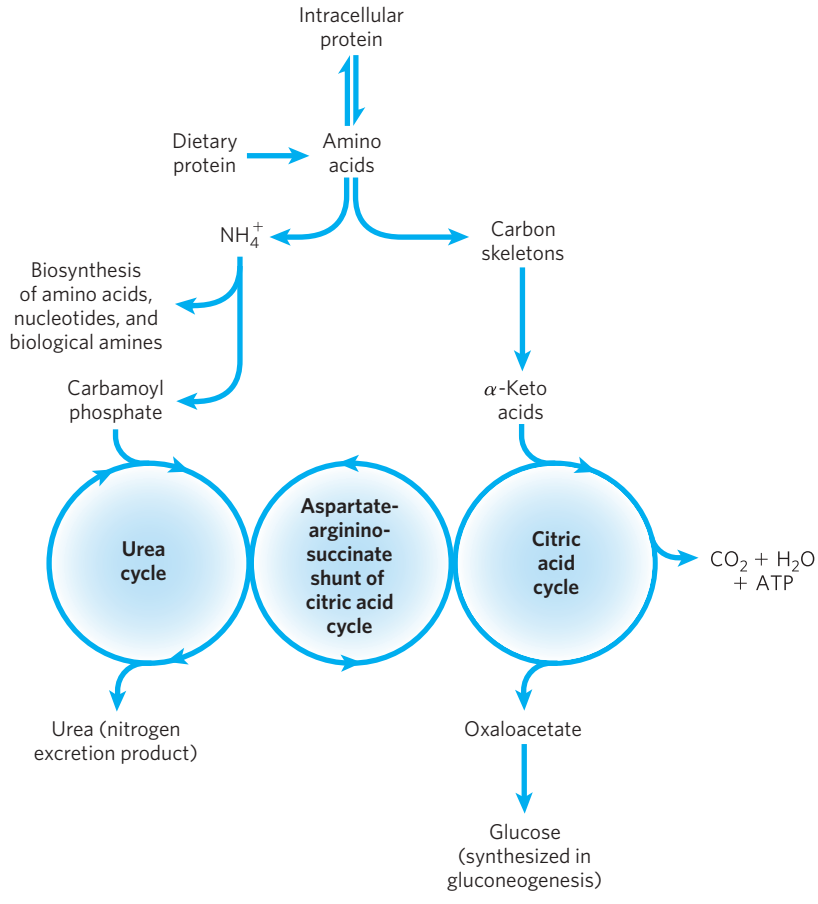

FIGURE 18–1 Overview of amino acid catabolism in mammals. The amino groups and the carbon skeleton take separate but interconnected pathways.

18.1 Metabolic Fates of Amino Groups

Nitrogen, N_2, is abundant in the atmosphere but is too inert for use in most biochemical processes. Because only a few microorganisms can convert N_2 to biologically useful forms such as NH_3 (Chapter 22), amino groups are carefully husbanded in biological systems.

Figure 18–2a provides an overview of the catabolic pathways of ammonia and amino groups in vertebrates. Amino acids derived from dietary protein are the source of most amino groups. Most amino acids are metabolized in the liver. Some of the ammonia generated in this process is recycled and used in a variety of biosynthetic pathways; the excess is either excreted directly or converted to urea or uric acid for excretion, depending on the organism (Fig. 18–2b). Excess ammonia generated in other (extrahepatic) tissues travels to the liver (in the form of amino groups, as described below) for conversion to the excretory form.

Four amino acids play central roles in nitrogen metabolism: glutamate, glutamine, alanine, and aspartate. The special place of these four amino acids in nitrogen metabolism is not an evolutionary accident. These particular amino acids are the ones most easily converted into citric acid cycle intermediates: glutamate and glutamine to α-ketoglutarate, alanine to pyruvate, and aspartate to oxaloacetate. Glutamate and glutamine are especially important, acting as a kind of general collection point for amino groups. In the cytosol of liver cells (hepatocytes), amino groups from most amino acids are transferred to α-ketoglutarate to form glutamate, which enters mitochondria and gives up its amino group to form NH_4^+. Excess ammonia generated in most other tissues is converted to the amide nitrogen of glutamine, which passes to the liver, then into liver mitochondria. Glutamine or glutamate or both are present in higher concentrations than other amino acids in most tissues.

In skeletal muscle, excess amino groups are generally transferred to pyruvate to form alanine, another important molecule in the transport of amino groups to the liver. We will see in Section 18.2 that aspartate comes into play in the metabolic processes that occur once the amino groups are delivered to the liver.

We begin with a discussion of the breakdown of dietary proteins, then give a general description of the metabolic fates of amino groups.

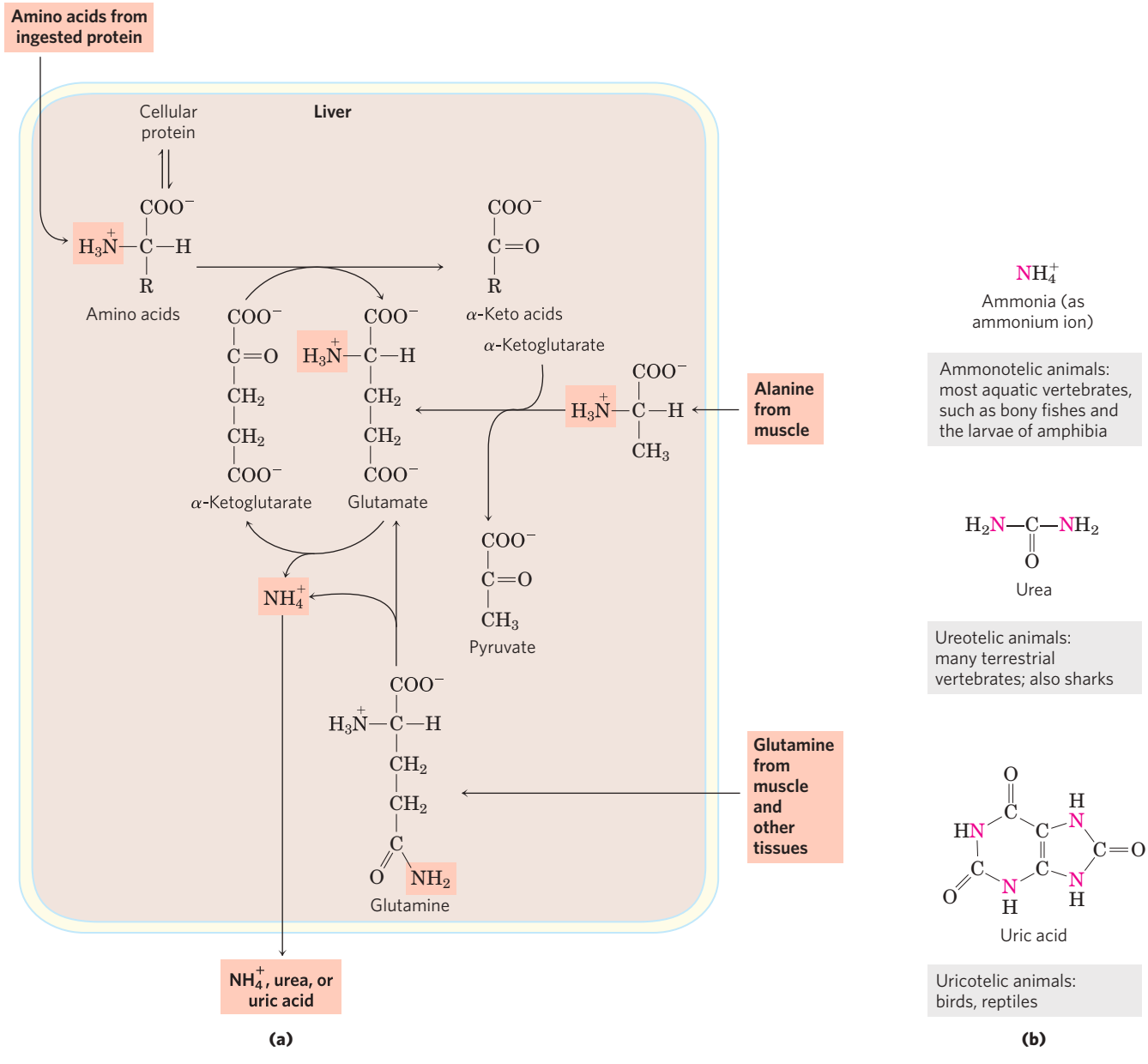

FIGURE 18–2 **Amino group catabolism. (a)** Overview of catabolism of amino groups (shaded) in vertebrate liver. **(b)** Excretory forms of nitrogen. Excess NH_4^+ is excreted as ammonia (microbes, bony fishes), urea (most terrestrial vertebrates), or uric acid (birds and terrestrial reptiles). Notice that the carbon atoms of urea and uric acid are highly oxidized; the organism discards carbon only after extracting most of its available energy of oxidation.

Dietary Protein Is Enzymatically Degraded to Amino Acids

In humans, the degradation of ingested proteins to their constituent amino acids occurs in the gastrointestinal tract. Entry of dietary protein into the stomach stimulates the gastric mucosa to secrete the hormone **gastrin**, which in turn stimulates the secretion of hydrochloric acid by the parietal cells and pepsinogen by the chief cells of the gastric glands **(Fig. 18–3a)**. The acidic gastric juice (pH 1.0 to 2.5) is both an antiseptic, killing most bacteria and other foreign cells, and a denaturing agent, unfolding globular proteins and rendering their internal peptide bonds more accessible to enzymatic hydrolysis. **Pepsinogen** (M_r 40,554), an inactive precursor, or zymogen (p. 231), is converted to active pepsin (M_r 34,614) by an autocatalytic cleavage (a cleavage mediated by the pepsinogen itself) that occurs only at low pH. In the stomach, pepsin hydrolyzes ingested proteins at peptide bonds on the amino-terminal side of the aromatic amino acid residues Phe, Trp, and Tyr (see Table 3–6), cleaving long polypeptide chains into a mixture of smaller peptides.

As the acidic stomach contents pass into the small intestine, the low pH triggers secretion of the hormone **secretin** into the blood. Secretin stimulates the pancreas

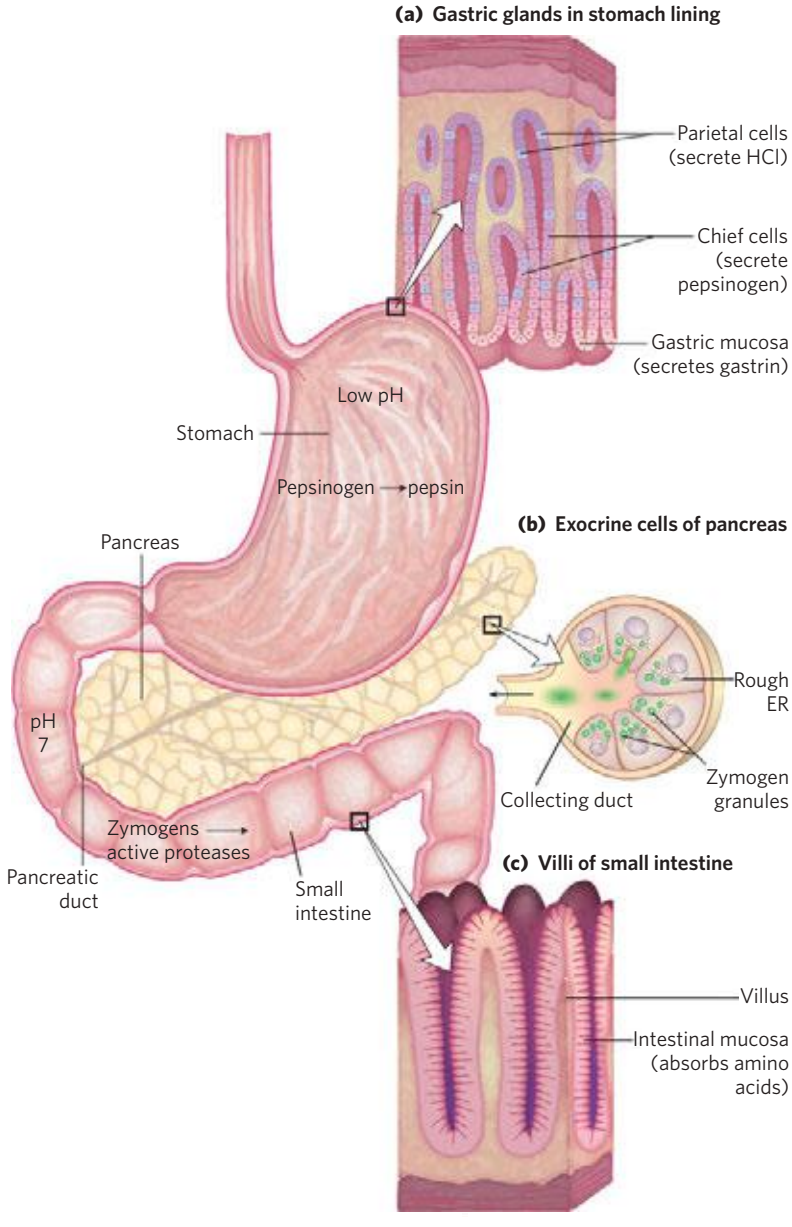

FIGURE 18–3 Part of the human digestive (gastrointestinal) tract. **(a)** The parietal cells and chief cells of the gastric glands secrete their products in response to the hormone gastrin. Pepsin begins the process of protein degradation in the stomach. **(b)** The cytoplasm of exocrine cells is completely filled with rough endoplasmic reticulum, the site of synthesis of the zymogens of many digestive enzymes. The zymogens are concentrated in membrane-enclosed transport particles called zymogen granules. When an exocrine cell is stimulated, its plasma membrane fuses with the zymogen granule membrane and zymogens are released into the lumen of the collecting duct by exocytosis. The collecting ducts ultimately lead to the pancreatic duct and thence to the small intestine. **(c)** Amino acids are absorbed through the epithelial cell layer (intestinal mucosa) of the villi and enter the capillaries. Recall that the products of lipid hydrolysis in the small intestine enter the lymphatic system after their absorption by the intestinal mucosa (see Fig. 17–1).

to secrete bicarbonate into the small intestine to neutralize the gastric HCl, abruptly increasing the pH to about 7. (All pancreatic secretions pass into the small intestine through the pancreatic duct.) The digestion of proteins now continues in the small intestine. Arrival of amino acids in the upper part of the intestine (duodenum) causes release into the blood of the hormone **cholecystokinin**, which stimulates secretion of several pancreatic enzymes with activity optima at pH 7 to 8. **Trypsinogen**, **chymotrypsinogen**, and **procarboxypeptidases A** and **B**—the zymogens of **trypsin**, **chymotrypsin**, and **carboxypeptidases A** and **B**—are synthesized and secreted by the exocrine cells of the pancreas (Fig. 18–3b). Trypsinogen is converted to its active form, trypsin, by **enteropeptidase**, a proteolytic enzyme secreted by intestinal cells. Free trypsin then catalyzes the conversion of additional trypsinogen to trypsin (see Fig. 6–38). Trypsin also

activates chymotrypsinogen, the procarboxypeptidases, and proelastase.

Why this elaborate mechanism for getting active digestive enzymes into the gastrointestinal tract? Synthesis of the enzymes as inactive precursors protects the exocrine cells from destructive proteolytic attack. The pancreas further protects itself against self-digestion by making a specific inhibitor, a protein called **pancreatic trypsin inhibitor** (p. 232), that effectively prevents premature production of active proteolytic enzymes within the pancreatic cells.

Trypsin and chymotrypsin further hydrolyze the peptides that were produced by pepsin in the stomach. This stage of protein digestion is accomplished very efficiently, because pepsin, trypsin, and chymotrypsin have different amino acid specificities (see Table 3–6). Degradation of the short peptides in the small intestine is then completed by other intestinal peptidases. These include carboxypeptidases A and B (both of which are zinc-containing enzymes), which remove successive carboxyl-terminal residues from peptides, and an **aminopeptidase** that hydrolyzes successive amino-terminal residues from short peptides. The resulting mixture of free amino acids is transported into the epithelial cells lining the small intestine (Fig. 18–3c), through which the amino acids enter the blood capillaries in the villi and travel to the liver. In humans, most globular proteins from animal sources are almost completely hydrolyzed to amino acids in the gastrointestinal tract, but some fibrous proteins, such as keratin, are only partly digested. In addition, the protein content of some plant foods is protected against breakdown by indigestible cellulose husks.

Acute pancreatitis is a disease caused by obstruction of the normal pathway by which pancreatic secretions enter the intestine. The zymogens of the proteolytic enzymes are converted to their catalytically active forms prematurely, *inside* the pancreatic cells, and attack the pancreatic tissue itself. This causes excruciating pain and damage to the organ that can prove fatal. ■

Pyridoxal Phosphate Participates in the Transfer of α-Amino Groups to α-Ketoglutarate

The first step in the catabolism of most L-amino acids, once they have reached the liver, is removal of the α-amino groups, promoted by enzymes called **aminotransferases** or **transaminases**. In these **transamination** reactions, the α-amino group is transferred to the α-carbon atom of α-ketoglutarate, leaving behind the corresponding α-keto acid analog of the amino acid **(Fig. 18–4)**. There is no net deamination (loss of amino groups) in these reactions, because the α-ketoglutarate becomes aminated as the α-amino acid is deaminated. The effect of transamination reactions is to collect the amino groups from many different amino acids in the form of L-glutamate. The glutamate then functions as an amino group donor for biosynthetic pathways or for excretion pathways that lead to the elimination of nitrogenous waste products.

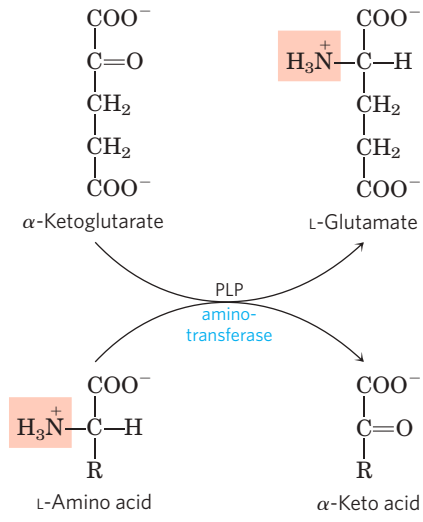

FIGURE 18–4 Enzyme-catalyzed transaminations. In many aminotransferase reactions, α-ketoglutarate is the amino group acceptor. All aminotransferases have pyridoxal phosphate (PLP) as cofactor. Although the reaction is shown here in the direction of transfer of the amino group to α-ketoglutarate, it is readily reversible.

Cells contain different types of aminotransferases. Many are specific for α-ketoglutarate as the amino group acceptor but differ in their specificity for the L-amino acid. The enzymes are named for the amino group donor (alanine aminotransferase, aspartate aminotransferase, for example). The reactions catalyzed by aminotransferases are freely reversible, having an equilibrium constant of about 1.0 ($\Delta G' \approx 0$ kJ/mol).

All aminotransferases have the same prosthetic group and the same reaction mechanism. The prosthetic group is **pyridoxal phosphate (PLP)**, the coenzyme form of pyridoxine, or vitamin B_6. We encountered pyridoxal phosphate in Chapter 15, as a coenzyme in the glycogen phosphorylase reaction, but its role in that reaction is not representative of its usual coenzyme function. Its primary role in cells is in the metabolism of molecules with amino groups.

Pyridoxal phosphate functions as an intermediate carrier of amino groups at the active site of aminotransferases. It undergoes reversible transformations between its aldehyde form, pyridoxal phosphate, which can accept an amino group, and its aminated form, pyridoxamine phosphate, which can donate its amino group to an α-keto acid **(Fig. 18–5a)**. Pyridoxal phosphate is generally covalently bound to the enzyme's active site through an aldimine (Schiff base) linkage to the ε-amino group of a Lys residue (Fig. 18–5b, d).

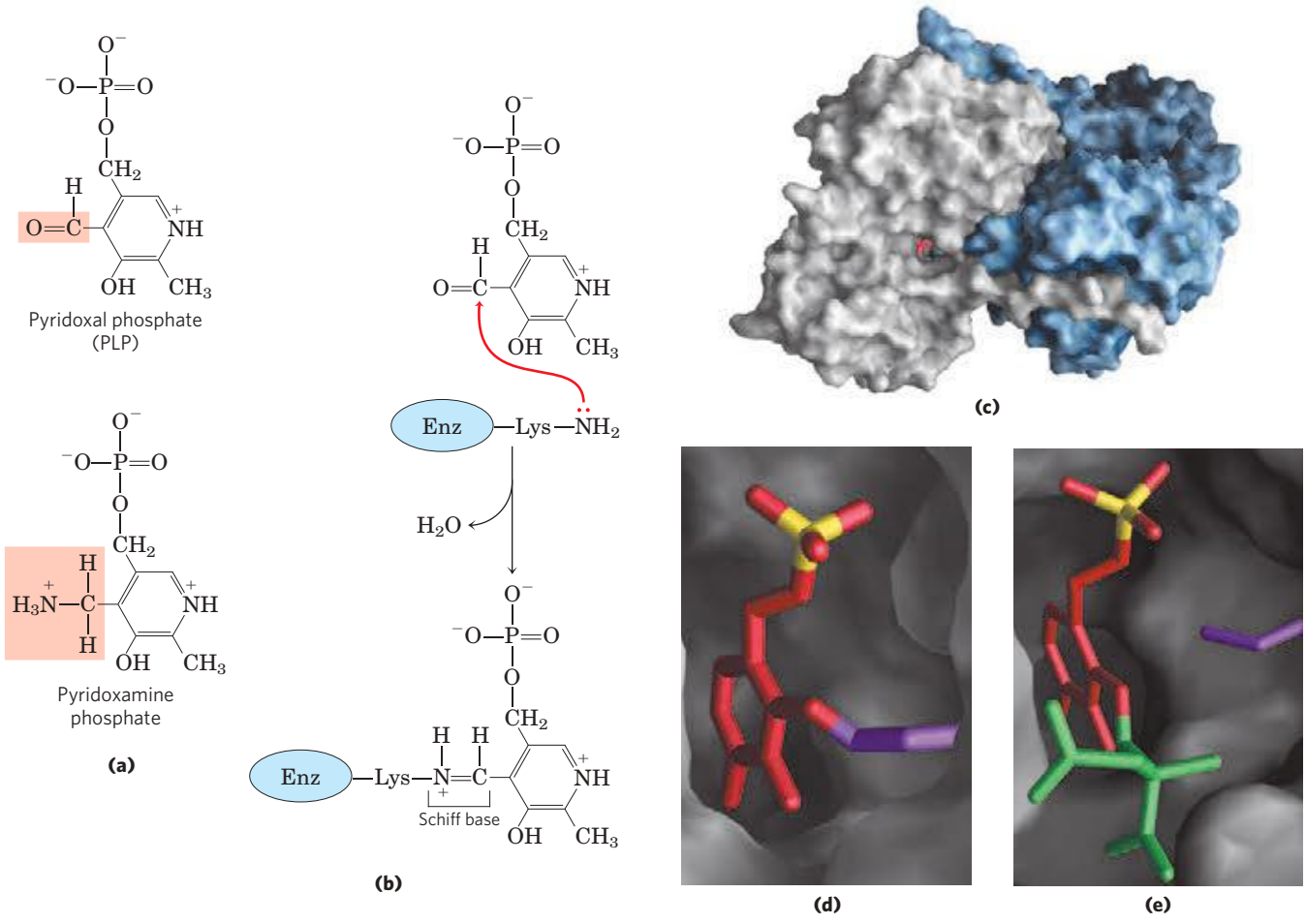

FIGURE 18–5 Pyridoxal phosphate, the prosthetic group of aminotransferases. (a) Pyridoxal phosphate (PLP) and its aminated form, pyridoxamine phosphate, are the tightly bound coenzymes of aminotransferases. The functional groups are shaded. **(b)** Pyridoxal phosphate is bound to the enzyme through noncovalent interactions and a Schiff-base (aldimine) linkage to a Lys residue at the active site. The steps in the formation of a Schiff base from a primary amine and a carbonyl group are detailed in Figure 14–6. **(c)** PLP (red) bound to one of the two active sites of the dimeric enzyme aspartate aminotransferase, a typical aminotransferase; **(d)** close-up view of the active site, with PLP (red, with yellow phosphorus) in aldimine linkage with the side chain of Lys^{258} (purple); **(e)** another close-up view of the active site, with PLP linked to the substrate analog 2-methylaspartate (green) via a Schiff base (PDB ID 1AJS).

Pyridoxal phosphate participates in a variety of reactions at the α, β, and γ carbons (C-2 to C-4) of amino acids. Reactions at the α carbon **(Fig. 18–6)** include racemizations (interconverting L- and D-amino acids) and decarboxylations, as well as transaminations. Pyridoxal phosphate plays the same chemical role in each of these reactions. A bond to the α carbon of the substrate is broken, removing either a proton or a carboxyl group. The electron pair left behind on the α carbon would form a highly unstable carbanion, but pyridoxal phosphate provides resonance stabilization of this intermediate (Fig. 18–6 inset). The highly conjugated structure of PLP (an electron sink) permits delocalization of the negative charge.

Aminotransferases (Fig. 18–5) are classic examples of enzymes catalyzing bimolecular Ping-Pong reactions (see Fig. 6–13b), in which the first substrate reacts and the product must leave the active site before the second substrate can bind. Thus the incoming amino acid binds to the active site, donates its amino group to pyridoxal phosphate, and departs in the form of an α-keto acid. The incoming α-keto acid then binds, accepts the amino group from pyridoxamine phosphate, and departs in the form of an amino acid.

Glutamate Releases Its Amino Group As Ammonia in the Liver

As we have seen, the amino groups from many of the α-amino acids are collected in the liver in the form of the amino group of L-glutamate molecules. These amino groups must next be removed from glutamate to prepare them for excretion. In hepatocytes, glutamate is transported from the cytosol into mitochondria, where it undergoes **oxidative deamination** catalyzed by **L-glutamate dehydrogenase** (M_r 330,000). In

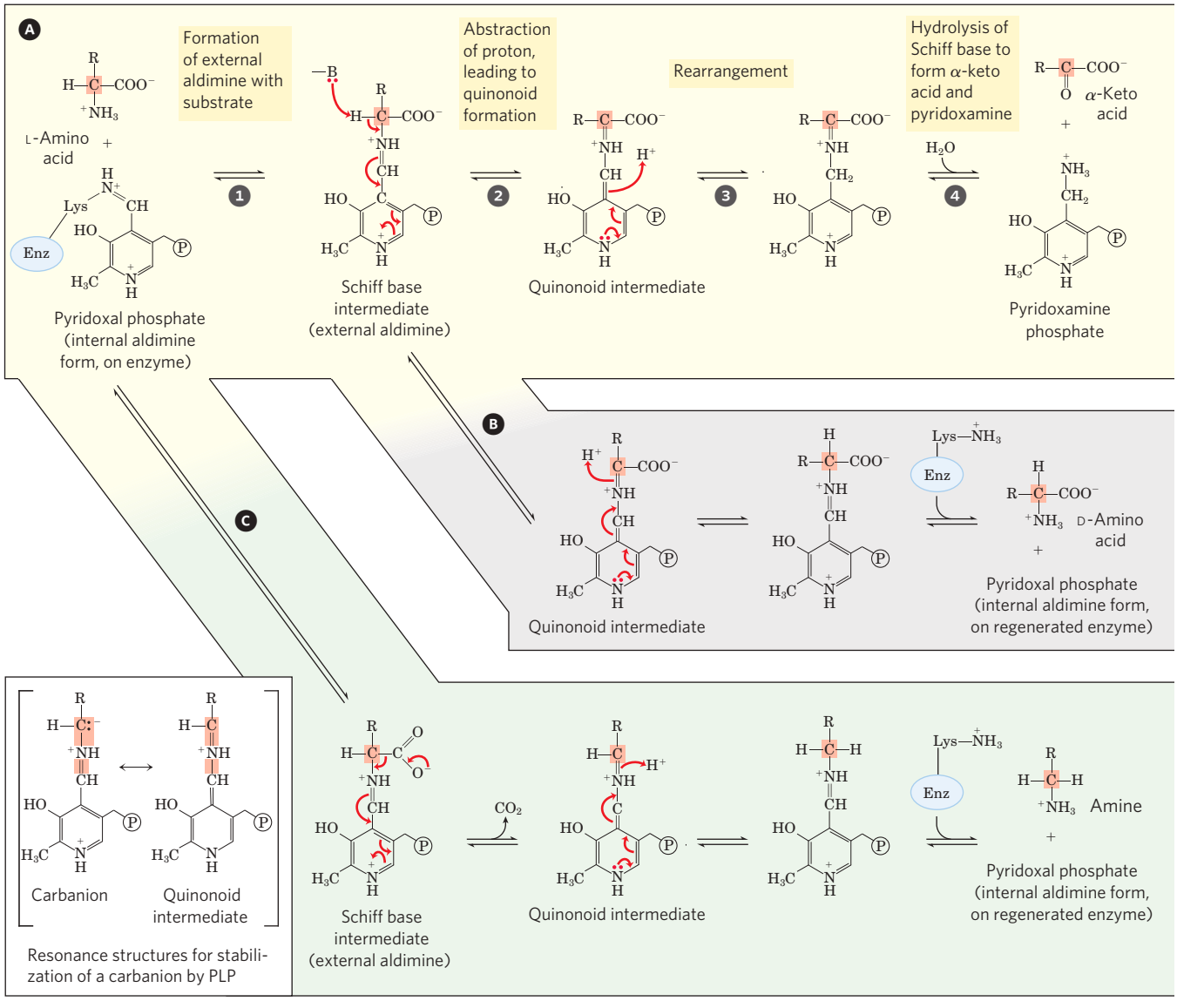

MECHANISM FIGURE 18–6 Some amino acid transformations at the α carbon that are facilitated by pyridoxal phosphate. Pyridoxal phosphate is generally bonded to the enzyme through a Schiff base, also called an internal aldimine. This activated form of PLP readily undergoes transimination to form a new Schiff base (external aldimine) with the α-amino group of the substrate amino acid (see Fig. 18–5b, d). Three alternative fates for the external aldimine are shown: Ⓐ transamination, Ⓑ racemization, and Ⓒ decarboxylation. The PLP–amino acid Schiff base is in conjugation with the pyridine ring, an electron sink that permits delocalization of an electron pair to avoid formation of an unstable carbanion on the α carbon (inset). A quinonoid intermediate is involved in all three types of reactions. The transamination route Ⓐ is especially important in the pathways described in this chapter. The pathway highlighted in yellow (shown left to right) represents only part of the overall reaction catalyzed by aminotransferases. To complete the process, a second α-keto acid replaces the one that is released, and this is converted to an amino acid in a reversal of the reaction steps (right to left). Pyridoxal phosphate is also involved in certain reactions at the β and γ carbons of some amino acids (not shown). **Pyridoxal Phosphate Reaction Mechanisms**

mammals, this enzyme is present in the mitochondrial matrix. It is the only enzyme that can use either NAD^+ or $NADP^+$ as the acceptor of reducing equivalents **(Fig. 18–7)**.

The combined action of an aminotransferase and glutamate dehydrogenase is referred to as **transdeamination**. A few amino acids bypass the transdeamination pathway and undergo direct oxidative deamination. The fate of the NH_4^+ produced by any of these deamination processes is discussed in detail in Section 18.2. The α-ketoglutarate formed from glutamate deamination can be used in the citric acid cycle and for glucose synthesis.

Glutamate dehydrogenase operates at an important intersection of carbon and nitrogen metabolism. An allosteric enzyme with six identical subunits, its activity

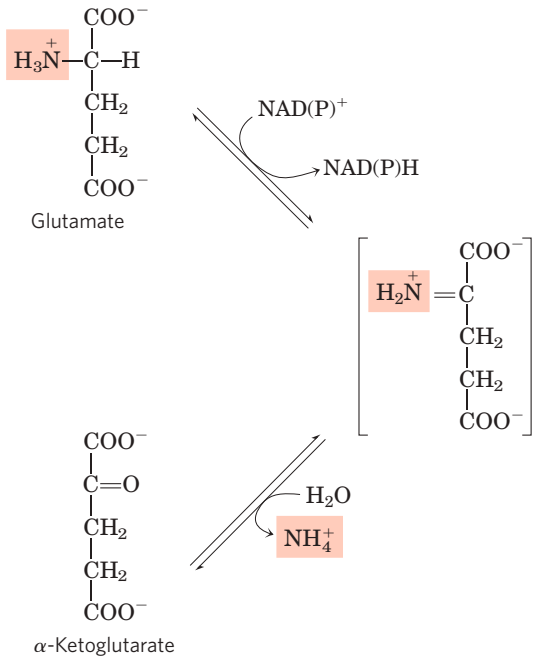

FIGURE 18–7 Reaction catalyzed by glutamate dehydrogenase. The glutamate dehydrogenase of mammalian liver has the unusual capacity to use either NAD^+ or $NADP^+$ as cofactor. The glutamate dehydrogenases of plants and microorganisms are generally specific for one or the other. The mammalian enzyme is allosterically regulated by GTP and ADP.

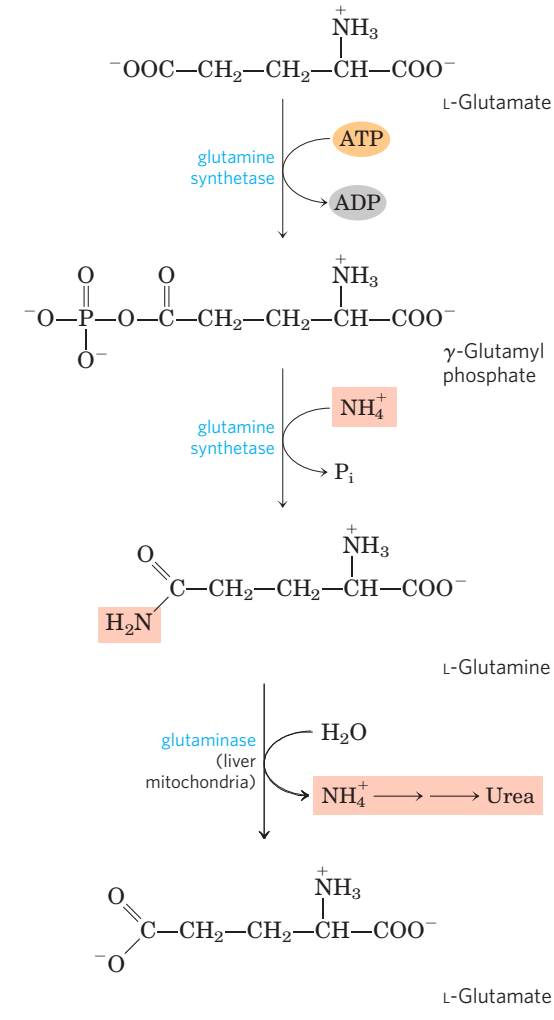

FIGURE 18–8 Ammonia transport in the form of glutamine. Excess ammonia in tissues is added to glutamate to form glutamine, a process catalyzed by glutamine synthetase. After transport in the bloodstream, the glutamine enters the liver and NH_4^+ is liberated in mitochondria by the enzyme glutaminase.

is influenced by a complicated array of allosteric modulators. The best-studied of these are the positive modulator ADP and the negative modulator GTP. The metabolic rationale for this regulatory pattern has not been elucidated in detail. Mutations that alter the allosteric binding site for GTP or otherwise cause permanent activation of glutamate dehydrogenase lead to a human genetic disorder called hyperinsulinism-hyperammonemia syndrome, characterized by elevated levels of ammonia in the bloodstream and hypoglycemia.

Glutamine Transports Ammonia in the Bloodstream

Ammonia is quite toxic to animal tissues (we examine some possible reasons for this toxicity later), and the levels present in blood are regulated. In many tissues, including the brain, some processes such as nucleotide degradation generate free ammonia. In most animals much of the free ammonia is converted to a nontoxic compound before export from the extrahepatic tissues into the blood and transport to the liver or kidneys. For this transport function, glutamate, critical to *intracellular* amino group metabolism, is supplanted by L-glutamine. The free ammonia produced in tissues is combined with glutamate to yield glutamine by the action of **glutamine synthetase**. This reaction requires ATP and occurs in two steps **(Fig. 18–8)**. First, glutamate and ATP react to form ADP and a γ-glutamyl phosphate intermediate, which then reacts with ammonia to produce glutamine and inorganic phosphate. Glutamine is a nontoxic transport form of ammonia; it is normally present in blood in much higher concentrations than other amino acids. Glutamine also serves as a source of amino groups in a variety of biosynthetic reactions. Glutamine synthetase is found in all organisms, always playing a central metabolic role. In microorganisms, the enzyme serves as an essential portal for the entry of fixed nitrogen into biological systems. (The roles of glutamine and glutamine synthetase in metabolism are further discussed in Chapter 22.)

In most terrestrial animals, glutamine in excess of that required for biosynthesis is transported in the blood to the intestine, liver, and kidneys for processing. In these tissues, the amide nitrogen is released as ammonium ion in the mitochondria, where the enzyme

glutaminase converts glutamine to glutamate and NH_4^+ (Fig. 18–8). The NH_4^+ from intestine and kidney is transported in the blood to the liver. In the liver, the ammonia from all sources is disposed of by urea synthesis. Some of the glutamate produced in the glutaminase reaction may be further processed in the liver by glutamate dehydrogenase, releasing more ammonia and producing carbon skeletons for metabolic fuel. However, most glutamate enters the transamination reactions required for amino acid biosynthesis and other processes (Chapter 22).

In metabolic acidosis (p. 688) there is an increase in glutamine processing by the kidneys. Not all the excess NH_4^+ thus produced is released into the bloodstream or converted to urea; some is excreted directly into the urine. In the kidney, the NH_4^+ forms salts with metabolic acids, facilitating their removal in the urine. Bicarbonate produced by the decarboxylation of α-ketoglutarate in the citric acid cycle can also serve as a buffer in blood plasma. Taken together, these effects of glutamine metabolism in the kidney tend to counteract acidosis. ■

Alanine Transports Ammonia from Skeletal Muscles to the Liver

Alanine also plays a special role in transporting amino groups to the liver in a nontoxic form, via a pathway called the **glucose-alanine cycle (Fig. 18–9)**. In muscle and certain other tissues that degrade amino acids for fuel, amino groups are collected in the form of glutamate by transamination (Fig. 18–2a). Glutamate can be converted to glutamine for transport to the liver, as described above, or it can transfer its α-amino group to pyruvate, a readily available product of muscle glycolysis, by the action of **alanine aminotransferase** (Fig. 18–9). The alanine so formed passes into the blood and travels to the liver. In the cytosol of hepatocytes, alanine aminotransferase transfers the amino group from alanine to α-ketoglutarate, forming pyruvate and glutamate. Glutamate can then enter mitochondria, where the glutamate dehydrogenase reaction releases NH_4^+ (Fig. 18–7), or can undergo transamination with oxaloacetate to form aspartate, another nitrogen donor in urea synthesis, as we shall see.

The use of alanine to transport ammonia from skeletal muscles to the liver is another example of the intrinsic economy of living organisms. Vigorously contracting skeletal muscles operate anaerobically, producing pyruvate and lactate from glycolysis as well as ammonia from protein breakdown. These products must find their way to the liver, where pyruvate and lactate are incorporated into glucose, which is returned to the muscles, and ammonia is converted to urea for excretion. The glucose-alanine cycle, in concert with the Cori cycle (see Box 14–2 and Fig. 23–19), accomplishes this transaction. The energetic burden of gluconeogenesis is thus imposed on the liver rather than the muscle, and all available ATP in muscle is devoted to muscle contraction.

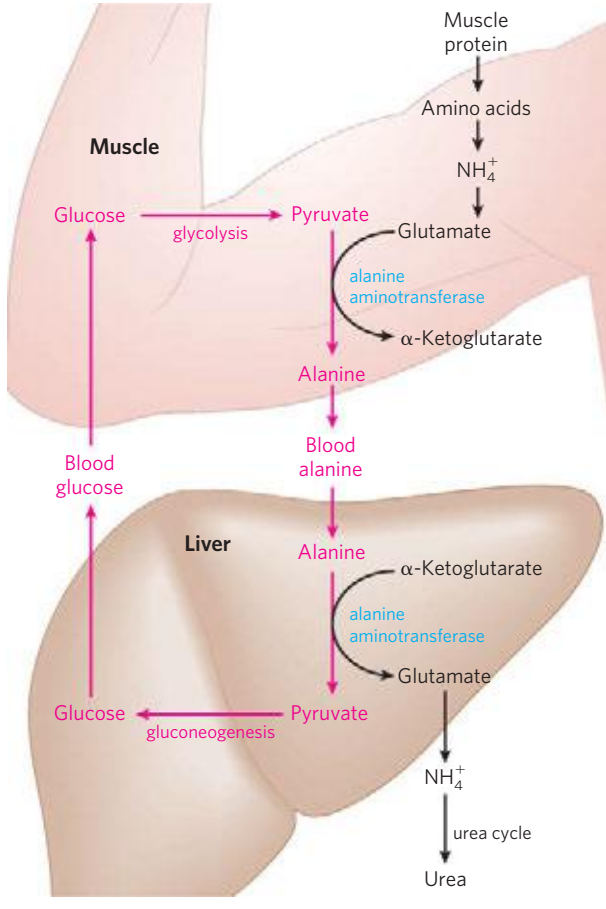

FIGURE 18–9 Glucose-alanine cycle. Alanine serves as a carrier of ammonia and of the carbon skeleton of pyruvate from skeletal muscle to liver. The ammonia is excreted and the pyruvate is used to produce glucose, which is returned to the muscle.

Ammonia Is Toxic to Animals

The catabolic production of ammonia poses a serious biochemical problem, because ammonia is very toxic. The molecular basis for this toxicity is not entirely understood. The terminal stages of ammonia intoxication in humans are characterized by onset of a comatose state accompanied by cerebral edema (an increase in the brain's water content) and increased cranial pressure, so research and speculation on ammonia toxicity have focused on this tissue. Speculation centers on a potential depletion of ATP in brain cells.

Ammonia readily crosses the blood-brain barrier, so any condition that raises the level of ammonia in the bloodstream will expose the brain to high concentrations too. The developing brain is more susceptible to the deleterious effects of ammonium ion than the adult brain. The damage from ammonium toxicity includes loss of neurons, altered synapse formation, and a general defect in cellular energy metabolism.

Ridding the cytosol of excess ammonia requires reductive amination of α-ketoglutarate to glutamate by glutamate dehydrogenase (the reverse of the reaction described earlier; Fig. 18–7) and conversion of glutamate to glutamine by glutamine synthetase. Both enzymes are present at high levels in the brain, although the glutamine synthetase reaction is almost certainly the more important pathway for removal of ammonia. High levels of NH_4^+ lead to increased levels of glutamine, which acts as an osmotically active solute (osmolyte) in brain astrocytes, star-shaped cells of the nervous system that provide nutrients, support, and insulation for neurons. This triggers an uptake of water into the astrocytes to maintain osmotic balance, leading to swelling of the cells and the brain, which in turn can lead to coma.

Depletion of glutamate in the glutamine synthetase reaction may have additional effects on the brain. Glutamate and its derivative γ-aminobutyrate (GABA; see Fig. 22–31) are important neurotransmitters; the sensitivity of the brain to ammonia may reflect a depletion of neurotransmitters as well as changes in cellular osmotic balance. ■

As we close this discussion of amino group metabolism, note that we have described several processes that deposit excess ammonia in the mitochondria of hepatocytes (Fig. 18–2). We now look at the fate of that ammonia.

SUMMARY 18.1 Metabolic Fates of Amino Groups

- Humans derive a small fraction of their oxidative energy from the catabolism of amino acids. Amino acids are derived from the normal breakdown (recycling) of cellular proteins, degradation of ingested proteins, and breakdown of body proteins in lieu of other fuel sources during starvation or in uncontrolled diabetes mellitus.
- Proteases degrade ingested proteins in the stomach and small intestine. Most proteases are initially synthesized as inactive zymogens.
- An early step in the catabolism of amino acids is the separation of the amino group from the carbon skeleton. In most cases, the amino group is transferred to α-ketoglutarate to form glutamate. This transamination reaction requires the coenzyme pyridoxal phosphate.
- Glutamate is transported to liver mitochondria, where glutamate dehydrogenase liberates the amino group as ammonium ion (NH_4^+). Ammonia formed in other tissues is transported to the liver as the amide nitrogen of glutamine or, in transport from skeletal muscle, as the amino group of alanine.
- The pyruvate produced by deamination of alanine in the liver is converted to glucose, which is transported back to muscle as part of the glucose-alanine cycle.

18.2 Nitrogen Excretion and the Urea Cycle

If not reused for the synthesis of new amino acids or other nitrogenous products, amino groups are channeled into a single excretory end product **(Fig. 18–10)**. Most aquatic species, such as the bony fishes, are **ammonotelic**, excreting amino nitrogen as ammonia. The toxic ammonia is simply diluted in the surrounding water. Terrestrial animals require pathways for nitrogen excretion that minimize toxicity and water loss. Most terrestrial animals are **ureotelic**, excreting amino nitrogen in the form of urea; birds and reptiles are **uricotelic**, excreting amino nitrogen as uric acid. (The pathway of uric acid synthesis is described in Fig. 22–48.) Plants recycle virtually all amino groups—they excrete nitrogen only under very unusual circumstances.

In ureotelic organisms, the ammonia deposited in the mitochondria of hepatocytes is converted to urea in the **urea cycle**. This pathway was discovered in 1932 by Hans Krebs (who later also discovered the citric acid cycle) and a medical student associate, Kurt Henseleit. Urea production occurs almost exclusively in the liver and is the fate of most of the ammonia channeled there. The urea passes into the bloodstream and thus to the kidneys and is excreted into the urine. The production of urea now becomes the focus of our discussion.

Urea Is Produced from Ammonia in Five Enzymatic Steps

The urea cycle begins inside liver mitochondria, but three of the subsequent steps take place in the cytosol; the cycle thus spans two cellular compartments (Fig. 18–10). The first amino group to enter the urea cycle is derived from ammonia in the mitochondrial matrix—most of this NH_4^+ arises by the pathways described in the previous section. The liver also receives some ammonia via the portal vein from the intestine, from the bacterial oxidation of amino acids. Whatever its source, the NH_4^+ generated in liver mitochondria is immediately used, together with CO_2 (as HCO_3^-) produced by mitochondrial respiration, to form carbamoyl phosphate in

FIGURE 18–10 Urea cycle and reactions that feed amino groups into the cycle. The enzymes catalyzing these reactions (named in the text) are distributed between the mitochondrial matrix and the cytosol. One amino group enters the urea cycle as carbamoyl phosphate, formed in the matrix; the other enters as aspartate, formed in the matrix by transamination of oxaloacetate and glutamate, catalyzed by aspartate aminotransferase. The urea cycle consists of four steps. ❶ Formation of citrulline from ornithine and carbamoyl phosphate (entry of the first amino group); the citrulline passes into the cytosol. ❷ Formation of argininosuccinate through a citrullyl-AMP intermediate (entry of the second amino group). ❸ Formation of arginine from argininosuccinate; this reaction releases fumarate, which enters the citric acid cycle. ❹ Formation of urea; this reaction also regenerates ornithine. The pathways by which NH_4^+ arrives in the mitochondrial matrix of hepatocytes were discussed in Section 18.1.

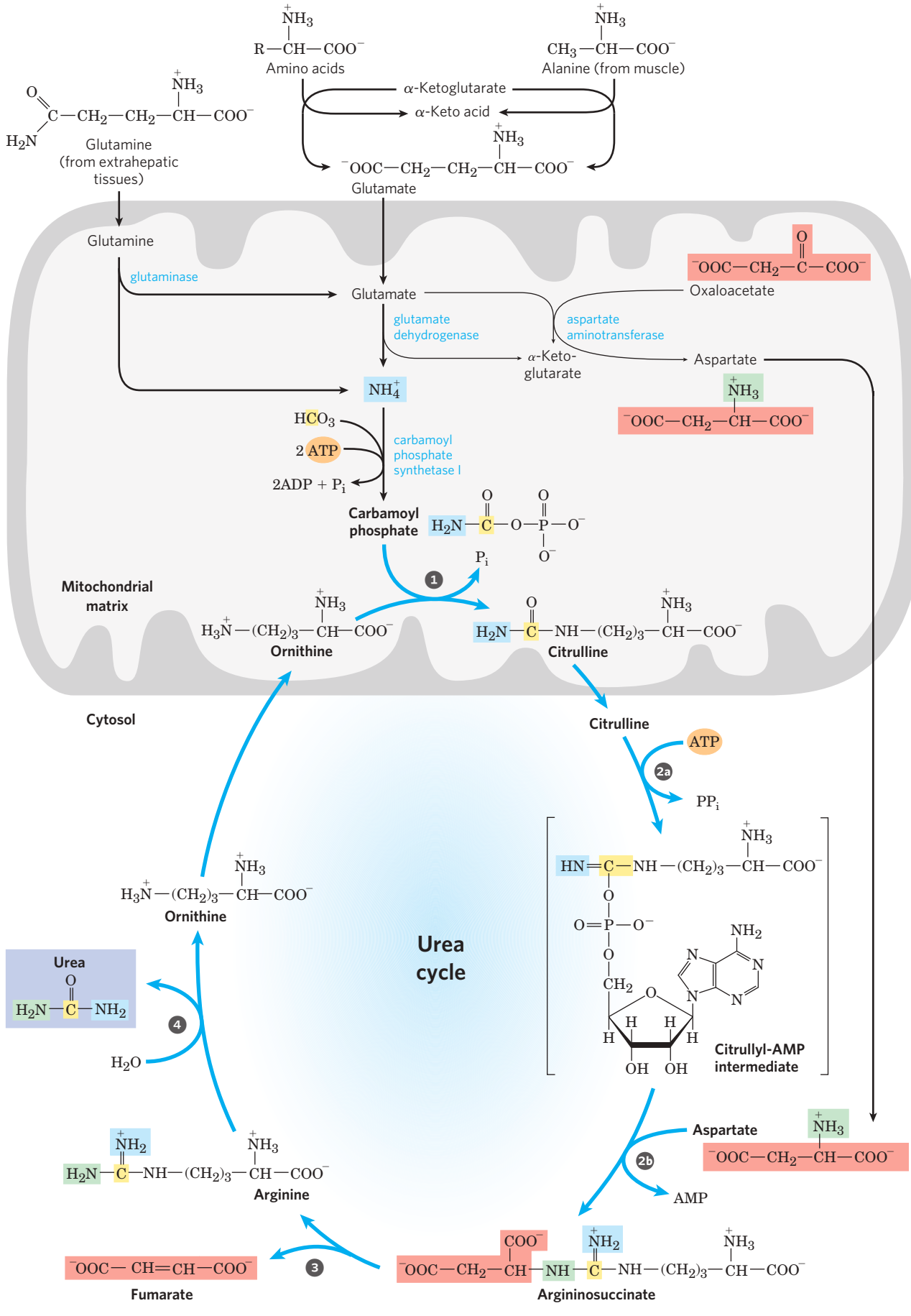
Amino acids
Alanine (from muscle)
α-Ketoglutarate
α-Keto acid
Glutamate
Glutamine
(from extrahepatic tissues)
Glutamine
glutaminase
Glutamate
Oxaloacetate
glutamate dehydrogenase
aspartate aminotransferase
α-Keto-glutarate
Aspartate
NH4+
HCO3
2 ATP
2ADP + Pi
carbamoyl phosphate synthetase I
Carbamoyl phosphate
Pi
1
Mitochondrial matrix
Ornithine
Citrulline
Cytosol
Citrulline
ATP
2a
PPi
Citrullyl-AMP intermediate
Urea cycle
Ornithine
Urea
4
H2O
Aspartate
2b
AMP
Arginine
3
Fumarate
Argininosuccinate

the matrix (**Fig. 18–11a**; see also Fig. 18–10). This ATP-dependent reaction is catalyzed by **carbamoyl phosphate synthetase I**, a regulatory enzyme (see below). The mitochondrial form of the enzyme is distinct from the cytosolic (II) form, which has a separate function in pyrimidine biosynthesis (Chapter 22).

The carbamoyl phosphate, which functions as an activated carbamoyl group donor, now enters the urea cycle. The cycle has only four enzymatic steps. First, carbamoyl phosphate donates its carbamoyl group to ornithine to form citrulline, with the release of P_i (Fig. 18–10, step ❶). The reaction is catalyzed by **ornithine transcarbamoylase**. Ornithine is not one of the 20 common amino acids found in proteins, but it is a key intermediate in nitrogen metabolism. It is synthesized from glutamate in a five-step pathway described in Chapter 22. Ornithine plays a role resembling that of oxaloacetate in the citric acid cycle, accepting material at each turn of the urea cycle. The citrulline produced in the first step of the urea cycle passes from the mitochondrion to the cytosol.

The next two steps bring in the second amino group. The source is aspartate generated in mitochondria by transamination and transported into the cytosol. A condensation reaction between the amino group of aspartate and the ureido (carbonyl) group of citrulline forms argininosuccinate (step ❷ in Fig. 18–10). This cytosolic reaction, catalyzed by **argininosuccinate synthetase**, requires ATP and proceeds through a citrullyl-AMP intermediate (Fig. 18–11b). The argininosuccinate is then cleaved by **argininosuccinase** (step ❸ in Fig. 18–10) to form free arginine and fumarate, the latter being converted to malate before entering mitochondria to join the pool of citric acid cycle intermediates. This is the only reversible step in the urea cycle. In the last reaction of the urea cycle (step ❹), the cytosolic enzyme **arginase** cleaves arginine to yield **urea** and ornithine. Ornithine is transported into the mitochondrion to initiate another round of the urea cycle.

As we noted in Chapter 16, the enzymes of many metabolic pathways are clustered (p. 636), with the product of one enzyme reaction being channeled directly to the next enzyme in the pathway. In the urea cycle, the mitochondrial and cytosolic enzymes seem to be clustered in this way. The citrulline transported out of the mitochondrion is not diluted into the general pool of metabolites in the cytosol but is passed directly to the active site of argininosuccinate synthetase. This channeling between enzymes continues for argininosuccinate, arginine, and ornithine. Only urea is released into the general cytosolic pool of metabolites.

The Citric Acid and Urea Cycles Can Be Linked

The fumarate produced in the argininosuccinase reaction is also an intermediate of the citric acid cycle.

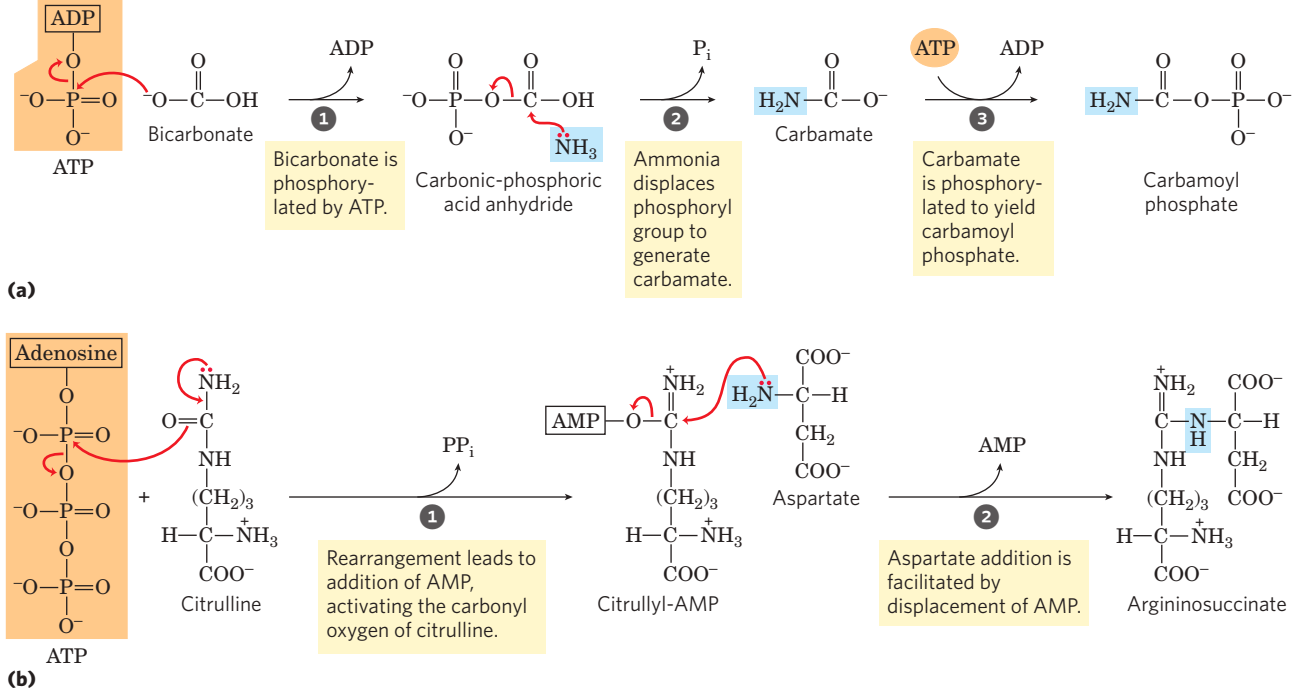

MECHANISM FIGURE 18–11 **Nitrogen-acquiring reactions in the synthesis of urea.** The urea nitrogens are acquired in two reactions, each requiring ATP. **(a)** In the reaction catalyzed by carbamoyl phosphate synthetase I, the first nitrogen enters from ammonia. The terminal phosphate groups of two molecules of ATP are used to form one molecule of carbamoyl phosphate. In other words, this reaction has two activation steps (❶ and ❸). Carbamoyl Phosphate Synthetase I Mechanism **(b)** In the reaction catalyzed by argininosuccinate synthetase, the second nitrogen enters from aspartate. Activation of the ureido oxygen of citrulline in step ❶ sets up the addition of aspartate in step ❷. Argininosuccinate Synthetase Mechanism

Thus, the cycles are, in principle, interconnected—in a process dubbed the "Krebs bicycle" **(Fig. 18–12)**. However, each cycle can operate independently, and communication between them depends on the transport of key intermediates between the mitochondrion and cytosol. Major transporters in the inner mitochondrial membrane include the malate–α-ketoglutarate transporter, the glutamate-aspartate transporter, and the glutamate-OH^- transporter. Together, these transporters facilitate the movement of malate and glutamate into the mitochondrial matrix and the movement of aspartate and α-ketoglutarate out to the cytosol.

Several enzymes of the citric acid cycle, including fumarase (fumarate hydratase) and malate dehydrogenase (p. 647), are also present as isozymes in the cytosol. There is no transporter to directly move the fumarate generated in cytosolic arginine synthesis back into the mitochondrial matrix. However, fumarate can be converted to malate in the cytosol. Fumarate and malate can be further metabolized in the cytosol or malate can be transported into mitochondria for use in the citric acid cycle. Aspartate formed in mitochondria by transamination between oxaloacetate and glutamate can be transported to the cytosol, where it serves as nitrogen donor in the urea cycle reaction catalyzed by argininosuccinate synthetase. These reactions, making up the **aspartate-argininosuccinate shunt**, provide metabolic links between the separate pathways by which the amino groups and carbon skeletons of amino acids are processed.

The use of aspartate as a nitrogen donor in the urea cycle may appear to be a relatively complicated way to introduce the second amino group into urea. However, we shall see in Chapter 22 that this pathway for nitrogen incorporation is one of the two common ways to introduce amino groups in the biosynthesis of molecules that contain them. In the urea cycle, additional pathway interconnections can help explain why aspartate is used as a nitrogen donor. The urea and citric acid cycles are closely tied to an additional process that brings NADH in the form of reducing equivalents into the mitochondrion. As detailed in the next chapter, the NADH produced by glycolysis, fatty acid oxidation, and other processes cannot be transported across

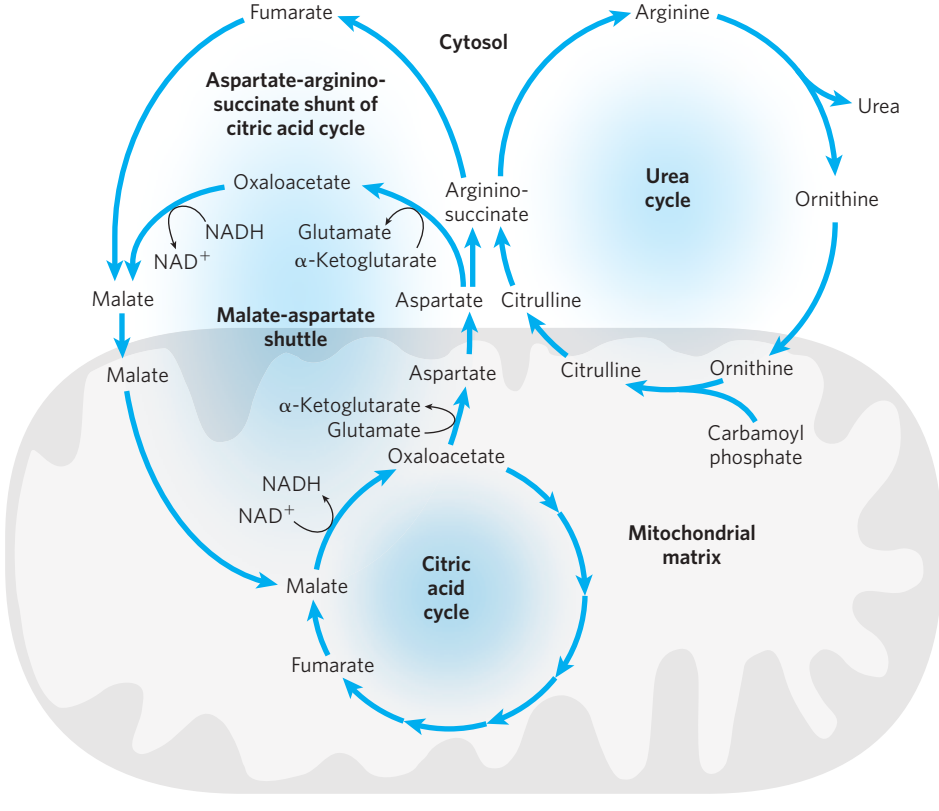

FIGURE 18–12 Links between the urea cycle and citric acid cycle. The interconnected cycles have been called the "Krebs bicycle." The pathways linking the citric acid and urea cycles are known as the aspartate-argininosuccinate shunt; these effectively link the fates of the amino groups and the carbon skeletons of amino acids. The interconnections are quite elaborate. For example, some citric acid cycle enzymes, such as fumarase and malate dehydrogenase, have both cytosolic and mitochondrial isozymes. Fumarate produced in the cytosol—whether by the urea cycle, purine biosynthesis, or other processes—can be converted to cytosolic malate, which is used in the cytosol, or transported into mitochondria to enter the citric acid cycle. These processes are further intertwined with the malate-aspartate shuttle, a set of reactions that brings reducing equivalents into the mitochondrion (see also Fig. 19–31). These different cycles and processes rely on a limited number of transporters in the inner mitochondrial membrane.

the mitochondrial inner membrane. Reducing equivalents are instead brought into the mitochondrion by converting aspartate to oxaloacetate in the cytosol, reducing the oxaloacetate to malate with NADH, and transporting the malate into the mitochondrial matrix via the malate–α-ketoglutarate transporter. Once inside the mitochondrion, the malate can be reconverted to oxaloacetate while generating NADH. The oxaloacetate is converted to aspartate in the matrix and transported out of the mitochondrion by the aspartate-glutamate transporter. This malate-aspartate shuttle completes yet another cycle that functions to keep the mitochondrion supplied with NADH (see Fig. 19–31).

These processes require that a balance be maintained in the cytosol between the concentrations of glutamate and aspartate. The enzyme that transfers amino groups between these key amino acids is aspartate aminotransferase, AAT (also called glutamate-oxaloacetate transaminase, GOT). This enzyme is among the most active enzymes in hepatocytes and other tissues. When tissue damage occurs, this easily assayed enzyme and others leak into the blood. Thus, measuring blood levels of liver enzymes is important in diagnosing a variety of medical conditions (Box 18–1).

The Activity of the Urea Cycle Is Regulated at Two Levels

The flux of nitrogen through the urea cycle in an individual animal varies with diet. When the dietary intake is primarily protein, the carbon skeletons of amino acids are used for fuel, producing much urea from the excess amino groups. During prolonged starvation, when breakdown of muscle protein begins to supply much of the organism's metabolic energy, urea production also increases substantially.

These changes in demand for urea cycle activity are met over the long term by regulation of the rates of synthesis of the four urea cycle enzymes and carbamoyl phosphate synthetase I in the liver. All five enzymes are synthesized at higher rates in starving animals and in animals on very-high-protein diets than in well-fed animals eating primarily carbohydrates and fats. Animals on protein-free diets produce lower levels of urea cycle enzymes.

On a shorter time scale, allosteric regulation of at least one key enzyme adjusts the flux through the urea cycle. The first enzyme in the pathway, carbamoyl phosphate synthetase I, is allosterically activated by ***N*-acetylglutamate**, which is synthesized from acetyl-CoA and glutamate by ***N*-acetylglutamate synthase (Fig. 18–13)**. In plants and microorganisms this enzyme catalyzes the first step in the de novo synthesis of arginine from glutamate (see Fig. 22–12), but in mammals *N*-acetylglutamate synthase activity in the liver has a purely regulatory function (mammals lack the other enzymes needed to convert glutamate to arginine). The steady-state levels of *N*-acetylglutamate are determined by the concentrations of glutamate and acetyl-CoA (the substrates for *N*-acetylglutamate synthase) and arginine (an activator of *N*-acetylglutamate synthase, and thus an activator of the urea cycle).

Pathway Interconnections Reduce the Energetic Cost of Urea Synthesis

If we consider the urea cycle in isolation, we see that the synthesis of one molecule of urea requires four high-energy phosphate groups (Fig. 18–10). Two ATP

BOX 18–1 MEDICINE Assays for Tissue Damage

Analyses of certain enzyme activities in blood serum give valuable diagnostic information for several disease conditions.

Alanine aminotransferase (ALT; also called glutamate-pyruvate transaminase, GPT) and aspartate aminotransferase (AST; also called glutamate-oxaloacetate transaminase, GOT) are important in the diagnosis of heart and liver damage caused by heart attack, drug toxicity, or infection. After a heart attack, a variety of enzymes, including these aminotransferases, leak from injured heart cells into the bloodstream. Measurements of the blood serum concentrations of the two aminotransferases by the SGPT and SGOT tests (S for serum)—and of another enzyme, **creatine kinase**, by the SCK test—can provide information about the severity of the damage. Creatine kinase is the first heart enzyme to appear in the blood after a heart attack; it also disappears quickly from the blood. GOT is the next to appear, and GPT follows later. Lactate dehydrogenase also leaks from injured or anaerobic heart muscle.

The SGOT and SGPT tests are also important in occupational medicine, to determine whether people exposed to carbon tetrachloride, chloroform, or other industrial solvents have suffered liver damage. Liver degeneration caused by these solvents is accompanied by leakage of various enzymes from injured hepatocytes into the blood. Aminotransferases are most useful in the monitoring of people exposed to these chemicals, because these enzyme activities are high in liver and thus are likely to be among the proteins leaked from damaged hepatocytes; also, they can be detected in the bloodstream in very small amounts.

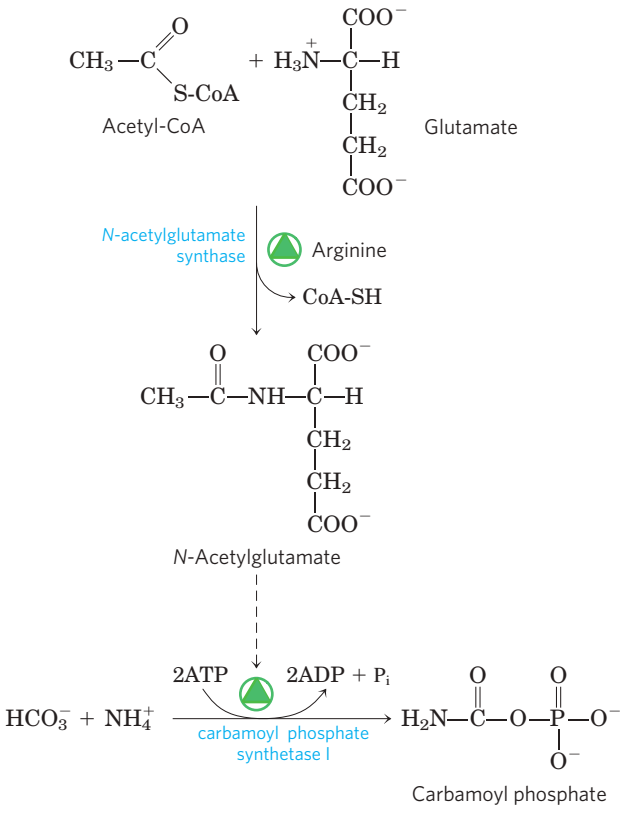

FIGURE 18–13 **Synthesis of *N*-acetylglutamate and its activation of carbamoyl phosphate synthetase I.**

molecules are required to make carbamoyl phosphate, and one ATP to make argininosuccinate—the latter ATP undergoing a pyrophosphate cleavage to AMP and PP_i, which is hydrolyzed to two P_i. The overall equation of the urea cycle is

$$2NH_4^+ + HCO_3^- + 3ATP^{4-} + H_2O \longrightarrow \text{urea} + 2ADP^{3-} + 4P_i^{2-} + AMP^{2-} + 2H^+$$

However, this apparent cost is ameliorated by the pathway interconnections detailed above. The fumarate generated by the urea cycle is converted to malate, and the malate is transported into the mitochondrion (Fig. 18–12). Inside the mitochondrial matrix, NADH is generated in the malate dehydrogenase reaction. Each NADH molecule can generate up to 2.5 ATP during mitochondrial respiration (Chapter 19), greatly reducing the overall energetic cost of urea synthesis.

Genetic Defects in the Urea Cycle Can Be Life-Threatening

People with genetic defects in any enzyme involved in urea formation cannot tolerate protein-rich diets. Amino acids ingested in excess of the minimum daily requirements for protein synthesis are deaminated in the liver, producing free ammonia that cannot be converted to urea and exported into the bloodstream, and, as we have seen, ammonia is highly toxic. The absence of a urea cycle enzyme can result in hyperammonemia or in the buildup of one or more urea cycle intermediates, depending on the enzyme that is missing. Given that most urea cycle steps are irreversible, the absent enzyme activity can often be identified by determining which cycle intermediate is present in especially elevated concentration in the blood and/or urine. Although the breakdown of amino acids can have serious health consequences in individuals with urea cycle deficiencies, a protein-free diet is not a treatment option. Humans are incapable of synthesizing half of the 20 common amino acids, and these **essential amino acids** (Table 18–1) must be provided in the diet.

A variety of treatments are available for individuals with urea cycle defects. Careful administration of the aromatic acids benzoate or phenylbutyrate in the diet can help lower the level of ammonia in the blood. Benzoate is converted to benzoyl-CoA, which combines with glycine to form hippurate (**Fig. 18–14**, left). The glycine used up in this reaction must be regenerated, and ammonia is thus taken up in the glycine synthase reaction. Phenylbutyrate is converted to phenylacetate by β oxidation. The phenylacetate is then converted to phenylacetyl-CoA, which combines with glutamine to form phenylacetylglutamine (Fig. 18–14, right). The resulting removal of glutamine triggers its further synthesis by glutamine synthetase (see Eqn 22–1) in a reaction that takes up ammonia. Both hippurate and phenylacetylglutamine are nontoxic compounds that are excreted in the urine. The pathways shown in Figure 18–14 make only minor contributions to normal metabolism, but they become prominent when aromatic acids are ingested.

TABLE 18–1 Nonessential and Essential Amino Acids for Humans and the Albino Rat

Nonessential	Conditionally essential*	Essential
Alanine	Arginine	Histidine
Asparagine	Cysteine	Isoleucine
Aspartate	Glutamine	Leucine
Glutamate	Glycine	Lysine
Serine	Proline	Methionine
	Tyrosine	Phenylalanine
		Threonine
		Tryptophan
		Valine

*Required to some degree in young, growing animals and/or sometimes during illness.

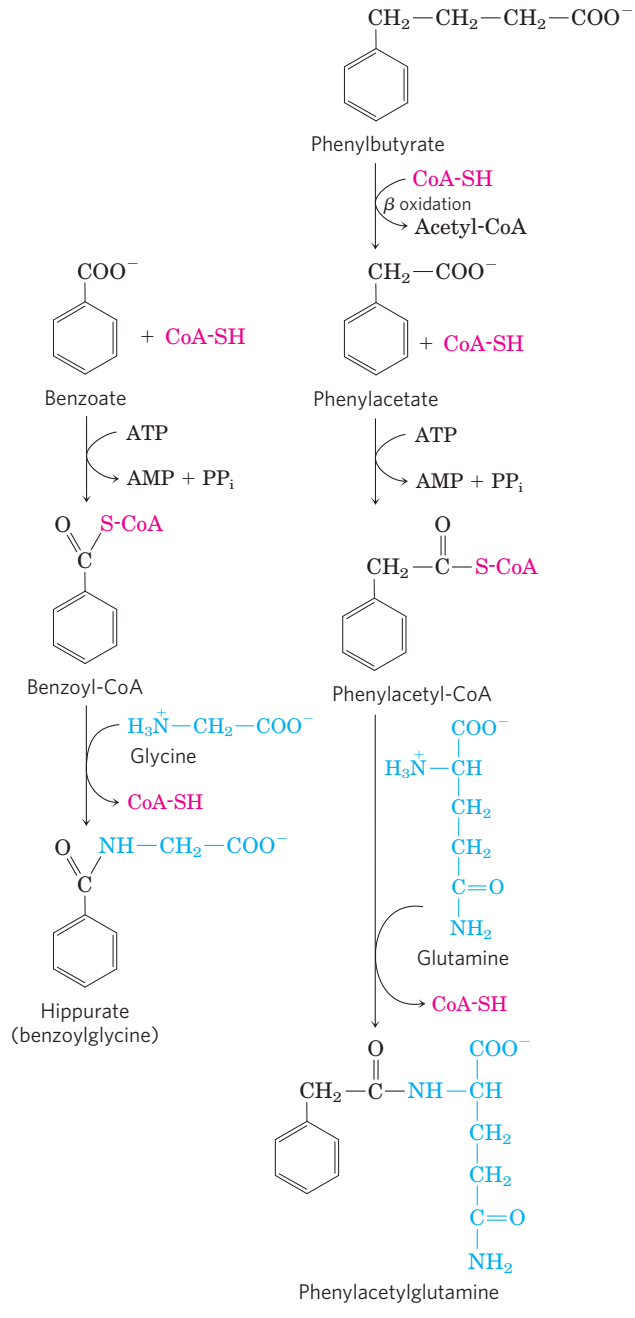

FIGURE 18–14 Treatment for deficiencies in urea cycle enzymes. The aromatic acids benzoate and phenylbutyrate, administered in the diet, are metabolized and combine with glycine and glutamine, respectively. The products are excreted in the urine. Subsequent synthesis of glycine and glutamine to replenish the pool of these intermediates removes ammonia from the bloodstream.

Other therapies are more specific to a particular enzyme deficiency. Deficiency of *N*-acetylglutamate synthase results in the absence of the normal activator of carbamoyl phosphate synthetase I (Fig. 18–13). This condition can be treated by administering carbamoyl glutamate, an analog of *N*-acetylglutamate that is effective in activating carbamoyl phosphate synthetase I.

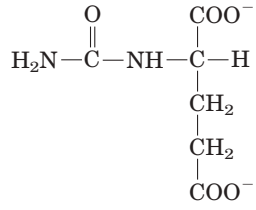

Carbamoyl glutamate

Supplementing the diet with arginine is useful in treating deficiencies of ornithine transcarbamoylase, argininosuccinate synthetase, and argininosuccinase. Many of these treatments must be accompanied by strict dietary control and supplements of essential amino acids. In the rare cases of arginase deficiency, arginine, the substrate of the defective enzyme, must be excluded from the diet. ■

SUMMARY 18.2 Nitrogen Excretion and the Urea Cycle

- Ammonia is highly toxic to animal tissues. In the urea cycle, ornithine combines with ammonia, in the form of carbamoyl phosphate, to form citrulline. A second amino group is transferred to citrulline from aspartate to form arginine—the immediate precursor of urea. Arginase catalyzes hydrolysis of arginine to urea and ornithine; thus ornithine is regenerated in each turn of the cycle.
- The urea cycle results in a net conversion of oxaloacetate to fumarate, both of which are intermediates in the citric acid cycle. The two cycles are thus interconnected.
- The activity of the urea cycle is regulated at the level of enzyme synthesis and by allosteric regulation of the enzyme that catalyzes the formation of carbamoyl phosphate.

18.3 Pathways of Amino Acid Degradation

The pathways of amino acid catabolism, taken together, normally account for only 10% to 15% of the human body's energy production; these pathways are not nearly as active as glycolysis and fatty acid oxidation. Flux through these catabolic routes also varies greatly, depending on the balance between requirements for biosynthetic processes and the availability of a particular amino acid. The 20 catabolic pathways converge to form only six major products, all of which enter the citric acid cycle **(Fig. 18–15)**. From here the carbon skeletons are diverted to gluconeogenesis or ketogenesis or are completely oxidized to CO_2 and H_2O.

All or part of the carbon skeletons of seven amino acids are ultimately broken down to acetyl-CoA. Five amino acids are converted to α-ketoglutarate, four to succinyl-CoA, two to fumarate, and two to oxaloacetate. Parts or all of six amino acids are converted to

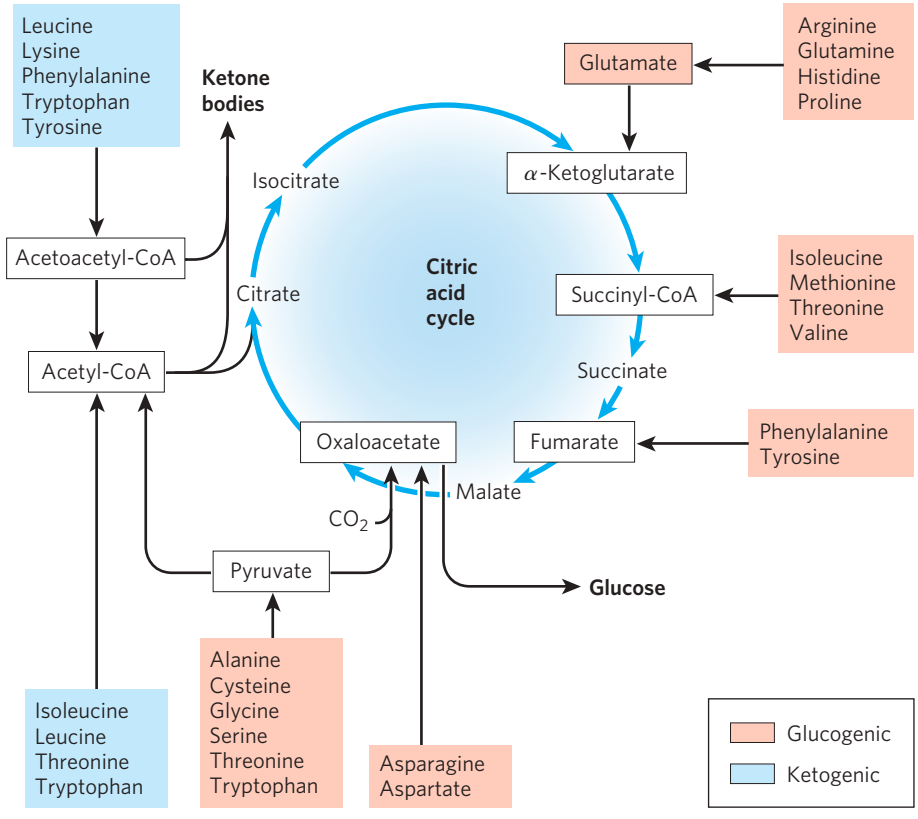

FIGURE 18–15 Summary of amino acid catabolism. Amino acids are grouped according to their major degradative end product. Some amino acids are listed more than once because different parts of their carbon skeletons are degraded to different end products. The figure shows the most important catabolic pathways in vertebrates, but there are minor variations among vertebrate species. Threonine, for instance, is degraded via at least two different pathways (see Figs 18–19, 18–27), and the importance of a given pathway can vary with the organism and its metabolic conditions. The glucogenic and ketogenic amino acids are also delineated in the figure, by color shading. Notice that five of the amino acids are both glucogenic and ketogenic. The amino acids degraded to pyruvate are also potentially ketogenic. Only two amino acids, leucine and lysine, are exclusively ketogenic.

pyruvate, which can be converted to either acetyl-CoA or oxaloacetate. We later summarize the individual pathways for the 20 amino acids in flow diagrams, each leading to a specific point of entry into the citric acid cycle. In these diagrams the carbon atoms that enter the citric acid cycle are shown in color. Note that some amino acids appear more than once, reflecting different fates for different parts of their carbon skeletons. Rather than examining every step of every pathway in amino acid catabolism, we single out for special discussion some enzymatic reactions that are particularly noteworthy for their mechanisms or their medical significance.

Some Amino Acids Are Converted to Glucose, Others to Ketone Bodies

The seven amino acids that are degraded entirely or in part to acetoacetyl-CoA and/or acetyl-CoA—phenylalanine, tyrosine, isoleucine, leucine, tryptophan, threonine, and lysine—can yield ketone bodies in the liver, where acetoacetyl-CoA is converted to acetoacetate and then to acetone and β-hydroxybutyrate (see Fig. 17–19). These are the **ketogenic** amino acids (Fig. 18–15). Their ability to form ketone bodies is particularly evident in uncontrolled diabetes mellitus, in which the liver produces large amounts of ketone bodies from both fatty acids and the ketogenic amino acids.

The amino acids that are degraded to pyruvate, α-ketoglutarate, succinyl-CoA, fumarate, and/or oxaloacetate can be converted to glucose and glycogen by pathways described in Chapters 14 and 15. They are the **glucogenic** amino acids. The division between ketogenic and glucogenic amino acids is not sharp; five amino acids—tryptophan, phenylalanine, tyrosine, threonine, and isoleucine—are both ketogenic and glucogenic. Catabolism of amino acids is particularly critical to the survival of animals with high-protein diets or during starvation. Leucine is an exclusively ketogenic amino acid that is very common in proteins. Its degradation makes a substantial contribution to ketosis under starvation conditions.

Several Enzyme Cofactors Play Important Roles in Amino Acid Catabolism

A variety of interesting chemical rearrangements occur in the catabolic pathways of amino acids. It is useful to begin our study of these pathways by noting the classes of reactions that recur and introducing their enzyme cofactors. We have already considered one important class: transamination reactions requiring pyridoxal phosphate. Another common type of reaction in amino acid catabolism is one-carbon transfers, which usually involve one of three cofactors: biotin, tetrahydrofolate, or *S*-adenosylmethionine **(Fig. 18–16)**. These cofactors transfer one-carbon groups in different oxidation states: biotin transfers carbon in its most oxidized state, CO_2 (see Fig. 14–19); tetrahydrofolate transfers one-carbon groups in intermediate oxidation states and sometimes as methyl groups; and *S*-adenosylmethionine transfers methyl groups, the most reduced state of carbon. The latter two cofactors are especially important in amino acid and nucleotide metabolism.

Tetrahydrofolate (**H_4 folate**), synthesized in bacteria, consists of substituted pterin (6-methylpterin), *p*-aminobenzoate, and glutamate moieties (Fig. 18–16).

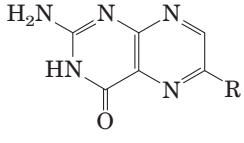

Pterin

The oxidized form, folate, is a vitamin for mammals; it is converted in two steps to tetrahydrofolate by the enzyme dihydrofolate reductase. The one-carbon group undergoing transfer, in any of three oxidation states, is bonded to N-5 or N-10 or both. The most reduced form of the cofactor carries a methyl group, a more oxidized form carries a methylene group, and the most oxidized forms carry a methenyl, formyl, or formimino group **(Fig. 18–17)**. Most forms of tetrahydrofolate are interconvertible and serve as donors of one-carbon units in a variety of metabolic reactions. The primary source of one-carbon units for tetrahydrofolate is the carbon removed in the conversion of serine to glycine, producing N^5,N^{10}-methylenetetrahydrofolate.

Although tetrahydrofolate can carry a methyl group at N-5, the transfer potential of this methyl group is insufficient for most biosynthetic reactions. ***S*-Adenosylmethionine (adoMet)** is the preferred cofactor for biological methyl group transfers. It is synthesized from ATP and methionine by the action of **methionine adenosyl transferase** (**Fig. 18–18**, step ❶). This reaction is unusual in that the nucleophilic sulfur atom of methionine attacks the 5′ carbon of the ribose moiety of ATP rather than one of the phosphorus atoms. Triphosphate is released and is cleaved to P_i and PP_i on the enzyme, and the PP_i is cleaved by inorganic pyrophosphatase; thus three bonds, including two bonds of high-energy phosphate groups, are broken in this reaction. The only other known reaction in which triphosphate is displaced from ATP occurs in the synthesis of coenzyme B_{12} (see Box 17–2, Fig. 3).

S-Adenosylmethionine is a potent alkylating agent by virtue of its destabilizing sulfonium ion. The methyl group is subject to attack by nucleophiles and is about 1,000 times more reactive than the methyl group of N^5-methyltetrahydrofolate.

Transfer of the methyl group from *S*-adenosylmethionine to an acceptor yields ***S*-adenosylhomocysteine** (Fig. 18–18, step ❷), which is subsequently broken down to homocysteine and adenosine (step ❸). Methionine is regenerated by transfer of a methyl group to homocysteine in a reaction catalyzed by methionine synthase (step ❹), and methionine is reconverted to *S*-adenosylmethionine to complete an activated-methyl cycle.

One form of methionine synthase common in bacteria uses N^5-methyltetrahydrofolate as a methyl donor.

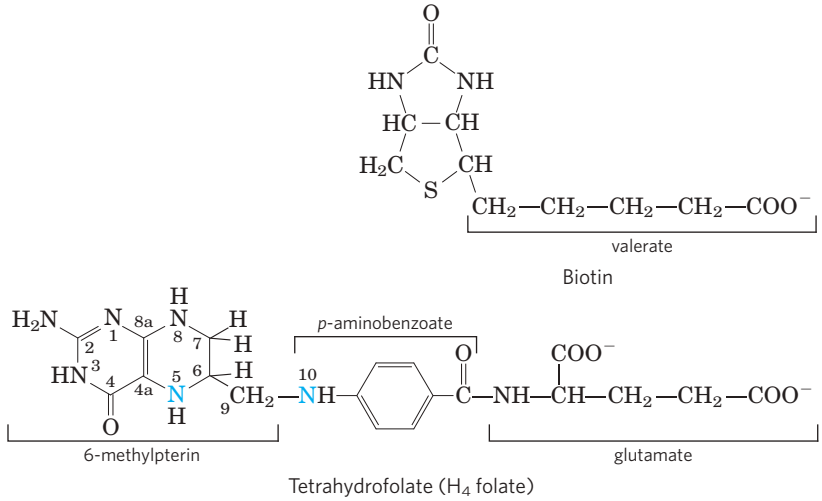

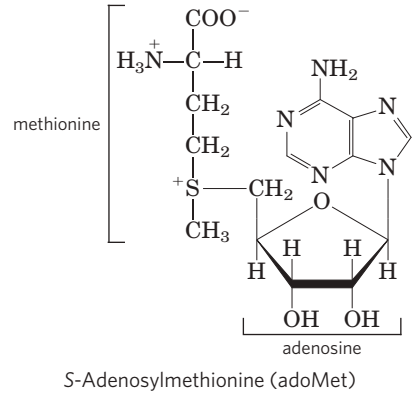

FIGURE 18–16 Some enzyme cofactors important in one-carbon transfer reactions. The nitrogen atoms to which one-carbon groups are attached in tetrahydrofolate are shown in blue.

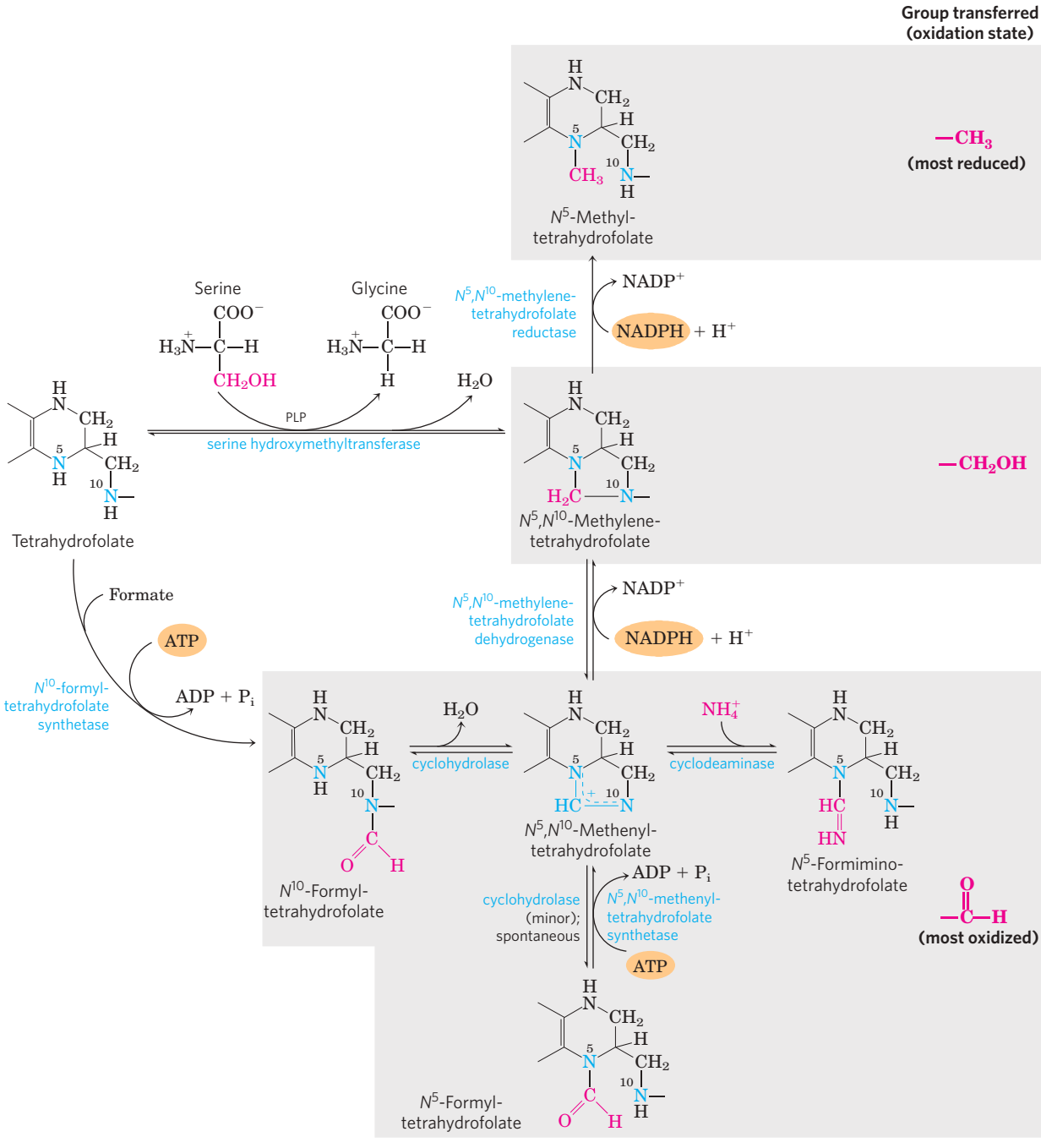

FIGURE 18–17 Conversions of one-carbon units on tetrahydrofolate. The different molecular species are grouped according to oxidation state, with the most reduced at the top and most oxidized at the bottom. All species within a single shaded box are at the same oxidation state. The conversion of N^5,N^{10}-methylenetetrahydrofolate to N^5-methyltetrahydrofolate is effectively irreversible. The enzymatic transfer of formyl groups, as in purine synthesis (see Fig. 22–35) and in the formation of formylmethionine in bacteria (Chapter 27), generally uses N^{10}-formyltetrahydrofolate rather than N^5-formyltetrahydrofolate. The latter species is significantly more stable and therefore a weaker donor of formyl groups. N^5-Formyltetrahydrofolate is a minor byproduct of the cyclohydrolase reaction, and can also form spontaneously. Conversion of N^5-formyltetrahydrofolate to N^5,N^{10}-methenyltetrahydrofolate requires ATP, because of an otherwise unfavorable equilibrium. Note that N^5-formiminotetrahydrofolate is derived from histidine in a pathway shown in Figure 18–26.

Another form of the enzyme present in some bacteria and mammals uses N^5-methyltetrahydrofolate, but the methyl group is first transferred to cobalamin, derived from coenzyme B_{12}, to form methylcobalamin as the methyl donor in methionine formation. This reaction and the rearrangement of L-methylmalonyl-CoA to succinyl-CoA (see Box 17–2, Fig. 1a) are the only known coenzyme B_{12}–dependent reactions in mammals. The vitamins B_{12} and folate are closely linked in these metabolic pathways. The B_{12} deficiency disease **pernicious anemia** is rare, seen only in individuals who have a defect in the intestinal absorption

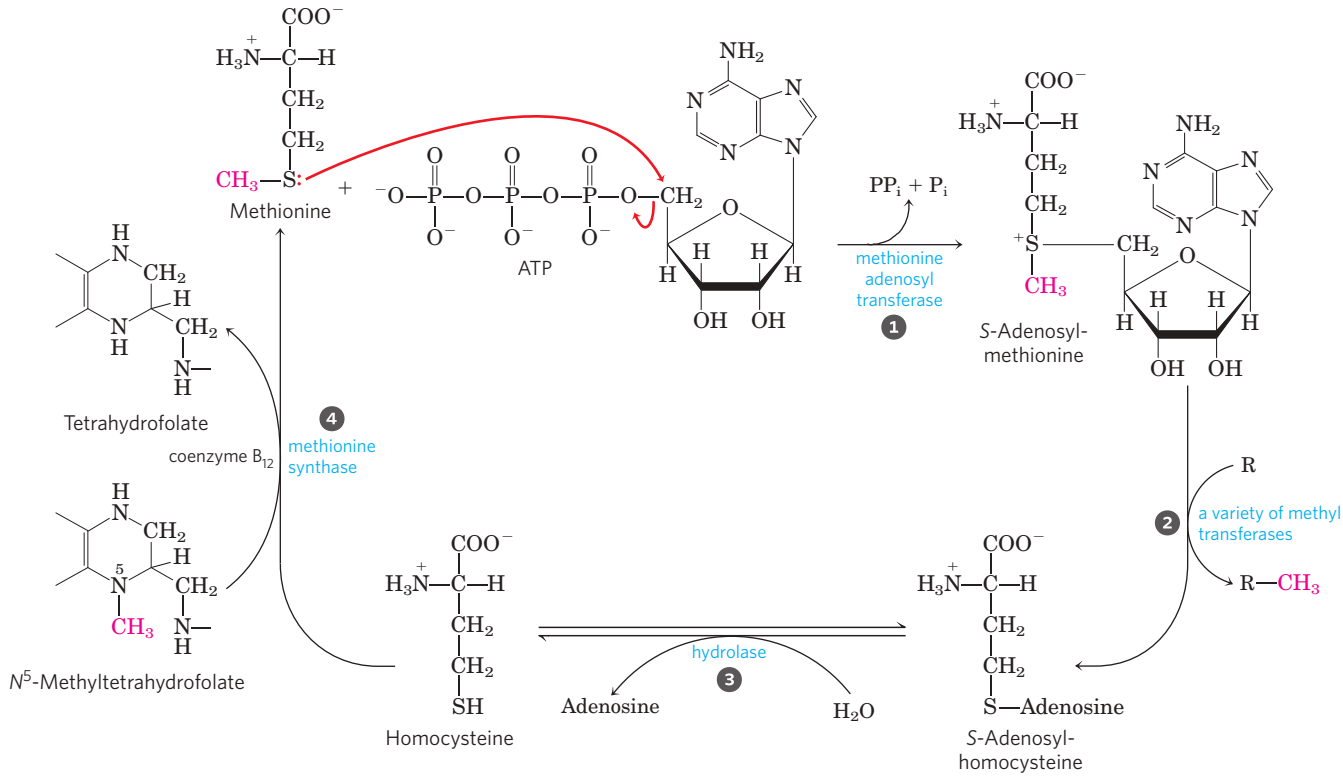

FIGURE 18–18 Synthesis of methionine and *S*-adenosylmethionine in an activated-methyl cycle. The steps are described in the text. In the methionine synthase reaction (step 4), the methyl group is transferred to cobalamin to form methylcobalamin, which in turn is the methyl donor in the formation of methionine. *S*-Adenosylmethionine, which has a positively charged sulfur (and is thus a sulfonium ion), is a powerful methylating agent in several biosynthetic reactions. The methyl group acceptor (step 2) is designated R.

pathways for this vitamin (see Box 17–2) or in strict vegetarians (B_{12} is not present in plants). The disease progresses slowly, because only small amounts of vitamin B_{12} are required and normal stores of B_{12} in the liver can last three to five years. Symptoms include not only anemia but a variety of neurological disorders.

The anemia can be traced to the methionine synthase reaction. As noted above, the methyl group of methylcobalamin is derived from N^5-methyltetrahydrofolate, and this is the only reaction in mammals that uses N^5-methyltetrahydrofolate. The reaction converting the N^5,N^{10}-methylene form to the N^5-methyl form of tetrahydrofolate is irreversible (Fig. 18–17). Thus, if coenzyme B_{12} is not available for the synthesis of methylcobalamin, metabolic folates become trapped in the N^5-methyl form. The anemia associated with vitamin B_{12} deficiency is called **megaloblastic anemia**. It manifests as a decline in the production of mature erythrocytes (red blood cells) and the appearance in the bone marrow of immature precursor cells, or **megaloblasts**. Erythrocytes are gradually replaced in the blood by smaller numbers of abnormally large erythrocytes called **macrocytes**. The defect in erythrocyte development is a direct consequence of the depletion of the N^5,N^{10}-methylenetetrahydrofolate, which is required for synthesis of the thymidine nucleotides needed for DNA synthesis (see Chapter 22). Folate deficiency, in which all forms of tetrahydrofolate are depleted, also produces anemia, for much the same reasons. The anemia symptoms of B_{12} deficiency can be alleviated by administering either vitamin B_{12} or folate.

However, it is dangerous to treat pernicious anemia by folate supplementation alone, because the neurological symptoms of B_{12} deficiency will progress. These symptoms do not arise from the defect in the methionine synthase reaction. Instead, the impaired methylmalonyl-CoA mutase (see Box 17–2 and Fig. 17–12) causes accumulation of unusual, odd-number fatty acids in neuronal membranes. The anemia associated with folate deficiency is thus often treated by administering both folate and vitamin B_{12}, at least until the metabolic source of the anemia is unambiguously defined. Early diagnosis of B_{12} deficiency is important because some of its associated neurological conditions may be irreversible.

Folate deficiency also reduces the availability of the N^5-methyltetrahydrofolate required for methionine synthase function. This leads to a rise in homocysteine levels in blood, a condition linked to heart disease, hypertension, and stroke. High levels of homocysteine may be responsible for 10% of all cases of heart disease. The condition is treated with folate supplements. ■

Tetrahydrobiopterin, another cofactor of amino acid catabolism, is similar to the pterin moiety of tetrahydrofolate, but it is not involved in one-carbon transfers; instead it participates in oxidation reactions. We

consider its mode of action when we discuss phenylalanine degradation (see Fig. 18–24).

Six Amino Acids Are Degraded to Pyruvate

The carbon skeletons of six amino acids are converted in whole or in part to pyruvate. The pyruvate can then be converted to acetyl-CoA and eventually oxidized via the citric acid cycle, or to oxaloacetate and shunted into gluconeogenesis. The six amino acids are alanine, tryptophan, cysteine, serine, glycine, and threonine **(Fig. 18–19)**. **Alanine** yields pyruvate directly on transamination with α-ketoglutarate, and the side chain of **tryptophan** is cleaved to yield alanine and thus pyruvate. **Cysteine** is converted to pyruvate in two steps; one removes the sulfur atom, the other is a transamination. **Serine** is converted to pyruvate by serine dehydratase. Both the β-hydroxyl and the α-amino groups of serine are removed in this single pyridoxal phosphate–dependent reaction **(Fig. 18–20a)**.

Glycine is degraded via three pathways, only one of which leads to pyruvate. Glycine is converted to serine by enzymatic addition of a hydroxymethyl group (Figs 18–19, 18–20b). This reaction, catalyzed by **serine hydroxymethyltransferase**, requires the coenzymes tetrahydrofolate and pyridoxal phosphate. The serine is converted to pyruvate as described above. In the second pathway, which predominates in animals, glycine undergoes oxidative cleavage to CO_2, NH_4^+, and a methylene group (—CH_2—) (Figs 18–19, 18–20c). This readily reversible reaction, catalyzed by **glycine cleavage enzyme** (also called glycine synthase), also requires tetrahydrofolate, which accepts the methylene group. In this oxidative cleavage pathway, the two carbon atoms of glycine do not enter the citric acid cycle. One carbon is lost as CO_2 and the other becomes the methylene group of N^5,N^{10}-methylenetetrahydrofolate (Fig. 18–17), a one-carbon group donor in certain biosynthetic pathways.

This second pathway for glycine degradation seems to be critical in mammals. Humans with serious defects in glycine cleavage enzyme activity suffer from a condition known as nonketotic hyperglycinemia. The condition is characterized by elevated serum levels of glycine, leading to severe mental deficiencies and death in

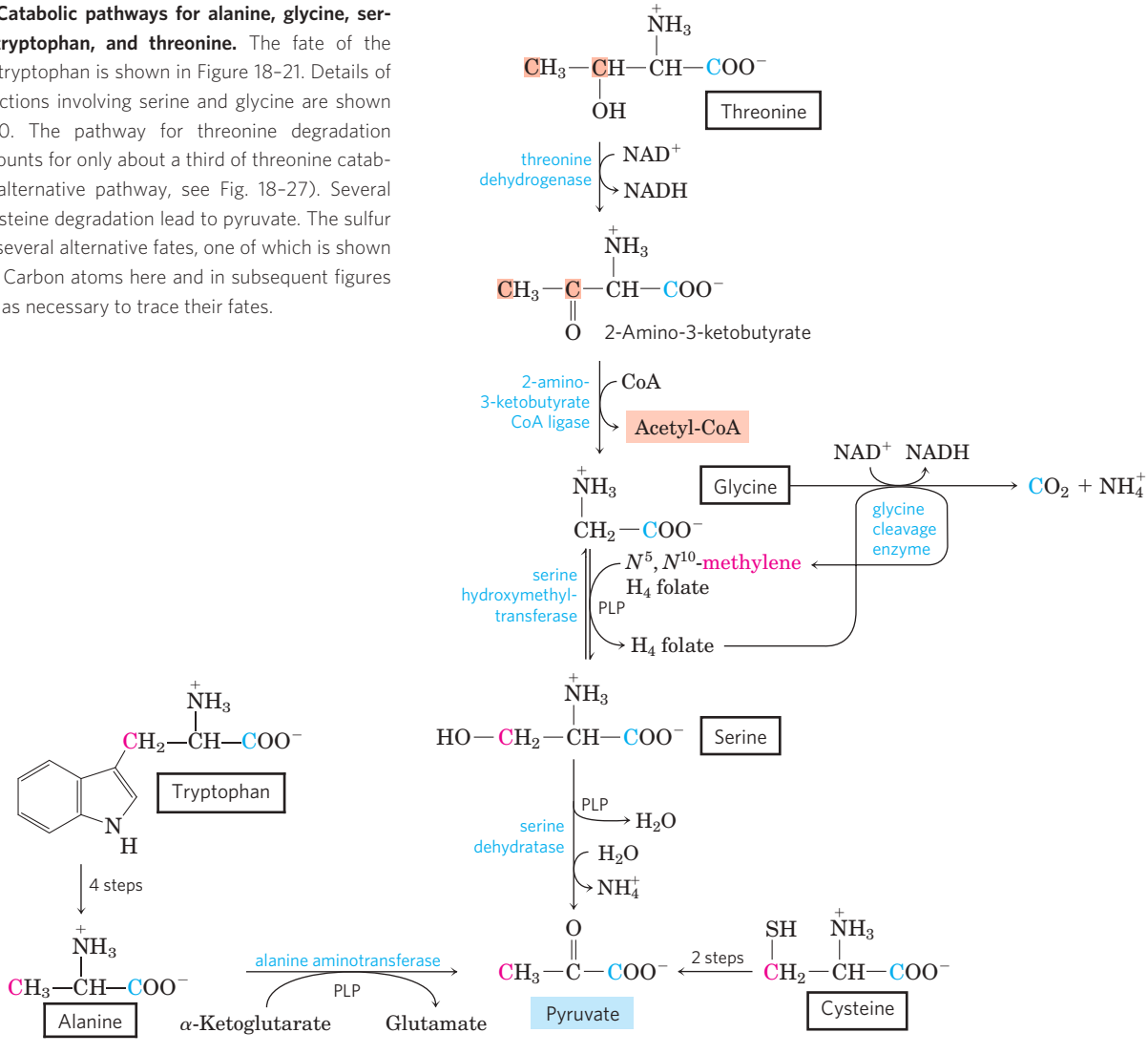

FIGURE 18–19 Catabolic pathways for alanine, glycine, serine, cysteine, tryptophan, and threonine. The fate of the indole group of tryptophan is shown in Figure 18–21. Details of most of the reactions involving serine and glycine are shown in Figure 18–20. The pathway for threonine degradation shown here accounts for only about a third of threonine catabolism (for the alternative pathway, see Fig. 18–27). Several pathways for cysteine degradation lead to pyruvate. The sulfur of cysteine has several alternative fates, one of which is shown in Figure 22–17. Carbon atoms here and in subsequent figures are color-coded as necessary to trace their fates.

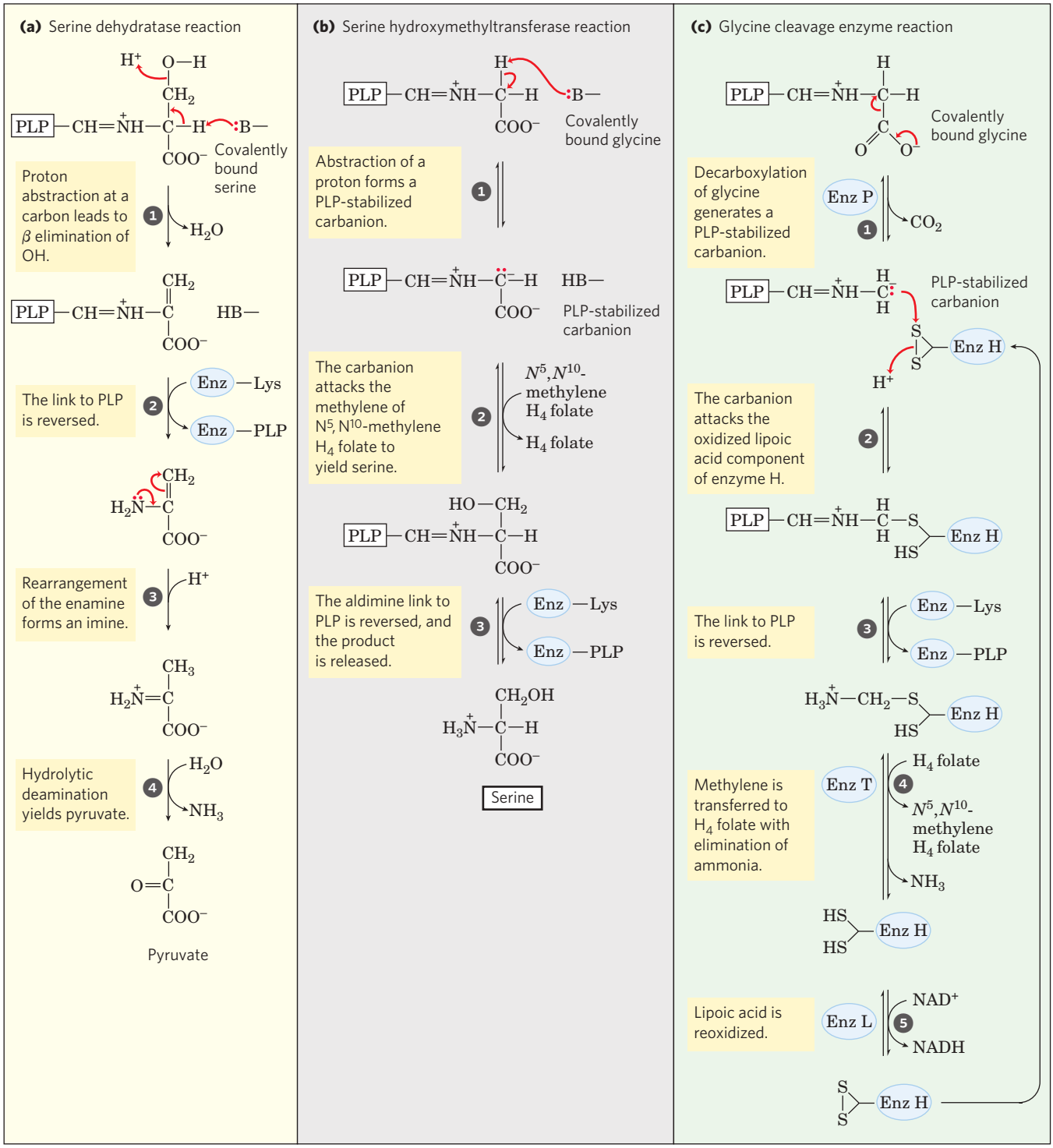

MECHANISM FIGURE 18–20 **Interplay of the pyridoxal phosphate and tetrahydrofolate cofactors in serine and glycine metabolism.** The first step in each of these reactions (not shown) involves the formation of a covalent imine linkage between enzyme-bound PLP and the substrate amino acid—serine in (a), glycine in (b) and (c). **(a)** A PLP-catalyzed elimination of water in the serine dehydratase reaction (step 1) begins the pathway to pyruvate. **(b)** In the serine hydroxymethyltransferase reaction, a PLP-stabilized carbanion (product of step 1) is a key intermediate in the reversible transfer of the methylene group (as —CH_2—OH) from N^5,N^{10}-methylenetetrahydrofolate to form serine. **(c)** The glycine cleavage enzyme is a multienzyme complex, with components P, H, T, and L. The overall reaction, which is reversible, converts glycine to CO_2 and NH_4^+, with the second glycine carbon taken up by tetrahydrofolate to form N^5,N^{10}-methylenetetrahydrofolate. Pyridoxal phosphate activates the α carbon of amino acids at critical stages in all these reactions, and tetrahydrofolate carries one-carbon units in two of them (see Figs 18-6, 18-17).

very early childhood. At high levels, glycine is an inhibitory neurotransmitter, perhaps explaining the neurological effects of the disease. Many genetic defects of amino acid metabolism have been identified in humans (Table 18–2). We shall encounter several more in this chapter. ■

In the third and final pathway of glycine degradation, the achiral glycine molecule is a substrate for the enzyme D-amino acid oxidase. The glycine is converted to glyoxylate, an alternative substrate for hepatic lactate dehydrogenase (p. 563). Glyoxylate is oxidized in an NAD^+-dependent reaction to oxalate:

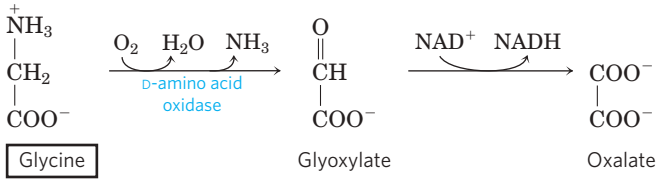

The primary function of D-amino acid oxidase, present at high levels in the kidney, is thought to be the detoxification of ingested D-amino acids derived from bacterial cell walls and from grilled foodstuffs (high heat causes some spontaneous racemization of the L-amino acids in proteins). Oxalate, whether obtained in foods or produced enzymatically in the kidneys, has medical significance. Crystals of calcium oxalate account for up to 75% of all kidney stones. ■

There are two significant pathways for **threonine** degradation. One pathway leads to pyruvate via glycine (Fig. 18–19). The conversion to glycine occurs in two steps, with threonine first converted to 2-amino-3-ketobutyrate by the action of threonine dehydrogenase. This is a relatively minor pathway in humans, accounting for 10% to 30% of threonine catabolism, but is more important in some other mammals. The major pathway in humans leads to succinyl-CoA and is described later.

In the laboratory, serine hydroxymethyltransferase will catalyze the conversion of threonine to glycine and acetaldehyde in one step, but this is not a significant pathway for threonine degradation in mammals.

Seven Amino Acids Are Degraded to Acetyl-CoA

Portions of the carbon skeletons of seven amino acids—**tryptophan**, **lysine**, **phenylalanine**, **tyrosine**, **leucine**, **isoleucine**, and **threonine**—yield acetyl-CoA and/or

TABLE 18–2 Some Human Genetic Disorders Affecting Amino Acid Catabolism

Medical condition	Approximate incidence (per 100,000 births)	Defective process	Defective enzyme	Symptoms and effects
Albinism	<3	Melanin synthesis from tyrosine	Tyrosine 3-monooxygenase (tyrosinase)	Lack of pigmentation; white hair, pink skin
Alkaptonuria	<0.4	Tyrosine degradation	Homogentisate 1,2-dioxygenase	Dark pigment in urine; late-developing arthritis
Argininemia	<0.5	Urea synthesis	Arginase	Mental retardation
Argininosuccinic acidemia	<1.5	Urea synthesis	Argininosuccinase	Vomiting; convulsions
Carbamoyl phosphate synthetase I deficiency	<0.5	Urea synthesis	Carbamoyl phosphate synthetase I	Lethargy; convulsions; early death
Homocystinuria	<0.5	Methionine degradation	Cystathionine β-synthase	Faulty bone development; mental retardation
Maple syrup urine disease (branched-chain ketoaciduria)	<0.4	Isoleucine, leucine, and valine degradation	Branched-chain α-keto acid dehydrogenase complex	Vomiting; convulsions; mental retardation; early death
Methylmalonic acidemia	<0.5	Conversion of propionyl-CoA to succinyl-CoA	Methylmalonyl-CoA mutase	Vomiting; convulsions; mental retardation; early death
Phenylketonuria	<8	Conversion of phenylalanine to tyrosine	Phenylalanine hydroxylase	Neonatal vomiting; mental retardation

acetoacetyl-CoA, the latter being converted to acetyl-CoA **(Fig. 18–21)**. Some of the final steps in the degradative pathways for leucine, lysine, and tryptophan resemble steps in the oxidation of fatty acids (see Fig. 17–9). Threonine (not shown in Fig. 18–21) yields some acetyl-CoA via the minor pathway illustrated in Figure 18–19.

The degradative pathways of two of these seven amino acids deserve special mention. Tryptophan breakdown is the most complex of all the pathways of amino acid catabolism in animal tissues; portions of tryptophan (four of its carbons) yield acetyl-CoA via acetoacetyl-CoA. Some of the intermediates in tryptophan catabolism are precursors for the synthesis of other biomolecules **(Fig. 18–22)**, including nicotinate, a precursor of NAD and NADP in animals; serotonin, a neurotransmitter in vertebrates; and indoleacetate, a growth factor in plants. Some of these biosynthetic pathways are described in more detail in Chapter 22 (see Figs 22–30, 22–31).

The breakdown of phenylalanine is noteworthy because genetic defects in the enzymes of this pathway lead to several inheritable human diseases **(Fig. 18–23)**, as discussed below. Phenylalanine and its oxidation product tyrosine (both with nine carbons) are degraded into two fragments, both of which can enter the citric acid cycle: four of the nine carbon atoms yield free acetoacetate, which is converted to acetoacetyl-CoA and thus acetyl-CoA, and a second four-carbon fragment is recovered as fumarate. Eight of the nine carbons of these two amino acids thus enter the citric acid cycle; the

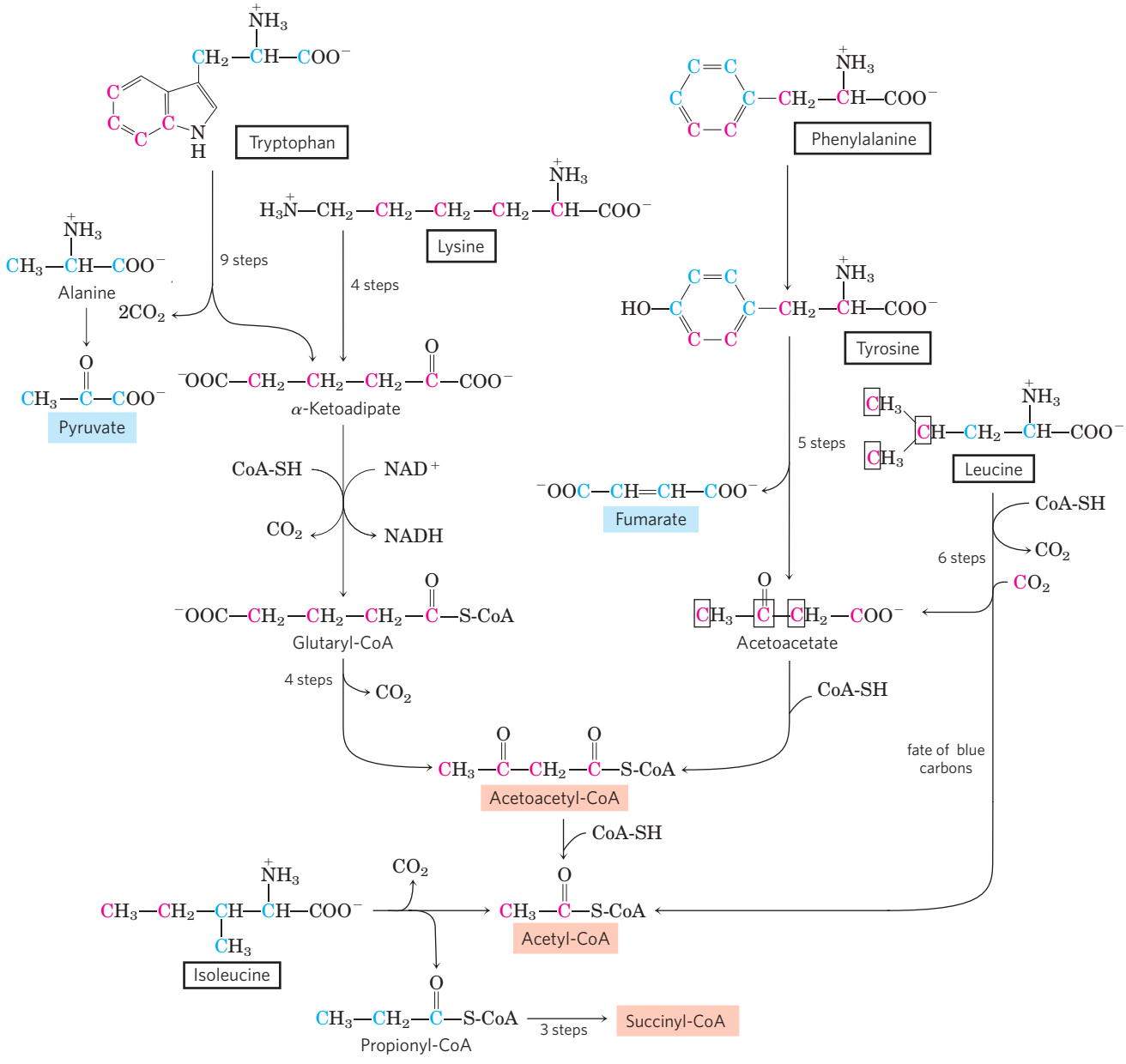

FIGURE 18–21 Catabolic pathways for tryptophan, lysine, phenylalanine, tyrosine, leucine, and isoleucine. These amino acids donate some of their carbons (red) to acetyl-CoA. Tryptophan, phenylalanine, tyrosine, and isoleucine also contribute carbons (blue) to pyruvate or citric acid cycle intermediates. The phenylalanine pathway is described in more detail in Figure 18-23. The fate of nitrogen atoms is not traced in this scheme; in most cases they are transferred to α-ketoglutarate to form glutamate.

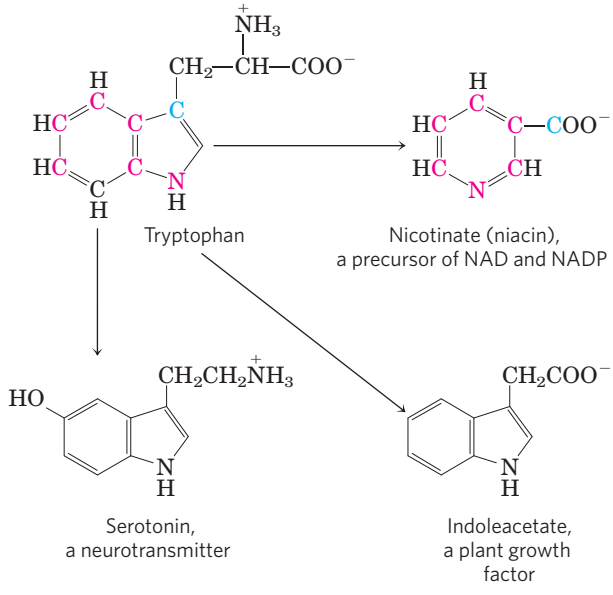

FIGURE 18–22 Tryptophan as precursor. The aromatic rings of tryptophan give rise to nicotinate (niacin), indoleacetate, and serotonin. Colored atoms trace the source of the ring atoms in nicotinate.

remaining carbon is lost as CO_2. Phenylalanine, after its hydroxylation to tyrosine, is also the precursor of dopamine, a neurotransmitter, and of norepinephrine and epinephrine, hormones secreted by the adrenal medulla (see Fig. 22–31). Melanin, the black pigment of skin and hair, is also derived from tyrosine.

Phenylalanine Catabolism Is Genetically Defective in Some People

Given that many amino acids are either neurotransmitters or precursors or antagonists of neurotransmitters, it is not surprising that genetic defects of amino acid metabolism can cause defective neural development and intellectual deficits. In most such diseases specific intermediates accumulate. For example, a genetic defect in **phenylalanine hydroxylase**, the first enzyme in the catabolic pathway for phenylalanine (Fig. 18–23), is responsible for the disease **phenylketonuria (PKU)**, the most common cause of elevated levels of phenylalanine in the blood (hyperphenylalaninemia).

Phenylalanine hydroxylase (also called phenylalanine-4-monooxygenase) is one of a general class of enzymes

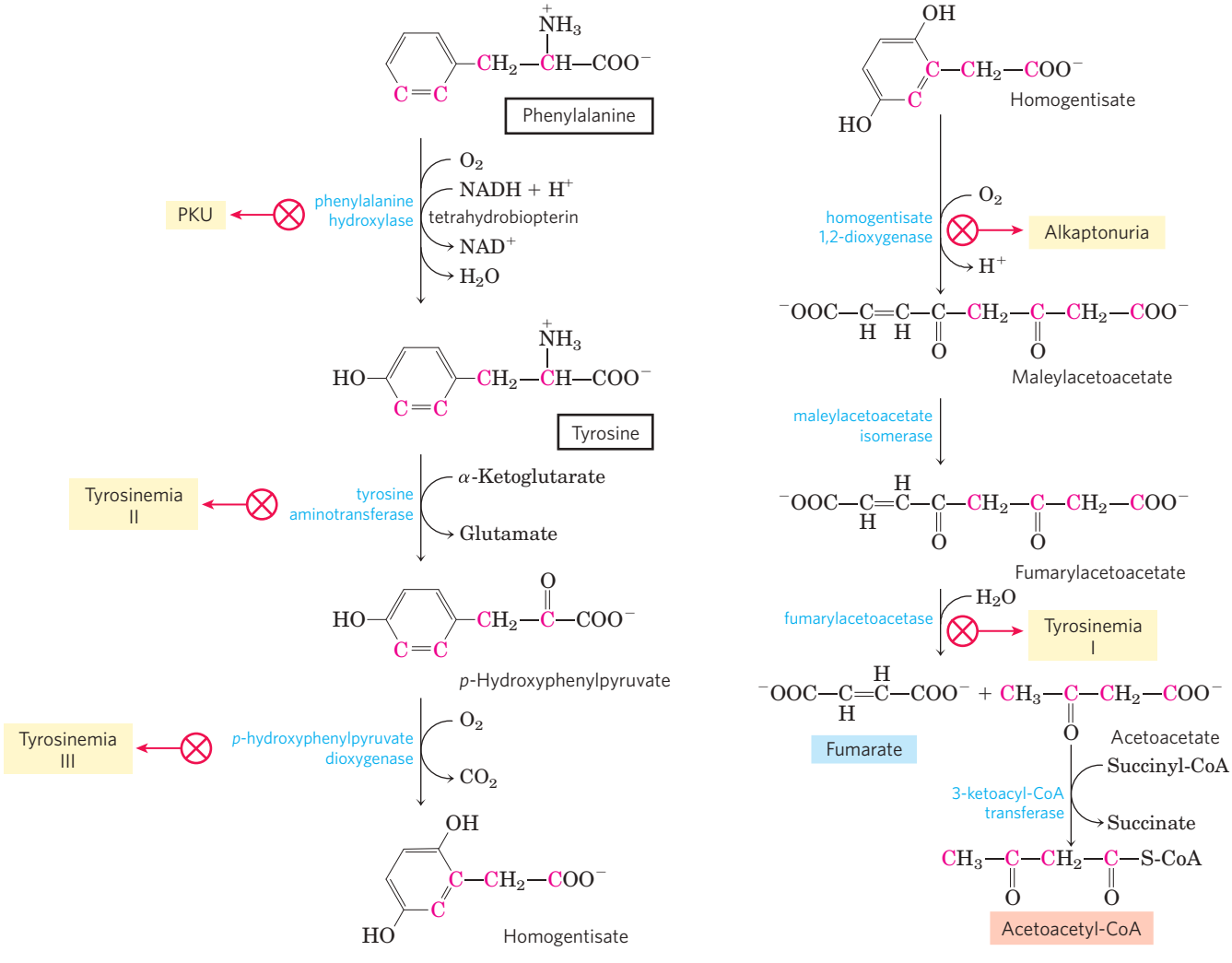

FIGURE 18–23 Catabolic pathways for phenylalanine and tyrosine. In humans these amino acids are normally converted to acetoacetyl-CoA and fumarate. Genetic defects in many of these enzymes cause inheritable human diseases (shaded yellow).

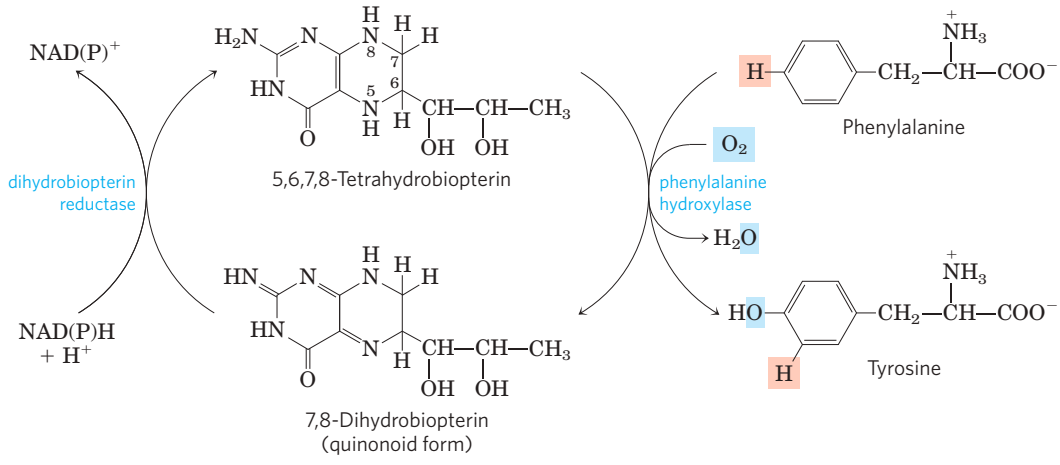

FIGURE 18–24 Role of tetrahydrobiopterin in the phenylalanine hydroxylase reaction. The H atom shaded pink is transferred directly from C-4 to C-3 in the reaction. This feature, discovered at the National Institutes of Health, is called the NIH shift.

called **mixed-function oxidases** (see Box 21–1), all of which catalyze simultaneous hydroxylation of a substrate by an oxygen atom of O_2 and reduction of the other oxygen atom to H_2O. Phenylalanine hydroxylase requires the cofactor tetrahydrobiopterin, which carries electrons from NADPH to O_2 and becomes oxidized to dihydrobiopterin in the process **(Fig. 18–24)**. It is subsequently reduced by the enzyme **dihydrobiopterin reductase** in a reaction that requires NADPH.

In individuals with PKU, a secondary, normally little-used pathway of phenylalanine metabolism comes into play. In this pathway phenylalanine undergoes transamination with pyruvate to yield **phenylpyruvate (Fig. 18–25)**. Phenylalanine and phenylpyruvate accumulate in the blood and tissues and are excreted in the urine—hence the name "phenylketonuria." Much of the phenylpyruvate, rather than being excreted as such, is either decarboxylated to phenylacetate or reduced to phenyllactate. Phenylacetate imparts a characteristic odor to the urine, which nurses have traditionally used to detect PKU in infants. The accumulation of phenylalanine or its metabolites in early life impairs normal development of the brain, causing severe intellectual deficits. This may be caused by excess phenylalanine competing with other amino acids for transport across the blood-brain barrier, resulting in a deficit of required metabolites.

Phenylketonuria was among the first inheritable metabolic defects discovered in humans. When this condition is recognized early in infancy, mental retardation can be prevented by rigid dietary control. The diet must supply only enough phenylalanine and tyrosine to meet the needs for protein synthesis. Consumption of protein-rich foods must be curtailed. Natural proteins, such as casein of milk, must first be hydrolyzed and much of the phenylalanine removed to provide an appropriate diet, at least through childhood. Because the artificial sweetener aspartame is a dipeptide of aspartate and the methyl ester of phenylalanine (see Fig. 1–24b), foods sweetened with aspartame bear warnings addressed to individuals on phenylalanine-controlled diets.

Phenylketonuria can also be caused by a defect in the enzyme that catalyzes the regeneration of tetrahydrobiopterin (Fig. 18–24). The treatment in this case is more complex than restricting the intake of phenylalanine and tyrosine. Tetrahydrobiopterin is also required for the formation of L-3,4-dihydroxyphenylalanine (L-dopa) and 5-hydroxytryptophan—precursors of the neurotransmitters norepinephrine and serotonin, respectively—and in phenylketonuria of this type, these precursors must be supplied in the diet. Supplementing the diet with tetrahydrobiopterin itself is ineffective because it is unstable and does not cross the blood-brain barrier.

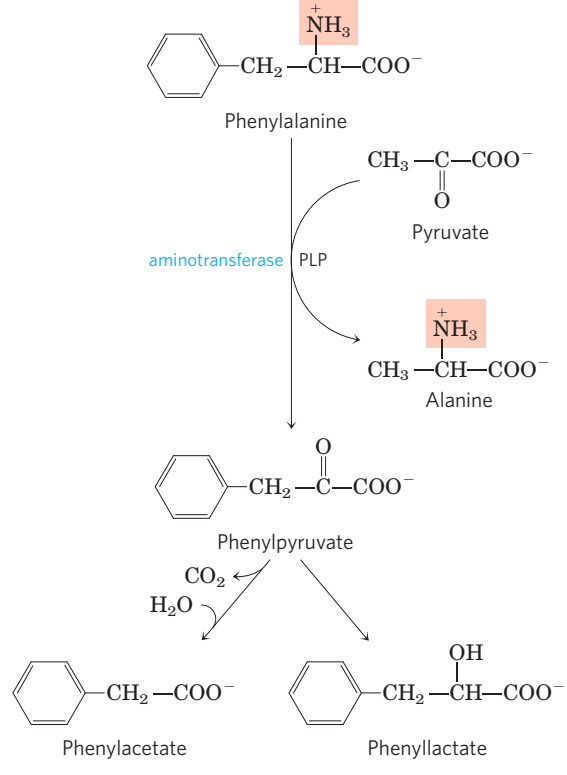

FIGURE 18–25 Alternative pathways for catabolism of phenylalanine in phenylketonuria. In PKU, phenylpyruvate accumulates in the tissues, blood, and urine. The urine may also contain phenylacetate and phenyllactate.

Screening newborns for genetic diseases can be highly cost-effective, especially in the case of PKU. The tests (no longer relying on urine odor) are relatively inexpensive, and the detection and early treatment of PKU in infants (eight to ten cases per 100,000 newborns) saves millions of dollars in later health care costs each year. More importantly, the emotional trauma avoided by early detection with these simple tests is inestimable.

Another inheritable disease of phenylalanine catabolism is **alkaptonuria**, in which the defective enzyme is **homogentisate dioxygenase** (Fig. 18–23). Less serious than PKU, this condition produces few ill effects, although large amounts of homogentisate are excreted and its oxidation turns the urine black. Individuals with alkaptonuria are also prone to develop a form of arthritis. Alkaptonuria is of considerable historical interest. Archibald Garrod discovered in the early 1900s that this condition is inherited, and he traced the cause to the absence of a single enzyme. Garrod was the first to make a connection between an inheritable trait and an enzyme—a great advance on the path that ultimately led to our current understanding of genes and the information pathways described in Part III. ■

Five Amino Acids Are Converted to α-Ketoglutarate

The carbon skeletons of five amino acids (proline, glutamate, glutamine, arginine, and histidine) enter the citric acid cycle as α-ketoglutarate **(Fig. 18–26)**. **Proline**, **glutamate**, and **glutamine** have five-carbon skeletons. The cyclic structure of proline is opened by oxidation of the carbon most distant from the carboxyl group to create a Schiff base, then hydrolysis of the Schiff base to a linear semialdehyde, glutamate γ-semialdehyde. This intermediate is further oxidized at the same carbon to produce glutamate. The action of glutaminase, or any of several enzyme reactions in which glutamine donates its amide nitrogen to an acceptor, converts glutamine to glutamate. Transamination or deamination of glutamate produces α-ketoglutarate.

Arginine and **histidine** contain five adjacent carbons and a sixth carbon attached through a nitrogen atom. The catabolic conversion of these amino acids to glutamate is therefore slightly more complex than the path from proline or glutamine (Fig. 18–26). Arginine is

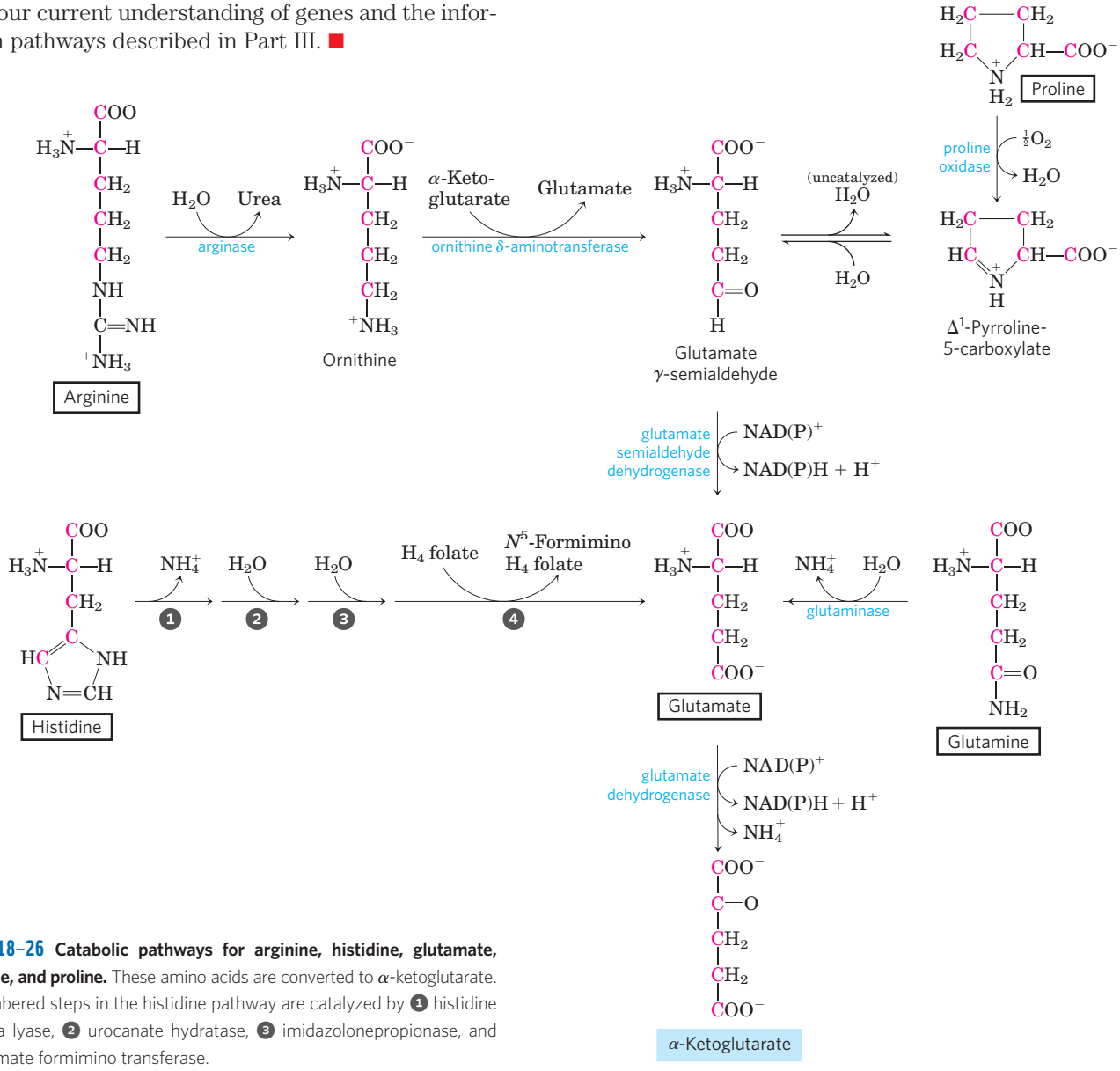

FIGURE 18–26 Catabolic pathways for arginine, histidine, glutamate, glutamine, and proline. These amino acids are converted to α-ketoglutarate. The numbered steps in the histidine pathway are catalyzed by ❶ histidine ammonia lyase, ❷ urocanate hydratase, ❸ imidazolonepropionase, and ❹ glutamate formimino transferase.

converted to the five-carbon skeleton of ornithine in the urea cycle (Fig. 18–10), and the ornithine is transaminated to glutamate γ-semialdehyde. Conversion of histidine to the five-carbon glutamate occurs in a multistep pathway; the extra carbon is removed in a step that uses tetrahydrofolate as cofactor.

Four Amino Acids Are Converted to Succinyl-CoA

The carbon skeletons of methionine, isoleucine, threonine, and valine are degraded by pathways that yield succinyl-CoA **(Fig. 18–27)**, an intermediate of the citric acid cycle. **Methionine** donates its methyl group to one of several possible acceptors through *S*-adenosylmethionine, and three of its four remaining carbon atoms are converted to the propionate of propionyl-CoA, a precursor of succinyl-CoA. **Isoleucine** undergoes transamination, followed by oxidative decarboxylation of the resulting α-keto acid. The remaining five-carbon skeleton is further oxidized to acetyl-CoA and propionyl-CoA. **Valine** undergoes transamination and decarboxylation, then a series of oxidation reactions that convert the remaining four carbons to propionyl-CoA. Some parts of the valine and isoleucine degradative pathways closely parallel steps in fatty acid degradation (see Fig. 17–9). In human tissues, **threonine** is also converted in two steps to propionyl-CoA. This is the primary pathway for threonine degradation in humans (see Fig. 18–19 for the alternative pathway). The mechanism of the first step is analogous to that catalyzed by serine dehydratase, and the serine and threonine dehydratases may actually be the same enzyme.

The propionyl-CoA derived from these three amino acids is converted to succinyl-CoA by a pathway described in Chapter 17: carboxylation to methylmalonyl-CoA, epimerization of the methylmalonyl-CoA, and conversion to succinyl-CoA by the coenzyme B_{12}–dependent methylmalonyl-CoA mutase (see Fig. 17–12). In the rare genetic disease known as methylmalonic acidemia, methylmalonyl-CoA mutase is lacking—with serious metabolic consequences (Table 18–2; Box 18–2).

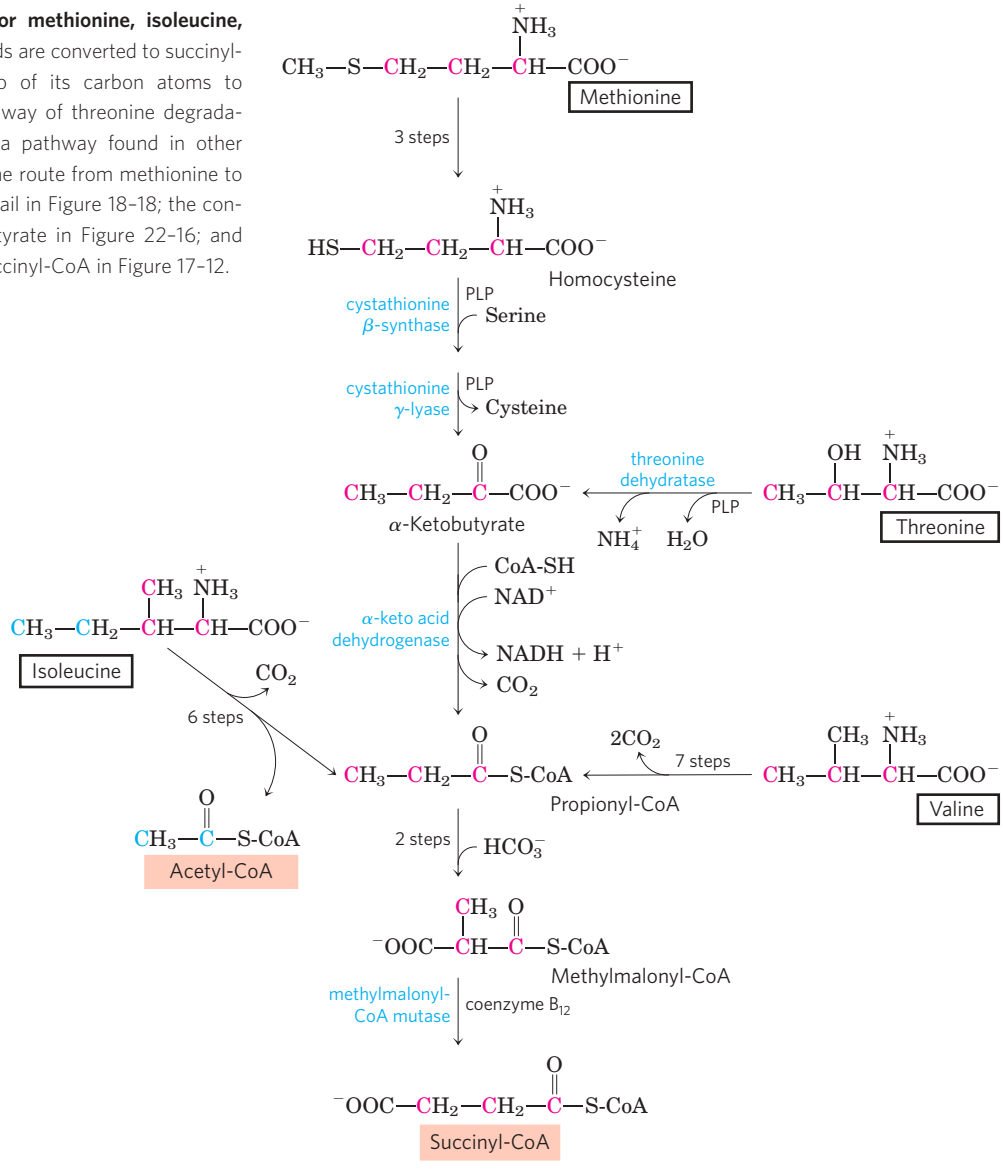

FIGURE 18–27 Catabolic pathways for methionine, isoleucine, threonine, and valine. These amino acids are converted to succinyl-CoA; isoleucine also contributes two of its carbon atoms to acetyl-CoA (see Fig. 18–21). The pathway of threonine degradation shown here occurs in humans; a pathway found in other organisms is shown in Figure 18–19. The route from methionine to homocysteine is described in more detail in Figure 18–18; the conversion of homocysteine to α-ketobutyrate in Figure 22–16; and the conversion of propionyl-CoA to succinyl-CoA in Figure 17–12.

Branched-Chain Amino Acids Are Not Degraded in the Liver

Although much of the catabolism of amino acids takes place in the liver, the three amino acids with branched side chains (leucine, isoleucine, and valine) are oxidized as fuels primarily in muscle, adipose, kidney, and brain tissue. These extrahepatic tissues contain an aminotransferase, absent in liver, that acts on all three branched-chain amino acids to produce the corresponding α-keto acids **(Fig. 18–28)**. The **branched-chain α-keto acid dehydrogenase complex** then catalyzes oxidative decarboxylation of all three α-keto acids, in each case releasing the carboxyl group as CO_2 and producing the acyl-CoA derivative. This reaction is formally analogous to two other oxidative decarboxylations encountered in Chapter 16: oxidation of pyruvate to acetyl-CoA by the pyruvate dehydrogenase complex (see Fig. 16–6) and oxidation of α-ketoglutarate to succinyl-CoA by the α-ketoglutarate dehydrogenase complex (p. 644). In fact, all three enzyme complexes are similar in structure and share essentially the same reaction mechanism. Five cofactors (thiamine pyrophosphate, FAD, NAD, lipoate, and coenzyme A) participate, and the three proteins in each complex catalyze homologous reactions. This is clearly a case in which enzymatic machinery that evolved to catalyze one reaction was "borrowed" by gene duplication and further evolved to catalyze similar reactions in other pathways.

Experiments with rats have shown that the branched-chain α-keto acid dehydrogenase complex is regulated by covalent modification in response to the content of branched-chain amino acids in the diet. With little or no excess dietary intake of branched-chain amino acids, the enzyme complex is phosphorylated and thereby inactivated by a protein kinase. Addition of excess branched-chain amino acids to the diet results in dephosphorylation and consequent activation of the enzyme. Recall that the pyruvate dehydrogenase complex is subject to similar regulation by phosphorylation and dephosphorylation (p. 654).

There is a relatively rare genetic disease in which the three branched-chain α-keto acids (as well as their precursor amino acids, especially leucine) accumulate in the blood and "spill over" into the urine. This condition, called **maple syrup urine disease** because of the characteristic odor imparted to the urine by the α-keto acids, results from a defective branched-chain α-keto acid dehydrogenase complex. Untreated, the disease results in abnormal development of the brain, mental retardation, and death in early infancy. Treatment entails rigid control of the diet, limiting the intake of valine, isoleucine, and leucine to the minimum required to permit normal growth. ■

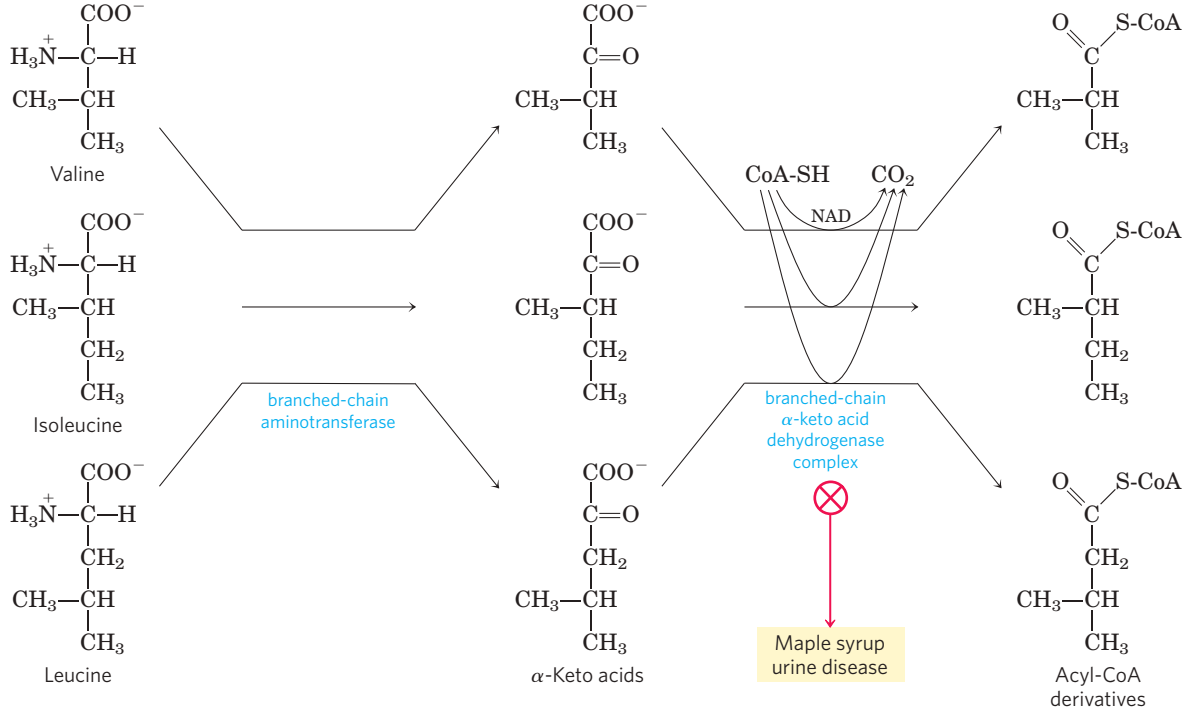

FIGURE 18–28 Catabolic pathways for the three branched-chain amino acids: valine, isoleucine, and leucine. All three pathways occur in extrahepatic tissues and share the first two enzymes, as shown here. The branched-chain α-keto acid dehydrogenase complex is analogous to the pyruvate and α-ketoglutarate dehydrogenase complexes and requires the same five cofactors (some not shown here). This enzyme is defective in people with maple syrup urine disease.

BOX 18–2 MEDICINE Scientific Sleuths Solve a Murder Mystery

Truth can sometimes be stranger than fiction—or at least as strange as a made-for-TV movie. Take, for example, the case of Patricia Stallings. Convicted of the murder of her infant son, she was sentenced to life in prison—but was later found innocent, thanks to the medical sleuthing of three persistent researchers.

The story began in the summer of 1989 when Stallings brought her three-month-old son, Ryan, to the emergency room of Cardinal Glennon Children's Hospital in St. Louis. The child had labored breathing, uncontrollable vomiting, and gastric distress. According to the attending physician, a toxicologist, the child's symptoms indicated that he had been poisoned with ethylene glycol, an ingredient of antifreeze, a conclusion apparently confirmed by analysis at a commercial lab.

After he recovered, the child was placed in a foster home, and Stallings and her husband, David, were allowed to see him in supervised visits. But when the infant became ill, and subsequently died, after a visit in which Stallings had been briefly left alone with him, she was charged with first-degree murder and held without bail. At the time, the evidence seemed compelling, as both the commercial lab and the hospital lab found large amounts of ethylene glycol in the boy's blood and traces of it in a bottle of milk Stallings had fed her son during the visit.

But without knowing it, Stallings had performed a brilliant experiment. While in custody, she learned she was pregnant; she subsequently gave birth to another son, David Stallings Jr., in February 1990. He was placed immediately in a foster home, but within two weeks he started having symptoms similar to Ryan's. David was eventually diagnosed with a rare metabolic disorder called methylmalonic acidemia (MMA). A recessive genetic disorder of amino acid metabolism, MMA affects about 1 in 48,000 newborns and presents symptoms almost identical with those caused by ethylene glycol poisoning.

Stallings couldn't possibly have poisoned her second son, but the Missouri state prosecutor's office was not impressed by the new developments and pressed forward with her trial anyway. The court wouldn't allow the MMA diagnosis of the second child to be introduced as evidence, and in January 1991 Patricia Stallings was convicted of assault with a deadly weapon and sentenced to life in prison.

Fortunately for Stallings, however, William Sly, chairman of the Department of Biochemistry and Molecular Biology at St. Louis University, and James Shoemaker, head of a metabolic screening lab at the university, got interested in her case when they heard about it from a television broadcast. Shoemaker performed his own analysis of Ryan's blood and didn't detect ethylene glycol. He and Sly then contacted Piero Rinaldo, a metabolic disease expert at Yale University School of Medicine whose lab is equipped to diagnose MMA from blood samples.

When Rinaldo analyzed Ryan's blood serum, he found high concentrations of methylmalonic acid, a breakdown product of the branched-chain amino acids isoleucine and valine, which accumulates in MMA patients because the enzyme that should convert it to the next product in the metabolic pathway is defective (Fig. 1).

Asparagine and Aspartate Are Degraded to Oxaloacetate

The carbon skeletons of **asparagine** and **aspartate** ultimately enter the citric acid cycle as malate in mammals or oxaloacetate in bacteria. The enzyme **asparaginase** catalyzes the hydrolysis of asparagine to aspartate, which undergoes transamination with α-ketoglutarate to yield glutamate and oxaloacetate **(Fig. 18–29)**. The oxaloacetate is converted to malate in the cytosol and then transported into the mitochondrial matrix through the malate–α-ketoglutarate transporter. In bacteria, the oxaloacetate produced in the transamination reaction can be used directly in the citric acid cycle.

We have now seen how the 20 common amino acids, after losing their nitrogen atoms, are degraded by dehydrogenation, decarboxylation, and other reactions to yield portions of their carbon backbones in the form of six central metabolites that can enter the citric acid cycle. Those portions degraded to acetyl-CoA are completely oxidized to carbon dioxide and water, with generation of ATP by oxidative phosphorylation.

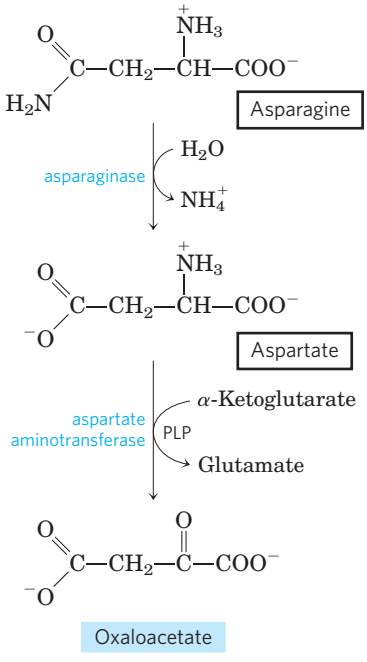

FIGURE 18–29 Catabolic pathway for asparagine and aspartate. Both amino acids are converted to oxaloacetate.

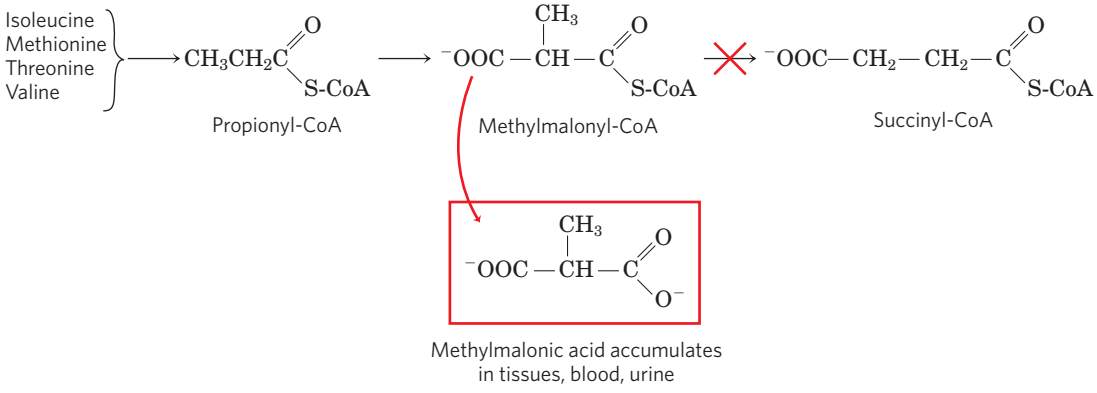

FIGURE 1 Children with a mutation (red X) that inactivates the enzyme methylmalony-CoA mutase cannot degrade isoleucine, methionine, threonine, and valine normally. Instead, a potentially fatal accumulation of methylmalonic acid occurs, with symptoms similar to those of ethylene glycol poisoning.

And particularly telling, he says, the child's blood and urine contained massive amounts of ketones, another metabolic consequence of the disease. Like Shoemaker, he did not find any ethylene glycol in a sample of the baby's bodily fluids. The bottle couldn't be tested, since it had mysteriously disappeared. Rinaldo's analyses convinced him that Ryan had died from MMA, but how to account for the results from two labs, indicating that the boy had ethylene glycol in his blood? Could they both be wrong?

When Rinaldo obtained the lab reports, what he saw was, he says, "scary." One lab said that Ryan Stallings' blood contained ethylene glycol, even though the blood sample analysis did not match the lab's own profile for a known sample containing ethylene glycol. "This was not just a matter of questionable interpretation. The quality of their analysis was unacceptable," Rinaldo says. And the second laboratory? According to Rinaldo, that lab detected an abnormal component in Ryan's blood and just "assumed it was ethylene glycol." Samples from the bottle had produced nothing unusual, says Rinaldo, yet the lab claimed evidence of ethylene glycol in that, too.

Rinaldo presented his findings to the case's prosecutor, George McElroy, who called a press conference the very next day. "I no longer believe the laboratory data," he told reporters. Having concluded that Ryan Stallings had died of MMA after all, McElroy dismissed all charges against Patricia Stallings on September 20, 1991.

As was the case for carbohydrates and lipids, the degradation of amino acids results ultimately in the generation of reducing equivalents (NADH and $FADH_2$) through the action of the citric acid cycle. Our survey of catabolic processes concludes in the next chapter with a discussion of respiration, in which these reducing equivalents fuel the ultimate oxidative and energy-generating process in aerobic organisms.

SUMMARY 18.3 Pathways of Amino Acid Degradation

- After the removal of amino groups, the carbon skeletons of amino acids undergo oxidation to compounds that can enter the citric acid cycle for oxidation to CO_2 and H_2O. The reactions of these pathways require several cofactors, including tetrahydrofolate and *S*-adenosylmethionine in one-carbon transfer reactions and tetrahydrobiopterin in the oxidation of phenylalanine by phenylalanine hydroxylase.
- Depending on their degradative end product, some amino acids can be converted to ketone bodies, some to glucose, and some to both. Thus amino acid degradation is integrated into intermediary metabolism and can be critical to survival under conditions in which amino acids are a significant source of metabolic energy.
- The carbon skeletons of amino acids enter the citric acid cycle through five intermediates: acetyl-CoA, α-ketoglutarate, succinyl-CoA, fumarate, and oxaloacetate. Some are also degraded to pyruvate, which can be converted to either acetyl-CoA or oxaloacetate.
- The amino acids producing pyruvate are alanine, cysteine, glycine, serine, threonine, and tryptophan. Leucine, lysine, phenylalanine, and tryptophan yield acetyl-CoA via acetoacetyl-CoA. Isoleucine, leucine, threonine, and tryptophan also form acetyl-CoA directly.
- Arginine, glutamate, glutamine, histidine, and proline produce α-ketoglutarate; isoleucine, methionine, threonine, and valine produce succinyl-CoA; four carbon atoms of phenylalanine

and tyrosine give rise to fumarate; and asparagine and aspartate produce oxaloacetate.

- The branched-chain amino acids (isoleucine, leucine, and valine), unlike the other amino acids, are degraded only in extrahepatic tissues.
- Several serious human diseases can be traced to genetic defects in the enzymes of amino acid catabolism.

Key Terms

Terms in bold are defined in the glossary.

aminotransferases 699
transaminases 699
transamination 699
pyridoxal phosphate (PLP) 699
oxidative deamination 700
L-glutamate dehydrogenase 700
glutamine synthetase 702
glutaminase 703
glucose-alanine cycle 703
ammonotelic 704
ureotelic 704
uricotelic 704
urea cycle 704
urea 704
creatine kinase 708
essential amino acids 709
ketogenic 711
glucogenic 711
tetrahydrofolate 712
***S*-adenosylmethionine (adoMet)** 712
tetrahydrobiopterin 714
phenylketonuria (PKU) 719
mixed-function oxidases 720
alkaptonuria 721
maple syrup urine disease 723

Further Reading

General

Amon, J., Titgemeyer, F., & Burkovski, A. (2010) Common patterns—unique features: nitrogen metabolism and regulation in Gram-positive bacteria. *FEMS Microbiol. Rev.* **34**, 588–605.

Arias, I.M., Alter, H.J., Boyer, J.L., Cohen, D.E., Fausto, N., Shafritz, D.A., & Wolkof, A.W. (2009) *The Liver: Biology and Pathobiology*, 5th edn, John Wiley & Sons, Hoboken, New Jersey.

Brosnan, J.T. (2001) Amino acids, then and now—a reflection on Sir Hans Krebs' contribution to nitrogen metabolism. *IUBMB Life* **52**, 265–270.

An interesting tour through the life of this important biochemist.

Frey, P.A. & Hegeman, A.D. (2006) *Enzymatic Reaction Mechanisms*, Oxford University Press, New York.

A good source for in-depth discussion of the classes of enzymatic reaction mechanisms described in the chapter.

Amino Acid Metabolism

Christen, P. & Metzler, D.E. (1985) *Transaminases*, Wiley-Interscience, Inc., New York.

Curthoys, N.P. & Watford, M. (1995) Regulation of glutaminase activity and glutamine metabolism. *Annu. Rev. Nutr.* **15**, 133–159.

Eliot, A.C. & Kirsch, J.F. (2004) Pyridoxal phosphate enzymes: mechanistic, structural and evolutionary considerations. *Annu. Rev. Biochem.* **73**, 383–415.

Fitzpatrick, P.F. (1999) Tetrahydropterin-dependent amino acid hydroxylases. *Annu. Rev. Biochem.* **68**, 355–382.

Kalhan, S.C. & Bier, D.M. (2008) Protein and amino acid metabolism in the human newborn. *Annu. Rev. Nutr.* **28**, 389–410.

Pencharz, P.B. & Ball, R.O. (2003) Different approaches to define individual amino acid requirements. *Annu. Rev. Nutr.* **23**, 101–116.

Determination of which amino acids are essential in the human diet is not a trivial problem, as this review relates.

The Urea Cycle

Braissant, O. (2010) Current concepts in the pathogenesis of urea cycle diosorders. *Mol. Genet. Metab.* **100**, S3–S12.

Brusilow, S.W. & Horwich, A.L. (2006) Urea cycle enzymes. In *Scriver's Online Metabolic and Molecular Bases of Inherited Disease* (Valle, D., Beaudet, A.L., Vogelstein, B., Kinzler, K.W., Antonarakis, S.E., Ballabio A., eds), http:// dx.doi.org/10.10 36/ ommbid, 108.

An authoritative source on this pathway.

Enns, G.M., Berry, S.A., Berry, G.T., Rhead, W.J., Brusilow, S.W., & Hamosh, A. (2007) Survival after treatment with phenylacetate and benzoate for urea-cycle disorders. *N. Engl. J. Med.* **356**, 2282–2292.

Kresge, N., Simoni R.D., & Hill, R.L. (2005) Four decades of research on the biosynthesis of urea: the work of Sarah Ratner. *J. Biol. Chem.* **280**, e34.

Morris, S.M. (2002) Regulation of enzymes of the urea cycle and arginine metabolism. *Annu. Rev. Nutr.* **22**, 87–105.

This review details what is known about some levels of regulation not covered in the chapter, such as hormonal and nutritional regulation.

Simoni, R.D., Hill, R.L., Vaughan, M., & Tabor, H. (2004) Transaminases: the work of Philip P. Cohen. *J. Biol. Chem.* **279**, e1.

Disorders of Amino Acid Degradation

Ledley, F.D., Levy, H.L., & Woo, S.L.C. (1986) Molecular analysis of the inheritance of phenylketonuria and mild hyperphenylalaninemia in families with both disorders. *N. Engl. J. Med.* **314**, 1276–1280.

Scriver, C.R., Kaufman, S., & Woo, S.L.C. (1988) Mendelian hyperphenylalaninemia. *Annu. Rev. Genet.* **22**, 301–321.

Valle, D., Beaudet, A.L., Vogelstein, B., Kinzler, K.W., Antonarakis, S.E., & Ballabio, A. (eds) (2006, updated 2011) *Scriver's Online Metabolic and Molecular Bases of Inherited Disease,* Part 8: Amino Acids, www.ommbid.com.

Werner, E.R., Blau, N., & Thöny, B. (2011) Tetrahydrobiopterin: biochemistry and pathophysiology. *Biochem. J.* **438**, 397–414.

Problems

1. Products of Amino Acid Transamination Name and draw the structure of the α-keto acid resulting when each of the following amino acids undergoes transamination with α-ketoglutarate: (a) aspartate, (b) glutamate, (c) alanine, (d) phenylalanine.

2. Measurement of Alanine Aminotransferase Activity The activity (reaction rate) of alanine aminotransferase is usually measured by including an excess of pure lactate dehydrogenase and NADH in the reaction system. The rate of alanine disappearance is equal to the rate of NADH disappearance measured spectrophotometrically. Explain how this assay works.

3. Alanine and Glutamine in the Blood Normal human blood plasma contains all the amino acids required for the synthesis of body proteins, but not in equal concentrations.

Alanine and glutamine are present in much higher concentrations than any other amino acids. Suggest why.

4. Distribution of Amino Nitrogen If your diet is rich in alanine but deficient in aspartate, will you show signs of aspartate deficiency? Explain.

5. Lactate versus Alanine as Metabolic Fuel: The Cost of Nitrogen Removal The three carbons in lactate and alanine have identical oxidation states, and animals can use either carbon source as a metabolic fuel. Compare the net ATP yield (moles of ATP per mole of substrate) for the complete oxidation (to CO_2 and H_2O) of lactate versus alanine when the cost of nitrogen excretion as urea is included.

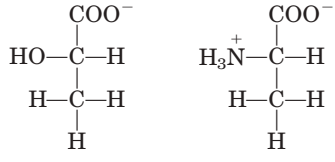

6. Ammonia Toxicity Resulting from an Arginine-Deficient Diet In a study conducted some years ago, cats were fasted overnight then given a single meal complete in all amino acids except arginine. Within 2 hours, blood ammonia levels increased from a normal level of 18 μg/L to 140 μg/L, and the cats showed the clinical symptoms of ammonia toxicity. A control group fed a complete amino acid diet or an amino acid diet in which arginine was replaced by ornithine showed no unusual clinical symptoms.

(a) What was the role of fasting in the experiment?

(b) What caused the ammonia levels to rise in the experimental group? Why did the absence of arginine lead to ammonia toxicity? Is arginine an essential amino acid in cats? Why or why not?

(c) Why can ornithine be substituted for arginine?

7. Oxidation of Glutamate Write a series of balanced equations, and an overall equation for the net reaction, describing the oxidation of 2 mol of glutamate to 2 mol of α-ketoglutarate and 1 mol of urea.

8. Transamination and the Urea Cycle Aspartate aminotransferase has the highest activity of all the mammalian liver aminotransferases. Why?

9. The Case against the Liquid Protein Diet A weight-reducing diet heavily promoted some years ago required the daily intake of "liquid protein" (soup of hydrolyzed gelatin), water, and an assortment of vitamins. All other food and drink were to be avoided. People on this diet typically lost 10 to 14 lb in the first week.

(a) Opponents argued that the weight loss was almost entirely due to water loss and would be regained very soon after a normal diet was resumed. What is the biochemical basis for this argument?

(b) A few people on this diet died. What are some of the dangers inherent in the diet, and how can they lead to death?

10. Ketogenic Amino Acids Which amino acids are exclusively ketogenic?

11. A Genetic Defect in Amino Acid Metabolism: A Case History A two-year-old child was taken to the hospital. His mother said that he vomited frequently, especially after feedings. The child's weight and physical development were below normal. His hair, although dark, contained patches of white. A urine sample treated with ferric chloride ($FeCl_3$) gave a green color characteristic of the presence of phenylpyruvate. Quantitative analysis of urine samples gave the results shown in the table.

	Concentration (mM)	
Substance	**Patient's urine**	**Normal urine**
Phenylalanine	7.0	0.01
Phenylpyruvate	4.8	0
Phenyllactate	10.3	0

(a) Suggest which enzyme might be deficient in this child. Propose a treatment.

(b) Why does phenylalanine appear in the urine in large amounts?

(c) What is the source of phenylpyruvate and phenyllactate? Why does this pathway (normally not functional) come into play when the concentration of phenylalanine rises?

(d) Why does the boy's hair contain patches of white?

12. Role of Cobalamin in Amino Acid Catabolism Pernicious anemia is caused by impaired absorption of vitamin B_{12}. What is the effect of this impairment on the catabolism of amino acids? Are all amino acids equally affected? (Hint: See Box 17–2.)

13. Vegetarian Diets Vegetarian diets can provide high levels of antioxidants and a lipid profile that can help prevent coronary disease. However, there can be some associated problems. Blood samples were taken from a large group of volunteer subjects who were vegans (strict vegetarians: no animal products), lactovegetarians (vegetarians who eat dairy products), or omnivores (individuals with a normal, varied diet including meat). In each case, the volunteers had followed the diet for several years. The blood levels of both homocysteine and methylmalonate were elevated in the vegan group, somewhat lower in the lactovegetarian group, and much lower in the omnivore group. Explain.

14. Pernicious Anemia Vitamin B_{12} deficiency can arise from a few rare genetic diseases that lead to low B_{12} levels despite a normal diet that includes B_{12}-rich meat and dairy sources. These conditions cannot be treated with dietary B_{12} supplements. Explain.

15. Pyridoxal Phosphate Reaction Mechanisms Threonine can be broken down by the enzyme threonine dehydratase, which catalyzes the conversion of threonine to α-ketobutyrate and ammonia. The enzyme uses PLP as a cofactor. Suggest a mechanism for this reaction, based on the mechanisms in Figure 18–6. Note that this reaction includes an elimination at the β carbon of threonine.

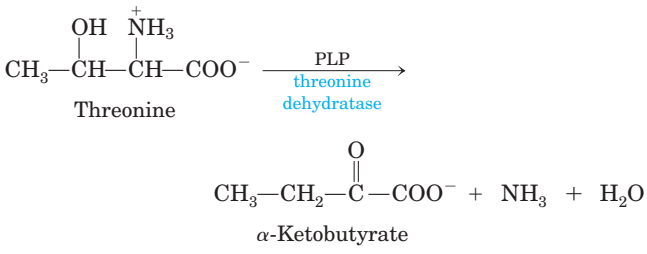

Threonine

α-Ketobutyrate

16. Pathway of Carbon and Nitrogen in Glutamate Metabolism When [2-^{14}C,^{15}N] glutamate undergoes oxidative degradation in the liver of a rat, in which atoms of the following metabolites will each isotope be found: (a) urea, (b) succinate, (c) arginine, (d) citrulline, (e) ornithine, (f) aspartate?

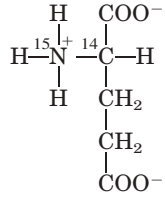

Labeled glutamate

17. Chemical Strategy of Isoleucine Catabolism Isoleucine is degraded in six steps to propionyl-CoA and acetyl-CoA.

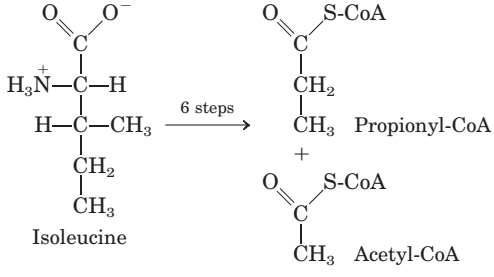

Isoleucine

Propionyl-CoA

Acetyl-CoA

(a) The chemical process of isoleucine degradation includes strategies analogous to those used in the citric acid cycle and the β oxidation of fatty acids. The intermediates of isoleucine degradation (I to V) shown below are not in the proper order. Use your knowledge and understanding of the citric acid cycle and β-oxidation pathway to arrange the intermediates in the proper metabolic sequence for isoleucine degradation.

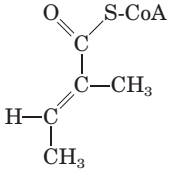

I

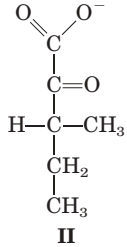

II

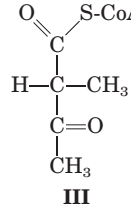

III

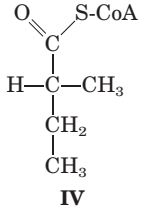

IV

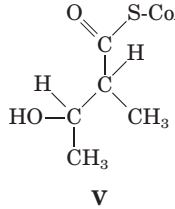

V

(b) For each step you propose, describe the chemical process, provide an analogous example from the citric acid cycle or β-oxidation pathway (where possible), and indicate any necessary cofactors.

18. Role of Pyridoxal Phosphate in Glycine Metabolism The enzyme serine hydroxymethyltransferase requires pyridoxal phosphate as cofactor. Propose a mechanism for the reaction catalyzed by this enzyme, in the direction of serine degradation (glycine production). (Hint: See Figs 18–19 and 18–20b.)

19. Parallel Pathways for Amino Acid and Fatty Acid Degradation The carbon skeleton of leucine is degraded by a series of reactions closely analogous to those of the citric acid cycle and β oxidation. For each reaction, (a) through (f), shown below, indicate its type, provide an analogous example from the citric acid cycle or β-oxidation pathway (where possible), and note any necessary cofactors.

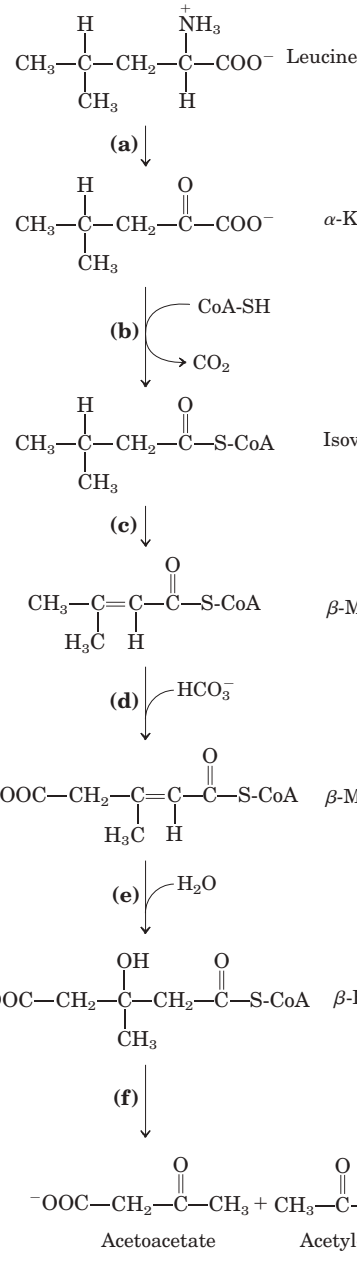

Data Analysis Problem

20. Maple Syrup Urine Disease Figure 18–28 shows the pathway for the degradation of branched-chain amino acids and the site of the biochemical defect that causes maple syrup urine disease. The initial findings that eventually led to the discovery of the defect in this disease were presented in three papers published in the late 1950s and early 1960s. This problem traces the history of the findings from initial clinical observations to proposal of a biochemical mechanism.

Menkes, Hurst, and Craig (1954) presented the cases of four siblings, all of whom died following a similar course of symptoms. In all four cases, the mother's pregnancy and the birth had been normal. The first 3 to 5 days of each child's life were also normal. But soon thereafter each child began having convulsions, and the children died between the ages of 11 days and 3 months. Autopsy showed considerable swelling of the brain in all cases. The children's urine had a strong, unusual "maple syrup" odor, starting from about the third day of life.

Menkes (1959) reported data collected from six more children. All showed symptoms similar to those described above, and died within 15 days to 20 months of birth. In one case, Menkes was able to obtain urine samples during the last months of the infant's life. When he treated the urine with 2,4-dinitrophenylhydrazone, which forms colored precipitates with keto compounds, he found three α-keto acids in unusually large amounts:

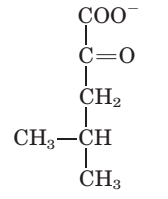
α-Ketoisocaproate

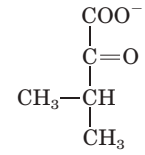
α-Ketoisovalerate

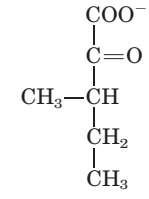
α-Keto-β-methyl-n-valerate

(a) These α-keto acids are produced by the deamination of amino acids. For each of the α-keto acids above, draw and name the amino acid from which it was derived.

Dancis, Levitz, and Westall (1960) collected further data that led them to propose the biochemical defect shown in Figure 18–28. In one case, they examined a patient whose urine first showed the maple syrup odor when he was 4 months old. At the age of 10 months (March 1956), the child was admitted to the hospital because he had a fever, and he showed grossly retarded motor development. At the age of 20 months (January 1957), he was readmitted and was found to have the degenerative neurological symptoms seen in previous cases of

	Urine (mg/24 h)			Plasma (mg/mL)	
	Normal	Patient		Normal	Patient
Amino acid(s)		**Mar. 1956**	**Jan. 1957**		**Jan. 1957**
Alanine	5–15	0.2	0.4	3.0–4.8	0.6
Asparagine and glutamine	5–15	0.4	0	3.0–5.0	2.0
Aspartic acid	1–2	0.2	1.5	0.1–0.2	0.04
Arginine	1.5–3	0.3	0.7	0.8–1.4	0.8
Cystine	2–4	0.5	0.3	1.0–1.5	0
Glutamic acid	1.5–3	0.7	1.6	1.0–1.5	0.9
Glycine	20–40	4.6	20.7	1.0–2.0	1.5
Histidine	8–15	0.3	4.7	1.0–1.7	0.7
Isoleucine	2–5	2.0	13.5	0.8–1.5	2.2
Leucine	3–8	2.7	39.4	1.7–2.4	14.5
Lysine	2–12	1.6	4.3	1.5–2.7	1.1
Methionine	2–5	1.4	1.4	0.3–0.6	2.7
Ornithine	1–2	0	1.3	0.6–0.8	0.5
Phenylalanine	2–4	0.4	2.6	1.0–1.7	0.8
Proline	2–4	0.5	0.3	1.5–3.0	0.9
Serine	5–15	1.2	0	1.3–2.2	0.9
Taurine	1–10	0.2	18.7	0.9–1.8	0.4
Threonine	5–10	0.6	0	1.2–1.6	0.3
Tryptophan	3–8	0.9	2.3	Not measured	0
Tyrosine	4–8	0.3	3.7	1.5–2.3	0.7
Valine	2–4	1.6	15.4	2.0–3.0	13.1

maple syrup urine disease; he died soon after. Results of his blood and urine analyses are shown in the table on page 729, along with normal values for each component.

(b) The table includes taurine, an amino acid not normally found in proteins. Taurine is often produced as a byproduct of cell damage. Its structure is:

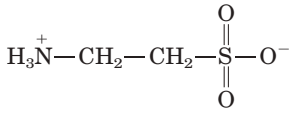

Based on its structure and the information in this chapter, what is the most likely amino acid precursor of taurine? Explain your reasoning.

(c) Compared with the normal values given in the table, which amino acids showed significantly elevated levels in the patient's blood in January 1957? Which ones in the patient's urine?

Based on their results and their knowledge of the pathway shown in Figure 18–28, Dancis and coauthors concluded: "although it appears most likely to the authors that the primary block is in the metabolic degradative pathway of the branched-chain amino acids, this cannot be considered established beyond question."

(d) How do the data presented here support this conclusion?

(e) Which data presented here do *not* fit this model of maple syrup urine disease? How do you explain these seemingly contradictory data?

(f) What data would you need to collect to be more secure in your conclusion?

References

Dancis, J., Levitz, M., & Westall, R. (1960) Maple syrup urine disease: branched-chain ketoaciduria. *Pediatrics* **25**, 72–79.

Menkes, J.H. (1959) Maple syrup disease: isolation and identification of organic acids in the urine. *Pediatrics* **23**, 348–353.

Menkes, J.H., Hurst, P.L., & Craig J.M. (1954) A new syndrome: progressive familial infantile cerebral dysfunction associated with an unusual urinary substance. *Pediatrics* **14**, 462–466.

19

Oxidative Phosphorylation and Photophosphorylation

Oxidative phosphorylation is the culmination of energy-yielding metabolism in aerobic organisms. All oxidative steps in the degradation of carbohydrates, fats, and amino acids converge at this final stage of cellular respiration, in which the energy of oxidation drives the synthesis of ATP. Photophosphorylation is the means by which photosynthetic organisms capture the energy of sunlight—the ultimate source of energy in the biosphere—and harness it to make ATP. Together, oxidative phosphorylation and photophosphorylation account for most of the ATP synthesized by most organisms most of the time. In eukaryotes, oxidative phosphorylation occurs in mitochondria, photophosphorylation in chloroplasts. The pathways to ATP synthesis in mitochondria and chloroplasts have challenged and fascinated biochemists for more than half a century, and the fascination has grown with our deepening appreciation of these fundamental mechanisms in living organisms, their conservation in evolution, and their structural bases.

Our current understanding of ATP synthesis in mitochondria and chloroplasts is based on the hypothesis, introduced by Peter Mitchell in 1961, that transmembrane differences in proton concentration are the reservoir for the energy extracted from biological oxidation reactions. This **chemiosmotic theory** has been accepted as one of the great unifying principles of twentieth-century biology. It provides insight into the processes of oxidative phosphorylation and photophosphorylation, and into such apparently disparate energy transductions as active transport across membranes and the motion of bacterial flagella.

Oxidative phosphorylation and photophosphorylation are mechanistically similar in three respects **(Fig. 19–1)**. (1) Both processes involve the flow of electrons through a chain of membrane-bound carriers. (2) The free energy made available by this "downhill" (exergonic) electron flow is coupled to the "uphill" transport of protons across a proton-impermeable membrane, conserving the free energy of fuel oxidation as a transmembrane electrochemical potential (p. 403). (3) The transmembrane flow of protons back down their concentration gradient through specific protein channels provides the free energy for synthesis of ATP, catalyzed by a membrane protein complex (ATP synthase) that couples proton flow to phosphorylation of ADP.

The chapter begins with mitochondrial oxidative phosphorylation. We first describe the components of the electron-transfer chain, their organization into large functional complexes in the inner mitochondrial membrane, the path of electron flow through them, and the proton movements that accompany this flow. We then consider the remarkable enzyme complex that, by "rota-

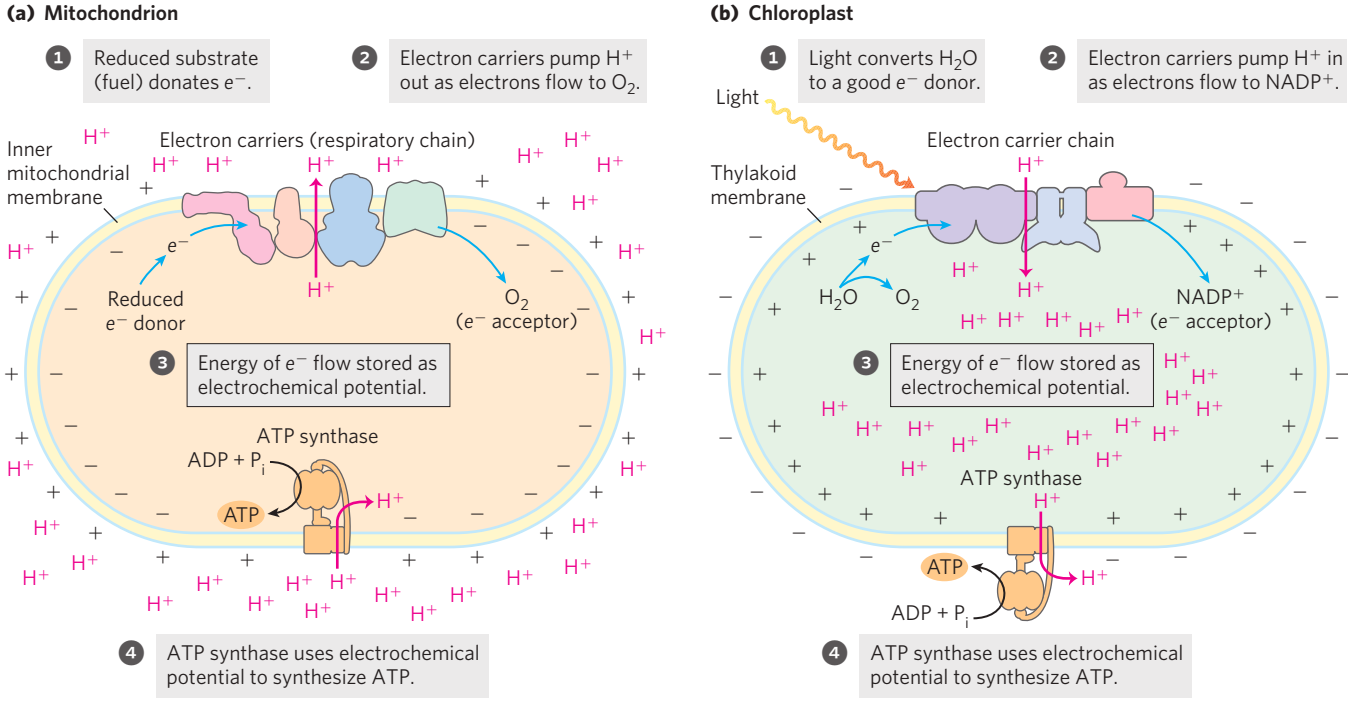

FIGURE 19–1 The chemiosmotic mechanism for ATP synthesis. (a) In mitochondria, electrons move through a chain of membrane-bound carriers (the respiratory chain) spontaneously, driven by the high reduction potential of oxygen and the relatively low reduction potentials of the various reduced substrates (fuels) that undergo oxidation in the mitochondrion. **(b)** In chloroplasts, the movement of electrons through a chain of membrane-bound carriers is driven by the energy of photons absorbed by the green pigment chlorophyll. In both organelles, electron flow creates an electrochemical potential by the transmembrane movement of protons and positive charge. In both cases this electrochemical potential drives ATP synthesis by a membrane-bound enzyme, ATP synthase, that is fundamentally similar in both mitochondria and chloroplasts, and in bacteria and archaea as well.

tional catalysis," captures the energy of proton flow in ATP, and the regulatory mechanisms that coordinate oxidative phosphorylation with the many catabolic pathways by which fuels are oxidized.

The metabolic role of mitochondria is so critical to cellular and organismal function that defects in mitochondrial function have very serious medical consequences. Mitochondria are central to neuronal and muscular function, and to the regulation of whole-body energy metabolism and body weight. Human neurodegenerative diseases, as well as cancer, diabetes, and obesity, are recognized as possible results of compromised mitochondrial function, and one theory of aging is based on gradual loss of mitochondrial integrity. ATP production is not the only important mitochondrial function; this organelle also acts in thermogenesis, steroid synthesis, and apoptosis (programmed cell death). The discovery of these diverse and important roles of mitochondria has stimulated much current research on the biochemistry of this organelle.

After discussing these various mitochondrial functions, we turn to photophosphorylation, looking first at the absorption of light by photosynthetic pigments, then at the light-driven flow of electrons from H_2O to $NADP^+$ and the molecular basis for coupling electron and proton flow. We also consider the similarities of structure and mechanism between the ATP synthases of chloroplasts and mitochondria, and the evolutionary basis for this conservation of mechanism. The remarkable ability of chloroplasts to make ATP by oxidizing a compound of unlimited availability (water), while producing a compound essential to most animal life (oxygen), poses a set of challenges equally fascinating to biologist, biochemist, and chemist. Determination of the structures of supramolecular complexes that carry out these processes in chloroplasts has provided invaluable physical and chemical clues to understanding the process of photosynthesis.

OXIDATIVE PHOSPHORYLATION

19.1 Electron-Transfer Reactions in Mitochondria

Albert L. Lehninger, 1917–1986

The discovery in 1948 by Eugene Kennedy and Albert Lehninger that mitochondria are the site of oxidative phosphorylation in eukaryotes marked the beginning of the modern phase of studies in biological energy transductions. Mitochondria, like gram-negative bacteria, have two membranes **(Fig. 19–2a)**. The outer mitochondrial membrane is readily permeable to

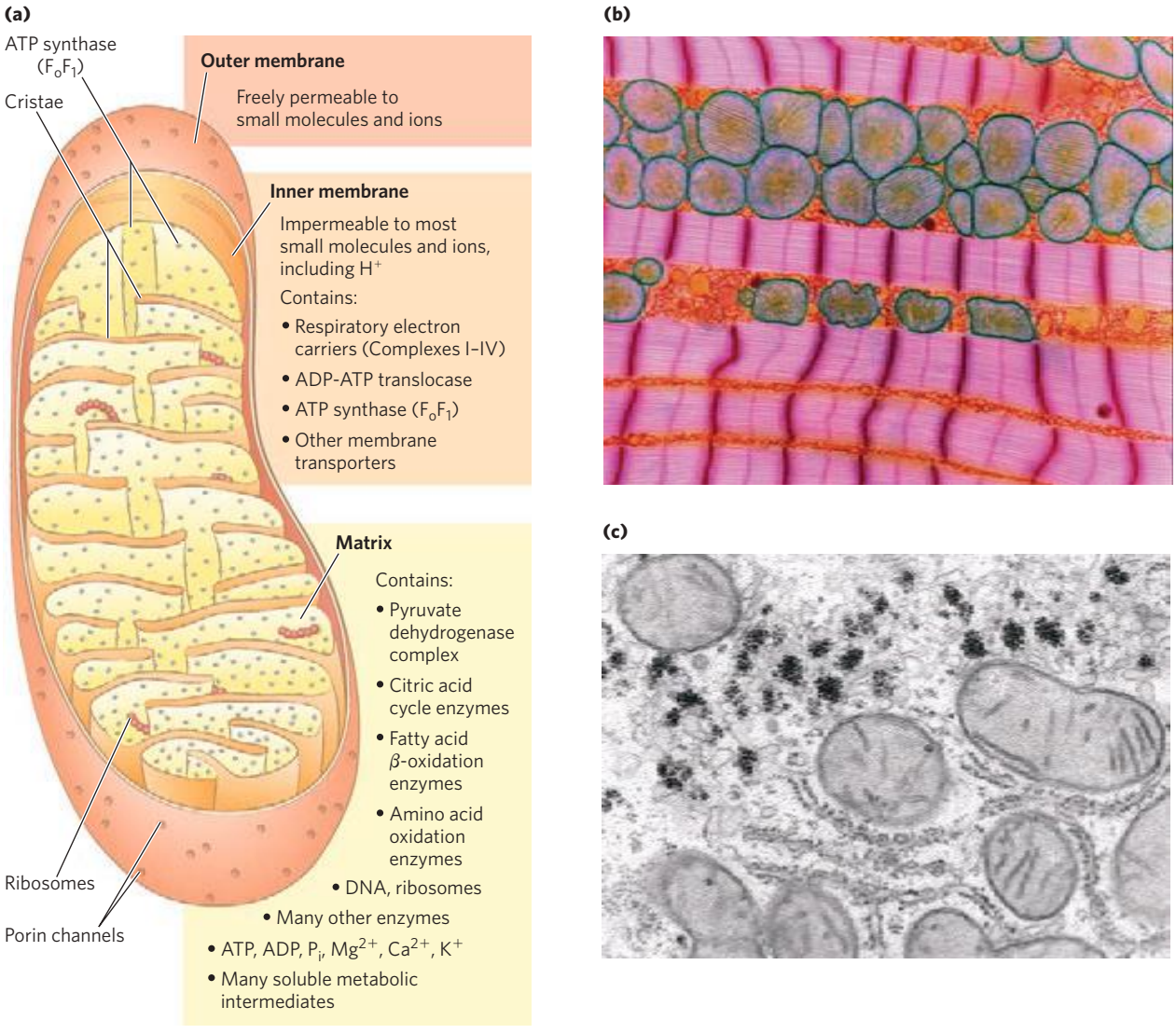

FIGURE 19–2 Biochemical anatomy of a mitochondrion. (a) The outer membrane has pores that make it permeable to small molecules and ions, but not to proteins. The convolutions (cristae) of the inner membrane provide a very large surface area. The inner membrane of a single liver mitochondrion may have more than 10,000 sets of electron-transfer systems (respiratory chains) and ATP synthase molecules, distributed over the membrane surface. **(b)** The mitochondria of heart muscle, which have more profuse cristae and thus a much larger area of inner membrane, contain more than three times as many sets of electron-transfer systems as **(c)** liver mitochondria. Muscle and liver mitochondria are about the size of a bacterium—1 to 2 μm long. The mitochondria of invertebrates, plants, and microbial eukaryotes are similar to those shown here, but with much variation in size, shape, and degree of convolution of the inner membrane.

small molecules (M_r <5,000) and ions, which move freely through transmembrane channels formed by a family of integral membrane proteins called porins. The inner membrane is impermeable to most small molecules and ions, including protons (H^+); the only species that cross this membrane do so through specific transporters. The inner membrane bears the components of the respiratory chain and the ATP synthase.

The mitochondrial matrix, enclosed by the inner membrane, contains the pyruvate dehydrogenase complex and the enzymes of the citric acid cycle, the fatty acid β-oxidation pathway, and the pathways of amino acid oxidation—all the pathways of fuel oxidation except glycolysis, which takes place in the cytosol. The selectively permeable inner membrane segregates the intermediates and enzymes of cytosolic metabolic pathways from those of metabolic processes occurring in the matrix. However, specific transporters carry pyruvate, fatty acids, and amino acids or their α-keto derivatives into the matrix for access to the machinery of the citric acid cycle. ADP and P_i are specifically transported into the matrix as newly synthesized ATP is transported out. The best current inventory of proteins in mammalian mitochondria lists about 1,100, at least 300 of which have unknown functions.

The bean-shaped representation of a mitochondrion in Figure 19–2 is an oversimplification, derived in part from early studies in which thin sections of cells were observed in the electron microscope. Three-dimensional images obtained either by reconstruction from serial sections or by confocal microscopy reveal greater variation in mitochondrial size and shape. In living cells

stained with mitochondrion-specific fluorescent dyes, large numbers of variously shaped mitochondria are seen, clustered about the nucleus (see Fig. 19–42).

Tissues with a high demand for aerobic metabolism (brain, skeletal and heart muscle, and eye, for example) contain many hundreds or thousands of mitochondria per cell, and in general, mitochondria of cells with high metabolic activity have more, and more densely packed, cristae (Fig. 19–1b). In tissues with less-active metabolism (skin, for example) there are fewer mitochondria, each with fewer cristae. During cell growth and division, mitochondria divide by fission (like bacteria), and under some circumstances individual mitochondria fuse to form larger, more-extended structures.

Electrons Are Funneled to Universal Electron Acceptors

Oxidative phosphorylation begins with the entry of electrons into the chain of electron carriers called the **respiratory chain**. Most of these electrons arise from the action of dehydrogenases that collect electrons from catabolic pathways and funnel them into universal electron acceptors—nicotinamide nucleotides (NAD^+ or $NADP^+$) or flavin nucleotides (FMN or FAD) (see Figs 13–24, 13–27).

Nicotinamide nucleotide–linked dehydrogenases catalyze reversible reactions of the following general types:

$$\text{Reduced substrate} + NAD^+ \rightleftharpoons \text{oxidized substrate} + NADH + H^+$$

$$\text{Reduced substrate} + NADP^+ \rightleftharpoons \text{oxidized substrate} + NADPH + H^+$$

Most dehydrogenases that act in catabolism are specific for NAD^+ as electron acceptor (Table 19–1). Some are in the cytosol, others are in mitochondria, and still others have mitochondrial and cytosolic isozymes.

NAD-linked dehydrogenases remove two hydrogen atoms from their substrates. One of these is transferred as a hydride ion ($:H^-$) to NAD^+, the other is released as H^+ in the medium (see Fig. 13–24). NADH and NADPH are water-soluble electron carriers that associate *reversibly* with dehydrogenases. NADH carries electrons from catabolic reactions to their point of entry into the respiratory chain, the NADH dehydrogenase complex described below. NADPH generally supplies electrons to anabolic reactions. Cells maintain separate pools of NADPH and NADH, with different redox potentials. This is accomplished by holding the ratio of [reduced form]/[oxidized form] relatively high for NADPH and relatively low for NADH. Neither NADH nor NADPH can cross the inner mitochondrial membrane, but the electrons they carry can be shuttled across indirectly, as we shall see.

Flavoproteins contain a very tightly, sometimes covalently, bound flavin nucleotide, either FMN or FAD (see Fig. 13–27). The oxidized flavin nucleotide can accept either one electron (yielding the semiquinone form) or two (yielding $FADH_2$ or $FMNH_2$). Electron transfer occurs because the flavoprotein has a higher reduction potential than the compound oxidized. Recall that reduction potential is a quantitative measure of the relative tendency of a given chemical species to accept electrons in an oxidation-reduction reaction (p. 530). The standard reduction potential of a flavin nucleotide, unlike that of NAD or NADP, depends on the protein with which it is associated. Local interactions

TABLE 19–1 Some Important Reactions Catalyzed by NAD(P)H-Linked Dehydrogenases

Reaction*	Location†
NAD-linked	
α-Ketoglutarate + CoA + $NAD^+ \rightleftharpoons$ succinyl-CoA + CO_2 + NADH + H^+	M
L-Malate + $NAD^+ \rightleftharpoons$ oxaloacetate + NADH + H^+	M and C
Pyruvate + CoA + $NAD^+ \rightleftharpoons$ acetyl-CoA + CO_2 + NADH + H^+	M
Glyceraldehyde 3-phosphate + P_i + $NAD^+ \rightleftharpoons$ 1,3-bisphosphoglycerate + NADH + H^+	C
Lactate + $NAD^+ \rightleftharpoons$ pyruvate + NADH + H^+	C
β-Hydroxyacyl-CoA + $NAD^+ \rightleftharpoons$ β-ketoacyl-CoA + NADH + H^+	M
NADP-linked	
Glucose 6-phosphate + $NADP^+ \rightleftharpoons$ 6-phosphogluconate + NADPH + H^+	C
L-Malate + $NADP^+ \rightleftharpoons$ pyruvate + CO_2 + NADPH + H^+	C
NAD- or NADP-linked	
L-Glutamate + H_2O + $NAD(P)^+ \rightleftharpoons$ α-ketoglutarate + NH_4^+ + NAD(P)H	M
Isocitrate + $NAD(P)^+ \rightleftharpoons$ α-ketoglutarate + CO_2 + NAD(P)H + H^+	M and C

*These reactions and their enzymes are discussed in Chapters 14 through 18.

†M designates mitochondria; C, cytosol.

with functional groups in the protein distort the electron orbitals in the flavin ring, changing the relative stabilities of oxidized and reduced forms. The relevant standard reduction potential is therefore that of the particular flavoprotein, not that of isolated FAD or FMN. The flavin nucleotide should be considered part of the flavoprotein's active site rather than a reactant or product in the electron-transfer reaction. Because flavoproteins can participate in either one- or two-electron transfers, they can serve as intermediates between reactions in which two electrons are donated (as in dehydrogenations) and those in which only one electron is accepted (as in the reduction of a quinone to a hydroquinone, described below).

Electrons Pass through a Series of Membrane-Bound Carriers

The mitochondrial respiratory chain consists of a series of sequentially acting electron carriers, most of which are integral proteins with prosthetic groups capable of accepting and donating either one or two electrons. Three types of electron transfers occur in oxidative phosphorylation: (1) direct transfer of electrons, as in the reduction of Fe^{3+} to Fe^{2+}, (2) transfer as a hydrogen atom ($H^+ + e^-$), and (3) transfer as a hydride ion ($:H^-$), which bears two electrons. The term **reducing equivalent** is used to designate a single electron equivalent transferred in an oxidation-reduction reaction.

In addition to NAD and flavoproteins, three other types of electron-carrying molecules function in the respiratory chain: a hydrophobic quinone (ubiquinone) and two different types of iron-containing proteins (cytochromes and iron-sulfur proteins). **Ubiquinone** (also called **coenzyme Q**, or simply **Q**) is a lipid-soluble benzoquinone with a long isoprenoid side chain **(Fig. 19–3)**. The closely related compounds plastoquinone (of plant chloroplasts) and menaquinone (of bacteria) play roles analogous to that of ubiquinone, carrying electrons in membrane-associated electron-transfer chains. Ubiquinone can accept one electron to become the semiquinone radical ($^{\bullet}QH$) or two electrons to form ubiquinol (QH_2) (Fig. 19–3) and, like flavoprotein carriers, it can act at the junction between a two-electron donor and a one-electron acceptor. Because ubiquinone is both small and hydrophobic, it is freely diffusible within the lipid bilayer of the inner mitochondrial membrane and can shuttle reducing equivalents between other, less mobile electron carriers in the membrane. And because it carries both electrons and protons, it plays a central role in coupling electron flow to proton movement.

The **cytochromes** are proteins with characteristic strong absorption of visible light, due to their iron-containing heme prosthetic groups **(Fig. 19–4a)**. Mitochondria contain three classes of cytochromes, designated *a*, *b*, and *c*, which are distinguished by differences in their light-absorption spectra. Each type of cytochrome in its reduced (Fe^{2+}) state has three absorption bands in the visible range (Fig. 19–4b). The longest-wavelength band

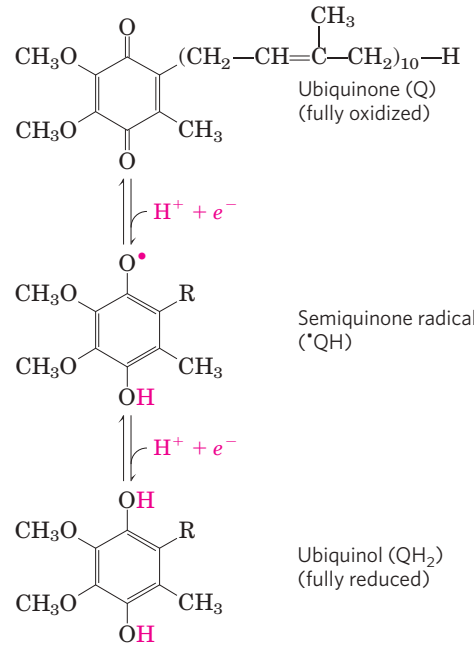

FIGURE 19–3 Ubiquinone (Q, or coenzyme Q). Complete reduction of ubiquinone requires two electrons and two protons, and occurs in two steps through the semiquinone radical intermediate.

is near 600 nm in type *a* cytochromes, near 560 nm in type *b*, and near 550 nm in type *c*. To distinguish among closely related cytochromes of one type, the exact absorption maximum is sometimes used in the names, as in cytochrome b_{562}.

The heme cofactors of *a* and *b* cytochromes are tightly, but not covalently, bound to their associated proteins; the hemes of *c*-type cytochromes are covalently attached through Cys residues (Fig. 19–4). As with the flavoproteins, the standard reduction potential of the heme iron atom of a cytochrome depends on its interaction with protein side chains and is therefore different for each cytochrome. The cytochromes of type *a* and *b* and some of type *c* are integral proteins of the inner mitochondrial membrane. One striking exception is the cytochrome *c* of mitochondria, a soluble protein that associates through electrostatic interactions with the outer surface of the inner membrane.

In **iron-sulfur proteins**, the iron is present not in heme but in association with inorganic sulfur atoms or with the sulfur atoms of Cys residues in the protein, or both. These iron-sulfur (Fe-S) centers range from simple structures with a single Fe atom coordinated to four Cys —SH groups to more complex Fe-S centers with two or four Fe atoms **(Fig. 19–5)**. **Rieske iron-sulfur proteins** (named after their discoverer, John S. Rieske) are a variation on this theme, in which one Fe atom is coordinated to two His residues rather than two Cys residues. All iron-sulfur proteins participate in one-electron transfers in which one iron atom of the iron-sulfur cluster is oxidized or reduced. At least eight Fe-S proteins function in mitochondrial electron transfer. The reduction potential

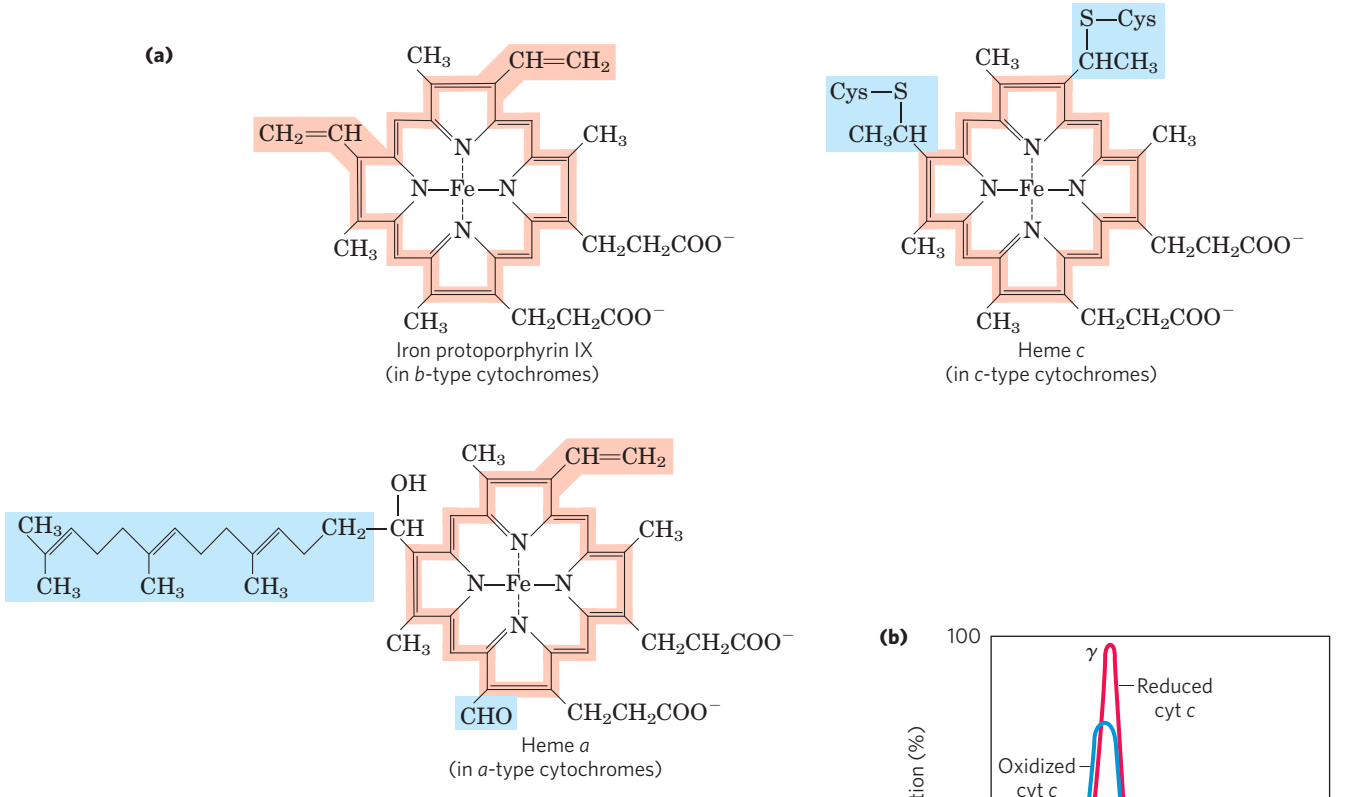

FIGURE 19–4 Prosthetic groups of cytochromes. (a) Each group consists of four five-membered, nitrogen-containing rings in a cyclic structure called a porphyrin. The four nitrogen atoms are coordinated with a central Fe ion, either Fe^{2+} or Fe^{3+}. Iron protoporphyrin IX is found in *b*-type cytochromes and in hemoglobin and myoglobin (see Fig. 4–17). Heme *c* is covalently bound to the protein of cytochrome *c* through thioether bonds to two Cys residues. Heme *a*, found in *a*-type cytochromes, has a long isoprenoid tail attached to one of the five-membered rings. The conjugated double-bond system (shaded light red) of the porphyrin ring has delocalized π electrons that are relatively easily excited by photons with the wavelengths of visible light, which accounts for the strong absorption by hemes (and related compounds) in the visible region of the spectrum. **(b)** Absorption spectra of cytochrome *c* (cyt *c*) in its oxidized (blue) and reduced (red) forms. The characteristic α, β, and γ bands of the reduced form are labeled.

of Fe-S proteins varies from −0.65 V to +0.45 V, depending on the microenvironment of the iron within the protein.

In the overall reaction catalyzed by the mitochondrial respiratory chain, electrons move from NADH, succinate, or some other primary electron donor through flavoproteins, ubiquinone, iron-sulfur proteins, and cytochromes, and finally to O_2. A look at the methods used to determine the sequence in which the carriers act is instructive, as the same general approaches have been used to study other electron-transfer chains, such as those of chloroplasts.

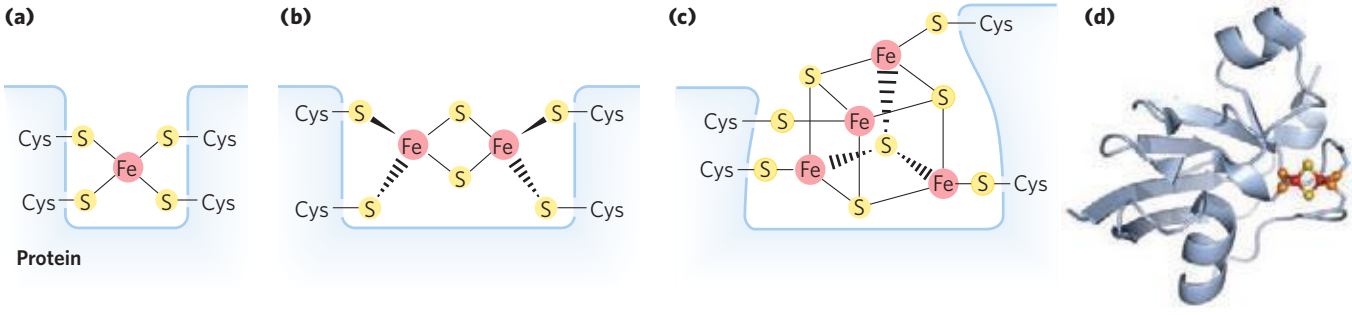

FIGURE 19–5 Iron-sulfur centers. The Fe-S centers of iron-sulfur proteins may be as simple as **(a)**, with a single Fe ion surrounded by the S atoms of four Cys residues. Other centers include both inorganic and Cys S atoms, as in **(b)** 2Fe-2S or **(c)** 4Fe-4S centers. **(d)** The ferredoxin of the cyanobacterium *Anabaena* 7120 has one 2Fe-2S center (PDB ID 1FRD); Fe is red, inorganic S is yellow, and the S of Cys is orange. (Note that in these designations only the inorganic S atoms are counted. For example, in the 2Fe-2S center (b), each Fe ion is actually surrounded by four S atoms.) The exact standard reduction potential of the iron in these centers depends on the type of center and its interaction with the associated protein.

TABLE 19–2 Standard Reduction Potentials of Respiratory Chain and Related Electron Carriers

Redox reaction (half-reaction)	$E'°$ (V)
$2H^+ + 2e^- \longrightarrow H_2$	−0.414
$NAD^+ + H^+ + 2e^- \longrightarrow NADH$	−0.320
$NADP^+ + H^+ + 2e^- \longrightarrow NADPH$	−0.324
NADH dehydrogenase (FMN) + $2H^+ + 2e^- \longrightarrow$ NADH dehydrogenase ($FMNH_2$)	−0.30
Ubiquinone + $2H^+ + 2e^- \longrightarrow$ ubiquinol	0.045
Cytochrome b (Fe^{3+}) + $e^- \longrightarrow$ cytochrome b (Fe^{2+})	0.077
Cytochrome c_1 (Fe^{3+}) + $e^- \longrightarrow$ cytochrome c_1 (Fe^{2+})	0.22
Cytochrome c (Fe^{3+}) + $e^- \longrightarrow$ cytochrome c (Fe^{2+})	0.254
Cytochrome a (Fe^{3+}) + $e^- \longrightarrow$ cytochrome a (Fe^{2+})	0.29
Cytochrome a_3 (Fe^{3+}) + $e^- \longrightarrow$ cytochrome a_3 (Fe^{2+})	0.35
$\frac{1}{2}O_2 + 2H^+ + 2e^- \longrightarrow H_2O$	0.8166

First, the standard reduction potentials of the individual electron carriers have been determined experimentally (Table 19–2). We would expect the carriers to function in order of increasing reduction potential, because electrons tend to flow spontaneously from carriers of lower $E'°$ to carriers of higher $E'°$. The order of carriers deduced by this method is NADH → Q → cytochrome b → cytochrome c_1 → cytochrome c → cytochrome a → cytochrome a_3 → O_2. Note, however, that the order of standard reduction potentials is not necessarily the same as the order of *actual* reduction potentials under cellular conditions, which depend on the concentration of reduced and oxidized forms (see Eqn 13–5, p. 531). A second method for determining the sequence of electron carriers involves reducing the entire chain of carriers experimentally by providing an electron source but no electron acceptor (no O_2). When O_2 is suddenly introduced into the system, the rate at which each electron carrier becomes oxidized (measured spectroscopically) reveals the order in which the carriers function. The carrier nearest O_2 (at the end of the chain) gives up its electrons first, the second carrier from the end is oxidized next, and so on. Such experiments have confirmed the sequence deduced from standard reduction potentials.

In a final confirmation, agents that inhibit the flow of electrons through the chain have been used in combination with measurements of the degree of oxidation of each carrier. In the presence of O_2 and an electron donor, carriers that function before the inhibited step become fully reduced, and those that function after this step are completely oxidized **(Fig. 19–6)**. By using several inhibitors that block different steps in the chain, investigators have determined the entire sequence; it is the same as deduced in the first two approaches.

Electron Carriers Function in Multienzyme Complexes

The electron carriers of the respiratory chain are organized into membrane-embedded supramolecular complexes that can be physically separated. Gentle treatment of the inner mitochondrial membrane with detergents allows the resolution of four unique electron-carrier complexes, each capable of catalyzing

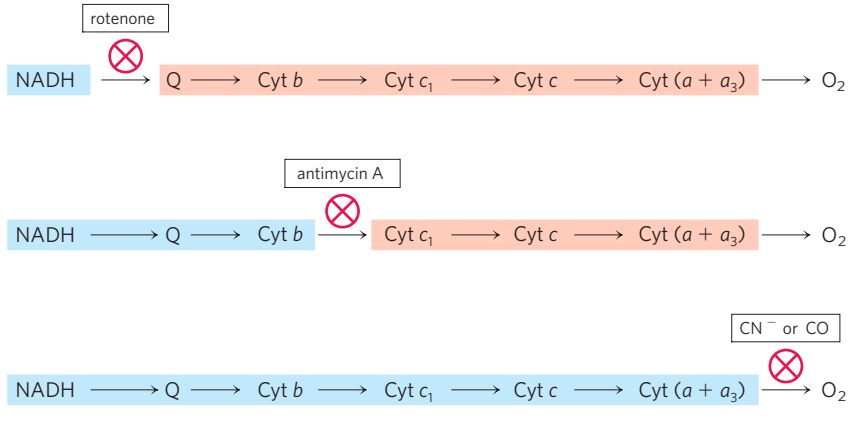

FIGURE 19–6 Method for determining the sequence of electron carriers. This method measures the effects of inhibitors of electron transfer on the oxidation state of each carrier. In the presence of an electron donor and O_2, each inhibitor causes a characteristic pattern of oxidized/reduced carriers: those before the block become reduced (blue), and those after the block become oxidized (light red).

TABLE 19–3 The Protein Components of the Mitochondrial Electron-Transfer Chain

Enzyme complex/protein	Mass (kDa)	Number of subunits*	Prosthetic group(s)
I NADH dehydrogenase	850	43 (14)	FMN, Fe-S
II Succinate dehydrogenase	140	4	FAD, Fe-S
III Ubiquinone:cytochrome *c* oxidoreductase	250	11	Hemes, Fe-S
Cytochrome *c*†	13	1	Heme
IV Cytochrome oxidase	160	13 (3–4)	Hemes; Cu_A, Cu_B

*Number of subunits in the bacterial equivalents in parentheses.

†Cytochrome *c* is not part of an enzyme complex; it moves between Complexes III and IV as a freely soluble protein.

electron transfer through a portion of the chain (Table 19–3; **Fig. 19–7**). Complexes I and II catalyze electron transfer to ubiquinone from two different electron donors: NADH (Complex I) and succinate (Complex II). Complex III carries electrons from reduced ubiquinone to cytochrome *c*, and Complex IV completes the sequence by transferring electrons from cytochrome *c* to O_2.

We now look in more detail at the structure and function of each complex of the mitochondrial respiratory chain.

Complex I: NADH to Ubiquinone **Figure 19–8** illustrates the relationship between Complexes I and II, and the enzymes of fatty acid β-oxidation, and ubiquinone. **Complex I**, also called **NADH:ubiquinone oxidoreductase** or **NADH dehydrogenase**, is a large enzyme composed of 42 different polypeptide chains, including an FMN-containing flavoprotein and at least six iron-sulfur centers. Complex I is L-shaped, with one arm of the L in the membrane and the other extending into the matrix. As shown in **Figure 19–9**, Complex I catalyzes two simultaneous and obligately coupled processes: (1) the exergonic transfer to ubiquinone of a hydride ion from NADH and a proton from the matrix, expressed by

$$NADH + H^+ + Q \longrightarrow NAD^+ + QH_2 \quad (19–1)$$

and (2) the endergonic transfer of four protons from the matrix to the intermembrane space. Complex I is therefore a proton pump driven by the energy of electron transfer, and the reaction it catalyzes is **vectorial**: it moves protons in a specific direction from one location (the matrix, which becomes negatively charged with the departure of protons) to another (the intermembrane space, which becomes positively charged). To emphasize the vectorial nature of the process, the overall reaction is often written with subscripts that indicate the location of the protons: P for the positive side of the inner membrane (the intermembrane space), N for the negative side (the matrix):

$$NADH + 5H^+_N + Q \longrightarrow NAD^+ + QH_2 + 4H^+_P \quad (19–2)$$

Amytal (a barbiturate drug), rotenone (a plant product commonly used as an insecticide), and piericidin A (an antibiotic) inhibit electron flow from the Fe-S centers of Complex I to ubiquinone (Table 19–4) and therefore block the overall process of oxidative phosphorylation.

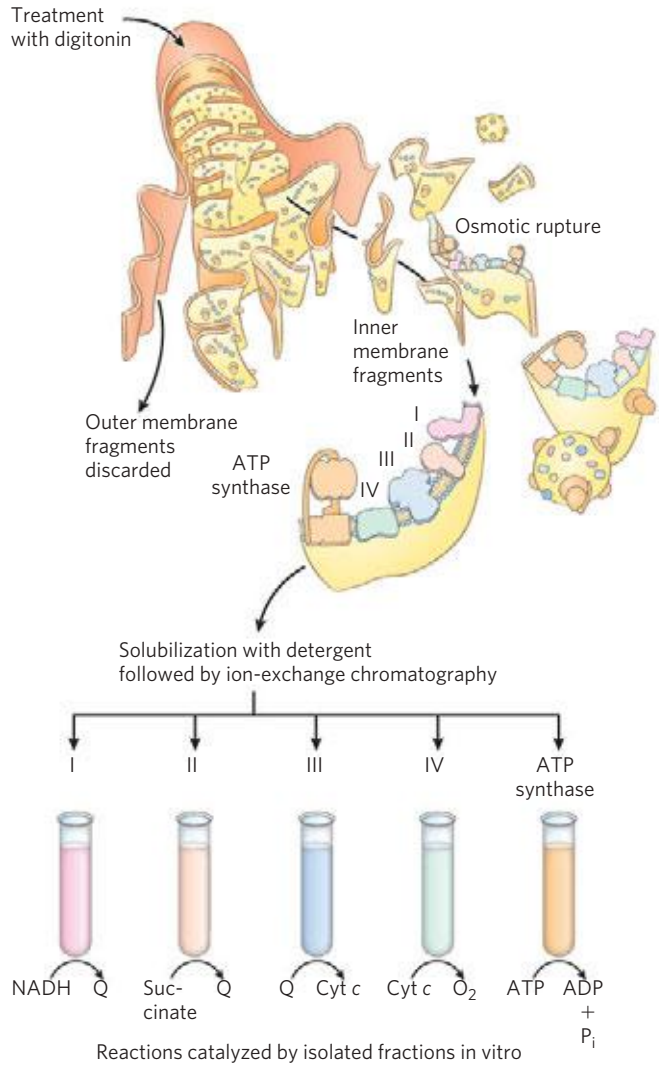

FIGURE 19–7 Separation of functional complexes of the respiratory chain. The outer mitochondrial membrane is first removed by treatment with the detergent digitonin. Fragments of inner membrane are then obtained by osmotic rupture of the mitochondria, and the fragments are gently dissolved in a second detergent. The resulting mixture of inner membrane proteins is resolved by ion-exchange chromatography into different complexes (I through IV) of the respiratory chain, each with its unique protein composition (see Table 19–3), and the enzyme ATP synthase (sometimes called Complex V). The isolated Complexes I through IV catalyze transfers between donors (NADH and succinate), intermediate carriers (Q and cytochrome *c*), and O_2, as shown. In vitro, isolated ATP synthase has only ATP-hydrolyzing (ATPase), not ATP-synthesizing, activity.

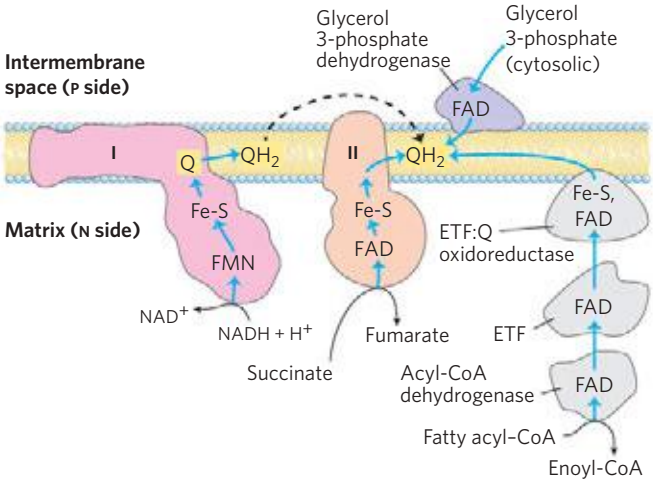

FIGURE 19–8 Path of electrons from NADH, succinate, fatty acyl-CoA, and glycerol 3-phosphate to ubiquinone. Ubiquinone (Q) is the point of entry for electrons derived from reactions in the cytosol, from fatty acid oxidation, and from succinate oxidation (in the citric acid cycle). Electrons from NADH pass through a flavoprotein with the cofactor FMN to a series of Fe-S centers (in Complex I) and then to Q. Electrons from succinate pass through a flavoprotein with the cofactor FAD and several Fe-S centers (in Complex II) on the way to Q. Glycerol 3-phosphate donates electrons to a flavoprotein (glycerol 3-phosphate dehydrogenase) on the outer face of the inner mitochondrial membrane, from which they pass to Q. Acyl-CoA dehydrogenase (the first enzyme of β oxidation) transfers electrons to electron-transferring flavoprotein (ETF), from which they pass to Q via ETF : ubiquinone oxidoreductase.

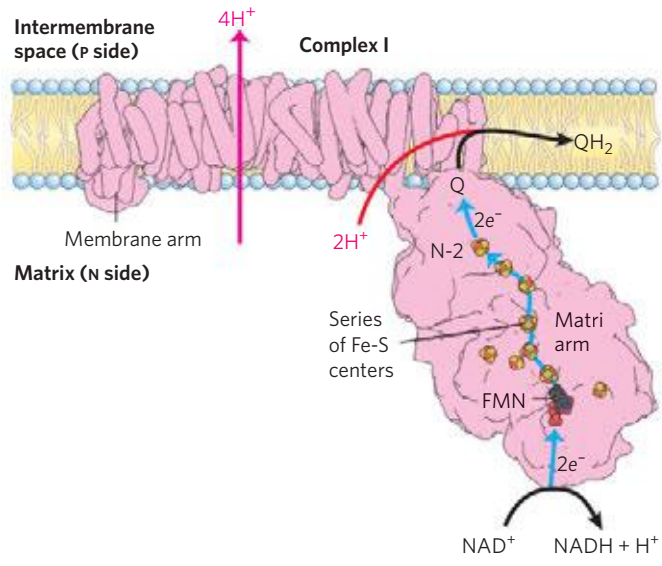

FIGURE 19–9 NADH : ubiquinone oxidoreductase (Complex I). (PDB ID 3M9S) Complex I (the crystal structure from the bacterium *Thermus thermophilus* is shown) catalyzes the transfer of a hydride ion from NADH to FMN, from which two electrons pass through a series of Fe-S centers to the Fe-S center N-2 in the matrix arm of the complex. Electron transfer from N-2 to ubiquinone on the membrane arm forms QH_2, which diffuses into the lipid bilayer. This electron transfer also drives the expulsion from the matrix of four protons per pair of electrons. The detailed mechanism that couples electron and proton transfer in Complex I is not yet known, but probably involves a Q cycle similar to that in Complex III in which QH_2 participates twice per electron pair (see Fig. 19–12). Proton flux produces an electrochemical potential across the inner mitochondrial membrane (N side negative, P side positive).

TABLE 19–4 Agents That Interfere with Oxidative Phosphorylation or Photophosphorylation

Type of interference	Compound*	Target/mode of action
Inhibition of electron transfer	Cyanide, Carbon monoxide	Inhibit cytochrome oxidase
	Antimycin A	Blocks electron transfer from cytochrome *b* to cytochrome c_1
	Myxothiazol, Rotenone, Amytal, Piericidin A	Prevent electron transfer from Fe-S center to ubiquinone
	DCMU	Competes with Q_B for binding site in PSII
Inhibition of ATP synthase	Aurovertin	Inhibits F_1
	Oligomycin, Venturicidin	Inhibits F_o and CF_o
	DCCD	Blocks proton flow through F_o and CF_o
Uncoupling of phosphorylation from electron transfer	FCCP, DNP	Hydrophobic proton carriers
	Valinomycin	K^+ ionophore
	Thermogenin	In brown adipose tissue, forms proton-conducting pores in inner mitochondrial membrane
Inhibition of ATP-ADP exchange	Atractyloside	Inhibits adenine nucleotide translocase

*DCMU is 3-(3,4-dichlorophenyl)-1,1-dimethylurea; DCCD, dicyclohexylcarbodiimide; FCCP, cyanide-*p*-trifluoromethoxyphenylhydrazone; DNP, 2,4-dinitrophenol.

Complex II: Succinate to Ubiquinone We encountered **Complex II** in Chapter 16 as **succinate dehydrogenase**, the only membrane-bound enzyme in the citric acid cycle (p. 646). Although smaller and simpler than Complex I, it contains five prosthetic groups of two types and four different protein subunits **(Fig. 19–10)**. Subunits C and D are integral membrane proteins, each with three transmembrane helices. They contain a heme group, heme *b*, and a binding site for ubiquinone, the final electron acceptor in the reaction catalyzed by Complex II. Subunits A and B extend into the matrix; they contain three 2Fe-2S centers, bound FAD, and a binding site for the substrate, succinate. The path of electron transfer from the succinate-binding site to FAD, then through the Fe-S centers to the Q-binding site, is more than 40 Å long, but none of the individual electron-transfer distances exceeds about 11 Å—a reasonable distance for rapid electron transfer (Fig. 19–10).

The heme *b* of Complex II is apparently not in the direct path of electron transfer; it may serve instead to reduce the frequency with which electrons "leak" out of the system, moving from succinate to molecular oxygen to produce the **reactive oxygen species (ROS)** hydrogen peroxide (H_2O_2) and the **superoxide radical** ($^{\bullet}O_2^-$), as described below. Humans with point mutations in Complex II subunits near heme *b* or the quinone-binding site suffer from hereditary paraganglioma. This inherited condition is characterized by benign tumors of the head and neck, commonly in the carotid body, an organ that senses O_2 levels in the blood. These mutations result in greater production of ROS and perhaps greater tissue damage during succinate oxidation. ■

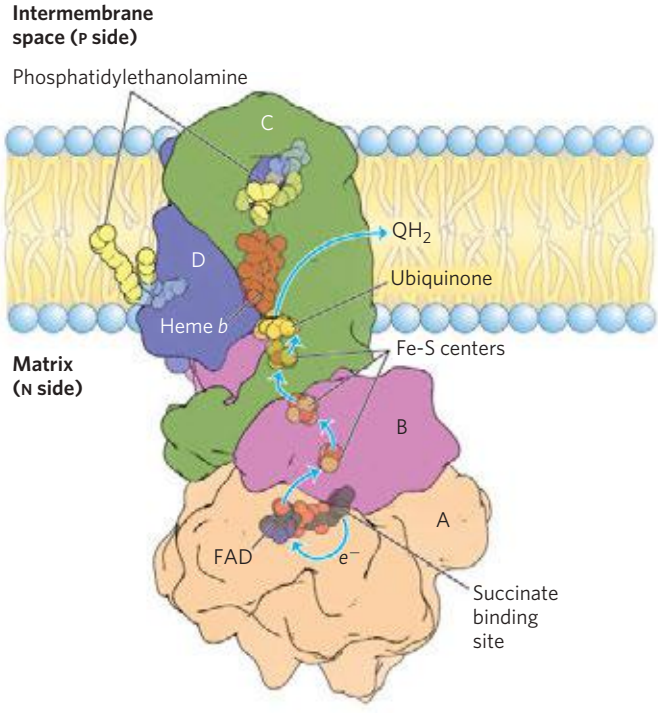

FIGURE 19–10 Structure of Complex II (succinate dehydrogenase). (PDB ID 1ZOY) This complex (shown here is the porcine heart enzyme) has two transmembrane subunits, C and D; the cytoplasmic extensions contain subunits A and B. Just behind the FAD in subunit A is the binding site for succinate. Subunit B has three Fe-S centers, ubiquinone is bound to subunit B, and heme *b* is sandwiched between subunits C and D. Two phosphatidylethanolamine molecules are so tightly bound to subunit D that they show up in the crystal structure. Electrons move (blue arrows) from succinate to FAD, then through the three Fe-S centers to ubiquinone. The heme *b* is not on the main path of electron transfer but protects against the formation of reactive oxygen species (ROS) by electrons that go astray.

Other substrates for mitochondrial dehydrogenases pass electrons into the respiratory chain at the level of ubiquinone, but not through Complex II. The first step in the β oxidation of fatty acyl–CoA, catalyzed by the flavoprotein **acyl-CoA dehydrogenase** (see Fig. 17–8), involves transfer of electrons from the substrate to the FAD of the dehydrogenase, then to electron-transferring flavoprotein (ETF), which in turn passes its electrons to **ETF : ubiquinone oxidoreductase** (Fig. 19–8). This enzyme transfers electrons into the respiratory chain by reducing ubiquinone. Glycerol 3-phosphate, formed either from glycerol released by triacylglycerol breakdown or by the reduction of dihydroxyacetone phosphate from glycolysis, is oxidized by **glycerol 3-phosphate dehydrogenase** (see Fig. 17–4). This enzyme is a flavoprotein located on the outer face of the inner mitochondrial membrane, and like succinate dehydrogenase and acyl-CoA dehydrogenase, it channels electrons into the respiratory chain by reducing ubiquinone (Fig. 19–8). The important role of glycerol 3-phosphate dehydrogenase in shuttling reducing equivalents from cytosolic NADH into the mitochondrial matrix is described in Section 19.2 (see Fig. 19–32). The effect of each of these electron-transferring enzymes is to contribute to the pool of reduced ubiquinone. QH_2 from all these reactions is reoxidized by Complex III.

Complex III: Ubiquinone to Cytochrome *c* The next respiratory complex, **Complex III**, also called **cytochrome bc_1 complex** or **ubiquinone : cytochrome *c* oxidoreductase**, couples the transfer of electrons from ubiquinol (QH_2) to cytochrome *c* with the vectorial transport of protons from the matrix to the intermembrane space. The determinations of the complete structure of this huge complex **(Fig. 19–11)** and of Complex IV (below) by x-ray crystallography, achieved between 1995 and 1998, were landmarks in the study of mitochondrial electron transfer, providing the structural framework to integrate the many biochemical observations on the functions of the respiratory complexes.

The functional unit of Complex III is a dimer, with the two monomeric units of cytochrome *b* surrounding a "cavern" in the middle of the membrane, in which ubiquinone is free to move from the matrix side of the membrane (site Q_N on one monomer) to the intermembrane space (site Q_P of the other monomer) as it shuttles electrons and protons across the inner mitochondrial membrane (Fig. 19–11b).

Based on the structure of Complex III and detailed biochemical studies of the redox reactions, a reasonable

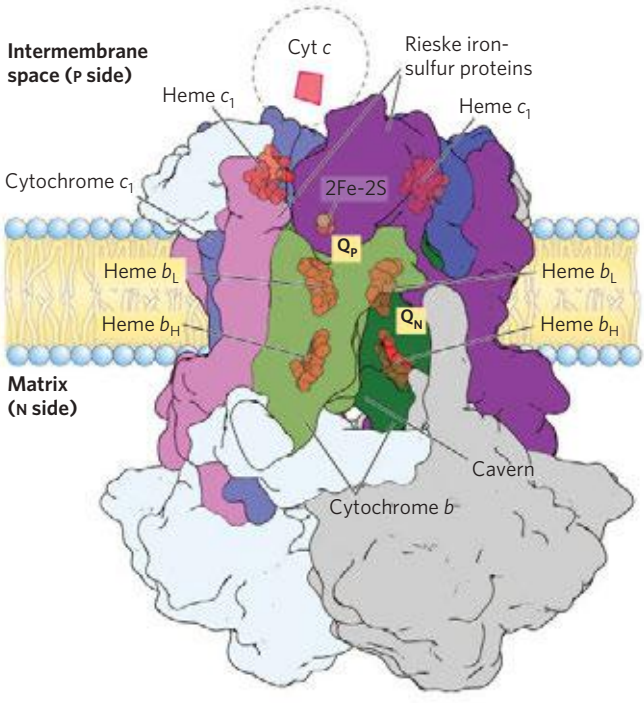

FIGURE 19–11 Cytochrome bc_1 complex (Complex III). (PDB ID 1BGY) The complex is a dimer of identical monomers, each with 11 different subunits. The functional core of each monomer is three subunits: cytochrome *b* (green) with its two hemes (b_H and b_L), the Rieske iron-sulfur protein (purple) with its 2Fe-2S centers, and cytochrome c_1 (blue) with its heme. This cartoon view of the complex shows how cytochrome c_1 and the Rieske iron-sulfur protein project from the P surface and can interact with cytochrome *c* (not part of the functional complex) in the intermembrane space. The complex has two distinct binding sites for ubiquinone, Q_N and Q_P, which correspond to the sites of inhibition by two drugs that block oxidative phosphorylation. Antimycin A, which blocks electron flow from heme b_H to Q, binds at Q_N, close to heme b_H on the N (matrix) side of the membrane. Myxothiazol, which prevents electron flow from QH_2 to the Rieske iron-sulfur protein, binds at Q_P, near the 2Fe-2S center and heme b_L on the P side. The dimeric structure is essential to the function of Complex III. The interface between monomers forms two caverns, each containing a Q_P site from one monomer and a Q_N site from the other. The ubiquinone intermediates move within these sheltered caverns.

Complex III crystallizes in two distinct conformations (not shown). In one, the Rieske Fe-S center is close to its electron acceptor, the heme of cytochrome c_1, but relatively distant from cytochrome *b* and the QH_2-binding site at which the Rieske Fe-S center receives electrons. In the other, the Fe-S center has moved away from cytochrome c_1 and toward cytochrome *b*. The Rieske protein is thought to oscillate between these two conformations as it is first reduced, then oxidized.

model, the **Q cycle**, has been proposed for the passage of electrons and protons through the complex. The net equation for the redox reactions of the Q cycle **(Fig. 19–12)** is

$$QH_2 + 2 \text{ cyt } c_1 \text{ (oxidized)} + 2H^+_N \longrightarrow Q + 2 \text{ cyt } c_1 \text{ (reduced)} + 4H^+_P \quad (19\text{–}3)$$

The Q cycle accommodates the switch between the two-electron carrier ubiquinol (the reduced form of ubiquinone) and the one-electron carriers—hemes b_L and b_H of cytochrome *b* and cytochromes c_1 and *c*—and results in the uptake of two protons on the N side, and the release of four protons on the P side per pair of electrons passing through Complex III to cytochrome *c*. Two of the protons released on the P side are electrogenic; the other two are electroneutral, balanced by the two charges (electrons) passed to cytochrome *c* on the P side. Although the path of electrons through this segment of the respiratory chain is complicated, the net effect of the transfer is simple: QH_2 is

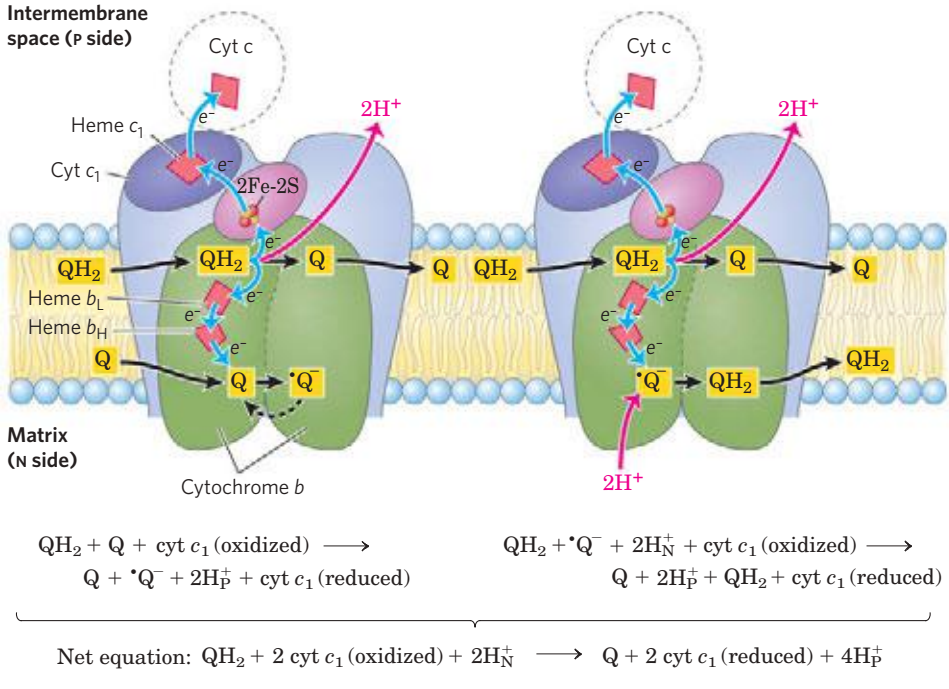

FIGURE 19–12 The Q cycle, shown in two stages. The path of electrons through Complex III is shown by blue arrows. The movement of various forms of ubiquinone is shown with black arrows. In the first stage (left), Q on the N side is reduced to the semiquinone radical, which moves back into position to accept another electron. In the second stage (right), the semiquinone radical is converted to QH_2. Meanwhile, on the P side of the membrane, two molecules of QH_2 are oxidized to Q, releasing two protons per Q molecule (four protons in all) into the intermembrane space. Each QH_2 donates one electron (via the Rieske Fe-S center) to cytochrome c_1, and one electron (via cytochrome *b*) to a molecule of Q near the N side, reducing it in two steps to QH_2. This reduction also consumes two protons per Q, which are taken up from the matrix (N side). Reduced cyt c_1 passes electrons one at a time to cyt *c*, which dissociates and carries electrons to Complex IV.

oxidized to Q, two molecules of cytochrome *c* are reduced, and protons are moved from the P side to the N side.

Cytochrome *c* is a soluble protein of the intermembrane space. After its single heme accepts an electron from Complex III, cytochrome *c* moves to Complex IV to donate the electron to a binuclear copper center.

Complex IV: Cytochrome *c* to O_2 In the final step of the respiratory chain, **Complex IV**, also called **cytochrome oxidase**, carries electrons from cytochrome *c* to molecular oxygen, reducing it to H_2O. Complex IV is a large enzyme (13 subunits; M_r 204,000) of the inner mitochondrial membrane. Bacteria contain a form that is much simpler, with only three or four subunits, but still capable of catalyzing both electron transfer and proton pumping. Comparison of the mitochondrial and bacterial complexes suggests that three subunits are critical to the function **(Fig. 19–13)**.

Mitochondrial subunit II contains two Cu ions complexed with the —SH groups of two Cys residues in a binuclear center (Cu_A; Fig. 19–13b) that resembles the 2Fe-2S centers of iron-sulfur proteins. Subunit I contains two heme groups, designated *a* and a_3, and another copper ion (Cu_B). Heme a_3 and Cu_B form a second binuclear center that accepts electrons from heme *a* and transfers them to O_2 bound to heme a_3.

Electron transfer through Complex IV is from cytochrome *c* to the Cu_A center, to heme *a*, to the heme a_3–Cu_B center, and finally to O_2 **(Fig. 19–14)**. For every four electrons passing through this complex, the enzyme consumes four "substrate" H^+ from the matrix (N side) in converting O_2 to $2H_2O$. It also uses the energy of this redox reaction to pump one proton outward into the intermembrane space (P side) for each electron that passes through, adding to the electrochemical potential

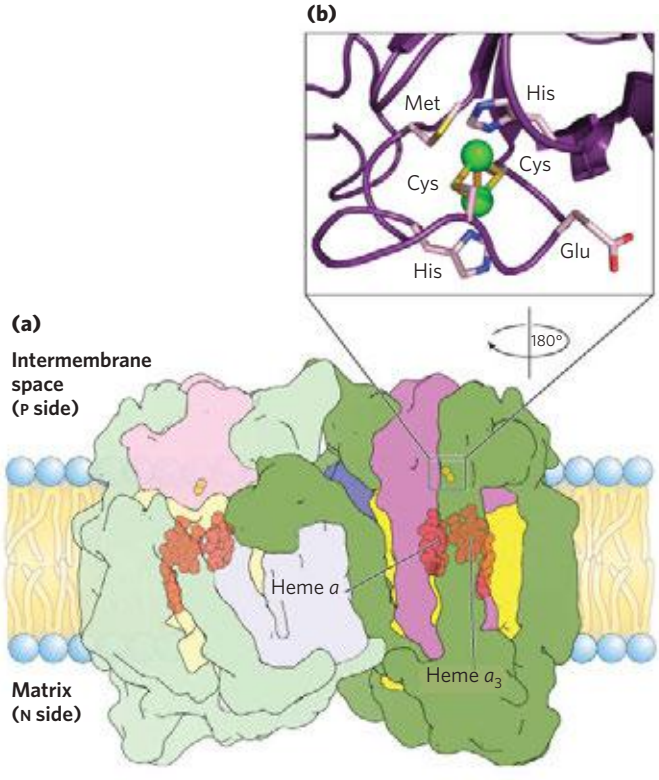

FIGURE 19–13 Structure of cytochrome oxidase (Complex IV). This complex from bovine mitochondria has 13 subunits, but only four core proteins are shown here (PDB ID 1OCC). **(a)** Complex IV, with four subunits in each of two identical units of a dimer. Subunit I (yellow) has two heme groups, *a* and a_3, near a single copper ion, Cu_B (not visible here). Heme a_3 and Cu_B form a binuclear Fe-Cu center. Subunit II (purple) contains two Cu ions complexed with the —SH groups of two Cys residues in a binuclear center, Cu_A, that resembles the 2Fe-2S centers of iron-sulfur proteins. This binuclear center and the cytochrome *c*–binding site are located in a domain of subunit II that protrudes from the P side of the inner membrane (into the intermembrane space). Subunit III (blue) is essential for rapid proton movement through subunit II. The role of subunit IV (green) is not yet known. **(b)** The binuclear center of Cu_A. The Cu ions (green spheres) share electrons equally. When the center is reduced, the ions have the formal charges $Cu^{1+}Cu^{1+}$; when oxidized, $Cu^{1.5+}Cu^{1.5+}$. Six amino acid residues are ligands around the Cu ions: two His, two Cys, Glu, and Met.

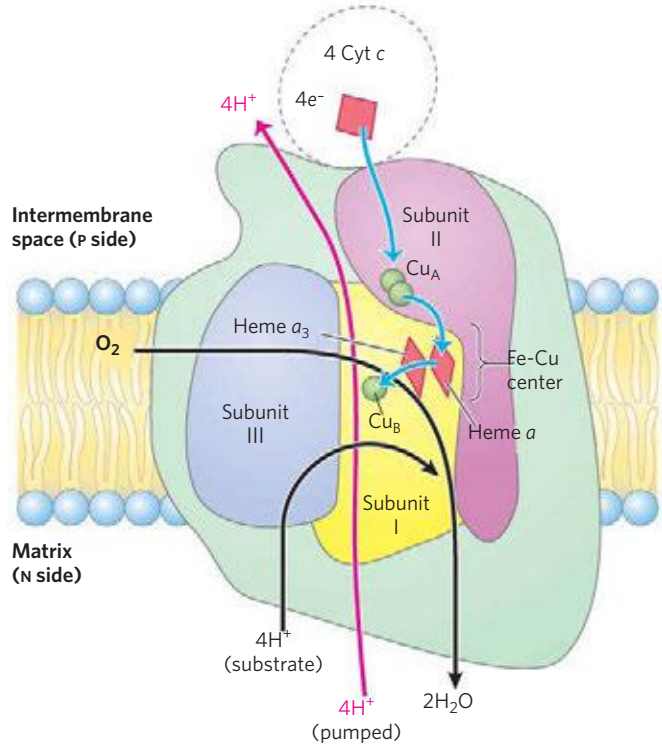

FIGURE 19–14 Path of electrons through Complex IV. The three proteins critical to electron flow are subunits I, II, and III. The larger green structure includes the other 10 proteins in the complex. Electron transfer through Complex IV begins with cytochrome *c* (top). Two molecules of reduced cytochrome *c* each donate an electron to the binuclear center Cu_A. From here electrons pass through heme *a* to the Fe-Cu center (heme a_3 and Cu_B). Oxygen now binds to heme a_3 and is reduced to its peroxy derivative (O_2^{2-}; not shown here) by two electrons from the Fe-Cu center. Delivery of two more electrons from cytochrome *c* (top, making four electrons in all) converts the O_2^{2-} to two molecules of water, with consumption of four "substrate" protons from the matrix. At the same time, four protons are pumped from the matrix by an as yet unknown mechanism.

produced by redox-driven proton transport through Complexes I and III. The overall reaction catalyzed by Complex IV is

$$4\ \text{cyt}\ c\ (\text{reduced}) + 8H^+_N + O_2 \longrightarrow 4\ \text{cyt}\ c\ (\text{oxidized}) + 4H^+_P + 2H_2O \quad (19\text{–}4)$$

This four-electron reduction of O_2 involves redox centers that carry only one electron at a time, and it must occur without the release of incompletely reduced intermediates such as hydrogen peroxide or hydroxyl free radicals—very reactive species that would damage cellular components. The intermediates remain tightly bound to the complex until completely converted to water.

Mitochondrial Complexes May Associate in Respirasomes

There is growing experimental evidence that in the intact mitochondrion, the respiratory complexes tightly associate with each other in the inner membrane to form **respirasomes**, functional combinations of two or more different electron-transfer complexes. For example, when Complex III is gently extracted from mitochondrial membranes, it is found to be associated with Complex I and remains associated during gentle electrophoresis. Supercomplexes of Complex III and IV can also be isolated, and when viewed with the electron microscope are of the right size and shape to accommodate the crystal structures of both complexes **(Fig. 19–15)**. Proteins of a family synthesized under the control of the hypoxia-inducible factor HIF are found associated with respirasomes and may be essential for their assembly or stability. HIF mediates changes in the composition of Complex IV under hypoxic conditions (see Fig. 19–34). The kinetics of electron flow through the series of respiratory complexes would be very different in the two extreme cases of tight versus no association: (1) if complexes were tightly associated, electron transfers would essentially occur through a solid state, and (2) if the complexes functioned separately, electrons would be carried between them by ubiquinone and cytochrome *c*. The kinetic evidence supports electron transfer through a solid state, and thus the respirasome model.

Cardiolipin, the lipid that is especially abundant in the inner mitochondrial membrane (see Figs 10–9 and 11–2), may be critical to the integrity of respirasomes; its removal with detergents, or its absence in certain yeast mutants, results in defective mitochondrial electron transfer and a loss of affinity between the respiratory complexes.

The Energy of Electron Transfer Is Efficiently Conserved in a Proton Gradient

The transfer of two electrons from NADH through the respiratory chain to molecular oxygen can be written as

$$NADH + H^+ + \tfrac{1}{2}O_2 \longrightarrow NAD^+ + H_2O \quad (19\text{–}5)$$

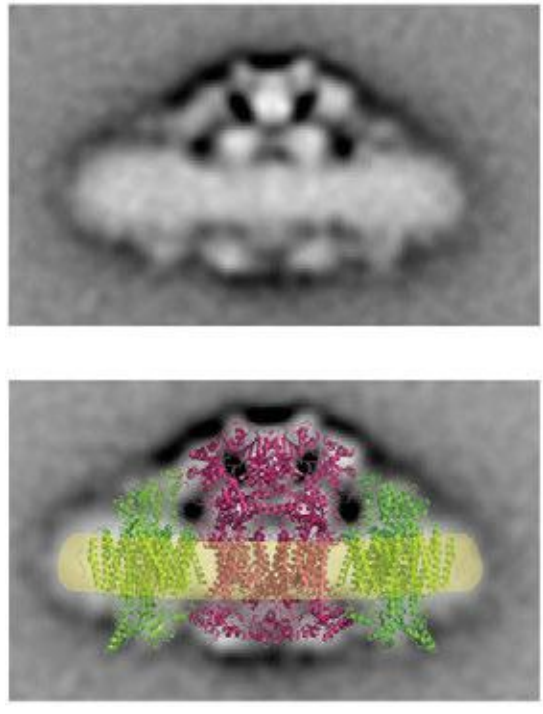

FIGURE 19–15 A putative respirasome composed of Complexes III and IV. (a) Purified supercomplexes containing Complexes III and IV, from yeast, visualized by electron microscopy after staining with uranyl acetate. The electron densities of hundreds of images were averaged to yield this composite view. **(b)** The x-ray–derived structures of one molecule of Complex III (red; from yeast) and two of Complex IV (green; from bovine heart) could be fitted to the electron-density map to suggest one possible mode of interaction of these complexes in a respirasome. This view is in the plane of the bilayer (yellow).

This net reaction is highly exergonic. For the redox pair NAD^+/NADH, E'° is −0.320 V, and for the pair O_2/H_2O, E'° is 0.816 V. The $\Delta E'^\circ$ for this reaction is therefore 1.14 V, and the standard free-energy change (see Eqn 13–7, p. 531) is

$$\begin{aligned}\Delta G'^\circ &= -n\mathcal{F}\Delta E'^\circ \\ &= -2(96.5\ \text{kJ/V·mol})(1.14\ \text{V}) \\ &= -220\ \text{kJ/mol (of NADH)}\end{aligned} \quad (19\text{–}6)$$

This *standard* free-energy change is based on the assumption of equal concentrations (1 M) of NADH and NAD^+. In actively respiring mitochondria, the actions of many dehydrogenases keep the actual [NADH]/[NAD^+] ratio well above unity, and the real free-energy change for the reaction shown in Equation 19–5 is therefore substantially greater (more negative) than −220 kJ/mol. A similar calculation for the oxidation of succinate shows that electron transfer from succinate (E'° for fumarate/succinate = 0.031 V) to O_2 has a smaller, but still negative, standard free-energy change of about −150 kJ/mol.

Much of this energy is used to pump protons out of the matrix. For each pair of electrons transferred to O_2, four protons are pumped out by Complex I, four by

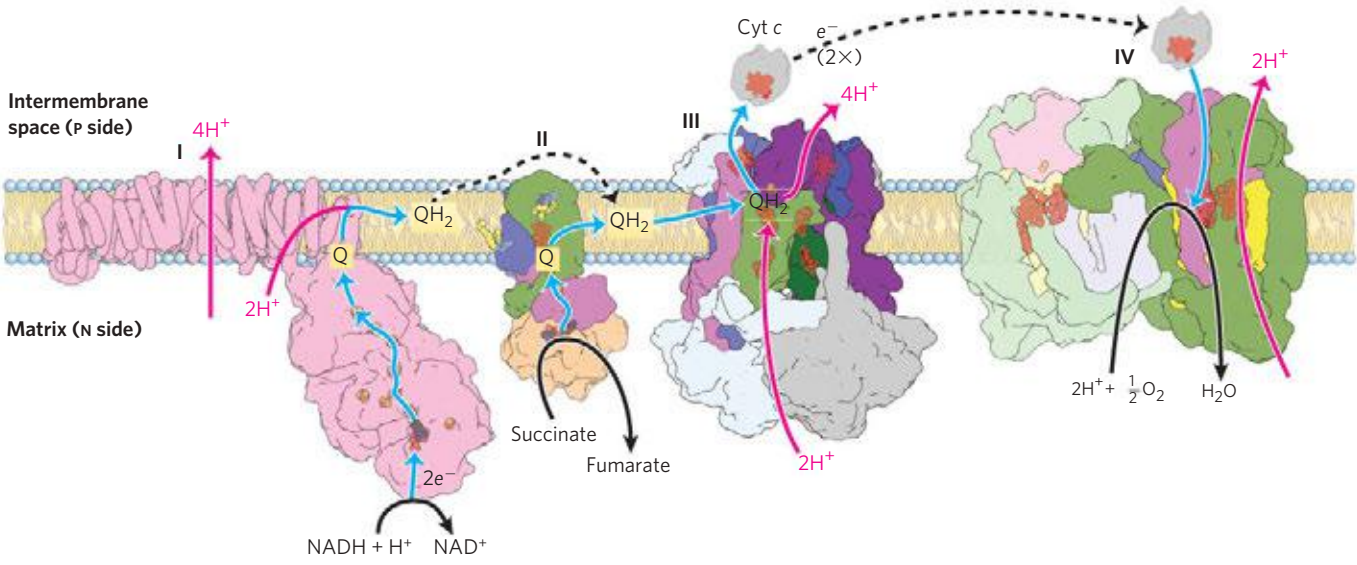

FIGURE 19–16 Summary of the flow of electrons and protons through the four complexes of the respiratory chain. Electrons reach Q through Complexes I and II. The reduced Q (QH_2) serves as a mobile carrier of electrons and protons. It passes electrons to Complex III, which passes them to another mobile connecting link, cytochrome *c*. Complex IV then transfers electrons from reduced cytochrome *c* to O_2. Electron flow through Complexes I, III, and IV is accompanied by proton flow from the matrix to the intermembrane space. Recall that electrons from β oxidation of fatty acids can also enter the respiratory chain through Q (see Fig. 19–8). The structures shown here are from several sources: Complex I, *Thermus thermophilus* (PDB ID 3M9S); Complex II, porcine heart (PDB ID 1ZOY); Complex III, bovine heart (PDB ID 1BGY); cytochrome *c*, equine heart (PDB ID 1HRC); Complex IV, bovine heart (PDB ID 1OCC).

Complex III, and two by Complex IV **(Fig. 19–16)**. The *vectorial* equation for the process is therefore

$$NADH + 11H_N^+ + \tfrac{1}{2}O_2 \longrightarrow NAD^+ + 10H_P^+ + H_2O \qquad (19–7)$$

The electrochemical energy inherent in this difference in proton concentration and separation of charge represents a temporary conservation of much of the energy of electron transfer. The energy stored in such a gradient, termed the **proton-motive force**, has two components: (1) the *chemical potential energy* due to the difference in concentration of a chemical species (H^+) in the two regions separated by the membrane, and (2) the *electrical potential energy* that results from the separation of charge when a proton moves across the membrane without a counterion **(Fig. 19–17)**.

As we showed in Chapter 11, the free-energy change for the creation of an electrochemical gradient by an ion pump is

$$\Delta G = RT \ln (C_2/C_1) + Z\mathcal{F}\Delta\psi \qquad (19–8)$$

where C_2 and C_1 are the concentrations of an ion in two regions, and $C_2 > C_1$; Z is the absolute value of its electrical charge (1 for a proton); and $\Delta\psi$ is the transmembrane difference in electrical potential, measured in volts.

For protons at 25 °C,

$$\ln (C_2/C_1) = 2.3(\log [H^+]_P - \log [H^+]_N)$$
$$= 2.3(pH_N - pH_P) = 2.3\ \Delta pH$$

and Equation 19–8 reduces to

$$\Delta G = 2.3RT\ \Delta pH + \mathcal{F}\Delta\psi \qquad (19–9)$$
$$= (5.70\ kJ/mol)\Delta pH + (96.5\ kJ/V\cdot mol)\Delta\psi$$

In actively respiring mitochondria, the measured $\Delta\psi$ is 0.15 to 0.20 V and the pH of the matrix is about 0.75 unit more alkaline than that of the intermembrane space.

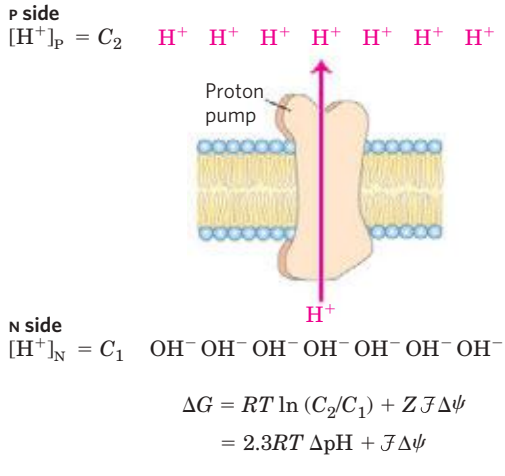

FIGURE 19–17 Proton-motive force. The inner mitochondrial membrane separates two compartments of different $[H^+]$, resulting in differences in chemical concentration (ΔpH) and charge distribution ($\Delta\psi$) across the membrane. The net effect is the proton-motive force (ΔG), which can be calculated as shown here. This is explained more fully in the text.

WORKED EXAMPLE 19–1 Energetics of Electron Transfer

Calculate the amount of energy conserved in the proton gradient across the inner mitochondrial membrane per pair of electrons transferred through the respiratory chain from NADH to oxygen. Assume $\Delta\psi$ is 0.15 V and the pH difference is 0.75 unit.

Solution: Equation 19–9 gives the free-energy change when *one* mole of protons moves across the inner membrane. Substituting the measured values for ΔpH (0.75 unit) and $\Delta\psi$ (0.15 V) in this equation gives $\Delta G = 19$ kJ/mol (of protons). Because the transfer of two electrons from NADH to O_2 is accompanied by the outward pumping of 10 protons (Eqn 19–7), roughly 200 kJ (of the 220 kJ released by oxidation of 1 mol of NADH) is conserved in the proton gradient.

When protons flow spontaneously *down* their electrochemical gradient, energy is made available to do work. In mitochondria, chloroplasts, and aerobic bacteria, the electrochemical energy in the proton gradient drives the synthesis of ATP from ADP and P_i. We return to the energetics and stoichiometry of ATP synthesis driven by the electrochemical potential of the proton gradient in Section 19.2.

Reactive Oxygen Species Are Generated during Oxidative Phosphorylation

Several steps in the path of oxygen reduction in mitochondria have the potential to produce highly reactive free radicals that can damage cells. The passage of electrons from QH_2 to Complex III and the passage of electrons from Complexes I and II to QH_2 involve the radical $^{\bullet}Q^{-}$ as an intermediate. The $^{\bullet}Q^{-}$ can, with a low probability, pass an electron to O_2 in the reaction

$$O_2 + e^- \longrightarrow {}^{\bullet}O_2^-$$

The superoxide free radical thus generated is highly reactive; its formation also leads to production of the even more reactive hydroxyl free radical, $^{\bullet}OH$ **(Fig. 19–18)**.

Reactive oxygen species can wreak havoc, reacting with and damaging enzymes, membrane lipids, and nucleic acids. In actively respiring mitochondria, 0.1% to as much as 4% of the O_2 used in respiration forms $^{\bullet}O_2^-$—more than enough to have lethal effects unless the free radical is quickly disposed of. Factors that slow the flow of electrons through the respiratory chain increase the formation of superoxide, perhaps by prolonging the lifetime of $^{\bullet}O_2^-$ generated in the Q cycle. The formation of ROS is favored when two conditions are met: (1) mitochondria are not making ATP (for lack of ADP or O_2) and therefore have a large proton-motive force and a high ratio of QH_2/Q, and (2) there is a high NADH/NAD^+ ratio in the matrix. In these situations, the mitochondrion is under oxidative stress—more electrons are available to enter the respiratory chain than can be immediately passed through to oxygen. When the supply of electron donors (NADH) is matched with that of electron acceptors, there is less oxidative stress, and ROS production is much reduced. Although overproduction of ROS is clearly detrimental, *low* levels of ROS may be used by the cell as a signal reflecting the insufficient supply of oxygen (hypoxia), triggering metabolic adjustments (see Fig. 19–34).

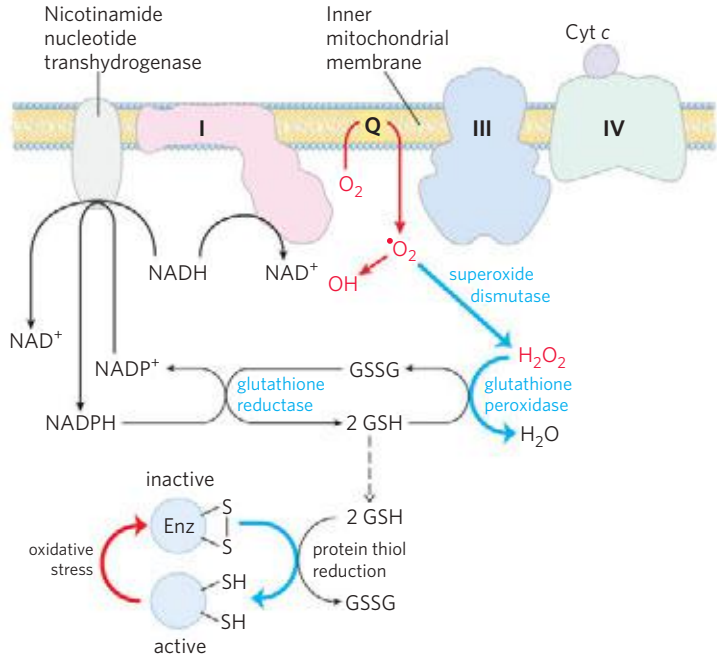

FIGURE 19–18 ROS formation in mitochondria and mitochondrial defenses. When the rate of electron entry into the respiratory chain and the rate of electron transfer through the chain are mismatched, superoxide radical ($^{\bullet}O_2^-$) production increases at Complexes I and III as the partially reduced ubiquinone radical ($^{\bullet}Q^-$) donates an electron to O_2. Superoxide acts on aconitase, a 4Fe-4S protein, to release Fe^{2+}. In the presence of Fe^{2+}, the Fenton reaction leads to formation of the highly reactive hydroxyl free radical ($^{\bullet}OH$). The reactions shown in blue defend the cell against the damaging effects of superoxide. Reduced glutathione (GSH; see Fig. 22-29) donates electrons for the reduction of H_2O_2 and of the oxidized Cys residues (—S—S—) of enzymes and other proteins, and GSH is regenerated from the oxidized form (GSSG) by reduction with NADPH.

To prevent oxidative damage by $^{\bullet}O_2^-$, cells have several forms of the enzyme **superoxide dismutase**, which catalyzes the reaction

$$2\ {}^{\bullet}O_2^- + 2H^+ \longrightarrow H_2O_2 + O_2$$

The hydrogen peroxide (H_2O_2) thus generated is rendered harmless by the action of **glutathione peroxidase** (Fig. 19–18). Glutathione reductase recycles the oxidized glutathione to its reduced form, using electrons from the NADPH generated by nicotinamide nucleotide transhydrogenase (in the mitochondrion) or by the pentose phosphate pathway (in the cytosol; see Fig. 14–21). Reduced glutathione also serves to keep protein sulfhydryl groups in their

BOX 19–1 Hot, Stinking Plants and Alternative Respiratory Pathways

Many flowering plants attract insect pollinators by releasing odorant molecules that mimic an insect's natural food sources or potential egg-laying sites. Plants pollinated by flies or beetles that normally feed on or lay their eggs in dung or carrion sometimes use foul-smelling compounds to attract these insects.

One family of stinking plants is the Araceae, which includes philodendrons, arum lilies, and skunk cabbages. These plants have tiny flowers densely packed on an erect structure, the spadix, surrounded by a modified leaf, the spathe. The spadix releases odors of rotting flesh or dung. Before pollination the spadix also heats up, in some species to as much as 20 to 40 °C above the ambient temperature. Heat production (thermogenesis) helps evaporate odorant molecules for better dispersal, and because rotting flesh and dung are usually warm from the hyperactive metabolism of scavenging microbes, the heat itself might also attract insects. In the case of the eastern skunk cabbage (Fig. 1), which flowers in late winter or early spring when snow still covers the ground, thermogenesis allows the spadix to grow up through the snow.

FIGURE 1 Eastern skunk cabbage.

How does a skunk cabbage heat its spadix? The mitochondria of plants, fungi, and unicellular eukaryotes have electron-transfer systems that are essentially the same as those in animals, but they also have an alternative respiratory pathway. A cyanide-resistant QH_2 oxidase transfers electrons from the ubiquinone pool directly to oxygen, bypassing the two proton-translocating steps of Complexes III and IV (Fig. 2). Energy that might have been conserved as ATP is instead released as heat. Plant mitochondria also have an alternative NADH dehydrogenase, insensitive to the Complex I inhibitor rotenone (see

reduced state, preventing some of the deleterious effects of oxidative stress (Fig. 19–18). Nicotinamide nucleotide transhydrogenase is critical in this process: it produces the NADPH essential for glutathione reductase activity.

Plant Mitochondria Have Alternative Mechanisms for Oxidizing NADH

Plant mitochondria supply the cell with ATP during periods of low illumination or darkness by mechanisms entirely analogous to those used by nonphotosynthetic organisms. In the light, the principal source of mitochondrial NADH is a reaction in which glycine, produced by a process known as photorespiration, is converted to serine (see Fig. 20–21):

$$2\ \text{Glycine} + NAD^+ \longrightarrow \text{serine} + CO_2 + NH_3 + NADH + H^+$$

For reasons discussed in Chapter 20, plants must carry out this reaction even when they do not need NADH for ATP production. To regenerate NAD^+ from unneeded NADH, mitochondria of plants (and of some fungi and protists) transfer electrons from NADH directly to ubiquinone and from ubiquinone directly to O_2, bypassing Complexes III and IV and their proton pumps. In this process the energy in NADH is dissipated as heat, which can sometimes be of value to the plant (Box 19–1). Unlike cytochrome oxidase (Complex IV), the alternative QH_2 oxidase is not inhibited by cyanide. Cyanide-resistant NADH oxidation is therefore the hallmark of this unique plant electron-transfer pathway.

SUMMARY 19.1 Electron-Transfer Reactions in Mitochondria

- Chemiosmotic theory provides the intellectual framework for understanding many biological energy transductions, including oxidative phosphorylation and photophosphorylation. The mechanism of energy coupling is similar in both cases: the energy of electron flow is conserved by the concomitant pumping of protons across the membrane, producing an electrochemical gradient, the proton-motive force.
- In mitochondria, hydride ions removed from substrates (such as α-ketoglutarate and malate) by NAD-linked dehydrogenases donate electrons to the respiratory (electron-transfer) chain, which transfers the electrons to molecular O_2, reducing it to H_2O.
- Reducing equivalents from NADH are passed through a series of Fe-S centers to ubiquinone,

Table 19–4), that transfers electrons from NADH in the matrix directly to ubiquinone, bypassing Complex I and its associated proton pumping. And plant mitochondria have yet another NADH dehydrogenase, on the external face of the inner membrane, that transfers electrons from NADPH or NADH in the intermembrane space to ubiquinone, again bypassing Complex I. Thus when electrons enter the alternative respiratory pathway through the rotenone-insensitive NADH dehydrogenase, the external NADH dehydrogenase, or succinate dehydrogenase (Complex II), and pass to O_2 via the cyanide-resistant alternative oxidase, energy is not conserved as ATP but is released as heat. A skunk cabbage can use the heat to melt snow, produce a foul stench, or attract beetles or flies.

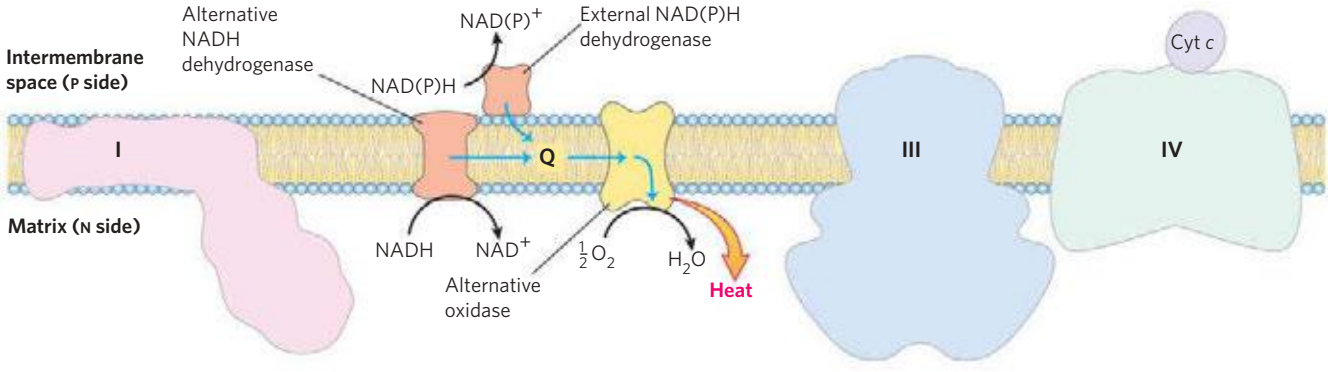

FIGURE 2 Electron carriers of the inner membrane of plant mitochondria. Electrons can flow through Complexes I, III, and IV, as in animal mitochondria, or through plant-specific alternative carriers by the paths shown with blue arrows.

which transfers the electrons to cytochrome *b*, the first carrier in Complex III. In this complex, electrons take two separate paths through two *b*-type cytochromes and cytochrome c_1 to an Fe-S center. The Fe-S center passes electrons, one at a time, through cytochrome *c* and into Complex IV, cytochrome oxidase. This copper-containing enzyme, which also contains cytochromes a and a_3, accumulates electrons, then passes them to O_2, reducing it to H_2O.

- Some electrons enter this chain of carriers through alternative paths. Succinate is oxidized by succinate dehydrogenase (Complex II), which contains a flavoprotein that passes electrons through several Fe-S centers to ubiquinone. Electrons derived from the oxidation of fatty acids pass to ubiquinone via the electron-transferring flavoprotein.
- Potentially harmful reactive oxygen species produced in mitochondria are inactivated by a set of protective enzymes, including superoxide dismutase and glutathione peroxidase.
- Plants, fungi, and unicellular eukaryotes have, in addition to the typical cyanide-sensitive path for electron transfer, an alternative, cyanide-resistant NADH oxidation pathway.

19.2 ATP Synthesis

How is a concentration gradient of protons transformed into ATP? We have seen that electron transfer releases, and the proton-motive force conserves, more than enough free energy (about 200 kJ) per "mole" of electron pairs to drive the formation of a mole of ATP, which requires about 50 kJ (p. 519). Mitochondrial oxidative phosphorylation therefore poses no thermodynamic problem. But what is the chemical mechanism that couples proton flux with phosphorylation?

The **chemiosmotic model**, proposed by Peter Mitchell, is the paradigm for this mechanism. According to the model **(Fig. 19–19)**, the electrochemical energy inherent in the difference in proton concentration and the separation of charge across the inner mitochondrial membrane—the proton-motive force—drives the synthesis of ATP as protons flow passively back into the matrix through a proton pore in **ATP synthase**. To emphasize this crucial role of the proton-motive force, the equation for ATP synthesis is sometimes written

$$\mathrm{ADP} + \mathrm{P_i} + n\mathrm{H_P^+} \longrightarrow \mathrm{ATP} + \mathrm{H_2O} + n\mathrm{H_N^+} \qquad (19\text{–}10)$$

Mitchell used "chemiosmotic" to describe enzymatic reactions that involve, simultaneously, a chemical reaction

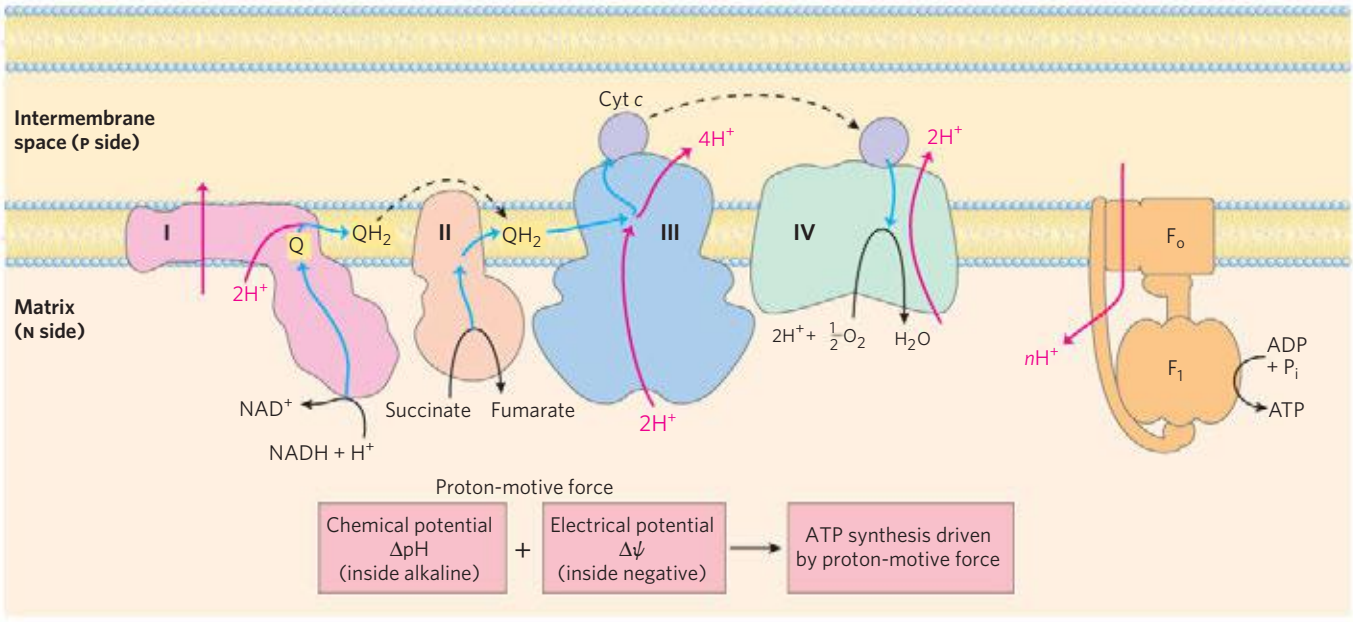

FIGURE 19–19 Chemiosmotic model. In this simple representation of the chemiosmotic theory applied to mitochondria, electrons from NADH and other oxidizable substrates pass through a chain of carriers arranged asymmetrically in the inner membrane. Electron flow is accompanied by proton transfer across the membrane, producing both a chemical gradient (ΔpH) and an electrical gradient ($\Delta\psi$) (combined, the proton-motive force). The inner mitochondrial membrane is impermeable to protons; protons can reenter the matrix only through proton-specific channels (F_o). The proton-motive force that drives protons back into the matrix provides the energy for ATP synthesis, catalyzed by the F_1 complex associated with F_o.

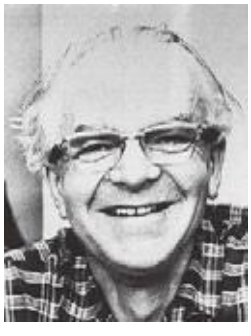

Peter Mitchell, 1920–1992

and a transport process, and the overall process is sometimes referred to as "chemiosmotic coupling." Coupling refers to the *obligate* connection between mitochondrial ATP synthesis and electron flow through the respiratory chain; neither of the two processes can proceed without the other. The operational definition of coupling is shown in **Figure 19–20**. When isolated mitochondria are suspended in a buffer containing ADP, P_i, and an oxidizable substrate such as succinate, three easily measured processes occur: (1) the substrate is oxidized (succinate yields fumarate), (2) O_2 is consumed, and (3) ATP is synthesized. Oxygen consumption and ATP synthesis depend on the presence of an oxidizable substrate (succinate in this case) as well as ADP and P_i.

Because the energy of substrate oxidation drives ATP synthesis in mitochondria, we would expect inhibitors of the passage of electrons to O_2 (such as cyanide, carbon monoxide, and antimycin A) to block ATP synthesis (Fig. 19–20a). More surprising is the finding that the converse is also true: inhibition of ATP synthesis blocks electron transfer in intact mitochondria. This obligatory coupling can be demonstrated in isolated mitochondria by providing O_2 and oxidizable substrates, but not ADP (Fig. 19–20b). Under these conditions, no ATP synthesis can occur and electron transfer to O_2 does not proceed. Henry Lardy, who pioneered the use of antibiotics to explore mitochondrial function, demonstrated coupling of oxidation and phosphorylation by using oligomycin and venturicidin, toxic antibiotics that bind to the ATP synthase in mitochondria. These compounds are potent inhibitors of both ATP synthesis *and* the transfer of electrons through the chain of carriers to O_2 (Fig. 19–20b). Because oligomycin is known to interact not directly with the electron carriers but with ATP synthase, it follows that electron transfer and ATP synthesis are obligately coupled: neither reaction occurs without the other.

Henry Lardy, 1917–2010

Chemiosmotic theory readily explains the dependence of electron transfer on ATP synthesis in mitochondria. When the flow of protons into the matrix through the proton channel of ATP synthase is blocked (with oligomycin, for example), no path exists for the return of protons to the matrix, and the continued extrusion of protons driven by the activity of the respiratory chain generates a large proton gradient. The proton-motive force builds up until the cost (free energy) of pumping protons out of the matrix against this gradient equals or exceeds the energy released by the transfer of electrons from

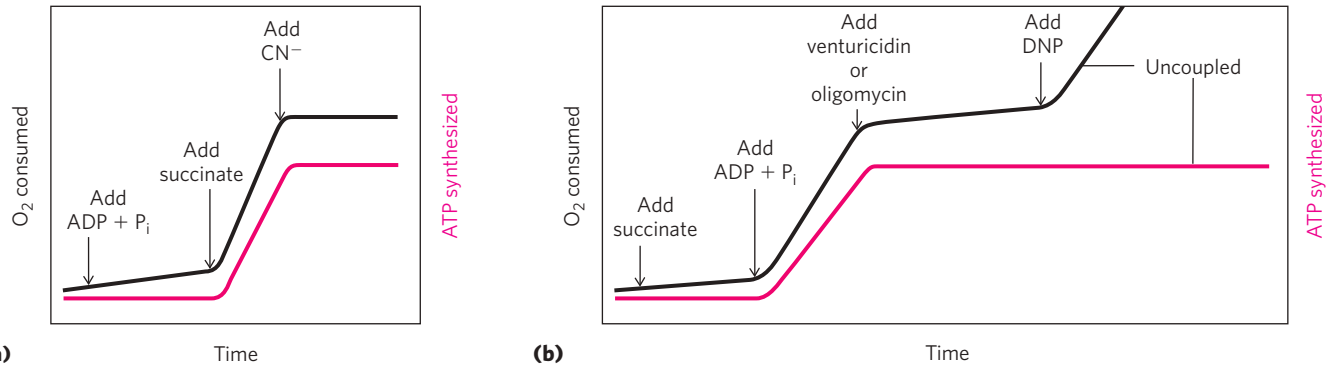

FIGURE 19–20 Coupling of electron transfer and ATP synthesis in mitochondria. In experiments to demonstrate coupling, mitochondria are suspended in a buffered medium and an O_2 electrode monitors O_2 consumption. At intervals, samples are removed and assayed for the presence of ATP. **(a)** Addition of ADP and P_i alone results in little or no increase in either respiration (O_2 consumption; black) or ATP synthesis (red). When succinate is added, respiration begins immediately and ATP is synthesized. Addition of cyanide (CN^-), which blocks electron transfer between cytochrome oxidase (Complex IV) and O_2, inhibits both respiration and ATP synthesis. **(b)** Mitochondria provided with succinate respire and synthesize ATP only when ADP and P_i are added. Subsequent addition of venturicidin or oligomycin, inhibitors of ATP synthase, blocks both ATP synthesis and respiration. Dinitrophenol (DNP) is an uncoupler, allowing respiration to continue without ATP synthesis.

NADH to O_2. At this point electron flow must stop; the free energy for the overall process of electron flow coupled to proton pumping becomes zero, and the system is at equilibrium.

Certain conditions and reagents, however, can uncouple oxidation from phosphorylation. When intact mitochondria are disrupted by treatment with detergent or by physical shear, the resulting membrane fragments can still catalyze electron transfer from succinate or NADH to O_2, but no ATP synthesis is coupled to this respiration. Certain chemical compounds cause uncoupling without disrupting mitochondrial structure. Chemical uncouplers include 2,4-dinitrophenol (DNP) and carbonylcyanide-*p*-trifluoromethoxyphenylhydrazone (FCCP) (Table 19–4; **Fig. 19–21**), weak acids with hydrophobic properties that permit them to diffuse readily across mitochondrial membranes. After entering the matrix in the protonated form, they can release a proton, thus dissipating the proton gradient. Resonance stabilization delocalizes the charge on the anionic forms, making them sufficiently permeant to diffuse back across the membrane, where they can pick up a proton and repeat the process. Ionophores such as valinomycin (see Fig. 11–44) allow inorganic ions to pass easily through membranes. Ionophores uncouple electron transfer from oxidative phosphorylation by dissipating the electrical contribution to the electrochemical gradient across the mitochondrial membrane.

A prediction of the chemiosmotic theory is that, because the role of electron transfer in mitochondrial ATP synthesis is simply to pump protons to create the electrochemical potential of the proton-motive force, an artificially created proton gradient should be able to replace electron transfer in driving ATP synthesis. This has been experimentally confirmed

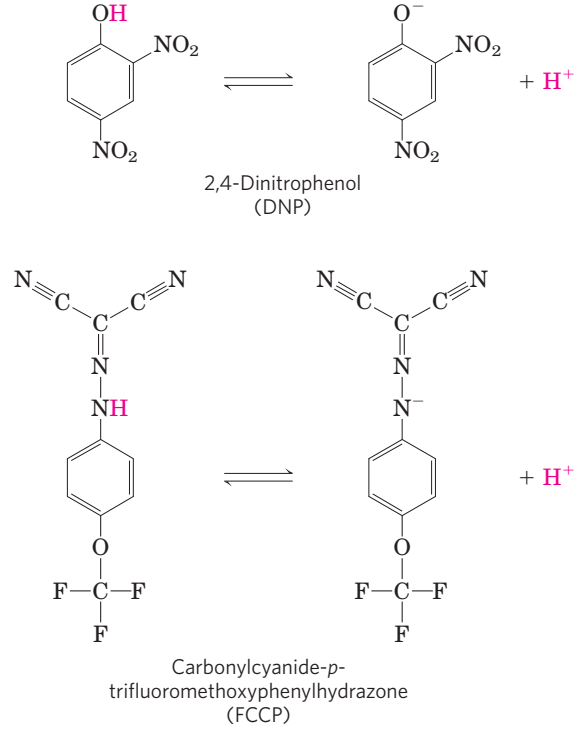

FIGURE 19–21 Two chemical uncouplers of oxidative phosphorylation. Both DNP and FCCP have a dissociable proton and are very hydrophobic. They carry protons across the inner mitochondrial membrane, dissipating the proton gradient. Both also uncouple photophosphorylation (see Fig. 19–65).

(Fig. 19–22). Mitochondria manipulated so as to impose a difference of proton concentration and a separation of charge across the inner membrane synthesize ATP *in the absence of an oxidizable substrate*; the proton-motive force alone suffices to drive ATP synthesis.

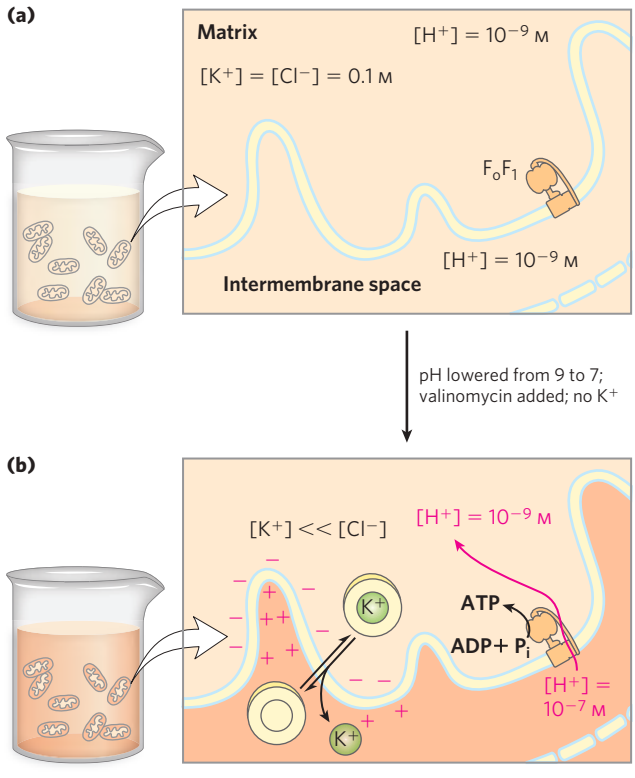

FIGURE 19–22 Evidence for the role of a proton gradient in ATP synthesis. An artificially imposed electrochemical gradient can drive ATP synthesis in the absence of an oxidizable substrate as electron donor. In this two-step experiment, **(a)** isolated mitochondria are first incubated in a pH 9 buffer containing 0.1 M KCl. Slow leakage of buffer and KCl into the mitochondria eventually brings the matrix into equilibrium with the surrounding medium. No oxidizable substrates are present. **(b)** Mitochondria are now separated from the pH 9 buffer and resuspended in pH 7 buffer containing valinomycin but no KCl. The change in buffer creates a difference of two pH units across the inner mitochondrial membrane. The outward flow of K^+, carried (by valinomycin) down its concentration gradient without a counter-ion, creates a charge imbalance across the membrane (matrix negative). The sum of the chemical potential provided by the pH difference and the electrical potential provided by the separation of charges is a proton-motive force large enough to support ATP synthesis in the absence of an oxidizable substrate.

ATP Synthase Has Two Functional Domains, F_o and F_1

Mitochondrial ATP synthase is an F-type ATPase (see Fig. 11–39) similar in structure and mechanism to the ATP synthases of chloroplasts and bacteria. This large enzyme complex of the inner mitochondrial membrane catalyzes the formation of ATP from ADP and P_i, driven by the flow of protons from the P to the N side of the membrane (Eqn 19–10). ATP synthase, also called Complex V, has two distinct components: F_1, a peripheral membrane protein, and F_o (*o* denoting oligomycin-sensitive), which is integral to the membrane. F_1, the first factor recognized as essential for oxidative phosphorylation, was identified and purified by Efraim Racker and his colleagues in the early 1960s.


Efraim Racker, 1913–1991

In the laboratory, small membrane vesicles formed from inner mitochondrial membranes carry out ATP synthesis coupled to electron transfer. When F_1 is gently extracted, the "stripped" vesicles still contain intact respiratory chains and the F_o portion of ATP synthase. The vesicles can catalyze electron transfer from NADH to O_2 but cannot produce a proton gradient: F_o has a proton pore through which protons leak as fast as they are pumped by electron transfer, and without a proton gradient the F_1-depleted vesicles cannot make ATP. Isolated F_1 catalyzes ATP hydrolysis (the reversal of synthesis) and was therefore originally called **F_1 ATPase**. When purified F_1 is added back to the depleted vesicles, it reassociates with F_o, plugging its proton pore and restoring the membrane's capacity to couple electron transfer and ATP synthesis.

ATP Is Stabilized Relative to ADP on the Surface of F_1

Isotope exchange experiments with purified F_1 reveal a remarkable fact about the enzyme's catalytic mechanism: on the enzyme surface, the reaction ADP + P_i $\rightleftharpoons$ ATP + H_2O is readily reversible—the free-energy change for ATP synthesis is close to zero! When ATP is hydrolyzed by F_1 in the presence of ^{18}O-labeled water, the P_i released contains an ^{18}O atom. Careful measurement of the ^{18}O content of P_i formed in vitro by F_1-catalyzed hydrolysis of ATP reveals that the P_i has not one, but three or four ^{18}O atoms **(Fig. 19–23)**. This indicates that the terminal pyrophosphate bond in ATP is cleaved and re-formed repeatedly before P_i leaves the enzyme surface. With P_i free to tumble in its binding site, each hydrolysis inserts ^{18}O randomly at one of the four positions in the molecule. This exchange reaction occurs in unenergized F_oF_1 complexes (with no proton gradient) and with isolated F_1—the exchange does not require the input of energy.

Kinetic studies of the initial rates of ATP synthesis and hydrolysis confirm the conclusion that $\Delta G'^\circ$ for ATP synthesis on the enzyme is near zero. From the measured rates of hydrolysis ($k_1 = 10\ s^{-1}$) and synthesis ($k_{-1} = 24\ s^{-1}$), the calculated equilibrium constant for the reaction

$$\text{Enz-ATP} \rightleftharpoons \text{Enz-(ADP + } P_i\text{)}$$

is

$$K'_{eq} = \frac{k_{-1}}{k_1} = \frac{24\ s^{-1}}{10\ s^{-1}} = 2.4$$

From this K'_{eq}, the calculated apparent $\Delta G'^\circ$ is close to zero. This is much different from the K'_{eq} of about 10^5 ($\Delta G'^\circ = -30.5$ kJ/mol) for the hydrolysis of ATP free in solution (not on the enzyme surface).

What accounts for the huge difference? ATP synthase stabilizes ATP relative to ADP + P_i by binding

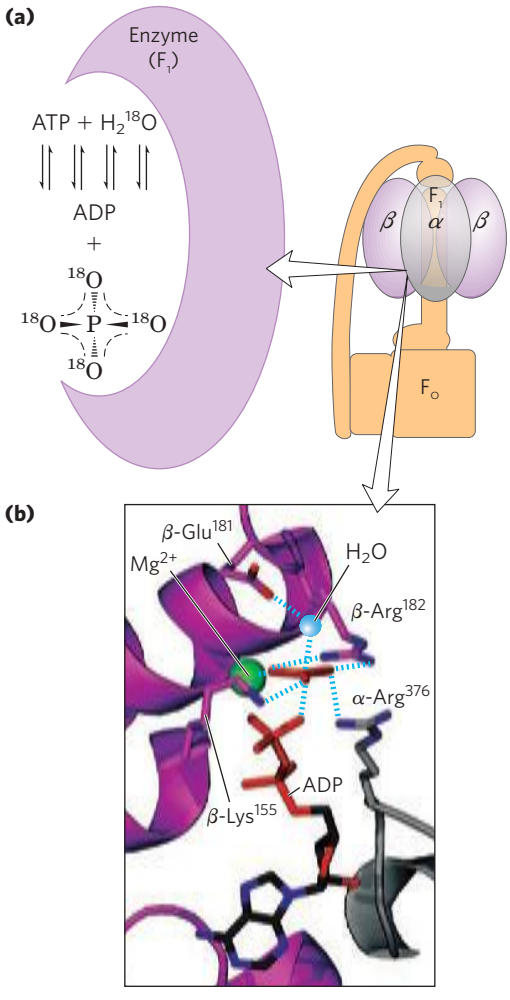

FIGURE 19–23 Catalytic mechanism of F_1. (a) ^{18}O-exchange experiment. F_1 solubilized from mitochondrial membranes is incubated with ATP in the presence of ^{18}O-labeled water. At intervals, a sample of the solution is withdrawn and analyzed for the incorporation of ^{18}O into the P_i produced from ATP hydrolysis. In minutes, the P_i contains three or four ^{18}O atoms, indicating that both ATP hydrolysis and ATP synthesis have occurred several times during the incubation. **(b)** The likely transition state complex for ATP hydrolysis and synthesis by ATP synthase (derived from PDB ID 1BMF). The α subunit is shown in gray, β in purple. The positively charged residues β-Arg^{182} and α-Arg^{376} coordinate two oxygens of the pentavalent phosphate intermediate; β-Lys^{155} interacts with a third oxygen, and the Mg^{2+} ion further stabilizes the intermediate. The blue sphere represents the leaving group (H_2O). These interactions result in the ready equilibration of ATP and ADP + P_i in the active site.

ATP more tightly, releasing enough energy to counterbalance the cost of making ATP. Careful measurements of the binding constants show that F_oF_1 binds ATP with very high affinity ($K_d \leq 10^{-12}$ M) and ADP with much lower affinity ($K_d \approx 10^{-5}$ M). The difference in K_d corresponds to a difference of about 40 kJ/mol in binding energy, and this binding energy drives the equilibrium toward formation of the product ATP.

The Proton Gradient Drives the Release of ATP from the Enzyme Surface

Although ATP synthase equilibrates ATP with ADP + P_i, in the absence of a proton gradient the newly synthesized ATP does not leave the surface of the enzyme. It is the proton gradient that causes the enzyme to release the ATP formed on its surface. The reaction coordinate diagram of the process **(Fig. 19–24)** illustrates the difference between the mechanism of ATP synthase and that of many other enzymes that catalyze endergonic reactions.

For the continued synthesis of ATP, the enzyme must cycle between a form that binds ATP very tightly and a form that releases ATP. Chemical and

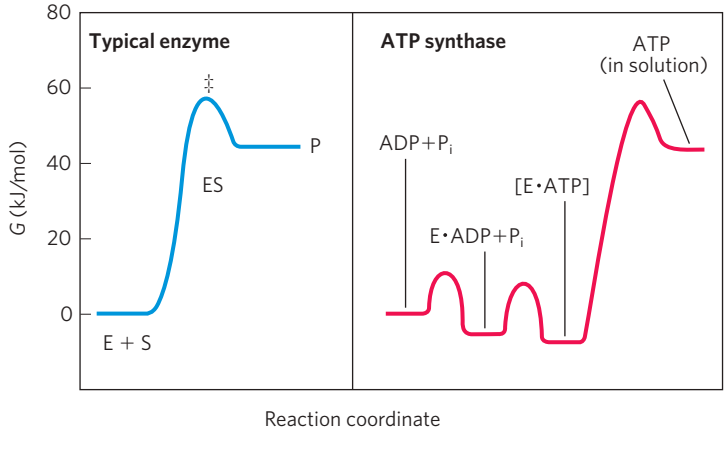

FIGURE 19–24 Reaction coordinate diagrams for ATP synthase and for a more typical enzyme. In a typical enzyme-catalyzed reaction (left), reaching the transition state (‡) between substrate and product is the major energy barrier to overcome. In the reaction catalyzed by ATP synthase (right), release of ATP from the enzyme, not formation of ATP, is the major energy barrier. The free-energy change for the formation of ATP from ADP and P_i in aqueous solution is large and positive, but on the enzyme surface, the very tight binding of ATP provides sufficient binding energy to bring the free energy of the enzyme-bound ATP close to that of ADP + P_i, so the reaction is readily reversible. The equilibrium constant is near 1. The free energy required for the release of ATP is provided by the proton-motive force.

crystallographic studies of the ATP synthase have revealed the structural basis for this alternation in function.

Each β Subunit of ATP Synthase Can Assume Three Different Conformations

Mitochondrial F_1 has nine subunits of five different types, with the composition $\alpha_3\beta_3\gamma\delta\varepsilon$. Each of the three β subunits has one catalytic site for ATP synthesis. The crystallographic determination of the F_1 structure by John E. Walker and colleagues revealed structural details very helpful in explaining the catalytic mechanism of the enzyme. The knoblike portion of F_1 is a flattened sphere, 8 nm high and 10 nm across, consisting of alternating α and β subunits arranged like the sections of an orange **(Fig. 19–25a, b, c)**. The polypeptides that make up the stalk in the F_1 crystal structure are asymmetrically arranged, with one domain of the single γ subunit making up a central shaft that passes through F_1, and another domain of γ associated primarily with one of the three β subunits, designated β-empty (Fig. 19–25b). Although the amino acid sequences of the three β subunits are identical, *their conformations differ*, in part because of the association of the γ subunit with just one of the three. The structures of the δ and ε subunits are not revealed in these crystallographic studies.

John E. Walker

The conformational differences among β subunits extend to differences in their ATP/ADP-binding sites. When researchers crystallized the protein in the presence of ADP and App(NH)p, a close structural analog of ATP that cannot be hydrolyzed by the ATPase activity of F_1, the binding site of one of the three β subunits was filled with App(NH)p, the second was filled with ADP, and the third was empty. The corresponding β subunit conformations are designated β-ATP, β-ADP, and β-empty (Fig. 19–25b). This difference in nucleotide binding among the three subunits is critical to the mechanism of the complex.

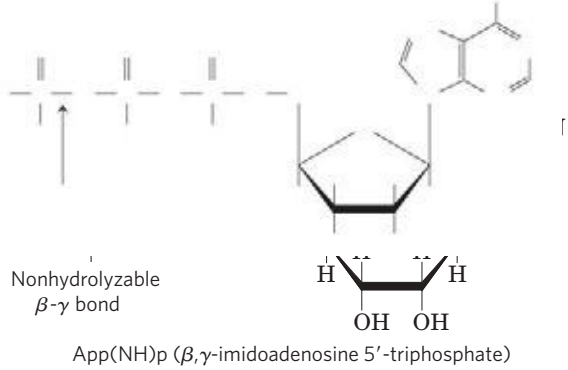

App(NH)p (β,γ-imidoadenosine 5′-triphosphate)

The F_o complex, with its proton pore, is composed of three subunits, a, b, and c, in the proportion ab_2c_n., where n ranges from 8 to 15 in various organisms; in yeast, it is 10. Subunit c is a small (M_r 8,000), very hydrophobic polypeptide, consisting almost entirely of two transmembrane helices, with a small loop extending from the matrix side of the membrane. The crystal structure of the yeast F_oF_1, solved in 1999, shows 10 c subunits, each with two transmembrane helices roughly perpendicular to the plane of the membrane and arranged in two concentric circles. The inner circle is made up of the amino-terminal helices of each c subunit; the outer circle, about 55 Å in diameter, is made up of the carboxyl-terminal helices. *The c subunits in this c ring rotate together as a unit around an axis perpendicular to the membrane*. The ε and γ subunits of F_1 form a leg-and-foot that projects from the bottom (membrane) side of F_1 and stands firmly on the ring of c subunits. The a subunit consists of several hydrophobic helices that span the membrane in close association with one of the c subunits in the c ring. The schematic drawing in Figure 19–25a combines the structural information from studies of bovine F_1, yeast F_oF_1, and the c ring of *Ilyobacter tartaricus*.

Rotational Catalysis Is Key to the Binding-Change Mechanism for ATP Synthesis

On the basis of detailed kinetic and binding studies of the reactions catalyzed by F_oF_1, Paul Boyer proposed a **rotational catalysis** mechanism in which the three active sites of F_1 take turns catalyzing ATP synthesis **(Fig. 19–26)**. A given β subunit starts in the β-ADP conformation, which binds ADP and P_i from the surrounding medium. The subunit now changes conformation, assuming the β-ATP form that tightly binds and stabilizes ATP, bringing about the ready equilibration of ADP + P_i with ATP on the enzyme surface. Finally, the subunit changes to the β-empty conformation, which has very low affinity for ATP, and the newly synthesized ATP leaves the enzyme surface. Another round of catalysis begins when this subunit again assumes the β-ADP form and binds ADP and P_i.

The conformational changes central to this mechanism are driven by the passage of protons through the F_o portion of ATP synthase. The streaming of protons through the F_o pore causes the cylinder of c subunits and the attached γ subunit to rotate about the long axis of γ, which is perpendicular to the plane of the membrane. The γ subunit passes through the center of the $\alpha_3\beta_3$ spheroid, which is held stationary relative to the

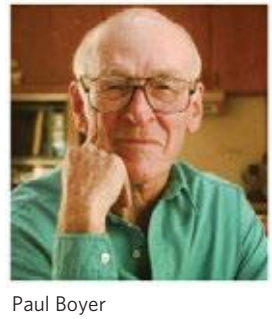

Paul Boyer

FIGURE 19–25 Mitochondrial ATP synthase complex. (a) A cartoon view of the F_oF_1 complex. **(b)** (PDB ID 1BMF and PDB ID 1JNV) F_1 viewed from above (that is, from the N side of the membrane), showing the three β (shades of purple) and three α (shades of gray) subunits and the central shaft (γ subunit, green). Each β subunit, near its interface with the neighboring α subunit, has a nucleotide-binding site critical to the catalytic activity. The single γ subunit associates primarily with one of the three $\alpha\beta$ pairs, forcing each of the three β subunits into slightly different conformations, with different nucleotide-binding sites. In the crystalline enzyme, one subunit (β-ADP) has ADP (yellow) in its binding site, the next (β-ATP) has ATP (red), and the third (β-empty) has no bound nucleotide.

(c) The entire enzyme viewed from the side (in the plane of the membrane). The F_1 portion (PDB IDs 1BMF, 1JNV, and 2A7U) has three α and three β subunits arranged like the segments of an orange around a central shaft, the γ subunit (green). (Two α subunits and one β subunit have been omitted to reveal the γ subunit and the binding sites for ATP and ADP on the β subunits.) The δ subunit confers oligomycin sensitivity on the ATP synthase, and the ε subunit may serve to inhibit its ATPase activity under some circumstances. The F_o subunit consists of one a subunit and two b subunits (PDB ID 2CLY and PDB ID 1B9U), which anchor the F_oF_1 complex in the membrane and act as a stator, holding the α and β subunits in place. F_o also includes the c ring, made up of a number (8 to 15, depending on the species) of identical c subunits, small, hydrophobic proteins. The c ring and the a subunit interact to provide a transmembrane path for protons. Each c subunit has an Asp residue near the middle of the membrane, which can bind or give up a proton. In this structure (PDB ID 1YCE), we have shown the homologous c_{11} ring of the Na^+-ATPase of *Ilyobacter tartaricus*, for which the structure is well established. The Na^+-binding sites in it, which correspond to the proton-binding sites of the F_oF_1 complex, are shown with their bound Na^+ ions (red spheres). **(d)** A view of F_o perpendicular to the membrane. Each of the c subunits in F_o has a critical Asp residue near the middle of the membrane, which undergoes protonation/deprotonation during the catalytic cycle of the ATP synthase. As in (c), red spheres represent the Na^+- or proton-binding sites in Asp residues.

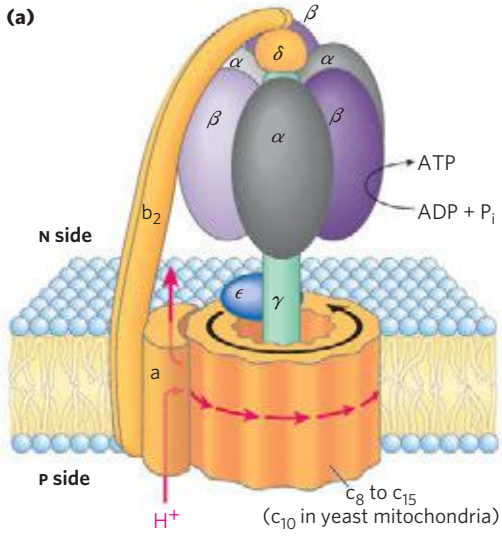

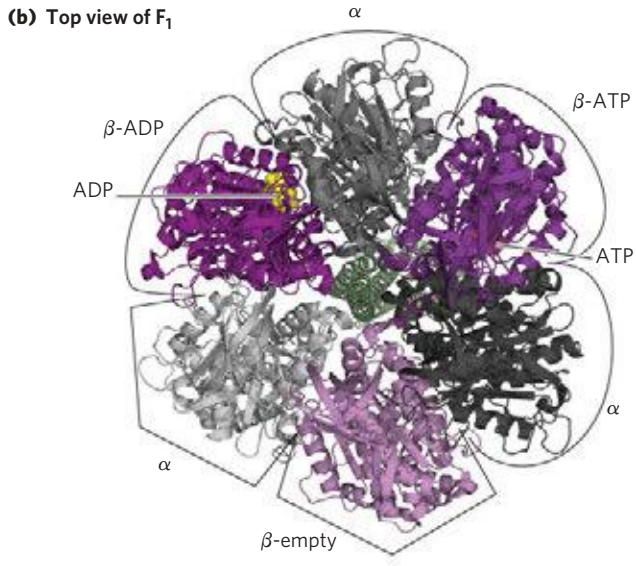

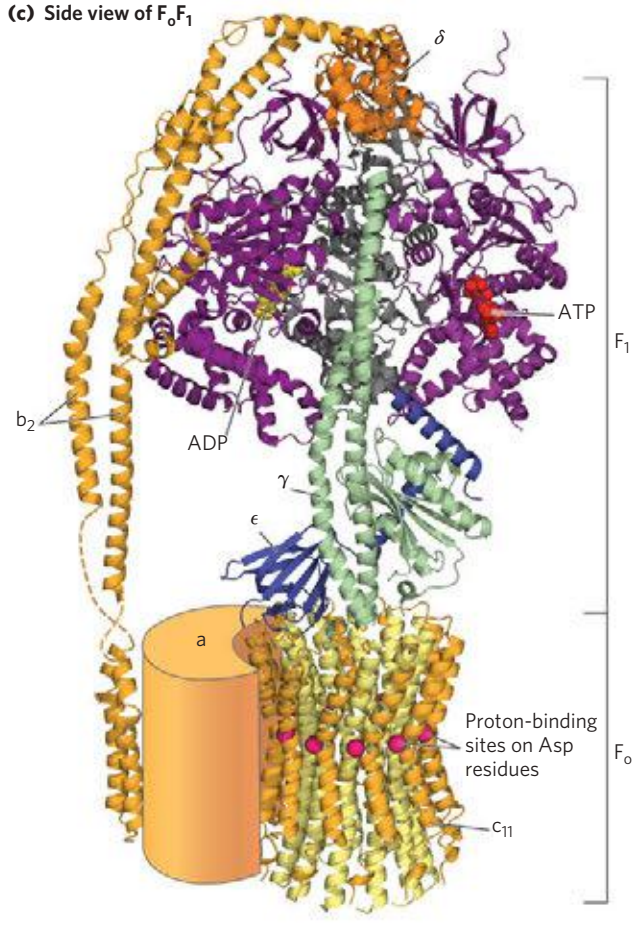

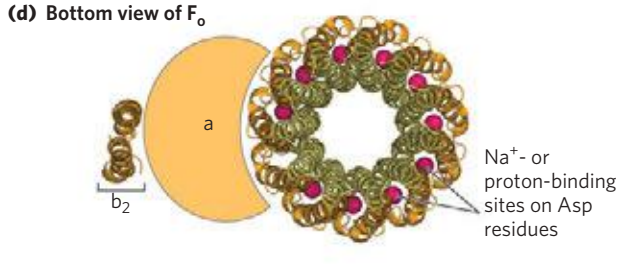

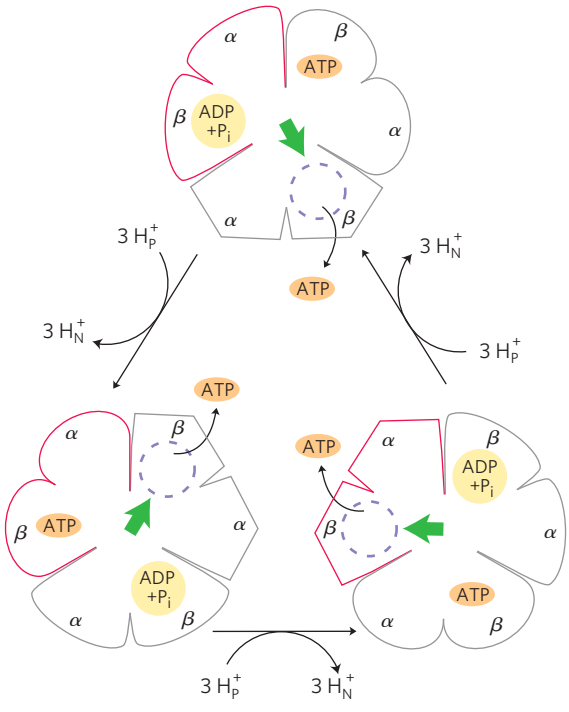

FIGURE 19–26 Binding-change model for ATP synthase. The F_1 complex has three nonequivalent adenine nucleotide–binding sites, one for each pair of α and β subunits. At any given moment, one of these sites is in the β-ATP conformation (which binds ATP tightly), a second is in the β-ADP (loose-binding) conformation, and a third is in the β-empty (very-loose-binding) conformation. The proton-motive force causes rotation of the central shaft—the γ subunit, shown as a green arrowhead—which comes into contact with each $\alpha\beta$ subunit pair in succession. This produces a cooperative conformational change in which the β-ATP site is converted to the β-empty conformation, and ATP dissociates; the β-ADP site is converted to the β-ATP conformation, which promotes condensation of bound ADP + P_i to form ATP; and the β-empty site becomes a β-ADP site, which loosely binds ADP + P_i entering from the solvent. This model, based on experimental findings, requires that at least two of the three catalytic sites alternate in activity; ATP cannot be released from one site unless and until ADP and P_i are bound at the other.

membrane surface by the b_2 and δ subunits (Fig. 19–25a). With each rotation of 120°, γ comes into contact with a different β subunit, and the contact forces that β subunit into the β-empty conformation.

The three β subunits interact in such a way that when one assumes the β-empty conformation, its neighbor to one side *must* assume the β-ADP form, and the other neighbor the β-ATP form. Thus one complete rotation of the γ subunit causes each β subunit to cycle through all three of its possible conformations, and for each rotation, three ATP are synthesized and released from the enzyme surface.

One strong prediction of this **binding-change model** is that the γ subunit should rotate in one direction when F_oF_1 is synthesizing ATP and in the opposite direction when the enzyme is hydrolyzing ATP. This prediction of rotation with ATP hydrolysis was confirmed in elegant experiments in the laboratories of Masasuke Yoshida and Kazuhiko Kinosita, Jr. The rotation of γ in a single F_1 molecule was observed microscopically by attaching a long, thin, fluorescent actin polymer to γ and watching it move relative to $\alpha_3\beta_3$ immobilized on a microscope slide as ATP was hydrolyzed. (The expected reversal of the rotation when ATP is being synthesized could not be tested in this experiment; there is no proton gradient to drive ATP synthesis.) When the entire F_oF_1 complex (not just F_1) was used in a similar experiment, the entire ring of c subunits rotated with γ **(Fig. 19–27)**. The "shaft" rotated in the predicted direction through 360°. The rotation was not smooth, but occurred in three discrete steps of 120°. As calculated from the known rate of ATP hydrolysis by one F_1 molecule and from the frictional drag on the long

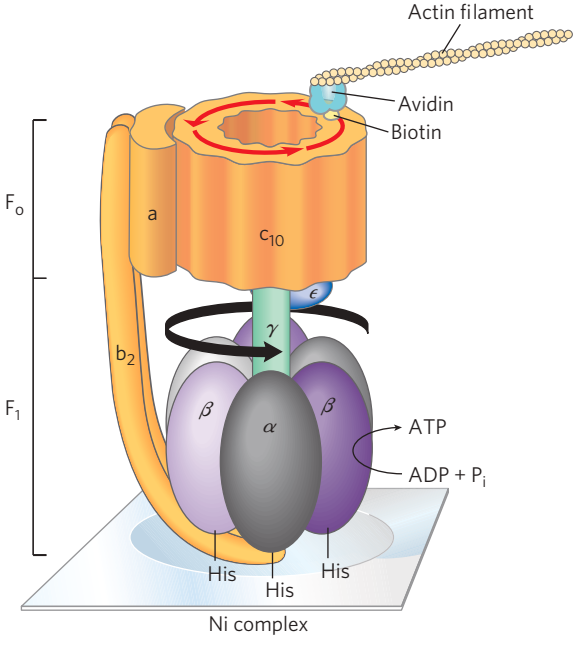

FIGURE 19–27 Experimental demonstration of rotation of F_o and γ. F_1 genetically engineered to contain a run of His residues adheres tightly to a microscope slide coated with a Ni complex; biotin is covalently attached to a c subunit of F_o. The protein avidin, which binds biotin very tightly, is covalently attached to long filaments of actin labeled with a fluorescent probe. Biotin-avidin binding now attaches the actin filaments to the c subunit. When ATP is provided as substrate for the ATPase activity of F_1, the labeled filament is seen to rotate continuously in one direction, proving that the F_o cylinder of c subunits rotates. In another experiment, a fluorescent actin filament was attached directly to the γ subunit. The series of fluorescence micrographs (read left to right) shows the position of the actin filament at intervals of 133 ms. Note that as the filament rotates, it makes a discrete jump about every eleventh frame. Presumably the cylinder and shaft move as one unit.

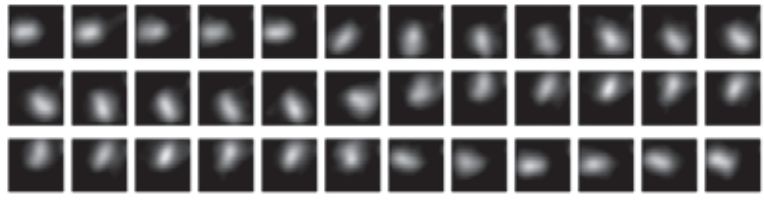

actin polymer, the efficiency of this mechanism in converting chemical energy into motion is close to 100%. It is, in Boyer's words, "a splendid molecular machine!"

How Does Proton Flow through the F_o Complex Produce Rotary Motion?

One feasible model to explain how proton flow and rotary motion are coupled in the F_o complex is shown in **Figure 19–28**. The individual subunits in F_o are arranged in a circle about a central core that is probably filled with membrane lipids. In each c subunit, there is a critical Asp (or Glu) residue located at about the middle of the membrane. Protons cross the membrane through a path made up of both a and c subunits. The a subunit has a proton half-channel leading from the cytosol (P side) to the middle of the membrane, where it ends near the Asp residue of the adjoining c subunit. A proton diffuses from the cytosolic side (where the proton concentration is relatively high) down this half-channel and binds to the Asp residue, displacing a positively charged Arg residue that had been associated with the Asp. This Arg residue swings aside, forming an interaction with the Asp on the adjacent c subunit in the ring and displacing the proton from that Asp; this adjacent proton exits through the second half-channel to the N side, where the proton concentration is relatively low, completing the movement of one proton equivalent from outside to inside the matrix. Now another proton has entered the half-channel on the cytosolic side, moved to the Asp of the next c subunit, and protonated it, again displacing Arg, which in turn displaces a proton from the next c subunit, and so forth. The rotary movement of the c ring is the result of thermal (Brownian) motion, made unidirectional by the large difference in proton concentration across the membrane. The number of protons that must be transferred to produce one complete rotation of the c ring is equal to the number of c subunits in the ring. Studies of the c ring with atomic force microscopy (Box 19–2) or x-ray diffraction have shown that the number of c subunits is different in different organisms **(Fig. 19–29)**. In animal mitochondria this number is 8, in yeast mitochondria and in *E. coli* it is 10, and the number of c subunits can range as high as 15 in the cyanobacterium *Spirulina platensis*. The rate of rotation in intact mitochondria has been estimated at about 6,000 rpm—100 rotations per second!

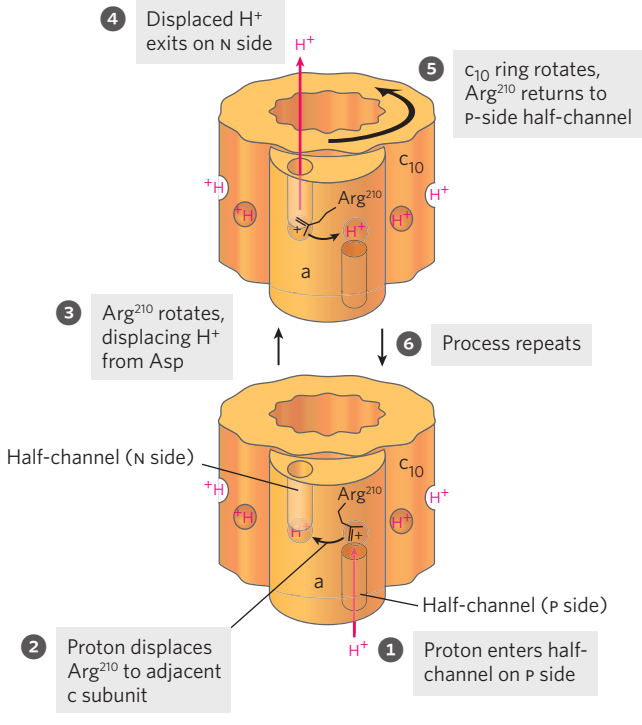

FIGURE 19–28 A model for proton-driven rotation of the c ring. The a subunit of the F_o complex of the ATP synthase (see Fig. 19-25a) has two hydrophilic half-channels for protons, one leading from the P side to the middle of the membrane, and another leading from the middle of the membrane to the N side (matrix). The individual c subunits in F_o (10 in the yeast enzyme) are arranged in a circle about a central core. Each c subunit has a critical Asp residue about midway across the membrane, which can donate or accept a proton (red H^+). The a subunit has a positively charged Arg side chain that forms an electrostatic interaction with the negatively charged carboxylate of Asp on the adjoining c subunit. This c subunit is initially positioned so that a proton that enters the half-channel on the P side (where the proton concentration is relatively high) encounters and protonates the Asp residue, weakening its interaction with Arg. The Arg side chain rotates toward the protonated Asp residue in the next c subunit, and displaces its carboxyl proton, as a new electrostatic Arg-Asp interaction forms. The displaced proton moves through the second half-channel in subunit a and is released on the N side. The c subunit with its unprotonated Asp residue moves so that its Arg-Asp pair faces the half-channel on the P side, and a second cycle begins: proton entry, protonation of Asp, Arg movement, and proton exit. Rotation of the ring occurs by thermal (Brownian) motion and is effectively ratcheted; the orientation of the proton gradient dictates the direction of proton flow and makes the rotation of the c ring essentially unidirectional.

Chemiosmotic Coupling Allows Nonintegral Stoichiometries of O_2 Consumption and ATP Synthesis

Before the general acceptance of the chemiosmotic model for oxidative phosphorylation, the assumption was that the overall reaction equation would take the following form:

$$x\text{ADP} + x\text{P}_i + \tfrac{1}{2}\text{O}_2 + \text{H}^+ + \text{NADH} \longrightarrow x\text{ATP} + \text{H}_2\text{O} + \text{NAD}^+ \qquad (19\text{–}11)$$

with the value of x—sometimes called the **P/O ratio** or the **P/2e^- ratio**—always an integer. When intact mitochondria are suspended in solution with an oxidizable substrate such as succinate or NADH and are provided with O_2, ATP synthesis is readily measurable, as is the decrease in O_2. In principle, these two measurements should yield the number of ATP synthesized per ½O_2 consumed, the P/O ratio. Measurement of P/O, however,

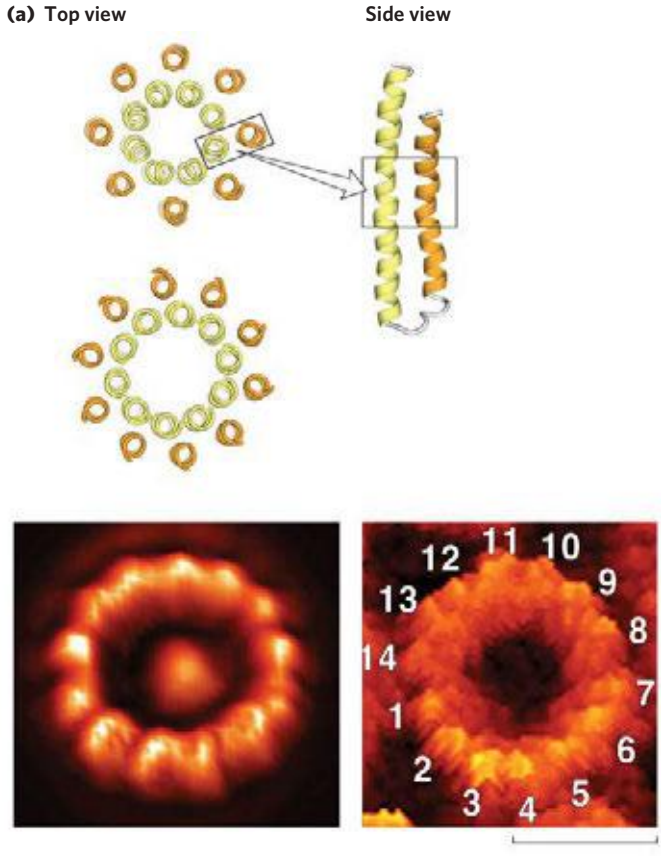

FIGURE 19–29 Different organisms have different numbers of c subunits in the c ring of the F_o complex. The structure of the c ring from several species has been determined by x-ray crystallography. Each helix in the inner ring is half of a hairpin-shaped c subunit; the outer ring of helices is the other half of the hairpin structure. Views of the c ring perpendicular to the membrane show the number of c subunits for **(a)** bovine mitochondria (8) and **(b)** yeast mitochondria (10). Atomic force microscopy has been used to visualize the c rings of **(c)** the thermophilic bacterium *Bacillus* species TA2.A1 (13) and **(d)** spinach (14). According to the model in Fig. 19–28, different numbers of c subunits in the c ring should result in different ratios of ATP formed per pair of electrons passing through the respiratory chain (different P/O ratios).

is complicated by the fact that intact mitochondria *consume* ATP in many unrelated reactions taking place in the matrix, and they consume O_2 for purposes other than oxidative phosphorylation. The contribution of these interfering reactions must be carefully measured, and the calculation of P/O must be corrected for their contributions. Most experiments have yielded P/O (ATP to $\frac{1}{2}O_2$) ratios of between 2 and 3 when NADH was the electron donor, and between 1 and 2 when succinate was the donor. Given the assumption that P/O should have an integral value, most experimenters agreed that the P/O ratios must be 3 for NADH and 2 for succinate, and for years those values appeared in research papers and textbooks.

With introduction of the chemiosmotic paradigm for coupling ATP synthesis to electron transfer, there was no

BOX 19–2 METHODS Atomic Force Microsc

In atomic force microscopy (AFM), the sharp tip of a microscopic probe attached to a flexible cantilever is drawn across an uneven surface such as a membrane (Fig. 1). Electrostatic and van der Waals interactions between the tip and the sample produce a force that moves the probe up and down (in the z dimension) as it encounters hills and valleys in the sample. A laser beam reflected from the cantilever detects motions of as little as 1 Å. In one type of atomic force microscope, the force on the probe is held constant (relative to a standard force, on the order of piconewtons) by a feedback circuit that causes the platform holding the sample to rise or fall to keep the force constant. A series of scans in the x and y dimensions (the plane of the membrane) yields a three-dimensional contour map of the surface with resolution near the atomic scale—0.1 nm in the vertical dimension, 0.5 to 1.0 nm in the lateral dimensions.

In favorable cases, AFM can be used to study single membrane protein molecules, such as the c subunits of the F_o complex (Fig. 19–29c, d).

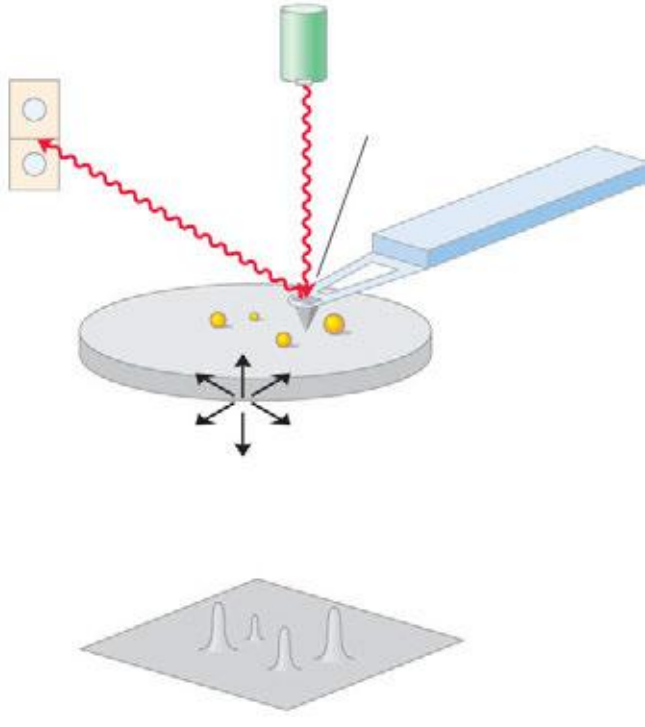

FIGURE 1 The principle of atomic force microscopy.

theoretical requirement for P/O to be integral. The relevant questions about stoichiometry became, How many protons are pumped outward by electron transfer from one NADH to O_2, and how many protons must flow inward through the F_oF_1 complex to drive the synthesis of one ATP? The measurement of proton fluxes is technically complicated; the investigator must take into account the buffering capacity of mitochondria, nonproductive leakage of protons across the inner membrane, and use of the proton gradient for functions other than ATP synthesis, such as driving the transport of substrates across the inner mitochondrial membrane (described below). The consensus experimental values for number of protons pumped out per pair of electrons are 10 for NADH and 6 for succinate (which sends electrons into the respiratory chain at the level of ubiquinone). The most widely accepted experimental value for number of protons required to drive the synthesis of an ATP molecule is 4, of which 1 is used in transporting P_i, ATP, and ADP across the mitochondrial membrane (see below). If 10 protons are pumped out per NADH and 4 must flow in to produce 1 ATP, the proton-based P/O ratio is 2.5 for NADH as the electron donor and 1.5 (6/4) for succinate.

The Proton-Motive Force Energizes Active Transport

Although the primary role of the proton gradient in mitochondria is to furnish energy for the synthesis of ATP, the proton-motive force also drives several transport processes essential to oxidative phosphorylation. The inner mitochondrial membrane is generally impermeable to charged species, but two specific systems transport ADP and P_i into the matrix and ATP out to the cytosol **(Fig. 19–30)**.

The **adenine nucleotide translocase**, integral to the inner membrane, binds ADP^{3-} in the intermembrane space and transports it into the matrix in exchange for an ATP^{4-} molecule simultaneously transported outward (see Fig. 13–11 for the ionic forms of ATP and ADP). Because this antiporter moves four negative charges out for every three moved in, its activity is favored by the transmembrane electrochemical gradient, which gives the matrix a net negative charge; the proton-motive force drives ATP-ADP exchange. Adenine nucleotide translocase is specifically inhibited by atractyloside, a toxic glycoside formed by a species of thistle. If the transport of ADP into and ATP out of mitochondria is inhibited, cytosolic ATP cannot be regenerated from ADP, explaining the toxicity of atractyloside.

A second membrane transport system essential to oxidative phosphorylation is the **phosphate translocase**, which promotes symport of one $H_2PO_4^-$ and one H^+ into the matrix. This transport process, too, is favored by the transmembrane proton gradient (Fig. 19–30). Notice that the process requires movement of one proton from the P to the N side of the inner membrane, consuming some of the energy of electron transfer. A complex of the

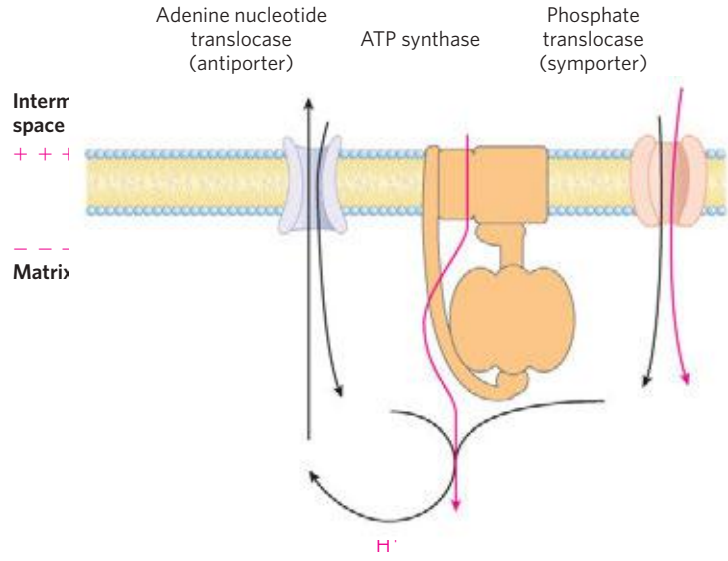

FIGURE 19–30 Adenine nucleotide and phosphate translocases. Transport systems of the inner mitochondrial membrane carry ADP and P_i into the matrix and newly synthesized ATP into the cytosol. The adenine nucleotide translocase is an antiporter; the same protein moves ADP into the matrix and ATP out. The effect of replacing ATP^{4-} with ADP^{3-} in the matrix is the net efflux of one negative charge, which is favored by the charge difference across the inner membrane (outside positive). At pH 7, P_i is present as both HPO_4^{2-} and $H_2PO_4^-$; the phosphate translocase is specific for $H_2PO_4^-$. There is no net flow of charge during symport of $H_2PO_4^-$ and H^+, but the relatively low proton concentration in the matrix favors the inward movement of H^+. Thus the proton-motive force is responsible both for providing the energy for ATP synthesis and for transporting substrates (ADP and P_i) into and product (ATP) out of the mitochondrial matrix. All three of these transport systems can be isolated as a single membrane-bound complex (ATP synthasome).

ATP synthase and both translocases, the **ATP synthasome**, can be isolated from mitochondria by gentle dissection with detergents, suggesting that the functions of these three proteins are very tightly integrated.

WORKED EXAMPLE 19–2 Stoichiometry of ATP Production: Effect of c Ring Size

(a) If *bovine* mitochondria have 8 c subunits per c ring, what is the predicted ratio of ATP formed per NADH oxidized? (b) What is the predicted value for *yeast* mitochondria, with 10 c subunits? (c) What are the comparable values for electrons entering the respiratory chain from $FADH_2$?

Solution: (a) The question asks us to determine how many ATP are produced per NADH. This is another way of asking us to calculate the P/O ratio, or x in Equation 19–11. If the c ring has 8 c subunits, then one full rotation will transfer 8 protons to the matrix and produce 3 ATP molecules. But this synthesis also requires the transport of 3 P_i into the matrix, at a cost of 1 proton each, adding 3 more protons to the total number required. This brings the total cost to (11 protons)/

(3 ATP) = 3.7 protons/ATP. The consensus value for the number of protons pumped out per pair of electrons transferred from NADH is 10 (see Fig. 19–19). So, oxidizing 1 NADH produces (10 protons)/(3.7 protons/ATP) = 2.7 ATP.

(b) If the c ring has 10 c subunits, then one full rotation will transfer 10 protons to the matrix and produce 3 ATP molecules. Adding in the 3 protons to transport the 3 P_i into the matrix brings the total cost to (13 protons)/(3 ATP) = 4.3 protons/ATP. Oxidizing 1 NADH produces (10 protons)/(4.3 protons/ATP) = 2.3 ATP.

(c) When electrons enter the respiratory chain from $FADH_2$ (at ubiquinone), only 6 protons are available to drive ATP synthesis. This changes the calculation for bovine mitochondria to (6 protons)/(3.7 protons/ATP) = 1.6 ATP per pair of electrons from $FADH_2$. For yeast mitochondria, the calculation is (6 protons)/(4.3 protons/ATP) = 1.4 ATP per pair of electrons from $FADH_2$.

These calculated values of x or the P/O ratio define a range that includes the experimental values of 2.5 ATP/NADH and 1.5 ATP/$FADH_2$, and we therefore use these values throughout this book.

Shuttle Systems Indirectly Convey Cytosolic NADH into Mitochondria for Oxidation

The NADH dehydrogenase of the inner mitochondrial membrane of animal cells can accept electrons only from NADH in the matrix. Given that the inner membrane is not permeable to NADH, how can the NADH generated by glycolysis in the cytosol be reoxidized to NAD^+ by O_2 via the respiratory chain? Special shuttle systems carry reducing equivalents from cytosolic NADH into mitochondria by an indirect route. The most active NADH shuttle, which functions in liver, kidney, and heart mitochondria, is the **malate-aspartate shuttle (Fig. 19–31)**. The reducing equivalents of cytosolic NADH are first transferred to cytosolic oxaloacetate to yield malate, catalyzed by cytosolic malate dehydrogenase. The malate thus formed passes through

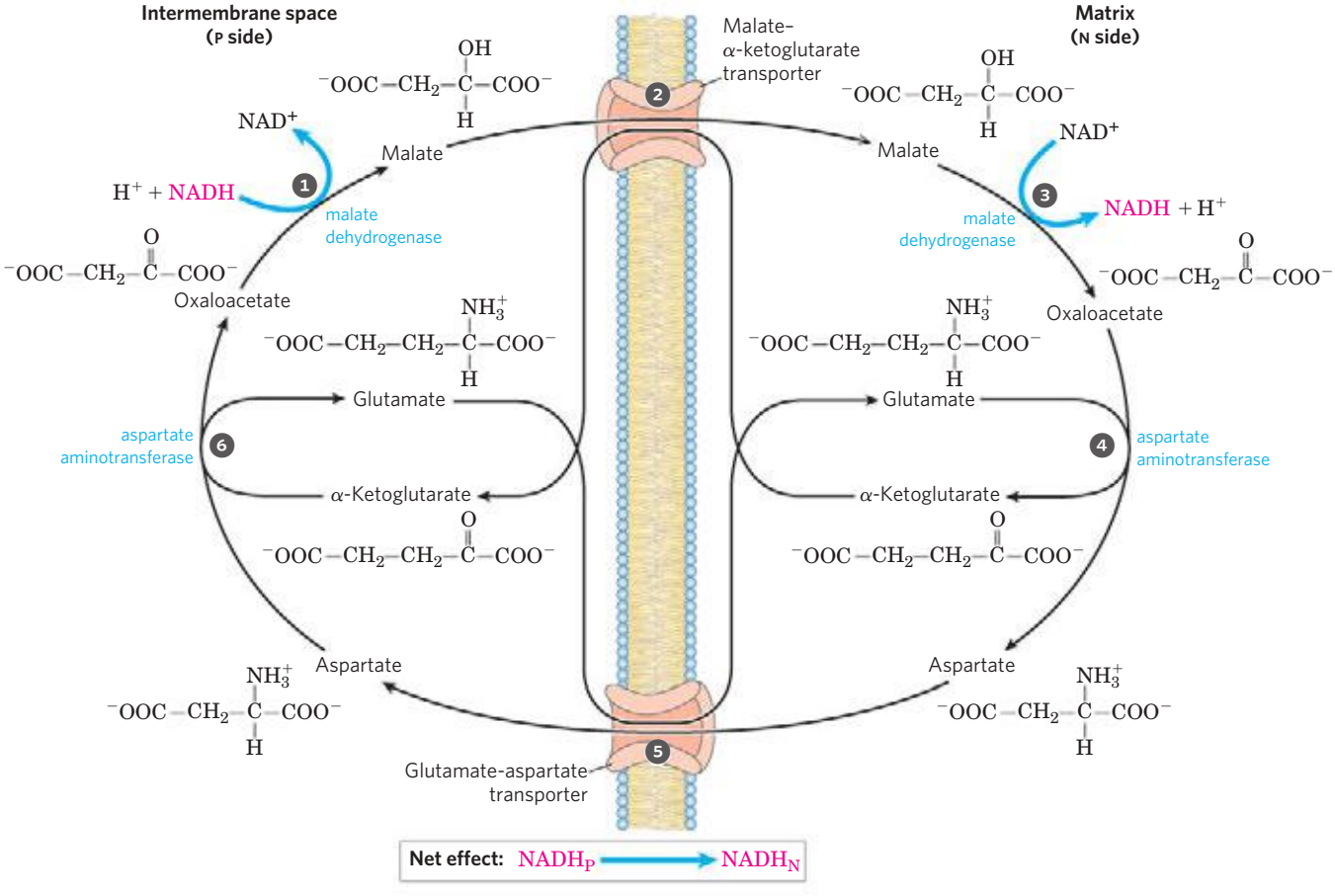

FIGURE 19–31 Malate-aspartate shuttle. This shuttle for transporting reducing equivalents from cytosolic NADH into the mitochondrial matrix is used in liver, kidney, and heart. ❶ NADH in the cytosol enters the intermembrane space through openings in the outer membrane (porins), then passes two reducing equivalents to oxaloacetate, producing malate. ❷ Malate crosses the inner membrane via the malate-α-ketoglutarate transporter. ❸ In the matrix, malate passes two reducing equivalents to NAD^+, and the resulting NADH is oxidized by the respiratory chain; the oxaloacetate formed from malate cannot pass directly into the cytosol. ❹ Oxaloacetate is first transaminated to aspartate, and ❺ aspartate can leave via the glutamate-aspartate transporter. ❻ Oxaloacetate is regenerated in the cytosol, completing the cycle.

the inner membrane via the malate–α-ketoglutarate transporter. Within the matrix the reducing equivalents are passed to NAD^+ by the action of matrix malate dehydrogenase, forming NADH; this NADH can pass electrons directly to the respiratory chain. About 2.5 molecules of ATP are generated as this pair of electrons passes to O_2. Cytosolic oxaloacetate must be regenerated by transamination reactions and the activity of membrane transporters to start another cycle of the shuttle.

Skeletal muscle and brain use a different NADH shuttle, the **glycerol 3-phosphate shuttle** (Fig. 19–32). It differs from the malate-aspartate shuttle in that it delivers the reducing equivalents from NADH to ubiquinone and thus into Complex III, not Complex I (Fig. 19–8), providing only enough energy to synthesize 1.5 ATP molecules per pair of electrons.

The mitochondria of plants have an *externally* oriented NADH dehydrogenase that can transfer electrons directly from cytosolic NADH into the respiratory chain at the level of ubiquinone. Because this pathway bypasses the NADH dehydrogenase of Complex I and the associated proton movement, the yield of ATP from cytosolic NADH is less than that from NADH generated in the matrix (Box 19–1).

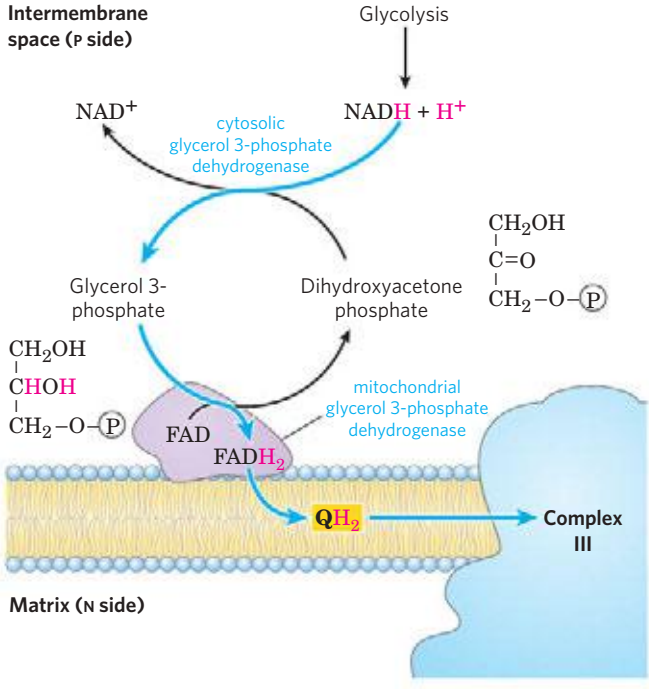

FIGURE 19–32 Glycerol 3-phosphate shuttle. This alternative means of moving reducing equivalents from the cytosol to the mitochondrial matrix operates in skeletal muscle and the brain. In the cytosol, dihydroxyacetone phosphate accepts two reducing equivalents from NADH in a reaction catalyzed by cytosolic glycerol 3-phosphate dehydrogenase. An isozyme of glycerol 3-phosphate dehydrogenase bound to the outer face of the inner membrane then transfers two reducing equivalents from glycerol 3-phosphate in the intermembrane space to ubiquinone. Note that this shuttle does not involve membrane transport systems.

SUMMARY 19.2 ATP Synthesis

- The flow of electrons through Complexes I, III, and IV results in pumping of protons across the inner mitochondrial membrane, making the matrix alkaline relative to the intermembrane space. This proton gradient provides the energy (in the form of the proton-motive force) for ATP synthesis from ADP and P_i by ATP synthase (F_oF_1 complex) in the inner membrane.
- ATP synthase carries out "rotational catalysis," in which the flow of protons through F_o causes each of three nucleotide-binding sites in F_1 to cycle from (ADP + P_i)–bound to ATP-bound to empty conformations.
- ATP formation on the enzyme requires little energy; the role of the proton-motive force is to push ATP from its binding site on the synthase.
- The ratio of ATP synthesized per ½O_2 reduced to H_2O (the P/O ratio) is about 2.5 when electrons enter the respiratory chain at Complex I, and 1.5 when electrons enter at ubiquinone. This ratio may vary somewhat in different organisms based on the number of c subunits in the F_o complex.
- Energy conserved in a proton gradient can drive solute transport uphill across a membrane.
- The inner mitochondrial membrane is impermeable to NADH and NAD^+, but NADH equivalents are moved from the cytosol to the matrix by either of two shuttles. NADH equivalents moved in by the malate-aspartate shuttle enter the respiratory chain at Complex I and yield a P/O ratio of 2.5; those moved in by the glycerol 3-phosphate shuttle enter at ubiquinone and give a P/O ratio of 1.5.

19.3 Regulation of Oxidative Phosphorylation

Oxidative phosphorylation produces most of the ATP made in aerobic cells. Complete oxidation of a molecule of glucose to CO_2 yields 30 or 32 ATP (Table 19–5). By comparison, glycolysis under anaerobic conditions (lactate fermentation) yields only 2 ATP per glucose. Clearly, the evolution of oxidative phosphorylation provided a tremendous increase in the energy efficiency of catabolism. Complete oxidation to CO_2 of the coenzyme A derivative of palmitate (16:0), which also occurs in the mitochondrial matrix, yields 108 ATP per palmitoyl-CoA (see Table 17–1). A similar calculation can be made for the ATP yield from oxidation of each of the amino acids (Chapter 18). Aerobic oxidative pathways that result in electron transfer to O_2 accompanied by oxidative phosphorylation therefore account for the vast majority of the ATP produced in catabolism, so the regulation of ATP production by oxidative phosphorylation to match the cell's fluctuating needs for ATP is absolutely essential.

TABLE 19–5 ATP Yield from Complete Oxidation of Glucose

Process	Direct product	Final ATP
Glycolysis	2 NADH (cytosolic) 2 ATP	3 or 5* 2
Pyruvate oxidation (two per glucose)	2 NADH (mitochondrial matrix)	5
Acetyl-CoA oxidation in citric acid cycle (two per glucose)	6 NADH (mitochondrial matrix) 2 $FADH_2$ 2 ATP or 2 GTP	15 3 2
Total yield per glucose		30 or 32

*The number depends on which shuttle system transfers reducing equivalents into the mitochondrion.

Oxidative Phosphorylation Is Regulated by Cellular Energy Needs

The rate of respiration (O_2 consumption) in mitochondria is tightly regulated; it is generally limited by the availability of ADP as a substrate for phosphorylation. Dependence of the rate of O_2 consumption on the availability of the P_i acceptor, ADP (Fig. 19–20b), the **acceptor control** of respiration, can be remarkable. In some animal tissues, the **acceptor control ratio**, the ratio of the maximal rate of ADP-induced O_2 consumption to the basal rate in the absence of ADP, is at least 10.

The intracellular concentration of ADP is one measure of the energy status of cells. Another, related measure is the **mass-action ratio** of the ATP-ADP system, $[ATP]/([ADP][P_i])$. Usually this ratio is very high, so the ATP-ADP system is almost fully phosphorylated. When the rate of some energy-requiring process (protein synthesis, for example) increases, the rate of breakdown of ATP to ADP and P_i increases, lowering the mass-action ratio. With more ADP available for oxidative phosphorylation, the rate of respiration increases, causing regeneration of ATP. This continues until the mass-action ratio returns to its normal high level, at which point respiration slows again. The rate of oxidation of cellular fuels is regulated with such sensitivity and precision that the $[ATP]/([ADP][P_i])$ ratio fluctuates only slightly in most tissues, even during extreme variations in energy demand. In short, ATP is formed only as fast as it is used in energy-requiring cellular activities.

An Inhibitory Protein Prevents ATP Hydrolysis during Hypoxia

We have already encountered ATP synthase as an ATP-driven proton pump (see Fig. 11–39), catalyzing the reverse of ATP synthesis. When a cell is hypoxic (deprived of oxygen), as in a heart attack or stroke, electron transfer to oxygen slows, and so does the pumping of protons. The proton-motive force soon collapses. Under these conditions, the ATP synthase could operate in reverse, hydrolyzing ATP to pump protons outward and causing a disastrous drop in ATP levels. This is prevented by a small (84 amino acids) protein inhibitor, IF_1, which simultaneously binds to two ATP synthase molecules, inhibiting their ATPase activity **(Fig. 19–33)**. IF_1 is inhibitory only in its dimeric form, which is favored at pH lower than 6.5. In a cell starved for oxygen, the main source of ATP becomes glycolysis, and the pyruvic or lactic acid thus formed lowers the pH in the cytosol and the mitochondrial matrix. This favors IF_1 dimerization, leading to inhibition of the ATPase activity of ATP synthase and thereby preventing wasteful hydrolysis of ATP. When aerobic metabolism resumes, production of pyruvic acid slows, the pH of the cytosol rises, the IF_1 dimer is destabilized, and the inhibition of ATP synthase is lifted. IF_1 is one of a growing number of proteins known to be intrinsically disordered (p. 141); it acquires a favored conformation only upon interaction with the ATP synthase.

Hypoxia Leads to ROS Production and Several Adaptive Responses

In hypoxic cells there is an imbalance between the input of electrons from fuel oxidation in the mitochondrial matrix and transfer of electrons to molecular oxygen,

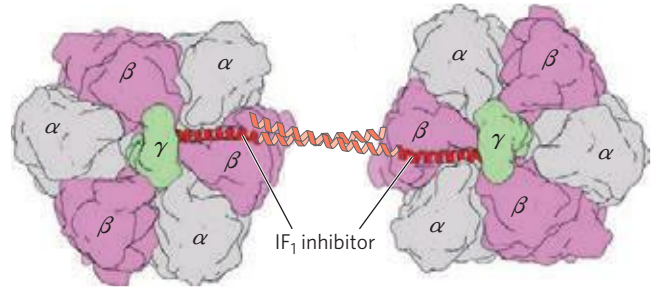

FIGURE 19–33 Structure of bovine F_1-ATPase in a complex with its regulatory protein IF_1. (Derived from PDB ID 1OHH) Two F_1 molecules are viewed here as in Figure 19–25c. The inhibitor IF_1 (red) binds to the $\alpha\beta$ interface of the subunits in the diphosphate (ADP) conformation (α-ADP and β-ADP), freezing the two F_1 complexes and thereby blocking ATP hydrolysis (and synthesis). (Parts of IF_1 that failed to resolve in the crystals of F_1 are shown in light red as they occur in crystals of isolated IF_1.) This complex is stable only at the low cytosolic pH characteristic of cells that are producing ATP by glycolysis; when aerobic metabolism resumes, the cytosolic pH rises, the inhibitor is destabilized, and ATP synthase becomes active.

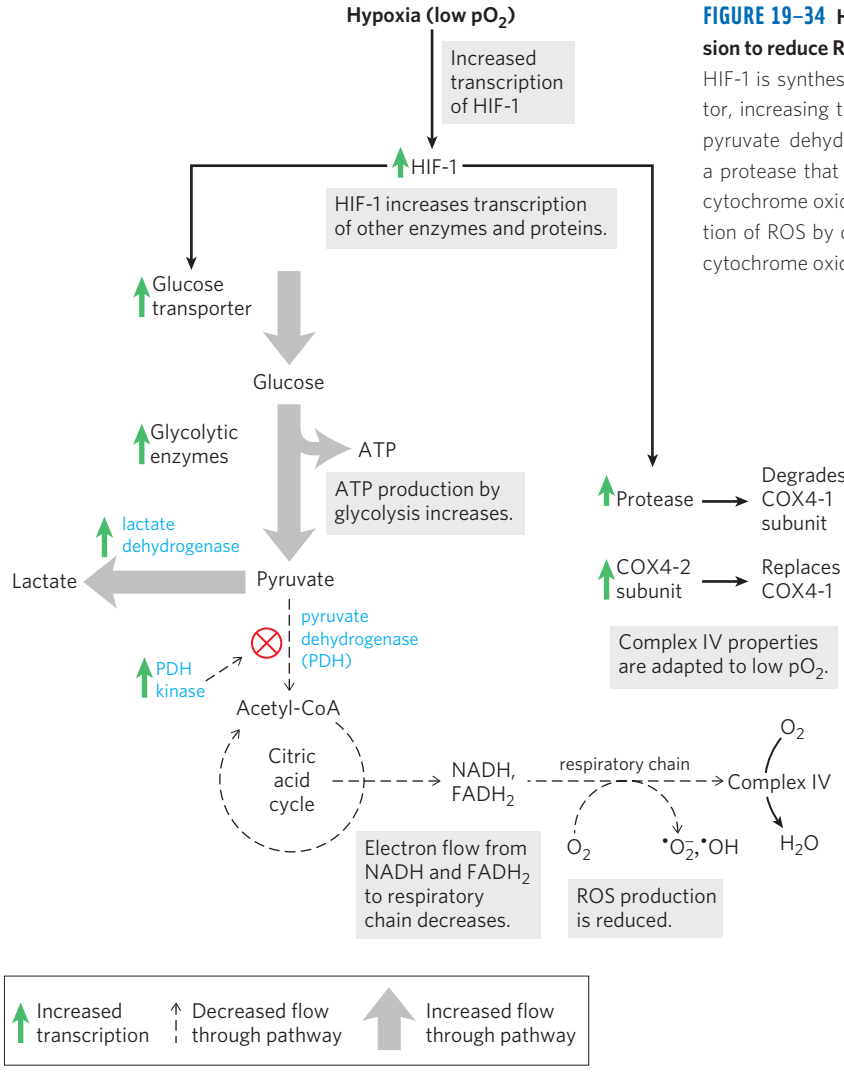

FIGURE 19–34 Hypoxia-inducible factor (HIF-1) regulates gene expression to reduce ROS formation. Under conditions of low oxygen (hypoxia), HIF-1 is synthesized in greater amounts and acts as a transcription factor, increasing the synthesis of glucose transporter, glycolytic enzymes, pyruvate dehydrogenase kinase (PDH kinase), lactate dehydrogenase, a protease that degrades the cytochrome oxidase subunit COX4-1, and cytochrome oxidase subunit COX4-2. These changes counter the formation of ROS by decreasing the supply of NADH and $FADH_2$ and making cytochrome oxidase of Complex IV more effective.

leading to increased formation of reactive oxygen species. In addition to the glutathione peroxidase system (Fig. 19–18), cells have two other lines of defense against ROS **(Fig. 19–34)**. One is regulation of pyruvate dehydrogenase (PDH), the enzyme that delivers acetyl-CoA to the citric acid cycle (Chapter 16). Under hypoxic conditions, PDH kinase phosphorylates mitochondrial PDH, inactivating it and slowing the delivery of $FADH_2$ and NADH from the citric acid cycle to the respiratory chain. A second means of preventing ROS formation is the replacement of one subunit of Complex IV, known as COX4-1, with another subunit, COX4-2, that is better suited to hypoxic conditions. With COX4-1, the catalytic properties of Complex IV are optimal for respiration at normal oxygen concentrations; with COX4-2, Complex IV is optimized for operation under hypoxic conditions.

The changes in PDH activity and the COX4-2 content of Complex IV are both mediated by HIF-1, the hypoxia-inducible factor. HIF-1 (another intrinsically disordered protein) accumulates in hypoxic cells and, acting as a transcription factor, triggers increased synthesis of PDH kinase, COX4-2, and a protease that degrades COX4-1. Recall that HIF-1 also mediates the changes in glucose transport and glycolytic enzymes that produce the Pasteur effect (see Box 14–1).

When these mechanisms for dealing with ROS are insufficient, due to genetic mutation affecting one of the protective proteins or under conditions of very high rates of ROS production, mitochondrial function is compromised. Mitochondrial damage is thought to be involved in aging, heart failure, certain rare cases of diabetes (described below), and several maternally inherited genetic diseases that affect the nervous system. ■

ATP-Producing Pathways Are Coordinately Regulated

The major catabolic pathways have interlocking and concerted regulatory mechanisms that allow them to function together in an economical and self-regulating manner to produce ATP and biosynthetic precursors. The relative concentrations of ATP and ADP control not only the rates of electron transfer and oxidative phosphorylation but also the rates of the citric acid cycle, pyruvate oxidation, and glycolysis **(Fig. 19–35)**. Whenever ATP consumption increases, the rate of electron

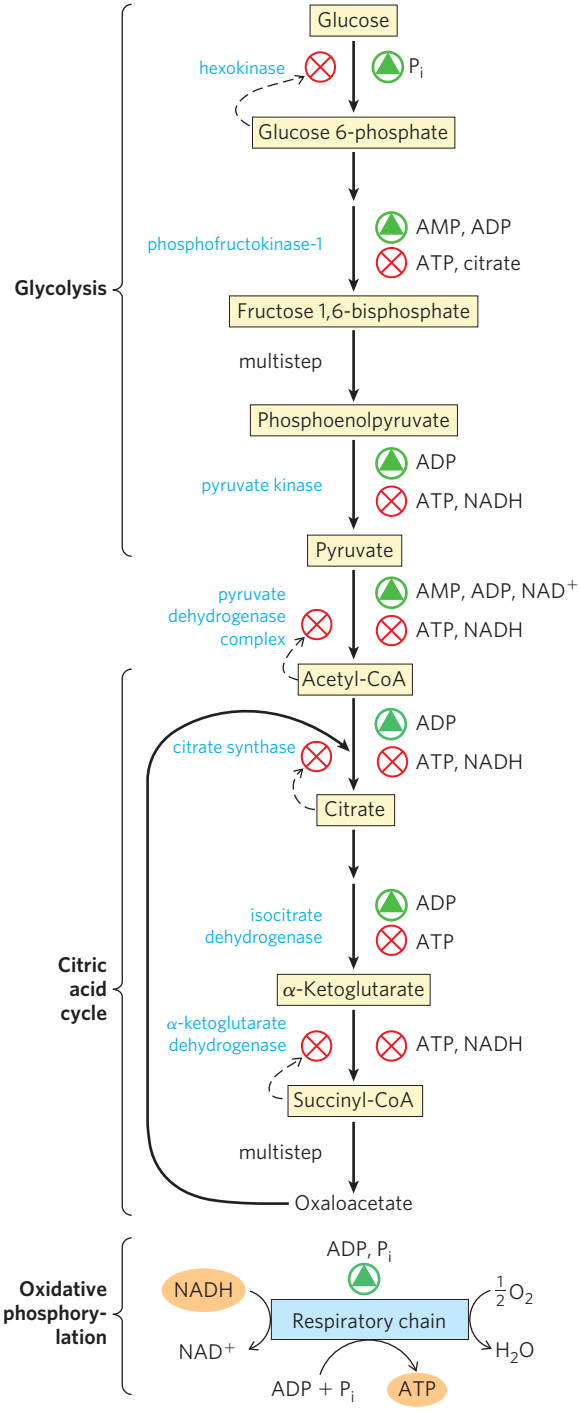

FIGURE 19–35 Regulation of the ATP-producing pathways. This diagram shows the interlocking regulation of glycolysis, pyruvate oxidation, the citric acid cycle, and oxidative phosphorylation by the relative concentrations of ATP, ADP, and AMP, and by NADH. High [ATP] (or low [ADP] and [AMP]) produces low rates of glycolysis, pyruvate oxidation, acetate oxidation via the citric acid cycle, and oxidative phosphorylation. All four pathways are accelerated when the use of ATP and the formation of ADP, AMP, and P_i increase. The interlocking of glycolysis and the citric acid cycle by citrate, which inhibits glycolysis, supplements the action of the adenine nucleotide system. In addition, increased levels of NADH and acetyl-CoA also inhibit the oxidation of pyruvate to acetyl-CoA, and a high [NADH]/[NAD^+] ratio inhibits the dehydrogenase reactions of the citric acid cycle (see Fig. 16–19).

transfer and oxidative phosphorylation increases. Simultaneously, the rate of pyruvate oxidation via the citric acid cycle increases, increasing the flow of electrons into the respiratory chain. These events can in turn evoke an increase in the rate of glycolysis, increasing the rate of pyruvate formation. When conversion of ADP to ATP lowers the ADP concentration, acceptor control slows electron transfer and thus oxidative phosphorylation. Glycolysis and the citric acid cycle are also slowed, because ATP is an allosteric inhibitor of the glycolytic enzyme phosphofructokinase-1 (see Fig. 15–16) and of pyruvate dehydrogenase (see Fig. 16–19).

Phosphofructokinase-1 is also inhibited by citrate, the first intermediate of the citric acid cycle. When the cycle is "idling," citrate accumulates within mitochondria, then is transported into the cytosol. When the concentrations of both ATP and citrate rise, they produce a concerted allosteric inhibition of phosphofructokinase-1 that is greater than the sum of their individual effects, slowing glycolysis.

SUMMARY 19.3 Regulation of Oxidative Phosphorylation

- Oxidative phosphorylation is regulated by cellular energy demands. The intracellular [ADP] and the mass-action ratio [ATP]/([ADP][P_i]) are measures of a cell's energy status.
- In hypoxic (oxygen-deprived) cells, a protein inhibitor blocks ATP hydrolysis by the reverse activity of ATP synthase, preventing a drastic drop in [ATP].
- The adaptive responses to hypoxia, mediated by HIF-1, slow electron transfer into the respiratory chain and modify Complex IV to act more efficiently under low-oxygen conditions.
- ATP and ADP concentrations set the rate of electron transfer through the respiratory chain via a series of interlocking controls on respiration, glycolysis, and the citric acid cycle.

19.4 Mitochondria in Thermogenesis, Steroid Synthesis, and Apoptosis

Although ATP production is a central role for the mitochondrion, this organelle has other functions that, in specific tissues or under specific circumstances, are also crucial. In adipose tissue, mitochondria generate heat to protect vital organs from low ambient temperature; in the adrenal glands and the gonads, mitochondria are the sites of steroid hormone synthesis; and in most or all tissues they are key participants in apoptosis (programmed cell death).

Uncoupled Mitochondria in Brown Adipose Tissue Produce Heat

We noted above that respiration slows when the cell is adequately supplied with ATP. There is a remarkable

and instructive exception to this general rule. Most newborn mammals, including humans, have a type of adipose tissue called **brown adipose tissue** (**BAT**; p. 944) in which fuel oxidation serves, not to produce ATP, but to generate heat to keep the newborn warm. This specialized adipose tissue is brown because of the presence of large numbers of mitochondria and thus high concentrations of cytochromes, with heme groups that are strong absorbers of visible light.

The mitochondria of brown adipocytes are much like those of other mammalian cells, except in having a unique protein in their inner membrane. **Thermogenin**, also called **uncoupling protein 1** (the product of the *UCP1* gene), provides a path for protons to return to the matrix without passing through the F_oF_1 complex **(Fig. 19–36)**. As a result of this short-circuiting of protons, the energy of oxidation is not conserved by ATP formation but is dissipated as heat, which contributes to maintaining the body temperature (see Fig. 23–16). Hibernating animals also depend on the activity of uncoupled BAT mitochondria to generate heat during their long dormancy (see Box 17–1). We will return to the role of thermogenin when we discuss the regulation of body mass in Chapter 23 (pp. 961–962).

Mitochondrial P-450 Oxygenases Catalyze Steroid Hydroxylations

Mitochondria are the site of biosynthetic reactions that produce steroid hormones, including the sex hormones, glucocorticoids, mineralocorticoids, and vitamin D hormone. These compounds are synthesized from cholesterol or a related sterol in a series of hydroxylations catalyzed by enzymes of the **cytochrome P-450** family, all of which have a critical heme group (its absorption at 450 nm gives this family its name). In the hydroxylation reactions, one atom of molecular oxygen is incorporated into the substrate and the second is reduced to H_2O:

$$R{-}H + O_2 + NADPH + H^+ \longrightarrow R{-}OH + H_2O + NADP^+$$

There are dozens of P-450 enzymes, all situated in the inner mitochondrial membrane with their catalytic site exposed to the matrix. Steroidogenic cells are packed with mitochondria specialized for steroid synthesis; the mitochondria are generally larger than those in other tissues and have more extensive and highly convoluted inner membranes **(Fig. 19–37)**.

The path of electron flow in the mitochondrial P-450 system is complex, involving a flavoprotein and an iron-sulfur protein that carry electrons from NADPH to the P-450 heme **(Fig. 19–38)**. All P-450 enzymes have a heme that interacts with O_2 and a substrate-binding site that confers specificity.

Another large family of P-450 enzymes is found in the endoplasmic reticulum of hepatocytes. These enzymes catalyze reactions similar to the mitochondrial P-450 reactions, but their substrates include a wide variety of hydrophobic compounds, many of which are **xenobiotics**—compounds not found in nature but synthesized industrially. The P-450 enzymes of the ER have very broad and overlapping substrate specificities. Hydroxylation of the hydrophobic compounds makes them more water soluble, and they can then be cleared by the kidneys and excreted in urine. Among the substrates for these P-450 oxygenases are many commonly used prescription drugs. Metabolism by P-450 enzymes limits the drugs' lifetime in the bloodstream and their therapeutic effects. Humans differ in their genetic complement of P-450 enzymes in the ER, and in the extent to which certain P-450 enzymes have been induced, such as by a history of ethanol ingestion. In principle, therefore, an individual's genetics and personal history could figure into determinations of therapeutic

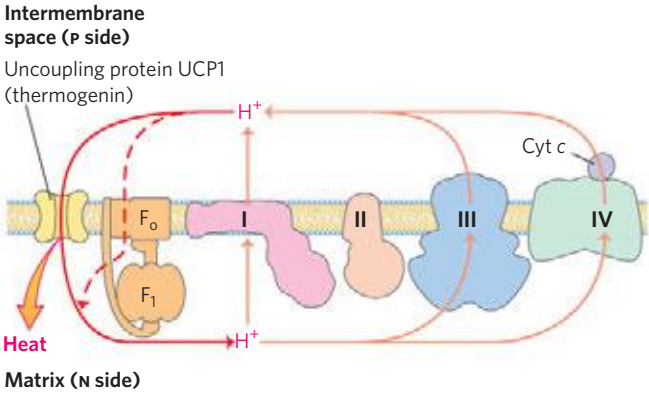

FIGURE 19–36 Heat generation by uncoupled mitochondria. The uncoupling protein (thermogenin) in the mitochondria of brown adipose tissue, by providing an alternative route for protons to reenter the mitochondrial matrix, causes the energy conserved by proton pumping to be dissipated as heat.

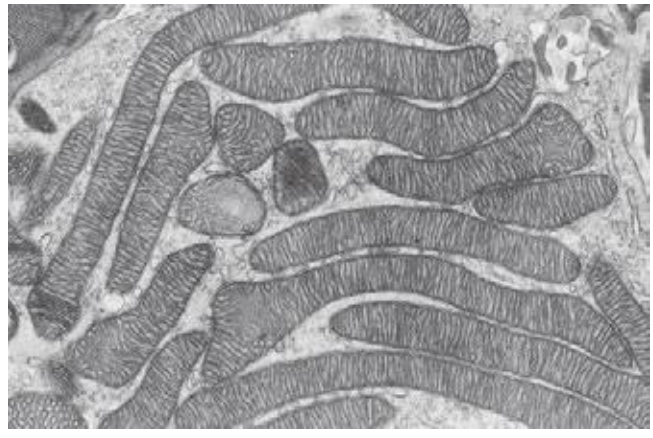

FIGURE 19–37 Mitochondria of adrenal gland, specialized for steroid synthesis. As seen in this electron micrograph of a thin section of adrenal gland, the mitochondria are profuse and have extensive cristae, providing a large surface for the P-450 enzymes of the inner membrane.

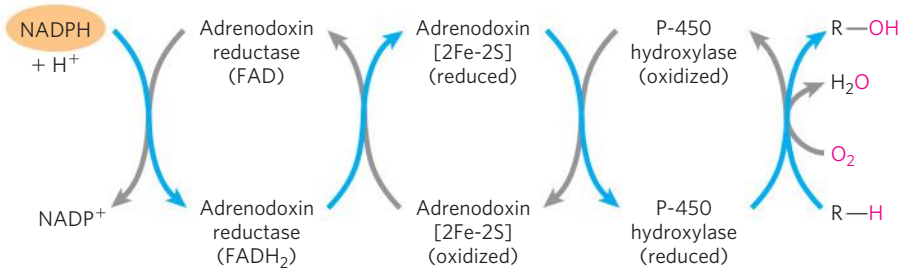

FIGURE 19–38 Path of electron flow in mitochondrial cytochrome P-450 reactions in adrenal gland. Two electrons are transferred from NADPH to the FAD-containing flavoprotein adrenodoxin reductase, which passes the electrons, one at a time, to adrenodoxin, a small, soluble 2Fe-2S protein. Adrenodoxin passes single electrons to the cytochrome P-450 hydroxylase, which interacts directly with O_2 and the substrate (R—H) to form the products, H_2O and R—OH.

drug dose; in practice, this precise tailoring of dosage is not yet economically feasible, but it may become so. ■

Mitochondria Are Central to the Initiation of Apoptosis

Apoptosis, also called **programmed cell death**, is a process in which individual cells die for the good of the organism (for example, in the course of normal embryonic development), and the organism conserves the cells' molecular components (amino acids, nucleotides, and so forth). Apoptosis may be triggered by an external signal, acting at a plasma membrane receptor, or by internal events such as DNA damage, viral infection, oxidative stress from the accumulation of ROS, or another stress such as a heat shock.

Mitochondria play a critical role in triggering apoptosis. When a stressor gives the signal for cell death, one early consequence is an increase in the permeability of the outer mitochondrial membrane, allowing cytochrome *c* to escape from the intermembrane space into the cytosol **(Fig. 19–39)**. The increased permeability is due to the opening of the **permeability transition pore complex (PTPC)**, a multisubunit protein in the outer membrane; its opening and closing are affected by several proteins that stimulate or suppress apoptosis. When released into the cytosol, cytochrome *c* interacts with monomers of the protein **Apaf-1 (apoptosis protease activating factor-1)**, causing the formation of an **apoptosome** composed of seven Apaf-1 and seven cytochrome *c* molecules. The apoptosome provides the platform on which the protease procaspase-9 is activated to caspase-9, a member of a family of highly specific proteases (the **caspases**) involved in apoptosis. They share a critical *C*ys residue at their active site, and all cleave proteins only on the carboxyl-terminal

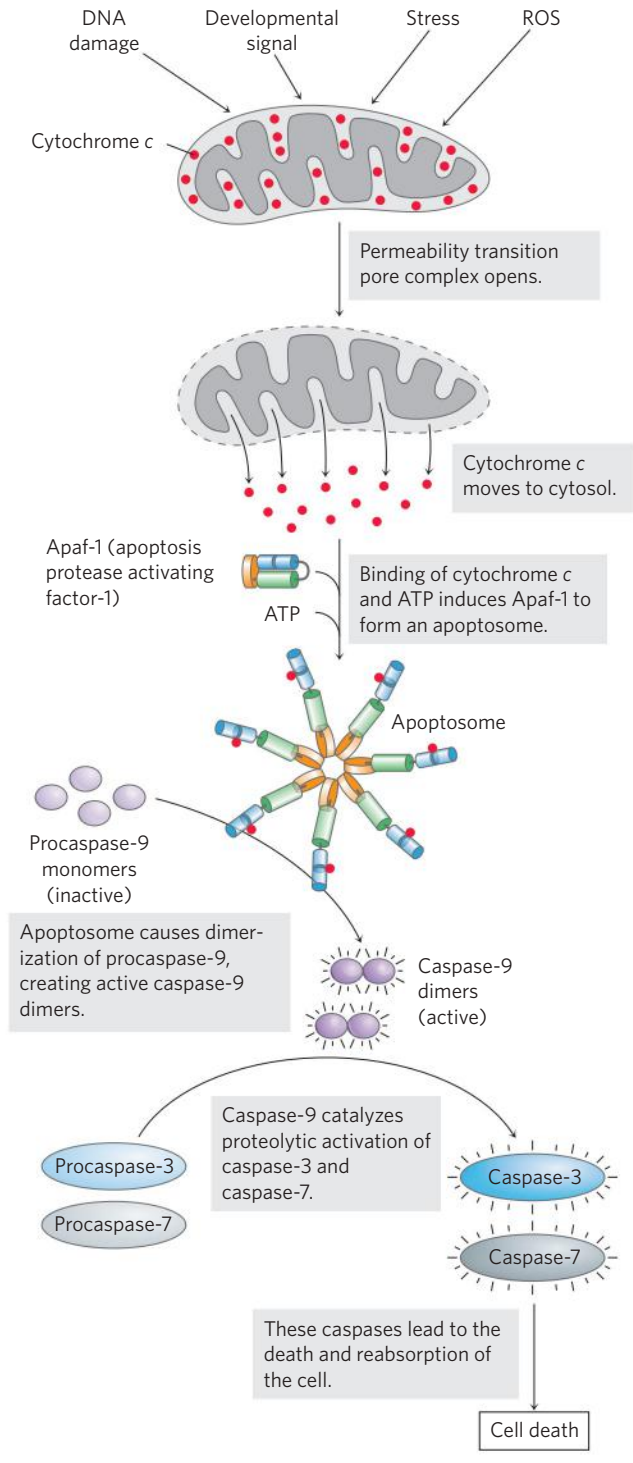

FIGURE 19–39 Role of cytochrome *c* in apoptosis. Cytochrome *c* is a small, soluble, mitochondrial protein, located in the intermembrane space, that carries electrons between Complex III and Complex IV during respiration. In a completely separate role, as outlined here, it acts as a trigger for apoptosis by stimulating the activation of a family of proteases called caspases.

side of *Asp* residues, thus the name "caspases." Activated caspase-9 initiates a cascade of proteolytic activations, with one caspase activating a second, and it in turn activating a third, and so forth (see Fig. 12–52). (This role of cytochrome *c* in apoptosis is a clear case of "moonlighting," in that one protein plays two very different roles in the cell; see Box 16–1.)

SUMMARY 19.4 Mitochondria in Thermogenesis, Steroid Synthesis, and Apoptosis

- In the brown adipose tissue of newborns, electron transfer is uncoupled from ATP synthesis and the energy of fuel oxidation is dissipated as heat.
- Hydroxylation reaction steps in the synthesis of steroid hormones in steroidogenic tissues (adrenal gland, gonads, liver, and kidney) take place in specialized mitochondria.
- Mitochondrial cytochrome *c*, released into the cytosol, participates in activation of caspase-9, one of the proteases involved in apoptosis.

19.5 Mitochondrial Genes: Their Origin and the Effects of Mutations

Mitochondria contain their own genome, a circular, double-stranded DNA (mtDNA) molecule. Each of the hundreds or thousands of mitochondria in a typical cell has about five copies of this genome. The human mitochondrial chromosome **(Fig. 19–40)** contains 37 genes (16,569 bp), including 13 that encode subunits of proteins of the respiratory chain (Table 19–6); the remaining genes code for rRNA and tRNA molecules essential to the protein-synthesizing machinery of mitochondria. The great majority of mitochondrial proteins—about 1,100 different types—are encoded by nuclear genes, synthesized on cytoplasmic ribosomes, then imported into and assembled in the mitochondria (Chapter 27).

Mitochondria Evolved from Endosymbiotic Bacteria

The existence of mitochondrial DNA, ribosomes, and tRNAs supports the hypothesis of the endosymbiotic origin of mitochondria (see Fig. 1–38), which holds that the first organisms capable of aerobic metabolism, including respiration-linked ATP production, were bacteria. Primitive eukaryotes that lived anaerobically (by fermentation) acquired the ability to carry out oxidative phosphorylation when they established a symbiotic relationship with bacteria living in their cytosol. After much evolution and the movement of many bacterial genes into the nucleus of the "host" eukaryote, the endosymbiotic bacteria eventually became mitochondria.

This hypothesis presumes that early free-living bacteria had the enzymatic machinery for oxidative phosphorylation and predicts that their modern bacterial descendants must have respiratory chains closely similar

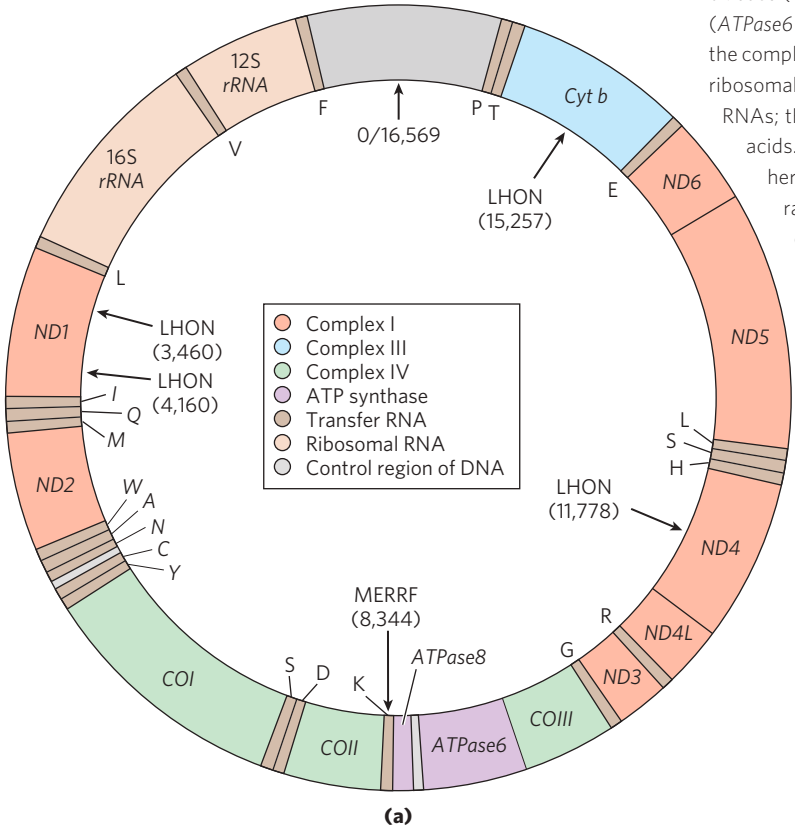

(a)

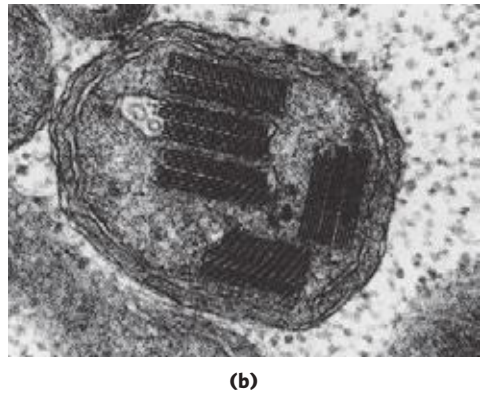

(b)

FIGURE 19–40 Mitochondrial genes and mutations. (a) Map of human mitochondrial DNA, showing the genes that encode proteins of Complex I, the NADH dehydrogenase (*ND1* to *ND6*); the cytochrome *b* of Complex III (*Cyt b*); the subunits of cytochrome oxidase (Complex IV) (*COI* to *COIII*); and two subunits of ATP synthase (*ATPase6* and *ATPase8*). The colors of the genes correspond to those of the complexes shown in Figure 19–7. Also included here are the genes for ribosomal RNAs (*rRNA*) and for some mitochondrion-specific transfer RNAs; tRNA specificity is indicated by the one-letter codes for amino acids. Arrows indicate the positions of mutations that cause Leber's hereditary optic neuropathy (LHON) and myoclonic epilepsy and ragged-red fiber disease (MERRF). Numbers in parentheses indicate the position of the altered nucleotides (nucleotide 1 is at the top of the circle and numbering proceeds counterclockwise). **(b)** Electron micrograph of an abnormal mitochondrion from the muscle of an individual with MERRF, showing the paracrystalline protein inclusions sometimes present in the mutant mitochondria.

TABLE 19–6 Respiratory Proteins Encoded by Mitochondrial Genes in Humans

Complex	Number of subunits	Number of subunits encoded by mitochondrial DNA
I NADH dehydrogenase	43	7
II Succinate dehydrogenase	4	0
III Ubiquinone:cytochrome *c* oxidoreductase	11	1
IV Cytochrome oxidase	13	3
V ATP synthase	8	2

to those of modern eukaryotes. They do. Aerobic bacteria carry out NAD-linked electron transfer from substrates to O_2, coupled to the phosphorylation of cytosolic ADP. The dehydrogenases are located in the bacterial cytosol and the respiratory chain in the plasma membrane. The electron carriers translocate protons outward across the plasma membrane as electrons are transferred to O_2. Bacteria such as *Escherichia coli* have F_oF_1 complexes in their plasma membranes; the F_1 portion protrudes into the cytosol and catalyzes ATP synthesis from ADP and P_i as protons flow back into the cell through the proton channel of F_o.

The respiration-linked extrusion of protons across the bacterial plasma membrane also provides the driving force for other processes. Certain bacterial transport systems bring about uptake of extracellular nutrients (lactose, for example) against a concentration gradient, in symport with protons (see Fig. 11–41). And the rotary motion of bacterial flagella is provided by "proton turbines," molecular rotary motors driven not by ATP but directly by the transmembrane electrochemical potential generated by respiration-linked proton pumping **(Fig. 19–41)**. It seems likely that the chemiosmotic mechanism evolved early, before the emergence of eukaryotes.

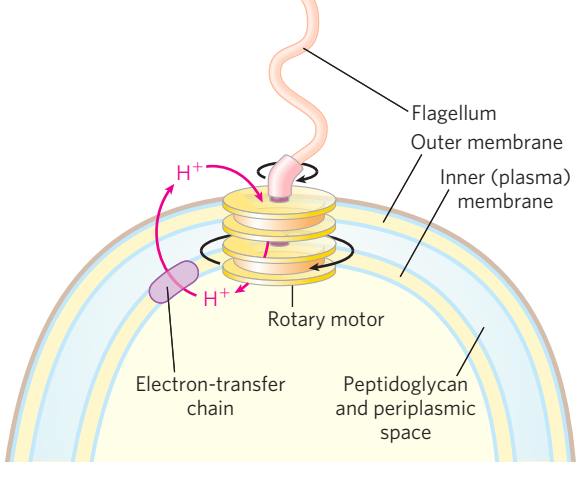

FIGURE 19–41 Rotation of bacterial flagella by proton-motive force. The shaft and rings at the base of the flagellum make up a rotary motor that has been called a "proton turbine." Protons ejected by electron transfer flow back into the cell through the turbine, causing rotation of the shaft of the flagellum. This motion differs fundamentally from the motion of muscle and of eukaryotic flagella and cilia, for which ATP hydrolysis is the energy source.

Mutations in Mitochondrial DNA Accumulate throughout the Life of the Organism

The respiratory chain is the major producer of reactive oxygen species in cells, so mitochondrial contents, including the mitochondrial genome, suffer the greatest exposure to, and damage by, ROS. Moreover, the mitochondrial DNA replication system is less effective than the nuclear system at correcting mistakes made during replication and at repairing DNA damage. As a consequence of these two factors, defects in mtDNA accumulate over time. One theory of aging is that this gradual accumulation of defects with increasing age is the primary cause of many of the "symptoms" of aging, which include, for example, progressive weakening of skeletal and heart muscle.

A unique feature of mitochondrial inheritance is the variation among individual cells, and between one individual organism and another, in the effects of a mtDNA mutation. A typical cell has hundreds or thousands of mitochondria, each with multiple copies of its own genome **(Fig. 19–42)**. Animals inherit essentially all of their mitochondria from the female parent. Eggs are large and contain 10^5 or 10^6 mitochondria, but sperm are

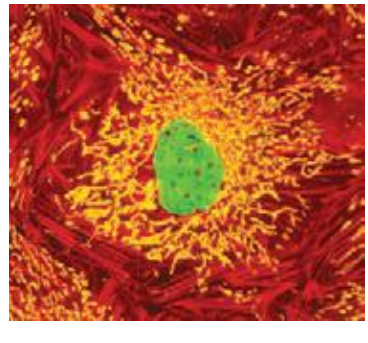

FIGURE 19–42 Single cells contain many mitochondria. A typical animal cell has hundreds or thousands of mitochondria, some fraction of which may contain genomes with mutations that affect mitochondrial function. This ovine (sheep) kidney epithelial cell was cultured in the laboratory, fixed, and then stained with fluorescent probes that show mitochondria as gold, microfilaments of actin as red, and nuclei as green when observed in the fluorescence microscope.

much smaller and contain far fewer mitochondria—perhaps 100 to 1,000. Furthermore, there is an active mechanism for targeting sperm-derived mitochondria for degradation in the fertilized egg. Just after fertilization, maternal phagosomes migrate to the site of sperm entry, engulf sperm mitochondria, and degrade them.

Suppose that, in a female organism, damage to one mitochondrial genome occurs in a germ cell from which oocytes develop, such that the germ cell contains mainly mitochondria with wild-type genes but one mitochondrion with a mutant gene. During the course of oocyte maturation, as this germ cell and its descendants repeatedly divide, the defective mitochondrion replicates and its progeny, all defective, are randomly distributed to daughter cells. Eventually, the mature egg cells contain different proportions of the defective mitochondria. When an egg cell is fertilized and undergoes the many divisions of embryonic development, the resulting somatic cells differ in their proportion of mutant mitochondria **(Fig. 19–43a)**. This **heteroplasmy** (in contrast to **homoplasmy**, in which every mitochondrial genome in every cell is the same) results in mutant phenotypes of varying degrees of severity. Cells (and tissues) containing mostly wild-type mitochondria have the wild-type phenotype; they are essentially normal. Other heteroplasmic cells will have intermediate phenotypes, some almost normal, others (with a high proportion of mutant mitochondria) abnormal (Fig. 19–41b). If the abnormal phenotype is associated with a disease (see below), individuals with the same mtDNA mutation may have disease symptoms of differing severity—depending on the number and distribution of affected mitochondria.

Some Mutations in Mitochondrial Genomes Cause Disease

A growing number of human diseases have been attributed to mutations in mitochondrial genes that reduce the cell's capacity to produce ATP. Some tissues and cell types—neurons, myocytes of both skeletal and cardiac muscle, and β cells of the pancreas—are less able than others to tolerate lowered ATP production and are therefore more affected by mutations in mitochondrial proteins.

A group of genetic diseases known as the **mitochondrial encephalomyopathies** affect primarily the brain and skeletal muscle. These diseases are invariably inherited from the mother, because, as noted above, a developing embryo derives all its mitochondria from the egg. The rare disease **Leber's hereditary optic neuropathy (LHON)** affects the central nervous system, including the optic nerves, causing bilateral loss of vision in early adulthood. A single base change in the mitochondrial gene *ND4* (Fig. 19–40a) changes an Arg residue to a His residue in a polypeptide of Complex I, and the result is mitochondria partially defective in electron transfer from NADH to ubiquinone. Although these mitochondria can produce some ATP by electron transfer from succinate, they apparently cannot supply sufficient ATP to support the very active metabolism of neurons. One result is damage to the

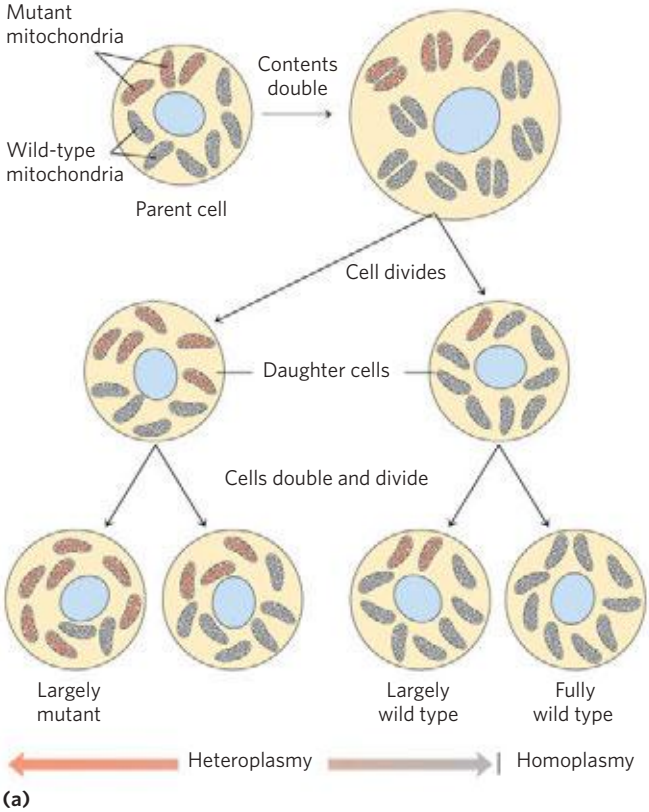

(a)

FIGURE 19–43 Heteroplasmy in mitochondrial genomes. (a) When a mature egg cell is fertilized, all of the mitochondria in the resulting diploid cell (zygote) are maternal; none come from the sperm. If some fraction of the maternal mitochondria have a mutant gene, the random distribution of mitochondria during subsequent cell divisions yields some daughter cells with mostly mutant mitochondria, some with mostly wild-type mitochondria, and some in between; thus the daughter cells show varying degrees of heteroplasmy. **(b)** Different degrees of heteroplasmy produce different cellular phenotypes. This section of human muscle tissue is from an individual with defective cytochrome oxidase. The cells have been stained to make wild-type cells blue and cells with mutant cytochrome oxidase brown. As the micrograph shows, different cells in the same tissue are affected to different degrees by the mitochondrial mutation.

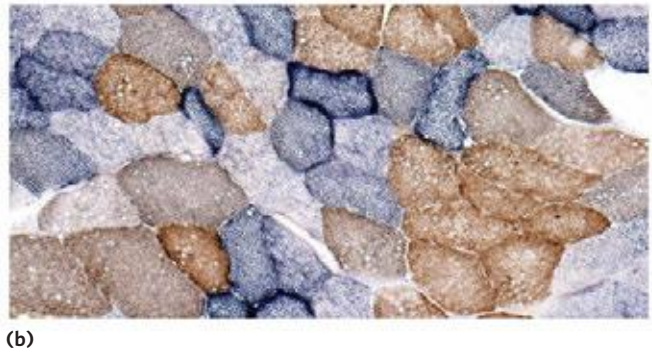

(b)

optic nerve, leading to blindness. A single base change in the mitochondrial gene for cytochrome *b*, a component of Complex III, also produces LHON, demonstrating that the pathology results from a general reduction of mitochondrial function, not specifically from a defect in electron transfer through Complex I.

A mutation (in *ATP6*) that affects the proton pore in ATP synthase leads to low rates of ATP synthesis while leaving the respiratory chain intact. The oxidative stress due to the continued supply of electrons from NADH increases the production of ROS, and the damage to mitochondria caused by ROS sets up a vicious cycle. Half of individuals with this mutant gene die within days or months of birth.

Myoclonic epilepsy with ragged-red fiber disease (MERRF) is caused by a mutation in the mitochondrial gene that encodes a tRNA specific for lysine ($tRNA^{Lys}$). This disease, characterized by uncontrollable muscular jerking, apparently results from defective production of several of the proteins that require mitochondrial tRNAs for their synthesis. Skeletal muscle fibers of individuals with MERRF have abnormally shaped mitochondria that sometimes contain paracrystalline structures (Fig. 19–40b). Other mutations in mitochondrial genes are believed to be responsible for the progressive muscular weakness that characterizes mitochondrial myopathy and for enlargement and deterioration of the heart muscle in hypertrophic cardiomyopathy. According to one hypothesis on the progressive changes that accompany aging, the accumulation of mutations in mtDNA during a lifetime of exposure to DNA-damaging agents such as $\cdot O_2^-$ results in mitochondria that cannot supply sufficient ATP for normal cellular function. Mitochondrial disease can also result from mutations in any of the ~1,100 nuclear genes that encode mitochondrial proteins. ■

Diabetes Can Result from Defects in the Mitochondria of Pancreatic β Cells

The mechanism that regulates the release of insulin from pancreatic β cells hinges on the ATP concentration in those cells. When blood glucose is high, β cells take up glucose and oxidize it by glycolysis and the citric acid cycle, raising [ATP] above a threshold level **(Fig. 19–44)**. When [ATP] exceeds this threshold, an ATP-gated K^+ channel in the plasma membrane closes, depolarizing the membrane and triggering insulin release (see Fig. 23–27). Pancreatic β cells with defects in oxidative phosphorylation cannot increase [ATP] above this threshold, and the resulting failure of insulin release effectively produces diabetes. For example, defects in the gene for glucokinase, the hexokinase IV isozyme present in β cells, lead to a rare form of diabetes, MODY2 (see Box 15–3); low glucokinase activity prevents the generation of above-threshold [ATP], blocking insulin secretion. Mutations in the mitochondrial $tRNA^{Lys}$ or $tRNA^{Leu}$ genes also compromise mitochondrial ATP production, and type 2 diabetes mellitus is common among individuals with these defects (although these cases make up a very small fraction of all cases of diabetes).

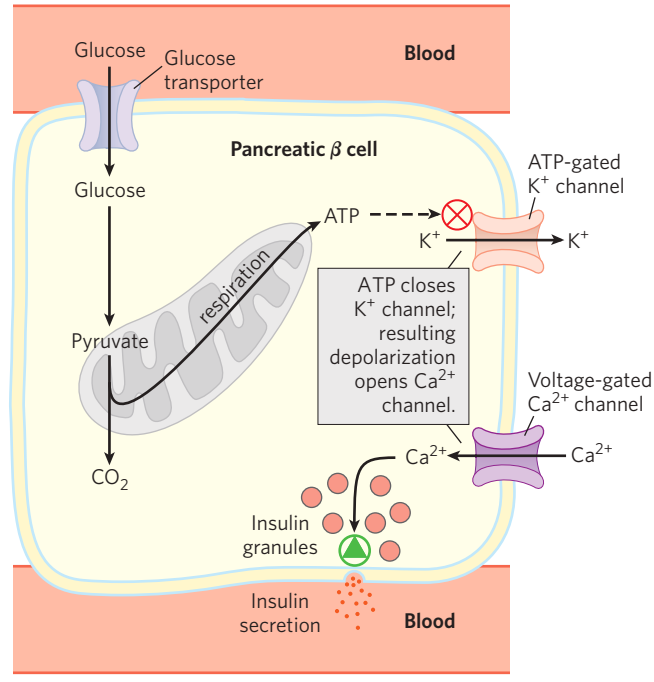

FIGURE 19–44 Defective oxidative phosphorylation in pancreatic β cells blocks insulin secretion. In the normal situation depicted here, when blood glucose rises, the production of ATP in β cells increases. ATP, by blocking K^+ channels, depolarizes the plasma membrane and thus opens the voltage-gated Ca^{2+} channels. The resulting influx of Ca^{2+} triggers exocytosis of insulin-containing secretory vesicles, releasing insulin. When oxidative phosphorylation in β cells is defective, [ATP] is never sufficient to trigger this process, and insulin is not released.

When nicotinamide nucleotide transhydrogenase, which is part of the mitochondrial defense against ROS (see Fig. 19–18), is genetically defective, the accumulation of ROS damages mitochondria, slowing ATP production and blocking insulin release by β cells (Fig. 19–44). Damage caused by ROS, including damage to mtDNA, may also underlie other human diseases; there is some evidence for its involvement in Alzheimer, Parkinson, and Huntington diseases and in heart failure, as well as in aging. ■

SUMMARY 19.5 Mitochondrial Genes: Their Origin and the Effects of Mutations

- A small proportion of human mitochondrial proteins, 13 in all, are encoded by the mitochondrial genome and synthesized in mitochondria. About 1,100 mitochondrial proteins are encoded in nuclear genes and imported into mitochondria after their synthesis.
- Mitochondria arose from aerobic bacteria that entered into an endosymbiotic relationship with ancestral eukaryotes.

- Mutations in the mitochondrial genome accumulate over the life of the organism. Mutations in the genes that encode components of the respiratory chain, ATP synthase, and the ROS-scavenging system, and even in tRNA genes, can cause a variety of human diseases, which often most severely affect muscle, heart, pancreatic β cells, and brain.

PHOTOSYNTHESIS: HARVESTING LIGHT ENERGY

We now turn to another reaction sequence in which the flow of electrons is coupled to the synthesis of ATP: light-driven phosphorylation. The capture of solar energy by photosynthetic organisms and its conversion to the chemical energy of reduced organic compounds is the ultimate source of nearly all biological energy on Earth. Photosynthetic and heterotrophic organisms live in a balanced steady state in the biosphere **(Fig. 19–45)**. Photosynthetic organisms trap solar energy and form ATP and NADPH, which they use as energy sources to make carbohydrates and other organic compounds from CO_2 and H_2O; simultaneously, they release O_2 into the atmosphere. Aerobic heterotrophs (humans, for example, as well as plants during dark periods) use the O_2 so formed to degrade the energy-rich organic products of photosynthesis to CO_2 and H_2O, generating ATP. The CO_2 returns to the atmosphere, to be used again by photosynthetic organisms. Solar energy thus provides the driving force for the continuous cycling of CO_2 and O_2 through the biosphere and provides the reduced substrates—fuels, such as glucose—on which nonphotosynthetic organisms depend.

Photosynthesis occurs in a variety of bacteria and in unicellular eukaryotes (algae) as well as in plants. Although the process in these organisms differs in detail, the underlying mechanisms are remarkably similar, and much of our understanding of photosynthesis in vascular plants is derived from studies of simpler organisms. The overall equation for photosynthesis in plants describes an oxidation-reduction reaction in which H_2O donates electrons (as hydrogen) for the reduction of CO_2 to carbohydrate (CH_2O):

$$CO_2 + H_2O \xrightarrow{\text{light}} O_2 + (CH_2O)$$

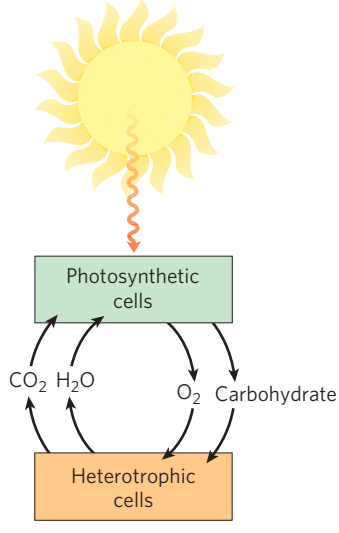

FIGURE 19–45 Solar energy as the ultimate source of all biological energy. Photosynthetic organisms use the energy of sunlight to manufacture glucose and other organic products, which heterotrophic cells use as energy and carbon sources.

19.6 General Features of Photophosphorylation

Unlike NADH (the major electron donor in oxidative phosphorylation), H_2O is a poor donor of electrons; its standard reduction potential is 0.816 V, compared with −0.320 V for NADH. Photophosphorylation differs from oxidative phosphorylation in requiring the input of energy in the form of light to *create* a good electron donor and a good electron acceptor (see Fig. 19–1). In photophosphorylation, electrons flow through a series of membrane-bound carriers including cytochromes, quinones, and iron-sulfur proteins, while protons are pumped across a membrane to create an electrochemical potential. Electron transfer and proton pumping are catalyzed by membrane complexes homologous in structure and function to Complex III of mitochondria. The electrochemical potential they produce is the driving force for ATP synthesis from ADP and P_i, catalyzed by a membrane-bound ATP synthase complex closely similar to that of mitochondria and bacteria.

Photosynthesis in plants encompasses two processes: the **light-dependent reactions**, or **light reactions**, which occur only when plants are illuminated, and the **carbon-assimilation reactions** (or **carbon-fixation reactions**), sometimes misleadingly called the dark reactions, which are driven by products of the light reactions **(Fig. 19–46)**. In the light reactions, chlorophyll and other pigments of photosynthetic cells absorb light energy and conserve it as ATP and NADPH; simultaneously, O_2 is evolved. In the carbon-assimilation reactions, ATP and NADPH are used to reduce CO_2 to form triose phosphates, starch, and sucrose, and other products derived from them. In this chapter we are concerned only with the light-dependent reactions that lead to the synthesis of ATP and NADPH. The reduction of CO_2 is described in Chapter 20.

Photosynthesis in Plants Takes Place in Chloroplasts

In photosynthetic eukaryotic cells, both the light-dependent and the carbon-assimilation reactions take place in the chloroplasts **(Fig. 19–47)**, intracellular organelles that are variable in shape and generally a few micrometers in diameter. Like mitochondria, they are surrounded by two membranes, an outer membrane that is permeable to small molecules and ions, and an inner membrane that encloses the internal compartment.

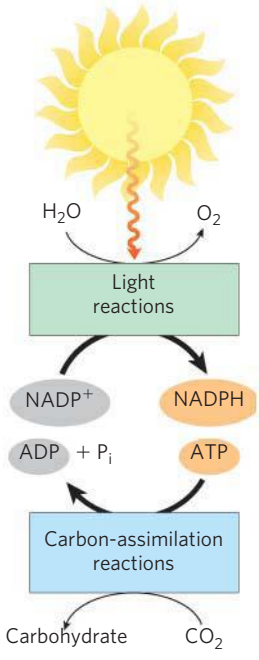

FIGURE 19–46 The light reactions of photosynthesis generate energy-rich NADPH and ATP at the expense of solar energy. NADPH and ATP are used in the carbon-assimilation reactions, which occur in light or darkness, to reduce CO_2 to form trioses and more complex compounds (such as glucose) derived from trioses.

This compartment contains many flattened, membrane-surrounded vesicles or sacs, the **thylakoids**, usually arranged in stacks called **grana** (Fig. 19–47b). Embedded in the thylakoid membranes (commonly called **lamellae**) are the photosynthetic pigments and the enzyme complexes that carry out the light reactions and ATP synthesis. The **stroma** (the aqueous phase enclosed by the inner membrane) contains most of the enzymes required for the carbon-assimilation reactions.

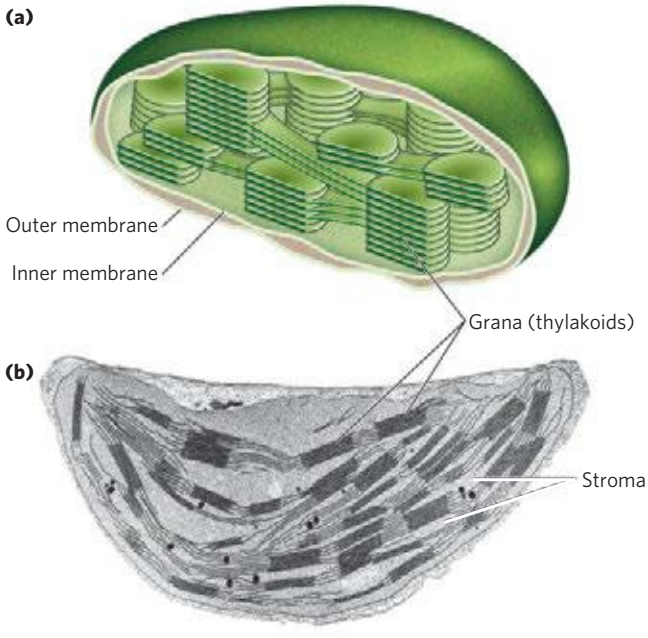

FIGURE 19–47 Chloroplast. (a) Schematic diagram. **(b)** Electron micrograph at high magnification showing grana, stacks of thylakoid membranes.

Light Drives Electron Flow in Chloroplasts

In 1937 Robert Hill found that when leaf extracts containing chloroplasts were illuminated, they (1) evolved O_2 and (2) reduced a nonbiological electron acceptor added to the medium, according to the **Hill reaction**:

$$2H_2O + 2A \xrightarrow{\text{light}} 2AH_2 + O_2$$

where A is the artificial electron acceptor, or **Hill reagent**. One Hill reagent, the dye 2,6-dichlorophenolindophenol, is blue when oxidized (A) and colorless when reduced (AH_2), making the reaction easy to follow.

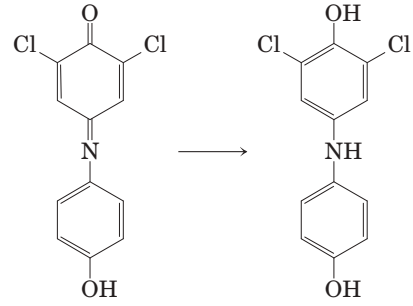

Dichlorophenolindophenol

When a leaf extract supplemented with the dye was illuminated, the blue dye became colorless and O_2 was evolved. In the dark, neither O_2 evolution nor dye reduction took place. This was the first evidence that absorbed light energy causes electrons to flow from H_2O to an electron acceptor. Moreover, Hill found that CO_2 was neither required nor reduced to a stable form under these conditions; O_2 evolution could be dissociated from CO_2 reduction. Several years later Severo Ochoa showed that $NADP^+$ is the biological electron acceptor in chloroplasts, according to the equation

$$2H_2O + 2NADP^+ \xrightarrow{\text{light}} 2NADPH + 2H^+ + O_2$$

To understand this photochemical process, we must first consider the more general topic of the effects of light absorption on molecular structure.

SUMMARY 19.6 General Features of Photophosphorylation

- Photosynthesis takes place in the chloroplasts of algae and plants, structures enclosed in double membranes and filled with stacked membranous discs (thylakoid membranes) containing the photosynthetic machinery.
- The light reactions of photosynthesis are those directly dependent on the absorption of light; the resulting photochemistry takes electrons from H_2O

and drives them through a series of membrane-bound carriers, producing NADPH and ATP.

- The carbon-assimilation reactions of photosynthesis reduce CO_2 with electrons from NADPH and energy from ATP, forming trioses, hexoses, and a wide variety of carbohydrates derived from them.

19.7 Light Absorption

Visible light is electromagnetic radiation of wavelengths 400 to 700 nm, a small part of the electromagnetic spectrum **(Fig. 19–48)**, ranging from violet to red. The energy of a single **photon** (a quantum of light) is greater at the violet end of the spectrum than at the red end; shorter wavelength (and higher frequency) corresponds to higher energy. The energy, E, in a single photon of visible light is given by the Planck equation:

$$E = h\nu = hc/\lambda$$

where h is Planck's constant (6.626×10^{-34} J·s), ν is the frequency of the light in cycles/s, c is the speed of light (3.00×10^8 m/s), and λ is the wavelength in meters. The energy of a photon of visible light ranges from 150 kJ/einstein for red light to ~300 kJ/einstein for violet light.

WORKED EXAMPLE 19–3 Energy of a Photon

The light used by vascular plants for photosynthesis has a wavelength of about 700 nm. Calculate the energy in a "mole" of photons (an einstein) of light of this wavelength, and compare this with the energy needed to synthesize a mole of ATP.

Solution: The energy in a single photon is given by the Planck equation. At a wavelength of 700×10^{-9} m, the energy of a photon is

$$E = hc/\lambda = \frac{[(6.626 \times 10^{-34}\ \text{J·s})(3.00 \times 10^8\ \text{m/s})]}{(7.00 \times 10^{-7}\ \text{m})} = 2.84 \times 10^{-19}\ \text{J}$$

An einstein of light is Avogadro's number (6.022×10^{23}) of photons; thus the energy of one einstein of photons at 700 nm is given by

$$(2.84 \times 10^{-19}\ \text{J/photon})(6.022 \times 10^{23}\ \text{photons/einstein}) = 17.1 \times 10^4\ \text{J/einstein} = 171\ \text{kJ/einstein}.$$

So, a "mole" of photons of red light has about five times the energy needed to produce a mole of ATP from ADP and P_i (30.5 kJ/mol).

When a photon is absorbed, an electron in the absorbing molecule (chromophore) is lifted to a higher energy level. This is an all-or-nothing event: to be absorbed, the photon must contain a quantity of energy (a **quantum**) that exactly matches the energy of the electronic transition. A molecule that has absorbed a photon is in an **excited state**, which is generally unstable. An electron lifted into a higher-energy orbital usually returns rapidly to its lower-energy orbital; the excited molecule decays to the stable **ground state**, giving up the absorbed quantum as light or heat or using it to do chemical work. Light emission accompanying decay of excited molecules (called **fluorescence**) is always at a longer wavelength (lower energy) than that of the absorbed light (see Box 12–3). An alternative mode of decay important in photosynthesis involves direct transfer of excitation energy from an excited molecule to a neighboring molecule. Just as the photon is a quantum of light energy, so the **exciton** is a quantum of energy passed from an excited molecule to another molecule in a process called **exciton transfer**.

Chlorophylls Absorb Light Energy for Photosynthesis

The most important light-absorbing pigments in the thylakoid membranes are the **chlorophylls**, green pigments with polycyclic, planar structures resembling the protoporphyrin of hemoglobin (see Fig. 5–1), except that Mg^{2+}, not Fe^{2+}, occupies the central position **(Fig. 19–49)**. The four inward-oriented nitrogen atoms of chlorophyll are coordinated with the Mg^{2+}. All chlorophylls have a long **phytol** side chain, esterified to a

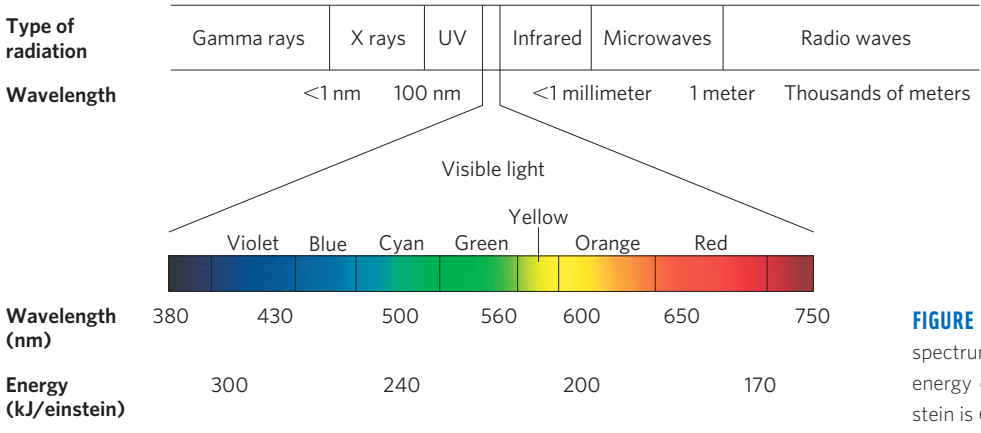

FIGURE 19–48 Electromagnetic radiation. The spectrum of electromagnetic radiation, and the energy of photons in the visible range. One einstein is 6.022×10^{23} photons.

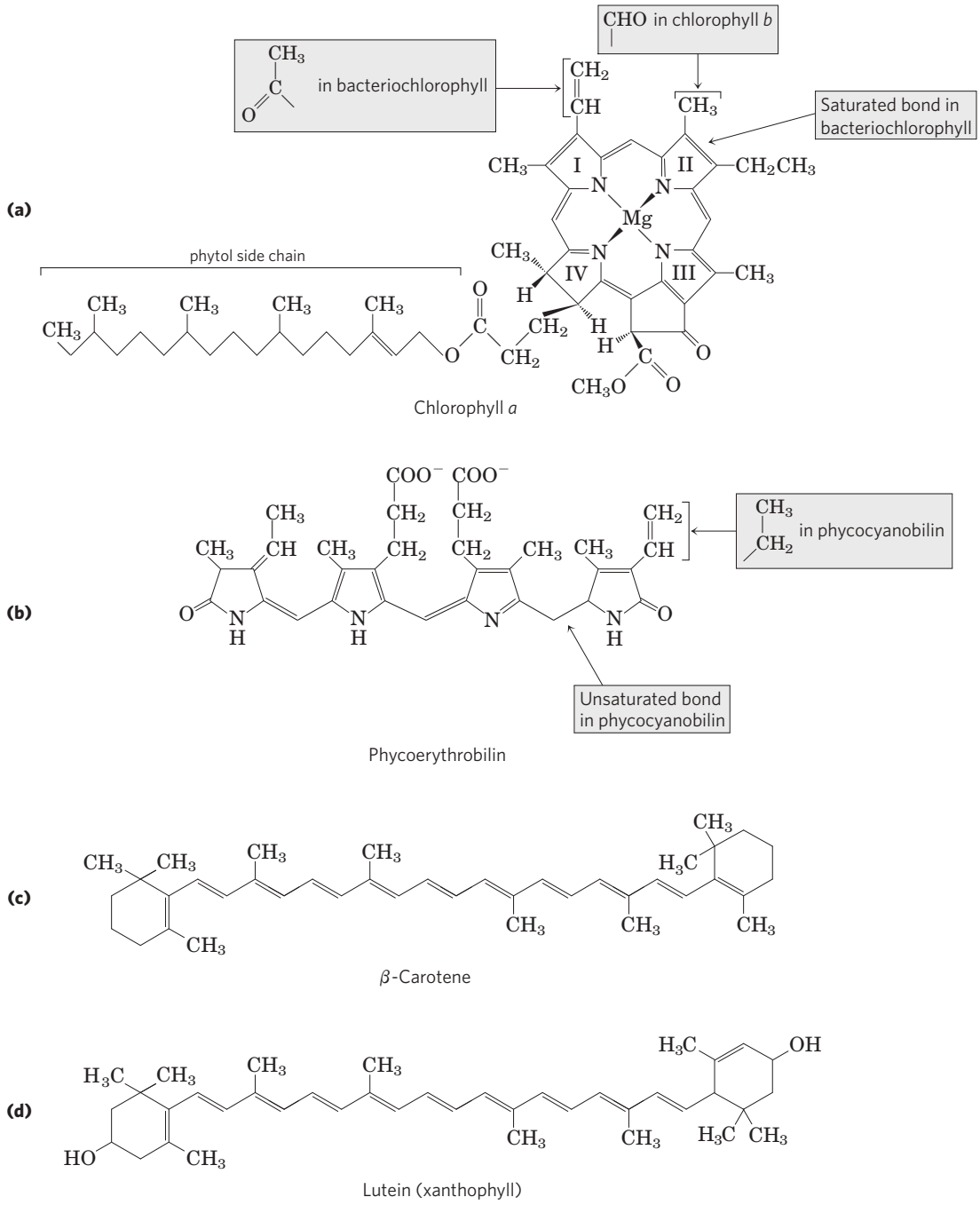

FIGURE 19–49 Primary and secondary photopigments. (a) Chlorophylls *a* and *b* and bacteriochlorophyll are the primary gatherers of light energy. **(b)** Phycoerythrobilin and phycocyanobilin (phycobilins) are the antenna pigments in cyanobacteria and red algae. **(c)** β-Carotene (a carotenoid) and **(d)** lutein (a xanthophyll) are accessory pigments in plants. The conjugated systems (alternating single and double bonds) in these molecules largely account for the absorption of visible light.

carboxyl-group substituent in ring IV, and chlorophylls also have a fifth five-membered ring not present in heme.

The heterocyclic five-ring system that surrounds the Mg^{2+} has an extended polyene structure, with alternating single and double bonds. Such polyenes characteristically show strong absorption in the visible region of the spectrum **(Fig. 19–50)**; the chlorophylls have unusually high molar extinction coefficients (see Box 3–1) and are therefore particularly well-suited for absorbing visible light during photosynthesis.

Chloroplasts always contain both chlorophyll *a* and chlorophyll *b* (Fig. 19–49a). Although both are green, their absorption spectra are sufficiently different (Fig. 19–50) that they complement each other's range of light absorption in the visible region. Most plants contain about twice as much chlorophyll *a* as chlorophyll *b*. The pigments in

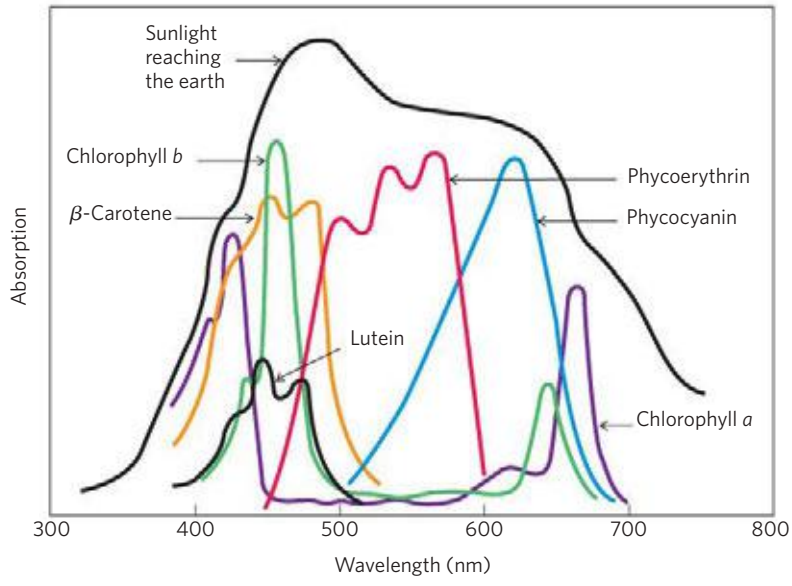

FIGURE 19–50 Absorption of visible light by photopigments. Plants are green because their pigments absorb light from the red and blue regions of the spectrum, leaving primarily green light to be reflected. Compare the absorption spectra of the pigments with the spectrum of sunlight reaching the earth's surface; the combination of chlorophylls (*a* and *b*) and accessory pigments enables plants to harvest most of the energy available in sunlight.

The relative amounts of chlorophylls and accessory pigments are characteristic of a particular plant species. Variation in the proportions of these pigments is responsible for the range of colors of photosynthetic organisms, from the deep blue-green of spruce needles, to the greener green of maple leaves, to the red, brown, or purple color of some species of multicellular algae and the leaves of some foliage plants favored by gardeners.

algae and photosynthetic bacteria include chlorophylls that differ only slightly from the plant pigments.

Chlorophyll is always associated with specific binding proteins, forming **light-harvesting complexes (LHCs)** in which chlorophyll molecules are fixed in relation to each other, to other protein complexes, and to the membrane. One light-harvesting complex (LHCII; **Fig. 19–51**) contains seven molecules of chlorophyll *a*, five of chlorophyll *b*, and two of the accessory pigment lutein (see below).

Cyanobacteria and red algae employ **phycobilins** such as phycoerythrobilin and phycocyanobilin (Fig. 19–49b) as their light-harvesting pigments. These open-chain tetrapyrroles have the extended polyene system found in chlorophylls, but not their cyclic structure or central Mg^{2+}. Phycobilins are covalently linked to specific binding proteins, forming **phycobiliproteins**, which associate in highly ordered complexes called phycobilisomes **(Fig. 19–52)** that constitute the primary light-harvesting structures in these microorganisms.

Accessory Pigments Extend the Range of Light Absorption

In addition to chlorophylls, thylakoid membranes contain secondary light-absorbing pigments, or **accessory pigments**, called carotenoids. **Carotenoids** may be yellow, red, or purple. The most important are **β-carotene**, which is a red-orange isoprenoid, and the yellow carotenoid **lutein** (Fig. 19–49c, d). The carotenoid pigments absorb light at wavelengths not absorbed by the chlorophylls (Fig. 19–50) and thus are supplementary light receptors.

Experimental determination of the effectiveness of light of different colors in promoting photosynthesis

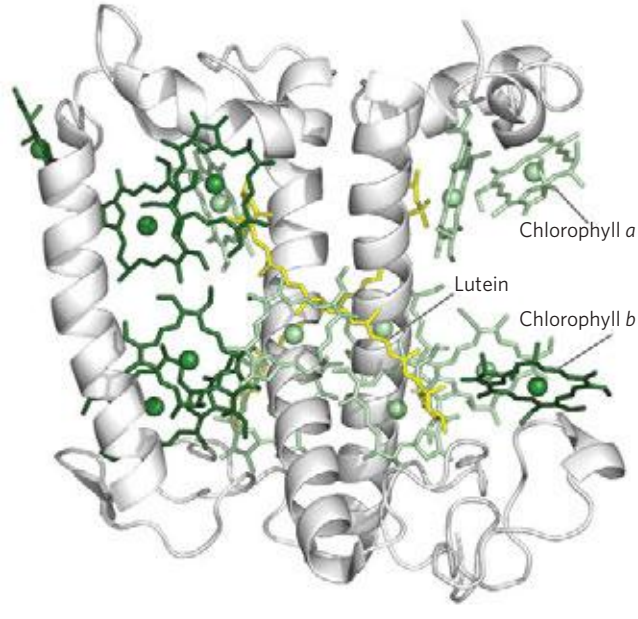

FIGURE 19–51 A light-harvesting complex, LHCII. (PDB ID 2BHW) The functional unit is an LHC trimer, with 36 chlorophyll and 6 lutein molecules. Shown here is a monomer, viewed in the plane of the membrane, with its three transmembrane α-helical segments, seven chlorophyll a molecules (light green), five chlorophyll *b* molecules (dark green), and two molecules of the accessory pigment lutein (yellow), which form an internal cross-brace.

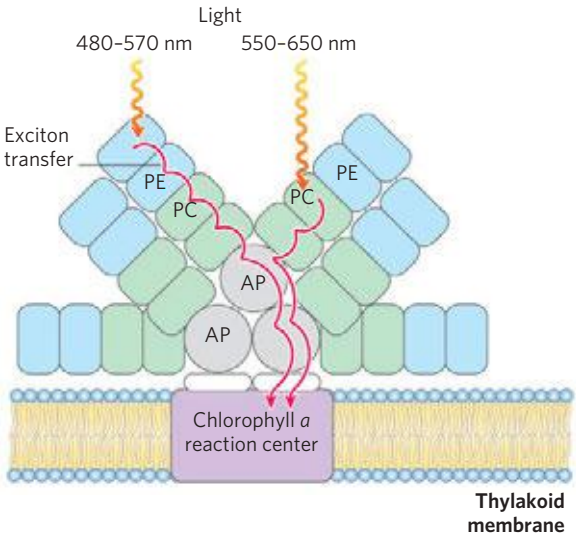

FIGURE 19–52 A phycobilisome. In these highly structured assemblies found in cyanobacteria and red algae, phycobilin pigments bound to specific proteins form complexes called phycoerythrin (PE), phycocyanin (PC), and allophycocyanin (AP). The energy of photons absorbed by PE or PC is conveyed through AP (a phycocyanobilin-binding protein) to chlorophyll *a* of the reaction center by exciton transfer, a process discussed in the text.

yields an **action spectrum** **(Fig. 19–53)**, often useful in identifying the pigment primarily responsible for a biological effect of light. By capturing light in a region of the spectrum not used by other organisms, a photosynthetic organism can claim a unique ecological niche. For example, the phycobilins in red algae and cyanobacteria absorb light in the range 520 to 630 nm (Fig. 19–50), allowing them to occupy niches where light of lower or higher wavelength has been filtered out by the pigments of other organisms living in the water above them, or by the water itself.

Chlorophyll Funnels the Absorbed Energy to Reaction Centers by Exciton Transfer

The light-absorbing pigments of thylakoid or bacterial membranes are arranged in functional arrays called **photosystems**. In spinach chloroplasts, for example, each photosystem contains about 200 chlorophyll and 50 carotenoid molecules. All the pigment molecules in a photosystem can absorb photons, but only a few chlorophyll molecules associated with the **photochemical reaction center** are specialized to transduce light into chemical energy. The other pigment molecules in a photosystem are called **light-harvesting** or **antenna molecules**. They absorb light energy and transmit it rapidly and efficiently to the reaction center **(Fig. 19–54)**.

The chlorophyll molecules in light-harvesting complexes have light-absorption properties that are subtly different from those of free chlorophyll. When isolated chlorophyll molecules in vitro are excited by light, the

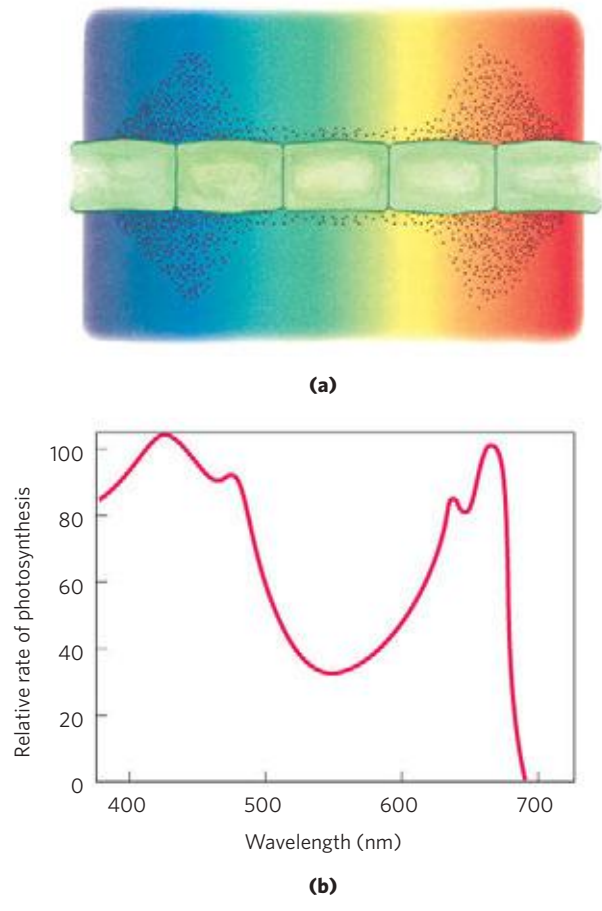

FIGURE 19–53 Two ways to determine the action spectrum for photosynthesis. (a) Results of a classic experiment performed by T. W. Englemann in 1882 to determine the wavelength of light that is most effective in supporting photosynthesis. Englemann placed cells of a filamentous photosynthetic alga on a microscope slide and illuminated them with light from a prism, so that one part of the filament received mainly blue light, another part yellow, another red. To determine which algal cells carried out photosynthesis most actively, Englemann also placed on the microscope slide bacteria known to migrate toward regions of high O_2 concentration. After a period of illumination, the distribution of bacteria showed highest O_2 levels (produced by photosynthesis) in the regions illuminated with violet and red light.

(b) Results of a similar experiment that used modern techniques (an oxygen electrode) for the measurement of O_2 production. An action spectrum (as shown here) describes the relative rate of photosynthesis for illumination with a constant number of photons of different wavelengths. An action spectrum is useful because, by comparison with absorption spectra (such as those in Fig. 19–50), it suggests which pigments can channel energy into photosynthesis.

absorbed energy is quickly released as fluorescence and heat, but when chlorophyll in intact leaves is excited by visible light (**Fig. 19–55**, step ❶), very little fluorescence is observed. Instead, the excited antenna chlorophyll transfers energy directly to a neighboring chlorophyll molecule, which becomes excited as the first molecule returns to its ground state (step ❷). This transfer of energy, exciton transfer, extends to a third, fourth, or subsequent neighbor, until one of a special pair of

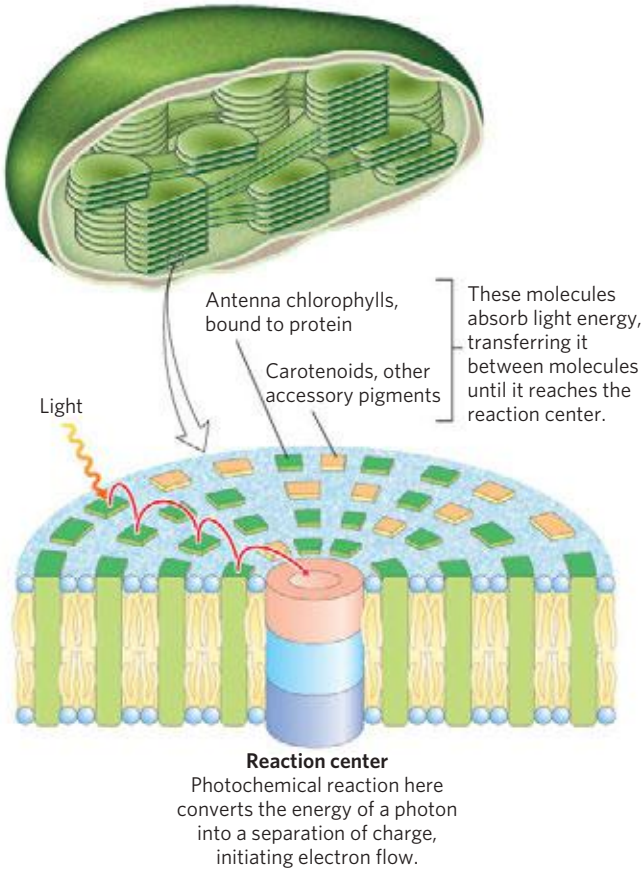

FIGURE 19–54 Organization of photosystems in the thylakoid membrane. Photosystems are tightly packed in the thylakoid membrane, with several hundred antenna chlorophylls and accessory pigments surrounding a photoreaction center. Absorption of a photon by any of the antenna chlorophylls leads to excitation of the reaction center by exciton transfer (red arrow). Also embedded in the thylakoid membrane are the cytochrome b_6f complex and ATP synthase (see Fig. 19–61).

chlorophyll *a* molecules at the photochemical reaction center is excited (step ❸). In this excited chlorophyll molecule, an electron is promoted to a higher-energy orbital. This electron then passes to a nearby electron acceptor that is part of the electron-transfer chain, leaving the reaction-center chlorophyll with a missing electron (an "electron hole," denoted by + in Fig. 19–55) (step ❹). The electron acceptor acquires a negative charge in this transaction. The electron lost by the reaction-center chlorophyll is replaced by an electron from a neighboring electron-donor molecule (step ❺), which thereby becomes positively charged. In this way, *excitation by light causes electric charge separation and initiates an oxidation-reduction chain.*

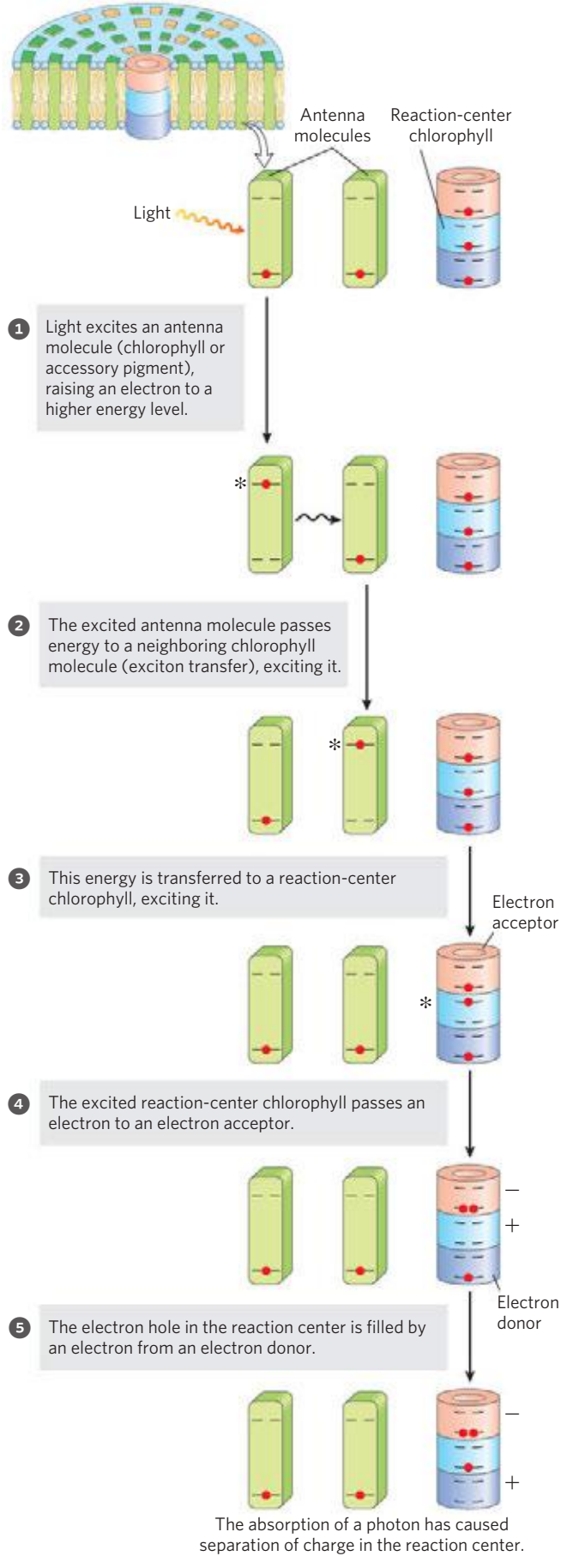

FIGURE 19–55 Exciton and electron transfer. This generalized scheme shows conversion of the energy of an absorbed photon into separation of charges at the reaction center. The steps are further described in the text. Note that step ❶ may repeat between successive antenna molecules until the exciton reaches a reaction-center chlorophyll. The asterisk (*) represents the excited state of a molecule.

SUMMARY 19.7 Light Absorption

- A photon of visible light possesses enough energy to bring about photochemical reactions, which in photosynthetic organisms lead eventually to ATP synthesis.
- In the light reactions of plants, absorption of a photon excites chlorophyll molecules and other (accessory) pigments, which funnel the energy into reaction centers in the thylakoid membranes. In the reaction centers, photoexcitation results in a charge separation that produces a strong electron donor (reducing agent) and a strong electron acceptor.

19.8 The Central Photochemical Event: Light-Driven Electron Flow

Light-driven electron transfer in plant chloroplasts during photosynthesis is accomplished by multienzyme systems in the thylakoid membrane. Our current picture of photosynthetic mechanisms is a composite, drawn from studies of plant chloroplasts and a variety of bacteria and algae. Determination of the molecular structures of bacterial photosynthetic complexes (by x-ray crystallography) has given us a much improved understanding of the molecular events in photosynthesis in general.

Bacteria Have One of Two Types of Single Photochemical Reaction Center

One major insight from studies of photosynthetic bacteria came in 1952 when Louis Duysens found that illumination of the photosynthetic membranes of the purple bacterium *Rhodospirillum rubrum* with a pulse of light of a specific wavelength (870 nm) caused a temporary decrease in the absorption of light at that wavelength; a pigment was "bleached" by 870 nm light. Later studies by Bessel Kok and Horst Witt showed similar bleaching of plant chloroplast pigments by light of 680 and 700 nm. Furthermore, addition of the (nonbiological) electron acceptor $[Fe(CN)_6]^{3-}$ (ferricyanide) caused bleaching at these wavelengths *without illumination*. These findings indicated that bleaching of the pigments was due to the loss of an electron from a photochemical reaction center. The pigments were named for the wavelength of maximum bleaching: P870, P680, and P700.

Photosynthetic bacteria have relatively simple phototransduction machinery, with one of two general types of reaction center. One type (found in purple bacteria) passes electrons through **pheophytin** (chlorophyll lacking the central Mg^{2+} ion) to a quinone. The other (in green sulfur bacteria) passes electrons through a quinone to an iron-sulfur center. Cyanobacteria and plants have two photosystems (PSI, PSII), one of each type, acting in tandem. Biochemical and biophysical studies have revealed many of the molecular details of reaction centers of bacteria, which therefore serve as prototypes for the more complex phototransduction systems of plants.

The Pheophytin-Quinone Reaction Center (Type II Reaction Center) The photosynthetic machinery in purple bacteria consists of three basic modules **(Fig. 19–56a)**: a single reaction center (P870), a cytochrome bc_1 electron-transfer complex similar to Complex III of the mitochondrial electron-transfer chain, and an ATP synthase, also similar to that of mitochondria. Illumination drives electrons through pheophytin and a quinone to the cytochrome bc_1 complex; after passing through the complex, electrons flow through cytochrome c_2 back to the reaction center, restoring its preillumination state. This light-driven cyclic flow of electrons provides the energy for proton pumping by the cytochrome bc_1 complex. Powered by the resulting proton gradient, ATP synthase produces ATP, exactly as in mitochondria.

The three-dimensional structures of the reaction centers of purple bacteria (*Rhodopseudomonas viridis* and *Rhodobacter sphaeroides*), deduced from x-ray crystallography, shed light on how phototransduction takes place in a pheophytin-quinone reaction center. The *R. viridis* reaction center **(Fig. 19–57a)** is a large protein complex containing four polypeptide subunits and 13 cofactors: two pairs of bacterial chlorophylls, a pair of pheophytins, two quinones, a nonheme iron, and four hemes in the associated *c*-type cytochrome.

The extremely rapid sequence of electron transfers shown in Figure 19–57b has been deduced from physical studies of the bacterial pheophytin-quinone centers, using brief flashes of light to trigger phototransduction and a variety of spectroscopic techniques to follow the flow of electrons through several carriers. A pair of bacteriochlorophylls—the "special pair," designated $(Chl)_2$—is the site of the initial photochemistry in the bacterial reaction center. Energy from a photon absorbed by one of the many antenna chlorophyll molecules surrounding the reaction center reaches $(Chl)_2$ by exciton transfer. When these two chlorophyll molecules—so close that their bonding orbitals overlap—absorb an exciton, the redox potential of $(Chl)_2$ is shifted, by an amount equivalent to the energy of the photon, converting the special pair to a very strong electron donor. The $(Chl)_2$ donates an electron that passes through a neighboring chlorophyll monomer to pheophytin (Pheo). This produces two radicals, one positively charged (the special pair of chlorophylls) and one negatively charged (the pheophytin):

$$(Chl)_2 + 1 \text{ exciton} \longrightarrow (Chl)_2^* \qquad \text{(excitation)}$$

$$(Chl)_2^* + Pheo \longrightarrow {}^{\bullet}(Chl)_2^+ + {}^{\bullet}Pheo^- \qquad \text{(charge separation)}$$

The pheophytin radical now passes its electron to a tightly bound molecule of quinone (Q_A), converting it to

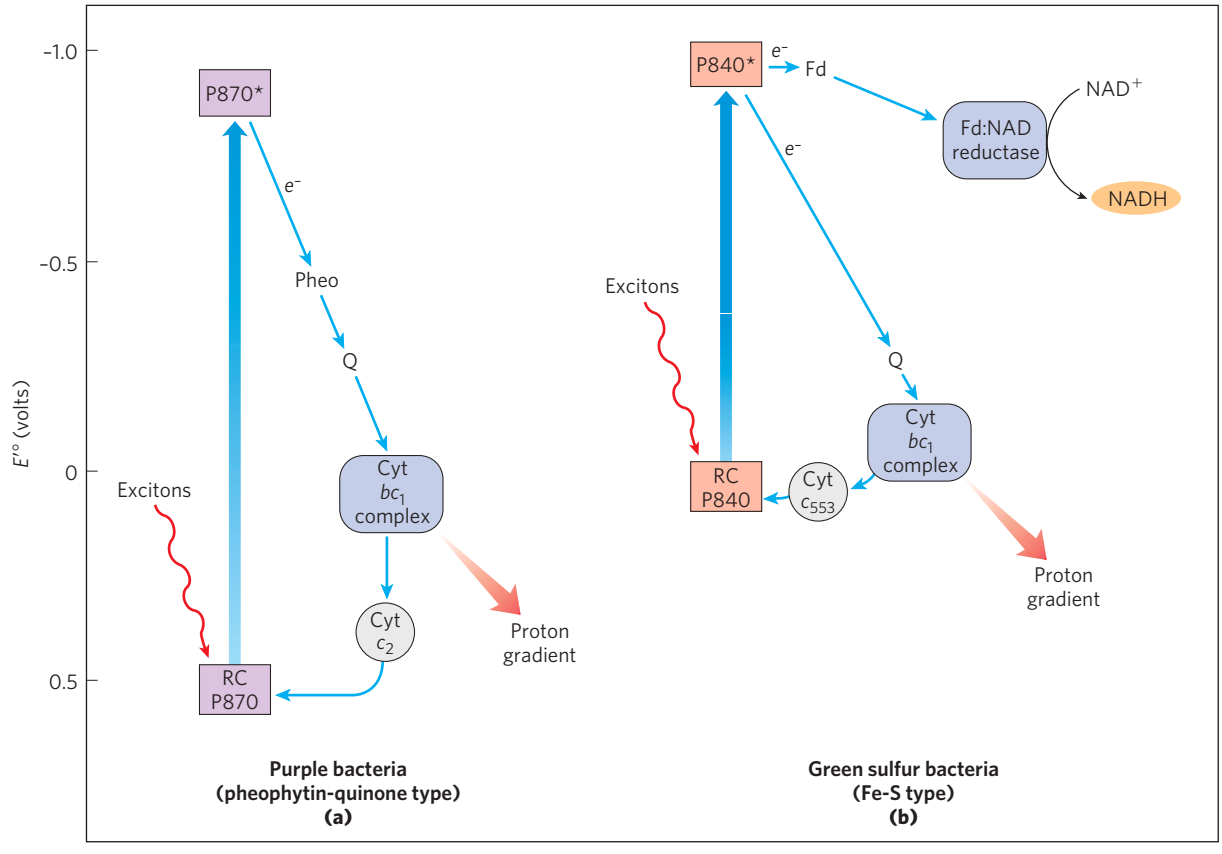

FIGURE 19–56 Functional modules of photosynthetic machinery in purple bacteria and green sulfur bacteria. (a) In purple bacteria, light energy drives electrons from the reaction-center P870 through pheophytin (Pheo), a quinone (Q), and the cytochrome bc_1 complex, then through cytochrome c_2 and thus back to the reaction center. Electron flow through the cytochrome bc_1 complex causes proton pumping, creating an electrochemical potential that powers ATP synthesis. **(b)** Green sulfur bacteria have two routes for electrons driven by excitation of P840: a cyclic route through a quinone to the cytochrome bc_1 complex and back to the reaction center via cytochrome *c*, and a noncyclic route from the reaction center through the iron-sulfur protein ferredoxin (Fd), then to NAD^+ in a reaction catalyzed by ferredoxin:NAD reductase.

a semiquinone radical, which immediately donates its extra electron to a second, loosely bound quinone (Q_B). Two such electron transfers convert Q_B to its fully reduced form, Q_BH_2, which is free to diffuse in the membrane bilayer, away from the reaction center:

$$2\ {}^{\bullet}\text{Pheo}^- + 2H^+ + Q_B \longrightarrow 2\ \text{Pheo} + Q_BH_2$$
(quinone reduction)

The hydroquinone (Q_BH_2), carrying in its chemical bonds some of the energy of the photons that originally excited P870, enters the pool of reduced quinone (QH_2) dissolved in the membrane and moves through the lipid phase of the bilayer to the cytochrome bc_1 complex.

Like the homologous Complex III in mitochondria, the cytochrome bc_1 complex of purple bacteria carries electrons from a quinol donor (QH_2) to an electron acceptor, using the energy of electron transfer to pump protons across the membrane, producing a proton-motive force. The path of electron flow through this complex is believed to be very similar to that through mitochondrial Complex III, involving a Q cycle (Fig. 19–12) in which protons are consumed on one side of the membrane and released on the other. The ultimate electron acceptor in purple bacteria is the electron-depleted form of P870, ${}^{\bullet}(\text{Chl})_2^+$ (Fig. 19–56a). Electrons move from the cytochrome bc_1 complex to P870 via a soluble *c*-type cytochrome, cytochrome c_2. The electron-transfer process completes the cycle, returning the reaction center to its unbleached state, ready to absorb another exciton from antenna chlorophyll.

A remarkable feature of this system is that all the chemistry occurs in the *solid state*, with reacting species held close together in the right orientation for reaction. The result is a very fast and efficient series of reactions.

The Fe-S Reaction Center (Type I Reaction Center) Photosynthesis in green sulfur bacteria involves the same three modules as in purple bacteria, but the process differs in several respects and involves additional enzymatic reactions (Fig. 19–56b). Excitation causes an electron to move from the reaction center to the cytochrome bc_1 complex via a quinone carrier. Electron transfer through this complex powers proton transport and creates the proton-motive force used for ATP synthesis, just as in

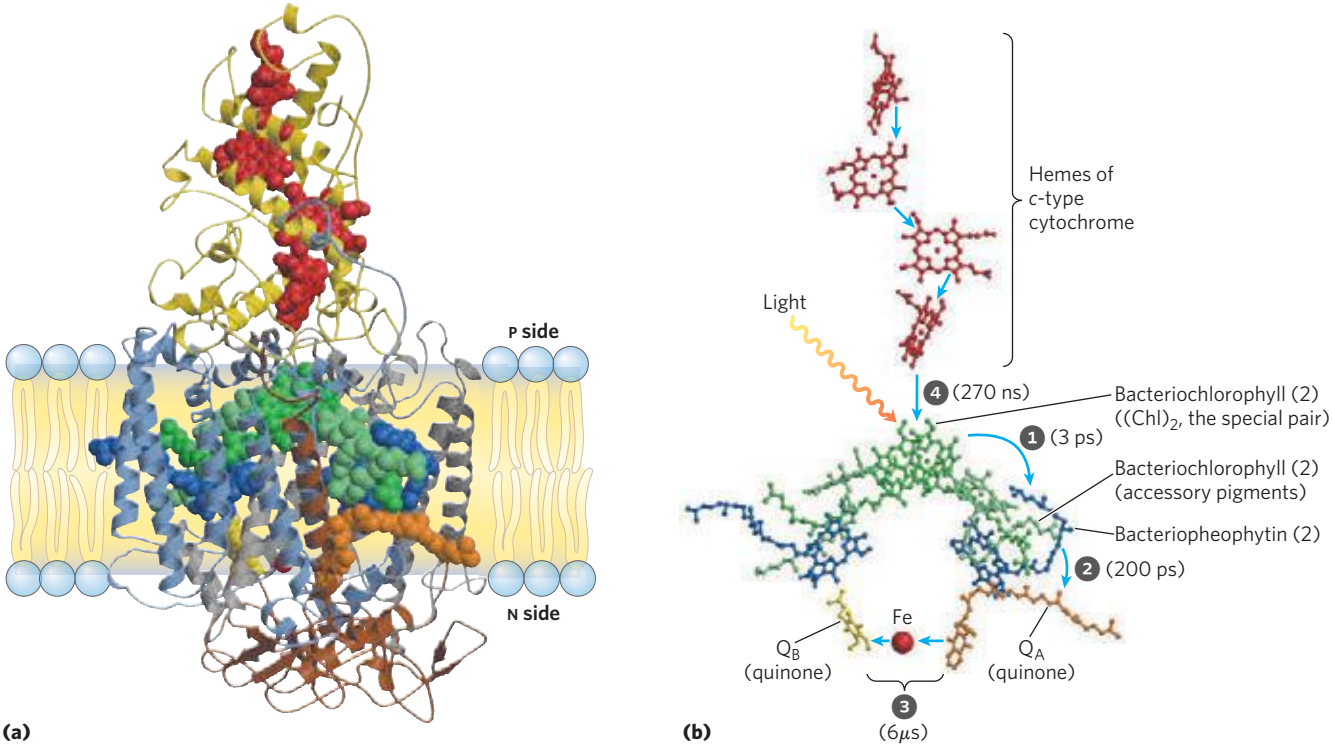

FIGURE 19–57 Photoreaction center of the purple bacterium *Rhodopseudomonas viridis*. (PDB ID 1PRC) **(a)** The system has four components: three subunits, H, M, and L (brown, blue, and gray, respectively), with a total of 11 transmembrane helical segments, and a fourth protein, cytochrome *c* (yellow), associated with the complex at the membrane surface. Subunits L and M are paired transmembrane proteins that together form a cylindrical structure with roughly bilateral symmetry about its long axis. Shown as space-filling models (and in (b) as ball-and-stick structures) are the prosthetic groups that participate in the photochemical events. Bound to the L and M chains are two pairs of bacteriochlorophyll molecules (green); one of the pairs—the "special pair," $(Chl)_2$—is the site of the first photochemical changes after light absorption. Also incorporated in the system are a pair of pheophytin *a* (Pheo *a*) molecules (blue); two quinones, menaquinone (Q_A) and ubiquinone (Q_B) (orange and yellow), also arranged with bilateral symmetry; and a single nonheme Fe (red) located approximately on the axis of symmetry between the quinones. Shown at the top of the figure are four heme groups (red) associated with the *c*-type cytochrome of the reaction center

(b) Sequence of events following excitation of the special pair of bacteriochlorophylls (all components colored as in (a)), with the time scale of the electron transfers in parentheses. ❶ The excited special pair passes an electron to pheophytin, ❷ from which the electron moves rapidly to the tightly bound menaquinone, Q_A. ❸ This quinone passes electrons much more slowly to the diffusible ubiquinone, Q_B, through the nonheme Fe. Meanwhile, ❹ the "electron hole" in the special pair is filled by an electron from a heme of cytochrome *c*.

purple bacteria and in mitochondria. However, in contrast to the cyclic flow of electrons in purple bacteria, some electrons flow from the reaction center to an iron-sulfur protein, **ferredoxin**, which then passes electrons via ferredoxin:NAD reductase to NAD^+, producing NADH. The electrons taken from the reaction center to reduce NAD^+ are replaced by the oxidation of H_2S to elemental S, then to SO_4^{2-}, in the reaction that defines the green sulfur bacteria. This oxidation of H_2S by bacteria is chemically analogous to the oxidation of H_2O by oxygenic plants.

Kinetic and Thermodynamic Factors Prevent the Dissipation of Energy by Internal Conversion

The complex construction of reaction centers is the product of evolutionary selection for efficiency in the photosynthetic process. The excited state $(Chl)_2^*$ could in principle decay to its ground state by internal conversion, a very rapid process (10 picoseconds; 1 ps = 10^{-12} s) in which the energy of the absorbed photon is converted to heat (molecular motion). Reaction centers are constructed to prevent the inefficiency that would result from internal conversion. The proteins of the reaction center hold the bacteriochlorophylls, bacteriopheophytins, and quinones in a fixed orientation relative to each other, allowing the photochemical reactions to take place in a virtually solid state. This accounts for the high efficiency and rapidity of the reactions; nothing is left to chance collision or random diffusion. Exciton transfer from antenna chlorophyll to the special pair of the reaction center is accomplished in less than 100 ps with >90% efficiency. Within 3 ps of the excitation of P870, pheophytin has received an electron and become a negatively charged radical; less than 200 ps later, the electron has reached the quinone Q_B (Fig. 19–57b). The electron-transfer reactions not only are fast but are thermodynamically "downhill"; the excited special pair $(Chl)_2^*$ is a

very good electron donor ($E'^\circ = -1\,\text{V}$) and each successive electron transfer is to an acceptor of substantially less negative E'°. The standard free-energy change for the process is therefore negative and large; recall from Chapter 13 that $\Delta G'^\circ = -n\,\Delta E'^\circ$; here, $\Delta E'^\circ$ is the difference between the standard reduction potentials of the two half-reactions

$$(1)\ (\text{Chl})_2^* \longrightarrow {}^\bullet(\text{Chl})_2^+ + e^- \quad E'^\circ = -1.0\,\text{V}$$
$$(2)\ \text{Q} + 2\text{H}^+ + 2e^- \longrightarrow \text{QH}_2 \quad E'^\circ = -0.045\,\text{V}$$

Thus

$$\Delta E'^\circ = -0.045\,\text{V} - (-1.0\,\text{V}) \approx 0.95\,\text{V}$$

and

$$\Delta G'^\circ = -2(96.5\,\text{kJ/V}\cdot\text{mol})(0.95\,\text{V}) = -180\,\text{kJ/mol}$$

The combination of fast kinetics and favorable thermodynamics makes the process virtually irreversible and highly efficient. The overall energy yield (the percentage of the photon's energy conserved in QH_2) is >30%, with the remainder of the energy dissipated as heat and entropy.

In Plants, Two Reaction Centers Act in Tandem

The photosynthetic apparatus of modern cyanobacteria, algae, and vascular plants is more complex than the one-center bacterial systems, and it seems to have evolved through the combination of two simpler bacterial photocenters. The thylakoid membranes of chloroplasts have two different kinds of photosystems, each with its own type of photochemical reaction center and set of antenna molecules. The two systems have distinct and complementary functions **(Fig. 19–58)**. **Photosystem II (PSII)** is a pheophytin-quinone type of system (like the single photosystem of purple bacteria) containing roughly equal amounts of chlorophylls *a* and *b*. Excitation of its reaction-center P680 drives electrons through the cytochrome b_6f complex with concomitant movement of protons across the thylakoid

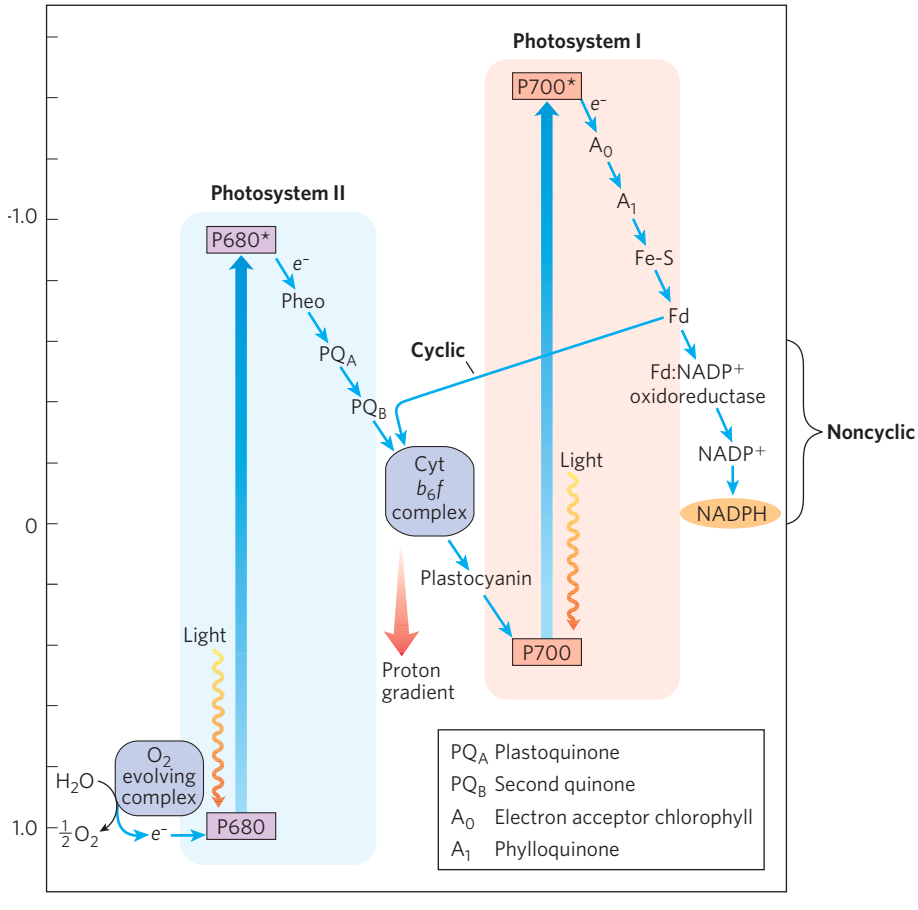

FIGURE 19–58 Integration of photosystems I and II in chloroplasts. This "Z scheme" shows the pathway of electron transfer from H_2O (lower left) to $NADP^+$ (far right) in noncyclic photosynthesis. The position on the vertical scale of each electron carrier reflects its standard reduction potential. To raise the energy of electrons derived from H_2O to the energy level required to reduce $NADP^+$ to NADPH, each electron must be "lifted" twice (heavy arrows) by photons absorbed in PSII and PSI. One photon is required per electron in each photosystem. After excitation, the high-energy electrons flow "downhill" through the carrier chains shown. Protons move across the thylakoid membrane during the water-splitting reaction and during electron transfer through the cytochrome b_6f complex, producing the proton gradient that is essential to ATP formation. An alternative path of electrons is cyclic electron transfer, in which electrons move from ferredoxin back to the cytochrome b_6f complex, instead of reducing $NADP^+$ to NADPH. The cyclic pathway produces more ATP and less NADPH than the noncyclic.

membrane. **Photosystem I (PSI)** is structurally and functionally related to the type I reaction center of green sulfur bacteria. It has a reaction center designated P700 and a high ratio of chlorophyll *a* to chlorophyll *b*. Excited P700 passes electrons to the Fe-S protein ferredoxin, then to $NADP^+$, producing NADPH. The thylakoid membranes of a single spinach chloroplast have many hundreds of each kind of photosystem.

These two reaction centers in plants act in tandem to catalyze the light-driven movement of electrons from H_2O to $NADP^+$ (Fig. 19–58). Electrons are carried between the two photosystems by the soluble protein **plastocyanin**, a one-electron carrier functionally similar to cytochrome *c* of mitochondria. To replace the electrons that move from PSII through PSI to $NADP^+$, cyanobacteria and plants oxidize H_2O (as green sulfur bacteria oxidize H_2S), producing O_2 (Fig. 19–58, bottom left). This process is called **oxygenic photosynthesis** to distinguish it from the anoxygenic photosynthesis of purple and green sulfur bacteria. All O_2-evolving photosynthetic cells—those of plants, algae, and cyanobacteria—contain both PSI and PSII; organisms with only one photosystem do not evolve O_2. The diagram in Figure 19–58, often called the **Z scheme** because of its overall form, outlines the pathway of electron flow between the two photosystems and the energy relationships in the light reactions. The Z scheme thus describes the complete route by which electrons flow from H_2O to $NADP^+$, according to the equation

$$2H_2O + 2NADP^+ + 8\,\text{photons} \longrightarrow O_2 + 2NADPH + 2H^+$$

For every two photons absorbed (one by each photosystem), one electron is transferred from H_2O to $NADP^+$. To form one molecule of O_2, which requires transfer of four electrons from two H_2O to two $NADP^+$, a total of eight photons must be absorbed, four by each photosystem.

The mechanistic details of the photochemical reactions in PSII and PSI are essentially similar to those of the two bacterial photosystems, with several important additions. In PSII, two very similar proteins, D1 and D2, form an almost symmetric dimer, to which all the electron-carrying cofactors are bound **(Fig. 19–59)**. Excitation of P680 in PSII produces $P680^*$, an excellent electron donor that, within picoseconds, transfers an electron to pheophytin, giving it a negative charge ($^\bullet Pheo^-$). With the loss of its electron, $P680^*$ is transformed into a radical cation, $P680^+$. $^\bullet Pheo^-$ very rapidly passes its extra electron to a protein-bound **plastoquinone**, $\mathbf{PQ_A}$ (or Q_A), which in turn passes its electron to another, more loosely bound plastoquinone, PQ_B (or Q_B). When PQ_B has acquired two electrons in two such transfers from PQ_A and two protons from the solvent water, it is in its fully reduced quinol form, PQ_BH_2. The overall reaction initiated by light in PSII is

$$4\,P680 + 4H^+ + 2\,PQ_B + 4\,\text{photons} \longrightarrow 4\,P680^+ + 2\,PQ_BH_2 \quad (19\text{–}12)$$

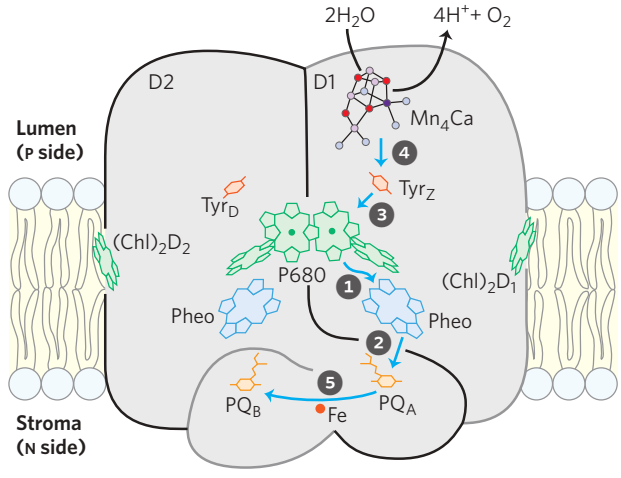

FIGURE 19–59 Photosystem II of the cyanobacterium *Synechococcus elongates*. The monomeric form of the complex shown here has two major transmembrane proteins, D1 and D2, each with its set of cofactors. Although the two subunits are nearly symmetric, electron flow occurs through only one of the two branches of cofactors, that on the right (on D1). The arrows show the path of electron flow from the Mn_4Ca ion cluster of the water-splitting enzyme to the quinone PQ_B. The photochemical events occur in the sequence indicated by the step numbers. Notice the close similarity between the positions of cofactors here and the positions in the bacterial photoreaction center shown in Figure 19–57. The role of the Tyr residues and the detailed structure of the Mn_4Ca cluster are discussed later (see Fig. 19–64b).

Eventually, the electrons in PQ_BH_2 pass through the cytochrome b_6f complex (Fig. 19–58). The electron initially removed from P680 is replaced with an electron obtained from the oxidation of water, as described below. The binding site for plastoquinone is the point of action of many commercial herbicides that kill plants by blocking electron transfer through the cytochrome b_6f complex and preventing photosynthetic ATP production.

The photochemical events that follow excitation of PSI at the reaction-center P700 are formally similar to those in PSII. The excited reaction-center $P700^*$ loses an electron to an acceptor, A_0 (believed to be a special form of chlorophyll, functionally homologous to the pheophytin of PSII), creating A_0^- and $P700^+$ (Fig. 19–58, right side); again, excitation results in charge separation at the photochemical reaction center. $P700^+$ is a strong oxidizing agent, which quickly acquires an electron from plastocyanin, a soluble Cu-containing electron-transfer protein. A_0^- is an exceptionally strong reducing agent that passes its electron through a chain of carriers that leads to $NADP^+$. First, **phylloquinone** (A_1) accepts an electron and passes it to an iron-sulfur protein (through three Fe-S centers in PSI). From here, the electron moves to **ferredoxin** (Fd), another iron-sulfur protein loosely associated with the thylakoid membrane. Spinach ferredoxin (M_r 10,700) contains a 2Fe-2S center (Fig. 19–5) that undergoes one-electron oxidation and reduction reactions. The fourth electron carrier in the chain is the flavoprotein

ferredoxin:NADP$^+$ oxidoreductase, which transfers electrons from reduced ferredoxin (Fd_{red}) to $NADP^+$:

$$2Fd_{red} + 2H^+ + NADP^+ \longrightarrow 2Fd_{ox} + NADPH + H^+$$

This enzyme is homologous to the ferredoxin:NAD reductase of green sulfur bacteria (Fig. 19–56b).

Antenna Chlorophylls Are Tightly Integrated with Electron Carriers

The electron-carrying cofactors of PSI and the light-harvesting complexes are part of a supramolecular complex **(Fig. 19–60a)**, the structure of which has been

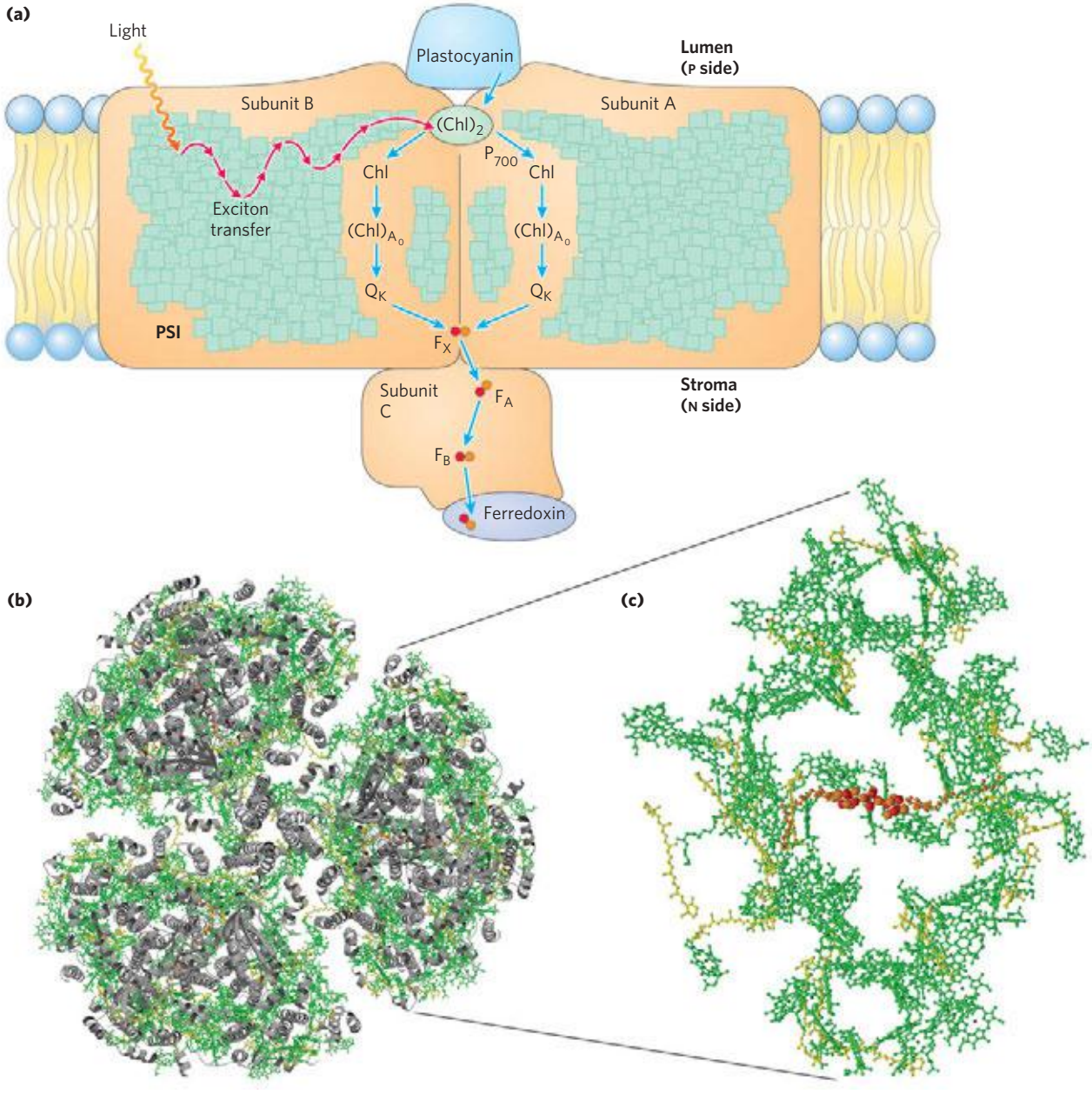

FIGURE 19–60 The supramolecular complex of PSI and its associated antenna chlorophylls. (a) Schematic drawing of the essential proteins and cofactors in a single unit of PSI. A large number of antenna chlorophylls surround the reaction center and convey to it (red arrows) the energy of absorbed photons. The result is excitation of the pair of chlorophyll molecules that constitute P700, greatly decreasing its reduction potential; P700 then passes an electron through two nearby chlorophylls to phylloquinone (Q_K; also called A_1). Reduced phylloquinone is reoxidized as it passes two electrons, one at a time (blue arrows), to an Fe-S protein (F_X) near the N side of the membrane. From F_X, electrons move through two more Fe-S centers (F_A and F_B) to the Fe-S protein ferredoxin in the stroma. Ferredoxin then donates electrons to $NADP^+$ (not shown), reducing it to NADPH, one of the forms in which the energy of photons is trapped in chloroplasts.

(b) The trimeric structure (derived from PDB ID 1JBO), viewed from the thylakoid lumen perpendicular to the membrane, showing all protein subunits (gray) and cofactors. **(c)** A monomer of PSI with all the proteins omitted, revealing the antenna and reaction-center chlorophylls (green with dark green Mg^{2+} ions in the center), carotenoids (yellow), and Fe-S centers of the reaction center (space-filling red and orange structures). The proteins in the complex hold the components rigidly in orientations that maximize efficient exciton transfers between excited antenna molecules and the reaction center.

solved crystallographically. The protein consists of three identical complexes, each composed of 11 different proteins (Fig. 19–60b). In this remarkable structure the many antenna chlorophyll and carotenoid molecules are precisely arrayed around the reaction center (Fig. 19–60c). The reaction center's electron-carrying cofactors are therefore tightly integrated with antenna chlorophylls. This arrangement allows very rapid and efficient exciton transfer from antenna chlorophylls to the reaction center. In contrast to the single path of electrons in PSII, the electron flow initiated by absorption of a photon is believed to occur through both branches of carriers in PSI.

The Cytochrome b_6f Complex Links Photosystems II and I

Electrons temporarily stored in plastoquinol as a result of the excitation of P680 in PSII are carried to P700 of PSI via the cytochrome b_6f complex and the soluble protein plastocyanin (Fig. 19–58, center). Like Complex III of mitochondria, the cytochrome b_6f complex **(Fig. 19–61)** contains a *b*-type cytochrome with two heme groups (designated b_H and b_L), a Rieske iron-sulfur protein (M_r 20,000), and cytochrome *f* (named for the Latin *frons*, "leaf"). Electrons flow through the cytochrome

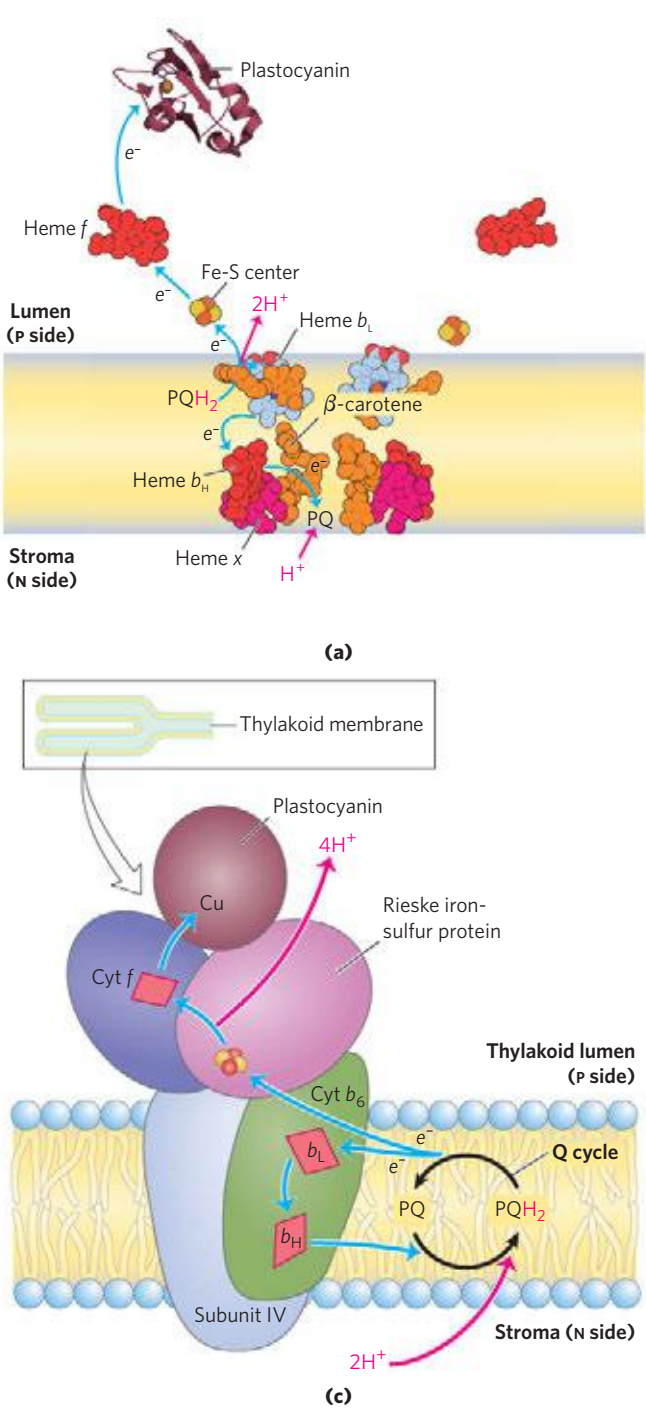

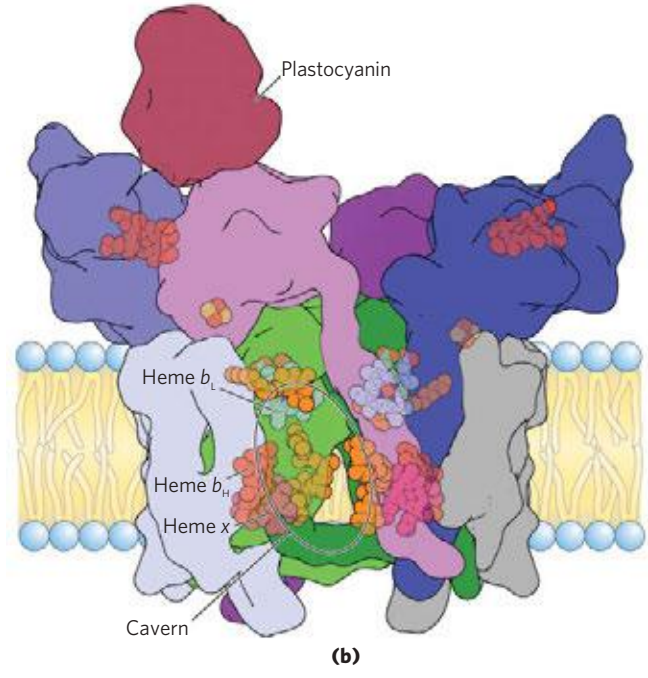

FIGURE 19–61 Electron and proton flow through the cytochrome b_6f complex. (a) The crystal structure of the complex (PDB ID 1FV5) reveals the positions of the cofactors involved in electron transfers. In addition to the hemes of cytochrome *b* (heme b_H and b_L; also called heme b_N and b_P, respectively, because of their proximity to the N and P sides of the bilayer) and cytochrome *f* (heme *f*), there is a fourth (heme *x*) near heme b_H; there is also a β-carotene of unknown function. Two sites bind plastoquinone: the PQH_2 site near the P side of the bilayer, and the PQ site near the N side. The Fe-S center of the Rieske protein lies just outside the bilayer on the P side, and the heme *f* site is on a protein domain that extends well into the thylakoid lumen. The electron path is shown for one of the monomers, but both sets of carriers in the dimer carry electrons to plastocyanin (PDB ID 2Q5B). **(b)** The complex is a homodimer arranged to create a cavern connecting the PQH_2 and PQ sites (compare this with the structure of mitochondrial Complex III in Fig. 19–11). This cavern allows plastoquinone to move between the sites of its oxidation and reduction.

(c) Plastoquinol (PQH_2) formed in PSII is oxidized by the cytochrome b_6f complex in a series of steps like those of the Q cycle in the cytochrome bc_1 complex (Complex III) of mitochondria (see Fig. 19–12). One electron from PQH_2 passes to the Fe-S center of the Rieske protein, the other to heme b_L of cytochrome b_6. The net effect is passage of electrons from PQH_2 to the soluble protein plastocyanin, which carries them to PSI.

b_6f complex from PQ_BH_2 to cytochrome *f*, then to plastocyanin, and finally to P700, thereby reducing it.

Like Complex III of mitochondria, cytochrome b_6f conveys electrons from a reduced quinone—a mobile, lipid-soluble carrier of two electrons (Q in mitochondria, PQ_B in chloroplasts)—to a water-soluble protein that carries one electron (cytochrome *c* in mitochondria, plastocyanin in chloroplasts). As in mitochondria, the function of this complex involves a Q cycle (Fig. 19–12) in which electrons pass, one at a time, from PQ_BH_2 to cytochrome b_6. This cycle results in the pumping of protons across the membrane; in chloroplasts, the direction of proton movement is from the stromal compartment to the thylakoid lumen, up to four protons moving for each pair of electrons. The result is production of a proton gradient across the thylakoid membrane as electrons pass from PSII to PSI. Because the volume of the flattened thylakoid lumen is small, the influx of a small number of protons has a relatively large effect on lumenal pH. The measured difference in pH between the stroma (pH 8) and the thylakoid lumen (pH 5) represents a 1,000-fold difference in proton concentration—a powerful driving force for ATP synthesis.

Cyclic Electron Flow between PSI and the Cytochrome b_6f Complex Increases the Production of ATP Relative to NADPH

Electron flow from PSII through the cytochrome b_6f complex, then through PSI to $NADP^+$, is sometimes called **noncyclic electron flow**, to distinguish it from **cyclic electron flow**, which occurs to varying degrees depending primarily on the light conditions. The noncyclic path produces a proton gradient, which is used to drive ATP synthesis, and NADPH, which is used in reductive biosynthetic processes. Cyclic electron flow involves only PSI, not PSII (Fig. 19–58). Electrons passing from P700 to ferredoxin do not continue to $NADP^+$, but move back through the cytochrome b_6f complex to plastocyanin. (This electron path parallels that in green sulfur bacteria, shown in Fig. 19–56b.) Plastocyanin then donates electrons to P700, which transfers them to ferredoxin. In this way, electrons are repeatedly recycled through the cytochrome b_6f complex and the reaction center of PSI, each electron propelled around the cycle by the energy of one photon. Cyclic electron flow is not accompanied by net formation of NADPH or evolution of O_2. However, it *is* accompanied by proton pumping by the cytochrome b_6f complex and by phosphorylation of ADP to ATP, referred to as **cyclic photophosphorylation**. The overall equation for cyclic electron flow and photophosphorylation is simply

$$ADP + P_i \xrightarrow{\text{light}} ATP + H_2O$$

By regulating the partitioning of electrons between $NADP^+$ reduction and cyclic photophosphorylation, a plant adjusts the ratio of ATP to NADPH produced in the light-dependent reactions to match its needs for these products in the carbon-assimilation reactions and other biosynthetic processes. As we shall see in Chapter 20, the carbon-assimilation reactions require ATP and NADPH in the ratio 3:2.

This regulation of electron-transfer pathways is part of a short-term adaptation to changes in light color (wavelength) and quantity (intensity), as further described below.

State Transitions Change the Distribution of LHCII between the Two Photosystems

The energy required to excite PSI (P700) is less (light of longer wavelength, lower energy) than that needed to excite PSII (P680). If PSI and PSII were physically contiguous, excitons originating in the antenna system of PSII would migrate to the reaction center of PSI, leaving PSII chronically underexcited and interfering with the operation of the two-center system. This imbalance in the supply of excitons is prevented by separation of the two photosystems in the thylakoid membrane **(Fig. 19–62)**. PSII is located almost exclusively in the tightly appressed membrane stacks of thylakoid grana; its associated light-harvesting complex (LHCII) mediates the tight association of adjacent membranes in the grana. PSI and the ATP synthase complex are located almost exclusively in the nonappressed thylakoid membranes (the stromal lamellae), where they have access to the contents of the stroma, including ADP and $NADP^+$. The cytochrome b_6f complex is present primarily in the grana.

The association of LHCII with PSI and PSII depends on light intensity and wavelength, which can change in the short term, leading to **state transitions** in the chloroplast. In state 1, a critical Ser residue in LCHII is not phosphorylated, and LHCII associates with PSII. Under conditions of intense or blue light, which favor absorption by PSII, that photosystem reduces plastoquinone to plastoquinol (PQH_2) faster than PSI can oxidize it. The resulting accumulation of PQH_2 activates a protein kinase that triggers the transition to state 2 by phosphorylating a Thr residue on LHCII **(Fig. 19–63)**. Phosphorylation weakens the interaction of LHCII with PSII, and some LHCII dissociates and moves to the stromal lamellae; here it captures photons (excitons) for PSI, speeding the oxidation of PQH_2 and reversing the imbalance between electron flow in PSI and PSII. In less intense light (in the shade, with more red light), PSI oxidizes PQH_2 faster than PSII can make it, and the resulting increase in [PQ] triggers dephosphorylation of LHCII, reversing the effect of phosphorylation.

The state transition in LCHII localization is mutually regulated with the transition from cyclic to noncyclic photophosphorylation, described above; the path of electrons is primarily noncyclic in state 1 and primarily cyclic in state 2.

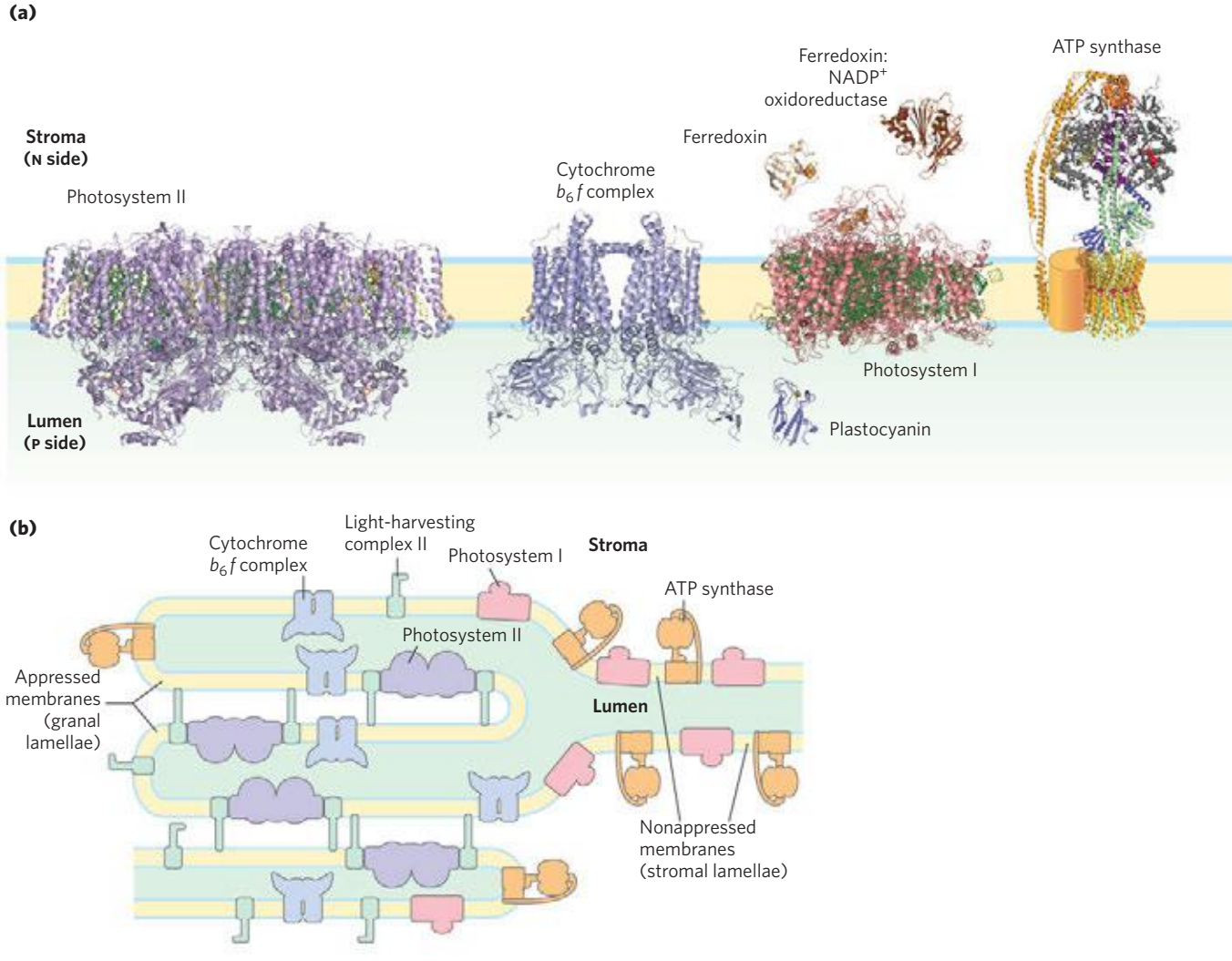

FIGURE 19–62 Localization of PSI and PSII in thylakoid membranes. **(a)** The structures of the complexes and soluble proteins of the photosynthetic apparatus of a vascular plant or alga, drawn to the same scale. The structures are photosystem II (PDB ID 2AXT), cytochrome b_{6f}, complex (PDB ID 2E74), plastocyanin (PDB ID 1AG6), photosystem I (PDB ID 1QZV), ferredoxin (PDB ID 1A70), and ferredoxin:NADP reductase (PDB ID 1QG0). The ATP synthase is the composite shown in Figure 19–25c. **(b)** Light-harvesting complex LHCII and ATP synthase are located both in appressed regions of the thylakoid membrane (granal lamellae, in which several membranes are in contact) and in nonappressed regions (stromal lamellae), and have ready access to ADP and $NADP^+$ in the stroma. PSII is present almost exclusively in the appressed regions, and PSI almost exclusively in nonappressed regions, exposed to the stroma. LHCII is the "adhesive" that holds appressed lamellae together (see Fig. 19–63).

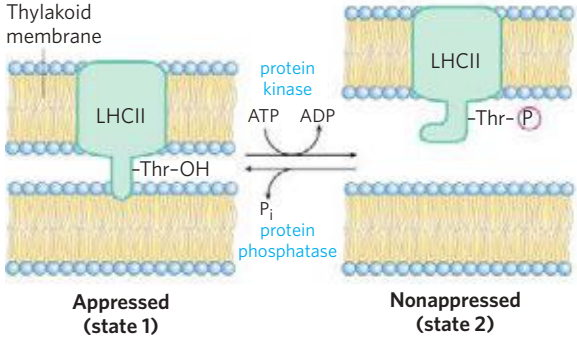

FIGURE 19–63 Balancing of electron flow in PSI and PSII by state transition. A hydrophobic domain of LHCII in one thylakoid lamella inserts into the neighboring lamella and closely appresses the two membranes (state 1). Accumulation of plastoquinol (not shown) stimulates a protein kinase that phosphorylates a Thr residue in the hydrophobic domain of LHCII, which reduces its affinity for the neighboring thylakoid membrane and converts appressed regions to nonappressed regions (state 2). A specific protein phosphatase reverses this regulatory phosphorylation when the $[PQ]/[PQH_2]$ ratio increases.

Water Is Split by the Oxygen-Evolving Complex

The ultimate source of the electrons passed to NADPH in plant (oxygenic) photosynthesis is water. Having given up an electron to pheophytin, $P680^+$ (of PSII) must acquire an electron to return to its ground state in preparation for capture of another photon. In principle, the required electron might come from any number of organic or inorganic compounds. Photosynthetic bacteria use a variety of electron donors for this purpose—

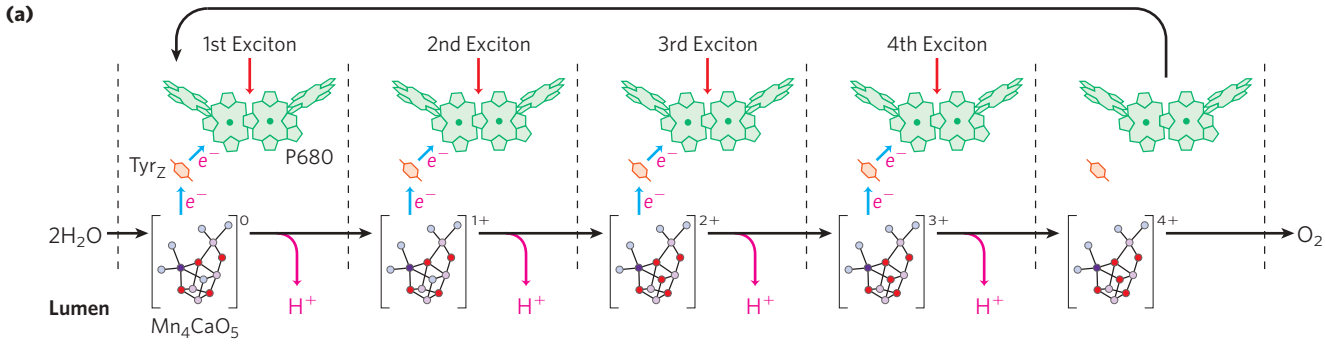

FIGURE 19–64 Water-splitting activity of the oxygen-evolving complex. (a) Shown here is the process that produces a four-electron oxidizing agent—a multinuclear center with four Mn ions, one Ca ion, and four oxygen atoms—in the water-splitting complex of PSII. The sequential absorption of four photons (excitons), each absorption causing the loss of one electron from the Mn_4Ca cluster, produces an oxidizing agent that can remove four electrons from two molecules of water, producing O_2. The electrons lost from the Mn_4Ca cluster pass one at a time to an oxidized Tyr residue in a PSII protein, then to $P680^+$. **(b)** The metallic center of the water-splitting complex, obtained by x-ray crystallography (PDB ID 3ARC). Tyr^{161}, known to participate in the oxidation of water, is seen hydrogen-bonded to a network of water molecules, including several directly in contact with the Mn_4Ca cluster. This is the site of one of the most important reactions in the biosphere!

acetate, succinate, malate, or sulfide—depending on what is available in a particular ecological niche. About 3 billion years ago, evolution of primitive photosynthetic bacteria (the progenitors of the modern cyanobacteria) produced a photosystem capable of taking electrons from a donor that is always available—water. Two water molecules are split, yielding four electrons, four protons, and molecular oxygen:

$$2H_2O \longrightarrow 4H^+ + 4e^- + O_2$$

A single photon of visible light does not have enough energy to break the bonds in water; four photons are required in this photolytic cleavage reaction.

The four electrons abstracted from water do not pass directly to $P680^+$, which can accept only one electron at a time. Instead, a remarkable molecular device, the **oxygen-evolving complex** (also called the **water-splitting complex**), passes four electrons *one at a time* to $P680^+$ **(Fig. 19–64)**. The immediate electron donor to $P680^+$ is a Tyr residue (often designated Z or Tyr_Z) in subunit D1 of the PSII reaction center. The Tyr residue loses both a proton and an electron, generating the electrically neutral Tyr free radical, $^\bullet$Tyr:

$$4\ P680^+ + 4\ Tyr \longrightarrow 4\ P680 + 4\ {}^\bullet Tyr \quad (19–13)$$

The Tyr radical regains its missing electron and proton by oxidizing a cluster of four manganese ions and one calcium ion in the water-splitting complex. With each single-electron transfer, the Mn_4Ca cluster becomes more oxidized; four single-electron transfers, each corresponding to the absorption of one photon, produce a charge of 4+ on the Mn_4Ca cluster (Fig. 19–64):

$$4\ {}^\bullet Tyr + [Mn_4Ca]^0 \longrightarrow 4\ Tyr + [Mn_4Ca]^{4+} \quad (19–14)$$

In this state, the Mn_4Ca cluster can take four electrons from a pair of water molecules, releasing $4H^+$ and O_2:

$$[Mn_4Ca]^{4+} + 2H_2O \longrightarrow [Mn_4Ca]^0 + 4H^+ + O_2 \quad (19–15)$$

Because the four protons produced in this reaction are released into the thylakoid lumen, the oxygen-evolving complex acts as a proton pump, driven by electron transfer. The sum of Equations 19–12 through 19–15 is

$$2H_2O + 2PQ_B + 4\ photons \longrightarrow O_2 + 2PQ_BH_2 \quad (19–16)$$

The detailed structure of the oxygen-evolving cluster has been obtained by high-resolution x-ray crystallography. The metal cluster takes the shape of a chair (Fig. 19–64b). The seat and legs of the chair are made up of three Mn ions, one Ca ion, and four O atoms; the fourth Mn and another O form the back of the chair. Four water molecules are also seen in the crystal structure, two associated with one of the Mn ions, the other two with the Ca ion. It is possible that one or more of these water molecules is the one that undergoes oxidation to produce O_2. This metal cluster is associated with a peripheral membrane protein (M_r 33,000) on the lumenal side of the thylakoid membrane that presumably stabilizes the cluster. The Tyr residue designated Z, through which electrons move between water and the PSII reaction center, is part of a network of hydrogen-bonded water molecules that includes the four associated with the Mn_4Ca cluster. The detailed mechanism of water oxidation by the Mn_4Ca cluster is not known but is under intense investigation. The reaction is central to life on Earth and may involve novel bioinorganic chemistry. Determination of the structure of the polymetallic center has inspired several reasonable and testable hypotheses. Stay tuned.

SUMMARY 19.8 The Central Photochemical Event: Light-Driven Electron Flow

- Bacteria have a single reaction center; in purple bacteria, it is of the pheophytin-quinone type, and in green sulfur bacteria, the Fe-S type.
- Structural studies of the reaction center of a purple bacterium have provided information about light-driven electron flow from an excited special pair of chlorophyll molecules, through pheophytin, to quinones. Electrons then pass from quinones through the cytochrome bc_1 complex, and back to the photoreaction center.
- An alternative path, in green sulfur bacteria, sends electrons from reduced quinones to NAD^+.
- Cyanobacteria and plants have two different photoreaction centers, arranged in tandem.
- Plant photosystem I passes electrons from its excited reaction center, P700, through a series of carriers to ferredoxin, which then reduces $NADP^+$ to NADPH.
- The reaction center of plant photosystem II, P680, passes electrons to plastoquinone, and the electrons lost from P680 are replaced by electrons from H_2O (electron donors other than H_2O are used in other organisms).
- Flow of electrons through the photosystems produces NADPH and ATP. Cyclic electron flow produces ATP only and allows variability in the proportions of NADPH and ATP formed.
- The localization of PSI and PSII between the granal and stromal lamellae can change and is indirectly controlled by light intensity, optimizing the distribution of excitons between PSI and PSII for efficient energy capture.
- The light-driven splitting of H_2O is catalyzed by a Mn- and Ca-containing protein complex; O_2 is produced. The reduced plastoquinone carries electrons to the cytochrome b_6f complex; from here they pass to plastocyanin, and then to P700 to replace those lost during its photoexcitation.
- Electron flow through the cytochrome b_6f complex drives protons across the plasma membrane, creating a proton-motive force that provides the energy for ATP synthesis by an ATP synthase.

19.9 ATP Synthesis by Photophosphorylation

The combined activities of the two plant photosystems move electrons from water to $NADP^+$, conserving some of the energy of absorbed light as NADPH (Fig. 19–58). Simultaneously, protons are pumped across the thylakoid membrane and energy is conserved as an electrochemical potential. We turn now to the process by which this proton gradient drives the synthesis of ATP, the other energy-conserving product of the light-dependent reactions.

Daniel Arnon, 1910–1994

In 1954 Daniel Arnon and his colleagues discovered that ATP is generated from ADP and P_i during photosynthetic electron transfer in illuminated spinach chloroplasts. Support for these findings came from the work of Albert Frenkel, who detected light-dependent ATP production in pigment-containing membranous structures called **chromatophores**, derived from photosynthetic bacteria. Investigators concluded that some of the light energy captured by the photosynthetic systems of these organisms is transformed into the phosphate bond energy of ATP. This process is called **photophosphorylation**, to distinguish it from oxidative phosphorylation in respiring mitochondria.

A Proton Gradient Couples Electron Flow and Phosphorylation

Several properties of photosynthetic electron transfer and photophosphorylation in chloroplasts indicate that a proton gradient plays the same role as in mitochondrial oxidative phosphorylation. (1) The reaction centers, electron carriers, and ATP-forming enzymes are located in a proton-impermeable membrane—the thylakoid membrane—which must be intact to support photophosphorylation. (2) Photophosphorylation can be uncoupled from electron flow by reagents that promote the passage of protons through the thylakoid membrane. (3) Photophosphorylation can be blocked by venturicidin and similar agents that inhibit the formation of ATP from ADP and P_i by the mitochondrial ATP synthase (Table 19–4). (4) ATP synthesis is catalyzed by F_oF_1 complexes, located on the outer surface of the thylakoid membranes, that are very similar in structure and function to the F_oF_1 complexes of mitochondria.

Electron-transferring molecules in the chain of carriers connecting PSII and PSI are oriented asymmetrically in the thylakoid membrane, so photoinduced electron flow results in the net movement of protons across the membrane, from the stromal side to the thylakoid lumen **(Fig. 19–65)**. In 1966 André Jagendorf showed that a pH gradient across the thylakoid membrane (alkaline outside) could furnish the driving force to generate ATP. His early observations provided some of the most important experimental evidence in support of Mitchell's chemiosmotic hypothesis.

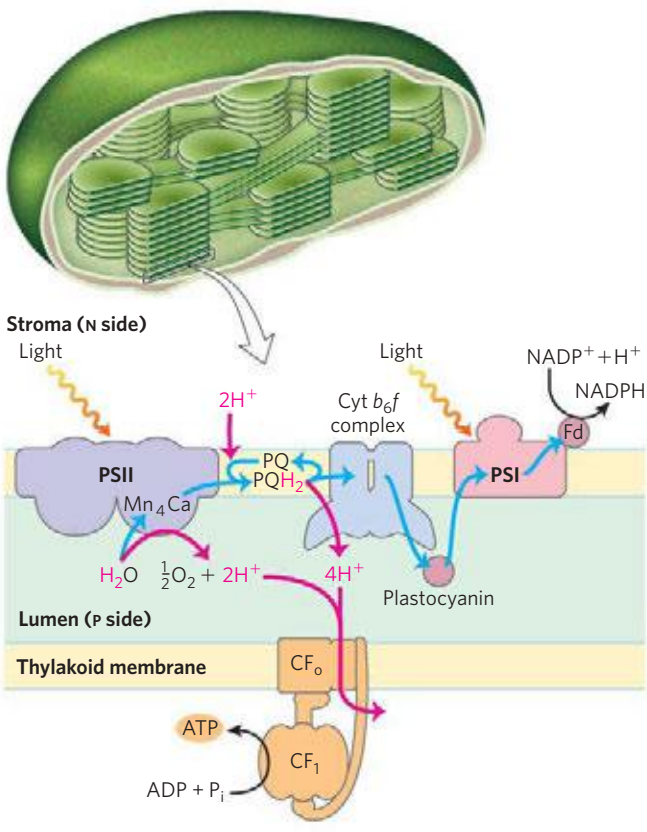

FIGURE 19–65 Proton and electron circuits during photophosphorylation. Electrons (blue arrows) move from H_2O through PSII, through the intermediate chain of carriers, through PSI, and finally to $NADP^+$. Protons (red arrows) are pumped into the thylakoid lumen by the flow of electrons through the carriers linking PSII and PSI, and reenter the stroma through proton channels formed by the F_o (designated CF_o) of ATP synthase. The F_1 subunit (CF_1) catalyzes synthesis of ATP.

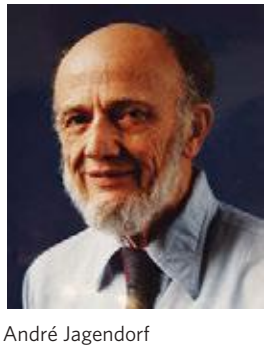

André Jagendorf

Jagendorf incubated chloroplasts, in the dark, in a pH 4 buffer; the buffer slowly penetrated into the inner compartment of the thylakoids, lowering their internal pH. He added ADP and P_i to the dark suspension of chloroplasts and then suddenly raised the pH of the outer medium to 8, momentarily creating a large pH gradient across the membrane. As protons moved out of the thylakoids into the medium, ATP was generated from ADP and P_i. Because the formation of ATP occurred in the dark (with no input of energy from light), this experiment showed that a pH gradient across the membrane is a high-energy state that, as in mitochondrial oxidative phosphorylation, can mediate the transduction of energy from electron transfer into the chemical energy of ATP.

The Approximate Stoichiometry of Photophosphorylation Has Been Established

As electrons move from water to $NADP^+$ in plant chloroplasts, about 12 H^+ move from the stroma to the thylakoid lumen per four electrons passed (that is, per O_2 formed). Four of these protons are moved by the oxygen-evolving complex, and up to eight by the cytochrome b_6f complex. The measurable result is a 1,000-fold difference in proton concentration across the thylakoid membrane ($\Delta pH = 3$). Recall that the energy stored in a proton gradient (the electrochemical potential) has two components: a proton concentration difference (ΔpH) and an electrical potential ($\Delta\psi$) due to charge separation. In chloroplasts, ΔpH is the dominant component; counter-ion movement apparently dissipates most of the electrical potential. In illuminated chloroplasts, the energy stored in the proton gradient per mole of protons is

$$\Delta G = 2.3RT\,\Delta pH + Z\mathcal{F}\,\Delta\psi = -17 \text{ kJ/mol}$$

so the movement of 12 mol of protons across the thylakoid membrane represents conservation of about 200 kJ of energy—enough energy to drive the synthesis of several moles of ATP ($\Delta G'^\circ = 30.5$ kJ/mol). Experimental measurements yield values of about 3 ATP per O_2 produced.

At least eight photons must be absorbed to drive four electrons from H_2O to NADPH (one photon per electron at each reaction center). The energy in eight photons of visible light is more than enough for the synthesis of three molecules of ATP.

ATP synthesis is not the only energy-conserving reaction of photosynthesis in plants; the NADPH formed in the final electron transfer is also energetically rich. The overall equation for noncyclic photophosphorylation (a term explained below) is

$$2H_2O + 8 \text{ photons} + 2NADP^+ + \sim 3ADP^+ + \sim 3P_i \longrightarrow O_2 + \sim 3ATP + 2NADPH \quad (19\text{–}17)$$

The ATP Synthase of Chloroplasts Is Like That of Mitochondria

The enzyme responsible for ATP synthesis in chloroplasts is a large complex with two functional components, CF_o and CF_1 (*C* denoting its location in chloroplasts). CF_o is a transmembrane proton pore composed of several integral membrane proteins and is homologous to mitochondrial F_o. CF_1 is a peripheral membrane protein complex very similar in subunit composition, structure, and function to mitochondrial F_1.

Electron microscopy of sectioned chloroplasts shows ATP synthase complexes as knoblike projections on the *outside* (stromal, or N) surface of thylakoid membranes; these complexes correspond to the ATP synthase complexes seen to project on the *inside*

(matrix, or N) surface of the inner mitochondrial membrane. Thus the relationship between the orientation of the ATP synthase and the direction of proton pumping is the same in chloroplasts and mitochondria. In both cases, the F_1 portion of ATP synthase is located on the more alkaline (N) side of the membrane through which protons flow down their concentration gradient; the direction of proton flow relative to F_1 is the same in both cases: P to N **(Fig. 19–66)**.

The mechanism of chloroplast ATP synthase is also believed to be essentially identical to that of its mitochondrial analog; ADP and P_i readily condense to form ATP on the enzyme surface, and the release of this enzyme-bound ATP requires a proton-motive force. Rotational catalysis sequentially engages each of the three β subunits of the ATP synthase in ATP synthesis, ATP release, and ADP + P_i binding (Figs 19–26, 19–27).

The chloroplast ATP synthase of spinach, with 14 c subunits in its F_o complex, is predicted to have a lower ratio of ATP formed to electrons transferred, compared with the bovine, yeast, or *E. coli* F_o complexes, with 8, 10, and 10 c subunits, respectively (Fig. 19–29).

SUMMARY 19.9 ATP Synthesis by Photophosphorylation

- In plants, both the water-splitting reaction and electron flow through the cytochrome b_6f complex are accompanied by proton pumping across the thylakoid membrane. The proton-motive force thus created drives ATP synthesis by a CF_oCF_1 complex similar to the mitochondrial F_oF_1 complex.
- The catalytic mechanism of CF_oCF_1 is very similar to that of the ATP synthases of mitochondria and bacteria. Physical rotation driven by the proton gradient is accompanied by ATP synthesis at sites that cycle through three conformations, one with high affinity for ATP, one with high affinity for ADP + P_i and one with low affinity for both nucleotides.

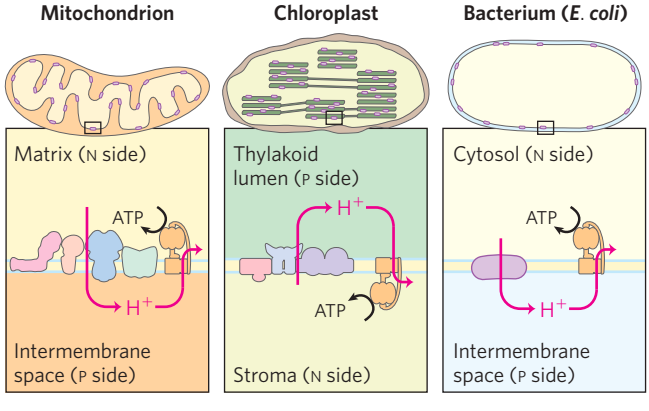

FIGURE 19–66 Orientation of the ATP synthase is fixed relative to the proton gradient. Superficially, the direction of proton pumping may seem to be different in chloroplasts relative to mitochondria and bacteria. In mitochondria and bacteria, protons are pumped *out of* the organelle or cell, and F_1 is on the *inside* of the membrane; in plant thylakoids, protons are pumped *into* the flattened discs within chloroplasts, and CF_1 is on the *outside* of the disc membrane. However, exactly the same mechanism of energy conversion (from proton gradient to ATP) occurs in all three cases. ATP is synthesized in the matrix of mitochondria, the stroma of chloroplasts, and the cytosol of bacteria.

19.10 The Evolution of Oxygenic Photosynthesis

The appearance of oxygenic photosynthesis on Earth about 2.5 billion years ago was a crucial event in the evolution of the biosphere. Until then, the earth had been essentially devoid of molecular oxygen and lacked the ozone layer that protects living organisms from solar UV radiation. Oxygenic photosynthesis made available a nearly limitless supply of reducing agent (H_2O) to drive the production of organic compounds by reductive biosynthetic reactions. And mechanisms evolved that allowed organisms to use O_2 as a terminal electron acceptor in highly energetic electron transfers from organic substrates, employing the energy of oxidation to support their metabolism. The complex photosynthetic apparatus of a modern vascular plant is the culmination of a series of evolutionary events, the most recent of which was the acquisition by eukaryotic cells of a cyanobacterial endosymbiont.

Chloroplasts Evolved from Ancient Photosynthetic Bacteria

Chloroplasts in modern organisms resemble mitochondria in several properties, and are believed to have originated by the same mechanism that gave rise to mitochondria: endosymbiosis. Like mitochondria, chloroplasts contain their own DNA and protein-synthesizing machinery. Some of the polypeptides of chloroplast proteins are encoded by chloroplast genes and synthesized in the chloroplast; others are encoded by nuclear genes, synthesized outside the chloroplast, and imported (Chapter 27). When plant cells grow and divide, chloroplasts give rise to new chloroplasts by division, during which their DNA is replicated and divided between daughter chloroplasts. The machinery and mechanism for light capture, electron flow, and ATP synthesis in modern cyanobacteria are similar in many respects to those in plant chloroplasts. These observations led to the now widely accepted hypothesis that the evolutionary progenitors of modern plant cells were primitive eukaryotes that engulfed photosynthetic cyanobacteria and established stable endosymbiotic relationships with them (see Fig. 1–38).

At least half of the photosynthetic activity on Earth now occurs in microorganisms—algae, other photosynthetic eukaryotes, and photosynthetic bacteria. Cyanobacteria have PSII and PSI in tandem, and the PSII has

an associated water-splitting activity resembling that of plants. However, the other groups of photosynthetic bacteria have single reaction centers and do not split H_2O or produce O_2. Many are obligate anaerobes and cannot tolerate O_2; they must use some compound other than H_2O as electron donor. Some photosynthetic bacteria use inorganic compounds as electron (and hydrogen) donors. For example, green sulfur bacteria use hydrogen sulfide:

$$2H_2S + CO_2 \xrightarrow{\text{light}} (CH_2O) + H_2O + 2S$$

These bacteria, instead of producing molecular O_2, form elemental sulfur as the oxidation product of H_2S. (They further oxidize the S to SO_4^{2-}.) Other photosynthetic bacteria use organic compounds such as lactate as electron donors:

$$2 \text{ Lactate} + CO_2 \xrightarrow{\text{light}} (CH_2O) + H_2O + 2 \text{ pyruvate}$$

The fundamental similarity of photosynthesis in plants and bacteria, despite the differences in the electron donors they employ, becomes more obvious when the equation of photosynthesis is written in the more general form

$$2H_2D + CO_2 \xrightarrow{\text{light}} (CH_2O) + H_2O + 2D$$

in which H_2D is an electron (and hydrogen) donor and D is its oxidized form. H_2D may be water, hydrogen sulfide, lactate, or some other organic compound, depending on the species. Most likely, the bacteria that first developed photosynthetic ability used H_2S as their electron source.

The ancient relatives of modern cyanobacteria probably arose by the combination of genetic material from two types of photosynthetic bacteria, with systems of the type seen in modern purple bacteria (with a PSII-like electron path) and green sulfur bacteria (with an electron path resembling that in PSI). The bacterium with two independent photosystems may have used one in one set of conditions, the other in different conditions. Over time, a mechanism to connect the two photosystems for simultaneous use evolved, and the PSII-like system acquired the water-splitting capacity found in modern cyanobacteria.

Modern cyanobacteria can synthesize ATP by oxidative phosphorylation or by photophosphorylation, although they have neither mitochondria nor chloroplasts. The enzymatic machinery for both processes is in a highly convoluted plasma membrane **(Fig. 19–67)**. Three protein components function in both processes, giving evidence that the processes have a common evolutionary origin **(Fig. 19–68)**. First, the proton-pumping cytochrome b_6f complex carries electrons from plastoquinone to cytochrome c_6 in photosynthesis, and also carries electrons from ubiquinone to cytochrome c_6 in oxidative phosphorylation—the role played by cytochrome bc_1 in mitochondria. Second, cytochrome c_6, homologous to mitochondrial cytochrome c, carries electrons from Complex III to Complex IV in cyanobacteria; it can also carry electrons from the cytochrome b_6f complex to PSI—a role performed in plants by plastocyanin. We therefore see the functional homology between the cyanobacterial cytochrome b_6f complex and the mitochondrial cytochrome bc_1 complex, and between cyanobacterial cytochrome c_6 and plant plastocyanin. The third conserved component is the ATP synthase, which functions in oxidative phosphorylation and photophosphorylation in cyanobacteria, and in the mitochondria and chloroplasts of photosynthetic eukaryotes. The structure and remarkable mechanism of this enzyme have been strongly conserved throughout evolution.

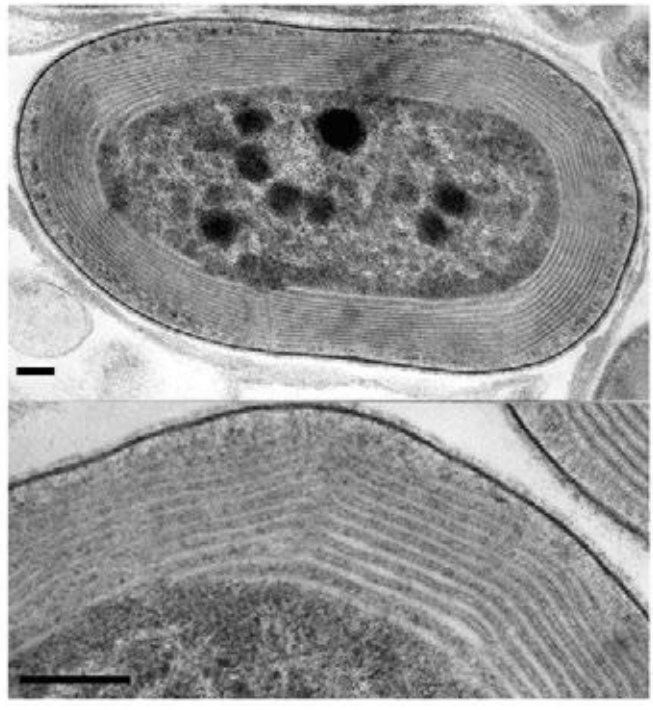

FIGURE 19–67 The photosynthetic membranes of a cyanobacterium. In these thin sections of a cyanobacterium, viewed with a transmission electron microscope, the multiple layers of the internal membranes are seen to fill half of the total volume of the cell. The extensive membrane system serves the same role as the thylakoids of vascular plants, providing a large surface area containing all of the photosynthetic machinery. (Bar = 100 nm.)

In *Halobacterium*, a Single Protein Absorbs Light and Pumps Protons to Drive ATP Synthesis

In some modern archaea, a quite different mechanism for converting the energy of light into an electrochemical gradient has evolved. The halophilic ("salt-loving") archaeon *Halobacterium salinarum* is descended from ancient evolutionary progenitors. This archaeon (commonly referred to as a halobacterium) lives only in brine ponds and salt lakes (Great Salt Lake and the Dead Sea, for example), where the

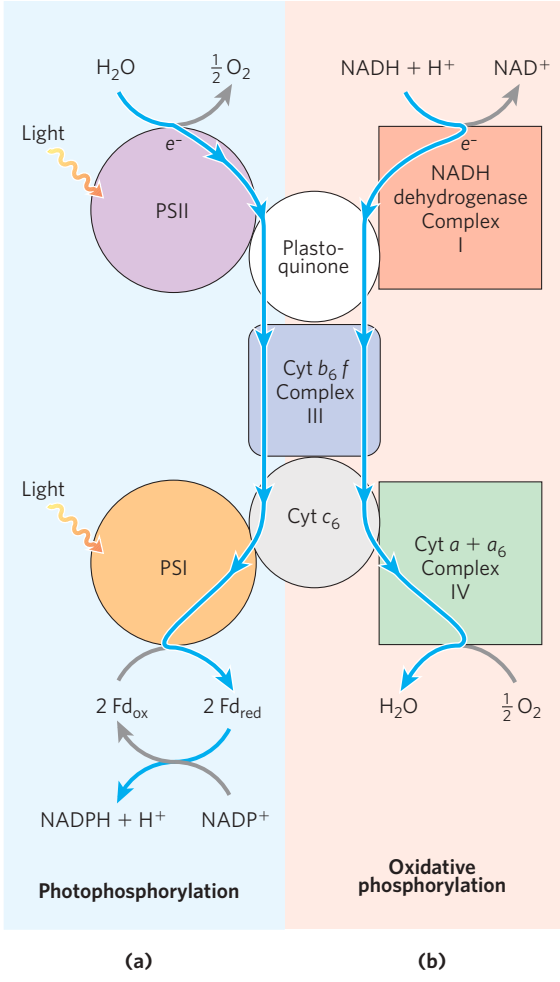

FIGURE 19–68 Dual roles of cytochrome b_6f and cytochrome c_6 in cyanobacteria reflect evolutionary origins. Cyanobacteria use cytochrome b_6f, cytochrome c_6, and plastoquinone for both oxidative phosphorylation and photophosphorylation. **(a)** In photophosphorylation, electrons flow (top to bottom) from water to $NADP^+$. **(b)** In oxidative phosphorylation, electrons flow from NADH to O_2. Both processes are accompanied by proton movement across the membrane, accomplished by a Q cycle.

high salt concentration—which can exceed 4 M—results from water loss by evaporation; indeed, halobacteria cannot live in NaCl concentrations lower than 3 M. These organisms are aerobes and normally use O_2 to oxidize organic fuel molecules. However, the solubility of O_2 is so low in brine ponds that sometimes oxidative metabolism must be supplemented by sunlight as an alternative source of energy.

The plasma membrane of *H. salinarum* contains patches of the light-absorbing pigment **bacteriorhodopsin**, which contains retinal (the aldehyde derivative of vitamin A; see Fig. 10–21) as a light-harvesting prosthetic group. When the cells are illuminated, all-*trans*-retinal bound to the bacteriorhodopsin absorbs a photon and undergoes photoisomerization to 13-*cis*-retinal, forcing a conformational change in the protein. The restoration of all-*trans*-retinal is accompanied by the outward movement of protons through the plasma membrane. Bacteriorhodopsin, with only 247 amino acid residues, is the simplest light-driven proton pump known. The difference in the three-dimensional structure of bacteriorhodopsin in the dark and after illumination **(Fig. 19–69a)** suggests a pathway by which a concerted series of proton "hops" could effectively move a proton across the membrane. The chromophore retinal is bound through a Schiff-base linkage to the ε-amino group of a Lys residue. In the dark, the nitrogen of this Schiff base is protonated; in the light, photoisomerization of retinal lowers the pK_a of this group and it releases its proton to a nearby Asp residue, triggering a series of proton hops that ultimately result in the release of a proton at the outer surface of the membrane (Fig. 19–69b).

The electrochemical potential across the membrane drives protons back into the cell through a membrane ATP synthase complex very similar to that of mitochondria and chloroplasts. Thus, when O_2 is limited, halobacteria can use light to supplement the ATP synthesized by oxidative phosphorylation. Halobacteria do not evolve O_2, nor do they carry out photoreduction of $NADP^+$; their phototransducing machinery is therefore much simpler than that of cyanobacteria or plants. Nevertheless, its proton-pumping mechanism may prove to be prototypical for the many other, more complex, ion pumps.

Bacteriorhodopsin

SUMMARY 19.10 The Evolution of Oxygenic Photosynthesis

- Modern cyanobacteria are derived from an ancient organism that acquired two photosystems, one of the type now found in purple bacteria, the other of the type found in green sulfur bacteria.
- Many photosynthetic microorganisms obtain electrons for photosynthesis not from water but from donors such as H_2S.
- Cyanobacteria with the tandem photosystems and a water-splitting activity that released oxygen into the atmosphere appeared on Earth about 2.5 billion years ago.
- Chloroplasts, like mitochondria, evolved from bacteria living endosymbiotically in early eukaryotic cells. The ATP synthases of bacteria, cyanobacteria, mitochondria, and chloroplasts share a common evolutionary precursor and a common enzymatic mechanism.
- An entirely different mechanism for converting light energy to a proton gradient has evolved in the modern archaea, in which the light-harvesting pigment is retinal.

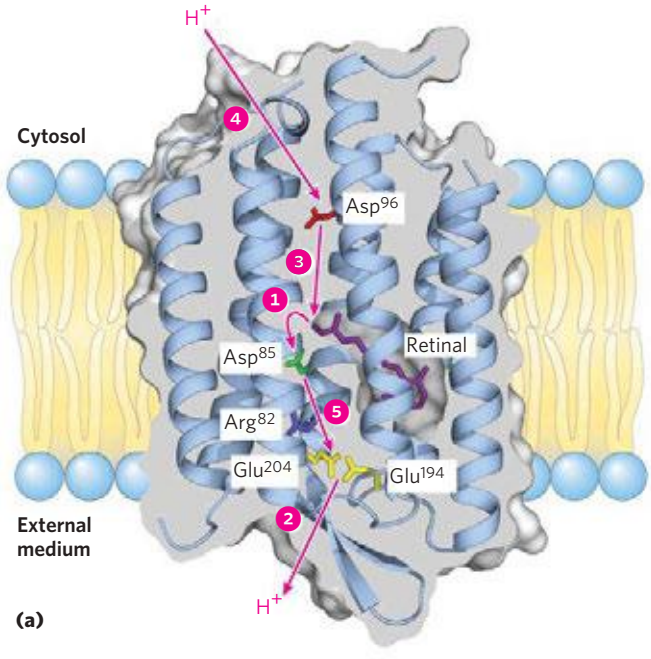

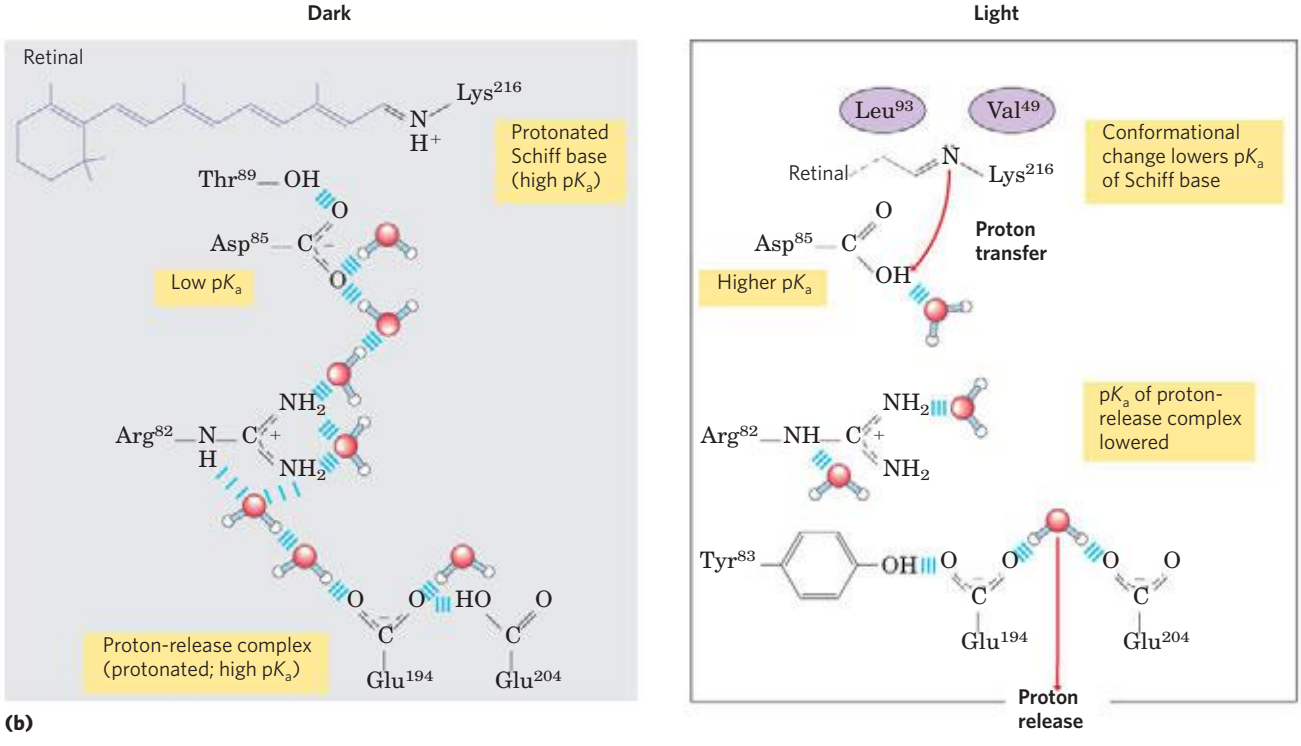

FIGURE 19–69 A different mechanism for light-driven proton pumping evolved independently in a halophilic archaeon. (a) Bacteriorhodopsin (M_r 26,000) of *Halobacterium halobium* has seven membrane-spanning α helices (PDB ID 1C8R). The chromophore all-*trans*-retinal (purple) is covalently attached via a Schiff base to the ε-amino group of a Lys residue deep in the membrane interior. Running through the protein are a series of Asp and Glu residues and a series of closely associated water molecules that together provide the transmembrane path for protons (red arrows). Steps ❶ through ❺ indicate proton movements, described below.

(b) In the dark (left panel), the Schiff base is protonated. Illumination (right panel) photoisomerizes the retinal, forcing subtle conformational changes in the protein that alter the distance between the Schiff base and its neighboring amino acid residues. Interaction with these neighbors (Leu^{93} and Val^{49}) lowers the pK_a of the protonated Schiff base, and the base gives up its proton to a nearby carboxyl group on Asp^{85} (step ❶ in (a)). This initiates a series of concerted proton hops between water molecules (see Fig. 2–14) in the interior of the protein, which ends with ❷ the release of a proton that was shared by Glu^{194} and Glu^{204} near the extracellular surface. (Tyr^{83} forms a hydrogen bond with Glu^{194} that facilitates this proton release.) ❸ The Schiff base reacquires a proton from Asp^{96}, which ❹ takes up a proton from the cytosol. ❺ Finally, Asp^{85} gives up its proton, leading to reprotonation of the Glu^{204}-Glu^{194} pair. The system is now ready for another round of proton pumping.

Key Terms

Terms in bold are defined in the glossary.

chemiosmotic theory 731
respiratory chain 734
flavoprotein 734
reducing equivalent 735
ubiquinone (coenzyme Q, Q) 735
cytochromes 735
iron-sulfur protein 735
Rieske iron-sulfur protein 735
Complex I 738
vectorial 738
Complex II 740
succinate dehydrogenase 740
reactive oxygen species (ROS) 740
superoxide radical ($^{\bullet}O_2^-$) 740
Complex III 740
cytochrome bc_1 complex 740
Q cycle 741
Complex IV 742
cytochrome oxidase 742
proton-motive force 744
ATP synthase 747
F_1 ATPase 750
rotational catalysis 752
binding-change model 754
P/O ratio 755
P/2e^- ratio 755

Further Reading

History and General Background

Arnon, D.I. (1984) The discovery of photosynthetic phosphorylation. *Trends Biochem. Sci.* **9**, 258–262.

Harold, F.M. (1986) *The Vital Force: A Study in Bioenergetics*, W. H. Freeman and Company, New York.

A very readable synthesis of the principles of bioenergetics and their application to energy transductions.

Heldt, H.-W. & Piechulla, B. (2010) *Plant Biochemistry*, 4th edn, Elsevier, New York.

A textbook of plant biochemistry with excellent discussions of photophosphorylation.

Lane, N. (2005) *Power, Sex, Suicide: Mitochondria and the Meaning of Life*, Oxford University Press, Oxford.

An entry-level description of the roles of mitochondria in energy conservation and in apoptosis.

Mitchell, P. (1979) Keilin's respiratory chain concept and its chemiosmotic consequences. *Science* **206**, 1148–1159.

Mitchell's Nobel lecture, outlining the evolution of the chemiosmotic hypothesis.

Scheffler, I.E. (2008) *Mitochondria*, 2nd edn, John Wiley & Sons, Hoboken, NJ.

An excellent survey of mitochondrial structure and function.

Slater, E.C. (1987) The mechanism of the conservation of energy of biological oxidations. *Eur. J. Biochem.* **166**, 489–504.

A clear and critical account of the evolution of the chemiosmotic model.

OXIDATIVE PHOSPHORYLATION

Electron-Transfer Reactions in Mitochondria

Adam-Vizi, V. & Chinopoulos, C. (2006) Bioenergetics and the formation of mitochondrial reactive oxygen species. *Trends Pharmacol.* **27**, 639–645.

Cramer, W.A., Hasan, S.S., & Yamashita, E. (2011) The Q cycle of cytochrome *bc* complexes: a structure perspective. *Biochim. Biophys. Acta* **1807**, 788–802.

Advanced discussion of the Q cycle in oxidative phosphorylation and photophosphorylation.

Dudkina, N.V., Kouřil, R., Peters, K., Braun, H.-P., & Boekema, E.J. (2010) Structure and function of mitochondrial supercomplexes. *Biochim. Biophys. Acta* **1797,** 664–670.

Efremov, R.S., Baradaran, R., & Sazanov, L.A. (2010) The architecture of respiratory complex I. *Nature* **465**, 441–447.

Hamanaka, R.B. & Chandel, N.S. (2010) Mitochondrial reactive oxygen species regulate cellular signaling and dictate biological outcomes. *Trends Biochem. Sci.* **35**, 505–513.

Millar, A.H., Whelan, J., Soole, K.L., & Day, D.A. (2011) Organization and regulation of mitochondrial respiration in plants. *Annu. Rev. Plant Biol.* **62**, 79–104.

Sun, F., Huo, X., Zhai, Y., Wang, A., Xu, J., Su, D., Bartlam, M., & Rao, Z. (2005) Crystal structure of mitochondrial respiratory protein Complex II. *Cell* **121**, 1043–1057.

Tsukihara, T., Aoyama, H., Yamashita, E., Tomizaki, T., Yamaguchi, H., Shinzawa-Itoh, K., Nakashima, R., Yaono, R., & Yoshikawa, S. (1996) The whole structure of the 13-subunit oxidized cytochrome *c* oxidase at 2.8 Å. *Science* **272**, 1136–1144.

The solution by x-ray crystallography of the structure of this huge membrane protein.

Xia, D., Yu, C.-A., Kim, H., Xia, J.-Z., Kachurin, A.M., Zhang, L., Yu, L., & Deisenhofer, J. (1997) Crystal structure of the cytochrome bc_1 complex from bovine heart mitochondria. *Science* **277**, 60–66.

Report revealing the crystallographic structure of Complex III.

Yoshikawa, S., Muramoto, K., & Shinzawa-Itoh, K. (2011) Proton-pumping mechanism of cytochrome *c* oxidase. *Annu. Rev. Biophys.* **40**, 205–223.

ATP Synthesis

Abrahams, J.P., Leslie, A.G.W., Lutter, R., & Walker, J.E. (1994) The structure of F_1-ATPase from bovine heart mitochondria determined at 2.8 Å resolution. *Nature* **370**, 621–628.

Boyer, P.D. (1997) The ATP synthase—a splendid molecular machine. *Annu. Rev. Biochem.* **66**, 717–749.

An account of the historical development and current state of the binding-change model, written by its principal architect.

Hinkle, P.C., Kumar, M.A., Resetar, A., & Harris, D.L. (1991) Mechanistic stoichiometry of mitochondrial oxidative phosphorylation. *Biochemistry* **30**, 3576–3582.

A careful analysis of experimental results and theoretical considerations on the question of nonintegral P/O ratios.

Okuno, D., Iino, R., & Noji, H. (2011) Rotation and structure of F_oF_1-ATP synthase. *J. Biochem.* **149**, 655–664.

Silverstein, T. (2005) The mitochondrial phosphate-to-oxygen ratio is not an integer. *Biochem. Mol. Biol. Educ.* **33**, 416–417.

von Ballmoos, C., Wiedenmann, A., & Dimroth, P. (2009) Essentials for ATP synthesis by F_1F_o ATP synthase. *Annu. Rev. Biochem.* **78**, 649–672.

Watt, I.N., Montgomery, M.G., Runswick, M.J., Leslie, A.G.W., & Walker, J.E. (2010) Bioenergetic cost of making an adenosine

triphosphate molecule in animal mitochondria. *Proc. Natl. Acad. Sci. USA* **107**, 16,823–16,827.

Regulation of Oxidative Phosphorylation

Taylor, C.T. (2008) Mitochondria and cellular oxygen sensing in the HIF pathway. *Biochem. J.* **409**, 19–26.

Mitochondria in Thermogenesis, Steroid Synthesis, and Apoptosis

Azzu, V. & Brand, M.D. (2010) The on-off switches of the mitochondrial uncoupling proteins. *Trends Biochem. Sci.* **35**, 298–307.

Intermediate-level review of how cold, overfeeding, and starvation affect the expression of thermogenin genes.

Wang, C. & Youle, R.J. (2009) The role of mitochondria in apoptosis. *Annu. Rev. Genet.* **43**, 95–118.

Mitochondrial Genes: Their Origin and Effects of Mutations

Abou-Sleiman, P.M., Muqit, M.M.K., & Wood, N.W. (2006) Expanding insights of mitochondrial dysfunction in Parkinson's disease. *Nat. Rev. Neurosci.* **7**, 207–219.

Becker, T., Böttinger, L., & Pfanner, N. (2012) Mitochondrial protein import: from transport pathways to an integrated network. *Trends Biochem. Sci.* **37**, 85–91.

Intermediate-level review of how proteins encoded in the nucleus get into mitochondria.

Chen, Z.J. & Butow, R.A. (2005) The organization and inheritance of the mitochondrial genome. *Nat. Rev. Genet.* **6**, 815–825.

Intermediate-level review.

Seyfried, T.N. & Shelton, L.M. (2010) Cancer as a metabolic disease. *Nutr. Metab.* **7**, 7–29.

Impaired energy metabolism is typical of a wide variety of cancers; a review of the role of mitochondria.

PHOTOSYNTHESIS

Light-Driven Electron Flow

Barber, J. & Anderson, J.M. (eds). (2002) Photosystem II: Molecular Structure and Function. Proceedings of a Meeting, 13–14 March 2002. *Philos. Trans. R. Soc. (Biol. Sci.)* **357** (1426).

A collection of 16 papers on photosystem II.

Biochim. Biophys. Acta Bioenerg. (2007) **1767** (6).

This journal issue contains 10 reviews on the structure and function of photosystems.

Busch, A. & Hipler, M. (2011) The structure and function of eukaryotic photosystem I. *Biochim. Biophys. Acta* **1807**, 864–877.

Huber, R. (1990) A structural basis of light energy and electron transfer in biology. *Eur. J. Biochem.* **187**, 283–305.

Huber's Nobel lecture, describing the physics and chemistry of phototransductions; an exceptionally clear and well-illustrated discussion, based on crystallographic studies of reaction centers.

Johnson, G.N. (2011) Physiology of PSI cyclic electron transport in higher plants. *Biochim. Biophys. Acta* **1807**, 906–911.

Review of the paths and roles of cyclic photophosphorylation.

Kramer, D.M., Avenson, T.J., & Edwards, G.E. (2007) Dynamic flexibility in the light reactions of photosynthesis governed by both electron and proton transfer reactions. *Trends Plant Sci.* **9**, 349–357.

Intermediate-level review of regulation of state transitions.

Rochaix, J.-D. (2011) Regulation of photosynthetic electron transport. *Biochim. Biophys. Acta* **1807**, 878–886.

Intermediate-level review of plant's responses to changes in quality and quantity of light.

Umena, Y., Kawakami, K., Shen, J.-R., & Kamiya, N. (2011) Crystal structure of oxygen-evolving photosystem II at a resolution of 1.9 Å. *Nature* **473**, 55–61.

ATP Synthesis by Photophosphorylation

Jagendorf, A.T. (1967) Acid-base transitions and phosphorylation by chloroplasts. *Fed. Proc.* **26**, 1361–1369.

Classic experiment establishing the ability of a proton gradient to drive ATP synthesis in the dark.

The Evolution of Oxygenic Photosynthesis

Hohmann-Marriott, M.F. & Blankenship, R.E. (2011) Evolution of photosynthesis. *Annu. Rev. Plant Biol.* **62**, 515–548.

Nelson, N. (2011) Photosystems and global effects of oxygenic photosynthesis. *Biochim. Biophys. Acta* **1807**, 856–863.

Intermediate-level review of the evolutionary forces that shaped oxygenic photosynthesis.

Problems

1. Oxidation-Reduction Reactions The NADH dehydrogenase complex of the mitochondrial respiratory chain promotes the following series of oxidation-reduction reactions, in which Fe^{3+} and Fe^{2+} represent the iron in iron-sulfur centers, Q is ubiquinone, QH_2 is ubiquinol, and E is the enzyme:

(1) $NADH + H^+ + E\text{-}FMN \longrightarrow NAD^+ + E\text{-}FMNH_2$

(2) $E\text{-}FMNH_2 + 2Fe^{3+} \longrightarrow E\text{-}FMN + 2Fe^{2+} + 2H^+$

(3) $2Fe^{2+} + 2H^+ + Q \longrightarrow 2Fe^{3+} + QH_2$

Sum: $NADH + H^+ + Q \longrightarrow NAD^+ + QH_2$

For each of the three reactions catalyzed by the NADH dehydrogenase complex, identify (a) the electron donor, (b) the electron acceptor, (c) the conjugate redox pair, (d) the reducing agent, and (e) the oxidizing agent.

2. All Parts of Ubiquinone Have a Function In electron transfer, only the quinone portion of ubiquinone undergoes oxidation-reduction; the isoprenoid side chain remains unchanged. What is the function of this chain?

3. Use of FAD Rather Than NAD^+ in Succinate Oxidation All the dehydrogenases of glycolysis and the citric acid cycle use NAD^+ ($E'°$ for NAD^+/NADH is −0.32 V) as electron acceptor except succinate dehydrogenase, which uses covalently bound FAD ($E'°$ for FAD/$FADH_2$ in this enzyme is 0.050 V). Suggest why FAD is a more appropriate electron acceptor than NAD^+ in the dehydrogenation of succinate, based on the $E'°$ values of fumarate/succinate ($E'° = 0.031$ V), NAD^+/NADH, and the succinate dehydrogenase FAD/$FADH_2$.

4. Degree of Reduction of Electron Carriers in the Respiratory Chain The degree of reduction of each carrier in the respiratory chain is determined by conditions in the mitochondrion. For example, when NADH and O_2 are abundant, the steady-state degree of reduction of the carriers decreases as electrons pass from the substrate to O_2. When electron transfer is blocked, the carriers before the block become more reduced and those beyond the block become more oxidized (see Fig. 19–6). For each of the conditions below, predict the state of oxidation of ubiquinone and cytochromes b, c_1, c, and $a + a_3$.

(a) Abundant NADH and O_2, but cyanide added

(b) Abundant NADH, but O_2 exhausted

(c) Abundant O_2, but NADH exhausted
(d) Abundant NADH and O_2

5. Effect of Rotenone and Antimycin A on Electron Transfer Rotenone, a toxic natural product from plants, strongly inhibits NADH dehydrogenase of insect and fish mitochondria. Antimycin A, a toxic antibiotic, strongly inhibits the oxidation of ubiquinol.

(a) Explain why rotenone ingestion is lethal to some insect and fish species.

(b) Explain why antimycin A is a poison.

(c) Given that rotenone and antimycin A are equally effective in blocking their respective sites in the electron-transfer chain, which would be a more potent poison? Explain.

6. Uncouplers of Oxidative Phosphorylation In normal mitochondria the rate of electron transfer is tightly coupled to the demand for ATP. When the rate of use of ATP is relatively low, the rate of electron transfer is low; when demand for ATP increases, electron-transfer rate increases. Under these conditions of tight coupling, the number of ATP molecules produced per atom of oxygen consumed when NADH is the electron donor—the P/O ratio—is about 2.5.

(a) Predict the effect of a relatively low and a relatively high concentration of uncoupling agent on the rate of electron transfer and the P/O ratio.

(b) Ingestion of uncouplers causes profuse sweating and an increase in body temperature. Explain this phenomenon in molecular terms. What happens to the P/O ratio in the presence of uncouplers?

(c) The uncoupler 2,4-dinitrophenol was once prescribed as a weight-reducing drug. How could this agent, in principle, serve as a weight-reducing aid? Uncoupling agents are no longer prescribed, because some deaths occurred following their use. Why might the ingestion of uncouplers lead to death?

7. Effects of Valinomycin on Oxidative Phosphorylation When the antibiotic valinomycin is added to actively respiring mitochondria, several things happen: the yield of ATP decreases, the rate of O_2 consumption increases, heat is released, and the pH gradient across the inner mitochondrial membrane increases. Does valinomycin act as an uncoupler or as an inhibitor of oxidative phosphorylation? Explain the experimental observations in terms of the antibiotic's ability to transfer K^+ ions across the inner mitochondrial membrane.

8. Mode of Action of Dicyclohexylcarbodiimide (DCCD) When DCCD is added to a suspension of tightly coupled, actively respiring mitochondria, the rate of electron transfer (measured by O_2 consumption) and the rate of ATP production dramatically decrease. If a solution of 2,4-dinitrophenol is now added to the preparation, O_2 consumption returns to normal but ATP production remains inhibited.

(a) What process in electron transfer or oxidative phosphorylation is affected by DCCD?

(b) Why does DCCD affect the O_2 consumption of mitochondria? Explain the effect of 2,4-dinitrophenol on the inhibited mitochondrial preparation.

(c) Which of the following inhibitors does DCCD most resemble in its action: antimycin A, rotenone, or oligomycin?

9. Compartmentalization of Citric Acid Cycle Components Isocitrate dehydrogenase is found only in the mitochondrion, but malate dehydrogenase is found in both the cytosol and mitochondrion. What is the role of cytosolic malate dehydrogenase?

10. The Malate–α-Ketoglutarate Transport System The transport system that conveys malate and α-ketoglutarate across the inner mitochondrial membrane (see Fig. 19–31) is inhibited by *n*-butylmalonate. Suppose *n*-butylmalonate is added to an aerobic suspension of kidney cells using glucose exclusively as fuel. Predict the effect of this inhibitor on (a) glycolysis, (b) oxygen consumption, (c) lactate formation, and (d) ATP synthesis.

11. Cellular ADP Concentration Controls ATP Formation Although both ADP and P_i are required for the synthesis of ATP, the rate of synthesis depends mainly on the concentration of ADP, not P_i. Why?

12. Time Scales of Regulatory Events in Mitochondria Compare the likely time scales for the adjustments in respiratory rate caused by (a) increased [ADP] and (b) reduced pO_2. What accounts for the difference?

13. The Pasteur Effect When O_2 is added to an anaerobic suspension of cells consuming glucose at a high rate, the rate of glucose consumption declines greatly as the O_2 is used up, and accumulation of lactate ceases. This effect, first observed by Louis Pasteur in the 1860s, is characteristic of most cells capable of both aerobic and anaerobic glucose catabolism.

(a) Why does the accumulation of lactate cease after O_2 is added?

(b) Why does the presence of O_2 decrease the rate of glucose consumption?

(c) How does the onset of O_2 consumption slow down the rate of glucose consumption? Explain in terms of specific enzymes.

14. Respiration-Deficient Yeast Mutants and Ethanol Production Respiration-deficient yeast mutants (p^-; "petites") can be produced from wild-type parents by treatment with mutagenic agents. The mutants lack cytochrome oxidase, a deficit that markedly affects their metabolic behavior. One striking effect is that fermentation is not suppressed by O_2—that is, the mutants lack the Pasteur effect (see Problem 13). Some companies are very interested in using these mutants to ferment wood chips to ethanol for energy use. Explain the advantages of using these mutants rather than wild-type yeast for large-scale ethanol production. Why does the absence of cytochrome oxidase eliminate the Pasteur effect?

15. Advantages of Supercomplexes for Electron Transfer There is growing evidence that mitochondrial Complexes I, II, III, and IV are part of a larger supercomplex. What might be the advantage of having all four complexes within a supercomplex?

16. How Many Protons in a Mitochondrion? Electron transfer translocates protons from the mitochondrial matrix to the external medium, establishing a pH gradient across the inner membrane (outside more acidic than inside). The tendency of protons to diffuse back into the matrix is the driving force for ATP synthesis by ATP synthase. During oxidative phosphorylation by a suspension of mitochondria in a medium of pH 7.4, the pH of the matrix has been measured as 7.7.

(a) Calculate $[H^+]$ in the external medium and in the matrix under these conditions.

(b) What is the outside-to-inside ratio of $[H^+]$? Comment on the energy inherent in this concentration difference. (Hint: See Eqn 11–4, p. 410.)

(c) Calculate the number of protons in a respiring liver mitochondrion, assuming its inner matrix compartment is a sphere of diameter 1.5 μm.

(d) From these data, is the pH gradient alone sufficient to generate ATP?

(e) If not, suggest how the necessary energy for synthesis of ATP arises.

17. Rate of ATP Turnover in Rat Heart Muscle Rat heart muscle operating aerobically fills more than 90% of its ATP needs by oxidative phosphorylation. Each gram of tissue consumes O_2 at the rate of 10.0 μmol/min, with glucose as the fuel source.

(a) Calculate the rate at which the heart muscle consumes glucose and produces ATP.

(b) For a steady-state concentration of ATP of 5.0 μmol/g of heart muscle tissue, calculate the time required (in seconds) to completely turn over the cellular pool of ATP. What does this result indicate about the need for tight regulation of ATP production? (Note: Concentrations are expressed as micromoles per gram of muscle tissue because the tissue is mostly water.)

18. Rate of ATP Breakdown in Insect Flight Muscle ATP production in the flight muscle of the fly *Lucilia sericata* results almost exclusively from oxidative phosphorylation. During flight, 187 mL of O_2/h·g of body weight is needed to maintain an ATP concentration of 7.0 μmol/g of flight muscle. Assuming that flight muscle makes up 20% of the weight of the fly, calculate the rate at which the flight-muscle ATP pool turns over. How long would the reservoir of ATP last in the absence of oxidative phosphorylation? Assume that reducing equivalents are transferred by the glycerol 3-phosphate shuttle and that O_2 is at 25 °C and 101.3 kPa (1 atm).

19. Mitochondrial Disease and Cancer Mutations in the genes that encode certain mitochondrial proteins are associated with a high incidence of some types of cancer. How might defective mitochondria lead to cancer?

20. Variable Severity of a Mitochondrial Disease Individuals with a disease caused by a specific defect in the mitochondrial genome may have symptoms ranging from mild to severe. Explain why.

21. Transmembrane Movement of Reducing Equivalents Under aerobic conditions, extramitochondrial NADH must be oxidized by the mitochondrial electron-transfer chain. Consider a preparation of rat hepatocytes containing mitochondria and all the cytosolic enzymes. If [4-^{3}H]NADH is introduced, radioactivity soon appears in the mitochondrial matrix. However, if [7-^{14}C]NADH is introduced, no radioactivity appears in the matrix. What do these observations reveal about the oxidation of extramitochondrial NADH by the electron-transfer chain?

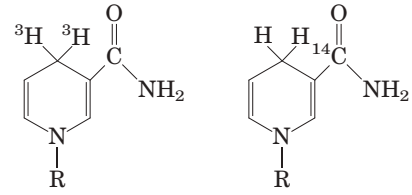

[4-^{3}H]NADH [7-^{14}C]NADH

22. High Blood Alanine Level Associated with Defects in Oxidative Phosphorylation Most individuals with genetic defects in oxidative phosphorylation are found to have relatively high concentrations of alanine in their blood. Explain this in biochemical terms.

23. NAD Pools and Dehydrogenase Activities Although both pyruvate dehydrogenase and glyceraldehyde 3-phosphate dehydrogenase use NAD^+ as their electron acceptor, the two enzymes do not compete for the same cellular NAD pool. Why?

24. Diabetes as a Consequence of Mitochondrial Defects Glucokinase is essential in the metabolism of glucose in pancreatic β cells. Humans with two defective copies of the glucokinase gene exhibit a severe, neonatal diabetes, whereas those with only one defective copy of the gene have a much milder form of the disease (mature onset diabetes of the young, MODY2). Explain this difference in terms of the biology of the β cell.

25. Effects of Mutations in Mitochondrial Complex II Single nucleotide changes in the gene for succinate dehydrogenase (Complex II) are associated with midgut carcinoid tumors. Suggest a mechanism to explain this observation.

26. Photochemical Efficiency of Light at Different Wavelengths The rate of photosynthesis, measured by O_2 production, is higher when a green plant is illuminated with light of wavelength 680 nm than with light of 700 nm. However, illumination by a combination of light of 680 nm and 700 nm gives a higher rate of photosynthesis than light of either wavelength alone. Explain.

27. Balance Sheet for Photosynthesis In 1804 Theodore de Saussure observed that the total weight of oxygen and dry organic matter produced by plants is greater than the weight of carbon dioxide consumed during photosynthesis. Where does the extra weight come from*ff*

28. Role of H_2S in Some Photosynthetic Bacteria Illuminated purple sulfur bacteria carry out photosynthesis in the presence of H_2O and $^{14}CO_2$, but only if H_2S is added and O_2 is absent. During the course of photosynthesis, measured by formation of

[^{14}C]carbohydrate, H_2S is converted to elemental sulfur, but no O_2 is evolved. What is the role of the conversion of H_2S to sulfur? Why is no O_2 evolved?

29. Boosting the Reducing Power of Photosystem I by Light Absorption When photosystem I absorbs red light at 700 nm, the standard reduction potential of P700 changes from 0.40 V to about −1.2 V. What fraction of the absorbed light is trapped in the form of reducing power?

30. Electron Flow through Photosystems I and II Predict how an inhibitor of electron passage through pheophytin would affect electron flow through (a) photosystem II and (b) photosystem I. Explain your reasoning.

31. Limited ATP Synthesis in the Dark In a laboratory experiment, spinach chloroplasts are illuminated in the absence of ADP and P_i, then the light is turned off and ADP and P_i are added. ATP is synthesized for a short time in the dark. Explain this finding.

32. Mode of Action of the Herbicide DCMU When chloroplasts are treated with 3-(3,4-dichlorophenyl)-1,1-dimethylurea (DCMU, or diuron), a potent herbicide, O_2 evolution and photophosphorylation cease. Oxygen evolution, but not photophosphorylation, can be restored by addition of an external electron acceptor, or Hill reagent. How does DCMU act as a weed killer? Suggest a location for the inhibitory action of this herbicide in the scheme shown in Figure 19–58. Explain.

33. Effect of Venturicidin on Oxygen Evolution Venturicidin is a powerful inhibitor of the chloroplast ATP synthase, interacting with the CF_o part of the enzyme and blocking proton passage through the CF_oCF_1 complex. How would venturicidin affect oxygen evolution in a suspension of well-illuminated chloroplasts? Would your answer change if the experiment were done in the presence of an uncoupling reagent such as 2,4-dinitrophenol (DNP)? Explain.

34. Bioenergetics of Photophosphorylation The steady-state concentrations of ATP, ADP, and P_i in isolated spinach chloroplasts under full illumination at pH 7.0 are 120.0, 6.0, and 700.0 μM, respectively.

(a) What is the free-energy requirement for the synthesis of 1 mol of ATP under these conditions?

(b) The energy for ATP synthesis is furnished by light-induced electron transfer in the chloroplasts. What is the minimum voltage drop necessary (during transfer of a pair of electrons) to synthesize ATP under these conditions? (You may need to refer to Eqn 13–7, p. 531.)

35. Light Energy for a Redox Reaction Suppose you have isolated a new photosynthetic microorganism that oxidizes H_2S and passes the electrons to NAD^+. What wavelength of light would provide enough energy for H_2S to reduce NAD^+ under standard conditions? Assume 100% efficiency in the photochemical event, and use E'° of −243 mV for H_2S and −320 mV for NAD^+. See Figure 19–48 for the energy equivalents of wavelengths of light.

36. Equilibrium Constant for Water-Splitting Reactions The coenzyme $NADP^+$ is the terminal electron acceptor in chloroplasts, according to the reaction

$$2H_2O + 2NADP^+ \longrightarrow 2NADPH + 2H^+ + O_2$$

Use the information in Table 19–2 to calculate the equilibrium constant for this reaction at 25 °C. (The relationship between K'_{eq} and $\Delta G'^\circ$ is discussed on p. 508.) How can the chloroplast overcome this unfavorable equilibrium?

37. Energetics of Phototransduction During photosynthesis, eight photons must be absorbed (four by each photosystem) for every O_2 molecule produced:

$$2H_2O + 2NADP^+ + 8\ \text{photons} \longrightarrow 2NADPH + 2H^+ + O_2$$

Assuming that these photons have a wavelength of 700 nm (red) and that the light absorption and use of light energy are 100% efficient, calculate the free-energy change for the process.

38. Electron Transfer to a Hill Reagent Isolated spinach chloroplasts evolve O_2 when illuminated in the presence of potassium ferricyanide (a Hill reagent), according to the equation

$$2H_2O + 4Fe^{3+} \longrightarrow O_2 + 4H^+ + 4Fe^{2+}$$

where Fe^{3+} represents ferricyanide and Fe^{2+}, ferrocyanide. Is NADPH produced in this process? Explain.

39. How Often Does a Chlorophyll Molecule Absorb a Photon? The amount of chlorophyll *a* (M_r 892) in a spinach leaf is about 20 μg/cm^2 of leaf surface. In noonday sunlight (average energy reaching the leaf is 5.4 J/cm^2 · min), the leaf absorbs about 50% of the radiation. How often does a single chlorophyll molecule absorb a photon? Given that the average lifetime of an excited chlorophyll molecule in vivo is 1 ns, what fraction of the chlorophyll molecules are excited at any one time?

40. Effect of Monochromatic Light on Electron Flow The extent to which an electron carrier is oxidized or reduced during photosynthetic electron transfer can sometimes be observed directly with a spectrophotometer. When chloroplasts are illuminated with 700 nm light, cytochrome *f*, plastocyanin, and plastoquinone are oxidized. When chloroplasts are illuminated with 680 nm light, however, these electron carriers are reduced. Explain.

41. Function of Cyclic Photophosphorylation When the [NADPH]/[$NADP^+$] ratio in chloroplasts is high, photophosphorylation is predominantly cyclic (see Fig. 19–58). Is O_2 evolved during cyclic photophosphorylation? Is NADPH produced? Explain. What is the main function of cyclic photophosphorylation?

Data Analysis Problem

42. Photophosphorylation: Discovery, Rejection, and Rediscovery In the 1930s and 1940s, researchers were beginning to make progress toward understanding the mechanism

of photosynthesis. At the time, the role of "energy-rich phosphate bonds" (today, "ATP") in glycolysis and cellular respiration was just becoming known. There were many theories about the mechanism of photosynthesis, especially about the role of light. This problem focuses on what was then called the "primary photochemical process"—that is, on what it is, exactly, that the energy from captured light produces in the photosynthetic cell. Interestingly, one important part of the modern model of photosynthesis was proposed early on, only to be rejected, ignored for several years, then finally revived and accepted.

In 1944, Emerson, Stauffer, and Umbreit proposed that "the function of light energy in photosynthesis is the formation of 'energy-rich' phosphate bonds" (p. 107). In their model (hereafter, the "Emerson model"), the free energy necessary to drive both CO_2 fixation *and* reduction came from these "energy-rich phosphate bonds" (i.e., ATP), produced as a result of light absorption by a chlorophyll-containing protein.

This model was explicitly rejected by Rabinowitch (1945). After summarizing Emerson and coauthors' findings, Rabinowitch stated: "Until more positive evidence is provided, we are inclined to consider as more convincing a general argument against this hypothesis, which can be derived from energy considerations. Photosynthesis is eminently a problem of energy *accumulation*. What good can be served, then, by converting light quanta (even those of red light, which amount to about 43 kcal per Einstein) into 'phosphate quanta' of only 10 kcal per mole? This appears to be a start in the wrong direction—toward *dissipation* rather than toward accumulation of energy" (Vol. I, p. 228). This argument, along with other evidence, led to the abandonment of the Emerson model until the 1950s, when it was found to be correct—albeit in a modified form.

For each piece of information from Emerson and coauthors' article presented in (a) through (d), answer the following three questions:

1. How does this information support the Emerson model, in which light energy is used directly by chlorophyll *to make ATP*, and the ATP then provides the energy to drive CO_2 fixation and reduction?
2. How would Rabinowitch explain this information, based on his model (and most other models of the day), in which light energy is used directly by chlorophyll *to make reducing compounds*? Rabinowitch wrote: "Theoretically, there is no reason why *all* electronic energy contained in molecules excited by the absorption of light should not be available for oxidation-reduction" (Vol. I, p. 152). In this model, the reducing compounds are then used to fix and reduce CO_2, and the energy for these reactions comes from the large amounts of free energy released by the reduction reactions.
3. How is this information explained by our modern understanding of photosynthesis?

(a) Chlorophyll contains a Mg^{2+} ion, which is known to be an essential cofactor for many enzymes that catalyze phosphorylation and dephosphorylation reactions.

(b) A crude "chlorophyll protein" isolated from photosynthetic cells showed phosphorylating activity.

(c) The phosphorylating activity of the "chlorophyll protein" was inhibited by light.

(d) The levels of several different phosphorylated compounds in photosynthetic cells changed dramatically in response to light exposure. (Emerson and coworkers were not able to identify the specific compounds involved.)

As it turned out, the Emerson and Rabinowitch models were both partly correct and partly incorrect.

(e) Explain how the two models relate to our current model of photosynthesis.

In his rejection of the Emerson model, Rabinowitch went on to say: "The difficulty of the phosphate storage theory appears most clearly when one considers the fact that, in weak light, eight or ten quanta of light are sufficient to reduce one molecule of carbon dioxide. If each quantum should produce one molecule of high-energy phosphate, the accumulated energy would be only 80–100 kcal per Einstein—while photosynthesis requires *at least* 112 kcal per mole, and probably more, because of losses in irreversible partial reactions" (Vol. 1, p. 228).

(f) How does Rabinowitch's value of 8 to 10 photons per molecule of CO_2 reduced compare with the value accepted today? You need to consult Chapter 20 for some of the information required here.

(g) How would you rebut Rabinowitch's argument, based on our current knowledge about photosynthesis?

References

Emerson, R.L., Stauffer, J.F., & Umbreit, W.W. (1944) Relationships between phosphorylation and photosynthesis in *Chlorella. Am. J. Botany* **31**, 107–120.

Rabinowitch, E.I. (1945) *Photosynthesis and Related Processes*, Interscience Publishers, New York.

this page left intentionally blank

20

Carbohydrate Biosynthesis in Plants and Bacteria

We have now reached a turning point in our study of cellular metabolism. Thus far in Part II we have described how the major metabolic fuels—carbohydrates, fatty acids, and amino acids—are degraded through converging *catabolic* pathways to enter the citric acid cycle and yield their electrons to the respiratory chain, and how this exergonic flow of electrons to oxygen is coupled to the endergonic synthesis of ATP. We now turn to *anabolic* pathways, which use chemical energy in the form of ATP and NADH or NADPH to synthesize cellular components from simple precursor molecules. Anabolic pathways are generally reductive rather than oxidative. Catabolism and anabolism proceed simultaneously in a dynamic steady state, so the energy-yielding degradation of cellular components is counterbalanced by biosynthetic processes, which create and maintain the intricate orderliness of living cells.

Plants must be especially versatile in their handling of carbohydrates, for several reasons. First, plants are autotrophs, able to convert inorganic carbon (as CO_2) into organic compounds. Second, biosynthesis occurs primarily in plastids, membrane-bounded organelles unique to photosynthetic organisms, and the movement of intermediates between cellular compartments is an important aspect of metabolism. Third, plants are not motile: they cannot move to find better supplies of water, sunlight, or nutrients. They must have sufficient metabolic flexibility to allow them to adapt to changing conditions in the place where they are rooted. Finally, plants have thick cell walls made of carbohydrate polymers, which must be assembled outside the plasma membrane and which constitute a significant proportion of the cell's carbohydrate.

The chapter begins with a description of the process by which CO_2 is assimilated into trioses and hexoses, then considers photorespiration, an important side reaction during CO_2 fixation, and the ways in which certain plants avoid this side reaction. We then look at how the biosynthesis of sucrose (for sugar transport) and starch (for energy storage) is accomplished by mechanisms analogous to those employed by animal cells to make glycogen. The next topic is the synthesis of the cellulose of plant cell walls and the peptidoglycan of bacterial cell walls, illustrating the problems of energy-dependent biosynthesis outside the plasma membrane. Finally, we discuss how the various pathways that share pools of common intermediates are segregated within organelles yet integrated with one another.

20.1 Photosynthetic Carbohydrate Synthesis

The synthesis of carbohydrates in animal cells always employs precursors having at least three carbons, all of which are less oxidized than the carbon in CO_2. Plants and photosynthetic microorganisms, by contrast, can synthesize carbohydrates from CO_2 and water, reducing CO_2 at the expense of the energy and reducing power furnished by the ATP and NADPH that are generated by the light-dependent reactions of photosynthesis **(Fig. 20–1)**. Plants (and other autotrophs) can use CO_2 as the sole source of the carbon atoms required for the biosynthesis of cellulose and starch, lipids and proteins, and the many other organic components of plant cells. By contrast, heterotrophs cannot bring

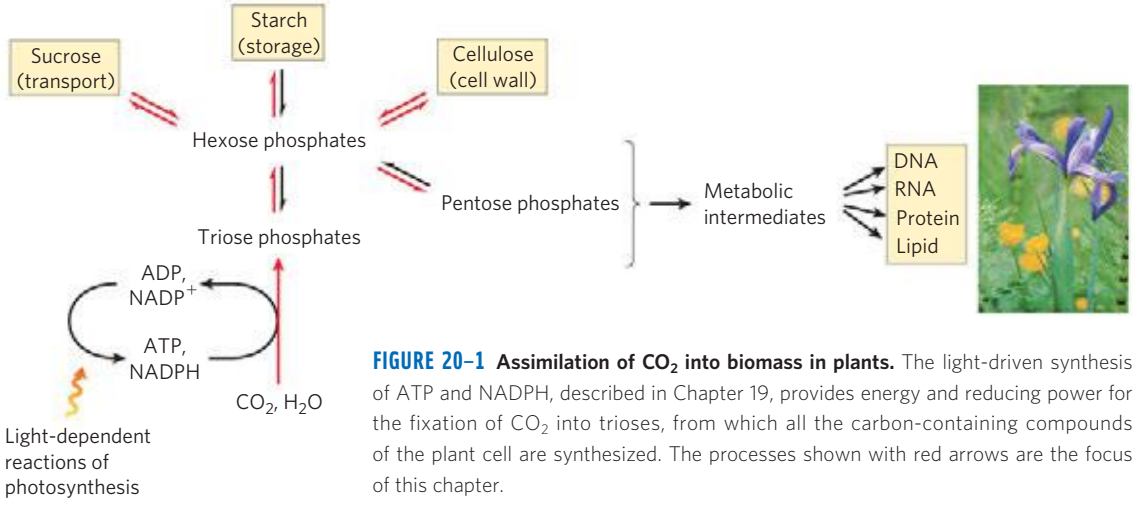

FIGURE 20–1 Assimilation of CO_2 into biomass in plants. The light-driven synthesis of ATP and NADPH, described in Chapter 19, provides energy and reducing power for the fixation of CO_2 into trioses, from which all the carbon-containing compounds of the plant cell are synthesized. The processes shown with red arrows are the focus of this chapter.

about the net reduction of CO_2 to achieve a net synthesis of glucose.

Green plants contain in their chloroplasts unique enzymatic machinery that catalyzes the conversion of CO_2 to simple (reduced) organic compounds, a process called **CO_2 assimilation**. This process has also been called **CO_2 fixation** or **carbon fixation**, but we reserve these terms for the specific reaction in which CO_2 is incorporated (fixed) into a three-carbon organic compound, the triose phosphate 3-phosphoglycerate. This simple product of photosynthesis is the precursor of more complex biomolecules, including sugars, polysaccharides, and the metabolites derived from them, all of which are synthesized by metabolic pathways similar to those of animal tissues. Carbon dioxide is assimilated via a cyclic pathway, its key intermediates constantly regenerated. The pathway was elucidated in the early 1950s by Melvin Calvin, Andrew Benson, and James A. Bassham, and is often called the **Calvin cycle** or, more descriptively, the **photosynthetic carbon reduction cycle**.

Melvin Calvin, 1911–1997

Carbohydrate metabolism is more complex in plant cells than in animal cells or in nonphotosynthetic microorganisms. In addition to the universal pathways of glycolysis and gluconeogenesis, plants have the unique reaction sequences for reduction of CO_2 to triose phosphates and the associated reductive pentose phosphate pathway—all of which must be coordinately regulated to ensure proper allocation of carbon to energy production and synthesis of starch and sucrose. Key enzymes are regulated, as we shall see, by (1) reduction of disulfide bonds by electrons flowing from photosystem I and (2) changes in pH and Mg^{2+} concentration that result from illumination. When we look at other aspects of plant carbohydrate metabolism, we also find enzymes that are modulated by (3) conventional allosteric regulation by one or more metabolic intermediates and (4) covalent modification (phosphorylation).

Plastids Are Organelles Unique to Plant Cells and Algae

Most of the biosynthetic activities in plants (including CO_2 assimilation) occur in **plastids**, a family of self-reproducing organelles bounded by a double membrane and containing a small genome that encodes some of their proteins. Most proteins destined for plastids are encoded in nuclear genes, which are transcribed and translated like other nuclear genes; then the proteins are imported into plastids. Plastids reproduce by binary fission, replicating their genome (a single circular DNA molecule) and using their own enzymes and ribosomes to synthesize the proteins encoded by that genome. **Chloroplasts** (see Fig. 19–47) are the sites of CO_2 assimilation. The enzymes for this process are contained in the stroma, the soluble phase bounded by the inner chloroplast membrane. **Amyloplasts** are colorless plastids (that is, they lack chlorophyll and other pigments found in chloroplasts). They have no internal membranes analogous to the photosynthetic membranes (thylakoids) of chloroplasts, and in plant tissues rich in starch these plastids are packed with starch granules **(Fig. 20–2)**. Chloroplasts can be converted to

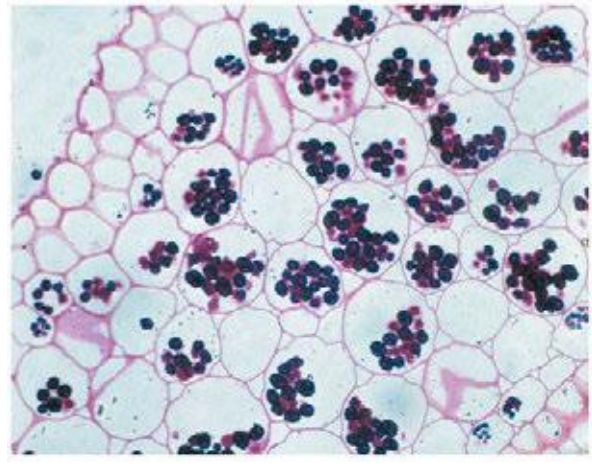

FIGURE 20–2 Amyloplasts filled with starch (dark granules) are stained with iodine in this section of *Ranunculus* root cells. Starch granules in various tissues range from 1 to 100 μm in diameter.

proplastids by the loss of their internal membranes and chlorophyll, and proplastids are interconvertible with amyloplasts **(Fig. 20–3)**. In turn, both amyloplasts and proplastids can develop into chloroplasts. The relative abundance of the plastid types depends on the type of plant tissue and on the intensity of illumination. Cells of green leaves are rich in chloroplasts, whereas amyloplasts dominate in nonphotosynthetic tissues that store starch in large quantities, such as potato tubers.

The inner membranes of all types of plastids are impermeable to polar and charged molecules. Traffic across these membranes is mediated by sets of specific transporters.

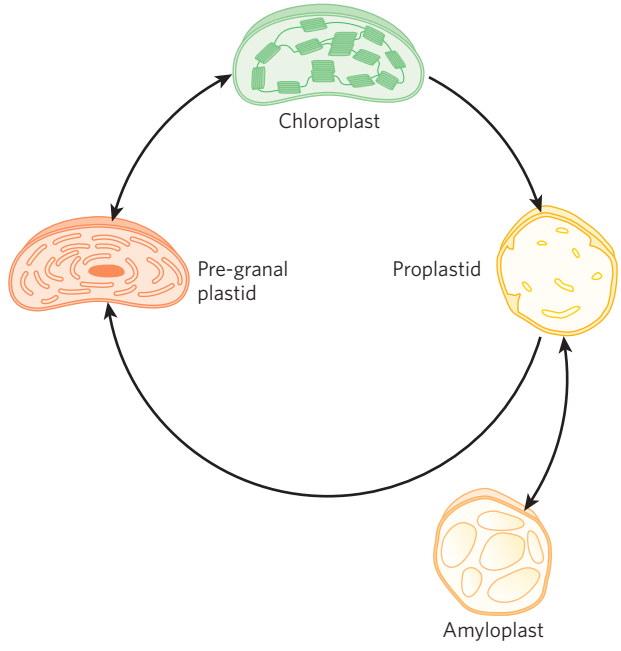

FIGURE 20–3 Plastids: their origins and interconversions. All types of plastids are bounded by a double membrane, and some (notably the mature chloroplast) have extensive internal membranes. The internal membranes can be lost (when a mature chloroplast becomes a proplastid) and resynthesized (as a proplastid gives rise to a pre-granal plastid and then a mature chloroplast). Proplastids in nonphotosynthetic tissues (such as root) give rise to amyloplasts, which contain large quantities of starch. All plant cells have plastids, and these organelles are the sites, not only of photosynthesis, but of other processes, including the synthesis of essential amino acids, thiamine, pyridoxal phosphate, flavins, and vitamins A, C, E, and K.

Carbon Dioxide Assimilation Occurs in Three Stages

The first stage in the assimilation of CO_2 into biomolecules **(Fig. 20–4)** is the **carbon-fixation reaction**: condensation of CO_2 with a five-carbon acceptor, **ribulose 1,5-bisphosphate**, to form two molecules of **3-phosphoglycerate**. In the second stage, the 3-phosphoglycerate is reduced to triose phosphates. Overall, three molecules of CO_2 are fixed to three molecules of ribulose 1,5-bisphosphate to form six molecules of glyceraldehyde 3-phosphate (18 carbons) in equilibrium with dihydroxyacetone phosphate. In the third stage, five of the six molecules of triose phosphate (15 carbons) are used to regenerate three molecules of ribulose 1,5-bisphosphate (15 carbons), the starting material. The sixth molecule of triose phosphate, the net product of photosynthesis, can be used to make hexoses for fuel and building materials, sucrose for transport to nonphotosynthetic tissues, or starch for storage. Thus the overall process is cyclical, with the continuous conversion of CO_2 to triose and hexose phosphates. Fructose 6-phosphate is a key intermediate in stage 3 of CO_2 assimilation; it stands at a branch point, leading either to regeneration of ribulose 1,5-bisphosphate or to synthesis of starch. The pathway from hexose phosphate to pentose bisphosphate involves many of the same reactions used in animal cells for the conversion of pentose phosphates to hexose phosphates during the nonoxidative phase of the **pentose phosphate pathway** (see Fig. 14–23). In the photosynthetic assimilation of CO_2, essentially the same set of reactions operates in the other direction, converting hexose phosphates to pentose phosphates. This **reductive pentose phosphate cycle** uses the same enzymes as the oxidative pathway, and several more enzymes that make the reductive cycle irreversible. All 13 enzymes of the pathway are in the chloroplast stroma.

Stage 1: Fixation of CO_2 into 3-Phosphoglycerate An important clue to the nature of the CO_2-assimilation mechanisms in photosynthetic organisms came in the late 1940s. Calvin and his associates illuminated a suspension of green algae in the presence of radioactive carbon dioxide ($^{14}CO_2$) for

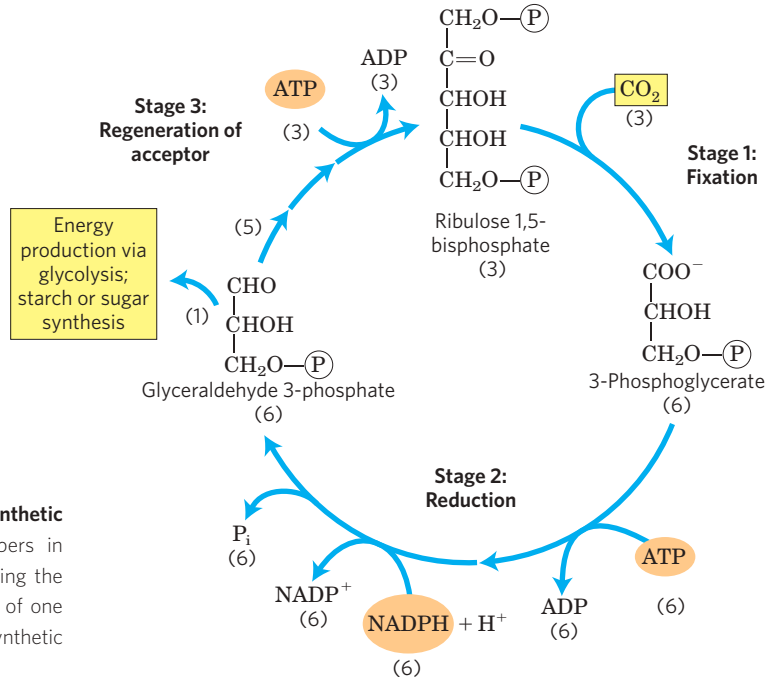

FIGURE 20–4 The three stages of CO_2 assimilation in photosynthetic organisms. Stoichiometries of three key intermediates (numbers in parentheses) reveal the fate of carbon atoms entering and leaving the cycle. As shown here, three CO_2 are fixed for the net synthesis of one molecule of glyceraldehyde 3-phosphate. This cycle is the photosynthetic carbon reduction cycle, or the Calvin cycle.

just a few seconds, then quickly killed the cells, extracted their contents, and with the help of chromatographic methods searched for the metabolites in which the labeled carbon first appeared. The first compound that became labeled was **3-phosphoglycerate**, with the ^{14}C predominantly located in the carboxyl carbon atom. These experiments strongly suggested that 3-phosphoglycerate is an early intermediate in photosynthesis. The many plants in which this three-carbon compound is the first intermediate are called **C_3 plants**, in contrast to the C_4 plants described below.

The enzyme that catalyzes incorporation of CO_2 into an organic form is **ribulose 1,5-bisphosphate carboxylase/oxygenase**, a name mercifully shortened to **rubisco**. As a carboxylase, rubisco catalyzes the covalent attachment of CO_2 to the five-carbon sugar ribulose 1,5-bisphosphate and cleavage of the unstable six-carbon intermediate to form two molecules of 3-phosphoglycerate, one of which bears the carbon introduced as CO_2 in its carboxyl group (Fig. 20–4). The enzyme's oxygenase activity is discussed in Section 20.2.

There are two distinct forms of rubisco. Form I is found in vascular plants, algae, and cyanobacteria; form II is confined to certain photosynthetic bacteria. Plant rubisco, the crucial enzyme in the production of biomass from CO_2, has a complex form I structure **(Fig. 20–5a)**, with eight identical large subunits (M_r 53,000; encoded in the chloroplast genome, or plastome), each containing a catalytic site, and eight identical small subunits (M_r 14,000; encoded in the nuclear genome) of uncertain function. The form II rubisco of photosynthetic bacteria is simpler in structure, having two subunits that in many respects resemble the large subunits of the plant enzyme (Fig. 20–5b). This similarity is consistent with the endosymbiont hypothesis for the origin of chloroplasts (p. 36). The plant enzyme has an exceptionally low turnover number; only three molecules of CO_2 are fixed per second per molecule of rubisco at 25 °C. To achieve high rates of CO_2 fixation, plants therefore need large amounts of this enzyme. In fact, rubisco makes up almost 50% of soluble protein in chloroplasts and is probably one of the most abundant enzymes in the biosphere.

Central to the proposed mechanism for plant rubisco is a carbamoylated Lys side chain with a bound Mg^{2+} ion. The Mg^{2+} ion brings together and orients the reactants at

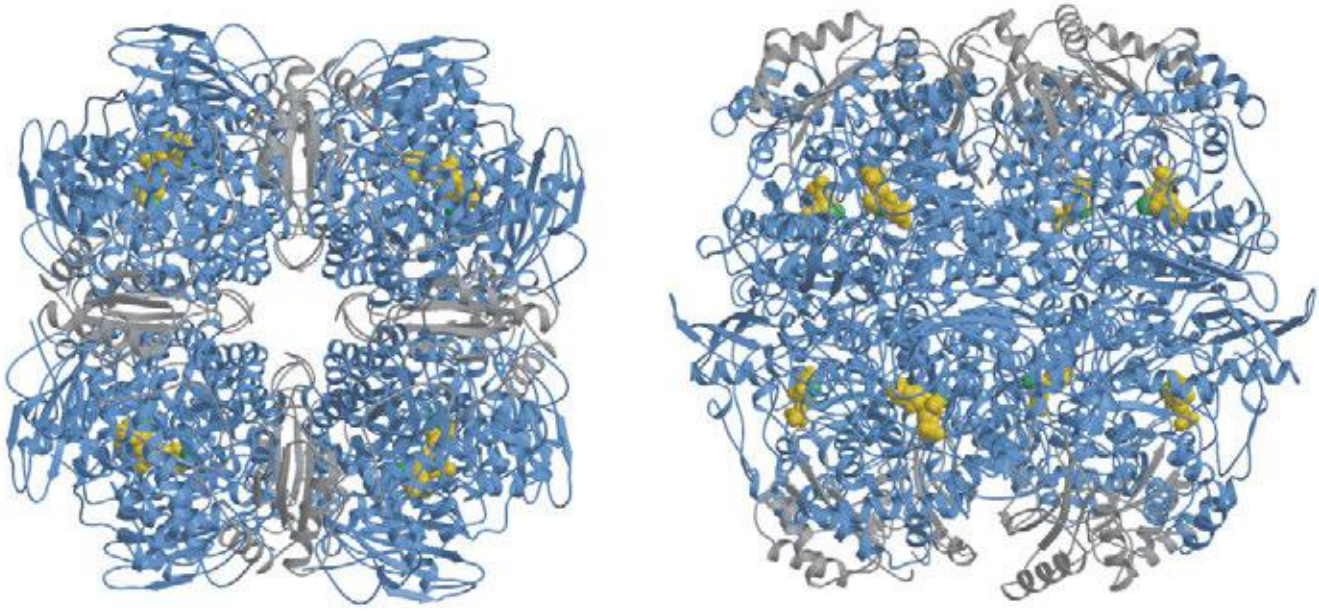

FIGURE 20–5 Structure of ribulose 1,5-bisphosphate carboxylase (rubisco). (a) Top and side views of a ribbon model of form I rubisco from spinach (PDB ID 8RUC). The enzyme has eight large subunits (blue) and eight small ones (gray), tightly packed into a structure of M_r greater than 500,000. Rubisco is present at a concentration of about 250 mg/mL in the chloroplast stroma, corresponding to an extraordinarily high concentration of active sites (~4 mM). A transition-state analog, 2-carboxyarabinitol bisphosphate, is shown in yellow bound to each of the eight substrate-binding sites. Mg^{2+} is shown in green. **(b)** Ribbon model of form II rubisco from the bacterium *Rhodospirillum rubrum* (PDB ID 9RUB). The subunits are in gray and blue.

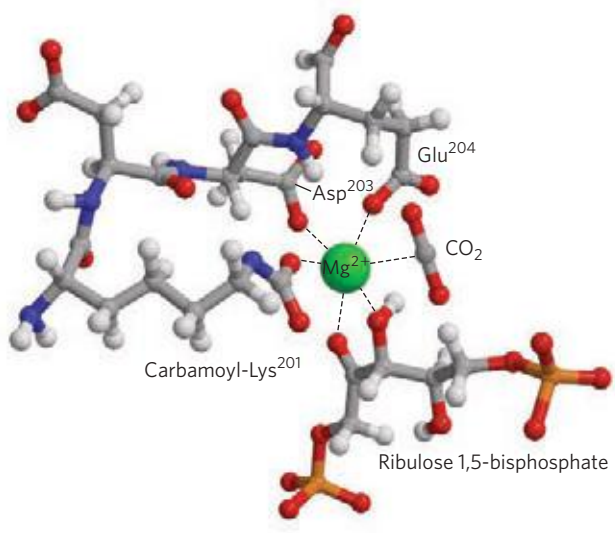

FIGURE 20–6 Central role of Mg^{2+} in the catalytic mechanism of rubisco. (Derived from PDB ID 1RXO) Mg^{2+} is coordinated in a roughly octahedral complex with six oxygen atoms: one oxygen in the carbamate on Lys^{201}; two in the carboxyl groups of Glu^{204} and Asp^{203}; two at C-2 and C-3 of the substrate, ribulose 1,5-bisphosphate; and one in the other substrate, CO_2. A water molecule occupies the CO_2-binding site in this crystal structure. In this figure a CO_2 molecule is modeled in its place. (Residue numbers refer to the spinach enzyme.)

the active site **(Fig. 20–6)** and polarizes the CO_2, opening it to nucleophilic attack by the five-carbon enediolate reaction intermediate formed on the enzyme **(Fig. 20–7)**. The resulting six-carbon intermediate breaks down to yield two molecules of 3-phosphoglycerate.

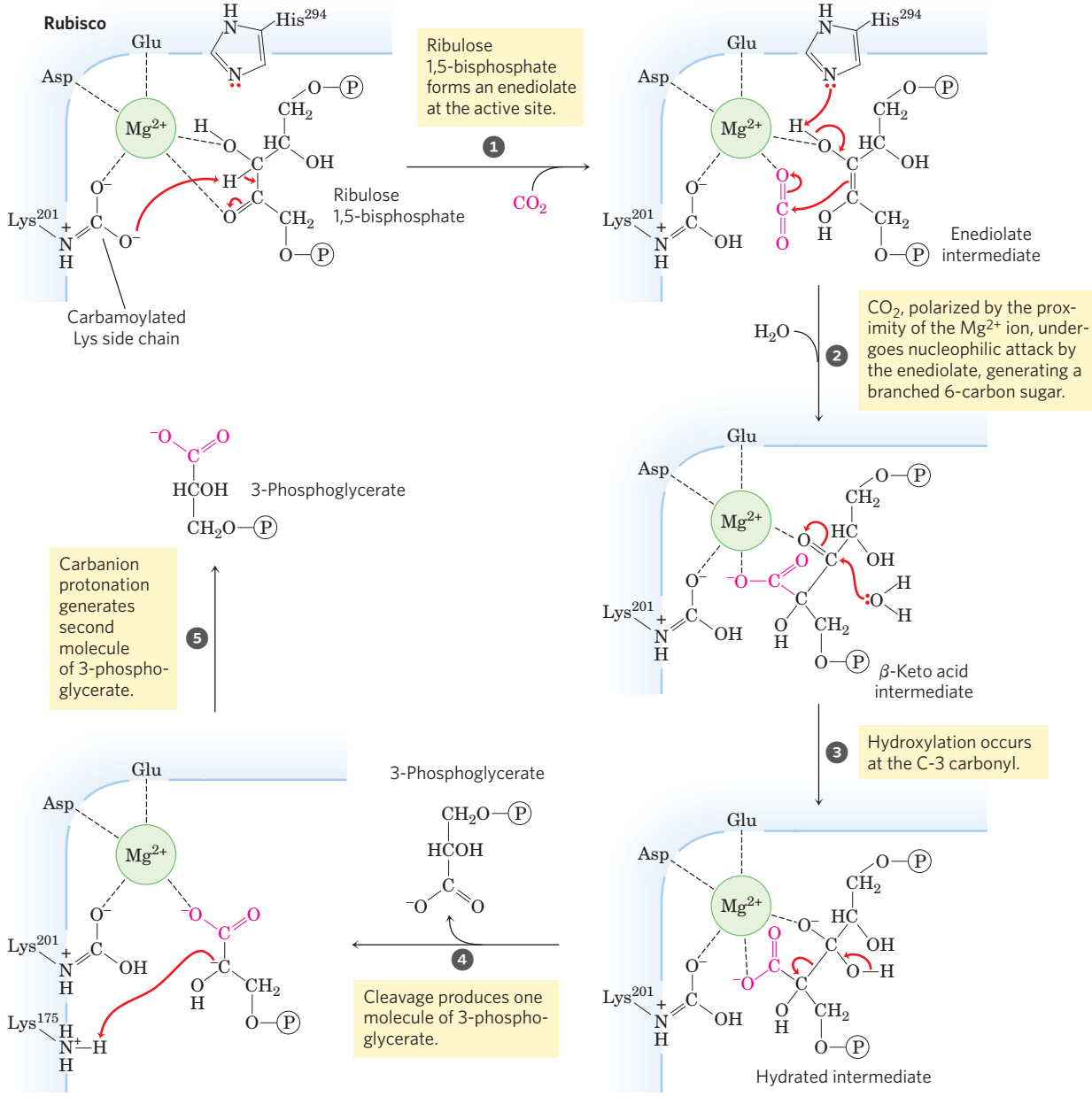

MECHANISM FIGURE 20–7 First stage of CO_2 assimilation: rubisco's carboxylase activity. The CO_2-fixation reaction is catalyzed by ribulose 1,5-bisphosphate carboxylase/oxygenase (rubisco). The overall reaction accomplishes the combination of one CO_2 and one ribulose 1,5-bisphosphate to form two molecules of 3-phosphoglycerate, one of which contains the carbon atom from CO_2 (red). Additional proton transfers (not shown), involving Lys^{201}, Lys^{175}, and His^{294}, occur in several of these steps. **Rubisco Mechanism; Rubisco Tutorial**

As the catalyst for the first step of photosynthetic CO_2 assimilation, rubisco is a prime target for regulation. The enzyme is inactive until carbamoylated on the ε amino group of Lys^{201} **(Fig. 20–8)**. Ribulose 1,5-bisphosphate inhibits carbamoylation by binding tightly to the active site and locking the enzyme in the "closed" conformation, in which Lys^{201} is inaccessible. **Rubisco activase** overcomes the inhibition by promoting ATP-dependent release of the ribulose 1,5-bisphosphate, exposing the Lys amino group to nonenzymatic carbamoylation by CO_2; this is followed by Mg^{2+} binding, which activates the rubisco. Rubisco activase in some species is activated by light through a redox mechanism similar to that shown in Figure 20.19.

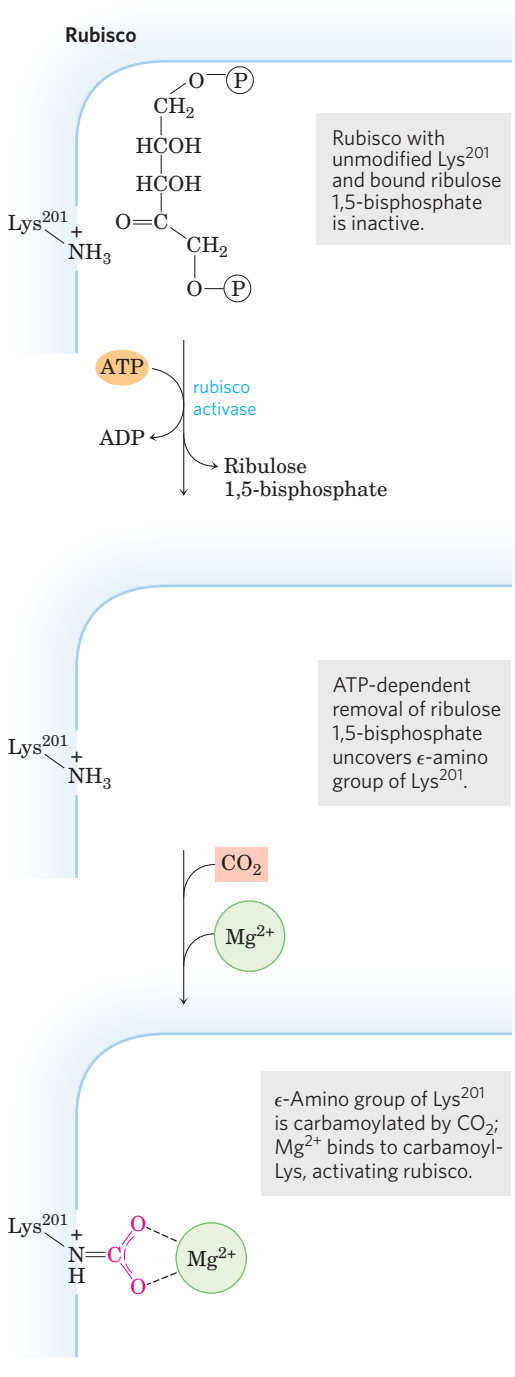

FIGURE 20–8 Role of rubisco activase in the carbamoylation of Lys^{201} of rubisco. When the substrate ribulose 1,5-bisphosphate is bound to the active site, Lys^{201} is not accessible. Rubisco activase couples ATP hydrolysis to expulsion of the bound sugar bisphosphate, exposing Lys^{201}; this Lys residue can now be carbamoylated with CO_2 in a reaction that is apparently not enzyme-mediated. Mg^{2+} is attracted to and binds to the negatively charged carbamoyl-Lys, and the enzyme is thus activated.

Another regulatory mechanism involves the "nocturnal inhibitor" 2-carboxyarabinitol 1-phosphate, a naturally occurring transition-state analog (p. 210) with a structure similar to that of the β-keto acid intermediate of the rubisco reaction (Fig. 20–7). This compound, synthesized in the dark in some plants, is a potent inhibitor of carbamoylated rubisco. It is either broken down when light returns or is expelled by rubisco activase, activating the rubisco.

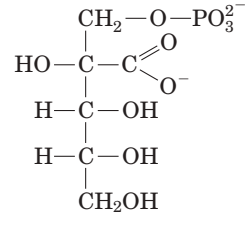

2-Carboxyarabinitol 1-phosphate

Stage 2: Conversion of 3-Phosphoglycerate to Glyceraldehyde 3-Phosphate The 3-phosphoglycerate formed in stage 1 is converted to glyceraldehyde 3-phosphate in two steps that are essentially the reversal of the corresponding steps in glycolysis, with one exception: the nucleotide cofactor for the reduction of 1,3-bisphosphoglycerate is NADPH rather than NADH **(Fig. 20–9)**. The chloroplast stroma contains all the glycolytic enzymes except phosphoglycerate mutase. The stromal and cytosolic enzymes are isozymes; both sets of enzymes catalyze the same reactions, but they are the products of different genes.

In the first step of stage 2, the stromal **3-phosphoglycerate kinase** catalyzes the transfer of a phosphoryl group from ATP to 3-phosphoglycerate, yielding 1,3-bisphosphoglycerate. Next, NADPH donates electrons in a reduction catalyzed by the chloroplast-specific isozyme of **glyceraldehyde 3-phosphate dehydrogenase**, producing glyceraldehyde 3-phosphate and P_i. The high concentrations of NADPH and ATP in the chloroplast stroma allow this thermodynamically unfavorable pair of reactions to proceed in the direction of 1,3-bisphosphoglycerate. Triose phosphate isomerase then interconverts glyceraldehyde 3-phosphate and dihydroxyacetone phosphate. Most of the triose phosphate thus produced is used to regenerate ribulose 1,5-bisphosphate; the rest is either converted to starch in the chloroplast and stored for later use or immediately exported to the cytosol and converted to sucrose for transport to growing regions of the plant. In

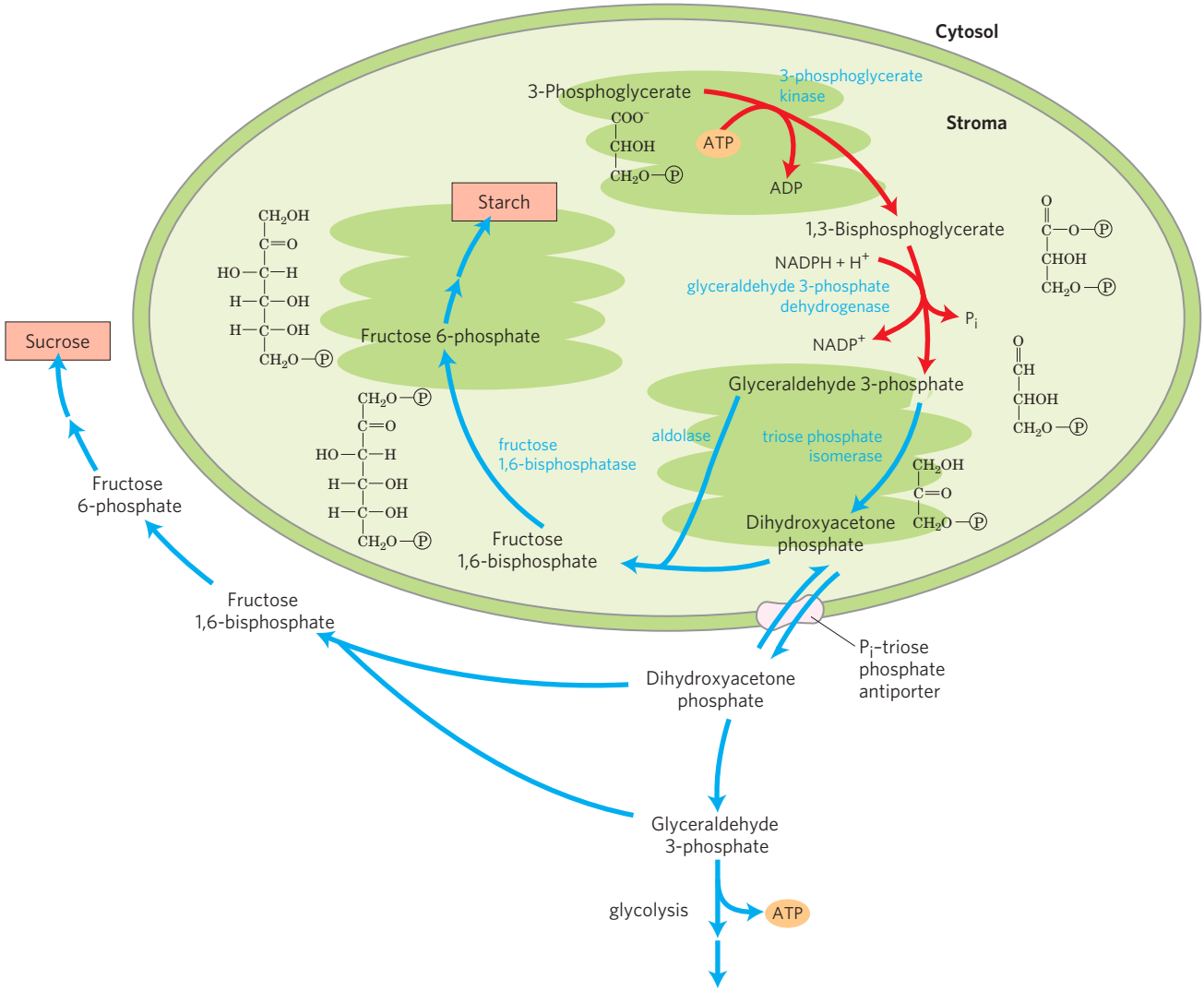

FIGURE 20–9 Second stage of CO_2 assimilation. 3-Phosphoglycerate is converted to glyceraldehyde 3-phosphate (red arrows). Also shown are the alternative fates of the fixed carbon of glyceraldehyde 3-phosphate (blue arrows). Most of the glyceraldehyde 3-phosphate is recycled to ribulose 1,5-bisphosphate as shown in Figure 20–10. A small fraction of the "extra" glyceraldehyde 3-phosphate may be used immediately as a source of energy, but most is converted to sucrose for transport or is stored in the chloroplast as starch. In the latter case, glyceraldehyde 3-phosphate condenses with dihydroxyacetone phosphate in the stroma to form fructose 1,6-bisphosphate, a precursor of starch. In other situations the glyceraldehyde 3-phosphate is converted to dihydroxyacetone phosphate, which leaves the chloroplast via a specific transporter (see Fig. 20–15) and, in the cytosol, can be degraded glycolytically to provide energy or used to form fructose 6-phosphate and hence sucrose.

developing leaves, a significant portion of the triose phosphate may be degraded by glycolysis to provide energy.

Stage 3: Regeneration of Ribulose 1,5-Bisphosphate from Triose Phosphates The first reaction in the assimilation of CO_2 into triose phosphates consumes ribulose 1,5-bisphosphate and, for continuous flow of CO_2 into carbohydrate, ribulose 1,5-bisphosphate must be constantly regenerated. This is accomplished in a series of reactions **(Fig. 20–10)** that, together with stages 1 and 2, constitute the cyclic pathway shown in Figure 20–4. The product of the first assimilation reaction (3-phosphoglycerate) thus undergoes transformations that regenerate ribulose 1,5-bisphosphate. The intermediates in this pathway include three-, four-, five-, six-, and seven-carbon sugars. In the following discussion, all step numbers refer to Figure 20–10.

Steps ❶ and ❹ are catalyzed by the same enzyme, **aldolase**. It first catalyzes the reversible condensation of glyceraldehyde 3-phosphate with dihydroxyacetone phosphate, yielding fructose 1,6-bisphosphate (step ❶); this is cleaved to fructose 6-phosphate and P_i by fructose 1,6-bisphosphatase (FBPase-1) in step ❷. The reaction is strongly exergonic and essentially irreversible. Step ❸ is catalyzed by **transketolase**, which contains thiamine pyrophosphate (TPP) as its prosthetic group (see Fig. 14–15a) and requires Mg^{2+}. Transketolase catalyzes the reversible transfer of a 2-carbon ketol group

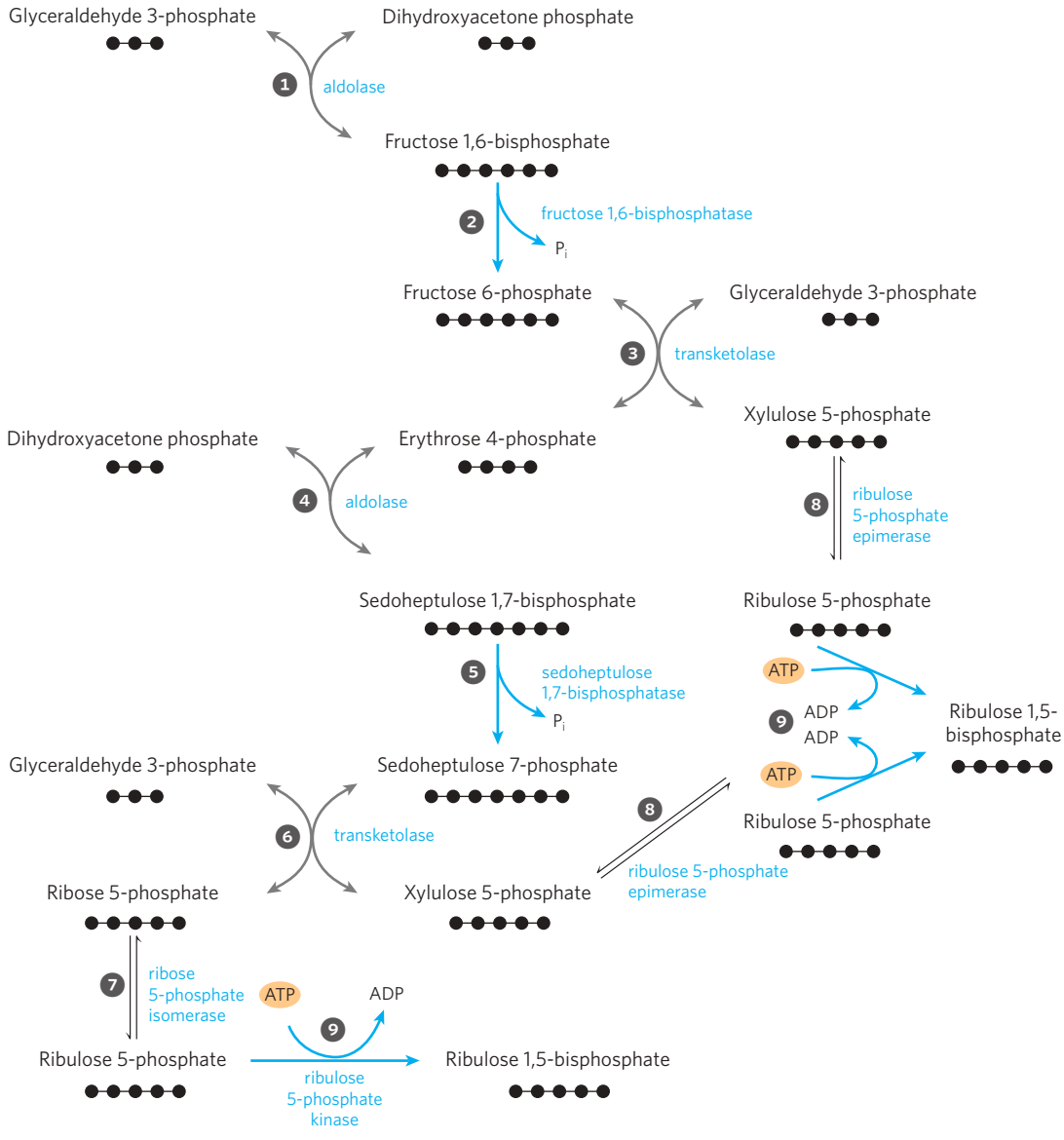

FIGURE 20–10 Third stage of CO_2 assimilation. This schematic diagram shows the interconversions of triose phosphates and pentose phosphates. Black dots represent the number of carbons in each compound. The starting materials are glyceraldehyde 3-phosphate and dihydroxyacetone phosphate. Reactions catalyzed by aldolase (❶ and ❹) and transketolase (❸ and ❻) produce pentose phosphates that are converted to ribulose 1,5-bisphosphate—ribose 5-phosphate by ribose 5-phosphate isomerase (❼) and xylulose 5-phosphate by ribulose 5-phosphate epimerase (❽). In step ❾, ribulose 5-phosphate is phosphorylated, regenerating ribulose 1,5-bisphosphate. The steps with blue arrows are exergonic and make the whole process irreversible: steps ❷ fructose 1,6-bisphosphatase, ❺ sedoheptulose bisphosphatase, and ❾ ribulose 5-phosphate kinase.

($CH_2OH—CO—$) from a ketose phosphate donor, fructose 6-phosphate, to an aldose phosphate acceptor, glyceraldehyde 3-phosphate **(Fig. 20–11a, b)**, forming the pentose xylulose 5-phosphate and the tetrose erythrose 4-phosphate. In step ❹, aldolase acts again, combining erythrose 4-phosphate with dihydroxyacetone phosphate to form the seven-carbon **sedoheptulose 1,7-bisphosphate**. An enzyme unique to plastids, sedoheptulose 1,7-bisphosphatase, converts the bisphosphate to sedoheptulose 7-phosphate (step ❺); this is the second irreversible reaction in the pathway. Transketolase now acts again, converting sedoheptulose 7-phosphate and glyceraldehyde 3-phosphate to two pentose phosphates in step ❻ (Fig. 20–11c). **Figure 20–12** shows how a two-carbon fragment is temporarily carried on the transketolase cofactor TPP and condensed with the three carbons of glyceraldehyde 3-phosphate in step ❻.

The pentose phosphates formed in the transketolase reactions—ribose 5-phosphate and xylulose 5-phosphate—are converted to **ribulose 5-phosphate** (steps ❼ and ❽), which in the final step ❾ of the cycle is phosphorylated to ribulose 1,5-bisphosphate by ribulose 5-phosphate kinase **(Fig. 20–13)**. This is the third very exergonic reaction of the pathway, as the phosphate anhydride bond in ATP is swapped for a phosphate ester in ribulose 1,5-bisphosphate.

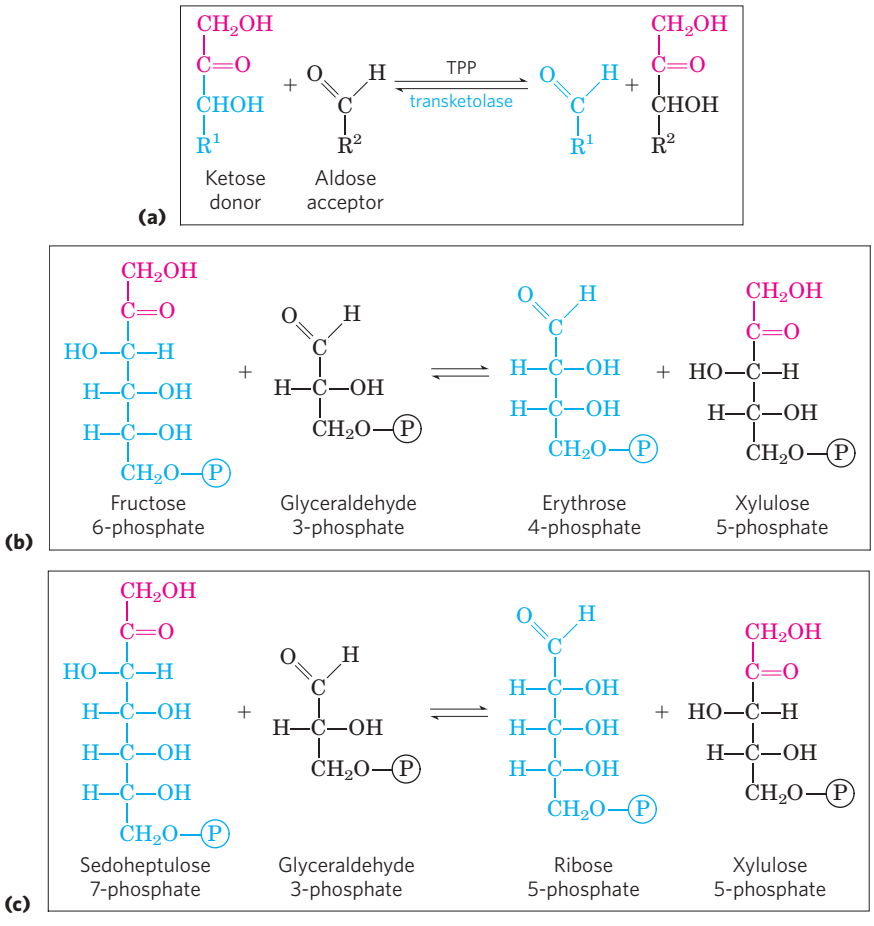

FIGURE 20–11 Transketolase-catalyzed reactions of the Calvin cycle. (a) General reaction catalyzed by transketolase: the transfer of a two-carbon group, carried temporarily on enzyme-bound TPP, from a ketose donor to an aldose acceptor. **(b)** Conversion of a hexose and a triose to a four-carbon and a five-carbon sugar (step ❸ of Fig. 20–10). **(c)** Conversion of seven-carbon and three-carbon sugars to two pentoses (step ❻ of Fig. 20–10).

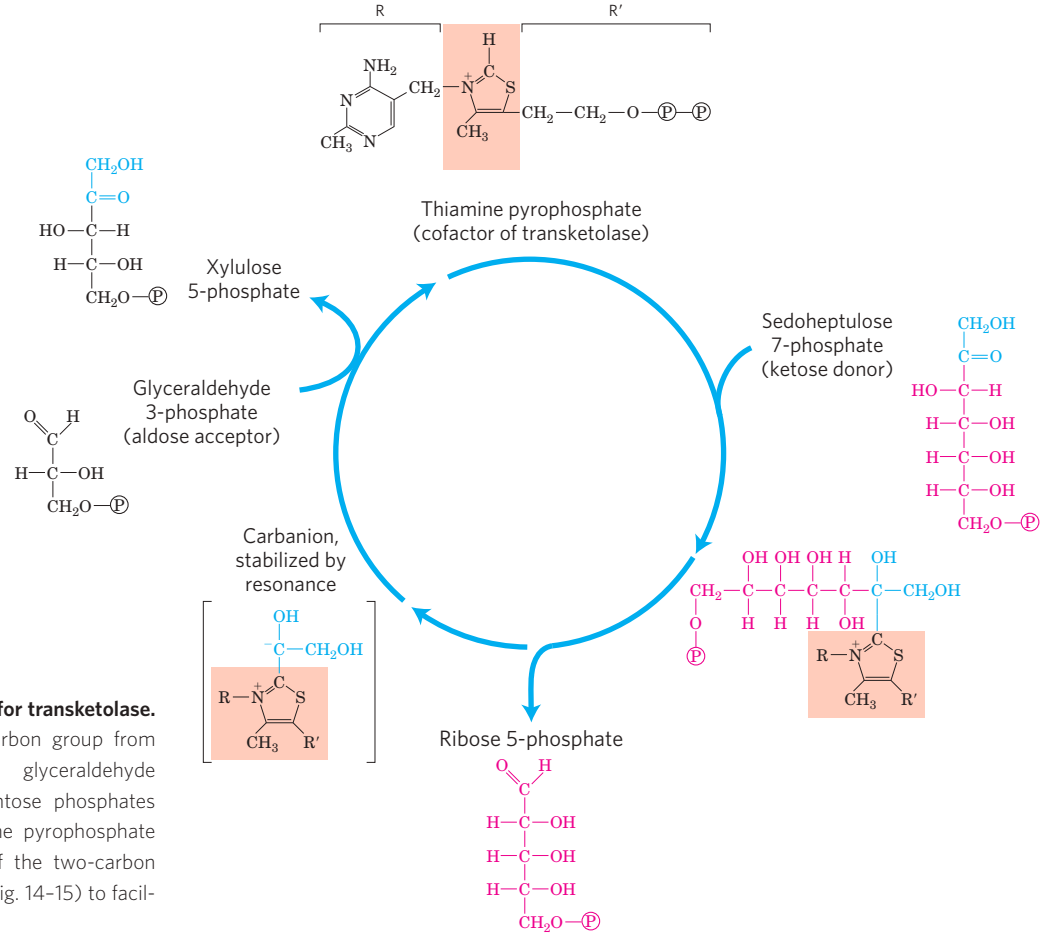

FIGURE 20–12 TPP as a cofactor for transketolase. Transketolase transfers a two-carbon group from sedoheptulose 7-phosphate to glyceraldehyde 3-phosphate, producing two pentose phosphates (step ❻ in Fig. 20–10). Thiamine pyrophosphate serves as a temporary carrier of the two-carbon unit and as an electron sink (see Fig. 14–15) to facilitate the reactions.

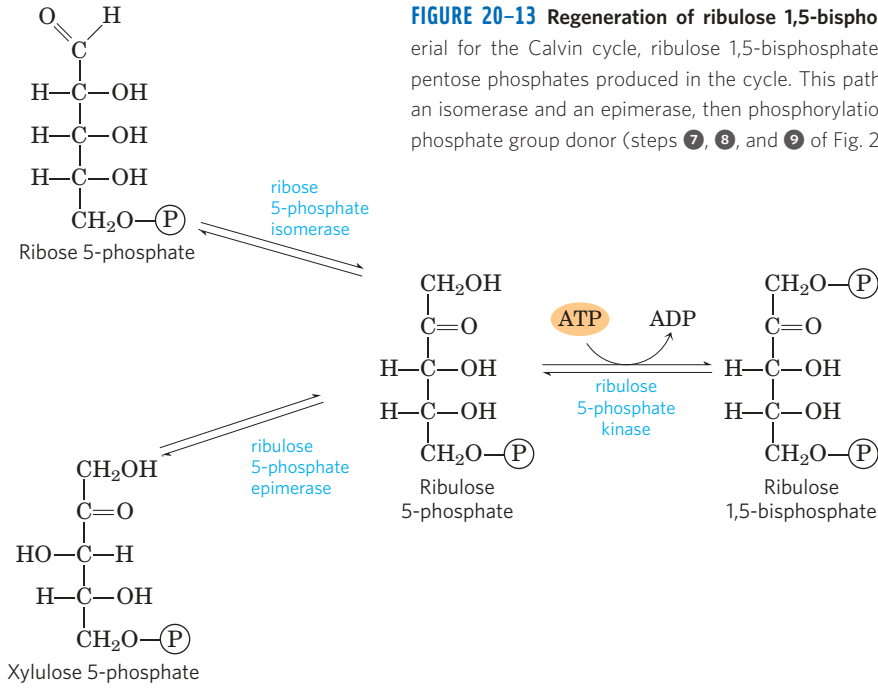

FIGURE 20–13 Regeneration of ribulose 1,5-bisphosphate. The starting material for the Calvin cycle, ribulose 1,5-bisphosphate, is regenerated from two pentose phosphates produced in the cycle. This pathway involves the action of an isomerase and an epimerase, then phosphorylation by a kinase, with ATP as phosphate group donor (steps ❼, ❽, and ❾ of Fig. 20–10).

Synthesis of Each Triose Phosphate from CO_2 Requires Six NADPH and Nine ATP

The net result of three turns of the Calvin cycle is the conversion of three molecules of CO_2 and one molecule of phosphate to a molecule of triose phosphate. The stoichiometry of the overall path from CO_2 to triose phosphate, with regeneration of ribulose 1,5-bisphosphate, is shown in **Figure 20–14**. Three molecules of ribulose 1,5-bisphosphate (a total of 15 carbons) condense with three CO_2 (3 carbons) to form six molecules of 3-phosphoglycerate (18 carbons). These six molecules of 3-phosphoglycerate are reduced to six molecules of glyceraldehyde 3-phosphate (which is in equilibrium with dihydroxyacetone phosphate), with the expenditure of six ATP (in the synthesis of 1,3-bisphosphoglycerate) and six NADPH (in the reduction of 1,3-bisphosphoglycerate to glyceraldehyde 3-phosphate). The isozyme of glyceraldehyde 3-phosphate dehydrogenase present in chloroplasts can use NADPH

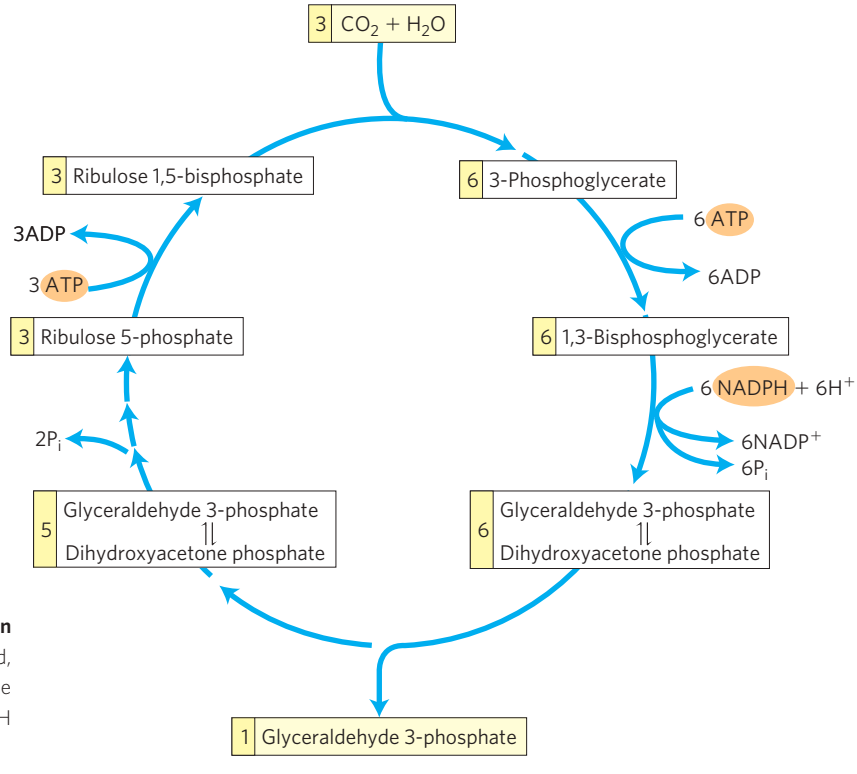

FIGURE 20–14 Stoichiometry of CO_2 assimilation in the Calvin cycle. For every three CO_2 molecules fixed, one molecule of triose phosphate (glyceraldehyde 3-phosphate) is produced and nine ATP and six NADPH are consumed.

as its electron carrier and normally functions in the direction of 1,3-bisphosphoglycerate reduction. The cytosolic isozyme uses NAD, as does the glycolytic enzyme of animals and other eukaryotes, and in the dark this isozyme acts in glycolysis to oxidize glyceraldehyde 3-phosphate. Both glyceraldehyde 3-phosphate dehydrogenase isozymes, like all enzymes, catalyze the reaction in both directions.

One molecule of glyceraldehyde 3-phosphate is the net product of the carbon-assimilation pathway. The other five triose phosphate molecules (15 carbons) are rearranged in steps ❶ to ❾ of Figure 20–10 to form three molecules of ribulose 1,5-bisphosphate (15 carbons). The last step in this conversion requires one ATP per ribulose 1,5-bisphosphate, or a total of three ATP. Thus, in summary, for every molecule of triose phosphate produced by photosynthetic CO_2 assimilation, six NADPH and nine ATP are required.

NADPH and ATP are produced in the light-dependent reactions of photosynthesis in about the same ratio (2:3) as they are consumed in the Calvin cycle. Nine ATP molecules are converted to ADP and phosphate in the generation of a molecule of triose phosphate; eight of the phosphates are released as P_i and combined with eight ADP to regenerate ATP. The ninth phosphate is incorporated into the triose phosphate itself. To convert the ninth ADP to ATP, a molecule of P_i must be imported from the cytosol, as we shall see.

In the dark, the production of ATP and NADPH by photophosphorylation, and the incorporation of CO_2 into triose phosphate (by the so-called dark reactions), cease. The "dark reactions" of photosynthesis were so named to distinguish them from the *primary* light-driven reactions of electron transfer to $NADP^+$ and synthesis of ATP, described in Chapter 19. They do not, in fact, occur at significant rates in the dark and are thus more appropriately called the **carbon-assimilation reactions**. Later in this section we describe the regulatory mechanisms that turn on carbon assimilation in the light and turn it off in the dark.

The chloroplast stroma contains all the enzymes necessary to convert the triose phosphates produced by CO_2 assimilation (glyceraldehyde 3-phosphate and dihydroxyacetone phosphate) to starch, which is temporarily stored in the chloroplast as insoluble granules. Aldolase condenses the trioses to fructose 1,6-bisphosphate; fructose 1,6-bisphosphatase produces fructose 6-phosphate; phosphohexose isomerase yields glucose 6-phosphate; and phosphoglucomutase produces glucose 1-phosphate, the starting material for starch synthesis (see Section 20.3).

All the reactions of the Calvin cycle except those catalyzed by rubisco, sedoheptulose 1,7-bisphosphatase, and ribulose 5-phosphate kinase also take place in animal tissues. Lacking these three enzymes, animals cannot carry out net conversion of CO_2 to glucose.

A Transport System Exports Triose Phosphates from the Chloroplast and Imports Phosphate

The inner chloroplast membrane is impermeable to most phosphorylated compounds, including fructose 6-phosphate, glucose 6-phosphate, and fructose 1,6-bisphosphate. It does, however, have a specific antiporter that catalyzes the one-for-one exchange of P_i with a triose phosphate, either dihydroxyacetone phosphate or 3-phosphoglycerate **(Fig. 20–15**; see also Fig. 20–9). This antiporter simultaneously moves P_i into the chloroplast, where it is used in photophosphorylation, and moves triose phosphate into the cytosol, where it can be used to synthesize sucrose, the form in which the fixed carbon is transported to distant plant tissues.

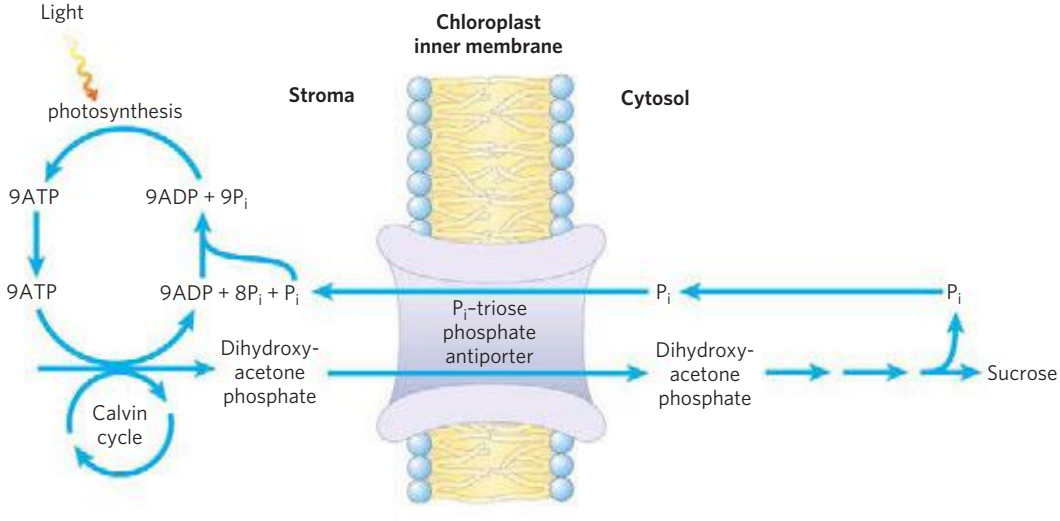

FIGURE 20-

chloroplast membrane. This transporter facilitates the exchange of cytosolic P_i for stromal dihydroxyacetone phosphate. The products of photosynthetic carbon assimilation are thus moved into the cytosol, ynthesis, and P_i required for photophosphorylation is moved into the stroma. This same antiporter can transport 3-phosphoglycerate and acts in the shuttle for exporting ATP and reducing equivalents (see Fig. 20–16).

Sucrose synthesis in the cytosol and starch synthesis in the chloroplast are the major pathways by which the excess triose phosphate from photosynthesis is "harvested." Sucrose synthesis (described below) releases four P_i molecules from the four triose phosphates required to make sucrose. For every molecule of triose phosphate removed from the chloroplast, one P_i is transported into the chloroplast, providing the ninth P_i mentioned above, to be used in regenerating ATP. If this exchange were blocked, triose phosphate synthesis would quickly deplete the available P_i in the chloroplast, slowing ATP synthesis and suppressing assimilation of CO_2 into starch.

The P_i–triose phosphate antiport system serves one additional function. ATP and reducing power are needed in the cytosol for a variety of synthetic and energy-requiring reactions. These requirements are met to an as yet undetermined degree by mitochondria, but a second potential source of energy is the ATP and NADPH generated in the chloroplast stroma during the light reactions. However, neither ATP nor NADPH can cross the chloroplast membrane. The P_i–triose phosphate antiport system has the indirect effect of moving ATP equivalents and reducing equivalents from the chloroplast to the cytosol **(Fig. 20–16)**. Dihydroxyacetone phosphate formed in the stroma is transported to the cytosol, where it is converted by glycolytic enzymes to 3-phosphoglycerate, generating ATP and NADH. 3-Phosphoglycerate reenters the chloroplast, completing the cycle.

Four Enzymes of the Calvin Cycle Are Indirectly Activated by Light

The reductive assimilation of CO_2 requires a lot of ATP and NADPH, and their stromal concentrations increase when chloroplasts are illuminated **(Fig. 20–17)**. The light-induced transport of protons across the thylakoid membrane (Chapter 19) also increases the stromal pH from about 7 to about 8, and it is accompanied by a flow of Mg^{2+} from the thylakoid compartment into the stroma, raising the $[Mg^{2+}]$ from 1 to 3 mM to 3 to 6 mM. Several

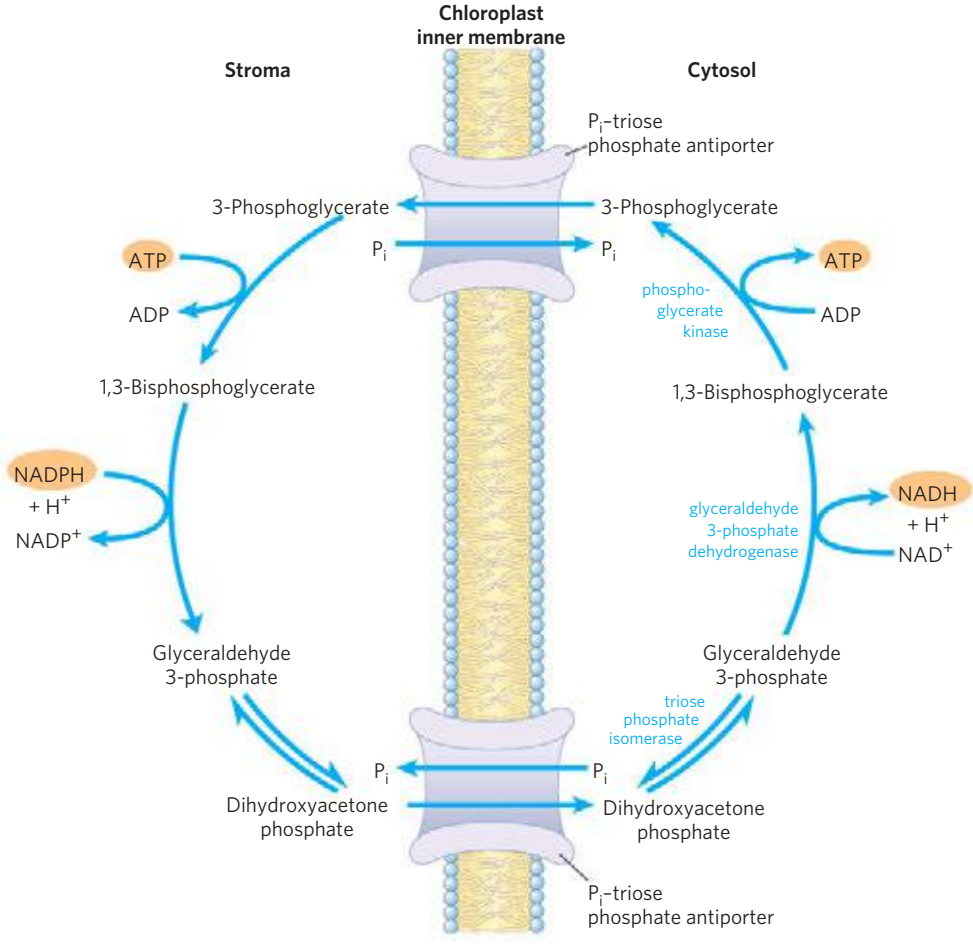

FIGURE 20–16 Role of the P_i–triose phosphate antiporter in the transport of ATP and reducing equivalents. Dihydroxyacetone phosphate leaves the chloroplast and is converted to glyceraldehyde 3-phosphate in the cytosol. The cytosolic glyceraldehyde 3-phosphate dehydrogenase and phosphoglycerate kinase reactions then produce NADH, ATP, and 3-phosphoglycerate. The latter reenters the chloroplast and is reduced to dihydroxyacetone phosphate, completing a cycle that effectively moves ATP and reducing equivalents (NAD(P)H) from chloroplast to cytosol.

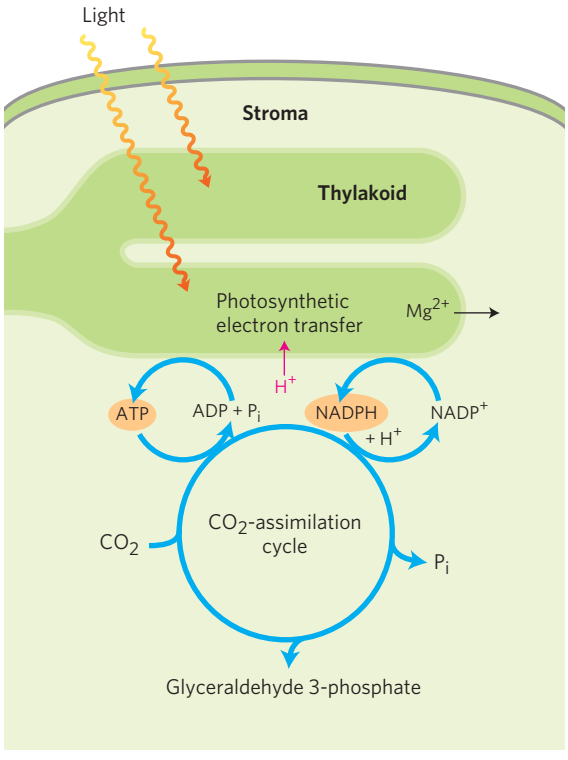

FIGURE 20–17 Source of ATP and NADPH. ATP and NADPH produced by the light reactions are essential substrates for the reduction of CO_2. The photosynthetic reactions that produce ATP and NADPH are accompanied by movement of protons (red) from the stroma into the thylakoid, creating alkaline conditions in the stroma. Magnesium ions pass from the thylakoid into the stroma, increasing the stromal [Mg^{2+}].

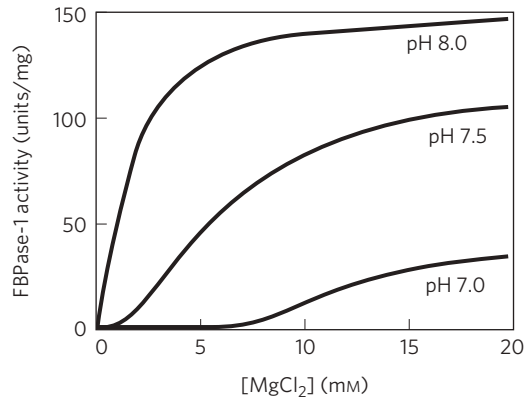

FIGURE 20–18 Activation of chloroplast fructose 1,6-bisphosphatase. Reduced fructose 1,6-bisphosphatase (FBPase-1) is activated by light and by the combination of high pH and high [Mg^{2+}] in the stroma, both of which are results of illumination.

stromal enzymes have evolved to take advantage of these light-induced conditions, which signal the availability of ATP and NADPH: the enzymes are more active in an alkaline environment and at high [Mg^{2+}]. For example, activation of rubisco by formation of the carbamoyllysine is faster at alkaline pH, and high stromal [Mg^{2+}] favors formation of the enzyme's active Mg^{2+} complex. Fructose 1,6-bisphosphatase requires Mg^{2+} and is very dependent on pH **(Fig. 20–18)**; its activity increases more than 100-fold when pH and [Mg^{2+}] rise during chloroplast illumination.

Four Calvin cycle enzymes are subject to a special type of regulation by light. Ribulose 5-phosphate kinase, fructose 1,6-bisphosphatase, sedoheptulose 1,7-bisphosphatase, and glyceraldehyde 3-phosphate dehydrogenase are activated by light-driven reduction of disulfide bonds between two Cys residues critical to their catalytic activities. When these Cys residues are disulfide-bonded (oxidized), the enzymes are inactive; this is the normal situation in the dark. With illumination, electrons flow from photosystem I to ferredoxin (see Fig. 19–58), which passes electrons to a small, soluble, disulfide-containing protein called **thioredoxin (Fig. 20–19)**, in a reaction catalyzed by **ferredoxin-thioredoxin reductase**. Reduced thioredoxin donates electrons for the reduction

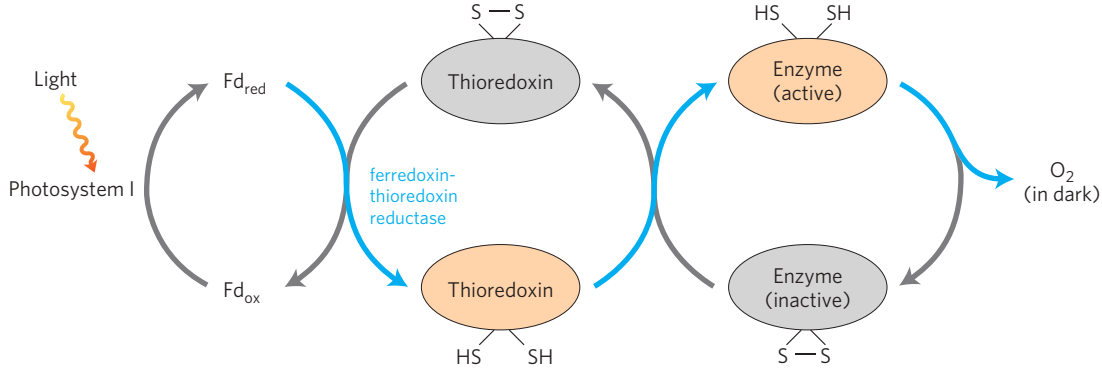

FIGURE 20–19 Light activation of several enzymes of the Calvin cycle. The light activation is mediated by thioredoxin, a small, disulfide-containing protein. In the light, thioredoxin is reduced by electrons moving from photosystem I through ferredoxin (Fd) (blue arrows), then thioredoxin reduces critical disulfide bonds in each of the enzymes sedoheptulose 1,7-bisphosphatase, fructose 1,6-bisphosphatase, ribulose 5-phosphate kinase, and glyceraldehyde 3-phosphate dehydrogenase, activating these enzymes. In the dark, the —SH groups undergo reoxidation to disulfides, inactivating the enzymes.

of the disulfide bonds of the light-activated enzymes, and these reductive cleavage reactions are accompanied by conformational changes that increase enzyme activities. At nightfall, the Cys residues in the four enzymes are reoxidized to their disulfide forms, the enzymes are inactivated, and ATP is not expended in CO_2 assimilation. Instead, starch synthesized and stored during the daytime is degraded to fuel glycolysis at night.

Glucose 6-phosphate dehydrogenase, the first enzyme in the *oxidative* pentose phosphate pathway, is also regulated by this light-driven reduction mechanism, but in the opposite sense. During the day, when photosynthesis produces plenty of NADPH, this enzyme is not needed for NADPH production. Reduction of a critical disulfide bond by electrons from ferredoxin *inactivates* the enzyme.

SUMMARY 20.1 Photosynthetic Carbohydrate Synthesis

- Photosynthesis in vascular plants takes place in chloroplasts. In the CO_2-assimilating reactions (the Calvin cycle), ATP and NADPH are used to reduce CO_2 to triose phosphates. These reactions occur in three stages: the fixation reaction itself, catalyzed by rubisco; reduction of the resulting 3-phosphoglycerate to glyceraldehyde 3-phosphate; and regeneration of ribulose 1,5-bisphosphate from triose phosphates.
- Rubisco condenses CO_2 with ribulose 1,5-bisphosphate, forming an unstable hexose bisphosphate that splits into two molecules of 3-phosphoglycerate. Rubisco is activated by covalent modification (carbamoylation of Lys^{201}) catalyzed by rubisco activase and is inhibited by a natural transition-state analog, the concentration of which rises in the dark and falls during daylight.
- Stromal isozymes of the glycolytic enzymes catalyze reduction of 3-phosphoglycerate to glyceraldehyde 3-phosphate; each molecule reduced requires one ATP and one NADPH.
- Stromal enzymes, including transketolase and aldolase, rearrange the carbon skeletons of triose phosphates, generating intermediates of three, four, five, six, and seven carbons and eventually yielding pentose phosphates. The pentose phosphates are converted to ribulose 5-phosphate, then phosphorylated to ribulose 1,5-bisphosphate to complete the Calvin cycle.
- The cost of fixing three CO_2 into one triose phosphate is nine ATP and six NADPH, which are provided by the light-dependent reactions of photosynthesis.
- An antiporter in the inner chloroplast membrane exchanges P_i in the cytosol for 3-phosphoglycerate or dihydroxyacetone phosphate produced by CO_2 assimilation in the stroma. Oxidation of dihydroxyacetone phosphate in the cytosol generates ATP and NADH, thus moving ATP and reducing equivalents from the chloroplast to the cytosol.
- Four enzymes of the Calvin cycle are activated indirectly by light and are inactive in the dark, so that hexose synthesis does not compete with glycolysis—which is required to provide energy in the dark.

20.2 Photorespiration and the C_4 and CAM Pathways

As we have seen, photosynthetic cells produce O_2 (by the splitting of H_2O) during the light-driven reactions (Chapter 19) and use CO_2 during the light-independent processes (described above), so the net gaseous change during photosynthesis is the uptake of CO_2 and release of O_2:

$$CO_2 + H_2O \longrightarrow O_2 + (CH_2O)$$

In the dark, plants also carry out **mitochondrial respiration**, the oxidation of substrates to CO_2 and the conversion of O_2 to H_2O. And there is another process in plants that, like mitochondrial respiration, consumes O_2 and produces CO_2 and, like photosynthesis, is driven by light. This process, **photorespiration**, is a costly side reaction of photosynthesis, a result of the lack of specificity of the enzyme rubisco. In this section we describe this side reaction and the strategies plants use to minimize its metabolic consequences.

Photorespiration Results from Rubisco's Oxygenase Activity

Rubisco is not absolutely specific for CO_2 as a substrate. Molecular oxygen (O_2) competes with CO_2 at the active site, and about once in every three or four turnovers, rubisco catalyzes the condensation of O_2 with ribulose 1,5-bisphosphate to form 3-phosphoglycerate and **2-phosphoglycolate** **(Fig. 20–20)**, a metabolically useless product. This is the oxygenase activity referred to in the full name of the enzyme: ribulose 1,5-bisphosphate carboxylase/oxygenase. The reaction with O_2 results in no fixation of carbon and seems to be a net liability to the cell; salvaging the carbons from 2-phosphoglycolate (by the pathway outlined below) consumes significant amounts of cellular energy and releases some previously fixed CO_2.

Given that the reaction with oxygen is deleterious to the organism, why did the evolution of rubisco produce an active site unable to discriminate well between CO_2 and O_2? Perhaps much of this evolution occurred before the time, about 2.5 billion years ago, when production of O_2 by photosynthetic organisms started to raise the oxygen content of the atmosphere. Before

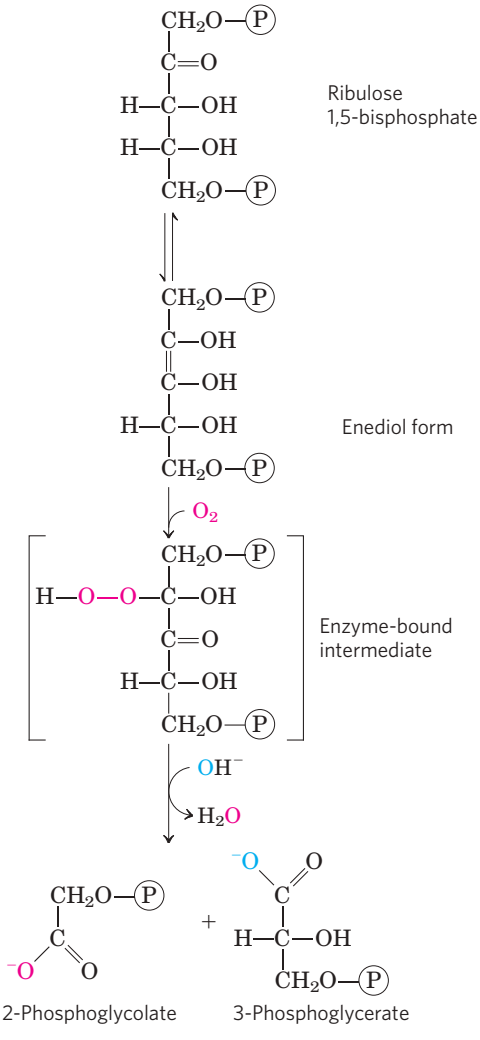

FIGURE 20–20 Oxygenase activity of rubisco. Rubisco can incorporate O_2 rather than CO_2 into ribulose 1,5-bisphosphate. The unstable intermediate thus formed splits into 2-phosphoglycolate (recycled as described in Fig. 20–21) and 3-phosphoglycerate, which can reenter the Calvin cycle.

that time, there was no selective pressure for rubisco to discriminate between CO_2 and O_2. The K_m for CO_2 is about 9 μM, and that for O_2 is about 350 μM. The modern atmosphere contains about 20% O_2 and only 0.04% CO_2, so an aqueous solution in equilibrium with air at room temperature contains about 250 μM O_2 and 11 μM CO_2—concentrations that allow significant O_2 "fixation" by rubisco and thus a significant waste of energy. The temperature dependence of the solubilities of O_2 and CO_2 is such that at higher temperatures, the ratio of O_2 to CO_2 in solution increases. In addition, the affinity of rubisco for CO_2 decreases with increasing temperature, exacerbating its tendency to catalyze the wasteful oxygenase reaction. And as CO_2 is consumed in the assimilation reactions, the ratio of O_2 to CO_2 in the air spaces of a leaf increases, further favoring the oxygenase reaction.

The Salvage of Phosphoglycolate Is Costly

The **glycolate pathway** converts two molecules of 2-phosphoglycolate to a molecule of serine (three carbons) and a molecule of CO_2 **(Fig. 20–21)**. In the

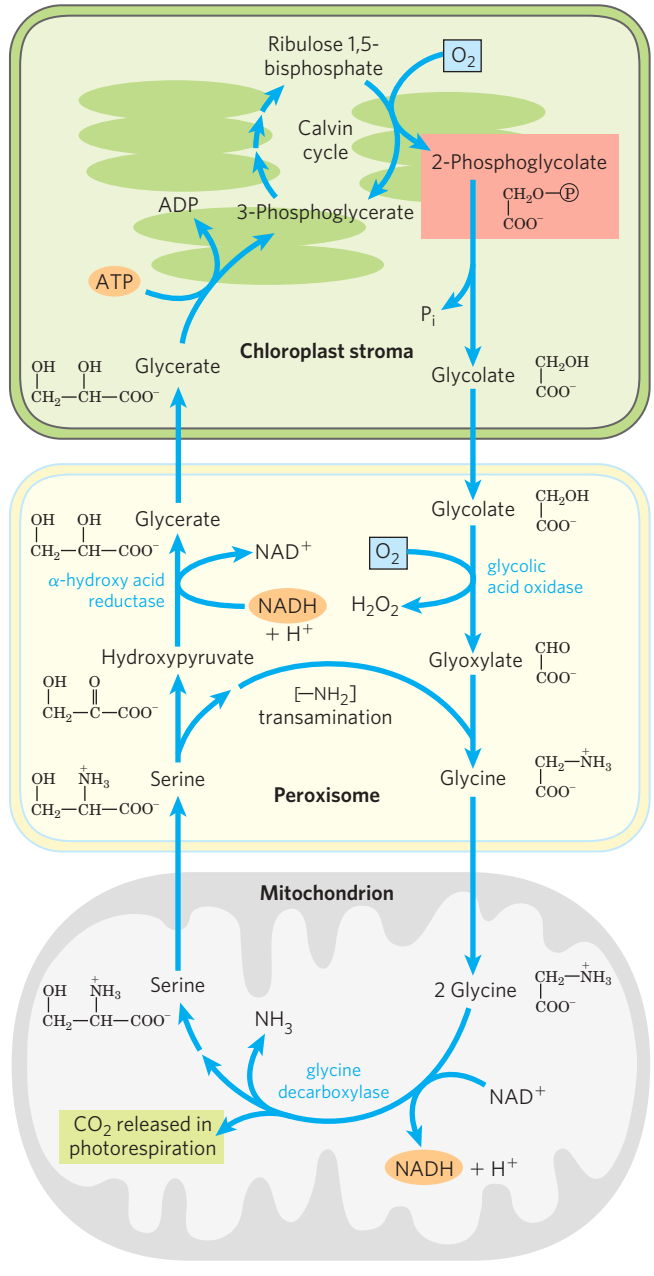

FIGURE 20–21 Glycolate pathway. This pathway, which salvages 2-phosphoglycolate (shaded light red) by its conversion to serine and eventually 3-phosphoglycerate, involves three cellular compartments. Glycolate formed by dephosphorylation of 2-phosphoglycolate in chloroplasts is oxidized to glyoxylate in peroxisomes and then transaminated to glycine. In mitochondria, two glycine molecules condense to form serine and the CO_2 released during photorespiration (shaded green). This reaction is catalyzed by glycine decarboxylase, an enzyme present at very high levels in the mitochondria of C_3 plants (see text). The serine is converted to hydroxypyruvate and then to glycerate in peroxisomes; glycerate reenters the chloroplasts to be phosphorylated, rejoining the Calvin cycle. Oxygen (shaded blue) is consumed at two steps during photorespiration.

chloroplast, a phosphatase converts 2-phosphoglycolate to glycolate, which is exported to the peroxisome. There, glycolate is oxidized by molecular oxygen, and the resulting aldehyde (glyoxylate) undergoes transamination to glycine. The hydrogen peroxide formed as a side product of glycolate oxidation is rendered harmless by peroxidases in the peroxisome. Glycine passes from the peroxisome to the mitochondrial matrix, where it undergoes oxidative decarboxylation by the glycine decarboxylase complex, an enzyme similar in structure and mechanism to two mitochondrial complexes we have already encountered: the pyruvate dehydrogenase complex and the α-ketoglutarate dehydrogenase complex (Chapter 16). The **glycine decarboxylase complex** oxidizes glycine to CO_2 and NH_3, with the concomitant reduction of NAD^+ to NADH and transfer of the remaining carbon from glycine to the cofactor tetrahydrofolate **(Fig. 20–22)**. The one-carbon unit carried on tetrahydrofolate is then transferred to a second glycine by serine hydroxymethyltransferase, producing serine. The net reaction catalyzed by the glycine decarboxylase complex and serine hydroxymethyltransferase is

$$2\ \text{Glycine} + NAD^+ + H_2O \longrightarrow \text{serine} + CO_2 + NH_3 + NADH + H^+$$

The serine is converted to hydroxypyruvate, to glycerate, and finally to 3-phosphoglycerate, which is used to regenerate ribulose 1,5-bisphosphate, completing the long, expensive cycle (Fig. 20–21).

In bright sunlight, the flux through the glycolate salvage pathway can be very high, producing about

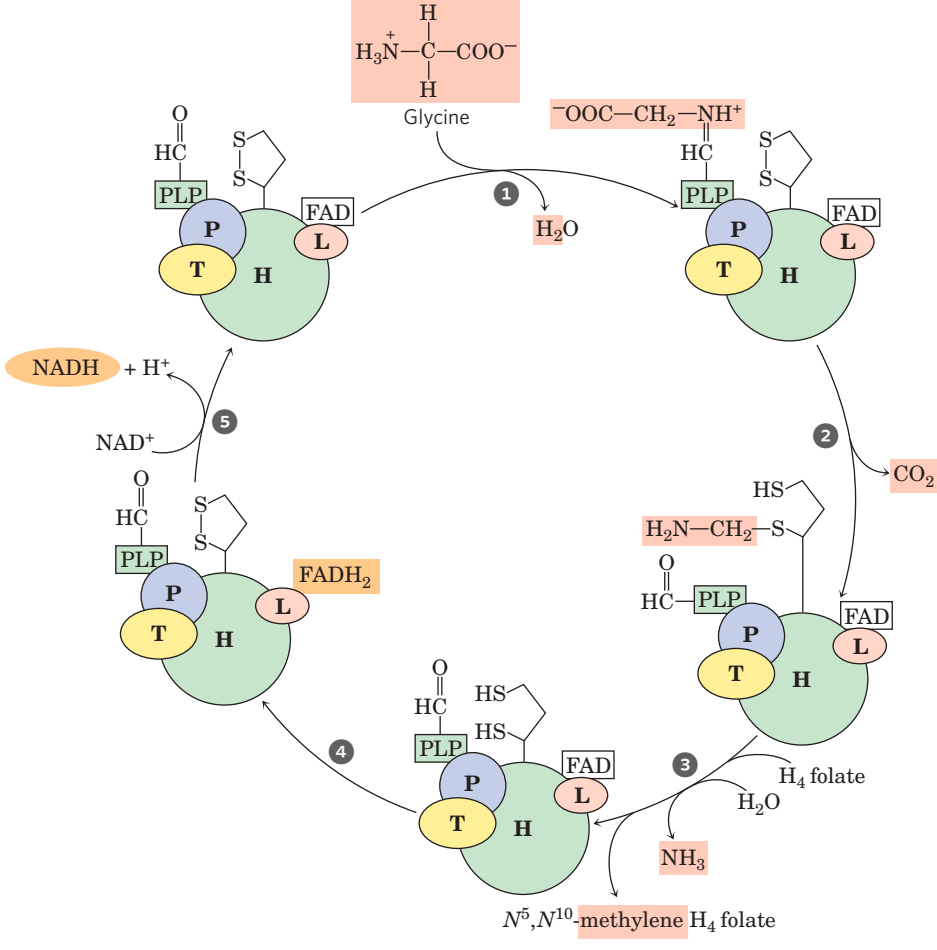

FIGURE 20–22 The glycine decarboxylase system. Glycine decarboxylase in plant mitochondria is a complex of four types of subunits, with the stoichiometry $P_4H_{27}T_9L_2$. Protein H has a covalently attached lipoic acid residue that can undergo reversible oxidation. Step ❶ is formation of a Schiff base between pyridoxal phosphate (PLP) and glycine, catalyzed by protein P (named for its bound PLP). In step ❷, protein P catalyzes oxidative decarboxylation of glycine, releasing CO_2; the remaining methylamine group is attached to one of the —SH groups of reduced lipoic acid. ❸ Protein T (which uses tetrahydrofolate (H_4 folate) as cofactor) now releases NH_3 from the methylamine moiety and transfers the remaining one-carbon fragment to tetrahydrofolate, producing N^5,N^{10}-methylenetetrahydrofolate. ❹ Protein L oxidizes the two —SH groups of lipoic acid to a disulfide, passing electrons through FAD to NAD^+ ❺, thus completing the cycle. The N^5,N^{10}-methylenetetrahydrofolate formed in this process is used by serine hydroxymethyltransferase to convert a molecule of glycine to serine, regenerating the tetrahydrofolate that is essential for the reaction catalyzed by protein T. The L subunit of glycine decarboxylase is identical to the dihydrolipoyl dehydrogenase (E_3) of pyruvate dehydrogenase and α-ketoglutarate dehydrogenase (see Fig. 16-6).

five times more CO_2 than is typically produced by all the oxidations of the citric acid cycle. To generate this large flux, mitochondria contain prodigious amounts of the glycine decarboxylase complex: the four proteins of the complex make up *half* of all the protein in the mitochondrial matrix in the leaves of pea and spinach plants! In nonphotosynthetic parts of a plant, such as potato tubers, mitochondria have very low concentrations of the glycine decarboxylase complex.

The combined activity of the rubisco oxygenase and the glycolate salvage pathway consumes O_2 and produces CO_2—hence the name **photorespiration**. This pathway is perhaps better called the **oxidative photosynthetic carbon cycle** or **C_2 cycle**, names that do not invite comparison with respiration in mitochondria. Unlike mitochondrial respiration, "photorespiration" does not conserve energy and may actually inhibit net biomass formation as much as 50%. This inefficiency has led to evolutionary adaptations in the carbon-assimilation processes, particularly in plants that have evolved in warm climates. The apparent inefficiency of rubisco, and its effect in limiting biomass production, has inspired efforts to genetically engineer a "better" rubisco, but this goal is not, as yet, within reach (Box 20–1).

In C_4 Plants, CO_2 Fixation and Rubisco Activity Are Spatially Separated

In many plants that grow in the tropics (and in temperate-zone crop plants native to the tropics, such as maize, sugarcane, and sorghum) a mechanism has evolved to circumvent the problem of wasteful photorespiration. The step in which CO_2 is fixed into a three-carbon product, 3-phosphoglycerate, is preceded by several steps, one of which is temporary fixation of CO_2 into a four-carbon compound. Plants that use this process are referred to as **C_4 plants**, and the assimilation process as **C_4 metabolism** or the **C_4 pathway**. Plants that use the carbon-assimilation method we have described thus far, in which the *first step* is reaction of CO_2 with ribulose 1,5-bisphosphate to form 3-phosphoglycerate, are called **C_3 plants**.

The C_4 plants, which typically grow at high light intensity and high temperatures, have several important characteristics: high photosynthetic rates, high growth rates, low photorespiration rates, low rates of water loss, and a specialized leaf structure. Photosynthesis in the leaves of C_4 plants involves two cell types: mesophyll and bundle-sheath cells **(Fig. 20–23a)**. There are three

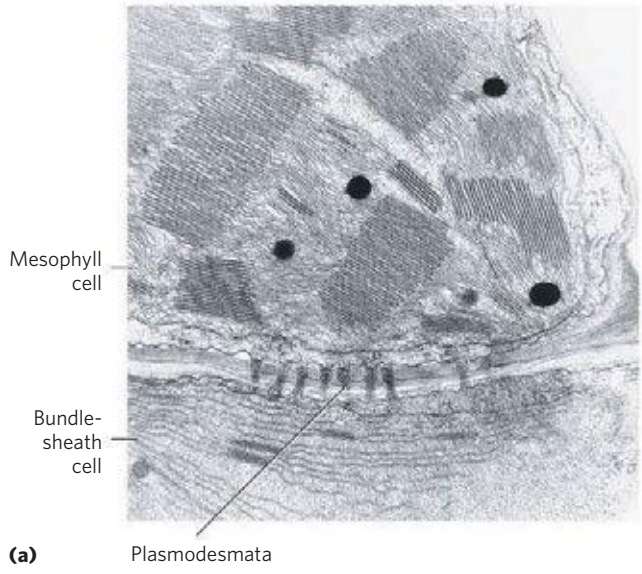

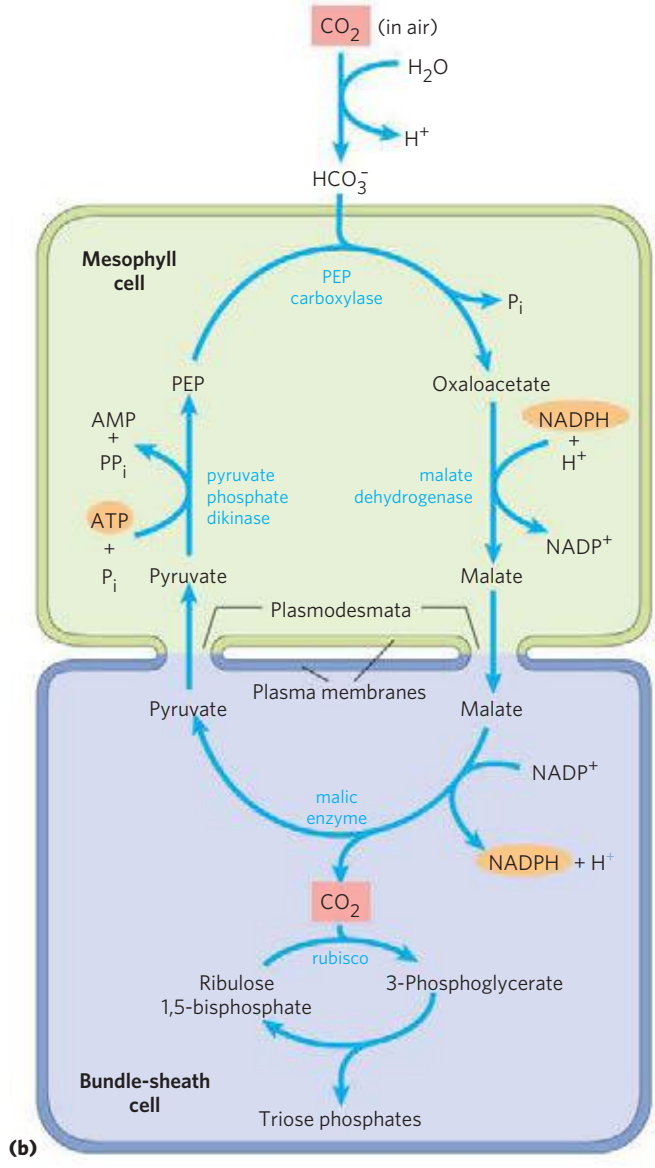

FIGURE 20–23 Carbon assimilation in C_4 plants. The C_4 pathway, involving mesophyll cells and bundle-sheath cells, predominates in plants of tropical origin. **(a)** Electron micrograph showing chloroplasts of adjacent mesophyll and bundle-sheath cells. The bundle-sheath cell contains starch granules. Plasmodesmata connecting the two cells are visible. **(b)** The C_4 pathway of CO_2 assimilation, which occurs through a four-carbon intermediate.

BOX 20–1 Will Genetic Engineering of Photosynthetic Organisms Increase Their Efficiency?

Three pressing world problems have prompted serious attention to the possibility of engineering plants to be more efficient in converting sunlight into biomass: the "greenhouse" effect of increasing atmospheric CO_2 on global climate change, the dwindling supply of oil for the generation of energy, and the need for more and better food for the world's growing population.

The concentration of CO_2 in the earth's atmosphere has risen steadily over the past 50 years (Fig. 1), the combined effect of the use of fossil fuels for energy and the clearing and burning of tropical forests to allow use of the land for agriculture. As atmospheric CO_2 increases, the atmosphere absorbs more heat radiated from the earth's surface and reradiates more toward the surface of the planet (and in all other directions). Retention of heat raises the temperature at the surface of the earth; this is the greenhouse effect. One way to limit the increase in atmospheric CO_2 would be to engineer plants or microorganisms with a greater capacity for sequestering CO_2.

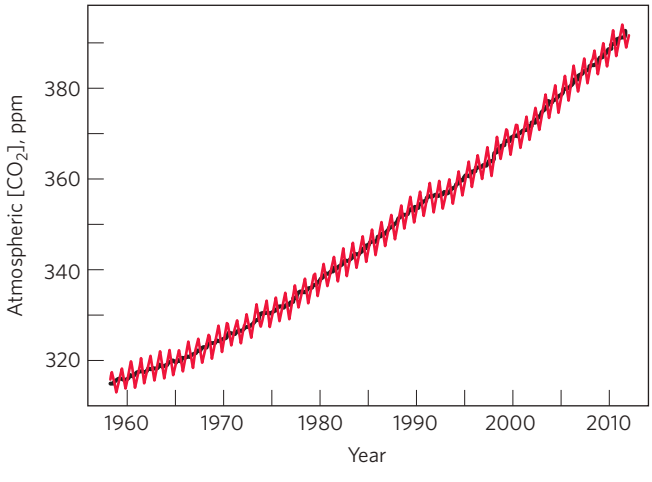

FIGURE 1 The concentration of CO_2 in the atmosphere measured at the Mauna Loa Observatory in Hawaii. Data from the National Oceanic and Atmospheric Administration and the Scripps Institution of Oceanography CO_2 Program.

The estimated amount of total carbon in all terrestrial systems (atmosphere, soil, biomass) is about 3,200 gigatons (GT)—3,200 billion metric tons. The atmosphere contains another 760 GT of CO_2.

The flux of carbon through these terrestrial reservoirs (Fig. 2) is largely due to the photosynthetic activities of plants and the degradative activities of microorganisms. Plants fix some 123 GT of carbon annually, then immediately release about half of that to the atmosphere as they respire. Much of the remainder is gradually released to the atmosphere by microbial action on dead plant materials, but biomass is sequestered in woody plants and trees for decades or centuries. Anthropogenic carbon flux, the amount of CO_2 released into the atmosphere by human activities, is 9 GT per year—small compared with total biomass, but enough to tip the balance of nature toward increased CO_2 in the atmosphere. It is estimated that the forests of North America sequester 0.7 GT of carbon annually, which represents about a tenth of the annual *global* production of CO_2 from fossil fuels. Clearly, preservation of forests and reforestation are effective ways to limit the flow of CO_2 back into the atmosphere.

A second approach to limiting the increase of atmospheric CO_2, while also addressing the need to replace dwindling fossil fuels, is to use renewable biomass as a source of ethanol to replace fossil fuels in internal combustion engines. This reduces the *unidirectional* movement of carbon from fossil fuels into the atmospheric pool of CO_2,, replacing it with the *cyclic* flow of CO_2 from ethanol to CO_2 and back to biomass. When maize, wheat, or switchgrass is fermented to ethanol for fuel, every increase in biomass

variants of C_4 metabolism, worked out in the 1960s by Marshall Hatch and Rodger Slack (Fig. 20–23b).

In plants of tropical origin, the first intermediate into which $^{14}CO_2$ is fixed is oxaloacetate, a four-carbon compound. This reaction, which occurs in the cytosol of leaf mesophyll cells, is catalyzed by **phosphoenolpyruvate carboxylase**, for which the substrate is HCO_3^-, not CO_2. The oxaloacetate thus formed is either reduced to malate at the expense of NADPH (as shown in Fig. 20–23b) or converted to aspartate by transamination:

Oxaloacetate + α-amino acid ⟶ L-aspartate + α-keto acid

The malate or aspartate formed in the mesophyll cells then passes into neighboring bundle-sheath cells through plasmodesmata, protein-lined channels that connect two plant cells and provide a path for movement of metabolites and even small proteins between cells. In the bundle-sheath cells, malate is oxidized and decarboxylated to yield pyruvate and CO_2 by the action of **malic enzyme**, reducing $NADP^+$. In plants that use aspartate as the CO_2 carrier, aspartate arriving in bundle-sheath cells is transaminated to form oxaloacetate and reduced to malate, then the CO_2 is released by malic enzyme or PEP carboxykinase. As labeling experiments show, the free CO_2 released in the bundle-sheath cells is

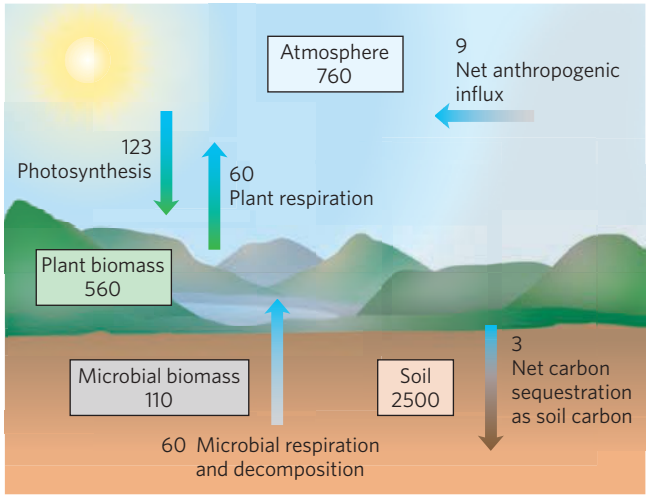

FIGURE 2 The terrestrial carbon cycle. Carbon stocks (boxes) are shown as gigatons (GT), and fluxes (arrows) are shown in GT per year. Animal biomass is negligible here—less than 0.5 GT.

production brought about by more efficient photosynthesis should result in a corresponding decrease in the use of fossil fuels.

Finally, engineering of food crops to yield more food per acre of land, or per hour of work, could improve human nutrition worldwide.

In principle, these goals might be accomplished by developing a rubisco that didn't also catalyze the wasteful reaction with O_2, or by increasing the turnover number for rubisco, or by increasing the level of rubisco or other enzymes in the pathway for carbon fixation. Rubisco, we have said, is an unusually inefficient enzyme, with a turnover number of 3 s^{-1} at 25°C; most enzymes have turnover numbers orders of magnitude larger. It also catalyzes the wasteful reaction with oxygen, which further reduces its efficiency in fixing CO_2 and producing biomass. If rubisco could be genetically engineered to turn over faster or to be more selective for CO_2 relative to O_2, would the effect be greater photosynthetic production of biomass and thus greater sequestration of CO_2, production of more nonfossil fuel, and improved nutrition?

We noted in Chapter 15 that the traditional view of metabolic pathways held that one step in any pathway was the slowest and therefore the limiting factor in material flow through the pathway. However, heroic efforts to engineer cells or organisms have often given discouraging results; organisms engineered to produce more of the "limiting" enzyme in a pathway often show little or no change in the flux through that pathway. The Calvin cycle is an instructive case in point. Increasing the amount of rubisco in plant cells through genetic engineering has little or no effect on the rate of CO_2 conversion into carbohydrate. Similarly, changes in the levels of enzymes known to be regulated by light and therefore suspected of playing key roles in the regulation of the pathway (fructose 1,6-bisphosphatase, 3-phosphoglycerate kinase, and glyceraldehyde 3-phosphate dehydrogenase) also lead to little or no significant improvement in photosynthetic rate. However, changed levels of sedoheptulose 1,7-bisphosphatase, not thought to be a regulatory enzyme, have a significant impact on photosynthesis. Metabolic control analysis (Section 15.2) suggests that this result is not unexpected; in the living organism, pathways can be limited by more than one step, since every change in one step results in compensating changes in other steps. Careful determination of the flux control coefficient (see Box 15–1) helps to pinpoint which enzymes in a pathway to target for genetic engineering. Clearly, genetic engineers and metabolic control analysts will need to work together on problems like this one!

the same CO_2 molecule originally fixed into oxaloacetate in the mesophyll cells. This CO_2 is now fixed again, this time by rubisco, in exactly the same reaction that occurs in C_3 plants: incorporation of CO_2 into C-1 of 3-phosphoglycerate.

The pyruvate formed by decarboxylation of malate in bundle-sheath cells is transferred back to the mesophyll cells, where it is converted to PEP by an unusual enzymatic reaction catalyzed by **pyruvate phosphate dikinase** (Fig. 20–23b). This enzyme is called a dikinase because two different molecules are simultaneously phosphorylated by one molecule of ATP: pyruvate to PEP, and phosphate to pyrophosphate. The pyrophosphate is subsequently hydrolyzed to phosphate, so two high-energy phosphate groups of ATP are used in regenerating PEP. The PEP is now ready to receive another molecule of CO_2 in the mesophyll cell.

The PEP carboxylase of mesophyll cells has a high affinity for HCO_3^- (which is favored relative to CO_2 in aqueous solution) and can fix CO_2 more efficiently than can rubisco. Unlike rubisco, it does not use O_2 as an alternative substrate, so there is no competition between CO_2 and O_2. The PEP carboxylase reaction, then, serves to fix and concentrate CO_2 in the form of malate. Release of CO_2 from malate in the bundle-sheath cells yields a sufficiently high local concentration of CO_2 for

rubisco to function near its maximal rate, and for suppression of the enzyme's oxygenase activity.

Once CO_2 is fixed into 3-phosphoglycerate in the bundle-sheath cells, the other reactions of the Calvin cycle take place exactly as described earlier. Thus in C_4 plants, mesophyll cells carry out CO_2 assimilation by the C_4 pathway and bundle-sheath cells synthesize starch and sucrose by the C_3 pathway.

Three enzymes of the C_4 pathway are regulated by light, becoming more active in daylight. Malate dehydrogenase is activated by the thioredoxin-dependent reduction mechanism shown in Figure 20–19; PEP carboxylase is activated by phosphorylation of a Ser residue; and pyruvate phosphate dikinase is activated by dephosphorylation. In the latter two cases, the details of how light effects phosphorylation or dephosphorylation are not known.

The pathway of CO_2 assimilation has a greater energy cost in C_4 plants than in C_3 plants. For each molecule of CO_2 assimilated in the C_4 pathway, a molecule of PEP must be regenerated at the expense of two phosphoanhydride bonds in ATP. Thus C_4 plants need five ATP molecules to assimilate one molecule of CO_2, whereas C_3 plants need only three (nine per triose phosphate). As the temperature increases (and the affinity of rubisco for CO_2 decreases, as noted above), a point is reached (at about 28 to 30 °C) at which the gain in efficiency from the elimination of photorespiration more than compensates for this energetic cost. C_4 plants (crabgrass, for example) outgrow most C_3 plants during the summer, as any experienced gardener can attest.

In CAM Plants, CO_2 Capture and Rubisco Action Are Temporally Separated

Succulent plants such as cactus and pineapple, which are native to very hot, very dry environments, have another variation on photosynthetic CO_2 fixation, which reduces loss of water vapor through the pores (stomata) by which CO_2 and O_2 must enter leaf tissue. Instead of separating the initial trapping of CO_2 and its fixation by rubisco across space (as do the C_4 plants), they separate these two events over time. At night, when the air is cooler and moister, the stomata open to allow entry of CO_2, which is then fixed into oxaloacetate by PEP carboxylase. The oxaloacetate is reduced to malate and stored in the vacuoles, to protect cytosolic and plastid enzymes from the low pH produced by malic acid dissociation. During the day the stomata close, preventing the water loss that would result from high daytime temperatures, and the CO_2 trapped overnight in malate is released as CO_2 by the NADP-linked malic enzyme. This CO_2 is now assimilated by the action of rubisco and the Calvin cycle enzymes. Because this method of CO_2 fixation was first discovered in stonecrops, perennial flowering plants of the family *Crassulaceae*, it is called *c*rassulacean *a*cid *m*etabolism, and the plants are called **CAM plants**.

SUMMARY 20.2 Photorespiration and the C_4 and CAM Pathways

- When rubisco uses O_2 rather than CO_2 as substrate, the 2-phosphoglycolate so formed is disposed of in an oxygen-dependent pathway. The result is increased consumption of O_2—photorespiration or, more accurately, the oxidative photosynthetic carbon cycle or C_2 cycle. The 2-phosphoglycolate is converted to glyoxylate, to glycine, and then to serine in a pathway that involves enzymes in the chloroplast stroma, the peroxisome, and the mitochondrion.
- In C_4 plants, the carbon-assimilation pathway minimizes photorespiration: CO_2 is first fixed in mesophyll cells into a four-carbon compound, which passes into bundle-sheath cells and releases CO_2 in high concentrations. The released CO_2 is fixed by rubisco, and the remaining reactions of the Calvin cycle occur as in C_3 plants.
- In CAM plants, CO_2 is fixed into malate in the dark and stored in vacuoles until daylight, when the stomata are closed (minimizing water loss) and malate serves as a source of CO_2 for rubisco.

20.3 Biosynthesis of Starch and Sucrose

During active photosynthesis in bright light, a plant leaf produces more carbohydrate (as triose phosphates) than it needs for generating energy or synthesizing precursors. The excess is converted to sucrose and transported to other parts of the plant, to be used as fuel or stored. In most plants, starch is the main storage form, but in a few plants, such as sugar beet and sugarcane, sucrose is the primary storage form. The synthesis of sucrose and starch occurs in different cellular compartments (cytosol and plastids, respectively), and these processes are coordinated by a variety of regulatory mechanisms that respond to changes in light level and photosynthetic rate. The synthesis of sucrose and starch is important to the plant but also to humans: starch provides more than 80% of human dietary calories worldwide.

ADP-Glucose Is the Substrate for Starch Synthesis in Plant Plastids and for Glycogen Synthesis in Bacteria

Starch, like glycogen, is a high molecular weight polymer of D-glucose in (α1→4) linkage. It is synthesized in chloroplasts for temporary storage as one of the stable end products of photosynthesis, and for long-term storage it is synthesized in the amyloplasts of the nonphotosynthetic parts of plants—seeds, roots, and tubers (underground stems).

The mechanism of glucose activation in starch synthesis is similar to that in glycogen synthesis. An activated **nucleotide sugar**, in this case **ADP-glucose**, is formed by condensation of glucose 1-phosphate with ATP in a reaction made essentially irreversible by the presence in plastids of inorganic pyrophosphatase (Fig. 15–31). **Starch synthase** then transfers glucose residues from ADP-glucose to preexisting starch molecules. The monomeric units are almost certainly added to the nonreducing end of the growing polymer, as they are in glycogen synthesis (see Fig. 15–32).

The amylose of starch is unbranched, but amylopectin has numerous (α1→6)-linked branches (see Fig. 7–13). Chloroplasts contain a branching enzyme, similar to glycogen-branching enzyme (see Fig. 15–33), that introduces the (α1→6) branches of amylopectin. Taking into account the hydrolysis by inorganic pyrophosphatase of the PP_i produced during ADP-glucose synthesis, the overall reaction for starch formation from glucose 1-phosphate is

$$\text{Starch}_n + \text{glucose 1-phosphate} + \text{ATP} \longrightarrow \text{starch}_{n+1} + \text{ADP} + 2P_i$$

$$\Delta G'^\circ = -50 \text{ kJ/mol}$$

Starch synthesis is regulated at the level of ADP-glucose formation, as discussed below.

Many types of bacteria store carbohydrate in the form of glycogen (essentially highly branched starch), which they synthesize in a reaction analogous to that catalyzed by glycogen synthase in animals. Bacteria, like plant plastids, use ADP-glucose as the activated form of glucose, whereas animal cells use UDP-glucose. Again, the similarity between plastid and bacterial metabolism is consistent with the endosymbiont hypothesis for the origin of organelles (p. 36).

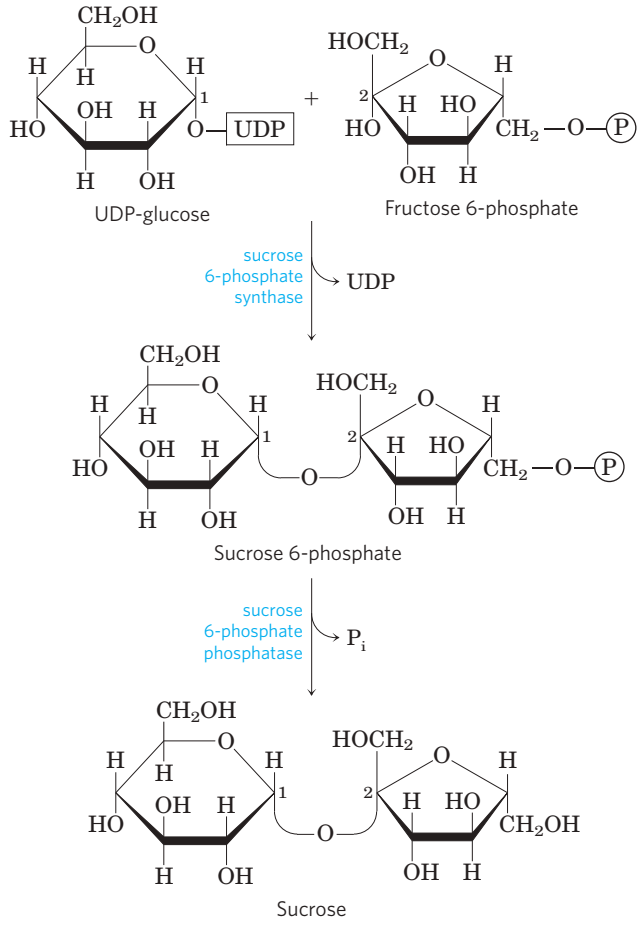

FIGURE 20–24 Sucrose synthesis. Sucrose is synthesized from UDP-glucose and fructose 6-phosphate, which are synthesized from triose phosphates in the plant cell cytosol by pathways shown in Figures 15–31 and 20–9. The sucrose 6-phosphate synthase of most plant species is allosterically regulated by glucose 6-phosphate and P_i.

UDP-Glucose Is the Substrate for Sucrose Synthesis in the Cytosol of Leaf Cells

Most of the triose phosphate generated by CO_2 fixation in plants is converted to sucrose **(Fig. 20–24)** or starch. In the course of evolution, sucrose may have been selected as the transport form of carbon because of its unusual linkage between the anomeric C-1 of glucose and the anomeric C-2 of fructose. This bond is not hydrolyzed by amylases or other common carbohydrate-cleaving enzymes, and the unavailability of the anomeric carbons prevents sucrose from reacting nonenzymatically (as does glucose) with amino acids and proteins.

Sucrose is synthesized in the cytosol, beginning with dihydroxyacetone phosphate and glyceraldehyde 3-phosphate exported from the chloroplast. After condensation of two triose phosphates to form fructose 1,6-bisphosphate (catalyzed by aldolase), hydrolysis by fructose 1,6-bisphosphatase yields fructose 6-phosphate. **Sucrose 6-phosphate synthase** then catalyzes the reaction of fructose 6-phosphate with **UDP-glucose** to form **sucrose 6-phosphate** (Fig. 20–24). Finally, **sucrose 6-phosphate phosphatase** removes the phosphate group, making sucrose available for export to other tissues. The reaction catalyzed by sucrose 6-phosphate synthase is a low-energy process ($\Delta G'^\circ = -5.7$ kJ/mol), but the hydrolysis of sucrose 6-phosphate to sucrose is sufficiently exergonic ($\Delta G'^\circ = -16.5$ kJ/mol) to make the overall synthesis of sucrose essentially irreversible. Sucrose synthesis is regulated and closely coordinated with starch synthesis, as we shall see.

One remarkable difference between the cells of plants and animals is the absence in the plant cell cytosol of the enzyme inorganic pyrophosphatase, which catalyzes the reaction

$$PP_i + H_2O \longrightarrow 2P_i \qquad \Delta G'^\circ = -19.2 \text{ kJ/mol}$$

For many biosynthetic reactions that liberate PP_i, pyrophosphatase activity makes the process more favorable energetically, tending to make these reactions irreversible.

In plants, this enzyme is present in plastids but absent from the cytosol. As a result, the cytosol of leaf cells contains a substantial concentration of PP_i—enough (~0.3 mM) to make reactions such as that catalyzed by UDP-glucose pyrophosphorylase (see Fig. 15–31) readily reversible. Recall from Chapter 14 (p. 550) that the cytosolic isozyme of phosphofructokinase in plants uses PP_i, not ATP, as the phosphoryl donor.

Conversion of Triose Phosphates to Sucrose and Starch Is Tightly Regulated

Triose phosphates produced by the Calvin cycle in bright sunlight, as we have noted, may be stored temporarily in the chloroplast as starch, or converted to sucrose and exported to nonphotosynthetic parts of the plant, or both. The balance between the two processes is tightly regulated, and both must be coordinated with the rate of carbon fixation. Five-sixths of the triose phosphate formed in the Calvin cycle must be recycled to ribulose 1,5-bisphosphate (Fig. 20–14); if more than one-sixth of the triose phosphate is drawn out of the cycle to make sucrose and starch, the cycle will slow or stop. However, *insufficient* conversion of triose phosphate to starch or sucrose would tie up phosphate, leaving a chloroplast deficient in P_i, which is also essential for operation of the Calvin cycle.

The flow of triose phosphates into sucrose is regulated by the activity of fructose 1,6-bisphosphatase (FBPase-1) and the enzyme that effectively reverses its action, PP_i-dependent phosphofructokinase (PP-PFK-1; p. 550). These enzymes are therefore critical points for determining the fate of triose phosphates produced by photosynthesis. Both enzymes are regulated by **fructose 2,6-bisphosphate (F26BP)**, which inhibits FBPase-1 and stimulates PP-PFK-1. In vascular plants, the concentration of F26BP varies inversely with the rate of photosynthesis **(Fig. 20–25)**. Phosphofructokinase-2, responsible for F26BP synthesis, is inhibited by dihydroxyacetone phosphate or 3-phosphoglycerate and stimulated by fructose 6-phosphate and P_i. During active photosynthesis, dihydroxyacetone phosphate is produced and P_i is consumed, resulting in inhibition of PFK-2 and lowered concentrations of F26BP. This favors greater flux of triose phosphate into fructose 6-phosphate formation and sucrose synthesis. With this regulatory system, sucrose synthesis occurs when the level of triose phosphate produced by the Calvin cycle exceeds that needed to maintain the operation of the cycle.

Sucrose synthesis is also regulated at the level of sucrose 6-phosphate synthase, which is allosterically activated by glucose 6-phosphate and inhibited by P_i. This enzyme is further regulated by phosphorylation and dephosphorylation; a protein kinase phosphorylates the enzyme on a specific Ser residue, making it less active, and a phosphatase reverses this inactivation by removing the phosphate **(Fig. 20–26)**. Inhibition of the kinase by glucose 6-phosphate, and of the phosphatase by P_i, enhances the effects of these two compounds on sucrose synthesis. When hexose phosphates are abundant, sucrose 6-phosphate synthase is activated by glucose 6-phosphate; when P_i is elevated (as when photosynthesis is slow), sucrose synthesis is slowed.

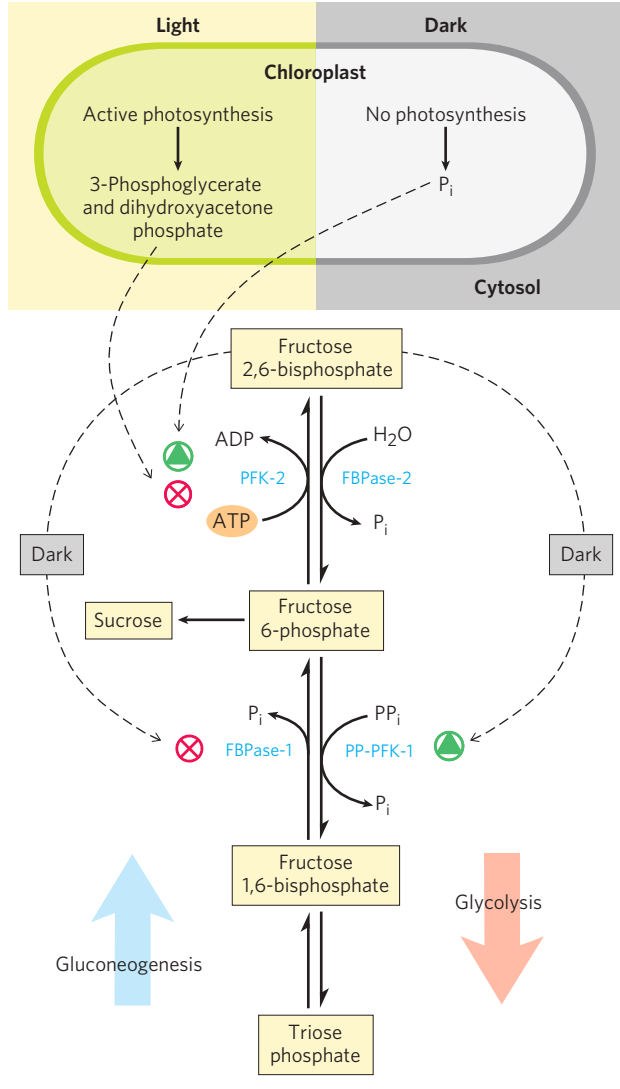

FIGURE 20–25 Fructose 2,6-bisphosphate as regulator of sucrose synthesis. The concentration of the allosteric regulator fructose 2,6-bisphosphate in plant cells is regulated by the products of photosynthetic carbon assimilation and by P_i. Dihydroxyacetone phosphate and 3-phosphoglycerate produced by CO_2 assimilation inhibit phosphofructokinase-2 (PFK-2), the enzyme that synthesizes the regulator; P_i stimulates PFK-2. The concentration of the regulator is therefore inversely proportional to the rate of photosynthesis. In the dark, the concentration of fructose 2,6-bisphosphate increases and stimulates the glycolytic enzyme PP_i-dependent phosphofructokinase-1 (PP-PFK-1), while inhibiting the gluconeogenic enzyme fructose 1,6-bisphosphatase (FBPase-1). When photosynthesis is active (in the light), the concentration of the regulator drops and the synthesis of fructose 6-phosphate and sucrose is favored.

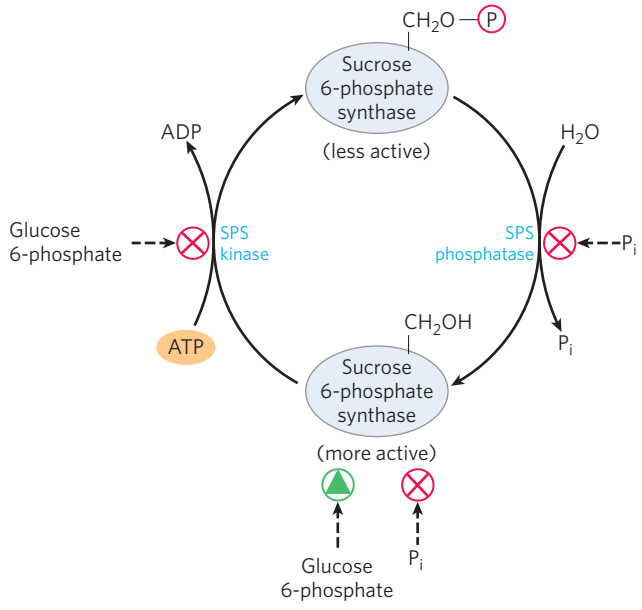

FIGURE 20–26 Regulation of sucrose phosphate synthase by phosphorylation. A protein kinase (SPS kinase) specific for sucrose phosphate synthase (SPS) phosphorylates a Ser residue in SPS, inactivating it; a specific phosphatase (SPS phosphatase) reverses this inhibition. The kinase is inhibited allosterically by glucose 6-phosphate, which also activates SPS allosterically. The phosphatase is inhibited by P_i, which also inhibits SPS directly. Thus when the concentration of glucose 6-phosphate is high as a result of active photosynthesis, SPS is activated and produces sucrose phosphate. A high P_i concentration, which occurs when photosynthetic conversion of ADP to ATP is slow, inhibits sucrose phosphate synthesis.

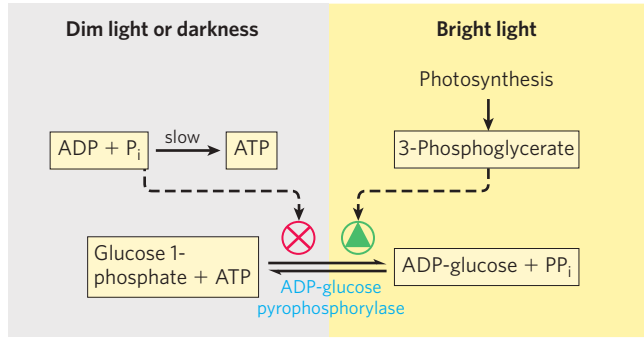

FIGURE 20–27 Regulation of ADP-glucose phosphorylase by 3-phosphoglycerate and P_i. This enzyme, which produces the precursor for starch synthesis, is rate-limiting in starch production. The enzyme is stimulated allosterically by 3-phosphoglycerate (3-PGA) and inhibited by P_i; in effect, the ratio [3-PGA]/[P_i], which rises with increasing rates of photosynthesis, controls starch synthesis at this step.

During active photosynthesis, triose phosphates are converted to fructose 6-phosphate, which is rapidly equilibrated with glucose 6-phosphate by phosphohexose isomerase. Because the equilibrium lies far toward glucose 6-phosphate, as soon as fructose 6-phosphate accumulates, the level of glucose 6-phosphate rises and sucrose synthesis is stimulated.

The key regulatory enzyme in starch synthesis is **ADP-glucose pyrophosphorylase (Fig. 20–27)**; it is activated by 3-phosphoglycerate (which accumulates during active photosynthesis) and inhibited by P_i (which accumulates when light-driven condensation of ADP and P_i slows). When sucrose synthesis slows, 3-phosphoglycerate formed by CO_2 fixation accumulates, activating this enzyme and stimulating the synthesis of starch.

SUMMARY 20.3 Biosynthesis of Starch and Sucrose

- Starch synthase in chloroplasts and amyloplasts catalyzes the addition of single glucose residues, donated by ADP-glucose, probably to the nonreducing end. Branches in amylopectin are introduced by a second enzyme.
- Sucrose is synthesized in the cytosol in two steps from UDP-glucose and fructose 1-phosphate.
- The partitioning of triose phosphates between sucrose synthesis and starch synthesis is regulated by fructose 2,6-bisphosphate (F26BP), an allosteric effector of the enzymes that determine the level of fructose 6-phosphate. F26BP concentration varies inversely with the rate of photosynthesis, and F26BP inhibits the synthesis of fructose 6-phosphate, the precursor to sucrose.

20.4 Synthesis of Cell Wall Polysaccharides: Plant Cellulose and Bacterial Peptidoglycan

Cellulose is a major constituent of plant cell walls, providing strength and rigidity and preventing the swelling of the cell and rupture of the plasma membrane that might result when osmotic conditions favor water entry into the cell. Each year, worldwide, plants synthesize more than 10^{11} metric tons of cellulose, making this simple polymer one of the most abundant compounds in the biosphere. The structure of cellulose is simple: linear polymers of thousands of ($\beta 1 \rightarrow 4$)-linked D-glucose units, assembled into bundles of about 36 chains, which aggregate side by side to form a microfibril **(Fig. 20–28)**.

The biosynthesis of cellulose is less well understood than that of glycogen or starch. As a major component of the plant cell wall, cellulose must be synthesized from intracellular precursors but deposited and assembled outside the plasma membrane. The enzymatic machinery for initiation, elongation, and export of cellulose chains is more complicated than that needed to synthesize starch or glycogen (which are not exported). Bacteria face a similar set of problems when they synthesize the complex polysaccharides that make up their cell walls, and they may employ some of the same mechanisms to solve these problems.

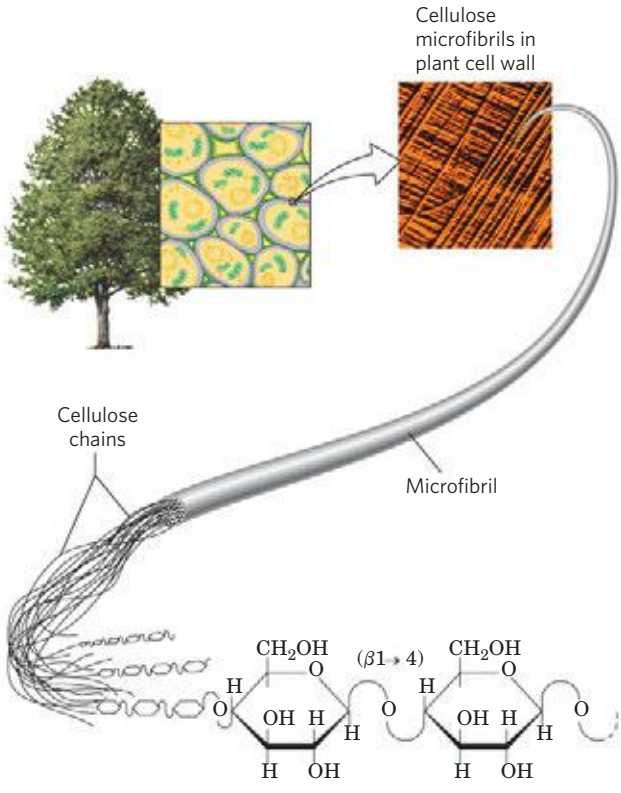

FIGURE 20–28 Cellulose structure. The plant cell wall is made up in part of cellulose molecules arranged side by side to form paracrystalline arrays—cellulose microfibrils. Many microfibrils combine to form a cellulose fiber, seen in the scanning electron microscope as a structure 5 to 12 nm in diameter, laid down on the cell surface in several layers distinguishable by the different orientations of their fibers.

Cellulose Is Synthesized by Supramolecular Structures in the Plasma Membrane

The complex enzymatic machinery that assembles cellulose chains spans the plasma membrane, with one part positioned to bind the substrate, UDP-glucose, in the cytosol and another part extending to the outside, responsible for elongating and crystallizing cellulose molecules in the extracellular space. Freeze-fracture electron microscopy shows these **terminal complexes**, also called **rosettes**, to be composed of six large particles arranged in a regular hexagon with a diameter of about 30 nm **(Fig. 20–29)**. Several proteins, including the catalytic subunit of **cellulose synthase**, make up the terminal complex. Much of the recent progress in understanding cellulose synthesis stems from genetic and molecular genetic studies of the plant *Arabidopsis thaliana*, which is especially amenable to genetic dissection and whose genome has been sequenced. The gene family that encodes this cellulose-synthesizing activity has been cloned and found to encode proteins with eight transmembrane segments and a central domain on the cytosolic side of the plasma membrane that includes sequences expected in a glycosyltransferase (Fig. 20–29).

In one working model of cellulose synthesis, cellulose chains are initiated by the formation of a lipid-linked intermediate unlike anything involved in starch or glycogen synthesis. As shown in step ❶ of Figure 20–29, glucose is transferred from UDP-glucose to a membrane lipid, probably the plant sterol sitosterol, on the inner face of the plasma membrane. Here, intracellular cellulose synthase adds several more glucose residues to the first one, in (β1→4) linkage, forming a short oligosac-

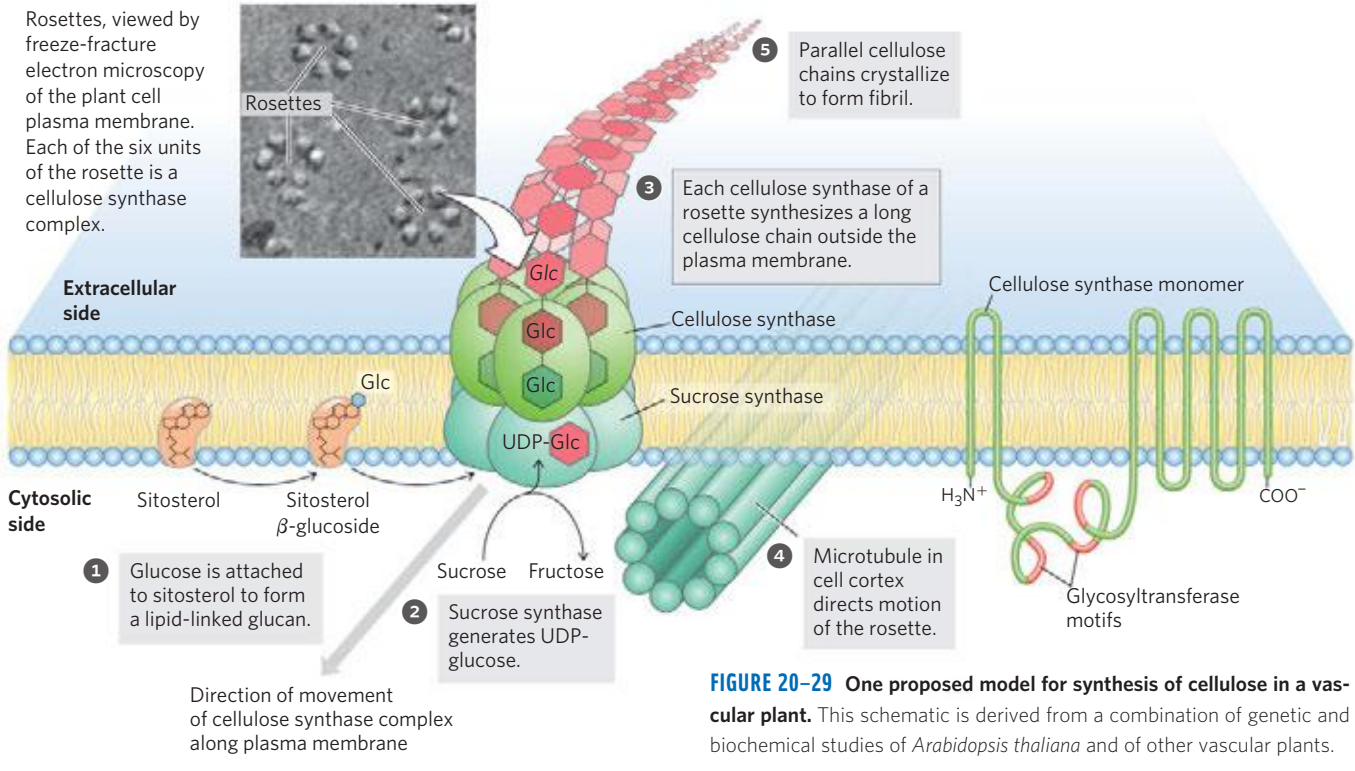

FIGURE 20–29 One proposed model for synthesis of cellulose in a vascular plant. This schematic is derived from a combination of genetic and biochemical studies of *Arabidopsis thaliana* and of other vascular plants.

charide chain attached to the sitosterol (sitosterol dextrin). Next, the whole sitosterol dextrin flips across to the outer face of the plasma membrane, where it now associates with another form of cellulose synthase.

The UDP-glucose used for cellulose synthesis (step ❷) is generated from sucrose produced during photosynthesis, by the reaction catalyzed by sucrose synthase (named for the reverse reaction):

$$\text{Sucrose} + \text{UDP} \longrightarrow \text{UDP-glucose} + \text{fructose}$$

Cellulose synthase spans the plasma membrane and uses cytosolic UDP-glucose as the precursor for extracellular cellulose synthesis. A membrane-bound form of sucrose synthase forms a complex with cellulose synthase, feeding UDP-glucose from sucrose directly into cell wall synthesis.

In step ❸ a second form of cellulose synthase extends the polymer to 500 to 15,000 glucose units, extruding it onto the outer surface of the cell. The action of the enzyme is processive: one enzyme molecule adds many glucose units before releasing the growing cellulose chain. The direction of chain growth (whether addition occurs at the reducing end or at the nonreducing end) has not been definitively established.

Each of the six globules of the rosette consists of multiple protein subunits that together synthesize six cellulose chains. The large enzyme complex that catalyzes this process (step ❹) actually moves along the plasma membrane, following the course of microtubules in the cortex, the cytoplasmic layer just under the membrane. Because these microtubules lie perpendicular to the axis of the plant's growth, the cellulose microfibrils are laid down across the axis of growth. The motion of the cellulose synthase complexes is believed to be driven by energy released in the polymerization reaction, not by a molecular motor such as kinesin.

The finished cellulose is in the form of crystalline microfibrils (Fig. 20–28), each consisting of 36 separate cellulose chains lying side by side, all with the same (parallel) orientation of nonreducing and reducing ends. It seems likely that the 36 separate polymers synthesized at one rosette arrive together on the outer surface of the cell, already aligned and (step ❺) ready to crystallize as a microfibril of the cell wall. When the 36 polymers reach some critical length, their synthesis is terminated by an unknown mechanism; crystallization into a microfibril follows.

In the activated precursor of cellulose (UDP-glucose), the glucose is α-linked to the nucleotide, but in the product (cellulose), glucose residues are ($\beta 1 \rightarrow 4$)-linked, so there is an inversion of configuration at the anomeric carbon (C-1) as the glycosidic bond forms. Glycosyltransferases that invert configuration are generally assumed to use a single-displacement mechanism, with nucleophilic attack by the acceptor species at the anomeric carbon of the donor sugar (UDP-glucose).

Certain bacteria (*Acetobacter*, *Agrobacteria*, *Rhizobia*, and *Sarcina*) and many simple eukaryotes also carry out cellulose synthesis, apparently by a mechanism similar to that in plants. If the bacteria use a membrane lipid to initiate new chains, it cannot be a sterol—bacteria do not contain sterols.

Lipid-Linked Oligosaccharides Are Precursors for Bacterial Cell Wall Synthesis

Like plants, many bacteria have thick, rigid extracellular walls that protect them from osmotic lysis. The **peptidoglycan** that gives bacterial envelopes their strength and rigidity is an alternating linear copolymer of *N*-acetylglucosamine (GlcNAc) and *N*-acetylmuramic acid (Mur2Ac), linked by ($\beta 1 \rightarrow 4$) glycosidic bonds and cross-linked by short peptides attached to the Mur2Ac **(Fig. 20–30)**. During assembly of the polysaccharide

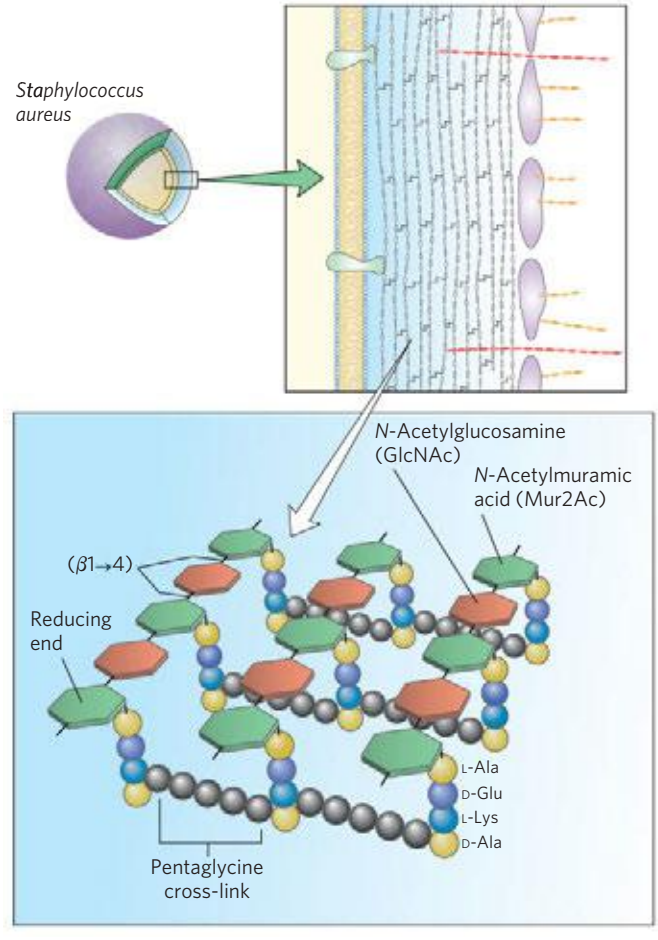

FIGURE 20–30 **Peptidoglycan structure.** This is the peptidoglycan of the cell wall of *Staphylococcus aureus*, a gram-positive bacterium. Peptides (strings of colored spheres) covalently link *N*-acetylmuramic acid residues in neighboring polysaccharide chains. Note the mixture of L and D amino acids in the peptides. Gram-positive bacteria such as *S. aureus* have a pentaglycine chain in the cross-link. Gram-negative bacteria, such as *E. coli*, lack the pentaglycine; instead, the terminal D-Ala residue of one tetrapeptide is attached directly to a neighboring tetrapeptide through either L-Lys or a lysine-like amino acid, diaminopimelic acid. The peptide bond of glutamate is unusual here; it involves the carboxyl group of the glutamate side chain.

backbone of this complex macromolecule, both GlcNAc and Mur2Ac are activated by attachment of a uridine nucleotide at their anomeric carbons. First, GlcNAc 1-phosphate condenses with UTP to form UDP-GlcNAc (**Fig. 20–31**, step ❶), which reacts with phosphoenolpyruvate to form UDP-Mur2Ac (step ❷); five amino acids are then added (step ❸). The Mur2Ac-pentapeptide moiety is transferred from the uridine nucleotide to the membrane lipid dolichol, a long-chain isoprenoid alcohol (see Fig. 10–22f) (step ❹), and a GlcNAc residue is donated by UDP-GlcNAc (step ❺). In many bacteria, five glycines are added in peptide linkage to the amino group of the Lys residue of the pentapeptide (step ❻). Finally, this disaccharide decapeptide is added to the nonreducing end of an existing peptidoglycan molecule (step ❼). A transpeptidation reaction cross-links adjacent polysaccharide chains (step ❽), contributing to a huge, strong, macromolecular wall around the bacterial cell. Many of the most effective antibiotics in use today act by inhibiting reactions in the synthesis of the peptidoglycan.

Many other oligosaccharides and polysaccharides are synthesized by similar routes in which sugars are activated for subsequent reactions by attachment to nucleotides. In the glycosylation of proteins, for example (see Fig. 27–39), the precursors of the carbohydrate moieties include sugar nucleotides and lipid-linked oligosaccharides.

SUMMARY 20.4 Synthesis of Cell Wall Polysaccharides: Plant Cellulose and Bacterial Peptidoglycan

- Cellulose synthesis takes place in terminal complexes (rosettes) in the plasma membrane. Each cellulose chain begins as a sitosterol dextrin formed inside the cell. It then flips to the outside, where the oligosaccharide portion is transferred to cellulose synthase in the rosette and is then

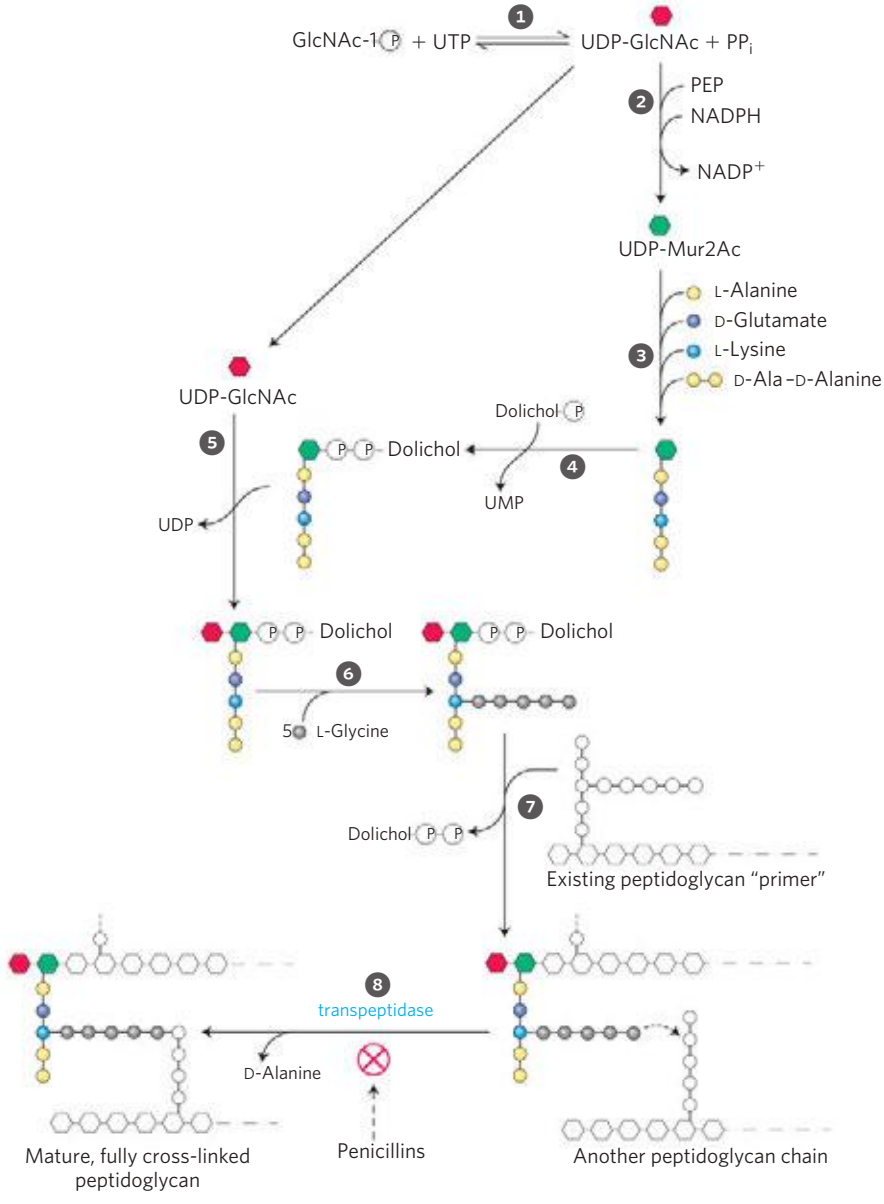

FIGURE 20–31 Synthesis of bacterial peptidoglycan. In the early steps of this pathway (❶ through ❹), *N*-acetylglucosamine (GlcNAc) and *N*-acetylmuramic acid (Mur2Ac) are activated by attachment of a uridine nucleotide (UDP) to their anomeric carbons and, in the case of Mur2Ac, of a long-chain isoprenoid alcohol (dolichol) through a phosphodiester bond. These activating groups participate in the formation of glycosidic linkages; they serve as excellent leaving groups. After steps ❺ and ❻, assembly of a disaccharide with a peptide side chain (10 amino acid residues), ❼ this precursor is transferred to the nonreducing end of an existing peptidoglycan chain, which serves as a primer for the polymerization reaction. Finally, ❽ in a transpeptidation reaction between the peptide side chains on two different peptidoglycan molecules, a Gly residue at the end of one chain displaces a terminal D-Ala in the other chain, forming a cross-link. This transpeptidation reaction is inhibited by the penicillins, which kill bacteria by weakening their cell walls (see Fig. 6–30).

extended. Each rosette produces 36 separate cellulose chains simultaneously and in parallel. The chains crystallize into one of the microfibrils that form the cell wall.

- Synthesis of the bacterial cell wall peptidoglycan also involves lipid-linked oligosaccharides formed inside the cell and flipped to the outside for assembly.

20.5 Integration of Carbohydrate Metabolism in the Plant Cell

Carbohydrate metabolism in a typical plant cell is more complex in several ways than that in a typical animal cell. The plant cell carries out the same processes that generate energy in animal cells (glycolysis, citric acid cycle, and oxidative phosphorylation); it can generate hexoses from three- or four-carbon compounds by gluconeogenesis; it can oxidize hexose phosphates to pentose phosphates with the generation of NADPH (the oxidative pentose phosphate pathway); and it can produce a polymer of (α1→4)-linked glucose (starch) and degrade it to generate hexoses. But besides these carbohydrate transformations that it shares with animal cells, the photosynthetic plant cell can fix CO_2 into organic compounds (the rubisco reaction); use the products of fixation to generate trioses, hexoses, and pentoses (the Calvin cycle); and convert acetyl-CoA generated from fatty acid breakdown to four-carbon compounds (the glyoxylate cycle) and the four-carbon compounds to hexoses (gluconeogenesis). These processes, unique to the plant cell, are segregated in several compartments not found in animal cells: the glyoxylate cycle in glyoxysomes, the Calvin cycle in chloroplasts, starch synthesis in amyloplasts, and organic acid storage in vacuoles. The integration of events among these various compartments requires specific transporters in the membranes of each organelle, to move products from one organelle to another or into the cytosol.

Gluconeogenesis Converts Fats and Proteins to Glucose in Germinating Seeds

Many plants store lipids and proteins in their seeds, to be used as sources of energy and as biosynthetic precursors during germination, before photosynthetic mechanisms have developed. Active gluconeogenesis in germinating seeds provides glucose for the synthesis of sucrose, polysaccharides, and many metabolites derived from hexoses. In plant seedlings, sucrose provides much of the chemical energy needed for initial growth.

We noted earlier (Chapter 14) that animal cells can carry out gluconeogenesis from three- and four-carbon precursors, but not from the two acetyl carbons of acetyl-CoA. Because the pyruvate dehydrogenase reaction is effectively irreversible (Section 16.1), animal cells have no way to convert acetyl-CoA to pyruvate or oxaloacetate. Unlike animals, plants and some microorganisms *can* convert acetyl-CoA derived from fatty acid oxidation to glucose **(Fig. 20–32)**. Some of the enzymes essential

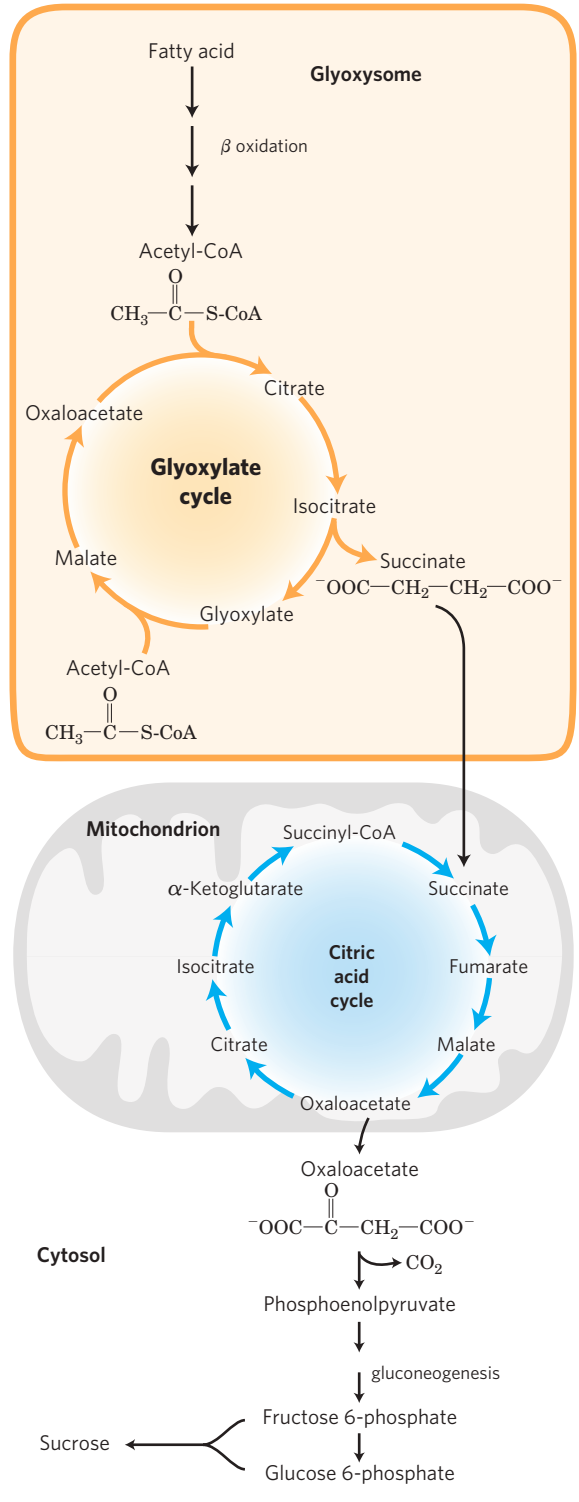

FIGURE 20–32 Conversion of stored fatty acids to sucrose in germinating seeds. This pathway begins in glyoxysomes. Succinate is produced and exported to mitochondria, where it is converted to oxaloacetate by enzymes of the citric acid cycle. Oxaloacetate enters the cytosol and serves as the starting material for gluconeogenesis and for the synthesis of sucrose, the transport form of carbon in plants.

to this conversion are sequestered in glyoxysomes, where glyoxysome-specific isozymes of β oxidation break down fatty acids to acetyl-CoA (see Fig. 16–24). The physical separation of the glyoxylate cycle and β-oxidation enzymes from the mitochondrial citric acid cycle enzymes prevents further oxidation of acetyl-CoA to CO_2. Instead, the acetyl-CoA is converted to succinate in the glyoxylate cycle (see Fig. 16–22). The succinate passes into the mitochondrial matrix, where it is converted by citric acid cycle enzymes to oxaloacetate, which moves into the cytosol. Cytosolic oxaloacetate is converted by gluconeogenesis to fructose 6-phosphate, the precursor of sucrose. Thus the integration of reaction sequences in three subcellular compartments is required for the production of fructose 6-phosphate or sucrose from stored lipids. Because only three of the four carbons in each molecule of oxaloacetate are converted to hexose in the cytosol, about 75% of the carbon in the fatty acids stored as seed lipids is converted to carbohydrate by the combined pathways of Figure 20–32. The other 25% is lost as CO_2 in the conversion of oxaloacetate to phosphoenolpyruvate. Hydrolysis of storage triacylglycerols also produces glycerol 3-phosphate, which can enter the gluconeogenic pathway after its oxidation to dihydroxyacetone phosphate **(Fig. 20–33)**.

Glucogenic amino acids (see Table 14–4) derived from the breakdown of stored seed proteins also yield precursors for gluconeogenesis, following transamination and oxidation to succinyl-CoA, pyruvate, oxaloacetate, fumarate, and α-ketoglutarate (Chapter 18)—all good starting materials for gluconeogenesis.

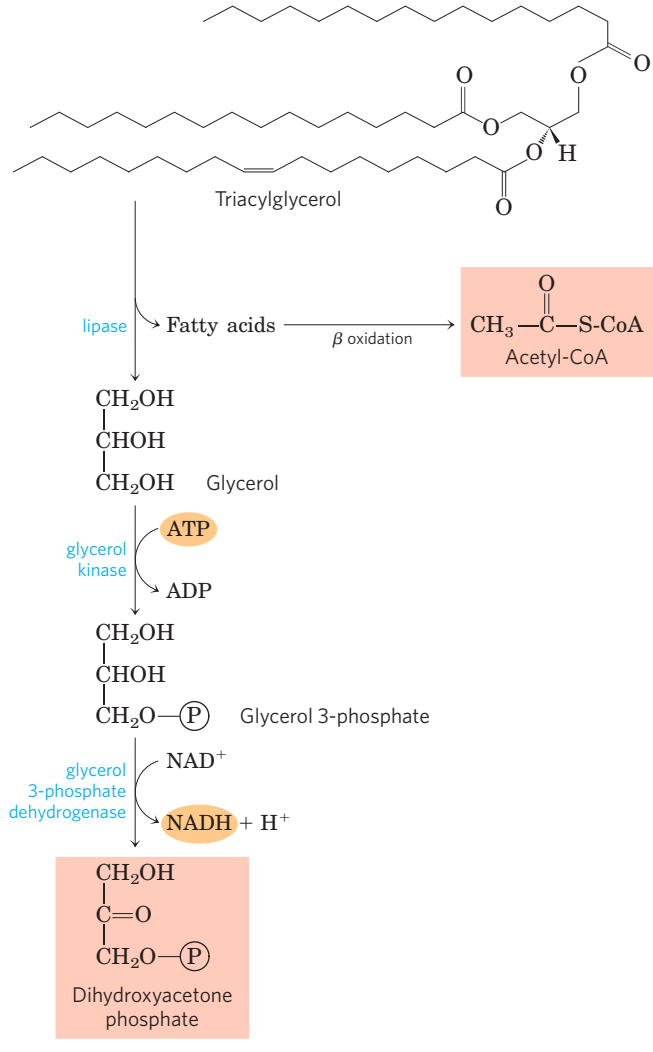

FIGURE 20–33 Conversion of the glycerol moiety of triacylglycerols to sucrose in germinating seeds. The glycerol of triacylglycerols is oxidized to dihydroxyacetone phosphate, which enters the gluconeogenic pathway at the triose phosphate isomerase reaction.

Pools of Common Intermediates Link Pathways in Different Organelles

Although we have described metabolic transformations in plant cells in terms of individual pathways, these pathways interconnect so completely that we should instead consider pools of metabolic intermediates shared among these pathways and connected by readily reversible reactions **(Fig. 20–34)**. One such **metabolite pool** includes the hexose phosphates glucose 1-phosphate, glucose 6-phosphate, and fructose 6-phosphate; a second includes the 5-phosphates of the pentoses ribose, ribulose, and xylulose; a third includes the triose phosphates dihydroxyacetone phosphate and glyceraldehyde 3-phosphate. Metabolite fluxes through these pools change in magnitude and direction in response to changes in the circumstances of the plant, and they vary with tissue type. Transporters in the membranes of each organelle move specific compounds in and out, and the regulation of these transporters presumably influences the degree to which the pools mix.

During daylight hours, triose phosphates produced in leaf tissue by the Calvin cycle move out of the chloroplast and into the cytosolic hexose phosphate pool, where they are converted to sucrose for transport to nonphotosynthetic tissues. In these tissues, sucrose is converted to starch for storage or is used as an energy source via glycolysis. In growing plants, hexose phosphates are also withdrawn from the pool for the synthesis of cell walls. At night, starch is metabolized by glycolysis to provide energy, essentially as in nonphotosynthetic organisms, and NADPH and ribose 5-phosphate are obtained through the oxidative pentose phosphate pathway.

SUMMARY 20.5 Integration of Carbohydrate Metabolism in the Plant Cell

- Plants can synthesize sugars from acetyl-CoA, the product of fatty acid breakdown, by the combined actions of the glyoxylate cycle and gluconeogenesis.
- The individual pathways of carbohydrate metabolism in plants overlap extensively; they

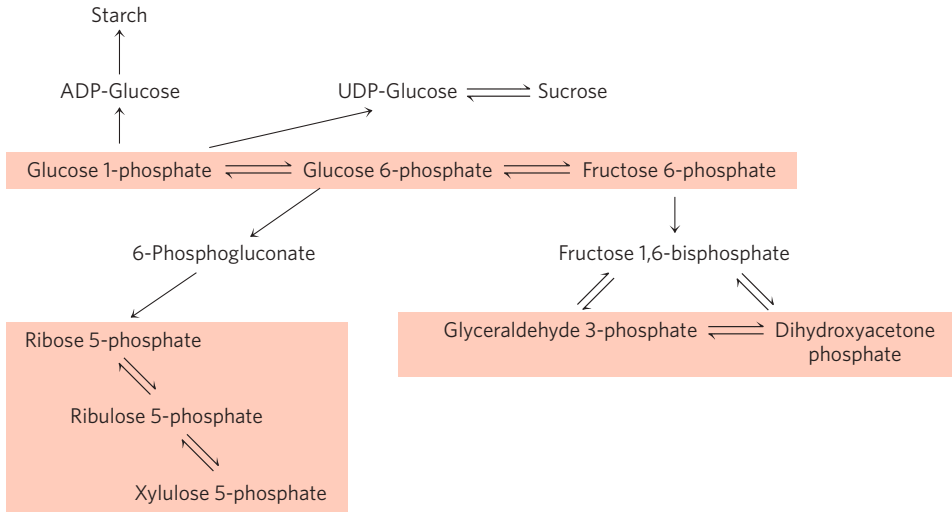

FIGURE 20–34 Pools of hexose phosphates, pentose phosphates, and triose phosphates. The compounds in each pool are readily interconvertible by reactions that have small standard free-energy changes. When one component of the pool is temporarily depleted, a new equilibrium is quickly established to replenish it. Movement of the sugar phosphates between intracellular compartments is limited; specific transporters must be present in an organelle membrane.

share pools of common intermediates, including hexose phosphates, pentose phosphates, and triose phosphates. Transporters in the membranes of chloroplasts, mitochondria, and amyloplasts mediate the movement of sugar phosphates between organelles. The direction of metabolite flow through the pools changes from day to night.

Key Terms

Terms in bold are defined in the glossary.

Calvin cycle 800
plastid 800
chloroplast 800
amyloplast 800
carbon-fixation reaction 801
ribulose 1,5-bisphosphate 801
3-phosphoglycerate 801
pentose phosphate pathway 801
reductive pentose phosphate cycle 801
C_3 plants 802
ribulose 1,5-bisphosphate carboxylase/oxygenase (rubisco) 802
rubisco activase 804
aldolase 805
transketolase 805
sedoheptulose 1,7-bisphosphate 806
ribulose 5-phosphate 806
carbon-assimilation reactions 809
thioredoxin 811
ferredoxin-thioredoxin reductase 811
photorespiration 812
2-phosphoglycolate 812
glycolate pathway 813
oxidative photosynthetic carbon cycle (C_2 cycle) 815
C_4 plants 815
phosphoenolpyruvate carboxylase 816
malic enzyme 816
pyruvate phosphate dikinase 817
CAM plants 818
nucleotide sugars 819
ADP-glucose 819
starch synthase 819
sucrose 6-phosphate synthase 819
fructose 2,6-bisphosphate 820
ADP-glucose pyrophosphorylase 821
cellulose synthase 822
peptidoglycan 823
metabolite pools 826

Further Reading

General References

Blankenship, R.E. (2002) *Molecular Mechanisms of Photosynthesis*, Blackwell Science, Oxford.

Very readable, well-illustrated, intermediate-level treatment of all aspects of photosynthesis, including the carbon metabolism covered in this chapter and the light-driven reactions described in Chapter 19.

Buchanan, B.B., Gruissem, W., & Jones, R.L. (eds). (2002) *Biochemistry and Molecular Biology of Plants*, American Society of Plant Physiology, Rockville, MD.

This wonderful, authoritative book covers all aspects of plant biochemistry and molecular biology. The following chapters cover carbohydrate structure and synthesis in greater depth: **Carpita, N. & McCann, M.**, Chapter 2, The cell wall (pp. 52–109); **Malkin, R. & Niyogi, K.**, Chapter 12, Photosynthesis (pp. 568–629); **Dennis, D.T. & Blakeley, S.D.**, Chapter 13, Carbohydrate Metabolism (pp. 630–675); **Siedow, J.N. & Day, D.A.**, Chapter 14, Respiration and Photorespiration (pp. 676–729).

Heldt, H.-W. & Piechulla, B. (2010) *Plant Biochemistry*, 4th edn., Academic Press, New York.

An *excellent* textbook of plant biochemistry.

Morton, O. (2007) *Eating the Sun: How Plants Power the Planet*, Harper, New York.

An engaging account of the discoveries in photosynthesis in the context of the history of science.

Photosynthetic Carbohydrate Synthesis

Andersson, I. & Backlund, A. (2008) Structure and function of rubisco. *Plant Physiol. Biochem.* **46**, 275–291.
Intermediate-level review.

Bassham, J.A. (2003) Mapping the carbon reduction cycle: a personal retrospective. *Photosynth. Res.* **76**, 35–52.

Benson, A.A. (2002) Following the path of carbon in photosynthesis: a personal story—history of photosynthesis. *Photosynth. Res.* **73**, 31–49.

Calvin, M. (1989) Forty years of photosynthesis and related activities. *Photosynth. Res.* **21**, 3–16.

Cleland, W.W., Andrews, T.J., Gutteridge, S., Hartman, F.C., & Lorimer, G.H. (1998) Mechanism of rubisco—the carbamate as general base. *Chem. Rev.* **98**, 549–561.
Review with a special focus on the carbamate at the active site.

Dietz, K.J., Link, G., Pistorius, E.K., & Scheibe, R. (2002) Redox regulation in oxygenic photosynthesis. *Prog. Botany* **63**, 207–245.

Hartman, F.C. & Harpel, M.R. (1994) Structure, function, regulation and assembly of D-ribulose-1,5-bisphosphate carboxylase/oxygenase. *Annu. Rev. Biochem.* **63**, 197–234.

Horecker, B.L. (2002) The pentose phosphate pathway. *J. Biol. Chem.* **277**, 47,965–47,971.

Jansson, C., Wullschleger, S.D., Kalluri, U.S., & Tuskan, G.A. (2010) Phytosequestration: carbon biosequestration by plants and the prospects of genetic engineering. *Bioscience* **60**, 685–696.
Global fluxes of carbon and the contribution of biomass to total terrestrial carbon.

Portis, A.R., Jr. (2003) Rubisco activase: rubisco's catalytic chaperone. *Photosynth. Res.* **75**, 11–27.
Structure, regulation, mechanism, and importance of rubisco activase.

Portis, A.R., Jr. & Parry, M.A.J. (2007) Discoveries in rubisco (ribulose 1,5-bisphosphate carboxylase/oxygenase): a historical perspective. *Photosynth. Res.* **94**, 121–143.

Raines, C.A. (2003) The Calvin cycle revisited. *Photosynth. Res.* **75**, 1–10.
Metabolic control analysis applied to the Calvin cycle.

Sage, R.F., Way, D.A., & Kubien, D.S. (2008) Rubisco, rubisco activase, and global climate change. *J. Exper. Bot.* **59**, 1581–1595.

Smith, A.M., Denyer, K., & Martin, C. (1997) The synthesis of the starch granule. *Annu. Rev. Plant Physiol. Plant Mol. Biol.* **48**, 67–87.
Review of the role of ADP-glucose pyrophosphorylase in the synthesis of amylose and amylopectin in starch granules.

Spreitzer, R.J. & Salvucci, M.E. (2002) Rubisco: structure, regulatory interactions, and possibilities for a better enzyme. *Annu. Rev. Plant Biol.* **53**, 449–475.
Advanced review on rubisco and rubisco activase.

Whitney, S.M., Houtz, R.L., & Alonso, H. (2011) Advancing our understanding and capacity to engineer nature's CO_2-sequestering enzyme, rubisco. *Plant Physiol.* **155**, 27–35.

Photorespiration and the C_4 and CAM Pathways

Ainsworth, E.A. & Long, S.P. (2005) What have we learned from 15 years of free-air CO_2 enrichment (FACE)? A meta-analytic review of the response of photosynthesis, canopy properties, and plant production to rising CO_2. *New Phytol.* **165**, 351–372.

Bauwe, H., Hagemann, M., & Fernie, A.R. (2010) Photorespiration: players, partners and origin. *Trends Plant Sci.* **15**, 330–336.

Black, C.C. & Osmond, C.B. (2003) Crassulacean acid metabolism and photosynthesis: working the night shift. *Photosynth. Res.* **76**, 329–341.

Douce, R., Bourguignon, J., Neuburger, M., & Rébeillé, F. (2001) The glycine decarboxylase system: a fascinating complex. *Trends Plant Sci.* **6**, 167–176.
Intermediate-level description of the structure and the reaction mechanism of the enzyme.

Hatch, M.D. (1987) C_4 photosynthesis: a unique blend of modified biochemistry, anatomy and ultrastructure. *Biochim. Biophys. Acta* **895**, 81–106.
Intermediate-level review by one of the discoverers of the C_4 pathway.

Hatch, M.D. & Slack, S.R. (1966) Photosynthesis by sugar-cane leaves: a new carboxylation reaction and the pathway of sugar formation. *Biochem. J.* **101**, 103–111.
The classic description of the path named for these authors.

Langdale, J.A. (2011) C4 cycles: past, present, and future research on C4 photosynthesis. *Plant Cell* **23**, 3879–3892.
Intermediate-level review

Tolbert, N.E. (1997) The C_2 oxidative photosynthetic carbon cycle. *Annu. Rev. Plant Physiol. Plant Mol. Biol.* **48**, 1–25.
A fascinating personal account of the development of our understanding of photorespiration, by one who was central in this development.

Biosynthesis of Starch and Sucrose

Doblin, M.S., Kurek, I., Javob-Wilk, D., & Delmer, D.P. (2002) Cellulose biosynthesis in plants: from genes to rosettes. *Plant Cell Physiol.* **43**, 1407–1420.

Huber, S.C. & Huber, J.L. (1996) Role and regulation of sucrose-phosphate synthase in higher plants. *Annu. Rev. Plant Physiol. Plant Mol. Biol.* **47**, 431–444.
Short review of factors that regulate this critical enzyme.

Keeling, P.L & Myers, A.M. (2010) Biochemistry and genetics of starch synthesis. *Annu. Rev. Food Sci. Technol.* **1**, 271–303.
Advanced review

Kotting, O., Kossmann, J., Zeeman, S.C., & Lloyd, J.R. (2010) Regulation of starch metabolism: the age of enlightenment? *Curr. Opin. Plant Biol.* **13**, 321–329.

Leloir, L.F. (1971) Two decades of research on the biosynthesis of saccharides. *Science* **172**, 1299–1303.
Leloir's Nobel address, including a discussion of the role of sugar nucleotides in metabolism.

Synthesis of Cellulose and Peptidoglycan

Endler, A. & Persson, S. (2011) Cellulose synthases and synthesis in *Arabidopsis*. *Mol. Plant* **4**, 199–211.

Joshi, C.P. & Mansfield, S.D. (2007) The cellulose paradox—simple molecule, complex biosynthesis. *Curr. Opin. Plant Biol.* **10**, 220–226.

Liepman, A.H., Andrews, T.J., Gutteridge, S., Hartman, F.C., & Lorimer, G.H. (2010) *Arabidopsis*—a powerful model system for plant cell wall research. *Plant J.* **61**, 1107–1121.

Scheible, W.-R. & Pauly, M. (2004) Glycosyltransferases and cell wall biosynthesis: novel players and insights. *Curr. Opin. Plant Biol.* **7**, 285–296.

Vollmer, W. & Seligman, S.J. (2009) Architecture of peptidoglycan: more data and more models. *Trends Microbiol.* **18**, 59–66.

Problems

1. Segregation of Metabolism in Organelles What are the advantages to the plant cell of having different organelles to carry out different reaction sequences that share intermediates?

2. Phases of Photosynthesis When a suspension of green algae is illuminated in the absence of CO_2 and then incubated with $^{14}CO_2$ in the dark, $^{14}CO_2$ is converted to [^{14}C]glucose for a brief time. What is the significance of this observation with regard to the CO_2-assimilation process, and how is it related to the light reactions of photosynthesis? Why does the conversion of $^{14}CO_2$ to [^{14}C]glucose stop after a brief time?

3. Identification of Key Intermediates in CO_2 Assimilation Calvin and his colleagues used the unicellular green alga *Chlorella* to study the carbon-assimilation reactions of photosynthesis. They incubated $^{14}CO_2$ with illuminated suspensions of algae and followed the time course of appearance of ^{14}C in two compounds, X and Y, under two sets of conditions. Suggest the identities of X and Y, based on your understanding of the Calvin cycle.

(a) Illuminated *Chlorella* were grown with unlabeled CO_2, then the light was turned off and $^{14}CO_2$ was added (vertical dashed line in the graph below). Under these conditions, X was the first compound to become labeled with ^{14}C; Y was unlabeled.

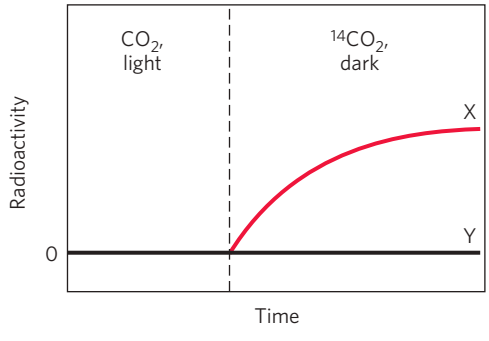

(b) Illuminated *Chlorella* cells were grown with $^{14}CO_2$. Illumination was continued until all the $^{14}CO_2$ had disappeared (vertical dashed line in the graph below). Under these conditions, X became labeled quickly but lost its radioactivity with time, whereas Y became more radioactive with time.

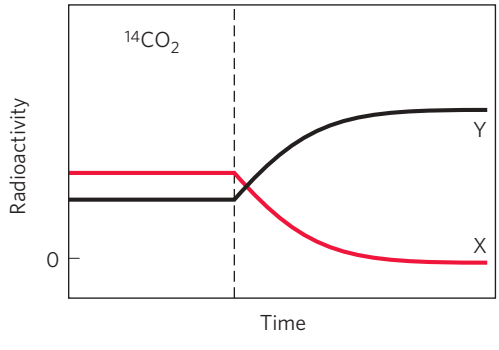

4. Regulation of the Calvin Cycle Iodoacetate reacts irreversibly with the free —SH groups of Cys residues in proteins.

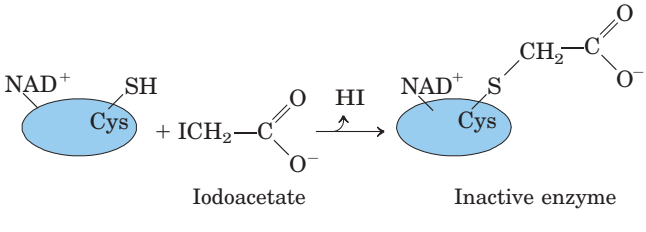

Predict which Calvin cycle enzyme(s) would be inhibited by iodoacetate, and explain why.

5. Thioredoxin in Regulation of Calvin Cycle Enzymes Motohashi and colleagues used thioredoxin as a hook to fish out from plant extracts the proteins that are activated by thioredoxin. To do this, they prepared a mutant thioredoxin in which one of the reactive Cys residues was replaced with a Ser. Explain why this modification was necessary for their experiments. Source: **Motohashi, K., Kondoh, A., Stumpp, M.T., & Hisabori, T.** (2001) Comprehensive survey of proteins targeted by chloroplast thioredoxin. *Proc. Natl. Acad. Sci. USA* **98**, 11,224–11,229.

6. Comparison of the Reductive and Oxidative Pentose Phosphate Pathways The *reductive* pentose phosphate pathway generates a number of intermediates identical to those of the *oxidative* pentose phosphate pathway (Chapter 14). What role does each pathway play in cells where it is active?

7. Photorespiration and Mitochondrial Respiration Compare the oxidative photosynthetic carbon cycle (C_2 cycle), also called *photorespiration*, with the *mitochondrial respiration* that drives ATP synthesis. Why are both processes referred to as respiration? Where in the cell do they occur, and under what circumstances? What is the path of electron flow in each?

8. Rubisco and the Composition of the Atmosphere N. E. Tolbert has argued that the dual specificity of rubisco for CO_2 and O_2 is not simply a leftover from evolution in a low-oxygen environment. He suggests that the relative activities of the carboxylase and oxygenase activities of rubisco actually have set, and now maintain, the ratio of CO_2 to O_2 in the earth's atmosphere. Discuss the pros and cons of this hypothesis, in molecular terms and in global terms. How does the existence of C_4 organisms bear on the hypothesis? Source: **Tolbert, N.E.** (1994) The role of photosynthesis and photorespiration in regulating atmospheric CO_2 and O_2. In *Regulation of Atmospheric CO_2 and O_2 by Photosynthetic Carbon Metabolism* (Tolbert, N.E., & Preiss, J., eds), pp. 8–33, Oxford University Press, New York.

9. Role of Sedoheptulose 1,7-Bisphosphatase What effect on the cell and the organism might result from a defect in sedoheptulose 1,7-bisphosphatase in (a) a human hepatocyte and (b) the leaf cell of a green plant?

10. Pathway of CO_2 Assimilation in Maize If a maize (corn) plant is illuminated in the presence of $^{14}CO_2$, after about 1 second, more than 90% of all the radioactivity incorporated in the leaves is found at C-4 of malate, aspartate, and oxaloacetate. Only after 60 seconds does ^{14}C appear at C-1 of 3-phosphoglycerate. Explain.

11. Identifying CAM Plants Given some $^{14}CO_2$ and all the tools typically present in a biochemistry research lab, how would you design a simple experiment to determine whether a plant is a typical C_4 plant or a CAM plant?

12. Chemistry of Malic Enzyme: Variation on a Theme Malic enzyme, found in the bundle-sheath cells of C_4 plants, carries out a reaction that has a counterpart in the citric acid cycle. What is the analogous reaction? Explain your choice.

13. The Cost of Storing Glucose as Starch Write the sequence of steps and the net reaction required to calculate the cost, in ATP molecules, of converting a molecule of cytosolic glucose 6-phosphate to starch and back to glucose 6-phosphate. What fraction of the maximum number of ATP molecules available from complete catabolism of glucose 6-phosphate to CO_2 and H_2O does this cost represent?

14. Inorganic Pyrophosphatase The enzyme inorganic pyrophosphatase contributes to making many biosynthetic reactions that generate inorganic pyrophosphate essentially irreversible in cells. By keeping the concentration of PP_i very low, the enzyme "pulls" these reactions in the direction of PP_i formation. The synthesis of ADP-glucose in chloroplasts is one reaction that is pulled in the forward direction by this mechanism. However, the synthesis of UDP-glucose in the plant cytosol, which produces PP_i, is readily reversible in vivo. How do you reconcile these two facts?

15. Regulation of Starch and Sucrose Synthesis Sucrose synthesis occurs in the cytosol and starch synthesis in the chloroplast stroma, yet the two processes are intricately balanced. What factors shift the reactions in favor of (a) starch synthesis and (b) sucrose synthesis?

16. Regulation of Sucrose Synthesis In the regulation of sucrose synthesis from the triose phosphates produced during photosynthesis, 3-phosphoglycerate and P_i play critical roles (see Fig. 20–25). Explain why the concentrations of these two regulators reflect the rate of photosynthesis.

17. Sucrose and Dental Caries The most prevalent infection in humans worldwide is dental caries, which stems from the colonization and destruction of tooth enamel by a variety of acidifying microorganisms. These organisms synthesize and live within a water-insoluble network of dextrans, called dental plaque, composed of (α1→6)-linked polymers of glucose with many (α1→3) branch points. Polymerization of dextran requires dietary sucrose, and the reaction is catalyzed by a bacterial enzyme, dextran-sucrose glucosyltransferase.

(a) Write the overall reaction for dextran polymerization.

(b) In addition to providing a substrate for the formation of dental plaque, how does dietary sucrose also provide oral bacteria with an abundant source of metabolic energy?

18. Differences between C_3 and C_4 Plants The plant genus *Atriplex* includes some C_3 and some C_4 species. From the data in the following plots (species 1, black curve; species 2, red curve), identify which is a C_3 plant and which is a C_4 plant. Justify your answer in molecular terms that account for the data in all three plots.

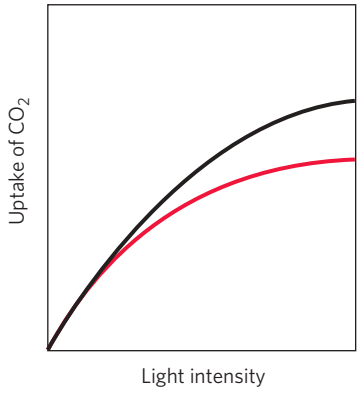

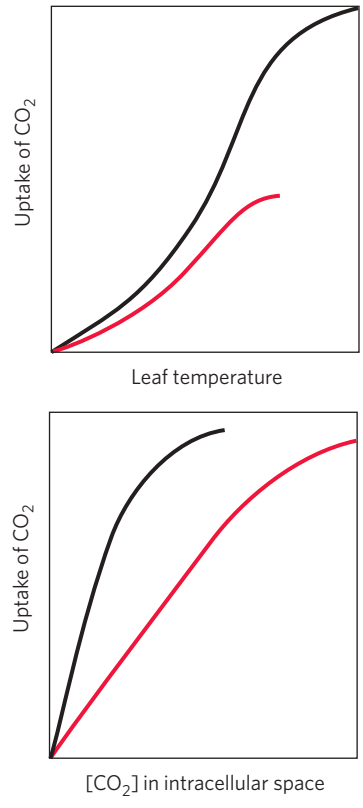

19. C_4 Pathway in a Single Cell In typical C_4 plants, the initial capture of CO_2 occurs in one cell type, and the Calvin cycle reactions occur in another (see Fig. 20–23). Voznesenskaya and colleagues[‡] have described a plant, *Bienertia cycloptera*—which grows in salty depressions of semidesert in Central Asia—that shows the biochemical properties of a C_4 plant but unlike typical C_4 plants does not segregate the reactions of CO_2 fixation into two cell types. PEP carboxylase and rubisco are present in the same cell. However, the cells have two types of chloroplasts, which are localized differently. One type, relatively poor in grana (thylakoids), is confined to the periphery; the more typical chloroplasts are clustered in the center of the cell, separated from the peripheral chloroplasts by large vacuoles. Thin cytosolic bridges pass through the vacuoles, connecting the peripheral and central cytosol. A micrograph of a *B. cycloptera* cell, with arrows pointing to peripheral chloroplasts, is shown below.

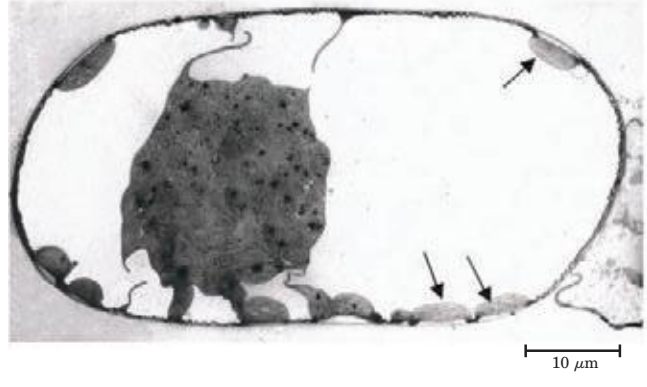

In this plant, where would you expect to find (a) PEP carboxylase, (b) rubisco, and (c) starch granules? Explain your answers with a model for CO_2 fixation in these C_4 cells. Source: **Voznesenskaya, E.V., Fraceschi, V.R., Kiirats, O., Artyusheva, E.G., Freitag, H., & Edwards, G.E.** (2002) Proof of C_4 photosynthesis without Kranz anatomy in *Bienertia cycloptera* (Chenopodiaceae). *Plant J.* **31**, 649–662.

Data Analysis Problem

20. Rubisco of Bacterial Endosymbionts of Hydrothermal Vent Animals Undersea hydrothermal vents support remarkable ecosystems. At these extreme depths there is no light to support photosynthesis, yet thriving vent communities are found. Much of their primary productivity occurs through chemosynthesis carried out by bacterial symbionts that live in specialized organs (trophosomes) of certain vent animals.

Chemosynthesis in these bacteria involves a process that is virtually identical to photosynthesis. Carbon dioxide is fixed by rubisco and reduced to glucose, and the necessary ATP and NADPH are produced by electron-transfer processes similar to those of the light-dependent reactions of photosynthesis. The key difference is that in chemosynthesis, the energy driving electron transfer comes from a highly exergonic chemical reaction rather than from light. Different chemosynthetic bacteria use different reactions for this purpose. The bacteria found in hydrothermal vent animals typically use the oxidation of H_2S (abundant in the vent water) by O_2, producing elemental sulfur. These bacteria also use the conversion of H_2S to sulfur as a source of electrons for chemosynthetic CO_2 reduction.

(a) What is the overall reaction for chemosynthesis in these bacteria? You do not need to write a balanced equation; just give the starting materials and products.

(b) Ultimately, these endosymbiotic bacteria obtain their energy from sunlight. Explain how this occurs.

Robinson and colleagues (2003) explored the properties of rubisco from the bacterial endosymbiont of the giant tube worm *Riftia pachyptila*. Rubisco, from any source, catalyzes the reaction of either CO_2 (Fig. 20–7) or O_2 (Fig. 20–20) with ribulose 1,5-bisphosphate. In general, rubisco reacts more readily with CO_2 than O_2. The degree of selectivity (Ω) can be expressed in the equation

$$\frac{V_{\text{carboxylation}}}{V_{\text{oxygenation}}} = \Omega \frac{[CO_2]}{[O_2]}$$

where V is the reaction velocity.

Robinson and coworkers measured the Ω value for the rubisco of the bacterial endosymbionts. They purified rubisco from tube-worm trophosomes, reacted it with mixtures of different ratios of O_2 and CO_2 in the presence of [1-^{3}H]ribulose 1,5-bisphosphate, and measured the ratio of [^{3}H]phosphoglycerate to [^{3}H]phosphoglycolate.

(c) The measured ratio of [^{3}H]phosphoglycerate to [^{3}H] phosphoglycolate is equal to the ratio $V_{\text{carboxylation}}/V_{\text{oxygenation}}$. Explain why.

(d) Why would [5-^{3}H]ribulose 1,5-bisphosphate not be a suitable substrate for this assay?

The Ω for the endosymbiont rubisco had a value of 8.6 ± 0.9.

(e) The atmospheric (molar) concentration of O_2 is 20% and that of CO_2 is about 380 parts per million. If the endosymbiont were to carry out chemosynthesis under these atmospheric conditions, what would be the value of $V_{\text{carboxylation}}/V_{\text{oxygenation}}$?

(f) Based on your answer to (e), would you expect Ω for the rubisco of a terrestrial plant to be higher than, equal to, or lower than 8.6? Explain your reasoning.

Two stable isotopes of carbon are commonly found in the environment: the more abundant ^{12}C and the rare ^{13}C. All rubisco enzymes catalyze the fixation of $^{12}CO_2$ faster than that of $^{13}CO_2$. As a result, the carbon in glucose is slightly enriched in ^{12}C compared with the isotopic composition of CO_2 in the environment. Several factors are involved in this "preferential" use of $^{12}CO_2$, but one factor is the fundamental physics of gases. The temperature of a gas is related to the kinetic energy of its molecules. Kinetic energy is given by $\frac{1}{2}mv^2$, where m is molecular mass and v is velocity. Thus, at the same temperature (same kinetic energy), the molecules of a lighter gas will be moving faster than those of a heavier gas.

(g) How could this contribute to rubisco's "preference" for $^{12}CO_2$ over $^{13}CO_2$? Some of the first convincing evidence that the tube-worm hosts were obtaining their fixed carbon from the endosymbionts was that the $^{13}C/^{12}C$ ratio in the animals was much closer to that of the bacteria than that of nonvent marine animals.

(h) Why is this more convincing evidence for a symbiotic relationship than earlier studies that simply showed the presence of rubisco in the bacteria found in trophosomes?

Reference

Robinson, J.J., Scott, K.M., Swanson, S.T., O'Leary, M.H., Horken, K., Tabita, F.R., & Cavanaugh, C.M. (2003) Kinetic isotope effect and characterization of form II RubisCO from the chemoautotrophic endosymbionts of the hydrothermal vent tubeworm *Riftia pachyptila*. *Limnol. Oceanogr.* **48**, 48–54.

this page left intentionally blank

21

Lipid Biosynthesis

Lipids play a variety of cellular roles, some only recently recognized. They are the principal form of stored energy in most organisms and major constituents of cellular membranes. Specialized lipids serve as pigments (retinal, carotene), cofactors (vitamin K), detergents (bile salts), transporters (dolichols), hormones (vitamin D derivatives, sex hormones), extracellular and intracellular messengers (eicosanoids, phosphatidylinositol derivatives), and anchors for membrane proteins (covalently attached fatty acids, prenyl groups, and phosphatidylinositol). The ability to synthesize a variety of lipids is essential to all organisms. This chapter describes the biosynthetic pathways for some of the most common cellular lipids, illustrating the strategies employed in assembling these water-insoluble products from water-soluble precursors such as acetate. Like other biosynthetic pathways, these reaction sequences are endergonic and reductive. They use ATP as a source of metabolic energy and a reduced electron carrier (usually NADPH) as a reductant.

We first describe the biosynthesis of fatty acids, the primary components of both triacylglycerols and phospholipids, then examine the assembly of fatty acids into triacylglycerols and the simpler membrane phospholipids. Finally, we consider the synthesis of cholesterol, a component of some membranes and the precursor of steroids such as the bile acids, sex hormones, and adrenocortical hormones.

21.1 Biosynthesis of Fatty Acids and Eicosanoids

After the discovery that fatty acid oxidation takes place by the oxidative removal of successive two-carbon (acetyl-CoA) units (see Fig. 17–8), biochemists thought the biosynthesis of fatty acids might proceed by a simple reversal of the same enzymatic steps. However, as they were to find out, fatty acid biosynthesis and breakdown occur by different pathways, are catalyzed by different sets of enzymes, and take place in different parts of the cell. Moreover, biosynthesis requires the participation of a three-carbon intermediate, **malonyl-CoA**, that is not involved in fatty acid breakdown.

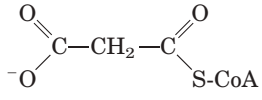

Malonyl-CoA

We focus first on the pathway of fatty acid synthesis, then turn our attention to regulation of the pathway and to the biosynthesis of longer-chain fatty acids, unsaturated fatty acids, and their eicosanoid derivatives.

Malonyl-CoA Is Formed from Acetyl-CoA and Bicarbonate

The formation of malonyl-CoA from acetyl-CoA is an irreversible process, catalyzed by **acetyl-CoA carboxylase**. The bacterial enzyme has three separate polypeptide subunits **(Fig. 21–1)**; in animal cells, all three activities are part of a single multifunctional polypeptide. Plant cells contain both types of acetyl-CoA carboxylase. In all cases, the enzyme contains a biotin prosthetic group covalently bound in amide linkage to the ε-amino group of a Lys residue in one of the three polypeptides or domains of the enzyme molecule. The two-step reaction catalyzed by this enzyme is very similar to other biotin-dependent carboxylation reactions, such as those catalyzed by pyruvate carboxylase (see Fig. 16–17) and propionyl-CoA carboxylase (see Fig. 17–12). A carboxyl group, derived from bicarbonate (HCO_3^-), is first transferred to biotin in an ATP-dependent reaction. The biotinyl group serves as a temporary carrier of CO_2, transferring it to acetyl-CoA in the second step to yield malonyl-CoA.

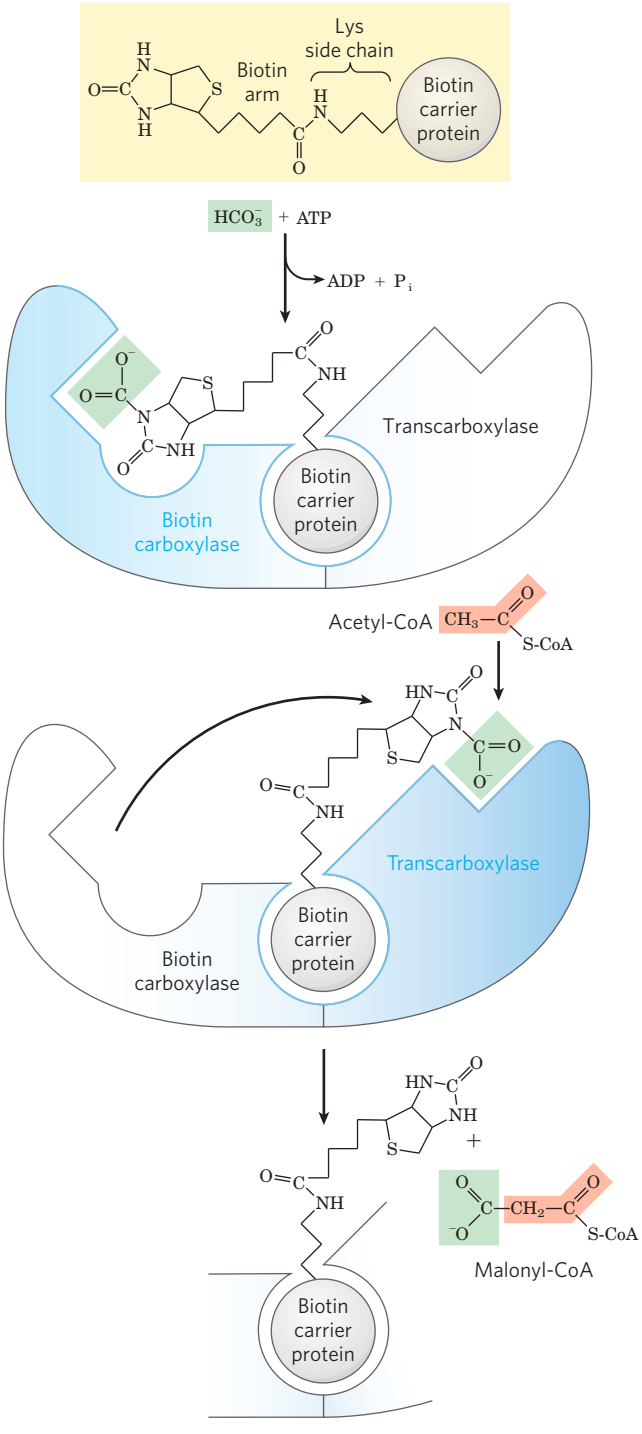

FIGURE 21–1 The acetyl-CoA carboxylase reaction. Acetyl-CoA carboxylase has three functional regions: biotin carrier protein (gray); biotin carboxylase, which activates CO_2 by attaching it to a nitrogen in the biotin ring in an ATP-dependent reaction (see Fig. 16–17); and transcarboxylase, which transfers activated CO_2 (shaded green) from biotin to acetyl-CoA, producing malonyl-CoA. The long, flexible biotin arm carries the activated CO_2 from the biotin carboxylase region to the transcarboxylase active site. The active enzyme in each step is shaded in blue.

Fatty Acid Synthesis Proceeds in a Repeating Reaction Sequence

In all organisms, the long carbon chains of fatty acids are assembled in a repeating four-step sequence **(Fig. 21–2)**, catalyzed by a system collectively referred to as **fatty acid synthase**. A saturated acyl group produced by each four-step series of reactions becomes the substrate for subsequent condensation with an activated malonyl group. With each passage through the cycle, the fatty acyl chain is extended by two carbons.

Both the electron-carrying cofactor and the activating groups in the reductive anabolic sequence differ from those in the oxidative catabolic process. Recall that in β oxidation, NAD^+ and FAD serve as electron acceptors and the activating group is the thiol (—SH) group of coenzyme A (see Fig. 17–8). By contrast, the reducing agent in the synthetic sequence is NADPH and the activating groups are two different enzyme-bound —SH groups, as described in the following section.

There are two major variants of fatty acid synthase: fatty acid synthase I (FAS I), found in vertebrates and fungi, and fatty acid synthase II (FAS II), found in plants and bacteria. The FAS I found in vertebrates consists of a single multifunctional polypeptide chain (M_r 240,000). The mammalian FAS I is the prototype. Seven active sites for different reactions lie in separate domains **(Fig. 21–3a)**. The mammalian polypeptide functions as a homodimer (M_r 480,000). The subunits appear to function independently. When all the active sites in one subunit are inactivated by mutation, fatty acid synthesis is only modestly reduced. A somewhat different FAS I is found in yeast and other fungi, and is made up of two multifunctional polypeptides that form a complex with an architecture distinct from the vertebrate systems (Fig. 21–3b). Three of the seven required active sites are found on the α subunit and four on the β subunit.

With FAS I systems, fatty acid synthesis leads to a single product, and no intermediates are released. When the chain length reaches 16 carbons, that product (palmitate, 16:0; see Table 10–1) leaves the cycle. Carbons C-16 and C-15 of the palmitate are derived from the methyl and carboxyl carbon atoms, respectively, of an acetyl-CoA used directly to prime the system at the outset **(Fig. 21–4)**; the rest of the carbon atoms in the chain are derived from acetyl-CoA via malonyl-CoA.

FAS II, in plants and bacteria, is a dissociated system; each step in the synthesis is catalyzed by a separate and freely diffusible enzyme. Intermediates are also diffusible and may be diverted into other pathways (such as lipoic acid synthesis). Unlike FAS I, FAS II generates a variety of products, including saturated fatty acids of several lengths, as well as unsaturated, branched, and hydroxy fatty acids. An FAS II system is also found in vertebrate mitochondria. The discussion to follow will focus on the mammalian FAS I.

The Mammalian Fatty Acid Synthase Has Multiple Active Sites

The multiple domains of mammalian FAS I function as distinct but linked enzymes. The active site for each

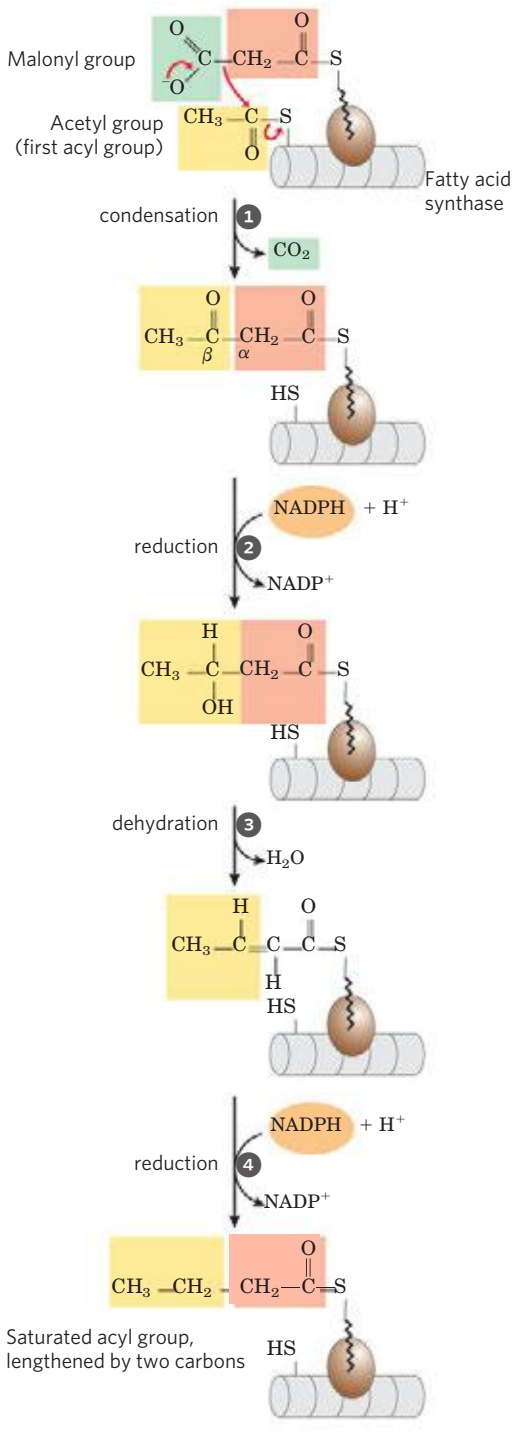

FIGURE 21–2 Addition of two carbons to a growing fatty acyl chain: a four-step sequence. Each malonyl group and acetyl (or longer acyl) group is activated by a thioester that links it to fatty acid synthase, a multienzyme system described later in the text. ❶ Condensation of an activated acyl group (an acetyl group from acetyl-CoA is the first acyl group) and two carbons derived from malonyl-CoA, with elimination of CO_2 from the malonyl group, extends the acyl chain by two carbons. The mechanism of the first step of this reaction is given to illustrate the role of decarboxylation in facilitating condensation. The β-keto product of this condensation is then reduced in three more steps nearly identical to the reactions of β oxidation, but in the reverse sequence: ❷ the β-keto group is reduced to an alcohol, ❸ elimination of H_2O creates a double bond, and ❹ the double bond is reduced to form the corresponding saturated fatty acyl group.

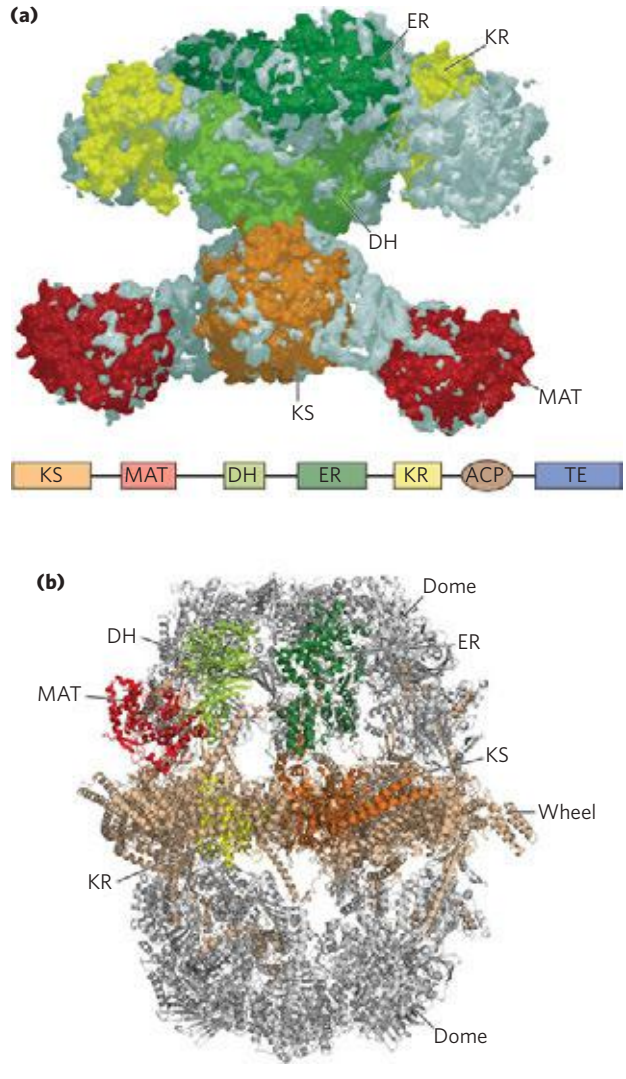

FIGURE 21–3 The structure of fatty acid synthase type I systems. Shown here are low-resolution structures of (a) the mammalian (porcine; dimer, derived from PDB ID 2CF2) and (b) fungal (derived from PDB IDs 2UV9, 2UVA, 2UVB, and 2UVC) enzyme systems. **(a)** All of the active sites in the mammalian system are located in different domains within a single large polypeptide chain. The different enzymatic activites are: β-ketoacyl-ACP synthase (KS), malonyl/acetyl-CoA–ACP transferase (MAT), β-hydroxyacyl-ACP dehydratase (DH), enoyl-ACP reductase (ER), and β-ketoacyl-ACP reductase (KR). ACP is the acyl carrier protein. The linear arrangement of the domains in the polypeptide is shown in the lower panel. The seventh domain (TE) is a thioesterase that releases the palmitate product from ACP when the synthesis is completed. The ACP and TE domains are disordered in the crystal and are therefore not shown in the structure. **(b)** In the structure of the FAS I from the fungus *Thermomyces lanuginosus*, the same active sites are divided between two multifunctional polypeptide chains that function together. Six copies of each polypeptide are found in the heterododecameric complex. A wheel of six α subunits, which include ACP as well as the KS and KR active sites, is found at the center of the complex. In the wheel, three subunits are found on one face, three on the other. On either side of the wheel are domes formed by trimers of the β subunits (containing the ER and DH active sites, as well as two domains with active sites analogous to MAT in the mammalian enzyme). The domains of one of each type of subunit are colored according to the active site colors of the mammalian enzyme in (a).

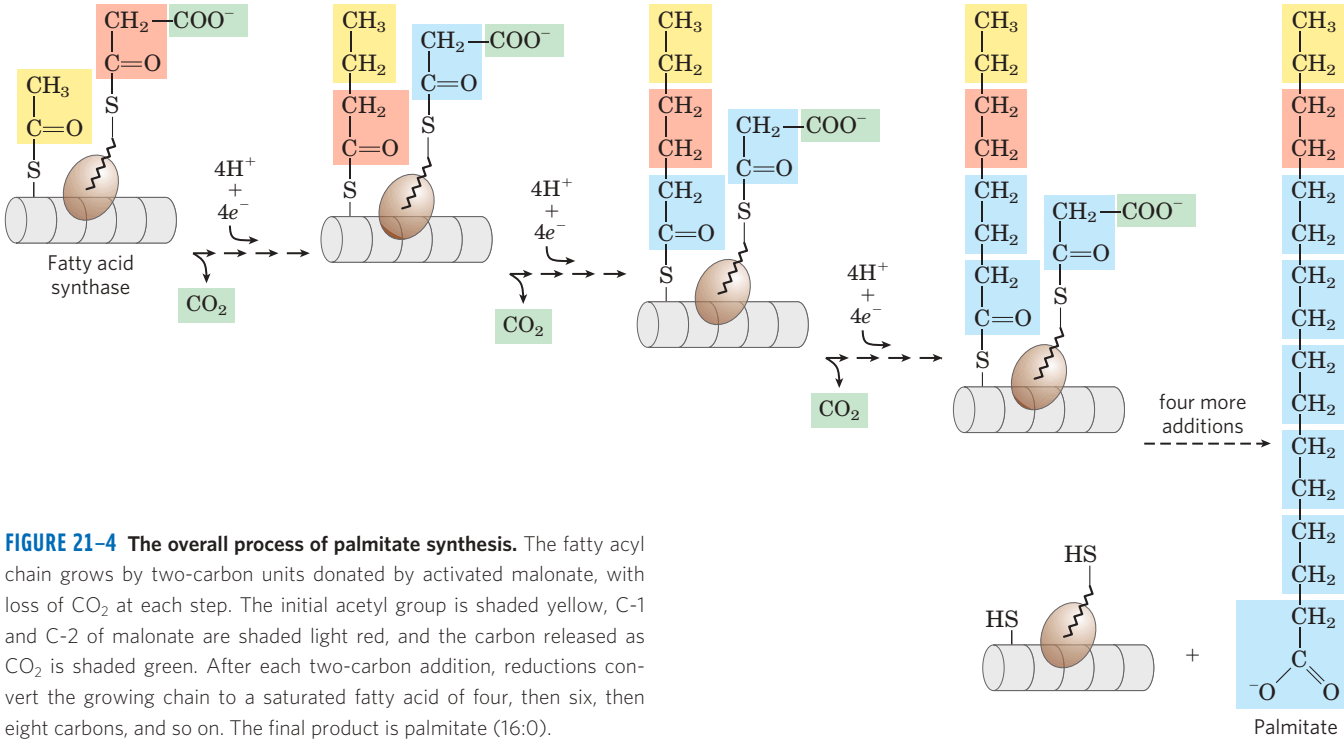

FIGURE 21–4 The overall process of palmitate synthesis. The fatty acyl chain grows by two-carbon units donated by activated malonate, with loss of CO_2 at each step. The initial acetyl group is shaded yellow, C-1 and C-2 of malonate are shaded light red, and the carbon released as CO_2 is shaded green. After each two-carbon addition, reductions convert the growing chain to a saturated fatty acid of four, then six, then eight carbons, and so on. The final product is palmitate (16:0).

enzyme is found in a separate domain within the larger polypeptide. Throughout the process of fatty acid synthesis, the intermediates remain covalently attached as thioesters to one of two thiol groups. One point of attachment is the —SH group of a Cys residue in one of the synthase domains (β-ketoacyl-ACP synthase; KS); the other is the —SH group of acyl carrier protein, a separate domain of the same polypeptide. Hydrolysis of thioesters is highly exergonic, and the energy released helps to make two different steps (❶ and ❺ in Fig. 21–6) in fatty acid synthesis (condensation) thermodynamically favorable.

Acyl carrier protein (ACP) is the shuttle that holds the system together. The *Escherichia coli* ACP is a small protein (M_r 8,860) containing the prosthetic group **4′-phosphopantetheine** (**Fig. 21–5**; compare this with the panthothenic acid and β-mercaptoethylamine moiety of coenzyme A in Fig. 8–38). The 4′-phosphopantetheine prosthetic group of *E. coli* ACP is believed to serve as a flexible arm, tethering the growing fatty acyl chain to the surface of the fatty acid synthase complex while carrying the reaction intermediates from one enzyme active site to the next. The ACP of mammals has a similar function and the same prosthetic group; as we have seen, however, it is embedded as a domain in a much larger multifunctional polypeptide.

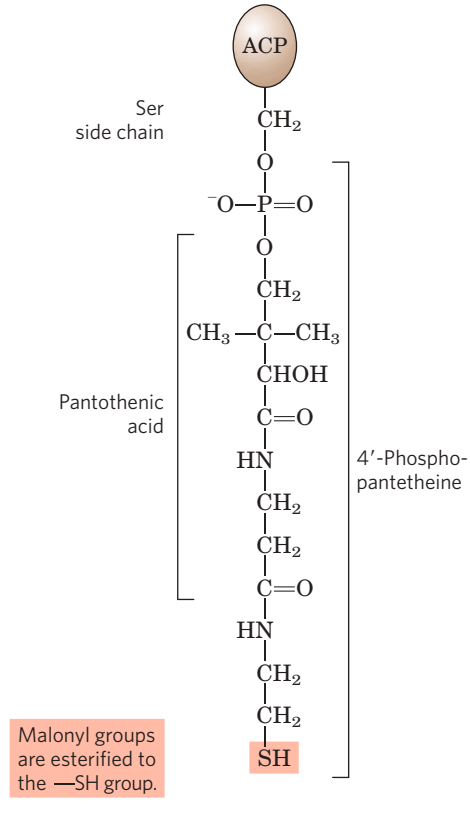

FIGURE 21–5 Acyl carrier protein (ACP). The prosthetic group is 4′-phosphopantetheine, which is covalently attached to the hydroxyl group of a Ser residue in ACP. Phosphopantetheine contains the B vitamin pantothenic acid, also found in the coenzyme A molecule. Its —SH group is the site of entry of malonyl groups during fatty acid synthesis.

Fatty Acid Synthase Receives the Acetyl and Malonyl Groups

Before the condensation reactions that build up the fatty acid chain can begin, the two thiol groups on the enzyme complex must be charged with the correct acyl groups (**Fig. 21–6**, top). First, the acetyl group of acetyl-CoA is

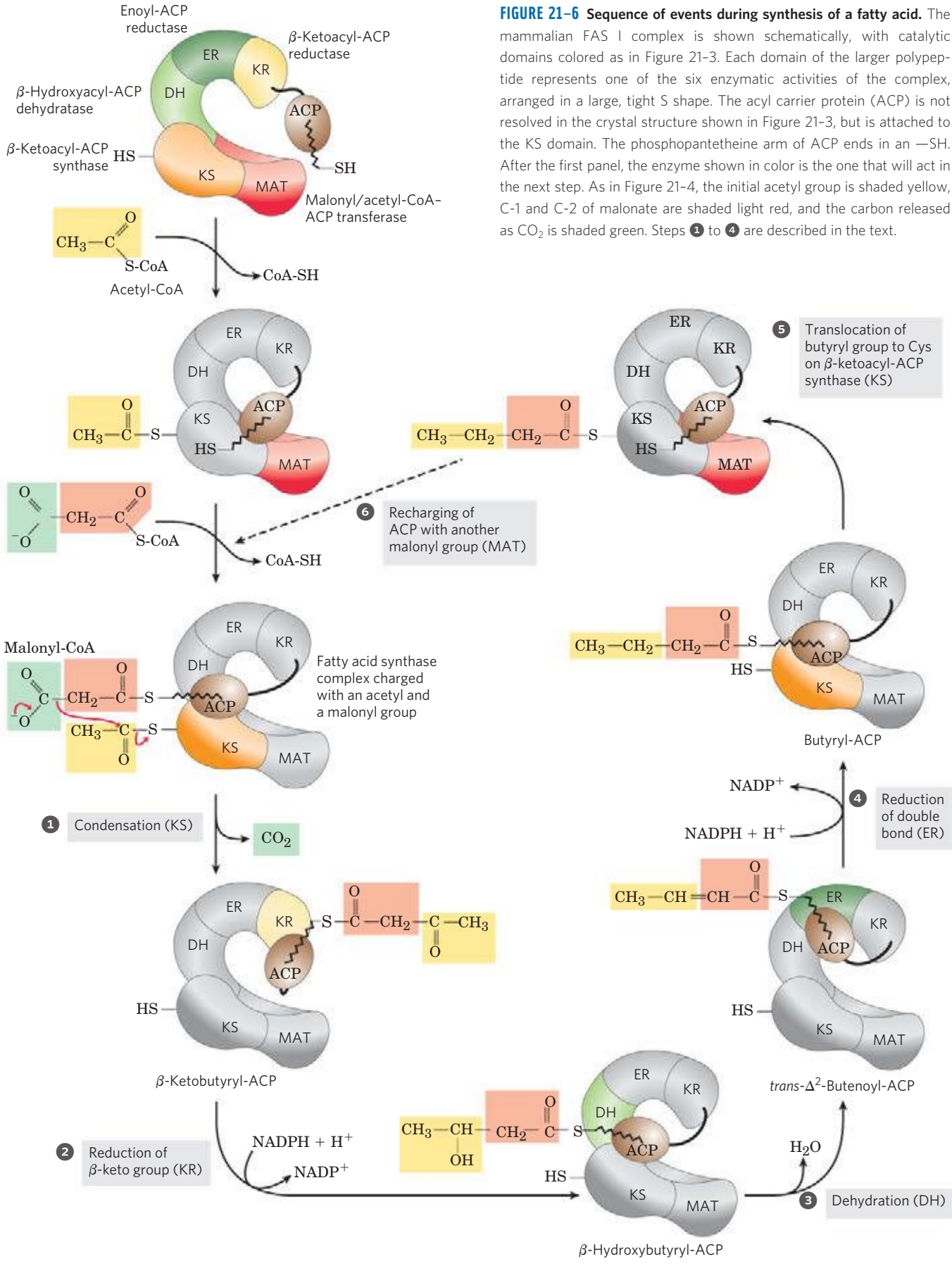

FIGURE 21–6 Sequence of events during synthesis of a fatty acid. The mammalian FAS I complex is shown schematically, with catalytic domains colored as in Figure 21–3. Each domain of the larger polypeptide represents one of the six enzymatic activities of the complex, arranged in a large, tight S shape. The acyl carrier protein (ACP) is not resolved in the crystal structure shown in Figure 21–3, but is attached to the KS domain. The phosphopantetheine arm of ACP ends in an —SH. After the first panel, the enzyme shown in color is the one that will act in the next step. As in Figure 21–4, the initial acetyl group is shaded yellow, C-1 and C-2 of malonate are shaded light red, and the carbon released as CO_2 is shaded green. Steps ❶ to ❹ are described in the text.

transferred to ACP in a reaction catalyzed by the **malonyl/acetyl-CoA–ACP transferase** (MAT in Fig. 21–6) domain of the multifunctional polypeptide. The acetyl group is then transferred to the Cys —SH group of the **β-ketoacyl-ACP synthase** (KS). The second reaction, transfer of the malonyl group from malonyl-CoA to the —SH group of ACP, is also catalyzed by malonyl/acetyl-CoA–ACP transferase. In the charged synthase complex, the acetyl and malonyl groups are activated for the chain-lengthening process. The first four steps of this process are now considered in some detail; all step numbers refer to Figure 21–6.

Step ❶ Condensation The first reaction in the formation of a fatty acid chain is a formal Claisen condensation involving the activated acetyl and malonyl groups to form **acetoacetyl-ACP**, an acetoacetyl group bound to ACP through the phosphopantetheine —SH group; simultaneously, a molecule of CO_2 is produced. In this reaction, catalyzed by β-ketoacyl-ACP synthase, the acetyl group is transferred from the Cys —SH group of the enzyme to the malonyl group on the —SH of ACP, becoming the methyl-terminal two-carbon unit of the new acetoacetyl group.

The carbon atom of the CO_2 formed in this reaction is the same carbon originally introduced into malonyl CoA from HCO_3^- by the acetyl-CoA carboxylase reaction (Fig. 21–1). Thus CO_2 is only transiently in covalent linkage during fatty acid biosynthesis; it is removed as each two-carbon unit is added.

Why do cells go to the trouble of adding CO_2 to make a malonyl group from an acetyl group, only to lose the CO_2 during the formation of acetoacetate? The use of activated malonyl groups rather than acetyl groups is what makes the condensation reactions thermodynamically favorable. The methylene carbon (C-2) of the malonyl group, sandwiched between carbonyl and carboxyl carbons, forms a good nucleophile. In the condensation step (step ❶), decarboxylation of the malonyl group facilitates the nucleophilic attack of the methylene carbon on the thioester linking the acetyl group to β-ketoacyl-ACP synthase, displacing the enzyme's —SH group. (This is a classic Claisen ester condensation; see Fig. 13–4.) Coupling the condensation to the decarboxylation of the malonyl group renders the overall process highly exergonic. A similar carboxylation-decarboxylation sequence facilitates the formation of phosphoenolpyruvate from pyruvate in gluconeogenesis (see Fig. 14–18).

By using activated malonyl groups in the synthesis of fatty acids and activated acetate in their degradation, the cell makes both processes energetically favorable, although one is effectively the reversal of the other. The extra energy required to make fatty acid synthesis favorable is provided by the ATP used to synthesize malonyl-CoA from acetyl-CoA and HCO_3^- (Fig. 21–1).

Step ❷ Reduction of the Carbonyl Group The acetoacetyl-ACP formed in the condensation step now undergoes reduction of the carbonyl group at C-3 to form D-β-hydroxybutyryl-ACP. This reaction is catalyzed by **β-ketoacyl-ACP reductase** (KR) and the electron donor is NADPH. Notice that the D-β-hydroxybutyryl group does not have the same stereoisomeric form as the L-β-hydroxyacyl intermediate in fatty acid oxidation (see Fig. 17–8).

Step ❸ Dehydration The elements of water are now removed from C-2 and C-3 of D-β-hydroxybutyryl-ACP to yield a double bond in the product, ***trans*-Δ²-butenoyl-ACP**. The enzyme that catalyzes this dehydration is **β-hydroxyacyl-ACP dehydratase** (DH).

Step ❹ Reduction of the Double Bond Finally, the double bond of *trans*-Δ²-butenoyl-ACP is reduced (saturated) to form **butyryl-ACP** by the action of **enoyl-ACP reductase** (ER); again, NADPH is the electron donor.

The Fatty Acid Synthase Reactions Are Repeated to Form Palmitate

Production of the four-carbon, saturated fatty acyl–ACP marks completion of one pass through the fatty acid synthase complex. In step ❺, the butyryl group is transferred from the phosphopantetheine —SH group of ACP to the Cys —SH group of β-ketoacyl-ACP synthase, which initially bore the acetyl group (Fig. 21–6). To start the next cycle of four reactions that lengthens the chain by two more carbons (step ❻), another malonyl group is linked to the now unoccupied phosphopantetheine —SH group of ACP **(Fig. 21–7)**. Condensation occurs as the butyryl group, acting like the acetyl group in the first cycle, is linked to two carbons of the malonyl-ACP group with concurrent loss of CO_2. The product of this condensation is a six-carbon acyl group, covalently bound to the phosphopantetheine —SH group. Its β-keto group is reduced in the next three steps of the synthase cycle to yield the saturated acyl group, exactly as in the first round of reactions—in this case forming the six-carbon product.

Seven cycles of condensation and reduction produce the 16-carbon saturated palmitoyl group, still bound to ACP. For reasons not well understood, chain elongation by the synthase complex generally stops at this point and free palmitate is released from the ACP by a hydrolytic activity (thioesterase; TE) in the multifunctional protein.

We can consider the overall reaction for the synthesis of palmitate from acetyl-CoA in two parts. First, the formation of seven malonyl-CoA molecules:

$$7\ \text{Acetyl-CoA} + 7CO_2 + 7\text{ATP} \longrightarrow 7\ \text{malonyl-CoA} + 7\text{ADP} + 7P_i \quad (21\text{–}1)$$

then seven cycles of condensation and reduction:

$$\text{Acetyl-CoA} + 7\ \text{malonyl-CoA} + 14\text{NADPH} + 14H^+ \longrightarrow \text{palmitate} + 7CO_2 + 8\ \text{CoA} + 14\text{NADP}^+ + 6H_2O \quad (21\text{–}2)$$

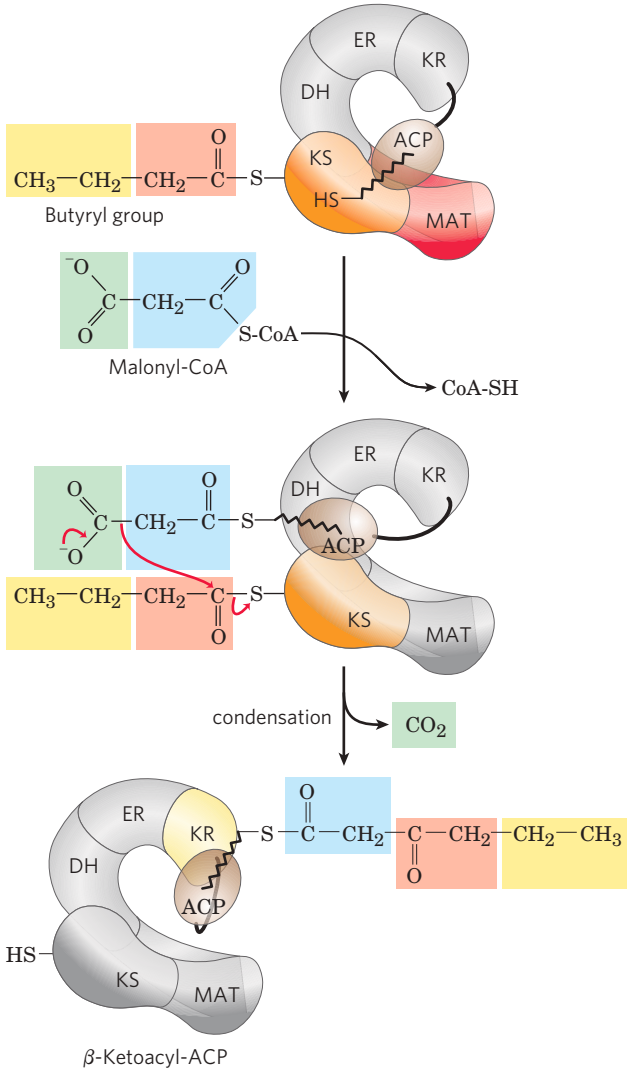

FIGURE 21–7 Beginning of the second round of the fatty acid synthesis cycle. The butyryl group is on the Cys —SH group. The incoming malonyl group is first attached to the phosphopantetheine —SH group. Then, in the condensation step, the entire butyryl group on the Cys —SH is exchanged for the carboxyl group of the malonyl residue, which is lost as CO_2 (green). This step is analogous to step ❶ in Figure 21-6. The product, a six-carbon β-ketoacyl group, now contains four carbons derived from malonyl-CoA and two derived from the acetyl-CoA that started the reaction. The β-ketoacyl group then undergoes steps ❷ through ❹, as in Figure 21-6.

Note that only six net water molecules are produced, because one is used to hydrolyze the thioester linking the palmitate product to the enzyme. The overall process (the sum of Eqns 21–1 and 21–2) is

$$8\ \text{Acetyl-CoA} + 7\ \text{ATP} + 14\text{NADPH} + 14\text{H}^+ \longrightarrow \text{palmitate} + 8\ \text{CoA} + 7\text{ADP} + 7\text{P}_i + 14\text{NADP}^+ + 6\text{H}_2\text{O} \quad (21\text{–}3)$$

The biosynthesis of fatty acids such as palmitate thus requires acetyl-CoA and the input of chemical energy in two forms: the group transfer potential of ATP and the reducing power of NADPH. The ATP is required to attach CO_2 to acetyl-CoA to make malonyl-CoA; the NADPH molecules are required to reduce the β-keto group and the double bond.

In nonphotosynthetic eukaryotes there is an additional cost to fatty acid synthesis, because acetyl-CoA is generated in the mitochondria and must be transported to the cytosol. As we will see, this extra step consumes two ATP per molecule of acetyl-CoA transported, increasing the energetic cost of fatty acid synthesis to three ATP per two-carbon unit.

Fatty Acid Synthesis Occurs in the Cytosol of Many Organisms but in the Chloroplasts of Plants

In most higher eukaryotes the fatty acid synthase complex is found exclusively in the cytosol **(Fig. 21–8)**, as are the biosynthetic enzymes for nucleotides, amino acids, and glucose. This location segregates synthetic processes from degradative reactions, many of which take place in the mitochondrial matrix. There is a corresponding segregation of the electron-carrying cofactors used in anabolism (generally a reductive process) and those used in catabolism (generally oxidative).

Usually, NADPH is the electron carrier for anabolic reactions, and NAD^+ serves in catabolic reactions. In hepatocytes, the [NADPH]/[$NADP^+$] ratio is very high (about 75) in the cytosol, furnishing a strongly reducing environment for the reductive synthesis of fatty acids and other biomolecules. The cytosolic [NADH]/[NAD^+] ratio is much smaller (only about 8×10^{-4}), so the NAD^+-dependent oxidative catabolism of glucose can take place in the same compartment, and at the same time, as fatty acid synthesis. The [NADH]/[NAD^+] ratio in the mitochondrion is much higher than in the cytosol, because of the flow of electrons to NAD^+ from the oxidation of fatty acids, amino acids, pyruvate, and acetyl-CoA. This high mitochondrial [NADH]/[NAD^+] ratio favors the reduction of oxygen via the respiratory chain.

In hepatocytes and adipocytes, cytosolic NADPH is largely generated by the pentose phosphate pathway (see Fig. 14–22) and by **malic enzyme (Fig. 21–9a)**. The NADP-linked malic enzyme that operates in the carbon-assimilation pathway of C_4 plants (see Fig. 20–23) is unrelated in function. The pyruvate produced in the reaction shown in Figure 21–9a reenters the mitochondrion. In hepatocytes and in the mammary gland of lactating animals, the NADPH required for fatty acid biosynthesis is supplied primarily by the pentose phosphate pathway (Fig. 21–9b).

In the photosynthetic cells of plants, fatty acid synthesis occurs not in the cytosol but in the chloroplast stroma (Fig. 21–8). This makes sense, given that NADPH is produced in chloroplasts by the light-dependent reactions of photosynthesis:

$$\text{H}_2\text{O} + \text{NADP}^+ \xrightarrow{\text{light}} \tfrac{1}{2}\text{O}_2 + \text{NADPH} + \text{H}^+$$

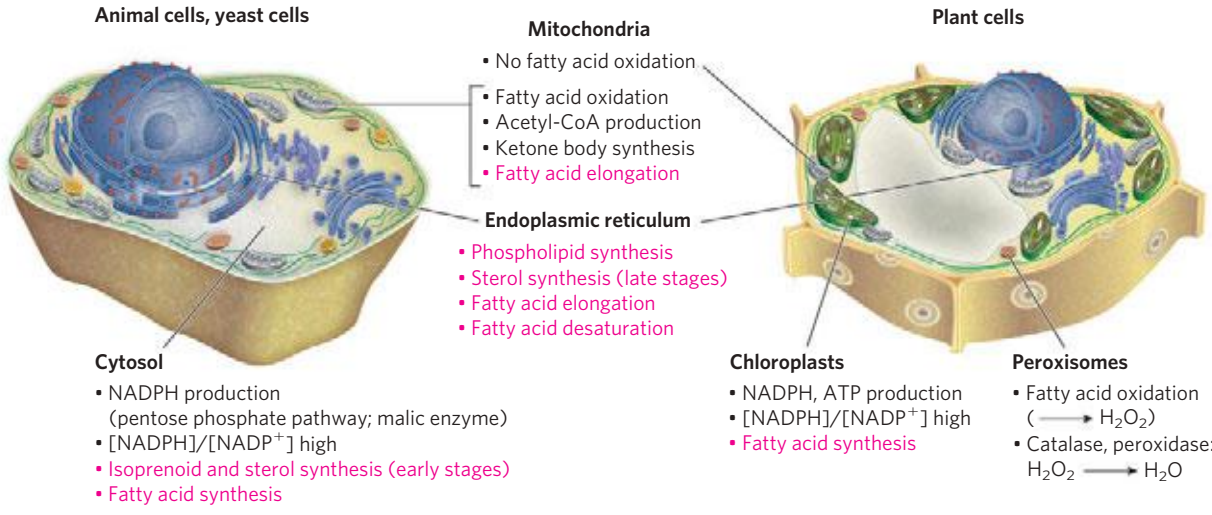

FIGURE 21–8 Subcellular localization of lipid metabolism. Yeast and vertebrate cells differ from higher plant cells in the compartmentation of lipid metabolism. Fatty acid synthesis takes place in the compartment in which NADPH is available for reductive synthesis (i.e., where the [NADPH]/[NADP+] ratio is high); this is the cytosol in animals and yeast, and the chloroplast in plants. Processes in red type are covered in this chapter.

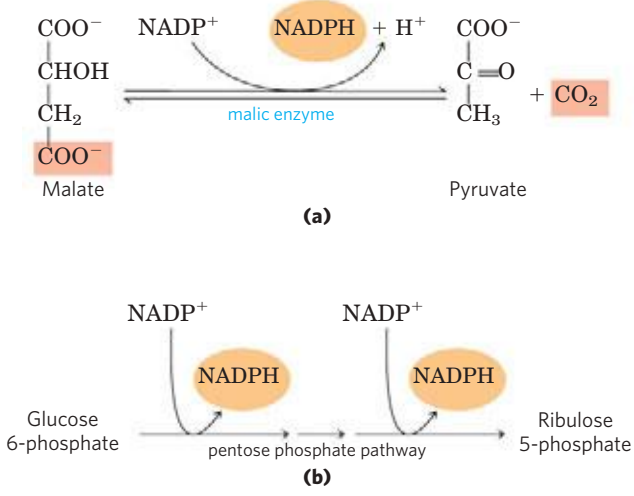

FIGURE 21–9 Production of NADPH. Two routes to NADPH, catalyzed by **(a)** malic enzyme and **(b)** the pentose phosphate pathway.

Acetate Is Shuttled out of Mitochondria as Citrate

In nonphotosynthetic eukaryotes, nearly all the acetyl-CoA used in fatty acid synthesis is formed in mitochondria from pyruvate oxidation and from the catabolism of the carbon skeletons of amino acids. Acetyl-CoA arising from the oxidation of fatty acids is not a significant source of acetyl-CoA for fatty acid biosynthesis in animals, because the two pathways are reciprocally regulated, as described below.

The mitochondrial inner membrane is impermeable to acetyl-CoA, so an indirect shuttle transfers acetyl group equivalents across the inner membrane **(Fig. 21–10)**. Intramitochondrial acetyl-CoA first reacts with oxaloacetate to form citrate, in the citric acid cycle reaction catalyzed by **citrate synthase** (see Fig. 16–7). Citrate then passes through the inner membrane on the **citrate transporter**. In the cytosol, citrate cleavage by **citrate lyase** regenerates acetyl-CoA and oxaloacetate in an ATP-dependent reaction. Oxaloacetate cannot return to the mitochondrial matrix directly, as there is no oxaloacetate transporter. Instead, cytosolic malate dehydrogenase reduces the oxaloacetate to malate, which can return to the mitochondrial matrix on the malate–α-ketoglutarate transporter in exchange for citrate. In the matrix, malate is reoxidized to oxaloacetate to complete the shuttle. However, most of the malate produced in the cytosol is used to generate cytosolic NADPH through the activity of malic enzyme (Fig. 21–9a). The pyruvate produced is transported to the mitochondria by the pyruvate transporter (Fig. 21–10), and converted back into oxaloacetate by pyruvate carboxylase in the matrix. The resulting cycle results in the consumption of two ATP (by citrate lyase and pyruvate carboxylase) for every molecule of acetyl-CoA delivered to fatty acid synthesis. After citrate cleavage to generate acetyl-CoA, conversion of the four remaining carbons to pyruvate and CO_2 via malic enzyme generates about half the NADPH required for fatty acid synthesis. The pentose phosphate pathway contributes the rest of the needed NADPH.

Fatty Acid Biosynthesis Is Tightly Regulated

When a cell or organism has more than enough metabolic fuel to meet its energy needs, the excess is generally converted to fatty acids and stored as lipids such as triacylglycerols. The reaction catalyzed by acetyl-CoA

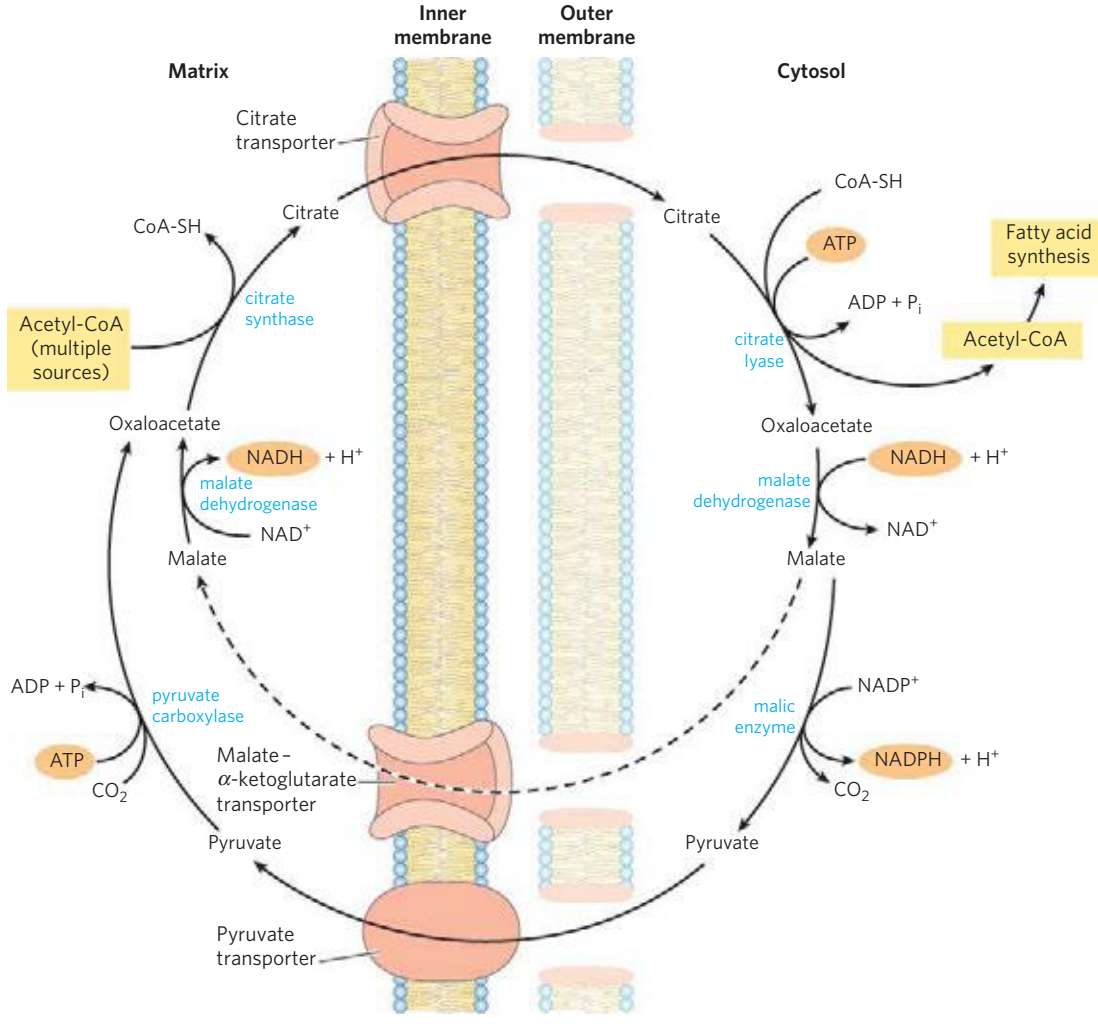

FIGURE 21–10 Shuttle for transfer of acetyl groups from mitochondria to the cytosol. The outer mitochondrial membrane is freely permeable to all these compounds. Pyruvate derived from amino acid catabolism in the mitochondrial matrix, or from glucose by glycolysis in the cytosol, is converted to acetyl-CoA in the matrix. Acetyl groups pass out of the mitochondrion as citrate; in the cytosol they are delivered as acetyl-CoA for fatty acid synthesis. Oxaloacetate is reduced to malate, which can return to the mitochondrial matrix and is converted to oxaloacetate. The major fate for cytosolic malate is oxidation by malic enzyme to generate cytosolic NADPH; the pyruvate produced returns to the mitochondrial matrix.

carboxylase is the rate-limiting step in the biosynthesis of fatty acids, and this enzyme is an important site of regulation. In vertebrates, palmitoyl-CoA, the principal product of fatty acid synthesis, is a feedback inhibitor of the enzyme; citrate is an allosteric activator **(Fig. 21–11a)**, increasing V_{max}. Citrate plays a central role in diverting cellular metabolism from the consumption (oxidation) of metabolic fuel to the storage of fuel as fatty acids. When the concentrations of mitochondrial acetyl-CoA and ATP increase, citrate is transported out of mitochondria; it then becomes both the precursor of cytosolic acetyl-CoA and an allosteric signal for the activation of acetyl-CoA carboxylase. At the same time, citrate inhibits the activity of phosphofructokinase-1 (see Fig. 15–16), reducing the flow of carbon through glycolysis.

Acetyl-CoA carboxylase is also regulated by covalent modification. Phosphorylation, triggered by the hormones glucagon and epinephrine, inactivates the enzyme and reduces its sensitivity to activation by citrate, thereby slowing fatty acid synthesis. In its active (dephosphorylated) form, acetyl-CoA carboxylase polymerizes into long filaments (Fig. 21–11b); phosphorylation is accompanied by dissociation into monomeric subunits and loss of activity.

The acetyl-CoA carboxylase of plants and bacteria is not regulated by citrate or by a phosphorylation-dephosphorylation cycle. The plant enzyme is activated by an increase in stromal pH and $[Mg^{2+}]$, which occurs on illumination of the plant (see Fig. 20–17). Bacteria do not use triacylglycerols as energy stores. In *E. coli*, the primary role of fatty acid synthesis is to provide precursors for membrane lipids; the regulation of this process is complex, involving guanine nucleotides (such as ppGpp) that coordinate cell growth with membrane formation (see Figs 8–39, 28–22).

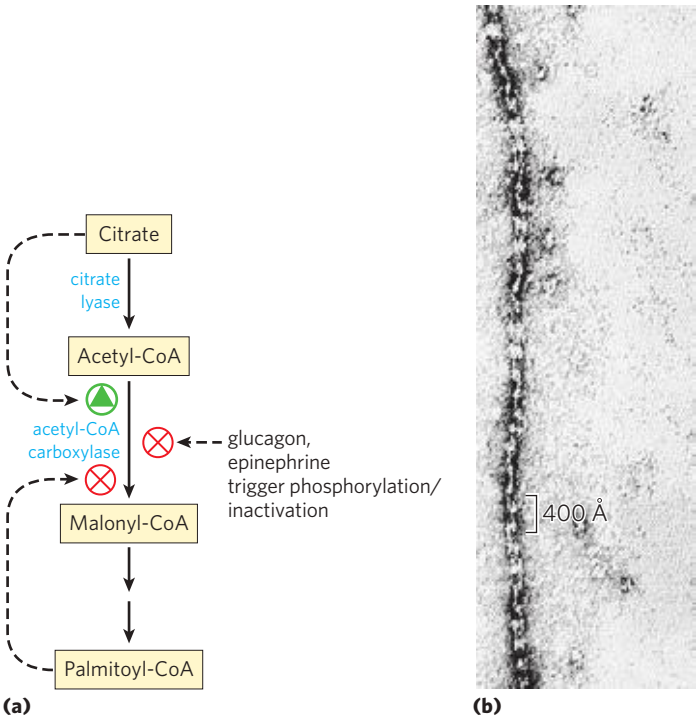

FIGURE 21–11 Regulation of fatty acid synthesis. (a) In the cells of vertebrates, both allosteric regulation and hormone-dependent covalent modification influence the flow of precursors into malonyl-CoA. In plants, acetyl-CoA carboxylase is activated by the changes in $[Mg^{2+}]$ and pH that accompany illumination (not shown here). **(b)** Filaments of acetyl-CoA carboxylase from chicken hepatocytes (the active, dephosphorylated form) as seen with the electron microscope.

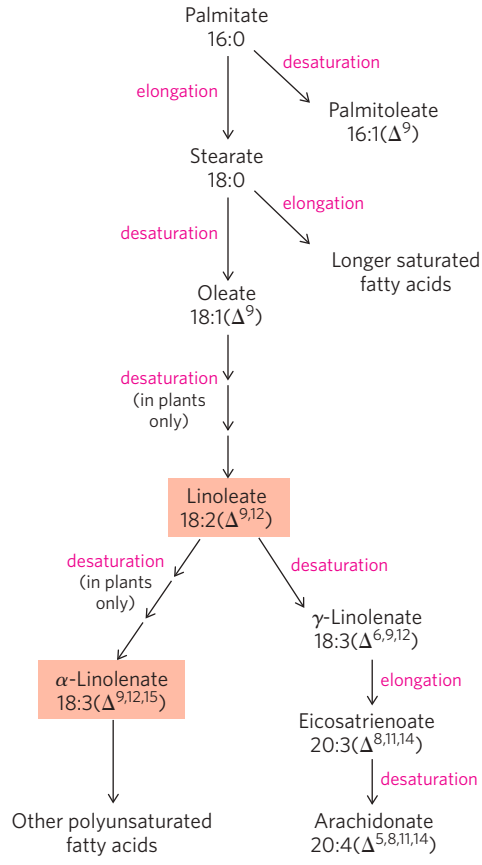

FIGURE 21–12 Routes of synthesis of other fatty acids. Palmitate is the precursor of stearate and longer-chain saturated fatty acids, as well as the monounsaturated acids palmitoleate and oleate. Mammals cannot convert oleate to linoleate or α-linolenate (shaded light red), which are therefore required in the diet as essential fatty acids. Conversion of linoleate to other polyunsaturated fatty acids and eicosanoids is outlined. Unsaturated fatty acids are symbolized by indicating the number of carbons and the number and position of the double bonds, as in Table 10–1.

In addition to the moment-by-moment regulation of enzymatic activity, these pathways are regulated at the level of gene expression. For example, when animals ingest an excess of certain polyunsaturated fatty acids, the expression of genes encoding a wide range of lipogenic enzymes in the liver is suppressed. This gene regulation is mediated by a family of nuclear receptor proteins called PPARs, which are described in more detail in Chapter 23 (see Fig. 23–42).

If fatty acid synthesis and β oxidation were to proceed simultaneously, the two processes would constitute a futile cycle, wasting energy. We noted earlier (see Fig. 17–13) that β oxidation is blocked by malonyl-CoA, which inhibits carnitine acyltransferase I. Thus during fatty acid synthesis, the production of the first intermediate, malonyl-CoA, shuts down β oxidation at the level of a transport system in the mitochondrial inner membrane. This control mechanism illustrates another advantage of segregating synthetic and degradative pathways in different cellular compartments.

Long-Chain Saturated Fatty Acids Are Synthesized from Palmitate

Palmitate, the principal product of the fatty acid synthase system in animal cells, is the precursor of other long-chain fatty acids **(Fig. 21–12)**. It may be lengthened to form stearate (18:0) or even longer saturated fatty acids by further additions of acetyl groups, through the action of **fatty acid elongation systems** present in the smooth endoplasmic reticulum and in mitochondria. The more active elongation system of the ER extends the 16-carbon chain of palmitoyl-CoA by two carbons, forming stearoyl-CoA. Although different enzyme systems are involved, and coenzyme A rather than ACP is the acyl carrier in the reaction, the mechanism of elongation in the ER is otherwise identical to that in palmitate synthesis: donation of two carbons by malonyl-CoA, followed by reduction, dehydration, and reduction to the saturated 18-carbon product, stearoyl-CoA.

Desaturation of Fatty Acids Requires a Mixed-Function Oxidase

Palmitate and stearate serve as precursors of the two most common monounsaturated fatty acids of animal tissues: palmitoleate, 16:1(Δ^9), and oleate, 18:1(Δ^9); both of these fatty acids have a single cis double bond

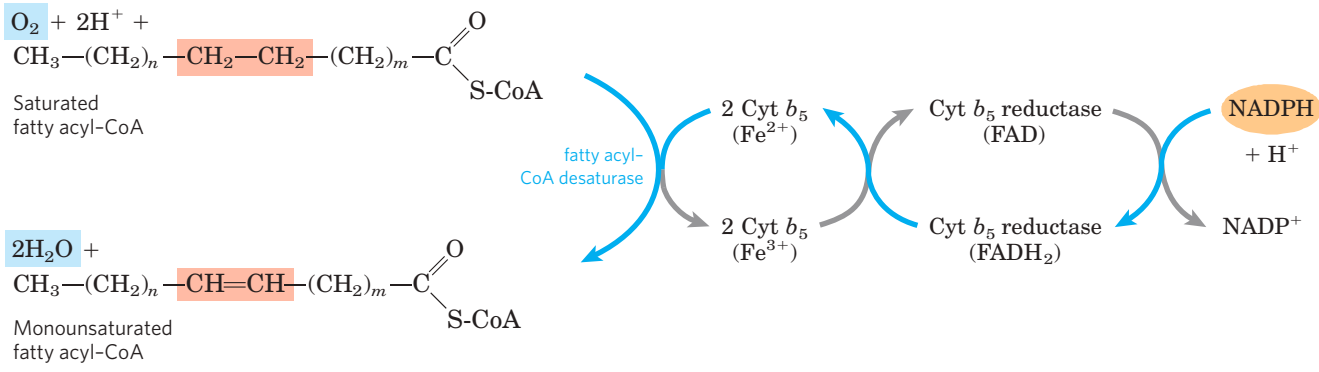

FIGURE 21–13 Electron transfer in the desaturation of fatty acids in vertebrates. Blue arrows show the path of electrons as two substrates—a fatty acyl-CoA and NADPH—undergo oxidation by molecular oxygen. These reactions take place on the lumenal face of the smooth ER. A similar pathway, but with different electron carriers, occurs in plants.

between C-9 and C-10 (see Table 10–1). The double bond is introduced into the fatty acid chain by an oxidative reaction catalyzed by **fatty acyl–CoA desaturase (Fig. 21–13)**, a **mixed-function oxidase** (Box 21–1). Two different substrates, the fatty acid and NADPH, simultaneously undergo two-electron oxidations. The path of electron flow includes a cytochrome (cytochrome b_5) and a flavoprotein (cytochrome b_5 reductase), both of which, like fatty acyl–CoA desaturase, are in the smooth ER. In plants, oleate ($18{:}1(\Delta^9)$) is produced by a **stearoyl-ACP desaturase (SCD)** that uses reduced ferredoxin as the electron donor in the chloroplast stroma.

The SCD of animals (mice) has an important role in the development of obesity and the insulin resistance that often accompanies obesity and precedes development of type 2 diabetes mellitus. Mice have four isozymes, SCD1 through SCD4, of which SCD1 is the best understood. Its synthesis is induced by dietary saturated fatty acids, and also by the action of SREBP and LXR, two protein regulators of lipid metabolism that activate transcription of lipid-synthesizing enzymes (described in Section 21.4). Mice with mutant forms of SCD1 are resistant to diet-induced obesity, and do not develop diabetes under conditions that cause both obesity and diabetes in mice with normal SCD1.

Mammalian hepatocytes can readily introduce double bonds at the Δ^9 position of fatty acids but cannot introduce additional double bonds between C-10 and the methyl-terminal end. Thus mammals cannot synthesize linoleate, $18{:}2(\Delta^{9,12})$, or α-linolenate, $18{:}3(\Delta^{9,12,15})$. Plants, however, can synthesize both; the desaturases that introduce double bonds at the Δ^{12} and Δ^{15} positions are located in the ER and the chloroplast. The ER enzymes act not on free fatty acids but on a phospholipid, phosphatidylcholine, that contains at least one oleate linked to the glycerol **(Fig. 21–14)**. Both plants and bacteria must synthesize polyunsaturated fatty acids to ensure membrane fluidity at reduced temperatures.

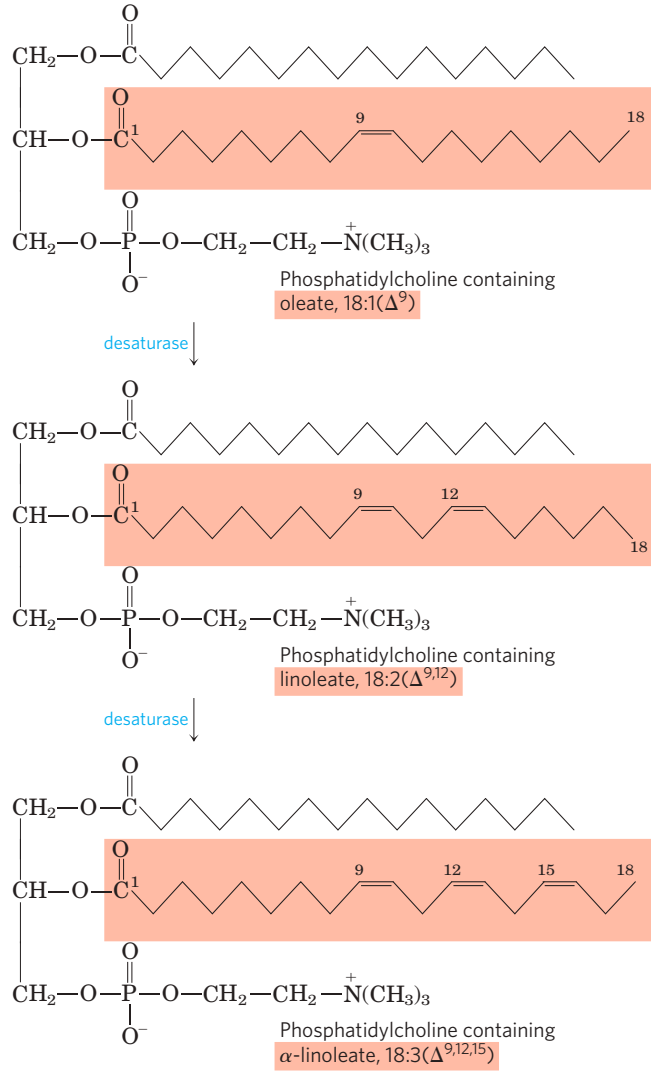

FIGURE 21–14 Action of plant desaturases. Desaturases in plants oxidize phosphatidylcholine-bound oleate to polyunsaturated fatty acids. Some of the products are released from the phosphatidylcholine by hydrolysis.

BOX 21–1 MEDICINE Mixed-Function Oxidases, Cytochrome P-450 Enzymes, and Drug Overdoses

In this chapter we encounter several enzymes that carry out oxidation-reduction reactions in which molecular oxygen is a participant. The stearoyl-CoA desaturase (SCD) that introduces a double bond into a fatty acyl chain (see Fig. 21–13) is one such enzyme.

The nomenclature for enzymes that catalyze reactions of this general type is often confusing to students. **Oxidase** is the general name for enzymes that catalyze oxidations in which molecular oxygen is the electron acceptor but oxygen atoms do not appear in the oxidized product. The enzyme that creates a double bond in fatty acyl–CoA during the oxidation of fatty acids in peroxisomes (see Fig. 17–14) is an oxidase of this type; a second example is the cytochrome oxidase of the mitochondrial electron-transfer chain (see Fig. 19–14). In the first case, the transfer of two electrons to H_2O produces hydrogen peroxide, H_2O_2; in the second, two electrons reduce $\frac{1}{2}O_2$ to H_2O. Many, but not all, oxidases are flavoproteins.

Oxygenases catalyze oxidative reactions in which oxygen atoms *are* directly incorporated into the product molecule, forming a new hydroxyl or carboxyl group, for example. **Dioxygenases** catalyze reactions in which both oxygen atoms of O_2 are incorporated into the organic product. An example of a dioxygenase is tryptophan 2,3-dioxygenase, which catalyzes the opening of the five-membered ring of tryptophan in the catabolism of this amino acid. When this reaction takes place in the presence of $^{18}O_2$, the isotopic oxygen atoms are found in the two carbonyl groups of the product (shown in red):

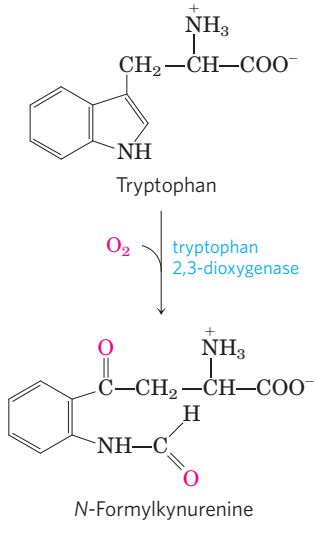

Monooxygenases, more common and more complex in their action, catalyze reactions in which only one of the two oxygen atoms of O_2 is incorporated into the organic product, the other being reduced to H_2O. Monooxygenases require two substrates to serve as reductants of the two oxygen atoms of O_2. The main substrate accepts one of the two oxygen atoms, and a cosubstrate furnishes hydrogen atoms to reduce the other oxygen atom to H_2O. The general reaction equation for monooxygenases is

$$AH + BH_2 + O{-}O \longrightarrow A{-}OH + B + H_2O$$

where AH is the main substrate and BH_2 the cosubstrate. Because most monooxygenases catalyze reactions in which the main substrate becomes hydroxylated, they are also called **hydroxylases**. They are also sometimes called **mixed-function oxidases** or **mixed-function oxygenases**, to indicate that they oxidize two different substrates simultaneously. (Note here the use of "oxidase," which violates the general definition given above).

There are different classes of monooxygenases, depending on the nature of the cosubstrate. Some use reduced flavin nucleotides ($FMNH_2$ or $FADH_2$), others use NADH or NADPH, and still others use α-ketoglutarate as the cosubstrate. The enzyme that hydroxylates the phenyl ring of phenylalanine to form tyrosine is a monooxygenase for which tetrahydrobiopterin serves as cosubstrate (see Fig. 18–23). (This is the enzyme that is defective in the human genetic disease phenylketonuria.)

The most numerous and most complex monooxygenation reactions are those employing a type of heme protein called **cytochrome P-450**. Like mitochondrial cytochrome oxidase, enzymes containing a cytochrome P-450 domain can react with O_2 and bind carbon monoxide, but they can be differentiated from cytochrome oxidase because the carbon monoxide complex of their reduced form absorbs light strongly at 450 nm—thus the name P-450.

Cytochrome P-450 enzymes catalyze hydroxylation reactions in which an organic substrate, RH, is hydroxylated to R—OH, incorporating one oxygen atom of O_2; the other oxygen atom is reduced to H_2O by reducing equivalents that are furnished by NADH or NADPH but are usually passed to cytochrome P-450 by an iron-sulfur protein. Figure 1 shows a simplified outline of the action of cytochrome P-450.

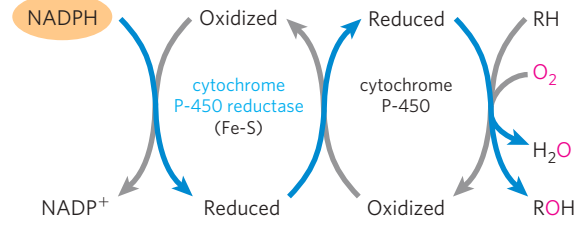

FIGURE 1

There is a large family of P-450–containing proteins of two general types: those highly specific for a single substrate (like typical enzymes) and those with more promiscuous binding sites that accept a variety of substrates, generally similar in being hydrophobic. In the adrenal cortex, for example, a specific cytochrome P-450 participates in the hydroxylation of steroids to yield the adrenocortical hormones (see Fig. 21–49). There are dozens of P-450 enzymes that act on very specific substrates in the biosynthetic pathways to steroid hormones and eicosanoids. Cytochrome P-450 enzymes with broader specificity are important in the hydroxylation of many different drugs, such as barbiturates and other xenobiotics (substances foreign to the organism), particularly if they are hydrophobic and relatively insoluble. The environmental carcinogen benzo[*a*]pyrene (found in cigarette smoke) undergoes cytochrome P-450–dependent hydroxylation during detoxification. Hydroxylation of xenobiotics, sometimes combined with the attachment of a polar compound such as glucuronic acid to the hydroxyl group, makes them more soluble in water and allows their excretion in the urine. Hydroxylation (and glucuronidation) inactivates most drugs, and the rate at which it occurs can determine how long a given dose of a drug remains in the blood at therapeutic levels. Humans differ in their levels of drug-metabolizing enzymes, both because of their genetics and because past exposure to substrates can induce the synthesis of higher levels of P-450 enzymes in a given individual. Both ethanol and barbiturate drugs share a P-450 enzyme. Long-term heavy drinking induces synthesis of that P-450 enzyme. Then, because the barbiturate is inactivated and cleared faster, larger doses of the drug are required to get the same therapeutic effect. If an individual takes this larger-than-usual dose of barbiturate and then also drinks alcohol, competition between the alcohol and the barbiturate for the limited amount of enzyme means that both alcohol and barbiturate are cleared more slowly. The resulting high levels of these two central nervous system depressants can be lethal. Similar complications arise when an individual takes two drugs that happen to be inactivated by the same P-450 enzyme; each drug increases the effective dose of the other by slowing its inactivation. It is therefore essential for physicians and pharmacists to know about all of a patient's prescribed and over-the-counter drugs and supplements (as well as a history of heavy drinking, or smoking, or exposure to environmental toxins).

Reactions described in this chapter that are catalyzed by mixed-function oxidases are those involved in fatty acyl–CoA desaturation (Fig. 21–13), leukotriene synthesis (Fig. 21–16), plasmalogen synthesis (Fig. 21–30), conversion of squalene to cholesterol (Fig. 21–37), and steroid hormone synthesis (Fig. 21–49).

Because they are necessary precursors for the synthesis of other products, linoleate and α-linolenate are **essential fatty acids** for mammals; they must be obtained from dietary plant material. Once ingested, linoleate may be converted to certain other polyunsaturated acids, particularly γ-linolenate, eicosatrienoate, and arachidonate (eicosatetraenoate), all of which can be made only from linoleate (Fig. 21–12). Arachidonate, $20{:}4(\Delta^{5,8,11,14})$, is an essential precursor of regulatory lipids, the eicosanoids. The 20-carbon fatty acids are synthesized from linoleate (and α-linolenate) by fatty acid elongation reactions analogous to those described on page 842.

Eicosanoids Are Formed from 20-Carbon Polyunsaturated Fatty Acids

Eicosanoids are a family of very potent biological signaling molecules that act as short-range messengers, affecting tissues near the cells that produce them. In response to hormonal or other stimuli, phospholipase A_2, present in most types of mammalian cells, attacks membrane phospholipids, releasing arachidonate from the middle carbon of glycerol. Enzymes of the smooth ER then convert arachidonate to **prostaglandins**, beginning with the formation of prostaglandin H_2 (PGH_2), the immediate precursor of many other prostaglandins and of thromboxanes **(Fig. 21–15a)**. The two reactions that lead to PGH_2 are catalyzed by a bifunctional enzyme, **cyclooxygenase (COX)**, also called **prostaglandin H_2 synthase**. In the first of two steps, the cyclooxygenase activity introduces molecular oxygen to convert arachidonate to PGG_2. The second step, catalyzed by the peroxidase activity of COX, converts PGG_2 to PGH_2.

Mammals have two isozymes of prostaglandin H_2 synthase, COX-1 and COX-2. These have different functions but closely similar amino acid sequences (60% to 65% sequence identity) and similar reaction mechanisms at both of their catalytic centers. COX-1 is responsible for the synthesis of the prostaglandins that regulate the secretion of gastric mucin, and COX-2 for the prostaglandins that mediate inflammation, pain, and fever.

Pain can be relieved by inhibiting COX-2. The first drug widely marketed for this purpose was aspirin (acetylsalicylate; Fig. 21–15b). The name aspirin (from *a* for acetyl and *spir* for *Spirsaüre,* the German

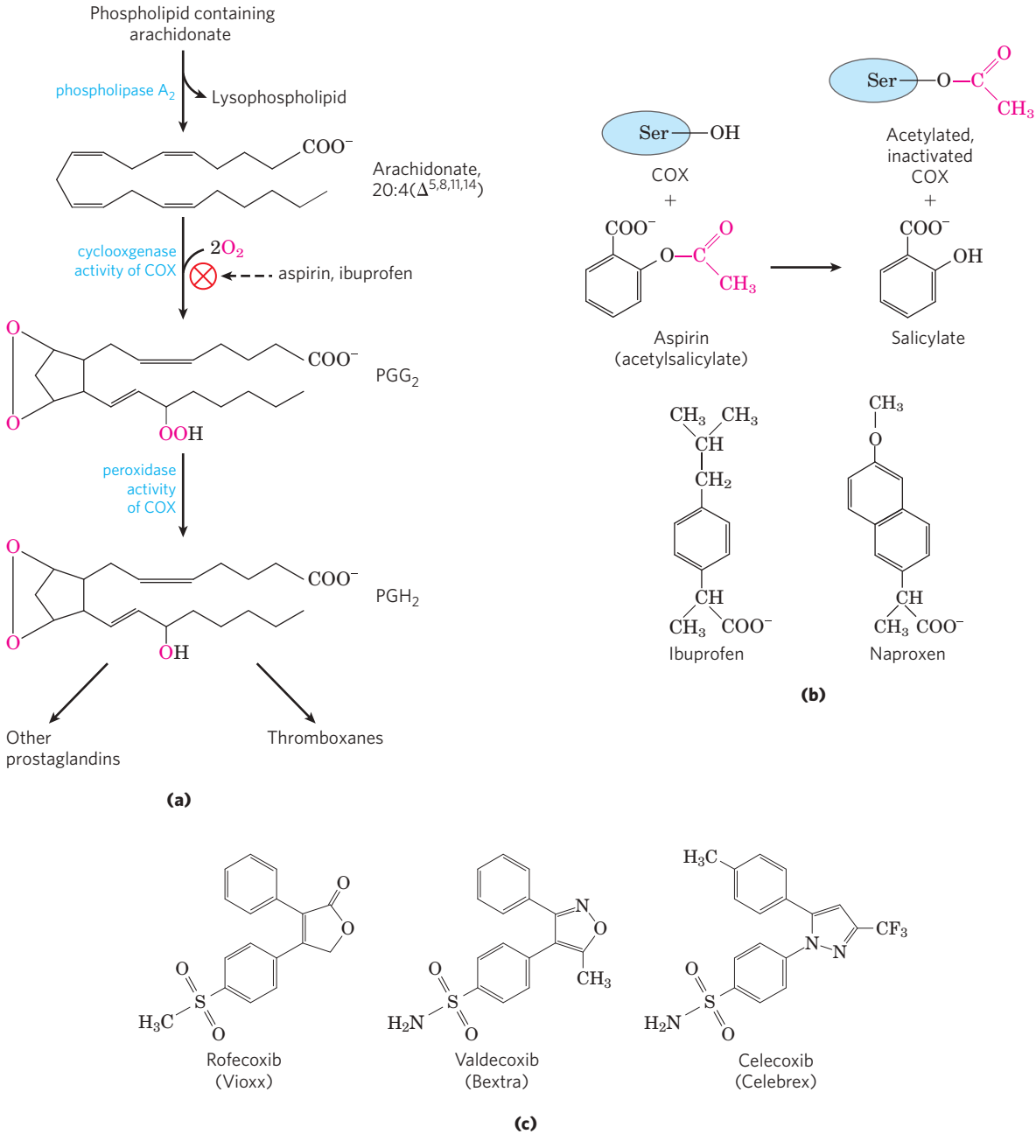

FIGURE 21–15 The "cyclic" pathway from arachidonate to prostaglandins and thromboxanes. (a) After arachidonate is released from phospholipids by the action of phospholipase A_2, the cyclooxygenase and peroxidase activities of COX (also called prostaglandin H_2 synthase) catalyze the production of PGH_2, the precursor of other prostaglandins and thromboxanes. **(b)** Aspirin inhibits the first reaction by acetylating an essential Ser residue on the enzyme. Ibuprofen and naproxen inhibit the same step, probably by mimicking the structure of the substrate or an intermediate in the reaction. **(c)** COX-2–specific cyclooxygenase inhibitors developed as pain relievers (see text). Vioxx was withdrawn from the market in 2004, and Bextra in 2005, because of their side effects on the cardiovascular system.

word for the salicylates prepared from the plant *Spiraea ulmaria*) appeared in 1899 when the drug was introduced by the Bayer company. Aspirin irreversibly inactivates the cyclooxygenase activity of both COX isozymes, by acetylating a Ser residue and blocking each enzyme's active site. The synthesis of prostaglandins and thromboxanes is thereby inhibited. Ibuprofen, another widely used *n*onsteroidal *a*nti*i*nflammatory *d*rug (NSAID; Fig. 21–15b), inhibits the same pair of enzymes. However, the inhibition of COX-1 can result in undesired side effects including stomach irritation and more serious conditions. In the 1990s, following discovery of the crystal structures of COX-1 and COX-2, NSAID compounds that had a greater specificity for COX-2 were developed as advanced therapies for severe pain. Three of these drugs were approved for use worldwide: rofecoxib (Vioxx), valdecoxib (Bextra), and celecoxib (Celebrex) (Fig. 21–15c). Launched in the late

1990s, the new compounds were initially a success for the pharmaceutical firms that produced them. However, enthusiasm turned to concern as field reports and clinical studies connected the drugs with an increased risk of heart attack and stroke. The reasons for the problems are still not clear, but some researchers speculated that the COX-2 inhibitors were altering the fine balance maintained between the hormone prostacyclin, which dilates blood vessels, prevents blood clotting, and is reduced by COX-2 inhibitors, and the thromboxanes, produced on the pathway involving COX-1, that help to form blood clots. Vioxx was withdrawn from the market in 2004, and Bextra was withdrawn soon after. As of early 2012, Celebrex is still on the market but is being used with increased caution.

Thromboxane synthase, present in blood platelets (thrombocytes), converts PGH_2 to thromboxane A_2, from which other **thromboxanes** are derived (Fig. 21–15a). Thromboxanes induce constriction of blood vessels and platelet aggregation, early steps in blood clotting. Low doses of aspirin, taken regularly, reduce the probability of heart attacks and strokes by reducing thromboxane production. ■

Thromboxanes, like prostaglandins, contain a ring of five or six atoms; the pathway from arachidonate to these two classes of compounds is sometimes called the "cyclic" pathway, to distinguish it from the "linear" pathway that leads from arachidonate to the **leukotrienes**, which are linear compounds **(Fig. 21–16)**. Leukotriene synthesis begins with the action of several lipoxygenases that catalyze the incorporation of molecular oxygen into arachidonate. These enzymes, found in leukocytes and in heart, brain, lung, and spleen, are mixed-function oxidases of the cytochrome P-450 family (Box 21–1). The various leukotrienes differ in the position of the peroxide group introduced by the lipoxygenases. This linear pathway from arachidonate, unlike the cyclic pathway, is not inhibited by aspirin or other NSAIDs.

Plants also derive important signaling molecules from fatty acids. As in animals, a key step in the initiation of signaling involves activation of a specific phospholipase. In plants, the fatty acid substrate that is released is α-linolenate. A lipoxygenase then catalyzes the first step in a pathway that converts linolenate to jasmonate, a substance known to have signaling roles in insect defense, resistance to fungal pathogens, and pollen maturation. Jasmonate (see Fig. 12–33) also affects seed germination, root growth, and fruit and seed development.

SUMMARY 21.1 Biosynthesis of Fatty Acids and Eicosanoids

- Long-chain saturated fatty acids are synthesized from acetyl-CoA by a cytosolic system of six enzymatic activities plus acyl carrier protein (ACP). There are two types of fatty acid synthase. FAS I, found in vertebrates and fungi, consists of multifunctional polypeptides. FAS II is a dissociated system found in bacteria and plants. Both contain two types of —SH groups (one furnished by the phosphopantetheine of ACP, the other by a Cys residue of β-ketoacyl-ACP synthase) that function as carriers of the fatty acyl intermediates.
- Malonyl-ACP, formed from acetyl-CoA (shuttled out of mitochondria) and CO_2, condenses with an acetyl bound to the Cys —SH to yield acetoacetyl-ACP, with release of CO_2. This is followed by reduction to the D-β-hydroxy derivative, dehydration to the *trans*-Δ^2-unsaturated acyl-ACP, and reduction to butyryl-ACP. NADPH is the electron donor for both reductions. Fatty acid synthesis is regulated at the level of malonyl-CoA formation.
- Six more molecules of malonyl-ACP react successively at the carboxyl end of the growing fatty acid chain to form palmitoyl-ACP—the end product of the fatty acid synthase reaction. Free palmitate is released by hydrolysis.
- Palmitate may be elongated to the 18-carbon stearate. Palmitate and stearate can be desaturated

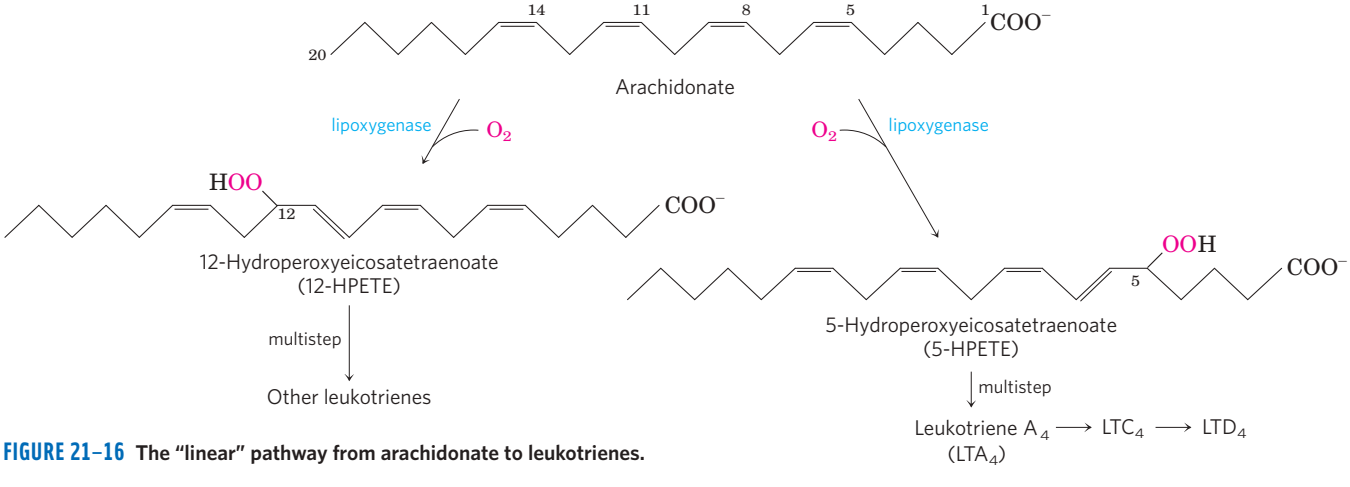

FIGURE 21–16 The "linear" pathway from arachidonate to leukotrienes.

to yield palmitoleate and oleate, respectively, by the action of mixed-function oxidases.

- Mammals cannot make linoleate and must obtain it from plant sources; they convert exogenous linoleate to arachidonate, the parent compound of eicosanoids (prostaglandins, thromboxanes, and leukotrienes), a family of very potent signaling molecules. The synthesis of prostaglandins and thromboxanes is inhibited by NSAIDs that act on the cyclooxygenase activity of prostaglandin H_2 synthase.

21.2 Biosynthesis of Triacylglycerols

Most of the fatty acids synthesized or ingested by an organism have one of two fates: incorporation into triacylglycerols for the storage of metabolic energy or incorporation into the phospholipid components of membranes. The partitioning between these alternative fates depends on the organism's current needs. During rapid growth, synthesis of new membranes requires the production of membrane phospholipids; when an organism has a plentiful food supply but is not actively growing, it shunts most of its fatty acids into storage fats. Both pathways begin at the same point: the formation of fatty acyl esters of glycerol. In this section we examine the route to triacylglycerols and its regulation, and the production of glycerol 3-phosphate in the process of glyceroneogenesis.

Triacylglycerols and Glycerophospholipids Are Synthesized from the Same Precursors

Animals can synthesize and store large quantities of triacylglycerols, to be used later as fuel (see Box 17–1). Humans can store only a few hundred grams of glycogen in liver and muscle, barely enough to supply the body's energy needs for 12 hours. In contrast, the total amount of stored triacylglycerol in a 70 kg man of average build is about 15 kg, enough to support basal energy needs for as long as 12 weeks (see Table 23–5). Triacylglycerols have the highest energy content of all stored nutrients—more than 38 kJ/g. Whenever carbohydrate is ingested in excess of the organism's capacity to store glycogen, the excess is converted to triacylglycerols and stored in adipose tissue. Plants also manufacture triacylglycerols as an energy-rich fuel, mainly stored in fruits, nuts, and seeds.

In animal tissues, triacylglycerols and glycerophospholipids such as phosphatidylethanolamine share two precursors (fatty acyl–CoA and L-glycerol 3-phosphate) and several biosynthetic steps. The vast majority of the glycerol 3-phosphate is derived from the glycolytic intermediate dihydroxyacetone phosphate (DHAP) by the action of the cytosolic NAD-linked **glycerol 3-phosphate dehydrogenase**; in liver and kidney, a small amount of glycerol 3-phosphate is also formed from glycerol by the action of **glycerol kinase** (Fig. 21–17). The other precursors of triacylglycerols are fatty acyl–CoAs, formed from fatty acids by **acyl-CoA synthetases**, the same

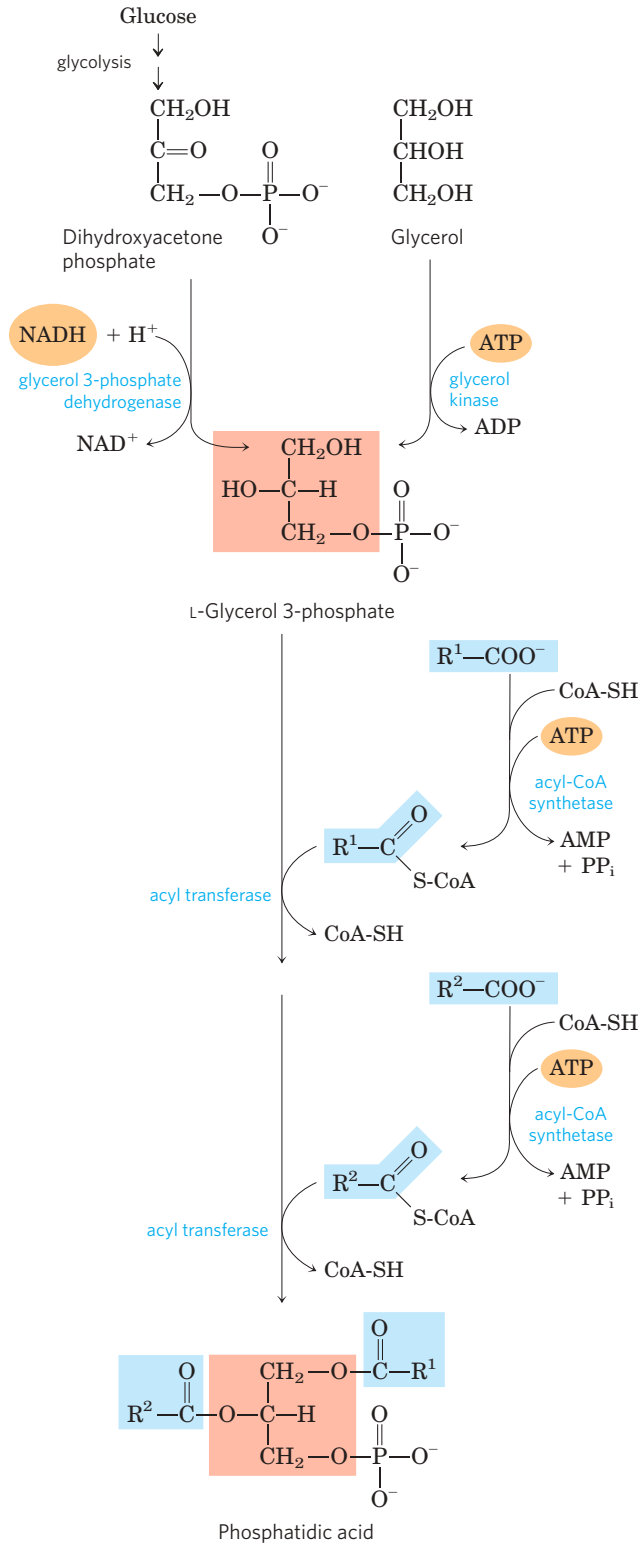

FIGURE 21–17 Biosynthesis of phosphatidic acid. A fatty acyl group is activated by formation of the fatty acyl-CoA, then transferred to ester linkage with L-glycerol 3-phosphate, formed in either of the two ways shown. Phosphatidic acid is shown here with the correct stereochemistry at C-2 of the glycerol molecule. (The intermediate product with only one esterified fatty acyl group is lysophosphatidic acid.) To conserve space in subsequent figures (and in Fig. 21–14), both fatty acyl groups of glycerophospholipids, and all three acyl groups of triacylglycerols, are shown projecting to the right.

enzymes responsible for the activation of fatty acids for β oxidation (see Fig. 17–5).

The first stage in the biosynthesis of triacylglycerols is the acylation of the two free hydroxyl groups of L-glycerol 3-phosphate by two molecules of fatty acyl–CoA to yield **diacylglycerol 3-phosphate**, more commonly called **phosphatidic acid** or phosphatidate (Fig. 21–17). Phosphatidic acid is present in only trace amounts in cells but is a central intermediate in lipid biosynthesis; it can be converted either to a triacylglycerol or to a glycerophospholipid. In the pathway to triacylglycerols, phosphatidic acid is hydrolyzed by **phosphatidic acid phosphatase** (also called lipin) to form a 1,2-diacylglycerol **(Fig. 21–18)**. Diacylglycerols are then converted to triacylglycerols by transesterification with a third fatty acyl–CoA.

Triacylglycerol Biosynthesis in Animals Is Regulated by Hormones

In humans, the amount of body fat stays relatively constant over long periods, although there may be minor short-term changes as caloric intake fluctuates. Carbohydrate, fat, or protein ingested in excess of energy needs is stored in the form of triacylglycerols that can be drawn upon for energy, enabling the body to withstand periods of fasting.

Biosynthesis and degradation of triacylglycerols are regulated such that the favored path depends on the metabolic resources and requirements of the moment. The rate of triacylglycerol biosynthesis is profoundly altered by the action of several hormones. Insulin, for example, promotes the conversion of carbohydrate to triacylglycerols **(Fig. 21–19)**. People with severe diabetes mellitus, due to failure of insulin secretion or action, not only are unable to use glucose properly but also fail to synthesize fatty acids from carbohydrates or amino acids. If the diabetes is untreated, these individuals have increased rates of fat oxidation and ketone body formation (Chapter 17) and therefore lose weight. ■

An additional factor in the balance between biosynthesis and degradation of triacylglycerols is that approximately 75% of all fatty acids released by lipolysis are reesterified to form triacylglycerols rather than used for fuel. This ratio persists even under starvation conditions, when energy metabolism is shunted from the use of carbohydrate to the oxidation of fatty acids. Some of this fatty acid recycling takes place in adipose tissue, with the reesterification occurring before release into the bloodstream; some takes place via a systemic cycle in

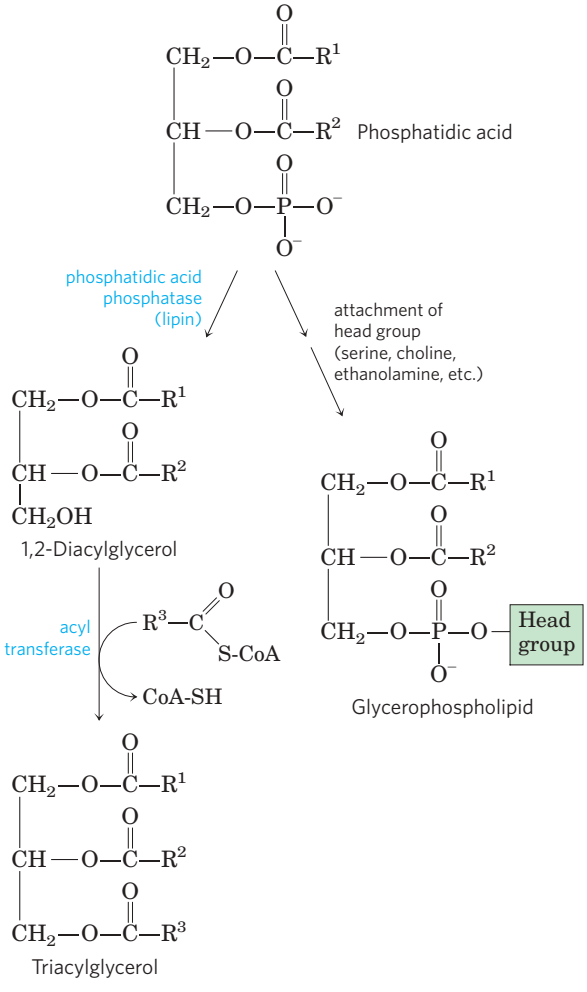

FIGURE 21–18 Phosphatidic acid in lipid biosynthesis. Phosphatidic acid is the precursor of both triacylglycerols and glycerophospholipids. The mechanisms for head-group attachment in phospholipid synthesis are described later in this section.

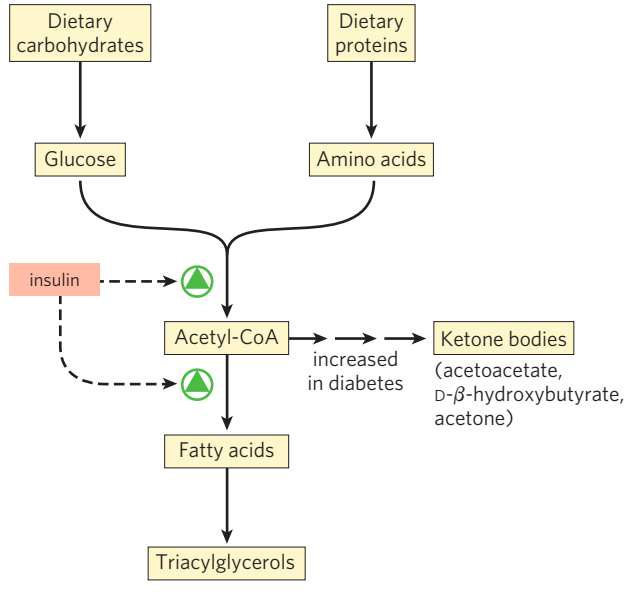

FIGURE 21–19 Regulation of triacylglycerol synthesis by insulin. Insulin stimulates conversion of dietary carbohydrates and proteins to fat. Individuals with diabetes mellitus either lack insulin or are insensitive to it. This results in diminished fatty acid synthesis, and the acetyl-CoA arising from catabolism of carbohydrates and proteins is shunted instead to ketone body production. People in severe ketosis smell of acetone, so the condition is sometimes mistaken for drunkenness (p. 959).

which free fatty acids are transported to liver, recycled to triacylglycerol, exported again to the blood (transport of lipids in the blood is discussed in Section 21.4), and taken up again by adipose tissue after release from triacylglycerol by extracellular lipoprotein lipase (**Fig. 21–20**; see also Fig. 17–1). Flux through this **triacylglycerol cycle** between adipose tissue and liver may be quite low when other fuels are available and the release of fatty acids from adipose tissue is limited, but as noted above, the proportion of released fatty acids that are reesterified remains roughly constant at 75% under all metabolic conditions. The level of free fatty acids in the blood thus reflects both the rate of release of fatty acids and the balance between the synthesis and breakdown of triacylglycerols in adipose tissue and liver.

When the mobilization of fatty acids is required to meet energy needs, release from adipose tissue is stimulated by the hormones glucagon and epinephrine (see Figs 17–3, 17–13). Simultaneously, these hormonal signals decrease the rate of glycolysis and increase the rate of gluconeogenesis in the liver (providing glucose for the brain, as further elaborated in Chapter 23). The released fatty acid is taken up by a number of tissues, including muscle, where it is oxidized to provide energy. Much of the fatty acid taken up by liver is not oxidized but is recycled to triacylglycerol and returned to adipose tissue.

The function of the apparently futile triacylglycerol cycle (futile cycles are discussed in Chapter 15) is not well understood. However, as we learn more about how the triacylglycerol cycle is sustained via metabolism in two separate organs and is coordinately regulated, some possibilities emerge. For example, the excess capacity in the triacylglycerol cycle (the fatty acid that is eventually reconverted to triacylglycerol rather than oxidized as fuel) could represent an energy reserve in the bloodstream during fasting, one that would be more rapidly mobilized in a "fight or flight" emergency than would stored triacylglycerol.

The constant recycling of triacylglycerols in adipose tissue even during starvation raises a second question: what is the source of the glycerol 3-phosphate required for this process? As noted above, glycolysis is suppressed in these conditions by the action of glucagon and epinephrine, so little DHAP is available, and glycerol released during lipolysis cannot be converted directly to glycerol 3-phosphate in adipose tissue, because these cells lack glycerol kinase (Fig. 21–17). So, how is sufficient glycerol 3-phosphate produced? The answer lies in a pathway discovered more than three decades ago and given little attention until recently, a pathway intimately linked to the triacylglycerol cycle and, in a larger sense, to the balance between fatty acid and carbohydrate metabolism.

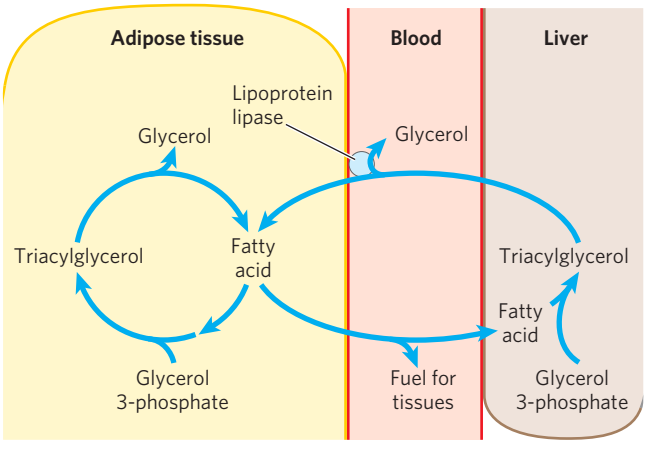

FIGURE 21–20 The triacylglycerol cycle. In mammals, triacylglycerol molecules are broken down and resynthesized in a triacylglycerol cycle during starvation. Some of the fatty acids released by lipolysis of triacylglycerol in adipose tissue pass into the bloodstream, and the remainder are used for resynthesis of triacylglycerol. Some of the fatty acids released into the blood are used for energy (in muscle, for example), and some are taken up by the liver and used in triacylglycerol synthesis. The triacylglycerol formed in the liver is transported in the blood back to adipose tissue, where the fatty acid is released by extracellular lipoprotein lipase, taken up by adipocytes, and reesterified into triacylglycerol.

Adipose Tissue Generates Glycerol 3-Phosphate by Glyceroneogenesis

Glyceroneogenesis is a shortened version of gluconeogenesis, from pyruvate to DHAP (see Fig. 14–17), followed by conversion of the DHAP to glycerol 3-phosphate by cytosolic NAD-linked glycerol 3-phosphate dehydrogenase **(Fig. 21–21)**. Glycerol 3-phosphate is subsequently used in triacylglycerol synthesis. Glyceroneogenesis was discovered in the 1960s by Lea Reshef, Richard Hanson, and John Ballard, and simultaneously by Eleazar Shafrir and his coworkers, who were intrigued by the presence of two gluconeogenic enzymes, pyruvate carboxylase and phosphoenolpyruvate (PEP) carboxykinase, in adipose tissue, where glucose is not synthesized. After a long period of inattention, interest in this pathway has been renewed by the demonstration of a link between glyceroneogenesis and type 2 diabetes, as we shall see.

Glyceroneogenesis has multiple roles. In adipose tissue, glyceroneogenesis coupled with reesterification of free fatty acids controls the rate of fatty acid release to the blood. In brown adipose tissue, the same pathway may control the rate at which free fatty acids are delivered to mitochondria for use in thermogenesis (see Fig. 19–36). And in fasting humans, glyceroneogenesis in the liver alone supports the synthesis of enough glycerol 3-phosphate to account for up to 65% of fatty acids reesterified to triacylglycerol.

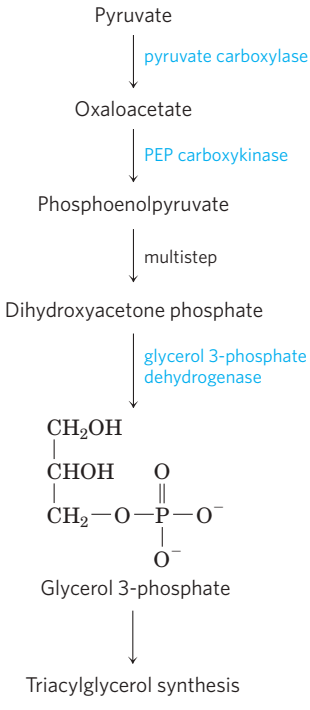

FIGURE 21–21 Glyceroneogenesis. The pathway is essentially an abbreviated version of gluconeogenesis, from pyruvate to dihydroxyacetone phosphate (DHAP), followed by conversion of DHAP to glycerol 3-phosphate, which is used for the synthesis of triacylglycerol.

Flux through the triacylglycerol cycle between liver and adipose tissue is controlled to a large degree by the activity of PEP carboxykinase, which limits the rate of both gluconeogenesis and glyceroneogenesis. Glucocorticoid hormones such as cortisol (a biological steroid derived from cholesterol; see Fig. 21–48) and dexamethasone (a synthetic glucocorticoid) regulate the levels of PEP carboxykinase reciprocally in the liver and adipose tissue. Acting through the glucocorticoid receptor, these steroid hormones increase the expression of the gene encoding PEP carboxykinase in the liver, thus increasing gluconeogenesis and glyceroneogenesis **(Fig. 21–22)**.

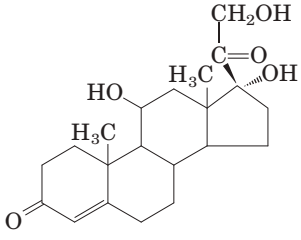

Cortisol

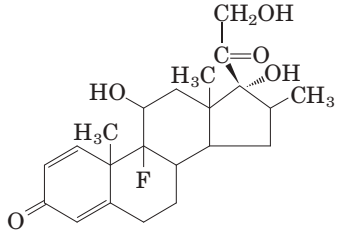

Dexamethasone

Stimulation of glyceroneogenesis leads to an increase in the synthesis of triacylglycerol molecules in the liver and their release into the blood. At the same time, glucocorticoids suppress the expression of the gene encoding PEP carboxykinase in adipose tissue. This results in a decrease in glyceroneogenesis in adipose tissue; recycling of fatty acids declines as a result, and more free fatty acids are released into the blood.

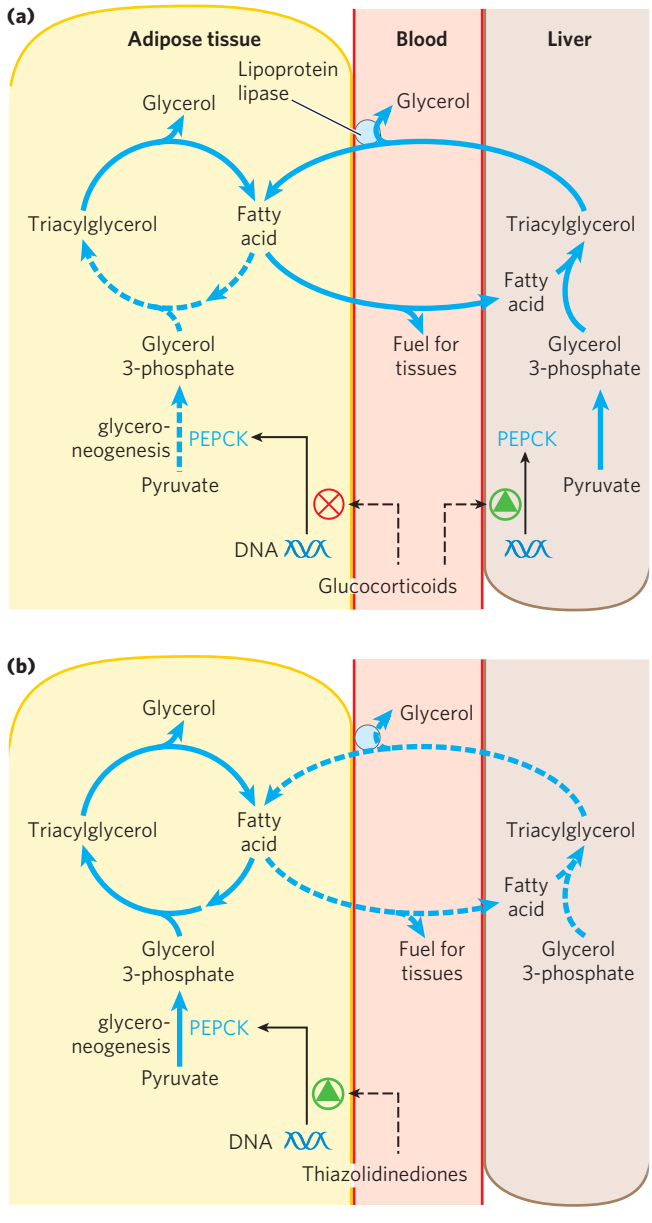

FIGURE 21–22 Regulation of glyceroneogenesis. (a) Glucocorticoid hormones stimulate glyceroneogenesis and gluconeogenesis in the liver, while suppressing glyceroneogenesis in the adipose tissue (by reciprocal regulation of the gene expressing PEP carboxykinase (PEPCK) in the two tissues); this increases the flux through the triacylglycerol cycle. The glycerol freed by the breakdown of triacylglycerol in adipose tissue is released to the blood and transported to the liver, where it is primarily converted to glucose, although some is converted to glycerol 3-phosphate by glycerol kinase. **(b)** A class of drugs called thiazolidinediones are now used to treat type 2 diabetes. In this disease, high levels of free fatty acids in the blood interfere with glucose utilization in muscle and promote insulin resistance. Thiazolidinediones activate a nuclear receptor called peroxisome proliferator-activated receptor γ (PPARγ), which induces the activity of PEP carboxykinase. Therapeutically, thiazolidinediones increase the rate of glyceroneogenesis, thus increasing the resynthesis of triacylglycerol in adipose tissue and reducing the amount of free fatty acid in the blood.

Thus glyceroneogenesis is regulated reciprocally in the liver and adipose tissue, affecting lipid metabolism in opposite ways: a lower rate of glyceroneogenesis in adipose tissue leads to more fatty acid release (rather than recycling), whereas a higher rate in the liver leads to more synthesis and export of triacylglycerols. The net result is an increase in flux through the triacylglycerol cycle. When the glucocorticoids are no longer present, flux through the cycle declines as the expression of PEP carboxykinase increases in adipose tissue and decreases in the liver.

Thiazolidinediones Treat Type 2 Diabetes by Increasing Glyceroneogenesis

The recent attention to glyceroneogenesis has arisen in part from the connection between this pathway and diabetes. High levels of free fatty acids in the blood interfere with glucose utilization in muscle and promote the insulin resistance that leads to type 2 diabetes. A new class of drugs called **thiazolidinediones** reduce the levels of fatty acids circulating in the blood and increase sensitivity to insulin. Thiazolidinediones promote the induction in adipose tissue of PEP carboxykinase (Fig. 21–22), leading to increased synthesis of the precursors of glyceroneogenesis. The therapeutic effect of thiazolidinediones is thus due, at least in part, to the increase in glyceroneogenesis, which in turn increases the resynthesis of triacylglycerol in adipose tissue and reduces the release of free fatty acid from adipose tissue into the blood. The benefits of one such drug, rosiglitazone (Avandia), are countered in part by an increased risk of heart attack, for reasons not yet clear. Assessment of this drug is continuing, and it is available only through a restricted distribution system.

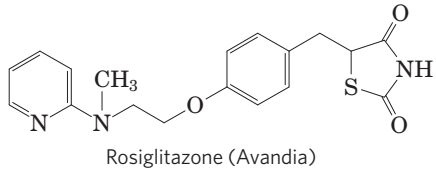

Rosiglitazone (Avandia)

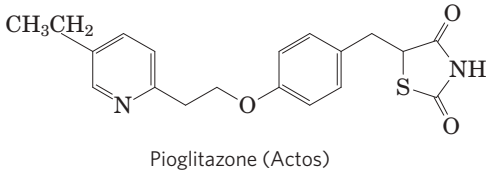

Pioglitazone (Actos)

Thiazolidinediones

SUMMARY 21.2 Biosynthesis of Triacylglycerols

- Triacylglycerols are formed by reaction of two molecules of fatty acyl–CoA with glycerol 3-phosphate to form phosphatidic acid; this product is dephosphorylated to a diacylglycerol, then acylated by a third molecule of fatty acyl–CoA to yield a triacylglycerol.
- The synthesis and degradation of triacylglycerol are hormonally regulated.
- Mobilization and recycling of triacylglycerol molecules results in a triacylglycerol cycle. Triacylglycerols are resynthesized from free fatty acids and glycerol 3-phosphate even during starvation. The dihydroxyacetone phosphate precursor of glycerol 3-phosphate is derived from pyruvate via glyceroneogenesis.

21.3 Biosynthesis of Membrane Phospholipids

In Chapter 10 we introduced two major classes of membrane phospholipids: glycerophospholipids and sphingolipids. Many different phospholipid species can be constructed by combining various fatty acids and polar head groups with the glycerol or sphingosine backbone (see Figs 10–9, 10–13). All the biosynthetic pathways follow a few basic patterns. In general, the assembly of phospholipids from simple precursors requires (1) synthesis of the backbone molecule (glycerol or sphingosine); (2) attachment of fatty acid(s) to the backbone through an ester or amide linkage; (3) addition of a hydrophilic head group to the backbone through a phosphodiester linkage; and, in some cases, (4) alteration or exchange of the head group to yield the final phospholipid product.

In eukaryotic cells, phospholipid synthesis occurs primarily on the surfaces of the smooth endoplasmic reticulum and the mitochondrial inner membrane. Some newly formed phospholipids remain at the site of synthesis, but most are destined for other cellular locations. The process by which water-insoluble phospholipids move from the site of synthesis to the point of their eventual function is not fully understood, but we will discuss some mechanisms that have emerged in recent years.

Cells Have Two Strategies for Attaching Phospholipid Head Groups

The first steps of glycerophospholipid synthesis are shared with the pathway to triacylglycerols (Fig. 21–17): two fatty acyl groups are esterified to C-1 and C-2 of L-glycerol 3-phosphate to form phosphatidic acid. Commonly but not invariably, the fatty acid at C-1 is saturated and that at C-2 is unsaturated. A second route to phosphatidic acid is the phosphorylation of a diacylglycerol by a specific kinase.

The polar head group of glycerophospholipids is attached through a phosphodiester bond, in which each of two alcohol hydroxyls (one on the polar head group and one on C-3 of glycerol) forms an ester with phosphoric acid **(Fig. 21–23)**. In the biosynthetic process, one of the hydroxyls is first activated by attachment of

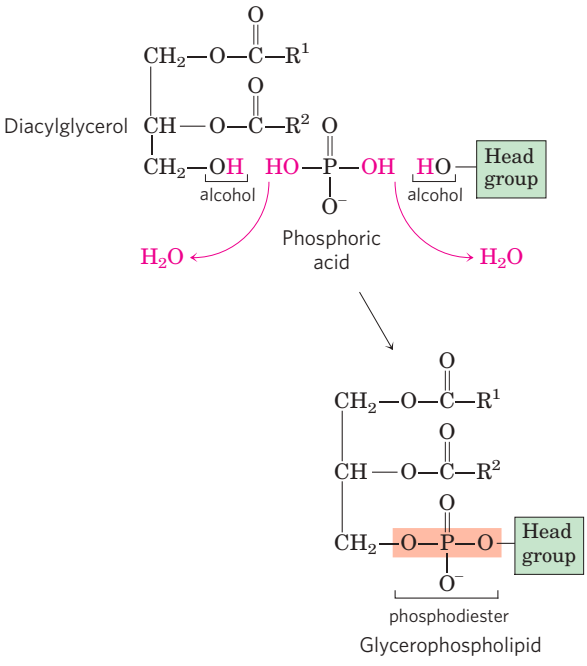

FIGURE 21–23 Head-group attachment. The phospholipid head group is attached to a diacylglycerol by a phosphodiester bond, formed when phosphoric acid condenses with two alcohols, eliminating two molecules of H_2O.

a nucleotide, cytidine diphosphate (CDP). Cytidine monophosphate (CMP) is then displaced in a nucleophilic attack by the other hydroxyl **(Fig. 21–24)**. The CDP is attached either to the diacylglycerol, forming the activated phosphatidic acid **CDP-diacylglycerol** (strategy 1), or to the hydroxyl of the head group (strategy 2). Eukaryotic cells employ both strategies, whereas bacteria use only the first. The central importance of cytidine nucleotides in lipid biosynthesis was discovered by Eugene P. Kennedy in the early 1960s, and this pathway is commonly referred to as the Kennedy pathway.

Phospholipid Synthesis in *E. coli* Employs CDP-Diacylglycerol

The first strategy for head-group attachment is illustrated by the synthesis of phosphatidylserine, phosphatidylethanolamine, and phosphatidylglycerol in *E. coli*. The diacylglycerol is activated by condensation of phosphatidic acid with cytidine triphosphate (CTP) to form CDP-diacylglycerol, with the elimination of pyrophosphate **(Fig. 21–25)**. Displacement of CMP through nucleophilic attack by the hydroxyl group of serine or by the C-1 hydroxyl of glycerol 3-phosphate yields **phosphatidylserine** or phosphatidylglycerol 3-phosphate, respectively. The latter is processed further by cleavage of the phosphate monoester (with release of P_i) to yield **phosphatidylglycerol**.

Phosphatidylserine and phosphatidylglycerol can serve as precursors of other membrane lipids in bacteria (Fig. 21–25). Decarboxylation of the serine moiety in

Eugene P. Kennedy, 1919–2011

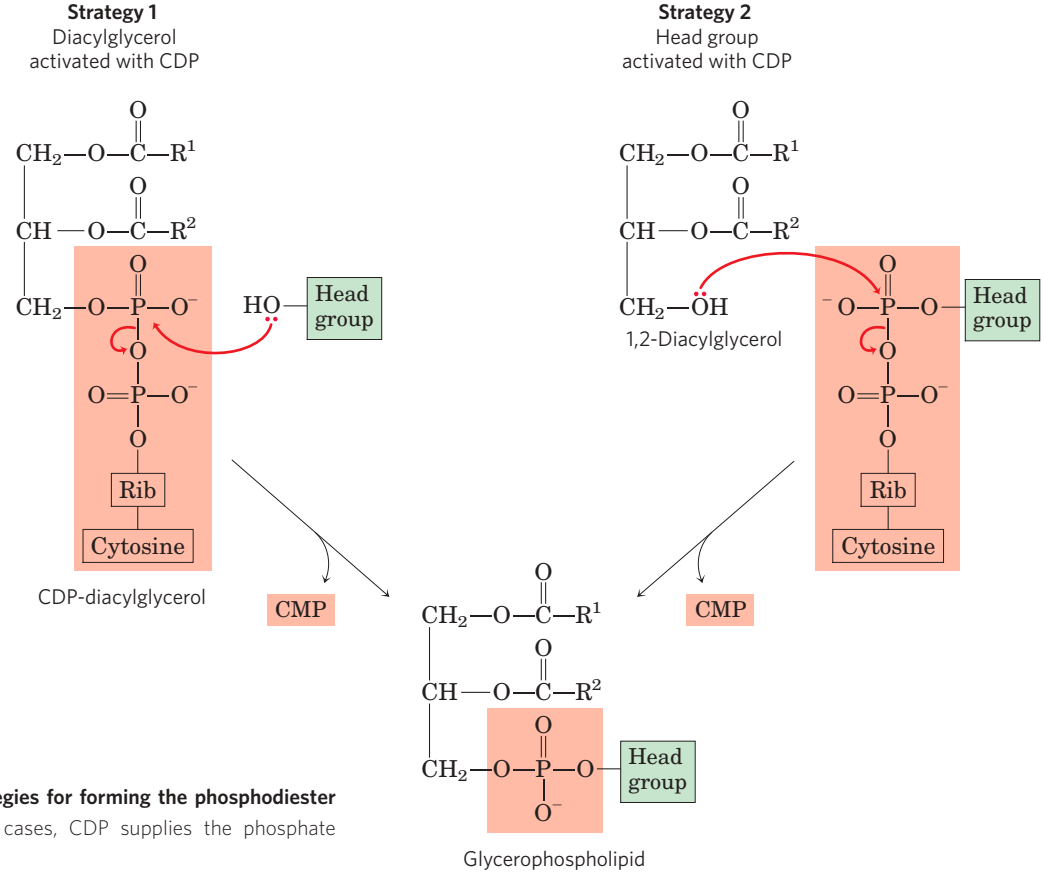

FIGURE 21–24 Two general strategies for forming the phosphodiester bond of phospholipids. In both cases, CDP supplies the phosphate group of the phosphodiester bond.

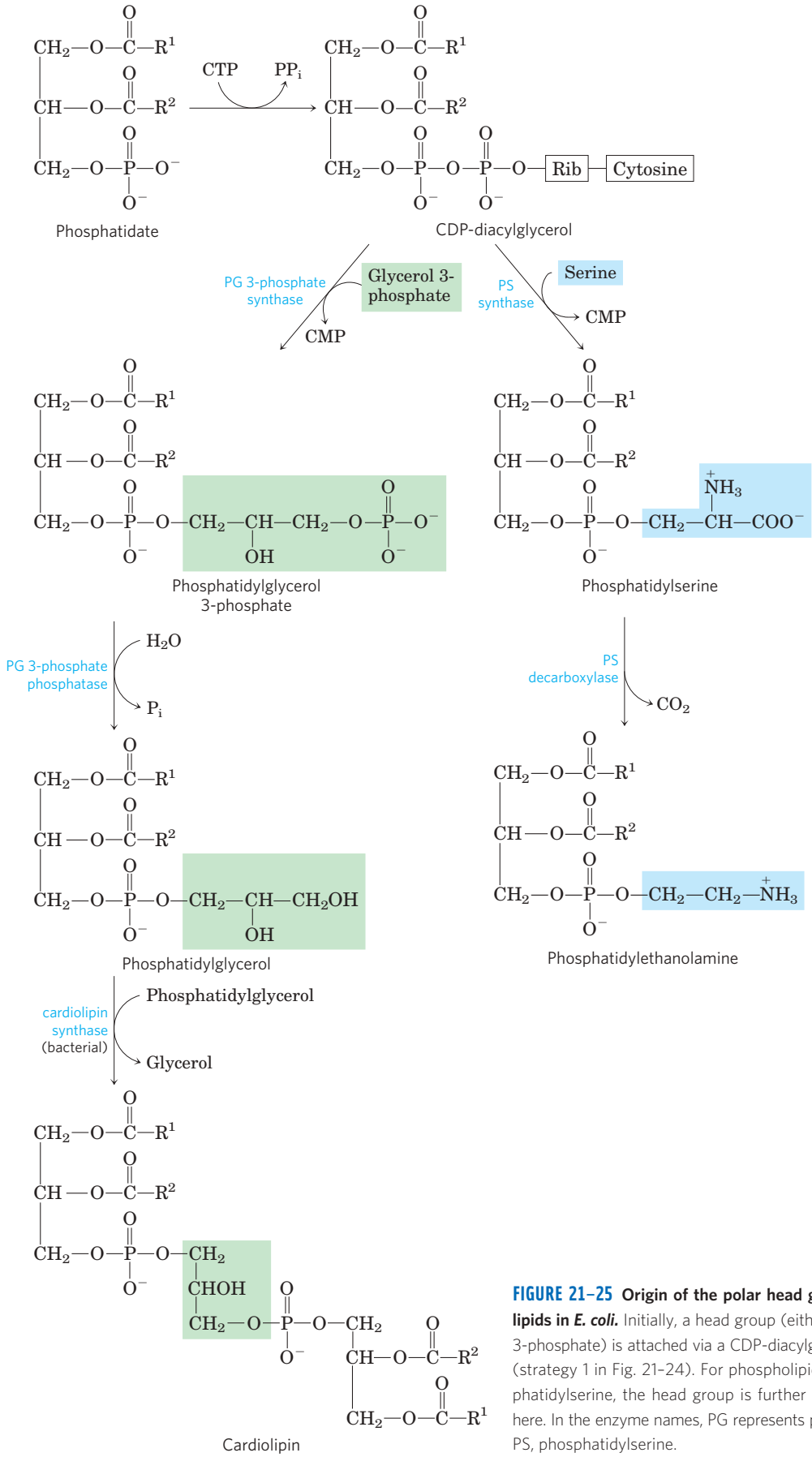

FIGURE 21–25 Origin of the polar head groups of phospholipids in *E. coli*. Initially, a head group (either serine or glycerol 3-phosphate) is attached via a CDP-diacylglycerol intermediate (strategy 1 in Fig. 21–24). For phospholipids other than phosphatidylserine, the head group is further modified, as shown here. In the enzyme names, PG represents phosphatidylglycerol; PS, phosphatidylserine.

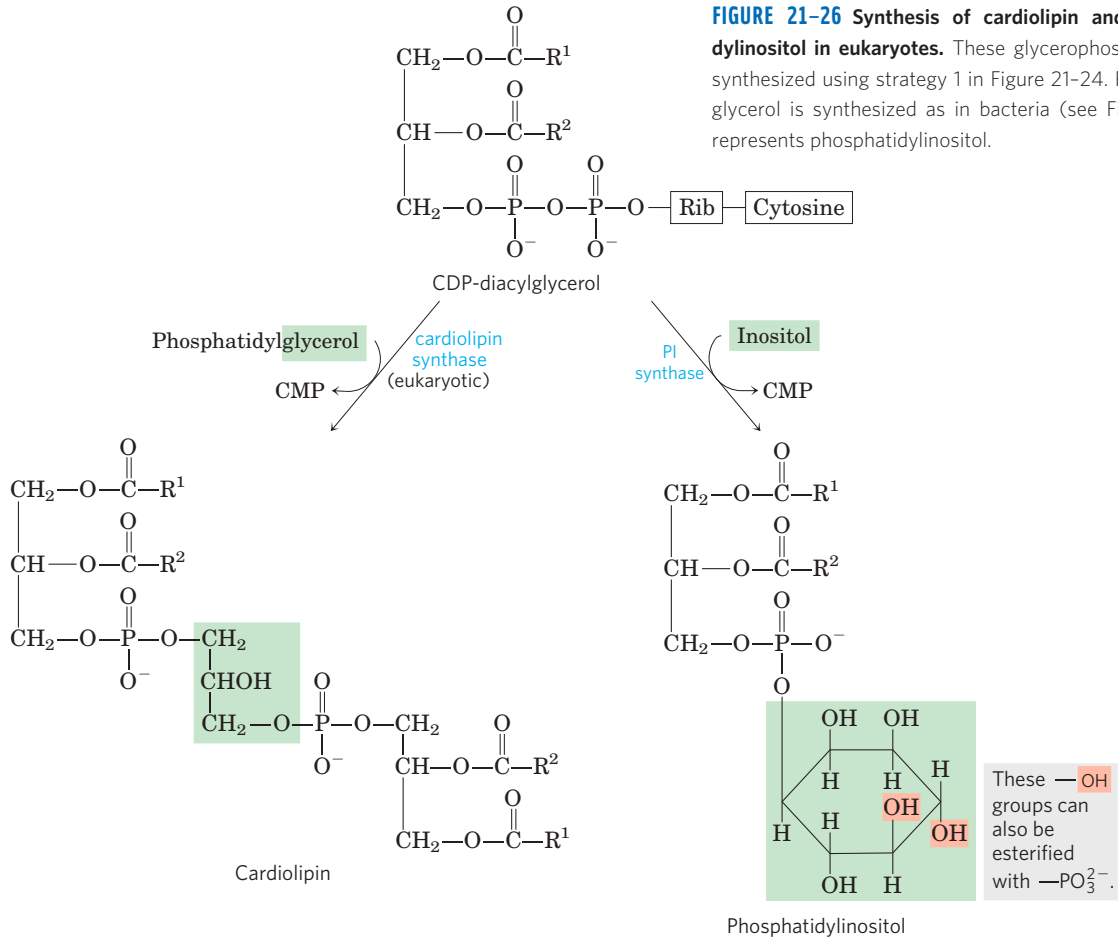

FIGURE 21–26 Synthesis of cardiolipin and phosphatidylinositol in eukaryotes. These glycerophospholipids are synthesized using strategy 1 in Figure 21–24. Phosphatidylglycerol is synthesized as in bacteria (see Fig. 21–25). PI represents phosphatidylinositol.

phosphatidylserine, catalyzed by phosphatidylserine decarboxylase, yields **phosphatidylethanolamine**. In *E. coli*, condensation of two molecules of phosphatidylglycerol, with elimination of one glycerol, yields **cardiolipin**, in which two diacylglycerols are joined through a common head group.

Eukaryotes Synthesize Anionic Phospholipids from CDP-Diacylglycerol

In eukaryotes, phosphatidylglycerol, cardiolipin, and the phosphatidylinositols (all anionic phospholipids; see Fig. 10–9) are synthesized by the same strategy used for phospholipid synthesis in bacteria. Phosphatidylglycerol is made exactly as in bacteria. Cardiolipin synthesis in eukaryotes differs slightly: phosphatidylglycerol condenses with CDP-diacylglycerol **(Fig. 21–26)**, not another molecule of phosphatidylglycerol as in *E. coli* (Fig. 21–25).

Phosphatidylinositol is synthesized by condensation of CDP-diacylglycerol with inositol (Fig. 21–26). Specific **phosphatidylinositol kinases** then convert phosphatidylinositol to its phosphorylated derivatives. Phosphatidylinositol and its phosphorylated products in the plasma membrane play a central role in signal transduction in eukaryotes (see Figs 12–10, 12–16).

Eukaryotic Pathways to Phosphatidylserine, Phosphatidylethanolamine, and Phosphatidylcholine Are Interrelated

Yeast, like bacteria, can produce phosphatidylserine by condensation of CDP-diacylglycerol and serine, and can synthesize phosphatidylethanolamine from phosphatidylserine in the reaction catalyzed by phosphatidylserine decarboxylase **(Fig. 21–27)**. Phosphatidylethanolamine may be converted to **phosphatidylcholine** (lecithin) by the addition of three methyl groups to its amino group; *S*-adenosylmethionine is the methyl group donor (see Fig. 18–18) for all three methylation reactions. The pathways to phosphatidylcholine and phosphatidylethanolamine in yeast are summarized in **Figure 21–28**. These paths are the major sources of phosphatidylethanolamine and phosphatidylcholine in all eukaryotic cells.

In mammals, phosphatidylserine is not synthesized from CDP-diacylglycerol; instead, it is derived from phosphatidylethanolamine or phosphatidylcholine via one of two head-group exchange reactions carried out

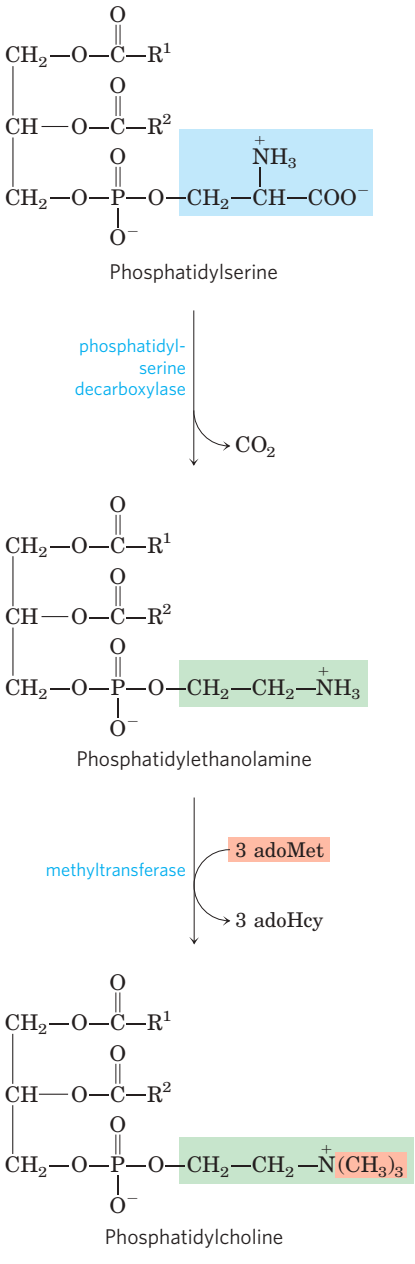

FIGURE 21–27 The major path from phosphatidylserine to phosphatidylethanolamine and phosphatidylcholine in all eukaryotes. AdoMet is *S*-adenosylmethionine; adoHcy, *S*-adenosylhomocysteine.

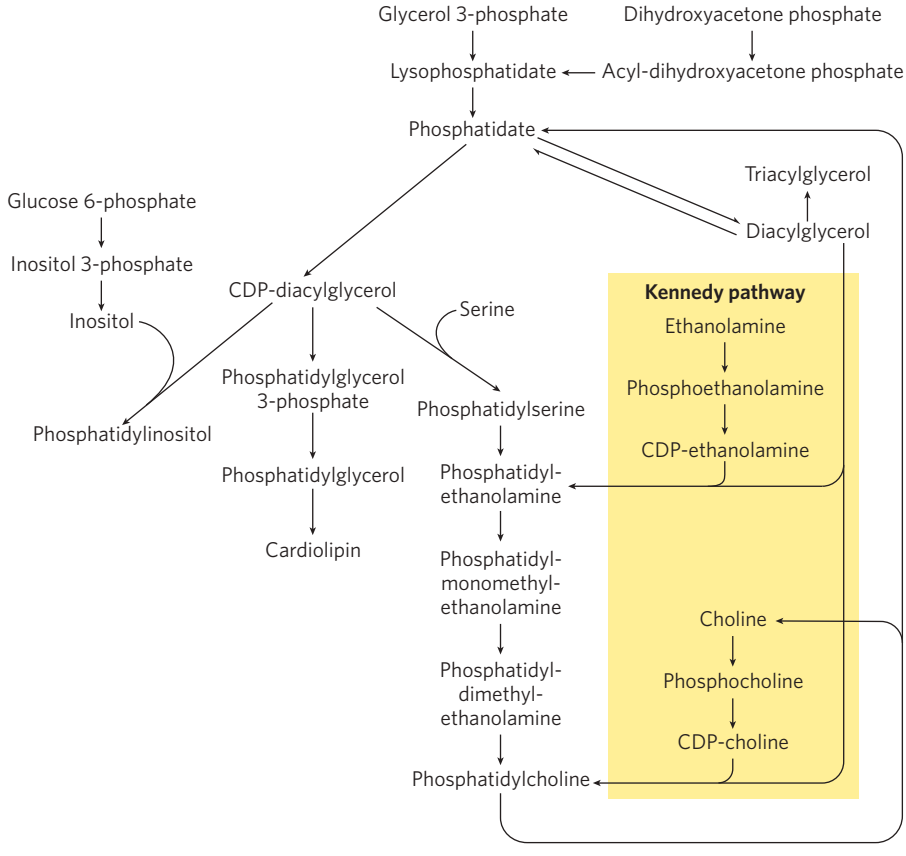

FIGURE 21–28 Summary of the pathways for synthesis of major phospholipids and triacylglycerides in a eukaryote (yeast). Phosphatidic acid is formed by transacylation of L-glycerol 3-phosphate with two fatty acyl groups donated from fatty acyl-CoA. The enzyme phosphatidic acid phosphatase (lipin) converts phosphatidic acid to diacylglycerol, which in the Kennedy pathway condenses with a CDP-activated head group (ethanolamine or choline) to form phosphatidylethanolamine or phosphatidylcholine. Alternatively, phosphatidic acid can be activated with a CDP moiety, which is displaced by condensation with a head group alcohol—inositol, glycerol 3-phosphate, or serine, forming phosphatidylinositol, phosphatidylglycerol, or phosphatidylserine. Decarboxylation of phosphatidylserine yields phosphatidylethanolamine, and methylation of phosphatidylethanolamine produces phosphatidylcholine. Not shown here are the head-group exchange reactions (see Fig. 21-29a) that interconvert phosphatidylethanolamine, phosphatidylserine, and phosphatidylcholine in mammals. Lysophosphatidic acid is phosphatidic acid missing one of the two fatty acyl groups.

in the endoplasmic reticulum **(Fig. 21–29a)**. Synthesis of phosphatidylethanolamine and phosphatidylcholine in mammals occurs by strategy 2 of Figure 21–24: phosphorylation and activation of the head group, followed by condensation with diacylglycerol. For example, choline is reused ("salvaged") by being phosphorylated then converted to CDP-choline by condensation with CTP. A diacylglycerol displaces CMP from CDP-choline, producing phosphatidylcholine (Fig. 21–29b). An analogous salvage pathway converts ethanolamine obtained in the diet to phosphatidylethanolamine. In the liver, phosphatidylcholine is also produced by methylation of phosphatidylethanolamine (with *S*-adenosylmethionine, as described above), but in all other tissues phosphatidylcholine is produced only by condensation of diacylglycerol and CDP-choline.

Plasmalogen Synthesis Requires Formation of an Ether-Linked Fatty Alcohol

The biosynthetic pathway to ether lipids, including **plasmalogens** and the **platelet-activating factor** (see Fig. 10–10), involves the displacement of an esterified fatty acyl group by a long-chain alcohol to form the ether linkage **(Fig. 21–30)**. Head-group attachment follows, by mechanisms essentially like those used in formation of the common ester-linked phospholipids. Finally, the characteristic double bond of plasmalogens (shaded blue in Fig. 21–30) is introduced by the action of a mixed-function oxidase similar to that responsible

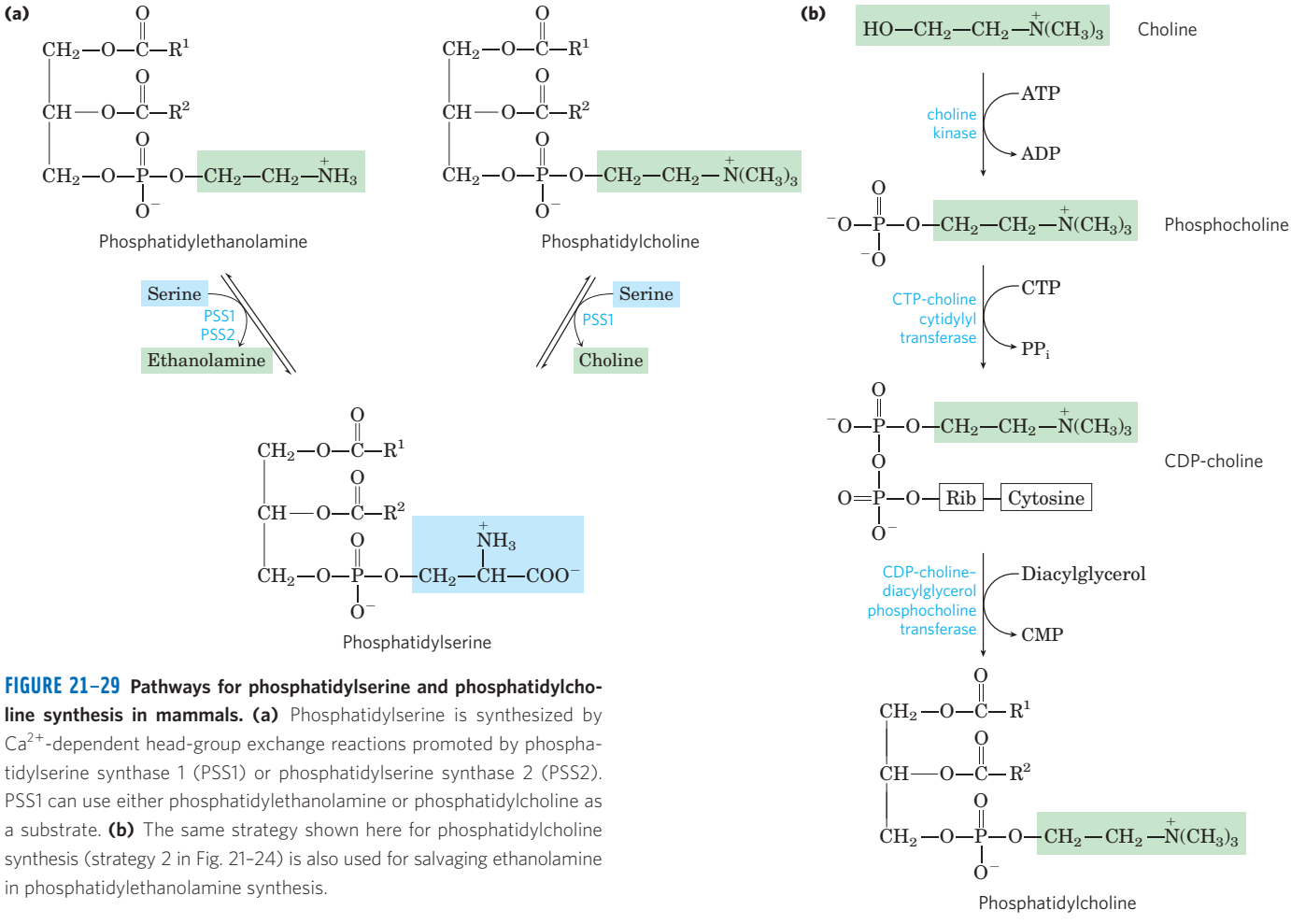

FIGURE 21–29 Pathways for phosphatidylserine and phosphatidylcholine synthesis in mammals. (a) Phosphatidylserine is synthesized by Ca^{2+}-dependent head-group exchange reactions promoted by phosphatidylserine synthase 1 (PSS1) or phosphatidylserine synthase 2 (PSS2). PSS1 can use either phosphatidylethanolamine or phosphatidylcholine as a substrate. **(b)** The same strategy shown here for phosphatidylcholine synthesis (strategy 2 in Fig. 21–24) is also used for salvaging ethanolamine in phosphatidylethanolamine synthesis.

for desaturation of fatty acids (Fig. 21–13). The peroxisome is the primary site of plasmalogen synthesis.

Sphingolipid and Glycerophospholipid Synthesis Share Precursors and Some Mechanisms

The biosynthesis of sphingolipids takes place in four stages: (1) synthesis of the 18-carbon amine **sphinganine** from palmitoyl-CoA and serine; (2) attachment of a fatty acid in amide linkage to yield ***N*-acylsphinganine**; (3) desaturation of the sphinganine moiety to form ***N*-acylsphingosine** (ceramide); and (4) attachment of a head group to produce a sphingolipid such as a **cerebroside** or **sphingomyelin (Fig. 21–31)**. The first few steps of this pathway occur in the endoplasmic reticulum, while the attachment of head groups in stage 4 occurs in the Golgi complex. The pathway shares several features with the pathways leading to glycerophospholipids: NADPH provides reducing power, and fatty acids enter as their activated CoA derivatives. In cerebroside formation, sugars enter as their activated nucleotide derivatives. Head-group attachment in sphingolipid synthesis has several novel aspects. Phosphatidylcholine, rather than CDP-choline, serves as the donor of phosphocholine in the synthesis of sphingomyelin.

In glycolipids—the cerebrosides and **gangliosides** (see Fig. 10–13)—the head-group sugar is attached directly to the C-1 hydroxyl of sphingosine in glycosidic linkage rather than through a phosphodiester bond. The sugar donor is a UDP-sugar (UDP-glucose or UDP-galactose).

Polar Lipids Are Targeted to Specific Cellular Membranes

After synthesis on the smooth ER, the polar lipids, including the glycerophospholipids, sphingolipids, and glycolipids, are inserted into specific cellular membranes in specific proportions, by mechanisms not yet understood. Membrane lipids are insoluble in water, so they cannot simply diffuse from their point of synthesis (the ER) to their point of insertion. Instead, they are transported from the ER to the Golgi complex, where additional synthesis can take place. They are then delivered in membrane vesicles that bud from the Golgi complex then move to and fuse with the target membrane. Sphingolipid transfer proteins carry ceramide from the ER to the Golgi complex, where sphingomyelin synthesis occurs. Cytosolic proteins also bind phospholipids and sterols and transport them between cellular membranes. These mechanisms contribute to the

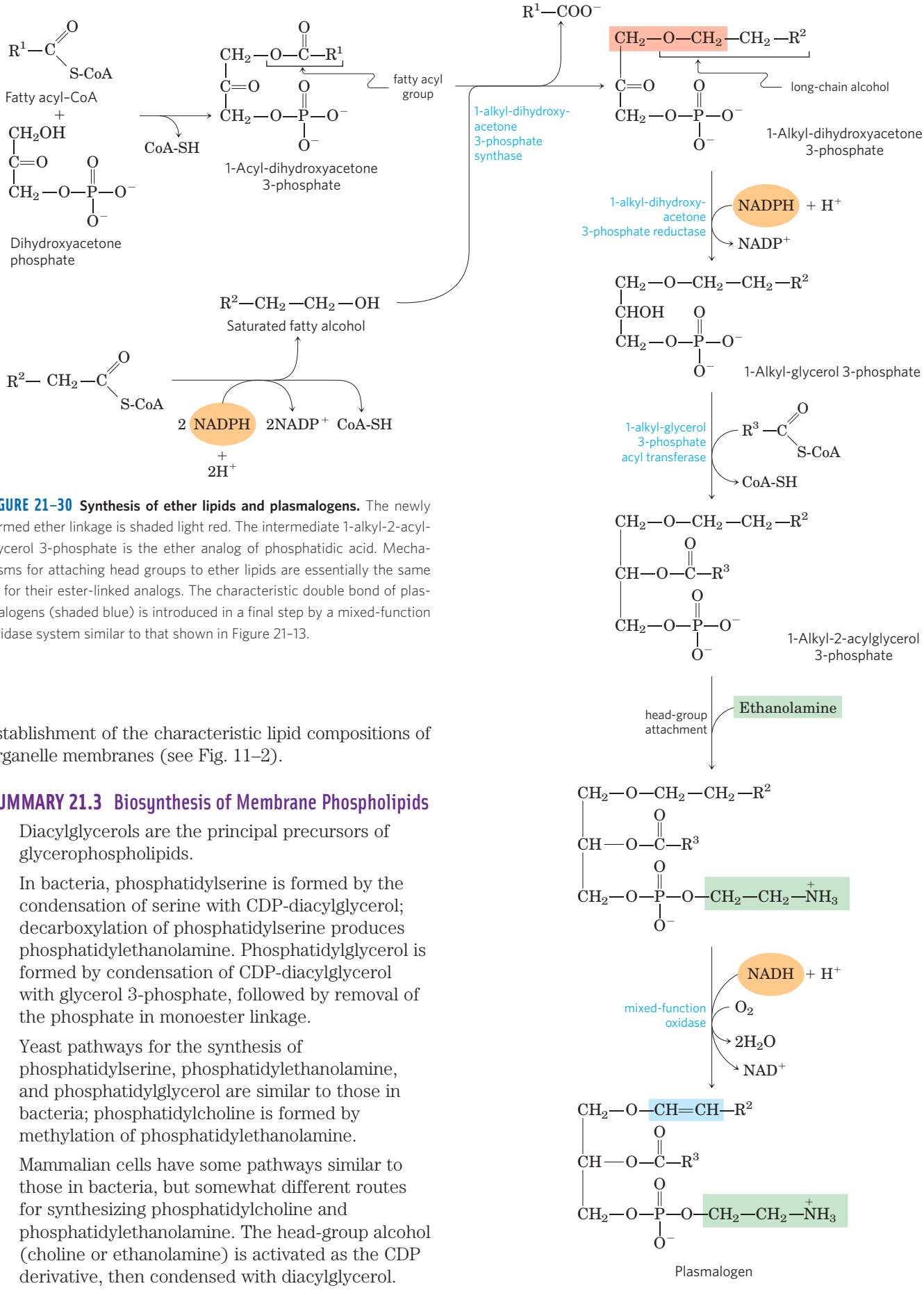

FIGURE 21–30 Synthesis of ether lipids and plasmalogens. The newly formed ether linkage is shaded light red. The intermediate 1-alkyl-2-acylglycerol 3-phosphate is the ether analog of phosphatidic acid. Mechanisms for attaching head groups to ether lipids are essentially the same as for their ester-linked analogs. The characteristic double bond of plasmalogens (shaded blue) is introduced in a final step by a mixed-function oxidase system similar to that shown in Figure 21–13.

establishment of the characteristic lipid compositions of organelle membranes (see Fig. 11–2).

SUMMARY 21.3 Biosynthesis of Membrane Phospholipids

- Diacylglycerols are the principal precursors of glycerophospholipids.
- In bacteria, phosphatidylserine is formed by the condensation of serine with CDP-diacylglycerol; decarboxylation of phosphatidylserine produces phosphatidylethanolamine. Phosphatidylglycerol is formed by condensation of CDP-diacylglycerol with glycerol 3-phosphate, followed by removal of the phosphate in monoester linkage.
- Yeast pathways for the synthesis of phosphatidylserine, phosphatidylethanolamine, and phosphatidylglycerol are similar to those in bacteria; phosphatidylcholine is formed by methylation of phosphatidylethanolamine.
- Mammalian cells have some pathways similar to those in bacteria, but somewhat different routes for synthesizing phosphatidylcholine and phosphatidylethanolamine. The head-group alcohol (choline or ethanolamine) is activated as the CDP derivative, then condensed with diacylglycerol.

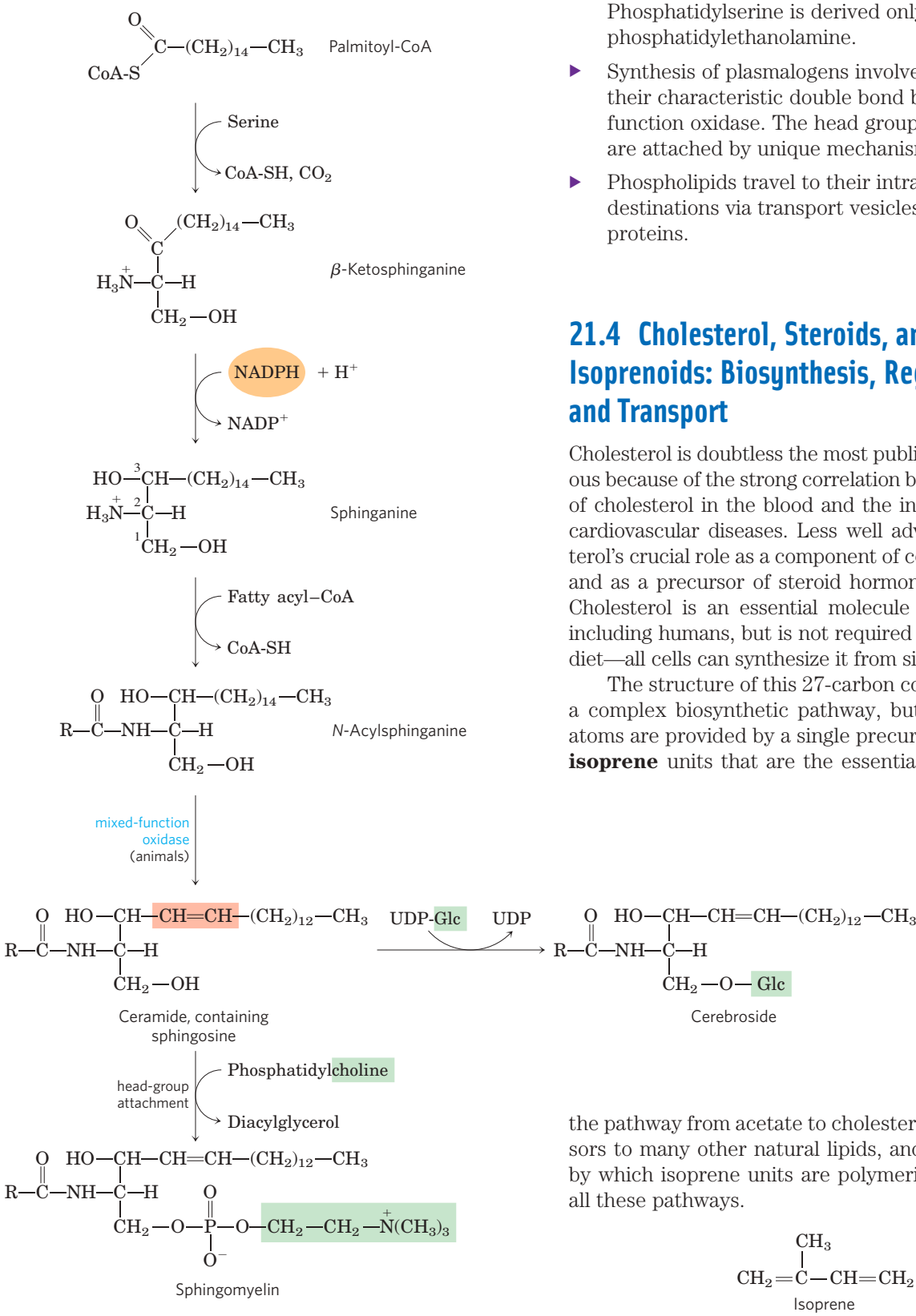

FIGURE 21–31 Biosynthesis of sphingolipids. Condensation of palmitoyl-CoA and serine (forming β-ketosphinganine) followed by reduction with NADPH yields sphinganine, which is then acylated to *N*-acylsphinganine (a ceramide). In animals, a double bond (shaded light red) is created by a mixed-function oxidase before the final addition of a head group: phosphatidylcholine, to form sphingomyelin, or glucose, to form a cerebroside.

Phosphatidylserine is derived only from phosphatidylethanolamine.

- Synthesis of plasmalogens involves formation of their characteristic double bond by a mixed-function oxidase. The head groups of sphingolipids are attached by unique mechanisms.
- Phospholipids travel to their intracellular destinations via transport vesicles or specific proteins.

21.4 Cholesterol, Steroids, and Isoprenoids: Biosynthesis, Regulation, and Transport

Cholesterol is doubtless the most publicized lipid, notorious because of the strong correlation between high levels of cholesterol in the blood and the incidence of human cardiovascular diseases. Less well advertised is cholesterol's crucial role as a component of cellular membranes and as a precursor of steroid hormones and bile acids. Cholesterol is an essential molecule in many animals, including humans, but is not required in the mammalian diet—all cells can synthesize it from simple precursors.

The structure of this 27-carbon compound suggests a complex biosynthetic pathway, but all of its carbon atoms are provided by a single precursor—acetate. The **isoprene** units that are the essential intermediates in the pathway from acetate to cholesterol are also precursors to many other natural lipids, and the mechanisms by which isoprene units are polymerized are similar in all these pathways.

We begin with an account of the main steps in the biosynthesis of cholesterol from acetate, and then discuss the transport of cholesterol in the blood, its uptake by cells, the normal regulation of cholesterol synthesis, and its regulation in those with defects in cholesterol uptake or transport. We next consider other cellular components

derived from cholesterol, such as bile acids and steroid hormones. Finally, an outline of the biosynthetic pathways to some of the many compounds derived from isoprene units, which share early steps with the pathway to cholesterol, illustrates the extraordinary versatility of isoprenoid condensations in biosynthesis.

Cholesterol Is Made from Acetyl-CoA in Four Stages

Cholesterol, like long-chain fatty acids, is made from acetyl-CoA. But the assembly plan of cholesterol is quite different from that of long-chain fatty acids. In early experiments, animals were fed acetate labeled with ^{14}C in either the methyl carbon or the carboxyl carbon. The pattern of labeling in the cholesterol isolated from the two groups of animals **(Fig. 21–32)** provided the blueprint for working out the enzymatic steps in cholesterol biosynthesis.

Synthesis takes place in four stages, as shown in **Figure 21–33**: ❶ condensation of three acetate units to form a six-carbon intermediate, mevalonate; ❷ conversion of mevalonate to activated isoprene units; ❸ polymerization of six 5-carbon isoprene units to form the 30-carbon linear squalene; and ❹ cyclization of squalene to form the four rings of the steroid nucleus, with a further series of changes (oxidations, removal or migration of methyl groups) to produce cholesterol.

Stage ❶ Synthesis of Mevalonate from Acetate The first stage in cholesterol biosynthesis leads to the intermediate **mevalonate (Fig. 21–34)**. Two molecules of acetyl-CoA condense to form acetoacetyl-CoA, which condenses with a third molecule of acetyl-CoA to yield the six-carbon compound **β-hydroxy-β-methylglutaryl-CoA (HMG-CoA)**. These first two reactions are catalyzed by **acetyl-CoA acetyl transferase** and **HMG-CoA synthase**, respectively. The cytosolic HMG-CoA synthase in this pathway is distinct from the mitochondrial isozyme that catalyzes HMG-CoA synthesis in ketone body formation (see Fig. 17–19).

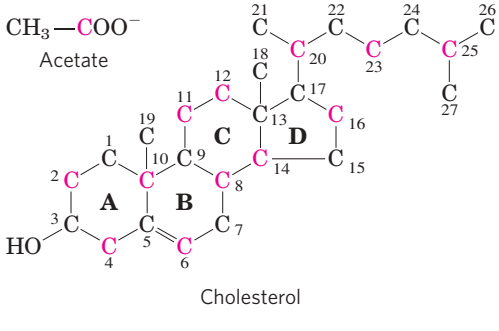

FIGURE 21–32 Origin of the carbon atoms of cholesterol. This can be deduced from tracer experiments with acetate labeled in the methyl carbon (black) or the carboxyl carbon (red). The individual rings in the fused-ring system are designated A through D.

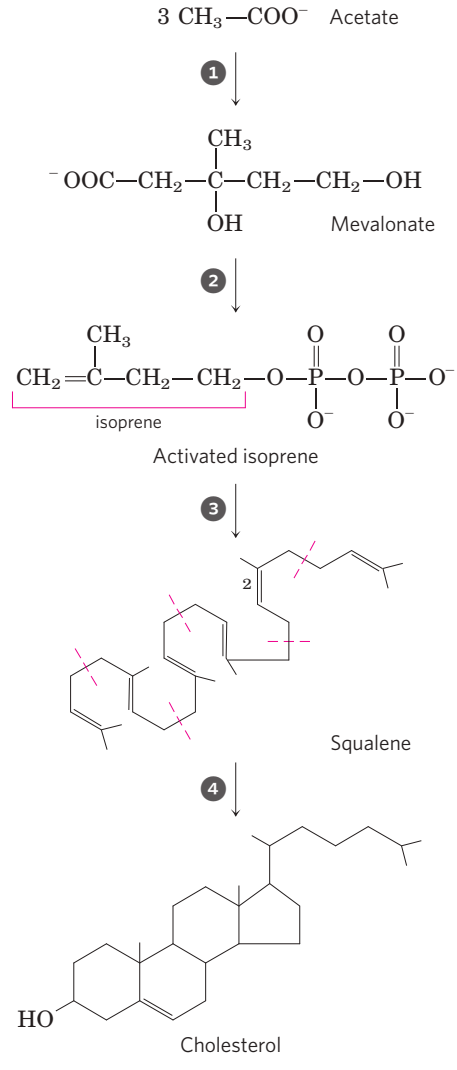

FIGURE 21–33 Summary of cholesterol biosynthesis. The four stages are discussed in the text. Isoprene units in squalene are set off by red dashed lines.

The third reaction is the committed step: reduction of HMG-CoA to mevalonate, for which each of two molecules of NADPH donates two electrons. **HMG-CoA reductase**, an integral membrane protein of the smooth ER, is the major point of regulation on the pathway to cholesterol, as we shall see.

Stage ❷ Conversion of Mevalonate to Two Activated Isoprenes In the next stage of cholesterol synthesis, three phosphate groups are transferred from three ATP molecules to mevalonate **(Fig. 21–35)**. The phosphate attached to the C-3 hydroxyl group of mevalonate in the intermediate 3-phospho-5-pyrophosphomevalonate is a good leaving group; in the next step, both this phosphate and the nearby carboxyl group leave, producing a double bond in the five-carbon product, **Δ^3-isopentenyl pyrophosphate**. This is the first of the two activated isoprenes central to cholesterol formation. Isomerization

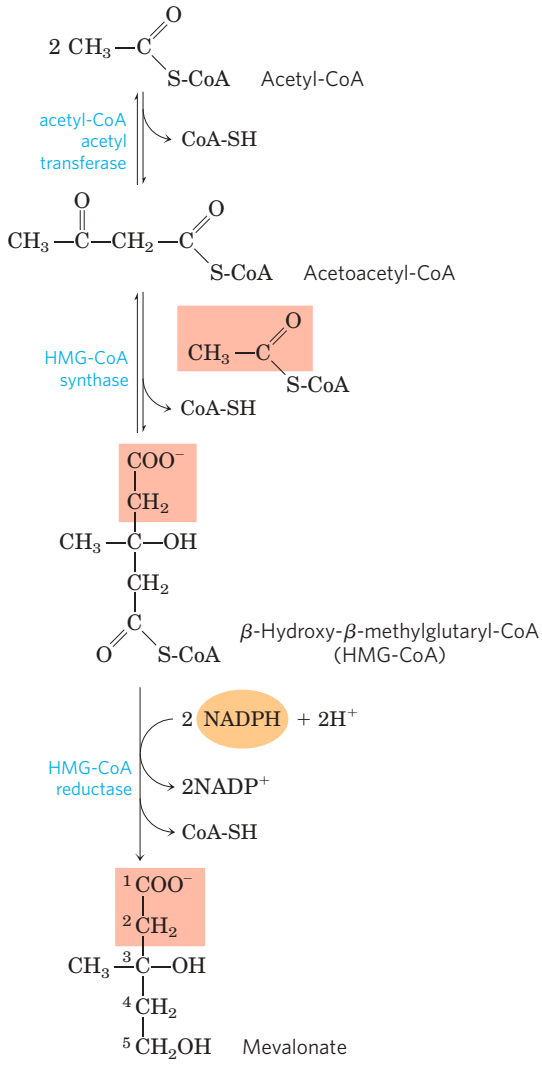

FIGURE 21–34 Formation of mevalonate from acetyl-CoA. The origin of C-1 and C-2 of mevalonate from acetyl-CoA is shaded light red.

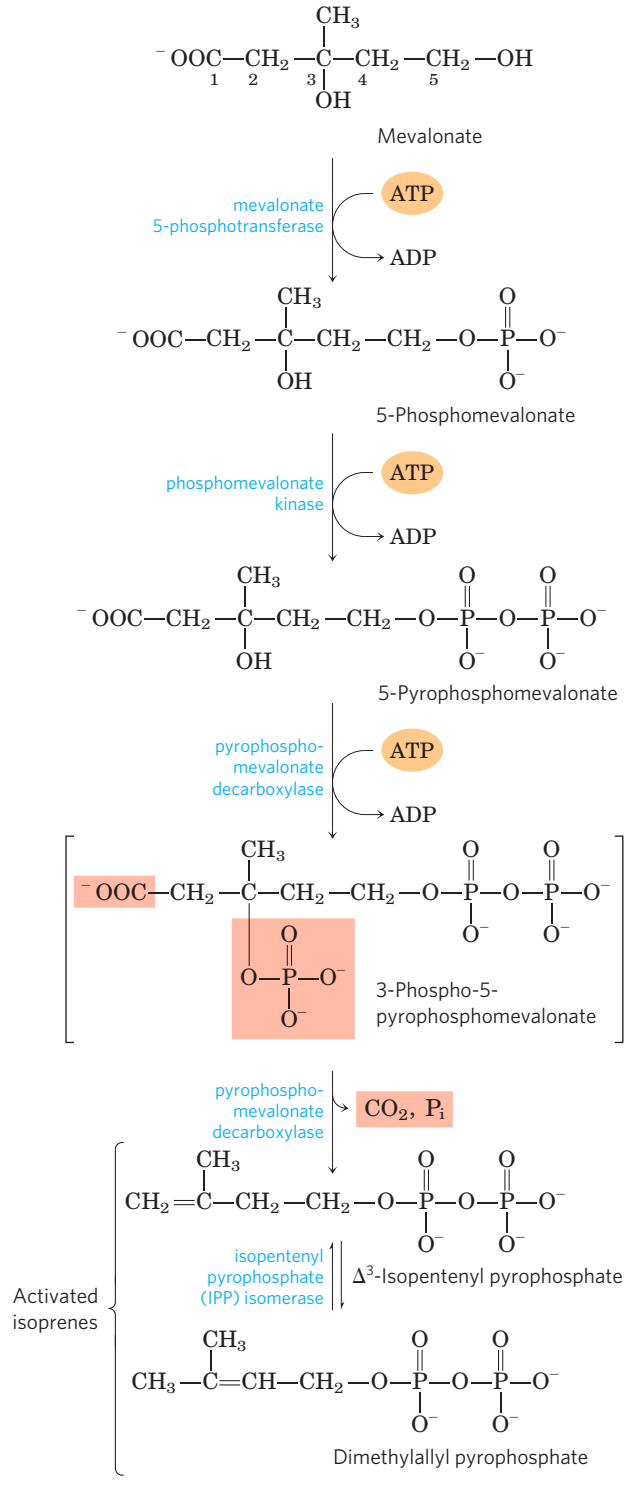

FIGURE 21–35 Conversion of mevalonate to activated isoprene units. Six of these activated units combine to form squalene (see Fig. 21–36). The leaving groups of 3-phospho-5-pyrophosphomevalonate are shaded light red. The bracketed intermediate is hypothetical.

of Δ^3-isopentenyl pyrophosphate yields the second activated isoprene, **dimethylallyl pyrophosphate**. Synthesis of isopentenyl pyrophosphate in the cytoplasm of plant cells follows the pathway described here. However, plant chloroplasts and many bacteria use a mevalonate-independent pathway. This alternative pathway does not occur in animals, so it is an attractive target for the development of new antibiotics.

Stage ❸ Condensation of Six Activated Isoprene Units to Form Squalene Isopentenyl pyrophosphate and dimethylallyl pyrophosphate now undergo a head-to-tail condensation, in which one pyrophosphate group is displaced and a 10-carbon chain, **geranyl pyrophosphate**, is formed **(Fig. 21–36)**. (The "head" is the end to which pyrophosphate is joined.) Geranyl pyrophosphate undergoes another head-to-tail condensation with isopentenyl pyrophosphate, yielding the 15-carbon intermediate **farnesyl pyrophosphate**. Finally, two molecules of farnesyl pyrophosphate join head to head, with the elimination of both pyrophosphate groups, to form **squalene**.

The common names of these intermediates derive from the sources from which they were first isolated.

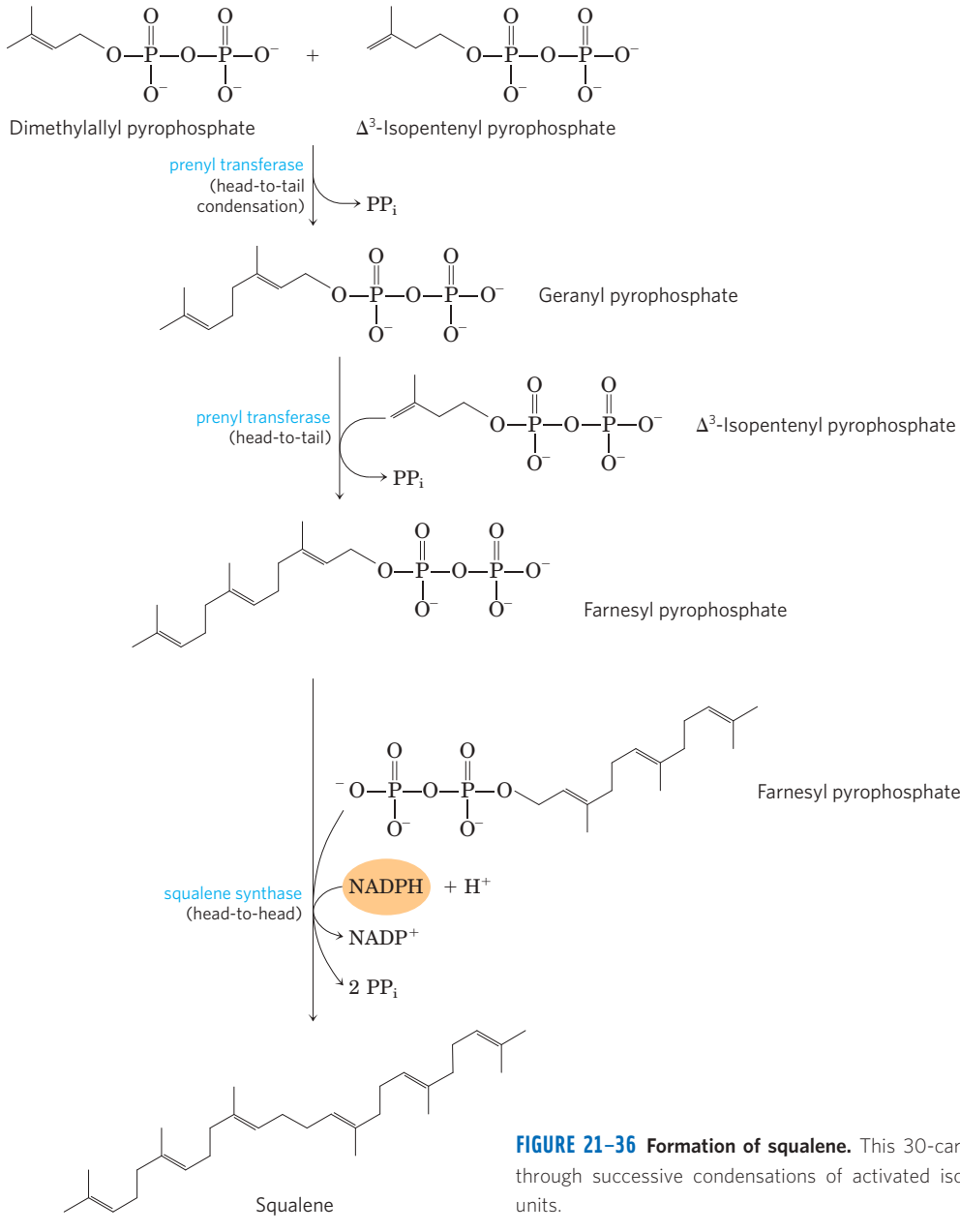

FIGURE 21–36 Formation of squalene. This 30-carbon structure arises through successive condensations of activated isoprene (five-carbon) units.

Geraniol, a component of rose oil, has the aroma of geraniums, and farnesol is an aromatic compound found in the flowers of the Farnese acacia tree. Many natural scents of plant origin are synthesized from isoprene units. Squalene, first isolated from the liver of sharks (genus *Squalus*), has 30 carbons, 24 in the main chain and 6 in the form of methyl group branches.

Stage ❹ Conversion of Squalene to the Four-Ring Steroid Nucleus When the squalene molecule is represented as in **Figure 21–37**, the relationship of its linear structure to the cyclic structure of the sterols becomes apparent. All sterols have the four fused rings that form the steroid nucleus, and all are alcohols, with a hydroxyl group at C-3—thus the name "sterol." The action of **squalene monooxygenase** adds one oxygen atom from O_2 to the end of the squalene chain, forming an epoxide. This enzyme is another mixed-function oxidase (Box 21–1); NADPH reduces the other oxygen atom of O_2 to H_2O. The double bonds of the product, **squalene 2,3-epoxide**, are positioned so that a remarkable concerted reaction can convert the linear squalene epoxide to a cyclic structure. In animal cells, this cyclization results in the formation of **lanosterol**, which contains the four rings characteristic of the steroid nucleus. Lanosterol is finally converted to cholesterol in a series of about 20 reactions that include the migration of some methyl groups and the removal of others. Elucidation of this extraordinary biosynthetic pathway, one of the most complex known, was accomplished by Konrad Bloch, Feodor Lynen, John Cornforth, and George Popják in the late 1950s.


Konrad Bloch, 1912–2000


Feodor Lynen, 1911–1979


John Cornforth

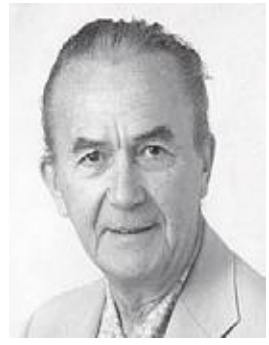
George Popják, 1914–1998

Cholesterol is the sterol characteristic of animal cells; plants, fungi, and protists make other, closely related sterols instead. They use the same synthetic pathway as far as squalene 2,3-epoxide, at which point the pathways diverge slightly, yielding other sterols, such as stigmasterol in many plants and ergosterol in fungi (Fig. 21–37).

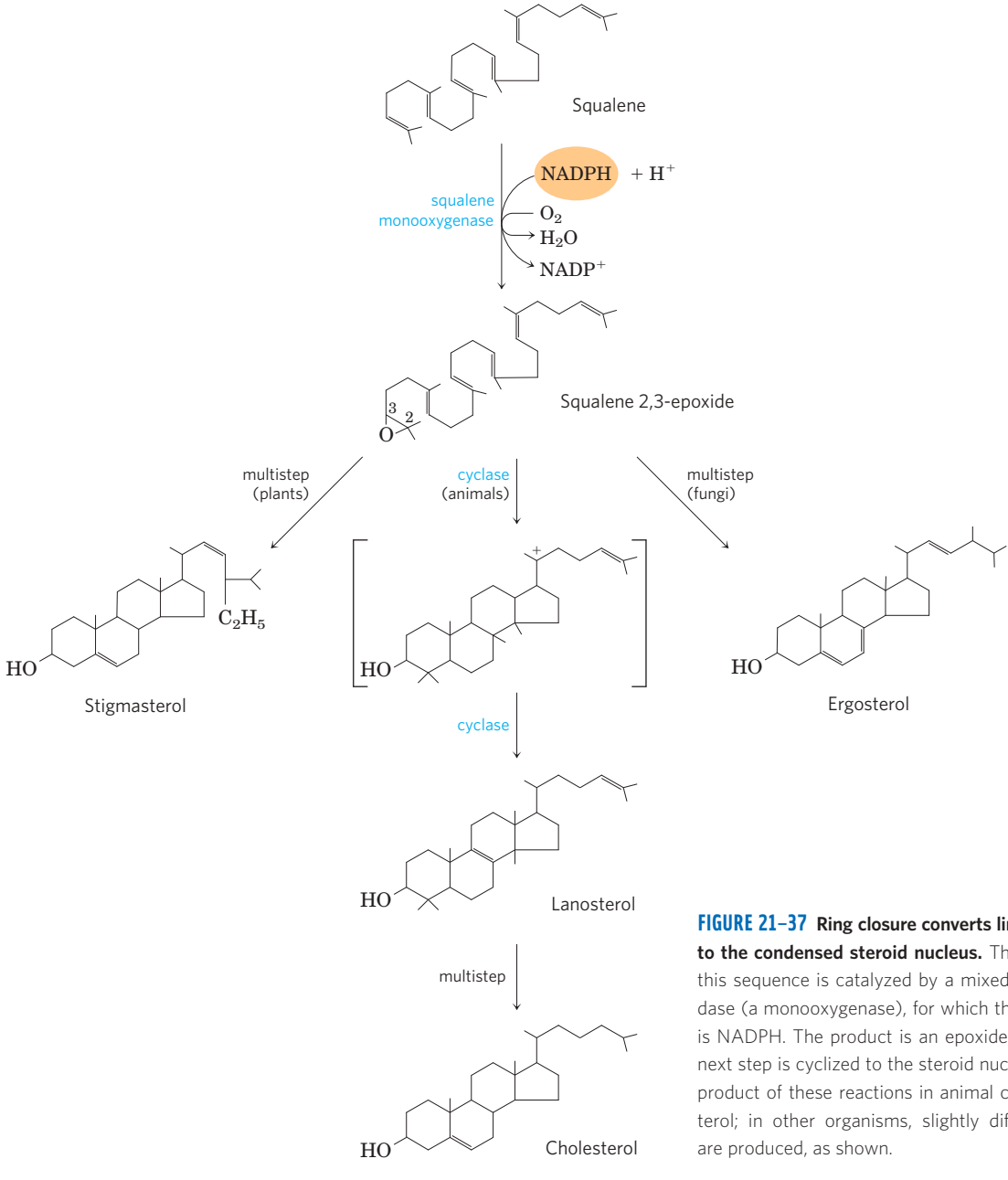

FIGURE 21–37 Ring closure converts linear squalene to the condensed steroid nucleus. The first step in this sequence is catalyzed by a mixed-function oxidase (a monooxygenase), for which the cosubstrate is NADPH. The product is an epoxide, which in the next step is cyclized to the steroid nucleus. The final product of these reactions in animal cells is cholesterol; in other organisms, slightly different sterols are produced, as shown.

WORKED EXAMPLE 21–1 Energetic Cost of Squalene Synthesis

What is the energetic cost of the synthesis of squalene from acetyl-CoA, in number of ATP per molecule of squalene synthesized?

Solution: In the pathway from acetyl-CoA to squalene, ATP is consumed only in the steps that convert mevalonate to the activated isoprene precursors of squalene. Three ATP molecules are used to create each of the six activated isoprenes required to construct squalene, for a total cost of 18 ATP molecules.

Cholesterol Has Several Fates

Most of the cholesterol synthesis in vertebrates takes place in the liver. A small fraction of the cholesterol made there is incorporated into the membranes of hepatocytes, but most of it is exported in one of three forms: bile acids, biliary cholesterol, or cholesteryl esters **(Fig. 21–38)**. Small quantities of oxysterols such as 25-hydroxycholesterol are formed in the liver, and act as regulators of cholesterol synthesis (see below). In other tissues, cholesterol is converted into steroid hormones (in the adrenal cortex and gonads, for example; see Fig. 10–19) or vitamin D hormone (i.e., in the liver and kidney; see Fig. 10–20). Such hormones are extremely potent biological signals acting through nuclear receptor proteins.

One of the three forms of cholesterol exported from the liver is bile, a fluid stored in the gallbladder and excreted into the small intestine to aid in the digestion of fat-containing meals. Its principal components are **bile acids** and their salts—both relatively hydrophilic cholesterol derivatives synthesized in the liver that serve as emulsifiers in the intestine, converting large particles of fat into tiny micelles and thereby greatly increasing the surface at which digestive lipases can act (see Fig. 17–1). Bile also contains much smaller amounts of cholesterol.

Cholesteryl esters are formed in the liver through the action of **acyl-CoA–cholesterol acyl transferase (ACAT)**. This enzyme catalyzes the transfer of a fatty acid from coenzyme A to the hydroxyl group of cholesterol (Fig. 21–38), converting the cholesterol to a more hydrophobic form and preventing it from entering membranes. Cholesteryl esters are transported in secreted lipoprotein particles to other tissues that use cholesterol, or they are stored in the liver in lipid droplets.

Cholesterol and Other Lipids Are Carried on Plasma Lipoproteins

Cholesterol and cholesteryl esters, like triacylglycerols and phospholipids, are essentially insoluble in water, yet must be moved from the tissue of origin to the tissues in which they will be stored or consumed. To facilitate their transport, they are carried in the blood plasma as **plasma lipoproteins**, macromolecular complexes of specific carrier proteins, called **apolipoproteins**, and various combinations of phospholipids, cholesterol, cholesteryl esters, and triacylglycerols.

Apolipoproteins ("apo" designates the protein in its lipid-free form) combine with lipids to form several

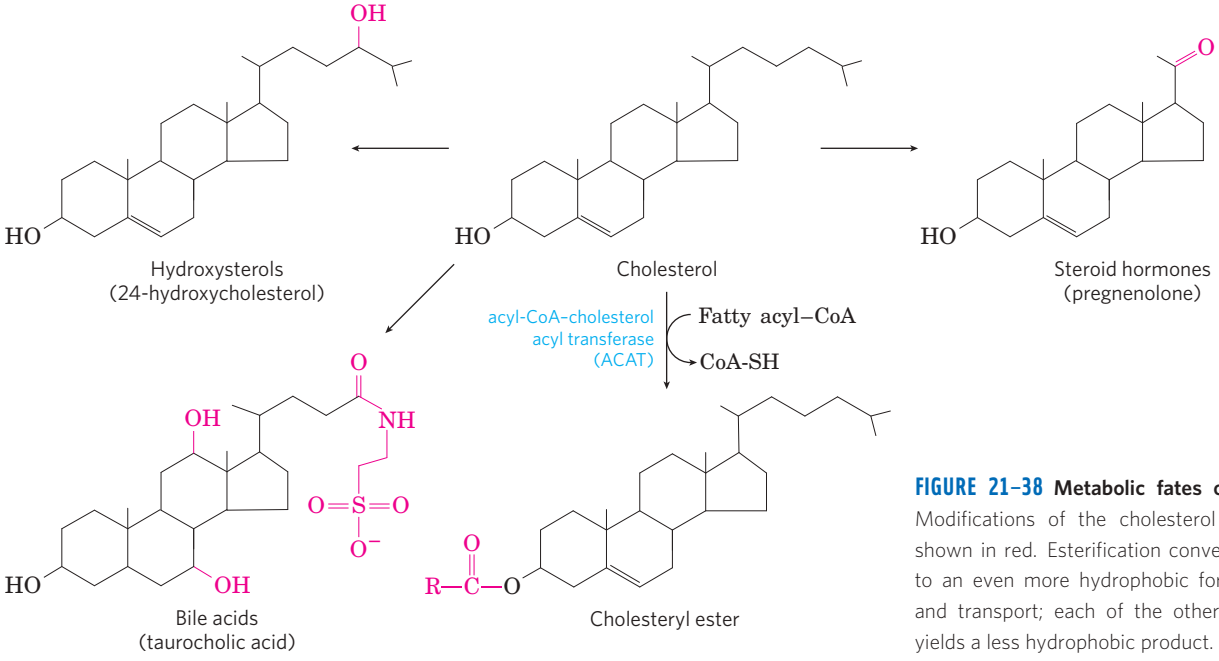

FIGURE 21–38 Metabolic fates of cholesterol. Modifications of the cholesterol structure are shown in red. Esterification converts cholesterol to an even more hydrophobic form for storage and transport; each of the other modifications yields a less hydrophobic product.

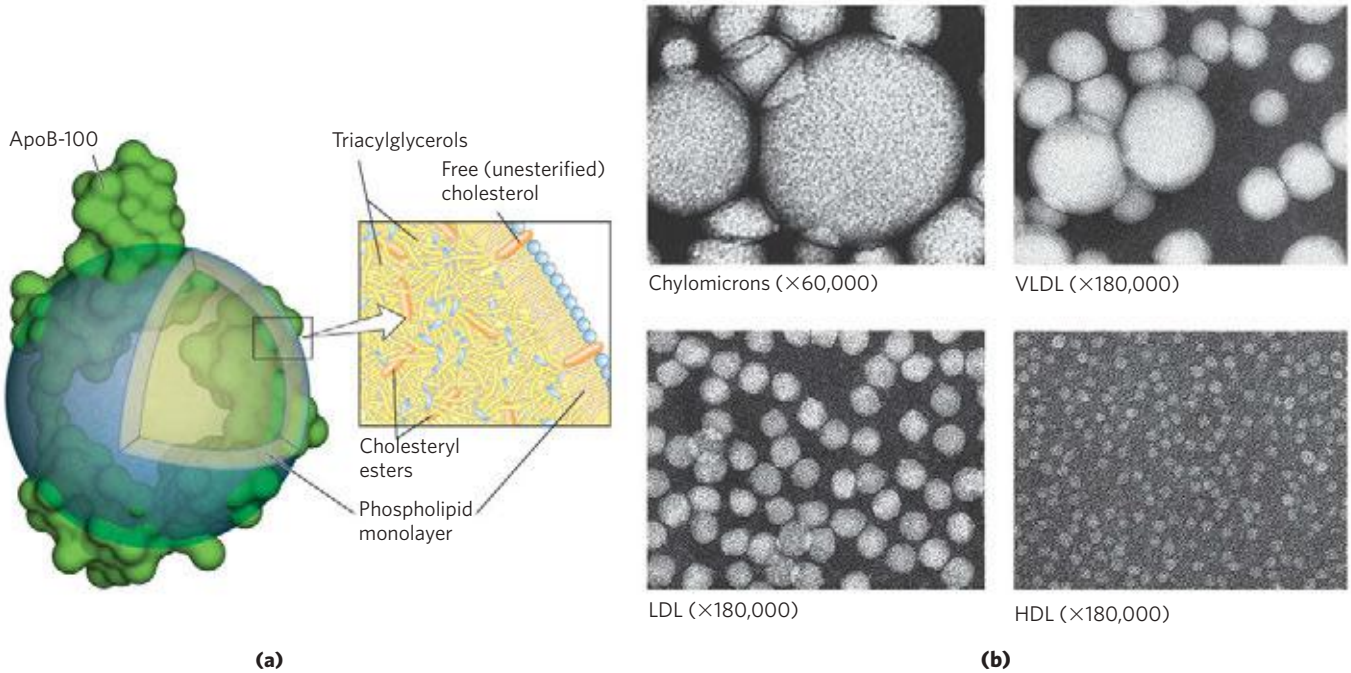

FIGURE 21–39 Lipoproteins. (a) Structure of a low-density lipoprotein (LDL). Apolipoprotein B-100 (apoB-100) is one of the largest single polypeptide chains known, with 4,636 amino acid residues (M_r 512,000). One particle of LDL contains a core with about 1,500 molecules of cholesteryl esters, surrounded by a shell composed of about 500 more molecules of cholesterol, 800 molecules of phospholipids, and one molecule of apoB-100. **(b)** Four classes of lipoproteins, visualized in the electron microscope after negative staining. Clockwise from top left: chylomicrons, 50 to 200 nm in diameter; VLDL, 28 to 70 nm; HDL, 8 to 11 nm; and LDL, 20 to 25 nm. The particle sizes given are those measured for these samples; particle sizes vary considerably in different preparations. For properties of lipoproteins, see Table 21–1.

classes of lipoprotein particles, spherical complexes with hydrophobic lipids in the core and hydrophilic amino acid side chains at the surface **(Fig. 21–39a)**. Different combinations of lipids and proteins produce particles of different densities, ranging from chylomicrons to high-density lipoproteins. These particles can be separated by ultracentrifugation (Table 21–1) and visualized by electron microscopy (Fig. 21–39b).

Each class of lipoprotein has a specific function, determined by its point of synthesis, lipid composition, and apolipoprotein content. At least ten distinct apolipoproteins are found in the lipoproteins of human plasma (Table 21–2), distinguishable by their size, their reactions with specific antibodies, and their characteristic distribution in the lipoprotein classes. These protein components act as signals, targeting lipoproteins to specific tissues or activating enzymes that act on the lipoproteins. They have also been implicated in disease; Box 21–2 describes a link between apoE and Alzheimer disease. **Figure 21–40** provides an overview of the formation and transport of the lipoproteins in mammals. The numbered steps in the following discussion refer to this figure.

Chylomicrons, discussed in Chapter 17 in connection with the movement of dietary triacylglycerols from the intestine to other tissues, are the largest of the lipoproteins and the least dense, containing a high proportion of triacylglycerols (see Fig. 17–2). ❶ Chylomicrons

TABLE 21–1 Major Classes of Human Plasma Lipoproteins: Some Properties

Lipoprotein	Density (g/mL)	Composition (wt %)				
		Protein	Phospholipids	Free cholesterol	Cholesteryl esters	Triacylglycerols
Chylomicrons	<1.006	2	9	1	3	85
VLDL	0.95–1.006	10	18	7	12	50
LDL	1.006–1.063	23	20	8	37	10
HDL	1.063–1.210	55	24	2	15	4

Source: Modified from Kritchevsky, D. (1986) Atherosclerosis and nutrition. *Nutr. Int.* 2, 290–297.

TABLE 21–2 Apolipoproteins of the Human Plasma Lipoproteins

Apolipoprotein	Polypeptide molecular weight	Lipoprotein association	Function (if known)
ApoA-I	28,100	HDL	Activates LCAT; interacts with ABC transporter
ApoA-II	17,400	HDL	Inhibits LCAT
ApoA-IV	44,500	Chylomicrons, HDL	Activates LCAT; cholesterol transport/clearance
ApoB-48	242,000	Chylomicrons	Cholesterol transport/clearance
ApoB-100	512,000	VLDL, LDL	Binds to LDL receptor
ApoC-I	7,000	VLDL, HDL	
ApoC-II	9,000	Chylomicrons, VLDL, HDL	Activates lipoprotein lipase
ApoC-III	9,000	Chylomicrons, VLDL, HDL	Inhibits lipoprotein lipase
ApoD	32,500	HDL	
ApoE	34,200	Chylomicrons, VLDL, HDL	Triggers clearance of VLDL and chylomicron remnants

Source: Modified from Vance, D.E. & Vance, J.E. (eds) (2008) *Biochemistry of Lipids and Membranes,* 5th edn, Elsevier Science Publishing.

are synthesized from dietary fats in the ER of enterocytes, epithelial cells that line the small intestine. The chylomicrons then move through the lymphatic system and enter the bloodstream via the left subclavian vein. The apolipoproteins of chylomicrons include apoB-48 (unique to this class of lipoproteins), apoE, and apoC-II (Table 21–2). ❷ ApoC-II activates lipoprotein lipase in the capillaries of adipose, heart, skeletal muscle, and lactating mammary tissues, allowing the release of free fatty acids (FFA) to these tissues. Chylomicrons thus carry dietary fatty acids to tissues where they will be consumed or stored as fuel. ❸ The remnants of chylomicrons (depleted of most of their triacylglycerols but still containing cholesterol, apoE, and apoB-48) move through the bloodstream to the liver. Receptors in the liver bind to the apoE in the chylomicron remnants and mediate their uptake by endocytosis. ❹ In the liver, the remnants release their cholesterol and are degraded in lysosomes. This pathway from dietary cholesterol to the liver is the **exogenous pathway** (blue arrows in Fig. 21–40).

When the diet contains more fatty acids and cholesterol than are needed immediately as fuel or precursors to other molecules, they are ❺ converted to triacylglycerols or cholesteryl esters in the liver and packaged with specific apolipoproteins into **very-low-density lipoprotein (VLDL)**. Excess carbohydrate in the diet can also be converted to triacylglycerols in the liver and exported as VLDL. In addition to triacylglycerols and cholesteryl esters, VLDL contains apoB-100, apoC-I,

BOX 21–2 MEDICINE ApoE Alleles Predict Incidence of Alzheimer Disease

In the human population there are three common variants, or alleles, of the gene encoding apolipoprotein E. The most common, accounting for about 78% of human apoE alleles, is *APOE3*; alleles *APOE4* and *APOE2* account for 15% and 7%, respectively. The *APOE4* allele is particularly common in humans with Alzheimer disease, and the link is highly predictive. Individuals who inherit *APOE4* have an increased risk of late-onset Alzheimer disease. Those who are homozygous for *APOE4* have a 16-fold increased risk of developing the disease; for those who do, the mean age of onset is just under 70 years. For people who inherit two copies of *APOE3*, by contrast, the mean age of onset of Alzheimer disease exceeds 90 years.

The molecular basis for the association between apoE-4 and Alzheimer disease is not yet known. It is also not clear how apoE-4 might affect the growth of the amyloid fibers that appear to be the primary causative agents of the disease (see Fig. 4–32). Speculation has focused on a possible role for apoE in stabilizing the cytoskeletal structure of neurons. The apoE-2 and apoE-3 proteins bind to a number of proteins associated with neuronal microtubules, whereas apoE-4 does not. This may accelerate the death of neurons. Whatever the mechanism proves to be, these observations promise to expand our understanding of the biological functions of apolipoproteins.

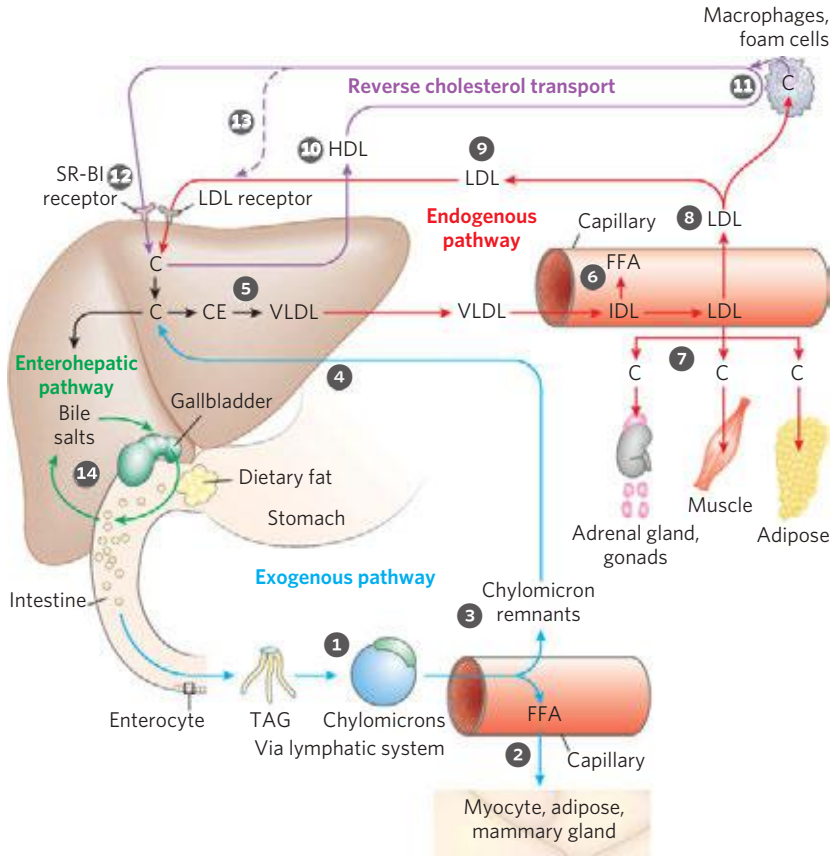

FIGURE 21–40 Lipoproteins and lipid transport. Lipids are transported in the bloodstream as lipoproteins, which exist as several variants that have different functions, different protein and lipid compositions (see Tables 21–1, 21–2), and thus different densities. Numbered steps are described in the text. In the exogenous pathway (blue arrows), dietary lipids are packaged into chylomicrons; much of their triacylglycerol content is released by lipoprotein lipase to adipose and muscle tissues during transport through capillaries. Chylomicron remnants (containing largely protein and cholesterol) are taken up by the liver. Bile salts produced in the liver aid in dispersing dietary fats, and are then reabsorbed in the enterohepatic pathway (green arrows). In the endogenous pathway (red arrows), lipids synthesized or packaged in the liver are delivered to peripheral tissues by VLDL. Extraction of lipid from VLDL (along with loss of some apolipoproteins) gradually converts some of it to LDL, which delivers cholesterol to extrahepatic tissues or returns to the liver. Excess cholesterol in extrahepatic tissues is transported back to the liver as HDL in reverse cholesterol transport (purple arrows). C represents cholesterol; CE represents cholesteryl ester.

apoC-II, apoC-III, and apoE (Table 21–2). VLDL is transported in the blood from the liver to muscle and adipose tissue. ❻ In the capillaries of these tissues, apoC-II activates lipoprotein lipase, which catalyzes the release of free fatty acids from triacylglycerols in the VLDL. Adipocytes take up these fatty acids, reconvert them to triacylglycerols, and store the products in intracellular lipid droplets; myocytes, in contrast, primarily oxidize the fatty acids to supply energy. When the insulin level is high (after a meal), VLDL serves primarily to convey lipids from the diet to adipose tissue for storage there. In the fasting state between meals, the fatty acids used to produce VLDL in the liver originate primarily from the adipose tissue, and the principal VLDL target is myocytes of the heart and skeletal muscle.

The loss of triacylglycerol converts some VLDL to VLDL remnants (also called intermediate-density lipoprotein, IDL). Further removal of triacylglycerol from IDL (remnants) produces **low-density lipoprotein (LDL)**. Rich in cholesterol and cholesteryl esters, and containing apoB-100 as their major apolipoprotein, ❼ LDL carries cholesterol to extrahepatic tissues such as muscle, adrenal glands, and adipose tissue. These tissues have plasma membrane LDL receptors that recognize apoB-100 and mediate the uptake of cholesterol and cholesteryl esters. ❽ LDL also delivers cholesterol to macrophages, sometimes converting them into foam cells (see Fig. 21–46). ❾ LDL not taken up by peripheral tissues and cells returns to the liver and is taken up via **LDL receptors** in the hepatocyte plasma membrane. Cholesterol that enters hepatocytes by this path may be incorporated into membranes, converted to bile acids, or reesterified by ACAT (Fig. 21–38) for storage within cytosolic lipid droplets. This pathway, from VLDL formation in the liver to LDL return to the liver, is the **endogenous pathway** of cholesterol metabolism and transport (red arrows in Fig. 21–40). Accumulation of excess intracellular cholesterol is prevented by reducing the rate of cholesterol synthesis when sufficient cholesterol is available from LDL in the blood. Regulatory mechanisms to

accomplish this are described below. We will return to Figure 21–40 and other pathways of lipoprotein transport after a discussion of LDL uptake by cells.

Cholesteryl Esters Enter Cells by Receptor-Mediated Endocytosis

Each LDL particle in the bloodstream contains apoB-100, which is recognized by LDL receptors present in the plasma membranes of cells that need to take up cholesterol. **Figure 21–41** shows such a cell, in which ❶ LDL receptors are synthesized in the Golgi complex and transported to the plasma membrane, where they are available to bind apoB-100. ❷ The binding of LDL to an LDL receptor initiates endocytosis, which ❸ conveys the LDL and its receptor into the cell within an endosome. ❹ The receptor-containing portions of the endosome membrane bud off and are returned to the cell surface, to function again in LDL uptake. ❺ The endosome fuses with a lysosome, which ❻ contains enzymes that hydrolyze the cholesteryl esters, releasing cholesterol and fatty acids into the cytosol. The apoB-100 protein is also degraded to amino acids that are released to the cytosol. ApoB-100 is also present in VLDL, but its receptor-binding domain is not available for binding to the LDL receptor; conversion of VLDL to LDL exposes the receptor-binding domain of apoB-100.

This pathway for the transport of cholesterol in blood and its **receptor-mediated endocytosis** by target tissues was elucidated by Michael Brown and Joseph Goldstein. They discovered that individuals with the genetic disease **familial hypercholesterolemia (FH)** have mutations in the LDL receptor that prevent the normal uptake of LDL by liver and peripheral tissues. The result of defective LDL uptake is very high blood levels of LDL (and of the cholesterol it carries). Individuals with FH have a greatly increased probability of developing atherosclerosis, a disease of

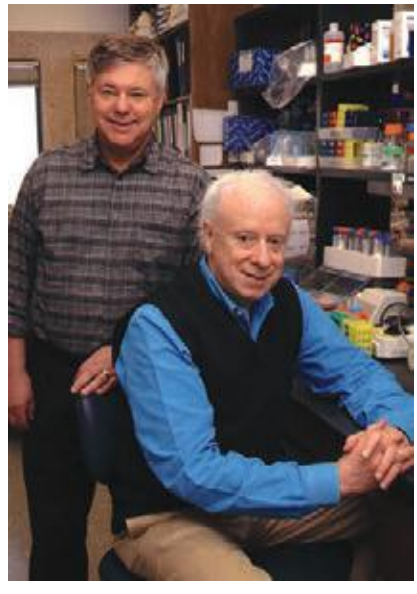

Michael Brown and Joseph Goldstein

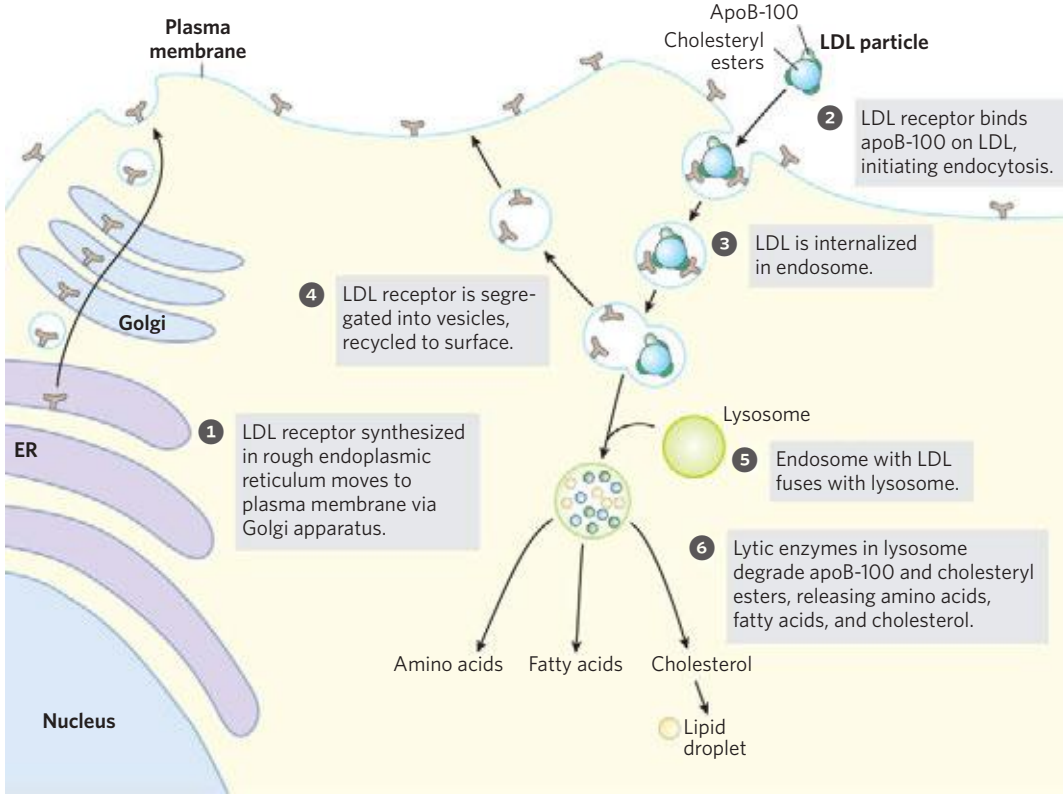

FIGURE 21–41 Uptake of cholesterol by receptor-mediated endocytosis.

the cardiovascular system in which blood vessels are occluded by cholesterol-rich plaques (see Fig. 21–46).

Niemann-Pick type-C (NPC) disease is an inherited defect in lipid storage, in which cholesterol is not transported out of the lysosomes and instead accumulates in lysosomes of liver, brain, and lung, bringing about early death. NPC is the result of a mutation in either of two genes (*NPC1*, *NPC2*) essential to moving cholesterol out of the lysosome and into the cytosol, where it can be further metabolized. *NPC1* encodes a transmembrane lysosomal protein, and *NPC2* encodes a soluble protein. These proteins act in tandem to transfer cholesterol out of the lysosome and into the cytosol for further processing or metabolism. ■

HDL Carries Out Reverse Cholesterol Transport

A fourth major lipoprotein in mammals, **high-density lipoprotein (HDL)**, originates in the liver and small intestine as small, protein-rich particles that contain relatively little cholesterol and no cholesteryl esters (⑩, Fig. 21–40). HDLs contain primarily apoA-I and other apolipoproteins (Table 21–2). They also contain the enzyme **lecithin-cholesterol acyl transferase (LCAT)**, which catalyzes the formation of cholesteryl esters from lecithin (phosphatidylcholine) and cholesterol **(Fig. 21–42)**. LCAT on the surface of nascent (newly forming) HDL particles converts the cholesterol and phosphatidylcholine of chylomicron and VLDL remnants encountered in the bloodstream to cholesteryl esters, which begin to form a core, transforming the disk-shaped nascent HDL to a mature, spherical HDL particle. ⑪ Nascent HDL can also pick up cholesterol from cholesterol-rich extrahepatic cells (including macrophages and foam cells formed from them; see below). ⑫ Mature HDL then returns to the liver, where the cholesterol is unloaded via the scavenger receptor SR-BI. ⑬ Some of the cholesteryl esters in HDL can also be transferred to LDL by the cholesteryl ester transfer protein. The HDL circuit is **reverse cholesterol transport** (purple arrows in Fig. 21–40). Much of this cholesterol is converted to bile salts in the liver and stored in the gallbladder. When a meal is ingested, bile salts are excreted into the intestine, where they disperse macroscopic pieces of fat into microscopic micelles that can be attacked by lipases. Bile salts are reabsorbed by the liver ⑭ and recirculate through the gallbladder in this **enterohepatic circulation** (green arrows in Fig. 21–40).

The mechanism of sterol unloading via the receptor SR-BI in liver and other tissues does not involve endocytosis, the mechanism used for LDL uptake. Instead, when HDL binds to SR-BI receptors in the plasma membranes of hepatocytes or steroidogenic tissues such as the adrenal gland, these receptors mediate partial and selective transfer of cholesterol and other lipids in HDL into the cell. Depleted HDL then dissociates to recirculate in the bloodstream and extract more lipids from remnants of chylomicrons and VLDL, and from cells overloaded with cholesterol, as described below.

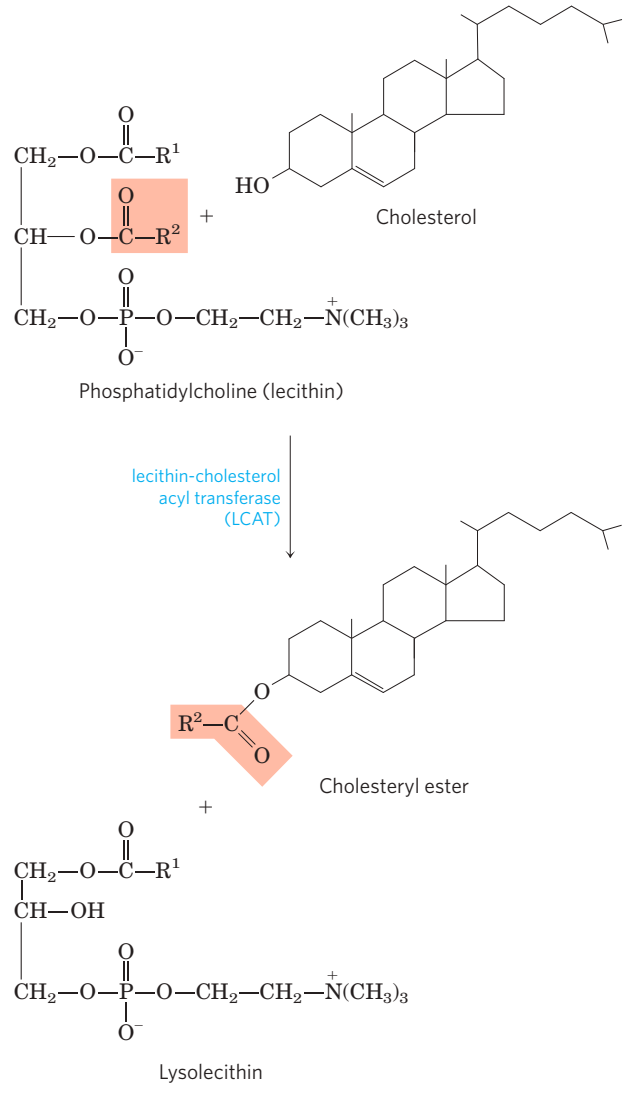

FIGURE 21–42 Reaction catalyzed by lecithin-cholesterol acyl transferase (LCAT). This enzyme is present on the surface of HDL and is stimulated by the HDL component apoA-I. Cholesteryl esters accumulate within nascent HDLs, converting them to mature HDLs.

Cholesterol Synthesis and Transport Are Regulated at Several Levels

Cholesterol synthesis is a complex and energy-expensive process. Excess cholesterol cannot be catabolized for use as fuel, and must therefore be excreted. Therefore, it is clearly advantageous to an organism to regulate the biosynthesis of cholesterol to complement dietary intake. In mammals, cholesterol production is regulated by intracellular cholesterol concentration, by the supply of ATP, and by the hormones glucagon and insulin. The committed step in the pathway to cholesterol (and a major site of regulation) is the conversion of HMG-CoA to mevalonate (Fig. 21–34), the reaction catalyzed by HMG-CoA reductase.

Short-term regulation of the *activity* of existing HMG-CoA reductase is accomplished by reversible covalent alteration—phosphorylation by the AMP-dependent protein kinase (AMPK), which senses high AMP concentration (indicating low ATP concentration). Thus, when ATP levels drop, the synthesis of cholesterol slows, and catabolic pathways for the generation of ATP are stimulated **(Fig. 21–43)**. Hormones that mediate global regulation of lipid and carbohydrate metabolism also act on HMG-CoA reductase; glucagon stimulates its phosphorylation (inactivation), and insulin promotes dephosphorylation, activating the enzyme and favoring cholesterol synthesis. These covalent regulatory mechanisms are probably not as important, quantitatively, as the mechanisms that affect the synthesis and degradation of the enzyme.

In the longer term, the *number of molecules* of HMG-CoA reductase is increased or decreased in response to the cellular concentrations of cholesterol. Regulation of HMG-CoA reductase synthesis by cholesterol is mediated by an elegant system of transcriptional regulation of the HMG-CoA gene **(Fig. 21–44)**. This gene, along with more than 20 other genes encoding enzymes that mediate the uptake and synthesis of cholesterol and unsaturated fatty acids, is controlled by a small family of proteins called **sterol regulatory element-binding proteins (SREBPs)**. When newly synthesized, these proteins are embedded in the ER. Only the soluble regulatory domain fragment of an SREBP functions as a transcriptional activator, using mechanisms discussed in Chapter 28. When cholesterol and oxysterol levels are high, SREBPs are held in the ER in a complex with another protein called **SREBP cleavage-activating protein (SCAP)**, which in turn is anchored in the ER membrane by its interaction with a third membrane protein, **Insig (*ins*ulin-*i*nduced *g*ene protein)** (Fig. 21–44a). SCAP and Insig act as sterol sensors. When sterol levels are high, the

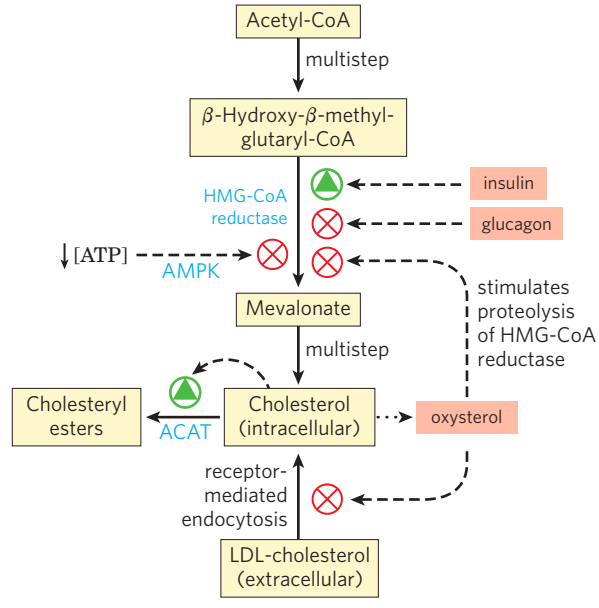

FIGURE 21–43 Regulation of cholesterol formation balances synthesis with dietary uptake and energy state. Insulin promotes dephosphorylation (activation) of HMG-CoA reductase; glucagon promotes its phosphorylation (inactivation); and the AMP-dependent protein kinase AMPK, when activated by low [ATP] relative to [AMP], phosphorylates and inactivates it. Oxysterol metabolites of cholesterol (for example, 24(*S*)-hydroxycholesterol) stimulate proteolysis of HMG-CoA reductase.

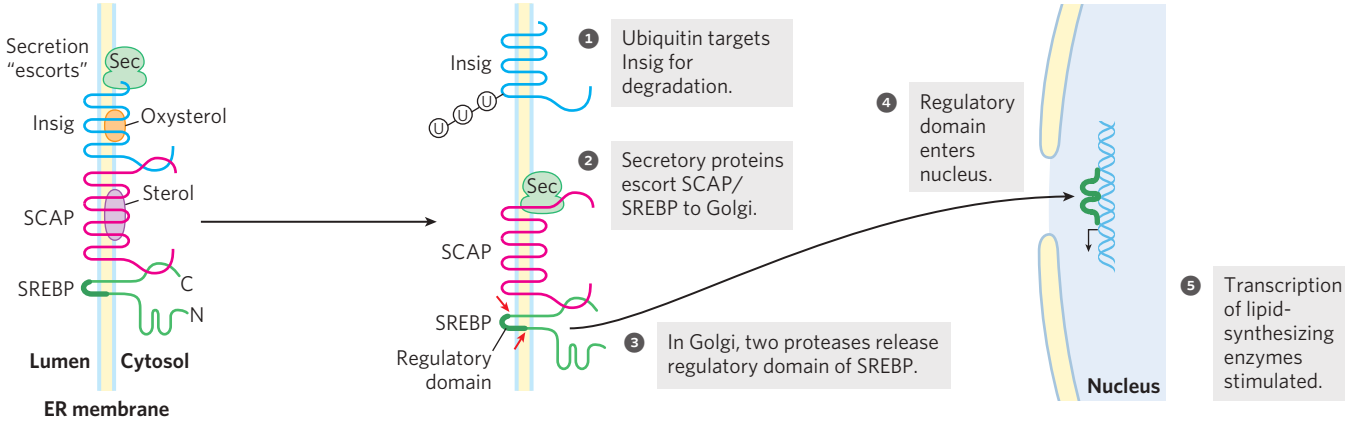

(a) High [sterol] in ER SCAP/SREBP retained in ER, bound to Insig

(b) Low [sterol] in ER Regulatory domain of SREBP released by proteolysis

(c) Increased cholesterol synthesis in ER

FIGURE 21–44 Regulation of cholesterol synthesis by SREBP. Sterol regulatory element-binding proteins (SREBPs, shown in green) are embedded in the ER when first synthesized, in a complex with the protein SREBP cleavage-activating protein (SCAP, red), which is in turn bound to Insig (blue). (*N* and *C* represent the amino and carboxyl termini of the proteins.) **(a)** When bound to SCAP and Insig, SREBPs are inactive. **(b)** When sterol levels decline, sterol-binding sites on Insig and SCAP are unoccupied, the complex migrates to the Golgi complex, and SREBP is cleaved to produce a regulatory domain, which **(c)** acts in the nucleus to increase the transcription of sterol-regulated genes. Insig is targeted for degradation by the attachment of several ubiquitin molecules.

Insig-SCAP-SREBP complex is retained in the ER membrane. When the level of sterols in the cell declines (Fig. 21–44b), the SCAP-SREBP complex is escorted by secretory proteins to the Golgi complex. There, two proteolytic cleavages of SREBP release a regulatory fragment, which enters the nucleus and activates transcription of its target genes, including HMG-CoA reductase, the LDL receptor protein, and a number of other proteins needed for lipid synthesis. When sterol levels increase sufficiently, the proteolytic release of SREBP amino-terminal domains is again blocked, and proteasome degradation of the existing active domains results in a rapid shutdown of the gene targets.

In the long term, the level of HMG-CoA reductase is also regulated by proteolytic degradation of the enzyme itself. High levels of cellular cholesterol are sensed by Insig, which triggers attachment of ubiquitin molecules to HMG-CoA reductase, leading to its degradation by proteasomes (see Fig. 27–48).

Liver X receptor (LXR) is a nuclear transcription factor activated by oxysterol ligands (reflecting high cholesterol levels), which integrates the metabolism of fatty acids, sterols, and glucose. LXRα is expressed primarily in liver, adipose tissue, and macrophages; LXRβ is present in all tissues. When bound to an oxysterol ligand, LXRs form heterodimers with a second type of nuclear receptor, the **retinoid X receptors (RXR)**, and the LXR-RXR dimer activates transcription from a set of genes **(Fig. 21–45)** including those for acetyl-CoA carboxylase (the first enzyme in fatty acid synthesis); fatty acid synthase; the cytochrome P-450 enzyme CYP7A1, required for sterol conversion to bile acid; apoproteins involved in cholesterol transport (apoC-I, apoC-II, apoD, and apoE); the ABC transporters ABCA1 and ABCG1, involved in reverse cholesterol transport (see below); GLUT4, the insulin-stimulated glucose transporter of muscle and adipose tissue; and SREBP1C. The transcriptional regulators LXR and SREBP therefore work together to achieve and maintain cholesterol homeostasis; SREBPs are activated by low levels of cellular cholesterol, and LXRs are activated by high cholesterol levels.

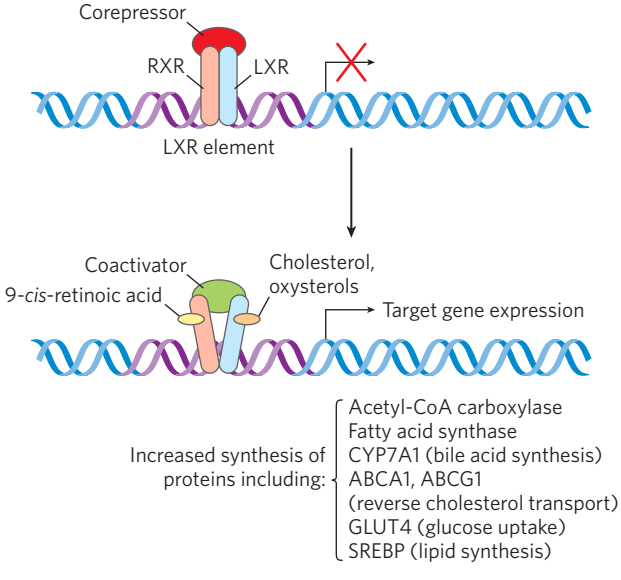

FIGURE 21–45 Action of RXR-LXR dimer on expression of genes for lipid and glucose metabolism. When their ligands are absent, RXR and LXR associate with a corepressor protein, preventing transcription of the genes associated with the LXR element (LXRE). When their respective ligands are present (9-*cis*-retinoic acid for RXR, cholesterol or oxysterols for LXR), the dimer dissociates from the corepressor, then associates with a coactivator protein. This complex binds to the LXR element and turns on the expression of the associated genes. Regulation of gene expression is a topic discussed in more detail in Chapter 28.

Finally, two other regulatory mechanisms influence cellular cholesterol level: (1) high intracellular concentrations of cholesterol activate ACAT, which increases esterification of cholesterol for storage, and (2) high cellular cholesterol levels diminish (via SREBP) transcription of the gene that encodes the LDL receptor, reducing production of the receptor and thus the uptake of cholesterol from the blood.

Dysregulation of Cholesterol Metabolism Can Lead to Cardiovascular Disease

When the sum of cholesterol synthesized and cholesterol obtained in the diet exceeds the amount required for the synthesis of membranes, bile salts, and steroids, pathological accumulations of cholesterol (plaques) can obstruct blood vessels, a condition called **atherosclerosis**. Heart failure due to occluded coronary arteries is a leading cause of death in industrialized societies. Atherosclerosis is linked to high levels of cholesterol in the blood, and particularly to high levels of LDL-cholesterol ("bad cholesterol"); there is a *negative* correlation between HDL ("good cholesterol") levels and arterial disease. Plaque formation in blood vessels is initiated when LDL containing partially oxidized fatty acyl groups adheres to and accumulates in the extracellular matrix of epithelial cells lining arteries **(Fig. 21–46)**. Immune cells (monocytes) are attracted to regions with such LDL accumulations, and they differentiate into macrophages, which take up the oxidized LDL and the cholesterol they contain. Macrophages cannot limit their uptake of sterols, and with increasing accumulation of cholesteryl esters and free cholesterol, the macrophages become **foam cells** (they appear foamy in the microscope). As excess free cholesterol accumulates in foam cells and their membranes, they undergo apoptosis. Over long periods of time, arteries become progressively occluded as plaques consisting of extracellular matrix material, scar tissue formed from smooth muscle tissue, and foam cell remnants gradually become larger. Occasionally a plaque breaks loose from the site of its formation and is carried through the blood to a narrowed region of an artery in the brain or the heart, causing a stroke or a heart attack.

In familial hypercholesterolemia, blood levels of cholesterol are extremely high and severe atherosclerosis

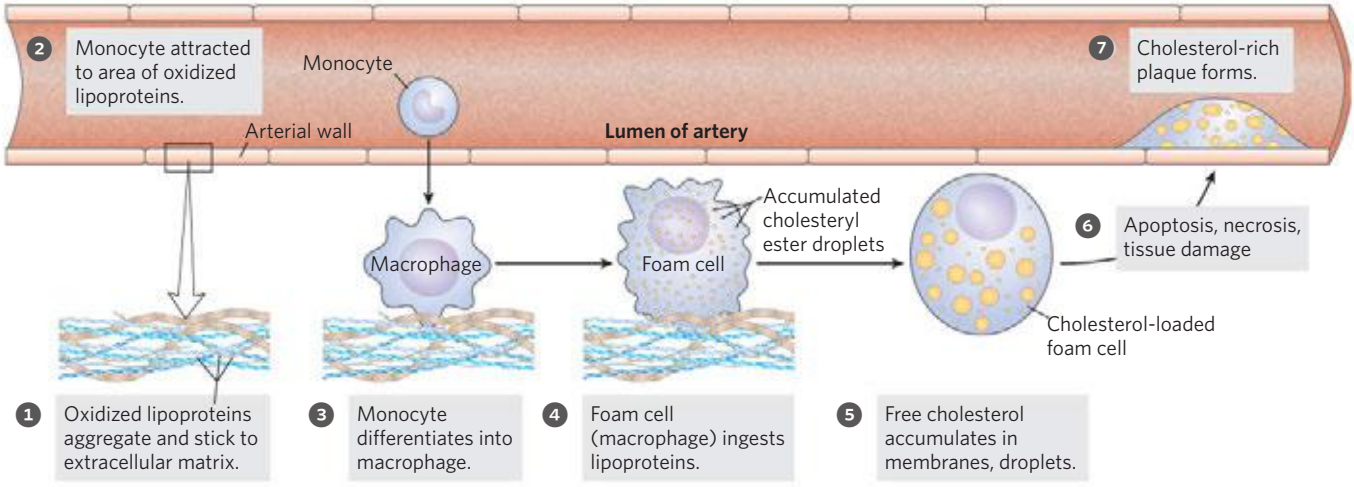

FIGURE 21–46 **Role of foam cells in formation of atherosclerotic plaques.**

BOX 21–3 MEDICINE The Lipid Hypothesis and the Development of Statins

Coronary heart disease is the leading cause of death in developed countries. The coronary arteries that bring blood to the heart become narrowed due to the formation of fatty deposits called atherosclerotic plaques (containing cholesterol, fibrous proteins, calcium deposits, blood platelets, and cell debris). Developing the link between artery occlusion (atherosclerosis) and blood cholesterol levels was a project of the twentieth century, triggering a dispute that was resolved only with the development of effective cholesterol-lowering drugs. The Framingham Heart Study is a longitudinal study, begun in 1948 and continuing today, aimed at identifying factors correlated with cardiovascular disease. About 5,000 participants from the city of Framingham, Massachusetts, underwent periodic physical examinations and lifestyle interviews. By 2002, participants of the third generation were included in the study. This monumental study led to the identification of risk factors for cardiovascular disease, including smoking, obesity, physical inactivity, diabetes, high blood pressure, and high blood cholesterol.

In 1913, N. N. Anitschkov, an experimental pathologist in St. Petersburg, Russia, published a study showing that rabbits fed a diet rich in cholesterol developed lesions very similar to the atherosclerotic plaques seen in aging humans. Anitschkov continued his work over the next few decades, publishing it in prominent western journals. Nevertheless, the work was not accepted as a model for human atherosclerosis, due to a prevailing view that the disease was a simple consequence of aging and could not be prevented. The link between serum cholesterol and atherosclerosis (the lipid hypothesis) was gradually strengthened, until some researchers in the 1960s openly suggested that therapeutic intervention might be helpful. However, controversy persisted until the results of a large study of cholesterol lowering, sponsored by the United States National Institutes of Health, was published in 1984: the Coronary Primary Prevention Trial. This study conclusively showed a statistically significant decrease in heart attacks and strokes as a result of decreasing cholesterol level. The study made use of a bile acid–binding resin, cholestyramine, to control cholesterol. The results triggered a search for more effective therapeutic interventions. Some controversy persisted until the development of the statins in the late 1980s and 1990s.

Dr. Akira Endo, working at the Sankyo company in Tokyo, discovered the first statin and reported the work in 1976. Endo had been interested in cholesterol metabolism for some time, and speculated in 1971 that the fungi being screened at that time for new antibiotics might also contain an inhibitor of cholesterol synthesis. Over a period of several years, he screened more than 6,000 fungal cultures until a positive result was found. The compound that resulted was named compactin (Fig. 1). The compound eventually proved effective in

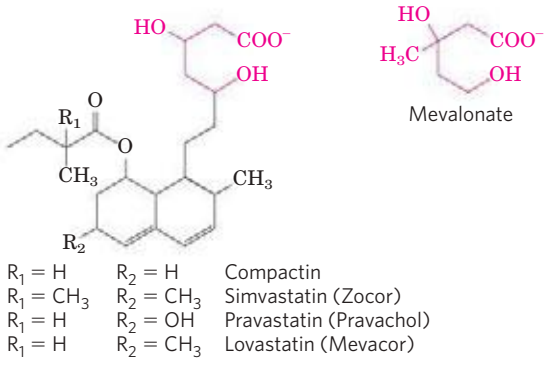

FIGURE 1 **Statins as inhibitors of HMG-CoA reductase.** A comparison of the structures of mevalonate and four pharmaceutical compounds (statins) that inhibit HMG-CoA reductase.

develops in childhood. These individuals have a defective LDL receptor and lack receptor-mediated uptake of cholesterol carried by LDL. Consequently, cholesterol is not cleared from the blood; it accumulates in foam cells and contributes to the formation of atherosclerotic plaques. Endogenous cholesterol synthesis continues despite the excessive cholesterol in the blood, because extracellular cholesterol cannot enter cells to regulate intracellular synthesis (Fig. 21–44). A class of drugs called **statins**, some isolated from natural sources and some synthesized by the pharmaceutical industry, is used to treat patients with familial hypercholesterolemia and other conditions involving elevated serum cholesterol. The statins resemble mevalonate (Box 21–3) and are competitive inhibitors of HMG-CoA reductase. ■

Reverse Cholesterol Transport by HDL Counters Plaque Formation and Atherosclerosis

HDL plays a critical role in the reverse cholesterol transport pathway **(Fig. 21–47)**, reducing the potential damage from foam cell buildup. Depleted HDL (low in cholesterol) picks up cholesterol stored in extrahepatic tissues (including foam cells at nascent plaques) and carries it to the liver. Two ATP-binding cassette (ABC) transporters are involved in cholesterol exit from cells. In this process, apoA-I interacts with an ABC transporter (ABCA1) in a cholesterol-rich cell. ABCA-1 transports a load of cholesterol from inside the cell to the outer surface of the plasma membrane, where lipid-free or lipid-poor apoA-I picks it up and transports it to the liver. Another ABC transporter (ABCG1) interacts

Akira Endo

Alfred Alberts

P. Roy Vagelos

reducing cholesterol levels in dogs and monkeys, and the work came to the attention of Michael Brown and Joseph Goldstein at the University of Texas–Southwestern medical school. Brown and Goldstein began to work with Endo, and confirmed his results. Some dramatic results in the first limited clinical trials convinced several pharmaceutical firms to join the hunt for statins. A team at Merck led by Alfred Alberts and P. Roy Vagelos began screening fungal cultures and found a positive result after screening just 18 cultures. The new statin was eventually called lovastatin (Fig. 1). A rumor that compactin, at very high doses, was carcinogenic in dogs almost sidelined the race to develop statins in 1980, but the benefits to patients with familial hypercholesterolemia were already evident. After much consultation with experts around the world and the U.S. Food and Drug Administration, Merck proceeded carefully to develop lovastatin. Extensive testing over the next two decades revealed no carcinogenic effects from lovastatin or from the newer generations of statins that have appeared since.

Statins inhibit HMG-CoA reductase in part by mimicking the structure of mevalonate (Fig. 1), and thus inhibit cholesterol synthesis. Lovastatin treatment lowers serum cholesterol by as much as 30% in individuals with hypercholesterolemia resulting from one defective copy of the gene for the LDL receptor. When combined with an edible resin that binds bile acids and prevents their reabsorption from the intestine, the drug is even more effective.

Statins are now the most widely used drugs for lowering serum cholesterol levels. Side effects are always a concern with drugs, but statins represent a case where many of the side effects are positive. These drugs can improve blood flow, enhance the stability of atherosclerotic plaques (so they don't rupture and obstruct blood flow), reduce platelet aggregation, and reduce vascular inflammation. Some of these effects occur before cholesterol levels drop in patients taking statins for the first time, and may be related to a secondary inhibition of isoprenoid synthesis by statins. Not all the effects of statins are positive. A few patients, usually among those taking statins in combination with other cholesterol-lowering drugs, experience muscle pain or weakness that can become severe and even debilitating. A fairly long list of other side effects has been documented in patients; most are rare. However, for the vast majority of patients, the statin-mediated decrease in the risks associated with coronary heart disease can be dramatic. As with all medications, statins should be used only in consultation with a physician.

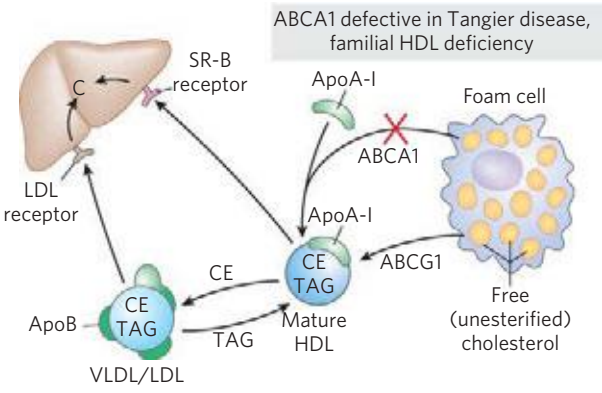

FIGURE 21–47 Reverse cholesterol transport. ApoA-I and HDLs pick up excess cholesterol from peripheral cells, with the participation of ABCA1 and ABCG1 transporters, and return it to the liver. In individuals with genetically defective ABCA1, the failure of reverse cholesterol transport leads to severe and early cardiovascular diseases: Tangier disease and familial HDL deficiency disease.

with mature HDL, facilitating the movement of cholesterol out of the cell and into the HDL. This efflux process is particularly critical when it involves reverse cholesterol transport away from foam cells at the sites of plaques that form in blood vessels in individuals with cardiovascular disease.

In **familial HDL deficiency**, HDL levels are very low, and in **Tangier disease** they are almost undetectable (Fig. 21–47). Both genetic disorders are the result of mutations in the ABCA1 protein. ApoA-I in cholesterol-depleted HDL cannot take up cholesterol from cells that lack ABCA1 protein, and apoA-I and cholesterol-poor HDL are rapidly removed from the blood and destroyed. Both familial HDL deficiency and Tangier disease are very rare (worldwide, fewer than 100 families with Tangier disease are known), but the existence of these diseases establishes a role for ABCA1 and ABCG1 proteins in the regulation of plasma HDL levels. ■

Steroid Hormones Are Formed by Side-Chain Cleavage and Oxidation of Cholesterol

Humans derive all their steroid hormones from cholesterol **(Fig. 21–48)**. Two classes of steroid hormones are synthesized in the cortex of the adrenal gland: **mineralocorticoids**, which control the reabsorption of inorganic ions (Na^+, Cl^-, and HCO_3^-) by the kidney, and **glucocorticoids**, which help regulate gluconeogenesis and reduce the inflammatory response. Sex hormones are produced in male and female gonads and the placenta. They include **progesterone**, which regulates the female reproductive cycle, and **androgens** (such as testosterone) and **estrogens** (such as estradiol), which influence the development of secondary sexual characteristics in males and females, respectively. Steroid hormones are effective at very low concentrations and are therefore synthesized in relatively small quantities.

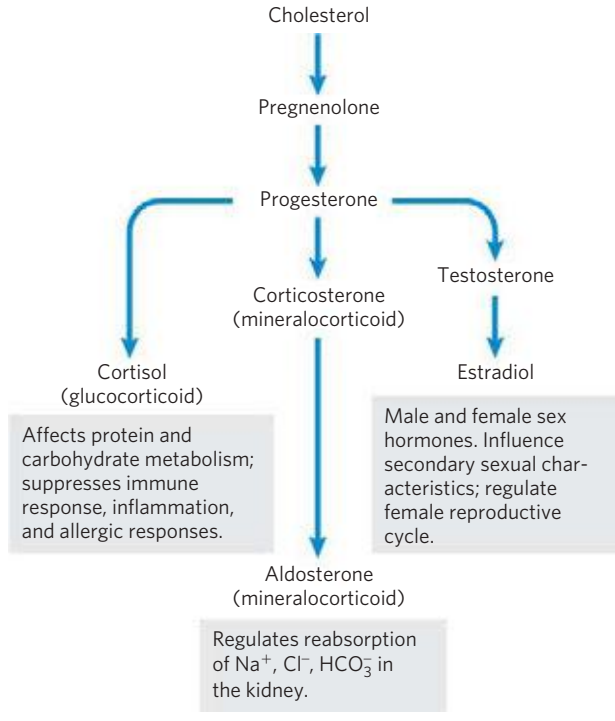

FIGURE 21–48 Some steroid hormones derived from cholesterol. The structures of some of these compounds are shown in Figure 10–19.

In comparison with the bile salts, their production consumes relatively little cholesterol.

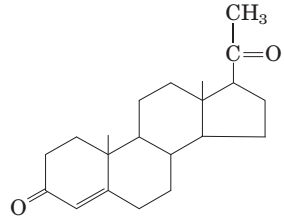

Progesterone

Synthesis of steroid hormones requires removal of some or all of the carbons in the "side chain" on C-17 of the D ring of cholesterol. Side-chain removal takes place in the mitochondria of steroidogenic tissues. Removal involves the hydroxylation of two adjacent carbons in the side chain (C-20 and C-22) followed by cleavage of the bond between them **(Fig. 21–49)**. Formation of the various hormones also involves the introduction of oxygen atoms. All the hydroxylation and oxygenation reactions in steroid biosynthesis are catalyzed by mixed-function oxidases (Box 21–1) that use NADPH, O_2, and mitochondrial cytochrome P-450.

Intermediates in Cholesterol Biosynthesis Have Many Alternative Fates

In addition to its role as an intermediate in cholesterol biosynthesis, isopentenyl pyrophosphate is the activated precursor of a huge array of biomolecules with diverse biological roles **(Fig. 21–50)**. They include vitamins A, E, and K; plant pigments such as carotene and the phytol

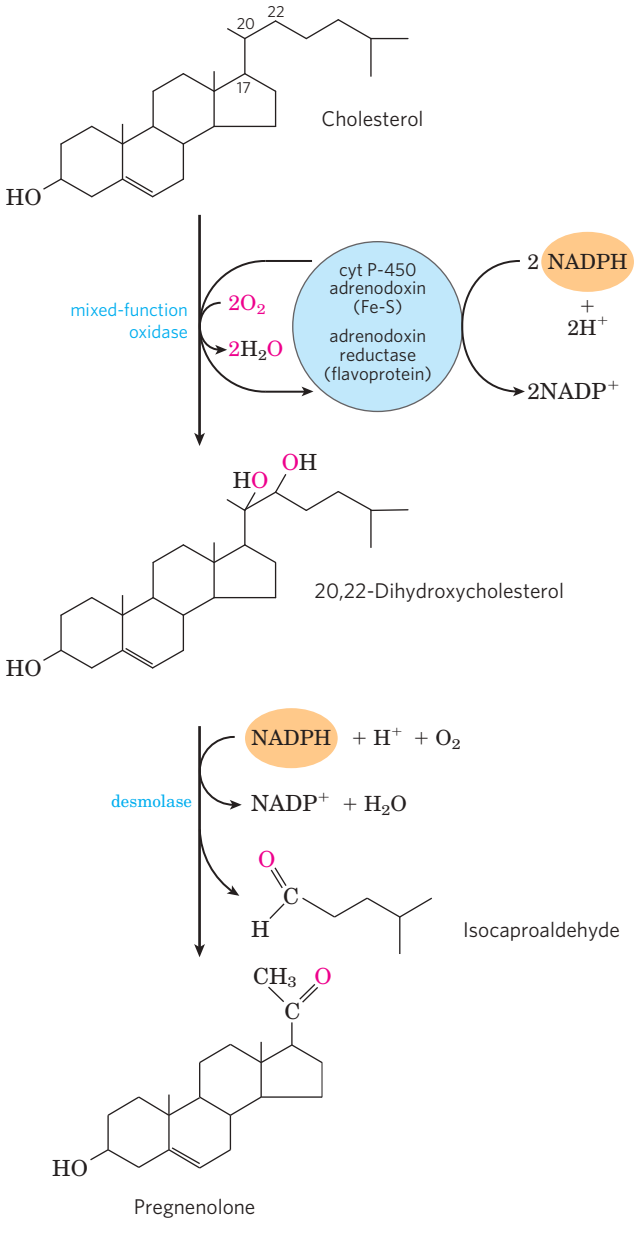

FIGURE 21–49 Side-chain cleavage in the synthesis of steroid hormones. Cytochrome P-450 acts as electron carrier in this mixed-function oxidase system that oxidizes adjacent carbons. The process also requires the electron-transferring proteins adrenodoxin and adrenodoxin reductase. This system for cleaving side chains is found in mitochondria of the adrenal cortex, where active steroid production occurs. Pregnenolone is the precursor of all other steroid hormones (see Fig. 21–48).

chain of chlorophyll; natural rubber; many essential oils (such as the fragrant principles of lemon oil, eucalyptus, and musk); insect juvenile hormone, which controls metamorphosis; dolichols, which serve as lipid-soluble carriers in complex polysaccharide synthesis; and ubiquinone and plastoquinone, electron carriers in mitochondria and chloroplasts. Collectively, these molecules are called isoprenoids. More than 20,000 different isoprenoid molecules have been discovered in nature, and hundreds of new ones are reported each year.

Prenylation (covalent attachment of an isoprenoid; see Fig. 27–35) is a common mechanism by which proteins are anchored to the inner surface of cellular membranes in mammals (see Fig. 11–15). In some of these proteins the attached lipid is the 15-carbon farnesyl group; others have the 20-carbon geranylgeranyl group. Different enzymes attach the two types of lipids. It is possible that prenylation reactions target proteins to different membranes, depending on which lipid is attached. Protein prenylation is another important role for the isoprene derivatives of the pathway to cholesterol.

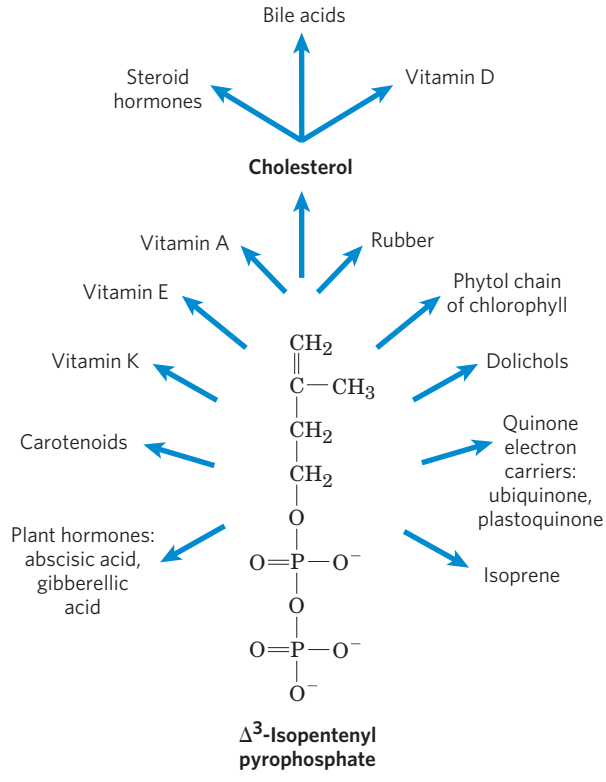

FIGURE 21–50 Overview of isoprenoid biosynthesis. The structures of most of the end products shown here are given in Chapter 10.

SUMMARY 21.4 Cholesterol, Steroids, and Isoprenoids: Biosynthesis, Regulation and Transport

- Cholesterol is formed from acetyl-CoA in a complex series of reactions, through the intermediates β-hydroxy-β-methylglutaryl-CoA, mevalonate, and two activated isoprenes, dimethylallyl pyrophosphate and isopentenyl pyrophosphate. Condensation of isoprene units produces the noncyclic squalene, which is cyclized to yield the steroid ring system and side chain.
- Cholesterol and cholesteryl esters are carried in the blood as plasma lipoproteins. VLDL carries cholesterol, cholesteryl esters, and triacylglycerols from the liver to other tissues, where the triacylglycerols are degraded by lipoprotein lipase, converting VLDL to LDL. The LDL, rich in cholesterol and its esters, is taken up by receptor-mediated endocytosis, in which the apolipoprotein B-100 of LDL is recognized by receptors in the plasma membrane.

- Cholesterol synthesis and transport are under complex regulation by hormones, cellular cholesterol content, and energy level (AMP concentration). HMG-CoA reductase is regulated allosterically and by covalent modification. Furthermore, both its synthesis and degradation rates are controlled by a complex of three proteins: Insig, SCAP, and SREBP, which sense cholesterol levels and trigger increased synthesis or degradation of HMG-CoA reductase. The number of LDL receptors per cell is also regulated by cholesterol content.
- Dietary conditions or genetic defects in cholesterol metabolism may lead to atherosclerosis and heart disease. In reverse cholesterol transport, HDL removes cholesterol from peripheral tissues, carrying it to the liver. By reducing the cholesterol content of foam cells, HDL protects against atherosclerosis.
- The steroid hormones (glucocorticoids, mineralocorticoids, and sex hormones) are produced from cholesterol by alteration of the side chain and introduction of oxygen atoms into the steroid ring system. In addition to cholesterol, a wide variety of isoprenoid compounds are derived from mevalonate through condensations of isopentenyl pyrophosphate and dimethylallyl pyrophosphate.
- Prenylation of certain proteins targets them for association with cellular membranes and is essential for their biological activity.

Key Terms

Terms in bold are defined in the glossary.

malonyl-CoA 833
acetyl-CoA carboxylase 833
fatty acid synthase 834
acyl carrier protein (ACP) 836
fatty acyl–CoA desaturase 843
mixed-function oxidases 843
stearoyl-ACP desaturase (SCD) 843
mixed-function oxygenases 844
cytochrome P-450 844
essential fatty acids 845
prostaglandin 845
cyclooxygenase (COX) 845
prostaglandin H_2 synthase 845
thromboxane synthase 847
thromboxane 847
leukotriene 847
glycerol 3-phosphate dehydrogenase 848
triacylglycerol cycle 850
glyceroneogenesis 850
thiazolidinediones 852
phosphatidylserine 853
phosphatidylglycerol 853
phosphatidyl-ethanolamine 855
cardiolipin 855
phosphatidylcholine 855
plasmalogen 856
platelet-activating factor 856
cerebroside 857
sphingomyelin 857
ganglioside 857
isoprene 859
mevalonate 860
β-hydroxy-β-methylglutaryl-CoA (HMG-CoA) 860
HMG-CoA synthase 860
HMG-CoA reductase 860
squalene 861
bile acids 864
cholesteryl esters 864
apolipoproteins 864
chylomicron 865
exogenous pathway 866
very-low-density lipoprotein (VLDL) 866
low-density lipoprotein (LDL) 867
endogenous pathway 867
LDL receptors 867
receptor-mediated endocytosis 868
high-density lipoprotein (HDL) 869
reverse cholesterol transport 869
enterohepatic circulation 869
sterol regulatory element-binding proteins (SREBPs) 870
SREBP cleavage-activating protein (SCAP) 870
insulin-induced gene protein (Insig) 870
liver X receptor (LXR) 871
retinoid X receptor (RXR) 871
atherosclerosis 871
foam cell 871
statin 873

Further Reading

The general references in Chapters 10 and 17 are also useful.

General

Vance, D.E. & Vance, J.E. (eds) (2008) *Biochemistry of Lipids, Lipoproteins, and Membranes*, 5th edn, New Comprehensive Biochemistry, Elsevier Science Publishing Co., Inc., New York.
Excellent reviews of lipid structure, biosynthesis, and function.

Biosynthesis of Fatty Acids and Eicosanoids

Chan, D.I. & Vogel, H.J. (2010) Current understanding of fatty acid biosynthesis and the acyl carrier protein. *Biochem. J.* **430**, 1–19.
Intermediate-level review

Maier, T., Jenni, S., & Ban, N. (2006) Architecture of mammalian fatty acid synthase at 4.5 Å resolution. *Science* **311**, 1258–1262.
The large multiprotein complexes that synthesize fatty acids in fungi have interesting and very different architectures compared with those in mammals.

Munday, M.R. (2002) Regulation of mammalian acetyl-CoA carboxylase. *Biochem. Soc. Trans.* **30**, 1059–1064.

Reshef, L., Olswang, Y., Cassuto, H., Blum, B., Croniger, C.M., Kalhan, S.C., Tilghman, S.M., & Hanson, R.M. (2003) Glyceroneogenesis and the triglyceride/fatty acid cycle. *J. Biol. Chem.* **278**, 30,413–30,416.

Sampath, H. & Ntambi, J.M. (2011) The role of stearoyl-CoA desaturase in obesity, insulin resistance, and inflammation. *Ann. N.Y. Acad. Sci.* **1243**, 47–53.
Brief review of roles of this enzyme in lipogenesis in several physiological processes.

Smith, W.L., Urade, Y., & Jakovsson, P.-J. (2011) Enzymes of the cyclooxygenase pathways of prostanoid biosynthesis. *Chem. Rev.* **111**, 5821–5865.
Advanced review.

Warner, T.D. & Mitchell, J.A. (2004) Cyclooxygenases: new forms, new inhibitors, and lessons from the clinic. *FASEB J.* **18**, 790–804.

White, S.W., Zheng, J., Zhang, Y.-M., & Rock, C.O. (2005) The structural biology of type II fatty acid biosynthesis. *Annu. Rev. Biochem.* **74**, 791–831.

Biosynthesis of Triacylglycerols and Membrane Phospholipids

Carman, G.M. & Han, G.-S. (2011) Regulation of phospholipid synthesis in the yeast *Saccharomyces cerevisiae*. *Annu. Rev. Biochem*. **89**, 859–883.
Advanced review.

Coleman, R.S. & Mashek, D.G. (2011) Mammalian triacylglycerol metabolism: synthesis, lipolysis, and signaling. *Chem. Rev*. **111**, 6359–6386.
Advanced review.

Dowhan, W. (1997) Molecular basis for membrane phospholipid diversity: why are there so many lipids? *Annu. Rev. Biochem.* **66**, 199–232.

Gibellini, F. & Smith, T.K. (2010) The Kennedy pathway—*de novo* synthesis of phosphatidylethanolamine and phosphatidylcholine. *IUBMB Life* **62**, 414–428.

Kennedy, E.P. (1962) The metabolism and function of complex lipids. *Harvey Lect.* **57**, 143–171.
A classic description of the role of cytidine nucleotides in phospholipid synthesis.

Raetz, C.R.H. & Dowhan, W. (1990) Biosynthesis and function of phospholipids in *Escherichia coli*. *J. Biol. Chem.* **265**, 1235–1238.
A brief review of bacterial biosynthesis of phospholipids and lipopolysaccharides.

Zechner, R., Zimmermann, R., Eichmann, T.O., Kohlwein, S.D., Haemmerle, G., Lass, A., & Madeo, R. (2012) Fat signals—lipases and lipolysis in lipid metabolism and signaling. *Cell Metab.* **15**, 279–291.

Biosynthesis of Cholesterol, Steroids, and Isoprenoids

Bloch, K. (1965) The biological synthesis of cholesterol. *Science* **150**, 19–28.
The author's Nobel address; a classic description of cholesterol synthesis in animals.

Boutte, Y. & Grebe, M. (2009) Cellular processes relying on sterol function in plants. *Curr. Opin. Plant Biol*. **12**, 705–713.
Review of synthesis and role of sterols in plants.

Brown, M.S. & Goldstein, J.L. (2009) Cholesterol feedback: from Schoenheimer's bottle to Scap's MELADL. *J. Lipid Res*. **50**, S15–S27.
Short historical summary of the roles of SCAP and SREBP in regulation of cholesterol synthesis.

Calandra, S., Tarugi, P., Speedy, H.E., Dean, A.F., Bertolini, S., & Shoulders, C.C. (2011) Mechanisms and genetic determinants regulating sterol absorption, circulating LDL levels, and sterol elimination: implications for classification and disease risk. *J. Lipid Res*. **52**, 1885–1926.
Extensive review of the role of LDL in human disease.

Calkin, A.C. & Tontonoz, P. (2012) Transcriptional integration of metabolism by the nuclear sterol-activated receptors LXR and FXR. *Nat. Rev. Mol. Cell Biol.* **13**, 213–224.
The role of these nuclear receptors in cholesterol metabolism and its integration into overall metabolism.

Chang, T.Y., Chang, C.C.Y., & Cheng, D. (1997) Acyl–coenzyme A: cholesterol acyltransferase. *Annu. Rev. Biochem.* **66**, 613–638.

Choi, S.H. & Ginsberg, H.N. (2011) Increased very low density lipoprotein (VLDL) secretion, hepatic steatosis, and insulin resistance. *Trends Endocrinol. Metab*. **22**, 353–363.
Review of insulin action of lipoprotein synthesis and circulation.

Getz, G.S. & Reardon, C.A. (2011) ABC transporters and the thickening cholesterol plot. *Curr. Opin. Lipidol.* **22**, 72–73.

Goldstein, J.L. & Brown, M.S. (2008) From fatty steak to fatty liver: 33 years of joint publications in the JCI. *J. Clin. Invest.* **118**, 1220–1222.
Short, excellent recap of seminal work on cholesterol and disease.

Goldstein, J.L. & Brown, M.S. (1990) Regulation of the mevalonate pathway. *Nature* **343**, 425–430.
Description of the allosteric and covalent regulation of the enzymes of the mevalonate pathway; includes a short discussion of the prenylation of Ras and other proteins.

Hanson, J.R. (2010) Classics of cholesterol biosynthesis. *Biochem. J.*, doi:10.1042/BJ20091543.
Review of the classic work of Popják and Cornforth on cholesterol synthesis.

Hegele, R.A. (2012) Plasma lipoproteins: genetic influences and clinical implications. *Nat. Rev. Genet*. **10**, 109–120.
Review of genetic basis for variations in plasma lipids and lipoproteins.

Jeon, T.-I. & Osborne, T.F. (2012) SREBPs: metabolic integrators in physiology and metabolism. *Trends Endocrinol. Metab.* **23**, 65–72.
Intermediate-level review of general roles of SREBPs, including cholesterol homeostasis.

Leduc, V., Jasmin-Belanger, S., & Poirier, J. (2010) APOE and cholesterol homeostasis in Alzheimer's disease. *Trends Mol. Med*. **16**, 469–477.

Maxfield, F.R. & Tabas, I. (2005) Role of cholesterol and lipid organization in disease. *Nature* **438**, 612–621.

Maxfield, F.R. & van Meer, G. (2010) Cholesterol, the central lipid of mammalian cells. *Curr. Opin. Cell Biol.* **22**, 422–429.

Miller, W.L. & Auchus, R.J. (2011) The molecular biology, biochemistry, and physiology of human steroidogenesis and its disorders. *Endocrine Rev.* **32**, 81–151.
Extensive, advanced review.

Miziorko, H.M. (2011) Enzymes of the mevalonate pathway of isoprenoid biosynthesis. *Arch. Biochem. Biophys*. **505**, 131–143.

Nes, D. (2011) Biosynthesis of cholesterol and other sterols. *Chem. Rev*. **111**, 6423–6451.

Olson, R.E. (1998) Discovery of the lipoproteins, their role in fat transport and their significance as risk factors. *J. Nutr.* **128** (2 Suppl.), 439S–443S.
Brief, clear, historical background on studies of lipoprotein function.

Raghow, R., Yellaturu, C., Deng, X., Park, E.A., & Elam, M.B. (2008) SREBPs: the crossroads of physiological and pathological lipid homeostasis. *Trends Endocrinol. Metab*. **19**, 65–73.

Russell, D.W. (2003) The enzymes, regulation, and genetics of bile acid synthesis. *Annu. Rev. Biochem.* **72**, 137–174.

Steinberg, D. (2006) An interpretive history of the cholesterol controversy, part V: the discovery of the statins and the end of the controversy. *J. Lipid Res.* **47**, 1339–1351.
The last in a five-part series detailing the history of the lipid controversy that led to the development of statins.

Tall, A.R., Yvan-Charvet, L., Terasaka, N., Pagler, T., & Wang, N. (2008) HDL, ABC transporters, and cholesterol efflux: implications for the treatment of atherosclerosis. *Cell Metab*. **7**, 365–375.
Reverse cholesterol transport: the role of ABC transporters.

Young, S.G. & Fielding, C.J. (1999) The ABCs of cholesterol efflux. *Nat. Genet.* **22**, 316–318.
A brief review of three papers in this journal issue that establish mutations in ABC1 as the cause of Tangier disease and familial HDL deficiency.

Shao, Y., Van Berkel, T.J.C., & Van Eck, M. (2010) Relative roles of various efflux pathways in net cholesterol efflux from macrophage foam cells in atherosclerotic lesions. *Curr. Opin. Lipidol*. **21**, 441–453.

Problems

1. Pathway of Carbon in Fatty Acid Synthesis Using your knowledge of fatty acid biosynthesis, provide an explanation for the following experimental observations:

(a) Addition of uniformly labeled [^{14}C]acetyl-CoA to a soluble liver fraction yields palmitate uniformly labeled with ^{14}C.

(b) However, addition of a *trace* of uniformly labeled [^{14}C]acetyl-CoA in the presence of an excess of unlabeled malonyl-CoA to a soluble liver fraction yields palmitate labeled with ^{14}C only in C-15 and C-16.

2. Synthesis of Fatty Acids from Glucose After a person has ingested large amounts of sucrose, the glucose and fructose that exceed caloric requirements are transformed to fatty acids for triacylglycerol synthesis. This fatty acid synthesis consumes acetyl-CoA, ATP, and NADPH. How are these substances produced from glucose?

3. Net Equation of Fatty Acid Synthesis Write the net equation for the biosynthesis of palmitate in rat liver, starting from mitochondrial acetyl-CoA and cytosolic NADPH, ATP, and CO_2.

4. Pathway of Hydrogen in Fatty Acid Synthesis Consider a preparation that contains all the enzymes and cofactors necessary for fatty acid biosynthesis from added acetyl-CoA and malonyl-CoA.

(a) If [2-^{2}H]acetyl-CoA (labeled with deuterium, the heavy isotope of hydrogen)

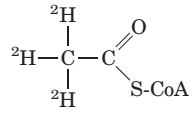

and an excess of unlabeled malonyl-CoA are added as substrates, how many deuterium atoms are incorporated into every molecule of palmitate? What are their locations? Explain.

(b) If unlabeled acetyl-CoA and [2-^{2}H]malonyl-CoA

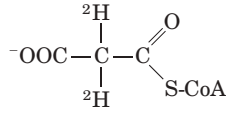

are added as substrates, how many deuterium atoms are incorporated into every molecule of palmitate? What are their locations? Explain.

5. Energetics of β-Ketoacyl-ACP Synthase In the condensation reaction catalyzed by β-ketoacyl-ACP synthase (see Fig. 21–6), a four-carbon unit is synthesized by the combination of a two-carbon unit and a three-carbon unit, with the release of CO_2. What is the thermodynamic advantage of this process over one that simply combines two two-carbon units?

6. Modulation of Acetyl-CoA Carboxylase Acetyl-CoA carboxylase is the principal regulation point in the biosynthesis of fatty acids. Some of the properties of the enzyme are described below.

(a) Addition of citrate or isocitrate raises the V_{max} of the enzyme as much as 10-fold.

(b) The enzyme exists in two interconvertible forms that differ markedly in their activities:

Protomer (inactive) $\rightleftharpoons$ filamentous polymer (active)

Citrate and isocitrate bind preferentially to the filamentous form, and palmitoyl-CoA binds preferentially to the protomer.

Explain how these properties are consistent with the regulatory role of acetyl-CoA carboxylase in the biosynthesis of fatty acids.

7. Shuttling of Acetyl Groups across the Mitochondrial Inner Membrane The acetyl group of acetyl-CoA, produced by the oxidative decarboxylation of pyruvate in the mitochondrion, is transferred to the cytosol by the acetyl group shuttle outlined in Figure 21–10.

(a) Write the overall equation for the transfer of one acetyl group from the mitochondrion to the cytosol.

(b) What is the cost of this process in ATPs per acetyl group?

(c) In Chapter 17 we encountered an acyl group shuttle in the transfer of fatty acyl–CoA from the cytosol to the mitochondrion in preparation for β oxidation (see Fig. 17–6). One result of that shuttle was separation of the mitochondrial and cytosolic pools of CoA. Does the acetyl group shuttle also accomplish this? Explain.

8. Oxygen Requirement for Desaturases The biosynthesis of palmitoleate (see Fig. 21–12) a common unsaturated fatty acid with a cis double bond in the Δ^9 position, uses palmitate as a precursor. Can palmitoleate synthesis be carried out under strictly anaerobic conditions? Explain.

9. Energy Cost of Triacylglycerol Synthesis Use a net equation for the biosynthesis of tripalmitoylglycerol (tripalmitin) from glycerol and palmitate to show how many ATPs are required per molecule of tripalmitin formed.

10. Turnover of Triacylglycerols in Adipose Tissue When [^{14}C]glucose is added to the balanced diet of adult rats, there is no increase in the total amount of stored triacylglycerols, but the triacylglycerols become labeled with ^{14}C. Explain.

11. Energy Cost of Phosphatidylcholine Synthesis Write the sequence of steps and the net reaction for the biosynthesis of phosphatidylcholine by the salvage pathway from oleate, palmitate, dihydroxyacetone phosphate, and choline. Starting from these precursors, what is the cost (in number of ATPs) of the synthesis of phosphatidylcholine by the salvage pathway?

12. Salvage Pathway for Synthesis of Phosphatidylcholine A young rat maintained on a diet deficient in methionine fails to thrive unless choline is included in the diet. Explain.

13. Synthesis of Isopentenyl Pyrophosphate If 2[^{14}C] acetyl-CoA is added to a rat liver homogenate that is synthesizing cholesterol, where will the ^{14}C label appear in Δ^3-isopentenyl pyrophosphate, the activated form of an isoprene unit?

14. Activated Donors in Lipid Synthesis In the biosynthesis of complex lipids, components are assembled by transfer of the appropriate group from an activated donor. For example, the activated donor of acetyl groups is acetyl-CoA. For each of the following groups, give the form of the activated donor: (a) phosphate; (b) D-glucosyl; (c) phosphoethanolamine; (d) D-galactosyl; (e) fatty acyl; (f) methyl; (g) the two-carbon group in fatty acid biosynthesis; (h) Δ^3-isopentenyl.

15. Importance of Fats in the Diet When young rats are placed on a totally fat-free diet, they grow poorly, develop a scaly dermatitis, lose hair, and soon die—symptoms that can be prevented if linoleate or plant material is included in the diet. What makes linoleate an essential fatty acid? Why can plant material be substituted?

16. Regulation of Cholesterol Biosynthesis Cholesterol in humans can be obtained from the diet or synthesized de novo. An adult human on a low-cholesterol diet typically synthesizes 600 mg of cholesterol per day in the liver. If the amount of cholesterol in the diet is large, de novo synthesis of cholesterol is drastically reduced. How is this regulation brought about?

17. Lowering Serum Cholesterol Levels with Statins Patients treated with a statin drug generally exhibit a dramatic lowering of serum cholesterol. However, the amount of the enzyme HMG-CoA reductase present in cells can increase substantially. Suggest an explanation for this effect.

18. Roles of Thiol Esters in Cholesterol Biosynthesis Draw a mechanism for each of the three reactions shown in Figure 21–34, detailing the pathway for the synthesis of mevalonate from acetyl-CoA.

19. Potential Side Effects of Treatment with Statins Although clinical trials have not yet been carried out to document benefits or side effects, some physicians have suggested that patients being treated with statins also take a supplement of coenzyme Q. Suggest a rationale for this recommendation.

Data Analysis Problem

20. Engineering *E. coli* to Produce Large Quantities of an Isoprenoid There is a huge variety of naturally occurring isoprenoids, some of which are medically or commercially important and produced industrially. The production methods include in vitro enzymatic synthesis, which is an expensive and low-yield process. In 1999, Wang, Oh, and Liao reported their experiments to engineer the easily grown bacterium *E. coli* to produce large amounts of astaxanthin, a commercially important isoprenoid.

Astaxanthin is a red-orange carotenoid pigment (an antioxidant) produced by marine algae. Marine animals such as shrimp, lobster, and some fish that feed on the algae get their orange color from the ingested astaxanthin. Astaxanthin is composed of eight isoprene units; its molecular formula is $C_{40}H_{52}O_4$:

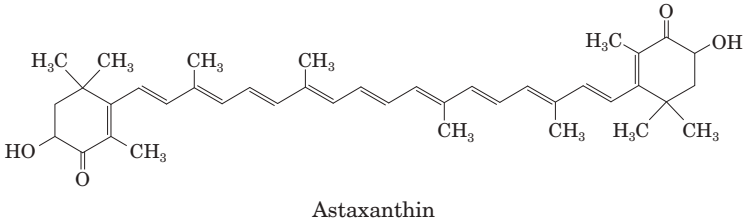

Astaxanthin

(a) Circle the eight isoprene units in the astaxanthin molecule. Hint: Use the projecting methyl groups as a guide.

Astaxanthin is synthesized by the pathway shown on the next page, starting with Δ^3-isopentenyl pyrophosphate (IPP). Steps ❶ and ❷ are shown in Figure 21–36, and the reaction catalyzed by IPP isomerase is shown in Figure 21–35.

(b) In step ❹ of the pathway, two molecules of geranylgeranyl pyrophosphate are linked to form phytoene. Is this a head-to-head or a head-to-tail joining? (See Figure 21–36 for details.)

(c) Briefly describe the chemical transformation in step ❺.

(d) The synthesis of cholesterol (Fig. 21–37) includes a cyclization (ring closure) that involves a net oxidation by O_2. Does the cyclization in step ❻ of the astaxanthin synthetic pathway require a net oxidation of the substrate (lycopene)? Explain your reasoning.

E. coli does not make large quantities of many isoprenoids, and does not synthesize astaxanthin. It is known to synthesize small amounts of IPP, DMAPP, geranyl pyrophosphate, farnesyl pyrophosphate, and geranylgeranyl pyrophosphate. Wang and colleagues cloned several of the *E. coli* genes that encode enzymes needed for astaxanthin synthesis in plasmids that allow their overexpression. These genes included *idi*, which encodes IPP isomerase, and *ispA*, which encodes a prenyl transferase that catalyzes steps ❶ and ❷.

To engineer an *E. coli* capable of the complete astaxanthin pathway, Wang and colleagues cloned several genes from other bacteria into plasmids that would allow their overexpression in *E. coli.* These genes included *crtE* from *Erwinia uredovora*, which encodes an enzyme that catalyzes step ❸; and *crtB*, *crtI*, *crtY*, *crtZ*, and *crtW* from *Agrobacterium aurantiacum*, which encode enzymes for steps ❹, ❺, ❻, ❼, and ❽, respectively.

The investigators also cloned the gene *gps* from *Archaeoglobus fulgidus*, overexpressed this gene in *E. coli*, and extracted the gene product. When this extract was reacted with [^{14}C]IPP and DMAPP, or geranyl pyrophosphate, or farnesyl pyrophosphate, only ^{14}C-labeled geranylgeranyl pyrophosphate was produced in all cases.

(e) Based on these data, which step(s) in the pathway are catalyzed by the enzyme encoded by *gps*? Explain your reasoning.

Wang and coworkers then constructed several *E. coli* strains overexpressing different genes and measured the orange color of the colonies (wild-type *E. coli* colonies are off-white) and the amount of astaxanthin produced. Their results are shown below.

Strain	Gene(s) overexpressed	Orange color	Astaxanthin yield (μg/g dry weight)
1	*crtBIZYW*	−	ND
2	*crtBIZYW, ispA*	−	ND
3	*crtBIZYW, idi*	−	ND
4	*crtBIZYW, idi, ispA*	−	ND
5	*crtBIZYW, crtE*	+	32.8
6	*crtBIZYW, crtE, ispA*	+	35.3
7	*crtBIZYW, crtE, idi*	++	234.1
8	*crtBIZYW, crtE, idi, ispA*	+++	390.3
9	*crtBIZYW, gps*	+	35.6
10	*crtBIZYW, gps, idi*	+++	1,418.8

Note: ND, not determined.

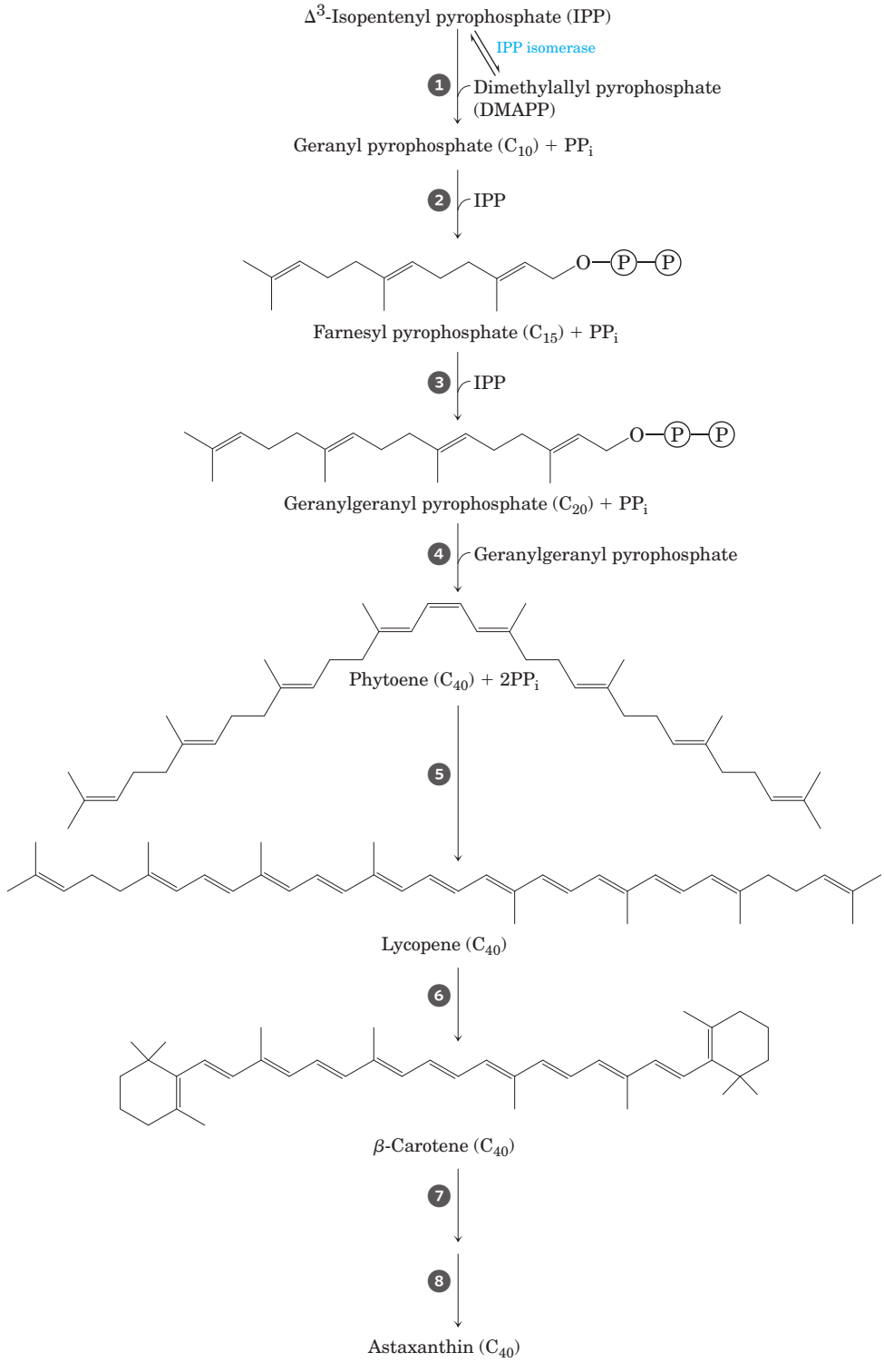

(f) Comparing the results for strains 1 through 4 with those for strains 5 through 8, what can you conclude about the expression level of an enzyme capable of catalyzing step ❸ of the astaxanthin synthetic pathway in wild-type *E. coli*? Explain your reasoning.

(g) Based on the data above, which enzyme is rate-limiting in this pathway, IPP isomerase or the enzyme encoded by *idi*? Explain your reasoning.

(h) Would you expect a strain overexpressing *crtBIZYW*, *gps*, and *crtE* to produce low (+), medium (++), or high (+++) levels of astaxanthin, as measured by its orange color? Explain your reasoning.

Reference

Wang, C.-W., Oh, M.-K., & Liao, J.C. (1999) Engineered isoprenoid pathway enhances astaxanthin production in *Escherichia coli*. *Biotechnol. Bioeng.* **62**, 235–241.

22

Biosynthesis of Amino Acids, Nucleotides, and Related Molecules

Nitrogen ranks behind only carbon, hydrogen, and oxygen in its contribution to the mass of living systems. Most of this nitrogen is bound up in amino acids and nucleotides. In this chapter we address all aspects of the metabolism of these nitrogen-containing compounds except amino acid catabolism, which is covered in Chapter 18.

Discussing the biosynthetic pathways for amino acids and nucleotides together is a sound approach, not only because both classes of molecules contain nitrogen (which arises from common biological sources) but because the two sets of pathways are extensively intertwined, with several key intermediates in common. Certain amino acids or parts of amino acids are incorporated into the structure of purines and pyrimidines, and in one case part of a purine ring is incorporated into an amino acid (histidine). The two sets of pathways also share much common chemistry, in particular a preponderance of reactions involving the transfer of nitrogen or one-carbon groups.

The pathways described here can be intimidating to the beginning biochemistry student. Their complexity arises not so much from the chemistry itself, which in many cases is well understood, but from the sheer number of steps and variety of intermediates. These pathways are best approached by maintaining a focus on metabolic principles we have already discussed, on key intermediates and precursors, and on common classes of reactions. Even a cursory look at the chemistry can be rewarding, for some of the most unusual chemical transformations in biological systems occur in these pathways; for instance, we find prominent examples of the rare biological use of the metals molybdenum, selenium, and vanadium. The effort also offers a practical dividend, especially for students of human or veterinary medicine. Many genetic diseases of humans and animals have been traced to an absence of one or more enzymes of amino acid and nucleotide metabolism, and many pharmaceuticals in common use to combat infectious diseases are inhibitors of enzymes in these pathways—as are a number of the most important agents in cancer chemotherapy.

Regulation is crucial in the biosynthesis of the nitrogen-containing compounds. Because each amino acid and each nucleotide is required in relatively small amounts, the metabolic flow through most of these pathways is not nearly as great as the biosynthetic flow leading to carbohydrate or fat in animal tissues. Because the different amino acids and nucleotides must be made in the correct ratios and at the right time for protein and nucleic acid synthesis, their biosynthetic pathways must be accurately regulated and coordinated with each other. And because amino acids and nucleotides are charged molecules, their levels must be regulated to maintain electrochemical balance in the cell. As discussed in earlier chapters, pathways can be controlled by changes in either the activity or the amounts of specific enzymes. The pathways we encounter in this chapter provide some of the best-understood examples of the regulation of enzyme activity. Control of the *amounts* of different enzymes in a cell (that is, of their synthesis and degradation) is a topic covered in Chapter 28.

22.1 Overview of Nitrogen Metabolism

The biosynthetic pathways leading to amino acids and nucleotides share a requirement for nitrogen. Because soluble, biologically useful nitrogen compounds are generally scarce in natural environments, most organisms maintain strict economy in their use of ammonia, amino acids, and nucleotides. Indeed, as we shall see, free

amino acids, purines, and pyrimidines formed during metabolic turnover of proteins and nucleic acids are often salvaged and reused. We first examine the pathways by which nitrogen from the environment is introduced into biological systems.

The Nitrogen Cycle Maintains a Pool of Biologically Available Nitrogen

Although Earth's atmosphere is four-fifths molecular nitrogen (N_2), relatively few species can convert this atmospheric nitrogen into forms useful to living organisms. In the biosphere, the metabolic processes of different species function interdependently to salvage and reuse biologically available nitrogen in a vast **nitrogen cycle (Fig. 22–1)**. The first step in the cycle is **fixation** (reduction) of atmospheric nitrogen by nitrogen-fixing bacteria to yield ammonia (NH_3 or NH_4^+). Although ammonia can be used by most living organisms, soil bacteria that derive their energy by oxidizing ammonia to nitrite (NO_2^-) and ultimately nitrate (NO_3^-) are so abundant and active that nearly all ammonia reaching the soil is oxidized to nitrate. This process is known as **nitrification**. Plants and many bacteria can take up and readily reduce nitrate and nitrite to ammonia through the action of nitrate and nitrite reductases. This ammonia is incorporated into amino acids by plants. Animals then use plants as a source of amino acids, both nonessential and essential, to build their proteins. When organisms die, microbial degradation of their proteins returns ammonia to the soil, where nitrifying bacteria again convert it to nitrite and nitrate. A balance is maintained between fixed nitrogen and atmospheric nitrogen by bacteria that reduce nitrate to N_2 under anaerobic conditions, a process called **denitrification** (Fig. 22–1). These soil bacteria use NO_3^- rather than O_2 as the ultimate electron acceptor in a series of reactions that (like oxidative phosphorylation) generates a transmembrane proton gradient, which is used to synthesize ATP.

The nitrogen cycle is short-circuited by a group of bacteria that promote anaerobic ammonia oxidation, or **anammox** (Fig. 22–1), a process that converts ammonia and nitrite to N_2. As much as 50% to 70% of the NH_3-to-N_2 conversion in the biosphere may occur through this pathway, undetected until the 1980s. The obligate anaerobes that promote anammox are fascinating in their own right and are providing some useful solutions to waste-treatment problems (Box 22–1).

Now let's examine the processes that generate the ammonia that is incorporated into microorganisms, plants, and the animals that eat them.

More than 90% of the NH_4^+ generated by vascular plants, algae, and microorganisms comes from nitrate assimilation, a two-step process. First NO_3^- is reduced to NO_2^- by **nitrate reductase**, then the NO_2^- is reduced to NH_4^+ in a six-electron transfer catalyzed by **nitrite reductase (Fig. 22–2)**. Both reactions involve chains of electron carriers and cofactors we have not yet encountered. Nitrate reductase is a large, soluble protein (M_r 220,000). Within the enzyme, a pair of electrons, donated by NADH, flows through —SH groups of cysteine, FAD, and a cytochrome (cyt b_{557}), then to a novel cofactor containing molybdenum, before reducing the substrate NO_3^- to NO_2^-.

The nitrite reductase of plants is located in the chloroplasts and receives its electrons from ferredoxin (which is reduced in the light-dependent reactions of photosynthesis; see Section 19.8). Six electrons, donated one at a time by ferredoxin, pass through a 4S-4Fe center in the enzyme, then through a novel heme-like molecule (siroheme) before reducing NO_2^- to NH_4^+ (Fig. 22–2). In nonphotosynthetic microbes, NADPH provides the electrons for this reaction.

Nitrogen Is Fixed by Enzymes of the Nitrogenase Complex

Only certain bacteria and archaea can fix atmospheric N_2. These organisms, called diazotrophs, include the cyanobacteria of soils and fresh and salt waters, methanogenic archaea (strict anaerobes that obtain energy and carbon by converting H_2 and CO_2 to methane), other kinds of free-living soil bacteria such as *Azotobacter* species, and the nitrogen-fixing bacteria that live as **symbionts** in the root nodules of leguminous plants. The first important product of nitrogen fixation is ammonia,

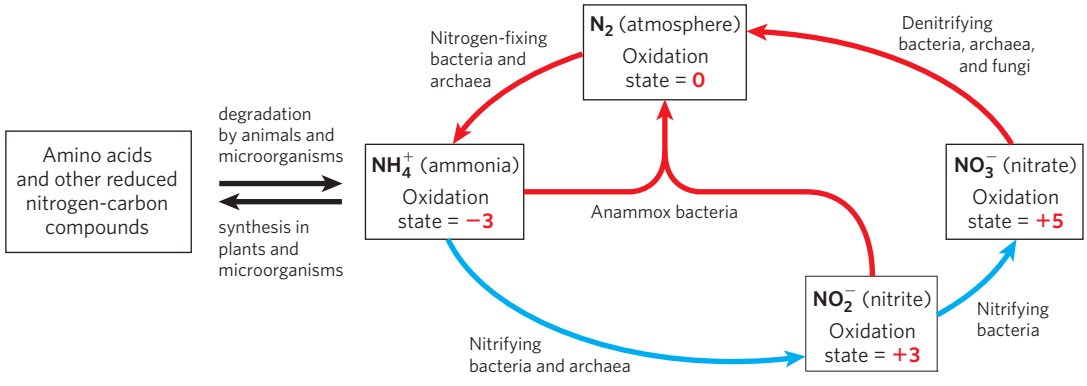

FIGURE 22–1 The nitrogen cycle. The total amount of nitrogen fixed annually in the biosphere exceeds 10^{11} kg. Reactions with red arrows occur largely or entirely in anaerobic environments.

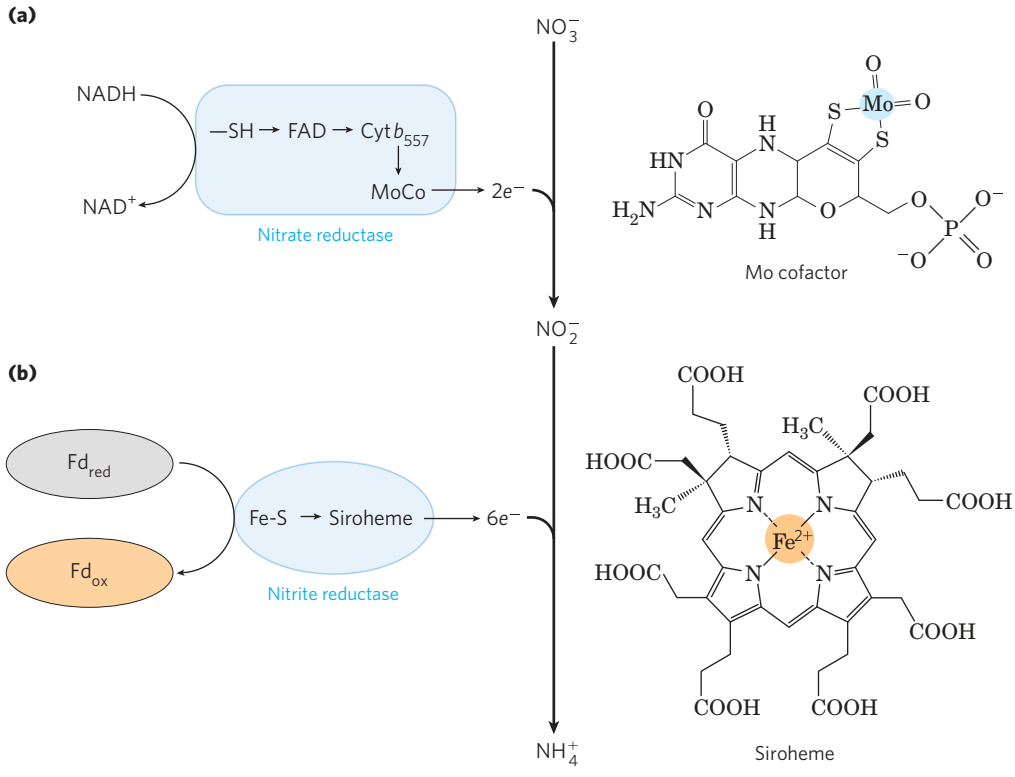

FIGURE 22–2 Nitrate assimilation by nitrate reductase and nitrite reductase. (a) Nitrate reductases of plants and bacteria catalyze the two-electron reduction of NO_3^- to NO_2^-, in which a novel Mo-containing cofactor plays a central role. NADH is the electron donor. **(b)** Nitrite reductase converts the product of nitrate reductase into NH_4^+ in a six-electron, eight-proton transfer process in which the metallic center in siroheme carries electrons, and the carboxyl groups of siroheme may donate protons. The initial source of electrons is reduced ferredoxin.

which can be used by all organisms either directly or after its conversion to other soluble compounds such as nitrites, nitrates, or amino acids.

The reduction of nitrogen to ammonia is an exergonic reaction:

$$N_2 + 3H_2 \longrightarrow 2NH_3 \qquad \Delta G'^\circ = -33.5 \text{ kJ/mol}$$

The N≡N triple bond, however, is very stable, with a bond energy of 930 kJ/mol. Nitrogen fixation therefore has an extremely high activation energy, and atmospheric nitrogen is almost chemically inert under normal conditions. Ammonia is produced industrially by the Haber process (named for its inventor, Fritz Haber), which requires temperatures of 400 to 500 °C and nitrogen and hydrogen at pressures of tens of thousands of kilopascals (several hundred atmospheres) to provide the necessary activation energy. Biological nitrogen fixation, however, must occur at biological temperatures and at 0.8 atm of nitrogen, and the high activation barrier is overcome by other means. This is accomplished, at least in part, by the binding and hydrolysis of ATP. The overall reaction can be written

$$N_2 + 10H^+ + 8e^- + 16ATP \longrightarrow 2NH_4^+ + 16ADP + 16P_i + H_2$$

Biological nitrogen fixation is carried out by a highly conserved complex of proteins called the **nitrogenase complex**; its central components are **dinitrogenase reductase** and **dinitrogenase** **(Fig. 22–3a)**. Dinitrogenase reductase (M_r 60,000) is a dimer of two identical subunits. It contains a single 4Fe-4S redox center (see Fig. 19–5), bound between the subunits, and can be oxidized and reduced by one electron. It also has two binding sites for ATP/ADP (one site on each subunit). Dinitrogenase (M_r 240,000), an $\alpha_2\beta_2$ tetramer, has two Fe-containing cofactors that transfer electrons (Fig. 22–3b). One, the **P cluster**, has a pair of 4Fe-4S centers; these share a sulfur atom, making an 8Fe-7S center. The second cofactor in dinitrogenase, the **FeMo cofactor**, is a novel structure composed of 7 Fe atoms, 9 inorganic S atoms, a Cys side chain, and a single carbon atom in the center of the FeS cluster. Also part of the cofactor is a molybdenum atom, with ligands that include three inorganic S atoms, a His side chain, and two oxygen atoms from a molecule of homocitrate that is an intrinsic part of the FeMo cofactor. There is also a form of nitrogenase that contains vanadium rather than molybdenum, and some bacterial species can produce both types. The vanadium-containing enzyme may be the primary nitrogen-fixing system under some conditions. The vanadium nitrogenase of *Azotobacter vinelandii* has the remarkable capacity to catalyze the reduction of carbon monoxide (CO) to ethylene (C_2H_4), ethane, and propane.

Nitrogen fixation is carried out by a highly reduced form of dinitrogenase and requires eight electrons: six for the reduction of N_2 and two to produce one molecule of H_2. Production of H_2 is an obligate part of the reaction mechanism, but its biological role in the process is not understood.

Dinitrogenase is reduced by the transfer of electrons from dinitrogenase reductase **(Fig. 22–4)**. The dinitrogenase tetramer has two binding sites for the reductase. The required eight electrons are transferred from reductase to dinitrogenase one at a time: a reduced reductase molecule binds to the dinitrogenase and transfers a single electron, then the oxidized reductase

BOX 22–1 Unusual Lifestyles of the Obscure but Abundant

Air-breathers that we are, we can easily overlook the bacteria and archaea that thrive in anaerobic environments. Although rarely featured in introductory biochemistry textbooks, these organisms constitute much of the biomass of this planet, and their contributions to the balance of carbon and nitrogen in the biosphere are essential to all forms of life.

As detailed in earlier chapters, the energy used to maintain living systems relies on the generation of proton gradients across membranes. Electrons derived from a reduced substrate are made available to electron carriers in membranes and pass through a series of electron transfers to a final electron acceptor. As a byproduct of this process, protons are released on one side of the membrane, generating the transmembrane proton gradient. The proton gradient is used to synthesize ATP or to drive other energy-requiring processes. For all eukaryotes, the reduced substrate is generally a carbohydrate (glucose or pyruvate) or a fatty acid and the electron acceptor is oxygen.

Many bacteria and archaea are much more versatile. In anaerobic environments such as marine and freshwater sediments, the variety of life strategies is extraordinary. Almost any available redox pair can be an energy source for some specialized organism or group of organisms. For example, a large number of lithotrophic bacteria (a lithotroph is a chemotroph that uses inorganic energy sources; see Fig. 1–5) have a hydrogenase that uses molecular hydrogen to reduce NAD^+:

$$H_2 + NAD^+ \xrightarrow{\text{hydrogenase}} NADH + H^+$$

The NADH is a source of electrons for a variety of membrane-bound electron acceptors, generating the proton gradient needed for ATP synthesis. Other lithotrophs oxidize sulfur compounds (H_2S, elemental sulfur, or thiosulfate) or ferrous iron. A widespread group of archaea called methanogens, all strict anaerobes, extract energy from the reduction of CO_2 to methane. And this is just a small sampling of what anaerobic organisms do for a living. Their metabolic pathways are replete with interesting reactions and highly specialized cofactors unknown in our own world of obligate aerobic metabolism. Study of these organisms can yield practical dividends. It can also provide clues about the origins of life on an early Earth, in an atmosphere that lacked molecular oxygen.

The nitrogen cycle depends on a wide range of specialized bacteria. There are two groups of nitrifying bacteria: those that oxidize ammonia to nitrites and those that oxidize the resulting nitrites to nitrates (see Fig. 22–1). Nitrate is second only to O_2 as a biological electron acceptor, and a great many bacteria and archaea can catalyze the denitrification of nitrates to nitrogen, which the nitrogen-fixing bacteria then convert back into ammonia. Ammonia is a major pollutant in sewage and in farm animal waste, and is a byproduct of fertilizer manufacture and oil refining. Waste-treatment plants have generally made use of communities of nitrifying and denitrifying bacteria to convert ammonia waste to atmospheric nitrogen. The process is expensive, requiring inputs of organic carbon and oxygen.

In the 1960s and 1970s, a few articles appeared in the research literature suggesting that ammonia could be oxidized to nitrogen anaerobically, using nitrite as an electron acceptor; this process was called anammox. The reports received little notice until bacteria promoting anammox were discovered in a waste-treatment system in Delft, the Netherlands, in the mid-1980s. A team of Dutch microbiologists led by Gijs Kuenen and Mike Jetten began to study these bacteria, which were soon identified as belonging to an unusual bacterial phylum, Planctomycetes. Some surprises were to follow.

The biochemistry underlying the anammox process was slowly unraveled (Fig. 1). Hydrazine (N_2H_4),

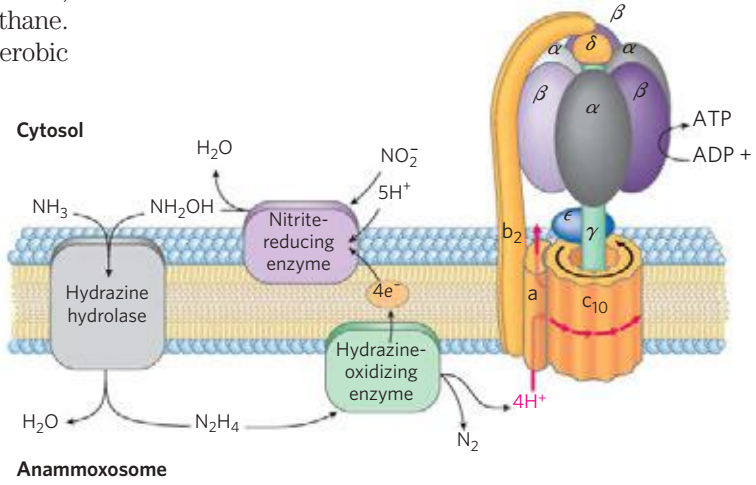

FIGURE 1 The anammox reactions. Ammonia and hydroxylamine are converted to hydrazine and H_2O by hydrazine hydrolase, and the hydrazine is oxidized by hydrazine-oxidizing enzyme, generating N_2 and protons. The protons generate a proton gradient for ATP synthesis. On the anammoxosome exterior, protons are used by the nitrite-reducing enzyme, producing hydroxylamine and completing the cycle. All of the anammox enzymes are embedded in the anammoxosome membrane.

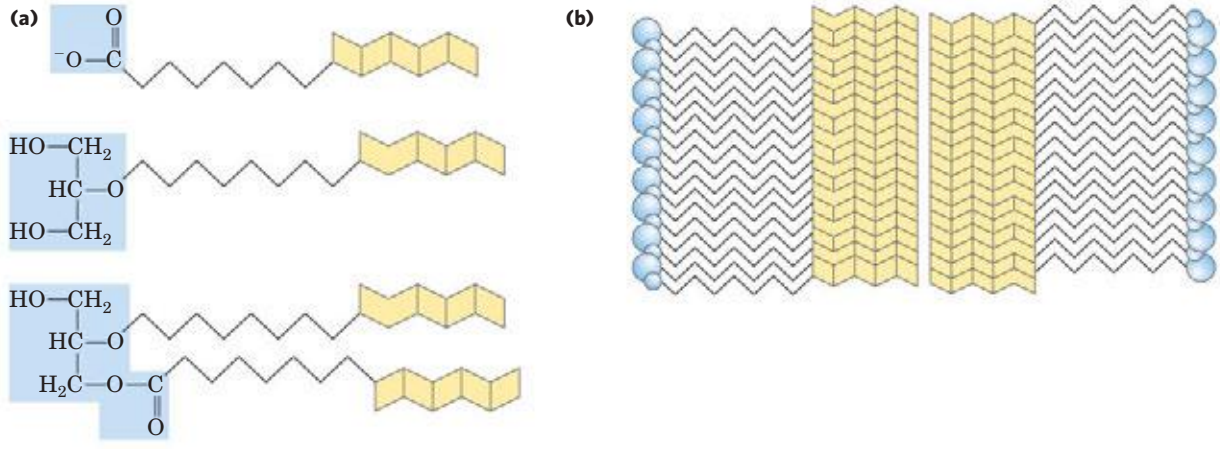

FIGURE 2 **(a)** Ladderane lipids of the anammoxosome membrane. The mechanism for synthesis of the unstable fused cyclobutane ring structures is unknown. **(b)** Ladderanes can stack to form a very dense, impermeable, hydrophobic membrane structure, allowing sequestration of the hydrazine produced in the anammox reactions.

a highly reactive molecule used as a rocket fuel, was an unexpected intermediate. As a small molecule, hydrazine is both highly toxic and difficult to contain. It readily diffuses across typical phospholipid membranes. The anammox bacteria solve this problem by sequestering hydrazine in a specialized organelle, dubbed the **anammoxosome**. The membrane of this organelle is composed of lipids known as **ladderanes** (Fig. 2), never before encountered in biology. The fused cyclobutane rings of ladderanes stack tightly to form a very dense barrier, greatly slowing the release of hydrazine. Cyclobutane rings are strained and difficult to synthesize; the bacterial mechanisms for synthesizing these lipids are not yet known.

The anammoxosome was a surprising finding. Bacterial cells generally do not have compartments, and the lack of a membrane-enclosed nucleus is often cited as the primary distinction between eukaryotes and bacteria. One type of organelle in a bacterium was interesting enough, but planctomycetes also have a nucleus: their chromosomal DNA is contained within a membrane (Fig. 3). Discovery of this subcellular organization has prompted further research to trace the origin of the planctomycetes and the evolution of eukaryotic nuclei. Planctomycetes are an ancient bacterial line with multiple genera, three of which are known to carry out the anammox reactions. Further study of this group may ultimately bring us closer to a key goal of evolutionary biology: a description of the organism affectionately referred to as LUCA—the last universal common ancestor of all life on our planet.

For now, the anammox bacteria offer a major advance in waste treatment, reducing the cost of ammonia removal by as much as 90% (the conventional denitrification steps are eliminated completely, and the aeration costs associated with nitrification are lower) and reducing the release of polluting byproducts. Clearly, a greater familiarity with the bacterial underpinnings of the biosphere can pay big dividends as we deal with the environmental challenges of the twenty-first century.

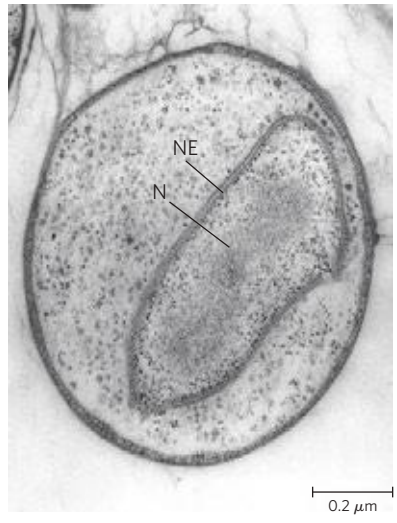

FIGURE 3 Transmission electron micrograph of a cross section through *Gemmata obscuriglobus*, showing the DNA in a nucleus (N) with enclosing nuclear envelope (NE). Bacteria of the *Gemmata* genus (phylum Planctomycetes) do not promote the anammox reactions.

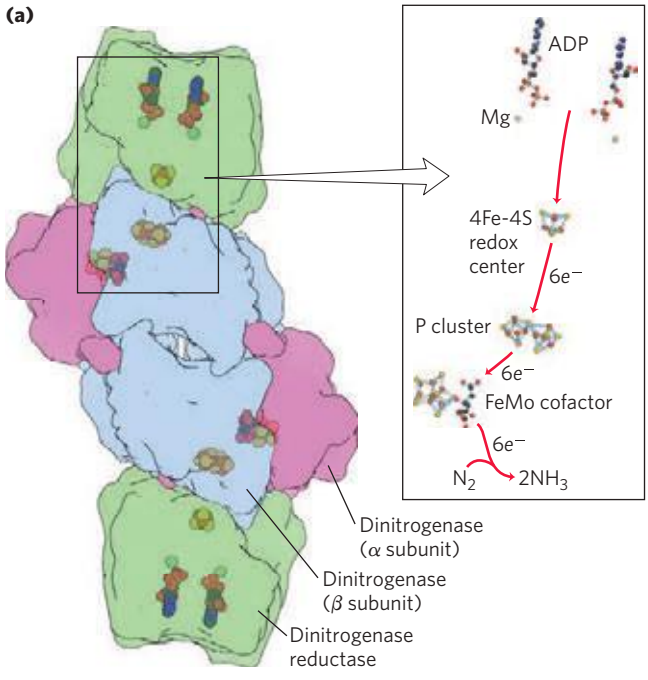

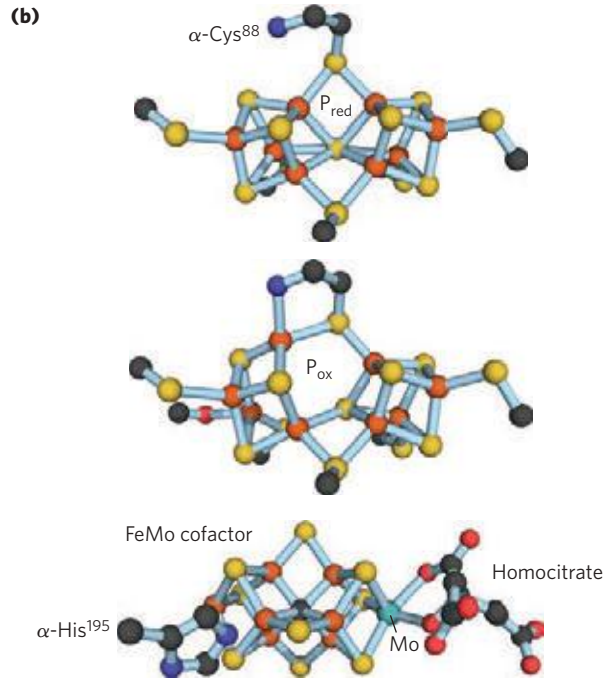

FIGURE 22–3 Enzymes and cofactors of the nitrogenase complex. (PDB ID 1FP6 and PDB ID 1M1N) **(a)** The holoenzyme consists of two identical dinitrogenase reductase molecules (green), each with a 4Fe-4S redox center and binding sites for two ATP, and two identical dinitrogenase heterodimers (purple and blue), each with a P cluster (Fe-S center) and an FeMo cofactor. In this structure, ADP is bound in the ATP site, to make the crystal more stable. **(b)** The electron-transfer cofactors. A P cluster is shown here in its reduced (top) and oxidized (middle) forms. The FeMo cofactor (bottom) has a Mo atom with three S ligands, a His ligand, and two oxygen ligands from a molecule of homocitrate. In some organisms, the Mo atom is replaced with a vanadium atom. (Fe is shown in orange, S in yellow.)

dissociates from dinitrogenase, in a repeating cycle. Each turn of the cycle requires the hydrolysis of two ATP molecules by the dimeric reductase. The immediate source of electrons to reduce dinitrogenase reductase varies, with reduced **ferredoxin** (see Section 19.8), reduced flavodoxin, and perhaps other sources playing a role. In at least one species, the ultimate source of electrons to reduce ferredoxin is pyruvate (Fig. 22–4).

The role of ATP in this process is somewhat unusual. Recall that ATP can contribute not only chemical energy, through the hydrolysis of one or more of its phosphoanhydride bonds, but also binding energy (p. 195), through noncovalent interactions that lower the activation energy. In the reaction carried out by dinitrogenase reductase, both ATP binding and ATP hydrolysis bring about protein conformational changes that help overcome the high activation energy of nitrogen fixation. The binding of two ATP molecules to the reductase shifts the reduction potential (E'°) of this protein from −300 to −420 mV, an enhancement of its reducing power that is

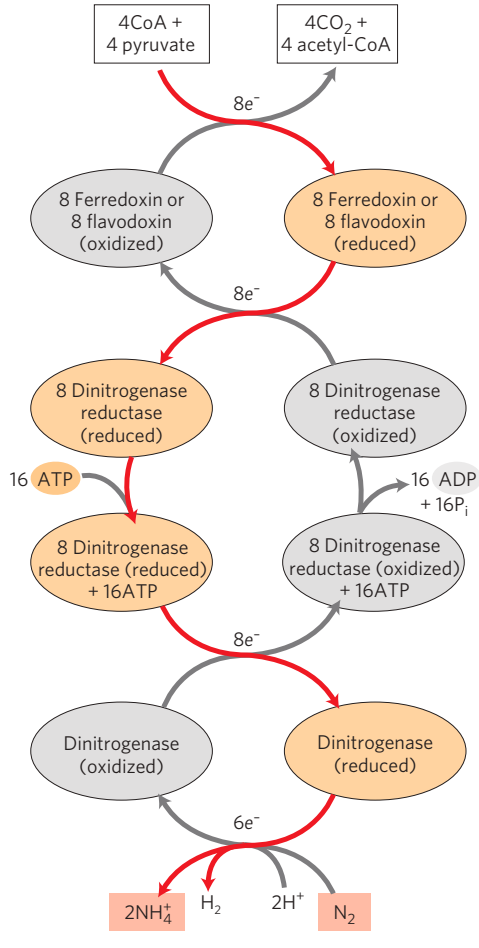

FIGURE 22–4 Electron path in nitrogen fixation by the nitrogenase complex. Electrons are transferred from pyruvate to dinitrogenase via ferredoxin (or flavodoxin) and dinitrogenase reductase. Dinitrogenase reductase reduces dinitrogenase one electron at a time, with at least six electrons required to fix one molecule of N_2. Two additional electrons are used to reduce $2H^+$ to H_2 in a process that obligatorily accompanies nitrogen fixation in anaerobes, making a total of eight electrons required per N_2 molecule. The subunit structures and metal cofactors of the dinitrogenase reductase and dinitrogenase proteins are described in the text and in Figure 22–3.

required to transfer electrons through dinitrogenase to N_2; the standard reduction potential for the half-reaction $N_2 + 6H^+ + 6e^- \longrightarrow 2NH_3$ is -0.34 V. The ATP molecules are then hydrolyzed just before the actual transfer of one electron to dinitrogenase.

ATP binding and hydrolysis change the conformation of nitrogenase reductase in two regions, which are structurally homologous with switch 1 and switch 2 regions of the GTP-binding proteins involved in biological signaling (see Box 12–2). ATP binding produces a conformational change that brings the 4Fe-4S center of the reductase closer to the P cluster of dinitrogenase (from 18 Å to 14 Å away), which facilitates electron transfer between the reductase and dinitrogenase. The details of electron transfer from the P cluster to the FeMo cofactor, and the means by which eight electrons are accumulated by nitrogenase, are not known, nor are the intermediates in the reaction known with certainty; two reasonable hypotheses are being tested, both involving the Mo atom as a central player **(Fig. 22–5)**.

The nitrogenase complex is remarkably unstable in the presence of oxygen. The reductase is inactivated in air, with a half-life of 30 seconds; dinitrogenase has a half-life of only 10 minutes in air. Free-living bacteria that fix nitrogen cope with this problem in a variety of ways. Some live only anaerobically or repress nitrogenase synthesis when oxygen is present. Some aerobic species, such as *Azotobacter vinelandii*, partially uncouple electron transfer from ATP synthesis so that oxygen is burned off as rapidly as it enters the cell (see Box 19–1). When fixing nitrogen, cultures of these bacteria actually increase in temperature as a result of their efforts to rid themselves of oxygen.

The symbiotic relationship between leguminous plants and the nitrogen-fixing bacteria in their root nodules **(Fig. 22–6)** takes care of both the energy requirements and the oxygen lability of the nitrogenase complex. The energy required for nitrogen fixation was probably the evolutionary driving force for this plant-bacteria association. The bacteria in root nodules have access to a large reservoir of energy in the form of abundant carbohydrate and citric acid cycle intermediates made available by the plant. This may allow the bacteria to fix hundreds of times more nitrogen than do their free-living cousins under

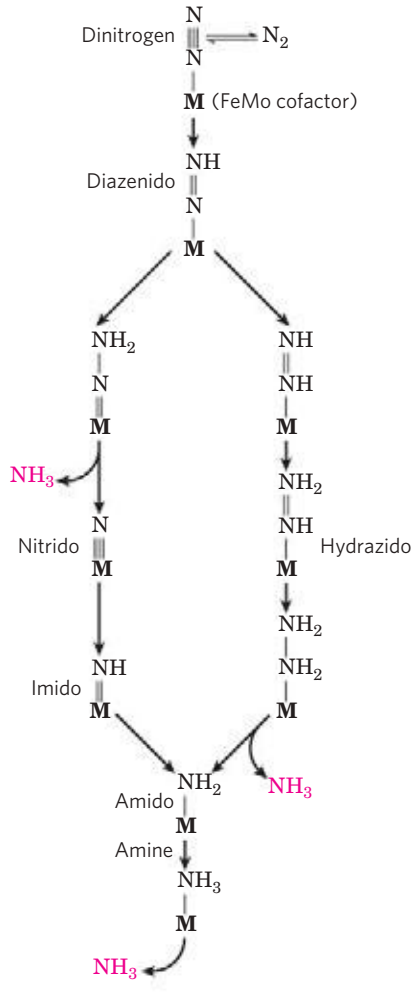

FIGURE 22–5 Two reasonable hypotheses for the intermediates involved in N_2 reduction. In both scenarios, the FeMo cofactor (abbreviated as **M** here) plays a central role, binding directly to one of the nitrogen atoms of N_2 and remaining bound throughout the sequence of reduction steps.

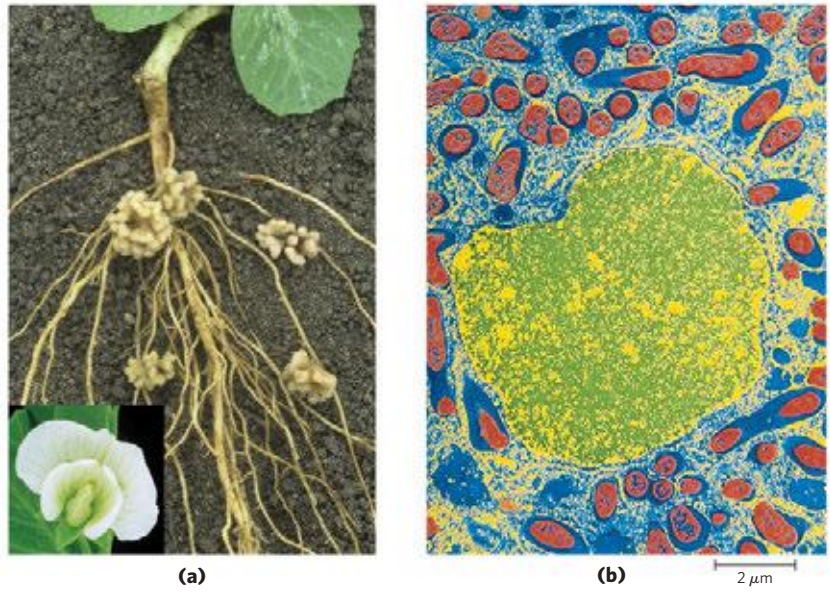

FIGURE 22–6 Nitrogen-fixing nodules. (a) Root nodules of the common pea, *Pisum saliva*, a legume. The flower of this plant is shown in the inset. **(b)** Artificially colorized electron micrograph of a thin section through a pea root nodule. Symbiotic nitrogen-fixing bacteria, or bacteroids (red), live inside the nodule cell, surrounded by the peribacteroid membrane (blue). Bacteroids produce the nitrogenase complex that converts atmospheric nitrogen (N_2) to ammonium (NH_4^+); without the bacteroids, the plant is unable to utilize N_2. The infected root cell provides some factors essential for nitrogen fixation, including leghemoglobin; this heme protein has a very high binding affinity for oxygen, which strongly inhibits nitrogenase. (The cell nucleus is shown in yellow/green. Not visible in this micrograph are other organelles of the infected root cell that are normally found in plant cells.)

conditions generally encountered in soils. To solve the oxygen-toxicity problem, the bacteria in root nodules are bathed in a solution of the oxygen-binding heme protein **leghemoglobin**, produced by the plant (although the heme may be contributed by the bacteria). Leghemoglobin binds all available oxygen so that it cannot interfere with nitrogen fixation, and efficiently delivers the oxygen to the bacterial electron-transfer system. The benefit to the plant, of course, is a ready supply of reduced nitrogen. In fact, the bacterial symbionts typically produce far more NH_3 than is needed by their symbiotic partner; the excess is released into the soil. The efficiency of the symbiosis between plants and bacteria is evident in the enrichment of soil nitrogen brought about by leguminous plants. This enrichment of NH_3 in the soil is the basis of crop rotation methods, in which plantings of nonleguminous plants (such as maize) that extract fixed nitrogen from the soil are alternated every few years with plantings of legumes such as alfalfa, peas, or clover.

Nitrogen fixation is energetically costly: 16 ATP and 8 electron pairs yield only 2 NH_3. It is therefore not surprising that the process is tightly regulated, so that NH_3 is produced only when needed. High [ADP], an indicator of low [ATP], is a strong inhibitor of nitrogenase. NH_4^+ represses the expression of the ~20 nitrogen fixation (*nif*) genes, effectively shutting down the pathway. Covalent alteration of nitrogenase is also used in some diazotrophs to control nitrogen fixation in response to the availability of NH_4^+ in the surroundings. Transfer of an ADP-ribosyl group from NADH to a specific Arg residue in the nitrogenase reductase shuts down N_2 fixation in *Rhodospirillum*, for example. This is the same covalent modification that we saw in the case of G protein inhibition by the toxins of cholera and pertussis (see Box 12–2).

Nitrogen fixation is the subject of intense study because of its immense practical importance. Industrial production of ammonia for use in fertilizers requires a large and expensive input of energy, and this has spurred a drive to develop recombinant or transgenic organisms that can fix nitrogen. In principle, recombinant DNA techniques (Chapter 9) might be used to transfer the DNA that encodes the enzymes of nitrogen fixation into non-nitrogen-fixing bacteria and plants. However, those genes alone will not suffice. About 20 genes are essential to nitrogenase activity in bacteria, many of them needed for the synthesis, assembly, and insertion of the cofactors. There is also the problem of protecting the enzyme in its new setting from destruction by oxygen. In all, there are formidable challenges in engineering new nitrogen-fixing plants. Success in these efforts will depend on overcoming the problem of oxygen toxicity in any cell that produces nitrogenase.

Ammonia Is Incorporated into Biomolecules through Glutamate and Glutamine

Reduced nitrogen in the form of NH_4^+ is assimilated into amino acids and then into other nitrogen-containing biomolecules. Two amino acids, **glutamate** and **glutamine**, provide the critical entry point. Recall that these same two amino acids play central roles in the catabolism of ammonia and amino groups in amino acid oxidation (Chapter 18). Glutamate is the source of amino groups for most other amino acids, through transamination reactions (the reverse of the reaction shown in Fig. 18–4). The amide nitrogen of glutamine is a source of amino groups in a wide range of biosynthetic processes. In most types of cells, and in extracellular fluids in higher organisms, one or both of these amino acids are present at higher concentrations—sometimes an order of magnitude or more higher—than other amino acids. An *Escherichia coli* cell requires so much glutamate that this amino acid is one of the primary solutes in the cytosol. Its concentration is regulated not only in response to the cell's nitrogen requirements but also to maintain an osmotic balance between the cytosol and the external medium.

The biosynthetic pathways to glutamate and glutamine are simple, and all or some of the steps occur in most organisms. The most important pathway for the assimilation of NH_4^+ into glutamate requires two reactions. First, **glutamine synthetase** catalyzes the reaction of glutamate and NH_4^+ to yield glutamine. This reaction takes place in two steps, with enzyme-bound γ-glutamyl phosphate as an intermediate (see Fig. 18–8):

(1) Glutamate + ATP $\longrightarrow$ γ-glutamyl phosphate + ADP

(2) γ-Glutamyl phosphate + NH_4^+ $\longrightarrow$ glutamine + P_i + H^+

Sum: Glutamate + NH_4^+ + ATP $\longrightarrow$ glutamine + ADP + P_i + H^+ (22–1)

Glutamine synthetase is found in all organisms. In addition to its importance for NH_4^+ assimilation in bacteria, it has a central role in amino acid metabolism in mammals, converting free NH_4^+, which is toxic, to glutamine for transport in the blood (Chapter 18).

In bacteria and plants, glutamate is produced from glutamine in a reaction catalyzed by **glutamate synthase**. (An alternative name for this enzyme, glutamate: oxoglutarate aminotransferase, yields the acronym GOGAT, by which the enzyme also is known.) α-Ketoglutarate, an intermediate of the citric acid cycle, undergoes reductive amination with glutamine as nitrogen donor:

α-Ketoglutarate + glutamine + NADPH + H^+ $\longrightarrow$ 2 glutamate + $NADP^+$ (22–2)

The net reaction of glutamine synthetase and glutamate synthase (Eqns 22–1 and 22–2) is

α-Ketoglutarate + NH_4^+ + NADPH + ATP $\longrightarrow$ L-glutamate + $NADP^+$ + ADP + P_i

Glutamate synthase is not present in animals, which instead maintain high levels of glutamate by processes such as the transamination of α-ketoglutarate during amino acid catabolism.

Glutamate can also be formed in yet another, albeit minor, pathway: the reaction of α-ketoglutarate and NH_4^+ to form glutamate in one step. This is catalyzed by

L-glutamate dehydrogenase, an enzyme present in all organisms. Reducing power is furnished by NADPH:

$$\alpha\text{-Ketoglutarate} + NH_4^+ + NADPH \longrightarrow \text{L-glutamate} + NADP^+ + H_2O$$

We encountered this reaction in the catabolism of amino acids (see Fig. 18–7). In eukaryotic cells, L-glutamate dehydrogenase is located in the mitochondrial matrix. The reaction equilibrium favors the reactants, and the K_m for NH_4^+ (~1 mM) is so high that the reaction probably makes only a modest contribution to NH_4^+ assimilation into amino acids and other metabolites. (Recall that the glutamate dehydrogenase reaction, in reverse (see Fig. 18–10), is one source of NH_4^+ destined for the urea cycle.) Concentrations of NH_4^+ high enough for the glutamate dehydrogenase reaction to make a significant contribution to glutamate levels generally occur only when NH_3 is added to the soil or when organisms are grown in a laboratory in the presence of high NH_3 concentrations. In general, soil bacteria and plants rely on the two-enzyme pathway outlined above (Eqns. 22–1, 22–2).

Glutamine Synthetase Is a Primary Regulatory Point in Nitrogen Metabolism

The activity of glutamine synthetase is regulated in virtually all organisms—as expected, given its central metabolic role as an entry point for reduced nitrogen. In enteric bacteria such as *E. coli*, the regulation is unusually complex. Type I enzyme (from bacteria) has 12 identical subunits of M_r 50,000 **(Fig. 22–7)** and is regulated both allosterically and by covalent modification. (Type II enzyme, from eukaryotes and some bacteria, has 10 identical subunits.) Alanine, glycine, and at least six end products of glutamine metabolism are allosteric inhibitors of the enzyme **(Fig. 22–8)**. Each inhibitor alone produces only partial inhibition, but the effects of multiple inhibitors are more than additive, and all eight together virtually shut down the enzyme. This is an example of cumulative feedback inhibition. This control mechanism provides a constant adjustment of glutamine levels to match immediate metabolic requirements.

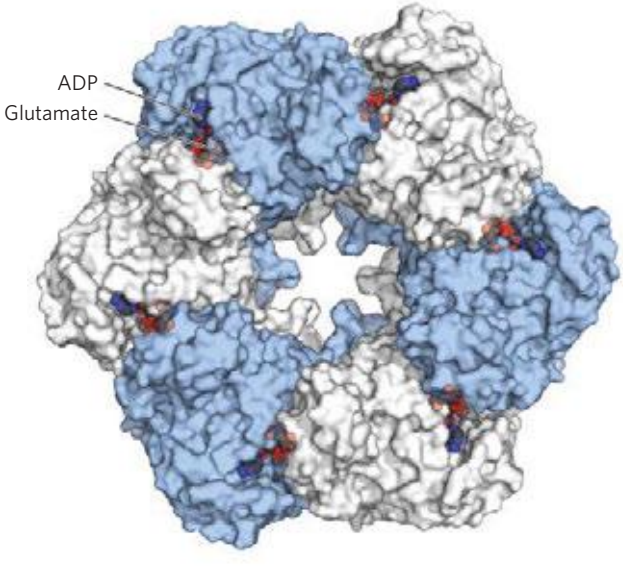

FIGURE 22–7 Subunit structure of bacterial type I glutamine synthetase. (PDB ID 2GLS) This view shows 6 of 12 the identical subunits; a second layer of 6 subunits lies directly beneath the six shown. Each of the 12 subunits has an active site, where ATP and glutamate are bound in orientations that favor transfer of a phosphoryl group from ATP to the side-chain carboxyl of glutamate. In this crystal structure, ADP occupies the ATP site.

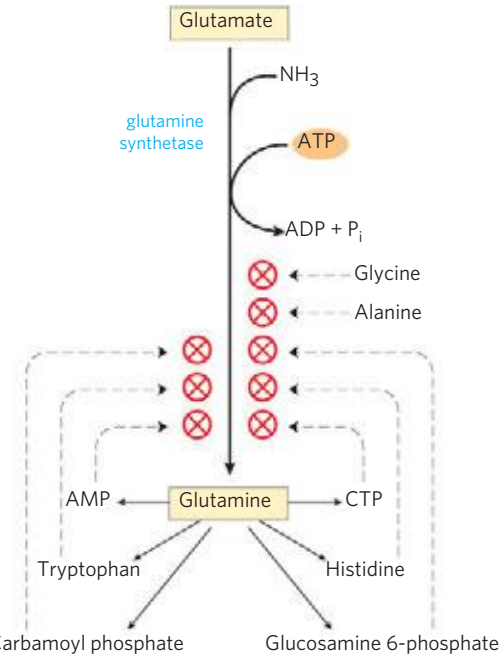

FIGURE 22–8 Allosteric regulation of glutamine synthetase. The enzyme undergoes cumulative regulation by six end products of glutamine metabolism. Alanine and glycine probably serve as indicators of the general status of amino acid metabolism in the cell.

Superimposed on the allosteric regulation is inhibition by adenylylation of (addition of AMP to) Tyr^{397}, located near the enzyme's active site **(Fig. 22–9)**. This covalent modification increases sensitivity to the allosteric inhibitors, and activity decreases as more subunits are adenylylated. Both adenylylation and deadenylylation are promoted by **adenylyltransferase** (AT in Fig. 22–9), part of a complex enzymatic cascade that responds to levels of glutamine, α-ketoglutarate, ATP, and P_i. The activity of adenylyltransferase is modulated by binding to a regulatory protein called P_{II}, and the activity of P_{II}, in turn, is regulated by covalent modification (uridylylation), again at a Tyr residue. The adenylyltransferase complex with uridylylated P_{II} (P_{II}-UMP) stimulates deadenylylation, whereas the same complex with deuridylylated P_{II} stimulates adenylylation of glutamine synthetase. Both uridylylation and deuridylylation of P_{II} are brought about by a single enzyme, **uridylyltransferase**. Uridylylation is inhibited by binding of glutamine and P_i to uridylyltransferase and is stimulated by binding of α-ketoglutarate and ATP to P_{II}.

The regulation does not stop there. The uridylylated P_{II} also mediates the activation of transcription of the gene encoding glutamine synthetase, thus increasing the cellular concentration of the enzyme; the deuridylylated

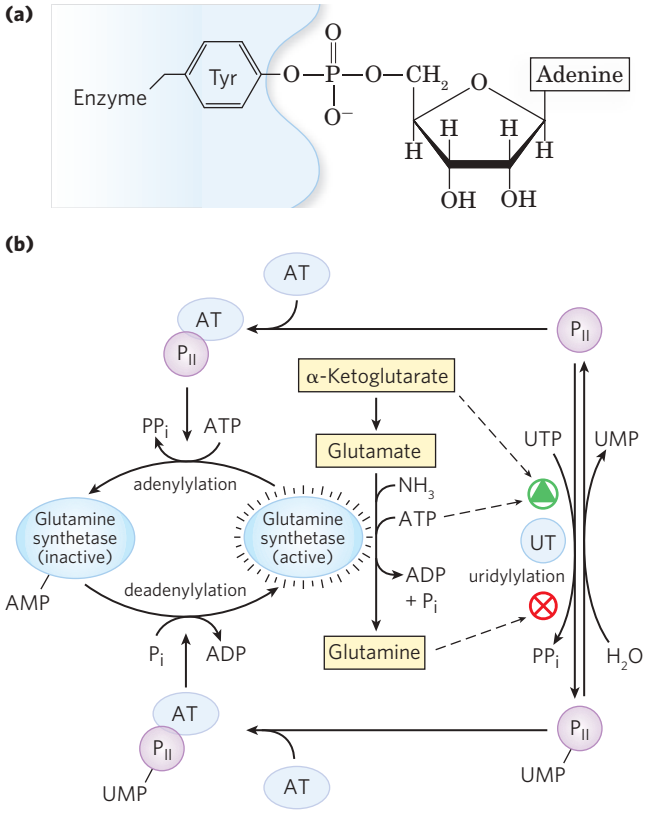

FIGURE 22–9 Second level of regulation of glutamine synthetase: covalent modifications. (a) An adenylylated Tyr residue. **(b)** Cascade leading to adenylylation (inactivation) of glutamine synthetase. AT represents adenylyltransferase; UT, uridylyltransferase. P_{II} is a regulatory protein, itself regulated by uridylylation. Details of this cascade are discussed in the text.

P_{II} brings about a decrease in transcription of the same gene. This mechanism involves an interaction of P_{II} with additional proteins involved in gene regulation, of a type described in Chapter 28. The net result of this elaborate system of controls is a decrease in glutamine synthetase activity when glutamine levels are high, and an increase in activity when glutamine levels are low and α-ketoglutarate and ATP (substrates for the synthetase reaction) are available. The multiple layers of regulation permit a sensitive response in which glutamine synthesis is tailored to cellular needs.

Several Classes of Reactions Play Special Roles in the Biosynthesis of Amino Acids and Nucleotides

The pathways described in this chapter include a variety of interesting chemical rearrangements. Several of these recur and deserve special note before we progress to the pathways themselves. These are (1) transamination reactions and other rearrangements promoted by enzymes containing pyridoxal phosphate; (2) transfer of one-carbon groups, with either tetrahydrofolate (usually at the —CHO and $—CH_2OH$ oxidation levels) or *S*-adenosylmethionine (at the $—CH_3$ oxidation level) as cofactor; and (3) transfer of amino groups derived from the amide nitrogen of glutamine. Pyridoxal phosphate (PLP), tetrahydrofolate (H_4 folate), and *S*-adenosylmethionine (adoMet) are described in some detail in Chapter 18 (see Figs 18–6, 18–17, and 18–18). Here we focus on amino group transfer involving the amide nitrogen of glutamine.

More than a dozen known biosynthetic reactions use glutamine as the major physiological source of amino groups, and most of these occur in the pathways outlined in this chapter. As a class, the enzymes catalyzing these reactions are called **glutamine amidotransferases**. All have two structural domains: one binding glutamine, the other binding the second substrate, which serves as amino group acceptor **(Fig. 22–10)**. A conserved Cys

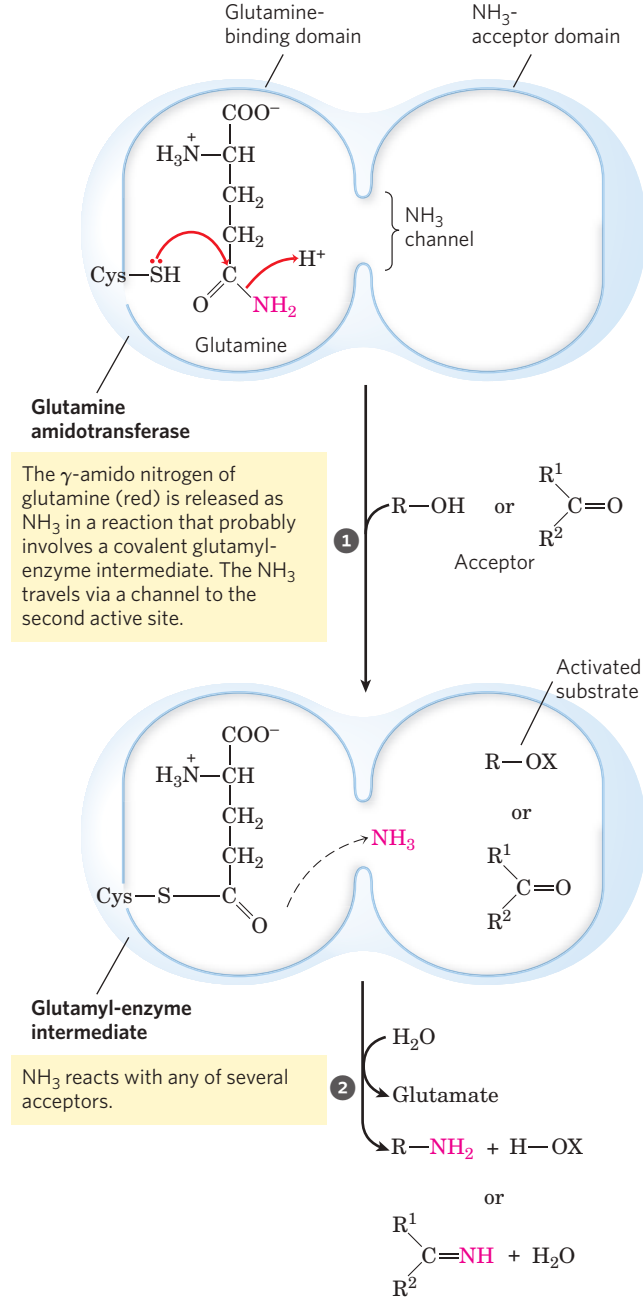

MECHANISM FIGURE 22–10 Proposed mechanism for glutamine amidotransferases. Each enzyme has two domains. The glutamine-binding domain contains structural elements conserved among many of these enzymes, including a Cys residue required for activity. The NH_3-acceptor (second-substrate) domain varies. Two types of amino acceptors are shown. X represents an activating group, typically a phosphoryl group derived from ATP, that facilitates displacement of a hydroxyl group from R—OH by NH_3.

residue in the glutamine-binding domain is believed to act as a nucleophile, cleaving the amide bond of glutamine and forming a covalent glutamyl-enzyme intermediate. The NH_3 produced in this reaction is not released, but instead is transferred through an "ammonia channel" to a second active site, where it reacts with the second substrate to form the aminated product. The covalent intermediate is hydrolyzed to the free enzyme and glutamate. If the second substrate must be activated, the usual method is the use of ATP to generate an acyl phosphate intermediate (R—OX in Fig. 22–10, with X as a phosphoryl group). The enzyme glutaminase acts in a similar fashion but uses H_2O as the second substrate, yielding NH_4^+ and glutamate (see Fig. 18–8).

SUMMARY 22.1 Overview of Nitrogen Metabolism

- The molecular nitrogen that makes up 80% of Earth's atmosphere is unavailable to most living organisms until it is reduced. This fixation of atmospheric N_2 takes place in certain free-living bacteria and in symbiotic bacteria in the root nodules of leguminous plants.
- In soil bacteria and vascular plants, the sequential action of nitrate reductase and nitrite reductase converts NO_3^- to NH_3, which can be assimilated into nitrogen-containing compounds.
- The nitrogen cycle entails formation of ammonia by bacterial fixation of N_2, nitrification of ammonia to nitrate by soil organisms, conversion of nitrate to ammonia by higher plants, synthesis of amino acids from ammonia by all organisms, and conversion of nitrate to N_2 by denitrifying soil bacteria. The anammox bacteria anaerobically oxidize ammonia to nitrogen, using nitrite as an electron acceptor.
- Fixation of N_2 as NH_3 is carried out by the nitrogenase complex, in a reaction that requires large investments of ATP and of reducing power. The nitrogenase complex is highly labile in the presence of O_2, and is subject to regulation by the supply of NH_3.
- In living systems, reduced nitrogen is incorporated first into amino acids and then into a variety of other biomolecules, including nucleotides. The key entry point is the amino acid glutamate. Glutamate and glutamine are the nitrogen donors in a wide range of biosynthetic reactions. Glutamine synthetase, which catalyzes the formation of glutamine from glutamate, is a main regulatory enzyme of nitrogen metabolism.
- The amino acid and nucleotide biosynthetic pathways make repeated use of the biological cofactors pyridoxal phosphate, tetrahydrofolate, and *S*-adenosylmethionine. Pyridoxal phosphate is required for transamination reactions involving glutamate and for other amino acid transformations. One-carbon transfers require *S*-adenosylmethionine and tetrahydrofolate. Glutamine amidotransferases catalyze reactions that incorporate nitrogen derived from glutamine.

22.2 Biosynthesis of Amino Acids

All amino acids are derived from intermediates in glycolysis, the citric acid cycle, or the pentose phosphate pathway **(Fig. 22–11)**. Nitrogen enters these pathways by way of glutamate and glutamine. Some pathways are simple, others are not. Ten of the amino acids are just one or several steps removed from the common metabolite from which they are derived. The biosynthetic pathways for others, such as the aromatic amino acids, are more complex.

Organisms vary greatly in their ability to synthesize the 20 common amino acids. Whereas most bacteria and plants can synthesize all 20, mammals can synthesize only about half of them—generally those

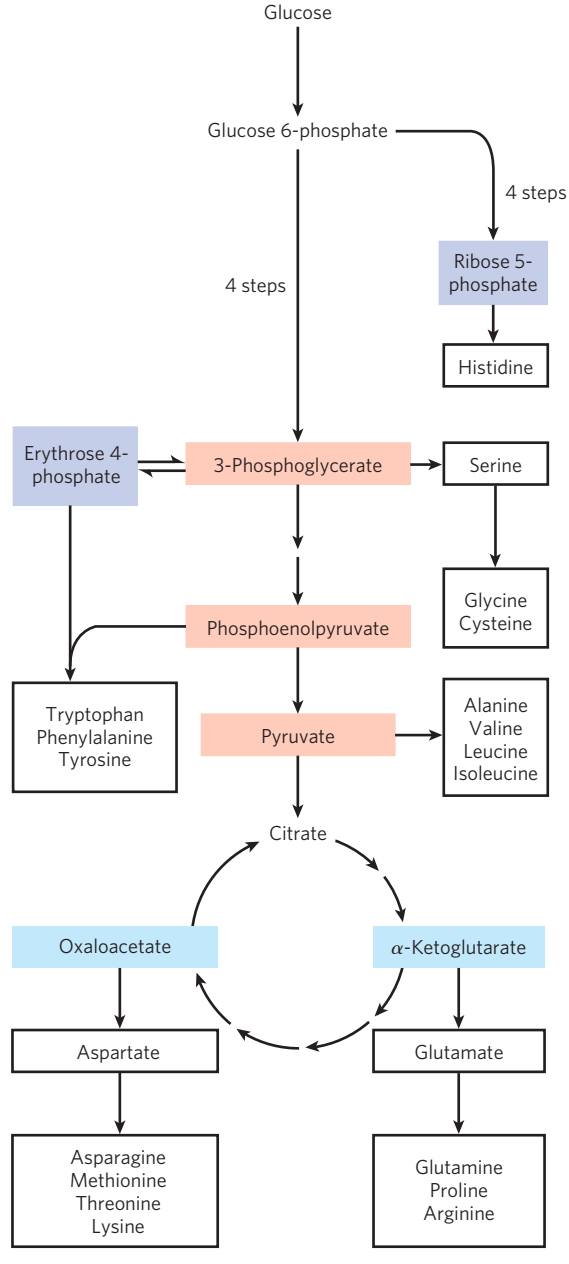

FIGURE 22–11 Overview of amino acid biosynthesis. The carbon skeleton precursors derive from three sources: glycolysis (light red), the citric acid cycle (blue), and the pentose phosphate pathway (purple).

with simple pathways. These are the **nonessential amino acids**, not needed in the diet (see Table 18–1). The remainder, the **essential amino acids**, must be obtained from food. Unless otherwise indicated, the pathways for the 20 common amino acids presented below are those operative in bacteria.

A useful way to organize these biosynthetic pathways is to group them into six families corresponding to their metabolic precursors (Table 22–1), and we use this approach to structure the detailed descriptions that follow. In addition to these six precursors, there is a notable intermediate in several pathways of amino acid and nucleotide synthesis: **5-phosphoribosyl-1-pyrophosphate (PRPP)**:

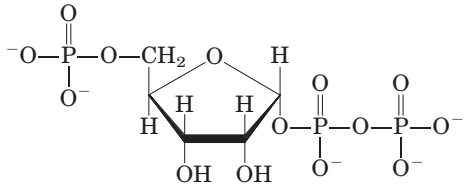

PRPP is synthesized from ribose 5-phosphate derived from the pentose phosphate pathway (see Fig. 14–22), in a reaction catalyzed by **ribose phosphate pyrophosphokinase**:

Ribose 5-phosphate + ATP ⟶
5-phosphoribosyl-1-pyrophosphate + AMP

This enzyme is allosterically regulated by many of the biomolecules for which PRPP is a precursor.

α-Ketoglutarate Gives Rise to Glutamate, Glutamine, Proline, and Arginine

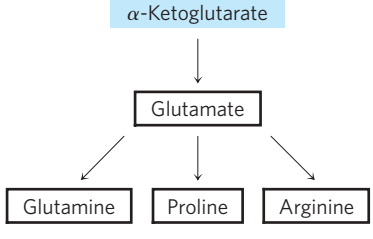

We have already described the biosynthesis of **glutamate** and **glutamine**. **Proline** is a cyclized derivative of glutamate **(Fig. 22–12)**. In the first step of proline synthesis, ATP reacts with the γ-carboxyl group of glutamate to form an acyl phosphate, which is reduced by NADPH or NADH to glutamate γ-semialdehyde. This intermediate undergoes rapid spontaneous cyclization and is then reduced further to yield proline.

Arginine is synthesized from glutamate via ornithine and the urea cycle in animals (Chapter 18). In principle, ornithine could also be synthesized from glutamate γ-semialdehyde by transamination, but the spontaneous cyclization of the semialdehyde in the proline pathway precludes a sufficient supply of this intermediate for ornithine synthesis. Bacteria have a de novo biosynthetic pathway for ornithine (and thus arginine) that parallels some steps of the proline pathway but includes two additional steps that avoid the problem of the spontaneous cyclization of glutamate γ-semialdehyde (Fig. 22–12). In the first step, the α-amino group of glutamate is blocked by an acetylation requiring acetyl-CoA; then, after the transamination step, the acetyl group is removed to yield ornithine.

The pathways to proline and arginine are somewhat different in mammals. Proline can be synthesized by the pathway shown in Figure 22–12, but it is also formed from arginine obtained from dietary or tissue protein. Arginase, a urea cycle enzyme, converts arginine to ornithine and urea (see Figs 18–10, 18–26). The ornithine is converted to glutamate γ-semialdehyde by the enzyme **ornithine δ-aminotransferase (Fig. 22–13)**. The semialdehyde cyclizes to Δ^1-pyrroline-5-carboxylate, which is then converted to proline (Fig. 22–12). The pathway for arginine synthesis shown in Figure 22–12 is absent in mammals. When arginine from dietary intake or protein turnover is insufficient for protein synthesis, the ornithine δ-aminotransferase reaction operates in the direction of ornithine formation. Ornithine is then converted to citrulline and arginine in the urea cycle.

TABLE 22–1 Amino Acid Biosynthetic Families, Grouped by Metabolic Precursor

α-Ketoglutarate	**Pyruvate**
Glutamate	Alanine
Glutamine	Valine*
Proline	Leucine*
Arginine	Isoleucine*
3-Phosphoglycerate	**Phosphoenolpyruvate and erythrose 4-phosphate**
Serine	
Glycine	
Cysteine	Tryptophan*
Oxaloacetate	Phenylalanine*
Aspartate	Tyrosine†
Asparagine	**Ribose 5-phosphate**
Methionine*	Histidine*
Threonine*	
Lysine*	

*Essential amino acids in mammals.
†Derived from phenylalanine in mammals.

Serine, Glycine, and Cysteine Are Derived from 3-Phosphoglycerate

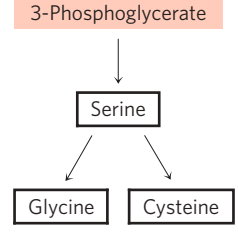

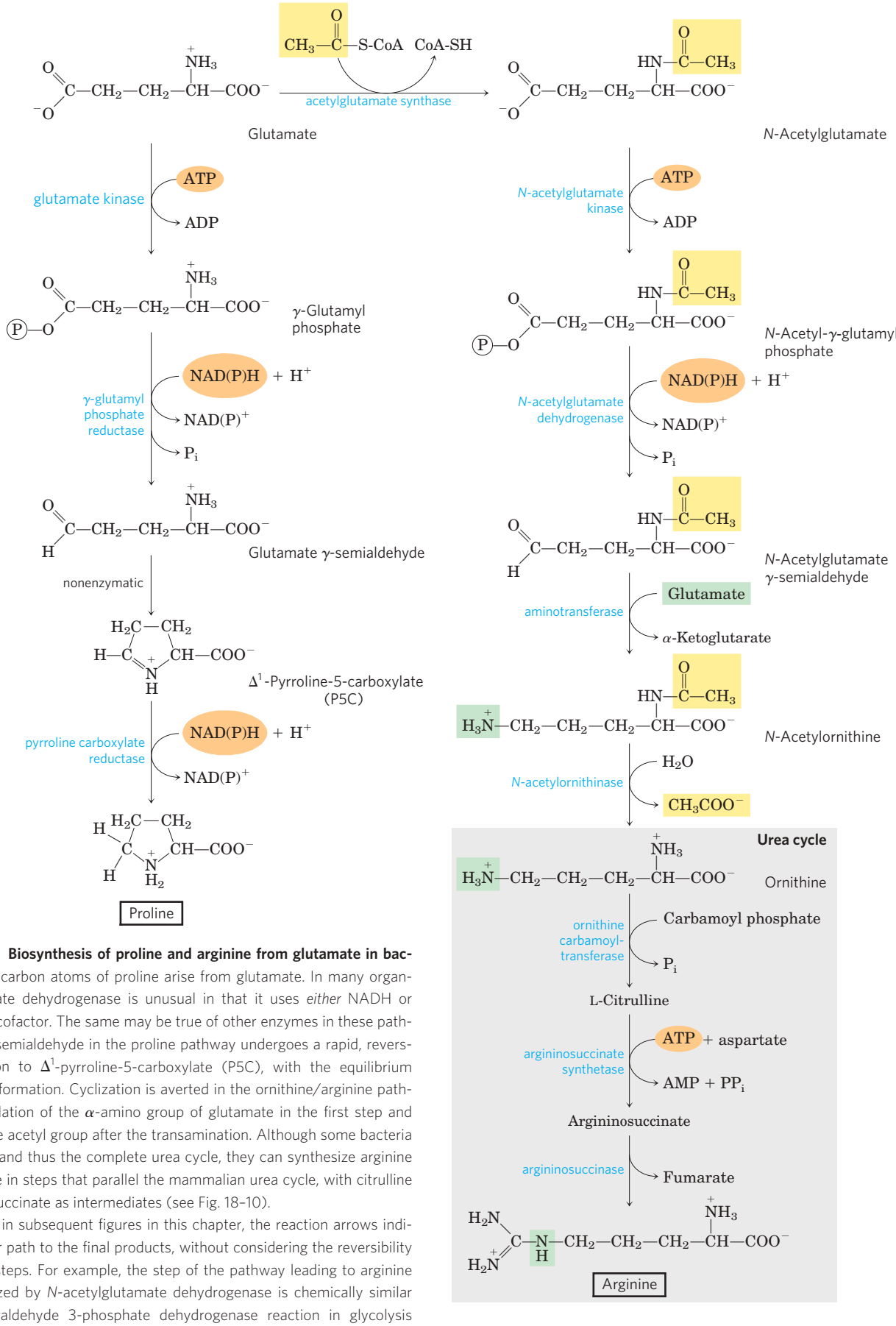

FIGURE 22–12 Biosynthesis of proline and arginine from glutamate in bacteria. All five carbon atoms of proline arise from glutamate. In many organisms, glutamate dehydrogenase is unusual in that it uses *either* NADH or NADPH as a cofactor. The same may be true of other enzymes in these pathways. The γ-semialdehyde in the proline pathway undergoes a rapid, reversible cyclization to Δ^1-pyrroline-5-carboxylate (P5C), with the equilibrium favoring P5C formation. Cyclization is averted in the ornithine/arginine pathway by acetylation of the α-amino group of glutamate in the first step and removal of the acetyl group after the transamination. Although some bacteria lack arginase and thus the complete urea cycle, they can synthesize arginine from ornithine in steps that parallel the mammalian urea cycle, with citrulline and argininosuccinate as intermediates (see Fig. 18–10).

Here, and in subsequent figures in this chapter, the reaction arrows indicate the linear path to the final products, without considering the reversibility of individual steps. For example, the step of the pathway leading to arginine that is catalyzed by *N*-acetylglutamate dehydrogenase is chemically similar to the glyceraldehyde 3-phosphate dehydrogenase reaction in glycolysis (see Fig. 14–8), and is readily reversible.

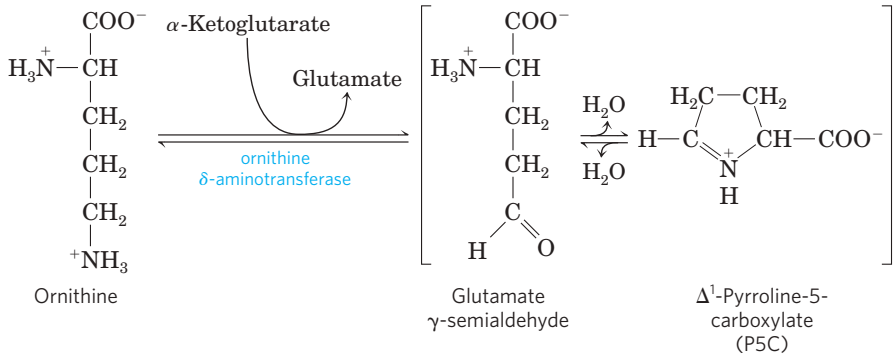

FIGURE 22–13 Ornithine δ-aminotransferase reaction: a step in the mammalian pathway to proline. This enzyme is found in the mitochondrial matrix of most tissues. Although the equilibrium favors P5C formation, the reverse reaction is the only mammalian pathway for synthesis of ornithine (and thus arginine) when arginine levels are insufficient for protein synthesis.

The major pathway for the formation of **serine** is the same in all organisms **(Fig. 22–14)**. In the first step, the hydroxyl group of 3-phosphoglycerate is oxidized by a dehydrogenase (using NAD^+) to yield 3-phosphohydroxypyruvate. Transamination from glutamate yields 3-phosphoserine, which is hydrolyzed to free serine by phosphoserine phosphatase.

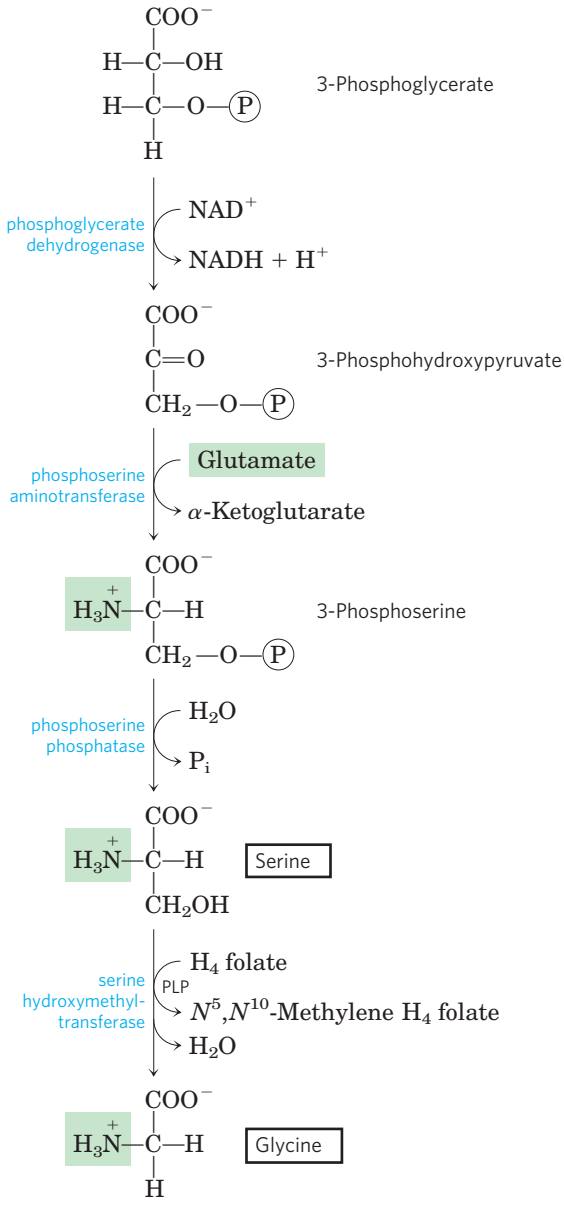

Serine (three carbons) is the precursor of **glycine** (two carbons) through removal of a carbon atom by **serine hydroxymethyltransferase** (Fig. 22–14). Tetrahydrofolate accepts the β carbon (C-3) of serine, which forms a methylene bridge between N-5 and N-10 to yield N^5,N^{10}-methylenetetrahydrofolate (see Fig. 18–17). The overall reaction, which is reversible, also requires pyridoxal phosphate. In the liver of vertebrates, glycine can be made by another route: the reverse of the reaction shown in Figure 18–20c, catalyzed by **glycine synthase** (also called **glycine cleavage enzyme**):

$$CO_2 + NH_4^+ + N^5,N^{10}\text{-methylenetetrahydrofolate} + NADH + H^+ \longrightarrow \text{glycine} + \text{tetrahydrofolate} + NAD^+$$

Plants and bacteria produce the reduced sulfur required for the synthesis of **cysteine** (and methionine, described later) from environmental sulfates; the pathway is shown on the right side of **Figure 22–15**. Sulfate is activated in two steps to produce 3′-phosphoadenosine 5′-phosphosulfate (PAPS), which undergoes an eight-electron reduction to sulfide. The sulfide is then used in the formation of cysteine from serine in a two-step pathway. Mammals synthesize cysteine from two amino acids: methionine furnishes the sulfur atom, and serine furnishes the carbon skeleton. Methionine is first converted to *S*-adenosylmethionine (see Fig. 18–18), which can lose its methyl group to any of a number of acceptors to form *S*-adenosylhomocysteine (adoHcy). This demethylated product is hydrolyzed to free homocysteine, which undergoes a reaction with serine, catalyzed by **cystathionine β-synthase**, to yield cystathionine **(Fig. 22–16)**. Finally, **cystathionine γ-lyase**, a PLP-requiring enzyme, catalyzes removal of ammonia and cleavage of cystathionine to yield free cysteine.

FIGURE 22–14 Biosynthesis of serine from 3-phosphoglycerate and of glycine from serine in all organisms. Glycine is also made from CO_2 and NH_4^+ by the action of glycine synthase, with N^5,N^{10}-methylenetetrahydrofolate as methyl group donor (see text).

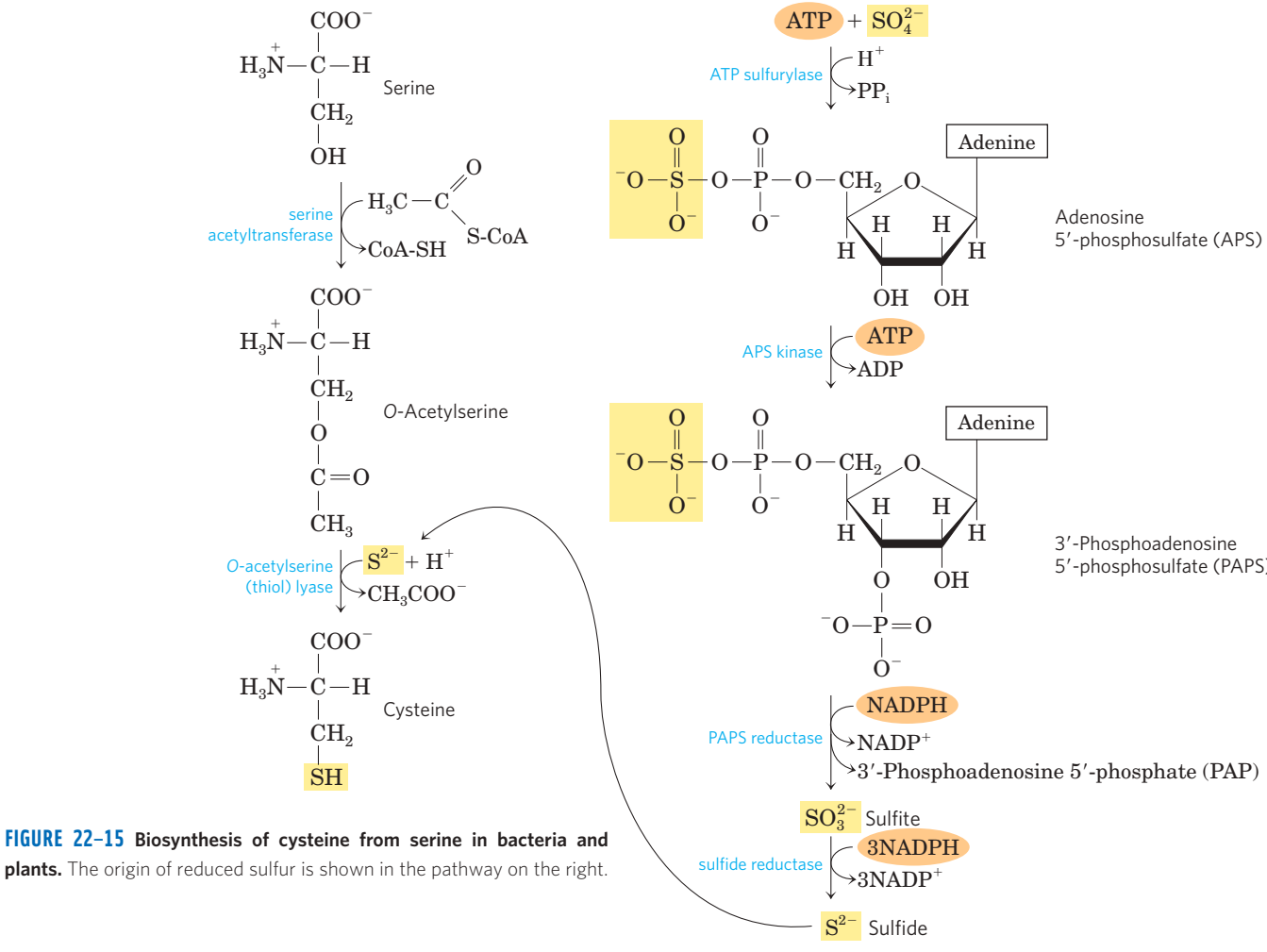

FIGURE 22–15 Biosynthesis of cysteine from serine in bacteria and plants. The origin of reduced sulfur is shown in the pathway on the right.

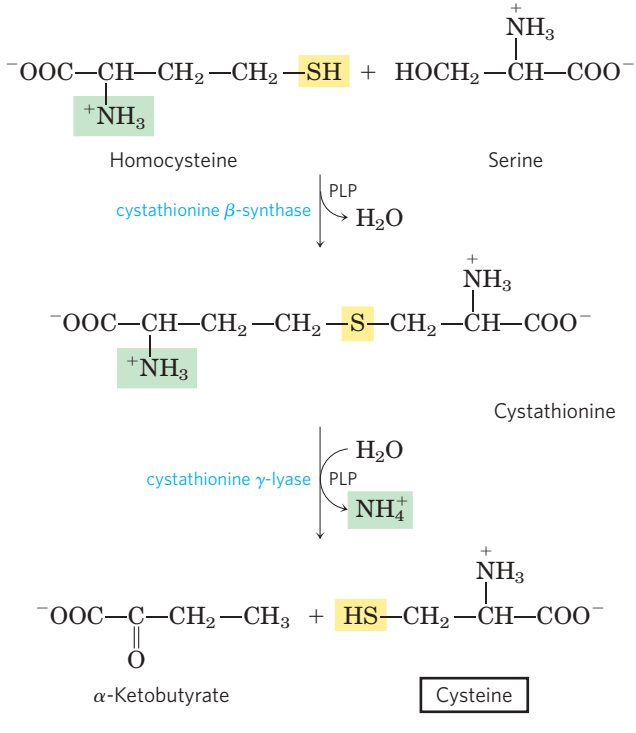

FIGURE 22–16 Biosynthesis of cysteine from homocysteine and serine in mammals. The homocysteine is formed from methionine, as described in the text.

Three Nonessential and Six Essential Amino Acids Are Synthesized from Oxaloacetate and Pyruvate

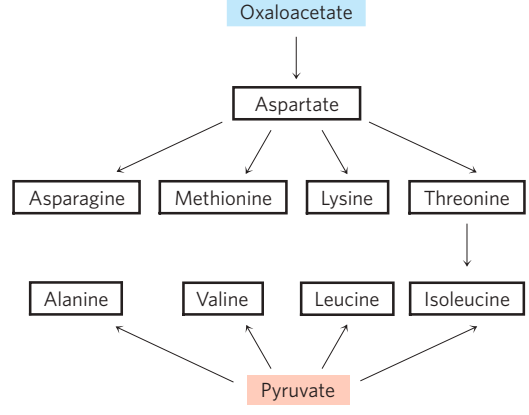

Alanine and **aspartate** are synthesized from pyruvate and oxaloacetate, respectively, by transamination from glutamate. **Asparagine** is synthesized by amidation of aspartate, with glutamine donating the NH_4^+. These are nonessential amino acids, and their simple biosynthetic pathways occur in all organisms.

For reasons incompletely understood, the malignant lymphocytes present in childhood acute lymphoblastic leukemia (ALL) require serum asparagine for growth. The chemotherapy for ALL is administered together with an L-asparaginase derived from bacteria,

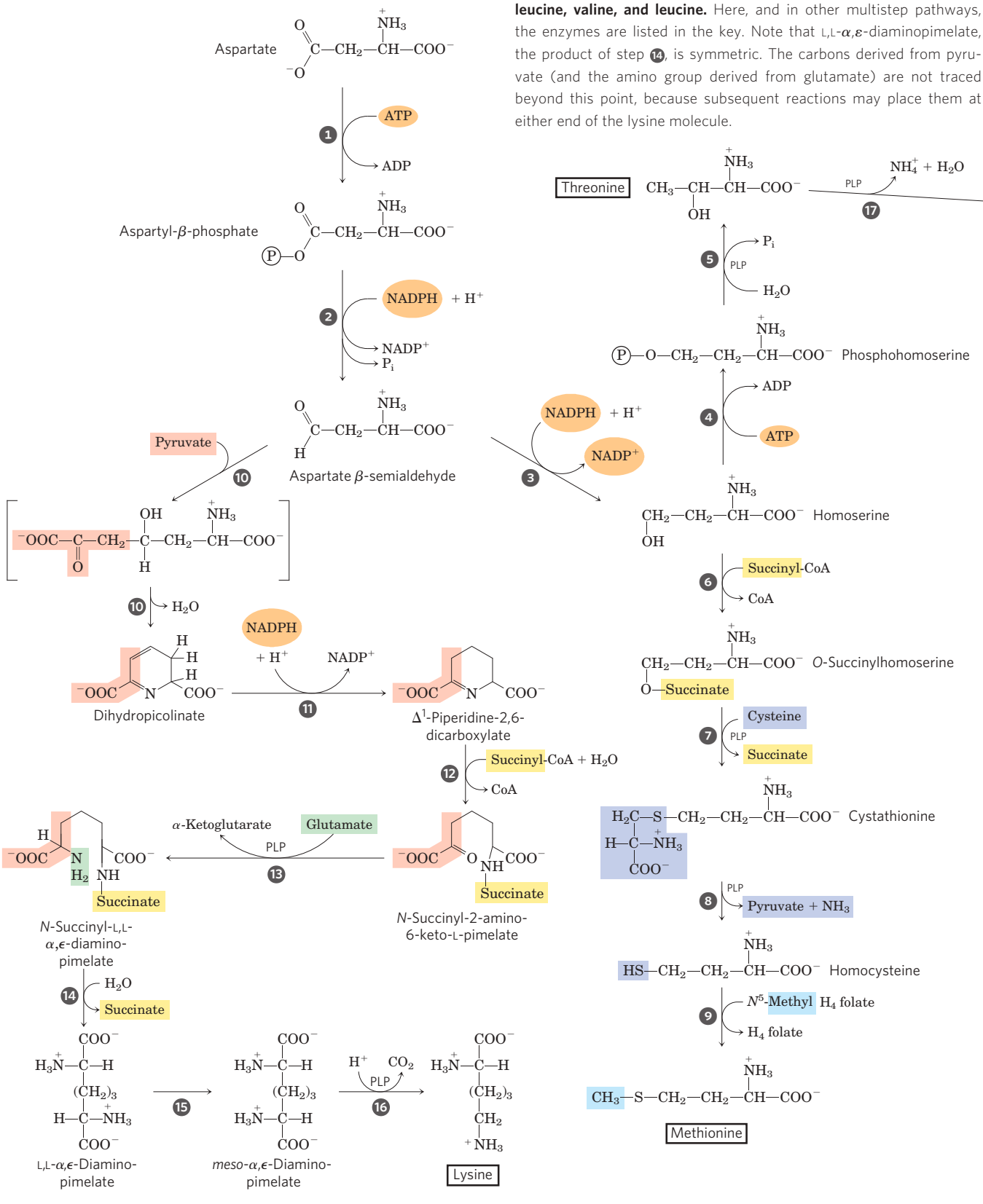

FIGURE 22–17 Biosynthesis of six essential amino acids from oxaloacetate and pyruvate in bacteria: methionine, threonine, lysine, isoleucine, valine, and leucine. Here, and in other multistep pathways, the enzymes are listed in the key. Note that L,L-α,ε-diaminopimelate, the product of step 14, is symmetric. The carbons derived from pyruvate (and the amino group derived from glutamate) are not traced beyond this point, because subsequent reactions may place them at either end of the lysine molecule.

with the enzyme functioning to reduce serum asparagine. The combined treatment results in a greater than 95% remission rate in cases of childhood ALL (L-asparaginase treatment alone produces remission in 40% to 60% of cases). However, the asparaginase treatment has some deleterious side effects, and about 10% of patients who achieve remission eventually suffer relapse, with tumors resistant to drug therapy. Researchers are now

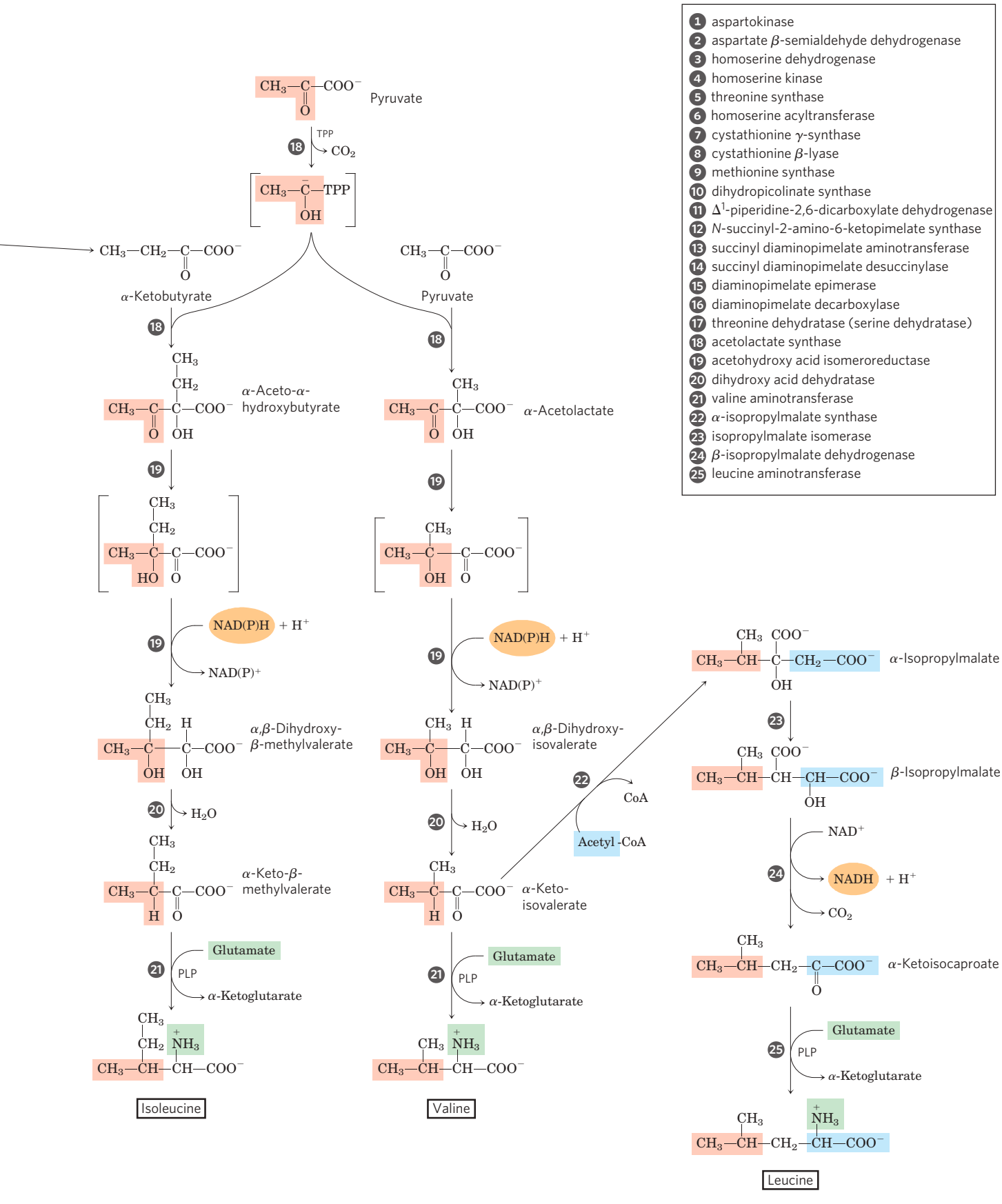

developing inhibitors of human asparagine synthetase to augment these therapies for childhood ALL. ■

Methionine, threonine, lysine, isoleucine, valine, and leucine are essential amino acids; humans cannot synthesize them. Their biosynthetic pathways are complex and interconnected **(Fig. 22–17)**. In some cases, the pathways in bacteria, fungi, and plants differ significantly. Figure 22–17 shows the bacterial pathways.

Aspartate gives rise to **methionine**, **threonine**, and **lysine**. Branch points occur at aspartate β-semialdehyde, an intermediate in all three pathways, and at homoserine, a precursor of threonine and methionine. Threonine, in turn, is one of the precursors of isoleucine. The **valine** and **isoleucine** pathways share four enzymes (Fig. 22–17, steps 18 to 21). Pyruvate gives rise to valine and isoleucine in pathways that begin with condensation of two carbons of pyruvate (in the form of hydroxyethyl thiamine pyrophosphate; see Fig. 14–15) with another molecule of pyruvate (the valine path) or with α-ketobutyrate (the isoleucine path). The α-ketobutyrate is derived from threonine in a reaction that requires pyridoxal phosphate (Fig. 22–17, step 17). An intermediate in the valine pathway, α-ketoisovalerate, is the starting point for a four-step branch pathway leading to **leucine** (steps 22 to 25).

Chorismate Is a Key Intermediate in the Synthesis of Tryptophan, Phenylalanine, and Tyrosine

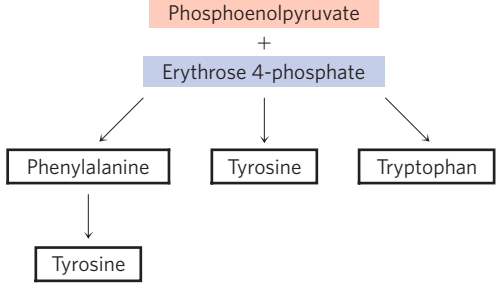

Aromatic rings are not readily available in the environment, even though the benzene ring is very stable. The branched pathway to tryptophan, phenylalanine, and tyrosine, occurring in bacteria, fungi, and plants, is the main biological route of aromatic ring formation. It proceeds through ring closure of an aliphatic precursor followed by stepwise addition of double bonds. The first four steps produce shikimate, a seven-carbon molecule derived from erythrose 4-phosphate and phosphoenolpyruvate **(Fig. 22–18)**. Shikimate is converted to chorismate in three steps that include the addition of three more carbons from another molecule of phosphoenolpyruvate. Chorismate is the first branch point of the pathway, with one branch leading to tryptophan, the other to phenylalanine and tyrosine.

In the **tryptophan** branch **(Fig. 22–19)**, chorismate is converted to anthranilate in a reaction in which glutamine donates the nitrogen that will become part of the indole ring. Anthranilate then condenses with PRPP. The indole ring of tryptophan is derived from the ring carbons and amino group of anthranilate plus two carbons derived from PRPP. The final reaction in the sequence is catalyzed by **tryptophan synthase**. This enzyme has an $\alpha_2\beta_2$ subunit structure and can be dissociated into two α subunits and a β_2 unit that catalyze different parts of the overall reaction:

$$\text{Indole-3-glycerol phosphate} \xrightarrow[\alpha\text{ subunit}]{} \text{indole} + \text{glyceraldehyde 3-phosphate}$$

$$\text{Indole} + \text{serine} \xrightarrow[\beta_2\text{ subunit}]{} \text{tryptophan} + H_2O$$

The second part of the reaction requires pyridoxal phosphate **(Fig. 22–20)**. Indole formed in the first part is not released by the enzyme, but instead moves through a channel from the α-subunit active site to one of the β-subunit active sites, where it condenses with a Schiff base intermediate derived from serine and PLP. Intermediate channeling of this type may be a feature of the entire pathway from chorismate to tryptophan. Enzyme active sites catalyzing different steps (sometimes not sequential steps) of the pathway to tryptophan are found on single polypeptides in some species of fungi and bacteria, but are separate proteins in other species. In addition, the activity of some of these enzymes requires a noncovalent association with other enzymes of the pathway. These observations suggest that all the pathway enzymes are components of a large, multienzyme complex in both bacteria and eukaryotes. Such complexes are generally not preserved intact when the enzymes are isolated using traditional biochemical methods, but evidence for the existence of multienzyme complexes is accumulating for this and other metabolic pathways (see Section 16.3).

In plants and bacteria, **phenylalanine** and **tyrosine** are synthesized from chorismate in pathways much less complex than the tryptophan pathway. The common intermediate is prephenate **(Fig. 22–21)**. The final step in both cases is transamination with glutamate.

Animals can produce tyrosine directly from phenylalanine through hydroxylation at C-4 of the phenyl group by **phenylalanine hydroxylase**; this enzyme also participates in the degradation of phenylalanine (see Figs 18–23, 18–24). Tyrosine is considered a conditionally essential amino acid, or as nonessential insofar as it can be synthesized from the essential amino acid phenylalanine.

Histidine Biosynthesis Uses Precursors of Purine Biosynthesis

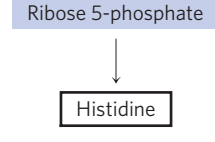

The pathway to **histidine** in all plants and bacteria differs in several respects from other amino acid biosynthetic pathways. Histidine is derived from three precursors **(Fig. 22–22)**: PRPP contributes five carbons, the purine ring of ATP contributes a nitrogen and a carbon, and glutamine supplies the second ring nitrogen. The key steps are condensation of ATP and PRPP, in which

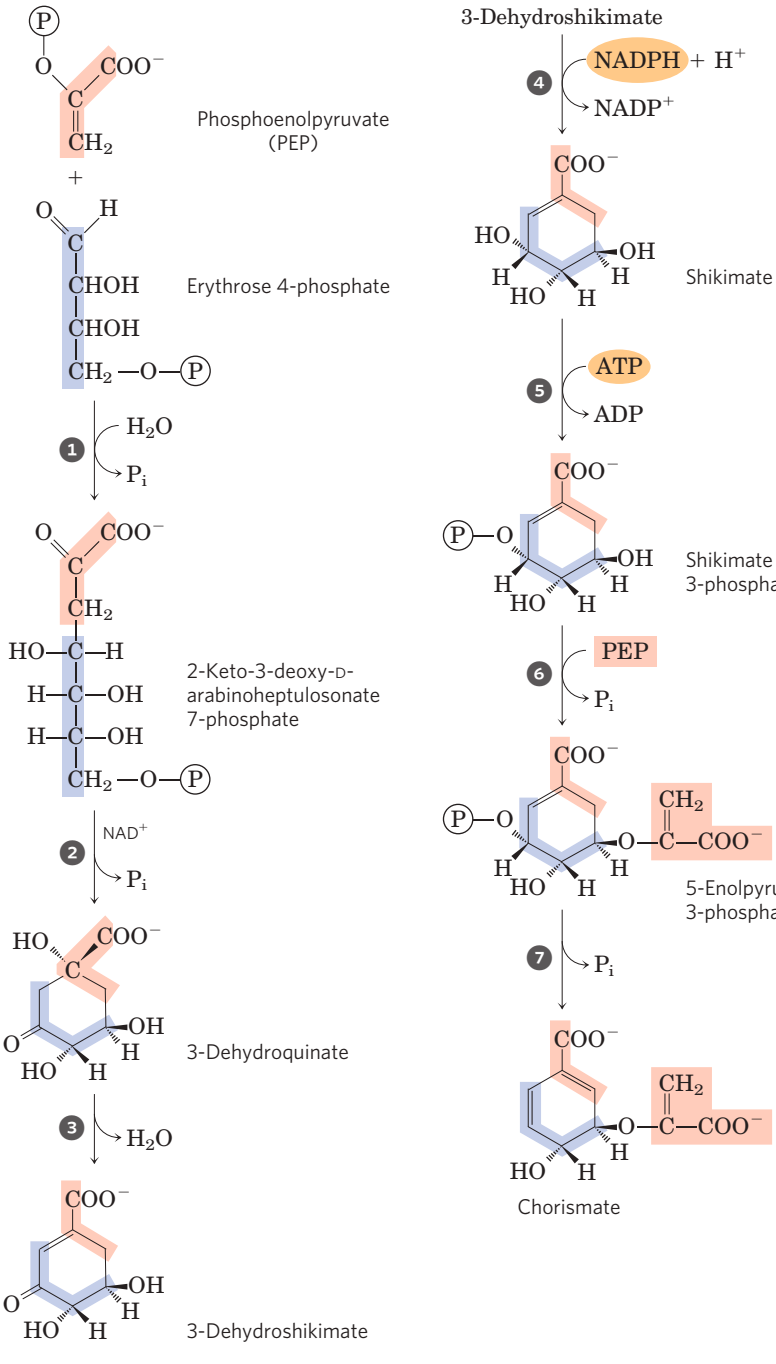

FIGURE 22–18 Biosynthesis of chorismate, an intermediate in the synthesis of aromatic amino acids in bacteria and plants. All carbons are derived from either erythrose 4-phosphate (light purple) or phosphoenolpyruvate (light red). Note that the NAD^+ required as a cofactor in step ❷ is released unchanged; it may be transiently reduced to NADH during the reaction, with formation of an oxidized reaction intermediate. Step ❻ is competitively inhibited by glyphosate ($^-OOC—CH_2—NH—CH_2—PO_3^{2-}$), the active ingredient in the widely used herbicide Roundup. The herbicide is relatively nontoxic to mammals, which lack this biosynthetic pathway. The chemical names quinate, shikimate, and chorismate are derived from the names of plants in which these intermediates have been found to accumulate.

N-1 of the purine ring is linked to the activated C-1 of the ribose of PRPP (step ❶ in Fig. 22–22); purine ring opening that ultimately leaves N-1 and C-2 of adenine linked to the ribose (step ❸); and formation of the imidazole ring, a reaction in which glutamine donates a nitrogen (step ❺). The use of ATP as a metabolite rather than a high-energy cofactor is unusual—but not wasteful, because it dovetails with the purine biosynthetic pathway. The remnant of ATP that is released after the transfer of N-1 and C-2 is 5-aminoimidazole-4-carboxamide ribonucleotide (AICAR), an intermediate of purine biosynthesis (see Fig. 22–35) that is rapidly recycled to ATP.

Amino Acid Biosynthesis Is under Allosteric Regulation

As detailed in Chapter 15, the control of flux through a metabolic pathway often reflects the activity of multiple enzymes in that pathway. In the case of amino acid synthesis, regulation takes place in part through feedback inhibition of the first reaction by the end product of the pathway. This first reaction is often catalyzed by an allosteric enzyme that plays an important role in the overall control of flux through that pathway. As an example, **Figure 22–23** shows the allosteric regulation of isoleucine synthesis from threonine (detailed in Fig. 22–17).

The end product, isoleucine, is an allosteric inhibitor of the first reaction in the sequence. In bacteria, such allosteric modulation of amino acid synthesis contributes to the minute-to-minute adjustment of pathway activity to cellular needs.

Allosteric regulation of an individual enzyme can be considerably more complex. An example is the remarkable set of allosteric controls exerted on glutamine synthetase of *E. coli* (Fig. 22–8). Six products derived from glutamine serve as negative feedback modulators of the enzyme, and the overall effects of these and other modulators are more than additive. Such regulation is called **concerted inhibition**.

Additional mechanisms contribute to the regulation of the amino acid biosynthetic pathways. Because the 20 common amino acids must be made in the correct proportions for protein synthesis, cells have developed ways not only of controlling the rate of synthesis of individual amino acids but also of coordinating their formation. Such coordination is especially well developed in fast-growing bacterial cells. **Figure 22–24** shows how *E. coli* cells coordinate the synthesis of lysine, methionine, threonine, and isoleucine, all made from aspartate. Several important types of inhibition patterns are evident. The step from aspartate to aspartyl-β-phosphate is catalyzed by three isozymes, each independently controlled by different modulators. This **enzyme multiplicity** prevents one biosynthetic end product from shutting down key steps in a pathway when other products of the same pathway are required. The steps from aspartate β-semialdehyde to homoserine and from threonine to α-ketobutyrate (detailed in Fig. 22–17) are also catalyzed by dual, independently controlled isozymes. One isozyme for the conversion of aspartate to aspartyl-β-phosphate is allosterically inhibited by two different modulators, lysine and isoleucine, whose action is more than additive—another example of concerted inhibition. The sequence from aspartate to isoleucine undergoes multiple, overlapping negative feedback inhibitions; for example, isoleucine inhibits the conversion of threonine to α-ketobutyrate (as described above), and threonine inhibits its own formation at three points: from homoserine, from aspartate β-semialdehyde, and from aspartate (steps ❹, ❸, and ❶ in Fig. 22–17). This overall regulatory mechanism is called **sequential feedback inhibition**.

Similar patterns are evident in the pathways leading to the aromatic amino acids. The first step of the

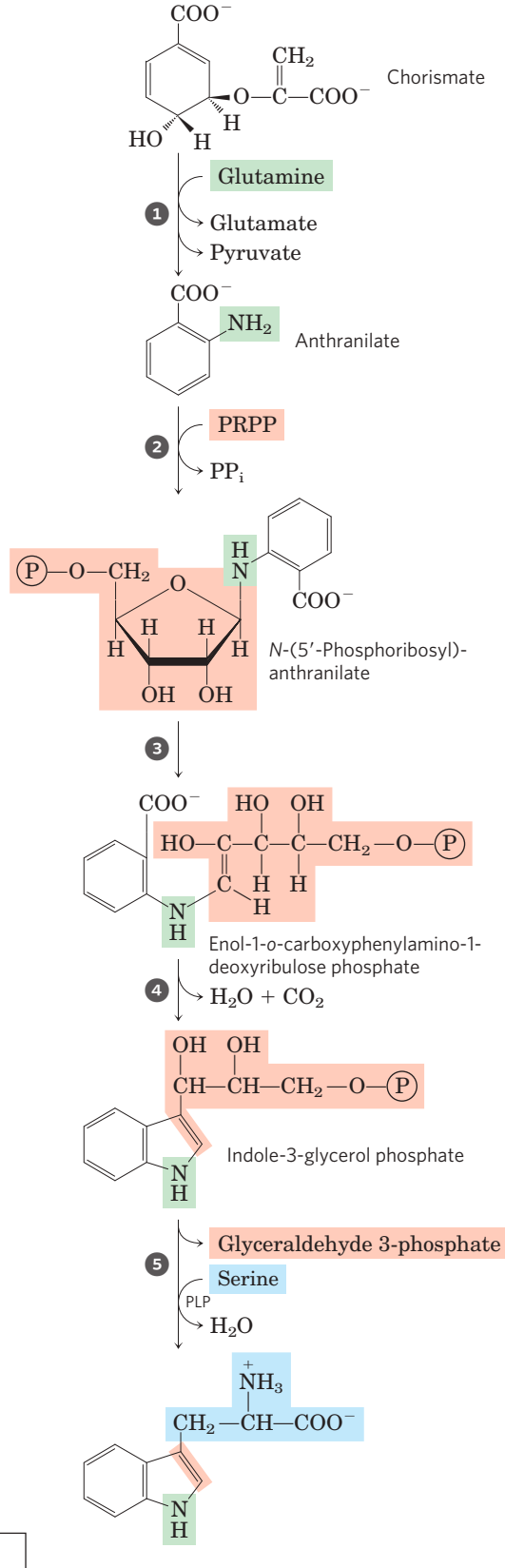

FIGURE 22–19 Biosynthesis of tryptophan from chorismate in bacteria and plants. In *E. coli*, enzymes catalyzing steps ❶ and ❷ are subunits of a single complex.

❶ anthranilate synthase
❷ anthranilate phosphoribosyltransferase
❸ *N*-(5′-phosphoribosyl)-anthranilate isomerase
❹ indole-3-glycerol phosphate synthase
❺ tryptophan synthase

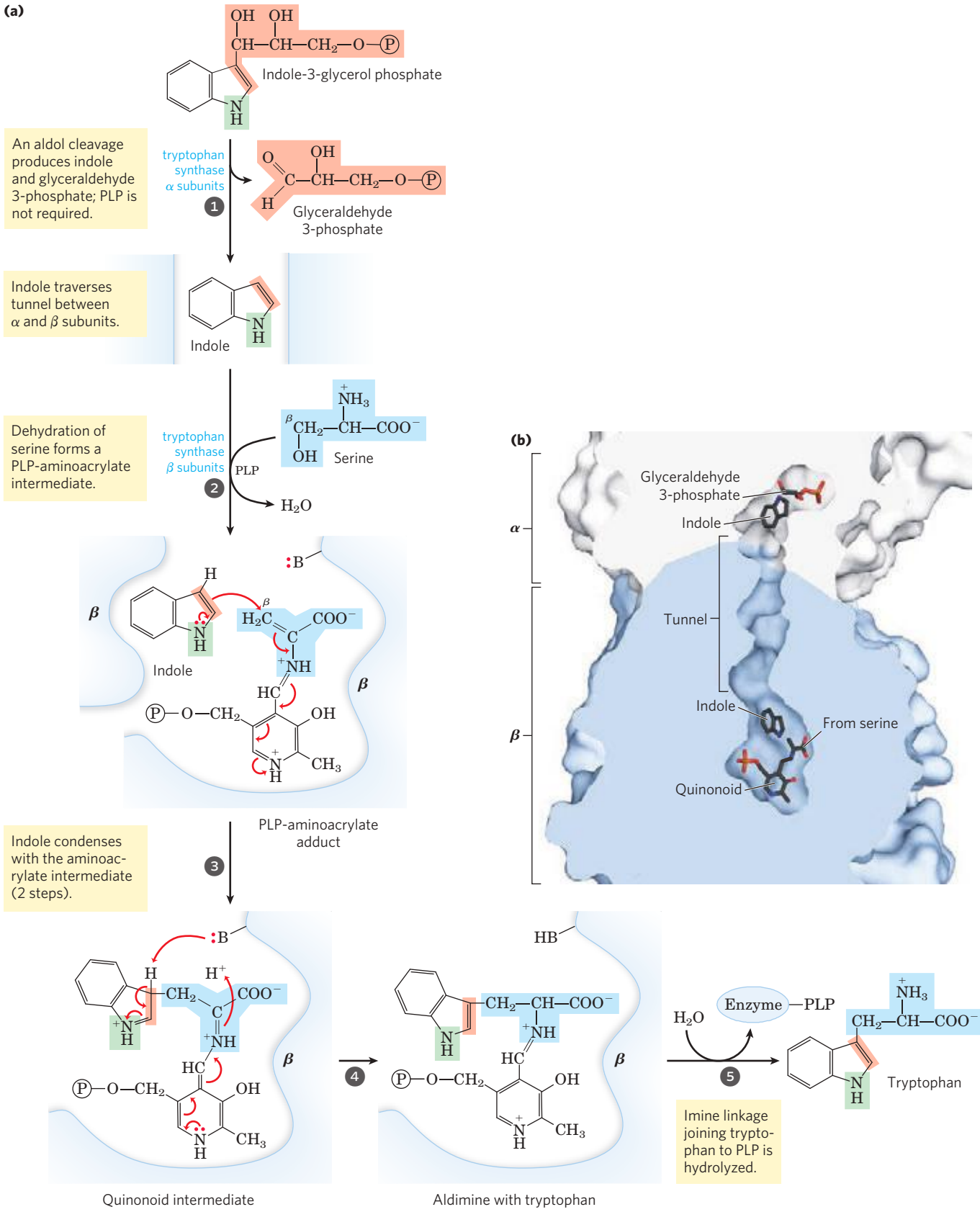

MECHANISM FIGURE 22–20 **Tryptophan synthase reaction. (a)** This enzyme catalyzes a multistep reaction with several types of chemical rearrangements. The PLP-facilitated transformations occur at the β carbon (C-3) of the amino acid, as opposed to the α-carbon reactions described in Figure 18–6. The β carbon of serine is attached to the indole ring system. **(b)** (PDB ID 1KFJ) Indole generated on the α subunit (white) moves through a tunnel to the β subunit (blue), where it condenses with the serine moiety. Tryptophan Synthase Mechanism

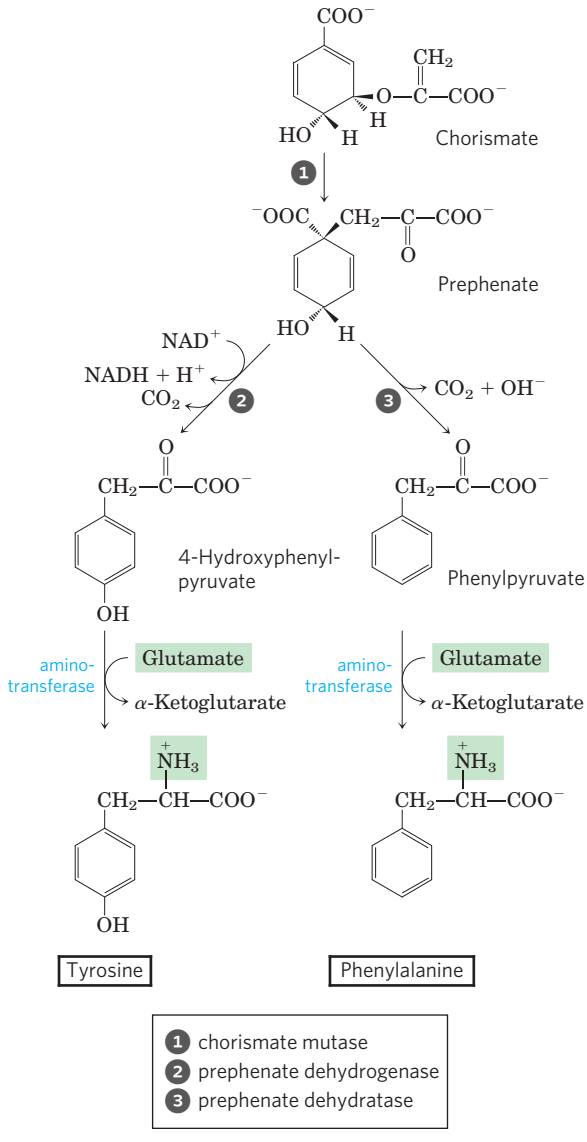

FIGURE 22–21 Biosynthesis of phenylalanine and tyrosine from chorismate in bacteria and plants. Conversion of chorismate to prephenate is a rare biological example of a Claisen rearrangement.

early pathway to the common intermediate chorismate is catalyzed by the enzyme 2-keto-3-deoxy-D-arabino-heptulosonate 7-phosphate (DAHP) synthase (❶ in Fig. 22–18). Most microorganisms and plants have three DAHP synthase isozymes. One is allosterically inhibited (feedback inhibition) by phenylalanine, another by tyrosine, and the third by tryptophan. This scheme helps the overall pathway to respond to cellular requirements for one or more of the aromatic amino acids. Additional regulation takes place after the pathway branches at chorismate. For example, the enzymes catalyzing the first two steps of the tryptophan branch are subject to allosteric inhibition by tryptophan.

SUMMARY 22.2 Biosynthesis of Amino Acids

- Plants and bacteria synthesize all 20 common amino acids. Mammals can synthesize about half; the others are required in the diet (essential amino acids).
- Among the nonessential amino acids, glutamate is formed by reductive amination of α-ketoglutarate and serves as the precursor of glutamine, proline, and arginine. Alanine and aspartate (and thus asparagine) are formed from pyruvate and oxaloacetate, respectively, by transamination. The carbon chain of serine is derived from 3-phosphoglycerate. Serine is a precursor of glycine; the β-carbon atom of serine is transferred to tetrahydrofolate. In microorganisms, cysteine is produced from serine and from sulfide produced by the reduction of environmental sulfate. Mammals produce cysteine from methionine and serine by a series of reactions requiring *S*-adenosylmethionine and cystathionine.
- Among the essential amino acids, the aromatic amino acids (phenylalanine, tyrosine, and tryptophan) form by a pathway in which chorismate occupies a key branch point. Phosphoribosyl pyrophosphate is a precursor of tryptophan and histidine. The pathway to histidine is interconnected with the purine synthetic pathway. Tyrosine can also be formed by hydroxylation of phenylalanine (and thus is considered conditionally essential). The pathways for the other essential amino acids are complex.
- The amino acid biosynthetic pathways are subject to allosteric end-product inhibition; the regulatory enzyme is usually the first in the sequence. Regulation of the various synthetic pathways is coordinated.

22.3 Molecules Derived from Amino Acids

In addition to their role as the building blocks of proteins, amino acids are precursors of many specialized biomolecules, including hormones, coenzymes, nucleotides, alkaloids, cell wall polymers, porphyrins, antibiotics, pigments, and neurotransmitters. We describe here the pathways to a number of these amino acid derivatives.

Glycine Is a Precursor of Porphyrins

The biosynthesis of **porphyrins**, for which glycine is a major precursor, is our first example because of the central importance of the porphyrin nucleus in heme proteins such as hemoglobin and the cytochromes. The porphyrins are constructed from four molecules of the monopyrrole derivative **porphobilinogen**, which itself is derived from two molecules of δ-aminolevulinate. There are two major pathways to δ-aminolevulinate. In higher eukaryotes **(Fig. 22–25a)**, glycine reacts with succinyl-CoA in the first step to yield α-amino-β-ketoadipate,

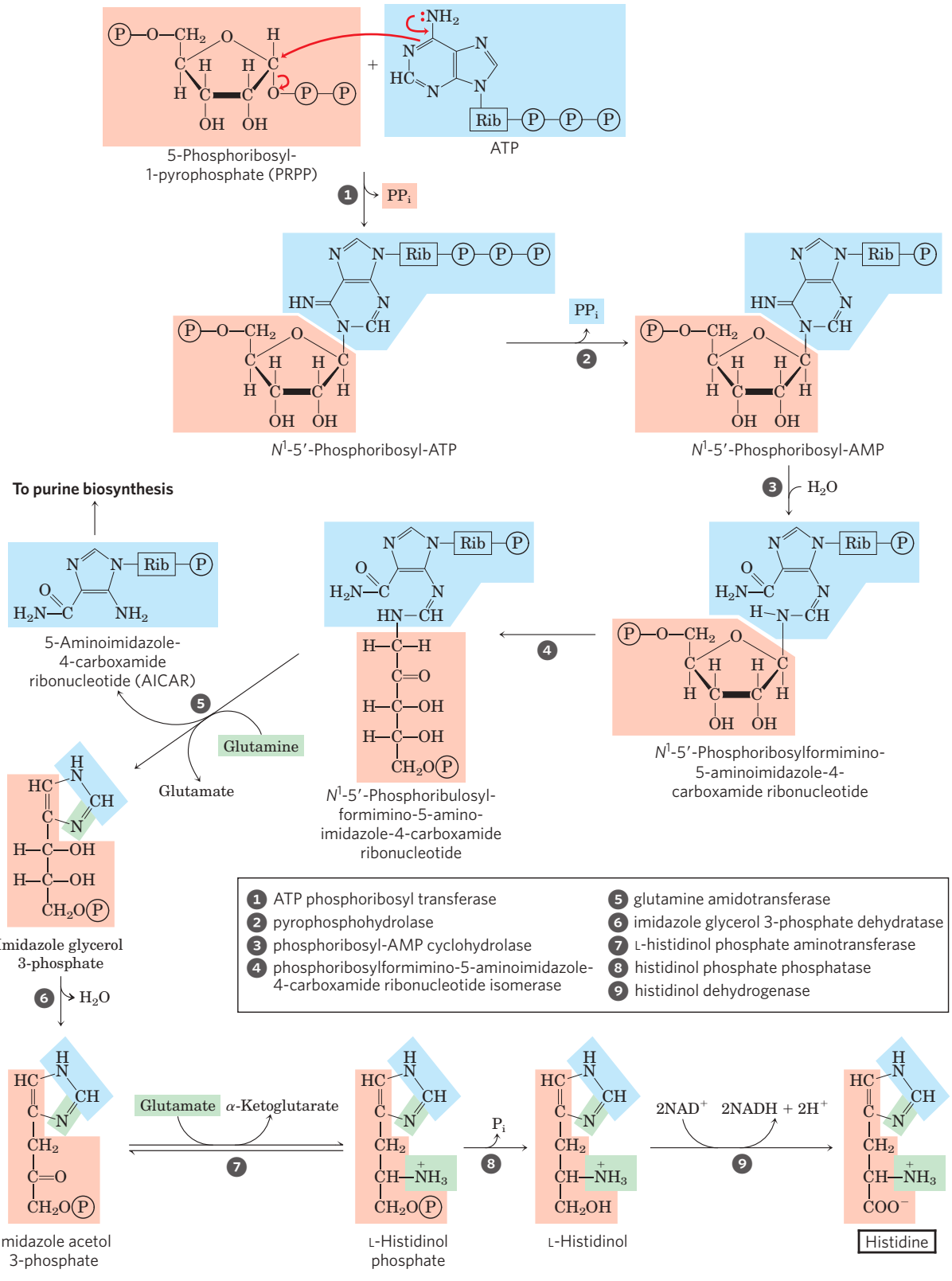

FIGURE 22–22 Biosynthesis of histidine in bacteria and plants. Atoms derived from PRPP and ATP are shaded light red and blue, respectively. Two of the histidine nitrogens are derived from glutamine and glutamate (green). Note that the derivative of ATP remaining after step ❺ (AICAR) is an intermediate in purine biosynthesis (see Fig. 22–35, step ❾), so ATP is rapidly regenerated.

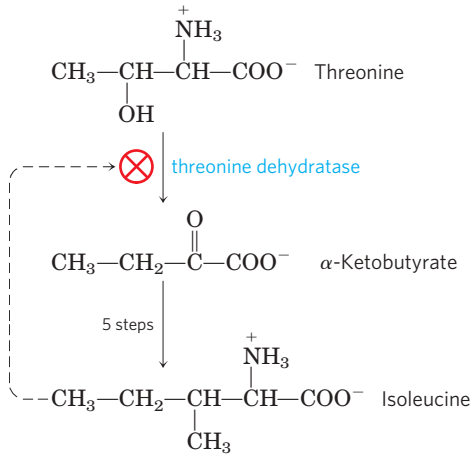

FIGURE 22–23 Allosteric regulation of isoleucine biosynthesis. The first reaction in the pathway from threonine to isoleucine is inhibited by the end product, isoleucine. This was one of the first examples of allosteric feedback inhibition to be discovered. The steps from α-ketobutyrate to isoleucine correspond to steps 18 through 21 in Figure 22–17 (five steps, because 19 is a two-step reaction).

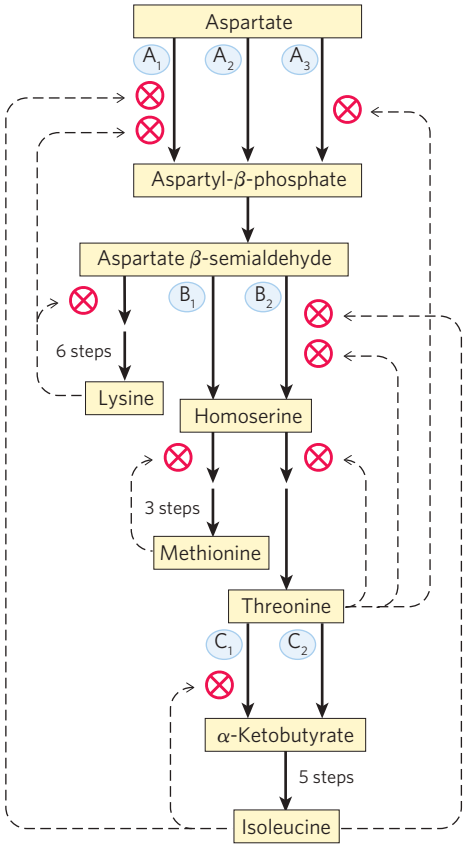

FIGURE 22–24 Interlocking regulatory mechanisms in the biosynthesis of several amino acids derived from aspartate in *E. coli*. Three enzymes (A, B, C) have either two or three isozyme forms, indicated by numerical subscripts. In each case, one isozyme (A_2, B_1, and C_2) has no allosteric regulation; these isozymes are regulated by changes in the amount of enzyme synthesized (Chapter 28). Synthesis of isozymes A_2 and B_1 is repressed when methionine levels are high, and synthesis of isozyme C_2 is repressed when isoleucine levels are high. Enzyme A is aspartokinase; B, homoserine dehydrogenase; C, threonine dehydratase.

which is then decarboxylated to δ-aminolevulinate. In plants, algae, and most bacteria, δ-aminolevulinate is formed from glutamate (Fig. 22–25b). The glutamate is first esterified to glutamyl-tRNA^{Glu} (see Chapter 27 on the topic of transfer RNAs); reduction by NADPH converts the glutamate to glutamate 1-semialdehyde, which is cleaved from the tRNA. An aminotransferase converts the glutamate 1-semialdehyde to δ-aminolevulinate.

In all organisms, two molecules of δ-aminolevulinate condense to form porphobilinogen and, through a series of complex enzymatic reactions, four molecules of porphobilinogen come together to form **protoporphyrin (Fig. 22–26)**. The iron atom is incorporated after the protoporphyrin has been assembled, in a step catalyzed by ferrochelatase. Porphyrin biosynthesis is regulated in higher eukaryotes by heme, which serves as a feedback inhibitor of early steps in the synthetic pathway. Genetic defects in the biosynthesis of porphyrins can lead to the accumulation of pathway intermediates, causing a variety of human diseases known collectively as **porphyrias** (Box 22–2).

Heme Is the Source of Bile Pigments

The iron-porphyrin (heme) group of hemoglobin, released from dying erythrocytes in the spleen, is degraded to yield free Fe^{2+} and, ultimately, **bilirubin**. This pathway is arresting for its capacity to inject color into human biochemistry.

The first step in the two-step pathway, catalyzed by heme oxygenase, converts heme to biliverdin, a linear (open) tetrapyrrole derivative **(Fig. 22–27)**. The other products of the reaction are free Fe^{2+} and CO. The Fe^{2+} is quickly bound by ferritin. Carbon monoxide is a poison that binds to hemoglobin (see Box 5–1), and the production of CO by heme oxygenase ensures that, even in the absence of environmental exposure, about 1% of an individual's heme is complexed with CO.

Biliverdin is converted to bilirubin in the second step, catalyzed by biliverdin reductase. You can monitor this reaction colorimetrically in a familiar in situ experiment. When you are bruised, the black and/or purple color results from hemoglobin released from damaged erythrocytes. Over time, the color changes to the green of biliverdin, and then to the yellow of bilirubin. Bilirubin is largely insoluble, and it travels in the bloodstream as a complex with serum albumin. In the liver, bilirubin is transformed to the bile pigment bilirubin diglucuronide. This product is sufficiently water-soluble to be secreted with other components of bile into the small intestine, where microbial enzymes convert it to several products, predominantly urobilinogen. Some urobilinogen is reabsorbed into the blood and transported to the kidney, where it is converted to urobilin, the compound that gives urine its yellow color (Fig. 22–27). Urobilinogen remaining in the intestine is converted (in another microbe-dependent reaction) to stercobilin (Fig. 22–27), which imparts the red-brown color to feces.

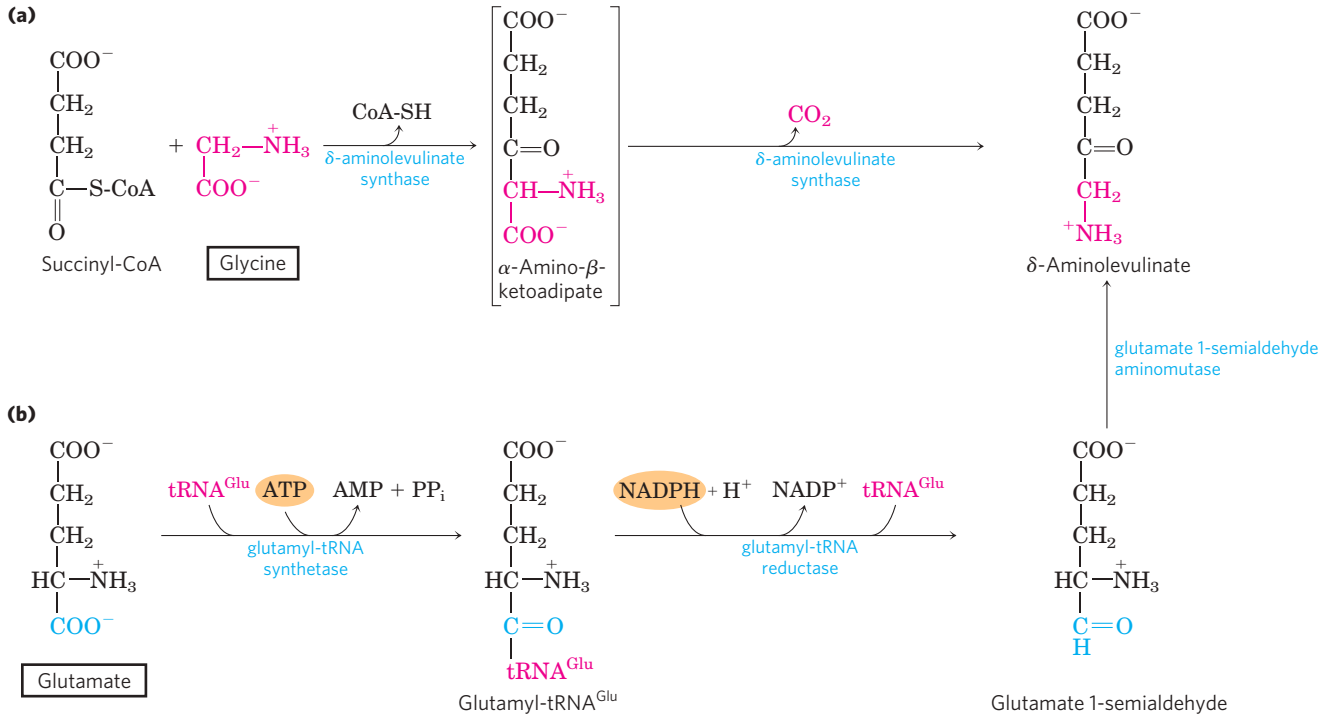

FIGURE 22–25 Biosynthesis of δ-aminolevulinate. (a) In most animals, including mammals, δ-aminolevulinate is synthesized from glycine and succinyl-CoA. The atoms furnished by glycine are shown in red. **(b)** In bacteria and plants, the precursor of δ-aminolevulinate is glutamate.

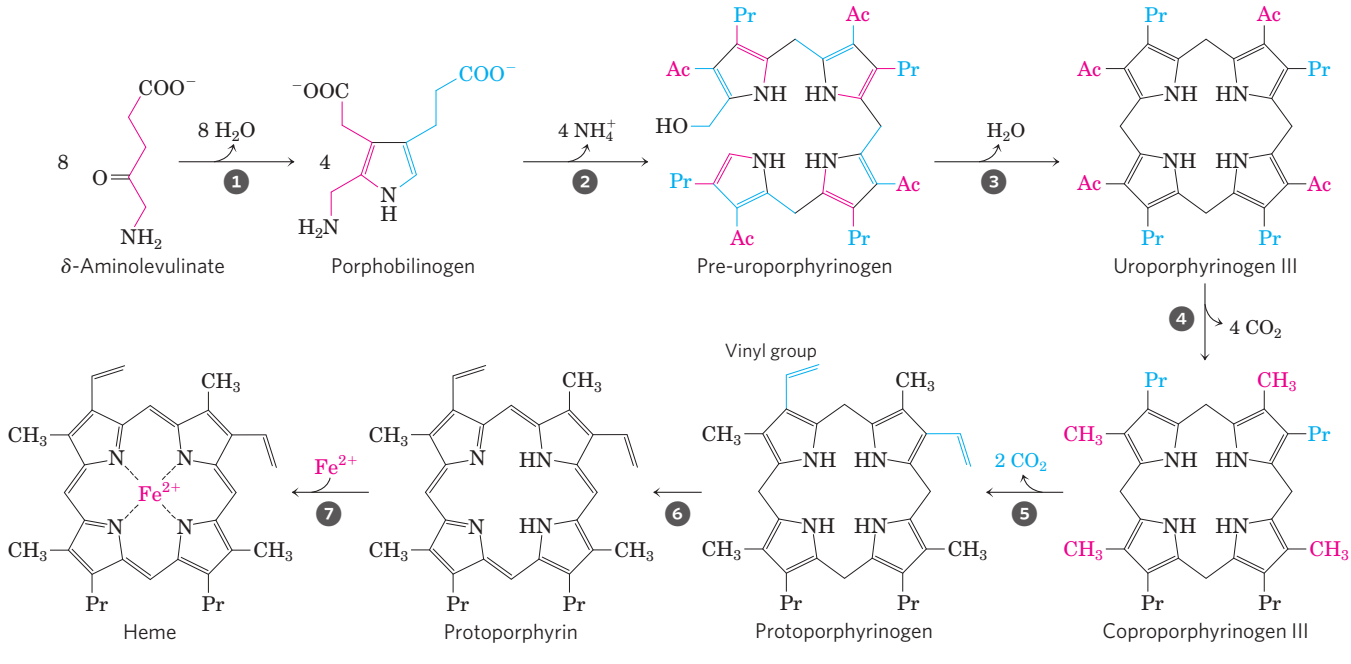

1. porphobilinogen synthase
2. uroporphyrinogen synthase
3. uroporphyrinogen III cosynthase
4. uroporphyrinogen decarboxylase
5. coproporphyrinogen oxidase
6. protoporphyrinogen oxidase
7. ferrochelatase

FIGURE 22–26 Biosynthesis of heme from δ-aminolevulinate. Ac represents acetyl (—CH_2COO^-); Pr, propionyl (—$CH_2CH_2COO^-$).

BOX 22–2 MEDICINE On Kings and Vampires

Porphyrias are a group of genetic diseases that result from defects in enzymes of the biosynthetic pathway from glycine to porphyrins; specific porphyrin precursors accumulate in erythrocytes, body fluids, and the liver. The most common form is acute intermittent porphyria. Most individuals inheriting this condition are heterozygotes and are usually asymptomatic, because the single copy of the normal gene provides a sufficient level of enzyme function. However, certain nutritional or environmental factors (as yet poorly understood) can cause a buildup of δ-aminolevulinate and porphobilinogen, leading to attacks of acute abdominal pain and neurological dysfunction. King George III, British monarch during the American Revolution, suffered several episodes of apparent madness that tarnished the record of this otherwise accomplished man. The symptoms of his condition suggest that George III suffered from acute intermittent porphyria.

One of the rarer porphyrias results in an accumulation of uroporphyrinogen I, an abnormal isomer of a protoporphyrin precursor. This compound stains the urine red, causes the teeth to fluoresce strongly in ultraviolet light, and makes the skin abnormally sensitive to sunlight. Many individuals with this porphyria are anemic because insufficient heme is synthesized. This genetic condition may have given rise to the vampire myths of folk legend.

The symptoms of most porphyrias are now readily controlled with dietary changes or the administration of heme or heme derivatives.

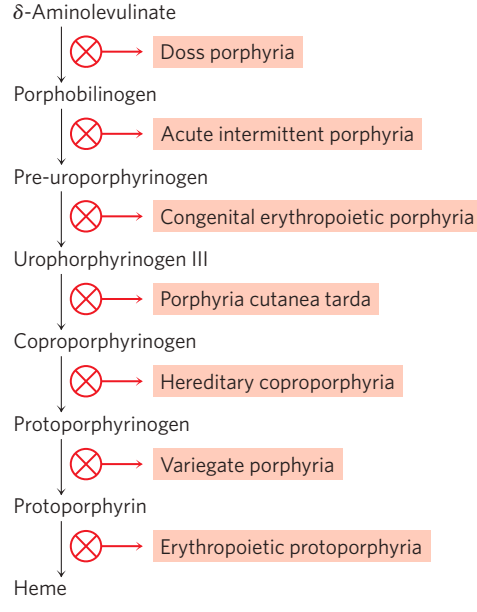

Impaired liver function or blocked bile secretion causes bilirubin to leak from the liver into the blood, resulting in a yellowing of the skin and eyeballs, a condition called jaundice. In cases of jaundice, determination of the concentration of bilirubin in the blood may be useful in the diagnosis of underlying liver disease. Newborn infants sometimes develop jaundice because they have not yet produced enough glucuronyl bilirubin transferase to process their bilirubin. A traditional treatment to reduce excess bilirubin, exposure to a fluorescent lamp, causes a photochemical conversion of bilirubin to compounds that are more soluble and easily excreted.

These pathways of heme breakdown play significant roles in protecting cells from oxidative damage and in regulating certain cellular functions. The CO produced by heme oxygenase is toxic at high concentrations, but at the very low concentrations generated during heme degradation it seems to have some regulatory and/or signaling functions. It acts as a vasodilator, much the same as (but less potent than) nitric oxide (discussed below). Low levels of CO also have some regulatory effects on neurotransmission. Bilirubin is the most abundant antioxidant in mammalian tissues and is responsible for most of the antioxidant activity in serum. Its protective effects seem to be especially important in the developing brain of newborn infants. The cell toxicity associated with jaundice may be due to bilirubin levels in excess of the serum albumin needed to solubilize it.

Given these varied roles of heme degradation products, the degradative pathway is subject to regulation, mainly at the first step. Humans have at least three isozymes of heme oxygenase (HO). HO-1 is highly regulated; the expression of its gene is induced by a wide range of stress conditions (shear stress, angiogenesis (uncontrolled development of blood vessels), hypoxia, hyperoxia, heat shock, exposure to ultraviolet light, hydrogen peroxide, and many other metabolic insults). HO-2 is found mainly in brain and testes, where it is continuously expressed. The third isozyme, HO-3, is not yet well characterized. ■

Amino Acids Are Precursors of Creatine and Glutathione

Phosphocreatine, derived from **creatine**, is an important energy buffer in skeletal muscle (see Box 23–2). Creatine is synthesized from glycine and arginine **(Fig. 22–28)**; methionine, in the form of *S*-adenosylmethionine, acts as methyl group donor.

Glutathione (GSH), present in plants, animals, and some bacteria, often at high levels, can be thought

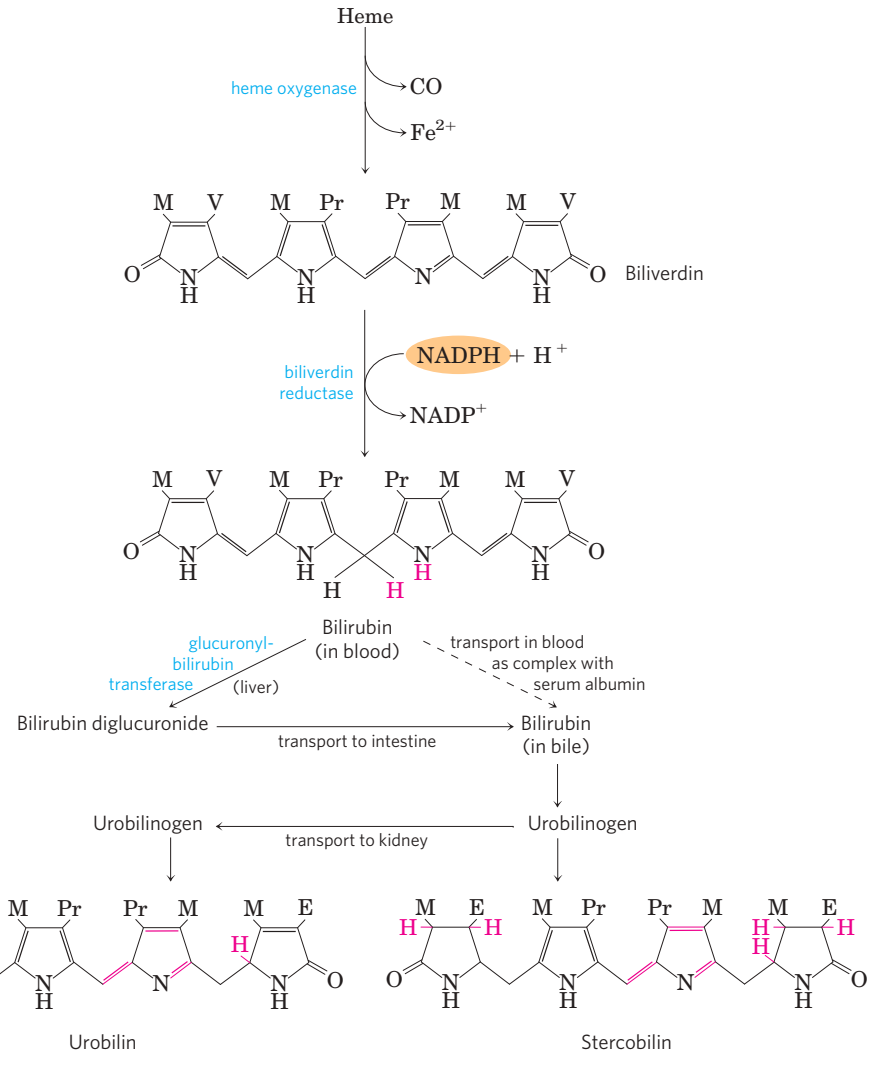

FIGURE 22–27 Bilirubin and its breakdown products. M represents methyl; V, vinyl; Pr, propionyl; E, ethyl. For ease of comparison, these structures are shown in linear form, rather than in their correct stereochemical conformations.

of as a redox buffer. It is derived from glutamate, cysteine, and glycine **(Fig. 22–29)**. The γ-carboxyl group of glutamate is activated by ATP to form an acyl phosphate intermediate, which is then attacked by the α-amino group of cysteine. A second condensation reaction follows, with the α-carboxyl group of cysteine activated to an acyl phosphate to permit reaction with glycine. The oxidized form of glutathione (GSSG), produced in the course of its redox activities, contains two glutathione molecules linked by a disulfide bond.

Glutathione probably helps maintain the sulfhydryl groups of proteins in the reduced state and the iron of heme in the ferrous (Fe^{2+}) state, and it serves as a reducing agent for glutaredoxin in deoxyribonucleotide synthesis (see Fig. 22–41). Its redox function is also used to remove toxic peroxides formed in the normal course of growth and metabolism under aerobic conditions:

$$2\ GSH + R{-}O{-}O{-}H \longrightarrow GSSG + H_2O + R{-}OH$$

This reaction is catalyzed by **glutathione peroxidase**, a remarkable enzyme in that it contains a covalently bound selenium (Se) atom in the form of selenocysteine (see Fig. 3–8a), which is essential for its activity.

D-Amino Acids Are Found Primarily in Bacteria

Although D-amino acids do not generally occur in proteins, they do serve some special functions in the structure of bacterial cell walls and peptide antibiotics. Bacterial peptidoglycans (see Fig. 20–30) contain both D-alanine and D-glutamate. D-Amino acids arise directly from the L isomers by the action of amino acid racemases, which have pyridoxal phosphate as cofactor (see Fig. 18–6). Amino acid racemization is uniquely important to bacterial metabolism, and enzymes such as alanine racemase are prime targets for pharmaceutical agents. One such agent, **L-fluoroalanine**, is being tested as an antibacterial drug. Another, **cycloserine**, is used to treat tuberculosis. Because these inhibitors also affect some PLP-requiring human enzymes, however, they have potentially undesirable side effects. ■

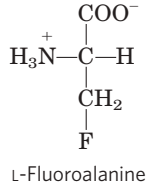
L-Fluoroalanine

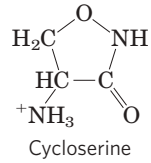
Cycloserine

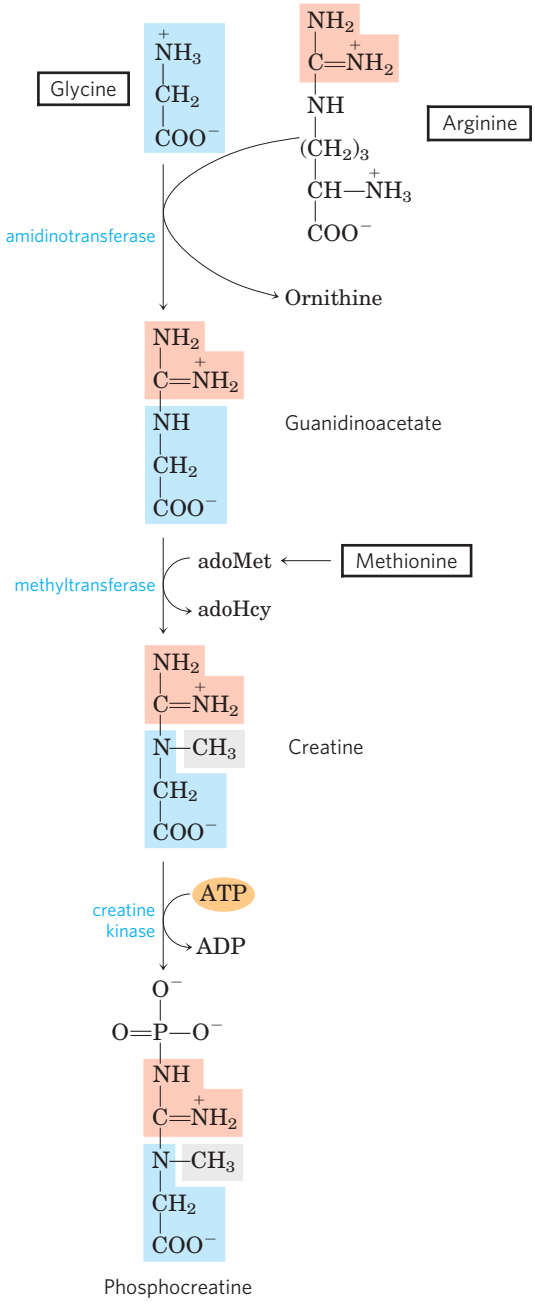

FIGURE 22–28 Biosynthesis of creatine and phosphocreatine. Creatine is made from three amino acids: glycine, arginine, and methionine. This pathway shows the versatility of amino acids as precursors of other nitrogenous biomolecules.

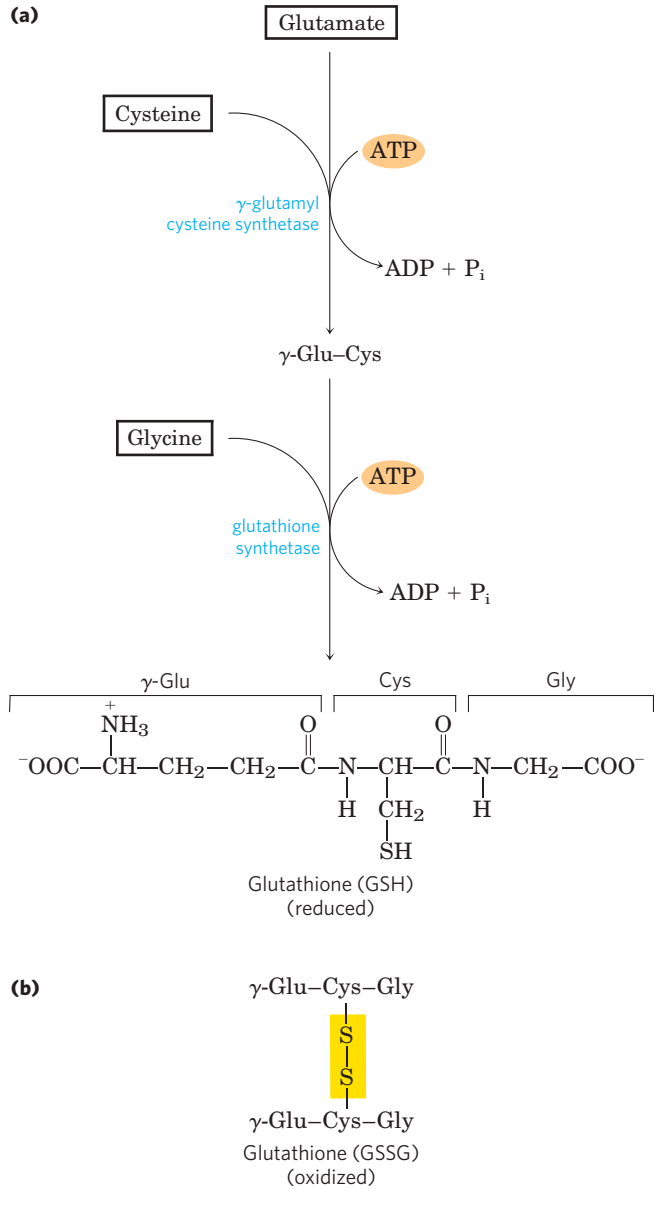

FIGURE 22–29 Glutathione metabolism. (a) Biosynthesis of glutathione. **(b)** Oxidized form of glutathione.

Aromatic Amino Acids Are Precursors of Many Plant Substances

Phenylalanine, tyrosine, and tryptophan are converted to a variety of important compounds in plants. The rigid polymer **lignin**, derived from phenylalanine and tyrosine, is second only to cellulose in abundance in plant tissues. The structure of the lignin polymer is complex and not well understood. Tryptophan is also the precursor of the plant growth hormone indole-3-acetate, or **auxin (Fig. 22–30a)**, which is important in the regulation of a wide range of biological processes in plants.

Phenylalanine and tyrosine also give rise to many commercially significant natural products, including the tannins that inhibit oxidation in wines; alkaloids such as morphine, which have potent physiological effects; and the flavoring of cinnamon oil (Fig. 22–30b), nutmeg, cloves, vanilla, cayenne pepper, and other products.

Biological Amines Are Products of Amino Acid Decarboxylation

Many important neurotransmitters are primary or secondary amines, derived from amino acids in simple pathways. In addition, some polyamines that

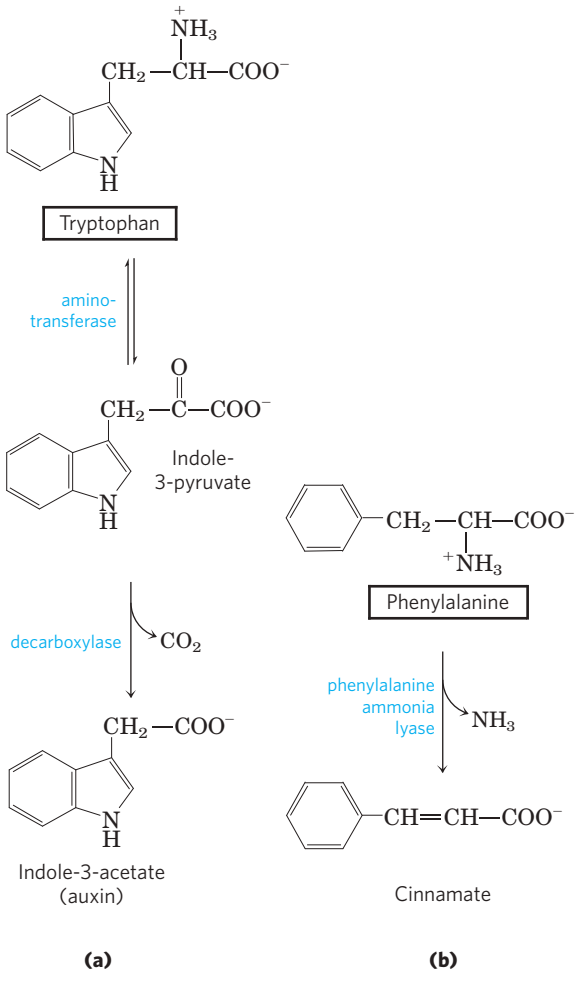

FIGURE 22–30 Biosynthesis of two plant substances from amino acids. **(a)** Indole-3-acetate (auxin) and **(b)** cinnamate (cinnamon flavor).

form complexes with DNA are derived from the amino acid ornithine, a component of the urea cycle. A common denominator of many of these pathways is amino acid decarboxylation, another PLP-requiring reaction (see Fig. 18–6).

The synthesis of some neurotransmitters is illustrated in **Figure 22–31**. Tyrosine gives rise to a family of catecholamines that includes **dopamine**, **norepinephrine**, and **epinephrine**. Levels of catecholamines are correlated with, among other things, changes in blood pressure. The neurological disorder Parkinson disease is associated with an underproduction of dopamine, and it has traditionally been treated by administering L-dopa. Overproduction of dopamine in the brain may be linked to psychological disorders such as schizophrenia.

Glutamate decarboxylation gives rise to **γ-aminobutyrate (GABA)**, an inhibitory neurotransmitter. Its underproduction is associated with epileptic seizures. GABA analogs are used in the treatment of epilepsy and hypertension. Levels of GABA can also be increased by administering inhibitors of the GABA-degrading enzyme GABA aminotransferase. Another important neurotransmitter, **serotonin**, is derived from tryptophan in a two-step pathway.

Histidine undergoes decarboxylation to **histamine**, a powerful vasodilator in animal tissues. Histamine is released in large amounts as part of the allergic response, and it also stimulates acid secretion in the stomach. A growing array of pharmaceutical agents are being designed to interfere with either the synthesis or the action of histamine. A prominent example is the histamine receptor antagonist **cimetidine** (Tagamet), a structural analog of histamine:

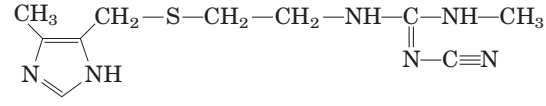

It promotes the healing of duodenal ulcers by inhibiting secretion of gastric acid.

Polyamines such as **spermine** and **spermidine**, involved in DNA packaging, are derived from methionine and ornithine by the pathway shown in **Figure 22–32**. The first step is decarboxylation of ornithine, a precursor of arginine (Fig. 22–12). **Ornithine decarboxylase**, a PLP-requiring enzyme, is the target of several powerful inhibitors used as pharmaceutical agents (see Box 6–3). ■

Arginine Is the Precursor for Biological Synthesis of Nitric Oxide

A surprise finding in the mid-1980s was the role of nitric oxide (NO)—previously known mainly as a component of smog—as an important biological messenger. This simple gaseous substance diffuses readily through membranes, although its high reactivity limits its range of diffusion to about a 1 mm radius from the site of synthesis. In humans NO plays a role in a range of physiological processes, including neurotransmission, blood clotting, and the control of blood pressure. Its mode of action is described in Chapter 12 (see Section 12.4).

Nitric oxide is synthesized from arginine in an NADPH-dependent reaction catalyzed by nitric oxide synthase **(Fig. 22–33)**, a dimeric enzyme structurally related to NADPH cytochrome P-450 reductase (see Box 21–1). The reaction is a five-electron oxidation. Each subunit of the enzyme contains one bound molecule of each of four different cofactors: FMN, FAD, tetrahydrobiopterin, and Fe^{3+} heme. NO is an unstable molecule and cannot be stored. Its synthesis is stimulated by interaction of nitric oxide synthase with Ca^{2+}-calmodulin (see Fig. 12–11).

SUMMARY 22.3 Molecules Derived from Amino Acids

- Many important biomolecules are derived from amino acids. Glycine is a precursor of porphyrins. Degradation of iron-porphyrin (heme) generates bilirubin, which is converted to bile pigments, with several physiological functions.

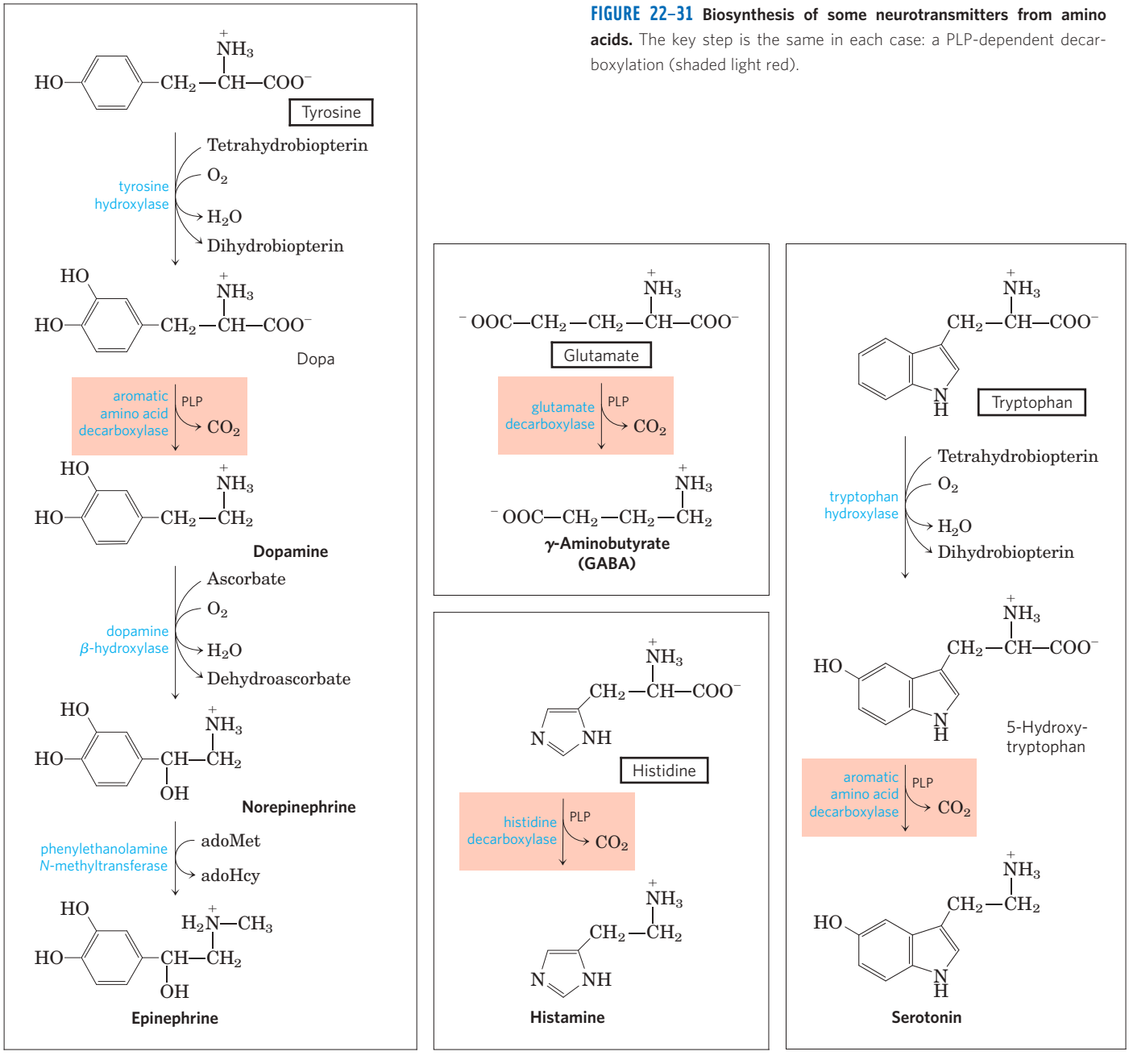

FIGURE 22–31 Biosynthesis of some neurotransmitters from amino acids. The key step is the same in each case: a PLP-dependent decarboxylation (shaded light red).

- Glycine and arginine give rise to creatine and phosphocreatine, an energy buffer. Glutathione, formed from three amino acids, is an important cellular reducing agent.
- Bacteria synthesize D-amino acids from L-amino acids in racemization reactions requiring pyridoxal phosphate. D-Amino acids are commonly found in certain bacterial walls and certain antibiotics.
- The aromatic amino acids give rise to many plant substances. The PLP-dependent decarboxylation of some amino acids yields important biological amines, including neurotransmitters.
- Arginine is the precursor of nitric oxide, a biological messenger.

22.4 Biosynthesis and Degradation of Nucleotides

As discussed in Chapter 8, nucleotides have a variety of important functions in all cells. They are the precursors of DNA and RNA. They are essential carriers of chemical energy—a role primarily of ATP and to some extent GTP. They are components of the cofactors NAD, FAD, *S*-adenosylmethionine, and coenzyme A, as well as of activated biosynthetic intermediates such as UDP-glucose and CDP-diacylglycerol. Some, such as cAMP and cGMP, are also cellular second messengers.

Two types of pathways lead to nucleotides: the **de novo pathways** and the **salvage pathways**. De novo

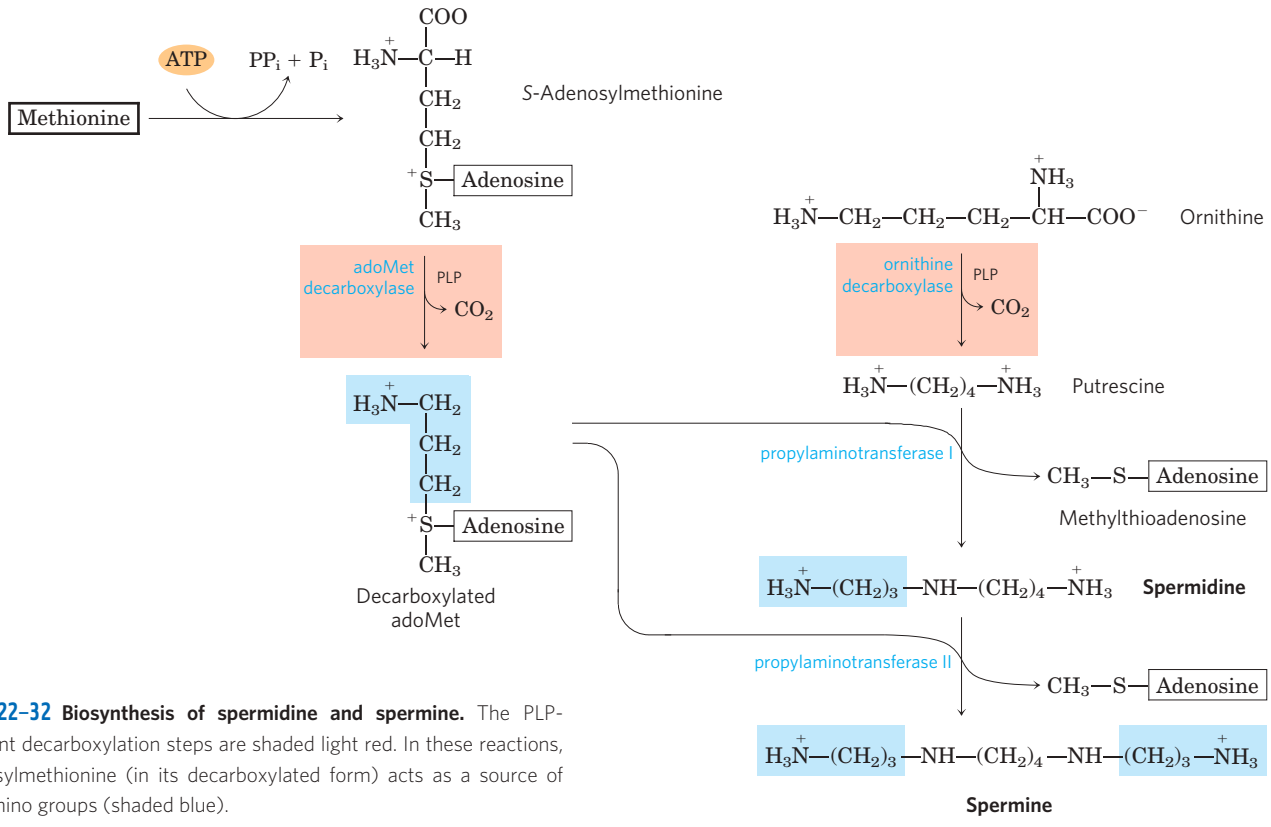

FIGURE 22–32 Biosynthesis of spermidine and spermine. The PLP-dependent decarboxylation steps are shaded light red. In these reactions, *S*-adenosylmethionine (in its decarboxylated form) acts as a source of propylamino groups (shaded blue).

synthesis of nucleotides begins with their metabolic precursors: amino acids, ribose 5-phosphate, CO_2, and NH_3. Salvage pathways recycle the free bases and nucleosides released from nucleic acid breakdown. Both types of pathways are important in cellular metabolism and both are discussed in this section.

The de novo pathways for purine and pyrimidine biosynthesis seem to be nearly identical in all living organisms. Notably, the free bases guanine, adenine, thymine, cytidine, and uracil are *not* intermediates in these pathways; that is, the bases are not synthesized and then attached to ribose, as might be expected. The purine ring structure is built up one or a few atoms at a time, attached to ribose throughout the process. The pyrimidine ring is synthesized as **orotate**, attached to ribose phosphate, and then converted to the common pyrimidine nucleotides required in nucleic acid synthesis. Although the free bases are not intermediates in the de novo pathways, they are intermediates in some of the salvage pathways.

Several important precursors are shared by the de novo pathways for synthesis of pyrimidines and purines. Phosphoribosyl pyrophosphate (PRPP) is important in both, and in these pathways the structure of ribose is retained in the product nucleotide, in contrast to its fate in the tryptophan and histidine biosynthetic pathways discussed earlier. An amino acid is an important precursor in each type of pathway: glycine for purines and

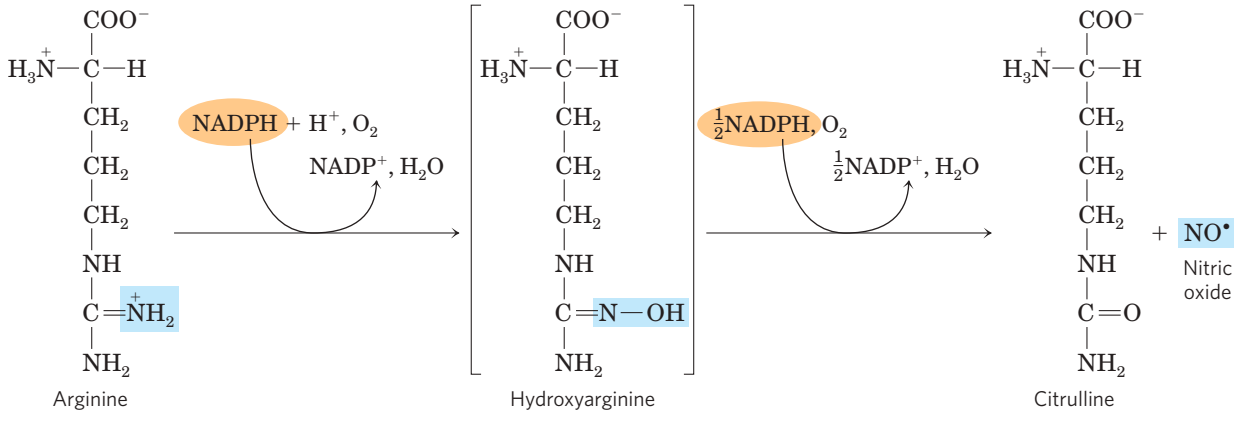

FIGURE 22–33 Biosynthesis of nitric oxide. Both steps are catalyzed by nitric oxide synthase. The nitrogen of the NO is derived from the guanidinium group of arginine.

aspartate for pyrimidines. Glutamine again is the most important source of amino groups—in five different steps in the de novo pathways. Aspartate is also used as the source of an amino group in the purine pathways, in two steps.

Two other features deserve mention. First, there is evidence, especially in the de novo purine pathway, that the enzymes are present as large, multienzyme complexes in the cell, a recurring theme in our discussion of metabolism. Second, the cellular pools of nucleotides (other than ATP) are quite small, perhaps 1% or less of the amounts required to synthesize the cell's DNA. Therefore, cells must continue to synthesize nucleotides during nucleic acid synthesis, and in some cases nucleotide synthesis may limit the rates of DNA replication and transcription. Because of the importance of these processes in dividing cells, agents that inhibit nucleotide synthesis have become particularly important in medicine.

We examine here the biosynthetic pathways of purine and pyrimidine nucleotides and their regulation, the formation of the deoxynucleotides, and the degradation of purines and pyrimidines to uric acid and urea. We end with a discussion of chemotherapeutic agents that affect nucleotide synthesis.

De Novo Purine Nucleotide Synthesis Begins with PRPP

John M. Buchanan, 1917–2007

The two parent purine nucleotides of nucleic acids are adenosine 5′-monophosphate (AMP; adenylate) and guanosine 5′-monophosphate (GMP; guanylate), containing the purine bases adenine and guanine. **Figure 22–34** shows the origin of the carbon and nitrogen atoms of the purine ring system, as determined by John M. Buchanan using isotopic tracer experiments in birds. The detailed pathway of purine biosynthesis was worked out primarily by Buchanan and G. Robert Greenberg in the 1950s.

In the first committed step of the pathway, an amino group donated by glutamine is attached at C-1 of PRPP **(Fig. 22–35)**. The resulting **5-phosphoribosylamine** is highly unstable, with a half-life of 30 seconds at pH 7.5. The purine ring is subsequently built up on this structure. The pathway described here is identical in all organisms, with the exception of one step that differs in higher eukaryotes, as noted below.

The second step is the addition of three atoms from glycine (Fig. 22–35, step ❷). An ATP is consumed to activate the glycine carboxyl group (in the form of an acyl phosphate) for this condensation reaction. The added glycine amino group is then formylated by N^{10}-formyltetrahydrofolate ❸, and a nitrogen is contributed by glutamine (step ❹), before dehydration and ring closure yield the five-membered imidazole ring of the purine nucleus, as 5-aminoimidazole ribonucleotide (AIR; step ❺).

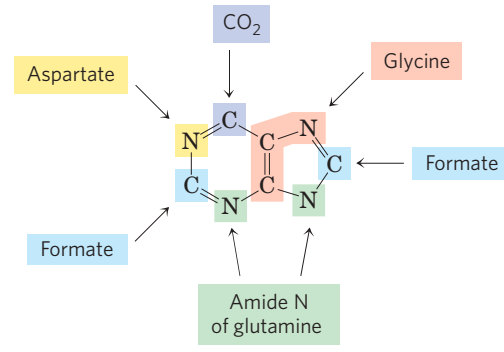

FIGURE 22–34 Origin of the ring atoms of purines. This information was obtained from isotopic experiments with ^{14}C- or ^{15}N-labeled precursors. Formate is supplied in the form of N^{10}-formyltetrahydrofolate.

At this point, three of the six atoms needed for the second ring in the purine structure are in place. To complete the process, a carboxyl group is first added (step ❻). This carboxylation is unusual in that it does not require biotin, but instead uses the bicarbonate generally present in aqueous solutions. A rearrangement transfers the carboxylate from the exocyclic amino group to position 4 of the imidazole ring (step ❼). Steps ❻ and ❼ are found only in bacteria and fungi. In higher eukaryotes, including humans, the 5-aminoimidazole ribonucleotide product of step ❺ is carboxylated directly to carboxyaminoimidazole ribonucleotide in one step instead of two (step ❻a). The enzyme catalyzing this reaction is AIR carboxylase.

Aspartate now donates its amino group in two steps (❽ and ❾): formation of an amide bond, followed by elimination of the carbon skeleton of aspartate (as fumarate). (Recall that aspartate plays an analogous role in two steps of the urea cycle; see Fig. 18–10.) The final carbon is contributed by N^{10}-formyltetrahydrofolate (step ❿), and a second ring closure takes place to yield the second fused ring of the purine nucleus (step ⓫). The first intermediate with a complete purine ring is **inosinate (IMP)**.

As in the tryptophan and histidine biosynthetic pathways, the enzymes of IMP synthesis seem to be organized as large, multienzyme complexes in the cell. Once again, evidence comes from the existence of single polypeptides with several functions, some catalyzing nonsequential steps in the pathway. In eukaryotic cells ranging from yeast to fruit flies to chickens, steps ❶, ❸, and ❺ in Figure 22–35 are catalyzed by a multifunctional protein. An additional multifunctional protein catalyzes steps ❿ and ⓫. In humans, a multifunctional enzyme combines the activities of AIR carboxylase and SAICAR synthetase (steps ❻a and ❽). In bacteria,

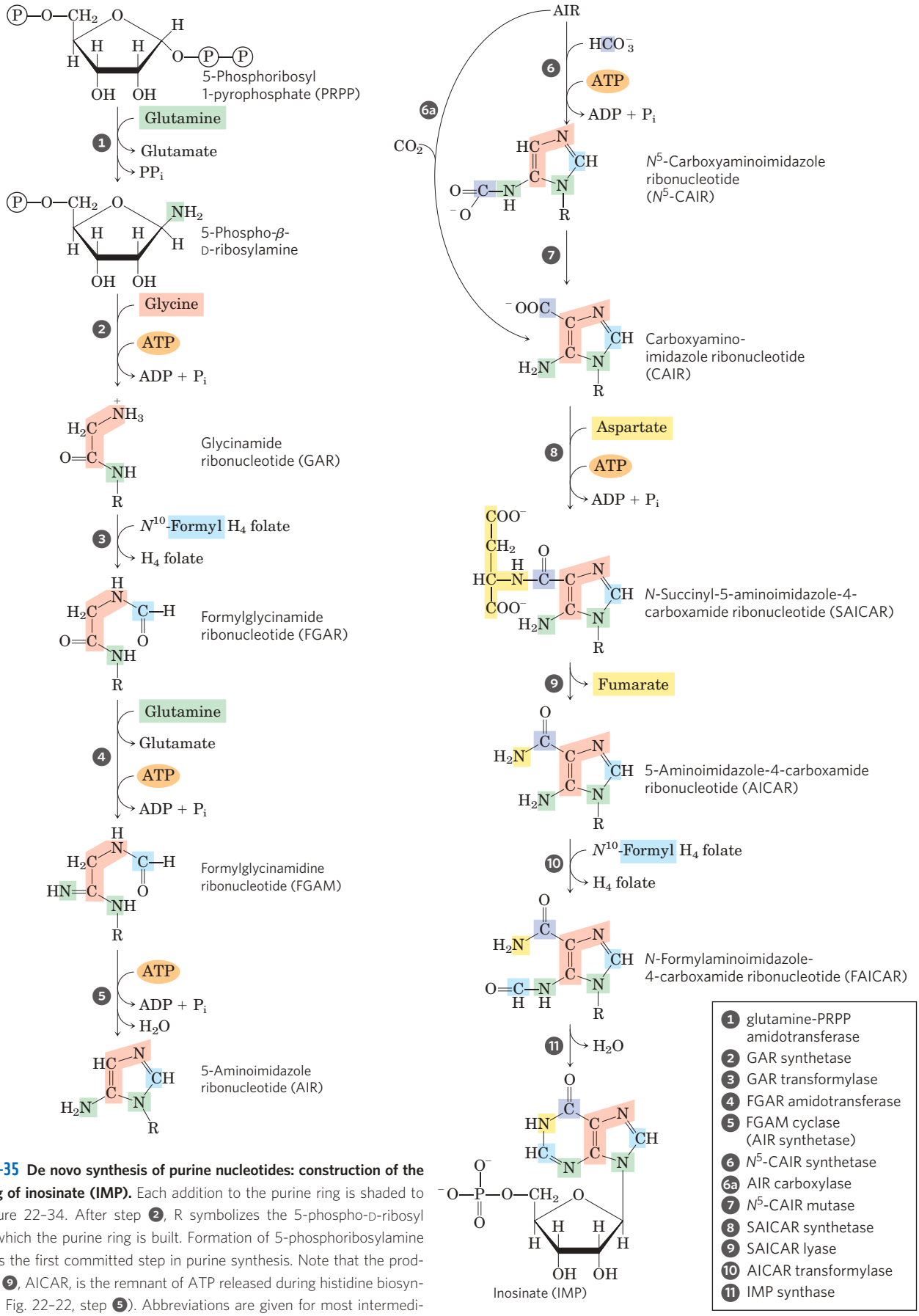

FIGURE 22–35 De novo synthesis of purine nucleotides: construction of the purine ring of inosinate (IMP). Each addition to the purine ring is shaded to match Figure 22–34. After step 2, R symbolizes the 5-phospho-D-ribosyl group on which the purine ring is built. Formation of 5-phosphoribosylamine (step 1) is the first committed step in purine synthesis. Note that the product of step 9, AICAR, is the remnant of ATP released during histidine biosynthesis (see Fig. 22–22, step 5). Abbreviations are given for most intermediates to simplify the naming of the enzymes. Step 6a is the alternative path from AIR to CAIR occurring in higher eukaryotes.

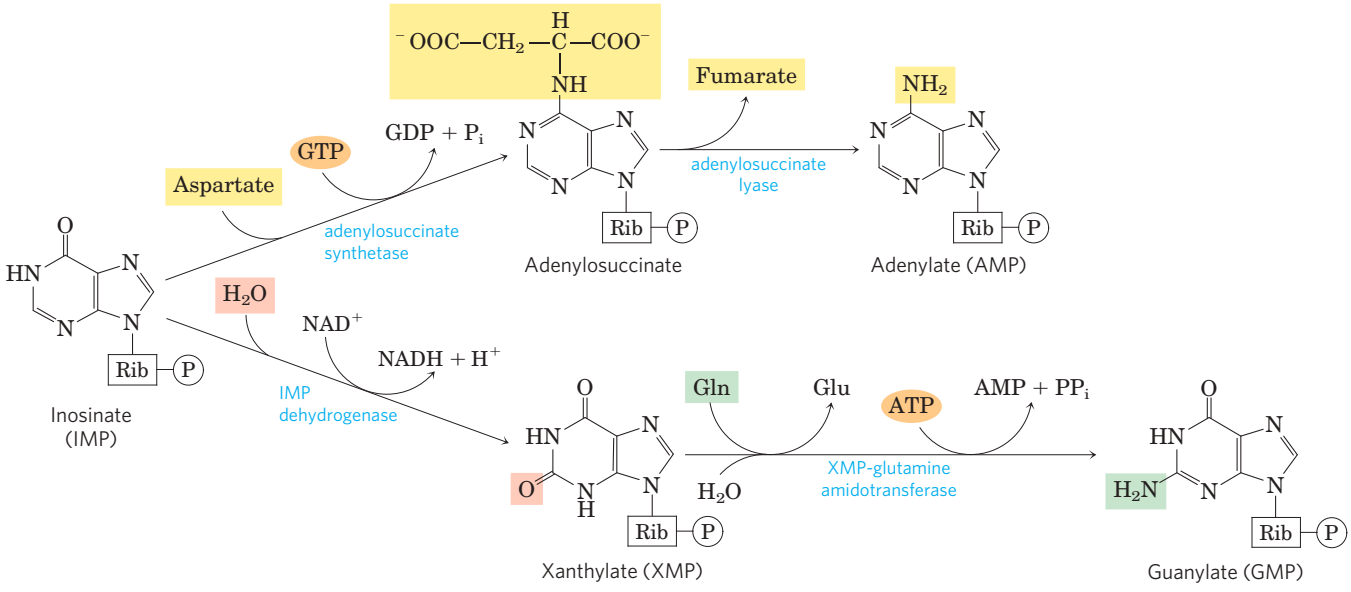

FIGURE 22–36 **Biosynthesis of AMP and GMP from IMP.**

these activities are found on separate proteins, but the proteins may form a large noncovalent complex. The channeling of reaction intermediates from one enzyme to the next permitted by these complexes is probably especially important for unstable intermediates such as 5-phosphoribosylamine.

Conversion of inosinate to adenylate requires the insertion of an amino group derived from aspartate **(Fig. 22–36)**; this takes place in two reactions similar to those used to introduce N-1 of the purine ring (Fig. 22–35, steps ❽ and ❾). A crucial difference is that GTP rather than ATP is the source of the high-energy phosphate in synthesizing adenylosuccinate. Guanylate is formed by the NAD^+-requiring oxidation of inosinate at C-2, followed by addition of an amino group derived from glutamine. ATP is cleaved to AMP and PP_i in the final step (Fig. 22–36).

Purine Nucleotide Biosynthesis Is Regulated by Feedback Inhibition

Three major feedback mechanisms cooperate in regulating the overall rate of de novo purine nucleotide synthesis and the relative rates of formation of the two end products, adenylate and guanylate **(Fig. 22–37)**. The first mechanism is exerted on the first reaction that is unique to purine synthesis: transfer of an amino group to PRPP to form 5-phosphoribosylamine. This reaction is catalyzed by the allosteric enzyme glutamine-PRPP amidotransferase, which is inhibited by the end products IMP, AMP, and GMP. AMP and GMP act synergistically in this concerted inhibition. Thus, whenever either AMP or GMP accumulates to excess, the first step in its biosynthesis from PRPP is partially inhibited.

In the second control mechanism, exerted at a later stage, an excess of GMP in the cell inhibits formation of xanthylate from inosinate by IMP dehydrogenase, without affecting the formation of AMP. Conversely, an accumulation of adenylate inhibits formation of adenylosuccinate by adenylosuccinate synthetase, without affecting the biosynthesis of GMP. When both products are present in sufficient quantities, IMP builds up, and it inhibits an earlier step in the pathway; this regulatory strategy is called **sequential feedback inhibition**. In the third mechanism, GTP is required in the conversion

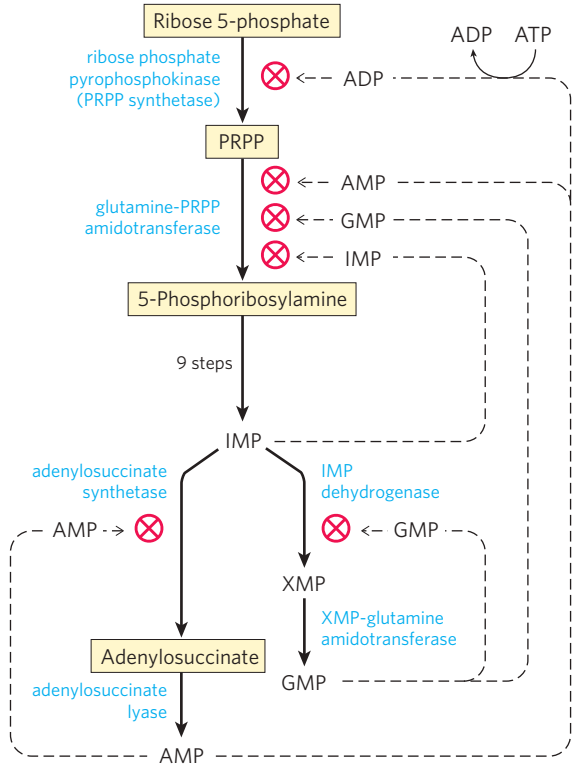

FIGURE 22–37 **Regulatory mechanisms in the biosynthesis of adenine and guanine nucleotides in *E. coli*.** Regulation of these pathways differs in other organisms.

of IMP to AMP, whereas ATP is required for conversion of IMP to GMP (Fig. 22–36), a reciprocal arrangement that tends to balance the synthesis of the two ribonucleotides.

The final control mechanism is the inhibition of PRPP synthesis by the allosteric regulation of ribose phosphate pyrophosphokinase. This enzyme is inhibited by ADP and GDP, in addition to metabolites from other pathways for which PRPP is a starting point.

Pyrimidine Nucleotides Are Made from Aspartate, PRPP, and Carbamoyl Phosphate

The common pyrimidine ribonucleotides are cytidine 5′-monophosphate (CMP; cytidylate) and uridine 5′-monophosphate (UMP; uridylate), which contain the pyrimidines cytosine and uracil. De novo pyrimidine nucleotide biosynthesis **(Fig. 22–38)** proceeds in a somewhat different manner from purine nucleotide synthesis; the six-membered pyrimidine ring is made first and then attached to ribose 5-phosphate. Required in this process is carbamoyl phosphate, also an intermediate in the urea cycle. However, as we noted in Chapter 18, in animals the carbamoyl phosphate required in urea synthesis is made in mitochondria by carbamoyl phosphate synthetase I, whereas the carbamoyl phosphate required in pyrimidine biosynthesis is made in the cytosol by a different form of the enzyme, **carbamoyl phosphate synthetase II**. In bacteria, a single enzyme supplies carbamoyl phosphate for the synthesis of arginine and pyrimidines. The bacterial enzyme has three separate active sites, spaced along a channel nearly 100 Å long **(Fig. 22–39)**. Bacterial carbamoyl phosphate synthetase provides a vivid illustration of the channeling of unstable reaction intermediates between active sites.

Carbamoyl phosphate reacts with aspartate to yield *N*-carbamoylaspartate in the first committed step of pyrimidine biosynthesis (Fig. 22–38). This reaction is catalyzed by **aspartate transcarbamoylase**. In bacteria, this step is highly regulated, and bacterial aspartate transcarbamoylase is one of the most thoroughly studied allosteric enzymes (see below). By removal of water from *N*-carbamoylaspartate, a reaction catalyzed by **dihydroorotase**, the pyrimidine ring is closed to form L-dihydroorotate. This compound is oxidized to the pyrimidine derivative orotate, a reaction in which NAD^+ is the ultimate electron acceptor. In eukaryotes, the first three enzymes in this pathway—carbamoyl phosphate synthetase II, aspartate transcarbamoylase, and dihydroorotase—are part of a single trifunctional protein. The protein, known by the acronym CAD, contains three identical polypeptide chains (each of M_r 230,000), each with active sites for all three reactions. This suggests that large, multienzyme complexes may be the rule in this pathway.

Once orotate is formed, the ribose 5-phosphate side chain, provided once again by PRPP, is attached to yield orotidylate (Fig. 22–38). Orotidylate is then

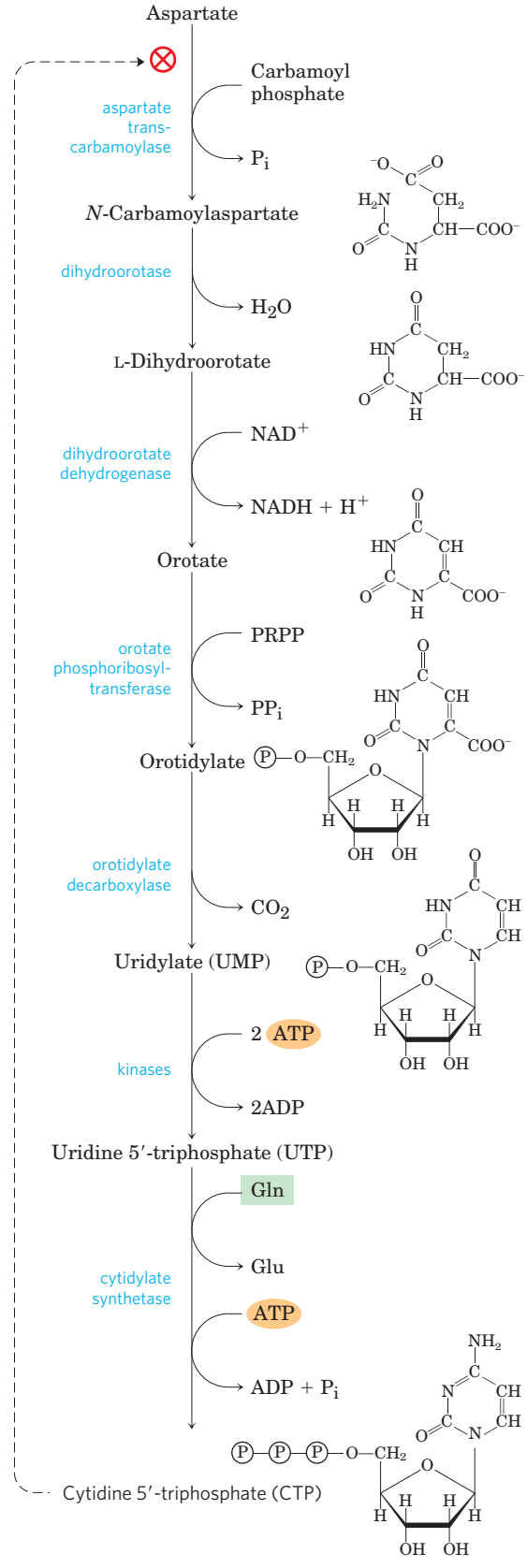

FIGURE 22–38 De novo synthesis of pyrimidine nucleotides: biosynthesis of UTP and CTP via orotidylate. The pyrimidine is constructed from carbamoyl phosphate and aspartate. The ribose 5-phosphate is then added to the completed pyrimidine ring by orotate phosphoribosyltransferase. The first step in this pathway (not shown here; see Fig. 18–11a) is the synthesis of carbamoyl phosphate from CO_2 and NH_4^+. In eukaryotes, the first step is catalyzed by carbamoyl phosphate synthetase II.

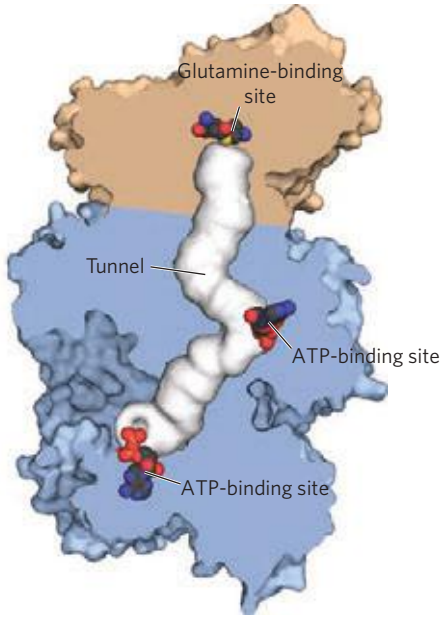

FIGURE 22–39 Channeling of intermediates in bacterial carbamoyl phosphate synthetase. (Derived from PDB ID 1M6V) The reaction catalyzed by this enzyme (and its mitochondrial counterpart) is illustrated in Figure 18–11a. The small and large subunits are shown in tan and blue, respectively; the tunnel between active sites (almost 100 Å long) is shown as white. In this reaction, a glutamine molecule binds to the small subunit, donating its amido nitrogen as NH_4^+ in a glutamine amidotransferase–type reaction. The NH_4^+ enters the tunnel, which takes it to a second active site, where it combines with bicarbonate in a reaction requiring ATP. The carbamate then reenters the tunnel to reach the third active site, where it is phosphorylated by ATP to carbamoyl phosphate. To solve this structure, the enzyme was crystallized with ornithine bound to the glutamine-binding site and ADP bound to the ATP-binding sites.

decarboxylated to uridylate, which is phosphorylated to UTP. CTP is formed from UTP by the action of **cytidylate synthetase**, by way of an acyl phosphate intermediate (consuming one ATP). The nitrogen donor is normally glutamine, although the cytidylate synthetases in many species can use NH_4^+ directly.

Pyrimidine Nucleotide Biosynthesis Is Regulated by Feedback Inhibition

Regulation of the rate of pyrimidine nucleotide synthesis in bacteria occurs in large part through aspartate transcarbamoylase (ATCase), which catalyzes the first reaction in the sequence and is inhibited by CTP, the end product of the sequence (Fig. 22–38). The bacterial ATCase molecule consists of six catalytic subunits and six regulatory subunits (see Fig. 6–33). The catalytic subunits bind the substrate molecules, and the allosteric subunits bind the allosteric inhibitor, CTP. The entire ATCase molecule, as well as its subunits, exists in two conformations, active and inactive. When CTP is not bound to the regulatory subunits, the enzyme is maximally active. As CTP accumulates and binds to the regulatory subunits, they undergo a change in conformation. This change is transmitted to the catalytic subunits, which then also shift to an inactive conformation.

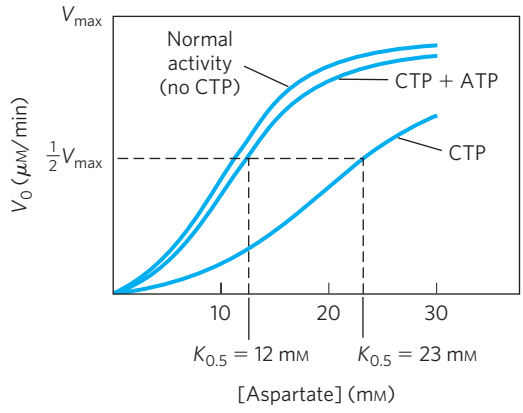

FIGURE 22–40 Allosteric regulation of aspartate transcarbamoylase by CTP and ATP. Addition of 0.8 mM CTP, the allosteric inhibitor of ATCase, increases the $K_{0.5}$ for aspartate (lower curve) thereby reducing the rate of conversion of aspartate to *N*-carbamoylaspartate. ATP at 0.6 mM fully reverses this inhibition by CTP (middle curve).

ATP prevents the changes induced by CTP. **Figure 22–40** shows the effects of the allosteric regulators on the activity of ATCase.

Nucleoside Monophosphates Are Converted to Nucleoside Triphosphates

Nucleotides to be used in biosynthesis are generally converted to nucleoside triphosphates. The conversion pathways are common to all cells. Phosphorylation of AMP to ADP is promoted by **adenylate kinase**, in the reaction

$$\text{ATP} + \text{AMP} \rightleftharpoons 2\ \text{ADP}$$

The ADP so formed is phosphorylated to ATP by the glycolytic enzymes or through oxidative phosphorylation.

ATP also brings about the formation of other nucleoside diphosphates by the action of a class of enzymes called **nucleoside monophosphate kinases**. These enzymes, which are generally specific for a particular base but nonspecific for the sugar (ribose or deoxyribose), catalyze the reaction

$$\text{ATP} + \text{NMP} \rightleftharpoons \text{ADP} + \text{NDP}$$

The efficient cellular systems for rephosphorylating ADP to ATP tend to pull this reaction in the direction of products.

Nucleoside diphosphates are converted to triphosphates by the action of a ubiquitous enzyme, **nucleoside diphosphate kinase**, which catalyzes the reaction

$$\text{NTP}_\text{D} + \text{NDP}_\text{A} \rightleftharpoons \text{NDP}_\text{D} + \text{NTP}_\text{A}$$

This enzyme is notable in that it is not specific for the base (purines or pyrimidines) or the sugar (ribose or deoxyribose). This nonspecificity applies to both phosphate acceptor (A) and donor (D), although the donor (NTP_D) is almost invariably ATP because it is present in higher concentration than other nucleoside triphosphates under aerobic conditions.

Ribonucleotides Are the Precursors of Deoxyribonucleotides

Deoxyribonucleotides, the building blocks of DNA, are derived from the corresponding ribonucleotides by direct reduction at the 2′-carbon atom of the D-ribose to form the 2′-deoxy derivative. For example, adenosine diphosphate (ADP) is reduced to 2′-deoxyadenosine diphosphate (dADP), and GDP is reduced to dGDP. This reaction is somewhat unusual in that the reduction occurs at a nonactivated carbon; no closely analogous chemical reactions are known. The reaction is catalyzed by **ribonucleotide reductase**, best characterized in *E. coli*, in which its substrates are ribonucleoside diphosphates.

The reduction of the D-ribose portion of a ribonucleoside diphosphate to 2′-deoxy-D-ribose requires a pair of hydrogen atoms, which are ultimately donated by NADPH via an intermediate hydrogen-carrying protein, **thioredoxin**. This ubiquitous protein serves a similar redox function in photosynthesis (see Fig. 20–19) and other processes. Thioredoxin has pairs of —SH groups that carry hydrogen atoms from NADPH to the ribonucleoside diphosphate. Its oxidized (disulfide) form is reduced by NADPH in a reaction catalyzed by **thioredoxin reductase** **(Fig. 22–41)**, and reduced thioredoxin is then used by ribonucleotide reductase to reduce the nucleoside diphosphates (NDPs) to deoxyribonucleoside diphosphates (dNDPs). A second source of reducing equivalents for ribonucleotide reductase is glutathione (GSH). Glutathione serves as the reductant for a protein closely related to thioredoxin, **glutaredoxin**, which then transfers the reducing power to ribonucleotide reductase (Fig. 22–41).

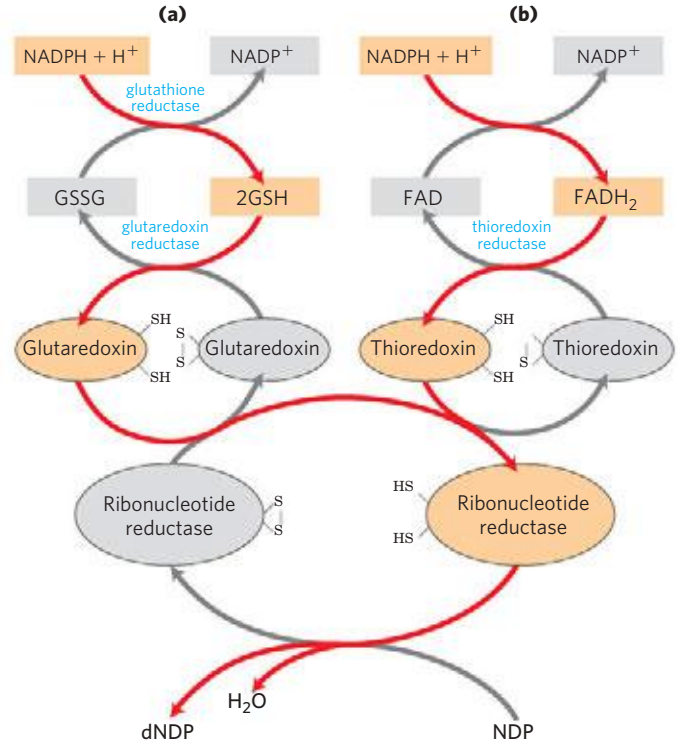

FIGURE 22–41 Reduction of ribonucleotides to deoxyribonucleotides by ribonucleotide reductase. Electrons are transmitted (red arrows) to the enzyme from NADPH via **(a)** glutaredoxin or **(b)** thioredoxin. The sulfide groups in glutaredoxin reductase are contributed by two molecules of bound glutathione (GSH; GSSG indicates oxidized glutathione). Note that thioredoxin reductase is a flavoenzyme, with FAD as prosthetic group.

Ribonucleotide reductase is notable in that its reaction mechanism provides the best-characterized example of the involvement of free radicals in biochemical transformations, once thought to be rare in biological systems. The enzyme in *E. coli* and most eukaryotes is an $\alpha_2\beta_2$ dimer, with catalytic subunits α_2 and radical-generation subunits β_2 **(Fig. 22–42)**. Each catalytic subunit contains two kinds of regulatory sites,

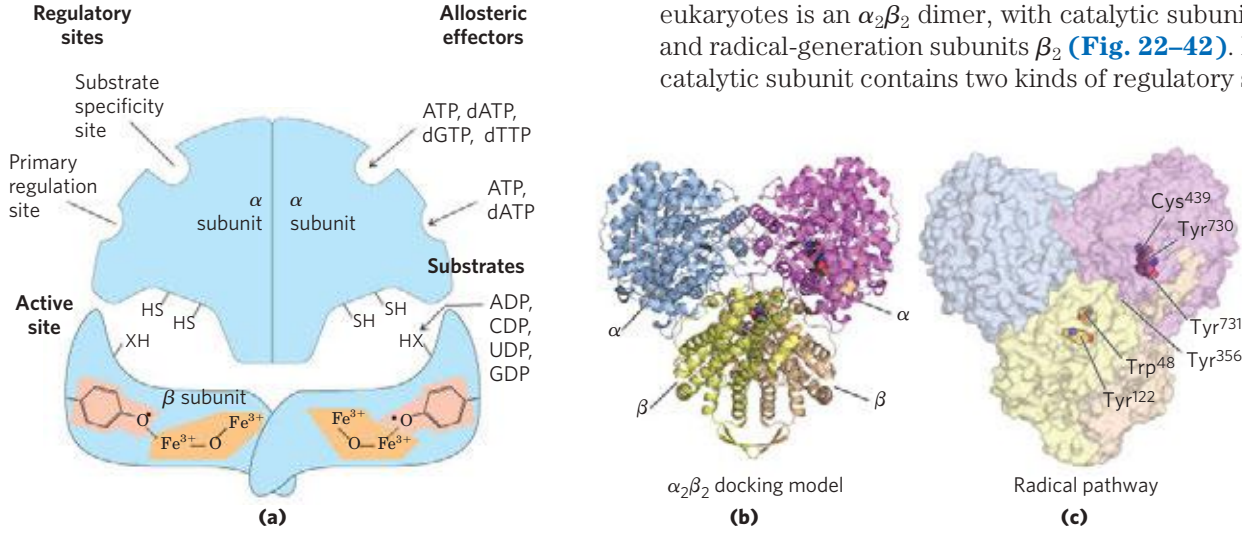

FIGURE 22–42 Ribonucleotide reductase. (a) A schematic diagram of the subunit structures. The catalytic subunit (α; also called R1) contains the two regulatory sites described in Fig. 22–44 and two Cys residues central to the reaction mechanism. The radical-generation subunits β (also called R2) contain the critical Tyr^{122} residue and the binuclear iron center. **(b)** Structures of α_2 and β_2 give the likely structure of $\alpha_2\beta_2$ (derived from PDB ID 3UUS). **(c)** The likely path of radical formation from the initial Tyr^{122} in a β subunit to the active-site Cys^{439}, which is used in the mechanism shown in Figure 22–43. Several aromatic amino acid residues participate in long-range radical transfer from the point of its formation at Tyr^{122} to the active site, where the nucleotide substrate is bound.

as described below. The two active sites of the enzyme are formed at the interface between the catalytic (α_2) and radical-generation (β_2) subunits. At each active site, an α subunit contributes two sulfhydryl groups required for activity and the β_2 subunits contribute a stable tyrosyl radical. The β_2 subunits also have a binuclear iron (Fe^{3+}) cofactor that helps generate and stabilize the Tyr^{122} radical (Fig. 22–42). The tyrosyl radical is too far from the active site to interact directly with the site, but several aromatic residues form a long-range radical transfer pathway to the active site (Fig. 22–42c). A likely mechanism for the ribonucleotide reductase reaction is illustrated in **Figure 22–43**. In *E. coli*, the sources of the required reducing equivalents for this reaction are thioredoxin and glutaredoxin, as noted above.

Three classes of ribonucleotide reductase have been reported. Their mechanisms (where known) generally conform to the scheme in Figure 22–43, but they differ in the identity of the group supplying the active-site radical and in the cofactors used to generate it. The *E. coli* enzyme (class I) requires oxygen to regenerate the tyrosyl radical if it is quenched, so this enzyme functions only in an aerobic environment. Class II enzymes, found in other microorganisms, have 5′-deoxyadenosylcobalamin (see Box 17–2) rather than a binuclear iron center. Class III enzymes have evolved to function in an anaerobic environment. *E. coli* contains a separate class III ribonucleotide reductase when grown anaerobically; this enzyme contains an iron-sulfur cluster (structurally distinct from the binuclear iron center of the class I enzyme) and requires NADPH and *S*-adenosylmethionine for activity. It uses nucleoside triphosphates rather than nucleoside diphosphates as substrates. The evolution of different classes of ribonucleotide reductase for production of DNA precursors in different environments reflects the importance of this reaction in nucleotide metabolism.

Regulation of *E. coli* ribonucleotide reductase is unusual in that not only its *activity* but its *substrate specificity* is regulated by the binding of effector molecules. Each α subunit has two types of regulatory

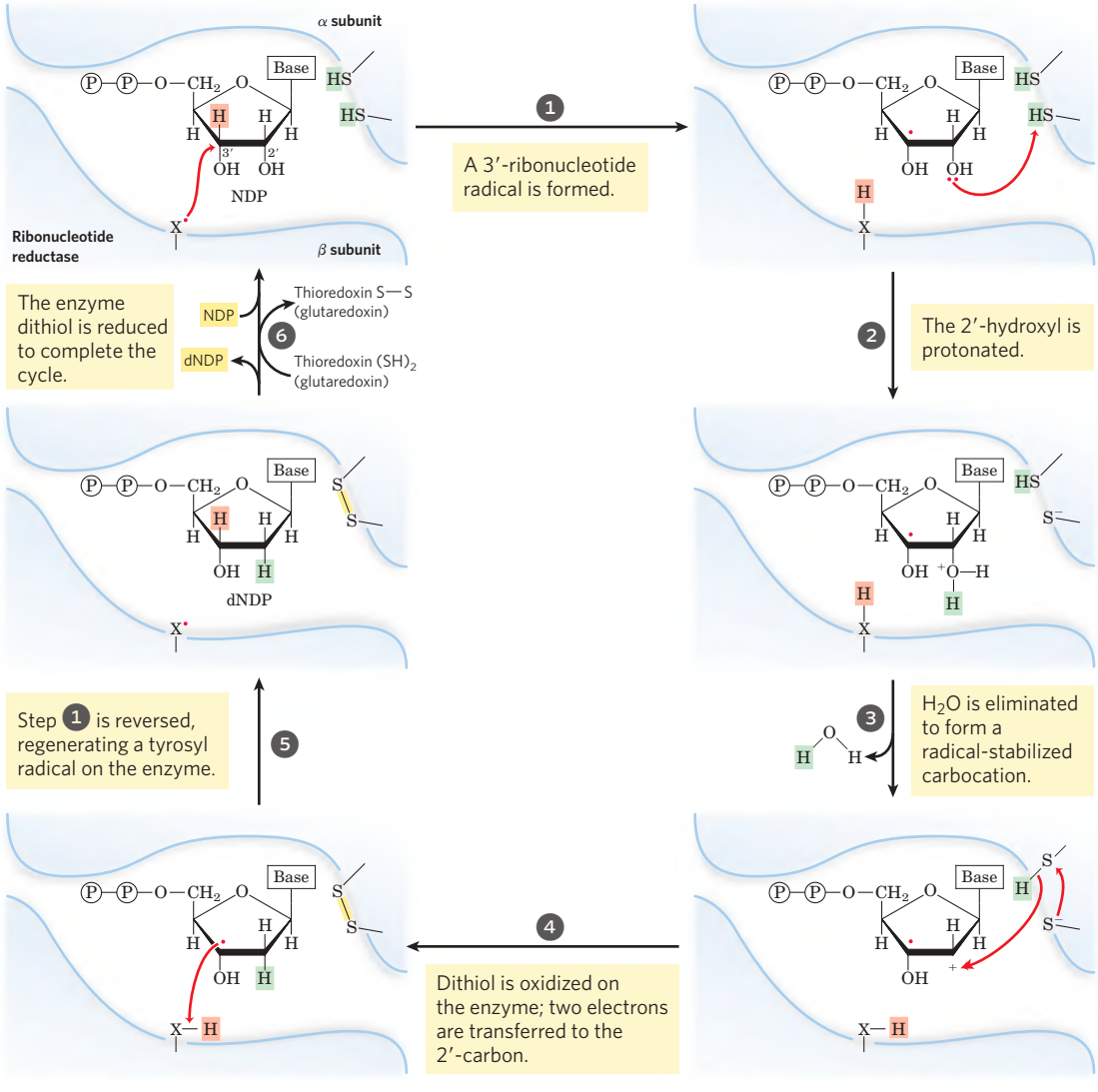

MECHANISM FIGURE 22–43 Proposed mechanism for ribonucleotide reductase. In the enzyme of *E. coli* and most eukaryotes, the active thiol groups are on the α subunit; the active-site radical (—X$^{\bullet}$) is on the β subunit and in *E. coli* is probably a thiyl radical of Cys^{439} (see Fig. 22–42).

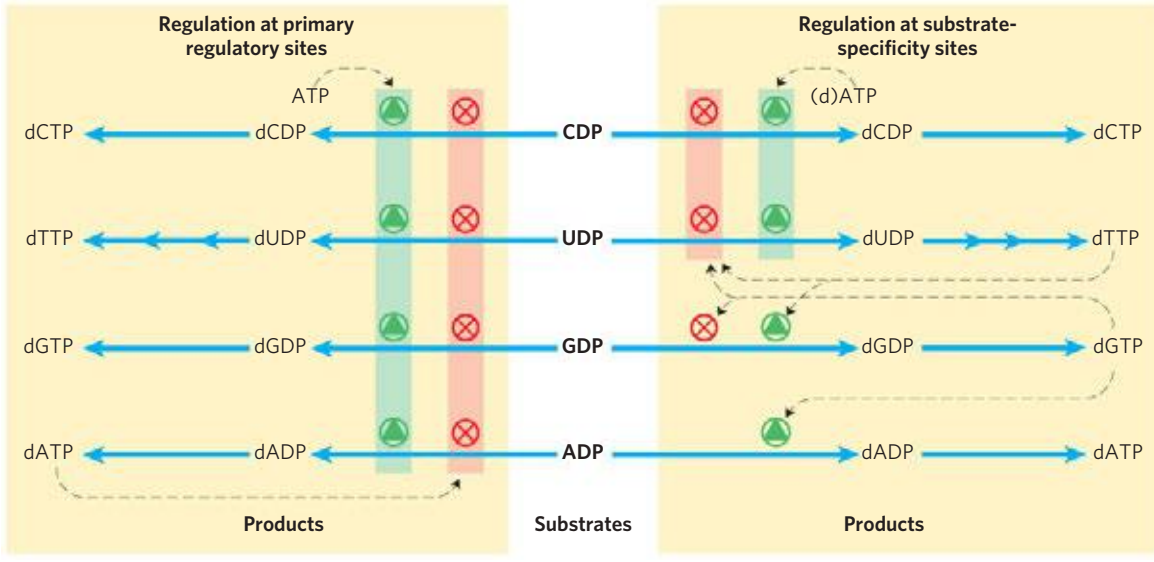

FIGURE 22–44 Regulation of ribonucleotide reductase by deoxynucleoside triphosphates. The overall activity of the enzyme is affected by binding at the primary regulatory site (left). The substrate specificity of the enzyme is affected by the nature of the effector molecule bound at the second type of regulatory site, the substrate-specificity site (right). The diagram indicates inhibition or stimulation of enzyme activity with the four different substrates. The pathway from dUDP to dTTP is described later (see Figs. 22–46, 22–47).

site (Fig. 22–42). One type affects overall enzyme activity and binds either ATP, which activates the enzyme, or dATP, which inactivates it. The second type alters substrate specificity in response to the effector molecule—ATP, dATP, dTTP, or dGTP—that is bound there **(Fig. 22–44)**. When ATP or dATP is bound, reduction of UDP and CDP is favored. When dTTP or dGTP is bound, reduction of GDP or ADP, respectively, is stimulated. The scheme is designed to provide a balanced pool of precursors for DNA synthesis. ATP is also a general activator for biosynthesis and ribonucleotide reduction. The presence of dATP in small amounts increases the reduction of pyrimidine nucleotides. An oversupply of the pyrimidine dNTPs is signaled by high levels of dTTP, which shifts the specificity to favor reduction of GDP. High levels of dGTP, in turn, shift the specificity to ADP reduction, and high levels of dATP shut the enzyme down. These effectors are thought to induce several distinct enzyme conformations with altered specificities.

These regulatory effects are accompanied by, and presumably mediated by, large structural rearrangements in the enzyme. When the active form of the *E. coli* enzyme ($\alpha_2\beta_2$) is inhibited by the addition of the allosteric inhibitor dATP, a ringlike $\alpha_4\beta_4$ structure forms, with alternating α_2 and β_2 subunits **(Fig. 22–45)**. In this altered structure, the radical-forming path from β to α is disrupted and the residues in the path are

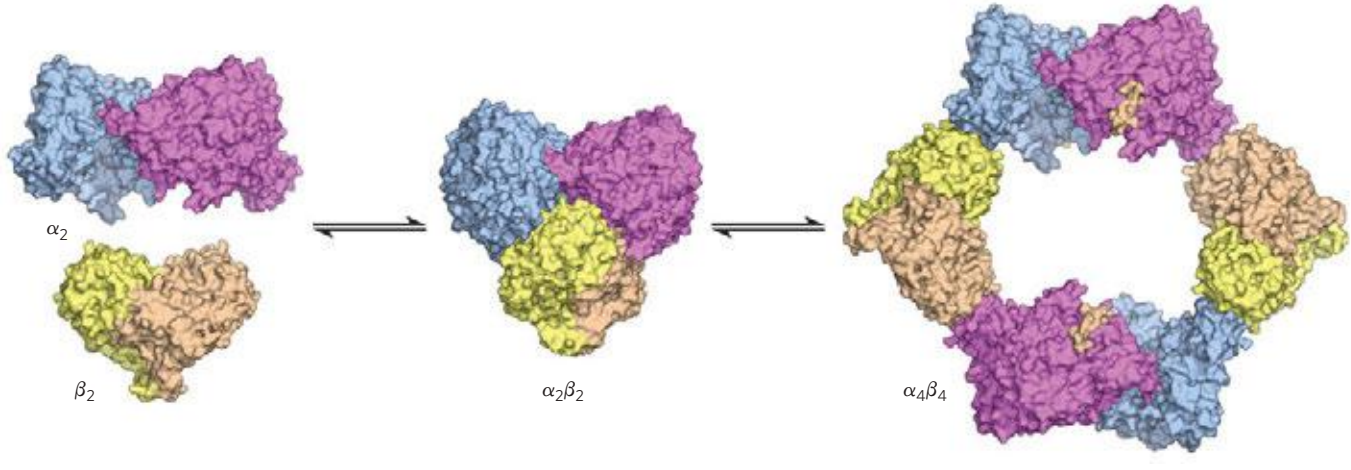

FIGURE 22–45 Oligomerization of ribonucleotide reductase induced by the allosteric inhibitor dATP. In high concentrations of dATP (50 μM), ring-shaped $\alpha_4\beta_4$ structures form (PDB ID 3UUS). In this conformation, the residues in the radical-forming path are exposed to the solvent, blocking the radical reaction and inhibiting the enzyme. The oligomerization is reversed at lower dATP concentrations.

exposed to solvent, effectively preventing radical transfer and thus inhibiting the reaction. The formation of ringlike $\alpha_4\beta_4$ structures is reversed when dATP levels are reduced. The yeast ribonucleotide reductase also undergoes oligomerization in the presence of dATP, forming a hexameric ring structure, $\alpha_6\beta_6$.

Thymidylate Is Derived from dCDP and dUMP

DNA contains thymine rather than uracil, and the de novo pathway to thymine involves only deoxyribonucleotides. The immediate precursor of thymidylate (dTMP) is dUMP. In bacteria, the pathway to dUMP begins with formation of dUTP, either by deamination of dCTP or by phosphorylation of dUDP **(Fig. 22–46)**. The dUTP is converted to dUMP by a dUTPase. The latter reaction must be efficient to keep dUTP pools low and prevent incorporation of uridylate into DNA.

Conversion of dUMP to dTMP is catalyzed by **thymidylate synthase**. A one-carbon unit at the hydroxymethyl (—CH_2OH) oxidation level (see Fig. 18–17) is transferred from N^5,N^{10}-methylenetetrahydrofolate to dUMP, then reduced to a methyl group **(Fig. 22–47)**. The reduction occurs at the expense of oxidation of tetrahydrofolate to dihydrofolate, which is unusual in tetrahydrofolate-requiring reactions. (The mechanism of this reaction is shown in Fig. 22–53.) The dihydrofolate is reduced to tetrahydrofolate by **dihydrofolate reductase**—a regeneration that is essential for the many processes that require tetrahydrofolate. In plants and at least one protist, thymidylate synthase and dihydrofolate reductase reside on a single bifunctional protein.

About 10% of the human population (and up to 50% of people in impoverished communities) suffers from folic acid deficiency. When the deficiency is severe, the symptoms can include heart disease, cancer, and some types of brain dysfunction. At least some of these symptoms arise from a reduction of thymidylate synthesis, leading to an abnormal incorporation of uracil into DNA. Uracil is recognized by DNA repair pathways (described in Chapter 25) and is cleaved from the DNA. The presence of high levels of uracil in DNA leads to strand breaks that can greatly affect the function and regulation of nuclear DNA, ultimately causing the observed effects on the heart and brain, as well as increased mutagenesis that leads to cancer. ■

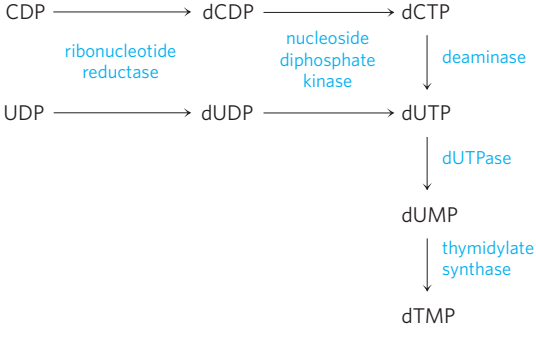

FIGURE 22–46 Biosynthesis of thymidylate (dTMP). The pathways are shown beginning with the reaction catalyzed by ribonucleotide reductase. Figure 22–47 gives details of the thymidylate synthase reaction.

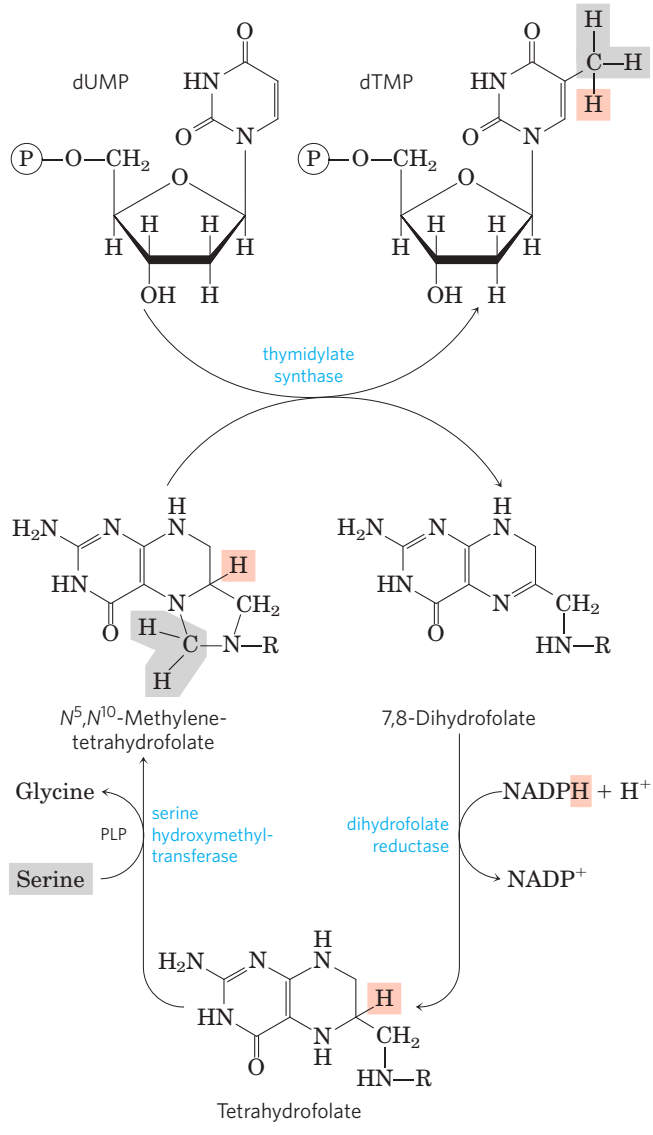

FIGURE 22–47 Conversion of dUMP to dTMP by thymidylate synthase and dihydrofolate reductase. Serine hydroxymethyltransferase is required for regeneration of the N^5,N^{10}-methylene form of tetrahydrofolate. In the synthesis of dTMP, all three hydrogens of the added methyl group are derived from N^5,N^{10}-methylenetetrahydrofolate (light red and gray).

Degradation of Purines and Pyrimidines Produces Uric Acid and Urea, Respectively

Purine nucleotides are degraded by a pathway in which they lose their phosphate through the action of **5′-nucleotidase (Fig. 22–48)**. Adenylate yields adenosine, which is deaminated to inosine by **adenosine deaminase**, and inosine is hydrolyzed to hypoxanthine (its purine base) and D-ribose. Hypoxanthine is

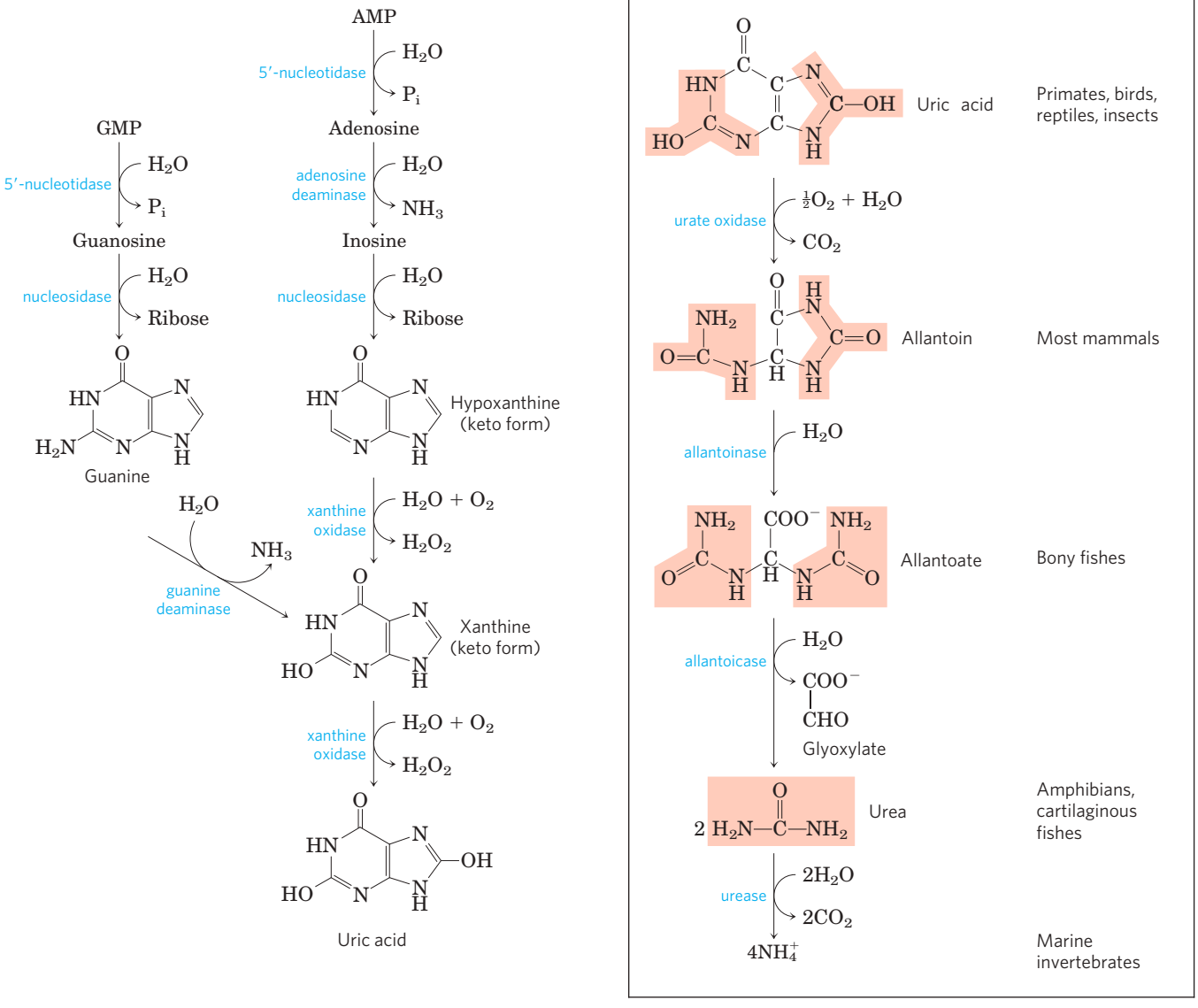

FIGURE 22–48 Catabolism of purine nucleotides. Note that primates excrete much more nitrogen as urea via the urea cycle (Chapter 18) than as uric acid from purine degradation. Similarly, fish excrete much more nitrogen as NH_4^+ than as urea produced by the pathway shown here.

oxidized successively to xanthine and then uric acid by **xanthine oxidase**, a flavoenzyme with an atom of molybdenum and four iron-sulfur centers in its prosthetic group. Molecular oxygen is the electron acceptor in this complex reaction.

GMP catabolism also yields uric acid as end product. GMP is first hydrolyzed to guanosine, which is then cleaved to free guanine. Guanine undergoes hydrolytic removal of its amino group to yield xanthine, which is converted to uric acid by xanthine oxidase (Fig. 22–48).

Uric acid is the excreted end product of purine catabolism in primates, birds, and some other animals. A healthy adult human excretes uric acid at a rate of about 0.6 g/24 h; the excreted product arises in part from ingested purines and in part from turnover of the purine nucleotides of nucleic acids. In most mammals and many other vertebrates, uric acid is further degraded to **allantoin** by the action of **urate oxidase**. In other organisms the pathway is further extended, as shown in Figure 22–48.

The pathways for degradation of pyrimidines generally lead to NH_4^+ production and thus to urea synthesis. Thymine, for example, is degraded to methylmalonylsemialdehyde **(Fig. 22–49)**, an intermediate of valine catabolism. It is further degraded through propionyl-CoA and methylmalonyl-CoA to succinyl-CoA (see Fig. 18–27).

Genetic aberrations in human purine metabolism have been found, some with serious consequences. For example, **adenosine deaminase (ADA) deficiency** leads to severe immunodeficiency disease in

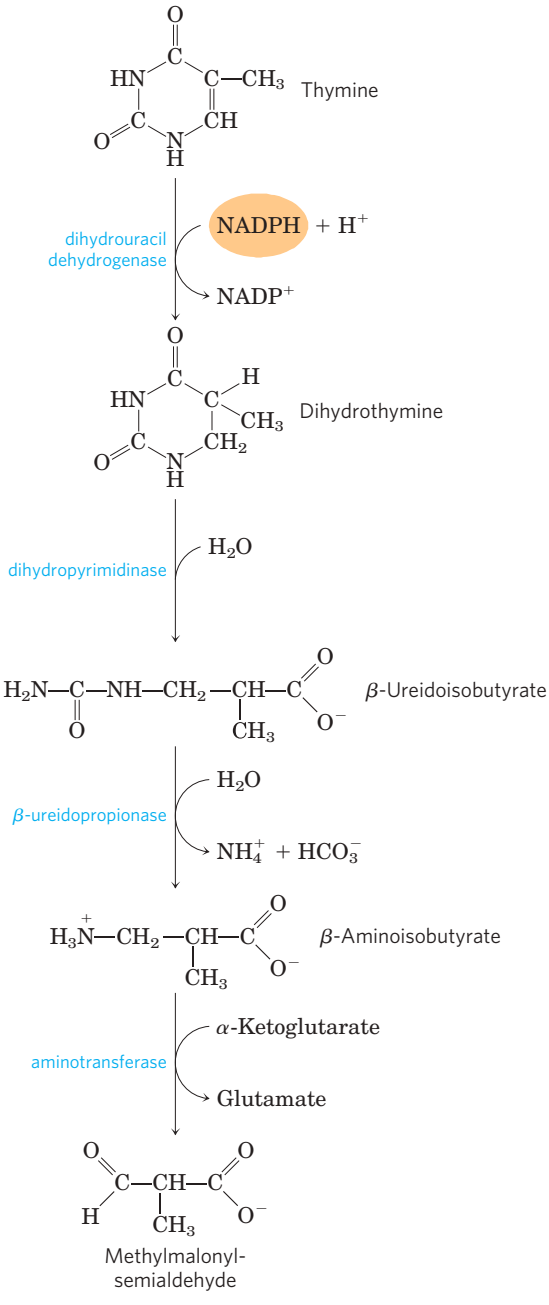

FIGURE 22–49 Catabolism of a pyrimidine. Shown here is the pathway for thymine. The methylmalonylsemialdehyde is further degraded to succinyl-CoA.

which T lymphocytes and B lymphocytes do not develop properly. Lack of ADA leads to a 100-fold increase in the cellular concentration of dATP, a strong inhibitor of ribonucleotide reductase (Fig. 22–44). High levels of dATP produce a general deficiency of other dNTPs in T lymphocytes. The basis for B-lymphocyte toxicity is less clear. Individuals with ADA deficiency lack an effective immune system and do not survive unless isolated in a sterile "bubble" environment. ADA deficiency was one of the first targets of human gene therapy trials (in 1990), which yielded mixed results. In more recent trials, some ADA-deficient individuals regained normal immune function after being given a functional gene for ADA. ■

Purine and Pyrimidine Bases Are Recycled by Salvage Pathways

Free purine and pyrimidine bases are constantly released in cells during the metabolic degradation of nucleotides. Free purines are in large part salvaged and reused to make nucleotides, in a pathway much simpler than the de novo synthesis of purine nucleotides described earlier. One of the primary salvage pathways consists of a single reaction catalyzed by **adenosine phosphoribosyltransferase**, in which free adenine reacts with PRPP to yield the corresponding adenine nucleotide:

$$\text{Adenine} + \text{PRPP} \longrightarrow \text{AMP} + \text{PP}_i$$

Free guanine and hypoxanthine (the deamination product of adenine; Fig. 22–48) are salvaged in the same way by **hypoxanthine-guanine phosphoribosyltransferase**. A similar salvage pathway exists for pyrimidine bases in microorganisms, and possibly in mammals.

A genetic lack of hypoxanthine-guanine phosphoribosyltransferase activity, seen almost exclusively in male children, results in a bizarre set of symptoms called **Lesch-Nyhan syndrome**. Children with this genetic disorder, which becomes manifest by the age of 2 years, are sometimes poorly coordinated and have intellectual deficits. In addition, they are extremely hostile and show compulsive self-destructive tendencies: they mutilate themselves by biting off their fingers, toes, and lips.

The devastating effects of Lesch-Nyhan syndrome illustrate the importance of the salvage pathways. Hypoxanthine and guanine arise constantly from the breakdown of nucleic acids. In the absence of hypoxanthine-guanine phosphoribosyltransferase, PRPP levels rise and purines are overproduced by the de novo pathway, resulting in high levels of uric acid production and goutlike damage to tissue (see below). The brain is especially dependent on the salvage pathways, and this may account for the central nervous system damage in children with Lesch-Nyhan syndrome. This syndrome is another potential target for gene therapy. ■

Excess Uric Acid Causes Gout

Long thought (erroneously) to be due to "high living," gout is a disease of the joints caused by an elevated concentration of uric acid in the blood and tissues. The joints become inflamed, painful, and arthritic, owing to the abnormal deposition of sodium urate crystals. The kidneys are also affected, as excess uric acid is deposited in the kidney tubules. Gout occurs predominantly in males. Its precise cause is not known, but it often involves an underexcretion of urate. A genetic deficiency of one or another enzyme of purine metabolism may also be a factor in some cases.

Gout is effectively treated by a combination of nutritional and drug therapies. Foods especially rich in nucleotides and nucleic acids, such as liver or glandular products, are withheld from the diet. Major alleviation

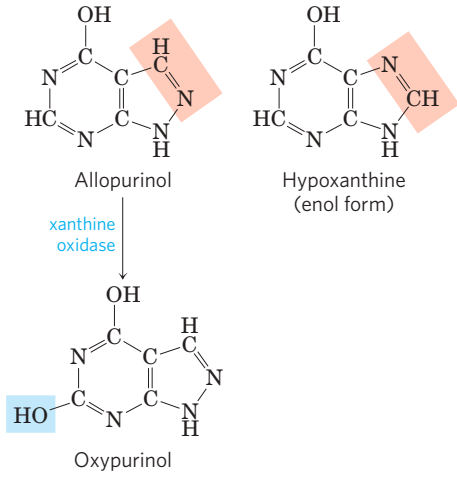

FIGURE 22–50 Allopurinol, an inhibitor of xanthine oxidase. Hypoxanthine is the normal substrate of xanthine oxidase. Only a slight alteration in the structure of hypoxanthine (shaded light red) yields the medically effective enzyme inhibitor allopurinol. At the active site, allopurinol is converted to oxypurinol, a strong competitive inhibitor that remains tightly bound to the reduced form of the enzyme.

of the symptoms is provided by the drug **allopurinol** **(Fig. 22–50)**, which inhibits xanthine oxidase, the enzyme that catalyzes the conversion of purines to uric acid. Allopurinol is a substrate of xanthine oxidase, which converts allopurinol to oxypurinol (alloxanthine). Oxypurinol inactivates the reduced form of the enzyme by remaining tightly bound in its active site. When xanthine oxidase is inhibited, the excreted products of purine metabolism are xanthine and hypoxanthine, which are more water-soluble than uric acid and less likely to form crystalline deposits. Allopurinol was developed by Gertrude Elion and George Hitchings, who also developed acyclovir, used in treating people with genital and oral herpes infections, and other purine analogs used in cancer chemotherapy. ■

Gertrude Elion, 1918–1999, and George Hitchings, 1905–1998

Many Chemotherapeutic Agents Target Enzymes in the Nucleotide Biosynthetic Pathways

The growth of cancer cells is not controlled in the same way as cell growth in most normal tissues. Cancer cells have greater requirements for nucleotides as precursors of DNA and RNA, and consequently are generally more sensitive than normal cells to inhibitors of nucleotide biosynthesis. A growing array of important chemotherapeutic agents—for cancer and other diseases—act by inhibiting one or more enzymes in these pathways. We describe here several well-studied examples that illustrate productive approaches to treatment and help us understand how these enzymes work.

The first set of agents includes compounds that inhibit glutamine amidotransferases. Recall that glutamine is a nitrogen donor in at least half a dozen separate reactions in nucleotide biosynthesis. The binding sites for glutamine and the mechanism by which NH_4^+ is extracted are quite similar in many of these enzymes. Most are strongly inhibited by glutamine analogs such as **azaserine** and **acivicin** **(Fig. 22–51)**. Azaserine, characterized by John Buchanan in the 1950s, was one of the first examples of a mechanism-based enzyme inactivator (suicide inactivator; p. 210 and Box 6–3). Acivicin shows promise as a cancer chemotherapeutic agent.

Other useful targets for pharmaceutical agents are thymidylate synthase and dihydrofolate reductase, enzymes that provide the only cellular pathway for thymine synthesis **(Fig. 22–52)**. One inhibitor that acts on thymidylate synthase, **fluorouracil**, is an important chemotherapeutic agent. Fluorouracil itself is not the enzyme inhibitor. In the cell, salvage pathways convert it to the deoxynucleoside monophosphate FdUMP, which binds to and inactivates the enzyme. Inhibition by FdUMP **(Fig. 22–53)** is a classic example of mechanism-based enzyme inactivation. Another prominent chemotherapeutic agent, **methotrexate**, is an inhibitor of dihydrofolate reductase.

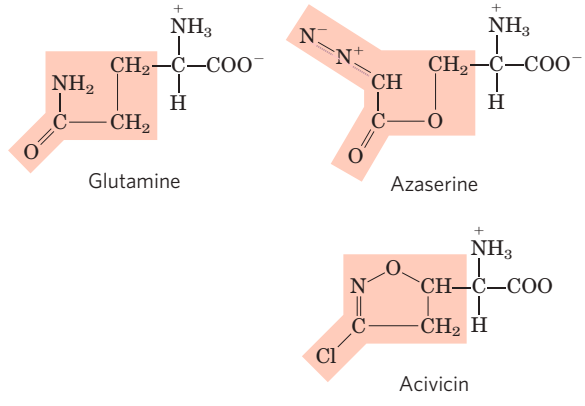

FIGURE 22–51 Azaserine and acivicin, inhibitors of glutamine amidotransferases. These analogs of glutamine interfere in several amino acid and nucleotide biosynthetic pathways.

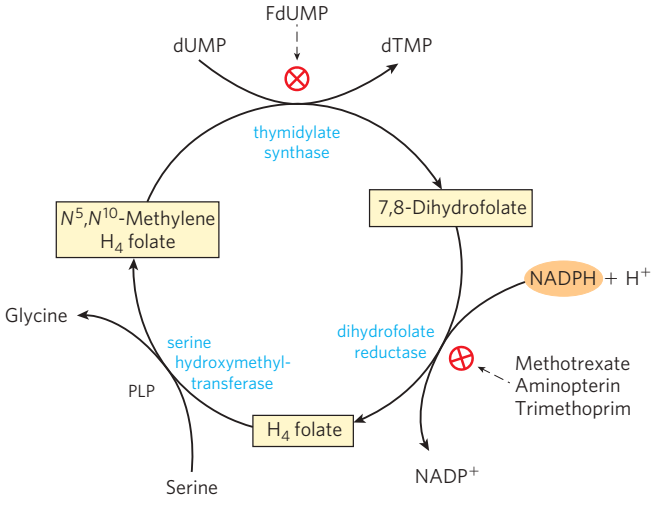

(a)

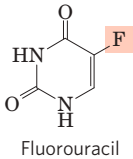

Fluorouracil

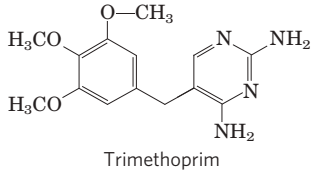

Trimethoprim

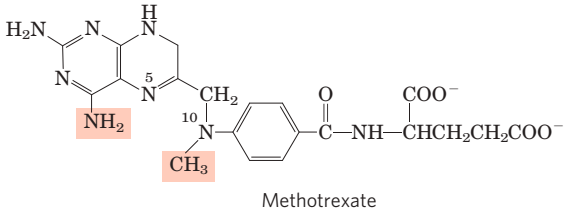

Methotrexate

(b)

FIGURE 22–52 Thymidylate synthesis and folate metabolism as targets of chemotherapy. (a) During thymidylate synthesis, N^5,N^{10}-methylenetetrahydrofolate is converted to 7,8-dihydrofolate; the N^5,N^{10}-methylenetetrahydrofolate is regenerated in two steps (see Fig. 22-47). This cycle is a major target of several chemotherapeutic agents. **(b)** Fluorouracil and methotrexate are important chemotherapeutic agents. In cells, fluorouracil is converted to FdUMP, which inhibits thymidylate synthase. Methotrexate, a structural analog of tetrahydrofolate, inhibits dihydrofolate reductase; the shaded amino and methyl groups replace a carbonyl oxygen and a proton, respectively, in folate (see Fig. 22-47). Another important folate analog, aminopterin, is identical to methotrexate except that it lacks the shaded methyl group. Trimethoprim, a tight-binding inhibitor of bacterial dihydrofolate reductase, was developed as an antibiotic.

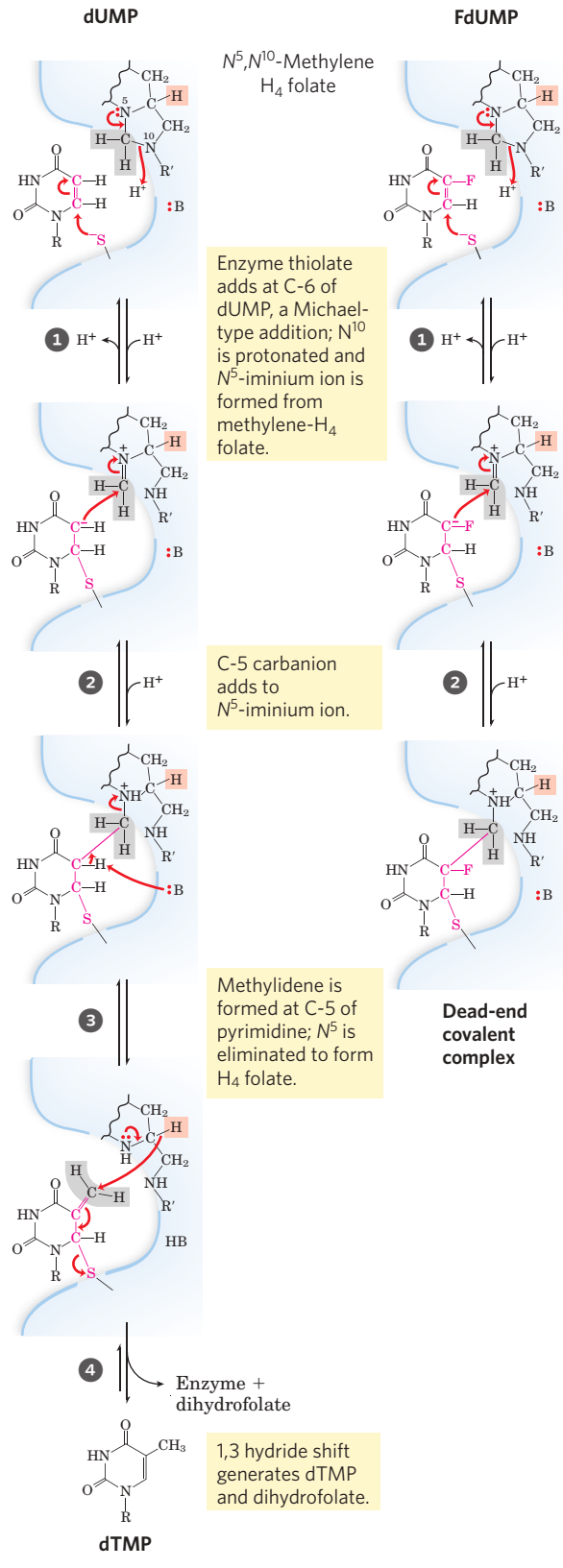

MECHANISM FIGURE 22–53 Conversion of dUMP to dTMP and its inhibition by FdUMP. The left side is the normal reaction mechanism of thymidylate synthase. The nucleophilic sulfhydryl group contributed by the enzyme in ❶ and the ring atoms of dUMP taking part in the reaction are shown in red; :B denotes an amino acid side chain that acts as a base to abstract a proton after step ❸. The hydrogens derived from the methylene group of N^5,N^{10}-methylenetetrahydrofolate are shaded in gray. The 1,3 hydride shift (step ❹), moves a hydride ion (shaded light red) from C-6 of H_4 folate to the methyl group of thymidine, resulting in the oxidation of tetrahydrofolate to dihydrofolate. This hydride shift is blocked when FdUMP is the substrate (right). Steps ❶ and ❷ proceed normally, but result in a stable complex—consisting of FdUMP linked covalently to the enzyme and to tetrahydrofolate—that inactivates the enzyme. Thymidylate Synthase Mechanism

This folate analog acts as a competitive inhibitor; the enzyme binds methotrexate with about 100 times higher affinity than dihydrofolate. **Aminopterin** is a related compound that acts similarly.

The medical potential of inhibitors of nucleotide biosynthesis is not limited to cancer treatment. All fast-growing cells (including bacteria and protists) are potential targets. **Trimethoprim**, an antibiotic developed by Hitchings and Elion, binds to bacterial dihydrofolate reductase nearly 100,000 times better than to the mammalian enzyme. It is used to treat certain urinary and middle-ear bacterial infections. Parasitic protists, such as the trypanosomes that cause African sleeping sickness (African trypanosomiasis), lack pathways for de novo nucleotide biosynthesis and are particularly sensitive to agents that interfere with their scavenging of nucleotides from the surrounding environment using salvage pathways. Allopurinol (Fig. 22–50) and several similar purine analogs have shown promise for the treatment of African trypanosomiasis and related afflictions. See Box 6–3 for another approach to combating African trypanosomiasis, made possible by advances in our understanding of metabolism and enzyme mechanisms. ■

SUMMARY 22.4 Biosynthesis and Degradation of Nucleotides

- The purine ring system is built up step-by-step beginning with 5-phosphoribosylamine. The amino acids glutamine, glycine, and aspartate furnish all the nitrogen atoms of purines. Two ring-closure steps form the purine nucleus.
- Pyrimidines are synthesized from carbamoyl phosphate and aspartate, and ribose 5-phosphate is then attached to yield the pyrimidine ribonucleotides.
- Nucleoside monophosphates are converted to their triphosphates by enzymatic phosphorylation reactions. Ribonucleotides are converted to deoxyribonucleotides by ribonucleotide reductase, an enzyme with novel mechanistic and regulatory characteristics. The thymine nucleotides are derived from dCDP and dUMP.
- Uric acid and urea are the end products of purine and pyrimidine degradation.
- Free purines can be salvaged and rebuilt into nucleotides. Genetic deficiencies in certain salvage enzymes cause serious disorders such as Lesch-Nyhan syndrome and ADA deficiency.
- Accumulation of uric acid crystals in the joints, possibly caused by another genetic deficiency, results in gout.
- Enzymes of the nucleotide biosynthetic pathways are targets for an array of chemotherapeutic agents used to treat cancer and other diseases.

Key Terms

Terms in bold are defined in the glossary.

nitrogen cycle 882
nitrogen fixation 882
anammox 882
symbionts 882
nitrogenase complex 883
P cluster 883
FeMo cofactor 883
leghemoglobin 888
glutamine synthetase 888
glutamate synthase 888
glutamine amidotransferases 890
5-phosphoribosyl-1-pyrophosphate (PRPP) 892
tryptophan synthase 898
porphyrin 902
porphyria 904
bilirubin 904
phosphocreatine 906
creatine 906
glutathione (GSH) 906
auxin 908
dopamine 909
norepinephrine 909
epinephrine 909
γ-aminobutyrate (GABA) 909
serotonin 909
histamine 909
cimetidine 909
spermine 909
spermidine 909
ornithine decarboxylase 909
de novo pathway 910
salvage pathway 910
inosinate (IMP) 912
carbamoyl phosphate synthetase II 915
aspartate transcarbamoylase 915
nucleoside monophosphate kinase 916
nucleoside diphosphate kinase 916
ribonucleotide reductase 917
thioredoxin 917
thymidylate synthase 920
dihydrofolate reductase 920
adenosine deaminase (ADA) deficiency 921
Lesch-Nyhan syndrome 922
allopurinol 923
azaserine 923
acivicin 923
fluorouracil 923
methotrexate 923
aminopterin 925

Further Reading

Nitrogen Fixation

Arp, D.J. & Stein, L.Y. (2003) Metabolism of inorganic N compounds by ammonia-oxidizing bacteria. *Crit. Rev. Biochem. Mol. Biol.* **38**, 491–495.

Burris, R.H. (1995) Breaking the N–N bond. *Annu. Rev. Plant Physiol. Plant Mol. Biol.* **46**, 1–19.

Eisenberg, D.S., Harindarpal, S., Gill, G., Pfluegl, M.U., & Rothstein, H. (2000) Structure-function relationships of glutamine synthetases. *Biochim. Biophys. Acta* **1477**, 122–145.

Fuerst, J.A. (2005) Intracellular compartmentation in planctomycetes. *Annu. Rev. Microbiol.* **59**, 299–328.
Advanced discussion of the structure and biochemistry of anammox.

Igarishi, R.Y. & Seefeldt, L.C. (2003) Nitrogen fixation: the mechanism of the Mo-dependent nitrogenase. *Crit. Rev. Biochem. Mol. Biol.* **38**, 351–384.

Lin, J.T. & Stewart, V. (1998) Nitrate assimilation in bacteria. *Adv. Microbiol. Physiol.* **39**, 1–30.

Patriarca, E.J., Tate, R., & Iaccarino, M. (2002) Key role of bacterial NH_4^+ metabolism in rhizobium-plant symbiosis. *Microbiol. Mol. Biol. Rev.* **66**, 203–222.

A good overview of ammonia assimilation in bacterial systems and its regulation.

Prell, J. & Poole, P. (2006) Metabolic changes of rhizobia in legume nodules. *Trends Microbiol.* **14**, 161–168.

A good summary of the intricate symbiotic relationship between rhizobial bacteria and their hosts.

Reese, D.C. & Howard, J.B. (2000) Nitrogenase: standing at the crossroads. *Curr. Opin. Chem. Biol.* **4**, 559–566.

Schwarz, G., Mendel, R.R., & Ribbe, M.W. (2009) Molybdenum cofactors, enzymes and pathways. *Nature* **460**, 839–847.

Seefeldt, L.C., Hoffman, B.M., & Dean, D.R. (2009) Mechanism of Mo-dependent nitrogenase. *Annu. Rev. Biochem.* **78**, 701–722.

Sinha, S.C. & Smith, J.L. (2001) The PRT protein family. *Curr. Opin. Struct. Biol.* **11**, 733–739.

Description of a protein family that includes many amidotransferases, with channels for the movement of NH_3 from one active site to another.

Amino Acid Biosynthesis

Frey, P.A. & Hegeman, A.D. (2007) *Enzymatic Reaction Mechanisms*, Oxford University Press, New York.

An updated summary of reaction mechanisms, including one-carbon metabolism and pyridoxal phosphate enzymes.

Neidhardt, F.C. (ed.). (1996) Escherichia coli *and* Salmonella: *Cellular and Molecular Biology*, 2nd edn, ASM Press, Washington, DC.

Volume 1 of this two-volume set has 13 chapters devoted to detailed descriptions of amino acid and nucleotide biosynthesis in bacteria. The Web-based version at www.ecosal.org is updated regularly. A valuable resource.

Pan P., Woehl, E., & Dunn, M.F. (1997) Protein architecture, dynamics and allostery in tryptophan synthase channeling. *Trends Biochem. Sci.* **22**, 22–27.

Richards, N.G.J. & Kilberg, M.S. (2006) Asparagine synthetase chemotherapy. *Annu. Rev. Biochem.* **75**, 629–654.

Stadtman, E.R. (2001) The story of glutamine synthetase regulation. *J. Biol. Chem.* **276**, 44,357–44,364.

Compounds Derived from Amino Acids

Ajioka R.S., Phillips, J.D., & Kushner, J.P. (2006) Biosynthesis of heme in mammals. *Biochim. Biophys. Acta Mol. Cell Res.* **1763**, 723–736.

Bredt, D.S. & Snyder, S.H. (1994) Nitric oxide: a physiologic messenger molecule. *Annu. Rev. Biochem.* **63**, 175–195.

Meister, A. & Anderson, M.E. (1983) Glutathione. *Annu. Rev. Biochem.* **52**, 711–760.

Morse, D. & Choi, A.M.K. (2002) Heme oxygenase-1—the "emerging molecule" has arrived. *Am. J. Respir. Cell Mol. Biol.* **27**, 8–16.

Rondon, M.R., Trzebiatowski, J.R., & Escalante-Semerena, J.C. (1997) Biochemistry and molecular genetics of cobalamin biosynthesis. *Prog. Nucleic Acid Res. Mol. Biol.* **56**, 347–384.

Stadtman, T.C. (1996) Selenocysteine. *Annu. Rev. Biochem.* **65**, 83–100.

Nucleotide Biosynthesis

Aiuti, A., Cattaneo, R., Galimberti, S., Benninghoff, U., Cassani, B., Callegaro, L., Scaramuzza, S., Andolfi, G., Mirolo, M., Brigida, I., et al. (2009) Gene therapy for immunodeficiency due to adenosine deaminase deficiency. *N. Engl. J. Med.* **360**, 447–458.

Ando, N., Brignole, E.J., Zimanyi, C.M., Funk, M.A., Yokoyama, K., Asturias, F.J., Stubbe, J., & Drennan, C.L. (2011) Structural interconversions modulate activity of *Escherichia coli,* ribonucleotide reductase. *Proc. Natl. Acad. Sci. USA* **108**, 21,046–21,051.

Carreras, C.W. & Santi, D.V. (1995) The catalytic mechanism and structure of thymidylate synthase. *Annu. Rev. Biochem.* **64**, 721–762.

Cotruvo, J.A., Jr. & Stubbe, J. (2011) Class I ribonucleotide reductases: metallocofactor assembly and repair in vitro and in vivo. *Annu. Rev. Biochem.* **80**, 733–767.

Fairman, J.W., Wijerathna, S.R., Ahmad, M.F., Xu, H., Nakano, R., Jha, S., Prendergast, J., Welin, M., Flodin, S., Roos, A., et al. (2011) Structural basis for allosteric regulation of human ribonucleotide reductase by nucleotide-induced oligomerization. *Nat. Struct. Mol. Biol.* **18**, 316–322.

Herrick, J. & Sclavi, B. (2007) Ribonucleotide reductase and the regulation of DNA replication: an old story and an ancient heritage. *Mol. Microbiol.* **63**, 22–34.

Holmgren, A. (1989) Thioredoxin and glutaredoxin systems. *J. Biol. Chem.* **264**, 13,963–13,966.

Kappock, T.J., Ealick, S.E., & Stubbe, J. (2000) Modular evolution of the purine biosynthetic pathway. *Curr. Opin. Chem. Biol.* **4**, 567–572.

Kornberg, A. & Baker, T.A. (1991) *DNA Replication*, 2nd edn, W. H. Freeman and Company, New York.

This text includes a good summary of nucleotide biosynthesis.

Licht, S., Gerfen, G.J., & Stubbe, J. (1996) Thiyl radicals in ribonucleotide reductases. *Science* **271**, 477–481.

Nordlund, P. & Reichard, P. (2006) Ribonucleotide reductases. *Annu. Rev. Biochem.* **75**, 681–706.

Schachman, H.K. (2000) Still looking for the ivory tower. *Annu. Rev. Biochem.* **69**, 1–29.

A lively description of research on aspartate transcarbamoylase, accompanied by delightful tales of science and politics.

Weeks, A., Lund, L., & Raushel, F.M. (2006) Tunneling of intermediates in enzyme-catalyzed reactions. *Curr. Opin. Chem. Biol.* **10**, 465–472.

Genetic Diseases

Löffler, M., Fairbanks, L.D., Zameitat, E., Marinaki, A.M., & Simmonds, H.A. (2005) Pyrimidine pathways in health and disease. *Trends Mol. Med.* **11**, 430-437.

Valle, D., Beaudet, A.L., Vogelstein, B., Kinzler, K.W., Antonarakis, S.E., & Ballabio, A. (eds). *Scriver's Online Metabolic and Molecular Bases of Inherited Disease*, www.ommbid.com. Published January 2006. Updated March 28, 2011.

This classic medical encyclopedia, last published in print in 2001 as a four-volume set, is now maintained online. It has good chapters on disorders of amino acid, porphyrin, and heme metabolism. See also the chapters on inborn errors of purine and pyrimidine metabolism.

Problems

1. ATP Consumption by Root Nodules in Legumes Bacteria residing in the root nodules of the pea plant consume more than 20% of the ATP produced by the plant. Suggest why these bacteria consume so much ATP.

2. Glutamate Dehydrogenase and Protein Synthesis The bacterium *Methylophilus methylotrophus* can synthesize protein from methanol and ammonia. Recombinant DNA techniques have improved the yield of protein by introducing into *M. methylotrophus* the glutamate dehydrogenase gene from *E. coli.* Why does this genetic manipulation increase the protein yield?

3. PLP Reaction Mechanisms Pyridoxal phosphate can help catalyze transformations one or two carbons removed

from the α carbon of an amino acid. The enzyme threonine synthase (see Fig. 22–17) promotes the PLP-dependent conversion of phosphohomoserine to threonine. Suggest a mechanism for this reaction.

4. Transformation of Aspartate to Asparagine There are two routes for transforming aspartate to asparagine at the expense of ATP. Many bacteria have an asparagine synthetase that uses ammonium ion as the nitrogen donor. Mammals have an asparagine synthetase that uses glutamine as the nitrogen donor. Given that the latter requires an extra ATP (for the synthesis of glutamine), why do mammals use this route?

5. Equation for the Synthesis of Aspartate from Glucose Write the net equation for the synthesis of aspartate (a nonessential amino acid) from glucose, carbon dioxide, and ammonia.

6. Asparagine Synthetase Inhibitors in Leukemia Therapy Mammalian asparagine synthetase is a glutamine-dependent amidotransferase. Efforts to identify an effective inhibitor of human asparagine synthetase for use in chemotherapy for patients with leukemia has focused not on the amino-terminal glutaminase domain but on the carboxyl-terminal synthetase active site. Explain why the glutaminase domain is not a promising target for a useful drug.

7. Phenylalanine Hydroxylase Deficiency and Diet Tyrosine is normally a nonessential amino acid, but individuals with a genetic defect in phenylalanine hydroxylase require tyrosine in their diet for normal growth. Explain.

8. Cofactors for One-Carbon Transfer Reactions Most one-carbon transfers are promoted by one of three cofactors: biotin, tetrahydrofolate, or *S*-adenosylmethionine (Chapter 18). *S*-Adenosylmethionine is generally used as a methyl group donor; the transfer potential of the methyl group in N^5-methyltetrahydrofolate is insufficient for most biosynthetic reactions. However, one example of the use of N^5-methyltetrahydrofolate in methyl group transfer is in methionine formation by the methionine synthase reaction (step ❾ of Fig. 22–17); methionine is the immediate precursor of *S*-adenosylmethionine (see Fig. 18–18). Explain how the methyl group of *S*-adenosylmethionine can be derived from N^5-methyltetrahydrofolate, even though the transfer potential of the methyl group in N^5-methyltetrahydrofolate is one-thousandth of that in *S*-adenosylmethionine.

9. Concerted Regulation in Amino Acid Biosynthesis The glutamine synthetase of *E. coli* is independently modulated by various products of glutamine metabolism (see Fig. 22–8). In this concerted inhibition, the extent of enzyme inhibition is greater than the sum of the separate inhibitions caused by each product. For *E. coli* grown in a medium rich in histidine, what would be the advantage of concerted inhibition?

10. Relationship between Folic Acid Deficiency and Anemia Folic acid deficiency, believed to be the most common vitamin deficiency, causes a type of anemia in which hemoglobin synthesis is impaired and erythrocytes do not mature properly. What is the metabolic relationship between hemoglobin synthesis and folic acid deficiency?

11. Nucleotide Biosynthesis in Amino Acid Auxotrophic Bacteria Wild-type *E. coli* cells can synthesize all 20 common amino acids, but some mutants, called amino acid auxotrophs, are unable to synthesize a specific amino acid and require its addition to the culture medium for optimal growth. Besides their role in protein synthesis, some amino acids are also precursors for other nitrogenous cell products. Consider the three amino acid auxotrophs that are unable to synthesize glycine, glutamine, and aspartate, respectively. For each mutant, what nitrogenous products other than proteins would the cell fail to synthesize?

12. Inhibitors of Nucleotide Biosynthesis Suggest mechanisms for the inhibition of (a) alanine racemase by L-fluoroalanine and (b) glutamine amidotransferases by azaserine.

13. Mode of Action of Sulfa Drugs Some bacteria require *p*-aminobenzoate in the culture medium for normal growth, and their growth is severely inhibited by the addition of sulfanilamide, one of the earliest sulfa drugs. Moreover, in the presence of this drug, 5-aminoimidazole-4-carboxamide ribonucleotide (AICAR; see Fig. 22–35) accumulates in the culture medium. These effects are reversed by addition of excess *p*-aminobenzoate.

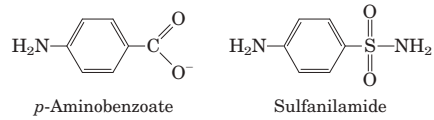

p-Aminobenzoate Sulfanilamide

(a) What is the role of *p*-aminobenzoate in these bacteria? (Hint: See Fig. 18–16.)

(b) Why does AICAR accumulate in the presence of sulfanilamide?

(c) Why are the inhibition and accumulation reversed by addition of excess *p*-aminobenzoate?

14. Pathway of Carbon in Pyrimidine Biosynthesis Predict the locations of ^{14}C in orotate isolated from cells grown on a small amount of uniformly labeled [^{14}C]succinate. Justify your prediction.

15. Nucleotides as Poor Sources of Energy Under starvation conditions, organisms can use proteins and amino acids as sources of energy. Deamination of amino acids produces carbon skeletons that can enter the glycolytic pathway and the citric acid cycle to produce energy in the form of ATP. Nucleotides, on the other hand, are not similarly degraded for use as energy-yielding fuels. What observations about cellular physiology support this statement? What aspect of the structure of nucleotides makes them a relatively poor source of energy?

16. Treatment of Gout Allopurinol (see Fig. 22–50), an inhibitor of xanthine oxidase, is used to treat chronic gout. Explain the biochemical basis for this treatment. Patients treated with allopurinol sometimes develop xanthine stones in the kidneys, although the incidence of kidney damage is much lower than in untreated gout. Explain this observation in the light of the following solubilities in urine: uric acid, 0.15 g/L; xanthine, 0.05 g/L; and hypoxanthine, 1.4 g/L.

17. Inhibition of Nucleotide Synthesis by Azaserine The diazo compound *O*-(2-diazoacetyl)-L-serine, known also as azaserine (see Fig. 22–51), is a powerful inhibitor of glutamine amidotransferases. If growing cells are treated with azaserine, what intermediates of nucleotide biosynthesis will accumulate? Explain.

Data Analysis Problem

18. Use of Modern Molecular Techniques to Determine the Synthetic Pathway of a Novel Amino Acid Most of the biosynthetic pathways described in this chapter were determined before the development of recombinant DNA technology and genomics, so the techniques were quite different from those that researchers would use today. Here we explore an example of the use of modern molecular techniques to investigate the pathway of synthesis of a novel amino acid, (2*S*)-4-amino-2-hydroxybutyrate (AHBA). The techniques mentioned here are described in various places in the book; this problem is designed to show how they can be integrated in a comprehensive study.

AHBA is a γ-amino acid that is a component of some aminoglycoside antibiotics, including the antibiotic butirosin. Antibiotics modified by the addition of an AHBA residue are often more resistant to inactivation by bacterial antibiotic-resistance enzymes. As a result, understanding how AHBA is synthesized and added to antibiotics is useful in the design of pharmaceuticals.

In an article published in 2005, Li and coworkers describe how they determined the synthetic pathway of AHBA from glutamate.

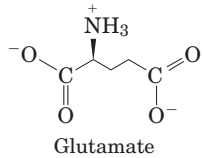

Glutamate

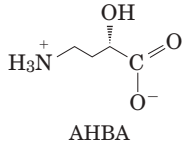

AHBA

(a) Briefly describe the chemical transformations needed to convert glutamate to AHBA. At this point, don't be concerned about the *order* of the reactions.

Li and colleagues began by cloning the butirosin biosynthetic gene cluster from the bacterium *Bacillus circulans*, which makes large quantities of butirosin. They identified five genes that are essential for the pathway: *btrI*, *btrJ*, *btrK*, *btrO*, and *btrV*. They cloned these genes into *E. coli* plasmids that allow overexpression of the genes, producing proteins with "histidine tags" fused to their amino termini to facilitate purification (see Section 9.1).

The predicted amino acid sequence of the BtrI protein showed strong homology to known acyl carrier proteins (see Fig. 21–5). Using mass spectrometry, Li and colleagues found a molecular mass of 11,812 for the purified BtrI protein (including the His tag). When the purified BtrI was incubated with coenzyme A and an enzyme known to attach CoA to other acyl carrier proteins, the majority molecular species had an M_r of 12,153.

(b) How would you use these data to argue that BtrI can function as an acyl carrier protein with a CoA prosthetic group?

Using standard terminology, Li and coauthors called the form of the protein lacking CoA apo-BtrI and the form with CoA (linked as in Fig. 21–5) holo-BtrI. When holo-BtrI was incubated with glutamine, ATP, and purified BtrJ protein, the holo-BtrI species of M_r 12,153 was replaced with a species of M_r 12,281, corresponding to the thioester of glutamate and holo-BtrI. Based on these data, the authors proposed the following structure for the M_r 12,281 species (γ-glutamyl-*S*-BtrI):

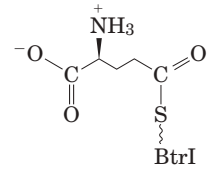

γ-Glutamyl-*S*-BtrI

(c) What other structure(s) is (are) consistent with the data above?

(d) Li and coauthors argued that the structure shown here (γ-glutamyl-*S*-BtrI) is likely to be correct because the α-carboxyl group must be removed at some point in the synthetic process. Explain the chemical basis of this argument. (Hint: See Fig. 18–6, reaction C.)

The BtrK protein showed significant homology to PLP-dependent amino acid decarboxylases, and BtrK isolated from *E. coli* was found to contain tightly bound PLP. When γ-glutamyl-*S*-BtrI was incubated with purified BtrK, a molecular species of M_r 12,240 was produced.

(e) What is the most likely structure of this species?

(f) Interestingly, when the investigators incubated glutamate and ATP with purified BtrI, BtrJ, and BtrK, they found a molecular species of M_r 12,370. What is the most likely structure of this species? Hint: Remember that BtrJ can use ATP to γ-glutamylate nucleophilic groups.

Li and colleagues found that BtrO is homologous to monooxygenase enzymes (see Box 21–1) that hydroxylate alkanes, using FMN as a cofactor, and BtrV is homologous to an NAD(P)H oxidoreductase. Two other genes in the cluster, *btrG* and *btrH*, probably encode enzymes that remove the γ-glutamyl group and attach AHBA to the target antibiotic molecule.

(g) Based on these data, propose a plausible pathway for the synthesis of AHBA and its addition to the target antibiotic. Include the enzymes that catalyze each step and any other substrates or cofactors needed (ATP, NAD, etc.).

Reference

Li, Y., Llewellyn, N.M., Giri, R., Huang, F., & Spencer, J.B. (2005) Biosynthesis of the unique amino acid side chain of butirosin: possible protective-group chemistry in an acyl carrier protein–mediated pathway. *Chem. Biol.* **12**, 665–675.

23

Hormonal Regulation and Integration of Mammalian Metabolism

In Chapters 13 through 22 we have discussed metabolism at the level of the individual cell, emphasizing central pathways common to almost all cells—bacterial, archaeal, and eukaryotic. We have seen how metabolic processes within cells are regulated at the level of individual enzyme reactions by substrate availability, by allosteric mechanisms, and by phosphorylation or other covalent modifications of enzymes.

To appreciate fully the significance of individual metabolic pathways and their regulation, we must view these pathways in the context of the whole organism. An essential characteristic of multicellular organisms is cell differentiation and division of labor. The specialized functions of the tissues and organs of complex organisms such as humans impose characteristic fuel requirements and patterns of metabolism. Hormonal signals integrate and coordinate the metabolic activities of different tissues and optimize the allocation of fuels and precursors to each organ.

In this chapter we focus on mammals, looking at the specialized metabolism of several major organs and tissues and the integration of metabolism in the whole organism. We begin by examining the broad range of hormones and hormonal mechanisms, then turn to the tissue-specific functions regulated by these mechanisms. We discuss the distribution of nutrients to various organs—emphasizing the central role played by the liver—and the metabolic cooperation among these organs. To illustrate the integrative role of hormones, we describe the interplay of insulin, glucagon, and epinephrine in coordinating fuel metabolism in muscle, liver, and adipose tissue. The metabolic disturbances in diabetes further illustrate the importance of hormonal regulation of metabolism. We discuss the long-term hormonal regulation of body mass and, finally, the role of obesity in development of the metabolic syndrome and diabetes.

23.1 Hormones: Diverse Structures for Diverse Functions

Hormones are small molecules or proteins that are produced in one tissue, released into the circulation, and carried to other tissues, where they act through receptors to bring about changes in cellular activities. They serve to coordinate the metabolic activities of several tissues or organs. Virtually every process in a complex organism is regulated by one or more hormones: maintenance of blood pressure, blood volume, and electrolyte balance; embryogenesis; sexual differentiation, development, and reproduction; hunger, eating behavior, digestion, and fuel allocation—to name but a few. We examine here the methods for detecting and measuring hormones and their interaction with receptors, and we consider a representative selection of hormone types.

The coordination of metabolism in mammals is achieved by the **neuroendocrine system**. Individual cells in one tissue sense a change in the organism's circumstances and respond by secreting a chemical messenger that passes to another cell in the same or different tissue, where the messenger binds to a receptor molecule and triggers a change in this second cell. These chemical messengers may relay information over very short or very long distances. In neuronal signaling **(Fig. 23–1a)**, the chemical messenger is a neurotransmitter (acetylcholine, for example) and may travel only a fraction of a micrometer, across the synaptic cleft to the next neuron in a network. In hormonal signaling, the messengers—hormones—are carried in the bloodstream to neighboring cells or to distant organs and tissues; they may travel a meter or more before encountering their target cell (Fig. 23–1b). Except for this anatomic difference, these two chemical signaling mechanisms are remarkably similar, and the same molecule can sometimes act as both neurotransmitter and hormone. Epinephrine and norepinephrine, for example, serve as neurotransmitters at certain synapses of the brain and neuromuscular junctions of smooth muscle and as hormones that regulate fuel metabolism in liver and muscle. The following discussion of cellular signaling emphasizes hormone action, drawing on discussions of fuel metabolism in earlier chapters, but most of the fundamental mechanisms described here also occur in neurotransmitter action.

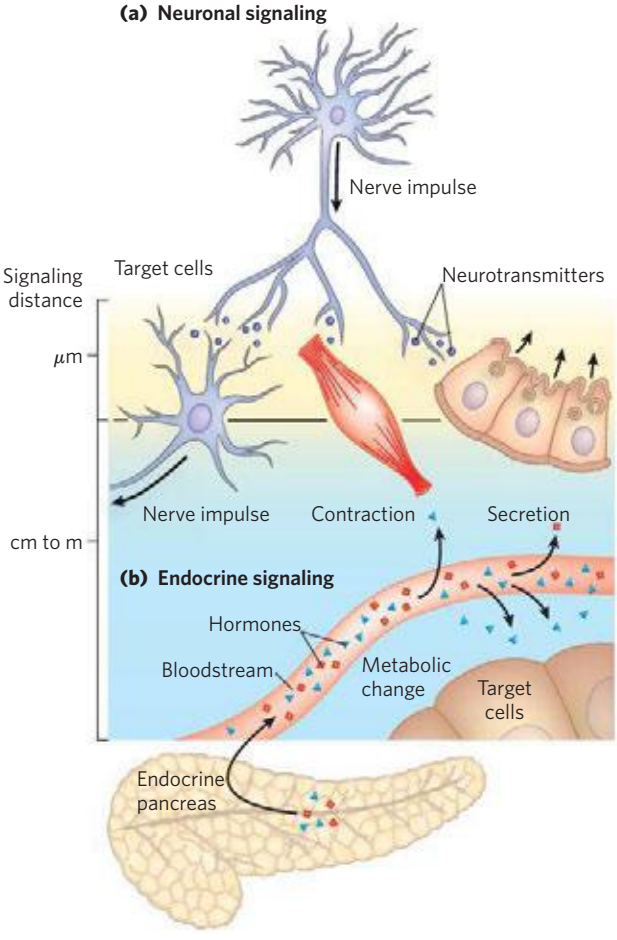

FIGURE 23–1 Signaling by the neuroendocrine system. (a) In neuronal signaling, electrical signals (nerve impulses) originate in the cell body of a neuron and travel very rapidly over long distances to the axon tip, where neurotransmitters are released and diffuse to the target cell. The target cell (another neuron, a myocyte, or a secretory cell) is only a fraction of a micrometer or a few micrometers away from the site of neurotransmitter release. **(b)** In endocrine signaling, hormones (such as insulin produced in pancreatic β cells) are secreted into the bloodstream, which carries them throughout the body to target tissues that may be a meter or more away from the secreting cell. Both neurotransmitters and hormones interact with specific receptors on or in their target cells, triggering responses.

The Detection and Purification of Hormones Requires a Bioassay

How is a hormone detected and isolated? First, researchers find that a physiological process in one tissue depends on a signal that originates in another tissue. Insulin, for example, was first recognized as a substance that is produced in the pancreas and affects the concentration of glucose in blood and urine (Box 23–1). Once a physiological effect of the putative hormone is discovered, a quantitative bioassay for the hormone can be developed. In the case of insulin, the assay consisted of injecting extracts of pancreas (a crude source of insulin) into experimental animals deficient in insulin, then quantifying the resulting changes in glucose concentration in blood and urine. To isolate a hormone, the biochemist fractionates extracts containing the putative hormone, with the same techniques used to purify other biomolecules (solvent fractionation, chromatography, and electrophoresis), and then assays each fraction for hormone activity. Once the chemical has been purified, its composition and structure can be determined.

This protocol for hormone characterization is deceptively simple. Hormones are extremely potent and are produced in very small amounts. Obtaining sufficient hormone to allow its chemical characterization often involves biochemical isolations on a heroic scale. When Andrew Schally and Roger Guillemin independently purified and characterized thyrotropin-releasing hormone (TRH) from the hypothalamus, Schally's group processed about 20 tons of hypothalamus from nearly two million sheep, and Guillemin's group extracted the hypothalamus from about a million pigs! TRH proved to be a simple derivative of the tripeptide Glu–His–Pro **(Fig. 23–2)**. Once the structure of the hormone was known, it could be chemically synthesized in large quantities for use in physiological and biochemical studies. For their work on hypothalamic hormones, Schally and Guillemin shared the Nobel Prize in Physiology or Medicine in 1977, along with Rosalyn Yalow, who (with Solomon A. Berson) developed the extraordinarily sensitive **radioimmunoassay (RIA)** for peptide hormones and used it to study hormone action. RIA revolutionized hormone research by making possible the rapid, quantitative, and specific measurement of hormones in minute amounts.

BOX 23–1 MEDICINE How Is a Hormone Discovered? The Arduous Path to Purified Insulin

Millions of people with type 1 diabetes mellitus inject themselves daily with pure insulin to compensate for the lack of production of this critical hormone by their own pancreatic β cells. Insulin injection is not a cure for diabetes, but it allows people who otherwise would have died young to lead long and productive lives. The discovery of insulin, which began with an accidental observation, illustrates the combination of serendipity and careful experimentation that led to the discovery of many of the hormones.

In 1889, Oskar Minkowski, a young assistant at the Medical College of Strasbourg, and Josef von Mering, at the Hoppe-Seyler Institute in Strasbourg, had a friendly disagreement about whether the pancreas, known to contain lipases, was important in fat digestion in dogs. To resolve the issue, they began an experiment on the digestion of fats. They surgically removed the pancreas from a dog, but before their experiment got any farther, Minkowski noticed that the dog was now producing far more urine than normal (a common symptom of untreated diabetes). Also, the dog's urine had glucose levels far above normal (another symptom of diabetes). These findings suggested that lack of some pancreatic product caused diabetes.

Minkowski tried unsuccessfully to prepare an extract of dog pancreas that would reverse the effect of removing the pancreas—that is, would lower the urinary or blood glucose levels. We now know that insulin is a protein and that the pancreas is very rich in proteases (trypsin and chymotrypsin), normally released directly into the small intestine to aid in digestion. These proteases doubtless degraded the insulin in the pancreatic extracts in Minkowski's experiments.

Despite considerable effort, no significant progress was made in the isolation or characterization of the "antidiabetic factor" until the summer of 1921, when Frederick G. Banting, a young scientist working in the laboratory of J. J. R. MacLeod at the University of Toronto, and a student assistant, Charles Best, took up the problem. By that time, several lines of evidence pointed to a group of specialized cells in the pancreas (the islets of Langerhans; see Fig. 23–26) as the source of the antidiabetic factor, which came to be called insulin (from Latin *insula*, "island").

Taking precautions to prevent proteolysis, Banting and Best (later aided by biochemist J. B. Collip) succeeded in December 1921 in preparing a purified pancreatic extract that cured the symptoms of experimental diabetes in dogs. On January 25, 1922 (just one month later!), their insulin preparation was injected into Leonard Thompson, a 14-year-old boy severely ill with diabetes mellitus. Within days, the levels of ketone bodies and glucose in Thompson's urine dropped dramatically; the extract saved his life and the lives of a number of other seriously ill children who also received these early preparations (Fig. 1). In 1923, Banting and MacLeod won the Nobel Prize for their isolation of insulin. Banting immediately announced that he would share his prize with Best; MacLeod shared his with Collip.

By 1923, pharmaceutical companies were supplying thousands of patients throughout the world with insulin extracted from porcine pancreas. With the development of genetic engineering techniques in the 1980s (Chapter 9), it became possible to produce unlimited quantities of human insulin by inserting the cloned human gene for insulin into a microorganism, which was then cultured on an industrial scale. Some patients with diabetes are now fitted with implanted insulin pumps, which release adjustable amounts of insulin on demand to meet changing needs at meal times and during exercise. There is a reasonable prospect that, in the future, transplantation of pancreatic tissue will provide diabetic patients with a source of insulin that responds as well as the normal pancreas, releasing insulin into the bloodstream only when blood glucose rises.

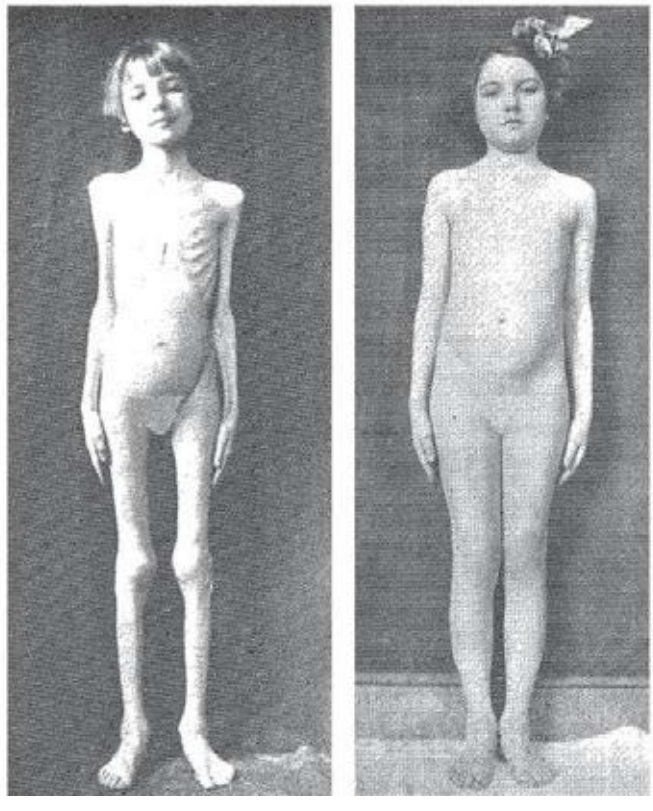

FIGURE 1 A child with type 1 diabetes before (left) and after (right) three months of treatment with an early preparation of insulin.

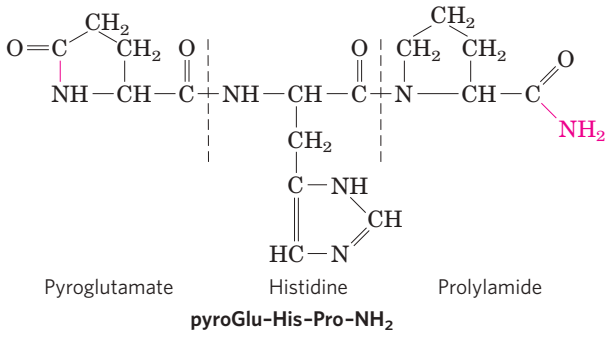

FIGURE 23–2 The structure of thyrotropin-releasing hormone (TRH). Purified (by heroic efforts) from extracts of hypothalamus, TRH proved to be a derivative of the tripeptide Glu-His-Pro. The side-chain carboxyl group of the amino-terminal Glu forms an amide (red bond) with the residue's α-amino group, creating pyroglutamate, and the carboxyl group of the carboxyl-terminal Pro is converted to an amide (red $—NH_2$). Such modifications are common among the small peptide hormones. In a typical protein of M_r ~50,000, the charges on the amino- and carboxyl-terminal groups contribute relatively little to the overall charge on the molecule, but in a tripeptide these two charges dominate the properties of the molecule. Formation of the amide derivatives removes these charges.

Hormone-specific antibodies are the key to the radioimmunoassay and its modern equivalent, the enzyme-linked immunosorbent assay (ELISA; see Fig. 5–26b). Purified hormone, injected into rabbits or mice, elicits antibodies that bind to the hormone with very high affinity and specificity. These antibodies may be purified and either radioisotopically labeled (for RIA) or conjugated with an enzyme that produces a colored product (for ELISA). The tagged antibodies are then allowed to interact with extracts containing the hormone. The fraction of antibody bound by the hormone in the extract is quantified by radiation detection or photometry. Because of the high affinity of the antibody for the hormone, such assays can be made sensitive to picograms of hormone in a sample.

Hormones Act through Specific High-Affinity Cellular Receptors

As we saw in Chapter 12, all hormones act through highly specific receptors in hormone-sensitive target cells, to which the hormones bind with high affinity. Each cell type has its own combination of hormone receptors, which define the range of its hormone responsiveness. Moreover, two cell types with the same type of receptor may have different intracellular targets of hormone action and thus may respond differently to the same hormone. The specificity of hormone action results from structural complementarity between the hormone and its receptor; this interaction is extremely selective, so even structurally similar hormones can have different effects if they preferentially bind to different receptors. The high affinity of the interaction allows cells to respond to very low concentrations of hormone. In the design of drugs intended to intervene in hormonal regulation, we need to know the relative specificity and affinity of the drug and the natural hormone. Recall that hormone-receptor interactions can be quantified by **Scatchard analysis** (see Box 12–1), which, under favorable conditions, yields a quantitative measure of affinity (the dissociation constant for the complex) and the number of hormone-binding sites in a preparation of receptor.

The intracellular consequences of ligand-receptor interaction are of at least five general types: (1) a second messenger (such as cAMP, cGMP, or inositol trisphosphate) generated inside the cell acts as an allosteric regulator of one or more enzymes, (2) a receptor tyrosine kinase is activated by the extracellular hormone, (3) a change in membrane potential results from the opening or closing of a hormone-gated ion channel, (4) an adhesion receptor on the cell surface conveys information from the extracellular matrix to the cytoskeleton, or (5) a steroid or steroidlike molecule causes a change in the level of expression (transcription of DNA into mRNA) of one or more genes, mediated by a nuclear hormone receptor protein (see Fig. 12–2).

Water-soluble peptide and amine hormones (insulin and epinephrine, for example) act extracellularly by binding to cell surface receptors that span the plasma membrane **(Fig. 23–3)**. When the hormone binds to its extracellular domain, the receptor undergoes a conformational change analogous to that produced in an allosteric enzyme by binding of an effector molecule. The

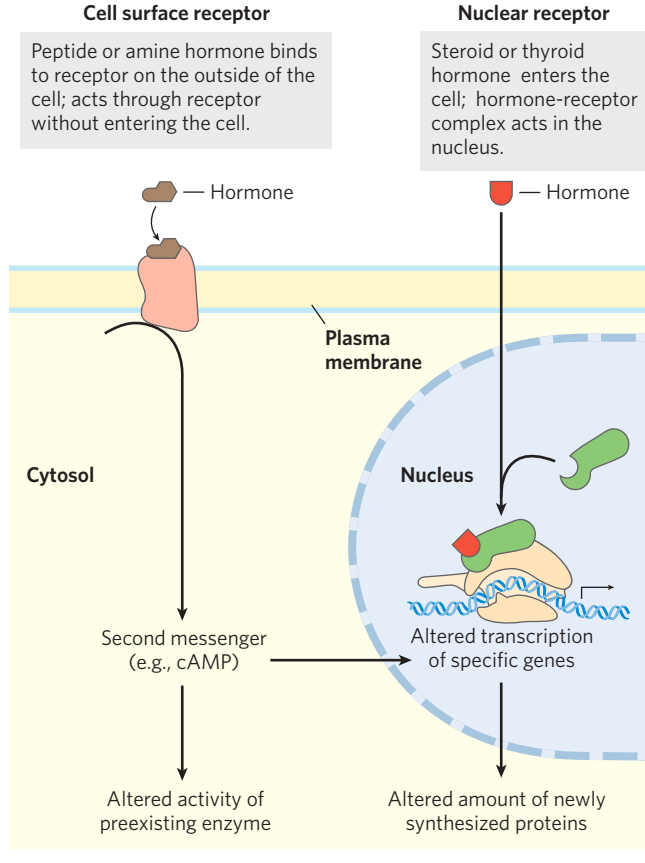

FIGURE 23–3 Two general mechanisms of hormone action. The peptide and amine hormones are faster acting than steroid and thyroid hormones.

conformational change triggers the downstream effects of the hormone.

A single hormone molecule, in forming a hormone-receptor complex, activates a catalyst that produces many molecules of second messenger, so the receptor serves not only as a signal transducer but also as a signal amplifier. The signal may be further amplified by a signaling cascade, a series of steps in which a catalyst activates a catalyst, resulting in very large amplifications of the original signal. A cascade of this type occurs in the regulation of glycogen synthesis and breakdown by epinephrine (see Fig. 12–7). Epinephrine activates (through its receptor) adenylyl cyclase, which produces many molecules of cAMP for each molecule of receptor-bound hormone. Cyclic AMP in turn activates cAMP-dependent protein kinase (protein kinase A), which activates glycogen phosphorylase *b* kinase, which activates glycogen phosphorylase *b*. The result is signal amplification: one epinephrine molecule causes the production of many thousands or millions of molecules of glucose 1-phosphate from glycogen.

Water-insoluble hormones (steroid, retinoid, and thyroid hormones) readily pass through the plasma membrane of their target cells to reach their receptor proteins in the nucleus (Fig. 23–3). With this class of hormones, the hormone-receptor complex itself carries the message: it interacts with DNA to alter the expression of specific genes, changing the enzyme complement of the cell and thereby changing cellular metabolism (see Fig. 12–30).

Hormones that act through plasma membrane receptors generally trigger very rapid physiological or biochemical responses. Just seconds after the adrenal medulla secretes epinephrine into the bloodstream, skeletal muscle responds by accelerating the breakdown of glycogen. By contrast, the thyroid hormones and the sex (steroid) hormones promote maximal responses in their target tissues only after hours or even days. These differences in response time correspond to different modes of action. In general, the fast-acting hormones lead to a change in the activity of one or more preexisting enzymes in the cell, by allosteric mechanisms or covalent modification. The slower-acting hormones generally alter gene expression, resulting in the synthesis of more (upregulation) or less (downregulation) of the regulated protein(s).

Hormones Are Chemically Diverse

Mammals have several classes of hormones, distinguishable by their chemical structures and their modes of action (Table 23–1). Peptide, catecholamine, and eicosanoid hormones act from outside the target cell via cell surface receptors. Steroid, vitamin D, retinoid, and thyroid hormones enter the cell and act through nuclear receptors. Nitric oxide (a gas) also enters the cell but activates a cytosolic enzyme, guanylyl cyclase (see Fig. 12–20).

Hormones can also be classified by the way they get from their point of release to their target tissue. **Endocrine** (from the Greek *endon*, "within," and *krinein*, "to release") hormones are released into the blood and carried to target cells throughout the body (insulin and glucagon are examples). **Paracrine** hormones are released into the extracellular space and diffuse to neighboring target cells (the eicosanoid hormones are of this type). **Autocrine** hormones affect the same cell that releases them, binding to receptors on the cell surface.

Mammals are hardly unique in possessing hormonal signaling systems. Insects and nematode worms have highly developed systems for hormonal regulation with fundamental mechanisms similar to those in mammals. Plants, too, use hormonal signals to coordinate the activities of their tissues (Chapter 12). The study of hormone action is not as advanced in plants as in animals, but we do know that some mechanisms are shared.

To illustrate the structural diversity and range of action of mammalian hormones, we consider representative examples of each major class listed in Table 23–1.

TABLE 23–1 Classes of Hormones

Type	Example	Synthetic path	Mode of action
Peptide	Insulin, glucagon	Proteolytic processing of prohormone	Plasma membrane receptors; second messengers
Catecholamine	Epinephrine	From tyrosine	
Eicosanoid	PGE_1	From arachidonate (20:4 fatty acid)	
Steroid	Testosterone	From cholesterol	Nuclear receptors; transcriptional regulation
Vitamin D	1α,25-Dihydroxyvitamin D_3	From cholesterol	
Retinoid	Retinoic acid	From vitamin A	
Thyroid	Triiodothyronine (T_3)	From Tyr in thyroglobulin	
Nitric oxide	Nitric oxide	From arginine + O_2	Cytosolic receptor (guanylyl cyclase) and second messenger (cGMP)

Peptide Hormones Peptide hormones may have from 3 to 200 or more amino acid residues. They include the pancreatic hormones insulin, glucagon, and somatostatin; the parathyroid hormone calcitonin; and all the hormones of the hypothalamus and pituitary (described below). These hormones are synthesized on ribosomes in the form of longer precursor proteins (prohormones), then packaged into secretory vesicles and proteolytically cleaved to form the active peptides. **Insulin** is a small protein (M_r 5,800) with two polypeptide chains, A and B, joined by two disulfide bonds. It is synthesized in the pancreas as an inactive single-chain precursor, preproinsulin **(Fig. 23–4)**, with an amino-terminal "signal sequence" that directs its passage into secretory vesicles. (Signal sequences are discussed in Chapter 27; see Fig. 27–38.) Proteolytic removal of the signal sequence and formation of three disulfide bonds produces proinsulin, which is stored in secretory granules (membrane vesicles filled with protein synthesized in the endoplasmic reticulum) in pancreatic β cells. When blood glucose is elevated sufficiently to trigger insulin secretion,

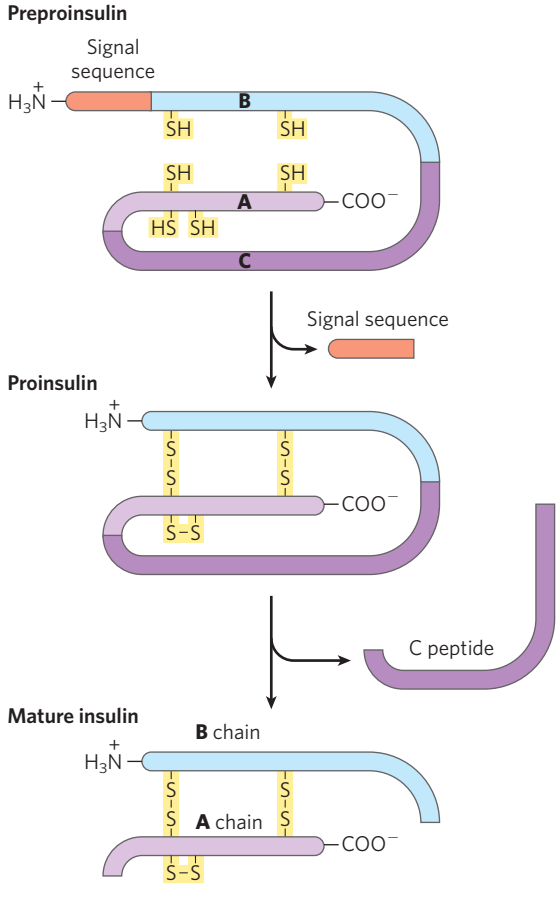

FIGURE 23–4 Insulin. Mature insulin is formed from its larger precursor preproinsulin by proteolytic processing. Removal of a 23 amino acid segment (the signal sequence) at the amino terminus of preproinsulin and formation of three disulfide bonds produces proinsulin. Further proteolytic cuts remove the C peptide from proinsulin to produce mature insulin, composed of A and B chains. The amino acid sequence of bovine insulin is shown in Figure 3–24.

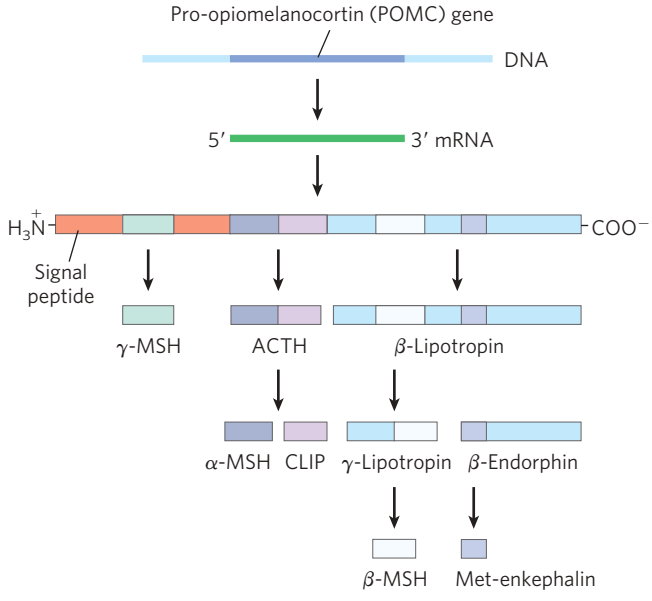

FIGURE 23–5 Proteolytic processing of the pro-opiomelanocortin (POMC) precursor. The initial gene product of the POMC gene is a long polypeptide that undergoes cleavage by a series of specific proteases to produce ACTH, β- and γ-lipotropin, α-, β-, and γ-MSH (melanocyte-stimulating hormone, or melanocortin), CLIP (corticotropin-like intermediary peptide), β-endorphin, and Met-enkephalin. The points of cleavage are paired basic residues, Arg–Lys, Lys–Arg, or Lys–Lys.

proinsulin is converted to active insulin by specific proteases, which cleave two peptide bonds to form the mature insulin molecule and C peptide, which are released into the blood by exocytosis.

In some cases, prohormone proteins, rather than yielding a single peptide hormone, produce several active hormones. Pro-opiomelanocortin (POMC) is a spectacular example of multiple hormones encoded by a single gene. The POMC gene encodes a large polypeptide that is progressively carved up into at least nine biologically active peptides **(Fig. 23–5)**. In many peptide hormones the terminal residues are modified, as in TRH (Fig. 23–2).

The concentration of peptide hormones in secretory granules is so high that the vesicle contents are virtually crystalline; when the contents are released by exocytosis, a large amount of hormone is released suddenly. The capillaries that serve peptide-producing endocrine glands are fenestrated (punctuated with tiny holes or "windows"), so the hormone molecules readily enter the bloodstream for transport to target cells elsewhere. As noted earlier, all peptide hormones act by binding to receptors in the plasma membrane. They cause the generation of a second messenger in the cytosol, which changes the activity of an intracellular enzyme, thereby altering the cell's metabolism.

Catecholamine Hormones The water-soluble compounds **epinephrine (adrenaline)** and **norepinephrine (noradrenaline)** are **catecholamines**, named for the structurally related compound catechol. They are synthesized from tyrosine (see Fig. 22–31).

Tyrosine ⟶ L-Dopa ⟶ Dopamine ⟶ Norepinephrine ⟶ Epinephrine

Catecholamines produced in the brain and in other neural tissues function as neurotransmitters, but epinephrine and norepinephrine are also hormones, synthesized and secreted by the adrenal glands. Like the peptide hormones, catecholamines are highly concentrated in secretory vesicles and released by exocytosis, and they act through surface receptors to generate intracellular second messengers. They mediate a wide variety of physiological responses to acute stress (see Table 23–6).

Eicosanoid Hormones The eicosanoid hormones (prostaglandins, thromboxanes, and leukotrienes) are derived from the 20-carbon polyunsaturated fatty acid arachidonate.

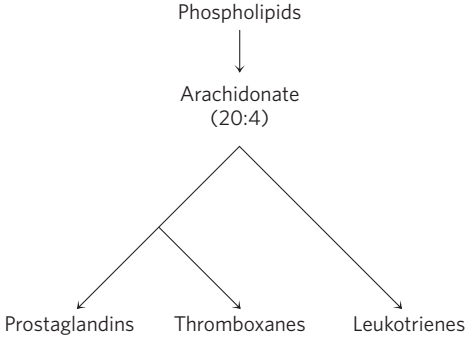

Unlike the hormones described above, they are not synthesized in advance and stored; they are produced, when needed, from arachidonate enzymatically released from membrane phospholipids by phospholipase A_2. The enzymes of the pathway leading to prostaglandins and thromboxanes are very widely distributed in mammalian tissues; most cells can produce these hormone signals, and cells of many tissues can respond to them through specific plasma membrane receptors. The eicosanoid hormones are paracrine hormones, secreted into the interstitial fluid (not primarily into the blood) and acting on nearby cells.

Prostaglandins promote the contraction of smooth muscle, including that of the intestine and uterus (and can therefore be used medically to induce labor). They also mediate pain and inflammation in all tissues. Many antiinflammatory drugs act by inhibiting steps in the prostaglandin synthetic pathway (see Fig. 21–15). Thromboxanes regulate platelet function and therefore blood clotting (see Fig. 6–39). Leukotrienes LTC_4 and LTD_4 act through plasma membrane receptors to stimulate contraction of smooth muscle in the intestine, pulmonary airways, and trachea. They are mediators of anaphylaxis, an immune overresponse that can include airway constriction, altered heartbeat, shock, and sometimes death. ■

Steroid Hormones The steroid hormones (adrenocortical hormones and sex hormones) are synthesized from cholesterol in several endocrine tissues.

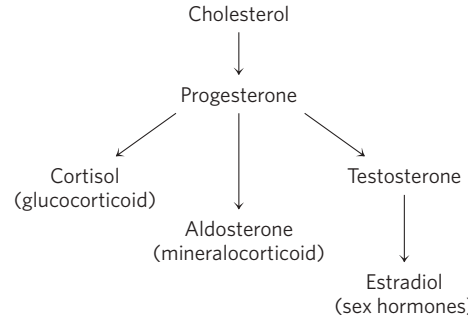

They travel to their target cells through the bloodstream, bound to carrier proteins. More than 50 corticosteroid hormones are produced in the adrenal cortex by reactions that remove the side chain from the D ring of cholesterol and introduce oxygen to form keto and hydroxyl groups. Many of these reactions involve cytochrome P-450 enzymes (see Box 21–1). The corticosteroids are of two general types, defined by their actions. Glucocorticoids (such as cortisol) primarily affect the metabolism of carbohydrates; mineralocorticoids (such as aldosterone) regulate the concentrations of electrolytes (K^+, Na^+, Ca^{2+}, Cl^-) in the blood. Androgens (such as testosterone) and estrogens (such as estradiol; see Fig. 10–19) are synthesized in the testes and ovaries. They affect sexual development, sexual behavior, and a variety of other reproductive and nonreproductive functions. Their synthesis also involves cytochrome P-450 enzymes that cleave the side chain of cholesterol and introduce oxygen atoms.

All steroid hormones act through nuclear receptors to change the level of expression of specific genes (see Fig. 12–30). They can also have more rapid effects, mediated by receptors in the plasma membrane.

Vitamin D Hormone Calcitriol (1α,25-dihydroxycalcitriol) is produced from vitamin D by enzyme-catalyzed hydroxylation in the liver and kidneys (see Fig. 10–20a). Vitamin D is obtained in the diet or by photolysis of 7-dehydrocholesterol in skin exposed to sunlight.

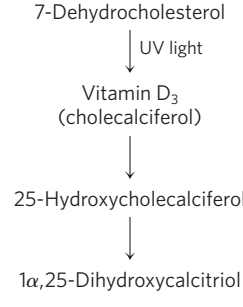

Calcitriol works in concert with parathyroid hormone in Ca^{2+} homeostasis, regulating [Ca^{2+}] in the blood and the balance between Ca^{2+} deposition and Ca^{2+} mobilization from bone. Acting through nuclear receptors, calcitriol activates the synthesis of an intestinal Ca^{2+}-binding protein essential for uptake of dietary Ca^{2+}. Inadequate dietary vitamin D or defects in the biosynthesis of calcitriol result in serious diseases such as rickets, in which bones are weak and malformed (see Fig. 10–20b). ■

Retinoid Hormones Retinoids are potent hormones that regulate the growth, survival, and differentiation of cells via nuclear retinoid receptors. The prohormone retinol is synthesized from β-carotene, primarily in liver (see Fig. 10–21), and many tissues convert retinol to the hormone retinoic acid (RA).

β-Carotene
↓
Vitamin A_1 (retinol)
↓
Retinoic acid

All tissues are retinoid targets, as all cell types have at least one form of nuclear retinoid receptor. In adults, the most significant targets include cornea, skin, epithelia of the lungs and trachea, and the immune system, in all of which there is continuing replacement of cells. RA regulates the synthesis of proteins essential for growth or differentiation. Excessive vitamin A (the precursor to retinoid hormones) can cause birth defects, and pregnant women are advised not to use the retinoid creams that have been developed for treatment of severe acne. ■

Thyroid Hormones The thyroid hormones T_4 (thyroxine) and T_3 (triiodothyronine) are synthesized from the precursor protein thyroglobulin (M_r 660,000). Up to 20 Tyr residues in thyroglobulin are enzymatically iodinated in the thyroid gland, then two iodotyrosine residues condense to form the precursor to thyroxine. When needed, thyroxine is released by proteolysis. Condensation of monoiodotyrosine with diiodothyronine produces T_3, which is also an active hormone released by proteolysis.

Thyroglobulin–Tyr
↓
Thyroglobulin–Tyr–I (iodinated Tyr residues)
↓ proteolysis
Thyroxine (T_4), triiodothyronine (T_3)

The thyroid hormones act through nuclear receptors to stimulate energy-yielding metabolism, especially in liver and muscle, by increasing the expression of genes encoding key catabolic enzymes.

Nitric Oxide ($NO^{\bullet}$) Nitric oxide is a relatively stable free radical synthesized from molecular oxygen and the guanidinium nitrogen of arginine (see Fig. 22–33) in a reaction catalyzed by **NO synthase**.

$$\text{Arginine} + 1\tfrac{1}{2}\text{NADPH} + 2O_2 \longrightarrow NO^{\bullet} + \text{citrulline} + 2H_2O + 1\tfrac{1}{2}NADP^+$$

This enzyme is found in many tissues and cell types: neurons, macrophages, hepatocytes, myocytes of smooth muscle, endothelial cells of the blood vessels, and epithelial cells of the kidney. NO acts near its point of release, entering the target cell and activating the cytosolic enzyme guanylyl cyclase, which catalyzes the formation of the second messenger cGMP (see Fig. 12–20). A cGMP-dependent protein kinase mediates the effects of NO by phosphorylating key proteins and altering their activities. For example, phosphorylation of contractile proteins in the smooth muscle surrounding blood vessels relaxes the muscle, thereby lowering blood pressure.

Hormone Release Is Regulated by a Hierarchy of Neuronal and Hormonal Signals

The changing levels of specific hormones regulate specific cellular processes, but what regulates the level of each hormone? The brief answer is that the central nervous system receives input from many internal and external sensors—signals about danger, hunger, dietary intake, blood composition and pressure, for example—and orchestrates the production of appropriate hormonal signals by the endocrine tissues. For a more complete answer, we must look at the hormone-producing systems of the human body and some of their functional interrelationships.

Figure 23–6 shows the anatomic location of the major endocrine glands in humans, and **Figure 23–7** represents the "chain of command" in the hormonal signaling hierarchy. The **hypothalamus**, a small region of

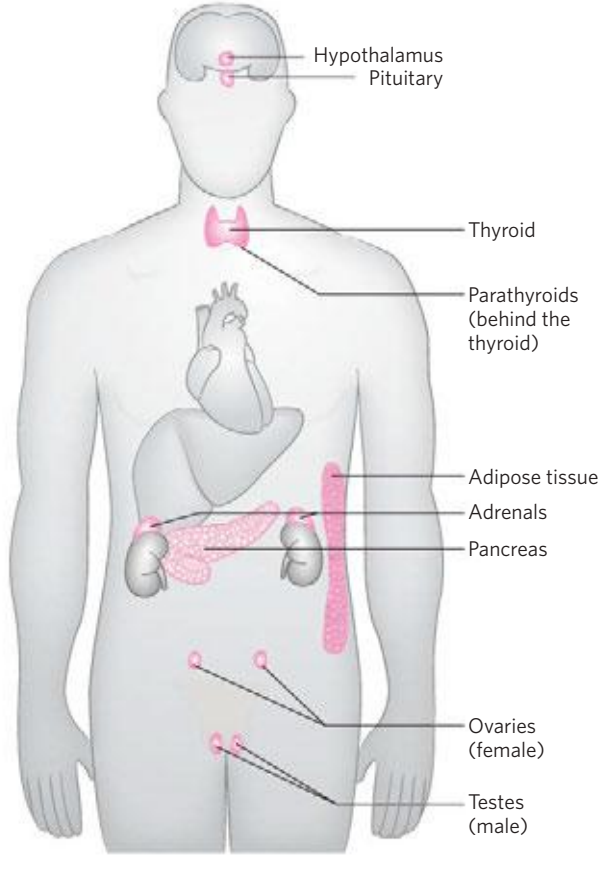

FIGURE 23–6 The major endocrine glands. The glands are shaded pink.

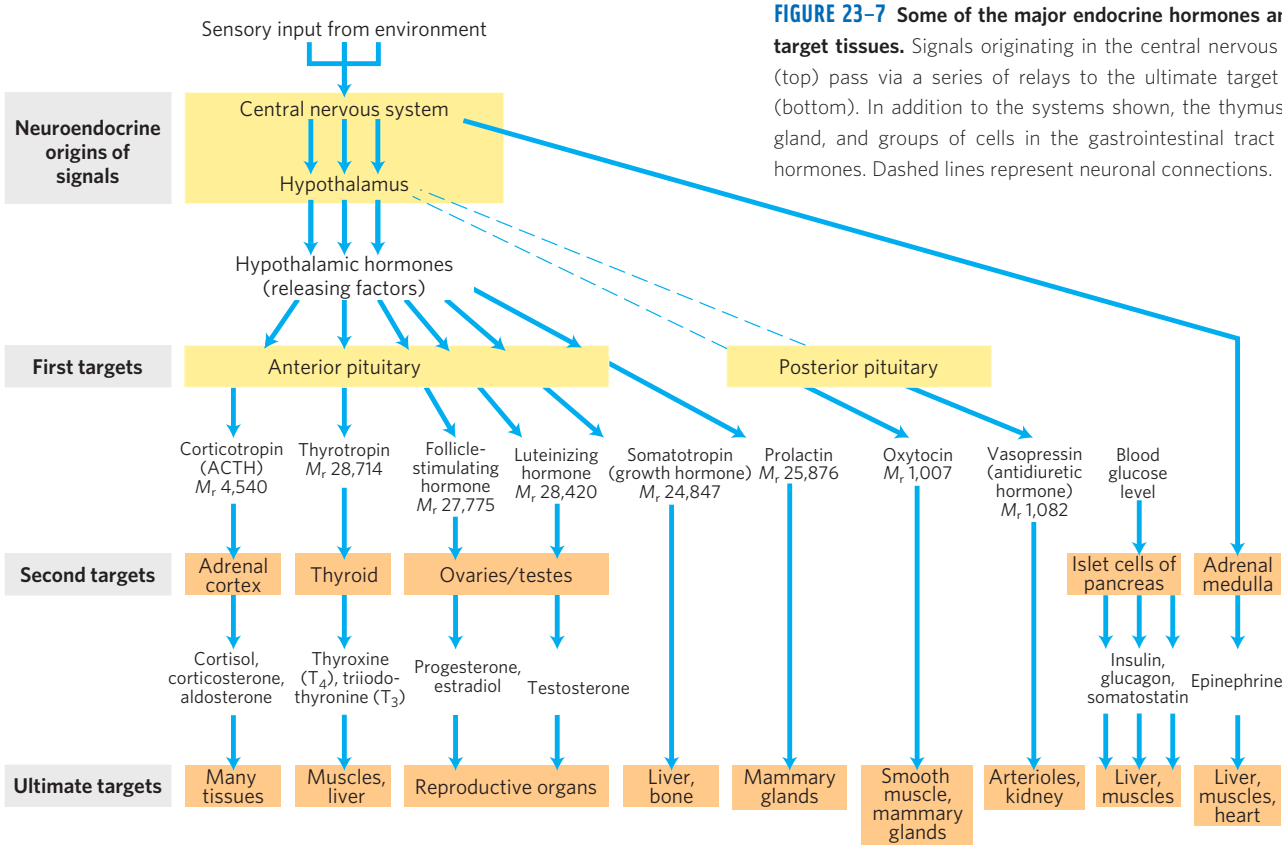

FIGURE 23–7 Some of the major endocrine hormones and their target tissues. Signals originating in the central nervous system (top) pass via a series of relays to the ultimate target tissues (bottom). In addition to the systems shown, the thymus, pineal gland, and groups of cells in the gastrointestinal tract secrete hormones. Dashed lines represent neuronal connections.

the brain **(Fig. 23–8)**, is the coordination center of the endocrine system; it receives and integrates messages from the central nervous system. In response to these messages, the hypothalamus produces regulatory hormones (releasing factors) that pass directly to the nearby pituitary gland through special blood vessels and neurons that connect the two glands (Fig. 23–8b). The pituitary gland has two functionally distinct parts. The **posterior pituitary** contains the axonal endings of many neurons that originate in the hypothalamus. These neurons produce the short peptide hormones oxytocin and vasopressin **(Fig. 23–9)**, which move down the axon to the nerve endings in the pituitary, where they are stored in secretory granules to await the signal for their release.

The **anterior pituitary** responds to hypothalamic hormones carried in the blood, producing **tropic hormones**, or **tropins** (from the Greek *tropos*, "turn"). These relatively long polypeptides activate the next rank of endocrine glands (Fig. 23–7), which includes the adrenal cortex, thyroid gland, ovaries, and testes. These glands in turn secrete their specific hormones, which are carried in the bloodstream to the target tissues. For example, corticotropin-releasing hormone secreted from the hypothalamus stimulates the anterior pituitary to release ACTH, which travels through the blood to the zona fasciculata of the adrenal cortex and triggers the release of cortisol. Cortisol, the ultimate hormone in this cascade, acts through its receptor in many types of target cells to alter their metabolism. In hepatocytes, one effect of cortisol is to increase the rate of gluconeogenesis.

Hormonal cascades such as those responsible for the release of cortisol and epinephrine result in large amplifications of the initial signal and allow exquisite fine-tuning of the output of the ultimate hormone **(Fig. 23–10)**. At each level in the cascade, a small signal elicits a larger response. For example, the initial electrical signal to the hypothalamus results in the release of a few *nanograms* of corticotropin-releasing hormone, which elicits the release of a few *micrograms* of corticotropin. Corticotropin acts on the adrenal cortex to cause the release of *milligrams* of cortisol, for an overall amplification of at least a millionfold.

At each level of a hormonal cascade, feedback inhibition of earlier steps in the cascade is possible; an unnecessarily elevated level of the ultimate hormone or of an intermediate hormone inhibits the release of earlier hormones in the cascade. These feedback mechanisms accomplish the same end as those that limit the output of a biosynthetic pathway (compare Fig. 23–10 with Fig. 22–37): a product is synthesized (or released) only until the necessary concentration is reached.

SUMMARY 23.1 Hormones: Diverse Structures for Diverse Functions

- Hormones are chemical messengers secreted by certain tissues into the blood or interstitial fluid, serving to regulate the activity of other cells or tissues.

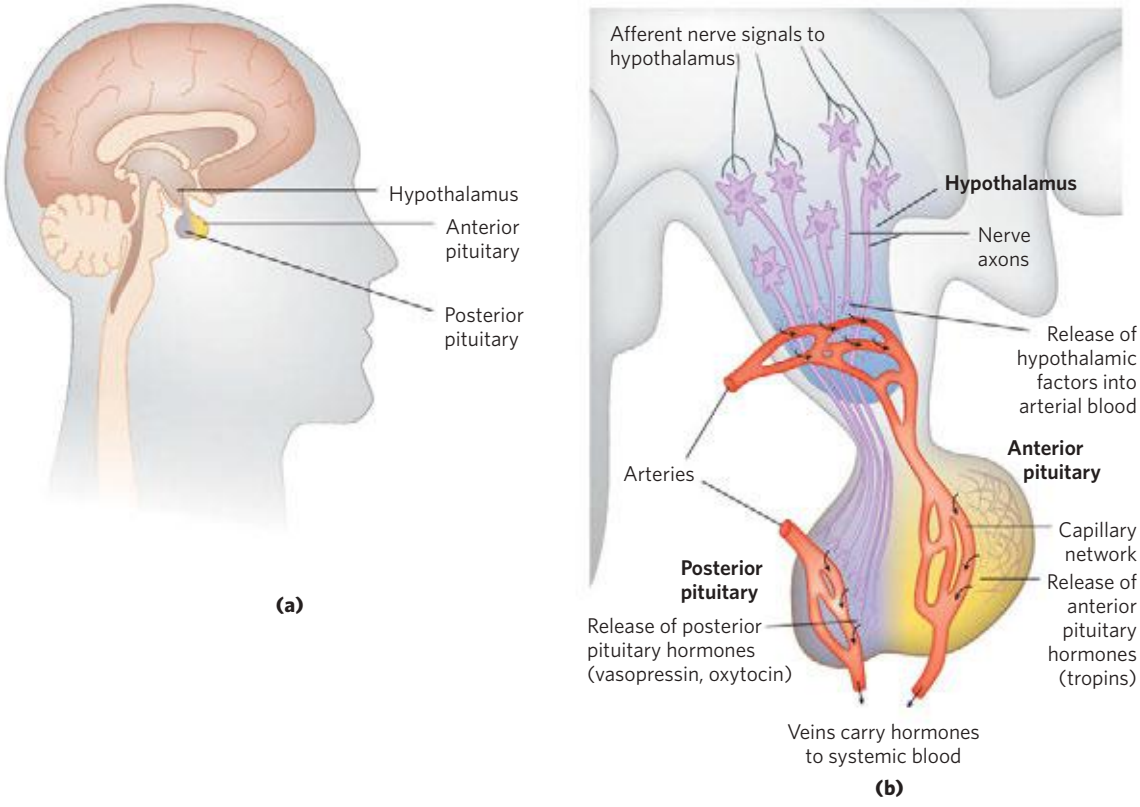

FIGURE 23–8 Neuroendocrine origins of hormone signals. (a) Location of the hypothalamus and pituitary gland. **(b)** Details of the hypothalamus-pituitary system. Signals from connecting neurons stimulate the hypothalamus to secrete releasing factors into a blood vessel that carries the hormones directly to a capillary network in the anterior pituitary. In response to each hypothalamic releasing factor, the anterior pituitary releases the appropriate hormone into the general circulation. Posterior pituitary hormones are synthesized in neurons arising in the hypothalamus, transported along axons to nerve endings in the posterior pituitary, and stored there until released into the blood in response to a neuronal signal.

- Radioimmunoassay and ELISA are two very sensitive techniques for detecting and quantifying hormones.
- Peptide, catecholamine, and eicosanoid hormones bind to specific receptors in the plasma membrane of target cells, altering the level of an intracellular second messenger, without actually entering the cell.

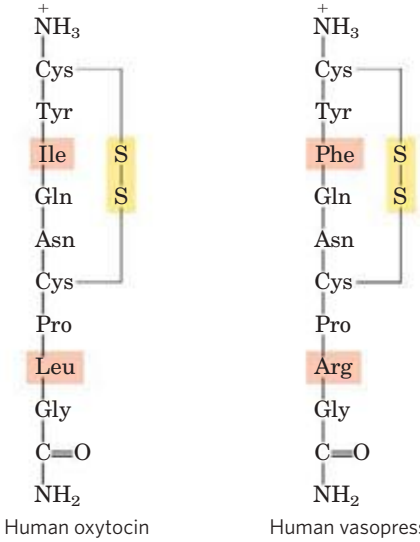

- Steroid, vitamin D, retinoid, and thyroid hormones enter target cells and alter gene expression by interacting with specific nuclear receptors.
- Some hormones are synthesized as prohormones and activated by enzymatic cleavage. In some cases, such as insulin, a single hormone is produced by proteolytic cleavages; in others, such as POMC, several distinct hormones are produced by cleavage of a single prohormone.
- Hormones are regulated by a hierarchy of interactions between the brain and endocrine glands: nerve impulses stimulate the hypothalamus to send specific hormones to the pituitary gland, thus stimulating (or inhibiting) the release of tropic

FIGURE 23–9 Two hormones of the posterior pituitary gland. The carboxyl-terminal residue of both peptides is glycinamide, —NH—CH_2—$CONH_2$ (as noted in Fig. 23-2, amidation of the carboxyl terminus is common in short peptide hormones). These two hormones, identical in all but two residues (shaded light red), have very different biological effects. Oxytocin acts on the smooth muscle of the uterus and mammary gland, causing uterine contractions during labor and promoting milk release during lactation. Vasopressin (also called antidiuretic hormone) increases water reabsorption in the kidney and promotes the constriction of blood vessels, thereby increasing blood pressure.

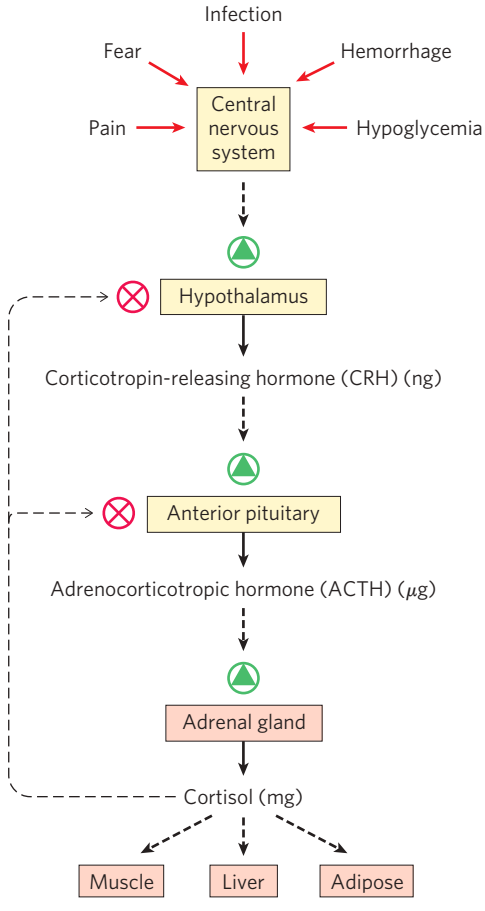

FIGURE 23–10 Cascade of hormone release following central nervous system input to the hypothalamus. Solid black arrows indicate hormone production and release; broken black arrows indicate the action of hormones on target tissues. In each endocrine tissue along the pathway, a stimulus from the level above is received, amplified, and transduced into the release of the next hormone in the cascade. The cascade is sensitive to regulation at several levels through feedback inhibition (thin, dashed arrows) by the ultimate hormone (in this case, cortisol). The product therefore regulates its own production, as in feedback inhibition of biosynthetic pathways within a single cell.

hormones. The anterior pituitary hormones in turn stimulate other endocrine glands (thyroid, adrenals, pancreas) to secrete their characteristic hormones, which in turn stimulate specific target tissues.

- Hormonal cascades, in which catalysts activate catalysts, amplify the initial stimulus by several orders of magnitude, often in a very short time (seconds).

23.2 Tissue-Specific Metabolism: The Division of Labor

Each tissue of the human body has a specialized function, reflected in its anatomy and metabolic activity **(Fig. 23–11)**. Skeletal muscle allows directed motion; adipose tissue stores and distributes energy in the form of fats, which serve as fuel throughout the body as well as thermal insulation; in the brain, cells pump ions across their plasma membranes to produce electrical signals. The liver plays a central processing and distributing role in metabolism and furnishes all other organs and tissues with an appropriate mix of nutrients via the bloodstream. The functional centrality of the liver is indicated by the common reference to all other tissues and organs as "extrahepatic." We therefore begin our discussion of the division of metabolic labor by considering the transformations of carbohydrates, amino acids, and fats in the mammalian liver. This is followed by brief descriptions of the primary metabolic functions of adipose tissue, muscle, brain, and the medium that interconnects all others: the blood.

The Liver Processes and Distributes Nutrients

During digestion in mammals, the three main classes of nutrients (carbohydrates, proteins, and fats) undergo enzymatic hydrolysis into their simple constituents. This breakdown is necessary because the epithelial cells lining the intestinal lumen absorb only relatively small molecules. Many of the fatty acids and monoacylglycerols released by digestion of fats in the intestine are reassembled within these epithelial cells into triacylglycerols (TAGs).

After being absorbed, most sugars and amino acids and some reconstituted TAGs pass from intestinal epithelial cells into blood capillaries and travel in the bloodstream to the liver; the remaining TAGs enter adipose tissue via the lymphatic system. The portal vein (Fig. 23–11) is a direct route from the digestive organs to the liver, and liver therefore has first access to ingested nutrients. The liver has two main cell types. Kupffer cells are phagocytes, important in immune function. **Hepatocytes**, of primary interest here, transform dietary nutrients into the fuels and precursors required by other tissues and export them via the blood. The kinds and amounts of nutrients supplied to the liver vary with several factors, including the diet and the time between meals. The demand of extrahepatic tissues for fuels and precursors varies among organs and with the level of activity and overall nutritional state of the individual.

To meet these changing circumstances, the liver has remarkable metabolic flexibility. For example, when the diet is rich in protein, hepatocytes supply themselves with high levels of enzymes for amino acid catabolism and gluconeogenesis. Within hours after a shift to a high-carbohydrate diet, the levels of these enzymes begin to drop and the hepatocytes increase their synthesis of enzymes essential to carbohydrate metabolism and fat synthesis. Liver enzymes turn over (are synthesized and degraded) at 5 to 10 times the rate of enzyme turnover in other tissues, such as muscle. Extrahepatic tissues also can adjust their metabolism to prevailing conditions, but none is as adaptable as the liver, and none is so central to the organism's overall metabolism. What follows is

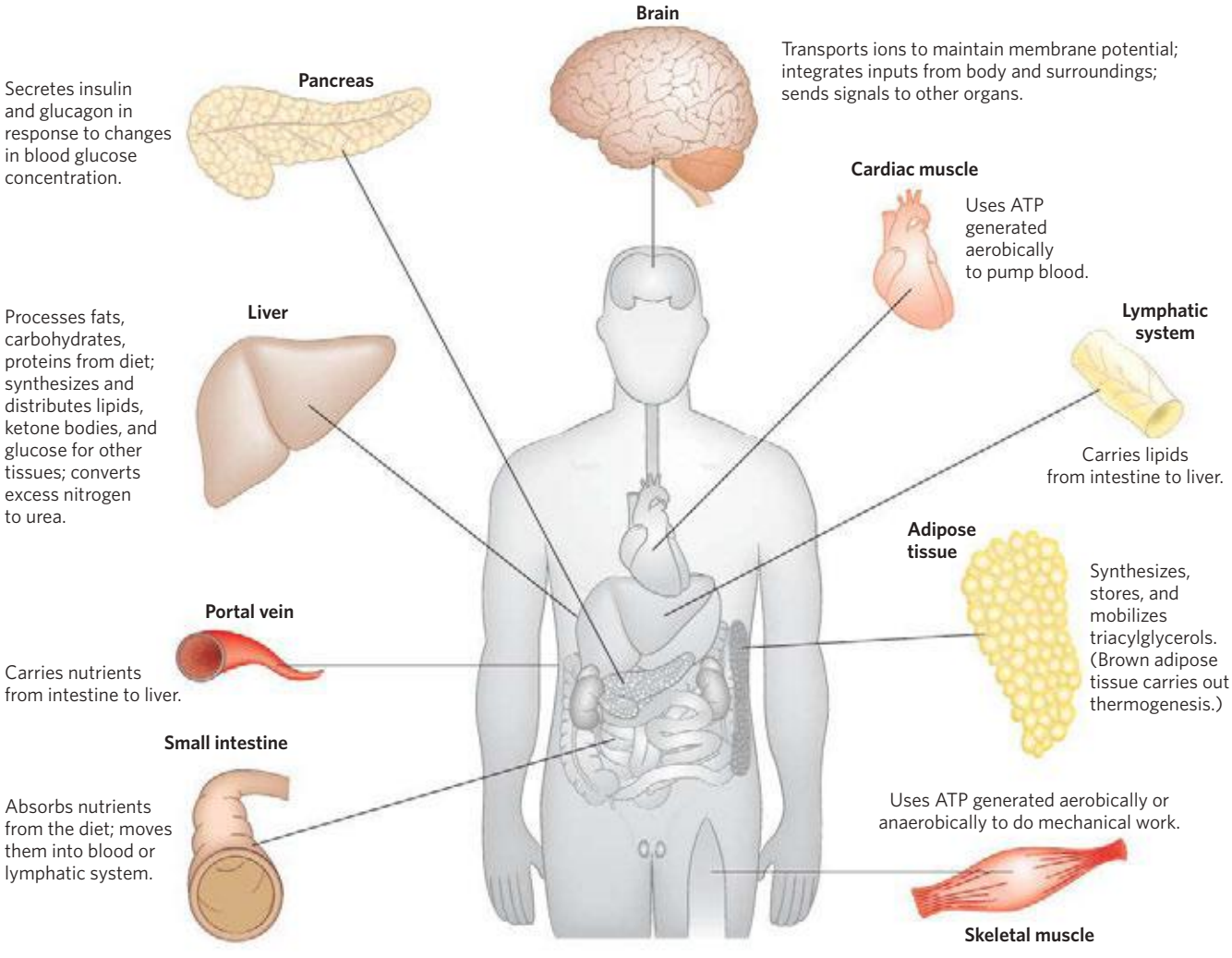

FIGURE 23–11 **Specialized metabolic functions of mammalian tissues.**

a survey of the possible fates of sugars, amino acids, and lipids that enter the liver from the bloodstream. To help you recall the metabolic transformations discussed here, Table 23–2 shows the major pathways and processes and indicates by figure number where each pathway is presented in detail. Here, we provide summaries of the pathways, referring to the numbered pathways and reactions in Figures 23–12 to 23–14.

Sugars The glucose transporter of hepatocytes (GLUT2) allows rapid, passive diffusion of glucose so that the concentration of glucose in a hepatocyte is essentially the same as that in the blood. Glucose entering hepatocytes is phosphorylated by hexokinase IV (glucokinase) to yield glucose 6-phosphate. Glucokinase has a much higher K_m for glucose (10 mM) than do the hexokinase isozymes in other cells (p. 603) and, unlike these other isozymes, it is not inhibited by its product, glucose 6-phosphate. The presence of glucokinase allows hepatocytes to continue phosphorylating glucose when the glucose concentration rises well above levels that would overwhelm other hexokinases. The high K_m of glucokinase also ensures that the phosphorylation of glucose in hepatocytes is minimal when the glucose concentration is low, preventing the liver from consuming glucose as fuel via glycolysis. This spares glucose for other tissues. Fructose, galactose, and mannose, all absorbed from the small intestine, are also converted to glucose 6-phosphate by enzymatic pathways examined in Chapter 14. Glucose 6-phosphate is at the crossroads of carbohydrate metabolism in the liver. It may take any of several major metabolic routes **(Fig. 23–12)**, depending on the current metabolic needs of the organism. By the action of various allosterically regulated enzymes, and through hormonal regulation of enzyme synthesis and activity, the liver directs the flow of glucose into one or more of these pathways.

❶ Glucose 6-phosphate is dephosphorylated by glucose 6-phosphatase to yield free glucose (see Fig. 15–30), which is exported to replenish blood glucose. Export is the predominant pathway when glucose 6-phosphate is in limited supply, because the blood glucose concentration must be kept sufficiently high (4 mM) to provide adequate energy for the brain and other tissues. ❷ Glucose 6-phosphate not immediately needed to form blood glucose is converted to

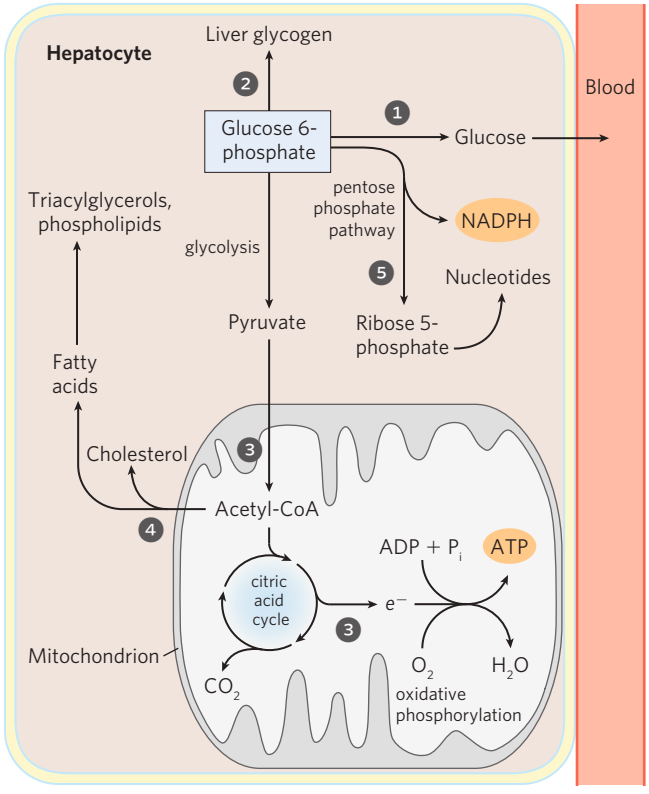

FIGURE 23–12 Metabolic pathways for glucose 6-phosphate in the liver. Here and in Figures 23–13 and 23–14, anabolic pathways are generally shown leading upward, catabolic pathways leading downward, and distribution to other organs horizontally. The numbered processes in each figure are described in the text.

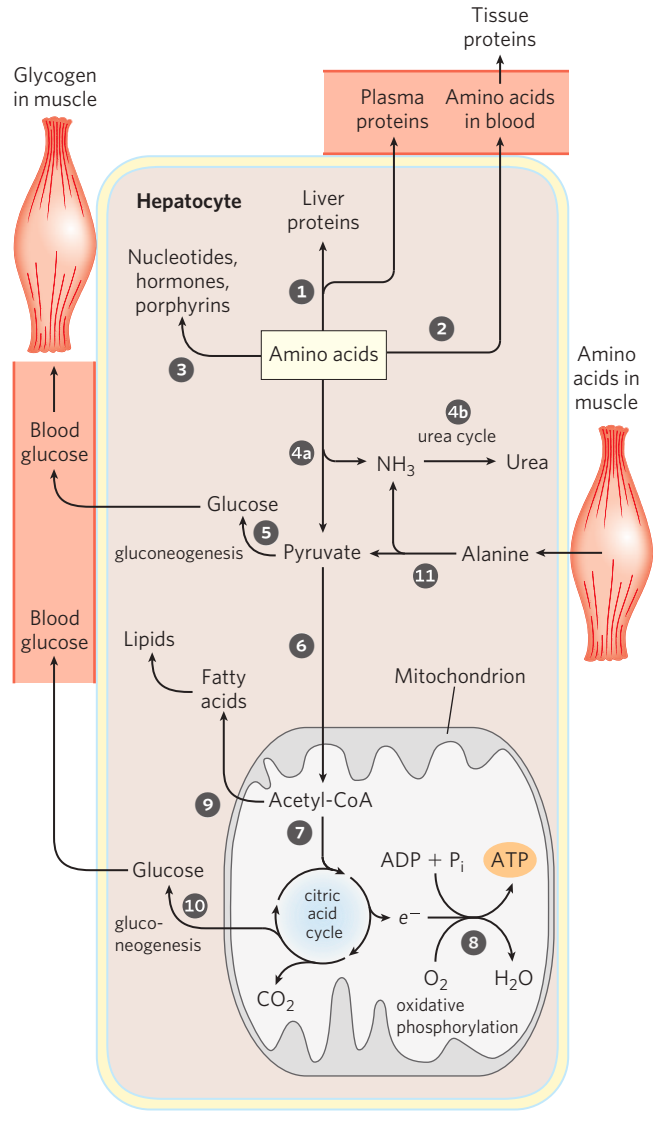

FIGURE 23–13 Metabolism of amino acids in the liver.

liver glycogen or has one of several other fates. Following glycolysis and the pyruvate dehydrogenase reaction, ❸ the acetyl-CoA so formed can be oxidized for ATP production by the citric acid cycle, with ensuing electron transfer and oxidative phosphorylation yielding ATP. (Normally, however, fatty acids are the preferred fuel for ATP production in hepatocytes.) ❹ Acetyl-CoA can also serve as the precursor of fatty acids, which are incorporated into TAGs and phospholipids, and of cholesterol. Much of the lipid synthesized in the liver is transported to other tissues by blood lipoproteins. ❺ Alternatively, glucose 6-phosphate can enter the pentose phosphate pathway, yielding both reducing power (NADPH), needed for the biosynthesis of fatty acids and cholesterol, and D-ribose 5-phosphate, a precursor for nucleotide biosynthesis. NADPH is also an essential cofactor in the detoxification and elimination of many drugs and other xenobiotics metabolized in the liver.

Amino Acids Amino acids that enter the liver follow several important metabolic routes **(Fig. 23–13)**. ❶ They are precursors for protein synthesis, a process discussed in Chapter 27. The liver constantly renews its own proteins, which have a relatively high turnover rate (average half-life of hours to days), and is also the site of biosynthesis of most plasma proteins. ❷ Alternatively, amino acids pass in the bloodstream to other organs to be used in the synthesis of tissue proteins. ❸ Other amino acids are precursors in the biosynthesis of nucleotides, hormones, and other nitrogenous compounds in the liver and other tissues.

❹a Amino acids not needed as biosynthetic precursors are transaminated or deaminated and degraded to yield pyruvate and citric acid cycle intermediates, with various fates; ❹b the ammonia released is converted to the excretory product urea. ❺ Pyruvate can be converted to glucose and glycogen via gluconeogenesis, or ❻ it can be converted to acetyl-CoA, which has several possible fates: ❼ oxidation via the citric acid cycle and ❽ oxidative phosphorylation to produce ATP or ❾ conversion to lipids for storage. ❿ Citric acid cycle intermediates can be siphoned off into glucose synthesis by gluconeogenesis.

The liver also metabolizes amino acids that arrive intermittently from other tissues. The blood is adequately supplied with glucose just after the digestion

TABLE 23–2 Pathways of Carbohydrate, Amino Acid, and Fat Metabolism Illustrated in Earlier Chapters

Pathway	Figure reference(s)
Citric acid cycle: acetyl-CoA ⟶ $2CO_2$	16–7
Oxidative phosphorylation: ATP synthesis	19–19
Carbohydrate catabolism	
Glycogenolysis: glycogen ⟶ glucose 1-phosphate ⟶ blood glucose	15–27; 15–28
Hexose entry into glycolysis: fructose, mannose, galactose ⟶ glucose 6-phosphate	14–11
Glycolysis: glucose ⟶ pyruvate	14–2
Pyruvate dehydrogenase reaction: pyruvate ⟶ acetyl-CoA	16–2
Lactic acid fermentation: glucose ⟶ lactate + 2ATP	14–4
Pentose phosphate pathway: glucose 6-phosphate ⟶ pentose phosphates + NADPH	14–22
Carbohydrate anabolism	
Gluconeogenesis: citric acid cycle intermediates ⟶ glucose	14–17
Glucose-alanine cycle: glucose ⟶ pyruvate ⟶ alanine ⟶ glucose	18–9
Glycogen synthesis: glucose 6-phosphate ⟶ glucose 1-phosphate ⟶ glycogen	15–32
Amino acid and nucleotide metabolism	
Amino acid degradation: amino acids ⟶ acetyl-CoA, citric acid cycle intermediates	18–15
Amino acid synthesis	22–11
Urea cycle: NH_3 ⟶ urea	18–10
Glucose-alanine cycle: alanine ⟶ glucose	18–9
Nucleotide synthesis: amino acids ⟶ purines, pyrimidines	22–35; 22–38
Hormone and neurotransmitter synthesis	22–31
Fat catabolism	
β Oxidation of fatty acids: fatty acids ⟶ acetyl-CoA	17–8
Oxidation of ketone bodies: β-hydroxybutyrate ⟶ acetyl-CoA ⟶ CO_2 via citric acid cycle	17–20
Fat anabolism	
Fatty acid synthesis: acetyl-CoA ⟶ fatty acids	21–6
Triacylglycerol synthesis: acetyl-CoA ⟶ fatty acids ⟶ triacylglycerol	21–18; 21–19
Ketone body formation: acetyl-CoA ⟶ acetoacetate, β-hydroxybutyrate	17–19
Cholesterol and cholesteryl ester synthesis: acetyl-CoA ⟶ cholesterol ⟶ cholesteryl esters	21–33 to 21–37
Phospholipid synthesis: fatty acids ⟶ phospholipids	21–17; 21–23 to 21–28

and absorption of dietary carbohydrate or, between meals, by the conversion of liver glycogen to blood glucose. During the interval between meals, especially if prolonged, some muscle protein is degraded to amino acids. These amino acids donate their amino groups (by transamination) to pyruvate, the product of glycolysis, to yield alanine, which ⓫ is transported to the liver and deaminated. Hepatocytes convert the resulting pyruvate to blood glucose (via gluconeogenesis ❺), and the ammonia to urea for excretion ❹b. One benefit of this glucose-alanine cycle (see Fig. 18–9) is the smoothing out of fluctuations in blood glucose between meals. The amino acid deficit incurred in muscles is made up after the next meal by incoming dietary amino acids.

Lipids The fatty acid components of lipids entering hepatocytes also have several different fates **(Fig. 23–14)**. ❶ Some are converted to liver lipids. ❷ Under most circumstances, fatty acids are the primary oxidative fuel in the liver. Free fatty acids may be activated and oxidized to yield acetyl-CoA and NADH. ❸ The acetyl-CoA is further oxidized via the citric acid cycle, and ❹ oxidations in the cycle drive the synthesis of ATP by oxidative phosphorylation. ❺ Excess acetyl-CoA, not required by the liver, is converted to acetoacetate and β-hydroxybutyrate; these ketone bodies circulate in the blood to other tissues to be used as fuel for the citric acid cycle. Ketone bodies, unlike fatty acids, can pass the blood-brain barrier, providing the brain with a source of acetyl-CoA for energy-yielding oxidation. Ketone bodies can supply a significant fraction of the energy in some extrahepatic tissues—up to one-third in the heart and as much as 60% to 70% in the brain during prolonged fasting. ❻ Some of the acetyl-CoA derived from fatty acids (and from glucose) is used for the biosynthesis of cholesterol, which is required for membrane synthesis. Cholesterol is also the precursor of all steroid hormones and of the bile salts, which are essential for the digestion and absorption of lipids.

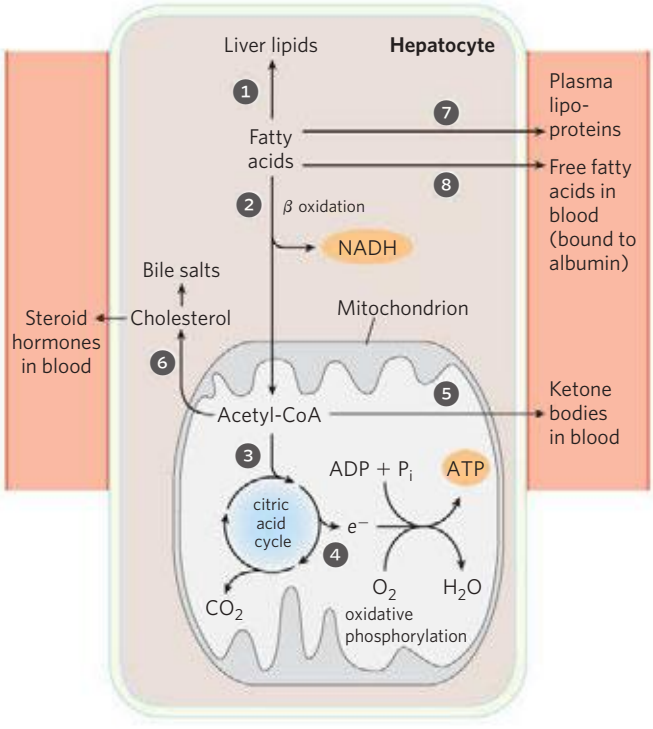

FIGURE 23–14 **Metabolism of fatty acids in the liver.**

The other two metabolic fates of lipids involve specialized mechanisms for the transport of insoluble lipids in blood. ❼ Fatty acids are converted to the phospholipids and TAGs of plasma lipoproteins, which carry lipids to adipose tissue for storage. ❽ Some free fatty acids are bound to serum albumin and carried to the heart and skeletal muscles, which take up and oxidize free fatty acids as a major fuel. Serum albumin is the most abundant plasma protein; one molecule can carry up to 10 molecules of free fatty acid.

The liver thus serves as the body's distribution center, exporting nutrients in the correct proportions to other organs, smoothing out fluctuations in metabolism caused by intermittent food intake, and processing excess amino groups into urea and other products to be disposed of by the kidneys. Certain nutrients are stored in the liver, including iron ions and vitamin A. The liver also detoxifies foreign organic compounds, such as drugs, food additives, preservatives, and other possibly harmful agents with no food value. Detoxification often involves the cytochrome P-450–dependent hydroxylation of relatively insoluble organic compounds, making them sufficiently soluble for further breakdown and excretion (see Box 21–1).

Adipose Tissues Store and Supply Fatty Acids

There are two distinct types of adipose tissue, white and brown **(Fig. 23–15)**, with quite distinct roles, and we focus first on the more abundant of the two. **White adipose tissue (WAT)** is amorphous and widely distributed in the body: under the skin, around the deep blood vessels, and in the abdominal cavity. The **adipocytes** of

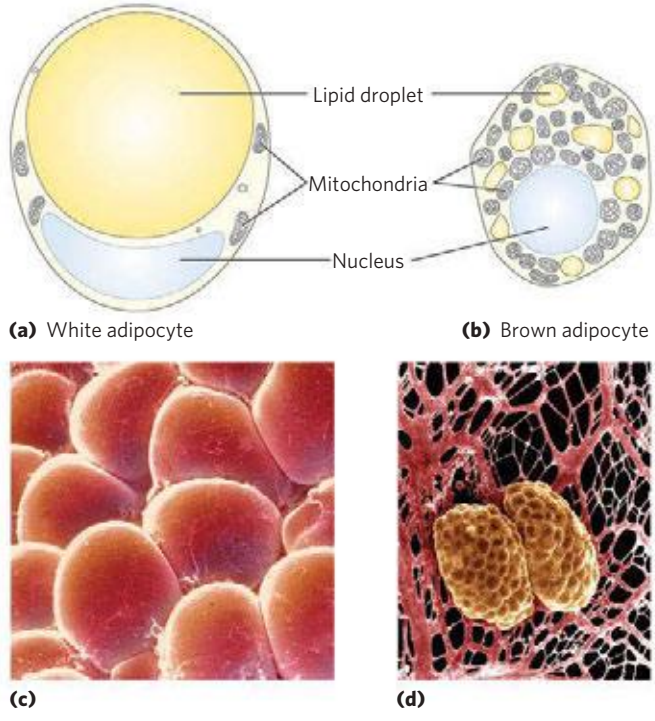

FIGURE 23–15 **Adipocytes of white and brown adipose tissue.** Schematic views of typical mouse adipocytes from **(a)** white adipose tissue (WAT) and **(b)** brown adipose tissue (BAT). White adipocytes are larger and contain a single huge lipid droplet, which squeezes the mitochondria and nucleus against the plasma membrane. In brown adipocytes, mitochondria are much more prominent, the nucleus is near the center of the cell, and multiple small fat droplets are present. Below are shown scanning electron micrographs of adipocytes in **(c)** WAT and **(d)** BAT. In fat tissues, capillaries and collagen fibers form a supporting network around spherical adipocytes.

WAT are large (diameter 30 to 70 μm), spherical cells, completely filled with a single large lipid (TAG) droplet that constitutes about 65% of the cell mass and squeezes the mitochondria and nucleus into a thin layer against the plasma membrane (Fig. 23–15a, c). In humans, WAT typically makes up about 15% of the mass of a healthy young adult. The adipocytes are metabolically very active, responding quickly to hormonal stimuli in a metabolic interplay with the liver, skeletal muscles, and heart.

Like other cell types, adipocytes have an active glycolytic metabolism, oxidize pyruvate and fatty acids via the citric acid cycle, and carry out oxidative phosphorylation. During periods of high carbohydrate intake, adipose tissue can convert glucose (via pyruvate and acetyl-CoA) to fatty acids, convert the fatty acids to TAGs, and store the TAGs as large fat globules—although in humans, much of the fatty acid synthesis occurs in hepatocytes. Adipocytes store TAGs arriving from the liver (carried in the blood as VLDL; see Fig. 21–40) and from the intestinal tract (carried in chylomicrons), particularly after meals rich in fat.

When the demand for fuel rises (between meals, for example), lipases in adipocytes hydrolyze stored TAGs to release free fatty acids, which can travel in the bloodstream to skeletal muscle and the heart. The release of

fatty acids from adipocytes is greatly accelerated by epinephrine, which stimulates the cAMP-dependent phosphorylation of perilipin and thus gives lipases specific for tri-, di-, and monoglycerides access to TAGs in the lipid droplet (see Fig. 17–3). Hormone-sensitive lipase is also stimulated by phosphorylation, but this is not the main cause of increased lipolysis. Insulin counterbalances this effect of epinephrine, decreasing the activity of the lipase.

The breakdown and synthesis of TAGs in adipose tissue constitute a substrate cycle; up to 70% of the fatty acids released by the three lipases are reesterified in adipocytes, re-forming TAGs. Recall from Chapter 15 that such substrate cycles allow fine regulation of the rate and direction of flow of intermediates through a bidirectional pathway. In adipose tissue, glycerol liberated by adipocyte lipases cannot be reused in the synthesis of TAGs, because adipocytes lack glycerol kinase. Instead, the glycerol phosphate required for TAG synthesis is made from pyruvate by glyceroneogenesis, involving the cytosolic PEP carboxykinase (see Fig. 21–22).

In addition to its central function as a fuel depot, adipose tissue plays an important role as an endocrine organ, producing and releasing hormones that signal the state of energy reserves and coordinate metabolism of fats and carbohydrates throughout the body. We return to this function later in the chapter when we discuss the hormonal regulation of body mass.

Brown Adipose Tissue Is Thermogenic

In small vertebrates and hibernating animals, a significant proportion of the adipose tissue is **brown adipose tissue (BAT)**, distinguished from WAT by its smaller (diameter 20 to 40 μm), differently shaped (polygonal, not round) adipocytes (Fig. 23–15b, d). Like white adipocytes, brown adipocytes store TAGs, but in several smaller lipid droplets per cell rather than as a single central droplet. BAT cells have more mitochondria and a richer supply of capillaries and innervation than WAT cells, and it is the cytochromes of mitochondria and the hemoglobin in capillaries that give BAT its characteristic brown color. A unique feature of brown adipocytes is their strong expression of the gene *UCP1*, which encodes **thermogenin**, the mitochondrial uncoupling protein (see Fig. 19–36). Thermogenin activity is responsible for one of the principal functions of BAT: **thermogenesis**.

In brown adipocytes, fatty acids stored in lipid droplets are released, enter mitochondria, and undergo complete conversion to CO_2 via β oxidation and the citric acid cycle. The reduced $FADH_2$ and NADH so generated pass their electrons through the respiratory chain to molecular oxygen. In WAT, protons pumped out of the mitochondria during electron transfer reenter the matrix through ATP synthase, with the energy of electron transfer conserved in ATP synthesis. In BAT, thermogenin provides an alternative route for protons to reenter the matrix that bypasses ATP synthase; the energy of the proton gradient is thus dissipated as heat, which can maintain the body (especially the nervous system and viscera) at its optimal temperature when the ambient temperature is relatively low.

In the human fetus, differentiation of fibroblast preadipocytes into BAT begins at the twentieth week of gestation, and at the time of birth BAT represents 1% to 5% of total body mass. The brown fat deposits are located where the heat generated by thermogenesis can ensure that vital tissues—blood vessels to the head, major abdominal blood vessels, and the viscera, including the pancreas, adrenal glands, and kidneys—are not chilled as the newborn enters a world of lower ambient temperature **(Fig. 23–16)**.

At birth, WAT development begins and BAT begins to disappear. Young adult humans have much-diminished deposits of BAT, from 3% of all adipose tissue in males to 7% in females, making up less than 0.1% of body mass. However, adults apparently have BAT that can be activated by cold exposure and suppressed by increasing the core body temperature (Fig. 23–16b). Adipocytes of BAT produce heat by oxidation of their own fatty acids, but they take up and oxidize both fatty acids and glucose from the blood at rates out of proportion to their mass. In fact, the detection of BAT by PET scanning depends on the adipocytes' relatively high rate of *glucose* uptake and metabolism (Fig. 23–16b). Humans with pheochromocytoma (tumors of the adrenal gland) overproduce epinephrine and norepinephrine, and one effect is differentiation of preadipocytes into discrete regions of BAT, localized roughly as in newborns. In the adaptation to warm or cold surroundings, and in the normal differentiation of WAT and BAT, the nuclear transcription factor PPARγ (described later in the chapter) plays a central role.

Muscles Use ATP for Mechanical Work

Metabolism in the cells of skeletal muscle—**myocytes**—is specialized to generate ATP as the immediate source of energy for contraction. Moreover, skeletal muscle is adapted to do its mechanical work in an intermittent fashion, on demand. Sometimes skeletal muscles must work at their maximum capacity for a short time, as in a 100 m sprint; at other times more prolonged work is required, as in running a marathon or in extended physical labor.

There are two general classes of muscle tissue, which differ in physiological role and fuel utilization. **Slow-twitch muscle**, also called red muscle, provides relatively low tension but is highly resistant to fatigue. It produces ATP by the relatively slow but steady process of oxidative phosphorylation. Red muscle is very rich in mitochondria and is served by very dense networks of blood vessels, which bring the oxygen essential to ATP production. **Fast-twitch muscle**, or white muscle, has fewer mitochondria than red muscle and is less well supplied with blood vessels, but it can develop greater tension and do so faster. White muscle is quicker to fatigue because when active, it uses ATP faster than it can

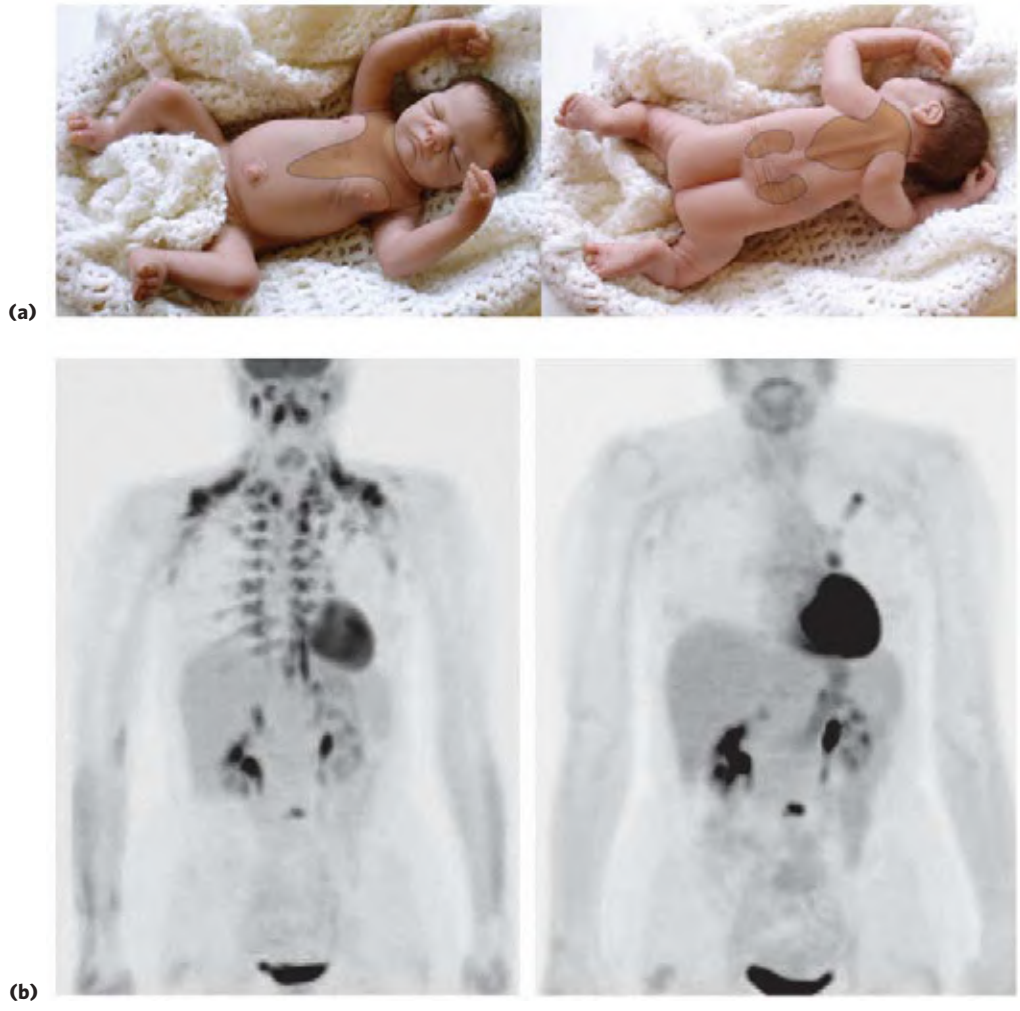

FIGURE 23–16 Brown adipose tissue in infants and adults. (a) At birth, human infants have brown fat distributed as shown here, to protect the spine, major blood vessels, and the internal organs. **(b)** PET scans of a 45-year-old woman injected with ^{18}F-deoxyglucose (to detect tissue that rapidly metabolizes glucose; see Fig. 23–23) reveal tumors of the left lung and lymph node, the right adrenal gland, and a lumbar vertebra (left). The heart and bladder were also intensely labeled as expected, but in addition there was striking metabolic activity in the regions that normally have brown fat in infants. When the same patient was warmed for 48 hours before the PET scan (right), these typical brown fat areas were not active, indicating that this adult had brown fat deposits, which were metabolically active only when the core body temperature was relatively low.

replace it. There is a genetic component to the proportion of red and white muscle in any individual; with training, the endurance of fast-twitch muscle can be improved.

Skeletal muscle can use free fatty acids, ketone bodies, or glucose as fuel, depending on the degree of muscular activity **(Fig. 23–17)**. In resting muscle, the primary fuels are free fatty acids from adipose tissue and ketone bodies from the liver. These are oxidized and degraded to yield acetyl-CoA, which enters the citric acid cycle for oxidation to CO_2. The ensuing transfer of electrons to O_2 provides the energy for ATP synthesis by oxidative phosphorylation. Moderately active muscle uses blood glucose in addition to fatty acids and ketone bodies. The glucose is phosphorylated, then degraded by glycolysis to pyruvate, which is converted to acetyl-CoA and oxidized via the citric acid cycle and oxidative phosphorylation.

In maximally active fast-twitch muscles, the demand for ATP is so great that the blood flow cannot provide O_2 and fuels fast enough to supply sufficient ATP by

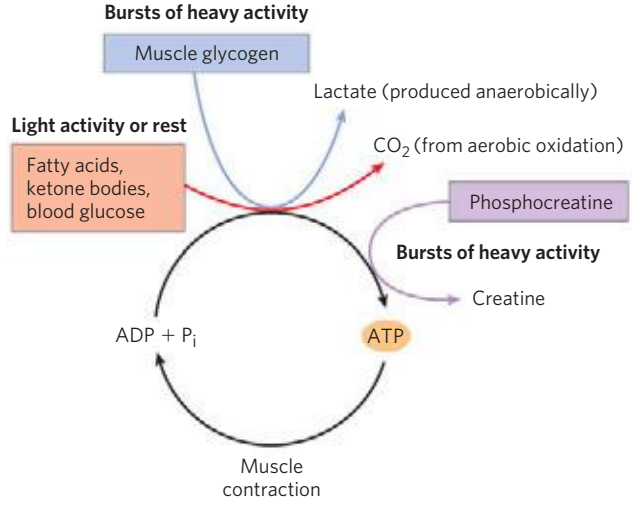

FIGURE 23–17 Energy sources for muscle contraction. Different fuels are used for ATP synthesis during bursts of heavy activity and during light activity or rest. Phosphocreatine can rapidly supply ATP.

BOX 23–2 Creatine and Creatine Kinase: Invaluable Diagnostic Aids and the Muscle Builder's Friends

In animal tissues that have a high and fluctuating need for ATP, primarily skeletal muscle, cardiac muscle, and brain, there are several isozymes of creatine kinase. A cytosolic isozyme is present in regions of high ATP use (myofibrils and sarcoplasmic reticulum, for example). By converting ADP produced during periods of high ATP use back to ATP, this isozyme prevents the accumulation of ADP to concentrations that could inhibit ATP-using enzymes by mass action. Another isozyme of creatine kinase is located in regions where the inner and outer membranes of mitochondria come into contact. This mitochondrial isozyme (mCK) probably serves to shuttle ATP equivalents produced in the mitochondria to cytosolic sites of ATP use (Fig. 1). The species that diffuses from the mitochondrion to ATP-consuming activities in the cytosol is therefore creatine phosphate, not ATP. The mCK isozyme colocalizes with the adenine nucleotide transporter (in the inner mitochondrial membrane) and porin (in the outer mitochondrial membrane), suggesting that these three components may function together to transport ATP formed in the mitochondria into the cytosol.

In knockout mice lacking the mitochondrial isozyme, myocytes compensate by producing more mitochondria, closely associated with myofibrils and sarcoplasmic reticulum, allowing quick diffusion of mitochondrial ATP to those sites of ATP use. Nevertheless, these mice have reduced capacity for running, indicating a defect in some aspect of energy-supplying metabolism.

Creatine and phosphocreatine spontaneously break down to form creatinine (Fig. 2). To maintain high creatine levels, these losses have to be replaced, either by dietary creatine, obtained primarily from meats (muscle) and dairy products, or by the de novo synthesis of creatine from glycine, arginine, and methionine (Fig. 22–28), which occurs primarily in liver and kidney. De novo synthesis of creatine is a major consumer of these amino acids, particularly in

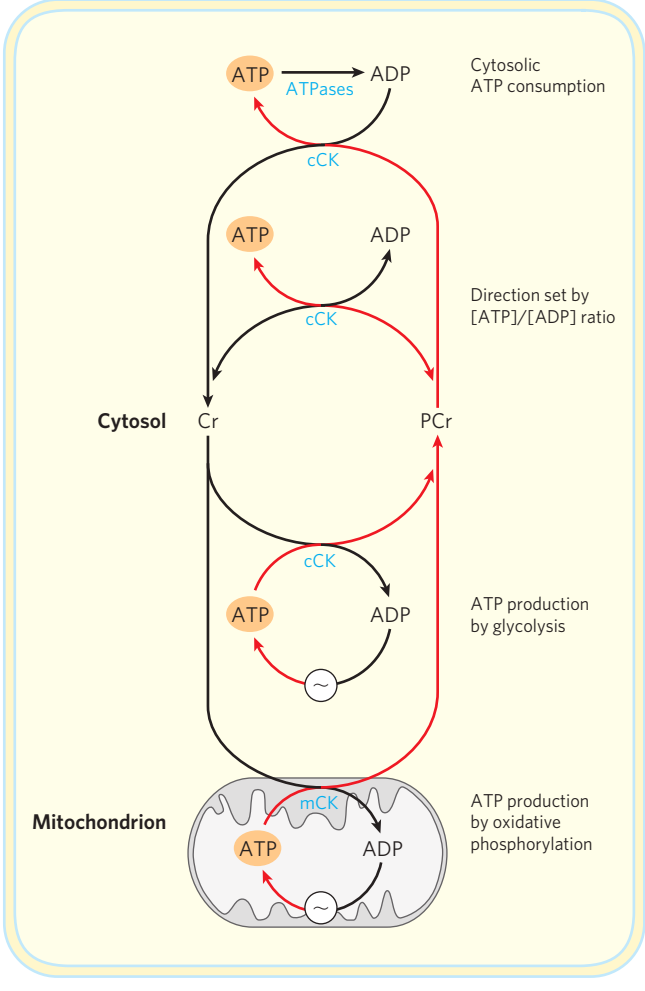

FIGURE 1 Mitochondrial creatine kinase (mCK) transfers a phosphoryl group from ATP to creatine (Cr) to form creatine phosphate (PCr), which diffuses to sites of ATP use, where cytosolic creatine kinase (cCK) then passes the phosphoryl group back into ATP. Cytosolic CK can also use ATP produced by glycolysis to synthesize PCr. During periods of little ATP demand, the pools of ATP and PCr are replenished in preparation for the next period of intense demand for ATP. In resting muscle, the concentration of PCr is 3 to 5 times that of ATP, buffering the cell against rapid depletion of ATP during short bursts of ATP demand.

aerobic respiration alone. Under these conditions, stored muscle glycogen is broken down to lactate by fermentation (p. 548). Each glucose unit degraded yields three ATP, because phosphorolysis of glycogen produces glucose 6-phosphate (via glucose 1-phosphate), sparing the ATP normally consumed in the hexokinase reaction. Lactic acid fermentation thus responds more quickly than oxidative phosphorylation to an increased need for ATP, supplementing basal ATP production by aerobic oxidation of other fuels via the citric acid cycle and respiratory chain. The use of blood glucose and muscle glycogen as fuels for muscular activity is greatly enhanced by the secretion of epinephrine, which stimulates both the release of glucose from liver glycogen and the breakdown of glycogen in muscle tissue. (Epinephrine mediates the so-called fight-or-flight response, discussed more fully below.)

The relatively small amount of glycogen (about 1% of the total weight of skeletal muscle) limits the amount of glycolytic energy available during all-out exertion. Moreover, the accumulation of lactate and consequent decrease in pH in maximally active muscles reduces their efficiency. Skeletal muscle, however, contains another source of ATP, phosphocreatine (10 to 30 mM),

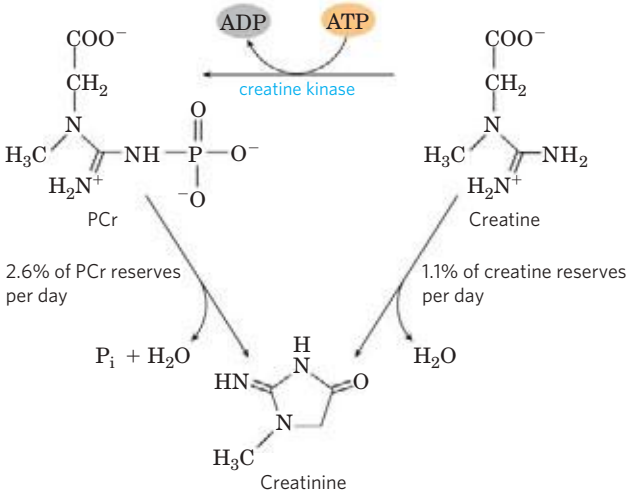

FIGURE 2 Spontaneous (nonenzymatic) formation of creatinine from phosphocreatine or creatine consumes a few percent of total creatine per day, which must be replaced by biosynthesis or from the diet.

FIGURE 3 Body builders often take supplemental creatine to supply creatine phosphate in new muscle tissue.

vegans, for whom this is the only source of creatine; plants do not contain creatine. Muscle tissue has a specific system to take up creatine, exported by liver or kidney, from the blood into cells, against a substantial concentration gradient. Efficient uptake of dietary creatine requires continuous exercise; without exercise, creatine supplementation is of little value.

Heart muscle contains a unique isozyme of creatine kinase (the MB isozyme), which is not normally found in the blood but appears there when released from heart muscle damaged by a heart attack. The blood level of MB begins to rise within 2 hours of the heart attack, typically peaks 12 to 36 hours after the heart attack, and returns to normal levels in 3 to 5 days. Measurement of the MB isozyme in blood therefore confirms the diagnosis of a heart attack and indicates approximately when it occurred.

Body builders who are adding muscle mass have a greater need for creatine and commonly take creatine supplements of up to 20 g per day for a few days, followed by lower maintenance doses. The combination of exercise and creatine supplementation increases muscle mass (Fig. 3) and improves performance in high-intensity, short-duration work. Children with inborn errors in the enzymes of creatine synthesis or uptake suffer severe intellectual disability and seizures. These individuals have much-reduced levels of brain creatine as measured by NMR (see Fig. 23–18). Creatine supplementation raises their brain creatine and creatine phosphate concentrations and brings about partial improvement of the symptoms.

In the healthy kidney, creatinine from creatine breakdown is efficiently cleared from the blood into the urine. When renal function is defective, creatinine levels in the blood rise above the normal range of 0.8 to 1.4 mg/dL. Elevated blood creatinine is associated with renal failure in diabetes and other conditions in which renal function is temporarily or permanently compromised. Renal clearance of creatinine varies slightly with age, race, and gender, so correcting the calculation for those factors yields a more sensitive measure of the extent of renal function, the **glomerular filtration rate (GFR)**.

which can rapidly regenerate ATP from ADP by the creatine kinase reaction:

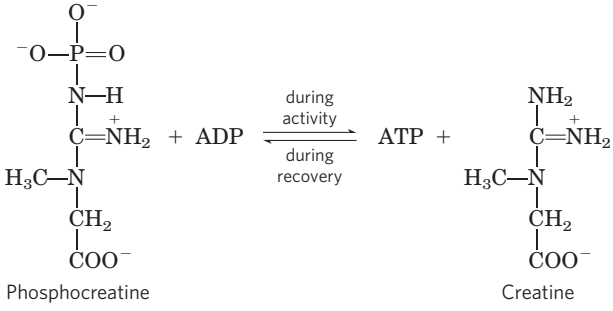

During periods of active contraction and glycolysis, this reaction proceeds predominantly in the direction of ATP synthesis; during recovery from exertion, the same enzyme resynthesizes phosphocreatine from creatine and ATP. Given the relatively high levels of ATP and phosphocreatine in muscle, these compounds can be detected in intact muscle, in real time, by NMR spectroscopy **(Fig. 23–18)**. Creatine serves to shuttle ATP equivalents from the mitochondrion to sites of ATP consumption and can be the limiting factor in the development of new muscle tissue (Box 23–2).

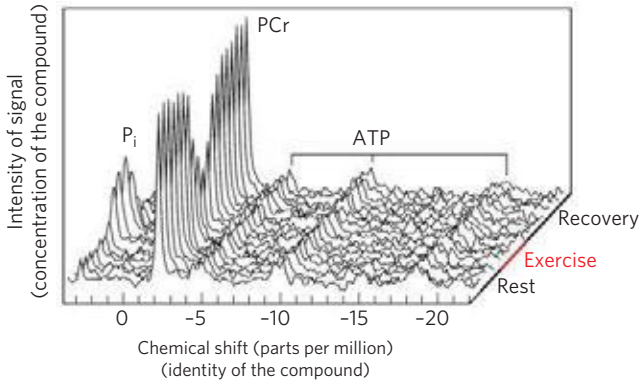

FIGURE 23–18 Phosphocreatine buffers ATP concentration during exercise. A "stack plot" of magnetic resonance spectra (of ^{31}P) showing inorganic phosphate (P_i), phosphocreatine (PCr), and ATP (each of its three phosphates giving a signal). The series of plots represents the passage of time, from a period of rest to one of exercise, and then of recovery. Note that the ATP signal hardly changes during exercise, kept high by continued respiration and by the reservoir of phosphocreatine, which diminishes during exercise. During recovery, when ATP production by catabolism is greater than ATP utilization by the (now resting) muscle, the phosphocreatine reservoir is refilled.

After a period of intense muscular activity, the individual continues breathing heavily for some time, using much of the extra O_2 for oxidative phosphorylation in the liver. The ATP produced is used for gluconeogenesis (in the liver) from lactate that has been carried in the blood from the muscles. The glucose thus formed returns to the muscles to replenish their glycogen, completing the Cori cycle (**Fig. 23–19**; see also Box 15–4).

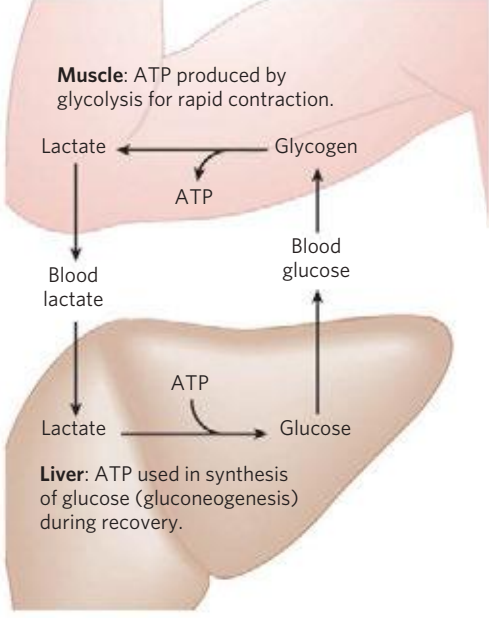

FIGURE 23–19 Metabolic cooperation between skeletal muscle and the liver: the Cori cycle. Extremely active muscles use glycogen as their energy source, generating lactate via glycolysis. During recovery, some of this lactate is transported to the liver and converted to glucose via gluconeogenesis. This glucose is released to the blood and returned to the muscles to replenish their glycogen stores. The overall pathway (glucose ⟶ lactate ⟶ glucose) constitutes the Cori cycle.

Actively contracting skeletal muscle generates heat as a byproduct of imperfect coupling of the chemical energy of ATP with the mechanical work of contraction. This heat production can be put to good use when ambient temperature is low: skeletal muscle carries out **shivering thermogenesis**, rapidly repeated muscle contraction that produces heat but little motion, helping to maintain the body at its preferred temperature of 37 °C.

Heart muscle differs from skeletal muscle in that it is continuously active in a regular rhythm of contraction and relaxation and it has a completely aerobic metabolism at all times. Mitochondria are much more abundant in heart muscle than in skeletal muscle, making up almost half the volume of the cells **(Fig. 23–20)**. The heart uses mainly free fatty acids, but also some glucose and ketone bodies taken up from the blood, as sources of energy; these fuels are oxidized via the citric acid cycle and oxidative phosphorylation to generate ATP. Like skeletal muscle, heart muscle does not store lipids or glycogen in large amounts. It does have small amounts of reserve energy in the form of phosphocreatine, enough for a few seconds of contraction. Because the heart is normally aerobic and obtains its energy from oxidative phosphorylation, the failure of O_2 to reach part of the heart muscle when the blood vessels are blocked by lipid deposits (atherosclerosis) or blood clots (coronary thrombosis) can cause that region of the heart muscle to die. This is what happens in myocardial infarction, more commonly known as a heart attack. ■

The Brain Uses Energy for Transmission of Electrical Impulses

The metabolism of the brain is remarkable in several respects. The neurons of the adult mammalian brain

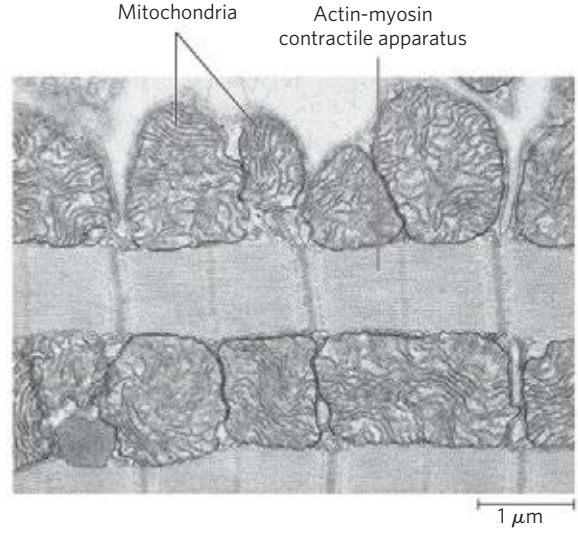

FIGURE 23–20 Electron micrograph of heart muscle. In the profuse mitochondria of heart tissue, pyruvate (from glucose), fatty acids, and ketone bodies are oxidized to drive ATP synthesis. This steady aerobic metabolism allows the human heart to pump blood at a rate of nearly 6 L/min, or about 350 L/h—or 200 × 10^6 L of blood over 70 years.

normally use only glucose as fuel **(Fig. 23–21)**. (Astrocytes, the other major cell type in the brain, can oxidize fatty acids.) The brain has a very active respiratory metabolism **(Fig. 23–22)**; it uses O_2 at a fairly constant rate, accounting for almost 20% of the total O_2 consumed by the body at rest. Because the brain contains very little glycogen, it is constantly dependent on incoming glucose in the blood. Should blood glucose fall significantly below a critical level for even a short time, severe and sometimes irreversible changes in brain function may result.

Although the neurons of the brain cannot directly use free fatty acids or lipids from the blood as fuels, they can, when necessary, use β-hydroxybutyrate (a ketone body), formed from fatty acids in the liver. The capacity of the brain to oxidize β-hydroxybutyrate via acetyl-CoA becomes important during prolonged fasting or starvation, after liver glycogen has been depleted, because it allows the brain to use body fat as an energy source. This spares muscle proteins—until they become the brain's ultimate source of glucose (via gluconeogenesis in the liver) during severe starvation.

Neurons oxidize glucose by glycolysis and the citric acid cycle, and the flow of electrons from these oxidations through the respiratory chain provides almost all the ATP used by these cells. Energy is required to create and maintain an electrical potential across the neuronal plasma membrane. The membrane contains an electrogenic ATP-driven antiporter, the Na^+K^+ ATPase, which simultaneously pumps 2 K^+ ions into and 3 Na^+ ions out of the neuron (see Fig. 11–38). The resulting transmembrane potential changes transiently as an electrical signal (action potential) sweeps from one end of a neuron to the other (see Fig. 12–26). Action potentials are the chief mechanism of information transfer in the nervous system, so depletion of ATP in neurons would have disastrous effects on all activities coordinated by neuronal signaling.

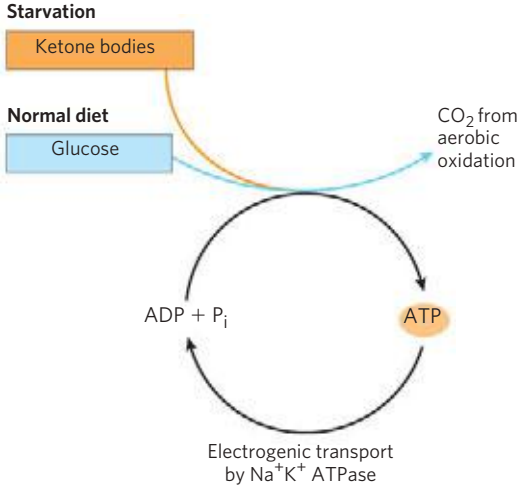

FIGURE 23–21 The fuels that supply ATP in the brain. The energy source used by the brain varies with nutritional state. The ketone body used during starvation is β-hydroxybutyrate. Electrogenic transport by the Na^+K^+ ATPase maintains the transmembrane potential essential to information transfer among neurons.

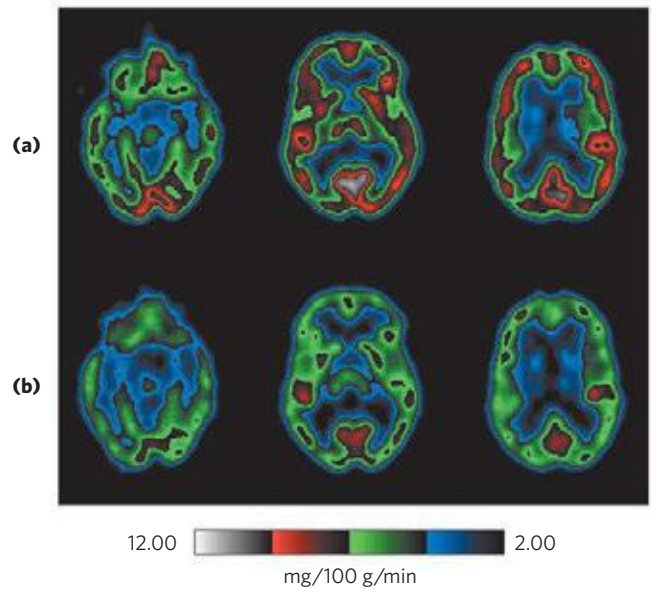

FIGURE 23–22 Glucose metabolism in the brain. The technique of positron emission tomography (PET) scanning shows metabolic activity in specific regions of the brain. PET scans allow visualization of isotopically labeled glucose in precisely localized regions of the brain of a living person, in real time. A positron-emitting glucose analog (2-[^{18}F]-fluoro-2-deoxy-D-glucose) is injected into the bloodstream; a few seconds later, a PET scan shows how much of the glucose has been taken up by each region of the brain—a measure of metabolic activity. Shown here are PET scans of front-to-back cross sections of the brain at three levels, from the top (at the left) downward (to the right). The scans compare glucose metabolism when the experimental subject **(a)** is rested and **(b)** has been deprived of sleep for 48 hours.

Blood Carries Oxygen, Metabolites, and Hormones

Blood mediates the metabolic interactions among all tissues. It transports nutrients from the small intestine to the liver and from the liver and adipose tissue to other organs; it also transports waste products from the extrahepatic tissues to the liver for processing and to the kidneys for excretion. Oxygen moves in the bloodstream from the lungs to the tissues, and CO_2 generated by tissue respiration returns via the bloodstream to the lungs for exhalation. Blood also carries hormonal signals from one tissue to another. In its role as signal carrier, the circulatory system resembles the nervous system: both regulate and integrate the activities of different organs.

The average adult human has 5 to 6 L of blood. Almost half of this volume is occupied by three types of blood cells **(Fig. 23–23)**: **erythrocytes** (red cells), filled with hemoglobin and specialized for carrying O_2 and CO_2; much smaller numbers of **leukocytes**

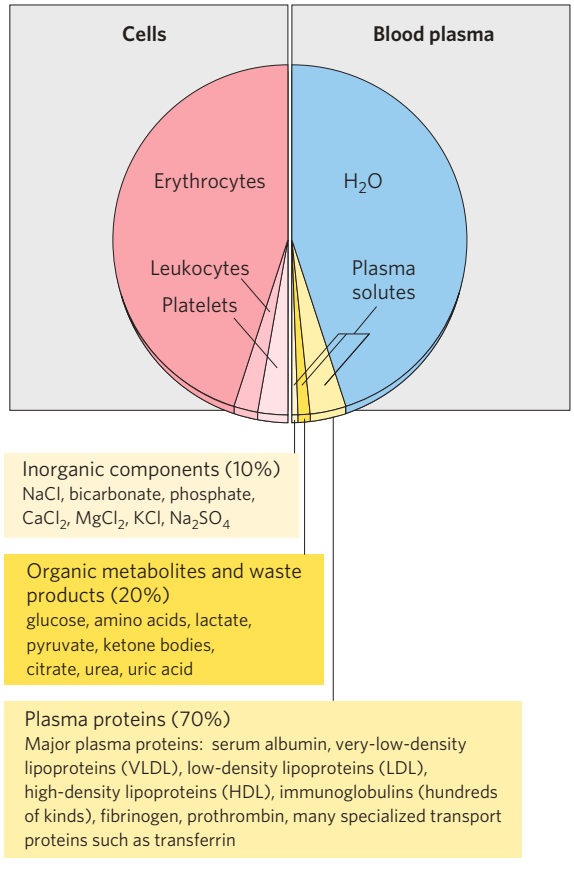

FIGURE 23–23 The composition of blood (by weight). Whole blood can be separated into blood plasma and cells by centrifugation. About 10% of blood plasma is solutes, of which about 10% consists of inorganic salts, 20% small organic molecules, and 70% plasma proteins. The major dissolved components are listed. Blood contains many other substances, often in trace amounts. These include other metabolites, enzymes, hormones, vitamins, trace elements, and bile pigments. Measurements of the concentrations of components in blood plasma are important in the diagnosis and treatment of many diseases.

(white cells) of several types (including **lymphocytes**, also found in lymphatic tissue), which are central to the immune system to defend against infections; and **platelets**, which help to mediate blood clotting. The liquid portion is the **blood plasma**, which is 90% water and 10% solutes. Dissolved or suspended in the plasma is a large variety of proteins, lipoproteins, nutrients, metabolites, waste products, inorganic ions, and hormones. More than 70% of the plasma solids are **plasma proteins**, primarily immunoglobulins (circulating antibodies), serum albumin, apolipoproteins involved in the transport of lipids, transferrin (for iron transport), and blood-clotting proteins such as fibrinogen and prothrombin.

The ions and low molecular weight solutes in blood plasma are not fixed components but are in constant flux between blood and various tissues. Dietary uptake of the inorganic ions that are the predominant electrolytes of blood and cytosol (Na^+, K^+, and Ca^{2+}) is, in general, counterbalanced by their excretion in the urine. For many blood components, something near a dynamic steady state is achieved: the concentration of the component changes little, although a continuous flux occurs between the digestive tract, blood, and urine. The plasma levels of Na^+, K^+, and Ca^{2+} remain close to 140, 5, and 2.5 mM, respectively, with little change in response to dietary intake. Any significant departure from these values can result in serious illness or death. The kidneys play an especially important role in maintaining ion balance by selectively filtering waste products and excess ions out of the blood while preventing the loss of essential nutrients and ions.

The human erythrocyte loses its nucleus and mitochondria during differentiation. It therefore relies on glycolysis alone for its supply of ATP. The lactate produced by glycolysis returns to the liver, where gluconeogenesis converts it to glucose, to be stored as glycogen or recirculated to the peripheral tissues. The erythrocyte has constant access to glucose in the bloodstream.

The concentration of glucose in plasma is subject to tight regulation. We have noted the constant requirement of the brain for glucose and the role of the liver in maintaining blood glucose in the normal range, 60 to 90 mg/100 mL of whole blood (~4.5 mM). (Because erythrocytes make up a significant fraction of blood volume, their removal by centrifugation leaves a supernatant fluid, the plasma, containing the "blood glucose" in a smaller volume. To convert blood glucose to plasma glucose concentration, multiply the blood glucose level by 1.14.) When blood glucose in a human drops to 40 mg/100 mL (the hypoglycemic condition), the person experiences discomfort and mental confusion **(Fig. 23–24)**; further reductions lead to coma, convulsions, and, in extreme hypoglycemia, death. Maintaining the normal concentration of glucose in blood is therefore a very high priority of the organism, and a variety of regulatory mechanisms have evolved to achieve that end. Among the most important regulators of blood glucose are the hormones insulin, glucagon, and epinephrine, as discussed in the next section. ■

SUMMARY 23.2 Tissue-Specific Metabolism: The Division of Labor

- In mammals there is a division of metabolic labor among specialized tissues and organs. The liver is the central distributing and processing organ for nutrients. Sugars and amino acids produced in digestion cross the intestinal epithelium and enter the blood, which carries them to the liver. Some triacylglycerols derived from ingested lipids also make their way to the liver, where the constituent fatty acids are used in a variety of processes.
- Glucose 6-phosphate is the key intermediate in carbohydrate metabolism. It may be polymerized into glycogen, dephosphorylated to blood glucose, or converted to fatty acids via acetyl-CoA. It may

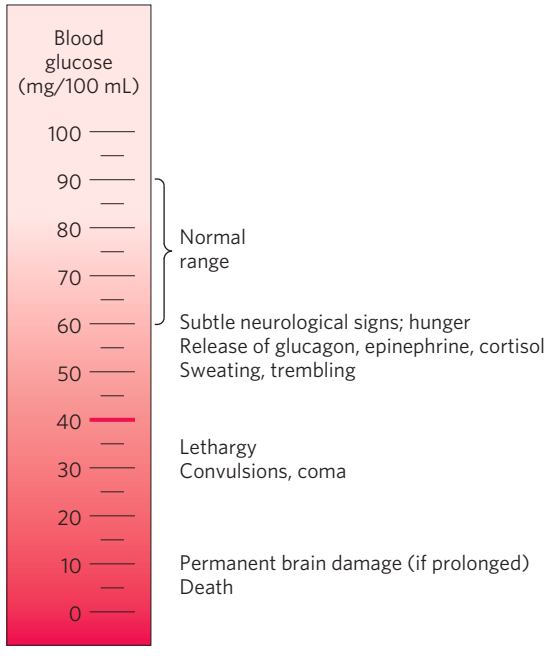

FIGURE 23–24 Physiological effects of low blood glucose in humans. Blood glucose levels of 40 mg/100 mL and below constitute severe hypoglycemia.

undergo oxidation by glycolysis, the citric acid cycle, and respiratory chain to yield ATP, or enter the pentose phosphate pathway to yield pentoses and NADPH.

- Amino acids are used to synthesize liver and plasma proteins, or their carbon skeletons are converted to glucose and glycogen by gluconeogenesis; the ammonia formed by deamination is converted to urea.
- The liver converts fatty acids to triacylglycerols, phospholipids, or cholesterol and its esters for transport as plasma lipoproteins to adipose tissue for storage. Fatty acids can also be oxidized to yield ATP or to form ketone bodies, which are circulated to other tissues.
- White adipose tissue stores large reserves of triacylglycerols and releases them into the blood in response to epinephrine or glucagon. Brown adipose tissue is specialized for thermogenesis, the result of fatty acid oxidation in uncoupled mitochondria.
- Skeletal muscle is specialized to produce and use ATP for mechanical work. During low to moderate muscular activity, oxidation of fatty acids and glucose is the primary source of ATP. During strenuous muscular activity, glycogen is the ultimate fuel, supplying ATP through lactic acid fermentation. During recovery, the lactate is reconverted (through gluconeogenesis) to glycogen and glucose in the liver for use in replenishing muscle glycogen supplies. Phosphocreatine is an immediate source of ATP during active contraction.
- Heart muscle obtains nearly all its ATP from oxidative phosphorylation, with fatty acids as the primary fuel.
- The neurons of the brain use only glucose and β-hydroxybutyrate as fuels, the latter being important during fasting or starvation. The brain uses most of its ATP for the active transport of Na^+ and K^+ to maintain the electrical potential across the neuronal membrane.
- The blood transfers nutrients, waste products, and hormonal signals among tissues and organs. It is made up of cells (erythrocytes, leukocytes, and platelets) and electrolyte-rich water (plasma) containing many proteins.

23.3 Hormonal Regulation of Fuel Metabolism

The minute-by-minute adjustments that keep the blood glucose level near 4.5 mM involve the combined actions of insulin, glucagon, epinephrine, and cortisol on metabolic processes in many body tissues but especially in liver, muscle, and adipose tissue. Insulin signals these tissues that blood glucose is higher than necessary; as a result, cells take up excess glucose from the blood and convert it to glycogen and triacylglycerols for storage. Glucagon signals that blood glucose is too low, and tissues respond by producing glucose through glycogen breakdown and (in the liver) gluconeogenesis and by oxidizing fats to reduce the use of glucose. Epinephrine is released into the blood to prepare the muscles, lungs, and heart for a burst of activity. Cortisol mediates the body's response to longer-term stresses. We discuss these hormonal regulations in the context of three normal metabolic states—well fed, fasted, and starving—and look at the metabolic consequences of diabetes mellitus, a disorder that results from derangements in the signaling pathways that control glucose metabolism.

Insulin Counters High Blood Glucose

Acting through plasma membrane receptors (see Figs 12–15, 12–16), insulin stimulates glucose uptake by muscle and adipose tissue (Table 23–3), where the glucose is converted to glucose 6-phosphate. In the liver, insulin also activates glycogen synthase and inactivates glycogen phosphorylase, so that much of the glucose 6-phosphate is channeled into glycogen.

Insulin also stimulates the storage of excess fuel as fat in adipose tissue **(Fig. 23–25)**. In the liver, insulin activates both the oxidation of glucose 6-phosphate to pyruvate via glycolysis and the oxidation of pyruvate to acetyl-CoA. The excess of acetyl-CoA not needed for energy production is used for fatty acid synthesis, and the fatty acids are exported from the liver as the TAGs

TABLE 23–3 Effects of Insulin on Blood Glucose: Uptake of Glucose by Cells and Storage as Triacylglycerols and Glycogen

Metabolic effect	Target enzyme
↑ Glucose uptake (muscle, adipose)	↑ Glucose transporter (GLUT4)
↑ Glucose uptake (liver)	↑ Glucokinase (increased expression)
↑ Glycogen synthesis (liver, muscle)	↑ Glycogen synthase
↓ Glycogen breakdown (liver, muscle)	↓ Glycogen phosphorylase
↑ Glycolysis, acetyl-CoA production (liver, muscle)	↑ PFK-1 (by ↑ PFK-2) ↑ Pyruvate dehydrogenase complex
↑ Fatty acid synthesis (liver)	↑ Acetyl-CoA carboxylase
↑ Triacylglycerol synthesis (adipose tissue)	↑ Lipoprotein lipase

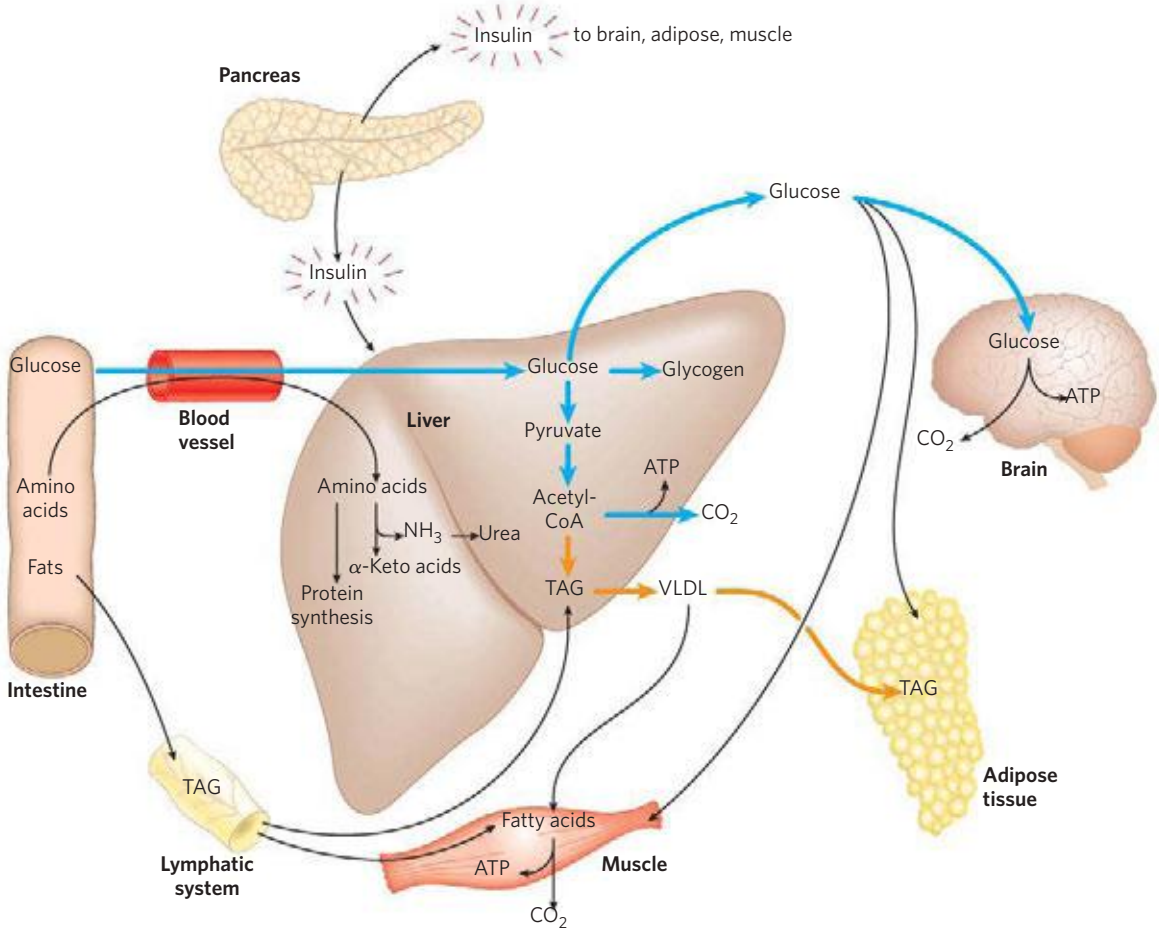

FIGURE 23–25 The well-fed state: the lipogenic liver. Immediately after a calorie-rich meal, glucose, fatty acids, and amino acids enter the liver. Blue arrows follow the path of glucose; orange arrows follow the path of lipids. Insulin released in response to the high blood glucose concentration stimulates glucose uptake by the tissues. Some glucose is exported to the brain for its energy needs and some to adipose and muscle tissue. In the liver, excess glucose is oxidized to acetyl-CoA, which is used to synthesize fatty acids for export as triacylglycerols in VLDLs to adipose and muscle tissue. The NADPH necessary for lipid synthesis is obtained by oxidation of glucose in the pentose phosphate pathway. Excess amino acids are converted to pyruvate and acetyl-CoA, which are also used for lipid synthesis. Dietary fats move via the lymphatic system, as chylomicrons, from the intestine to the liver, muscle, and adipose tissues.

of plasma lipoproteins (VLDL; see Fig. 21–40) to adipose tissue. Insulin stimulates the synthesis of TAGs in adipocytes, from fatty acids released from the VLDL triacylglycerols. These fatty acids are ultimately derived from the excess glucose taken up from blood by the liver. In summary, the effect of insulin is to favor the conversion of excess blood glucose to two storage forms: glycogen (in the liver and muscle) and triacylglycerols (in adipose tissue).

Besides acting directly on muscle and liver to change their metabolism of carbohydrates and fats, insulin can act in the brain to signal these tissues indirectly, as described later.

Pancreatic β Cells Secrete Insulin in Response to Changes in Blood Glucose

When glucose enters the bloodstream from the intestine after a carbohydrate-rich meal, the resulting increase in blood glucose causes increased secretion of insulin (and decreased secretion of glucagon) by the pancreas. Insulin release is largely regulated by the level of glucose in the blood supplying the pancreas. The peptide hormones insulin, glucagon, and somatostatin are produced by clusters of specialized pancreatic cells, the islets of Langerhans **(Fig. 23–26)**. Each cell type of the islets produces a single hormone: α cells produce glucagon; β cells, insulin; and δ cells, somatostatin.

As shown in **Figure 23–27**, when blood glucose rises, ❶ GLUT2 transporters carry glucose into the

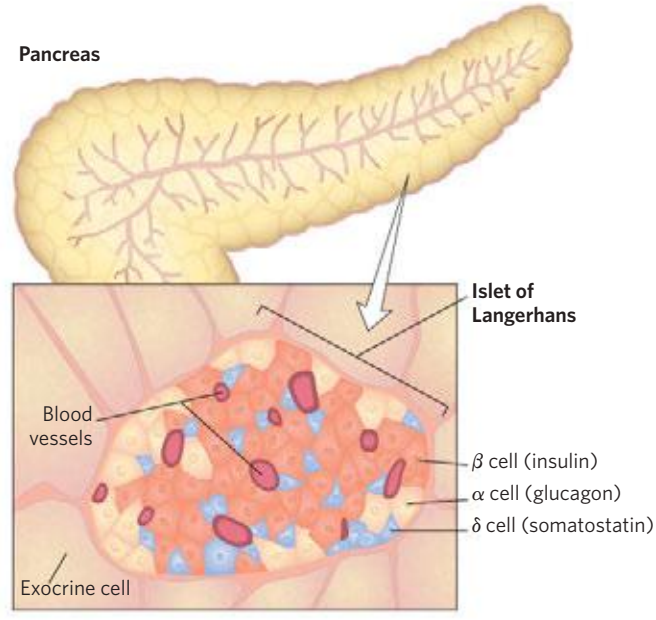

FIGURE 23–26 The endocrine system of the pancreas. The pancreas contains both exocrine cells (see Fig. 18–3b), which secrete digestive enzymes in the form of zymogens, and clusters of endocrine cells, the islets of Langerhans. The islets contain α, β, and δ cells (also known as A, B, and D cells, respectively), each cell type secreting a specific peptide hormone.

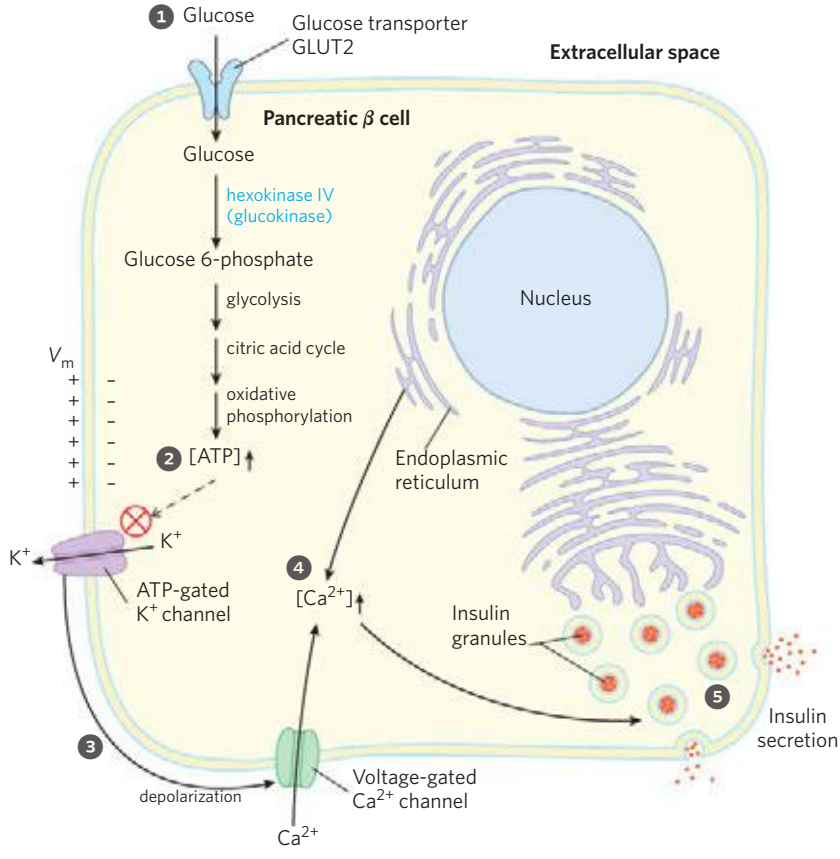

FIGURE 23–27 Glucose regulation of insulin secretion by pancreatic β cells. When the blood glucose level is high, active metabolism of glucose in the β cell raises intracellular [ATP], closing K^+ channels in the plasma membrane and thus depolarizing the membrane. In response to this membrane-depolarization triggered by high [ATP], voltage-gated Ca^{2+} channels open, allowing Ca^{2+} to flow into the cell. (Ca^{2+} is also released from the endoplasmic reticulum, in response to the initial elevation of [Ca^{2+}] in the cytosol.) Cytosolic [Ca^{2+}] is now high enough to trigger insulin release by exocytosis. The numbered processes are discussed in the text.

β cells, where it is immediately converted to glucose 6-phosphate by hexokinase IV (glucokinase) and enters glycolysis. With the higher rate of glucose catabolism, ❷ [ATP] increases, causing the closing of **ATP-gated K^+ channels** in the plasma membrane. ❸ Reduced efflux of K^+ depolarizes the membrane. (Recall from Section 12.6 that exit of K^+ through an open K^+ channel hyperpolarizes the membrane; closing the K^+ channel therefore effectively depolarizes the membrane.) Membrane depolarization opens voltage-gated Ca^{2+} channels, and ❹ the resulting increase in cytosolic [Ca^{2+}] triggers ❺ the release of insulin by exocytosis. The brain integrates inputs on energy supply and demand, and signals from the parasympathetic and sympathetic nervous system also affect (stimulate and inhibit, respectively) insulin release. A simple feedback loop limits hormone release: insulin lowers blood glucose by stimulating glucose uptake by the tissues; the reduced blood glucose is detected by the β cell as a diminished flux through the hexokinase reaction; this slows or stops the release of insulin. This feedback regulation holds blood glucose concentration nearly constant despite large fluctuations in dietary intake.

The activity of ATP-gated K^+ channels is central to the regulation of insulin secretion by β cells. The channels are octamers of four identical Kir6.2 subunits and four identical SUR1 subunits and are constructed along the same lines as the K^+ channels of bacteria and those of other eukaryotic cells (see Figs 11–47 and 11–48). The four Kir6.2 subunits form a cone around the K^+ channel and function as the selectivity filter and ATP-gating mechanism **(Fig. 23–28)**. When [ATP] rises (indicating increased blood glucose), the K^+ channels close, depolarizing the plasma membrane and triggering insulin release as shown in Figure 23–27.

The **sulfonylurea drugs**, oral medications used in the treatment of type 2 diabetes mellitus, bind to the SUR1 (*sulfonylurea receptor*) subunits of the K^+ channels, closing the channels and stimulating insulin release. The first generation of these drugs (tolbutamide, for example) was developed in the 1950s. The second-generation drugs, including glyburide (Micronase), glipizide (Glucotrol), and glimepiride (Amaryl), are more potent and have fewer side effects. (The sulfonylurea moiety is screened light red in the following structures.) The sulfonylureas are sometime used in combination with injected insulin but often suffice alone for controlling type 2 diabetes.

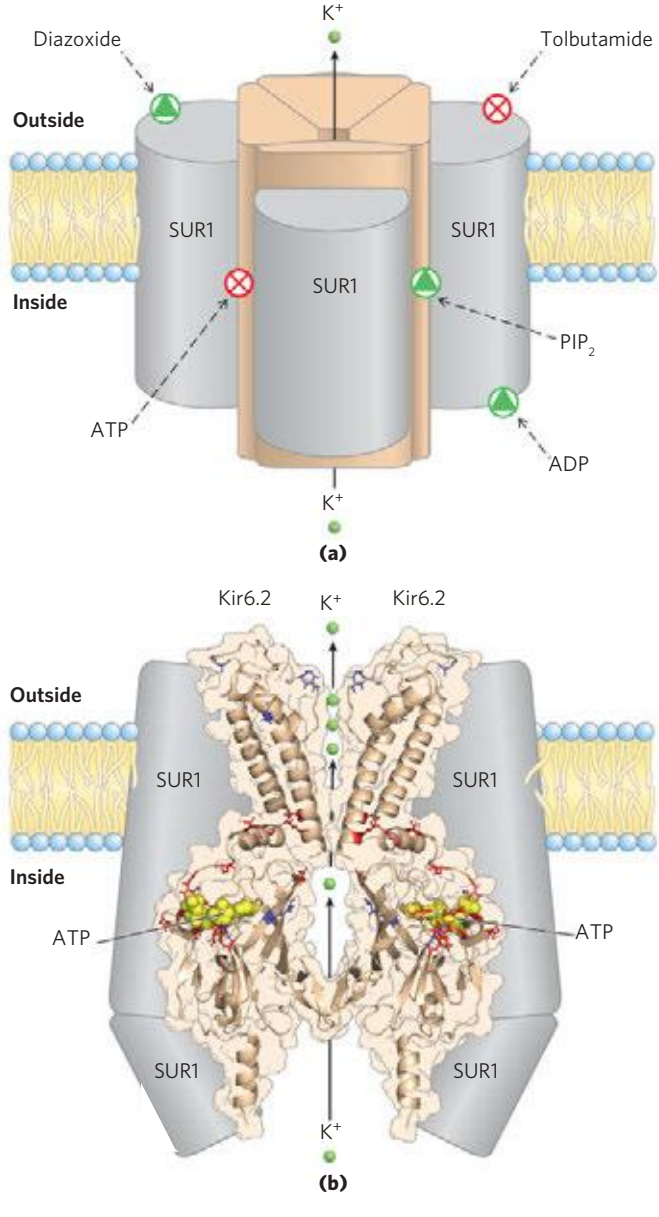

FIGURE 23–28 ATP-gated K^+ channels in β cells. (a) The ATP-gated channel, viewed in the plane of the membrane. The channel is formed by four identical Kir6.2 subunits, and outside those are four SUR1 (sulfonylurea receptor) subunits. The SUR1 subunits have binding sites for ADP and the drug diazoxide, which favor the open channel, and tolbutamide, a sulfonylurea drug that favors the closed channel. The Kir6.2 subunits constitute the actual channel, and they contain, on the cytosolic side, binding sites for ATP and phosphatidylinositol 4,5-bisphosphate (PIP_2), which favor the closed and the open channel, respectively. **(b)** The structure of the Kir6.2 portion of the channel, viewed in the plane of the membrane. For clarity, only two transmembrane domains and two cytosolic domains are shown. Three K^+ ions (green) are shown in the region of the selectivity filter. Mutation in certain amino acid residues (shown in red) leads to neonatal diabetes; mutation in others (shown in blue) leads to hyperinsulinism of infancy. This structure (coordinates courtesy of Frances Ashford and her colleagues at the University of Oxford) was obtained not directly by crystallography but by mapping the known Kir6.2 sequence onto the crystal structures of a bacterial Kir channel (KirBac1.1; PDB ID 1P7B) and the amino and carboxyl domains of another Kir protein, Kir3.1 (PDB ID 1U4E). Compare this structure with the gated K^+ channel in Figure 11–48.

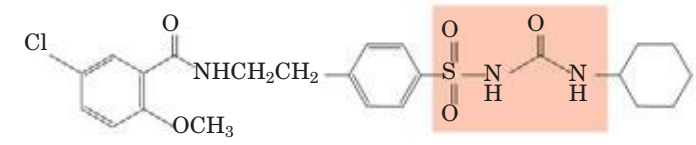

Glyburide

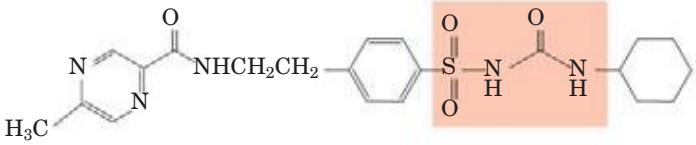

Glipizide

Mutations in the ATP-gated K^+ channels of β cells are, fortunately, rare. Mutations in Kir6.2 that result in constantly *open* K^+ channels (red residues in Fig. 23–28b) lead to neonatal diabetes mellitus, with severe hyperglycemia that requires insulin therapy. Other mutations in Kir6.2 or SUR1 (blue residues in Fig. 23–28b) produce permanently *closed* K^+ channels and continuous release of insulin. If untreated, individuals with these mutations develop congenital hyperinsulinemia (hyperinsulinism of infancy); excessive insulin causes severe hypoglycemia (low blood glucose) leading to irreversible brain damage. One effective treatment is surgical removal of part of the pancreas to reduce insulin production. ■

Glucagon Counters Low Blood Glucose

Several hours after the intake of dietary carbohydrate, blood glucose levels fall slightly because of the ongoing oxidation of glucose by the brain and other tissues. Lowered blood glucose triggers secretion of **glucagon** and decreases insulin release **(Fig. 23–29)**.

Glucagon causes an *increase* in blood glucose concentration in several ways (Table 23–4). Like epinephrine, it stimulates the net breakdown of liver glycogen by activating glycogen phosphorylase and inactivating glycogen synthase; both effects are the result of phosphorylation of the regulated enzymes, triggered by cAMP. Glucagon inhibits glucose breakdown by glycolysis in the liver and stimulates glucose synthesis by gluconeogenesis. Both effects result from lowering the concentration of fructose 2,6-bisphosphate, an allosteric inhibitor of the gluconeogenic enzyme fructose 1,6-bisphosphatase (FBPase-1) and an activator of the glycolytic enzyme phosphofructokinase-1. Recall that [fructose 2,6-bisphosphate] is ultimately controlled by a cAMP-dependent protein phosphorylation reaction (see Fig. 15–19) Glucagon also inhibits the glycolytic enzyme pyruvate kinase (by promoting its cAMP-dependent phosphorylation), thus blocking the conversion of phosphoenolpyruvate to pyruvate and preventing oxidation of pyruvate via the citric acid cycle. The resulting

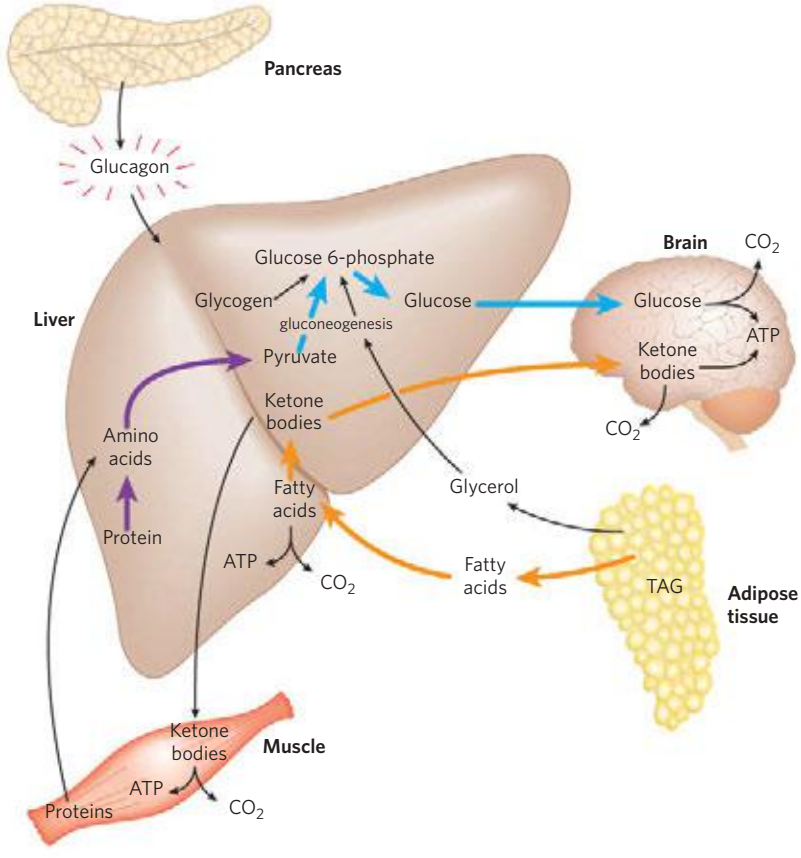

FIGURE 23–29 The fasting state: the glucogenic liver. After some hours without a meal, the liver becomes the principal source of glucose for the brain. Liver glycogen is broken down, and the glucose 1-phosphate produced is converted to glucose 6-phosphate, then to free glucose, which is released into the bloodstream. Amino acids from the degradation of proteins in liver and muscle, and glycerol from the breakdown of TAGs in adipose tissue, are used for gluconeogenesis. The liver uses fatty acids as its principal fuel, and excess acetyl-CoA is converted to ketone bodies for export to other tissues; the brain is especially dependent on this fuel when glucose is in short supply (see Fig. 23–21). (Blue arrows follow the path of glucose; orange arrows, the path of lipids; and purple arrows, the path of amino acids.)

TABLE 23–4 Effects of Glucagon on Blood Glucose: Production and Release of Glucose by the Liver

Metabolic effect	Effect on glucose metabolism	Target enzyme
↑ Glycogen breakdown (liver)	Glycogen ⟶ glucose	↑ Glycogen phosphorylase
↓ Glycogen synthesis (liver)	Less glucose stored as glycogen	↓ Glycogen synthase
↓ Glycolysis (liver)	Less glucose used as fuel in liver	↓ PFK-1
↑ Gluconeogenesis (liver)	Amino acids, Glycerol, Oxaloacetate ⟶ glucose	↑ FBPase-2 ↓ Pyruvate kinase ↑ PEP carboxykinase
↑ Fatty acid mobilization (adipose tissue)	Less glucose used as fuel by liver, muscle	↑ Hormone-sensitive lipase
		↑ PKA (perilipin–Ⓟ)
↑ Ketogenesis	Provides alternative to glucose as energy source for brain	↓ Acetyl-CoA carboxylase

accumulation of phosphoenolpyruvate favors gluconeogenesis. This effect is augmented by glucagon's stimulation of the synthesis of the gluconeogenic enzyme PEP carboxykinase. By stimulating glycogen breakdown, preventing glycolysis, and promoting gluconeogenesis in hepatocytes, glucagon enables the liver to export glucose, restoring blood glucose to its normal level.

Although its primary target is the liver, glucagon (like epinephrine) also affects adipose tissue, activating TAG breakdown by causing cAMP-dependent phosphorylation of perilipin and hormone-sensitive lipase. The activated lipase liberates free fatty acids, which are exported to the liver and other tissues as fuel, sparing glucose for the brain. The net effect of glucagon is therefore to stimulate glucose synthesis and release by the liver and to mobilize fatty acids from adipose tissue, to be used instead of glucose by tissues other than the brain. All these effects of glucagon are mediated by cAMP-dependent protein phosphorylation.

During Fasting and Starvation, Metabolism Shifts to Provide Fuel for the Brain

The fuel reserves of a healthy adult human are of three types: glycogen stored in the liver and, in smaller quantities, in muscles; large quantities of triacylglycerols in adipose tissues; and tissue proteins, which can be degraded when necessary to provide fuel (Table 23–5).

TABLE 23–5 Available Metabolic Fuels in a Normal-Weight, 70 kg Man and in an Obese, 140 kg Man at the Beginning of a Fast

Type of fuel	Weight (kg)	Caloric equivalent (thousands of kcal (kJ))	Estimated survival (months)*
Normal-weight, 70 kg man			
Triacylglycerols (adipose tissue)	15	140 (590)	
Proteins (mainly muscle)	6	24 (100)	
Glycogen (muscle, liver)	0.23	0.90 (3.8)	
Circulating fuels (glucose, fatty acids, triacylglycerols, etc.)	0.023	0.10 (0.42)	
Total		165 (690)	3
Obese, 140 kg man			
Triacylglycerols (adipose tissue)	80	750 (3,100)	
Proteins (mainly muscle)	8	32 (130)	
Glycogen (muscle, liver)	0.23	0.92 (3.8)	
Circulating fuels	0.025	0.11 (0.46)	
Total		783 (3,200)	14

*Survival time is calculated on the assumption of a basal energy expenditure of 1,800 kcal/day.

Two hours after a meal, the blood glucose level is diminished slightly, and tissues receive glucose released from liver glycogen. There is little or no synthesis of triacylglycerols. By four hours after a meal, blood glucose has fallen further, insulin secretion has slowed, and glucagon secretion has increased. These hormonal signals mobilize triacylglycerols from adipose tissue, which now become the primary fuel for muscle and liver. **Figure 23–30** shows the responses to prolonged fasting. ❶ To provide glucose for the brain, the liver degrades certain proteins—those most expendable in an organism not ingesting food. Their nonessential amino acids are transaminated or deaminated (Chapter 18), and ❷ the extra amino groups are converted to urea, which is exported via the bloodstream to the kidneys and excreted in the urine.

Also in the liver, and to some extent in the kidneys, the carbon skeletons of glucogenic amino acids are converted to pyruvate or intermediates of the citric acid cycle. ❸ These intermediates (as well as the glycerol derived from TAGs in adipose tissue) provide the starting materials for gluconeogenesis in the liver, ❹ yielding glucose for export to the brain. ❺ Fatty acids released from adipose tissue are oxidized to acetyl-CoA in the liver, but as oxaloacetate is depleted by the use of citric acid cycle intermediates for gluconeogenesis, ❻ entry of

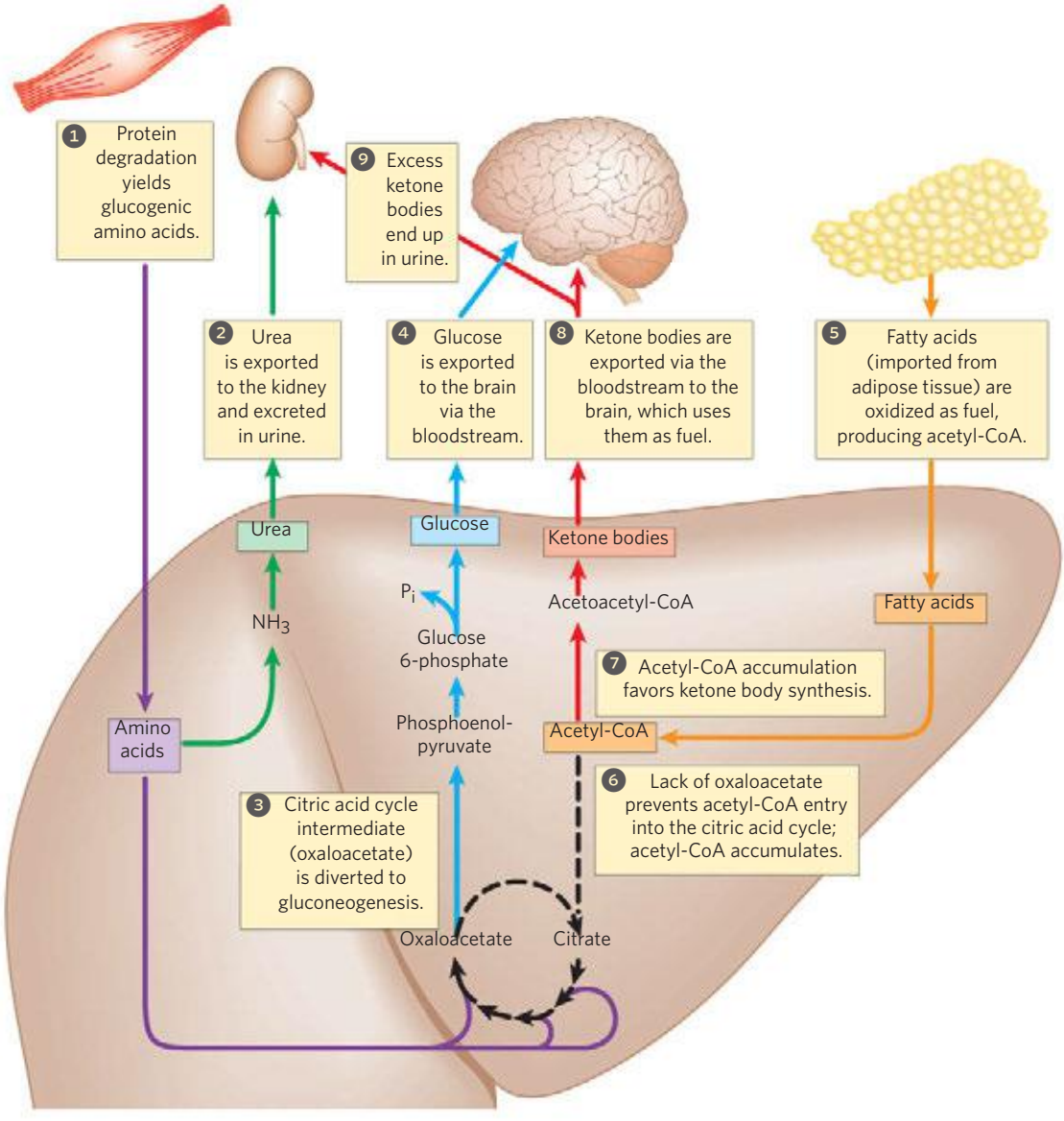

FIGURE 23–30 Fuel metabolism in the liver during prolonged fasting or in uncontrolled diabetes mellitus. The numbered steps are described in the text. After depletion of stored carbohydrates (glycogen), gluconeogenesis in the liver becomes the main source of glucose for the brain (blue arrows). NH_3 from amino acid deamination is converted into urea and excreted (green arrows). Glucogenic amino acids from protein breakdown (purple arrows) provide substrates for gluconeogenesis), and glucose is exported to the brain. Fatty acids from adipose tissue are imported into the liver and oxidized to acetyl-CoA (orange arrows), and acetyl-CoA is the starting material for ketone body formation in the liver and export to brain to serve as the principal energy source (red arrows). When the concentration of ketone bodies in the blood exceeds the ability of the kidneys to reabsorb ketones, these compounds begin to appear in the urine.

acetyl-CoA into the cycle is inhibited and acetyl-CoA accumulates. ❼ This favors the formation of acetoacetyl-CoA and ketone bodies. After a few days of fasting, the levels of ketone bodies in the blood rise **(Fig. 23–31)** as they are exported from the liver to the heart, skeletal muscle, and brain, which use these fuels instead of glucose (Fig. 23–30, ❽).

Acetyl-CoA is a critical regulator of the fate of pyruvate: it allosterically inhibits pyruvate dehydrogenase and stimulates pyruvate carboxylase. In these ways, acetyl-CoA prevents its own further production from pyruvate while stimulating the conversion of pyruvate to oxaloacetate, the first step in gluconeogenesis.

Triacylglycerols stored in the adipose tissue of a normal-weight adult could provide enough fuel to maintain a basal rate of metabolism for about three months; a very obese adult has enough stored fuel to endure a fast of more than a year (Table 23–5). When fat reserves are gone, the degradation of *essential* proteins begins; this leads to loss of heart and liver function and, in prolonged starvation, to death. Stored fat can provide adequate energy (calories) during a fast or rigid diet, but vitamins and minerals must be provided, and sufficient dietary glucogenic amino acids are needed to replace those being used for gluconeogenesis. Rations for those on a weight-reduction diet are commonly fortified with vitamins, minerals, and amino acids or proteins.

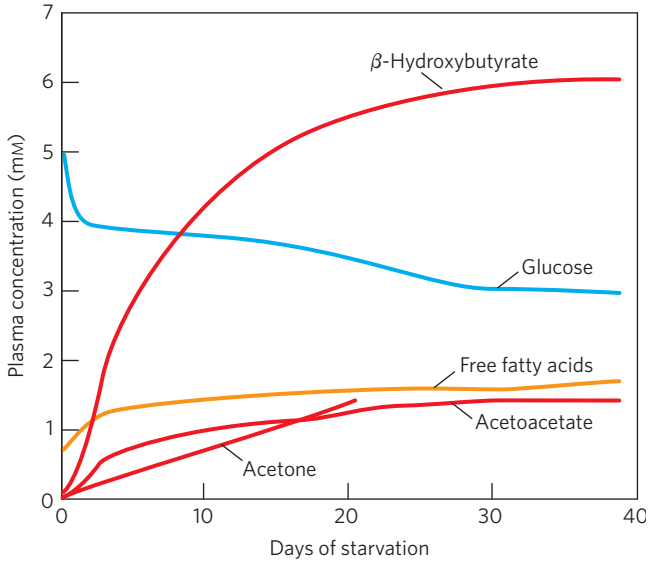

FIGURE 23–31 Plasma concentrations of fatty acids, glucose, and ketone bodies during six weeks of starvation. Despite the hormonal mechanisms for maintaining the level of glucose in blood, glucose begins to diminish within 2 days of fasting (blue). The level of ketone bodies, almost unmeasurable before the fast, rises dramatically after 2 to 4 days of fasting (red), with β-hydroxybutyrate as the major contributor. These water-soluble ketones, acetoacetate and β-hydroxybutyrate, supplement glucose as an energy source for the brain during a long fast. Acetone, a minor ketone body, is not metabolized but is eliminated in the breath. A much smaller rise in blood fatty acids (orange) also occurs, but this rise does not contribute to energy metabolism in the brain, as fatty acids do not cross the blood-brain barrier.

Epinephrine Signals Impending Activity

When an animal is confronted with a stressful situation that requires increased activity—fighting or fleeing, in the extreme case—neuronal signals from the brain trigger the release of epinephrine and norepinephrine from the adrenal medulla. Both hormones dilate the respiratory passages to facilitate the uptake of O_2, increase the rate and strength of the heartbeat, and raise the blood pressure, thereby promoting the flow of O_2 and fuels to the tissues (Table 23–6). This is the "fight or flight" response.

Epinephrine acts primarily on muscle, adipose, and liver tissues. It activates glycogen phosphorylase and inactivates glycogen synthase by cAMP-dependent phosphorylation of the enzymes, thus stimulating the conversion of *liver* glycogen to blood glucose, the fuel for anaerobic muscular work. Epinephrine also promotes the anaerobic breakdown of *muscle* glycogen by lactic acid fermentation, stimulating glycolytic ATP formation. The stimulation of glycolysis is accomplished by raising the concentration of fructose 2,6-bisphosphate, a potent allosteric activator of the key glycolytic enzyme phosphofructokinase-1. Epinephrine also stimulates fat mobilization in adipose tissue, activating (by cAMP-dependent phosphorylation) hormone-sensitive lipase and moving aside the perilipin covering the lipid droplet surface (see Fig. 17–3). Finally, epinephrine stimulates glucagon secretion and inhibits insulin secretion, reinforcing its effect of mobilizing fuels and inhibiting fuel storage.

Cortisol Signals Stress, Including Low Blood Glucose

A variety of stressors (anxiety, fear, pain, hemorrhage, infection, low blood glucose, starvation) stimulate release of the corticosteroid hormone **cortisol** from the adrenal cortex. Cortisol acts on muscle, liver, and adipose tissue to supply the organism with fuel to withstand the stress. Cortisol is a relatively slow-acting hormone that alters metabolism by changing the kinds and amounts of certain enzymes synthesized in its target cells rather than by regulating the activity of existing enzyme molecules.

In adipose tissue, cortisol leads to an increase in the release of fatty acids from stored TAGs. The exported fatty acids serve as fuel for other tissues, and the glycerol is used for gluconeogenesis in the liver. Cortisol stimulates the breakdown of nonessential muscle proteins and the export of amino acids to the liver, where they serve as precursors for gluconeogenesis. In the liver, cortisol promotes gluconeogenesis by stimulating synthesis of the key enzyme PEP carboxykinase; glucagon has the same effect, whereas insulin has the opposite effect. Glucose produced in this way is stored in the liver as glycogen or exported immediately to tissues that need glucose for fuel. The net effect of these metabolic changes is to restore blood glucose to its normal level and to increase glycogen stores, ready to support the fight-or-flight response commonly associated with stress. The effects of

TABLE 23–6 Physiological and Metabolic Effects of Epinephrine: Preparation for Action

Immediate effect	Overall effect
Physiological	
↑ Heart rate ↑ Blood pressure ↑ Dilation of respiratory passages	Increase delivery of O_2 to tissues (muscle)
Metabolic	
↑ Glycogen breakdown (muscle, liver) ↓ Glycogen synthesis (muscle, liver) ↑ Gluconeogenesis (liver)	Increase production of glucose for fuel
↑ Glycolysis (muscle)	Increases ATP production in muscle
↑ Fatty acid mobilization (adipose tissue)	Increases availability of fatty acids as fuel
↑ Glucagon secretion ↓ Insulin secretion	Reinforce metabolic effects of epinephrine

cortisol therefore counterbalance those of insulin. During extended periods of stress, the continued release of cortisol loses its positive adaptive value and begins to cause damage to muscle and bone and to impair endocrine and immune function.

Diabetes Mellitus Arises from Defects in Insulin Production or Action

Diabetes mellitus is a relatively common disease: nearly 6% of the U.S. population shows some degree of abnormality in glucose metabolism that is indicative of diabetes or a tendency toward the condition. There are two major clinical classes of diabetes mellitus: **type 1 diabetes**, sometimes referred to as insulin-dependent diabetes mellitus (IDDM), and **type 2 diabetes**, or non–insulin-dependent diabetes mellitus (NIDDM), also called insulin-resistant diabetes.

Type 1 diabetes begins early in life, and symptoms quickly become severe. This disease responds to insulin injection, because the metabolic defect stems from an autoimmune destruction of pancreatic β cells and a consequent inability to produce sufficient insulin. Type 1 diabetes requires both insulin therapy and careful, lifelong control of the balance between dietary intake and insulin dose. Characteristic symptoms of type 1 (and type 2) diabetes are excessive thirst and frequent urination (polyuria), leading to the intake of large volumes of water (polydipsia) ("diabetes mellitus" means "excessive excretion of sweet urine"). These symptoms are due to the excretion of large amounts of glucose in the urine, a condition known as **glucosuria**.

Type 2 diabetes is slow to develop (typically in older, obese individuals), and the symptoms are milder and often go unrecognized at first. This is really a group of diseases in which the regulatory activity of insulin is disordered: insulin is produced, but some feature of the insulin-response system is defective. Individuals with this disorder are insulin-resistant. The connection between type 2 diabetes and obesity (discussed below) is an active and exciting area of research.

Individuals with either type of diabetes are unable to take up glucose efficiently from the blood; recall that insulin triggers the movement of GLUT4 glucose transporters to the plasma membrane in muscle and adipose tissue (see Fig. 12–16). With glucose unavailable, fatty acids become the principal fuel, which leads to another characteristic metabolic change in diabetes: excessive but incomplete oxidation of fatty acids in the liver. The acetyl-CoA produced by β oxidation cannot be completely oxidized by the citric acid cycle, because the high [NADH]/[NAD^+] ratio produced by β oxidation inhibits the cycle (recall that three steps of the cycle convert NAD^+ to NADH). Accumulation of acetyl-CoA leads to overproduction of the ketone bodies, acetoacetate and β-hydroxybutyrate, which cannot be used by extrahepatic tissues as fast as they are made in the liver. In addition to β-hydroxybutyrate and acetoacetate, the blood of individuals with diabetes also contains acetone, which results from the spontaneous decarboxylation of acetoacetate:

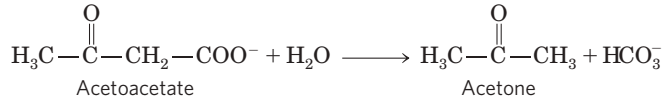

Acetone is volatile and is exhaled, and in uncontrolled diabetes the breath has a characteristic odor sometimes mistaken for ethanol. A diabetic individual who is experiencing mental confusion due to high blood glucose is occasionally misdiagnosed as intoxicated, an error that can be fatal. The overproduction of ketone bodies, called **ketosis**, results in greatly increased concentrations of ketone bodies in the blood (ketonemia) and urine (ketonuria).

The ketone bodies are carboxylic acids, which ionize, releasing protons. In uncontrolled diabetes this acid production can overwhelm the capacity of the blood's bicarbonate buffering system and produce a lowering of blood pH called **acidosis** or, in combination with ketosis, **ketoacidosis**, a potentially life-threatening condition.

Biochemical measurements on blood and urine samples are essential in the diagnosis and treatment of diabetes. A sensitive diagnostic criterion is provided by the **glucose-tolerance test**. The individual fasts overnight, then drinks a test dose of 100 g of glucose dissolved in a glass of water. The blood glucose concentration is measured before the test dose and at 30 min intervals for several hours thereafter. A healthy individual assimilates the glucose readily, the blood glucose rising to no more than about 9 or 10 mM; little or no glucose appears in the urine. In diabetes, individuals assimilate the test dose of glucose poorly; their blood glucose level rises dramatically and returns to the fasting level very slowly. Because the blood glucose levels exceed the kidney threshold (about 10 mM), glucose also appears in the urine. ■

SUMMARY 23.3 Hormonal Regulation of Fuel Metabolism

- The concentration of glucose in blood is hormonally regulated. Fluctuations in blood glucose (normally 60 to 90 mg/100 mL, or about 4.5 mM) due to dietary intake or vigorous exercise are counterbalanced by a variety of hormonally triggered changes in metabolism in several organs.
- High blood glucose elicits the release of insulin, which speeds the uptake of glucose by tissues and favors the storage of fuels as glycogen and triacylglycerols while inhibiting fatty acid mobilization in adipose tissue.
- Low blood glucose triggers release of glucagon, which stimulates glucose release from liver glycogen and shifts fuel metabolism in liver and muscle to fatty acid oxidation, sparing glucose for use by the brain. In prolonged fasting, triacylglycerols become the principal fuel; the liver converts the fatty acids to ketone bodies for export to other tissues, including the brain.
- Epinephrine prepares the body for increased activity by mobilizing glucose from glycogen and other precursors, releasing it into the blood.
- Cortisol, released in response to a variety of stressors (including low blood glucose), stimulates gluconeogenesis from amino acids and glycerol in the liver, thus raising blood glucose and counterbalancing the effects of insulin.
- In diabetes, insulin is either not produced or not recognized by the tissues, and the uptake of blood glucose is compromised. When blood glucose levels are high, glucose is excreted. Tissues then depend on fatty acids for fuel (producing ketone bodies) and degrade cellular proteins to provide glucogenic amino acids for glucose synthesis. Uncontrolled diabetes is characterized by high glucose levels in the blood and urine and the production and excretion of ketone bodies.

23.4 Obesity and the Regulation of Body Mass

In the U.S. population, 30% of adults are obese and another 35% are overweight, as defined in terms of body mass index (BMI), calculated as (weight in kg)/(height in m)^2. A BMI below 25 is considered normal; an individual with a BMI of 25 to 30 is overweight; a BMI greater than 30 indicates **obesity**. Obesity is life-threatening. It significantly increases the chances of developing type 2 diabetes as well as heart attack, stroke, and cancers of the colon, breast, prostate, and endometrium. Consequently, there is great interest in understanding how body mass and the storage of fats in adipose tissue are regulated. ■

To a first approximation, obesity is the result of taking in more calories in the diet than are expended by the body's fuel-consuming activities. The body can deal with an excess of dietary calories in three ways: (1) convert excess fuel to fat and store it in adipose tissue, (2) burn excess fuel by extra exercise, and (3) "waste" fuel by diverting it to heat production (thermogenesis) by uncoupled mitochondria. In mammals, a complex set of hormonal and neuronal signals acts to keep fuel intake and energy expenditure in balance so as to hold the amount of adipose tissue at a suitable level. Dealing effectively with obesity requires understanding these various checks and balances under normal conditions and how these homeostatic mechanisms can fail.

Adipose Tissue Has Important Endocrine Functions

One early hypothesis to explain body-mass homeostasis, the "adiposity negative-feedback" model, postulated a mechanism that inhibits eating behavior and increases energy expenditure whenever body weight exceeds a certain value (the set point); the inhibition is relieved when body weight drops below the set point **(Fig. 23–32)**. This model predicts that a feedback signal originating in adipose tissue influences the brain centers that control eating behavior and activity (metabolic and motor activity). The first such factor, leptin, was discovered in 1994, and subsequent research revealed that adipose tissue is an important endocrine organ that produces peptide hormones, known as **adipokines**. Adipokines may act locally (autocrine and paracrine action) or systemically (endocrine action), carrying information about the adequacy of the energy reserves (TAGs) stored in adipose tissue to other tissues and to the brain. Normally, adipokines produce changes in fuel metabolism and feeding behavior that reestablish adequate fuel reserves and maintain body mass. When adipokines are over- or underproduced, the resulting dysregulation may result in life-threatening disease.

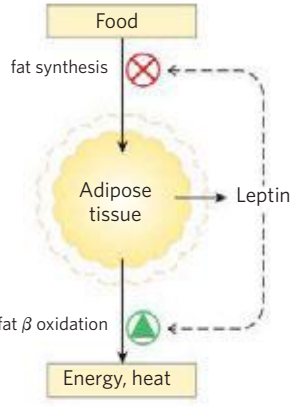

FIGURE 23–32 Set-point model for maintaining constant mass. When the mass of adipose tissue increases (dashed outline), released leptin inhibits feeding and fat synthesis and stimulates oxidation of fatty acids. When the mass of adipose tissue decreases (solid outline), lowered leptin production favors greater food intake and less fatty acid oxidation.

Leptin (Greek *leptos*, "thin") is an adipokine (167 amino acids) that, on reaching the brain, acts on receptors in the hypothalamus to curtail appetite. Leptin was first identified as the product of a gene designated *OB* (obese) in laboratory mice. Mice with two defective copies of this gene (*ob*/*ob* genotype; lowercase letters signify a mutant form of the gene) show the behavior and physiology of animals in a constant state of starvation: their plasma cortisol levels are elevated; they are unable to stay warm, exhibit unrestrained appetite, grow abnormally, and do not reproduce. As a consequence of the unrestrained appetite, they become severely obese, weighing as much as three times more than normal mice **(Fig. 23–33)**. They also have metabolic disturbances very similar to those seen in diabetes, and they are insulin-resistant. When leptin is injected into *ob*/*ob* mice, they eat less, lose weight, and increase their locomotor activity and thermogenesis.

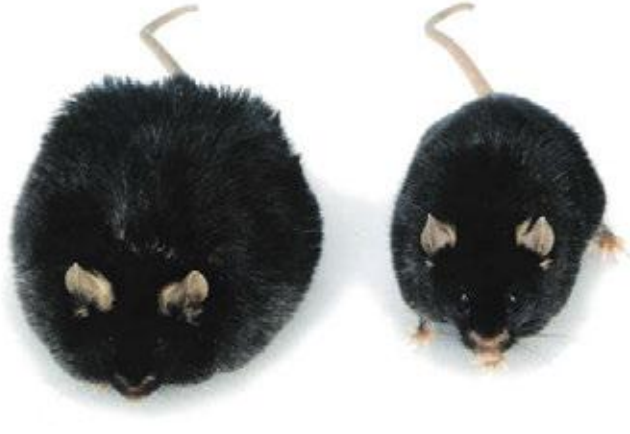

FIGURE 23–33 Obesity caused by defective leptin production. Both of these mice, which are the same age, have defects in the *OB* gene. The mouse on the right was injected daily with purified leptin and weighs 35 g. The mouse on the left got no leptin and consequently ate more food and was less active; it weighs 67 g.

A second mouse gene, designated *DB* (diabetic), also has a role in appetite regulation. Mice with two defective copies (*db*/*db*) are obese and diabetic. The *DB* gene encodes the **leptin receptor**. When the receptor is defective, the signaling function of leptin is lost.

The leptin receptor is expressed primarily in regions of the brain known to regulate feeding behavior—neurons of the arcuate nucleus of the hypothalamus **(Fig. 23–34a)**. Leptin carries the message that fat reserves are sufficient, and it promotes a reduction in

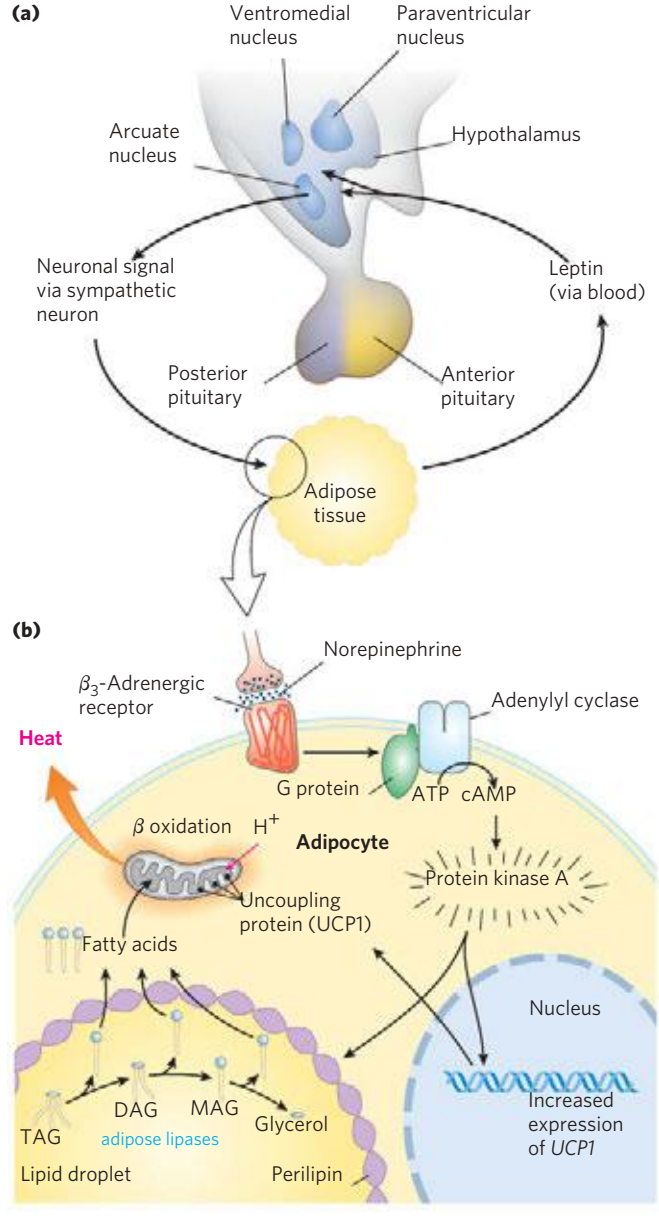

FIGURE 23–34 Hypothalamic regulation of food intake and energy expenditure. (a) Role of the hypothalamus in its interaction with adipose tissue. The hypothalamus receives input (leptin) from adipose tissue and responds with neuronal signals to adipocytes. **(b)** Effects of neuronal stimulation of the adipocyte include activation of protein kinase A, which triggers mobilization of fatty acids from TAG and their uncoupled oxidation in mitochondria, generating heat but not ATP.

fuel intake and increased expenditure of energy. Leptin-receptor interaction in the hypothalamus alters the release of neuronal signals to the region of the brain that affects appetite. Leptin also stimulates the sympathetic nervous system, increasing blood pressure, heart rate, and thermogenesis by uncoupling the mitochondria of brown adipocytes (Fig. 23–34b). Recall that thermogenin, or UCP1, forms a channel in the inner mitochondrial membrane that allows protons to reenter the mitochondrial matrix without passing through the ATP synthase complex. This permits continual oxidation of fuel (fatty acids in a brown adipocyte) without ATP synthesis, dissipating energy as heat and consuming dietary calories or stored fats in potentially very large amounts.

Leptin Stimulates Production of Anorexigenic Peptide Hormones

Two types of neurons in the arcuate nucleus control fuel intake and metabolism **(Fig. 23–35)**. The **orexigenic** (appetite-stimulating) neurons stimulate eating by producing and releasing **neuropeptide Y (NPY)**, which causes the next neuron in the circuit to send the signal to the brain: Eat! The blood level of NPY rises during starvation and is elevated in both *ob/ob* and *db/db* mice. The high NPY concentration presumably contributes to the obesity of these mice, who eat voraciously.

The **anorexigenic** (appetite-suppressing) neurons in the arcuate nucleus produce ***α*-melanocyte–stimulating hormone** (***α*-MSH**; also known as melanocortin), formed from its polypeptide precursor pro-opiomelanocortin (POMC; Fig. 23–5). Release of *α*-MSH causes the next neuron in the circuit to send the signal to the brain: Stop eating!

The amount of leptin released by adipose tissue depends on both the number and the size of adipocytes. When weight loss decreases the mass of lipid tissue, leptin levels in the blood decrease, the production of NPY increases, and the processes in adipose tissue shown in Figure 23–34 are reversed. Uncoupling is diminished, slowing thermogenesis and saving fuel, and fat mobilization slows in response to reduced signaling by cAMP. Consumption of more food combined with more efficient utilization of fuel results in replenishment of the fat reserve in adipose tissue, bringing the system back into balance.

Leptin may also be essential to the normal development of hypothalamic neuronal circuits. In mice, the outgrowth of nerve fibers from the arcuate nucleus during early brain development is slower in the absence of leptin, affecting both the orexigenic and (to a lesser extent) anorexigenic outputs of the hypothalamus. It is possible that the leptin levels *during development* of these circuits determine the details of the hardwiring of this regulatory system.

Leptin Triggers a Signaling Cascade That Regulates Gene Expression

The leptin signal is transduced by a mechanism also used by receptors for interferon and growth factors, the JAK-STAT system (**Fig. 23–36**; see Fig. 12–18). The leptin receptor, which has a single transmembrane segment, dimerizes when leptin binds to the extracellular domains of two monomers. Both monomers are phosphorylated on a Tyr residue of their intracellular domain by a **Janus kinase (JAK)**. The Ⓟ–Tyr residues become docking

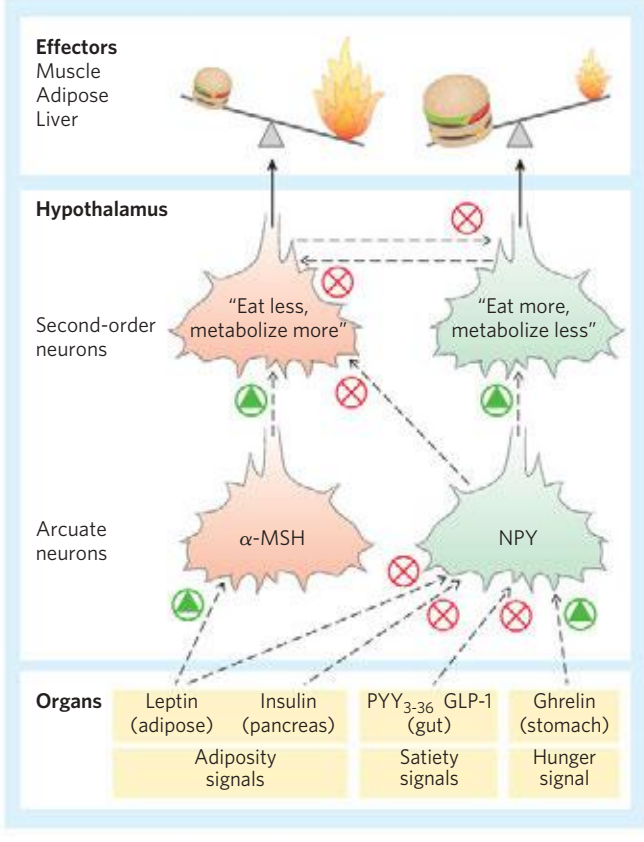

FIGURE 23–35 Hormones that control eating. In the arcuate nucleus of the hypothalamus, two sets of neurosecretory cells receive hormonal input and relay neuronal signals to the cells of muscle, adipose tissue, and liver. Leptin and insulin are released from adipose tissue and pancreas, respectively, in proportion to the mass of body fat. The two hormones act on anorexigenic neurosecretory cells to trigger release of *α*-MSH (melanocyte-stimulating hormone); *α*-MSH carries the signal to second-order neurons in the hypothalamus, which puts out the signals to eat less and metabolize more fuel. Leptin and insulin also act on orexigenic neurosecretory cells to inhibit the release of NPY, reducing the "eat more" signal sent to the tissues. As described later in the text, the gastric hormone ghrelin *stimulates* appetite by activating the NPY-expressing cells; PYY_{3-36}, released from the colon, *inhibits* these neurons and thereby decreases appetite. Each of the two types of neurosecretory cells inhibits hormone production by the other, so any stimulus that activates orexigenic cells inactivates anorexigenic cells, and vice versa. This strengthens the effect of stimulatory inputs.

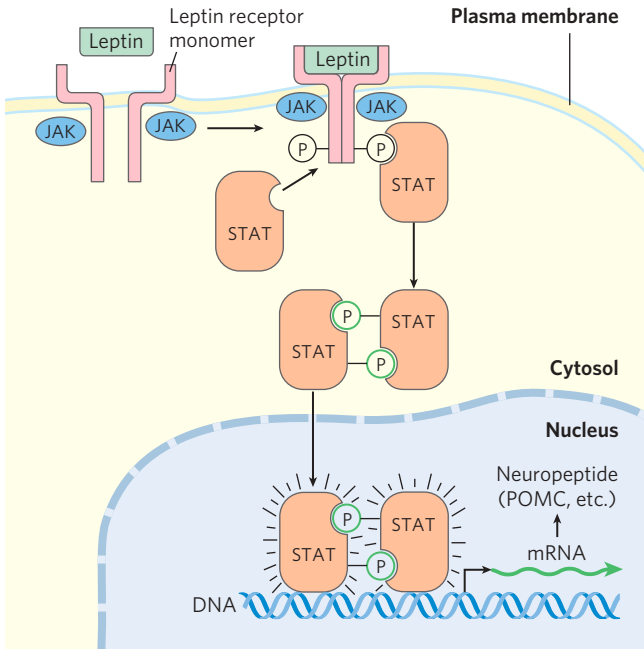

FIGURE 23–36 The JAK-STAT mechanism of leptin signal transduction in the hypothalamus. Leptin binding induces dimerization of the leptin receptor, followed by phosphorylation of specific Tyr residues in the receptor's cytosolic domain, catalyzed by Janus kinase (JAK). STATs bound to the phosphorylated leptin receptor are now phosphorylated on Tyr residues by a separate activity of JAK. The STATs dimerize, binding each other's Ⓟ-Tyr residues, and enter the nucleus. Here, they bind specific regulatory regions in the DNA and alter the expression of certain genes. The products of these genes ultimately influence the organism's feeding behavior and energy expenditure.

sites for three proteins that are *s*ignal *t*ransducers and *a*ctivators of *t*ranscription (**STATs** 3, 5, and 6; sometimes called fat-STATS). The docked STATs are then phosphorylated on Tyr residues by the same JAK. After phosphorylation, the STATs dimerize, then move to the nucleus, where they bind to specific DNA sequences and stimulate the expression of target genes, including the gene for POMC, from which α-MSH is produced.

The increased catabolism and thermogenesis triggered by leptin are due in part to increased synthesis of the mitochondrial uncoupling protein thermogenin (product of the *UCP1* gene) in brown adipocytes. Leptin stimulates the synthesis of thermogenin by altering synaptic transmissions from neurons in the arcuate nucleus to adipose and other tissues via the sympathetic nervous system. The resulting increased release of norepinephrine in these tissues acts through β_3-adrenergic receptors to stimulate transcription of the *UCP1* gene. The resulting uncoupling of electron transfer from oxidative phosphorylation consumes fat and is thermogenic (Fig. 23–34).

Might human obesity be the result of insufficient leptin production, and therefore treatable by the injection of leptin? Blood levels of leptin are in fact usually much *higher* in obese animals (including humans) than in animals of normal body mass (except, of course, in *ob/ob* mutants, which cannot make leptin). Some downstream element in the leptin response system must be defective in obese individuals, and the elevation in leptin is the result of an (unsuccessful) attempt to overcome the leptin resistance. In those very rare humans with extreme obesity who have a defective leptin gene (*OB*), leptin injection does result in dramatic weight loss. In the vast majority of obese individuals, however, the *OB* gene is intact. In clinical trials, the injection of leptin did not have the weight-reducing effect observed in obese *ob/ob* mice. Clearly, most cases of human obesity involve one or more factors in addition to leptin.

The Leptin System May Have Evolved to Regulate the Starvation Response

The leptin system probably evolved to adjust an animal's activity and metabolism during periods of fasting and starvation, not as a means to restrict weight gain. The *reduction* in leptin level triggered by nutritional deficiency reverses the thermogenic processes illustrated in Figure 23–34, allowing fuel conservation. In the hypothalamus, decreased leptin signal also triggers decreased production of thyroid hormone (slowing basal metabolism), decreased production of sex hormones (preventing reproduction), and increased production of glucocorticoids (mobilizing the body's fuel-generating resources). By minimizing energy expenditure and maximizing the use of endogenous reserves of energy, these leptin-mediated responses may allow an animal to survive periods of severe nutritional deprivation. In liver and muscle, leptin stimulates **AMP-activated protein kinase (AMPK)** and through its action inhibits fatty acid synthesis and activates fatty acid oxidation, favoring energy-generating processes.

Insulin Acts in the Arcuate Nucleus to Regulate Eating and Energy Conservation

Insulin secretion may reflect both the size of fat reserves (adiposity) and the current energy balance (blood glucose level). In addition to its endocrine actions on various tissues, insulin acts in the central nervous system (in the hypothalamus) to inhibit eating (Fig. 23–35). Insulin receptors in the orexigenic neurons of the arcuate nucleus *inhibit* the release of NPY, and insulin receptors in the anorexigenic neurons *stimulate* α-MSH production, thereby decreasing fuel intake and increasing thermogenesis. By mechanisms discussed in Section 23.3, insulin also signals muscle, liver, and adipose tissues to increase the conversion of glucose to acetyl-CoA, providing the starting material for fat synthesis.

The actions of leptin and insulin are not wholly independent. Leptin makes the cells of liver and muscle more sensitive to insulin. One hypothesis to explain this effect suggests cross talk between the protein tyrosine kinases activated by leptin and those activated by insulin

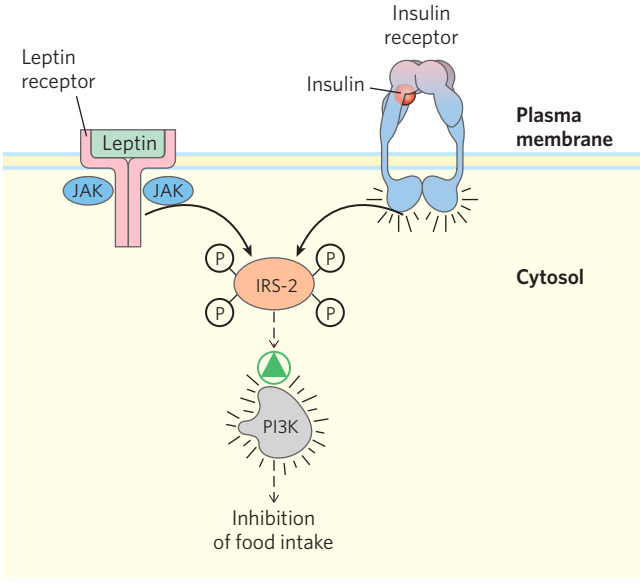

FIGURE 23–37 A possible mechanism for cross talk between receptors for insulin and leptin. The insulin receptor has intrinsic Tyr kinase activity (see Fig. 12–15), and the leptin receptor, when occupied by its ligand, is phosphorylated by a soluble Tyr kinase (JAK). One possible explanation for the observed interaction between leptin and insulin is that both may phosphorylate the same substrate—in the case shown here, insulin receptor substrate-2 (IRS-2). When phosphorylated, IRS-2 activates PI3K, which has downstream consequences that include inhibition of food intake. IRS-2 serves here as an integrator of the input from two receptors.

(Fig. 23–37); common second messengers in the two signaling pathways allow leptin to trigger some of the same downstream events that are triggered by insulin, through insulin receptor substrate-2 (IRS-2) and phosphatidylinositol 3-kinase (PI3K) (see Fig. 12–16).

Adiponectin Acts through AMPK to Increase Insulin Sensitivity

Adiponectin is a peptide hormone (224 amino acids) produced almost exclusively in adipose tissue, an adipokine that sensitizes other organs to the effects of insulin, protects against atherosclerosis, and inhibits inflammatory responses (monocyte adhesion, macrophage transformation, and the proliferation and migration of the cells of vascular smooth muscle). Adiponectin circulates in the blood and powerfully affects the metabolism of fatty acids and carbohydrates in liver and muscle. It increases the uptake of fatty acids from the blood by myocytes and the rate at which fatty acids undergo β oxidation in muscle. It also blocks fatty acid synthesis and gluconeogenesis in hepatocytes, and stimulates glucose uptake and catabolism in muscle and liver.

These effects of adiponectin are indirect and not fully understood, but AMPK clearly mediates many of them. Acting through its plasma membrane receptor, adiponectin triggers phosphorylation and activation of AMPK. Recall that AMPK is activated by factors that signal the need to shift metabolism away from biosynthesis and toward energy generation **(Fig. 23–38)**. When activated, AMPK phosphorylates target proteins critical to the metabolism of lipids and carbohydrates, with profound effects on the metabolism of the whole animal **(Fig. 23–39)**. Adiponectin receptors are also present in the brain; the hormone activates AMPK in the hypothalamus, stimulating food intake and reducing energy expenditure.

One enzyme regulated by AMPK in the liver and in white adipose tissue is acetyl-CoA carboxylase, which produces malonyl-CoA, the first intermediate committed to fatty acid synthesis. Malonyl-CoA is a powerful inhibitor of the enzyme carnitine acyltransferase I, which starts the process of β oxidation by transporting fatty acids into the mitochondrion (see Fig. 17–6). By phosphorylating and inactivating acetyl-CoA carboxylase, AMPK inhibits fatty acid synthesis while relieving the inhibition (by malonyl-CoA) of β oxidation (see Fig. 17–13). Cholesterol synthesis is also inhibited by AMPK, which phosphorylates and inactivates HMG-CoA reductase, an enzyme in the path to cholesterol (see Fig. 21–34). Similarly, AMPK inhibits fatty acid synthase and acyl transferase, effectively blocking the synthesis of triacylglycerols. In short, lipid synthesis is inhibited and lipid use as fuel is stimulated.

Mice with defective adiponectin genes are less sensitive to insulin than those with normal adiponectin, and they show poor glucose tolerance: ingestion of dietary carbohydrate causes a long-lasting rise in blood glucose. These metabolic defects resemble those of humans with type 2 diabetes, who are similarly **insulin-insensitive** and clear glucose from the blood only slowly. Indeed, individuals with obesity or type 2 diabetes have lower blood adiponectin levels than nondiabetic controls. Moreover, drugs used in the treatment of type 2 diabetes—the thiazolidinediones, such as rosiglitazone (Avandia) and pioglitazone (Actos) (p. 852)—increase the expression of adiponectin mRNA

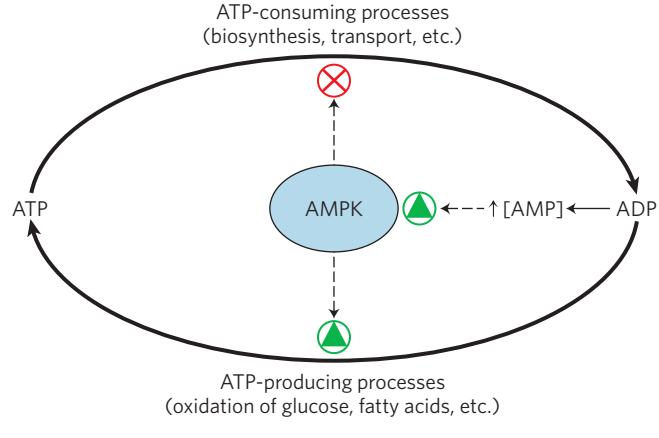

FIGURE 23–38 The role of AMP-activated protein kinase (AMPK) in regulating ATP metabolism. ADP produced in synthetic reactions is converted to AMP by adenylate kinase. AMP activates AMPK, which regulates ATP-consuming and ATP-generating pathways by phosphorylating key enzymes (see Fig. 23–39).

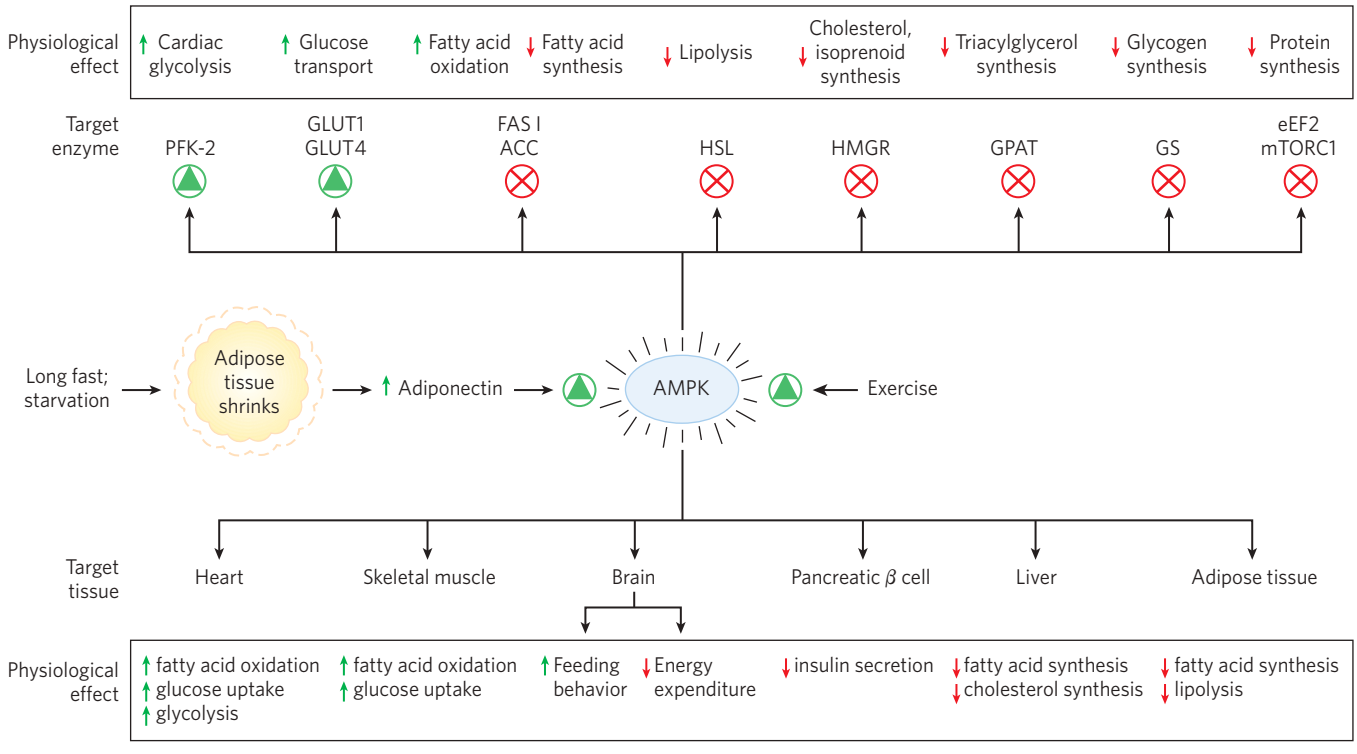

FIGURE 23–39 Formation of adiponectin and its actions through AMPK. Extended fasting or starvation results in decreased reserves of triacylglycerols in adipose tissue, which triggers adiponectin production and release from adipocytes. The rise in plasma adiponectin acts through its plasma membrane receptors in various cell types and organs to inhibit energy-consuming processes and stimulate energy-producing processes. Adiponectin acts through its receptors in the brain to stimulate feeding behavior and inhibit energy-consuming physical activity, and to inhibit thermogenesis in brown fat. Adiponectin exerts its metabolic effects by activating AMPK, which regulates (by phosphorylation) specific enzymes in key metabolic processes (see Fig. 15-8). PFK-2, phosphofructokinase-2; GLUT1 and GLUT4, glucose transporters; FAS I, fatty acid synthase I; ACC, acetyl-CoA carboxylase; HSL, hormone-sensitive lipase; HMGR, HMG-CoA reductase; GPAT, an acyl transferase; GS, glycogen synthase; eEF2, eukaryotic elongation factor 2 (required for protein synthesis; see Chapter 27); mTOR1, mammalian target of rapamycin (a protein kinase that regulates protein synthesis on the basis of nutrient availability; see Fig. 23-40). Thiazolidinedione drugs activate the transcription factor PPARγ (see Figs 23-41 and 23-42), which then turns on adiponectin synthesis, indirectly activating AMPK. Exercise, through conversion of ATP to ADP and AMP, also stimulates AMPK.

in adipose tissue and increase blood adiponectin levels in experimental animals; they also activate AMPK (Fig. 23–39). (In 2011 the FDA concluded that Avandia use was associated with an increased risk of heart attacks, and it therefore limited the use of the drug to those diabetes patients for whom other available treatments were ineffective.) It seems likely that adiponectin will prove to be an important link between type 2 diabetes and its most important predisposing factor, obesity. ■

mTORC1 Activity Coordinates Cell Growth with the Supply of Nutrients and Energy

The activity of a second novel protein kinase helps to mediate cell proliferation and increased cell size in response to growth factors and energy and nutrient availability. The highly conserved Ser/Thr kinase **mTORC1** is activated by abundant energy and nutrient supplies (such as high concentrations of branched-chain amino acids). When activated, mTORC1 phosphorylates several transcription factors, leading to increased expression of genes encoding the enzymes of lipid synthesis and mitochondrial proliferation and increased ribosome biogenesis **(Fig. 23–40)**. Fasting results in inactivation of mTORC1, leading to increased breakdown of protein and glycogen in liver and muscle and mobilization of triglycerides in adipose tissue. Chronic activation of mTORC1 by overeating results in excess deposition of triglycerides in adipose tissue and also in liver and muscle. This abnormal lipid accumulation in liver and muscle may contribute to insulin insensitivity and type 2 diabetes, as described in Section 23.5. Mutations that produce constantly activated mTORC1 are also commonly associated with human cancers.

Diet Regulates the Expression of Genes Central to Maintaining Body Mass

Proteins in a family of ligand-activated transcription factors, the **peroxisome proliferator-activated receptors (PPARs)**, respond to changes in dietary lipid by

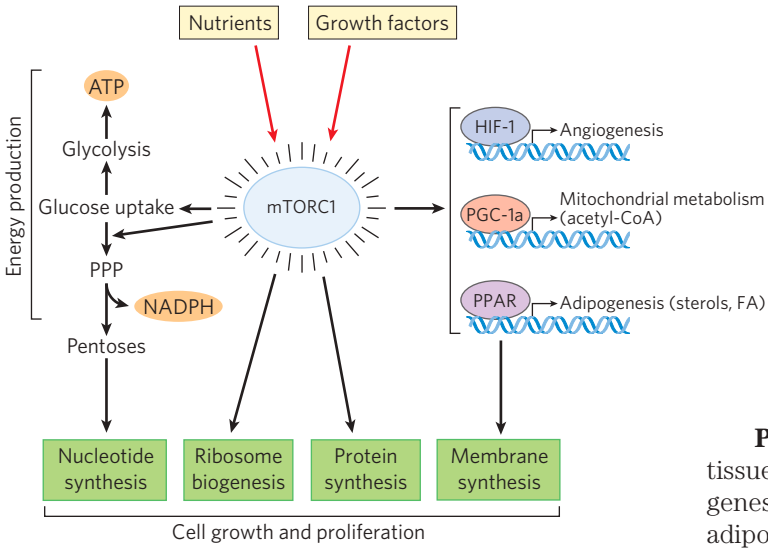

FIGURE 23–40 mTORC1 stimulates cell growth and proliferation when adequate nutrition is available. mTORC1 is a Ser/Thr protein kinase activated by growth factors and metabolites that signal a state of adequate nutrition. By phosphorylating key target proteins, mTORC1 activates energy (ATP and NADPH) production for biosynthesis and stimulates the synthesis of proteins and lipids, allowing cell growth and proliferation. (PPP is pentose phosphate pathway; FA is fatty acids.)

altering the expression of genes involved in fat and carbohydrate metabolism. These transcription factors were first recognized for their roles in peroxisome synthesis—thus their name. Their normal ligands are fatty acids or fatty acid derivatives, but they can also bind synthetic agonists and can be activated in the laboratory by genetic manipulation. PPARα, PPARδ, and PPARγ are members of this nuclear receptor superfamily. They act in the nucleus by forming heterodimers with another nuclear receptor, RXR (retinoid X receptor), binding to regulatory regions of DNA near the genes under their control and changing the rate of transcription of those genes **(Fig. 23–41)**.

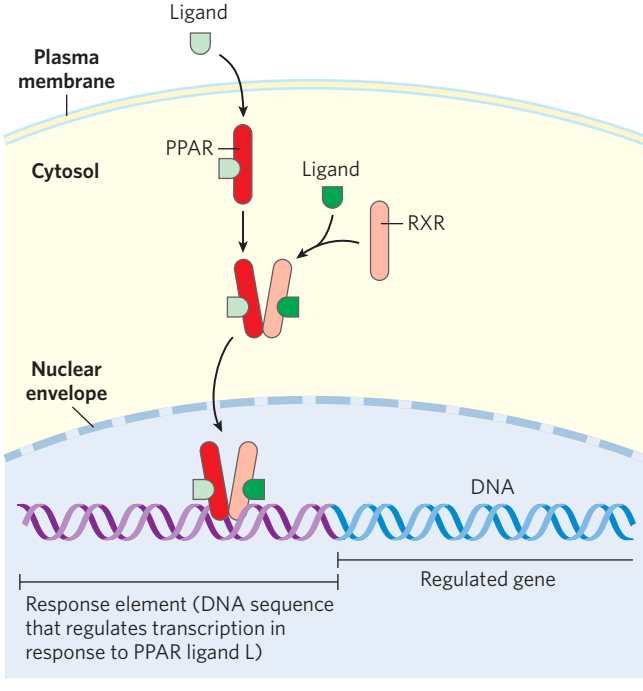

FIGURE 23–41 Mode of action of PPARs. PPARs are transcription factors that, when bound to their cognate ligand (L), form heterodimers with the nuclear receptor RXR. The dimer binds specific regions of DNA known as response elements, stimulating transcription of genes in those regions.

PPARγ, expressed primarily in liver and adipose tissue (both brown and white), is involved in turning on genes necessary to the differentiation of fibroblasts into adipocytes and genes that encode proteins required for lipid synthesis and storage in adipocytes **(Fig. 23–42)**. PPARγ is activated by the thiazolidinedione drugs that are used to treat type 2 diabetes (discussed below).

PPARα is expressed in liver, kidney, heart, skeletal muscle, and brown adipose tissue. The ligands that activate this transcription factor include eicosanoids, free fatty acids, and the class of drugs called fibrates, such as fenofibrate (TriCor) and ciprofibrate (Modalim), which are used to treat coronary heart disease by raising HDL and lowering blood triacylglycerols. In hepatocytes, PPARα turns on the genes necessary for the uptake and β oxidation of fatty acids and formation of ketone bodies during fasting.

PPARδ and **PPARβ** are key regulators of fat oxidation, which act by sensing changes in dietary lipid. PPARδ acts in liver and muscle, stimulating the transcription of at least nine genes encoding proteins for β oxidation and for energy dissipation through uncoupling of mitochondria. Normal mice overfed on high-fat diets accumulate massive amounts of white fat, and fat droplets accumulate in the liver. But when the same overfeeding experiment is carried out with mice that have a genetically altered, always active PPARδ, this fat accumulation is prevented. In mice with a nonfunctioning leptin receptor (*db/db*), activated PPARδ prevents the development of obesity that would otherwise occur. By stimulating fatty acid breakdown in uncoupled mitochondria, PPARδ causes fat depletion, weight loss, and thermogenesis. Seen in this light, thermogenesis is both a means of keeping warm and a defense against obesity. Clearly, PPARδ is a potential target for drugs to treat obesity.

Short-Term Eating Behavior Is Influenced by Ghrelin and PYY$_{3–36}$

Ghrelin is a peptide hormone (28 amino acids) produced in cells lining the stomach. It was originally recognized as the stimulus for the release of growth hormone (*ghre* is the Proto-Indo-European root of "grow"), then subsequently shown to be a powerful appetite stimulant

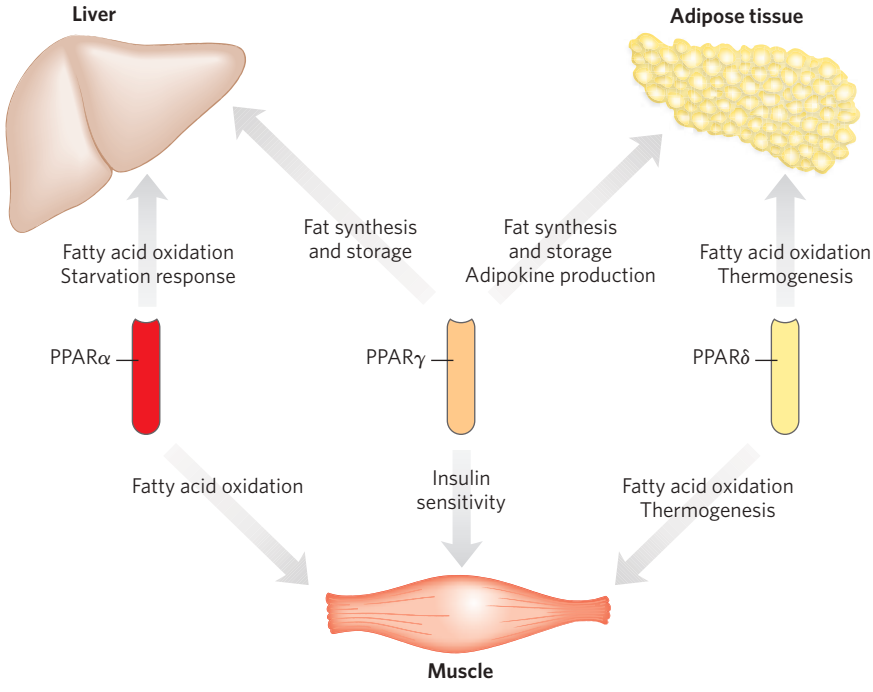

FIGURE 23–42 Metabolic integration by PPARs. The three PPAR isoforms regulate lipid and glucose homeostasis through their coordinated effects on gene expression in liver, muscle, and adipose tissue. PPARα and PPARδ (and its closely related isoform PPARβ) regulate lipid utilization; PPARγ regulates lipid storage and the insulin sensitivity of various tissues.

that works on a shorter time scale (between meals) than leptin and insulin. Ghrelin receptors are located in the pituitary gland (presumably mediating growth hormone release) and in the hypothalamus (affecting appetite), as well as in heart muscle and adipose tissue. Ghrelin acts through a G protein–coupled receptor to generate the second messenger IP_3, which mediates ghrelin action. The concentration of ghrelin in the blood varies strikingly between meals, peaking just before a meal and dropping sharply just after the meal **(Fig. 23–43)**. Injection of ghrelin into humans produces immediate sensations of intense hunger. Individuals with Prader-Willi syndrome, whose blood levels of ghrelin are exceptionally high, have an uncontrollable appetite, leading to extreme obesity that often results in death before the age of 30.

$PYY_{3–36}$ is a peptide hormone (2 amino-terminal Y residues plus 34 amino acids) secreted by endocrine cells in the lining of the small intestine and colon in response to food entering from the stomach. The level of $PYY_{3–36}$ in the blood rises after a meal and remains high for some hours. It is carried in the blood to the arcuate nucleus, where it acts on orexigenic neurons, inhibiting NPY release and reducing hunger (Fig. 23–35). Humans injected with $PYY_{3–36}$ feel little hunger and eat less than normal amounts for about 12 hours.

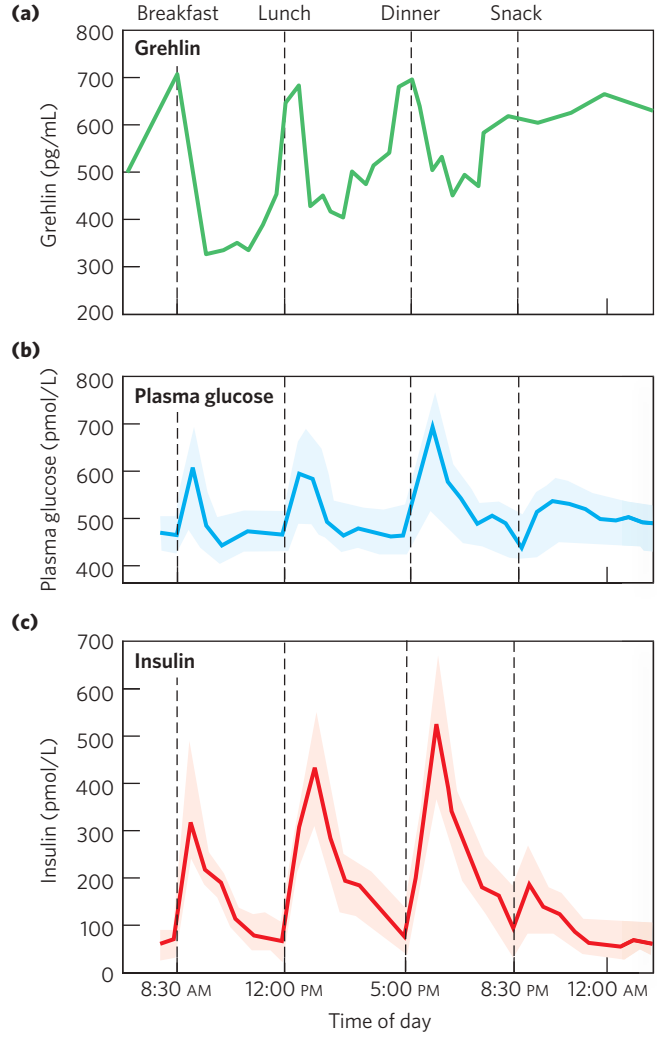

FIGURE 23–43 Variations in blood concentrations of glucose, ghrelin, and insulin relative to meal times. (a) Plasma levels of ghrelin rise sharply just *before* the normal time for meals (7 AM breakfast, 12 noon lunch, 5:30 PM dinner) and drop precipitously just after meals, paralleling the subjective feelings of hunger. **(b)** Blood glucose rises sharply *after* a meal, **(c)** followed immediately by a rise in insulin levels in response to the increase in blood glucose concentration.

Microbial Symbionts in the Gut Influence Energy Metabolism and Adipogenesis

Lean and obese individuals harbor different combinations of microbial symbionts in the gut. Investigation of this observation led to the discovery that certain microorganisms of the gut release fermentation products, namely the short-chain fatty acids acetate, propionate, butyrate, and lactate, which enter the bloodstream and trigger metabolic changes in adipose tissue. Propionate, for example, drives the expansion of WAT by acting on G protein–coupled receptors (GPR43 and GPR41) in the plasma membranes of several cell types, including adipocytes. These receptors trigger differentiation of precursor cells into adipocytes and inhibit lipolysis in existing adipocytes, leading to an increase in WAT mass—obesity.

These findings suggest possible approaches to the prevention of obesity that involve altering the makeup of the microbial community in the gut, either by direct addition of microbial species (probiotics) that disfavor adipogenesis or by adding to the diet nutrients (prebiotics) that favor the dominance of the probiotic microbes. For example, certain polymers of fructose (fructans) that are indigestible to animals favor such a microbial community in mice and lead to decreased fat storage in WAT and liver (and to the decrease in insulin sensitivity associated with obesity and lipid deposition in the liver; see below).

Endocrine cells present in the lining of the GI tract secrete products—the anorexigenic peptides $PYY_{3–36}$ and glucagon-like peptide-1 (GLP-1) and the orexigenic peptide ghrelin—that modulate food intake and energy expenditure in the animal. Interaction with specific microbes in the gut, or with their fermentation products, may be the trigger for release of these peptides. The investigations of effects of diet on microbial symbionts of the gut, and of the effects of microbial products on energy metabolism and adipogenesis, may lead to a deeper understanding of the effects of diet and microbial symbionts on the development of obesity and of its pathological sequels, the metabolic syndrome and type 2 diabetes.

This interlocking system of neuroendocrine controls of food intake and metabolism presumably evolved to protect against starvation and to eliminate counterproductive accumulation of fat (extreme obesity). The difficulty most people face in trying to lose weight testifies to the remarkable effectiveness of these controls.

SUMMARY 23.4 Obesity and the Regulation of Body Mass

- Obesity is increasingly common in the United States and other developed countries and predisposes people toward several life-threatening conditions, including cardiovascular disease and type 2 diabetes.
- Adipose tissue produces leptin, a hormone that regulates feeding behavior and energy expenditure so as to maintain adequate reserves of fat. Leptin production and release increase with the number and size of adipocytes.
- Leptin acts on receptors in the arcuate nucleus of the hypothalamus, causing the release of anorexigenic (appetite-suppressing) peptides, including α-MSH, that act in the brain to inhibit eating. Leptin also stimulates sympathetic nervous system action on adipocytes, leading to uncoupling of mitochondrial oxidative phosphorylation, with consequent thermogenesis.
- The signal-transduction mechanism for leptin involves phosphorylation of the JAK-STAT system. On phosphorylation by JAK, STATs can bind to regulatory regions in nuclear DNA and alter the expression of genes for proteins that set the level of metabolic activity and determine feeding behavior. Insulin acts on receptors in the arcuate nucleus, with results similar to those caused by leptin.
- The hormone adiponectin stimulates fatty acid uptake and oxidation and inhibits fatty acid synthesis. It also sensitizes muscle and liver to insulin. Adiponectin's actions are mediated by AMPK, which is also activated by low [AMP] and exercise.
- Ghrelin, a hormone produced in the stomach, acts on orexigenic (appetite-stimulating) neurons in the arcuate nucleus to produce hunger before a meal. $PYY_{3–36}$, a peptide hormone of the intestine, acts at the same site to lessen hunger after a meal.
- The specific types of microbial symbionts in the gut can influence adipogenesis, the increase in the mass of body fat.

23.5 Obesity, the Metabolic Syndrome, and Type 2 Diabetes

In the industrialized world, where the food supply is more than adequate, there is a growing epidemic of obesity and the type 2 diabetes associated with it. As many as 300 million people in the world now have diabetes, and reasonable projections predict a dramatic rise in cases over the next decade, following the world epidemic of obesity. The pathology of diabetes includes cardiovascular disease, renal failure, blindness, poor healing in the extremities that requires amputations, and neuropathy. In 2011, the global mortality from diabetes was estimated at 4 million, a number that is sure to rise in coming years. Clearly, it is essential to understand type 2 diabetes and its relationship to obesity and to find countermeasures that prevent or reverse the damage done by this disease. ■

In Type 2 Diabetes the Tissues Become Insensitive to Insulin

The hallmark of type 2 diabetes is the development of insulin resistance: a state in which more insulin is needed to bring about the biological effects

produced by a lower amount of insulin in the normal, healthy state. In the early stages of the disease, pancreatic β cells secrete enough insulin to overcome the lower insulin sensitivity of muscle and liver. But the β cells eventually fail, and the lack of insulin becomes apparent in the body's inability to regulate blood glucose. The intermediate stage, preceding type 2 diabetes mellitus, is sometimes called the **metabolic syndrome**, or **syndrome X**. This is typified by obesity, especially in the abdomen; hypertension (high blood pressure); abnormal blood lipids (high TAG and LDL, low HDL); slightly high blood glucose; and a reduced ability to clear glucose in the glucose-tolerance test. Individuals with metabolic syndrome often also show changes in blood proteins, changes that are associated with abnormal clotting (high fibrinogen concentration) or inflammation (high concentrations of the C-reactive peptide, which typically increases with an inflammatory response). About 27% of the adult population in the United States has these symptoms of metabolic syndrome.

What predisposes individuals with metabolic syndrome to develop type 2 diabetes? According to the "lipid toxicity" hypothesis **(Fig. 23–44)**, the action of PPARγ on adipocytes normally keeps the cells ready to synthesize and store triacylglycerols—the adipocytes are insulin-sensitive and produce leptin, which leads to their continued intracellular deposition of TAG. However, excess caloric intake in obese individuals causes adipocytes to become filled with TAG, leaving adipose tissue unable to meet any further demand for TAG storage. Lipid-filled adipose tissue releases protein factors that attract macrophages, which infiltrate the tissue and may come to represent as much as 50% of the adipose tissue by mass. Macrophages trigger the inflammatory response, which impairs TAG deposition in adipocytes and favors release of free fatty acids into the blood. These excess fatty acids enter liver and muscle cells, where they are converted to TAGs that accumulate as lipid droplets. This ectopic (Greek *ektopos*, "out of place") deposition of TAGs leads to insulin insensitivity in liver and muscle, the hallmark of type 2 diabetes.

Moreover, according to this hypothesis, excess stored fatty acids and TAGs are toxic to liver and muscle. Some individuals are less well equipped genetically to handle this burden of ectopic lipids and are more susceptible to the cellular damage that leads to the development of type 2 diabetes. Insulin resistance probably involves impairment of several of the mechanisms by which

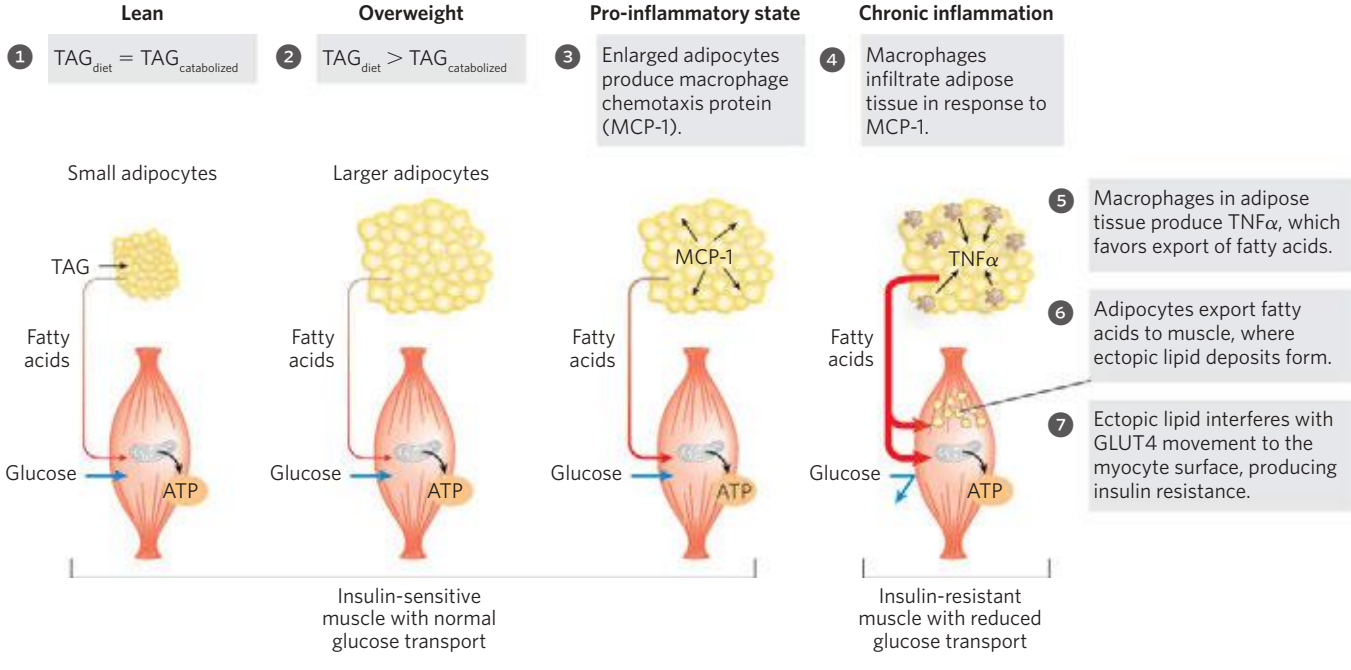

FIGURE 23-44 Overloading adipocytes with triacylglycerols triggers inflammation in fat tissue and ectopic lipid deposition and insulin resistance in muscle. In an individual of healthy body mass, triacylglycerol (TAG) uptake in the diet equals TAG oxidation for energy. In overweight individuals, excess caloric intake results in enlarged adipocytes, engorged with TAG and unable to store more. Enlarged adipocytes secrete MCP-1 (monocyte chemotaxis protein-1), attracting macrophages. Macrophages infiltrate adipose tissue and produce TNF α (tumor necrosis factor α), which triggers lipid breakdown and fatty acid release into the blood. The fatty acids released from adipose tissue enter muscle cells, where they accumulate in small lipid droplets. This ectopic storage of lipids somehow causes insulin resistance, perhaps by triggering lipid-activated protein kinases that inactivate some element in the insulin-signaling pathway. GLUT4 glucose transporters leave the muscle cell surface, preventing glucose entry into muscle; the myocyte has now become insulin-resistant. It cannot use blood glucose for its fuel, so fatty acids are mobilized from adipose tissue and become the primary fuel. The increased influx of fatty acids into muscle leads to further deposition of ectopic lipids. In some individuals, insulin resistance develops into type 2 diabetes. Other individuals are genetically less susceptible to the deleterious effects of ectopic lipid storage or are genetically better equipped to manage this storage and do not develop diabetes.

insulin acts on metabolism, which include changes in protein levels and changes in the activities of signaling enzymes and transcription factors. For example, both adiponectin synthesis in adipocytes and adiponectin level in the blood decrease with obesity and increase with weight loss.

Several of the drugs that are effective in improving insulin sensitivity in type 2 diabetes are known to act on specific proteins in signaling pathways, and their actions are consistent with the lipotoxicity model. Thiazolidinediones bind to PPARγ, turning on a set of adipocyte-specific genes and promoting the differentiation of preadipocytes to small adipocytes, thereby increasing the body's capacity for absorbing fatty acids from the diet and storing them as TAGs.

There are clearly genetic factors that predispose toward type 2 diabetes. Although 80% of individuals with type 2 diabetes are obese, most obese individuals do not develop type 2 diabetes. Given the complexity of the regulatory mechanisms we have discussed in this chapter, it is not surprising that the genetics of diabetes is complex, involving interactions between variant genes and environmental factors, including diet and lifestyle. At least 10 genetic loci have been reliably linked to type 2 diabetes; variation in any of these "diabetogenes" alone would cause a relatively small increase in the likelihood of developing type 2 diabetes. For example, people with a variant PPARγ in which an Ala residue replaces Pro at position 12 are at a slightly, though significantly, increased risk of developing type 2 diabetes. ■

Type 2 Diabetes Is Managed with Diet, Exercise, and Medication

Studies show that three factors improve the health of individuals with type 2 diabetes: dietary restriction, regular exercise, and drugs that increase insulin sensitivity or insulin production. Dietary restriction (and accompanying weight loss) reduces the overall burden of handling fatty acids. The lipid composition of the diet influences, through PPARs and other transcription factors, the expression of genes that encode proteins involved in fatty acid oxidation and in energy expenditure via thermogenesis. Exercise activates AMPK, as does adiponectin; AMPK shifts metabolism toward fat oxidation and inhibits fat synthesis.

Several classes of drugs are used in the management of type 2 diabetes, some of which we have discussed earlier in the chapter (Table 23–7). Sulfonylureas act on the ATP-gated K^+ channels in β cells to stimulate insulin release. Biguanides such as metformin (Glucophage) activate AMPK, mimicking the effects of adiponectin. Thiazolidinediones act through PPARγ to increase the concentration of adiponectin in plasma and to stimulate adipocyte differentiation, thereby increasing the capacity for TAG storage. Inhibitors of dipeptide protease IV (DPP IV) prevent the proteolytic degradation of GLP-1, a peptide hormone produced in the gut that stimulates pancreatic insulin secretion. Inhibition of the peptidase prolongs the action of GLP-1, effectively increasing insulin secretion.

TABLE 23–7 Treatments for Type 2 Diabetes Mellitus

Intervention/treatment	Direct target	Effect of treatment
Weight loss	Adipose tissue; reduces TAG content	Reduces lipid burden; increases capacity for lipid storage in adipose tissue; restores insulin sensitivity
Exercise	AMPK, activated by increasing [AMP]/[ATP]	Aids weight loss; see Fig. 23–39
Sulfonylureas: glipizide (Glucotrol), glyburide (several brands), glimepiride (Amaryl)	Pancreatic β cells; K^+ channels blocked	Stimulates insulin secretion by pancreas; see Fig. 23–27
Biguanides: metformin (Glucophage)	AMPK, activated	Increases glucose uptake by muscle; decreases glucose production in liver
Thiazoladinediones: troglitazone (Rezulin),* rosiglitazone (Avandia),† pioglitazone (Actos)	PPARγ	Stimulates expression of genes, potentiating the action of insulin in liver, muscle, adipose tissue; increases glucose uptake; decreases glucose synthesis in liver
GLP-1 modulators: exenatide (Byetta), sitagliptin (Januvia)	Glucagon-like peptide-1, dipeptide protease IV	Enhances insulin secretion by pancreas

*Voluntarily withdrawn because of side effects.

†Prescriptions limited to patients not helped by other treatment, because of possible increased risk of cardiovascular disease.

The combination of weight loss and exercise is the preferred way to *prevent* development of the metabolic syndrome and type 2 diabetes. Recent findings concerning BAT in adults suggest an interesting possibility for aiding weight loss and reducing the amount of TAG that must be stored. The protein PRDM16 is expressed strongly, and perhaps uniquely, in brown adipose tissue. When overexpressed in the adipose tissue of mice, PRDM16 induces the differentiation of preadipocytes in white adipose tissue into *brown* adipocytes, with high levels of thermogenin and strikingly uncoupled respiration. Such cells could, in principle, consume fatty acids above the amount needed for ATP production, converting the energy of oxidation to heat. Given the widespread and increasing occurrence of type 2 diabetes, the possibility of stimulating fat oxidation by activating BAT certainly deserves exploration. ■

SUMMARY 23.5 Obesity, the Metabolic Syndrome, and Type 2 Diabetes

- The metabolic syndrome, which includes obesity, hypertension, elevated blood lipids, and insulin resistance, is often the prelude to type 2 diabetes.
- The insulin resistance that characterizes type 2 diabetes may be a consequence of abnormal lipid storage in muscle and liver, in response to a lipid intake that cannot be accommodated by adipose tissue.
- Expression of the enzymes of lipid synthesis is under tight and complex regulation. PPARs are transcription factors that determine the rate of synthesis of many enzymes involved in lipid metabolism and adipocyte differentiation.
- Effective treatments for type 2 diabetes include exercise, appropriate diet, and drugs that increase insulin sensitivity or insulin production.

Key Terms

Terms in bold are defined in the glossary.

hormone 929
neuroendocrine system 930
radioimmunoassay (RIA) 930
Scatchard analysis 932
endocrine 933
paracrine 933
autocrine 933
insulin 934
epinephrine 934
norepinephrine 934
catecholamines 934
eicosanoid hormones 935
steroid hormones 935
vitamin D hormone 935
retinoid hormones 936
thyroid hormones 936
nitric oxide ($NO^{\bullet}$) 936
NO synthase 936
hypothalamus 936
posterior pituitary 937
anterior pituitary 937
tropic hormone (tropin) 937
hepatocyte 939
white adipose tissue (WAT) 943
adipocyte 943
brown adipose tissue (BAT) 944
thermogenin (UCP1) 944
thermogenesis 944
myocyte 944
slow-twitch muscle 944
fast-twitch muscle 944
glomular filtration rate (GFR) 947
shivering thermogenesis 948
erythrocyte 949
leukocyte 949
lymphocytes 950
platelets 950
blood plasma 950
plasma proteins 950
ATP-gated K^+ channels 954
sulfonylurea drugs 954
glucagon 955
cortisol 958
diabetes mellitus 959
type 1 diabetes 959
type 2 diabetes 959
glucosuria 959
ketosis 959
acidosis 960
ketoacidosis 960
glucose-tolerance test 960
obesity 960
adipokines 960
leptin 961
leptin receptor 961
orexigenic 962
neuropeptide Y (NPY) 962
anorexigenic 962
α-melanocyte–stimulating hormone (α-MSH) 962
JAK (Janus kinase) 962
STAT (signal transducer and activator of transcription) 963
AMP-activated protein kinase (AMPK) 963
adiponectin 964
mTORC1 965
PPAR (peroxisome proliferator-activated receptor) 965
ghrelin 966
$PYY_{3–36}$ 967
metabolic syndrome 969

Further Reading

General Background and History

Blumenthal, S. (2009) The insulin immunoassay after 50 years: a reassessment. *Perspect. Biol. Med.* **52**, 343–354.

Fascinating historical account of development of the radioimmunoassay by Yalow and Berson and its use in studies of insulin and diabetes.

Chew, S.L. & Leslie, D. (2006) *Clinical Endocrinology and Diabetes: An Illustrated Colour Text*, Churchill Livingstone, Edinburgh.

Schmidt, T.J. (2010) Biochemistry of hormones. In *Textbook of Biochemistry with Clinical Correlations*, 7th edn (Devlin, T.M., ed.), pp. 883–938, John Wiley & Sons, Inc., New York.

Tissue-Specific Metabolism

Brosnan, J.T. & and Brosnan, M.E. (2007) Creatine: endogenous metabolite, dietary, and therapeutic supplement. *Annu. Rev. Nutr.* **27**, 241–261.

Cannon, B. & Nedergaard, K. (2004) Brown adipose tissue: function and physiological significance. *Physiol. Rev.* **84**, 277–359.

Elia, M. (1995) General integration and regulation of metabolism at the organ level. *Proc. Nutr. Soc.* **54**, 213–234.

Enerbäck, S. (2010) Human brown adipose tissue (minireview). *Cell Metab.* **11**, 248–252.

Randle, P.J. (1995) Metabolic fuel selection: general integration at the whole-body level. *Proc. Nutr. Soc.* **54**, 317–327.

Ravussin, E. & Galgani, J.E. (2011) The implication of brown adipose tissue for humans. *Annu. Rev. Nutr.* **31**, 33–37.

Hormonal Regulation of Fuel Metabolism

Cahill, G.F., Jr. (2006) Fuel metabolism in starvation. *Annu. Rev. Nutr.* **26**, 1–22.

Desvergne, B., Michalik, L., & Wahli, W. (2006) Transcriptional regulation of metabolism. *Physiol. Rev.* **86**, 465–514.

Feige, J.N. & Auwerx, J. (2007) Transcriptional coregulators in the control of energy homeostasis. *Trends Cell Biol.* **17**, 292–301.

Hardie, D.G. & Sakamoto, K. (2006) AMPK: a key sensor of fuel and energy status in skeletal muscle. *Physiology* **21**, 48–60.

Kadowaki, T., Yamauchi, T., Kubota, N., Hara, K., Ueki, K., & Tobe, K. (2006) Adiponectin and adiponectin receptors in insulin resistance, diabetes, and the metabolic syndrome. *J. Clin. Invest.* **116**, 1784–1792.

Kola, B., Boscaro, M., Rutter, G.A., Grossman, A.B., & Korbonits, M. (2006) Expanding role of AMPK in endocrinology. *Trends Endocrinol. Metab.* **17**, 205–215.

Kraemer, D.K., Al-Khalili, L., Guigas, B., Leng, Y., Garcia-Roves, P.M., & Krook, A. (2007) Role of AMP kinase and PPARδ in the regulation of lipid and glucose metabolism in human skeletal muscle. *J. Biol. Chem.* **282**, 19,313–19,320.

Lin, H.V. & Accill, D. (2011) Hormonal regulation of hepatic glucose production in health and disease. *Cell Metab.* **14**, 9–19.

Advanced review of the mechanisms that regulate production of glucose by the liver.

Maccarrone, M., Gasperi, V., Catani, M.V., Diep, T.A., Dainese, E., Hansen, H.S., & Avigliano, L. (2010) The endocannabinoid system and its relevance for nutrition. *Annu. Rev. Nutr.* **30**, 423–440.

Nguyen, A.D., Herzog, H., & Sainsbury, A. (2011) Neuropeptide Y and peptide YY: important regulators of energy metabolism. *Curr. Opin. Endocrinol. Diabetes. Obes.* **18**, 56–60.

Intermediate-level survey of the effects of NPY and PYY in the brain on energy metabolism in the mouse.

Nichols, C.G. (2006) K_{ATP} channels as molecular sensors of cellular metabolism. *Nature* **440**, 470–476.

Control of Body Mass

Ahima, R.S. (2005) Central actions of adipocyte hormones. *Trends Endocrinol. Metab.* **16**, 307–313.

A decrease in leptin is an important signal for the switch between fed and fasted states.

Ahima, R.S. (2006) Ghrelin—a new player in glucose homeostasis? *Cell Metab.* **3**, 301–307.

Azzu, V. & Brand, M.D. (2010) The on-off switches of the mitochondrial uncoupling proteins. *Trends Biochem. Sci.* **35**, 298–307.

Intermediate-level review of how cold, overfeeding, and starvation affect the expression of thermogenin genes.

Biddinger, S.B. & Kahn, C.R. (2006) From mice to men: insights into the insulin resistance syndromes. *Annu. Rev. Physiol.* **68**, 123–158.

Review of the structure, function, and role of uncoupling proteins.

Delzenne, N.M. & Cani, P.D. (2011) Interaction between obesity and the gut microbiota: relevance in nutrition. *Annu. Rev. Nutr.* **31**, 15–31.

Friedman, J.M. (2002) The function of leptin in nutrition, weight, and physiology. *Nutr. Rev.* **60**, S1–S14.

Intermediate-level review of all aspects of leptin biology.

Howell, J.J. & Manning, B.D. (2011) mTOR couples cellular nutrient sensing to metabolic homeostasis. *Trends Endocrinol. Metab.* **22**, 94–102.

Intermediate-level review of how mTORC1 mediates the metabolic responses to fluctuations in nutrient availability.

Jequier, E. & Tappy, L. (1999) Regulation of body weight in humans. *Physiol. Rev*. **79**, 451–480.

Detailed review of the role of leptin in body-weight regulation, the control of food intake, and the roles of white and brown adipose tissues in energy expenditure.

Klok, M.D., Jakobsdottir, S., & Drent, M.L. (2007) Role of leptin and ghrelin in the regulation of food intake and body weight. *Obes. Rev.* **8**, 21–34.

Marx, J. (2003) Cellular warriors at the battle of the bulge. *Science* **299**, 846–849.

Short review of biochemistry of weight control and introduction to several papers in the same issue of *Science* on obesity in humans.

Morton, G.J., Cummings, D.E., Baskin, D.G., Barsh, G.S., & Schwartz, M.W. (2006) Central nervous system control of food intake and body weight. *Nature* **443**, 289–295.

Zoncu, R., Efeyan, A., & Sabatini, D.M. (2011) mTOR: from growth signal integration to cancer, diabetes and ageing. *Nat. Rev. Mol. Cell Biol.* **12**, 21–35.

Obesity, the Metabolic Syndrome, and Type 2 Diabetes

Attie, A.D. & Scherer, P.E. (2009) Adipocyte metabolism and obesity. *J. Lipid Res.* **50**, S395–S399.

Barish, G.D., Narkar, V.A., & Evans, R.M. (2006) PPARδ: a dagger in the heart of the metabolic syndrome. *J. Clin. Invest.* **116**, 590–597.

Clee, S.M. & Attie, A.D. (2007) The genetic landscape of type 2 diabetes in mice. *Endocrinol. Rev.* **28**, 48–83.

Cypess, A.M. & Kahn, C.R. (2010) Brown fat as a therapy for obesity and diabetes. *Curr. Opin. Endocrinol. Diabetes. Obes.* **17**, 143–149.

Intermediate-level discussion of the possibility of stimulating fat oxidation by BAT as a treatment for obesity.

Guilherme, A., Virbasius, J.V., Puri, V., & Czech, M.P. (2008) Adipocyte dysfunctions linking obesity to insulin resistance and type 2 diabetes. *Nat. Rev. Mol. Cell Biol.* **9**, 367–377.

Harper, M.E., Green, K., & Brand, M.D. (2008) The efficiency of cellular energy transduction and its implications for obesity. *Annu. Rev. Nutr.* **28**, 13–33.

Kasuga, M. (2006) Insulin resistance and pancreatic β cell failure. *J. Clin. Invest.* **116**, 1756–1760.

Introduction to a series of reviews about type 2 diabetes in this issue of the journal.

Klein, J., Perwitz, N., Kraus, D., & Fasshauer, M. (2006) Adipose tissue as source and target for novel therapies. *Trends Endocrinol. Metab.* **17**, 26–32.

Intermediate-level review.

Lusis, A.J., Attie, A.D., & Reue, K. (2008) Metabolic syndrome: from epidemiology to systems biology. *Nat. Rev. Genet.* **9**, 819–830.

McAllister, E.J., Dhurandhar, N.V., Keith, S.W., Aronne, L.J., Barger, J., Baskin, M., Benca, R.M., Biggio, J., Boggiano, M.M., Eisenmann, J.C., et al. (2009) Ten putative contributors to the obesity epidemic. *Crit. Rev. Food Sci. Nutr.* **49**, 868–913.

Advanced and lengthy review of factors responsible for the international epidemic of obesity.

Muoio, D.M. & Newgard, C.B. (2008) Molecular and metabolic mechanisms of insulin resistance and β-cell failure in diabetes. *Nat. Rev. Mol. Cell Biol.* **9**, 193–205.

Savage, D.B., Petersen, K.F., & Shulman, G.I. (2007) Disordered lipid metabolism and the pathogenesis of insulin resistance. *Physiol. Rev.* **87**, 507–520.

Semple, R.K., Chatterjee, V.K.K., & O'Rahilly, S. (2006) PPARγ and human metabolic disease. *J. Clin. Invest.* **116**, 581–589.

Sharma, A.M. & Staels, B. (2007) Peroxisome proliferator-activated receptor γ and adipose tissue—understanding obesity-related changes in regulation of lipid and glucose metabolism. *J. Clin. Endocrinol. Metab.* **92**, 386–395.

Verdin, E., Hirschey, M.D., Finley, L.W., & Haigis, M.C. (2010) Sirtuin regulation of mitochondria: energy production, apoptosis, and signaling. *Trends Biochem. Sci.* **35**, 669–675.

Vidal-Puig, A., & Unger, R.H. (2010). *Biochim. Biophys. Acta,* **180**, 207–208.

This entire issue of the journal is about lipotoxicity and the metabolic syndrome.

Virtue, S. & Vidal-Puig, A. (2008) It's not how fat you are, it's what you do with it that counts. *PLoS Biol.*, **6**, e237. (doi:10.1371/journal.pbio.0060237)

Voight, B.F., Scott, L.J., Steinthorsdottir, V., Morris, A.P., Dina C., Welch, R.P., Zeggini, E., Huth, C., Aulchencko, Y.S., Thorleifsson, G., et al. (2010) Twelve type 2 diabetes susceptibility loci identified through large-scale association analysis. *Nat. Genet.* **42**, 579–589.

Results of a large survey (47,000 individuals) to identify genes that predispose humans toward type 2 diabetes.

Whittle, A.J., Lopez, M., & Vidal-Puig, A. (2011) Using brown adipose tissue to treat obesity—the central issue. *Trends Mol. Med.* **8**, 405–411.

Intermediate-level review of the possibility of treating obesity by stimulating brown fat activity.

Xu, H., Barnes, G.T., Yang, Q., Tan, G., Yang, D., Chou, C.J., Sole, J., Nichols, A., Ross, J.S., Tartaglia, L.A., & Chen, H. (2003) Chronic inflammation in fat plays a crucial role in the development of obesity-related insulin resistance. *J. Clin. Invest.* **112**, 1821–1830.

Problems

1. Peptide Hormone Activity Explain how two peptide hormones as structurally similar as oxytocin and vasopressin can have such different effects (see Fig. 23–9).

2. ATP and Phosphocreatine as Sources of Energy for Muscle During muscle contraction, the concentration of phosphocreatine in skeletal muscle drops while the concentration of ATP remains fairly constant. However, in a classic experiment, Robert Davies found that if he first treated muscle with 1-fluoro-2,4-dinitrobenzene (p. 98), the concentration of ATP declined rapidly while the concentration of phosphocreatine remained unchanged during a series of contractions. Suggest an explanation.

3. Metabolism of Glutamate in the Brain Brain tissue takes up glutamate from the blood, transforms it into glutamine, and releases the glutamine into the blood. What is accomplished by this metabolic conversion? How does it take place? The amount of glutamine produced in the brain can actually exceed the amount of glutamate entering from the blood. How does this extra glutamine arise? (Hint: You may want to review amino acid catabolism in Chapter 18; recall that NH_4^+ is very toxic to the brain.)

4. Proteins as Fuel during Fasting When muscle proteins are catabolized in skeletal muscle during a fast, what are the fates of the amino acids?

5. Absence of Glycerol Kinase in Adipose Tissue Glycerol 3-phosphate is required for the biosynthesis of triacylglycerols. Adipocytes, specialized for the synthesis and degradation of triacylglycerols, cannot use glycerol directly because they lack glycerol kinase, which catalyzes the reaction

$$\text{Glycerol} + \text{ATP} \longrightarrow \text{glycerol 3-phosphate} + \text{ADP}$$

How does adipose tissue obtain the glycerol 3-phosphate necessary for triacylglycerol synthesis?

6. Oxygen Consumption during Exercise A sedentary adult consumes about 0.05 L of O_2 in 10 seconds. A sprinter, running a 100 m race, consumes about 1 L of O_2 in 10 seconds. After finishing the race, the sprinter continues to breathe at an elevated (but declining) rate for some minutes, consuming an extra 4 L of O_2 above the amount consumed by the sedentary individual.

(a) Why does the need for O_2 increase dramatically during the sprint?

(b) Why does the demand for O_2 remain high after the sprint is completed?

7. Thiamine Deficiency and Brain Function Individuals with thiamine deficiency show some characteristic neurological signs and symptoms, including loss of reflexes, anxiety, and mental confusion. Why might thiamine deficiency be manifested by changes in brain function?

8. Potency of Hormones Under normal conditions, the human adrenal medulla secretes epinephrine ($C_9H_{13}NO_3$) at a rate sufficient to maintain a concentration of 10^{-10} M in circulating blood. To appreciate what that concentration means, calculate the diameter of a round swimming pool, with a water depth of 2.0 m, that would be needed to dissolve 1.0 g (about 1 teaspoon) of epinephrine to a concentration equal to that in blood.

9. Regulation of Hormone Levels in the Blood The half-life of most hormones in the blood is relatively short. For example, when radioactively labeled insulin is injected into an animal, half of the labeled hormone disappears from the blood within 30 min.

(a) What is the importance of the relatively rapid inactivation of circulating hormones?

(b) In view of this rapid inactivation, how is the level of circulating hormone kept constant under normal conditions?

(c) In what ways can the organism make rapid changes in the level of a circulating hormone?

10. Water-Soluble versus Lipid-Soluble Hormones On the basis of their physical properties, hormones fall into one of two categories: those that are very soluble in water but relatively insoluble in lipids (e.g., epinephrine) and those that are relatively insoluble in water but highly soluble in lipids (e.g., steroid hormones). In their role as regulators of cellular activity, most water-soluble hormones do not enter their target cells. The lipid-soluble hormones, by contrast, do enter their target cells and ultimately act in the nucleus. What is the correlation between solubility, the location of receptors, and the mode of action of these two classes of hormones?

11. Metabolic Differences between Muscle and Liver in a "Fight-or-Flight" Situation When an animal confronts a "fight-or-flight" situation, the release of epinephrine promotes glycogen breakdown in the liver, heart, and skeletal muscle. The end product of glycogen breakdown in the liver is glucose; the end product in skeletal muscle is pyruvate.

(a) What is the reason for the different products of glycogen breakdown in the two tissues?

(b) What is the advantage to an animal that must fight or flee of these specific glycogen breakdown routes?

12. Excessive Amounts of Insulin Secretion: Hyperinsulinism Certain malignant tumors of the pancreas cause excessive production of insulin by the β cells. Affected individuals exhibit shaking and trembling, weakness and fatigue, sweating, and hunger.

(a) What is the effect of hyperinsulinism on the metabolism of carbohydrates, amino acids, and lipids by the liver?

(b) What are the causes of the observed symptoms? Suggest why this condition, if prolonged, leads to brain damage.

13. Thermogenesis Caused by Thyroid Hormones Thyroid hormones are intimately involved in regulating the basal metabolic rate. Liver tissue of animals given excess thyroxine shows an increased rate of O_2 consumption and increased heat output (thermogenesis), but the ATP concentration in the tissue is normal. Different explanations have been offered for the thermogenic effect of thyroxine. One is that excess thyroxine causes uncoupling of oxidative phosphorylation in mitochondria. How could such an effect account for the observations? Another explanation suggests that the thermogenesis is due to an increased rate of ATP utilization by the thyroxine-stimulated tissue. Is this a reasonable explanation? Why?

14. Function of Prohormones What are the possible advantages of synthesizing hormones as prohormones?

15. Sources of Glucose during Starvation The typical human adult uses about 160 g of glucose per day, 120 g of which is used by the brain. The available reserve of glucose (~20 g of circulating glucose and ~190 g of glycogen) is adequate for about one day. After the reserve has been depleted during starvation, how would the body obtain more glucose?

16. Parabiotic *ob/ob* Mice By careful surgery, researchers can connect the circulatory systems of two mice so that the same blood circulates through both animals. In these **parabiotic** mice, products released into the blood by one animal reach the other animal via the shared circulation. Both animals are free to eat independently. If a mutant *ob/ob* mouse (both copies of the *OB* gene are defective) and a normal *OB/OB* mouse (two good copies of the *OB* gene) were made parabiotic, what would happen to the weight of each mouse?

17. Calculation of Body Mass Index A portly biochemistry professor weighs 260 lb (118 kg) and is 5 feet 8 inches (173 cm) tall. What is his body mass index? How much weight would he have to lose to bring his body mass index down to 25 (normal)?

18. Insulin Secretion Predict the effects on insulin secretion by pancreatic β cells of exposure to the potassium ionophore valinomycin (Fig. 11-44). Explain your prediction.

19. Effects of a Deleted Insulin Receptor A strain of mice specifically lacking the insulin receptor of liver is found to have mild fasting hyperglycemia (blood glucose = 132 mg/dL, vs. 101 mg/dL in controls) and a more striking hyperglycemia in the fed state (glucose = 363 mg/dL, vs. 135 mg/dL in controls). The mice have higher than normal levels of glucose 6-phosphatase in the liver and elevated levels of insulin in the blood. Explain these observations.

20. Decisions on Drug Safety The drug Avandia (rosiglitazone) is effective in lowering blood glucose in patients with type 2 diabetes but also carries an increased risk of heart attack. If it were your responsibility to decide whether this drug should remain on the market (labeled with suitable warnings of its side effects) or should be withdrawn, what factors would you weigh in making your decision?

21. Type 2 Diabetes Medication The drugs acarbose (Precose) and miglitol (Glyset), used in the treatment of type 2 diabetes mellitus, inhibit α-glucosidases in the brush border of the small intestine. These enzymes degrade oligosaccharides derived from glycogen or starch to monosaccharides. Suggest a possible mechanism for the salutary effect of these drugs for individuals with diabetes. What side effects, if any, would you expect from these drugs. Why? (Hint: Review lactose intolerance, pp. 561–562).

Data Analysis Problem

22. Cloning the Pancreatic β-Cell Sulfonylurea Receptor Glyburide, a member of the sulfonylurea family of drugs shown on p. 955, is used to treat type 2 diabetes. It binds to and closes the ATP-gated K^+ channel shown in Figures 23–27 and 23–28.

(a) Given the mechanism shown in Figure 23–27, would treatment with glyburide result in increased or decreased insulin secretion by pancreatic β cells? Explain your reasoning.

(b) How does treatment with glyburide help reduce the symptoms of type 2 diabetes?

(c) Would you expect glyburide to be useful for treating type 1 diabetes? Why or why not?

Aguilar-Bryan and coauthors (1995) cloned the gene for the sulfonylurea receptor (SUR) portion of the ATP-gated K^+ channel from hamsters. The research team went to great lengths to ensure that the gene they cloned was in fact the SUR-encoding gene. Here we explore how it is possible for researchers to demonstrate that they have actually cloned the gene of interest rather than another gene.

The first step was to obtain pure SUR protein. As was already known, drugs such as glyburide bind SUR with very high affinity (K_d < 10 nM), and SUR has a molecular weight of 140 to 170 kDa. Aguilar-Bryan and coworkers made use of the high-affinity glyburide binding to tag the SUR protein with a radioactive label that would serve as a marker to purify the protein from a cell extract. First, they made a radiolabeled derivative of glyburide, using radioactive iodine (^{125}I):

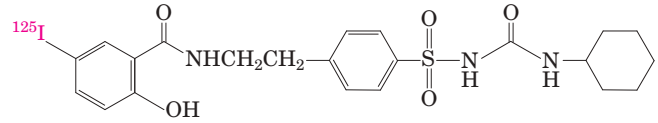

[^{125}I]5-Iodo-2-hydroxyglyburide

(d) In preliminary studies, the ^{125}I-labeled glyburide derivative (hereafter, [^{125}I]glyburide) was shown to have the same K_d and binding characteristics as unaltered glyburide. Why was it necessary to demonstrate this (what alternative possibilities did it rule out)?

Even though [^{125}I]glyburide bound to SUR with high affinity, a significant amount of the labeled drug would probably

dissociate from the SUR protein during purification. To prevent this, [^{125}I]glyburide had to be covalently cross-linked to SUR. There are many methods for covalent cross-linking; Aguilar-Bryan and coworkers used UV light. When aromatic molecules are exposed to short-wave UV, they enter an excited state and readily form covalent bonds with nearby molecules. By cross-linking the radiolabeled glyburide to the SUR protein, the researchers could simply track the ^{125}I radioactivity to follow SUR through the purification procedure.

Aguilar-Bryan and colleagues treated hamster HIT cells (which express SUR) with [^{125}I]glyburide and UV light, purified the ^{125}I-labeled 140 kDa protein, and sequenced its amino-terminal 25 amino acid segment; they found the sequence PLAFCGTENHSAAYRVDQGVLNNGC. The investigators then generated antibodies that bound to two short peptides in this sequence, one that bound to PLAFCGTE and the other to HSAAYRVDQGV, and showed that these antibodies bound the purified ^{125}I-labeled 140 kDa protein.

(e) Why was it necessary to include this antibody-binding step?

Next, the researchers designed PCR primers based on the sequences above and cloned a gene from a hamster cDNA library that encoded a protein that included these sequences (see Chapter 9 on biotechnology methods). The cloned putative *SUR* cDNA hybridized to an mRNA of the appropriate length that was present in cells known to contain SUR. The putative *SUR* cDNA did not hybridize to any mRNA fraction of the mRNAs isolated from hepatocytes, which do not express SUR.

(f) Why was it necessary to include this putative *SUR* cDNA–mRNA hybridization step?

Finally, the cloned gene was inserted into and expressed in COS cells, which do not normally express the *SUR* gene. The investigators mixed these cells with [^{125}I]glyburide with or without a large excess of unlabeled glyburide, exposed the cells to UV light, and measured the radioactivity of the 140 kDa protein produced. Their results are shown in the table.

Experiment	Cell type	Added putative *SUR* cDNA?	Added excess unlabeled glyburide?	^{125}I label in 140 kDa protein
1	HIT	No	No	+ + +
2	HIT	No	Yes	−
3	COS	No	No	−
4	COS	Yes	No	+ + +
5	COS	Yes	Yes	−

(g) Why was no ^{125}I-labeled 140 kDa protein found in experiment 2?

(h) How would you use the information in the table to argue that the cDNA encoded SUR?

(i) What other information would you want to collect to be more confident that you had cloned the *SUR* gene?

Reference

Aguilar-Bryan, L., Nichols, C.G., Wechsler, S.W., Clement, J.P. IV, Boyd, A.E. III, González, G., Herrera-Sosa, H., Nguy, K., Bryan, J., & Nelson, D.A. (1995) Cloning of the β cell high-affinity sulfonylurea receptor: a regulator of insulin secretion. *Science* **268**, 423–426.

this page left intentionally blank